DIGITAL ACCESS TO SCHOLARSHIP AT HARVARD
DASH.HARVARD.EDU

HARVARD LIBRARY
Office for Scholarly Communication

Two Views on Gravity: F-Theory and Holography

The Harvard community has made this article openly available. Please share how this access benefits you. Your story matters

Citation	Kang, Jinwoo. 2019. Two Views on Gravity: F-Theory and Holography. Doctoral dissertation, Harvard University, Graduate School of Arts & Sciences.
Citable link	http://nrs.harvard.edu/urn-3:HUL.InstRepos:42029691
Terms of Use	This article was downloaded from Harvard University's DASH repository, and is made available under the terms and conditions applicable to Other Posted Material, as set forth at http://nrs.harvard.edu/urn-3:HUL.InstRepos:dash.current.terms-of-use#LAA

Two Views on Gravity: F-theory and Holography

A DISSERTATION PRESENTED
BY
JINWOO KANG
TO
THE DEPARTMENT OF PHYSICS

IN PARTIAL FULFILLMENT OF THE REQUIREMENTS
FOR THE DEGREE OF
DOCTOR OF PHILOSOPHY
IN THE SUBJECT OF
PHYSICS

HARVARD UNIVERSITY
CAMBRIDGE, MASSACHUSETTS
APRIL 2019

©2019 – Jinwoo Kang
all rights reserved.

Thesis advisor: Professor Daniel Jafferis Jinwoo Kang

Two Views on Gravity: F-theory and Holography

Abstract

We investigate two different views towards gravitational theories using mathematical frameworks. First, we study gravitational theories with supersymmetries in various dimensions from top-down approach via F-theory or M-theory compactifications. We utilize the geometry of elliptic fibrations to investigate such compactifications. The other viewpoint does not require to study theories with supersymmetries. With the framework of von Neumann algebras, we study gravitational theories in the bulk and its boundary conformal field theories.

We consider the construction of supergravity theories in three to six dimensions via the compactifcation of M-theory and F-theory on elliptically-fibered manifolds. Interesting gauge theory sectors arise when such manifolds have singularities. We study the resolutions of singularities of these spaces which give the window onto the low energy physics of effective supergravity.

We consider elliptically-fibered Calabi–Yau threefolds that give rise to supergravities with simple gauge groups, with a particular emphasis on F_4, G_2, Spin(7), and Spin(8), or semi-simple gauge groups of the form SO(4), Spin(4), $SU(2) \times G_2$, $SU(2) \times SU(3)$, $SU(2) \times Sp(4)$, $SU(2) \times Sp(4)/\mathbb{Z}_2$, $SU(2) \times SU(4)$, and $SU(2) \times SU(4)/\mathbb{Z}_2$. For such models we enumerate the spectra in five-dimensions and six-dimensions with eight supercharges via M-theory and F-theory compactifications and determine the structure of the Coulomb branch for these 5d theories. Furthermore we verify that all local

anomalies in 6d are canceled. For theories with an abelian gauge group we introduced a new, general model for an elliptic fibration that realizes this $U(1)$ symmetry.

The physical spectra often depends on topological invariants of the elliptic fibration. In particular, when the effective theory is required to be supersymmetric, the elliptic fibration must be Calabi–Yau. In the more general case, when the fibration is not assumed to be Calabi–Yau, we utilized the resolution of singularities to determine a host of topological invariants and characteristic numbers for elliptic fibrations that correspond to a physical gauge group with a simple non-abelian factor. These include the Euler characteristic, Hodge numbers, Chern numbers, Pontryagin numbers, Todd genus, holomorphic genera, L-genus, A-genus, and the M-theory curvature invariant.

In a different vein, infinite-dimensional von Neumann algebras of various types are used to understand the local algebras in quantum field theories. Utilizing such von Neumann algebras, one can study holographic quantum field theories and their gravity duals by incorporating toy models from quantum error correction.

We reformulate the entanglement wedge reconstruction in the language of infinite-dimensional von Neumann algebras. Using the frame of Tomita–Takasaki theory, we can also write the infinite-dimensional analog of the relative entropies. Using these techniques, we show that for a general infinite-dimensional Hilbert space, the entanglement wedge reconstruction is identical to the equivalence in relative entropies between the boundary and the bulk.

Contents

I Introduction **1**

1 Introduction **2**
- 1.1 String theory . . . 6
- 1.2 M-theory and dualities to string theories . . . 12
- 1.3 Compactifications to various dimensions . . . 17
- 1.4 F-theory . . . 20
- 1.5 F/M-theory compactifications . . . 27
- 1.6 Canonical problems in F/M-theory . . . 29
- 1.7 Von Neuman algebras in quantum gravity . . . 31

2 Geometry of Elliptic Fibrations, Characteristic Numbers, and 5D/6D Supergravity Theories **34**
- 2.1 Elliptic fibrations and fiber types . . . 51
- 2.2 Weierstrass models, Tate's algorithm, and Mordell–Weil group . . . 59
- 2.3 Lie groups Lie algebra, representations from an elliptic fibrations . . . 71
- 2.4 The geometry of crepant resolutions and Couomb branches . . . 83
- 2.5 Non-simply-connected simple groups in F-theory . . . 85
- 2.6 Collisions of singularities and semi-smple groups in F-theory . . . 87
- 2.7 Intersection theory and pushforward formulae . . . 89
- 2.8 Euler characteristic and Hodge numbers . . . 100
- 2.9 Characteristic numbers of the fourfolds . . . 104
- 2.10 Weak coupling limit and brane geometry . . . 111
- 2.11 Tadpole matching and Whitney branes . . . 115
- 2.12 $5d\,\mathcal{N}=1$ supergravity theories . . . 117
- 2.13 $6d\,\mathcal{N}=(1,0)$ supergravity theories . . . 122

3 Entanglement entropy, Holography, and von Neumann Algebra **131**
- 3.1 Bounded and Unbounded Operators . . . 137
- 3.2 Example of a strongly convergent sequence of operators . . . 146
- 3.3 Infinite-dimensional von Neumann algebras . . . 150
- 3.4 Definition of von Neumann algebras . . . 158
- 3.5 Review of Tomita-Takesaki theory . . . 164

3.6 The three-qutrit code and a finite tensor network 170

II Weak Coupling Limit and a Rank One Mordell–Weil Group 173

4 A New Model for Elliptic Fibrations with a Rank One Mordell–Weil Group **176**
4.1 Summary and the layouts 177
4.2 $Q_7(\mathscr{L}, \mathscr{S})$ model and Jacobian fibration 179
4.3 Properties of a $Q_7(\mathscr{L}, \mathscr{S})$ elliptic fibration 190
4.4 Weak coupling limit of a $Q_7(\mathscr{L}, \mathscr{S})$ model 204
4.5 Conclusion and discussion 212

III Topological Invariants and Characteristic Numbers 215

5 Euler characteristics of crepant resolutions of Weierstrass models **221**
5.1 Stratey and organization of the chapter 225
5.2 Euler Characteristic of Elliptic Fibrations 229
5.3 The Euler Characteristic as the Degree of the Top Chern Class 233
5.4 Pushforwards and Computing the Euler Characteristic 240
5.5 Jacobi's Partial Fraction Identity 246
5.6 Hodge Numbers of Elliptically Fibered Calabi–Yau Threefolds 248
5.7 An Illustrative Example: SU(2)-Models 250
5.8 Tables of Results 254
5.9 Discussion 263

6 Characteristic numbers of crepant resolutions of Weierstrass models **265**
6.1 Strategy and roadmaps of results 266
6.2 Geometric discussion 271
6.3 Invariance of characteristic numbers 275
6.4 Pushforward of blowups and projective bundles. 277
6.5 *G*-models 285

7 Characteristic numbers of elliptic fibrations with non-trivial Mordell–Weil groups **291**
7.1 Models with multisections and organization of the chapter 292
7.2 Descriptions of the elliptic fibrations considered 295
7.3 Pushforward theorems 303
7.4 Collection of results 308

IV Geometric Perspective on 5d/6d Supergravity Theories with Simple Gauge Groups 316

8 The Geometry of F_4-Models 320
8.1 Summary of results . . . 321
8.2 Step 8 of Tate's algorithm . . . 335
8.3 The crepant resolution . . . 337
8.4 Fiber structure . . . 341
8.5 Topological invariants . . . 356
8.6 A double cover of a ruled surface branch along $2b$ fibers . . . 365
8.7 Application to M-theory and F-theory in 5 and 6 dimensions . . . 367
8.8 Conclusion . . . 378

9 The Geometry of G_2, Spin(7), and Spin(8)-models 382
9.1 Step 6 of Tate's algorithm characterizing the fiber I_0^* . . . 390
9.2 Summary of results . . . 393
9.3 G_2-models . . . 415
9.4 Spin(7)-models . . . 426
9.5 Spin(8)-model . . . 441
9.6 Application to five-dimensional and six-dimensional supergravity theories . . . 454

V 5d and 6d Spectra and Anomalies of Semi-simple Gauge Group Models 462

10 Flopping and Slicing: SO(4) and Spin(4)-models 470
10.1 Models considered . . . 470
10.2 Summary of results . . . 478
10.3 SO(4)-model . . . 497
10.4 Spin(4)-model . . . 508

11 The Geometry of $SU(2) \times G_2$-models 524
11.1 Summary and organization of the chapter . . . 526
11.2 Geometric Results . . . 539
11.3 The Crepant Resolutions and Fiber Structures . . . 553
11.4 Deriving the matter representation of an $SU(2) \times G_2$-model . . . 573
11.5 *5d* and *6d* Supergravity Theories with Eight Supercharges . . . 579
11.6 Counting hypermultiplets: numerical oddities . . . 585

12 48 CREPANT PATHS TO $SU(2)\times SU(3)$ **593**
12.1 Summary and organization of this chapter . . . 596
12.2 The many faces of the $SU(2)\times SU(3)$-model . . . 604
12.3 Geometry . . . 609
12.4 Hyperplane arrangements and geography of flops . . . 618
12.5 The $I_2^s+I_3^s$ Model . . . 628
12.6 The III+IV^s Model . . . 647
12.7 *5d* and *6d* supergravity theories with eight supercharges . . . 664
12.8 Fiber enhancement . . . 673

13 MORDELL-WEIL TORSION, ANOMALIES, AND PHASE TRANSITIONS **691**
13.1 Summary of results . . . 695
13.2 $(SU(2)\times Sp(4))/\mathbb{Z}_2$-model . . . 712
13.3 $SU(2)\times Sp(4)$-model . . . 723
13.4 $(SU(2)\times SU(4))/\mathbb{Z}_2$-model . . . 736
13.5 $SU(2)\times SU(4)$-model . . . 753

VI Entanglement Entropy, Holography, and Infinite-dimensional von Neumann Algebra 772

14 HOLOGRAPHIC RELATIVE ENTROPY IN INFINITE-DIMENSIONAL HILBERT SPACES 775
14.1 The Main Theorem: Bulk Reconstruction and Relative Entropy . . . 776
14.2 Proof of Theorem 14.1.1 . . . 782
14.3 Proof of Theorem 3.0.1 . . . 794
14.4 Discussion . . . 801

15 ENTANGLEMENT WEDGE RECONSTRUCTION OF INFINITE-DIM VON NEUMANN ALGEBRAS **816**
15.1 The isometry between two infinite-dimensional Hilbert spaces . . . 821
15.2 Defining von Neumann algebras . . . 823
15.3 Definition of the tensor network map . . . 829
15.4 Properties of the tensor network map . . . 834
15.5 Cyclic and separating vectors . . . 840
15.6 M_{code} is a hyperfinite type II_1 factor . . . 844
15.7 The relative Tomita operator . . . 847
15.8 Computing relative entropy for hyperfinite von Neumann algebras . . . 854
15.9 Conclusion and outlook . . . 872

VII Conclusion **875**

16 Conclusion **876**

References **886**

Citations to Previously Published Work

The contents of Part II are based on the following papers:

> **Chapter 4**: "A New Model for Elliptic Fibrations with a Rank One Mordell-Weil Group: I. Singular Fibers and Semi-Stable Degenerations," Mboyo Esole, Monica Jinwoo Kang, and Shing-Tung Yau, arXiv:1410.0003 [hep-th].

The contents of Part III are based on the following papers:

> **Chapter 5**: "The Geometry of F_4-Models," Mboyo Esole, Patrick Jefferson, and Monica Jinwoo Kang, arXiv:1704.08251 [hep-th].
>
> **Chapter 6**: "The Geometry of G_2, Spin(7), and Spin(8)-models," Mboyo Esole, Ravi Jagadeesan, and Monica Jinwoo Kang, arXiv:1709.04913 [hep-th].

The contents of Part III are based on the following papers:

> **Chapter 7**: "Euler Characteristics of Crepant Resolutions of Weierstrass Models," Mboyo Esole, Patrick Jefferson, and Monica Jinwoo Kang, To appear in Comm. Math. Phys., arXiv:1703.00905 [math.AG].
>
> **Chapter 8**: "Characteristic numbers of crepant resolutions of Weierstrass models," Mboyo Esole and Monica Jinwoo Kang, arXiv:1807.08755 [hep-th].
>
> **Chapter 9**: "Characteristic numbers of elliptic fibrations with non-trivial Mordell-Weil groups," Mboyo Esole and Monica Jinwoo Kang, arXiv:1808.07054 [hep-th].

The contents of Part III are based on the following papers:

> **Chapter 10**: "Flopping and Slicing: SO(4) and Spin(4)-models," Mboyo Esole and Monica Jinwoo Kang, arXiv:1802.04802 [hep-th].
>
> **Chapter 11**: "The Geometry of the $SU(2)\times G_2$-model," Mboyo Esole and Monica Jinwoo Kang, JHEP **1902**, 091 (2019), arXiv:1805.03214 [hep-th].

Chapter 12: "48 Crepant Paths to SU(2)×SU(3)," Mboyo Esole, Ravi Jagadeesan, and Monica Jinwoo Kang, arXiv:1905.05174 [hep-th].

Chapter 13: "Mordell-Weil Torsion, Anomalies, and Phase Transitions," Mboyo Esole, Monica Jinwoo Kang, and Shing-Tung Yau, arXiv: 1712.02337 [hep-th].

The contents of Part III are based on the following papers:

Chapter 14: "Holographic Relative Entropy in Infinite-dimensional Hilbert Spaces," Monica Jinwoo Kang and David Kolchmeyer, arXiv:1811.05482 [hep-th].

Chapter 15: "Entanglement Wedge Reconstruction of Infinite-dimensional von Neumann algebras using Tensor Networks," Monica Jinwoo Kang and David Kolchmeyer, To appear.

To my beloved parents and brother
for their endless encouragement, love, and inspiration
who have shown me that everything is possible.

항상 웃음을 잃지 않고 노력하면 이룰 수 있다고 가르쳐준
어머니 이영순과 아버지 강기흥께
그리고 수학의 아름다움을 보여주고 항상 든든한 버팀목이 되어준
동생 강성경에게 이 논문을 바칩니다.

Acknowledgments

First, I must thank my advisor Daniel Jafferis for his guidance throughout my graduate career. The path which my graduate studies have taken is rooted in him, and he has inspired me to be an independent thinker.

I would also like to thank Mboyo Esole, who has guided me both academically and emotionally. I have learned so much from him from thinking geometrically and elaborating on ideas to how to feel more optimistic in life. He has been a true mentor, a respectful collaborator, and a very close caring friend. It was a real pleasure to work with him and get to know him. Further, it has been a privilege to observe the care which he bestows on those around him.

I have benefited greatly from the wisdom of Shing-Tung Yau, who has been a constant source of inspiration. His kindness was a light that provided comfort to my graduate studies. It goes without saying that I extend my gratitude to my collaborators Ravi Jagadeesan, Patrick Jefferson, and David Kolchmeyer. It has been always wonderful to learn about different perspectives from my collaborators.

My lasting memories of the experience at the string theory group at Harvard will be dominated by Delilah Gates, Daniel Harlow, Temple He, Guglielmo Lockhart, Prahar Mitra, Maria Rodriguez, and David Vegh. From physics discussions to everyday chitchat, they have provided me mirth and gaiety. I want to especially thank Daniel Harlow for his astute perspective in physics and constant

encouragement. He has instigated many research ideas and shined me new directions. I also want to acknowledge Temple He for his constant support and joyous discussions. Furthermore, I am deeply thankful to Nicole D'Aleo who not only helped to arrange everything from reimbursements to application materials but also gave strong moral support as a close friend.

The physics department of Harvard provided a very passionate and encouraging environment. I want to particularly thank Melissa Franklin for guiding me with advice through many important decisions in my career. Her positive energy and support made me be stronger and dedicated to physics. Without her, my graduate career would not have been possible.

Throughout my graduate studies, I have also benefited from discussions with many professors and postdocs, including Murad Alim, Louise Anderson, Paolo Aluffi, Ibrahima Bah, Vijay Balasubramanian, Richard Derryberry, Ron Donagi, Sergei Gukov, Babak Haghighat, Craig Lawrie, Kimyeong Lee, Noppadol Mekareeya, Hirosi Ooguri, Steven Rayan, Shu-Heng Shao, Wati Taylor, Cumrun Vafa, Stefan Vandoren, Wen-bin Yan, and Piljin Yi. I want to especially thank Sergei Gukov for all the discussions and his patience in explaining any physics question I had in person or via email. I would like to extend my thanks to Craig Lawrie, who was always available for discussions and gave me warm support.

Growing up in Korea, I have been fortunate to be supervised by Young H. Kim and Young Cheol Jeon in Korea Science Academy who have shown me the elegance of physics and mathematics. They have encouraged me to try every academic path I aspire to, regardless of my gender.

I would also like to express my gratitude to my amazing friends, Sangguen Cho, Jihee Kim, Taeho Kim, Joon Park, and Yoonsang Yoon for much love, joy, and encouragement. They were more than

happy to listen to my life stories whether it was good or bad, and I did not have to miss my home as an international student due to their existence.

Lastly and most importantly, mere words cannot adequately express the gratitude that I have for my parents, Youngsoon Lee and Kiheung Kang, and my brother Sungkyung Kang. Their love and endless encouragement throughout the last seven years of graduate studies have formed the bedrock out of which this thesis has grown. I owe the person that I am today to their abiding support. Without Sungkyung, much more than this thesis would not exist.

Part I

Introduction

All that the human mind has produced—the brightest in genius, the most persevering in application, has been lavished on the details of the law of gravity.

Charles Babbage

1

Introduction

The vast edifice of modern physics is without doubt the most predictive prescription ever devised by mankind to describe the world around us. Despite stellar accomplishments, such as the experimental verification of accuracy to one part per billion of the fine structure constant of the electron, there still remain many open questions, and not just questions of detail, but fundamental, foundational questions. The main question relevant for this thesis can be illustrated by a simple thought experi-

ment, as follows. Ask the students in any high school physics class what the simplest of the four fundamental forces that unpin our universe is and the universal response is gravity. Ask the professors at any university what the most complicated of the four fundamental forces is and the answer will also, universally, be gravity. How to reconcile this vast jump between a theory that appears simple in one's youth, and becomes most troublesome as one ages? The goal of this thesis will be to shed some light on the difficulties involved with gravity, and to present approaches to understanding gravity which will open a window onto its elusive nature.

Of course, the reason why the high school students cannot yet appreciate the subtlety of gravity is that there are yet to be exposed unto the quantum world, where it comes to conflict. It is in this world, beyond the classical paradise of general relativity, that the bugbears of gravity come into being. To wit, the difficulty is in the study of *quantum gravity*.

The theory of quantum gravity is vital to understand when the gravitational force is of equal strength with other forces, namely strong, weak, and electromagnetic forces. The latter, non-gravitational forces, are described by the Standard Model, which is the pinnacle of quantum field theory combining them, whereas the former is described via the general relativity that describes classical gravity in our spacetime; any theory of quantum gravity must encompass both of these theoretical frameworks. As we endeavor to unveil the fundamental truth underlying the interactions of the fundamental forces and their completions, we naturally try to understand how gravity warps the spacetime so strongly in a manner where quantum mechanics is at play. One of the examples is a black hole, which has been the source of inspiration of various modern physics and has been observed directly for the first time only very recently, where relativistic quantum gravitational effects are ex-

pected to become relevant. These effects, where quantum gravity is at play of its highest effect, are not yet currently observed as they are negligible at scales accessible for the current era of technology.[1] However, these effects are responsible for the evaporation of the black holes and further, the beginning of the universe near the Big Bang.

General relativity describes gravity where the quantum properties are disregarded; it is conceptually rooted in understanding spacetime in a geometric manner. More precisely, general relativity can be regarded as an adequate description of classical gravity and spacetime along with their mutual relation. Quantum mechanics, on the other hand, has been formulated as a study of dynamics and fields. It has replaced our understanding of physics and replaced classical mechanics thereby redefining the general theory of motion and further sets our notions of matter and causality. Thus the twin peaks that are the two different conceptual frameworks governing modern physics are general relativity and quantum physics.

A quest for a theory describing quantum gravity is thus, in essence, a quest to understand the nature of spacetime. The quantum regime becomes relevant when one looks at sufficiently small regions of spacetime; when one approaches the Planck scale the spacetime is resolved into quantized discrete 'lumps', and the usual notions associated to a continuous spacetime break down. In particular, time evolution is no longer viable at such a scale. Quantum gravity requires addressing the question of the nature of spacetimes at these scales, which are precisely where the gravitational force becomes equivalently strong as the forces controlling particle physics. One natural avenue by which

[1] Evidently, the image of black hole is finally observed with a diameter encompassing only twelve pixels in 2019 thereby giving the general relativity, established in 1916 by Einstein, a direct confirmation.

one could attempt to construct a theory of quantum gravity is thus to quantize the fundamental degrees of freedom of general relativity. The gravitational field in general relativity is the dynamical spacetime metric tensor, and so a quantization of this field corresponds to a quantization of the geometry. In a theory of quantum gravity the spacetime itself will have quantum properties, and one of the principle challenges in understanding any such theory is to make sense of such "quantum geometry."

Throughout the last few decades, physicists have tried to build theories of quantum gravity encapturing both general relativity and quantum field theory, and yet, we have found only one to be successful: *String theory*. String theory is the ultimate pinnacle of the conceptual revolution in physics combining the general covariance principles of general relativity and the quantization of quantum mechanics, and it is constructed with a one-dimensional object "strings" instead of a zero-dimensional point particle, unlike quantum field theory. By virtue of the non-trivial extent of the string, there is a natural discretization of spacetime at scales close to the size of the string, which can be taken near the Planck scale.[2] In this way the string intrinsically captures the quantized geometry necessary to talk about a theory of quantum gravity. However, there have been different approaches in understanding quantum gravity such as via a direct quantization of general relativity with non-perturbative canonical quantization and via capturing the quantum properties of gravity in form of a graviton dynamics with covariant quantization. The former is known as loop quantum gravity and the latter is known as string theory. At the level of our current knowledge, string theory is the

[2]Strictly speaking, string theory is involving a string scale which is slightly smaller than the Planck scale. The strings are modeled to be on the order of the Planck length.

only known way to consistently answer physical questions involving all four fundamental forces.

String theory has been developed for several decades with many successes and has further has been an inspiration to probe quantum gravity via studying an emergent gravity and spacetime using the technique of holography with its famed AdS/CFT correspondence [224]. Many scenarios and toy models studied for emergent gravity are of an information-theoretical, quantum-computational type, as it elucidates its quantum complexity and the information stored in the spacetime via entanglement [166, 193].

String theory is therefore geometric in nature as it is a theory of spacetime. While string theory require much investigation and consolidation, there have been many successful outcomes such as the aforementioned AdS/CFT correspondence [224], mirror symmetries of Calabi–Yau manifolds [67], black hole microstate ensembles [284], Gromov-Witten invariants and instanton calculus [304], matrix models and combinatorics [27], Moonshine conjectures [48], and integrable structures in super Yang-Mills theory [33].

1.1 String theory

String theory is a ten-dimensional theory that is constructed via quantization of strings, which are one-dimensional physical objects.[3] In contrast to quantum field theory, which quantizes a point particle, string theory thereby is UV-complete without spacetime divergences. Much like how the study of point particles can be phrased as the study of their worldline, in string theory the object which

[3] We only consider superstring theories, which are known to be consistent. Bosonic string theories suffer from tachyons and thus are not considered in this thesis.

captures the dynamics is the two-dimensional worldsheet traced out by the string moving through spacetime. In the language of string theory, the particles that we observe in the world around us are then defined as the Fourier modes of string quanta at a large distance. That is, if one observes a small string from a far distance, or equivalently at a low energy scale, then it appears, for all intents and purposes, like a point particle, as one cannot resolve the extent of the string at such a low scale. This gives a folklore theorem of quantum gravity that the spectrum is comprised of massless states and their towers of excitations thereby giving a complete set of the spectrum of particles. The towers then describe the "massive" states where the mass scale is set by string tension of the fundamental string, which is of the order of Planck mass. This encompasses the string theory to be a theory with fundamental objects living in "quantum spacetime" of the theory where the scale is set to be of string scale.

There are two different types of strings, open strings and closed strings, depending on the existence of boundaries of their worldsheet. The closed string provides the massless modes that correspond to a "quantized" graviton as a symmetric two-tensor. The open string realizes the gauge bosons of Yang–Mills theory. In this way we can see that string theory incorporates all four fundamental forces.

Indeed, one natural question is why to consider one-dimensional strings instead of higher dimensional membranes. While this is justified as only the strings can be quantized consistently, there do exist non-fundamental heavy objects of higher dimensions in string theory, which are known as branes. Branes can be seen as subspaces of ten-dimensional spacetimes of which open strings end. It is a physical generalization of the magnetic monopoles and thus a solitonic object. It naturally

follows that super Yang–Mills theories are then the low energy theories confined to such an object.

String theory is anomaly-free in ten-dimensions [146]. In fact there is not a unique anomaly-free string theory, rather, there are five perturbative string theories: type I, type IIA, type IIB, heterotic of type SO(32), and heterotic of type $E_8 \times E_8$. These string theories preserve either 16 or 32 supercharges and require closed strings, and these theories are characterized with respect to the types of strings admitted, the number of supercharges, and the chirality of the theory in Table 1.1.

Types of string theory	Types of strings	Number of supercharges	Chirality
Type I	Open + closed strings	16	Chiral
Type IIA	Open + closed strings	32	Non-chiral
Type IIB	Open + closed strings	32	Chiral
Heterotic	Closed strings only	16	Chiral

Table 1.1: There are five different types of string theories in ten-dimensions. Both types of heterotic theories, with either $E_8 \times E_8$ or SO(32), share the same features and hence are written together.

These five string theories are all dual to each other [305]. The existence of these dualities implies that seemingly different superstring theories are actually physically equivalent. In other words, each string theory describes physics that is phrased differently via various degrees of freedom but they are all transferable to one another. The two distinctively well-known dualities are T-duality and S-duality. S-duality is the oldest duality known in physics and it is defined as relating two theories with strong and weak couplings. More precisely, when one of the theories at a small coupling g_1 while the other theory is at a large coupling g_2 are related via $g_1 = 1/g_2$, we call that the two theories are *S-dual* to each other. Via S-duality we can understand the strongly coupled regime of a theory by investigating a weakly coupled regime of the other theory, and hence it is also known as a strong-weak duality. This duality is originated from quantum field theory generalizing the electromagnetic

duality of Maxwell's equations, which is famously known as Montonen-Olive duality [238], and it is first established to be possible in the context of string theory [255, 275]. T-duality, on the other hand, is a newer duality that is discovered in the context of string theory. The two theories describing the same physics are *T-dual* when one of the theories describes strings propagating in an imaginary spacetime shaped like a circle of some radius R, while the other theory describes strings propagating on a spacetime shaped like a circle of radius proportional to $1/R$ [271].

While there are five types of perturbative string theories that are dual to one another, M-theory and F-theory describe non-perturbative theories that provide the perturbative theories as a weak coupling regime of their moduli spaces. That is, all of the five consistent superstring theories are just different limiting cases of a single eleven-dimensional theory called M-theory. Using the M-theory, an eleven-dimensional theory, we can establish an S-duality between type IIA theory and heterotic theory of type $E_8 \times E_8$. Using S-duality and T-duality altogether, the five perturbative string theories are connected as depicted in Figure 1.1. F-theory is best described as a theory that provides a geometric toolkit via elliptic fibration to understand the dynamics of string theory.

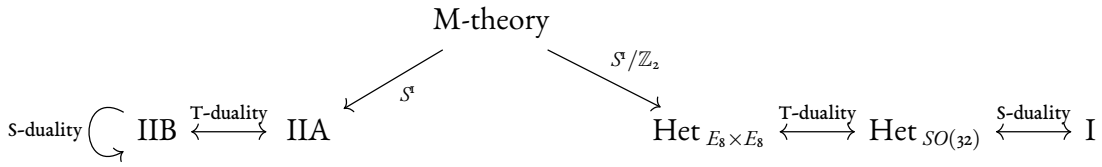

Figure 1.1: The five perturbative string theories, type I, type IIA, type IIB, heterotic $E_8 \times E_8$, and heterotic SO(32) are all dual to each other. We incorcorate a non-perturbative picture from M-theory, an eleven-dimensional supergravity theory, to depict the duality between the type IIA theory and heterotic theory of type $E_8 \times E_8$ via compactifications on a circle and an interval respectively. The rest of the theories are connected via S- and T-dualities, as shown.

For the purposes of this thesis, the relevant perturbative string theory will be type IIB theory. The feature, which will be taken advantage of, is that type IIB theory maps to itself under S-duality, as depicted in Figure 1.1. First, we note that type IIB theory has the following bosonic field content:

$$\lambda_s, \quad C_0, \quad B_{\mu\nu}, \quad C_{\mu\nu}, \quad C_{\mu\nu\rho\lambda}, \tag{1.1}$$

where the first one is the coupling constant set by a dilaton φ via $\lambda_s = e^{-\varphi}$, B is the Kalb-Ramond two-form coupled to fundamental strings in the Neveu-Schwarz sector, and the three C fields are Ramond-Ramond fields (which are in turn, even forms) that are coupled to D(-1)-brane, D1-brane, and D3-brane respectively. C_0, in particular, is an axion. The first two fields, an axion and a dilaton, can naturally be composited together as a complex field living on the upper half plane

$$\tau = C_0 + \frac{i}{\lambda_s}. \tag{1.2}$$

This τ is known as the axio-dilaton.

Furthermore, the S-duality of type IIB theory extends to a full $SL(2, \mathbb{Z})$ symmetry that acts on the axio-dilaton as

$$\tau \longrightarrow \frac{a\tau + b}{c\tau + d} \quad \text{where} \quad \begin{pmatrix} a & b \\ c & d \end{pmatrix} \in SL(2, \mathbb{Z}). \tag{1.3}$$

Type IIB theory has two-form fields $B_{\mu\nu}$ and $C_{\mu\nu}$, which, respectively, coupled electrically to the

fundamental string (also called the F1-brane) and the D1-brane. Under an $SL(2,\mathbb{Z})$ transformation

$$\lambda_s \longrightarrow \frac{1}{\lambda_s}\,, \tag{1.4}$$

these two fields are exchanged.[4] This transformation swaps the tensions of the fundamental string and the D1-brane, and thus it is necessary that the potentials coupled to these extended objects are also exchanged. On the other hand, there is only a single four-form field, $C_{\mu\nu\rho\lambda}$, and thus it must map to itself under the transformation, which is given in equation (1.4). That is, the D3-brane which couples to the four-form must be self-dual under the given transformation. As a consequence of this it is immediate that the $U(N)$ $\mathcal{N}=4$ super-Yang–Mills theory living on the worldvolume of a stack of N D3-branes must be invariant under an $SL(2,\mathbb{Z})$ symmetry, as the D3-branes are simply mapped onto themselves. The worldvolume theory enjoys invariance under the transformations

$$\tau \to \tau + 1\,, \quad \tau \to -\frac{1}{\tau} \tag{1.5}$$

of its complexified coupling constant (or the axio-dilaton), τ. Since the D5-brane and the NS5-brane are the magnetic duals of the fundamental string and of the D1-brane they are also necessarily exchanged by the transformation given by the equation (1.4).

This duality, which is called the S-duality of type IIB theory, is changing the fundamental string into what one would perturbatively think of as a composite heavy object, the D1-brane. We note

[4] This is not the full $SL(2,\mathbb{Z})$ symmtery. This is a tranformation concerning only the S-duality with the matrix corresponding to $\begin{pmatrix} 0 & -1 \\ 1 & 0 \end{pmatrix}$ with $C_0 = 0$.

that because the duality replaces fundamental objects with composite objects one has to be careful with the definition of a Feynman path integral – to perform the integral one must pick a particular duality frame, and integrate over the fundamental degrees of freedom in that frame. The notion of what is light, or fundamental, that goes into the definition of the path integral is not necessarily a duality invariant notion.

One of the key observations for this thesis is that the $SL(2,\mathbb{Z})$ S-duality of type IIB theory can be interpreted as the $SL(2,\mathbb{Z})$ complex structure transformations of the torus. This insight allows one to write down the vacuum solutions of the type IIB theory by utilizing the machinery of elliptic fibrations. However, before we turn to this subject, it is necessary to introduce further notions of compactifications and duality.

1.2 M-theory and dualities to string theories

We have just seen that there exist five perturbative superstring theories that are related to each other by dualities. In fact, there is a sixth theory that exists in the duality chain that is in eleven-dimensions; this is known as an eleven-dimensional supergravity theory that is not a theory of strings. All of these duality-related perturbative theories indicate that there exists a non-perturbative completion to which these perturbative theories are limits. This non-perturbative theory is called *M-theory*, which is an eleven-dimensional theory which is subjected to much exploration. While M-theory lacks description in terms of quantized fundamental strings, it does contain, similar to the perturbative theories discussed above, non-perturbative solitonic branes. The most straightforward

limit of M-theory is a type IIA theory, where the former is compactified on an S^1. This reduces the eleven-dimensional theory into an effective ten-dimensional theory, and we will now summarize how the field content of the type IIA theory arises from a parent 11d theory.

The radius of the circle and the IIA string coupling constant are identified as [305]

$$R^3 \sim g_s^2. \tag{1.6}$$

M-theory has a three-form field $C_{\mu\nu\rho}$, a 3-dimensional world volume object, which is associated with the M2-brane. Then this M2-brane wraps around the S^1 yielding a string, which is identified as IIA string. An M2-brane not wrapping around the circle gives rise to a D2-brane. The magnetic version of the M2-brane is the M5-brane in M-theory. Let us consider an M5-brane around this S^1. Then we get D4-branes. When M5-branes are not wrapping around the circle, we get the NS 5-brane of type IIA theory, which is a magnetic dual object to the string. In type IIA theory, there are also D6-branes and D8-branes. First of all, D6-brane is the Kaluza-Klein monopole, which happens when the circle shrinks at a point. Consider the Taub-NUT geometry, which looks like $\mathbb{R}^3 \times S^1$ asymptotically, where the circle shrinks in the middle. Then such a point on $\mathbb{R}^3$ is the D6-brane, as represented in Figure 1.2. The D6-branes are codimension-three objects. On the other hand, D8-branes are codimension-one objects, which dramatically impact on the global topology of the space.

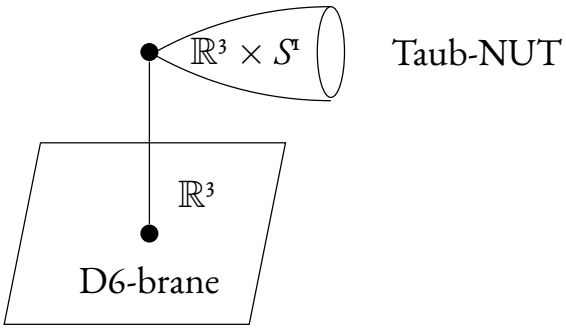

Figure 1.2: D6-brane is the object where the circle shrinks from the Taub-NUT space.

Let's connect M-theory to other theories than type IIA theory. First of all, there is another theory in ten-dimensions: type IIB theory. In order to connect M-theory to IIB theory, we have to use the T-duality that relates type IIA theory and type IIB theories in nine-dimensions via compactifications on circles. From this, we can expect that M-theory on a T^2 is identical to type IIB theory on a circle in nine-dimensions, as represented in Figure 1.3.

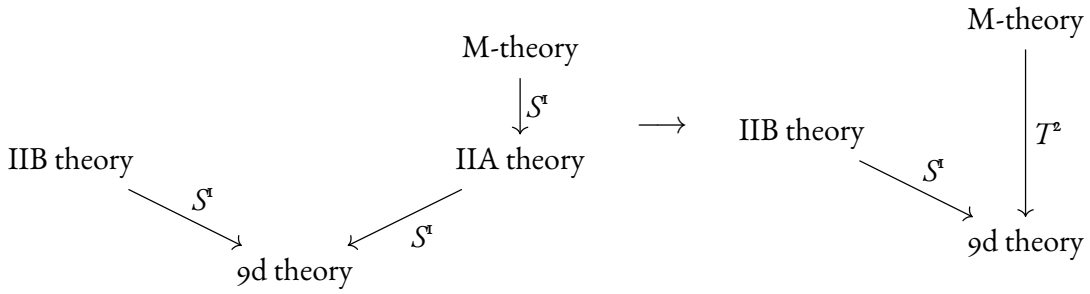

Figure 1.3: M-theory and IIB theory yield the same 9d theory

The axio-dilaton of type IIB theory, which is given by equation (1.2), carries two real parameters to be compactified on a circle and the nine-dimensional IIB theory has another one real parameter

that is the radius of the circle

$$(R^{\text{IIB}}\,,\ \tau). \tag{1.7}$$

On the other hand, M-theory is also parametrized by three real parameters:

$$(A\,,\ \widetilde{\tau}), \tag{1.8}$$

where A is the area of the T^2, and $\widetilde{\tau}$ is the complex structure of the torus that has a symmetry under $\widetilde{\tau} \longrightarrow \widetilde{\tau} + 1$ [273]. The axion C_0 is the gauge degrees of freedom that is periodically valued. As we go around the 7-brane (which has a codimension-two world volume), C_0 shifts by 1. It follows that τ shifts by 1. It follows that this τ respects the symmetry of $\tau \longrightarrow \tau + 1$. Then it has the same symmetry with $\widetilde{\tau}$ from M-theory and hence we relate these two τs:

$$\widetilde{\tau} = \tau. \tag{1.9}$$

Then we related the other real variables,

$$\frac{1}{2\pi R^{\text{IIB}}} = m_p^3 A, \tag{1.10}$$

where m_p is the Planck mass [273].

In fact, the $\widetilde{\tau}$ has a full $SL(2,\mathbb{Z})$ symmetry, not just a shift symmetry. Suppose we take $C_0 = 0$,

then

$$\lambda_s \longrightarrow \frac{1}{\lambda_s}, \tag{1.11}$$

which gives a strong-weak duality. Indeed, type IIB theory is self-dual under the strong-weak duality.

We now consider how these two different two-form fields of type IIB theory arise by considering M-theory compactified in a torus. That is, we will consider a compactification of type IIB theory on an S^1, and look at the components of the two 10d two-forms that do not extend along the S^1, and thus they behave like 9d two-forms. These equally can be understood from the perspective of the M-theory three-form, $C_{\mu\nu\rho}$. To get a two-form one of the directions in $C_{\mu\nu\rho}$ must lie along one of the directions inside the T^2 on which we are compactifying. A torus T^2 has two distinct one-cycles, the A and B cycles, and the two two-forms $B_{\mu\nu}$ and $C_{\mu\nu}$ arise from wrapping $C_{\mu\nu\rho}$ with one direction along each of these cycles. Realizing the $SL(2,\mathbb{Z})$ transformation, given by equation (1.4), as a modular transformation of the complex structure of the torus, one can see that the A and B cycles are exchanged. Generally this process involves wrapping the M2-brane, which couples electrically to the three-form, along the cycle $pA + qB$ of the torus. For $(p,q) = (1,0)$ the resulting string is the fundamental string, and $(p,q) = (0,1)$ is the D1-brane. The $SL(2,\mathbb{Z})$ symmetry of the torus can be thought of, in this way, as generating the $SL(2,\mathbb{Z})$ self-duality symmetry of type IIB theory from M-theory. Wrapping on a general (p,q)-cycle (with p and q coprime) gives rise to a bound state of F-strings and D1-branes.

It is important to note that the 11d M-theory picture is not always the most useful way to study

string theory. In M-theory on T^2 with area A gets mapped to type IIB theory on an S^1 with radius R^{IIB} such that

$$R^{\text{IIB}} \sim 1/A. \tag{1.12}$$

This is consistent with the fact that the Kaluza–Klein modes of type IIB theory, which are the winding modes in type IIA language, which in the M-theory uplift is then an M2-brane wrapping also the other cycle, i.e. wrapping the entire torus. If we consider M-theory on a T^2 and we shrink $A \to 0$ then the theory is not 9d, as one would naively think, but because of (1.12) it is, in fact, 10d type IIB theory. In this way, M-theory would naively miss type IIB, and knowing about T-duality of type IIA theory is an additional ingredient that is obscured from the pure M-theory point of view.

1.3 Compactifications to various dimensions

If we wish to consider theories lower than ten-dimensions, then we are required to make some of the ten-dimensions to be small. In this way, if one is at sufficiently low energy, then one cannot resolve the size of the extra dimensions, and thus the observed effective theories are in lower-dimensions. This procedure is known as *strings compactifications*. In this section, we review when such compactifications can give rise to supersymmetric effective field theories.

Consider the ten-dimensional spacetime to be of the form

$$\mathbb{R}^{1,9-d} \times M_d\,, \tag{1.13}$$

where M_d is a compact d-dimensional oriented Riemannian manifold, known as the internal space. This string background preserves some spacetime supersymmetry if there exists a covariantly constant spinor on the internal manifold, that is, some spinor ξ such that

$$\nabla_I \xi = 0 \,. \tag{1.14}$$

To determine if there exists a covariantly constant spinor one can check whether there exists a subgroup of the holonomy group of the internal manifold such that the spin representation branches to a sum of irreducible representations of the subgroup which includes a summand which is the trivial representation. Then one can consider specific manifolds M_d of "reduced holonomy", that is, the holonomy group of that manifold is a subgroup of the generic holonomy group for an oriented Riemannian manifold; these manifolds will give supersymmetric compactifications. The generic holonomy group for such an M_d is $SO(d)$; we will now give the relevant subgroups for each d. These are reviewed by Joyce in [181].

- $d = 1$: All one-dimensional manifolds have trivial holonomy and so preserve supersymmetry.
- $d = 2$: The holonomy group is $SO(2)$ or $U(1)$, and only the trivial subgroup gives rise to a covariantly constant spinor. The only M_2 with trivial holonomy is T^2, and in general the only M_d with trivial holonomy is the d-torus, T^d, which will always admit covariantly constant spinors.
- $d = 3$: The holonomy group is $SO(3)$ or $SU(2)$ which has no relevant non-trivial subgroup.

The only option is then $M_3 = T^3$.

- $d = 4$: The holonomy group is $SO(4) \simeq SU(2) \times SU(2)$. The spin representation of $SO(4)$ is the $(2,1) \oplus (1,2)$, so we can see that we can choose one of the $SU(2)$ subgroups such that the trivial representation appears in the branching. A four-manifold with $SU(2) \simeq Sp(1)$ holonomy is hyperKähler, and is known as a $K3$ surface. One example of such a four-manifold is to take $T^4/\mathbb{Z}_2$ where the $\mathbb{Z}_2$ quotient acts on all coordinates like $x^i \to -x^i$.

- $d = 5$: This is the same as the $d = 4$ case, where one has to consider first the $SO(4)$ subgroup of $SO(5)$. This corresponds to $M_5 = K3 \times S^1$.

- $d = 6$: One interesting subgroup in this case is $SU(3) \subset SO(6)$, which implies that M_6 is a Calabi–Yau threefold, CY_3. Yau proved that such a space admits a Ricci-flat Kahler metric. We can also compactify on $K3 \times T^2$.

- $d = 7$: The subgroup $G_2 \subset SO(7)$ is such that the spinor representation decomposes as $8^s \to 7 \oplus 1$. Manifolds M_7 with such reduced holonomy are called G_2-manifolds. We also have the product spaces with even further reduced holonomy, for example, $CY_3 \times S^1$.

- $d = 8$: In this case we have two options for irreducible 8-manifolds – the reduced holonomy groups can be either $SU(4)$ or $Spin(7)$, which are Calabi–Yau fourfolds and $Spin(7)$-manifolds, respectively. The obvious product options built out of the above mentioned reduced holonomy manifolds such as $G_2 \times S^1$ and $CY_3 \times T^2$ also admit covariantly constant spinors.

d	Compactifiied space	Type IIA	Type IIB	Heterotic / Type I
10				
9		(1,1)	(2,0)	(1,0)
8		32 supercharges	32 supercharges	16 supercharges
7				
6	$K3$	(1,1)	(2,0)	(1,0)
		16 supercharges	16 supercharges	8 supercharges
5	$K3 \times S^1$	$\mathcal{N} = 2$	$\mathcal{N} = 2$	$\mathcal{N} = 1$
	$K3 \times T^2$	$\mathcal{N} = 4$	$\mathcal{N} = 4$	$\mathcal{N} = 2$
4	CY_3	$\mathcal{N} = 2$	$\mathcal{N} = 2$	$\mathcal{N} = 1$
		8 supercharges	8 supercharges	4 supercharges
3	G_2	$\mathcal{N} = 2$	$\mathcal{N} = 2$	$\mathcal{N} = 1$
	CY_3	4 supercharges	4 supercharges	2 supercharges

Table 1.2: Resulting theories of various dimensions compactified from superstring theories

The summary of the resulting theories in various dimensions is presented in Table 1.2. In fact, we can observe that we get theories with $\mathcal{N} = 0, 1, 2, 4, 8$. By the combinations of left and right sides with $(0, 1, 2, 4) \otimes (0, 1, 2, 4)$, we can have different holonomies acting on the left and right. By doing such we can build the rest $\mathcal{N} = 3, 5, 6$ theories. Note that $\mathcal{N} = 7$ theory does not exist as the supergravity becomes $\mathcal{N} = 8$.

1.4 F-theory

Previously we have observed that perturbative type IIB string theory is self-dual under the $SL(2, \mathbb{Z})$ symmetry. Such an S-duality can invert the string coupling constant, or axio-dilaton, which can lead to a dual description that is inherently strongly coupled. It would naively appear that we cannot allow the axio-dilaton to vary over spacetime, as there may be a region where the coupling becomes

large and the perturbative understanding is lost. In fact, in this section we will utilize the various dualities that we have been discussing to argue that there does exist a consistent way to write down such an axio-dilation varying compactifications of type IIB theory, by parametrizing the axio-dilaton variation as an auxiliary elliptic fibration over the compactification space.

To do so, let us first recall some of the known dualities. Heterotic string theory compactified on a T^4 is dual to type IIA theory compactified on $K3$, and heterotic theory compactified on T^3 is dual to M-theory compactified on $K3$. One can speculate as to whether this pattern continues further, and whether there exists a duality between heterotic theory compactified on a T^2 and some uplifted twelve-dimensional theory on $K3$. Naively this will not be possible as there does not exist a 12d supergravity theory that we can compactify on the $K3$ for the right-hand-side of the duality, however, there is a hint that this might be possible. We take M-theory on T^2 which we said is related to type IIB theory on an S^1. There is a limit where the radius of the S^1 goes to infinity, which is where the area of the T^2 goes to zero. While the T^2 is of zero volume, the data of it is not completely absent from the type IIB theory; for instance, the complex structure mode of the torus is a part of the type IIB theory. In this way, one can think of type IIB theory as a 12d theory, where two of the directions look like a zero-area torus.

Now we can consider a compactification of M-theory on some manifold which has a torus fibration over some base space, B. When we take the limit where the area of the torus fiber shrinks to zero volume we recover type IIB theory compactified on B. If we now take a $K3$ surface which admits a torus fibration over a 2d manifold then we can do this procedure to get an 8d theory which is the compactification of IIB on such a 2d manifold – this would be the candidate theory for the dual to

heterotic on T^2 that we speculated about above.

In fact, there exist $K3$ surfaces which are torus (or elliptic) fibrations over $\mathbb{P}^1$. Such a $K3$ surface has a realization via a Weierstrass equation

$$y^2 = x^3 + f_8(z_1, z_2)x + g_{12}(z_1, z_2)\,, \tag{1.15}$$

where f_8 and g_{12} are degrees 8 and 12 homogeneous polynomials in the projective coordinates, $[z_1 : z_2]$ of the base $\mathbb{P}^1$. To match with heterotic on T^2 we must count the moduli of this $K3$ surface. A polynomial of degree d has $d + 1$ parameters because there are $(d + 1)$ coefficients in the generic polynomial, which tells us that we naively have $9 + 13 = 22$ parameters from the complex structure moduli of the $K3$. An overall rescaling will remove one of these parameters, and then there is an $SL(2, \mathbb{Z})$ action which removes further three parameters. Thus the $K3$ surface has 18 complex parameters. The Kähler parameters are just the volumes of the T^2 fiber and the $\mathbb{P}^1$ base, however, since the theory requires the fiber to shrink into zero volume, the volume of T^2 is not a part of the theory. In turn, there is just one real Kähler parameter controlling the size of the $\mathbb{P}^1$.

The parameter space of the $K3$ is then given by

$$\frac{SO(18, 2)}{SO(18) \times SO(2)} \times R^+\,, \tag{1.16}$$

which is exactly the Narain moduli space for the compactification of heterotic on T^2. Furthermore,

we see that

$$A \sim \lambda_h \,, \tag{1.17}$$

so increasing the area of the $\mathbb{P}^1$ makes the heterotic theory strongly coupled.

We have just described a curious compactification of type IIB theory on a $\mathbb{P}^1$ which preserves only half of the supersymmetry, as it is dual to a heterotic compactification. By writing $K3$ as a torus fibration we allowed the complex structure modulus, τ, to depend on the holomorphic coordinate on the $\mathbb{P}^1$, z. Since

$$\tau = C_0 + \frac{i}{\lambda_s} \,, \tag{1.18}$$

we see that C_0 and λ_s now depend also on z. We do not usually consider such compactifications in superstring perturbation theory as there may be a point on spacetime where the string coupling becomes large, and then the perturbation theory breaks down. We can determine the points in $\mathbb{P}^1$ where $\tau \to \infty$, where we have no perturbative control of the theory. It turns out that when τ becomes infinite is exactly where the torus fibers of the elliptic fibration degenerate. This occurs at the discriminant locus, which is when

$$\Delta = 4f_8^3 + 27g_{12}^2 = 0 \,. \tag{1.19}$$

Since Δ is a degree 24 polynomial then there are 24 zeros of Δ distributed over the $\mathbb{P}^1$. We note that τ is actually not a well-defined function of z, as it undergoes $SL(2,\mathbb{Z})$ transformations when one moves on a path around one of these zeros of Δ.

Then we have constructed a theory in twelve-dimensions by identifying the τ as a shrunk torus on top of IIB theory. This theory is called ***F-theory***. This is a new type of compactification coming from string duality. Where $\tau \to 0, \infty$, we have monodromies. More precisely, we have monodromies from $\tau \to \tau + 1$, which is where D7-branes are wrapping around with $SL(2, \mathbb{Z})$ action. Hence we can determine that each point, each zero of Δ, is wrapped by D7-brane. Then via $SL(2, \mathbb{Z})$ action,

$$SL(2, \mathbb{Z}) \text{ action} : \quad \begin{pmatrix} p & r \\ q & s \end{pmatrix} \begin{pmatrix} 1 \\ 0 \end{pmatrix} = \begin{pmatrix} p \\ q \end{pmatrix}, \quad ps - rq = 1, \tag{1.20}$$

where p and q are relatively prime, we get a (p, q) 7-brane.

The 24 zeroes of Δ indicate that there are 24 7-branes present in the background. Since the base $\mathbb{P}^1$ is a compact manifold then we can see that not all of these 7-branes can be simultaneously viewed as D7-branes, in any duality frame. This is because the monodromy associated to a D7-brane shifts the axio-dilaton such that $\tau \to \tau + 1$, and thus one cannot cancel off all of the branch cuts emanating from the D7-branes. In this way, we can see that consistent compactifications of F-theory must generally have non-perturbative (p, q) 7-branes in the spectrum.

Note that each D7-brane has a U(1) gauge group. When the pinched points are brought together, we can have an enhancement of the gauge group. When we have a stack of N branes, the singularity is of A_{N-1} type and is described as

$$xy = z^n, \tag{1.21}$$

and hence we get an SU(N) gauge group.

In order to have a heterotic theory from this construction, we need to be able to put some D7-branes together to build an E_8. We can expect such to be possible by using singularities of type D and E. Unlike the F-theory perspective, it is more difficult to see such a geometric construction to yield these ADE type of gauge theories.

Let's consider M-theory on $K3$ that admits singularities of ADE type of Lie algebra. This is dual to heterotic theory on T^3. Let us consider the case of A_{N-1} as an example to demonstrate such is possible from M-theory. The geometry of type $\mathbb{C}_2/\mathbb{Z}_N$ gives a type A_{N-1} singularity. To consider the singularities of A_{N-1} type, we can think of having $(N-1)$ number of spheres, 2d cycles, touching each other as in Figure 1.4.

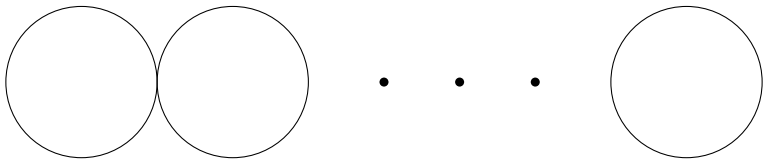

Figure 1.4: A chain of $(N-1)$ spheres touching each other, resulting from a resolution of an A_{N-1} type singularity

The size of these spheres are controlled by Kähler parameters of $\mathbb{P}^1$s: $\varphi_1, \varphi_2, \cdots, \varphi_{N-1}$. Furthermore, M-theory has 3-form fields $C_{\mu\nu\rho}$ that give for every independent 2-cycle a 2-form. So we can write the three-form fields in the basis of 2-forms $\omega^i_{\mu\nu}$ as

$$C_{\mu\nu\rho} = \sum_i A^i_\mu(x)\omega^i_{\mu\nu}, \tag{1.22}$$

where A^i_μ depends on the direction that is not compactified. Hence for a three-form field, we can de-

compose into a two-form and a one-form in the leftover space, which is the gauge field. This gauge field carries a $U(1)^{N-1}$ symmetry.

Now wrap M2-brane on one of the 2-cycles:

$$e^{i\int_{M2} C_{\mu\nu\rho}} \sim e^{i\oint A_\mu}. \tag{1.23}$$

The 3-form field $C_{\mu\nu\rho}$ is the one that is coupled to M2-brane, and hence on this gauge field A_μ, there will be a U(1) charge. Thus we get a charged object corresponding to this M2-brane wrapping around 2-cycle. Wrapping around just one 2-cycle, we are considering the geometry of $\mathbb{C}_2/\mathbb{Z}_2$. Then we have two possibilities: we can have an M2-brane or an anti-M2-brane, wrapping around with the opposite orientation. Hence we get two states: ± 1 charges of U(1) based on the orientation of M2-brane. They are charged massive vector multiplets $W^{\pm}$ where the mass is proportional to the area. More precisely, the mass of the vector multiplets is proportional to

$$m \sim TA, \tag{1.24}$$

where T is the tension of the M2-brane and A is the area. However, it is impossible to have a charged massive vector multiplet under a U(1) unless they are the W-bosons of a Higgsed non-abelian gauge group. As the area shrinks to zero, we get a massless vector multiplet. In other words, we get a U(1) with two charged objects that are opposite in charge, and we can conclude that this is SU(2). Thus we see that when we wrap an M2-brane on one 2-cycle that has A_1 singularity, we get a non-abelian

gauge symmetry SU(2). Giving vacuum expectation value to the scalar φ for this U(1), i.e. Higgsing the U(1), is equivalent to blowing up.

Now we can consider a general case of $(N-1)$ 2-cycles that had $U(1)^{N-1}$ symmetry. This will yield an SU(N) gauge symmetry. However, we do not have enough vectors as we have only $2(N-1)$ charged and $(N-1)$ neutral objects. We are required to wrap two touching $\mathbb{P}^1$s to bind and form a bound state to resolve such an issue.

We learned that we can wrap M2-branes on touching $\mathbb{P}^1$s to form a bound state. We can wrap many at once up to all $(N-1)$ of them. Each chain will give a charged object up to $\pm$ sign. This gives exact dimensions of SU(N): checking along all the chains up to the sign, we can get the full rank of SU(N). In this way, we can see the charge and degeneracies of the SU(N).

1.5 F/M-theory compactifications

Suppose we have two theories A and B compactified on M_1 and M_2 respectively, yielding the same theory on $\mathbb{R}^d$. Then there are parameters corresponding to scalar fields. We usually construct dualities by taking such a parameter to be a constant in the resulting d-dimensional compactified theory. We can think of this parameter to vary in different parts of $\mathbb{R}^d$ but still having the duality. Then we can vary the parameters point by point in $\mathbb{R}^d$. This is not guaranteed to work but if we vary them gradually and slowly, this may work. As long as we preserve the number of supersymmetries, all the cases are shown to have the duality and result in the same d-dimensional theory even if it breaks the adiabatic principle. Hence by taking this duality perspective, we can compactify further preserving

some supersymmetry to get lower-dimensional theories.

For example, type IIB theory with varying the coupling constant over $\mathbb{P}^1 \times S^1$ is dual to M-theory on $K3$ when the parameters are mapped point by point. On the other hand, we take the S^1 to have infinite size, which then corresponds to having the fibers of the elliptic fibration shrinking to zero size in F-theory. Moreover, M-theory on $K3$ is dual to heterotic on T^3. By taking the heterotic theory on $T^2 \times S^1$, we have the duality between the heterotic theory on T^2 and the type IIB theory on $\mathbb{P}^1$, which was explained earlier by building F-theory from IIB on $\mathbb{P}^1$.

$$\text{Heterotic on } T^3 \quad \longleftrightarrow \quad \text{M-theory on } K3 \quad \longleftrightarrow \quad \text{IIB on } \mathbb{P}^1 \times S^1$$

$$\text{Heterotic on } T^2 \quad \longleftrightarrow \quad \text{IIB on } \mathbb{P}^1 \text{ (F-theory on } K3)$$

Now consider F-theory on an elliptic manifold M^d_{ell}, then the resulting theory is a $(12 - d)$-dimensional theory. When we have an elliptic manifold, we can consider F-theory for any case that has a type IIB theory with a varying parameter via duality. Then we can construct the following duality that results in the same $(10 - d)$-dimensional theory.

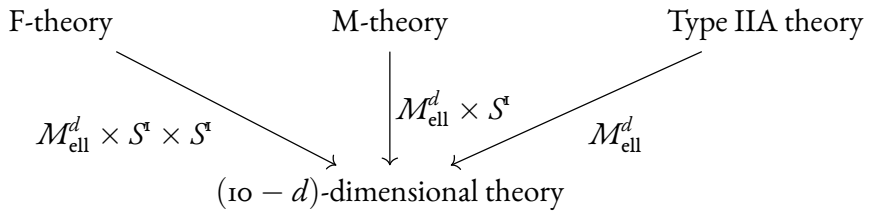

We can study these dualities for various dimensions. For a seven-dimensional theory via com-

pactification have either 32 or 16 supercharges as in Table 1.2. For six-dimensional theories, we can get theories with the same amount of supercharges or a theory with 8 supercharges. This can be achieved via the compactification of the heterotic theory on $K3$ or F-theory on elliptically-fibered Calabi–Yau threefolds. For a five-dimensional theory, we can have the same amount of supercharges. For a four-dimensional theory, the minimal amount of supercharges is now 4, which corresponds to a 4d $\mathcal{N} = 1$ theory. This theory can be achieved by compactifying heterotic theories on Calabi–Yau threefolds, F-theory on Calabi–Yau fourfolds, or M-theory on G_2-manifolds. These are summarized in Table 1.3.

$10 - d$	Number of supercharges
7	32, 16 supercharges
6	32, 16, 8 supercharges
5	32, 16, 8 supercharges
4	32, 16, 8, 4 supercharges

Table 1.3: Possible number of supercharges in lower-dimension theories via compactifications

1.6 Canonical problems in F/M-theory

A standard set of questions in F-theory and M-theory compactifications on an elliptically fibered Calabi-Yau threefold Y are the following [9, 45, 107, 124, 129]:

(i) **Birational geometry.** Does the singular Weierstrass model have a crepant resolution? How many crepant resolutions does it have? How are they flop-connected with each other? What is the graph of the flops?

(ii) **Fiber geometry.** What is the fiber structure of each crepant resolution? What are the vertical curves composing the singular fibers? What are their weights? What representation do they carry?

(iii) **Coulomb branch and charged hypermultiplets.** What is the structure of the Coulomb branch of the five-dimensional $\mathcal{N} = 1$ theory with Lie group $\mathfrak{g}$ and representation $\mathbf{R}$ geometrically engineered by an elliptic fibration Y? How many hypermultiplets transform under each of the irreducible components of $\mathbf{R}$? Can we completely fix the number of charged multiplets by comparing the triple intersection numbers and the prepotentials?

(iv) **Anomaly cancellations and uplift.** Is the five-dimensional theory always compatible with an uplift to an anomaly free six-dimensional theory? What are the conditions to ensure cancellations of anomalies of a six-dimensional $\mathcal{N} = (1, 0)$ supergravity obtained by compactification of F-theory on Y? Can we fix the number of multiplets by the six-dimensional anomaly cancellation conditions?

(v) **Topological invariants.** What is the Euler characteristic of a crepant resolution? What are the Hodge numbers of Y? What are the triple intersection numbers in each Coulomb branch?

These questions are closely related to each other and have been addressed recently for many geometries, such as the G_2, Spin(7), and Spin(8)-models [112] (Chapter 9), F_4-models [115] (Chapter 8), SU(n)-models [124, 125, 127, 129, 148], and also for (non-simply connected) semi-simple groups such as the SO(4) and Spin(4)-models [118] (Chapter 10), the $SU(2) \times G_2$-models [119] (Chapter 11), the

$SU(2)\times SU(3)$-models [113] (Chapter 12), the $SU(2)\times SU(4)$, $(SU(2)\times SU(4))/\mathbb{Z}_2$, $SU(2)\times Sp(4)$, and $(SU(2)\times Sp(4))/\mathbb{Z}_2$-models [121] (Chapter 13).

We first do not restrict ourselves to Calabi-Yau threefolds, but discuss the crepant resolutions and the Euler characteristic without fixing the base of the fibration in the spirit of [5, 6, 120, 125, 127]. The computation of topological invariants such as the triple intersection numbers and the Euler characteristic are streamlined by recent pushforward theorems [114].

For recent works in F-theory and birational geometry in physics, see for example [11, 14, 31, 41, 79, 93, 179, 198, 216], see also the recent review on F-theory [301] and reference within. We refer to [169] for a review of six-dimensional theories.

1.7 Von Neuman algebras in quantum gravity

Any theory compatible with special relativity on a continuous spacetime must transform covariantly with respect to translations, rotations, and boosts, where the latter two generate the Lorentz symmetry. In light of the fact that the Minkowski space has ten degrees of freedom – translation symmetry from the four spacetime directions, reflection symmetry giving three degrees of freedom, and boost symmetries from three spatial directions – ignoring the effect of gravity, every object invariant under these symmetries is invariant under relativity. In any continuous quantum field theory, the isometries of the fixed spacetime always enter the global symmetry group of the theory. Thus if one writes down any theory compatible with relativity, then the theory is required to possess such a symmetry, and this is known as *Poincaré symmetry*. The Poincaré group is the group of Minkowski spacetime

isometries.

When such a theory is quantized, the notion of Poincaré symmetry must be replaced by a more refined notion acting on the Hilbert space of the states of the quantum field theory. A requirement of more refined Poincaré symmetry into a von Neumann algebra follows from considering theories with general covariance. The physical description of theories that are not generally covariant is based on three fundamental notions in physics such as observables, states, and time evolution. The first two notions, observables and states, determine the kinematics of the theory whereas the time evolution is responsible for describing the dynamics of the theory. We recall that in quantum mechanics, a theory that does not satisfy a general covariance, there are two approaches to time evolution, which are sometimes called Schr"odinger and Heisenberg pictures. In the former it is the state of the theory that has time dependence and operators do not, whereas in the latter, the opposite is true; each of these pictures privileges time over the other, spatial, directions. Thus one can see it is not immediately compatible with general relativity. The von Neumann algebra captures the dynamics, that is the time evolution, in a generally covariant way. Thus, in the theory of gravity, where covariance is required to be satisfied, one cannot avoid such a formulation.

The dynamics of the theory of quantum gravity has to incorporate how quantum mechanical observables change over time, where the states of a quantum system are given by the one-dimensional subspaces of a Hilbert space. Then quantum dynamics involves the study of one-parameter automorphisms of the algebra of all bounded operators on the Hilbert space of observables, which is coming from the old Heisenberg picture, and involves careful examinations of the information, such as the entropy, of a thermal system. The thermal state, or equivalently a density function, of

a covariant theory with a Hamiltonian H is given by $\rho = e^{-\beta H}$ and such a state has a time evolution, which is the thermal time of ρ. Hence the time evolution is a state-dependent quantity. It is important to note that one of the fundamental properties of von Neumann algebras is that a state defines a one-parameter family of automorphisms. Compared to theories that are not generally covariant, where the theory is described fully by the Hamiltonian, or equivalently a representation of the Poincaré group, covariant theories are described by the algebras of observables and states that are gauge invariant, where a one-parameter group of automorphisms of the algebra inscribes the modular group and the physical time is the modular flow of the thermal state. Henceforth, von Neumann algebras, which have the modular flow as an intrinsic property independent from the states, are innately dynamical. Thus it is the natural generalization of the Poincaré symmetry that we consider for the theory of quantum gravity, which has a natural connection to (entanglement) entropy via the modular flow.

The most powerful method of advance that can be suggested at present is to employ all the resources of pure mathematics in attempts to perfect and generalize the mathematical formalism that forms the existing basis of theoretical physics, and after each success in this direction, to try to interpret the new mathematical features in terms of physical entities.

Paul Dirac

2

Geometry of Elliptic Fibrations, Characteristic Numbers, and 5d/6d Supergravity Theories

The geometric engineering of supergravity theories via string theory can be studied by utilizing the $SL(2,\mathbb{Z})$ transformation properties of the axio-dilation to write down an auxilliary elliptic fibration that captures the global features of the string theory background, including some effects of strong coupling. The details of the effective supergravity theory will be captured by this elliptic fibration, and there is a well-established dictionary between the physical features, like the spectrum and interactions, and the geometric properties of the fibration. In this section we will elucidate the pertinent details of elliptic fibrations, and the relationship with the low energy effective physics.

The study of elliptic fibrations started with Kodaira's seminal papers on minimal elliptic surfaces [200]. Kodaira classified the possible geometric singular fibers and the class of monodromies around them for minimal elliptic surfaces. He further derived a formula for the Euler characteristics of minimal elliptic surfaces. Néron also classified singular fibers of elliptic surfaces defined by Weierstrass models, though from an arithmetic point of view [251]. Following a theorem of Deligne [94], an elliptic fibration with a rational section has a birational Weierstrass model defined over the same base. Tate developed an algorithm to determine the type of singular fibers of a Weierstrass model by manipulating its coefficients [290].

There are new phenomena for higher dimensional elliptic fibrations with direct applications to stringy geometry and supergravity theories. First, components of the discriminant locus can intersect each other. This is what Miranda calls "collisions of singularities" in his study of regularizations of elliptic threefolds defined by Weierstrass models [236]. Secondly, if we start with Weierstrass models, crepant resolutions (when they exist) are not unique: different crepant resolutions of the same Weierstrass models are connected by a network of flops [176, 227, 306], see [112, 115, 125, 127, 129] for

explicit constructions. These two phenomena are closely related to each other. The collision of singularities are responsible for attaching a representation $\mathbf{R}$ of a Lie algebra $\mathfrak{g}$ to an elliptic fibration [38]. One can then determine a hyperplane arrangement $\mathrm{I}(\mathfrak{g}, \mathbf{R})$ whose chamber structures have an incidence graph isomorphic to the network of flops between different crepant resolutions of the underlying Weierstrass model. Each crepant resolution corresponds to a different chamber of the extended relative Mori cone of the elliptic fibration.[1]

Elliptic fibrations are commonly used in physics to geometrically engineer gauge theories via compactifications of M-theory and F-theory. In fact, certain theories are known only through their construction by elliptic fibrations. More precisely in M-theory and F-theory, elliptic fibrations are used as compactifying spaces which give rise to gauge theories coupled to supergravity theories in spacetimes of dimension less than or equal to eight [37, 243, 244]. The F-theory's algorithm attaches to a given elliptic fibration a Lie algebra $\mathfrak{g}$, a Lie group G, and a representation $\mathbf{R}$ of G. Although many aspects are well understood, the algorithm relating the geometry and physics is still a work in progress. The Lie algebra $\mathfrak{g}$ is uniquely determined by the dual graphs of the fibers over the generic points of irreducible components of the reduced discriminant locus. The Lie algebra $\mathfrak{g}$ is determined by the singular fibers over generic points of the discriminant locus. As the fundamental group of G is isomorphic to the Mordell–Weil group of the elliptic fibration, the global structure of the Lie group G depends on not only the Lie algebra but also the Mordell–Weil group of the fi-

[1] The use of the hyperplane arrangement $\mathrm{I}(\mathfrak{g}, \mathbf{R})$ as a combinatorial invariant of an elliptic fibration [125, 127, 148, 163] is directly inspired by the study of Coulomb phases of five dimensional gauge theories [176] and illustrates how ideas from stringy geometry improves our understanding of the topology and birational geometry of elliptic fibrations. These hyperplanes arrangements are also interesting independently of their connections to elliptic fibrations and gauge theories, as they have beautiful combinatorial properties that can be captured by generating functions [110, 111].

bration [20, 229, 292]. The representation **R** is captured at the intersections of components of the discriminant locus or in singularities. The weights of the representations are obtained by intersection numbers of rational curves forming the singular fibers with fibral divisors produced by rational curves moving over irreducible components of the discriminant locus. An elliptic fibration for which the F-theory algorithm returns a Lie group G is called a G-model. The geometry of G-models are well understood mostly when G is a simple group. The semi-simple case is more subtle because of the appearance of colliding singularities. Various semi-simple cases are studied in Part IV, Chapters 10 to 13.

The low energy theories derived by compactification of M-theory or F-theory on Calabi–Yau threefolds are respectively five-dimensional and six-dimensional supergravity theories with eight supercharges [66, 131]. We will refer to them as five-dimensional $(5d)$ $\mathcal{N} = 1$ [176] and six-dimensional $(6d)$ $\mathcal{N} = (1, 0)$ supergravity theories [149, 266, 269]. Similarly, when compactified on fourfolds, the resulting theories are three-dimensional or four-dimensional theories. In particular, when the fourfold is Calabi–Yau, the resulting theories have four supercharges: 3d $\mathcal{N} = 2$ or 4d $\mathcal{N} = 1$ supergravity theories.

In compactification of M-theory [83] on an elliptically-fibered threefolds to five-dimensional gauge supergravity theories, the different crepant resolutions of the underlying Weierstrass model are understood as different Coulomb phases of the same gauge theory, and flops become phase transitions between different Coulomb phases [176]. Triple intersection numbers are understood as Chern-Simons levels of the gauge theory and determine the couplings of vector multiplets and the graviphoton of the five-dimensional supergravity theory. In a five-dimensional $\mathcal{N} = 1$ supergravity

theory, the Chern-Simons levels and the kinetic terms of the vector multiplets and the graviphoton are controlled by a cubic prepotential, which admits a one-loop quantum correction but is protected by supersymmetry from additional corrections [176]. The one-loop quantum correction depends on the number of multiplets $n_{\mathbf{R}_i}$ charged under the irreducible representation $\mathbf{R}_i$ [176]. In an M-theory compactified on a Calabi–Yau threefold, the full prepotential (including the quantum correction) is given geometrically by the triple intersection numbers of the divisors [66, 131].

While our geometric computations are done relative to a base of arbitrary dimension and without assuming the Calabi–Yau condition, to discuss anomaly cancellations, we specifically require the elliptic fibration to be a Calabi–Yau threefold. In particular, this requires the base of the fibration B to be a rational surface. We denote its canonical class by K_B or just K when the context is clear. Our approach is rooted in geometry and can be summarized as follows [9, 112, 115, 124, 125, 127, 129].

1. We work with Weierstrass models. We first determine a crepant resolution.

2. We study the fibral structure of the resolved elliptic fibration. In particular, we identify the singular fibers appearing at collisions of singularities. They are composed of rational curves carrying weights of the representation $\mathbf{R}$ attached to the elliptic fibration.

3. Using intersection theory, we find the weights of the vertical curves at collisions of singularities and derive the representation $\mathbf{R}$. Each weight is minus the intersection number of the vertical curve with the fibral divisor not touching the section of the elliptic fibration. One interesting property of our approach is that for complex representations (such as the $(2, 4)$, or the $(1, 4)$ of $A_1 \oplus A_3$), the weights of the dual representation appear naturally as weights of

some vertical curves. Hence, quaternionic representations are not forced by hand (to respect the CPT invariance of an underlying physical theory) but are imposed by the geometry itself.

4. We determine the network of flops of each model by studying the hyperplane arrangement $\mathrm{I}(\mathfrak{g}, \mathbf{R})$. Crepant resolutions and flops are related to the structure of the extended Mori cone. The hyperplane arrangement $\mathrm{I}(\mathfrak{g}, \mathbf{R})$ is a combinatorial invariant that controls the behavior of the extended Mori cone. The chamber structure of $\mathrm{I}(\mathfrak{g}, \mathbf{R})$ corresponds to the $5d$ and $6d$ Coulomb branches. The $6d$ Coulomb branch is related to the $5d$ Coulomb branch after a circle compactification and dualizing tensor multiplets into vectors.

5. The crepant resolution allows us to compute the Euler characteristic of each models and the triple intersection polynomial of the fibral divisors. We determine the Euler characteristic by computing the pushforward of the total Chern class defined in homology [114]. Using pushforward theorems for blowups and projective bundles, we express all topological invariants in terms of the topology of the base. In the case of a Calabi–Yau threefold, we compute the Hodge numbers using the Euler characteristic and the Shioda-Tate-Wazir theorem [300, Corollary 4.1]. Even though the fiber structure of the models with a trivial Mordell–Weil group is much more complicated than the one with a $\mathbb{Z}_2$ Mordell–Weil group, the Euler characteristic of the former specializes to that of the latter (after imposing $aS + bT = -4K$ for $a, b \in \mathbb{N}$ depending on the gauge algebra[2]), since both are defined by the same sequence of blowups [114].

[2]For example, for $(\mathrm{SU}(2) \times \mathrm{SU}(4))/\mathbb{Z}_2$-model, the condition is given by $S + 2T = -4K$.

6. By comparing the triple intersection numbers with the one-loop quantum correction, we determine constraints on the number of hyperpmultiplets charged under irreducible components of **R**. (For example in the case of I_2+I_4-models, the fundamental representations are absent when the Mordell–Weil group is $\mathbb{Z}_2$; the possible gauge group and the corresponding representation are presented in Table 13.1.)

7. We check explicitly that the constraints obtained by identifying the triple intersection numbers with the one-loop prepotential are compatible with an uplift to an anomaly-free six-dimensional $\mathcal{N} = (1, 0)$ supergravity theory. In the theories with a trivial Mordell–Weil group, the triple intersection numbers did not completely fix the number of hypermultiplets transforming in a given irreducible representation. But all numbers are fixed by considering the constraints from the vanishing of the coefficient of $\mathbf{tr}R^4$ and $\mathbf{tr}F_a^4$ where R is the Riemann curvature two-form and F_a is the field strength of the vector field A_a.

We note that the first data we need is topological invariants such as the Euler characteristic of the compactifying space. We compute for the various simple models for the Euler characteristic of the ellipctic fibration and specify their values for the cases of threefolds and fourfolds. Furthermore, in the case of Calabi–Yau threefolds, we compute the Hodge numbers. They are computed in various cases of the semi-simple models as well. This is feasible because the Euler characteristic of the threefolds and fourfolds is invariant under the choic of crepant resoltuions. More generally, in contrast to the case of fivefolds, Chern and Pontryagin numbers of fourfolds are invariant under crepant birational maps. Hence we can only compute without considering all possible crepant resoltuions to

compute the invariants for the threefoldsand the fourfolds. We focus on these results in Part III:

1. Chapter 5 : Generating functions of Euler characteristics, the Euler characteristics of the eliptically-fibered threefolds and fourfolds, and Hodge numbers of Calabi–Yau threefolds realizing various simple groups [114],

2. Chapter 6 : Characteristic numbers of the eliptically-fibered fourfolds realizing various simple groups [116],

3. Chapter 7 : Characteristic numbers of elliptically-fibered fourfolds with multisections or non-trivial Mordell–Weil groups [117].

In particular in Chapter 6, we compute various invariants of the eliptically-fibered fourfolds, which can be used as a compactifying space to give rise to a 3d or 4d theories. We compute the Euler characteristic, the holomorphic genera, the Todd-genus, the L-genus, the $\hat{A}$-genus, and the curvature invariant X_8 that appears in M-theory. We also show that certain characteristic classes are independent on the choice of the Kodaria fiber characterizing the group G. That is the case of $\int_Y c_1^2 c_2$, the arithmetic genus, and the $\hat{A}$-genus. Thus, it is enough to know $\int_Y c_2^2$ and the Euler characteristic $\chi(Y)$ to determine all the Chern numbers of an elliptically-fibered fourfold.

In Chapter 7, we compute characteristic numbers of elliptically-fibered fourfolds with multisections or non-trivial Mordell–Weil groups. We first consider the models of type E_{9-d} with $d = 1, 2, 3, 4$ whose generic fibers are normal elliptic curves of degree d. We then analyze the characteristic numbers of the Q_7-model, which provides a smooth model for elliptic fibrations of rank one and generalizes the E_5, E_6, and E_7-models. Finally, we examine the characteristic numbers of G-

models with $G = \mathrm{SO}(n)$ with $n = 3, 4, 5, 6$ and $\mathrm{G} = \mathrm{PSU}(3)$ whose Mordell–Weil groups are respectively $\mathbb{Z}_2$ and $\mathbb{Z}_3$. In each case, we compute the Chern and Pontryagin numbers, the Euler characteristic, the holomorphic genera, the Todd-genus, the L-genus, the A-genus, and the eight-form curvature invariant from M-theory.

A representation $\mathbf{R}$ can be complex, pseudo-real (quaternionic) or real.[3] A hypermultiplet transforming in a reducible quaternionic representation $\mathbf{R} \oplus \overline{\mathbf{R}}$, such that $\mathbf{R}$ an irreducible complex representation of the gauge group, is called a *full hypermultiplet*. The completion of the complex representation $\mathbf{R}$ to the reducible quaternionic representation $\mathbf{R} \oplus \overline{\mathbf{R}}$ is required by the CPT theorem. A hypermultiplet transforming in an irreducible quaternionic representation is called a *half-hypermultiplet*. On a half-hypermultiplet, the pseudo-real representation of the gauge group requires the existence of an anti-linear map that squares to minus the identity. In six (resp. five) dimensional Lorentzian spacetime, this anti-linear map allows the introduction of a symplectic Majorana Weyl (resp. symplectic Majorana) condition that reduces by half the number of degrees of freedom. In our convention, we avoid the double counting that consists of writing a reducible representation $\mathbf{R} \oplus \overline{\mathbf{R}}$ even when $\mathbf{R}$ is an irreducible pseudo-real representation. A full hypermultiplet has multiplicity $n_{\mathbf{R}} + n_{\overline{\mathbf{R}}} = 2n_{\mathbf{R}}$ while a half-hypermultiplet has multiplicity $n_{\mathbf{R}}$. Since we do not double count half-hypermultiplets, we do not introduce factors of $1/2$ in the anomaly polynomial when $\mathbf{R}$ is pseudo-real. Still, a hypermultiplet in a pseudo-real representation contributes to the anomaly polynomial half as much as a full hypermultiplet.

[3] When a hypermultiplet is charged under an irreducible complex representation $\mathbf{R}$, its CPT dual is charged under the complex conjugate representation $\overline{R}$.

Comparing the triple intersection numbers with the one-loop prepotential gives constraints linear in $n_{\mathbf{R}_i}$ that are sometimes enough to completely determine all the numbers $n_{\mathbf{R}_i}$. This is for example the case for many models with a simple group [112, 115, 124] and also semi-simple models with a $\mathbb{Z}_2$ Mordell–Weil group, namely the SO(4)-model, the $(\mathrm{SU}(2) \times \mathrm{Sp}(4))/\mathbb{Z}_2$-model, and the $(\mathrm{SU}(2) \times \mathrm{SU}(4))/\mathbb{Z}_2$-model. The Spin(4), $\mathrm{SU}(2) \times \mathrm{Sp}(4)$, and $\mathrm{SU}(2) \times \mathrm{SU}(4)$-models have in addition hypermultiplets transforming in fundamental representations and equating the one-loop prepotential and the triple intersection numbers does not provide enough constraints to fix all $n_{\mathbf{R}_i}$. We can fix all $n_{\mathbf{R}_i}$ in different ways.

- Firstly, by using Witten's formula that asserts that the number of hypermultiplets transforming in the adjoint representation of an irreducible component G_a of the gauge group is the (arithmetic) genus of the curve S_a supporting that group. Witten's formula uses M2-branes to study the quantization of the curve S_a seen as a moduli space. Each (anti)-holomorphic 1-form on S_a is responsible for a hypermultiplet.

- Secondly, by using techniques of intersecting branes to directly count $n_{\mathbf{R}_i}$ as intersection numbers between components of the discriminant locus. This method assumes that the components intersect relatively well. For certain representations (such as the traceless second antisymmetric representation of $\mathrm{Sp}(2n)$, this method has to be completed with a generalization of Witten's formula.

- Finally, we can use the existence of an anomaly-free six-dimensional supergravity theory. Matching the triple intersection numbers with the one-loop prepotential and asking for the

vanishing of the coefficients of $\mathbf{tr}R^4$ and $\mathbf{tr}F_a^4$ in the anomaly polynomial of the $6d$ $\mathcal{N} = 1$ supergravity theory are enough to fix all the $n_{\mathbf{R}_i}$. Here R is the Riemann curvature two-form and F_a are the field-strength of the vector fields. The vanishing of these quartic terms is a necessary condition to cancel anomalies by the Green-Schwarz mechanism.

We find that the last method is the most satisfying and general as it only relies on basic aspects of supergravity theories in five and six dimensions: exactness of the one-loop quantum correction and the cancellation of anomalies of the six-dimensional theory. We checked that all three methods give the same result. In a six-dimensional uplifted theory, the number of hypermultiplets are the same, but we have to adjust the number of vector and tensor multiplets. The tensor multiplets and spinors require cancellations of anomalies.

The anomalies in six-dimensional theories can be formally summarized by an eight-form I_8 constructed from the Riemann curvature two-form R and the gauge curvature two-forms F_i (see [147, 270] and [22, 106, 272]). The Green-Schwarz mechanism consists of adding a counterterm depending on the Yang-Mills and gravitational Chern-Simons three-forms and modifying the gauge transformation of the appropriate antisymmetric self-dual or anti-self-dual two-forms simultaneously [270, 272]. This requires I_8 to factorize into a product of two four-forms. We check these conditions in detail and factorize the anomaly polynomial I_8 explicitly for each cases.

Before factoring the anomaly polynomial I_8, a necessary condition is the vanishing of the coefficients of the terms $\mathbf{tr}R^4$ and $\mathbf{tr}F_a^4$ from the quartic contribution of the pure gravitational and the pure gauge anomalies. The condition on the pure gravitational anomaly requires knowing the Euler

characteristic of the elliptic fibration due to the content of hypermultiplets. Due to the recent results on the pushforward of blowups [114], we can now easily compute such invariants using a crepant resolution of singularities with centers that are local complete intersections. In particular, we get results that are independent of the dimension of the base and provide the results for all n-folds.

Using the number of multiplets, we show that the pure gravitational and the pure gauge anomalies are canceled using the number of representations $n_{\mathbf{R}_i}$, which are restricted by matching triple intersection numbers with the one-loop quantum correction to the cubic prepotential (see Section 2.13.2). Assuming that the coefficients of $\mathbf{tr}R^4$ and $\mathbf{tr}F_a^4$ vanish, for the semi-simple gauge group with two simple components $G = G_1 \times G_2$, the anomaly polynomial is

$$I_8 = \frac{K^2}{8}(\mathbf{tr}R^2)^2 + \frac{1}{6}(X_1^{(2)} + X_2^{(2)})\mathbf{tr}R^2 - \frac{2}{3}(X_1^{(4)} + X_2^{(4)}) + 4Y_{12},$$

which we prove to reduce to a perfect square for all case considered, as expected from Sadov's work [269]. More precisely,

$$I_8 = \frac{1}{2}\left(\frac{K}{2}\mathbf{tr}R^2 - 2S\mathbf{tr}_2F_1^2 - 2T\mathbf{tr}_4F_2^2\right)^2.$$

The term that is squared is used as a magnetic source for the antisymmetric two-form in the gravitational multiplet that cancel the anomaly in the Green-Schwarz-Sognatti mechanism.

In summary, following Sadov, there is a geometric formulation of the Green-Schwarz mechanism for elliptically fibered Calabi–Yau threefolds [269]. Hence, the number of multiplets, which are

computed from the triple intersection numbers, can be used to check if the Green-Schwarz mechanism cancels the anomalies in the *6d* theory uplift. This method was introduced in [45] and implemented explicitly in [124] for SU(n)-models, and the following cases in this thesis:

1. Chapter 8 : F_4-models [115],
2. Chapter 9 : G_2, Spin(7), Spin(8)-models [112],
3. Chapter 10 : SO(4) and Spin(4)-models [118],
4. Chapter 11 : $SU(2) \times G_2$-models [119],
5. Chapter 12 : $SU(2) \times SU(3)$-models [113],
6. Chapter 13 : $SU(2) \times Sp(4)$, $(SU(2) \times Sp(4))/\mathbb{Z}_2$, $SU(2) \times SU(4)$, $(SU(2) \times SU(4))/\mathbb{Z}_2$-models [121].

An important aspect of the dictionary between elliptic fibrations and gauge theories is that the elliptic fibration also captures global aspects of the gauge theory: the fundamental group $\pi_1(G)$ of the gauge group is isomorphic to the Mordell–Weil group of the elliptic fibration [20, 229, 239], see also [31, and refs. within]. One natural question is how the Mordell–Weil group of the elliptic fibration affects these supergravity theories. These questions have their mathematical counterparts that are also interesting for their own sake. For example, what is the effect on the Coulomb branch of a five-dimensional gauge theory when a semi-simple group is quotiented by a subgroup of its center? This physics question translates in mathematics to the following: what happens to the extended Mori cone of an elliptically-fibered Calabi–Yau threefold when the Mordell–Weil group is purely

torsion? Moreover, would this five-dimensional theory with such a Mordell–Weil group still have a six-dimensional uplift with cancellation of anomalies?

For all the collisions we consider with the Mordell–Weil group $\mathbb{Z}_2$ in this thesis, namely Chapters 10 and 13, the Mordell–Weil group $\mathbb{Z}_2$ is an obstruction for the presence of fundamental representations. This change of matter content has also consequences for the cancellations of anomalies in the six-dimensional theory.

Given a complex Lie algebra $\mathfrak{g}$, there is a unique simply connected compact Lie group $\widetilde{G} = \exp(\mathfrak{g})$. We denote the center of $\widetilde{G}$ by $Z(\widetilde{G})$. All Lie groups sharing the same Lie algebra have the same universal cover $\widetilde{G} = \exp(\mathfrak{g})$ and are quotient of $\widetilde{G}$ by a subgroup H of its center $Z(\widetilde{G})$. The center of the group $\widetilde{G}/H$ is then $Z(\widetilde{G})/H$ and depends not only on the isomorphic class of H but also on the embedding of H in $Z(\widetilde{G})$. It follows that gauge groups with the same Lie algebra can have different centers and first homotopy groups. In a gauge theory, the center and the first homotopy group of the group play a crucial role in the description of non-local operators such as Wilson lines and 'tHooft operators. Since not all representations of the Lie algebra $\mathfrak{g}$ are coming from a representation of the Lie group, a non-trivial Mordell–Weil group places restrictions on the representation $\mathbf{R}$. The choice of the correct group depends on the Mordell–Weil and is constrained by the representation $\mathbf{R}$.

We can also investigate when the Mordell–Weil group is a $U(1)$. In chapter 4, we introduce a new model for elliptic fibrations endowed with a Mordell–Weil group of rank one. We call it a $\mathrm{Q}_7(\mathscr{L}, \mathscr{S})$ model. It naturally generalizes several previous models of elliptic fibrations popular in the F-theory literature.

1. Chapter 4: Q_7-Model – a new model for elliptic fibrations with a rank one Mordell–Weil group.

We use this model to determine the spectrum of singular fibers of an elliptic fibration of rank one and compute a generating function for its Euler characteristic. With a view toward string theory, we determine a semi-stable degeneration which is understood as a weak coupling limit in F-theory. We show that it satisfies a non-trivial topological relation at the level of homological Chern classes. This identity ensures that the D3 charge in F-theory is the same as the one in the weak coupling limit. The weak coupling limit is reviewed in Section 2.10

We work over the complex numbers and assume that the base B is a smooth projective variety, $\mathscr{L}$ is a line bundle over B, and $S = V(s)$ is a smooth irreducible subvariety of B given by the zero scheme of a section s of a line bundle $\mathscr{S}$. The locus of points of B over which the fiber is singular is called the discriminant locus of ϕ. Under mild assumptions, the discriminant is a Cartier divisor [101]. An elliptic fibration is a proper surjective morphism $\phi : Y \to B$ between algebraic varieties such that the generic fiber of ϕ is a smooth algebraic curve of genus one and ϕ is endowed with a rational section.

The local ring of a subvariety S of X is denoted $\mathscr{O}_{X,S}$, its maximal ideal is $\mathscr{M}_{X,S}$ and the quotient field is the residue field $\kappa(S) = \mathscr{O}_{X,S}/\mathscr{M}_{X,S}$. The local ring $\mathscr{O}_{X,S}$ is the stalk of the structure sheaf of X at the generic point η_S of S and $\kappa(S)$ is the function field of S. If S is a divisor, $\mathscr{O}_{X,S}$ is a one dimensional local domain. In case X is nonsingular along S, $\mathscr{O}_{X,S}$ is a discrete valuation ring and the order of vanishing is given by the usual valuation.

We denote the vanishing locus of the sections $f_1, \ldots, f_n$ by $V(f_1, \ldots, f_n)$. The tangent bundle of a variety X is denoted by TX and the normal bundle of a subvariety Z of a variety X is denoted by $N_Z X$. Let $\mathscr{V} \to B$ be a vector bundle over a variety B. We denote the by $\mathbb{P}(\mathscr{V})$ the projective bundle of lines in $\mathscr{V}$. We use Weierstrass models defined with respect to the projective bundle $\pi : X_0 = \mathbb{P}[\mathscr{O}_B \oplus \mathscr{L}^{\otimes 2} \oplus \mathscr{L}^{\otimes 3}] \to B$ where $\mathscr{L}$ is a line bundle of B. We denote the pullback of $\mathscr{L}$ with respect to π by $\pi^*\mathscr{L}$. We denote by $\mathscr{O}_{X_0}(1)$ the canonical line bundle on X_0, i.e., the dual of the tautological line bundle of X_0 (see [136, Appendix B.5]). The Weierstrass model $\phi : Y_0 \to B$ is defined as the zero-scheme of a section of $\mathscr{O}_{X_0}(3) \otimes \pi^*\mathscr{L}^{\otimes 6}$—Weierstrass models and Deligne's formulaire are studied in more detail in Section 2.2.1. Any elliptic fibration over a smooth variety defined with an algebraically closed field is birational to a (possibly singular) Weierstrass model [94, 246, 247]. For Weierstrass models, we use the notation of Tate as presented in Deligne's formulaire [94]. Tate's algorithm determines the type of the geometric fiber over the special point of a Weierstrass model over a discrete valuation ring by manipulating the coefficients of the Weierstrass model [290]. There are well-known formulas to compute the discriminant locus Δ and the j-invariant of a Weierstrass model. Tate's algorithem is studied in detail in Section 2.2.6. The type of singular fibers over a generic point of a divisor S of the base are classified by Kodaira and Néron. They are reviewed in Sections 2.1.1 and 2.2.5. We denote the geometric fibers of an elliptic surface by Kodaira symbols. To denote a generic fiber, we decorate the Kodaira fiber by an index "ns" , "ss" , or "s" that characterizes the degree of the field extension necessary to move from the generic fiber to the geometric generic fiber. We denote the type of the geometric generic fiber over an irreducible component of the discriminant locus by one of the Kodaira symbols I_n, IV, III, II, I_n^*, IV*, III*, and

II^* [200].

We use the conventions of Carter and denote an affine Dynkin diagram by $\tilde{\mathfrak{g}}$, where $\mathfrak{g}$ is the Dynkin diagram of a simple Lie algebra [70]. We write $\tilde{\mathfrak{g}}^t$ for the twisted Dynkin diagram whose Cartan matrix is the transpose of the Cartan matrix of $\tilde{\mathfrak{g}}$. This notation is only relevant when $\mathfrak{g}$ is not simply laced, that is, for $\mathfrak{g} = \mathrm{G}_2$, F_4, B_{3+k}, or C_{2+k}. Given a vector bundle $\mathscr{V}$, we denote by $\mathbb{P}[\mathscr{V}]$ the projective bundle of lines of $\mathscr{V}$. In intersection theory, we follow the conventions of Fulton [136].

Given a vector bundle $V \to B$ defined over a variety B, we denote by $\pi : \mathbb{P}[V] \to B$ the projectivization of a vector bundle $V \to B$. This is extended to weighted projective bundles, for which we write $\mathbb{P}_{\vec{w}}[V]$ where $\vec{w}$ are the weights of characterizing the weighted projective bundle. There are two conventions for projective bundles. We use the classical (pre-Grothendieck) convention in which a projective space $\mathbb{P}[V]$ is the space of directions of a vector space V in contrast to the space of hyperplanes. This is particularly important when dealing with Chern classes. Our convention on projective bundle matches Fulton's book on intersection theory. We denote by $\mathbb{P}[V]_{\mathscr{W}}$ the collection of hypersurfaces defined as the zero locus of a section of the line bundle $\mathscr{W}$ in the projective bundle $\mathbb{P}[V]$. We denote by $\mathscr{O}_{\mathbb{P}[V]}(-1)$ the tautological line bundle of $\mathbb{P}[V]$. Its dual is denoted $\mathscr{O}_{\mathbb{P}[V]}(1)$. We denote by $\mathscr{O}_{\mathbb{P}[V]}(n)$ the nth tensor product of $\mathscr{O}_{\mathbb{P}[V]}(1)$ (if $n > 0$) and of $\mathscr{O}_{\mathbb{P}[V]}(-1)$ if $n < 0$. When the context is clear, we abuse notations and write $\mathscr{O}(n)$ for $\mathscr{O}_{\mathbb{P}[V]}(n)$.

2.1 Elliptic fibrations and fiber types

2.1.1 Fiber types, dual graphs, Kodaira symbols

Definition 2.1.1 (Algebraic cycle)**.** An algebraic cycle of a Noetherian scheme X is a finite formal sum $\sum_i N_i V_i$ of subvarieties V_i with integer coefficients N_i. If all the subvarieties V_i have the same dimension d, the cycle is called a d-cycle. The free group generated by subvarieties of dimension d is denoted $Z_d(X)$. The group of all cycles, denoted $Z(X) = \bigoplus_d Z_d(X)$, is the free group generated by subvarieties of X.

Definition 2.1.2 (Degree of a zero-cycle[136, Chapter 1, Definition 1.4, p. 13])**.** Let X be a complete scheme. The *degree* of a zero-cycle $\sum N_i p_i$ of X is

$$\deg(\sum_i N_i p_i) = \sum_i N_i [\kappa(p_i) : k],$$

where $[\kappa(p_i) : k]$ is the degree of the field extension $\kappa(p_i) \to k$.

Let Θ be an algebraic one-cycle with irreducible decomposition $\Theta = \sum_i m_i \Theta_i$. We denote by $\Theta_i \cdot \Theta_j$ the zero-cycle defined by the intersection of Θ_i and Θ_j for $i \neq j$.

Definition 2.1.3 (n-points, tree)**.** A *n-point* of an algebraic one-cycle Θ is a point in $\bigcup_i \Theta_i$, which belongs to exactly n distinct irreducible components Θ_i. An algebraic one-cycle Θ is said to be a *tree* if it does not have n-points for $n > 2$. Two curves intersect transversally if their intersection consists of isolated reduced closed points.

Following Kodaira [200], we introduce the following definition:

Definition 2.1.4 (Fiber type)**.** The *type* of an algebraic one-cycle $\Theta \in Z_1(X)$ with irreducible decomposition $\Theta = \sum_i m_i \Theta_i$ consists of the isomorphism class of each irreducible curve Θ_i, together with the topological structure of the reduced polyhedron $\sum_i \Theta_i$.

The topological structure of the polyhedron $\sum_i \Theta_i$ is characterized by the underlying set of the scheme-theoretic intersection $\Theta_i \bigcap \Theta_j$ $(i \neq j)$ of the irreducible components Θ_i.

Definition 2.1.5 (Dual graph)**.** Given an algebraic one-cycle Θ with irreducible decomposition $\Theta = \sum_i m_i \Theta_i$, we associate a weighted graph (called the *dual graph* of Θ) such that

- the vertices are the irreducible components Θ_i of the fiber,
- the weight of the vertex corresponding to an irreducible component Θ_i is its multiplicity m_i
- the vertices corresponding to the irreducible components Θ_i and Θ_j $(i \neq j)$ are connected by $\hat{\Theta}_{i,j} = \deg[\Theta_i \bigcap \Theta_j]$ edges.[4]

The type of the geometric fiber over a codimension one point of a minimal elliptic fibration is called the *Kodaira type* of the fiber. As shown by Kodaira [200] and Néron [251], there are 10 Kodaira types, and we denote them with the notation of Kodaira.

Definition 2.1.6 (Kodaira symbols, See [200, Theorem 6.3])**.** Kodaira has introduced the following symbols characterizing the type of one-cycles appearing in the study of minimal elliptic surfaces. See Table 2.1 for a visualization of these fibers.

[4] The degree $\deg(\alpha_0)$ of a zero-cycle α_0 is defined by passing to the Chow ring and using the degree defined in [136, Definition 1.4].

1. Type I_0: a smooth curve of genus 1.

2. Type I_1: an irreducible nodal rational curve.

3. Type II: an irreducible cuspidal rational curve.

4. Type I_2: $\Theta = \Theta_1 + \Theta_2$ and $\Theta_1 \cdot \Theta_2 = p_1 + p_2$: two smooth rational curves intersecting transversally at two distinct points p_1 and p_2. The dual graph of I_2 is $\widetilde{A}_1$.

5. Type III: $\Theta = \Theta_1 + \Theta_2$ and $\Theta_1 \cdot \Theta_2 = 2p$: two smooth rational curves intersecting at a double point. Its dual graph is $\widetilde{A}_1$.

6. Type IV: $\Theta = \Theta_1 + \Theta_2 + \Theta_3$ and $\Theta_1 \cdot \Theta_2 = \Theta_1 \cdot \Theta_3 = \Theta_2 \cdot \Theta_3 = p$: a 3-star composed of smooth rational curves. Its dual graph is $\widetilde{A}_2$.

7. Type I_n ($n \geq 3$): $\Theta = \Theta_0 + \cdots \Theta_n$ with $\Theta_i \cdot \Theta_{i+1} = p_i$ $i = 0, \cdots, n-1$ and $\Theta_n \cdot \Theta_0 = p_n$. Its dual graph is the affine Dynkin diagram $\widetilde{A}_{n-1}$.

8. Type I_n^* ($n \geq 0$): $\Theta = \Theta_0 + \Theta_1 + 2\Theta_2 + \cdots + 2\Theta_{n+2} + \Theta_{n+3} + \Theta_{n+4}$, with $\Theta_i \cdot \Theta_{i+1} = p_i$ ($i = 1, \ldots, n+2$), $\Theta_0 \cdot \Theta_2 = p_0$, $\Theta_{n+4} \cdot \Theta_{n+2} = p_{n+4}$. The dual graph the affine Dynkin diagram $\widetilde{D}_{4+n}$.

9. Type IV*: $\Theta = \Theta_0 + \Theta_1 + 2\Theta_2 + 2\Theta_3 + 3\Theta_4 + 2\Theta_5 + \Theta_6$ with $\Theta_i \cdot \Theta_{i+1} = p_i$ ($i = 3, \ldots, 6$), $\Theta_1 \cdot \Theta_3 = p_1$, $\Theta_0 \cdot \Theta_2 = p_0$, $\Theta_2 \cdot \Theta_4 = p_2$. The dual graph is the affine Dynkin diagram $\widetilde{E}_6$.

10. Type III*: $\Theta = \Theta_0 + 2\Theta_1 + 2\Theta_2 + 3\Theta_3 + 4\Theta_4 + 3\Theta_5 + 2\Theta_6 + \Theta_7$ with $\Theta_i \cdot \Theta_{i+1} = p_i$ ($i = 3, \ldots, 6$), $\Theta_1 \cdot \Theta_3 = p_1$, $\Theta_0 \cdot \Theta_1 = p_0$, $\Theta_2 \cdot \Theta_4 = p_2$. The dual graph is the affine Dynkin

diagram $\widetilde{E}_7$.

11. Type II*: $\Theta = 2\Theta_1 + 3\Theta_2 + 4\Theta_3 + 6\Theta_4 + 5\Theta_5 + 4\Theta_6 + 3\Theta_7 + 2\Theta_8 + \Theta_0$, with $\Theta_i \cdot \Theta_{i+1} = p_i$ ($i = 3, \ldots, 7$), $\Theta_1 \cdot \Theta_3 = p_1$, $\Theta_8 \cdot \Theta_0 = p_8$, and $\Theta_2 \cdot \Theta_4 = p_2$. The dual graph the affine Dynkin diagram $\widetilde{E}_8$.

The dual graph of a Kodaira fiber is always an affine Dynkin diagram of type ADE (see Table 2.2), while the dual graph of a generic fiber itself can be the affine Dynkin diagram of a non-simply-laced simple Lie algebra.

Let G be a simply-connected simple Lie group with Dynkin diagram $\mathfrak{g}$. We denote by $\widetilde{\mathfrak{g}}$ the affine Dynkin diagram that reduces, upon removal of its extra node, to the Dynkin diagram $\mathfrak{g}$. Following Carter [70], we write $\widetilde{\mathfrak{g}}^t$ for its Langlands dual, namely, the twisted Dynkin diagram whose Cartan matrix is the transpose of the Cartan matrix of $\widetilde{\mathfrak{g}}$. In particular, $\widetilde{\mathfrak{g}}$ and $\widetilde{\mathfrak{g}}^t$ are distinct only when $\mathfrak{g}$ is not simply laced (that is, when $\mathfrak{g}$=B_k, C_k, G_2, or F_4).

Type	$v(c_4)$	$v(c_6)$	$v(\Delta)$	j	Monodromy	Fiber	Dual Graph
I_0	≥ 0	≥ 0	0	$\mathbb{C}$	I_2	Smooth	-
I_1	0	0	1	∞	$\begin{pmatrix} 1 & 1 \\ 0 & 1 \end{pmatrix}$		$\widetilde{\mathrm{A}}_0$
II	≥ 1	1	2	0	$\begin{pmatrix} 1 & 1 \\ -1 & 0 \end{pmatrix}$		$\widetilde{\mathrm{A}}_0$
III	1	≥ 2	3	1728	$\begin{pmatrix} 0 & 1 \\ -1 & 0 \end{pmatrix}$		$\widetilde{\mathrm{A}}_1$
IV	≥ 2	2	4	0	$\begin{pmatrix} 0 & 1 \\ -1 & -1 \end{pmatrix}$		$\widetilde{\mathrm{A}}_2$
I_n	0	0	$n > 1$	∞	$\begin{pmatrix} 1 & n \\ 0 & 1 \end{pmatrix}$	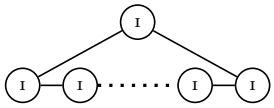	$\widetilde{\mathrm{A}}_{n-1}$
I_n^*	2	≥ 3	$n+6$	∞	$\begin{pmatrix} -1 & -n \\ 0 & -1 \end{pmatrix}$	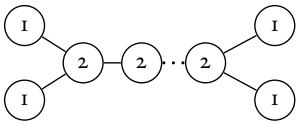	$\widetilde{\mathrm{D}}_{n+4}$
	≥ 2	3	$n+6$				
IV^*	≥ 3	4	8	0	$\begin{pmatrix} -1 & -1 \\ 1 & 0 \end{pmatrix}$	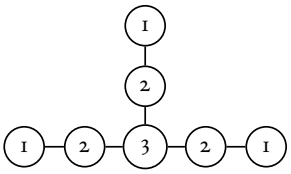	$\widetilde{\mathrm{E}}_6$
III^*	3	≥ 5	9	1728	$\begin{pmatrix} 0 & -1 \\ 1 & 0 \end{pmatrix}$	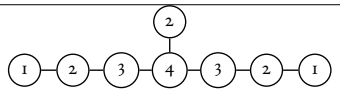	$\widetilde{\mathrm{E}}_7$
II^*	≥ 4	5	10	0	$\begin{pmatrix} 0 & -1 \\ 1 & 1 \end{pmatrix}$	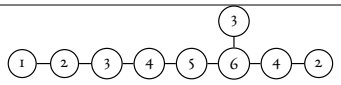	$\widetilde{\mathrm{E}}_8$

Table 2.1: Kodaira-Néron classification of geometric fibers over codimension one points of the base of an elliptic fibration [200, 251]. The j-invariant of the I_0^* is never ∞ and can take any finite value.

Tate's Step	1	2	3	4	5	6	7	8	9	10
Kodaira's symbol	I_0	$\mathrm{I}_{n>0}$	II	III	IV	I_0^*	$\mathrm{I}_{n>0}^*$	IV*	III*	II*
Néron's type	A	B_n	C_1	C_2	C_3	C_4	$\mathrm{C}_{5,n}$	C_6	C_7	C_8
Dual graph	–	$\widetilde{\mathrm{A}}_{n-1}$	$\widetilde{\mathrm{A}}_1$	$\widetilde{\mathrm{A}}_1$	$\widetilde{\mathrm{A}}_2$	$\widetilde{\mathrm{D}}_4$	$\widetilde{\mathrm{D}}_{4+n}$	$\widetilde{\mathrm{E}}_6$	$\widetilde{\mathrm{E}}_7$	$\widetilde{\mathrm{E}}_8$
$v(\Delta)$	0	n	2	3	4	6	$6+n$	8	9	10
$v(j)$	0	$-n$	0	0	0	0	$-n$	0	0	0
j	$j \in \mathbb{C}$	$j = \infty$	$j = 0$	$j = 1728$	$j = 0$	$j \in \mathbb{C}$	$j = \infty$	$j = 0$	$j = 1728$	$j = 0$

Table 2.2: Kodaira-Néron classification. When working over an algebraically closed field, the fiber type is determined uniquely by the valuation of the discriminant Δ and the j-invariant.

2.1.2 Elliptic fibrations, generic versus geometric fibers

Definition 2.1.7 (Elliptic fibrations)**.** A surjective proper morphism $\phi : Y \longrightarrow B$ between two algebraic varieties Y and B is called an elliptic fibration if the generic fiber of ϕ is a smooth projective curve of genus one and ϕ has a rational section. When B is a curve, Y is called an elliptic surface. When B is a surface, Y is said to be an elliptic threefold. In general, if B has dimension $n-1$, Y is called an elliptic n-fold.

The locus of singular fibers of ϕ is called the discriminant locus of ϕ and is denoted $\Delta(\phi)$ or simply Δ when the context is clear. If the base B is smooth, the discriminant locus is a divisor [101]. The singular fibers of a minimal elliptic surface have been classified by Kodaira and Néron. The dual graphs of these geometric fibers are affine Dynkin diagrams. We denote these singular fibers by their Kodaira symbols as described in Definition 2.1.6 and presented in Table 2.1.

The language of schemes streamlines many notions in the study of fibrations. We review some basic definitions.

Definition 2.1.8 (Fiber over a point)**.** Let $\phi : Y \longrightarrow B$ be a morphism of schemes. For any $p \in B$, the fiber over p is denoted Y_p and defined using a fibral product[5] as

$$Y_p = Y \times_B \operatorname{Spec} \kappa(\mathrm{p}).$$

The first projection $Y_p \longrightarrow Y$ induces an homeomorphism from Y_p onto $f^{-1}(p)$ [219, §3.1 Proposition 1.16] . The second projection gives Y_p the structure of a scheme over the residue field $\kappa(p)$.

If p is not a closed point[6], the residue field $\kappa(p)$ is not necessarily algebraically closed. Certain components of Y_p could be $\kappa(p)$-irreducible (i.e. irreducible when defined over $\kappa(p)$) while they become reducible after an appropriate field extension. An irreducible scheme over a field k is said to be *geometrically irreducible* when it stays irreducible after any field extension. The most refined description of the fiber Y_p is always the one corresponding to the algebraic closure $\overline{\kappa(p)}$ of $\kappa(p)$. This motivates the following definition.

Definition 2.1.9. The geometric fiber over p is the fiber $Y_p \times_{\kappa(p)} \overline{\kappa(p)}$, the fiber Y_p after the base change induced by the field extension $\kappa(p) \to \overline{\kappa(p)}$ to the algebraic closure of $\kappa(p)$.

By construction, a geometric fiber is always composed of geometrically irreducible components.

Definition 2.1.10. We say that the type of a fiber Y_p is *geometric* if it does not change after a field extension.

[5] Given three sets (A_1, A_2, and S) and two maps $\phi_1 : A_1 \to B$ and $\phi_2 : A_2 \to B$, we define the fibral product $A_1 \times_S A_2$ as the subset of $A_1 \times A_2$ composed of couples (a_1, a_2) such that $\phi_1(a_1) = \phi_2(a_2)$.

[6] For example, if p is the generic point of a subvariety of B.

Remark 2.1.11. To emphasize the difference between the fiber Y_p and its geometric fiber, we will refer to the fiber Y_p (defined with respect to the residue field $\kappa(p)$) as the *arithmetic fiber*.

For an elliptic n-fold, the Kodaira fibers are also the *geometric generic fibers* of the irreducible components of the reduced discriminant locus. While the dual graph of a Kodaira fiber is an affine Dynkin diagram of type $\widetilde{A}_k$, $\widetilde{D}_{4+k}$, $\widetilde{E}_6$, $\widetilde{E}_7$, or $\widetilde{E}_8$, the dual graph of the generic (arithmetic) fiber itself can also be a twisted Dynkin diagram of type $\widetilde{B}^t_{3+k}$, $\widetilde{C}^t_{2+k}$, $\widetilde{G}^t_2$, or $\widetilde{F}^t_4$. This is reviewed in Tables 2.3 and 2.4. These dual graphs are not geometric in the sense that after an appropriate base change they become $\widetilde{D}_{4+n}$, $\widetilde{A}_{2+2k}$ or $\widetilde{A}_{1+2k}$, and $\widetilde{E}_6$ respectively. The Kodaira fibers of the following type never need a field extension:

$$\mathrm{I}_1,\ \mathrm{II},\ \mathrm{III},\ \mathrm{III}^*,\ \text{and}\ \mathrm{II}^*.$$

The remaining Kodaira fibers (IV, $\mathrm{I}_{n>1}$, I^*_n, and IV^*) can come from fibers Y_p whose types are not geometric and require at least a field extension of degree 2 to describe a fiber with a geometric type. When the fiber Y_p has a geometric type, the type of the fiber is said to be *split*. Otherwise, the type of Y_p is said to be non-split. When that is the case we mark the fiber with an "ns" superscript: $\mathrm{IV}^{\mathrm{ns}}$, $\mathrm{I}^{\mathrm{ns}}_n$, $\mathrm{I}^{*\mathrm{ns}}_n$, $(n \geq 2)$ and $\mathrm{IV}^{*\mathrm{ns}}$. When a field extension is not needed, the fibers are marked with an "s" superscript ("split"): IV^{s}, $\mathrm{I}^{\mathrm{s}}_n$, $\mathrm{I}^{*\mathrm{s}}_n$, $(n \geq 2)$ and $\mathrm{IV}^{*\mathrm{s}}$. The fiber of type I^*_0 can be split, semi-split, or non-split if the Kodaira types require no field extension, a quadratic extension, or a cubic extension. The corresponding dual graphs are respectively $\widetilde{D}_4$, $\widetilde{B}^t_3$, and $\widetilde{G}^t_2$.

2.2 Weierstrass models, Tate's algorithm, and Mordell–Weil group

A *genus-one fibration* over a variety B is a surjective morphism $\phi : Y \to B$ onto B such that the general fiber is a smooth projective curve of genus one. A *rational section* of the genus-one fibration is a rational map $\sigma : B \to Y$ such that the image of $\phi \circ \sigma$ is dense in B and restrict to the identity on the domain of definition of σ. In particular, a rational section can be ill-defined over a divisor of B. The image of the base under a rational section gives a divisor of Y.

When the genus-one fibration admits a rational section, we call it an *elliptic fibration*. An elliptic fibration is birational to a Weierstrass model [94, 246].

2.2.1 Weierstrass models, Mordell–Weilgroup, and Deligne's formulaire

We follow the notation of Deligne [94]. Let $\mathscr{L}$ be a line bundle over a quasi-projective variety B. We define the following projective bundle (of lines):

$$\pi : X_6 = \mathbb{P}_B[\mathscr{O}_B \oplus \mathscr{L}^{\otimes 2} \oplus \mathscr{L}^{\otimes 3}] \longrightarrow B. \tag{2.1}$$

The relative projective coordinates of X_6 over B are denoted $[z : x : y]$, where z, x, and y are defined respectively by the natural injection of $\mathscr{O}_B$, $\mathscr{L}^{\otimes 2}$, and $\mathscr{L}^{\otimes 3}$ into $\mathscr{O}_B \oplus \mathscr{L}^{\otimes 2} \oplus \mathscr{L}^{\otimes 3}$. Hence, z is a section of $\mathscr{O}_{X_6}(1)$, x is a section of $\mathscr{O}_{X_6}(1) \otimes \pi^* \mathscr{L}^{\otimes 2}$, and y is a section of $\mathscr{O}_{X_6}(1) \otimes \pi^* \mathscr{L}^{\otimes 3}$.

Definition 2.2.1. *A Weierstrass model* is an elliptic fibration $\phi : Y \to B$ cut out by the zero locus of a section of the line bundle $\mathscr{O}(3) \otimes \pi^* \mathscr{L}^{\otimes 6}$ in X_6.

The most general Weierstrass equation is written in the notation of Tate as [94] $F = 0$ with

$$F = y^2z + a_1xyz + a_3yz^2 - (x^3 + a_2x^2z + a_4xz^2 + a_6z^3), \tag{2.2}$$

where a_i is a section of $\pi^*\mathscr{L}^{\otimes i}$ on B. Such a hypersurface is an elliptic fibration since over the generic point of the base, the fiber is a nonsingular cubic planar curve with a rational point ($x = z = 0$). The line bundle $\mathscr{L}$ is called the *fundamental line bundle* of the Weierstrass model $\phi : Y \to B$ and can be defined directly from the elliptic fibration Y as $\mathscr{L} = R^1\phi_*\mathscr{O}_Y$.

The rational section of the Weierstrass model is then $O : z = x = 0$, which is a point of inflection on the generic fiber. The group of rational sections of the elliptic fibration $\phi : Y \to B$ is called the *Mordell–Weil group* $MW(\phi)$. It is a finitely generated Abelian group. Its rank and torsion group are birational invariants of the elliptic fibration. The definition of $MW(\phi)$ assumes the choice of an identity element. For a Weierstrass equation, the canonical choice is the point of inflection $O : z = x = 0$.

Following Tate and Deligne, we introduce the following quantities [94]

$$\begin{cases} b_2 &= a_1^2 + 4a_2, \quad b_4 = a_1a_3 + 2a_4, \quad b_6 = a_3^2 + 4a_6 \\ b_8 &= a_1^2a_6 - a_1a_3a_4 + 4a_2a_6 + a_2a_3^2 - a_4^2 \\ c_4 &= b_2^2 - 24b_4, \quad c_6 = -b_2^3 + 36b_2b_4 - 216b_6 \\ \Delta &= -b_2^2b_8 - 8b_4^3 - 27b_6^2 + 9b_2b_4b_6, \quad j = c_4^3/\Delta \end{cases} \tag{2.3}$$

These quantities satisfy the following two relations

$$1728\Delta = c_4^3 - c_6^2, \quad 4b_8 = b_2 b_6 - b_4^2. \tag{2.4}$$

The b_i ($i = 2, 3, 4, 6$) and c_i ($i = 4, 6$) are sections of $\pi^* \mathscr{L}^{\otimes i}$. The discriminant Δ is a section of $\pi^* \mathscr{L}^{\otimes 12}$. Geometrically, the discriminant locus is the subvariety of B cut out by the equation $\Delta = 0$, and is the locus of points p of the base B such that the fiber over p (i.e. Y_p) is singular. Over a generic point of Δ, the fiber is a nodal cubic that degenerates to a cuspidal cubic over the codimension-two locus $c_4 = c_6 = 0$. Up to isomorphisms, the j-invariant $j = c_4^3/\Delta$ uniquely characterizes nonsingular elliptic curves.

If we complete the square in y in the Weierstrass equation, the equation becomes

$$zy^2 = x^3 + \tfrac{1}{4} b_2 x^2 z + \tfrac{1}{2} b_4 x z^2 + \tfrac{1}{4} b_6 z^3. \tag{2.5}$$

In addition, if we complete the cube in x gives the short form of the Weierstrass equation, the equation becomes

$$zy^2 = x^3 - \tfrac{1}{48} c_4 x z^2 - \tfrac{1}{864} c_6 z^3. \tag{2.6}$$

2.2.2 Quartic models of genus one curve and elliptic fibrations

We can think of an elliptic fibration as an elliptic curve over the function field of the base. From that point of view, the Mordell–Weil group is really just the group of rational points. Given a divisor of

degree two on a genus one curve, the Riemann-Roch theorem ensures that the curve can be embedded in the weighted projective space $\mathbb{P}_{2,1,1}$ as a quartic curve

$$u^2 = q_0 y^4 + q_1 y^3 z + q_2 y^2 z^2 + q_3 y z^3 + q_4 z^4. \tag{2.7}$$

For general values of the coefficients, this is a smooth genus one fibration. Genus one fibration of this type has been discussed recently by Braun and Morrison [59]. If we call $\mathscr{L}^2$ the line bundle over the base such that u is a section of $\mathscr{O}(2) \otimes \pi_* \mathscr{L}^2$, then equation (2.7) is of type $\mathbb{P}_{2,1,1}[\mathscr{L}^2 \oplus \mathscr{M} \oplus \mathscr{O}_B]_{\mathscr{O}(4)\otimes\pi^*\mathscr{L}^4}$ for some line bundle $\mathscr{M}$. Then y is a section of $\mathscr{O}(1) \otimes \pi_* \mathscr{M}$, z is a section of $\mathscr{O}(1)$, and the coefficient q_i $(i = 0, 1, 2, 3, 4)$ is a section of $\mathscr{L}^4 \otimes \mathscr{M}^{-i}$.

2.2.3 Fibrations with Mordell–Weil group of rank one

If we have a genus one curve endowed with a divisor of degree two that splits into two rational points, we can assume in equation (2.7) that q_4 is a perfect square and the quartic equation can be put in the following canonical form:

$$u(u + b_2 z^2) + y(-c_0 y^3 + c_1 z y^2 + c_2 y z^2 + c_3 z^3) = 0, \tag{2.8}$$

which has double points singularities at $u = y = b_2 = c_3 = 0$. These singularities can be resolved by blowing up the non-Cartier divisor $u = y = 0$. This is a small and thus crepant resolution[7]. It

[7] Since we blow up a divisor, we cannot change the canonical class. Hence, a small resolution is always crepant.

follows that any elliptic fibration with a Mordell–Weil group of rank one has a model for which the general fiber is a quartic curve in $Bl_{[0:0:1]}\mathbb{P}^2_{2,1,1}$.

Remark 2.2.2. If b_2 is a unit, we get an elliptic fibration of type E_7. This is a model of type $\mathbb{P}_{2,1,1}[\mathscr{L}^2 \oplus \mathscr{L} \oplus \mathscr{O}_B]_{\mathscr{O}(4)\otimes\pi^*\mathscr{L}^4}$. Such an elliptic fibration has generically rank one. We can normalize the equation to have $q_4 = 1$. We can take the identity element of the Mordell–Weil group to be the rational point $y = u - z^2 = 0$ and the generator of the Mordell–Weil group to be $y = u + z^2 = 0$. These two sections do not intersect.

Computing the Jacobian of genus one quartic curves is a classical problem that can be solved by invariant theory as developed already in the 19th century by Cayley. In his famous memoir [302], Weil has even traced solution to this problem to Hermite and Euler. Nagell's algorithm, which is discussed for example in chapter 8 of Cassel's book [75], provides a direct computation of the birational map to the Jacobian for a cubic with a rational point in characteristic different from two and three. More advanced tools are necessary when the characteristic is two or three. This problem has been treated in all generality in [18].

2.2.4 Elliptic fibrations with Mordell–Weil group $\mathbb{Z}_2$

A generic Weierstrass model with a Mordell–Weil torsion subgroup $\mathbb{Z}_2$ is given by the following theorem, which is a direct consequence of a classic result in the study of elliptic curves in number theory [175, §5 of Chap 4], and was first discussed in a string theoretic setting by Aspinwall and Morrison [20].

Theorem 2.2.3. *An elliptic fibration over a smooth base B and with Mordell–Weil group $\mathbb{Z}_2$ is birational to the following (singular) Weierstrass model:*

$$zy^2 = x(x^2 + a_2xz + a_4z^2). \tag{2.9}$$

The section $x = y = 0$ is the generator of the $\mathbb{Z}_2$ Mordell–Weil group and $x = z = 0$ is the neutral element of the Mordell–Weil group. The discriminant of this Weierstrass model is

$$\Delta = 16a_4^2(a_2^2 - 4a_4). \tag{2.10}$$

2.2.5 Singular fibers over generic points

Kodaira has classified the possible types of singular fibers of a minimal elliptic surface. Néron arrived to the same classification in an arithmetic setting based on Weierstrass models. For higher dimensional elliptic fibrations, one can define a notion of minimality and Kodaira's classification continues to hold for geometric fibers over generic points of the discriminant locus.

We recall that a fiber over a point p is scheme defined with respect to the residue field of the point p. If the point p is a closed point, its residue field is just the ground field and the fiber is always geometric when the ground field is algebraically closed. But if the point p is the generic point of an irreducible variety, its residue field might not be algebraically closed. In that case, some components of the singular fiber that are irreducible with respect to the residue field of p might become reducible after a field extension. Such a component is said to not be geometrically irreducible.

The fibers over generic points are classified by decorated Kodaira fibers where the decoration ("split", "non-split", "semi-split") keeps track of the minimal field extension needed to make all component of the singular fiber (and the divisors defined by intersection of components) geometrically irreducible. It is enough to consider only quadratic and cubic field extension. The split case corresponds to the case in which the fiber has components that are geometrically irreducible. Kodaira fibers of type I_1, II, III, III*, and II* are always geometric. Kodaira fibers of type $\mathrm{I}_{n\geq 2}$, IV, IV*, $\mathrm{I}^*_{n\geq 0}$ are said to be split when they have geometrically irreducible component or non-split otherwise. For these fibers, a quadratic field extension is required to make them geometrically irreducible. For the fiber I^*_0, the non-split and split cases require respectively a cubic and quadratic field extension.

The fiber of type I_2 is very special in the sense that its non-split and split type have the same number of irreducible components, but distinguished themselves by the splitting properties of their intersection points. The fiber of type I_2 is composed of two rational curves intersecting transversally at two distinct geometric points. Let κ be the residue field of the point p over which the fiber I_2 is considered. When the two points of intersection form a κ-irreducible divisor on each component, the curve (with respect to the residue field of p), the fiber is said to be non-split, otherwise, the divisor is the sum of two points that are rational with respect to the residue field of p and the fiber is said to be split. At the collision of two I_2 fibers, the generic fiber can be $\mathrm{I}_4^{\mathrm{ns}}$ or $\mathrm{I}_4^{\mathrm{s}}$. The difference between $\mathrm{I}_4^{\mathrm{ns}}$ or $\mathrm{I}_4^{\mathrm{s}}$ over a codimension-two loci evaporates when the base is a surface since then these fibers are located over closed points with residue fields that are algebraically closed. That means that the fibers over codimension-two points of an elliptic threefolds are always geometric.

While geometric fibers have dual graphs that are always ADE affine Dynkin diagrams, the fiber

type over generic points are twisted affine Dynkin diagram. We denoted an affine Dynkin diagram by $\widetilde{g}$ and its Langlands dual by $\widetilde{\mathfrak{g}}^t$, this is the unique twisted Dynkin diagram whose Cartan matrix is the transpose of the Cartan matrix of $\tilde{\mathfrak{g}}$.

If K_i are decorated Kodaira fibers and S_i are irreducible divisors of the base, a model of type $K_1 + K_2 + \cdots + K_n$ is an elliptic fibration for which there exists two irreducible components S_1 and S_2 in the discriminant locus such that the type of the fiber over the generic point of S_i is K_i and the fiber over the generic point of any other component of the discriminant locus is irreducible (Kodaira type II or I_1).

2.2.6 Tate's algorithm

Let R be a complete discrete valuation ring with valuation v, uniformizing parameter s, and perfect residue field $\kappa = R/(s)$. We are interested in the case where κ has characteristic zero. We recall that a discrete valuation ring has only three ideals, the zero ideal, the ring itself, and the principal ideal sR. We take the convention in which the ring itself is not a prime ideal. It follows that the scheme $\mathrm{Spec}(R)$ has only two points: the generic point (defined by the zero ideal) and the closed point (defined by the principal ideal sR).

Let E/R be an elliptic curve over R with Weierstrass equation

$$y^2 + a_1xy + a_3y = x^3 + a_2x^2 + a_4x + a_6, \quad a_i \in R.$$

The generic fiber is a regular elliptic curve. After a resolution of singularities, we have a regular

model $\mathscr{E}$ over R and the *special fiber* is the fiber over the closed point Spec $R/(s)$. Tate's algorithm determines the type of the geometric fiber over the closed point of Spec(R) by manipulating the valuations of the coefficients and the discriminant, and the arithmetic properties of some auxiliary polynomials. The type of the *geometric fiber* is denoted by its Kodaira's symbol (see Definition 2.1.6). The special fiber becomes geometric after a quadratic or a cubic field extension κ'/κ. Keeping track of the field extension used gives a classification of the special fiber as a κ-scheme—this is what we call the arithmetic fiber. The information on the required field extension needed to have geometrically irreducible components is already carefully encoded in Tate's original algorithm, as it is needed to compute the local index (denoted by c in Tate's notation). In the language of Néron's model, the local index c is the order of the component group; geometrically, the local index is the number of reduced components of the special fiber defined over κ. Following Tate, we use the convenient notation

$$a_{i,j} = a_i s^{-j}.$$

Tate's algorithm consists of the following eleven steps (see [290], [281, §IV.9], [256], [99], [107]). For Step 7, we use the more refined description of Papadopoulos [256, Part III, page 134] who also gives in [256, §1, page 122] an exhaustive list of errata of Tate's original paper [290]. Tate's algorithm is discussed in F-theory in [37, 186]. Subtleties in Step 6 and the distinction between two G_2-models depending on $[\kappa' : \kappa]$ are explained in [112]. We follow the presentation of [107]:

Step 1. $v(\Delta) = 0 \implies \mathrm{I}_0$.

Step 2. If $v(\Delta) \geq 1$, change coordinates so that $v(a_3) \geq 1$, $v(a_4) \geq 1$, and $v(a_6) \geq 1$.

If $v(b_2) = 0$, the type is $\mathrm{I}_{v(\Delta)}$. To have a fiber with geometric irreducible components, it is enough to work in the splitting field κ' of the following polynomial of $\kappa[T]$:

$$T^2 + a_1 T - a_2.$$

The discriminant of this quadric is b_2. If b_2 is a square in κ, then $\kappa' = \kappa$, otherwise $\kappa' \neq \kappa$:

(a) $\kappa' = \kappa \implies \mathrm{I}_n^{\mathrm{s}}$ (b) $\kappa' \neq \kappa \implies \mathrm{I}_n^{\mathrm{ns}}$

Step 3. $v(b_2) \geq 1$, $v(a_3) \geq 1$, $v(a_4) \geq 1$, and $v(a_6) = 1 \implies$ II.

Step 4. $v(b_2) \geq 1$, $v(a_3) \geq 1$, $v(a_4) = 1$, and $v(a_6) \geq 2 \implies$ III.

Step 5. $v(b_2) \geq 1$, $v(a_3) \geq 1$, $v(a_4) \geq 2$, $v(a_6) \geq 2$, and $v(b_6) = 2 \implies$ IV.

The fiber has geometric irreducible components over the splitting field κ' of the polynomial

$$T^2 + a_{3,1} T - a_{6,2}$$

Its discriminant is $b_{6,2}$. If $b_{6,2}$ is a square in κ, then $\kappa' = \kappa$ otherwise $\kappa' \neq \kappa$.

(a) $\kappa' = \kappa \implies \mathrm{IV}^{\mathrm{s}}$ (b) $\kappa' \neq \kappa \implies \mathrm{IV}^{\mathrm{ns}}$

Step 6. $v(b_2) \geq 1$, $v(a_3) \geq 1$, $v(a_4) \geq 2$, $v(a_6) \geq 3$, $v(b_6) \geq 3$, $v(b_8) \geq 3$. Then make a change of coordinates such that $v(a_1) \geq 1$, $v(a_2) \geq 1$, $v(a_3) \geq 2$, $v(a_4) \geq 2$, and $v(a_6) \geq 3$. Let

$$P(T) = T^3 + a_{2,1} T^2 + a_{4,2} T + a_{6,3}$$

If $P(T)$ is a separable polynomial in κ, that is if $P(T)$ has three distinct roots in a field extension of κ, then the type is I_0^*. The geometric fiber is defined over the splitting field κ' of $P(T)$ in κ. The type of the special fiber before to go to the splitting field depends on the degree of the field extension $\kappa' \to \kappa$:

- $[\kappa' : \kappa] = 6$ or $3 \implies \mathrm{I}_0^{*\mathrm{ns}}$ with dual graph $\widetilde{\mathrm{G}}_2^t$.
- $[\kappa' : \kappa] = 2 \implies \mathrm{I}_0^{*\mathrm{ss}}$ with dual graph $\widetilde{\mathrm{B}}_3^t$.
- $[\kappa' : \kappa] = 1 \implies \mathrm{I}_0^{*\mathrm{s}}$ with dual graph $\widetilde{\mathrm{D}}_4$.

where "ns", "ss", and "s" stand respectively for "non-split", "semi-split", and "split". In the notation of Liu, these fibers are respectively $\mathrm{I}_{0,3}^*$, $\mathrm{I}_{0,2}^*$, and I_0^*. The Galois group is the symmetric group S_3, the cyclic group $\mathbb{Z}/3\mathbb{Z}$, the cyclic group $\mathbb{Z}/2\mathbb{Z}$ or the identity when the degree is respectively 6, 3, 2, and 1.

Step 7. If $P(T)$ has a double root, then the type is I_n^* with $n \geq 1$. Make a change of coordinates such that the double root is at the origin. Then $v(a_1) \geq 1$, $\quad v(a_2) = 1, v(a_3) \geq 2$, $\quad v(a_4) \geq 3,$, $v(a_6) \geq 4$, and $v(\Delta) = n + 6$ $(n \geq 1)$. We now assume that, except for their valuations, the Weierstrass coefficients are generic. We then distinguish between even and odd values of n.

(a) If $n = 2\ell - 3$ $(\ell \geq 2)$, then $v(a_1) \geq 1, v(a_2) = 1, v(a_3) \geq \ell$, $\quad v(a_4) \geq \ell + 1$, $v(a_6) \geq 2\ell, v(b_6) = 2\ell, v(b_8) = 2\ell + 1$, and

$$T^2 + a_{3,\ell}T - a_{6,2\ell}$$

has two distinct roots in its splitting field κ'. If the two roots are rational ($[\kappa' : \kappa] = 1$) then we have $\mathrm{I}^{*s}_{2\ell-3}$ with dual graph $\widetilde{\mathrm{D}}_{2\ell+1}$, otherwise ($[\kappa' : \kappa] = 2$) we have the fiber type $\mathrm{I}^{*ns}_{2\ell-3}$ with dual graph $\widetilde{\mathrm{B}}^{t}_{2\ell}$.

(b) If $n = 2\ell - 2$ ($\ell \geq 2$) then, $v(a_1) \geq 1$, $\quad v(a_2) = 1, v(a_3) \geq \ell + 1$, $\quad v(a_4) \geq \ell + 1$, $v(a_6) \geq 2\ell + 1$, and $v(b_8) = 2\ell + 2$. The polynomial

$$a_{2,1}T^2 + a_{4,\ell+1}T - a_{6,2\ell+1}$$

has two distinct roots in its splitting field. If the two roots are rational then we have $\mathrm{I}^{*s}_{2\ell-2}$ with dual graph $\widetilde{\mathrm{D}}_{2\ell+2}$, otherwise $\mathrm{I}^{*ns}_{2\ell-2}$ with dual graph $\widetilde{\mathrm{B}}^{t}_{2\ell+1}$.

Step 8. If $P(T)$ has a triple root, change coordinates such that the triple root is zero. Then $v(a_1) \geq 1$, $v(a_2) \geq 2$, $v(a_3) \geq 2$, $v(a_4) \geq 3$, $v(a_6) \geq 4$.

Let

$$Q(T) = T^2 + a_{3,2}T - a_{6,4}$$

If Q has two distinct roots ($v(b_6) = 4$ or equivalently $v(\Delta) = 8$) the type is IV*.

The split type depends on the rationality of the roots. If $b_{6,4}$ is a perfect square modulo s, the fiber is IV$^{*\mathrm{s}}$ with dual graph $\widetilde{\mathrm{E}}_6$, otherwise the fiber is IV$^{*\mathrm{ns}}$ with dual graph $\widetilde{\mathrm{F}}^{t}_{4}$. The split form can be enforced with $v(a_6) \geq 5$ and $v(a_3) = 2$.

Step 9. If Q has a double root, we change coordinates so that the double root is at the origin. Then:

$$v(a_1) \geq 1, \quad v(a_2) \geq 2, \quad v(a_3) \geq 3, \quad v(a_4) = 3, \quad v(a_6) \geq 5 \implies \text{type III}^*.$$

Step 10. $v(a_1) \geq 1, \quad v(a_2) \geq 2, \quad v(a_3) \geq 3, \quad v(a_4) \geq 4, \quad v(a_6) = 5 \implies \text{type II}^*.$

Step 11. Else $v(a_i) \geq i$ and the equation is not minimal. Divide all the a_i by s^i and start again with the new equation.

2.3 Lie groups Lie algebra, representations from an elliptic fibrations

2.3.1 Convention

Our conventions for affine Dynkin diagrams are as follows. A projective Dynkin diagram is denoted M_k where M is A, B, C, D, E, F, or G, and k is the number of nodes. An affine Dynkin diagram that becomes a projective Dynkin diagram $\mathfrak{g}$ after removing a node of multiplicity one is denoted $\widetilde{\mathfrak{g}}$. We denote by $\widetilde{\mathfrak{g}}^t$ the (the possibly twisted) affine Dynkin diagram whose Cartan matrix is the transpose of the Cartan matrix of $\widetilde{\mathfrak{g}}$. The graph of $\widetilde{\mathfrak{g}}^t$ is obtained by exchanging the directions of all the arrows of $\widetilde{\mathfrak{g}}$. When the extra node is removed, the dual graph of $\widetilde{\mathfrak{g}}^t$ reduces to the dual graph of the Langlands dual of $\mathfrak{g}$. The affine Dynkin diagrams $\widetilde{\mathfrak{g}}^t$ and $\widetilde{\mathfrak{g}}$ are distinct only when $\mathfrak{g}$ is not simply laced (i.e., when $\mathfrak{g}$ is G_2, F_4, B_k, or C_k). The notation $\widetilde{\mathfrak{g}}^t$ follows Carter[8] [70, Appendix, p. 540-609] and is equivalent to the notation $\widetilde{\mathfrak{g}}^\vee$ used by MacDonald in §5 of [223]. The multiplicities define a zero vector of the extended Cartan matrix. In the notation of Kac [182], $\widetilde{B}^t_\ell$ ($\ell \geq 3$), $\widetilde{C}^t_\ell$ ($\ell \geq 2$), $\widetilde{G}^t_2$, and $\widetilde{F}^t_4$ are respectively denoted $A^{(2)}_{2\ell-1}$, $D^{(2)}_{\ell+1}$, $D^{(3)}_4$, and $E^{(2)}_6$; while $\widetilde{B}_\ell$ ($\ell \geq 3$), $\widetilde{C}_\ell$ ($\ell \geq 2$), $\widetilde{G}_2$, and

[8] There is a typo on page 570 of [70] in the first Dynkin diagram of $\widetilde{B}_\ell$ on the top of the page, where the arrow is in the wrong direction but correctly oriented in the rest of the page.

$\widetilde{F}_4$ are respectively denoted $B_\ell^{(1)}$, $C_\ell^{(1)}$, $G_2^{(1)}$, and $F_4^{(1)}$. When $\mathfrak{g}$ is non-simply laced, the affine Dynkin diagrams $\widetilde{\mathfrak{g}}^t$ and $\widetilde{\mathfrak{g}}$ differ from each by the directions of their arrows and also by the multiplicities of their nodes (see Figure 2.1).

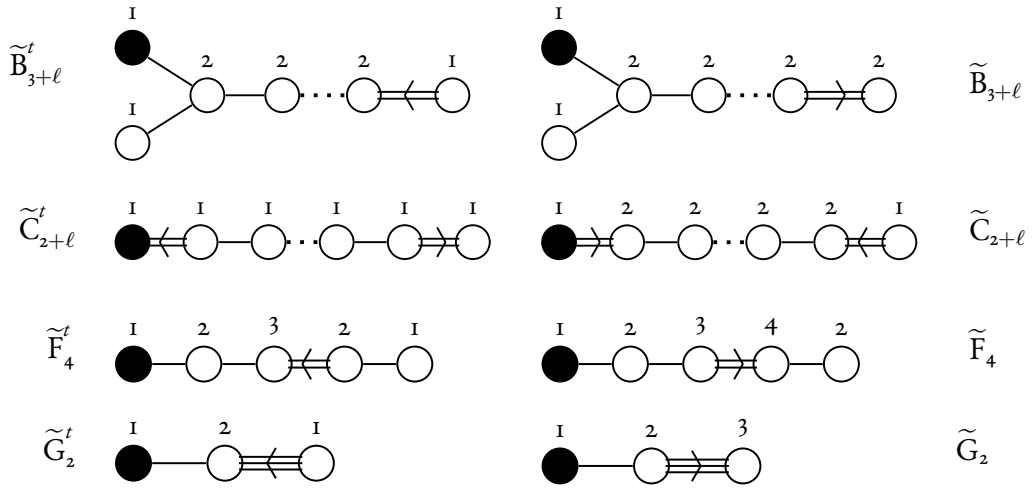

Figure 2.1: Twisted affine Lie algebras vs affine Lie algebras for non-simply laced cases. Only those on the left appears in the theory of elliptic fibrations as dual graphs of the fiber over the generic point of an irreducible component of the discriminant locus.

2.3.2 *G*-MODELS

G-models are used to geometrically engineer gauge theories in compactifications of M-theory and F-theory [37, 186, 243, 292]. They also play an important role in studying superconformal gauge theories (for a review see [169] and reference therein). *G*-models are typically defined by crepant resolutions of singular Weierstrass models given by Tate's algorithm and characterizing a specific (decorated) Kodaira fiber [13, 112, 114, 118–121, 124, 125, 127, 129, 215, 229].

Definition 2.3.1 ($\mathcal{K}$-model)**.** Let $\mathcal{K}$ be a fiber type. Let $S \subset B$ be a smooth divisor of a projective variety B. An elliptic fibration $\phi : Y \longrightarrow B$ over B is said to be a *$\mathcal{K}$-model* if the discriminant locus $\Delta(\phi)$ contains as an irreducible component a divisor $S \subset B$ such that the generic fiber over S is of type $\mathcal{K}$ and any other fiber away from S is irreducible.

The locus of points in the base that lie below singular fibers of a non-trivial elliptic fibration is a Cartier divisor Δ called the discriminant locus of the elliptic fibration. We denote the irreducible components of the reduced discriminant by Δ_i. If the elliptic fibration is minimal, the type of the fiber over the generic point of Δ_i of Δ has a dual graph that is an affine Dynkin diagram $\widetilde{\mathfrak{g}}_i^t$. If the generic fiber over Δ_i is irreducible, $\mathfrak{g}_i$ is the trivial Lie algebra since $\widetilde{\mathfrak{g}}_i^t = \widetilde{A}_0$. The Lie algebra $\mathfrak{g}$ associated with the elliptic fibration $\phi : Y \to B$ is then the direct sum $\mathfrak{g} = \bigoplus_i \mathfrak{g}_i$, where the Lie algebra $\mathfrak{g}_i$ is such that the affine Dynkin diagram $\widetilde{\mathfrak{g}}_i^t$ is the dual graph of the fiber over the generic point of Δ_i.

In F-theory, a Lie group $G(\phi)$ attached to a given elliptic fibration $\phi : Y \longrightarrow B$ depends on the type of generic singular fibers and the Mordell–Weil group $\mathrm{MW}(\phi)$ of the elliptic fibration [90].

When an elliptic $\phi : Y \to B$ has trivial Mordell–Weil group, the compact Lie group G associated with the elliptic fibration ϕ is semi-simple, simply connected, and is given by the formula $G := \exp(\bigoplus_i \mathfrak{g}_i)$, $\exp(\mathfrak{g})$ is the unique compact simply connected Lie group whose Lie algebra is $\mathfrak{g}$, the index i runs over all the irreducible components of the reduced discriminant locus. The Lie algebra $\mathfrak{g}_i$ is such that the affine Dynkin diagram $\widetilde{\mathfrak{g}}_i^t$ is the dual graph of the fiber over the generic point of the irreducible component Δ_i of the reduced discriminant of the elliptic fibration.

If the elliptic fibration has a Mordell–Weil group $T \times \mathbb{Z}^r$ with torsion subgroup T and rank r, then the group G is the quotient $\widetilde{G}/T \times U(1)^r$ where $\widetilde{G} = \exp(\bigoplus_i \mathfrak{g}_i)$. Defining the quotient $\widetilde{G}/T$ properly requires a choice of embedding of T in the center $Z(\widetilde{G})$ of the simply connected group $\widetilde{G}$. The center of G is then $Z(\widetilde{G})/T$. The representation $\mathbf{R}$ attached to the elliptic fibration constrains the possibilities and is sometimes enough to completely determine the embedding of T in $Z(\widetilde{G})$.

Hence, the Lie algebra $\mathfrak{g}$ associated to the elliptic fibration is then the Langlands dual $\mathfrak{g}^\vee = \bigoplus_i \mathfrak{g}_i^\vee$ of $\mathfrak{g} = \bigoplus_i \mathfrak{g}_i$. If we denote by $\exp(\mathfrak{g}^\vee)$ the unique (up to isomorphism) simply connected compact simple group whose Lie algebra is $\mathfrak{g}^\vee$, then the group associated to the elliptic fibration ϕ is:

$$G(\phi) := \frac{\exp(\mathfrak{g}^\vee)}{\mathrm{MW}_{\mathrm{tor}}(\phi)} \times U(1)^{\mathrm{rk\ MW}(\phi)},$$

where $\mathrm{rk\,MW}(\phi)$ is the rank of the Mordell–Weil group of ϕ and $\mathrm{MW}_{\mathrm{tor}}(\phi)$ is the torsion subgroup of the Mordell–Weil group of ϕ. Defining properly the quotient of $\exp(\mathfrak{g}^\vee)$ by the Mordell–Weil group requires a choice of embedding of the Mordell–Weil group in the center of $\exp(\mathfrak{g}^\vee)$ [229].

If the dual fibers of K_1 and K_2 are affine Dynkin diagrams of type $\widetilde{\mathfrak{g}}_1^t$ and $\widetilde{\mathfrak{g}}_2^t$, then the Lie algebra associated with the $K_1 + K_2$-model is

$$\mathfrak{g} = \mathfrak{g}_1 \oplus \mathfrak{g}_2.$$

Recall that a variety is said to be an elliptic n-fold if it is endowed with a proper surjective morphism $\phi : Y \to B$ to a variety of dimension $n - 1$ such that the generic fiber of ϕ is a smooth projective curve of genus one, and ϕ has a rational section. We can define G-models as the following:

Definition 2.3.2 (G-models)**.** Let G be a simple, simply-connected compact complex Lie group with Lie algebra $\mathfrak{g}$. A G-model is an elliptic fibration $\phi : Y \to B$ with a discriminant locus containing an irreducible component S such that

1. the generic fiber over any other component of the discriminant is irreducible (that is, of Kodaira type I_1 or II),

2. the fiber over the generic point of S has a dual graph that becomes of the same type as the Dynkin diagram of the Langlands dual of $\mathfrak{g}$ after removing the node corresponding to the component touching the section of the elliptic fibration.

If the reduced discriminant locus has a unique irreducible component S over which the generic fiber is not irreducible, the group $G(\phi)$ is simple. The relevant fiber $\widetilde{\mathfrak{g}}^t$ can be realized by resolving the singularities of a Weierstrass model derived from Tate's algorithm. The relation between the fiber type and the group $G(\phi)$ is not one-to-one. For example, an SU(2)-model can be given by a divisor S with a fiber of type $\mathrm{I}_2^{\mathrm{s}}$, $\mathrm{I}_2^{\mathrm{ns}}$, III, $\mathrm{IV}^{\mathrm{ns}}$, or $\mathrm{I}_3^{\mathrm{ns}}$. For that reason, a given decorated Kodaira fiber provides a more refined characterization of a G-model.

Example 2.3.3. For $n \geq 4$, an SU(n)-model is a $\mathrm{I}_n^{\mathrm{s}}$-model with a trivial Mordell–Weil group. For $n \geq 0$, a Spin($8+2n$)-model is an $\mathrm{I}_n^{*\mathrm{s}}$-model with trivial Mordell–Weil group. For $n \geq 1$, a Spin($7+2n$)-model is an $\mathrm{I}_n^{*\mathrm{ns}}$-model with trivial Mordell–Weil group. A G_2-model is an $\mathrm{I}_0^{*\mathrm{ns}}$-model with a trivial Mordell–Weil group. A Spin(7)-model is an $\mathrm{I}_0^{*\mathrm{ss}}$-model with a trivial Mordell–Weil group.

Example 2.3.4. The SO(3), SO(5), SO(6), and SO(7)-models are respectively $\mathrm{I}_2^{\mathrm{ns}}$, $\mathrm{I}_4^{\mathrm{ns}}$, $\mathrm{I}_4^{\mathrm{s}}$, and $\mathrm{I}_0^{*\mathrm{ss}}$-models with MW=$\mathbb{Z}/2\mathbb{Z}$. For $n \geq 0$, an SO$(8+2n)$-model is an $\mathrm{I}_n^{*\mathrm{s}}$-model with a Mordell–Weil group MW=$\mathbb{Z}/2\mathbb{Z}$. For $n \geq 1$, an SO$(7+2n)$-model is an $\mathrm{I}_n^{*\mathrm{ns}}$-model with Mordell–Weil group MW=$\mathbb{Z}/2\mathbb{Z}$.

Example 2.3.5. If the Mordell–Weil group is trivial, $\mathcal{K}$-models with $\mathcal{K} = \mathrm{I}_2^{\mathrm{s}}$, $\mathrm{I}_2^{\mathrm{ns}}$, III, $\mathrm{IV}^{\mathrm{ns}}$, or $\mathrm{I}_3^{\mathrm{ns}}$, are all SU(2)-models. An A_2-model can be given by a IV^{s}-model or a I_3-model. If the Mordell–Weil group is trivial, both a IV^{s}-model or a $\mathrm{I}_3^{\mathrm{s}}$-model give a SU(3)-model. A C_ℓ-model can be given by an $\mathrm{I}_{2\ell+2}^{\mathrm{ns}}$-model or an $\mathrm{I}_{2\ell+3}^{\mathrm{ns}}$-model, and if the Mordell–Weil group is trivial, these both give a USp(2ℓ)-model.

Remark 2.3.6. Not all singular Weierstrass models are G-models as the reducible singular fibers might not appear in codimension one. See, for example, the Jacobians of the elliptic fibrations discussed in [5, 6, 109, 120].

Definition 2.3.7 ($\mathcal{K}_1 + \cdots + \mathcal{K}_n$-model)**.** Let $\mathcal{K}_1, \mathcal{K}_2, \cdots, \mathcal{K}_n$ be Kodaira types and $S_1, \cdots, S_n$ be a smooth divisor of a projective variety B. An elliptic fibration $\phi : Y \longrightarrow B$ over B is said to be a $\mathcal{K}_1 + \cdots + \mathcal{K}_n$*-model* if the reduced discriminant locus $\Delta(\phi)$ contains components S_i as an irreducible component a divisor $S \subset B$ such that the generic fiber over S_i is of type $\mathcal{K}_i$ and any other generic fiber of a component of the discriminant locus different from the S_i is irreducible.

Fiber type	Dynkin diagram	Kodaira type
$\widetilde{A}_0$		$I_1, \quad II$
$\widetilde{A}_1$	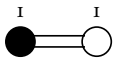	$I_2^s, \quad I_2^{ns}, \quad I_3^{ns}, \quad III, \quad IV^{ns}$
$\widetilde{A}_{\ell-1} \quad (\ell \geq 3)$	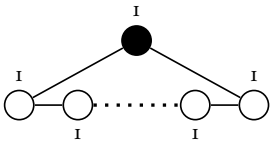	I_ℓ^s
$\widetilde{D}_{4+\ell} \quad (\ell \geq 0)$	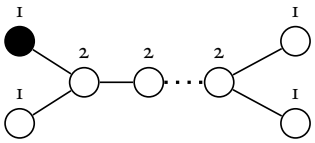	I_ℓ^{*s}
$\widetilde{E}_6$	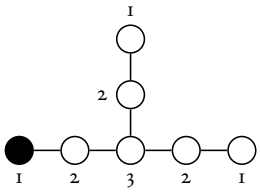	IV^{*s}
$\widetilde{E}_7$	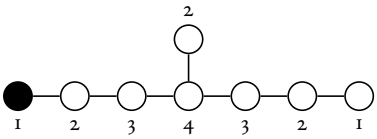	III^*
$\widetilde{E}_8$	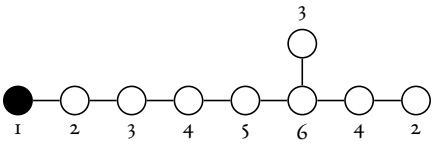	II^*
$\widetilde{B}^t_{3+\ell} \quad (\ell \geq 0)$	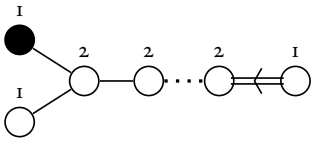	$\begin{cases} I_0^{*ss} & \text{for} \quad \ell = 0 \\ I_\ell^{*ns} & \text{for} \quad \ell \geq 1 \end{cases}$
$\widetilde{C}^t_{2+\ell} \quad (\ell \geq 0)$	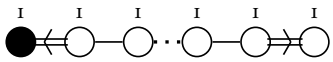	$I_{4+2\ell}^{ns}, \quad I_{5+2\ell}^{ns}$
$\widetilde{F}_4^t$	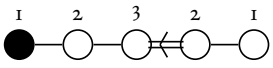	IV^{*ns}
$\widetilde{G}_2^t$	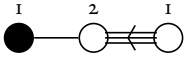	I_0^{*ns}

Table 2.3: Affine Dynkin diagrams appearing as dual graphs of decorated Kodaira fibers.

Fiber Type	Dual graph	Dual graph of Geometric fiber
$\widetilde{A}_1$	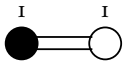	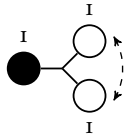
$I^{*ns}_{\ell-3}$ $\widetilde{B}^t_\ell$ $(\ell \geq 3)$	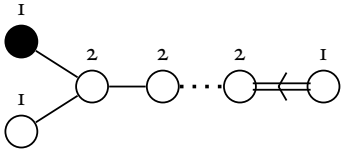	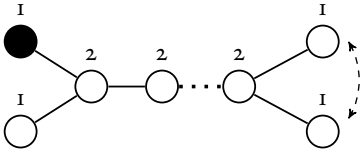
$I^{ns}_{2\ell+2}$ $\widetilde{C}^t_{\ell+1}$ $(\ell \geq 1)$	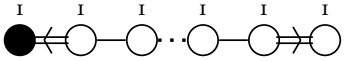	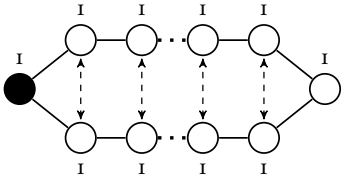
$I^{ns}_{2\ell+3}$ $\widetilde{C}^t_{\ell+1}$ $(\ell \geq 1)$		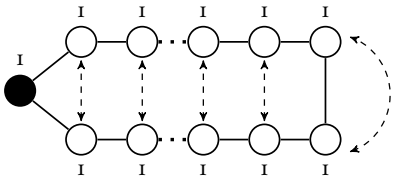
IV^{*ns} $\widetilde{F}^t_4$	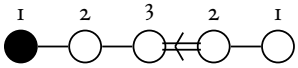	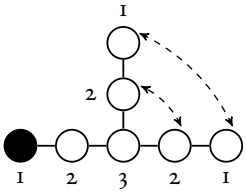
I^{*ss}_{o} $\widetilde{B}^t_3$	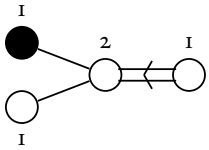	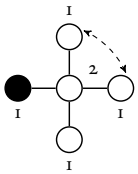
I^{*ns}_{o} $\widetilde{G}^t_2$	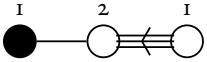	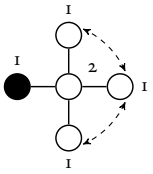

Table 2.4: Dual graphs for elliptic fibrations

.

Given a G-model, the generic fibers degenerate into fibers of different types over points of codimension two in the base, usually intersections of irreducible components Δ_i of the reduced discriminant or codimension-one singularities of the reduced discriminant.

Given an elliptic fibration $\phi : Y \to B$, if S is an irreducible component of the discriminant locus, the generic fiber over S can degenerate further over subvarieties of S. We distinguish between two types of degenerations. A degeneration is said to be *arithmetic* if it modifies the type of the fiber without changing the type of the geometric fiber. A degeneration is said to be *geometric* if it modifies the geometric type of the fiber. (This was covered in detail in Section 2.1.2.)

2.3.3 Geometric weights and representation from the elliptic fibration

Let $\phi : Y \to B$ be a smooth flat elliptic fibration whose discriminant has a unique component S over which the generic fiber is reducible with dual graph the affine Dynkin diagram $\tilde{\mathfrak{g}}^t$. We denote the irreducible components of the generic fiber over S as C_a. If $\mathfrak{g}$ is not simply laced, the curves C_a are not all geometrically irreducible. Let D_a be the fibral divisors over S. By definition, $\phi^*(S) = \sum_a m_a D_a$. The curve C_a can also be thought of as the generic fiber of D_a over S. Let C be a vertical curve of the elliptic fibration.

We define the weight of a vertical C with respect to a fibral divisor D_a as the intersection number

$$\varpi_a(C) := -\int_Y D_a \cdot C.$$

Using intersection of curves with fibral divisors to determine a representation from an elliptic fibra-

tion is a particularly robust algorithm since the intersections of divisors and curves are well-defined even in the presence of singularities [136]. We can ignore the intersection number of the divisor touching the section of the elliptic fibration as it is fixed in terms of the others, thus allowing us to write

$$\varpi(C) = \boxed{\varpi_1(C)\,,\ \varpi_2(C)\,,\ \cdots\,,\ \varpi_n(C)}.$$

We interpret $\varpi(C)$ as the weight of the vertical curve C in the basis of fundamental weights. This interpretation implies that the fibral divisors play the role of co-roots of $\mathfrak{g}$, while vertical curves are identified with elements of the weight lattice of $\mathfrak{g}$.

Definition 2.3.8 (Weight vector of a vertical curve)**.** Let C be a vertical curve, i.e. a curve contained in a fiber of the elliptic fibration. Let S be an irreducible component of the reduced discriminant of the elliptic fibration $\phi : Y \to B$. The pullback of $\phi^* S$ has irreducible components $D_0, D_1, \ldots, D_n$, where D_0 is the component touching the section of the elliptic fibration. The *weight vector* of C over S is by definition the vector $\varpi_S(C) = (-D_1 \cdot C, \ldots, -D_n \cdot C)$ of intersection numbers $D_i \cdot C$ for $i = 1, \ldots, n$.

The irreducible curves of the degenerations over codimension-two loci give weights of a representation $\mathbf{R}$. However, they only give a subset of weights. Hence, we need an algorithm that retrieves the full representation $\mathbf{R}$ given only a few of its weights. This problem can be addressed systematically using the notion of a saturated set of weights by Bourbaki [57, Chap.VIII.§7. Sect. 2].

Definition 2.3.9 (Saturated set of weights)**.** A set Π of integral weights is *saturated* if for any weight $\varpi \in \Pi$ and any simple root α, the weight $\varpi - i\alpha$ is also in Π for any i such that $0 \leq i \leq \langle \varpi, \alpha \rangle$. A saturated set has *highest weight* λ if $\lambda \in \Lambda^+$ and $\mu \prec \lambda$ for any $\mu \in \Pi$.

Definition 2.3.10 (Saturation of a subset)**.** Any subsets Π of weights is contained in a unique smallest saturated subset. We call it the saturation of Π.

Proposition 2.3.11.

(a) A saturated set of weights is invariant under the action of the Weyl group.

(b) The saturation of a set of weights Π *is finite if and only if the set* Π *is finite.*

(c) A saturated set with highest weight λ *consists of all dominant weights lower than or equal to* λ *and their conjugates under the Weyl group.*

Proof. See [174, Chap. III §13.4]. □

Theorem 2.3.12. *Let* Π *be a finite saturated set of weights. Then there exists a finite dimensional* $\mathfrak{g}$*-module whose set of weights is* Π.

Proof. [57, Chap.VIII.§7. Sect. 2, Corollary to Prop. 5]. □

It follows from the general theory of elliptic fibration that the intersection of the generic fibers with the fibral divisors gives the invariant form of the affine Lie algebra $\tilde{\mathfrak{g}}^t$, where $\mathfrak{g}$ is the Lie algebra of G. The matrix $\varpi_a(C_b)$ is the invariant form of the Lie algebra $\tilde{\mathfrak{g}}$ in the normalization where short roots have diagonal entries 2.

Definition 2.3.13 (Representation of a G-model)**.** To a G-model, we associate a representation $\mathbf{R}$ of the Lie algebra $\mathfrak{g}$ as follows. The weight vectors of the irreducible vertical rational curves of the fibers over codimension-two points form a set Π whose saturation defines uniquely a representation $\mathbf{R}$ by Theorem 2.3.12. We call this representation $\mathbf{R}$ the representation of the G-model.

Definition 2.3.13 is essentially a formalization of the method of Aspinwall and Gross [19, §4]. Note that we always get the adjoint representation as a summand of $\mathbf{R}$. There are subtleties when the divisor S is singular [10, 199].

The unique compact, connected, and simply connected Lie group with Lie algebra $\mathfrak{g}$ is

$$\widetilde{G} = \exp(\mathfrak{g}).$$

Assuming that the Mordell–Weil group has rank r and torsion subgroup H, the gauge group attached to the elliptic fibration requires the specification of an embedding of H in the center of $\widetilde{G}$

$$H \cong \widetilde{H} \subset Z(\widetilde{G}).$$

Then

$$G = U(1)^r \times \widetilde{G}/\widetilde{H}, \quad H \cong \widetilde{H}, \quad \widetilde{H} \trianglelefteq Z(\widetilde{G}).$$

Two different isomorphic subgroups of $Z(\widetilde{G})$ can give two different quotients $\widetilde{G}/\widetilde{H}$. The choice of the correct embedded is restricted by the representation $\mathbf{R}$ attached to the elliptic fibration since not all representation of Lie algebra of a group G is a representation of G.

2.4 The geometry of crepant resolutions and Couomb branches

2.4.1 Hyperplane arrangement $\mathrm{I}(\mathfrak{g}, \mathbf{R})$

Let $\mathfrak{g}$ be a semi-simple Lie algebra and $\mathbf{R}$ a representation of $\mathfrak{g}$. The kernel of each weight $\mathscr{w}$ of $\mathbf{R}$ defines a hyperplane $\mathscr{w}^{\perp}$ through the origin of the Cartan sub-algebra of $\mathfrak{g}$.

Definition 2.4.1 (hyperplane arrangement $\mathrm{I}(\mathfrak{g}, \mathbf{R})$)**.** The hyperplane arrangement $\mathrm{I}(\mathfrak{g}, \mathbf{R})$ is defined inside the dual fundamental Weyl chamber of $\mathfrak{g}$, i.e. the dual cone of the fundamental Weyl chamber of $\mathfrak{g}$, and its hyperplanes are the set of kernels of the weights of $\mathbf{R}$.

For each G-model, we associate the hyperplane arrangement $\mathrm{I}(\mathfrak{g}, \mathbf{R})$ using the representation $\mathbf{R}$ induced by the weights of vertical rational curves produced by degenerations of the generic fiber over codimension-two points of the base. We then study the incidence structure of the hyperplane arrangement $\mathrm{I}(\mathfrak{g}, \mathbf{R})$ [110–112, 115, 163].

2.4.2 Crepant resolutions, flops, and Coulomb branches

Each crepant resolution of a singular Weierstrass model is a relative minimal model (in the sense of the Minimal Model Program) over the Weierstrass model [227]. When the base of the fibration is a curve, the Weierstrass model has a unique crepant resolution. When the base is of dimension two or higher, a crepant resolution does not always exist; furthermore, when it does, it is not necessarily unique. Different crepant resolutions of the same Weierstrass model are connected by a finite sequence of flops.

Following F-theory, we attach to a given elliptic fibration a Lie algebra $\mathfrak{g}$, a representation $\mathbf{R}$ of $\mathfrak{g}$, and a hyperplane arrangement $\mathrm{I}(\mathfrak{g}, \mathbf{R})$. The Lie algebra $\mathfrak{g}$ and the representation $\mathbf{R}$ are determined by the fibers over codimension-one and codimension-two points, respectively, of the base in the discriminant locus. The hyperplane arrangement $\mathrm{I}(\mathfrak{g}, \mathbf{R})$ is defined inside the dual fundamental Weyl chamber of $\mathfrak{g}$ (i.e. the dual cone of the fundamental Weyl chamber of $\mathfrak{g}$), and its hyperplanes are the set of kernels of the weights of $\mathbf{R}$.

The network of flops is studied using the hyperplane arrangement $\mathrm{I}(\mathfrak{g}, \mathbf{R})$ inspired from the theory of Coulomb branches of five-dimensional supersymmetric gauge theories with eight supercharges [176]. The network of crepant resolutions is isomorphic to the network of Weyl chambers of the hyperplane arrangement $\mathrm{I}(\mathfrak{g}, \mathbf{R})$ defined by splitting the dual fundamental Weyl chamber of the Lie algebra $\mathfrak{g}$ by the hyperplanes dual to the weights of $\mathbf{R}$. The hyperplane arrangement $\mathrm{I}(\mathfrak{g}, \mathbf{R})$ and its relation to the Coulomb branches of supersymmetric gauge theories and the network of crepant resolutions are studied in [97, 110, 111, 118, 119, 121, 125, 127, 163, 176].

The algorithm that we use to determine the representation $\mathbf{R}$ works for any base of dimension two or higher and does not require to impose the Calabi–Yau condition. The algorithm consists of three steps. We start by identifying those vertical curves that are relative extremal curves appearing over divisors of S, over which the irreducible components of the generic fiber of S degenerate. We then associate to each of these curves a weight computed geometrically as minus of the intersections of the curve with the fibral divisors. Lastly, the representation $\mathbf{R}$ is then determined from these weights using the notion of saturated set of weights introduced by Bourbaki [57].

2.5 Non-simply-connected simple groups in F-theory

The classification of connected Lie groups over the complex or real numbers is based on the following theorem whose content can be traced back to Cartan and Lie. In what follows, all groups and Lie algebras are defined over the complex numbers or the real numbers. We refer to [55, Chap III, §6] for more information.

Theorem 2.5.1.

1. *Any connected Lie group G defined over the complex numbers or the real numbers is isomorphic to a quotient $\tilde{G}/K$ of its universal covering group $\tilde{G}$ by a discrete central subgroup K of $\tilde{G}$ isomorphic to the fundamental group of G.*

2. *Two connected Lie groups having the same Lie algebra are locally isomorphic. Two simply connected Lie groups having the same Lie algebra are isomorphic.*

3. *(Cartan–Lie theorem) If $\mathfrak{g}$ is a finite dimensional Lie algebra, there exists a simply connected Lie group whose associated Lie algebra is isomorphic to $\mathfrak{g}$.*

Proof. See [55, Chap III, §6.3, Theorem 3]. □

The center of G is isomorphic to the quotient $Z(\tilde{G})/K$. In particular, this implies that the fundamental group of any connected group is Abelian. The third assertion is the Cartan–Lie theorem (usually called Lie's third fundamental theorem).[9] The second assertion (without the simply con-

[9] Lie proved the local existence of a Lie group. Cartan proved the global existence and the simply connected property.

nected specialization) is Lie's second fundamental theorem. The following definition is inspired by the Cartan–Lie theorem (second assertion of Theorem 2.5.1).

Definition 2.5.2 (simply connected Lie group associated with a Lie algebra)**.** Given a finite dimensional Lie algebra $\mathfrak{g}$, the simply connected Lie group whose Lie algebra is isomorphic to $\mathfrak{g}$ is called the *simply connected Lie group associated with* $\mathfrak{g}$ and is denoted by $\exp(\mathfrak{g})$.

A direct consequence of Theorem 2.5.1 is that the classification of connected simple Lie groups reduces to the classification of simply connected simple Lie groups and of the subgroups of their centers. The centers of simply connected simple complex Lie groups are given in Table 2.5.

If $\mathfrak{g}$ is G_2, F_4, or E_8, there is a unique connected, simple, complex compact Lie group with Lie algebra $\mathfrak{g}$. If $\mathfrak{g}$ is A_{p-1} (with p a prime number), B_{3+n}, C_{2+n}, D_{5+2n}, E_6, E_7, there are two compact connected Lie groups with Lie algebra $\mathfrak{g}$, namely the simply connected group $G = \exp(\mathfrak{g})$ and the centerless group $G_{ad} := G/Z(G)$. For symplectic groups, we denote by $\mathrm{Sp}(2n)$ for the compact and connected simple complex Lie group with Lie algebra C_n, that is $\mathrm{Sp}(2n) \cong \mathrm{USp}(2n)$.

The case of A_{n-1} involves the classification of subgroups of $\mathbb{Z}/n\mathbb{Z}$. The subgroups of $\mathbb{Z}/n\mathbb{Z}$ are the cyclic groups $\mathbb{Z}/r\mathbb{Z}$ such that r is a divisor of n. There are three compact connected Lie groups with Lie algebra D_{5+2n} and four with Lie algebra D_{4+2n}. [10] Namely, the simply connected group $\mathrm{Spin}(8+2n)$, its $\mathbb{Z}/2\mathbb{Z}$ quotient $\mathrm{SO}(8+2n)$, and its centerless quotient $\mathrm{PSO}(8+2n)$.

[10] The Lie algebra D_{5+2n} has three distinct compact groups: $\mathrm{Spin}(10+4n)$, its $\mathbb{Z}/2\mathbb{Z}$ quotient $\mathrm{SO}(10+4n)$, and the centerless group $\mathrm{PSO}(10+4n)$. The center of $\mathrm{Spin}(8+4n)$ is $(\mathbb{Z}/2\mathbb{Z})^2 = \{\pm 1, \pm\Gamma_*\}$ with $\Gamma_*^2 = 1$. We have 4 distinct subgroups: the trivial group, the full group $(\mathbb{Z}/2\mathbb{Z})^2$, and three proper subgroups –each generated by a non-neutral element of $(\mathbb{Z}/2\mathbb{Z})^2$–each isomorphic to $\mathbb{Z}/2\mathbb{Z}$. As a result there are give compact groups with Lie algebra D_{4+2n}: the simply connected group $\mathrm{Spin}(8+4n)$, the orthogonal group $\mathrm{SO}(8+4n)$, the center less group $\mathrm{PSO}(8+4n)$, and two groups $\mathrm{HSpin}(8+4n)$ that are isomorphic to each other. One is a quotient of $\mathrm{Spin}(8+4n)$ by $\{1, \Gamma_*\}$ and the other is a quotient by $\{1, -\Gamma_*\}$.

$\mathfrak{g}$	$G = \exp(\mathfrak{g})$	Center $Z(G)$	$G_{Ad} := G/Z(G)$	Quotient with non-trivial center
A_{n-1}	$SU(n)$	$\mathbb{Z}/n\mathbb{Z}$	$PSU(n)$	$SU(n)/(\mathbb{Z}/r\mathbb{Z})$ with $r\|n$ and $r \neq 1, n$
B_{3+n}	$Spin(7+2n)$	$\mathbb{Z}/2\mathbb{Z}$	$SO(7+2n)$	-
C_{2+n}	$Sp(4+2n)$	$\mathbb{Z}/2\mathbb{Z}$	$PSp(4+2n)$	-
D_{4+2n}	$Spin(8+4n)$	$(\mathbb{Z}/2\mathbb{Z})^2$	$PSO(8+4n)$	$SO(8+4n)$, $HSpin^{\pm}(8+4n)$
D_{5+2n}	$Spin(10+4n)$	$\mathbb{Z}/4\mathbb{Z}$	$PSO(10+4n)$	$SO(10+4n)$
E_6	E_6	$\mathbb{Z}/3\mathbb{Z}$	$E_6/(\mathbb{Z}/3\mathbb{Z})$	-
E_7	E_7	$\mathbb{Z}/2\mathbb{Z}$	$E_7/(\mathbb{Z}/2\mathbb{Z})$	-
E_8	E_8	trivial	E_8	-
F_4	F_4	trivial	F_4	-
G_2	G_2	trivial	G_2	-

Table 2.5: Classification of connected compact simple complex Lie groups. The group $G = \exp(\mathfrak{g})$ is the unique simply connected compact group with Lie algebra $\mathfrak{g}$. We denote its center by Z. The group $G_{Ad} = G/Z$ is the unique centerless connected simple group with Lie algebra $\mathfrak{g}$. The group G and G_{Ad} are isomorphic when $Z(G)$ is the trivial group, that is for $\mathfrak{g} = G_2, F_4$, or E_8. G and G_{Ad} are the only connected compact simple groups with Lie algebra $\mathfrak{g}$ except in the case of $\mathfrak{g} = A_{n-1}$ with n a non-prime number and $\mathfrak{g} = D_{4+2n}$ where the orthogonal group $SO(8+4n)$ and the half spin group $HSpin(8+4n)$ are non-simply connected with center $\mathbb{Z}/2\mathbb{Z}$. The orthogonal group $SO(2m)$ is the quotient of $Spin(2n)$ by ± 1. The groups $HSpin^{\pm}(8+4m)$ are the $\mathbb{Z}/2\mathbb{Z}$ quotient of $Spin(8+4m)$ for which one of the half-spin representations is faithful. The group $HSpin^{\pm}(8+4m)$ are isomorphic to each other. The half-spin groups $HSpin^{\pm}(8+4m)$ are isomorphic to $SO(8+4m)$ if and only if $m = 0$.

2.6 Collisions of singularities and semi-smple groups in F-theory

The theory of elliptic surfaces is well understood since the seminal work of Kodaira and Néron [200, 251]. For an elliptic surface, the discriminant locus (i.e. the locus of singular fibers) is composed of isolated points and the singular fibers are classified by Kodaira symbols (see section 2.2.5).

When the elliptic fibration is of dimension three or higher, the discriminant locus can have intersecting components. Kodaira fibers now classify the type of the geometric fiber over the generic point of a normal irreducible component of the discriminant locus. Singularities of the discriminant locus are called *collisions of singularities* [236]. A typical example of collision of singularities are intersection points of irreducible components of the discriminant locus. Let S_1 and S_2 be two smooth

irreducible components of the discriminant locus with generic fibers of Kodaira type T_1 and T_2. The generic fiber at the intersection of S_1 and S_2 is denoted by $T_1 + T_2$. The type of the generic fiber at the collision does not have to be one of Kodaira's types [129, 236]. But it is usually a contraction of a Kodaira type or obtained by letting some of the nodes of a Kodaira fiber to coincide. We will assume throughout thes thesis that we work over the complex numbers.

In the early 1980s, Miranda introduced a systematic regularization procedure for elliptic threefolds defined by Weierstrass models [236]. He considers collisions of type $T_1 + T_2$ in which T_1 and T_2 are Kodaira fibers having the same j-invariant and such that the supporting divisors are smooth divisors intersecting transversally. Miranda's regularization produces elliptic fibrations that are flat fibrations and their j-invariant is a morphism. Miranda's work on threefolds was generalized to elliptic n-folds in Szydlo's Ph.D. thesis [286]. Elliptic fibrations resulting from Miranda's regularization are called *Miranda models* [100]. Miranda models were used by Dolgachev and Gross to study the Tate-Shafarevich group of elliptic threefolds [100]. Using tools from the Minimal Model Program, Hodge theory, and toric geometry, Nakayama studied in [248] the local fibration structure of elliptic threefolds defining a collision $\mathrm{I}_n + \mathrm{I}_m$ with normal transverse divisors in a nonsingular surface.

Miranda regularization is not usually a crepant resolution. But when it is, it provides interesting examples of elliptic Calabi–Yau threefolds yielding non-Abelian semi-simple gauge theories. Applications of Miranda model to F-theory was first studied by Bershadsky and Johansen [38] and have applications in the classification of six-dimensional Conformal Field Theories (CFTs).

In F-theory and M-theory, collisions of singularities are crucial for geometric engineering of gauge theories with semi-simple Lie groups, and matters charged under some representation of the Lie

group [243, 243, 292]. In recent years, we have improved our understanding of crepant resolutions of elliptic fibrations corresponding to simple Lie groups [112, 115, 124, 125, 127, 129]. We have extended these methods to the study of elliptic fibrations corresponding to semi-simple groups [113, 118–121], including the case in which the gauge group is not simply connected. Following a point of view that started in [5, 6, 109, 120], we work relatively to an arbitrary base and do not impose the Calabi–Yau condition.

This allows us to understand the geometry of these elliptic fibrations in a larger setting before to specialize to the particular cases relevant to string theory. In the case of Calabi–Yau threefolds, such analyses are closely related to basic questions on five dimensional and six dimensional supergravity theories since they are obtained by compactifications of M-theory and F-theory. In the case of the five-dimensional theory, we determine the matter content, the structure of the Coulomb branch, and the Chern-Simons levels. In its six-dimensional theory uplift, we determine the tensor branch, the matter content, and the fine detail of cancellations of gravitational, gauge, and mixed anomalies.

2.7 Intersection theory and pushforward formulae

2.7.1 A brief history of pushforward in string theory

Intersection theory in algebraic geometry as we know it today is presented in the seminal book of Fulton [136]. Chern classes are defined from Segre classes, which satisfy stronger functorial properties. The first formula computing the Chern classes of the tangent bundle of the blow-up of a nonsingular variety along a nonsingular center was conjectured by Todd and Segre, and proven by

Porteous [261]. A generalization of Porteous to singular varieties was obtained by Aluffi [4], who also provided user friendly descriptions of Porteous formula in the case of blow-ups whose centers are smooth complete intersections. Aluffi formula are center to this various parts of this thesis, and are reviewed in section 5.4.

The pushforward allows to compute intersection numbers of a fibration in terms of the Chow ring of its base. The first use of implicit pushforward methods in string theory is the computation of the Euler characteristic of a Weierstrass model by Sethi, Vafa and Witten for Calabi–Yau threefolds and fourfolds in terms of the Chow ring of its base [279]. Using efficient pushforward techniques, generating functions for the Euler characteristic of a smooth Weierstrass model was derived by Aluffi and Esole [5]. Intersection theory is instrumental in defining the induced D3-charges in presence of an orientifold [78], which is to constrain to satisfy a "tadpole condition". See [6, 109, 120] for additional examples of topological relations in the Chow ring motivated by string dualities and tapdole cancellations.

The first application of Porteous formula in string theory is [12]. Aluffi's formula was used to compute the Euler characteristic of an SU(5) model [129] in [226] and in the study of anomaly cancellations in six dimensional gauge theories in [118, 120, 121, 124]. Powerful methods to compute pushforwards in projective bundles using the functorial properties of the Segre class were obtained in [135], extended a point of view used in [5, 6]. Recently in [114], we introduced new theorems that streamline the computation of pushforwards of blowups as simple algebraic manipulations involving rational polynomials. These techniques allow a simple computations of pushforward of any analytic expression of the exceptional divisors of the blowup of a complete intersections of

smooth divisors. All these techniques are illustrated in [114] by computing the Euler characteristics of crepant resolutions of Weierstrass models.

Theorem 2.7.1 (Aluffi-Esole, [5]). *For a smooth Weierstrass model, we have*

$$\phi_* c(Y) = 12 \frac{L}{1+6L} c(B). \tag{2.11}$$

Theorem 2.7.2 (Esole–Jefferson–Kang,[114]). *The* SU(2)*-model over a base of arbitrary dimension, gives*

$$\phi_* c(Y) = \frac{2L + 3LS - S^2}{(1+S)(1+6L-2S)} c(B), \tag{2.12}$$

where S is the divisor supporting the fiber of type I_2 *or* III.

Theorem 2.7.3 (Esole–Fullwood–Yau, [109, Theorem 1.4]). *Let $\phi : Y \to B$ be an elliptic fibration defined by the complete intersection of two divisors of class $\mathscr{O}(2) \otimes \pi^* \mathscr{L}^{\otimes 2}$ in the projective bundle $\pi : \mathbb{P}\Big(\mathscr{O}_B \oplus \mathscr{L} \oplus \mathscr{L} \oplus \mathscr{L}\Big) \to B$. Then*

$$\phi_* c(Y) = \frac{4L(3+5L)}{(1+2L)^2} c(B), \tag{2.13}$$

where $L = c_1(\mathscr{L})$.

Theorem 2.7.4 (Esole–Kang–Yau, [120]). *Consider a projective variety B endowed with two line bundles $\mathscr{L}$ and $\mathscr{D}$. Let $\phi : Y \to B$ be a smooth elliptic fibration defined as the zero scheme of a section*

of the line bundle $\mathscr{O}(3) \otimes \pi^* \mathscr{L}^{\otimes 2} \otimes \pi^* \mathscr{D}$ *in the projective bundle* $\pi : \mathbb{P}\Big(\mathscr{O}_B \oplus \mathscr{L} \oplus \mathscr{D}\Big) \to B$. *Then*

$$\phi_* c(Y) = 6 \frac{(2L + 2L^2 - LD + D^2)}{(1 + 2L - 2D)(1 + 2L + D)} c(B), \tag{2.14}$$

where $D = c_1(\mathscr{D})$ *and* $L = c_1(\mathscr{L})$.

2.7.2 Definitions and notations

The first Chern class of $\mathscr{O}_{X_0}(1)$ is denoted H and the first Chern class of $\mathscr{L}$ is denoted L. The Chow group $A_*(X)$ of a nonsingular variety X is the group of divisors modulo rational equivalence [136, Chap. 1,§1.3]. We use $[V]$ to refer to the class of a subvariety V in $A_*(X)$. Given a class $\alpha \in A_*(X)$, the degree of α is denoted $\int_X \alpha$ (or simply $\int \alpha$ if X is clear from the context.) Only the zero component of α is relevant in computing $\int_X \alpha$—see [136, Definition 1.4, p. 13]. We use $c(X) = c(TX) \cap [X]$ to refer to the total homological Chern class of a nonsingular variety X, and likewise we use $c_i(TX)$ to denote the ith Chern class of the tangent bundle TX. Given two varieties X, Y and a proper morphism $f : X \to Y$, the proper pushforward associated to f is denoted f_*. If $g : X \to Y$ is a flat morphism, the pullback of g is denoted g^* and by definition $g^*[V] = [g^{-1}(V)]$, see [136, Chap 1, §1.7].

Definition 2.7.5 (Pushforward, [136, Chap. 1, p. 11])**.** Let $f : X \longrightarrow Y$ be a proper morphism. Let V be a subvariety of X, the image $W = f(V)$ a subvariety of Y, and the function field $R(V)$ an

extension of the function field $R(W)$. The pushforward $f_* : A_*(X) \to A_*(Y)$ is defined as follows

$$f_*[V] = \begin{cases} 0 & \text{if} \quad \dim V \neq \dim W, \\ [R(V) : R(W)]\,[V_2] & \text{if} \quad \dim V = \dim W, \end{cases}$$

where $[R(V) : R(W)]$ is the degree of the field extension $R(V)/R(W)$.

Definition 2.7.6 (Degree, [136, Chap. 1, p. 13])**.** The degree of a class α of $A_*(X)$ is denoted by $\int_X \alpha$ (or simply $\int \alpha$ if there is no ambiguity in the choice of X), and is defined to be the degree of its component in $A_0(X)$.

The total homological Chern class $c(X)$ of any nonsingular variety X of dimension d is defined as

$$c(X) = c(TX) \cap [X],$$

where TX is the tangent bundle of X and $[X]$ is the class of X in the Chow ring. The degree of $c(X)$ is the topological Euler characteristic of X:

$$\chi(X) = \int_X c(X).$$

The following Lemma gives an important functorial property of the degree.

Lemma 2.7.7 ([136, Chap. 1, p. 13])**.** *Let $f : X \longrightarrow Y$ be a proper map between varieties. For any class*

α in the Chow ring $A_*(X)$ of X:

$$\int_X \alpha = \int_Y f_*\alpha.$$

Lemma 2.7.7 means that an intersection number in X can be computed in Y through a pushforward of a proper map $f : X \longrightarrow Y$. This simple fact has far-reaching consequences as it allows us to express the topological invariants of an elliptic fibration in terms of those of the base.

Let X be a projective variety with at worst canonical Gorenstein singularities. We denote the canonical class by K_X.

Definition 2.7.8 (Crepant birational map)**.** A birational map $\phi : \widetilde{Y} \to Y$ between two algebraic varieties with $\mathbb{Q}$-Cartier canonical classes is said to be *crepant* if it preserves the canonical class, i.e. $K_{\widetilde{Y}} = \phi^* K_Y$.

Definition 2.7.9 (Resolution of singularities)**.** A resolution of singularities of a variety Y is a proper birational morphism $\phi : \widetilde{Y} \longrightarrow Y$ such that $\widetilde{Y}$ is nonsingular and ϕ is an isomorphism away from the singular locus of Y. In other words, $\widetilde{Y}$ is nonsingular and if U is the singular locus of Y, ϕ maps $\phi^{-1}(Y \setminus U)$ isomorphically onto $Y \setminus U$.

Definition 2.7.10 (Crepant resolution of singularities)**.** A *crepant resolution of singularities* is a resolution of singularities such that $K_Y = f^* K_X$.

2.7.3 Pushforward formulae

When pushing forward blowups of a projective bundle $\pi : X_0 = \mathbb{P}[\mathscr{O}_B \oplus \mathscr{L}^{\otimes 2} \oplus \mathscr{L}^{\otimes 3}] \longrightarrow B$, the key ingredients are the following three theorems. The first one is a theorem of Aluffi which gives

the Chern class after a blowup along a local complete intersection. Given a complete intersection Z of hypersurfaces $Z_i = V(z_i)$ in a variety X, we denote the blowup $\widetilde{X} = \mathrm{Bl}_Z X$ of X along Z with exceptional divisor $E = V(e)$ as

$$X \xleftarrow{(z_1, \ldots, z_n | e)} \widetilde{X}.$$

The second theorem is a pushforward theorem that provides a user-friendly method to compute invariant of the blowup space in terms of the original space. The last theorem is a direct consequence of functorial properties of the Segre class and gives a simple method to pushforward analytic expressions in the Chow ring of the projective bundle X_0 to the Chow ring of its base.

Theorem 2.7.11 (Aluffi, [4, Lemma 1.3]). *Let $Z \subset X$ be the complete intersection of d nonsingular hypersurfaces $Z_1, \cdots, Z_d$ meeting transversally in X. Let $f : \widetilde{X} \longrightarrow X$ be the blowup of X centered at Z. We denote the exceptional divisor of f by E. The total Chern class of $\widetilde{X}$ is then:*

$$c(T\widetilde{X}) = (1 + E) \left(\prod_{i=1}^{d} \frac{1 + f^* Z_i - E}{1 + f^* Z_i} \right) f^* c(TX). \tag{2.15}$$

Lemma 2.7.12 (See [4, 114]). *Let $f : \widetilde{X} \longrightarrow X$ be the blowup of X centered at Z. We denote the exceptional divisor of f by E. Then*

$$f_* E^n = (-1)^{d+1} h_{n-d}(Z_1, \ldots, Z_d) Z_1 \cdots Z_d,$$

where $h_i(x_1, \ldots, x_k)$ is the complete homogeneous symmetric polynomial of degree i in $(x_1, \ldots, x_k)$ with the convention that h_i is identically zero for $i < 0$ and $h_0 = 1$.

Theorem 2.7.13 (Esole–Jefferson–Kang, see [114]). *Let the nonsingular variety $Z \subset X$ be a complete intersection of d nonsingular hypersurfaces $Z_1, \cdots, Z_d$ meeting transversally in X. Let E be the class of the exceptional divisor of the blowup $f : \widetilde{X} \longrightarrow X$ centered at Z. Let $\widetilde{Q}(t) = \sum_a f^* Q_a t^a$ be a formal power series with $Q_a \in A_*(X)$. We define the associated formal power series $Q(t) = \sum_a Q_a t^a$, whose coefficients pullback to the coefficients of $\widetilde{Q}(t)$. Then the pushforward $f_* \widetilde{Q}(E)$ is*

$$f_* \widetilde{Q}(E) = \sum_{\ell=1}^{d} Q(Z_\ell) M_\ell, \quad \text{where} \quad M_\ell = \prod_{\substack{m=1 \\ m \neq \ell}}^{d} \frac{Z_m}{Z_m - Z_\ell}.$$

Theorem 2.7.14 (See [114]). *Let $\mathscr{L}$ be a line bundle over a variety B and $\pi : X_0 = \mathbb{P}[\mathscr{O}_B \oplus \mathscr{L}^{\otimes 2} \oplus \mathscr{L}^{\otimes 3}] \longrightarrow B$ a projective bundle over B. Let $\widetilde{Q}(t) = \sum_a \pi^* Q_a t^a$ be a formal power series in t such that $Q_a \in A_*(B)$. Define the auxiliary power series $Q(t) = \sum_a Q_a t^a$. Then*

$$\pi_* \widetilde{Q}(H) = -2 \left. \frac{Q(H)}{H^2} \right|_{H=-2L} + 3 \left. \frac{Q(H)}{H^2} \right|_{H=-3L} + \frac{Q(0)}{6L^2},$$

where $L = c_1(\mathscr{L})$ and $H = c_1(\mathscr{O}_{X_0}(1))$ is the first Chern class of the dual of the tautological line bundle of $\pi : X_0 = \mathbb{P}(\mathscr{O}_B \oplus \mathscr{L}^{\otimes 2} \oplus \mathscr{L}^{\otimes 3}) \to B$.

By adjunction, the Chern class of a Weierstrass model is

$$c(TY) = \frac{(1+H)(1+H+2L)(1+H+3L)}{1+3H+6L} c(TB). \tag{2.16}$$

Since all the blowups used in this thesis have centers that are complete intersections of two or

three smooth divisors, the following two Lemmas are all that is needed to compute pushforwards under such blowups when the base is a threefold. They are direct consequences of Lemma 2.7.12.

Lemma 2.7.15. *For a blowup $f : \widetilde{X} \longrightarrow X$ with center a transverse intersection of two divisors of class Z_1 and Z_2, we have*

$$f_*E = 0, \qquad f_*E^2 = -Z_1Z_2, \qquad f_*E^3 = -(Z_1 + Z_2)Z_1Z_2,$$
$$f_*E^4 = -(Z_1^2 + Z_2^2 + Z_1Z_2)Z_1Z_2, \quad f_*E^5 = -(Z_1 + Z_2)(Z_1^2 + Z_2^2)Z_1Z_2. \tag{2.17}$$

Lemma 2.7.16. *For a blowup $f : \widetilde{X} \longrightarrow X$ with center a transverse intersection of three divisors of class Z_1, Z_2, and Z_3, we have*

$$f_*E = 0, \qquad f_*E^2 = 0, \qquad f_*E^3 = Z_1Z_2Z_3,$$
$$f_*E^4 = (Z_1 + Z_2)Z_1Z_2Z_3, \quad f_*E^5 = (Z_1^2 + Z_2^2 + Z_3^2 + Z_1Z_2 + Z_1Z_3 + Z_2Z_3)Z_1Z_2Z_3. \tag{2.18}$$

Lemma 2.7.17 ([114, 134])**.** *Given the projective bundle $\pi : X_0 = \mathbb{P}(\mathscr{O}_B \oplus \mathscr{L}^{\otimes 2} \oplus \mathscr{L}^{\otimes 3}) \to B$, denoting the first Chern class of $\mathscr{L}$ by L, we have:*

$$\pi_*1 = 0, \quad \pi_*H = 0, \quad \pi_*H^2 = 1, \quad \pi_*H^3 = -5L, \quad \pi_*H^4 = 19L^2, \quad \pi_*H^5 = -65L^3,$$
$$\pi_*H^k = \left[(-2)^{k-1} - (-3)^{k-1}\right] L^{k-2} \quad n \geq 1.$$

Using Lemma 2.7.17, it is then direct to show that

$$\pi_*\Big(H^k(3H+6L)\Big) = -(-3)^k L^{k-1}, \quad k \geq 1 \tag{2.19}$$

2.7.4 Example: the second Chern class under a crepant birational map

We now look at the behavior of the second Chern class of a divisor V under a crepant blowup whose center is a complete intersection of n smooth divisors intersecting transversally in a smooth ambient space X.

Theorem 2.7.18. *Consider a smooth variety X and a blowup $f : \widetilde{X} \to X$ with center the complete intersection of $n \geq 2$ smooth divisors Z_i intersecting transversally. We denote the exceptional divisor by E. Consider a divisor V in X. If we ask for the restriction of the blowup to V to be crepant, then the class of V is such that its proper transform is $\widetilde{V} = f^*V - (n-1)E$. It follows that*

$$f_*\Big(c_2(T\widetilde{V}) \cdot \widetilde{V}\Big) = c_2(TV) \cdot V.$$

Proof. Using Aluffi's formula (Theorem 2.7.11) and the adjunction formula, we have

$$c(T\widetilde{V}) = (1+E)\Big(\prod_{i=1}^{n} \frac{(1+f^*Z_i - E)}{(1+f^*Z_i)}\Big)\frac{f^*c(TX)}{(1+f^*V-(n-1)E)}.$$

In the case $n-2$, by a direct expansion:

$$c_1(T\widetilde{V}) = f^*c_1(TX) - f^*V = f^*c_1(TV), \quad c_2(T\widetilde{V}) = f^*c_2(Y) - V(Y - Z_1 - Z_2) - V^2,$$

where $c_2(TV) = c_2(TX) - c_1V + V^2$. It follows that

$$f_*c_2(T\widetilde{V}) \cap \widetilde{V} = f_*\Big[f^*c_2(TV) \cap [V] + f^*Vf^*(Z_1 + Z_2)E - f^*(Z1 + Z2)E^2 + E^3\Big]$$

By applying Lemma 2.7.15, we find

$$f_*c_2(T\widetilde{V}) \cap (\widetilde{V}) = c_2(TV) \cap [V].$$

In the case $n = 3$, there is no contribution of order E^3 in $f_*c_2(T\widetilde{V}) \cap (\widetilde{V})$ and by Lemma 2.7.16 we have $f_*E = f_*E^2 = 0$.

$$f_*\left(c_2(T\widetilde{V}) \cdot \widetilde{V}\right) = f^*[c_2(V) \cdot V] + (2c_1V - 2c_2 - 4V^2 + VZ_1 + VZ_2 + VZ_3)E + (4V - 2Z_1 - 2Z_2 - 2Z_3)E^2.$$

In the case $n \geq 4$, the theorem is trivial because $c_2(T\widetilde{V}) \cdot \widetilde{V}$ is at most cubic in E and $f^*E^i = 0$ for $i \leq 3$ by Lemma 2.7.12. □

2.8 Euler characteristic and Hodge numbers

2.8.1 Batyrev's theorem and Euler characteristic of a crepant resolution

We denote the Chow ring of a nonsingular variety X by $A_*(X)$. The free group of generated by subvarieties of dimension r modulo rational equivalence is denoted by $A_r(X)$. The degree of a class α of $A_*(X)$ is denoted by $\int_X \alpha$ (or simply $\int \alpha$ if there is no ambiguity in the choice of X), and is defined to be the degree of its component in $A_0(X)$. The total homological Chern class $c(X)$ of any nonsingular variety X of dimension d is defined by:

$$c(X) = c(TX) \cap [X],$$

where TX is the tangent bundle of X and $[X]$ is the class of X in the Chow ring. The degree of $c(X)$ is the topological Euler characteristic of X:

$$\chi(X) = \int_X c(X).$$

Motivated by string geometry, Batyrev and Dais proposed in [30, Conjecture 1.3] the following conjecture.

Conjecture 2.8.1 (Batyrev and Dais, see [30])**.** *Hodge numbers of smooth crepant resolutions of an algebraic variety defined over the complex numbers with at worse Gorenstein canonical singularities do not depend on the choice of such a resolution.*

Using p-adic integration and the Weil conjecture, Batyrev proved the following slightly weaker proposition:

Theorem 2.8.2 (Batyrev, [29]). *Let X and Y be irreducible birational smooth n-dimensional projective algebraic varieties over $\mathbb{C}$. Assume that there exists a birational rational map $\phi : X - - \to Y$ which does not change the canonical class. Then X and Y have the same Betti numbers.*

Batyrev's result was strongly inspired by string dualities, in particular by the work of Dixon, Harvey, Vafa, and Witten [98]. Kontsevitch proved the Batyrev–Dais conjecture for the special case of Calabi–Yau varieties as a corollary of his newly invented theory of motivic integration; the proof relies on Hodge theory and geometrizes Batyrev's use of p-adic integration.

Theorem 2.8.3 (Kontsevitch, [Kontsevich]). *Let X and Y be birationally-equivalent smooth Calabi–Yau varieties. Then X and Y have the same Hodge numbers.*

As a direct consequence of Batyrev's theorem, the Euler characteristic of a crepant resolution of a variety with Gorenstein canonical singularities is independent on the choice of resolution. We identify the Euler characteristic as the degree (see Definition 2.1.2) of the total (homological) Chern class of a crepant resolution $f : \widetilde{Y} \longrightarrow Y$ of a Weierstrass model $Y \longrightarrow B$:

$$\chi(\widetilde{Y}) = \int c(\widetilde{Y}).$$

We then use the birational invariance of the degree under the pushfoward to express the Euler characteristic as a class in the Chow ring of the projective bundle X_0. We subsequently push this class

forward to the base to obtain a rational function depending upon only the total Chern class of the base $c(B)$, the first Chern class $c_1(\mathscr{L})$, and the class S of the divisor in B:

$$\chi(\widetilde{Y}) = \int_B \pi_* f_* c(\widetilde{Y}).$$

In view of Theorem 2.8.2, this Euler characteristic is independent of the choice of a crepant resolution. We discuss pushforwards and their role in the computation of the Euler characteristic in more detail in Section 5.4.

2.8.2 Hodge numbers for Calabi–Yau elliptic threefolds

Using motivitic integration, Kontsevich shows in his famous "String Cohomology" Lecture at Orsay that birational equivalent Calabi–Yau varieties have the same class in the completed Grothendieck ring [Kontsevich]. Hence, birational equivalent Calabi–Yau varieties have the same Hodge-Deligne polynomial, Hodge numbers, and Euler characteristic. In this section, we compute the Hodge numbers of crepant resolutions of Weierstrass models in the case of Calabi–Yau threefolds.

Theorem 2.8.4 (Kontsevich, (see [Kontsevich])). *Let X and Y be birational equivalent Calabi–Yau varieties over the complex numbers. Then X and Y have the same Hodge numbers.*

Remark 2.8.5. In Kontsevich's theorem, a Calabi–Yau variety is a nonsingular complete projective variety of dimension d with a trivial canonical divisor. To compute Hodge numbers in this section, we use the following stronger definition of a Calabi–Yau variety.

Definition 2.8.6. A *Calabi–Yau variety* is a smooth compact projective variety Y of dimension n with a trivial canonical class and such that $H^i(Y, \mathcal{O}_X) = 0$ for $1 \leq i \leq n-1$.

We first recall some basic definitions and relevant classical theorems.

Theorem 2.8.7 (Noether's formula)**.** *If B is a smooth compact, connected, complex surface with canonical class K_B and Euler number c_2, then*

$$\chi(\mathcal{O}_B) = 1 - h^{0,1}(B) + h^{0,2}(B), \quad \chi(\mathcal{O}_B) = \frac{1}{12}(K^2 + c_2).$$

When B is a smooth compact rational surface, we have a simple expression of $h^{1,1}(B)$ as a function of K^2 using the following lemma.

Lemma 2.8.8. *Let B be a smooth compact rational surface with canonical class K. Then*

$$h^{1,1}(B) = 10 - K^2. \tag{2.20}$$

Proof. Since B is a rational surface, $h^{0,1}(B) = h^{0,2}(B) = 0$. Hence $c_2 = 2 + h^{1,1}(B)$ and the lemma follows from Noether's formula. □

We now compute $h^{1,1}(Y)$ using the Shioda–Tate–Wazir theorem [300, Corollary 4.1].

Theorem 2.8.9 (Shioda-Tate-Wazir; see Corollary 4.1. of [300])**.** *Let $\phi : Y \to B$ be a smooth elliptic threefold. Then,*

$$\rho(Y) = \rho(B) + f + \operatorname{rank}(MW(\phi)) + 1,$$

where f is the number of geometrically irreducible fibral divisors not touching the zero section.

Theorem 2.8.10. *Let Y be a smooth Calabi–Yau threefold elliptically fibered over a smooth variety B with Mordell–Weil group of rank zero. Assuming the Mordell-Weil group of Y has rank zero, then*

$$h^{1,1}(Y) = h^{1,1}(B) + f + 1, \quad h^{2,1}(Y) = h^{1,1}(Y) - \frac{1}{2}\chi(Y),$$

where f is the number of geometrically irreducible fibral divisors not touching the zero section. In particular, if Y is a G-model with G being a semi-simple group, then f is the rank of G.

2.9 Characteristic numbers of the fourfolds

The theory of characteristic classes was founded in the 1930s and 1940s by Whitney, Stiefel, Pontryagin, and Chern [171, 234]. To these days, the most famous characteristic numbers are the Stiefel-Whitney numbers, the Pontryagin numbers, the Chern numbers, together with the Euler characteristic, which is the oldest topological invariant. The theory of characteristic classes relies deeply on sheaf theory as developed by Kodaira, Spencer, and Serre; and historically, also on Thom's theory of cobordism. Grothendieck introduced an axiomatic definition of Chern classes in the Chow ring of a variety using projective bundles. This establishes characteristic classes as familiar objects in intersection theory [136, Chap 3]. In a sense, any natural transformation from the complex vector bundles to the cohomology ring is a polynomial in the Chern numbers. In his seminal book, Hirzebruch expresses all characteristic classes in terms of Chern classes [171].

2.9.1 List of characteristic numbers

We compute the following six types of rational Chern and Pontryagin numbers for each G-models:

1. The Chern numbers

$$\int_Y c_1(TY)^4,\ \int_Y c_1(TY)^2 c_2(TY),\ \int_Y c_1(TY)c_3(TY),\ \int_Y c_2^2(TY),\ \text{and}\ \int_Y c_4(TY). \tag{2.21}$$

2. The holomorphic genera $\chi_p(Y) = \sum_{q=0}^{n}(-1)^q h^{p,q}(Y)$ [196]:

$$\begin{aligned}
\chi_0(Y) &= \int_Y \mathrm{Td}(TY) = \frac{1}{720}\int_Y(-c_4 + c_1c_3 + 3c_2^2 + 4c_1^2c_2 - c_1^4),\\
\chi_1(Y) &= \frac{1}{180}\int_Y(-31c_4 - 14c_1c_3 + 3c_2^2 + 4c_1^2c_2 - c_1^4),\\
\chi_2(Y) &= \frac{1}{120}\int_Y(79c_4 - 19c_1c_3 + 3c_2^2 + 4c_1^2c_2 - c_1^4).
\end{aligned} \tag{2.22}$$

   The holomorphic Euler characteristic χ_0 is a birational [162, Theorem II.8.19] and diffeomorphism invariant. The other holomorphic genera are diffeomorphism invariants and invariant under crepant birational maps.

3. The Pontryagin numbers of a fourfold are the numbers $\int_Y p_2(TY)$ and $\int_Y p_1^2(TY)$, where the Pontryagin classes $p_1(TY)$ and $p_2(TY)$ are defined as follows:

$$\begin{aligned}
p_1(TY) &= c_1^2(TY) - 2c_2(TY),\\
p_2(TY) &= c_2^2(TY) - 2c_1(TY)c_3(TY) + 2c_4(TY).
\end{aligned} \tag{2.23}$$

4. The Hirzebruch signature of a fourfold,

$$\sigma(Y) = \frac{1}{45}\int_Y \Big(7p_2(TY) - p_1^2(TY)\Big) = \frac{1}{45}\int_Y (-c_1^4 + 4c_1^2c_2 + 3c_2^2 - 14c_1c_3 + 14c_4). \quad (2.24)$$

The signature is the degree of the Hirzebruch L-genus. The L-genus is always an integer [234, Corrolary 19.5, p. 226] and depends only on the oriented homotopy type of the variety [234, Corrolary 19.6, p. 226].

5. The $\hat{\text{A}}$-genus of a fourfold,

$$\begin{aligned}\int_Y \hat{\text{A}}_2(TY) &= \frac{1}{5760}\int_Y \Big(7p_1^2(TY) - 4p_2(TY)\Big) \\ &= \frac{1}{5760}\int_Y \Big(7c_1^4 - 28c_1^2c_2 + 8c_1c_3 + 24c_2^2 - 8c_4\Big).\end{aligned} \quad (2.25)$$

By the Atiyah-Singer theorem, if the fourfold Y is a spin manifold, the degree of $\hat{\text{A}}_2$ gives the index of the Dirac operator on Y. We will see that the $\hat{\text{A}}$-genus is independent of our choice of a crepant resolution and is also independent of G.

6. We also compute the following form that plays an important role in many questions of anomaly cancellations, it detects the appearance of a non-vanishing contribution to the one-point function for the two, three, and four forms in type IIA, M, and F-theory [279, 293]:

$$X_8(Y) = \frac{1}{192}\int_Y \Big(p_1^2(TY) - 4p_2(TY)\Big). \quad (2.26)$$

In string theory, $X_8(Y)$ typically appears as a curvature invariant. As it is expressed by Pontryagin numbers, $X_8(Y)$ is an oriented diffeomorphism invariants and is also invariants under crepant birational maps.

2.9.2 Chern numbers of fourfolds are K-equivalence invariants

Crepant resolutions are in a sense the mildest form of desingularizations, since they do not modify a singular variety away from its singular locus and preserves the canonical class. Crepant resolutions are also relative minimal models over the underlying singular variety. When they exist, crepant resolutions are not necessarily unique for varieties of dimension three or higher. For G-models, the number of flops can be pretty big [110, 111, 163]. When two varieties are crepant resolutions of the same underlying singular variety, a natural question to ask is if their characteristic numbers are the same. For instance, the Betti numbers and the Hodge numbers are invariants under crepant birational maps [29, Kontsevich].

A key point that makes this computation possible is the fact that it is enough to know a single crepant resolution to compute the Chern and Pontryagin numbers of a given G-model. This is because the Chern numbers of a fourfold are invariants under crepant birational maps as proven in Theorem 2.9.6 using a result of Aluffi [3, p. 3368] and the birational invariance of the Todd genus. We would like to point out that such an invariance for the Chern numbers should not be taken for granted as it is not generally true that Chern and Pontryagin numbers are invariant under crepant birational maps. The first counter-example appears in dimension five (see Example 2.9.1). This fact motivated our choice to present the results only for fourfolds. For a projective five-fold, the Chern

numbers are

$$\int c_1^5, \quad \int c_1^3 c_2, \quad \int c_1^2 c_3, \quad \int c_1 c_4, \quad \int c_5, \quad \int c_1 c_2^2, \quad \int c_2 c_3,$$

where only the first five are invariant under K-equivalence by Aluffi's theorem (see Theorems 2.9.4 and 2.9.6). In fact, Goresky and MacPherson gave the following example of a five-dimensional Schubert variety with two different small resolutions with the same Chern numbers with the exception of $\int c_2 c_3$. For more information on K-invariance, see [298, 299].

Example 2.9.1 (Goresky and MacPherson, [140, Example 2, page 221]). Let X be the Schubert variety in the Grassmannian $G_2(\mathbb{C}^4)$ consisting of all complex two-planes $V \subset \mathbb{C}^4$ such that $\dim(V \cap \mathbb{C}^2) \geq 1$. This variety X has a singularity at the point $V = \mathbb{C}^2$, and it has a small resolution $\phi_1 : \widetilde{X}_1 \to X$ where $\widetilde{X}_1$ consists of all $(1,2)$- flags $V^1 \subset V^2 \subset \mathbb{C}^4$ such that $V^1 \subset \mathbb{C}^2$. It has a second small resolution $\phi_2 : \widetilde{X}_1 \to X$ which consists of all $(2,3)$ flags $V^2 \subset V^3 \subset \mathbb{C}^4$ such that $\mathbb{C}^2 \subset V^3$. Although $\widetilde{X}_1$ and $\widetilde{X}_2$ are homeomorphic, by a computation of Verdier, they do not have the same Chern classes.

Example 2.9.2 (Goresky and MacPherson, [140, Example 2, page 222]). Let X be a Schubert variety $X = \{V \in G_2(\mathbb{C}^5 | \dim(V \cap \mathbb{C}^3) \leq 1\}$. Let $\widetilde{X}_1$ be the variety of partial flags $V_1 \subset V_2 \subset \mathbb{C}^5$ such that $V_1 \subset \mathbb{C}^2$. Let $\tilde{X}_2$ be the variety of partial flags $V_2 \subset V_4 \subset \mathbb{C}^4$ such that $\mathbb{C}^3 \subset V_4$. Both $\widetilde{X}_1$ and $\widetilde{X}_2$ are small resolutions of X but their cohomology rings are not even abstractly isomorphic.

The following theorem of Libgober and Wood was known to Hirzebruch in the case of fourfolds.

Theorem 2.9.3 (Libgober and Wood, [218], Theorem 3). *For a compact complex manifold X, the Chern number $\int_X c_1 c_{n-1}$ is determined by the holomorphic genera and hence by the Hodge numbers.*

Even though Chern numbers other than the Euler characteristic are not topological invariants, some are invariant under crepant birational maps as proven by Aluffi.

Theorem 2.9.4 (Aluffi, [3, page 3368]). *For two nonsingular n-dimensional complete varieties X and Y connected by a crepant birational map*

$$\int_X c_1(TX)^i c_{n-i}(TX) = \int_Y c_1(TY)^i c_{n-i}(TY), \quad i = 0, 1, \ldots, n.$$

The following theorem is also used in this thesis.

Theorem 2.9.5 (Aluffi, [3, Corollary 1.2]). *Let $f : \widetilde{X} \to X$ be a crepant resolution. Then the class*

$$f_*\left(c(T\widetilde{X}) \cap [\widetilde{X}]\right),$$

in $(A_*X)_{\mathbb{Q}}$ is independent of X.

The following theorem assets that the Chern numbers of fourfolds are K-equivalence invariants. The proof is a simple application of Theorem 2.9.4 of Aluffi.

Theorem 2.9.6 (Esole–Kang, [116]). *The Chern and Pontryagin numbers of an algebraic variety of complex dimension four are K-equivalence invariants.*

Proof. The Chern numbers of a fourfold are $\int_Y c_1(TY)^4$, $\int_Y c_1(TY)^2 c_2(TY)$, $\int_Y c_1(TY)c_3(TY)$, $\int_Y c_2^2(TY)$, and $\int_Y c_4(TY)$. Hirzebruch showed that $\int_Y c_1(TY)c_3(TY)$ can be expressed by Hodge numbers. Moreover, from a result of Aluffi, we know that the Chern numbers $\int_Y c_1^i(TY)c_{n-i}(TY)$ are K-equivalence invariants. The Chern number $\int_Y c_2^2(TY)$ is also a K-equivalence invariant as it can be expressed as a linear combination of the holomorphic Euler characteristic (which is a birational invariant) and the $\int_Y c_1^i(TY)c_{n-i}(TY)$ for $i = 0, 1, 2, 3, 4$. It follows that all Chern numbers of a fourfold are K-equivalence invariants. The same is true for Pontryagin numbers since they are linear combinations of Chern numbers. □

Theorem 2.9.6 allows us to compute Chern numbers of G-models in the crepant resolution of our choice since it is independent of a choice of a crepant resolution.

The Chern number $\int_Y c_1(TY)^2 c_2(TY)$, the $\hat{A}$-genus, and the Todd-genus (the holomorphic Euler characteristic) are invariants of the choice of G. They can all be expressed as invariants of the divisor W defined by the vanishing locus of a smooth section of $\mathscr{L}$.

2.9.3 Independence of Chern numbers

By expressing χ_0 and $\hat{A}$ in terms of Chern numbers and using the identity $\int_Y c_1^4 = 0$, which holds for any crepant resolution of a Weierstrass model (see Theorem 6.1.1), we get the following expressions of $c_1^2 c_2$ and $c_1 c_3$:

$$\int_Y c_1^2 c_2 = 96(\chi_0(Y) - \hat{A}(Y)), \quad \int_Y c_1 c_3 = 384\hat{A}(Y) + 336\chi_0(Y) + \chi(Y) - 3\int_Y c_2^2. \tag{2.27}$$

For an elliptic fibration that is a crepant resolution of a Weierstrass model, this shows that $\int_Y c_1^2 c_2$ gives the same value as a smooth Weierstrass model with the same fundamental line bundle $\mathscr{L}$. It is therefore enough to compute only $\int_Y c_2^2$ and the Euler characteristic $\chi(Y) = \int_Y c_4$ to know all the Chern numbers of a crepant resolution of a Weierstrass model.

2.10 Weak coupling limit and brane geometry

In an F-theory compactification on an elliptic fourfold $Y \to B$, the number of D3 branes (N_{D3}) depends only on the Euler characteristic $\chi(Y)$ of the elliptic fibration Y and the G_4-flux [153]:

$$\text{D3 tadpole in F-theory}: \quad N_{D3} = \tfrac{1}{24}\chi(Y) - \frac{1}{2}\int_Y G_4 \wedge G_4. \tag{2.28}$$

This relation is derived from the duality between M-theory and F-theory. For IIB $\mathbb{Z}_2$ orientifold compactifications, the D3 tadpole depends on fluxes and the Euler characteristics of the cycles wrapped by the orientifolds and the D7-branes:

$$\text{D3 tadpole in type IIB}: \quad 2N_{D3} = \tfrac{1}{6}\chi(O) + \tfrac{1}{24}\sum_i \chi(D_i) + \frac{1}{2}\sum_i \int_{D_i} tr(F^2), \tag{2.29}$$

where O is an orientifold; D_i are surfaces wrapped by D7-branes; $\int_{D_i} tr(F^2)$ are fluxes localized on the D7-branes. The trace tr is taken in the adjunct representation. Since the number of D3 branes is independent of the string coupling and invariant under $\mathfrak{Sl}(2,\mathbb{Z})$, one would expect a matching

between the computation of the number of D3 branes in F-theory and in type IIB:

$$2\chi(Y) - 24\int_Y G_4 \wedge G_4 = 4\chi(O) + \sum_i \chi(D_i) + 12\sum_i \int_{D_i} tr(F^2). \tag{2.30}$$

Such a matching condition was first introduced in [78]. For configurations such that both G-fluxes and type IIB fluxes are zero, the matching of the D3 tadpole in type IIB and in F-theory will give a purely topological relation between Euler characteristics [78]:

$$\text{Tadpole matching condition}: \quad 2\chi(Y) = 4\chi(O) + \sum_i \chi(D_i). \tag{2.31}$$

When this topological condition holds, equation (2.30) also gives a relation between the fluxes in F-theory and in type IIB:

$$\text{Flux matching condition}: \quad \int_Y G_4 \wedge G_4 = -\frac{1}{2}\sum_i \int_{D_i} tr(F^2). \tag{2.32}$$

In general, the curvature contribution to the D3 tadpole in F-theory and type IIB theory do not have to match. For example, branes seen in the type IIB limit can recombine into a different configuration of branes plus fluxes [78].

2.10.1 Geometric definition of a weak coupling limit

Following the point of view of [6], the weak coupling limit of an elliptic fibration is a degeneration such that the generic fiber of the elliptic fibration becomes semi-stable as we reach $\varepsilon = 0$. A semi-

stable elliptic curve is a singular elliptic curve of type I_n. Such a singular elliptic curve has an infinite j-invariant. This explains the name "weak coupling limit" as an infinite j-invariant means that the imaginary part of τ goes to zero which in the F-theory description of type IIB string theory essentially means the string coupling is weak: $g_s \to 0$. If the semi-stable fiber is just a nodal curve I_1 as it is the case for a smooth Weierstrass model, we are in the case analyzed by Sen. In the case the degeneration gives a curve of type I_n with $n > 1$, each irreducible components of the semi-stable curve I_n describes a $\mathbb{P}^1$-bundle over the base and since two components intersects normally, all together they form a normal crossing variety Z. It follows that for a weak coupling limit defines with a generic fiber of type I_n naturally leads to a *semi-stable degeneration*. We will see it explicitly here. It is important to realize that an elliptic fibration can admit many non-equivalent weak coupling limits with different semi-stable curves I_n as illustrated in [6, 109].

2.10.2 Brane geometry at weak coupling

When taking a weak coupling limit, the discriminant locus can split into different components that are wrapped by orientifolds and branes. These branes can be singular and can split further into brane-image-brane pairs in the double cover of the base. We quickly review the most familiar ones by considering the following discriminant and j-invariant:

$$\Delta = \varepsilon^2 h^{2+n} \prod_i (\eta_i^2 - h\psi_i^2) \prod_j (\eta_j^2 - h\chi_j), \prod_k \varphi_k + O(\varepsilon^3), \tag{2.33}$$

$$j \propto \frac{h^{4-n}}{\varepsilon^2 \prod_i (\eta_i^2 - h\psi_i^2) \prod_j (\eta_j^2 - h\chi_j) \prod_k \varphi_k}. \tag{2.34}$$

The locus $h = 0$ is the orientifold locus as seen from the base of the elliptic fibration. As ε goes to zero, j goes to infinity and the string couplings goes to zero.

$$\lim_{\varepsilon \to 0} j = \infty \Longrightarrow Im(\tau) = \infty \iff g_s = 0.$$

At weak coupling, we get an orientifold on the double cover of the base branched at $h = 0$:

$$X: \quad \xi^2 = h, \tag{2.35}$$

which defines a section of the line bundle $\mathscr{L}^2$. The involution $\sigma : X \to X$ which sends ξ to $-\xi$ can be used to define a $\mathbb{Z}_2$ orientifold symmetry $\sigma\Omega(-)^{F_L}$ and the branched locus is therefore interpret as a $O7$ orientifold. The geometry of Sen's weak coupling limit can be summarized by the following diagram:

$$\text{Sen's limit} \qquad \begin{array}{ccc} T^2 & \longrightarrow & Y_{n+1} \\ & & \downarrow \pi \quad \searrow \text{Orientifold limit} \\ & & B_n \xleftarrow[1:2]{\sigma} X_n \end{array} \tag{2.36}$$

where $Y_{n+1} \to B_n$ is an elliptic fibration and $X_n \to B$ is a double cover. The different terms of Δ determine different type of D7-branes. We summarize them in table 2.6 where we have also included the orientifold.

Name	In the discriminant	In the double cover X
Orientifold	b^2	$\xi = 0$
Whitney brane	$\eta^2 - b\chi$	$\eta^2 - \xi^2\chi = 0$
Brane-image-brane pair	$\eta^2 - b\psi^2$	$(\eta + \xi\psi)(\eta - \xi\psi) = 0$
Invariant brane	η	$\eta = 0$

Table 2.6: Familiar types of brane found in Sen's weak coupling limit. The Whitney brane is the one observed in Sen's limit of a E_8 elliptic fibration. It can specialize into a brane-image-brane pair when χ is a perfect square and into two invariant branes on top of each other when $\chi = 0$.

2.11 Tadpole matching and Whitney branes

2.11.1 Generalized tadpole condition

The D3 tadpole matching condition presented in equation (2.31) is a topological condition that can be proven to hold in a much more general set up than anticipated from the assumptions of its string theory origin. It generalizes to a relation valid at the level of the total homological Chern classes for elliptic fibrations over bases of arbitrary dimension without even assuming the Calabi–Yau condition [5, 6, 109]:

$$\text{Generalized tadpole condition}: \quad 2\phi_* c(Y) = 4\rho_* c(O) + \sum \rho_* c(D_i). \tag{2.37}$$

The right-hand-side of this relation involves objects seen in the type IIB weak coupling limit defined by taking a degeneration of the elliptic fibration while the left-hand-side is the elliptic fibration. In that respect, it requires both a choice of an elliptic fibration and a choice of a degeneration. The most interesting case is the one involving a Weierstrass model (an E_8 elliptic fibration). In that case,

the degeneration is given by the original Sen's weak coupling limit and the corresponding generalized tadpole relation was proven in [5]. Sen's weak coupling limit was generalized geometrically in [6]. The method of [6] provides an easy way to define a weak coupling limit for families of elliptic fibrations that are not given by a Weierstrass model. It also gives a natural way to organize such limits using the fiber geometry of the elliptic fibration. A generalized tadpole relation is available for E_8, E_6 and E_7 elliptic fibration [5, 6], and D_5 elliptic fibration [109].

2.11.2 Whitney branes and Orientifold Euler characteristic

Since Whitney branes are singular, we have to be careful how we define their Euler characteristic or more generally their total Chern class. The appropriate definition has been worked out in [5, 78]. For a Whitney brane D_w, we have

$$c(D_w) := \rho_* c(\overline{D}_w) - c(S), \tag{2.38}$$

where $\overline{D}_w$ is the normalization of D_w and S is the locus of codimension-two singularities of the Whitney brane. The corresponding Euler characteristic is known as the *orientifold Euler characteristic* $\chi_o(D) = \chi(\overline{D}) - \chi(S)$. The original weak coupling limit discussed by Sen will satisfy the F theory-type IIB tadpole matching condition only thanks to the presence of the singularities of the Whitney brane [5, 78]. The orientifold Euler characteristic is also useful for certain weak coupling limits of E_7 and D_5 elliptic fibrations [6, 109].

2.12 $5d\ \mathcal{N} = 1$ SUPERGRAVITY THEORIES

The compactification of M-theory on a Calabi–Yau threefold Y yields a five dimensional supergravity theory with eight supercharges coupled to $h^{1,1}(Y)$ vector multiplets and $h^{2,1}(Y) + 1$ neutral hypermultiplets [66]. The gravity multiplet also contains a gauge field called the graviphoton. The kinetic terms of the vector multiplets and the graviphoton, together with the coefficients of the Chern Simons terms, are derived from the prepotential $\mathcal{F}(\varphi)$, which is a real function of the scalar fields of the vector multiplets. After integrating out massive charged vector and matter fields, the prepotential receives a one-loop quantum correction protected from additional quantum corrections by supersymmetry. The vector multiplets transform in the adjoint representation of the gauge group while the hypermultiplets transform in representation $\mathbf{R} = \bigoplus_i \mathbf{R}_i$ of the gauge group, where $\mathbf{R}_i$ are irreducible components of $\mathbf{R}$.

The Coulomb branches of the theory correspond to the chambers of the hyperplane arrangement $\mathrm{I}(\mathfrak{g}, \mathbf{R})$. By matching the crepant resolutions with the chambers of $\mathrm{I}(\mathfrak{g}, \mathbf{R})$, we determine which resolutions correspond to which phases of the Coulomb branch. The triple intersection numbers of the fibral divisors correspond to the coefficient of the Chern-Simons couplings of the five dimensional gauge theory and can be compared with the Intrilligator–Morrison–Seiberg (IMS) prepotential, which is the one-loop quantum contribution to the prepotential of the five-dimensional gauge theory. Since in field theory the Chern-Simons couplings are linear in the numbers $n_{\mathbf{R}_i}$ of hypermultiplets transforming in the irreducible representation $\mathbf{R}_i$ such that $\mathbf{R} = \bigoplus_i \mathbf{R}_i$, computing the triple intersection numbers provides a way to determine the numbers $n_{\mathbf{R}_i}$ from the topology of the ellip-

tic fibration. We observe by direct computation in each chamber that the numbers we find do not depend on the choice of the crepant resolution.

This idea of using the triple intersection numbers to determine the number of multiplets transforming in a given representation was used previously in [124] for SU(n)-models, in [115] (or Chapter 8) for F_4-models, in [112] (or Chapter 9) for G_2, Spin(7), and Spin(8)-models, in [118] (or Chapter 10) for SO(4)and Spin(4)-models, in [119] (or Chapter 11) for $SU(2) \times G_2$-models, in [113] (or Chapter 12) for $SU(2) \times SU(3)$-models, in [121] (or Chapter 13) for $SU(2) \times Sp(4)$, $SU(2) \times Sp(4)/\mathbb{Z}_2$, $SU(2) \times SU(4)$, and $SU(2) \times SU(4)/\mathbb{Z}_2$-models. This technique has been advocated by Grimm and Hayashi in [148].

Multiplet	Fields
Graviton	$(g_{\mu\nu}, A_\mu, \psi_\mu)$
Vector	(A_μ, ϕ, λ)
Hyper	(q, ζ)

Table 2.7: Supermultiplets for $\mathcal{N} = 1$ five dimensional supergravity. The indices μ and ν refer to the five dimensional spacetime coordinates. The tensor $g_{\mu\nu}$ is the metric of the five dimensional spacetime. The fields ψ_μ, λ, ζ are symplectic Majorana spinors. The field ψ_μ is the gravitino and A_μ is the graviphoton. The hyperscalar q is a quaternion composed of four real scalar fields.

2.12.1 5d PREPOTENTIAL

In the Coulomb phase of an $\mathcal{N} = 1$ supergravity theory in five dimension, the scalar fields of the vector multiplets are restricted to the Cartan sub-algebra of the Lie group as the Lie group is broken to $U(1)^r$ where r is the rank of the group. It follows that the charge of an hypermultiplet is simply given by a weight of the representation under which it transforms [176]. The 5d prepotential by

Intrilligator–Morrison–Seiberg (IMS) is the one-loop quantum contribution to the prepotential of a five-dimensional gauge theory with the matter fields in the representations $\mathbf{R}_i$ of the gauge group. Let φ be in the Cartan subalgebra of a Lie algebra $\mathfrak{g}$. The weights are in the dual space of the Cartan subalgebra. We denote the evaluation of a weight on a coroot vector φ as a scalar product $\langle \mu, \varphi \rangle$. We recall that the roots are the weights of the adjoint representation of $\mathfrak{g}$. Denoting the fundamental simple roots by α and the weights of $\mathbf{R}_i$ by ϖ we have

$$6\mathscr{F}_{\text{IMS}}(\varphi) = \frac{1}{2}\left(\sum_{\ell} |\langle \alpha_\ell, \varphi \rangle|^3 - \sum_i \sum_{\varpi \in \mathbf{R}_i} n_{\mathbf{R}_i} |\langle \varpi, \varphi \rangle|^3\right). \tag{2.39}$$

For all simple groups with the exception of SU(N) with $N \geq 3$, this is the full cubic prepotential as there are no non-trivial third Casimir invariants.

The open dual fundamental Weyl chamber is defined as the cone $\langle \alpha, \varphi \rangle > 0$, where α runs through the set of all simple positive roots. For a given choice of a group G and representations $\mathbf{R}_i$, we have to determine a Weyl chamber to remove the absolute values in the sum over the roots. We then consider the hyperplane arrangement $\langle \varpi, \varphi \rangle = 0$, where ϕ runs through all the weights of all the representations $\mathbf{R}_i$ and φ is an element of the coroot space. They define the hyperplane arrangement $\mathrm{I}(\mathfrak{g}, \mathbf{R} = \bigoplus_i \mathbf{R}_i)$ restricted to the dual fundamental Weyl chamber. If none of these hyperplanes intersect the interior of the dual Weyl chamber of $\mathfrak{g}$, we can safely remove the absolute values in the sum over the weights. Otherwise, we have hyperplanes partitioning the dual fundamental Weyl chamber into subchambers. Each of these subchambers is defined by the signs of the linear forms $\langle \varpi, \varphi \rangle$. Two such subchambers are adjacent when they differ by the sign of a unique linear

form. Within each of these subchambers, the prepotential is a cubic polynomial.

Each of the subchambers is called a *Coulomb phase* of the gauge theory. But as we go from one subchamber to an adjacent one, we have to go through one of the walls defined by the weights. The transition from one chamber to an adjacent chamber is a *phase transition* that geometrically corresponds to a flop between different crepant resolutions of the same singular Weierstrass model. The number of chambers of such a hyperplane arrangement is physically the number of phases of the Coulomb branch of the gauge theory.

2.12.2 Counting hypermultiplets: Witten's genus formula

M-theory compactified on an elliptically fibered Calabi–Yau threefold Y gives rise to a five-dimensional supergravity theory with eight supercharges coupled to $h^{2,1}(Y) + 1$ neutral hypermultiplets and $h^{1,1}(Y) - 1$ vector multiplets [66]. Taking into account the graviphoton, there are a total of $h^{1,1}(Y)$ gauge fields. The kinetic terms, the Chern-Simons coefficients of the vector multiplets, and the graviphoton are all completely determined by the intersection ring of the Calabi–Yau variety.

Witten determined the number of states appearing when a curve collapses to a point using a quantization argument [306]. In particular, he showed that the number of hypermultiplets transforming in the adjoint representation is the genus of the curve S over which the gauge group is localized. Aspinwall, Katz, and Morrison subsequently applied Witten's quantization argument to the case of non-simply laced groups in [1]. If S' is a d cover of S with ramification divisor R, then

number $n_{\mathbf{R}_0}$ of hypermultiplets transforming in the representation $\mathbf{R}_0$ is given by

$$n_{\mathbf{R}_0} = g' - g, \tag{2.40}$$

where g' is the genus of S' and g is the genus of S [1]. This method is shown to be consistent with the six-dimensional anomaly cancellation conditions [142].

Computing the right hand side of the equation(2.40) $g' - g$ is a classical exercise whose answer is given by the following theorem.

Theorem 2.12.1 (Riemann-Hurwitz, see [162, Chap. IV, Cor. 2.4 and Example 2.5.4.]). *Let $f : S' \to S$ be a finite, separable morphism of curves of degree d branched with ramification divisor R. If g' is the genus of S', g is the genus of S, and R is the ramification divisor, then*

$$g' - g = (d-1)(g-1) + \frac{1}{2}\deg R.$$

Physically, this is the number of charged hypermultiplets in the representation $\mathbf{R}_0$, as expected from Witten's quantization argument[11]:

$$n_{\mathbf{R}_0} = (d-1)\Big(g-1\Big) + \frac{1}{2}\deg R. \tag{2.41}$$

[11] This is a direct application of the Riemann-Hurwitz's theorem (Theorem 2.12.1) in the context of Witten's genus for non-simply laced groups [1]. See Section 3 of [143].

2.13 $6d\ \mathcal{N} = (1,0)$ SUPERGRAVITY THEORIES

The matter content of the six-dimensional $\mathcal{N} = (1,0)$ supergravity theory are given by [147]

$$\begin{aligned} \text{supergravity multiplets:} &\quad (g_{\mu\nu}, B^{-}_{\mu\nu}, \psi_{\mu}{}^{A-}) \\ \text{tensor multiplets:} &\quad (B^{+}_{\mu\nu}, \chi^{A+}, \sigma) \\ \text{vector multiplets:} &\quad (A_{\mu}, \lambda^{A-}) \\ \text{hypermultiplets:} &\quad (4\varphi, \zeta^{+}) \end{aligned}$$

where $\mu, \nu = 0, \ldots, 5$ label spacetime indices, $A = 1, 2$ labels the fundamental representation of the R-symmetry SU(2), and $\pm$ denotes the chirality of Weyl spinors or the self-duality $(+)$ or anti-self-duality $(-)$ of the field strength of antisymmetric two-forms. The gravitini $\psi_{\mu}{}^{A-}$, the tensorini χ^{A+}, and gaugini λ^{A-} are symplectic Majorana Weyl spinors. The hyperino ζ^{+} is a Weyl spinor invariant under the R-symmetry group $\mathrm{SU}(2)_R$. The scalar manifold of the tensor multiplets is the symmetric space $\mathrm{SO}(1, n_T)/\mathrm{SO}(n_T)$ where n_T is the number of tensor multiplets. The scalar manifold of the hypermultiplet is a quaternionic-Kähler manifold of quaternionic dimension n_H, where n_H is the number of hypermultiplets.

We consider a gauged six-dimensional $\mathcal{N} = (1,0)$ supergravity theory [147] with a semi-simple gauge group $G = \prod_a G_a$, $n_V^{(6)}$ vector multiplets, n_T tensor multiplets, and n_H hypermultiplets consisting of n_H° neutral hypermultiplets and $n_H^{c\!h}$ charged hypermultiplets under a representation $\bigoplus_i \mathbf{R}_i$ of the gauge group with $\mathbf{R}_i = \bigotimes_a \mathbf{R}_{i,a}$, where $\mathbf{R}_{i,a}$ is an irreducible representation of the simple component G_a of the semi-simple group G. The vector multiplets transform under the adjoint of the gauge group. CPT invariance requires the representation to be quaternionic, and hence we have

quaternions of dimension n_H for the hypermultiplets.

In particular, F-theory compactified on a Calabi–Yau threefold Y gives a six-dimensional supergravity theory with eight supercharges coupled to n_V vector, n_T tensor, and $n_H^\circ = h^{2,1}(Y) + 1$ neutral hypermultiplets. When the Calabi–Yau variety is elliptically-fibered with a gauge group G and a representation $\mathbf{R}$,

- the number of vectors: $n_V = \dim G$,
- the number of tensors: $n_T = 9 - K^2$,
- the number of hypers: $n_H = n_H^\circ + n_H^{ch}$ with neutral hypers $n_H^\circ = h^{2,1} + 1$,

where K is the canonical class of the base B of the elliptic fibration, and we have charged hypermultiplets transforming in the representation $\mathbf{R}$ of G. We consider the semisimple gauge group with simple components G_a such that $G = \sum_a G_a$. The base of the fibration is then necessarily a rational surface B whose canonical class is denoted K [269].

2.13.1 $5d\ \mathcal{N} = 1$ SUPERGRAVITY THEORIES AND THEIR $6d$ UPLIFTS

For a compactification on a Calabi–Yau threefold Y, the number of neutral hypermultiplets is $n_H^\circ = h^{2,1}(Y) + 1$ [66]. The number of each multiplet is

$$n_V^{(6)} = \dim G, \quad n_T = h^{1,1}(B) - 1 = 9 - K^2, \tag{2.42}$$

$$n_H = n_H^\circ + n_H^{ch} = h^{2,1}(Y) + 1 + \sum_i n_{\mathbf{R_i}} \left(\dim \mathbf{R_i} - \dim \mathbf{R_i}^{(0)} \right), \tag{2.43}$$

where the (elliptically fibered) base B is a rational surface. From the Hodge number $h^{2,1}(Y)$ of the Calabi–Yau threefolds, the number of hypernultiplets can be computed for each G-model.

F-theory on Y $\downarrow$ $6d\ \mathcal{N} = (1,0)$ sugra	M-theory on Y $\downarrow$ $5d\ \mathcal{N} = 1$ sugra	F-theory on $Y \times S^1$ $\downarrow$ $5d\ \mathcal{N} = 1$ sugra
$n_V^{(6)} = h^{1,1}(Y) - h^{1,1}(B) - 1$ $n_H^\circ = h^{2,1}(Y) + 1$ $n_T = h^{1,1}(B) - 1$	$n_V^{(5)} = n_V^{(6)} + n_T + 1 = h^{1,1}(Y) - 1$ $n_H^\circ = h^{2,1}(Y) + 1$	

Table 2.8: Compactification of F-theory and M-theory on a Calabi–Yau threefold Y. We assume that all tensor multiplets in the five dimensional theory are dualized to vector multiplets. The number of neutral hypermultiplets are the same in five and six dimensions, but $n_V^{(5)} = n_V^{(6)} + n_T + 1$.

2.13.2 Anomaly Cancellations in $6d\ \mathcal{N} = (1,0)$ supergravity theories

For anomalies in six dimensions, we have incorporated the viewpoints of [142, 147, 208, 237, 262, 269] and use the notation of [121]. We refer to [257] for an elegant general review.

Since we consider only local anomalies, we only have pure gravitational anomalies, pure gauge anomalies, and mixed gravitational and gauge anomalies. An effective way to address these anomalies are via using Green-Schwarz mechanism in six-dimensions. The anomaly polynomial I_8 has a pure gravitational contribution from the term proportional to the $\mathbf{tr}R^4$, which is given by $\propto (n_H - n_V^{(6)} + 29n_T - 273)\mathbf{tr}R^4$, where R is the Riemann tensor thought of as a 6×6 real matrix of two-form values.

In order to have vanishing gravitational anomalies, the coefficient of $\mathbf{tr}R^4$ is required to vanish

[262]:

$$n_H - n_V^{(6)} + 29n_T - 273 = 0. \tag{2.44}$$

The remainder terms of the anomaly polynomial I_8, is given by

$$\mathrm{I}_8 = \frac{K^2}{8}(\mathbf{tr}R^2)^2 + \frac{1}{6}\sum_a X_a^{(2)}\mathbf{tr}R^2 - \frac{2}{3}\sum_a X_a^{(4)} + 4\sum_{a<b} Y_{ab}, \tag{2.45}$$

where contributions from each simple gauge component $X_a^{(n)}$ for $n = 2, 4$ and the mixed contribution Y_{ab} are given by

$$X_a^{(n)} = \mathbf{tr}_{\mathbf{adj}}F_a^n - \sum_i n_{\mathbf{R}_{i,a}}\mathbf{tr}_{\mathbf{R}_{i,a}}F_a^n, \quad Y_{ab} = \sum_{i,j} n_{\mathbf{R}_{i,a},\mathbf{R}_{j,b}}\mathbf{tr}_{\mathbf{R}_{i,a}}F_a^2\mathbf{tr}_{\mathbf{R}_{j,b}}F_b^2, \tag{2.46}$$

where $n_{\mathbf{R}_{i,a},\mathbf{R}_{j,b}}$ is the number of hypermultiplets transforming in the representation $(\mathbf{R}_{i,a}, \mathbf{R}_{j,b})$ of the gauge group $G_a \times G_b$. Note that the mixed term by computing all possible pairs of the simple components of the gauge groups which are denoted by two indices.

It is important to note that when a representation is charged on more than a simple component of the group, it affects not only Y_{ab} but also $X_a^{(2)}$ and $X_a^{(4)}$. Consider a representation $(\mathbf{R}_1, \mathbf{R}_2)$ for of a semisimple group with two simple components $G = G_1 \times G_2$, where $\mathbf{R_a}$ is a representation of G_a. Then this representation contributes $\dim \mathbf{R}_2$ times to $n_{\mathbf{R}_1}$, and contributes $\dim \mathbf{R}_1$ times to $n_{\mathbf{R}_2}$:

$$n_{\mathbf{R}_1} = \cdots + \dim \mathbf{R}_2\, n_{\mathbf{R}_1,\mathbf{R}_2}, \quad n_{\mathbf{R}_2} = \cdots + \dim \mathbf{R}_1\, n_{\mathbf{R}_1,\mathbf{R}_2}. \tag{2.47}$$

Since the hypermultiplets of zero weights are neutral, we have to remove the neutral hypermultiplet contributions to get the charged dimension of the hypermultiplets in each irreducible representation. By denoting the zero weights of a representation $\mathbf{R_i}$ as $\mathbf{R_i^{(0)}}$, the charged dimension of the hypermultiplets in representation $\mathbf{R_i}$ is given by

$$\dim \mathbf{R_i} - \dim \mathbf{R_i^{(0)}}.$$

For a representation $\mathbf{R_i}$, $n_{\mathbf{R_i}}$ denotes the multiplicity of the representation $\mathbf{R_i}$. Then the number of charged hypermultiplets is given by [142]

$$n_H^{ch} = \sum_i n_{\mathbf{R_i}} \left(\dim \mathbf{R_i} - \dim \mathbf{R_i^{(0)}} \right). \tag{2.48}$$

The trace identities for a representation $\mathbf{R}_{i,a}$ of a simple group G_a are

$$\mathbf{tr}_{\mathbf{R_{i,a}}} F_a^2 = A_{\mathbf{R_{i,a}}} \mathbf{tr}_{\mathbf{F_a}} F_a^2, \quad \mathbf{tr}_{\mathbf{R_{i,a}}} F_a^4 = B_{\mathbf{R_{i,a}}} \mathbf{tr}_{\mathbf{F_a}} F_a^4 + C_{\mathbf{R_{i,a}}} (\mathbf{tr}_{\mathbf{F_a}} F_a^2)^2 \tag{2.49}$$

with respect to a reference representation $\mathbf{F_a}$ for each simple component G_a of the gauge group.[12] The coefficients $A_{\mathbf{R_{i,a}}}$, $B_{\mathbf{R_{i,a}}}$, and $C_{\mathbf{R_{i,a}}}$ depends on the gauge groups and are listed in [22, 106, 294].

Then we can write the gauge contribution terms with respect to the coefficients from trace identi-

[12] We denoted this representation as $\mathbf{F_a}$ as we picked the fundamental representations for convenience. However, any representation can be used as a reference representation.

ties:

$$X_a^{(2)} = \overbrace{\left(A_{a,\mathbf{adj}} - \sum_i n_{\mathbf{R}_{i,a}} A_{\mathbf{R}_{i,a}}\right)}^{A_a} \mathbf{tr}_{\mathbf{F}_a} F_a^2, \tag{2.50}$$

$$X_a^{(4)} = \overbrace{\left(B_{a,\mathbf{adj}} - \sum_i n_{\mathbf{R}_{i,a}} B_{\mathbf{R}_{i,a}}\right)}^{B_a} \mathbf{tr}_{\mathbf{F}_a} F_a^4 + \overbrace{\left(C_{a,\mathbf{adj}} - \sum_i n_{\mathbf{R}_{i,a}} C_{\mathbf{R}_{i,a}}\right)}^{C_a} (\mathbf{tr}_{\mathbf{F}_a} F_a^2)^2, \tag{2.51}$$

$$Y_{ab} = \sum_{i,j} n_{\mathbf{R}_{i,a},\mathbf{R}_{j,b}} A_{\mathbf{R}_{i,a}} A_{\mathbf{R}_{j,b}} \mathbf{tr}_{\mathbf{F}_a} F_a^2 \mathbf{tr}_{\mathbf{F}_b} F_b^2. \tag{2.52}$$

For each simple component G_a, the anomaly polynomial I_8 has a pure gauge contribution proportional to the quartic term $\mathbf{tr} F_a^4$, which is contained in equation (2.51). In order to have a vanishing pure gauge anomalies, the coefficients of these terms have to vanish:

$$B_{a,\mathbf{adj}} - \sum_i n_{\mathbf{R}_{i,a}} B_{\mathbf{R}_{i,a}} = 0. \tag{2.53}$$

For a representation $\mathbf{R}$ with only one quartic Casimir, we simply take $B_{\mathbf{R}} = 0$.

When the coefficients of all quartic terms ($\mathbf{tr} R^4$ and $\mathbf{tr} F_a^4$) vanish, the remaining part of the anomaly polynomial I_8 is [269]

$$\begin{cases} \mathrm{I}_8 = \frac{K^2}{8} (\mathbf{tr} R^2)^2 + \frac{1}{6} \sum_a X_a^{(2)} \mathbf{tr} R^2 - \frac{2}{3} \sum_a X_a^{(4)} + 4 \sum_{a<b} Y_{ab}, \\ X_a^{(2)} = \left(A_{a,\mathbf{adj}} - \sum_i n_{\mathbf{R}_{i,a}} A_{\mathbf{R}_{i,a}}\right) \mathbf{tr}_{\mathbf{F}_a} F_a^2, \quad X_a^{(4)} = \left(C_{a,\mathbf{adj}} - \sum_i n_{\mathbf{R}_{i,a}} C_{\mathbf{R}_{i,a}}\right) (\mathbf{tr}_{\mathbf{F}_a} F_a^2)^2, \\ Y_{ab} = \sum_{i,j} n_{\mathbf{R}_{i,a},\mathbf{R}_{j,b}} A_{\mathbf{R}_{i,a}} A_{\mathbf{R}_{j,b}} \mathbf{tr}_{\mathbf{F}_a} F_a^2 \mathbf{tr}_{\mathbf{F}_b} F_b^2, \quad (a \neq b). \end{cases} \tag{2.54}$$

The anomalies are canceled by the Green-Schwarz mechanism when I_8 factorizes [147, 270, 272].

For example, if the coefficients of $\mathbf{tr}R^4$ and $\mathbf{tr}F_a^4$ vanish and $G = G_1 \times G_2$, the remainder of the anomaly polynomial can be written as

$$I_8 = \frac{K^2}{8}(\mathbf{tr}R^2)^2 + \frac{1}{6}(X_1^{(2)} + X_2^{(2)})\mathbf{tr}R^2 - \frac{2}{3}(X_1^{(4)} + X_2^{(4)}) + 4Y_{12}. \tag{2.55}$$

If I_8 factors as $\frac{1}{2}\Omega_{ij}X_i^{(4)}X_j^{(4)}$, then the anomaly is cancelled by adding the counter term $\Omega_{ij}B_i \wedge X_j^{(4)}$ to the Lagrangian. The modification of the field strength $H^{(i)}$ of the antisymmetric tensor $B^{(i)}$ are $H^{(i)} = dB^{(i)} + \omega^{(i)}$, where $\omega^{(i)}$ is a proper combination of Yang-Mills and gravitational Chern-Simons terms.

More precisely, the modification of the field strength H of the antisymmetric tensor B for the general scenario is

$$H = dB + \frac{1}{2}K\omega_{3L} + 2\sum_a \frac{S_a}{\lambda_a}\omega_{a,3Y}, \tag{2.56}$$

where ω_{3L} and $\omega_{a,3Y}$ are respectively the gravitational Yang-Mills and Chern–Simons terms. If I_8 factors as

$$I_8 = X \cdot X, \tag{2.57}$$

then the anomaly is canceled by adding the following Green-Schwarz counter-term

$$\Delta L_{GS} \propto \frac{1}{2}B \wedge X, \tag{2.58}$$

which implies that X carries string charges. Following Sadov [269], to cancel the local anomalies, we consider

$$X = \frac{1}{2} K \mathbf{tr} R^2 + \sum_a \frac{2}{\lambda_a} S_a \mathbf{tr} F_a^2, \tag{2.59}$$

where the λ_a are normalization factors chosen such that the smallest topological charge of an embedded SU(2) instanton in G_a is one [35, 208, 257]. This forces λ_a to be the Dynkin index of the fundamental representation of G_a as summarized in Table 2.9 [257].

$\mathfrak{g}$	A_n	B_n	C_n	D_n	E_8	E_7	E_6	F_4	G_2
λ	1	2	1	2	60	12	6	6	2

Table 2.9: The normalization factors for each simple gauge algebra. See [208].

With all the local anomaly cancellation conditions in six-dimensions investigated, we can coalesce as the set of equations with number of charged hypermultiplets in each irreducible representations as unknwons. If the simple group G_a is supported on a divisor S_a, the local anomaly cancellation conditions are the following equations:

$$n_T = 9 - K^2, \tag{2.60a}$$

$$n_H - n_V^{(6)} + 29 n_T - 273 = 0, \tag{2.60b}$$

$$\left(B_{a,\mathbf{adj}} - \sum_i n_{\mathbf{R}_{i,a}} B_{\mathbf{R}_{i,a}} \right) = 0, \tag{2.60c}$$

$$\lambda_a \left(A_{a,\mathbf{adj}} - \sum_i n_{\mathbf{R}_{i,a}} A_{\mathbf{R}_{i,a}} \right) = 6K \cdot S_a, \tag{2.60d}$$

$$\lambda_a^2 \left(C_{a,\mathbf{adj}} - \sum_i n_{\mathbf{R}_{i,a}} C_{\mathbf{R}_{i,a}} \right) = -3 S_a^2, \tag{2.60e}$$

$$\lambda_a \lambda_b \sum_{i,j} n_{\mathbf{R}_{i,a},\mathbf{R}_{j,b}} A_{\mathbf{R}_{i,a}} A_{\mathbf{R}_{j,b}} = S_a \cdot S_b, \quad (a \neq b). \tag{2.60f}$$

Equation (2.60a) gives the number of tensor multiplets and assume that the base of the fibration is a rational surface, equation (2.60b) is required by the vanishing of the pure gravitational anomalies, equation (2.60c) ensures the cancellation of pure gauge anomalies, equations (2.60d) and (2.60e) are the conditions for cancellation of mixed gravitational-gauge anomalies.

Assuming the first three equations hold, cancelling the anomalies is equivalent to factoring the anomaly polynomial

$$\mathrm{I}_8 = \frac{K^2}{8}(\mathbf{tr} R^2)^2 + \frac{1}{6}(X_1^{(2)} + X_2^{(2)})\mathbf{tr} R^2 - \frac{2}{3}(X_1^{(4)} + X_2^{(4)}) + 4Y_{12}. \tag{2.61}$$

To summarize, for a compactification on an elliptically-fibered Calabi–Yau threefold Y, the number of multiplets is [142]

$$n_V^{(6)} = \dim G, \quad n_T = h^{1,1}(B) - 1 = 9 - K^2, \tag{2.62a}$$

$$n_H = n_H^\circ + n_H^{cb} = h^{2,1}(Y) + 1 + \sum_i n_{\mathbf{R}_i} \left(\dim \mathbf{R_i} - \dim \mathbf{R_i}^{(\circ)} \right), \tag{2.62b}$$

where $n_{\mathbf{R}_i}$ is a number of hypermultiplets charged under each irreducible representation $\mathbf{R_i}$ that satisfies equations (2.60).

Entropy is the price of structure.

Ilya Prigogine

3

Entanglement entropy, Holography, and von Neumann Algebra

Entanglement entropy has many applications in quantum field theory, ranging from the study of renormalization group flows [72, 73] to confinement [194] to topological orders [193, 217]. With the discovery of the Ryu–Takayangi formula [268], entanglement entropy has been especially useful

in studying holographic quantum field theories. For holographic theories, it is important to understand the emergent low-energy bulk physics in d-dimensions from the conformal field theory in $(d-1)$-dimensions. Since local bulk operators can be expressed as boundary operators smeared over either the entire spatial slice or compact spatial subregions [157, 158], a single bulk operator can be reconstructed in different subregions [2]. Quantum error correction provides a convenient setup where bulk operators are defined only on a code subspace of the physical Hilbert space of the conformal field theory. In order to resolve apparent inconsistencies with space-like commutativity of local operators in quantum field theory, bulk reconstruction was studied in the context of quantum error correcting codes [2]. Using the Ryu–Takayangi formula, [178] showed that the relative entropy of nearby states computed in a boundary subregion is equivalent to the relative entropy computed in the dual entanglement wedge [167], up to corrections on the order of Newton's constant G_N. These results were used in [102, 160] to argue that CFT operators in a boundary subregion can be used to reconstruct bulk operators in the entanglement wedge.

Much of the literature on entanglement entropy contains assumptions that are only true for quantum mechanical systems with finite-dimensional Hilbert spaces. For instance, entanglement entropy has often been defined by assuming that the Hilbert space $\mathcal{H}$ can be written as $\mathcal{H} = \mathcal{H}_A \otimes \mathcal{H}_{A^c}$, where A refers to a subregion of space and A^c refers to the complement of A. The entanglement entropy is the von Neumann entropy of the reduced density matrix one obtains after performing a partial trace on the Hilbert space $\mathcal{H}_{A^c}$. However, the infinite-dimensional Hilbert space $\mathcal{H}$ does not factorize in this way because the entanglement entropy contains a universal area-law divergence [307].

Von Neumann algebras are a mathematical structure that arise naturally in quantum field theory. Instead of assuming that the Hilbert space factorizes, we should characterize a causally complete region of spacetime[1] by an associated von Neumann algebra [155]. Formulating quantum field theory with von Neumann algebras is powerful because it allows one to make use of the mathematical machinery of Tomita-Takesaki theory to study entanglement. The modular operator is an important object in Tomita-Takesaki theory, and Araki [15] has used it to define relative entropy in quantum field theory. Theorem 3.5.8, a central result of Tomita-Takesaki theory, formalizes the notion of modular flow. A demonstration of how von Neumann algebras are associated with the left and right Rindler wedges of Minkowski space was provided by Bisognano and Wichmann in [43]. More recently, an explicit computation of mutual information for free fermions in 1+1 dimensions was performed in [221]. Moreover, the study of entanglement entropy has utilized results in the mathematical field of operator algebras [25, 220, 221].

Given the role that entanglement entropy plays in our understanding of holography and the role that von Neumann algebras play in our understanding of entanglement entropy, it is natural to ask whether statements in the bulk reconstruction literature can be recast in a way that dispenses with the fiction that the boundary Hilbert space can be written as $\mathcal{H} = \mathcal{H}_A \otimes \mathcal{H}_{A^c}$ for an arbitrary subregion A. In the context of quantum error correction with finite dimensional Hilbert spaces, [159] formulates and completes the equivalence of the Ryu–Takayangi formula, entanglement wedge reconstruction, and the equality of bulk and boundary relative entropies. With the exception of the

[1] The causal complement of a region R, denoted by R', is defined to be all of the points in spacetime which are spacelike separated from every point in R. A region R is causally complete if $R'' = R$. Note that any von Neumann algebra $\mathcal{M}$ satisfies $\mathcal{M} = \mathcal{M}''$, where the $'$ denotes the commutant.

Ryu–Takayangi formula, there are natural ways to generalize these statements to the case where the Hilbert space is infinite-dimensional. The Ryu–Takayangi formula, on the other hand, computes the entanglement entropy of an arbitrary subregion in the boundary field theory, which is infinite.

In Chapter 14, we prove that in the context of quantum error correction with infinite-dimensional Hilbert spaces, the equivalence of bulk and boundary relative entropies is a necessary and sufficient condition for entanglement wedge reconstruction. This is presented more precisely in Theorem 3.0.1. We define cyclic and separating states in Definitions 3.5.1 and 3.5.2, and relative entropy in Definition 3.5.6.

Theorem 3.0.1. *Let $u : \mathcal{H}_{code} \to \mathcal{H}_{phys}$ be an isometry[2] between two Hilbert spaces. Let M_{code} and M_{phys} be von Neumann algebras on $\mathcal{H}_{code}$ and $\mathcal{H}_{phys}$ respectively. Let M'_{code} and M'_{phys} respectively be the commutants of M_{code} and M_{phys}. Suppose that the set of cyclic and separating vectors with respect to M_{code} is dense in $\mathcal{H}_{code}$. Also suppose that if $|\Upsilon\rangle \in \mathcal{H}_{code}$ is cyclic and separating with respect to M_{code}, then $u|\Upsilon\rangle$ is cyclic and separating with respect to M_{phys}. Then the following two statements are equivalent:*

1. Bulk reconstruction

$$\forall \mathcal{O} \in M_{code}\, \forall \mathcal{O}' \in M'_{code}, \quad \exists \tilde{\mathcal{O}} \in M_{phys}\, \exists \tilde{\mathcal{O}}' \in M'_{phys} \quad \textit{such that}$$

$$\forall\, |\Theta\rangle \in \mathcal{H}_{code} \quad \begin{cases} u\mathcal{O}\,|\Theta\rangle = \tilde{\mathcal{O}} u\,|\Theta\rangle\,, \qquad u\mathcal{O}'\,|\Theta\rangle = \tilde{\mathcal{O}}' u\,|\Theta\rangle\,, \\ u\mathcal{O}^\dagger\,|\Theta\rangle = \tilde{\mathcal{O}}^\dagger u\,|\Theta\rangle\,, \quad u\mathcal{O}'^\dagger\,|\Theta\rangle = \tilde{\mathcal{O}}'^\dagger u\,|\Theta\rangle\,. \end{cases}$$

[2] This means that u is a norm-preserving map. The map u need not be a bijection. In general, $u^\dagger u$ is the identity on $\mathcal{H}_{code}$ and $uu^\dagger$ is a projection on $\mathcal{H}_{phys}$.

2. Boundary relative entropy equals bulk relative entropy

For any $|\Psi\rangle, |\Phi\rangle \in \mathcal{H}_{code}$ *with* $|\Psi\rangle$ *cyclic and separating with respect to* $\mathcal{M}_{code}$,

$$\mathcal{S}_{\Psi|\Phi}(\mathcal{M}_{code}) = \mathcal{S}_{u\Psi|u\Phi}(\mathcal{M}_{phys}), \text{ and } \mathcal{S}_{\Psi|\Phi}(\mathcal{M}'_{code}) = \mathcal{S}_{u\Psi|u\Phi}(\mathcal{M}'_{phys}),$$

where $\mathcal{S}_{\Psi|\Phi}(\mathcal{M})$ *is the relative entropy.*

Theorem 3.0.1 has two separate statements regarding bulk reconstruction and relative entropy. Early attempts to express bulk operators as nonlocal operators on the boundary were made in [157, 158], and [2] made the connection between bulk reconstruction and quantum error correction. The statement that relative entropy equals bulk relative entropy is due to [178].

Given the assumptions of Theorem 3.0.1, $\mathcal{M}_{code}$ may be viewed as a von Neumann subalgebra of $\mathcal{M}_{phys}$. For a specific setting when the relative entropy of two states defined with respect to $\mathcal{M}_{code}$ is identical to the relative entropy defined with respect to $\mathcal{M}_{phys}$, $\mathcal{M}_{code}$ is called a weakly sufficient subalgebra with respect to the two states. This particular case is studied in [260]. However, Theorem 3.0.1 is concerned with the case when the relative entropies agree for all states in the code subspace.

Von Neumann algebras acting on finite-dimensional Hilbert spaces must be of type I. Once infinite-dimensional Hilbert spaces are considered, the local operator algebras that arise in quantum field theory are generically of type III [137, 307]. An example of an infinite-dimensional von Neumann algebra is a type II_1 factor, which is defined and explained in Section 3.4.1.

More precisely, for a generic local quantum field theory, the von Neumann algebra associated

with any causally complete subregion is generically a type III_1 factor.[3] Assuming that this property of generic local QFTs applies in the bulk theory, one of the assumptions of Theorem 3.0.1 is no longer needed as seen in Remark 3.0.2 (see Section 14.4.5 for further discussion).

Remark 3.0.2. If $\mathcal{M}_{code}$ and $\mathcal{M}'_{code}$ are both type III_1 factors, then a result of Connes-Størmer [80] allows us to relax the assumption in Theorem 3.0.1 that the set of cyclic and separating vectors with respect to $\mathcal{M}_{code}$ is dense in $\mathcal{H}_{code}$.

Since AdS/CFT implies that information in the bulk is encoded redundantly in the boundary, quantum error correction is a natural framework in which to elucidate the connection between holographic quantum field theories and their gravity duals [2, 102, 160, 164]. Quantum error correction with finite-dimensional Hilbert spaces has been used to argue that entanglement wedge reconstruction is identical to the Ryu–Takayanagi formula and the equivalence of bulk and boundary relative entropies [102, 159]. In order to study a more realistic toy model where boundary subregions are characterized by infinite-dimensional von Neumann algebras, we should consider quantum error correcting codes defined on infinite-dimensional Hilbert spaces.

In chapter 15, we construct a Quantum Error Correcting Code (QECC) where the physical Hilbert space and the code subspace are infinite-dimensional and admit the action of infinite-dimensional von Neumann algebras. We describe a toy model that allows us to see how a von Neumann algebra on the code subspace is reconstructed on the physical Hilbert space. Furthermore, we show that in the context of operator-algebra quantum error correction, this QECC satisfies the following two

[3] In Section 2 of [184], we justify this statement on physical grounds and review the classification of factors.

statements:

- Entanglement wedge reconstruction [89, 167, 297],
- Relative entropy equals bulk relative entropy (JLMS formula [178]).

The technical assumptions that connect entanglement wedge reconstruction and the JLMS formula are presented in Theorem 3.0.1 above.

In particular, we first show that our QECC satisfies entanglement wedge reconstruction for a particular choice of von Neumann algebras acting on the code and physical Hilbert spaces, and then we invoke Theorem 1.1 in [185] to argue that our QECC also satisfies the JLMS formula.

We also show that relative entropies defined with respect to the infinite-dimensional von Neumann algebras we consider can be expressed as limits of relative entropies defined with respect to finite-dimensional subalgebras. Thus, another way to see that our QECC satisfies the JLMS formula is to note that our QECC satisfies the JLMS formula with respect to finite-dimensional von Neumann algebras. The JLMS formula for finite-dimensional algebras is studied in [159].

3.1 Bounded and Unbounded Operators

In this section, we review some results in functional analysis that are used in the proofs of Theorems 14.1.1 and 3.0.1. In particular, we explain how to define a function of a bounded self-adjoint operator and we review the spectral theorem (for unbounded operators). We mostly follow reference [264].

Definition 3.1.1. An *operator* on a Hilbert space $\mathcal{H}$ is a linear map from its domain, a linear subspace of $\mathcal{H}$, into $\mathcal{H}$.

Definition 3.1.2. A *bounded operator* is an operator $\mathcal{O}$ that satisfies $||\mathcal{O}|\psi\rangle|| \leq K||\,|\psi\rangle||\quad \forall\,|\psi\rangle \in \mathcal{H}$ for some $K \in \mathbb{R}$. We let $\mathcal{B}(\mathcal{H})$ denote the algebra of bounded operators on $\mathcal{H}$.

Definition 3.1.3. The *commutant* of a subset $S \subset \mathcal{B}(\mathcal{H})$ is the set S' of bounded operators that commute with all operators in S, i.e. $S' = \{\mathcal{O} \in \mathcal{B}(\mathcal{H}) : \mathcal{O}\mathcal{P} = \mathcal{P}\mathcal{O}\,\forall \mathcal{P} \in S\}$. The double commutant of S is the commutant of S'.

Definition 3.1.4. A *von Neumann algebra* is an algebra of bounded operators that contains the identity operator, is closed under hermitian conjugation, and is equal to its double commutant.

Theorem 3.1.5. *Let $\mathcal{O} \in \mathcal{B}(\mathcal{H})$. Let $\{|\Psi_n\rangle\} \in \mathcal{H}$ be a sequence of vectors such that its limit vanishes, i.e.* $\lim_{n\to\infty} |\Psi_n\rangle = 0$. *Then,* $\lim_{n\to\infty} \mathcal{O}\,|\Psi_n\rangle = 0$.

Theorem 3.1.5 implies that bounded operators define a continuous linear map on the Hilbert space. Any bounded operator that annihilates a dense subspace of the Hilbert space is identically zero.

Definition 3.1.6. A *densely defined operator* on a Hilbert space $\mathcal{H}$ is an operator whose domain is a dense subspace of $\mathcal{H}$.

3.1.1 Functions of bounded operators

In this section, we will explain how to understand functions of bounded operators.

Definition 3.1.7. The *spectrum* of $\mathcal{O} \in \mathcal{B}(\mathcal{H})$ is defined as

$$\sigma(\mathcal{O}) := \{\lambda \in \mathbb{C} : \mathcal{O} - \lambda I \text{ is not invertible}\},$$

where I denotes the identity operator.

We will make use of the mathematical facts that $\sigma(\mathcal{O})$ is a nonempty closed bounded subset of $\mathbb{C}$ and that when $\mathcal{O}$ is self-adjoint, $\sigma(\mathcal{O}) \subset \mathbb{R}$ and $||\mathcal{O}|| = \sup_{\lambda \in \sigma(\mathcal{O})} |\lambda|$ [180][264].

Definition 3.1.8. Let $\mathcal{O} \in \mathcal{B}(\mathcal{H})$ be a self-adjoint operator. We denote the set of continuous $\mathbb{R}$-valued functions defined on $\sigma(\mathcal{O})$ by $C(\sigma(\mathcal{O}))$.

Definition 3.1.9. For every self-adjoint operator $\mathcal{O} \in \mathcal{B}(\mathcal{H})$, we define the L_∞ norm (denoted by $||\cdot||_\infty$) of $f \in C(\sigma(\mathcal{O}))$ by

$$||f||_\infty = \sup_{x \in \sigma(\mathcal{O})} |f(x)|.$$

Theorem 3.1.10 ([264], page 121). *Given a self-adjoint operator $\mathcal{O} \in \mathcal{B}(\mathcal{H})$, the set of polynomials (with $\mathbb{R}$-valued coefficients) is dense in $C(\sigma(\mathcal{O}))$ in the L_∞ norm.*

Definition 3.1.11. For any polynomial $p(x) = \sum_{n=0}^{N} a_n x^n$ with $a_n \in \mathbb{R}$, we define $p(\mathcal{O}) := \sum_{n=0}^{N} a_n \mathcal{O}^n$ for $\mathcal{O} \in \mathcal{B}(\mathcal{H})$.

Theorem 3.1.12 ([264], page 223). *Let $p(x) = \sum_{n=0}^{N} a_n x^n$ with $a_n \in \mathbb{R}$. Let $\mathcal{O} \in \mathcal{B}(\mathcal{H})$.*[4] *Then*

$$\sigma(p(\mathcal{O})) = \{p(\lambda) | \lambda \in \sigma(\mathcal{O})\}.$$

Theorem 3.1.13 ([264], page 223). *For any self-adjoint operator $\mathcal{O} \in \mathcal{B}(\mathcal{H})$ and any polynomial $p \in C(\sigma(\mathcal{O}))$,*

$$||p(\mathcal{O})|| = ||p||_\infty.$$

[4] Note that $\mathcal{O}$ need not be self-adjoint.

Proof. $||p(\mathcal{O})|| = \sup_{\lambda \in \sigma(p(\mathcal{O}))} |\lambda| = \sup_{\lambda \in \sigma(\mathcal{O})} |p(\lambda)| = ||p||_\infty$. □

Let $\mathcal{O} \in \mathcal{B}(\mathcal{H})$ be self-adjoint. Let P denote the space of polynomials defined on $\mathbb{R}$ with $\mathbb{R}$-valued coefficients. Define a map $\tilde{\varphi}_{\mathcal{O}} : P \to \mathcal{B}(\mathcal{H})$ such that $\tilde{\varphi}_{\mathcal{O}}(p) = p(\mathcal{O})$ for any polynomial $p \in P$. The map $\tilde{\varphi}_{\mathcal{O}}$ is a bounded linear operator because $||\tilde{\varphi}_{\mathcal{O}}(p)|| = ||p||_\infty$. Hence, $\tilde{\varphi}_{\mathcal{O}}$ may be uniquely extended to a bounded linear operator $\varphi_{\mathcal{O}} : C(\sigma(\mathcal{O})) \to \mathcal{B}(\mathcal{H})$. For $f \in C(\sigma(\mathcal{O}))$, we define $f(\mathcal{O}) := \varphi_{\mathcal{O}}(f)$. If $\{p_n\} \in P$ denotes a sequence of polynomials such that $\lim_{n\to\infty} p_n = f$ (where the limit converges in the L_∞ norm), then we may also write

$$f(\mathcal{O}) = \lim_{n\to\infty} p_n(\mathcal{O}), \tag{3.1}$$

where the limit converges in the norm topology. If $f, g \in C(\sigma(\mathcal{O}))$, then one may show [264] that $f(\mathcal{O})g(\mathcal{O}) = (fg)(\mathcal{O})$ and that $(f^*)(\mathcal{O}) = f(\mathcal{O})^\dagger$.

Theorem 3.1.14 ([180], page 19). *Let M be a von Neumann algebra. Any operator in M is a linear combination of four unitary operators in M.*

Proof. Let $\mathcal{O} \in M$. We may write

$$\mathcal{O} = \frac{1}{2}(\mathcal{O} + \mathcal{O}^\dagger) - \frac{i}{2}(i(\mathcal{O} - \mathcal{O}^\dagger)).$$

This shows that $\mathcal{O}$ may be written as a linear combination of two self-adjoint operators in M. Next, let $\mathcal{Q} \in M$ be a self-adjoint operator that satisfies $||\mathcal{Q}|| < 1$. The condition $||\mathcal{Q}|| < 1$ is important

because the function $f(x) = \sqrt{1-x^2}$ is $\mathbb{R}$-valued and continuous only for $|x| < 1$. Define $U := \mathcal{Q} + i\sqrt{1-\mathcal{Q}^2}$. Then U is unitary, $U \in \mathcal{M}$, and $\mathcal{Q} = \frac{U+U^\dagger}{2}$. □

3.1.2 Unbounded operators

Unbounded operators are generically not defined on the entire Hilbert space. The domain of an operator $\mathcal{O}$ is denoted by $D(\mathcal{O})$. The definition of $\mathcal{O}^\dagger$ is subtle when $\mathcal{O}$ is unbounded, as $\mathcal{O}^\dagger$ may not be defined on the entire Hilbert space.

Definition 3.1.15. A densely defined operator $\mathcal{O}$ is *closed* when $\mathcal{O}(\lim_{n\to\infty} |\psi_n\rangle) = \lim_{n\to\infty} \mathcal{O}\,|\psi_n\rangle$ whenever both limits exist.

Definition 3.1.16. Let $\mathcal{O}$ be a densely defined operator on $\mathcal{H}$. The domain of the adjoint $\mathcal{O}^\dagger$ is defined by

$$D(\mathcal{O}^\dagger) = \{|\varphi\rangle : \exists\, |\eta\rangle \in \mathcal{H} \text{ such that } \langle\varphi|\mathcal{O}|\psi\rangle = \langle\eta|\psi\rangle \quad \forall\, |\psi\rangle \in D(\mathcal{O})\}.$$

For $|\varphi\rangle \in D(\mathcal{O}^\dagger)$ there is precisely one $|\eta\rangle$ that satisfies the above criteron. We define

$$\mathcal{O}^\dagger\,|\varphi\rangle := |\eta\rangle\,.$$

Theorem 3.1.17 ([264], page 252)**.** *If $\mathcal{O}$ is a densely defined operator on $\mathcal{H}$, then $\mathcal{O}^\dagger$ is closed. If $\mathcal{O}$ is closed, $D(\mathcal{O}^\dagger)$ is dense in $\mathcal{H}$.*

Definition 3.1.18. A densely defined operator $\mathcal{O}$ is *self-adjoint* when $\mathcal{O} = \mathcal{O}^\dagger$. In particular, $D(\mathcal{O}) = D(\mathcal{O}^\dagger)$.

Definition 3.1.19. A densely defined operator is *positive* when $\langle\psi|\mathcal{O}|\psi\rangle \geq 0 \quad \forall\, |\psi\rangle \in D(\mathcal{O})$.

Definition 3.1.20. Let $\mathcal{O}$ be a closed operator on a Hilbert space $\mathcal{H}$. $\lambda \in \mathbb{C}$ is in the *resolvent set* of $\mathcal{O}$ if $\lambda I - \mathcal{O}$ is a bijection of $D(\mathcal{O})$ onto $\mathcal{H}$. The *spectrum* of $\mathcal{O}$, denoted $\sigma(\mathcal{O})$, is defined to be the set of all complex numbers that are not in the resolvent set of $\mathcal{O}$.

Theorem 3.1.21. *Let $\mathcal{O}$ be a self-adjoint positive operator. Then the spectrum of $\mathcal{O}$ is a subset of* $[0, \infty)$.

Proof. For any $|\chi\rangle \in D(\mathcal{O})$ and any $\lambda = \lambda_1 + i\lambda_2$ for $\lambda_1, \lambda_2 \in \mathbb{R}$, note that[5]

$$||(\mathcal{O} - \lambda I)\,|\chi\rangle\,||^2 = \lambda_2^2||\,|\chi\rangle\,||^2 + ||(\mathcal{O} - \lambda_1)\,|\chi\rangle\,||^2 \geq \lambda_2^2||\,|\chi\rangle\,||^2. \tag{3.2}$$

Let us consider the case when $\lambda_2 \neq 0$. Then $\ker(\mathcal{O}-\lambda I) = \{0\}$ so that $\mathcal{O}-\lambda I$ is an injection. Using the fact that $D(\mathcal{O})$ is dense in $\mathcal{H}$, one may show that the orthocomplement of the range of $(\mathcal{O} - \lambda I)$ is trivial, implying that the range of $(\mathcal{O} - \lambda I)$ is dense in $\mathcal{H}$. Then, the previous equation implies that if $\{|\chi_n\rangle\} \in D(\mathcal{O})$ is a sequence such that $\lim_{n\to\infty}(\mathcal{O} - \lambda I)\,|\chi_n\rangle$ exists, then $\lim_{n\to\infty}|\chi_n\rangle$ also exists. Since $\mathcal{O}$ is a closed operator, the range of $(\mathcal{O} - \lambda I)$ is also closed. Thus, $(\mathcal{O} - \lambda I)$ is a bijection from $D(\mathcal{O})$ onto $\mathcal{H}$, demonstrating that λ is in the resolvent set of $\mathcal{O}$.

[5] To be explicit, we have that

$$\langle(\mathcal{O} - \lambda I)\chi|(\mathcal{O} - \lambda I)\chi\rangle = \langle(\mathcal{O} - \lambda_1 I)\chi|(\mathcal{O} - \lambda_1 I)\chi\rangle + \langle\lambda_2\chi|\lambda_2\chi\rangle + i\lambda_2\,\langle\chi|(\mathcal{O} - \lambda_1 I)\chi\rangle - i\lambda_2\,\langle(\mathcal{O} - \lambda_1 I)\chi|\chi\rangle\,.$$

The last two terms cancel because $\mathcal{O}$ is self-adjoint and λ_1 is real.

Now, consider the case when $\lambda \in \mathbb{R}, \lambda < 0$. For any $|\chi\rangle \in D(\mathcal{O})$,

$$||(\mathcal{O} - \lambda I)\,|\chi\rangle\,||^2 = |\lambda|^2||\,|\chi\rangle\,||^2 - 2\,\langle\chi|\mathcal{O}|\chi\rangle\,\lambda + ||\mathcal{O}\,|\chi\rangle\,||^2. \tag{3.3}$$

As $\mathcal{O}$ is a positive operator,

$$||(\mathcal{O} - \lambda I)\,|\chi\rangle\,||^2 \geq |\lambda|^2||\,|\chi\rangle\,||^2. \tag{3.4}$$

The same logic used in the previous case establishes that λ is in the resolvent set of $\mathcal{O}$. Hence, the spectrum of $\mathcal{O}$ must be a subset of $[0, \infty)$. □

Theorem 3.1.22 ([264], page 316). *Let $\mathcal{O}$ be a closed operator. Then $D(\mathcal{O}^\dagger\mathcal{O}) = \{|\psi\rangle : |\psi\rangle \in D(\mathcal{O}),\ \mathcal{O}\,|\psi\rangle \in D(\mathcal{O}^\dagger)\}$ is dense in the Hilbert space and $\mathcal{O}^\dagger\mathcal{O}$ is self-adjoint and positive.*

3.1.3 The spectral theorem for unbounded operators

In this section, we closely follow [264] (pages 262-263), to which we refer the reader for more details on the spectral theorem. Note that a projection $P \in \mathcal{B}(\mathcal{H})$ is idempotent and hermitian i.e. $P = P^2 = P^\dagger$.

Definition 3.1.23. A *projection valued measure* assigns a projection P_Ω to every Borel set $\Omega \subset \mathbb{R}$ such that

- $P_\emptyset = 0, P_{(-\infty,\infty)} = I$
- $P_{\Omega_1} P_{\Omega_2} = P_{\Omega_1 \cap \Omega_2}$

- If $\Omega = \cup_{n=1}^{\infty} \Omega_n$ with $\Omega_n \cap \Omega_m = \emptyset$ if $n \neq m$, then P_Ω is a strong limit of $\sum_{n=1}^{N} P_{\Omega_n}$.

Given any vector $|\psi\rangle \in \mathcal{H}$, $\langle\psi|P_\Omega|\psi\rangle$ defines an integration measure for Borel functions, which we will use in Definition 3.1.25.

Theorem 3.1.24 (**Spectral Theorem** [264], page 263)**.** *There is a one-to-one correspondence between self-adjoint operators $\mathcal{O}$ and projection valued measures $P_\Omega^{\mathcal{O}}$. The correspondence is given by*

$$\mathcal{O} = \int_{\mathbb{R}} \lambda \, d(P_\lambda^{\mathcal{O}}).$$

The notation means that we are integrating the function $f(\lambda) = \lambda$ on $\mathbb{R}$ with the projection-valued measure given by $P_\Omega^{\mathcal{O}}$. The integral converges strongly.[6]

Intuitively, $P_\Omega^{\mathcal{O}}$ is the projection onto the "eigenspace" spanned by all "eigenvalues" in Ω. We will need that $P^{\mathcal{O}}_{(-\infty,\infty)} = P^{\mathcal{O}}_{\sigma(\mathcal{O})}$, where $\sigma(\mathcal{O})$ denotes the spectrum of $\mathcal{O}$. For the details on how the spectral projections associated with a self-adjoint operator $\mathcal{O}$ are constructed, see Theorem VIII.4 and discussions afterwards in Section VIII.3 of [264].

Definition 3.1.25. Given a self-adjoint positive operator $\mathcal{O}$, the diagonal matrix element of $\log \mathcal{O}$ is given by

$$\langle\psi| \log \mathcal{O} |\psi\rangle := \int_0^\infty \log \lambda \, d(\langle\psi|P_\lambda^{\mathcal{O}}|\psi\rangle),$$

for all $|\psi\rangle \in \mathcal{H}$ such that the above integral converges, where $P_\Omega^{\mathcal{O}}$ is the unique projection valued measure associated with $\mathcal{O}$ by the spectral theorem.

[6] For any $|\psi\rangle \in D(\mathcal{O})$, the integral $\int_{\mathbb{R}} \lambda d(P_\lambda^{\mathcal{O}} |\psi\rangle)$ with vector-valued measure $P_\Omega^{\mathcal{O}} |\psi\rangle$ converges in the Hilbert space norm to $\mathcal{O}|\psi\rangle$. The integral does not converge for $|\psi\rangle \notin D(\mathcal{O})$.

Note that $\log x$ is continuous for $x \in (0, \infty)$. Thus, $\log x$ is a Borel function. One can define a self-adjoint operator using any real-valued Borel function on $\mathbb{R}$. See page 264 of [264].

Theorem 3.1.26. *Let $\mathcal{O}$ be a self-adjoint positive operator. For all $|\psi\rangle \in D(\mathcal{O})$ such that $\langle\psi| \log \mathcal{O}|\psi\rangle$ is defined,*

$$\langle\psi| \log \mathcal{O}|\psi\rangle \leq \langle\psi|\mathcal{O}|\psi\rangle - \langle\psi|\psi\rangle \,,$$

and the inequality is saturated if and only if $\mathcal{O}\,|\psi\rangle = |\psi\rangle$.

Proof. Assume $|\psi\rangle \neq 0$. For $x > 0$, note that $\log x \leq x - 1$. It follows that

$$\langle\psi| \log \mathcal{O}|\psi\rangle = \int_0^\infty \log \lambda \, d(\langle\psi|P^{\mathcal{O}}_\lambda|\psi\rangle) \leq \int_0^\infty \lambda \, d(\langle\psi|P^{\mathcal{O}}_\lambda|\psi\rangle) - \int_0^\infty 1 \, d(\langle\psi|P^{\mathcal{O}}_\lambda|\psi\rangle). \quad (3.5)$$

The first integral on the right hand side converges because $|\psi\rangle \in D(\mathcal{O})$. The second integral converges to $\langle\psi|\psi\rangle$ because the spectrum of $\mathcal{O}$ is a subset of $[0, \infty)$, which implies that $P^{\mathcal{O}}_{[0,\infty)} = P^{\mathcal{O}}_{(-\infty,\infty)} = I$. Hence,

$$\langle\psi| \log \mathcal{O}|\psi\rangle \leq \langle\psi|\mathcal{O}|\psi\rangle - \langle\psi|\psi\rangle \,. \quad (3.6)$$

As $\log x \leq x - 1$ is only saturated for $x = 1$, the inequality in equation (3.5) is only saturated when the measure $\langle\psi|P^{\mathcal{O}}_\Omega|\psi\rangle$ is such that $\langle\psi|P^{\mathcal{O}}_\Omega|\psi\rangle = 0$ when $1 \notin \Omega$. If $1 \neq \Omega$, then $\langle\psi|P^{\mathcal{O}}_\Omega|\psi\rangle = \langle P^{\mathcal{O}}_\Omega\psi|P^{\mathcal{O}}_\Omega\psi\rangle$ implies that $P^{\mathcal{O}}_\Omega\,|\psi\rangle = 0$. If $1 \in \Omega$, then the fact that $\int_{\mathbb{R}} 1 d(\langle\psi|P^{\mathcal{O}}_\lambda|\psi\rangle) = \langle\psi|\psi\rangle$ implies that $\langle P^{\mathcal{O}}_\Omega\psi|P^{\mathcal{O}}_\Omega\psi\rangle = \langle\psi|P^{\mathcal{O}}_\Omega|\psi\rangle = \langle\psi|\psi\rangle$. For $1 \in \Omega$, note that the Cauchy-Schwartz inequality $|\,\langle\psi|P^{\mathcal{O}}_\Omega|\psi\rangle\,| \leq ||\,|\psi\rangle\,|| \cdot ||P^{\mathcal{O}}_\Omega\,|\psi\rangle\,||$ is saturated, which implies that $P^{\mathcal{O}}_\Omega\,|\psi\rangle$ is a multiple

of $|\psi\rangle$, and this multiple must be 1. Thus, for $1 \in \Omega$, $P^{\mathcal{O}}_{\Omega} |\psi\rangle = |\psi\rangle$. This implies that

$$\mathcal{O} |\psi\rangle = \int_{\mathbb{R}} \lambda \, d(P^{\mathcal{O}}_{\lambda} |\psi\rangle) = |\psi\rangle \, . \tag{3.7}$$

□

3.2 Example of a strongly convergent sequence of operators

Let us give a nontrivial example a strongly convergent sequence in A_{code}. First we will make some preliminary definitions.

3.2.1 Preliminary definitions

Consider the Hilbert space of a single qutrit. Let $V(\theta) := \begin{pmatrix} e^{i\theta} & 0 & 0 \\ 0 & e^{-i\theta} & 0 \\ 0 & 0 & 1 \end{pmatrix}$ be a unitary operator defined on this Hilbert space. Let $|\gamma\rangle$ be any normalized state of a single qutrit. Then one may show that

$$\langle \gamma | V(\theta) | \gamma \rangle = 1 + z_\gamma (1 - \cos\theta) + i \hat{z}_\gamma \sin\theta \tag{3.8}$$

where z_γ and $\hat{z}_\gamma$ are real numbers that depend on $|\gamma\rangle$ and satisfy $|z_\gamma| \leq 1$, $|\hat{z}_\gamma| \leq 1$.

Furthermore, consider the expectation value of the operator $V(\theta) \otimes I$ in a two-qutrit Hilbert

space in the state $|\lambda\rangle = \frac{1}{\sqrt{3}}(|00\rangle + |11\rangle + |22\rangle)$

$$\langle\lambda|V(\theta)\otimes I|\lambda\rangle = \frac{2\cos\theta + 1}{3} = 1 - \frac{2}{3}(1-\cos\theta). \tag{3.9}$$

3.2.2 The example

We will define a sequence of operators in A_{code} that we wish to study. First, we define a sequence of angles $\{\theta_n\}$. We will specify the actual values of $\theta_n,\ n \in \mathbb{N}$ later. We define the sequence of operators $\{a_n\} \in A_{code}$ to be

$$a_1 = \left[V_{i_1}(\theta_1)\otimes I_{j_1}\right]\otimes I\cdots \tag{3.10}$$

$$a_2 = \left[V_{i_1}(\theta_1)\otimes I_{j_1}\right]\otimes\left[V_{i_2}(\theta_2)\otimes I_{j_2}\right]\otimes I\cdots \tag{3.11}$$

$$\vdots$$

$$a_n = \left[V_{i_1}(\theta_1)\otimes I_{j_1}\right]\otimes\left[V_{i_2}(\theta_2)\otimes I_{j_2}\right]\otimes\cdots\otimes\left[V_{i_n}(\theta_n)\otimes I_{j_n}\right]\otimes I\cdots \tag{3.12}$$

$$\vdots \tag{3.13}$$

Each square brackets contains the black qutrits associated with one collection in Figure 3.3. Each of the operators in the sequence is unitary, so they all are bounded and have unit norm. Now, we want to investigate the convergence of this sequence acting on a basis vector of $p\mathcal{H}_{code}$, such as the one given in equation (15.1). Define $|\psi_n\rangle := a_n |M, \{p,q\}\rangle$ for $n \in \mathbb{N}$. Choose $n, m \in \mathbb{N}$ with $m > n$. Then we have

$$|| \, |\psi_m\rangle - |\psi_n\rangle \, ||^2 = 2 - \langle\psi_m|\psi_n\rangle - \langle\psi_n|\psi_m\rangle = 2 - \langle M, \{p,q\}|a_m^\dagger a_n|M, \{p,q\}\rangle - \langle M, \{p,q\}|a_n^\dagger a_m|M, \{p,q\}\rangle \, . \tag{3.14}$$

Note that

$$a_n^\dagger a_m = \left[I_{i_1} \otimes I_{j_1}\right] \otimes \cdots \otimes \left[I_{i_n} \otimes I_{j_n}\right] \otimes \left[V_{i_{n+1}}(\theta_{n+1}) \otimes I_{j_{n+1}}\right] \otimes \cdots \otimes \left[V_{i_m}(\theta_m) \otimes I_{j_m}\right] \otimes I \cdots \tag{3.15}$$

$$\langle M, \{p,q\}|a_n^\dagger a_m|M, \{p,q\}\rangle = \prod_{k=n+1}^{m} Y_k \tag{3.16}$$

$$Y_k = \begin{cases} \langle p_k|V_{i_k}(\theta_k)|p_k\rangle & k \leq M \\ \langle \lambda \cdots |V_{i_k}(\theta_k) \otimes I_{j_k}|\lambda \cdots\rangle & k > M \end{cases} \tag{3.17}$$

Another way to write Y_k is

$$Y_k = 1 + x_k(1 - \cos\theta_k) + iy_k \sin\theta_k = r_k e^{i\varphi_k} \tag{3.18}$$

where x_k and y_k are real numbers satisfying $|x_k| \leq 1$, $|y_k| \leq 1$. One may show that

$$1 - 2|1 - \cos\theta_k| \leq r_k \leq 1 + (1 - \cos\theta_k)^2 + 2|1 - \cos\theta_k| + \sin^2\theta_k \tag{3.19}$$

and that, if $|\theta_k| < \frac{\pi}{2}$,

$$|\varphi_k| \leq \arctan \frac{|\sin\theta_k|}{1 - |1 - \cos\theta_k|}. \tag{3.20}$$

Up until now we did not specify the choice of angles θ_k. Now, we make a choice. First, we choose an arbitrary $\eta \in \mathbb{R}$ such that $0 < \eta < 1$. We choose θ_k such that each r_k satisfies

$$e^{-\eta^k} < r_k < e^{\eta^k} \tag{3.21}$$

and such that each φ_k satisfies

$$-\eta^k < \varphi_k < \eta^k. \tag{3.22}$$

We choose each θ_k to be nonzero.

Thus,

$$\prod_{k=n+1}^{m} r_k < e^{\sum_{k=n+1}^{m} \eta^k} < e^{\frac{\eta^{n+1}}{1-\eta}}, \tag{3.23}$$

$$\prod_{k=n+1}^{m} r_k > e^{-\sum_{k=n+1}^{m} \eta^k} > e^{-\frac{\eta^{n+1}}{1-\eta}}, \tag{3.24}$$

$$|\sum_{k=n+1}^{m} \varphi_k| < \frac{\eta^{n+1}}{1-\eta}. \tag{3.25}$$

Thus, the real part of $\prod_{k=n+1}^{m} Y_k$ is arbitrarily close to 1 for n sufficiently large. This means that $|| \, |\psi_m\rangle - |\psi_n\rangle \, ||$ is arbitrarily close to 0 for n sufficiently large and $m > n$. This is enough to show that the sequence $\{|\psi_n\rangle\}$ is Cauchy, meaning that $\lim_{n\to\infty} a_n \, |\mathcal{M}, \{p, q\}\rangle$ converges for every basis vector $|\mathcal{M}, \{p, q\}\rangle$. Hence, $\lim_{n\to\infty} a_n \, |\psi\rangle$ converges for every $|\psi\rangle \in p\mathcal{H}_{code}$. Since the sequence of norms $\{||a_n||\}$ is bounded from above (in particular $||a_n|| = 1 \quad \forall n \in \mathbb{N}$) then the sequence of operators $\{a_n\}$ converges strongly.

3.3 Infinite-dimensional von Neumann algebras

In this section, we provide background information on operator algebras, including the definitions of type I, II_1, II_∞, and III factors that elucidate their relevance to physics. We also prove theorems that are useful for constructing our infinite-dimensional QECC. First, we review the notion of Hilbert space and bounded operators in Section 3.3.1. With these notions, we recall basic theorems about Hilbert spaces, operators, and boundedness. Based on those, we explain the operator topologies in Section 3.3.2. Then we introduce relevant theorems and present definitions of von Neumann algebras in a physics-friendly manner in Section 3.4. We review the different types of von Neumann algebra factors in Section 3.4.1. This section mainly draws upon [180], [Landsman], and [264].

3.3.1 Hilbert Space and Bounded Operators

Definition 3.3.1. A *Hilbert space* is a complex vector space $\mathcal{H}$ with the inner product

$$\langle \cdot | \cdot \rangle : \mathcal{H} \times \mathcal{H} \to \mathbb{C}$$

that satisfies the following properties:

1. The inner product is linear in the second variable,
2. The inner product satisfies $\overline{\langle \xi | \eta \rangle} = \langle \eta | \xi \rangle$,
3. The inner product is positive definite ($\langle \xi | \xi \rangle > 0$ for $|\xi\rangle \neq 0$),
4. The vector space $\mathcal{H}$ is complete for the norm defined by $|| \, |\xi\rangle \, || = \sqrt{\langle \xi | \xi \rangle}$.

A Hilbert space is complete when all Cauchy sequences converge. A *pre-Hilbert space* has the same properties as a Hilbert space except that it is not complete.

Definition 3.3.2. A Hilbert space is *separable* when it has an orthonormal basis, or a sequence $\{|e_i\rangle\}$ of unit vectors such that $\langle e_i | e_j \rangle = 0 \quad \forall i \neq j$ and 0 is the only element of $\mathcal{H}$ orthogonal to all of the $|e_i\rangle$.

Definition 3.3.3. Given two Hilbert spaces $\mathcal{H}$ and $\mathcal{K}$, a linear operator $\mathcal{O} : \mathcal{H} \to \mathcal{K}$ is *bounded* when $||\mathcal{O} \, |\xi\rangle \, || \leq K || \, |\xi\rangle \, || \quad \forall \, |\xi\rangle \in \mathcal{H}$ for some number K. The infimum of all such K is called the *norm* of $\mathcal{O}$, i.e. $||\mathcal{O}||$. The set of bounded operators from $\mathcal{H} \to \mathcal{H}$ is denoted as $\mathcal{B}(\mathcal{H})$.

Theorem 3.3.4 (Uniform Boundedness Principle [282]). *Let* $\{\mathcal{O}_n\} \in \mathcal{B}(\mathcal{H})$ *be a sequence of operators such that* $\lim_{n\to\infty} \mathcal{O}_n |\chi\rangle$ *converges for every* $|\chi\rangle \in \mathcal{H}$*. Then, the sequence of norms* $\{||\mathcal{O}_n||\}$ *is bounded from above.*[7]

Theorem 3.3.5. *If* $\{\mathcal{O}_n\} \in \mathcal{B}(\mathcal{H})$ *is a sequence of operators whose norms are bounded from above and* $\lim_{n\to\infty} \mathcal{O}_n |\psi\rangle$ *converges for all* $|\psi\rangle$ *in a dense subspace of* $\mathcal{H}$*, then* $\lim_{n\to\infty} \mathcal{O}_n |\Upsilon\rangle$ *converges for all* $|\Upsilon\rangle \in \mathcal{H}$*.*

Proof. Note that $||(\mathcal{O}_n - \mathcal{O}_m)|\Upsilon\rangle|| \leq (||\mathcal{O}_n|| + ||\mathcal{O}_m||)||\,|\Upsilon\rangle - |\psi\rangle\,|| + ||(\mathcal{O}_n - \mathcal{O}_m)|\psi\rangle||$. We are given that $\{\mathcal{O}_n |\psi\rangle\}$ is a Cauchy sequence. Given $\varepsilon > 0$, choose $|\psi\rangle$ such that $(||\mathcal{O}_n|| + ||\mathcal{O}_m||)||\,|\Upsilon\rangle - |\psi\rangle\,|| < \frac{\varepsilon}{2}$. Then, choose N such that for all $n, m > N$, $||(\mathcal{O}_n - \mathcal{O}_m)|\psi\rangle|| < \frac{\varepsilon}{2}$. Hence, $\{\mathcal{O}_n |\Upsilon\rangle\}$ is a Cauchy sequence. □

Theorem 3.3.6 (Bounded Linear Transformation (BLT) Theorem [264]). *Suppose* $\mathcal{O}$ *is a bounded linear transformation from a pre-Hilbert space* $p\mathcal{H}$ *to a Hilbert space* $\mathcal{H}$*. Then* $\mathcal{O}$ *can be uniquely extended to a bounded linear operator (with the same norm) from the completion of* $p\mathcal{H}$ *to* $\mathcal{H}$*.*

Definition 3.3.7. An operator $\mathcal{O} \in \mathcal{B}(\mathcal{H})$ is

- *self-adjoint* if $\mathcal{O}^\dagger = \mathcal{O}$,
- a *projection* if $\mathcal{O} = \mathcal{O}^\dagger = \mathcal{O}^2$,
- *positive* if $\langle\xi|\mathcal{O}|\xi\rangle \geq 0 \quad \forall\, |\xi\rangle \in \mathcal{H}$ (thus $\mathcal{O}_1 \geq \mathcal{O}_2$ if $\mathcal{O}_1 - \mathcal{O}_2$ is positive),

[7] The Uniform Boundedness Principle is true in a more general setting, but we are only interested in the special case given here.

- an *isometry* if $\mathcal{O}^\dagger \mathcal{O} = 1$,
- *unitary* if $\mathcal{O}^\dagger \mathcal{O} = \mathcal{O}\mathcal{O}^\dagger = 1$,
- a *partial isometry* if $\mathcal{O}^\dagger \mathcal{O}$ is a projection.

One can also define an isometry more generally as a norm-preserving map from one Hilbert space to a different Hilbert space. An example is the isometry from $\mathcal{H}_{code}$ to $\mathcal{H}_{phys}$ considered in Theorem 3.0.1.

Definition 3.3.8. If $S \subset \mathcal{B}(\mathcal{H})$, then the *commutant* S' is $\{\mathcal{O} \in \mathcal{B}(\mathcal{H}) : \mathcal{O}\mathcal{P} = \mathcal{P}\mathcal{O} \quad \forall \mathcal{P} \in S\}$.

Theorem 3.3.9. *Let $|e_i\rangle$, $i \in \mathbb{N}$ be an orthonormal basis of a Hilbert space $\mathcal{H}$. Let $\mathcal{O} \in \mathcal{B}(\mathcal{H})$. Then*

$$\lim_{n\to\infty} \sum_{i=1}^{n} \sum_{j=1}^{n} |e_i\rangle \langle e_i|\mathcal{O}|e_j\rangle \langle e_j|\chi\rangle = \mathcal{O}|\chi\rangle \quad \forall |\chi\rangle \in \mathcal{H}. \tag{3.26}$$

Proof. For $n, m \in \mathbb{N}$, define

$$S_{n,m} := \sum_{i=1}^{n} \sum_{j=1}^{m} |e_i\rangle \langle e_i|\mathcal{O}|e_j\rangle \langle e_j| . \tag{3.27}$$

Let $|\chi\rangle \in \mathcal{H}$. Note that

$$\begin{aligned} S_{n,m}|\chi\rangle - \mathcal{O}|\chi\rangle = &\left[\sum_{i=1}^{n} |e_i\rangle \langle e_i| \mathcal{O} - \mathcal{O}\right] |\chi\rangle \\ &- \left[\sum_{i=1}^{n} |e_i\rangle \langle e_i| \mathcal{O} - \mathcal{O}\right] \sum_{j=m+1}^{\infty} |e_j\rangle \langle e_j|\chi\rangle + \left[\sum_{j=1}^{m} \mathcal{O}|e_j\rangle \langle e_j| - \mathcal{O}\right] |\chi\rangle . \end{aligned} \tag{3.28}$$

We will evaluate the norm of the above equation and use the triangle inequality on the right hand side. We need the inequality

$$\begin{aligned} &|| \left[\sum_{i=1}^{n} |e_i\rangle \langle e_i| \mathcal{O} - \mathcal{O} \right] \sum_{j=m+1}^{\infty} |e_j\rangle \langle e_j|\chi\rangle \, || \leq || \sum_{i=1}^{n} |e_i\rangle \langle e_i| \mathcal{O} - \mathcal{O}|| \cdot || \sum_{j=m+1}^{\infty} |e_j\rangle \langle e_j|\chi\rangle \, || \\ &\leq K|| \sum_{j=m+1}^{\infty} |e_j\rangle \langle e_j|\chi\rangle \, ||, \end{aligned} \tag{3.29}$$

where $K > 0$ is some constant. This inequality follows from the fact that the limit

$$\lim_{n\to\infty} \left[\sum_{i=1}^{n} |e_i\rangle \langle e_i| \mathcal{O} - \mathcal{O} \right] |\psi\rangle \tag{3.30}$$

converges for all $|\psi\rangle \in \mathcal{H}$, which implies that the set

$$\{|| \sum_{i=1}^{n} |e_i\rangle \langle e_i| \mathcal{O} - \mathcal{O}|| : n \in \mathbb{N}\}$$

is bounded (see Theorem 3.3.4). Thus,

$$\begin{aligned} ||S_{n,m} |\chi\rangle - \mathcal{O} |\chi\rangle \, || \leq & || \left[\sum_{i=1}^{n} |e_i\rangle \langle e_i| \mathcal{O} - \mathcal{O} \right] |\chi\rangle \, || \\ & + K|| \sum_{j=m+1}^{\infty} |e_j\rangle \langle e_j|\chi\rangle \, || + || \left[\sum_{j=1}^{m} \mathcal{O} |e_j\rangle \langle e_j| - \mathcal{O} \right] |\chi\rangle \, ||. \end{aligned} \tag{3.31}$$

Given any $\varepsilon > 0$, there exists an $M \in \mathbb{N}$ such that for $m > M$,

$$K||\sum_{j=m+1}^{\infty} |e_j\rangle \langle e_j|\chi\rangle || < \frac{\varepsilon}{3}, \quad || \left[\sum_{j=1}^{m} \mathcal{O} |e_j\rangle \langle e_j| - \mathcal{O}\right] |\chi\rangle || < \frac{\varepsilon}{3}. \tag{3.32}$$

There also exists an $N \in \mathbb{N}$ such that for $n > N$,

$$|| \left[\sum_{i=1}^{n} |e_i\rangle \langle e_i| \mathcal{O} - \mathcal{O}\right] |\chi\rangle || < \frac{\varepsilon}{3}. \tag{3.33}$$

Thus, there exist $N, M \in \mathbb{N}$ such that $||S_{n,m} |\chi\rangle - \mathcal{O} |\chi\rangle || < \varepsilon$ for $n > N$ and $m > M$. Hence,

$$\lim_{n\to\infty} \sum_{i=1}^{n} \sum_{j=1}^{n} |e_i\rangle \langle e_i|\mathcal{O}|e_j\rangle \langle e_j|\chi\rangle = \lim_{n\to\infty} S_{n,n} |\chi\rangle = \mathcal{O} |\chi\rangle \quad \forall |\chi\rangle \in \mathcal{H}. \tag{3.34}$$

□

Remark 3.3.10. Naively, the equation (3.26) in Theorem 3.3.9 can be thought of as a trivial consequence of the statement that for all $|\chi\rangle$ in $\mathcal{H}$,

$$\lim_{n\to\infty} \lim_{m\to\infty} \sum_{i=1}^{n} \sum_{j=1}^{m} |e_i\rangle \langle e_i|\mathcal{O}|e_j\rangle \langle e_j|\chi\rangle = \lim_{m\to\infty} \lim_{n\to\infty} \sum_{i=1}^{n} \sum_{j=1}^{m} |e_i\rangle \langle e_i|\mathcal{O}|e_j\rangle \langle e_j|\chi\rangle = \mathcal{O} |\chi\rangle$$

However despite the fact that the statement is always true, the equation (3.26) does not follow directly, which makes the Theorem 3.3.9 to be nontrivial. This can be easily demonstrated by the following counter example where the statement holds where the equation (3.26) does not hold. Con-

sider the double-sequence $a_{n,m} \in \mathbb{R}$, indexed by $n, m \in \mathbb{N}$, which is defined as

$$a_{n,m} := \frac{1}{\frac{m}{n} + \frac{n}{m}}. \tag{3.35}$$

One can check that

$$\lim_{n\to\infty} \lim_{m\to\infty} a_{n,m} = \lim_{m\to\infty} \lim_{n\to\infty} a_{n,m} = 0. \tag{3.36}$$

However, we get a nonzero limit of $a_{n,n}$ such that

$$\lim_{n\to\infty} a_{n,n} = \frac{1}{2}. \tag{3.37}$$

This demonstrates that the Theorem 3.3.9 is not a simple consequence of the definition of a limit. Our proof of Theorem 3.3.9 makes use of Theorem 3.3.4, which is demonstrated above in its proof.

3.3.2 Topologies on $\mathcal{B}(\mathcal{H})$

A topology on $\mathcal{B}(\mathcal{H})$ is a family of subsets of $\mathcal{B}(\mathcal{H})$ that are defined to be open. This family must contain both the empty set $\emptyset$ and $\mathcal{B}(\mathcal{H})$ itself. Furthermore, this family must be closed under finite intersections and arbitrary unions. There are various notions of open sets in $\mathcal{B}(\mathcal{H})$; we list their definitions below, closely following [180]. In this section $\mathcal{O}$ denotes an operator in $\mathcal{B}(\mathcal{H})$ and $|\xi_i\rangle$, $|\eta_i\rangle$ denote states in $\mathcal{H}$.

Definition 3.3.11. The *norm (or uniform) topology* is induced by the operator norm $||\mathcal{O}||$. It is the

smallest topology that contains the following basic neighborhoods:

$$\mathcal{N}(\mathcal{O}, \varepsilon) = \{\mathcal{P} \in \mathcal{B}(\mathcal{H}) : ||\mathcal{P} - \mathcal{O}|| < \varepsilon\}.$$

Definition 3.3.12. The *strong operator topology* is the smallest topology that contains the following basic neighborhoods:

$$\mathcal{N}(\mathcal{O}, |\xi_1\rangle, |\xi_2\rangle, \ldots, |\xi_n\rangle, \varepsilon) = \{\mathcal{P} \in \mathcal{B}(\mathcal{H}) : ||(\mathcal{P} - \mathcal{O})|\xi_i\rangle|| < \varepsilon \quad \forall i \in \{1, 2, \cdots, n\}\}.$$

A sequence of bounded operators $\{\mathcal{O}_n\}$ converges strongly if and only if $\lim_{n\to\infty} \mathcal{O}_n |\psi\rangle$ converges for all $|\psi\rangle \in \mathcal{H}$. Note that the hermitian conjugates $\mathcal{O}_n^\dagger$ need not converge strongly. We will sometimes use s-lim to denote a strong limit.

Definition 3.3.13. The *weak operator topology* is the smallest topology that contains the following basic neighborhoods:

$$\mathcal{N}(\mathcal{O}, |\xi_1\rangle, \ldots, |\xi_n\rangle, |\eta_1\rangle, \ldots, |\eta_n\rangle, \varepsilon) = \{\mathcal{P} \in \mathcal{B}(\mathcal{H}) : |\langle\eta_i|(\mathcal{P} - \mathcal{O})|\xi_i\rangle| < \varepsilon \quad \forall i \in \{1, 2, \cdots, n\}\}.$$

A sequence of bounded operators $\{\mathcal{O}_n\}$ converges weakly if and only if $\lim_{n\to\infty} \langle\chi|\mathcal{O}_n|\psi\rangle$ converges for all $|\chi\rangle, |\psi\rangle \in \mathcal{H}$. We will sometimes use w-lim to denote a weak limit.

Definition 3.3.14. The *ultraweak operator topology* is the smallest topology that contains the fol-

lowing basic neighborhoods:

$$\mathcal{N}(\mathcal{O}, \{|\xi_i\rangle\}, \{|\eta_i\rangle\}, \varepsilon) = \{\mathcal{P} \in \mathcal{B}(\mathcal{H}) : \sum_{i=1}^{\infty} |\, \langle\eta_i|(\mathcal{P} - \mathcal{O})|\xi_i\rangle \,| < \varepsilon\},$$

where the sequences $\{|\xi_i\rangle\}$ and $\{|\eta_i\rangle\}$ satisfy

$$\sum_{i=1}^{\infty}(||\,|\xi_i\rangle\,||^2 + ||\,|\eta_i\rangle\,||^2) < \infty.$$

Given topologies A and B, we say that topology A is stronger than topology B when every open set in topology B is also open in topology A. The relations between the various operator topologies are given in Figure 3.1.

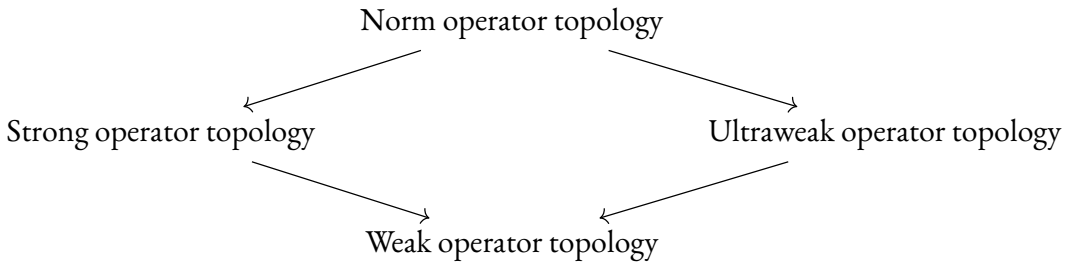

Figure 3.1: The norm operator topology is stronger than the strong operator topology and the ultraweak operator topology, which are both stronger than the weak operator topology.

3.4 Definition of von Neumann algebras

In this section, we define von Neumann algebras, factors, and hyperfinite von Neumann algebras.

Definition 3.4.1. A $\star$*-algebra* is an algebra of operators that is closed under hermitian conjugation.

Theorem 3.4.2 ([180], page 12). *Let M be a $\star$-subalgebra of $\mathcal{B}(\mathcal{H})$ that contains the identity operator. Then $M'' = \overline{M}$, where closure[8] is taken in the strong operator topology.*

Theorem 3.4.3 ([180], page 12). *If M is a $\star$-subalgebra of $\mathcal{B}(\mathcal{H})$ that contains the identity operator, then the following statements are equivalent:*

- $M = M''$,
- *M is closed in the strong operator topology,*
- *M is closed in the weak operator topology.*

Definition 3.4.4. A *von Neumann algebra* is an algebra that satisfies the statements in Theorem 3.4.3.

Given a $\star$-subalgebra of $\mathcal{B}(\mathcal{H})$ containing the identity, we can generate a von Neumann algebra by taking either the double commutant or the closure in the strong or weak topology.

Definition 3.4.5. A *factor* is a von Neumann algebra M with trivial center. That is,

$$M \cap M' = \{\lambda I : \lambda \in \mathbb{C}\},$$

where I denotes the identity operator.

Definition 3.4.6. A von Neumann algebra M is *hyperfinite* if $M = (\cup_n M_n)''$ for a sequence $\{M_n\}$ of finite-dimensional von Neumann subalgebras of M that satisfies $M_n \subset M_{n+1} \quad \forall n \in \mathbb{N}$.

[8] A set is closed if its complement is open. The closure of a set S, denoted $\overline{S}$, is the smallest closed set that contains S.

Note that the union of finitely many closed sets is also closed. However, the union of infinitely many closed sets need not be closed. In section 15.2, we define a hyperfinite von Neumann algebra by taking the closure of an infinite union of finite-dimensional von Neumann algebras. The closure introduces additional operators into the algebra.

Definition 3.4.7. If M is a von Neumann algebra, a non-zero projection $p \in M$ is called *minimal* if, for any other projection q, $q \leq p \implies (q = 0 \text{ or } q = p)$.

Definition 3.4.8. Let A be a $\star$-algebra that contains the identity operator I. Let $T : A \to \mathbb{C}$ be a linear function on A. The map T is

- *positive* if $T(\mathcal{O}^\dagger \mathcal{O}) \geq 0$ and $T(\mathcal{O}^\dagger) = T(\mathcal{O})^* \quad \forall \mathcal{O} \in A$,
- *normalized* if $T(I) = 1$,
- a *state* if T is positive and normalized,
- *faithful* if $T(\mathcal{O}^\dagger \mathcal{O}) = 0 \implies \mathcal{O} = 0 \quad \forall \mathcal{O} \in A$,
- *tracial* (or a *trace*) if $T(\mathcal{O}_1 \mathcal{O}_2) = T(\mathcal{O}_2 \mathcal{O}_1) \quad \forall \mathcal{O}_1, \mathcal{O}_2 \in A$.

Given any normalized Hilbert space vector $|\Psi\rangle$ and a von Neumann algebra $M \subset \mathcal{B}(\mathcal{H})$, one can naturally define an associated state $T_\Psi : M \to \mathbb{C}$ as

$$T_\Psi(\mathcal{O}) := \langle \Psi | \mathcal{O} | \Psi \rangle \quad \forall \mathcal{O} \in M.$$

For this reason, the term "state" is often used to refer to both Hilbert space vectors and positive, normalized linear functions of a von Neumann algebra.

3.4.1 Classification of von Neumann algebras

In this section, we review the classification of von Neumann algebra factors in a manner to have a direct consequence in physics. We first review type I factors, which are the only factors relevant for finite-dimensional Hilbert spaces. We then review type II factors. We explicitly construct type II_1 factors from our tensor network model in Section 15.2. We finally review type III factors. We explain why among type III factors we only expect type III_1 factors to arise as algebras in local quantum field theories.

Type I factors

Definition 3.4.9. A factor with a minimal projection is called a *type I factor*.

Definition 3.4.10. A type I factor that is isomorphic[9] to the algebra of bounded operators on a Hilbert space of dimension n is a *type I_n factor*.

Definition 3.4.11. A type I factor that is isomorphic to the algebra of bounded operators on an infinite-dimensional Hilbert space is a *type I_∞ factor*.

[9] We say that the von Neumann algebras M_1 and M_2, which may act on different Hilbert spaces, are *isomorphic* when there exists a bijection between M_1 and M_2 that preserves linear combinations, products, and adjoints. We refer the reader to section III.2.1 of [155] for more details.

Type II factors

Definition 3.4.12. *A type II_1 factor* is an infinite-dimensional factor M on $\mathcal{H}$ that admits a non-zero linear function $\mathrm{tr} : M \to \mathbb{C}$ satisfying the following properties:

- $\mathrm{tr}(\mathcal{O}_1\mathcal{O}_2) = \mathrm{tr}(\mathcal{O}_2\mathcal{O}_1) \quad \forall \mathcal{O}_1, \mathcal{O}_2 \in M$,
- $\mathrm{tr}(\mathcal{O}^\dagger\mathcal{O}) \geq 0 \quad \forall \mathcal{O} \in M$,
- tr is ultraweakly continuous.

Theorem 3.4.13 ([180], page 39). *Let M be a von Neumann algebra with a positive ultra-weakly continuous faithful normalized trace tr. Then M is a type II_1 factor if and only if $Tr = tr$ for all ultraweakly continuous normalized traces Tr.*

Theorem 3.4.14 ([180], page 109). *Up to isomorphisms, there is a unique hyperfinite type II_1 factor.*

Definition 3.4.15 ([180], page 57). A type II_∞ factor is a factor of the form $M \otimes \mathcal{B}(\mathcal{H})$ with M a type II_1 factor and $\dim \mathcal{H} = \infty$.

Type III factors

In order to define the von Neumann algebra of type III factor, we first recall the definition of the invariant using the modular operator, which is presented in section 15.7.

Definition 3.4.16. If M is a von Neumann algebra, the invariant $S(M)$ is the intersection over all faithful normal states φ of the spectra of their corresponding modular operators Δ_φ.

Note that each cyclic and separating vector in the Hilbert space defines a faithful normal state. Thus, for every cyclic and separating vector $|\Psi\rangle$, $S(\mathcal{M})$ is a subset of the spectrum of the modular operator Δ_Ψ. With the intersection $S(\mathcal{M})$, we can define the type III factor.

Definition 3.4.17. A factor $\mathcal{M}$ is of type III if and only if $0 \in S(\mathcal{M})$.

When $0 \in S(\mathcal{M})$, every modular operator Δ_Ψ is not a bijection of $D(\Delta_\Psi)$ onto $\mathcal{H}$.[10] It follows that the inverse of every modular operator is not defined on the entire Hilbert space. This is exactly desired for a local quantum field theory because the inverse of a modular operator is the modular operator defined with respect to the commutant:

$$\Delta_\Psi^{-1} = \Delta'_\Psi. \tag{3.38}$$

As shown in [307], Δ'_Ψ should not be bounded and thus should not be defined on the entire Hilbert space. If $0 \notin S(\mathcal{M})$, then there exists a state whose modular operator defined with respect to $\mathcal{M}'$ is bounded. Hence we expect the condition $0 \in S(\mathcal{M})$ to be satisfied by the algebras arising from a physical local quantum field theory.

[10] This is a direct consequence of the definitions of the spectrum and the resolvent set. We let $D(\mathcal{O})$ denote the domain of operator $\mathcal{O}$. See section 2.2 of [185] for more information.

Definition 3.4.18. The *spectrum* of $\mathcal{O} \in \mathcal{B}(\mathcal{H})$ is defined as

$$\sigma(\mathcal{O}) := \{\lambda \in \mathbb{C} : \mathcal{O} - \lambda I \text{ is not invertible}\},$$

where I denotes the identity operator.

Definition 3.4.19. Let $\mathcal{O}$ be a closed operator on a Hilbert space $\mathcal{H}$. $\lambda \in \mathbb{C}$ is in the *resolvent set* of $\mathcal{O}$ if $\lambda I - \mathcal{O}$ is a bijection of $D(\mathcal{O})$ onto $\mathcal{H}$. The *spectrum* of $\mathcal{O}$, denoted $\sigma(\mathcal{O})$, is defined to be the set of all complex numbers that are not in the resolvent set of $\mathcal{O}$.

Definition 3.4.20. A factor M is called type III_λ for $0 \leq \lambda \leq 1$ if

$$\lambda = 0 \implies S(M) = \{0\} \cup \{1\}, \tag{3.39}$$

$$0 < \lambda < 1 \implies S(M) = \{0\} \cup \{\lambda^n : n \in \mathbb{Z}\}, \tag{3.40}$$

$$\lambda = 1 \implies S(M) = \{0\} \cup \mathbb{R}^+. \tag{3.41}$$

We expect a local quantum field theory to have a continuous spectrum of the modular operator Δ_Ψ. Thus we see that the von Neumann algebra of type III_1 factor is the only factor that is relevant to physics among all possible type III factors.

We can also use $S(M)$ to characterize factors of types I or II. For such factors, $S(M)$ is given by the following theorem.

Theorem 3.4.21 ([285])**.** *Let M be a type I or type II factor on a separable Hilbert space. Let $S(M)$ be the invariant given in Definition 3.4.16. Then $S(M) = \{0, 1\}$ if M is of type I_∞ or II_∞ and $S(M) = \{1\}$ otherwise.*

3.5 Review of Tomita-Takesaki theory

Previous works on entanglement entropy and AdS/CFT [71, 74, 102, 178] have used the definition for the relative entropy as $S(\rho, \sigma) = \mathrm{Tr}\,(\rho \log \rho - \rho \log \sigma)$. Since $S(\rho, \sigma)$ does not increase upon performing a partial trace on ρ and σ, the relative entropy may be intuitively thought of as a measure of distinguishability between two states. Araki's definition of the relative entropy [15] also has a

monotonicity property, and it reduces to $S(\rho, \sigma)$ when the Hilbert space is finite-dimensional [307]. Hence, we might expect that statements about relative entropy in AdS/CFT can be reformulated for infinite-dimensional Hilbert spaces.

We want to understand the connection between entanglement wedge reconstruction and the equivalence of bulk and boundary relative entropies in infinite dimensional Hilbert spaces, using Tomita-Takesaki theory. Tomita-Takesaki theory provides us with the relative modular operator which is used to define the relative entropy. In this section, we review properties of the relative modular operator and the definition of the relative entropy, following [15, 180, 307].

Definition 3.5.1. A vector $|\Psi\rangle \in \mathcal{H}$ is said to be *cyclic* with respect to a von Neumann algebra M when the set of vectors $\mathcal{O}|\Psi\rangle$ for $\mathcal{O} \in M$ is dense in $\mathcal{H}$.

Definition 3.5.2. A vector $|\Psi\rangle \in \mathcal{H}$ is *separating* with respect to a von Neumann algebra M when zero is the only operator in M that annihilates $|\Psi\rangle$. That is, $\mathcal{O}|\Psi\rangle = 0 \implies \mathcal{O} = 0$ for $\mathcal{O} \in M$.

Given a von Neumann algebra $M \subset \mathcal{B}(\mathcal{H})$ and a vector $|\Psi\rangle \in \mathcal{H}$, we may define a map $e_\Psi : M \to \mathcal{H} : \mathcal{O} \mapsto \mathcal{O}|\Psi\rangle$. $\mathcal{H}$ is the closure of the image of e_Ψ iff $|\Psi\rangle$ is cyclic with respect to M. Also, $\ker e_\Psi = \{0\}$[11] iff $|\Psi\rangle$ is separating with respect to M.

Definition 3.5.3. Let $|\Psi\rangle, |\Phi\rangle \in \mathcal{H}$ and M be a von Neumann algebra. The *relative Tomita operator* is the operator $S_{\Psi|\Phi}$ that acts as

$$S_{\Psi|\Phi}|x\rangle := |y\rangle$$

[11] In other words, e_Ψ is an injective map.

for any sequence $\{\mathcal{O}_n\} \in M$ such that the limits $|x\rangle = \lim_{n\to\infty} \mathcal{O}_n |\Psi\rangle$ and $|y\rangle = \lim_{n\to\infty} \mathcal{O}_n^\dagger |\Phi\rangle$ both exist.

The relative Tomita operator $S_{\Psi|\Phi}$ is well-defined on a dense subset of the Hilbert space if and only if $|\Psi\rangle$ is cyclic and separating with respect to M.[12] Note that $S_{\Psi|\Phi}$ is a closed operator.

Theorem 3.5.4 ([180], page 94)**.** *Let $|\Psi\rangle, |\Phi\rangle \in \mathcal{H}$ both be cyclic and separating with respect to a von Neumann algebra M. Let $S_{\Psi|\Phi}$ and $S'_{\Psi|\Phi}$ be the relative Tomita operators defined with respect to M and its commutant M' respectively. Then*

$$S^\dagger_{\Psi|\Phi} = S'_{\Psi|\Phi},\ S'^\dagger_{\Psi|\Phi} = S_{\Psi|\Phi}. \tag{3.42}$$

Definition 3.5.5. Let $S_{\Psi|\Phi}$ be a relative Tomita operator and $|\Psi\rangle \in \mathcal{H}$ be cyclic and separating with respect to a von Neumann algebra M. The *relative modular operator* is

$$\Delta_{\Psi|\Phi} := S^\dagger_{\Psi|\Phi} S_{\Psi|\Phi}.$$

If $|\Phi\rangle$ is replaced with $\mathcal{O}' |\Phi\rangle$, where $\mathcal{O}' \in M'$ is unitary, then the relative modular operator remains unchanged [307]:

$$\Delta_{\Psi|\Phi} = \Delta_{\Psi|\mathcal{O}'\Phi}. \tag{3.43}$$

Definition 3.5.6 ([15])**.** Let $|\Psi\rangle, |\Phi\rangle \in \mathcal{H}$ and $|\Psi\rangle$ be cyclic and separating with respect to a von

[12] $S_{\Psi|\Phi}$ is well-defined if and only if $\lim_{n\to\infty} \mathcal{O}_n |\Psi\rangle = 0 \implies \lim_{n\to\infty} \mathcal{O}_n^\dagger |\Psi\rangle = 0$. See footnote 14 of [307] for a proof of why this is true. $S_{\Psi|\Phi}$ is densely defined because $|\Psi\rangle$ is cyclic with respect to M.

Neumann algebra M. Let $\Delta_{\Psi|\Phi}$ be a relative modular operator. The *relative entropy* with respect to M of $|\Psi\rangle$ is

$$\mathcal{S}_{\Psi|\Phi}(M) = -\langle\Psi| \log \Delta_{\Psi|\Phi} |\Psi\rangle .$$

Note that the relative entropy $\mathcal{S}_{\Psi|\Phi}(M)$ is nonnegative and it vanishes precisely when $|\Phi\rangle = \mathcal{O}'|\Psi\rangle$ for a unitary $\mathcal{O}' \in M'$.

Definition 3.5.7. Let M be a von Neumann algebra on $\mathcal{H}$ and $|\Psi\rangle$ be a cyclic and separating vector for M. The *Tomita operator* S_Ψ is

$$S_\Psi := S_{\Psi|\Psi},$$

where $S_{\Psi|\Psi}$ is the relative modular operator defined with respect to M. The *modular operator* $\Delta_\Psi = S_\Psi^\dagger S_\Psi$ and the *antiunitary operator* J_Ψ are the operators that appear in the polar decomposition of S_Ψ such that

$$S_\Psi = J_\Psi \Delta_\Psi^{1/2}.$$

Theorem 3.5.8 (Tomita-Takesaki [288])**.** *Let M be a von Neumann algebra on $\mathcal{H}$ and let $|\Psi\rangle$ be a cyclic and separating vector for M. Then*

- $J_\Psi M J_\Psi = M'$.
- $\Delta_\Psi^{it} M \Delta_\Psi^{-it} = M \quad \forall t \in \mathbb{R}$.

Theorem 3.5.8 is important because it allows us to interpret Δ_Ψ as the operator that generates a modular flow on M. Suppose that the Hilbert space $\mathcal{H}$ factorizes as $\mathcal{H} = \mathcal{H}_\ell \otimes \mathcal{H}_r$. For concrete-

ness, we may intuitively think of $\mathcal{H}_\ell$ as a Hilbert space that corresponds to the left Rindler wedge of Minkowski space, while $\mathcal{H}_r$ corresponds to the right Rindler wedge.

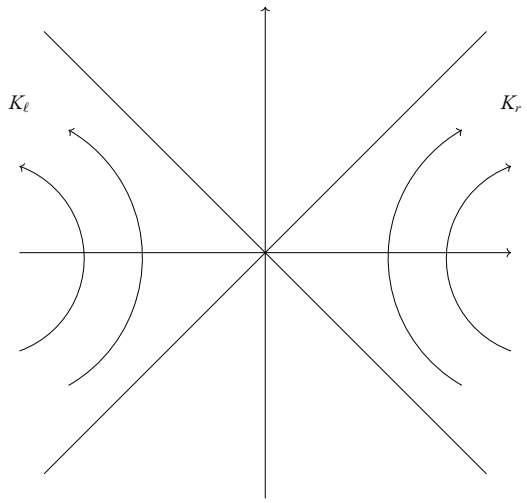

Figure 3.2: Two Rindler wedges in Minkowski space. The generators K_r and K_ℓ correspond to boosts, as shown.

For a given state $|\Psi\rangle \in \mathcal{H}$, if we define

$$\rho := |\Psi\rangle\langle\Psi|, \quad \rho_\ell := \mathrm{Tr}_r\, \rho, \quad \rho_r := \mathrm{Tr}_\ell\, \rho, \tag{3.44}$$

then the reduced density matrices ρ_ℓ and ρ_r generate a modular flow on operators that act on $\mathcal{H}_\ell$ and $\mathcal{H}_r$, respectively. The modular operator Δ_Ψ corresponding to the von Neumann algebra that acts nontrivially on $\mathcal{H}_\ell$ is then given by

$$\Delta_\Psi = \rho_\ell \otimes \rho_r^{-1}. \tag{3.45}$$

When $|\Psi\rangle$ is the vacuum and $\mathcal{H}_\ell$ and $\mathcal{H}_r$ correspond to Rindler wedges, we have that

$$\rho_\ell = e^{-2\pi K_\ell}, \quad \rho_r = e^{-2\pi K_r}, \tag{3.46}$$

where K_ℓ and K_r are the boost generators that act respectively on the left and right wedges (see Figure 3.2). The modular operator Δ_Ψ is then given by

$$\Delta_\Psi = e^{-2\pi(K_\ell - K_r)}. \tag{3.47}$$

In this context, Theorem 3.5.8 states that the modular flow maps operators in a Rindler wedge to operators in the same Rindler wedge. Thus, the algebraically defined modular flow in Theorem 3.5.8 has a geometric interpretation. This is an example of *modular covariance*, which is the property that the modular flow is a spacetime symmetry. The unitary group generated by the modular operator associated with the vacuum state implements the Lorentz boosts that leave the Rindler wedges invariant. The antiunitary operator J corresponds to the operator CRT, where C denotes charge conjugation, R is a reflection that maps one wedge into the other, and T is time reversal [32].

One of the findings of [178] is that bulk modular flow is dual to boundary modular flow. As an intermediate step in proving the equivalence of bulk and boundary entropies, we will also show that the bulk and boundary modular operators act on the code subspace in the same way. This is further evidence that the definitions and theorems of Tomita-Takesaki theory are relevant for understanding bulk reconstruction.

3.6 The three-qutrit code and a finite tensor network

The three-qutrit code is an example of a QECC. A code qutrit is isometrically mapped to a Hilbert space of three physical qutrits. The map is given by

$$\begin{cases} |0\rangle & \to \frac{1}{\sqrt{3}}(|\tilde{0}\tilde{0}\tilde{0}\rangle + |\tilde{1}\tilde{1}\tilde{1}\rangle + |\tilde{2}\tilde{2}\tilde{2}\rangle), \\ |1\rangle & \to \frac{1}{\sqrt{3}}(|\tilde{0}\tilde{1}\tilde{2}\rangle + |\tilde{1}\tilde{2}\tilde{0}\rangle + |\tilde{2}\tilde{0}\tilde{1}\rangle), \\ |2\rangle & \to \frac{1}{\sqrt{3}}(|\tilde{0}\tilde{2}\tilde{1}\rangle + |\tilde{1}\tilde{0}\tilde{2}\rangle + |\tilde{2}\tilde{1}\tilde{0}\rangle). \end{cases} \tag{3.48}$$

We can write this more succinctly as

$$|i\rangle \to \sum_{\tilde{a},\tilde{b},\tilde{c}} T_{i\tilde{a}\tilde{b}\tilde{c}} \, |\tilde{a}\tilde{b}\tilde{c}\rangle \, , \tag{3.49}$$

where i denotes an input leg and $\tilde{a}, \tilde{b}, \tilde{c}$ denote output legs. We can apply successive isometries to create an isometry from two code qutrits to four physical qutrits. We illustrate this with a tensor network, represented in Figure 3.3.

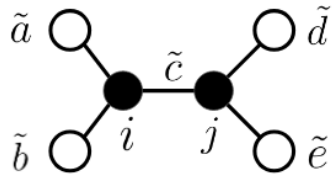

Figure 3.3: The black code subspace qutrits are mapped to the white physical qutrits via an isometry defined by this tensor network.

The isometry corresponding to Figure 3.3 is given by

$$|p\rangle_i |q\rangle_j \to \sum_{\tilde{x},\tilde{y},\tilde{z},\tilde{c},\tilde{w}} \sqrt{3} T_{p\tilde{x}\tilde{y}\tilde{c}} T_{q\tilde{z}\tilde{w}\tilde{c}} |\tilde{x}\rangle_{\tilde{a}} |\tilde{y}\rangle_{\tilde{b}} |\tilde{z}\rangle_{\tilde{d}} |\tilde{w}\rangle_{\tilde{e}} . \tag{3.50}$$

Throughout this chapter, we use subscripts to associate qutrits with specific nodes in Figures 3.3 or 15.1, and tildes are used to denote qutrits in the physical Hilbert space.

Let U be a unitary operator that acts on a two-qutrit state as

$$\begin{aligned} U|00\rangle &= |00\rangle \quad U|11\rangle = |20\rangle \quad U|22\rangle = |10\rangle \\ U|01\rangle &= |11\rangle \quad U|12\rangle = |01\rangle \quad U|20\rangle = |21\rangle \\ U|02\rangle &= |22\rangle \quad U|10\rangle = |12\rangle \quad U|21\rangle = |02\rangle , \end{aligned} \tag{3.51}$$

and define

$$|\lambda\rangle := \frac{1}{\sqrt{3}} \left[|00\rangle + |11\rangle + |22\rangle \right] . \tag{3.52}$$

Let $|\psi\rangle_{ij}$ be a vector in the Hilbert space of the black qutrits i, j in Figure 3.3, and let $|\tilde{\psi}\rangle_{\tilde{a}\tilde{b}\tilde{d}\tilde{e}}$ be its image under the isometry in equation (3.50). Let $U_{\tilde{a}\tilde{b}}$ ($U_{\tilde{d}\tilde{e}}$) be the unitary operator in equation (3.51) that acts on qutrits $\tilde{a}, \tilde{b}$ ($\tilde{d}, \tilde{e}$). One may compute that

$$U^\dagger_{\tilde{a}\tilde{b}} U^\dagger_{\tilde{d}\tilde{e}} |\tilde{\psi}\rangle_{\tilde{a}\tilde{b}\tilde{d}\tilde{e}} = |\psi\rangle_{\tilde{a}\tilde{d}} |\lambda\rangle_{\tilde{b}\tilde{e}} , \tag{3.53}$$

where $|\psi\rangle_{\tilde{a}\tilde{d}}$ is the same state as $|\psi\rangle_{ij}$, except on the white qutrits $\tilde{a}, \tilde{d}$. That is, starting with the state $|\tilde{\psi}\rangle_{\tilde{a}\tilde{b}\tilde{d}\tilde{e}}$ on the white qutrits, one can apply separate unitary transformations on white qutrits $\tilde{a}, \tilde{b}$

and $\tilde{d}, \tilde{e}$ to recover $|\psi\rangle_{ij}$ on white qutrits $\tilde{a}, \tilde{d}$ and the maximally entangled state $|\lambda\rangle$ on qutrits $\tilde{b}, \tilde{e}$.

Given an operator $\mathcal{O}$ that acts on qutrit i in Figure 3.3, we may define an operator $\tilde{\mathcal{O}}$ that acts on the adjacent white qutrits $\tilde{a}, \tilde{b}$ as follows:

$$\tilde{\mathcal{O}} := \sum_{p,q} \langle p|\mathcal{O}|q\rangle_i \left[U_{\tilde{a}\tilde{b}} |p\rangle_{\tilde{a}} \langle q|_{\tilde{a}} U^{\dagger}_{\tilde{a}\tilde{b}} \otimes I_{\tilde{d}\tilde{e}} \right]. \tag{3.54}$$

We say that $\mathcal{O}$, which acts on the code Hilbert space, is reconstructed as $\tilde{\mathcal{O}}$, which acts on the physical Hilbert space.

Part II

Weak Coupling Limit and a Rank One Mordell–Weil Group

In the third section of *Enumeratio Linearum Tertii Ordinis* (The Enumeration of Cubics), Sir Isaac Newton finds that all cubic curves can be put in one of the following four canonical forms [26, 152, 161, 252]:

$$yx^2 + Ax = By^3 + Cy^2 + Dy + E, \tag{3.55}$$

$$xy = Ax^3 + Bx^2 + Cx + D, \tag{3.56}$$

$$y^2 = Ax^3 + Bx^2 + Cx + D, \tag{3.57}$$

$$y = Ax^3 + Bx^2 + Cx + D. \tag{3.58}$$

The second and fourth forms are curves of genus zero as the variable y is a rational function of x. The first and third forms are curves of genus one. Since they have rational points, they are actually elliptic curves.

The third canonical form was called a *cubic hyperbola* by Newton. Today, it is universally known as a Weierstrass equation. Its Newton's polygon is a reflexive triangle with six lattice points on its boundary[13]. Its Mordell–Weil group is generically trivial. On the other hand, the first canonical form has two rational points along the line of infinity. This indicates that its Mordell–Weil group is non-trivial.

The first canonical form is not as famous as the Weierstrass model. But as we shall see in this paper, it corresponds to the general form of a cubic curve with a non-trivial Mordell–Weil group. This

[13] A reflexive polygon is a polygon with a unique lattice point in its interior. For a binary planar algebraic curve, the number of interior lattice points in their Newton's polygon gives the arithmetic genus of the curve.

remark is particularly powerful when this curve is used as a model for a fibration. The Newton's polygon of this curve is a reflexive quadrilateral with seven lattice points on its boundary. If we interpret the coefficients of this equation as parameters defined over a base space B, the first canonical form describes an elliptic fibration with a Mordell–Weil group of rank one. This fibration is generically smooth and can be used as a Jacobian for any elliptic fibration with a non-trivial Mordell–Weil group.

In Chapter 4, we introduce a new model for elliptic fibrations endowed with a Mordell–Weil group of rank one. We call it a $\mathrm{Q}_7(\mathscr{L}, \mathscr{S})$ model. It naturally generalizes several previous models of elliptic fibrations popular in the F-theory literature. The model is also explicitly smooth, thus relevant physical quantities can be computed in terms of topological invariants in straight manner. Since the general fiber is defined by a cubic curve, basic arithmetic operations on the curve can be done using the chord-tangent group law. We will use this model to determine the spectrum of singular fibers of an elliptic fibration of rank one and compute a generating function for its Euler characteristic. With a view toward string theory, we determine a semi-stable degeneration which is understood as a weak coupling limit in F-theory. We show that it satisfies a non-trivial topological relation at the level of homological Chern classes. This identity ensures that the D3 charge in F-theory is the same as the one in the weak coupling limit.

If I have seen further than others, it is by standing upon

the shoulders of giants.

Newton

4

A New Model for Elliptic Fibrations with a Rank One Mordell–Weil Group

The aim of this chapter is to introduce a new model for elliptic fibrations endowed with a Mordell–Weil group of rank one over a variety B. We call this model $\mathrm{Q}_7(\mathscr{L}, \mathscr{S})$. It is given by a smooth hypersurface in a projective bundle characterized by two line bundles $\mathscr{L}$ and $\mathscr{S}$. Its general fiber

is modeled by a plane cubic whose Newton's polygon is a reflexive quadrilateral with seven lattice points on its boundary. It generalizes both the E_6 elliptic fibration and the elliptic fibration introduced recently by Cacciatori, Cattaneo, and Van Geemen [64]. Ultimately, it can be traced back to Newton's first form of cubic curves.

4.1 Summary and the layouts

The $Q_7(\mathscr{L}, \mathscr{S})$ model allows for a particularly friendly derivation of several geometric, topological and arithmetic properties. We provide a classification of its singular fibers. Following [5, 6, 109], we derive a *generalized Sethi-Vafa-Witten formula* for these elliptic fibrations. This is a generating function for the Euler characteristic over a base of arbitrary dimension. We also explicitly construct a semi-stable degeneration of the $Q_7(\mathscr{L}, \mathscr{S})$ model. This degeneration will be understood in F-theory as a *weak coupling limit* mapping the elliptic fibration to an orientifold theory [78, 95, 123, 277]. Inspired by string dualities, we prove a topological relation in the Chow ring of such elliptic fibrations, connecting their homological total Chern class with that of several sub-varieties naturally produced by the semi-stable degeneration. In the context of F-theory, we show that this relation induces the non-trivial fact that the D_3 charge is the same in F-theory and its orientifold weak coupling limit. For previous works on elliptic fibrations with non-trivial Mordell–Weil groups in F-theory, see [6, 50, 51, 58, 59, 61, 62, 84, 85, 87, 88, 109, 150, 197, 210, 229, 232, 242, 257, 258, 296].

Recently, Morrison and Park have revisited the geometry of elliptic fibration with a Mordell–Weil group of rank one in the context of F-theory on Calabi–Yau threefolds [239]. In their treat-

ment, they navigate between two models: the Jacobian and its resolution. The Jacobian (given by a Weierstrass model) is useful to compute arithmetic properties of the elliptic fibration. They also need an explicit resolution of singularities to evaluate intersection numbers necessary in the discussion of cancellations of anomalies. More generally, in F-theory on an elliptic threefold, a smooth model is useful to compute several physical quantities that are expressed in terms of topological invariants. For example, the Euler characteristic is used in the discussion of anomaly cancellations and intersection numbers are interpreted as physical charges. In F-theory on an elliptic fourfold, the D3 tadpole depends on the Euler characteristic of the fourfold. For all these reasons, it will be useful to have a smooth model for an elliptic fibration with Mordell–Weil group of rank one. It would specially be useful if the the generic fiber is a cubic curve so that several arithmetic properties can be computed using the chord-tangent law without passing to the Jacobian.

4.1.1 Layout

In Section 4.2, we give the formal definition of a $\mathrm{Q}_7(\mathscr{L}, \mathscr{S})$ elliptic fibration. We then summarize the results of the chapter. Along the way we give an alternate derivation of the Jacobian formula in Section 4.2.3. In section 4.3, we collect some basic properties of the $\mathrm{Q}_7(\mathscr{L}, \mathscr{S})$ elliptic fibration. In particular, we study some limits that recovered well known elliptic fibrations such as the E_6 and the E_7 models. We also classify the singular fibers of a non-singular fibration of type $\mathrm{Q}_7(\mathscr{L}, \mathscr{S})$. Then, We prove the theorem on its Euler characteristic. In section 4.4, we consider the $\mathrm{Q}_7(\mathscr{L}, \mathscr{S})$ model in the context of F-theory on elliptic fourfolds and prove the existence of a weak coupling limit. We establish that this weak coupling gives an orientifold theory for which the tadpole matching

condition is satisfied. Then, We compute the spectrum of branes and see that it corresponds to an orientifold with a $Sp(1)$ stack and a Whitney brane. We present our conclusions in section 4.5.

4.2 $Q_7(\mathscr{L}, \mathscr{S})$ model and Jacobian fibration

4.2.1 Definition of a $Q_7(\mathscr{L}, \mathscr{S})$ model

The model of elliptic fibrations with Mordell–Weil group of rank one that we introduced in this chapter is an hypersurface cut by a section of the line bundle $\mathscr{O}(3) \otimes \pi^* \mathscr{L}^2 \otimes \pi^* \mathscr{S}$ in the projective bundle $\pi : \mathbb{P}[\mathscr{L} \oplus \mathscr{S} \oplus \mathscr{O}_B] \to B$, where $\mathscr{L}$ and $\mathscr{S}$ are two line bundles over the base B. The defining equation can be put in the following canonical form:

$$Q_7(\mathscr{L}, \mathscr{S}) : \quad y(x^2 - c_0 y^2) + z(c_1 y^2 + b_2 xz + c_2 yz + c_3 z^2) = 0. \tag{4.1}$$

The Newton's polygon of this cubic equation is a reflexive quadrilateral with seven lattice points on its boundary. For this reason, we denote this model $Q_7(\mathscr{L}, \mathscr{S})$.

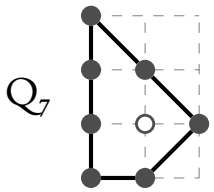

Figure 4.1: Newton polygon of a Q_7 reflexive polytope. A $Q_7(\mathscr{L}, \mathscr{S})$ model is described by a section of a line bundle $O(3) \otimes \pi^* \mathscr{L}^2 \otimes \pi^* \mathscr{S}$ in the projective bundle $\mathbb{P}[\mathscr{L}^2 \oplus \mathscr{S} \oplus \mathscr{O}_B]$. Its equation is automatically of type Q_7.

The coefficients are sections of the following line bundles:

Line bundles	$\mathscr{L}^2 \otimes \mathscr{S}^{-2}$	$\mathscr{L}^2 \otimes \mathscr{S}^{-1}$	$\mathscr{L}^2$	$\mathscr{L}^2 \otimes \mathscr{S}$	$\mathscr{L}^2 \otimes \mathscr{S}^2$
sections	c_0	c_1	c_2	c_3	b_2^2

The details of the projective bundle and the section characterizing the variety are enough to ensure that we get exactly the same Jacobian as the one of an elliptic fibration of rank one. In the defining equation, we denote the projective coordinates as $[x : y : z]$:

Line bundles	$\mathscr{O}(1) \otimes \pi^*\mathscr{L}$	$\mathscr{O}(1) \otimes \pi^*\mathscr{S}$	$\mathscr{O}(1)$	$\mathscr{O}(3) \otimes \pi^*\mathscr{L}^2 \otimes \pi^*\mathscr{S}$
sections	x	y	z	$Q_7(\mathscr{L}, \mathscr{S})$

The special case of $Q_7(\mathscr{L}, \mathscr{O}_B)$ gives the elliptic fibration recently introduced by Cacciatori, Cattaneo, and Van Geemen [64] while the case $Q_7(\mathscr{L}, \mathscr{L})$ is the usual E_6 elliptic fibration [5]. Two rational points of a $Q_7(\mathscr{L}, \mathscr{S})$ model are

$$O : y = z = 0 \quad \textit{and} \quad O' : y = b_2 x + c_3 z = 0. \tag{4.2}$$

These two points are on the line $y = 0$ which is tangent to the elliptic curve at O. There is also a degree-two divisor on each fiber given by $z = x^2 - c_0 y^2 = 0$, where c_0 is a section of $\mathscr{L}^2 \otimes \mathscr{S}^{-2}$. In the case of $Q_7(\mathscr{L}, \mathscr{L})$, c_0 is just a constant and we get two additional rational sections, $z = x \pm \sqrt{c_0} y = 0$, which are inverse of each other in the Mordell–Weil group.

4.2.2 The Jacobian fibration

Since $z = y = 0$ defines a section for the elliptic fibration $Q_7(\mathscr{L}, \mathscr{S})$, we can define a birationally equivalent Weierstrass model. We interpret the Jacobian of the fibration as the relative Picard scheme $Pic^0(Y/B)$ following [18] (see chapter 9 of [53]). Using the formula for the Jacobian of a family of plane cubics over an arbitrary base scheme [18], we get the following Weierstrass equation:

$$zy(y - b_2c_1z) = x^3 - c_2x^2z + (-c_0b_2^2 + c_3c_1)xz^2 + (c_3^2 + b_2^2c_2)c_0z^3, \tag{4.3}$$

which admits the rational point (see Section 4.2.3):

$$x = c_2 + \frac{c_3^2}{b_2^2}, \quad y = \frac{2c_3^3 + 2c_3c_0b_2^2 - b_2^4c_1}{2b_2^3}. \tag{4.4}$$

We can rewrite the Weierstrass form in the short form [94, 291]

$$zy^2 = x^3 + Fxz^2 + Gz^3,$$

with F and G exactly as in [239] modulo the redefinition $c_2 \mapsto -c_2$:

$$F = -b_2^2c_0 + c_1c_3 - \frac{1}{3}c_2^2, \quad G = \frac{2}{3}b_2^2c_0c_2 + \frac{1}{4}b_2^2c_1^2 + c_0c_3^2 + \frac{1}{3}c_1c_2c_3 - \frac{2}{27}c_2^3. \tag{4.5}$$

It is interesting to see that F and G are respectively sections of $\mathscr{L}^4$ and $\mathscr{L}^6$. In particular, the line bundle $\mathscr{S}$ has disappeared.

4.2.3 Alternative derivation of the Jacobian

The Jacobian of a genus one curve with a Mordell–Weil group of rank one can be easily obtained using the Riemann-Roch theorem as discussed for example in [239, 296]. In this section, we present a "quick and dirty trick" that reproduces the same result in an intuitive way. It also gives a simple arithmetic meaning to the section $\mathscr{S}$ that enters in the definition of the $\mathrm{Q}_7(\mathscr{L}, \mathscr{S})$.

Consider a Weierstrass model with a rational point P other than the point at infinity $O : x = z = 0$. Putting P at $y = 0$, the cubic $x^3 + a_2x^2 + a_4x + a_6$ has to factorize. By an appropriate translation of x, we can put the Weierstrass model in the following form:

$$y(y + a_1x + a_3) = (x + a_2)(x^2 + a_4). \tag{4.6}$$

We end up with a general Weierstrass model with the specialization $a_6 = a_2a_4$:

$$y^2 + a_1xy + a_3y = x^3 + a_2x^2 + a_4x + a_2a_4. \tag{4.7}$$

This specialization is too mild to factorize the discriminant but does gives two non-trivial rational sections:

$$(x, y) = (-a_2, 0) \text{ and } (x, y) = (-a_2, a_1a_2 - a_3). \tag{4.8}$$

These two points are inverse of each other for the Mordell–Weil group with the neutral element $x = z = 0$. Since we can write the Weierstrass model as:

$$y(y + a_1x + a_3) = (x + a_2)(x^2 + a_4), \tag{4.9}$$

we have conifold-like points at $y = y + a_1x + a_3 = x + a_2 = x^2 + a_4 = 0$. It corresponds to the point $y = x + a_2 = 0$ on each fiber over the codimension-2 locus in the base:

$$a_3 - a_1a_2 = a_4 + a_2^2 = 0. \tag{4.10}$$

Over this locus, the elliptic fiber can be put in this suggestive form:

$$a_3 - a_1a_2 = a_4 + a_2^2 = 0 \Longrightarrow (y + \tfrac{a_1}{2}(x + a_2))^2 = (x + a_2)^2(x - a_2 + \frac{a_1^2}{4}), \tag{4.11}$$

which shows that the elliptic curve has a A_1 singularity over $a_3 - a_1a_2 = a_4 + a_2^2 = 0$.

We now consider the case in which a_2 has an explicit rational part:

$$a_2 = c - \frac{p}{q}, \tag{4.12}$$

where c is integral and p/q is a reduced fraction. By taking appropriate choices for (a_1, a_3, a_4), we can still ensure that when we complete the square in y, the coefficients b_2, b_4 and b_6 are all integral. Since $b_2 = 4a_2 + a_1^2$, we can get rid of the fractional part of b_2 due to a_2 by taking $a_1 = 2\sqrt{p/q}$.

However, the point $(x, y) = (a_2, -a_1a_2 + a_3)$ will not be rational anymore because of the square root in a_1. We can solve this problem by requiring that p/q to be a perfect square ($p/q = r^2/s^2$). That is:

$$a_1 = 2\frac{r}{s}, \quad a_2 = c - \frac{r^2}{s^2}. \tag{4.13}$$

We can get rid of the fractional part of $b_4 = 2a_4 + a_1a_3$ by requiring a_3 to be proportional to s:

$$a_1 = 2\frac{r}{s}, \quad a_2 = c - \frac{r^2}{s^2}, \quad a_3 = 2st. \tag{4.14}$$

Since $b_6 = 4a_6 + a_3^2$ and $a_6 = a_2a_4$, we can ensure that b_6 is integral by taking a_4 to be proportional to s^2. Using $a_6 = a_2a_4$, we get our final form:

$$a_1 = 2\frac{r}{s}, \quad a_2 = c - \frac{r^2}{s^2}, \quad a_3 = 2st, \quad a_4 = s^2u, \quad a_6 = u(cs^2 - r^2). \tag{4.15}$$

$$E: \quad y^2 + 2\frac{r}{s}xy + 2sty = x^3 + (c - \frac{r^2}{s^2})x^2 + s^2ux + u(cs^2 - r^2). \tag{4.16}$$

This has a rational point of type $(x, y) = (-a_2, 0)$ with $a_2 = c - r^2/s^2$. This Weierstrass equation has coefficients that are rational expressions. But by construction, we can resolve this problem by completing the square in y:

$$E: \quad y(y + 2st) = x^3 + cx^2 + (s^2u + 2rt)x + u(cs^2 - r^2). \tag{4.17}$$

with the rational point

$$x = -c + \frac{r^2}{s^2}, \quad y = \frac{r^3 - rcs^2 + s^4 t}{s^3}. \tag{4.18}$$

Completing the square in y we get the canonical form of a Weierstrass model of rank 1:

$$E: \quad y^2 = x^3 + cx^2 + (s^2 u + 2rt)x + ucs^2 - ur^2 + s^2 t^2, \tag{4.19}$$

The corresponding short Weierstrass form is then

$$y^2 = x^3 + (-\tfrac{1}{3}c^2 + 2rt + s^2 u)x + (\tfrac{2}{27}c^3 + s^2 t^2 - r^2 u - \frac{2}{3}c(rt - s^2 u)), \tag{4.20}$$

which depends only on the variable (s^2, r, c, t, u). The reduced Weierstrass model is invariant under the involution:

$$(s^2, r, c, t, u) \leftrightarrow (-u, t, c, r, -s^2). \tag{4.21}$$

It is also invariant under the scaling symmetry

$$\alpha \cdot (s^2, r, c, t, u) = (\alpha^2 s^2, \alpha r, c, \frac{t}{\alpha}, \frac{u}{\alpha^2}). \tag{4.22}$$

It is the Jacobian of the Jacobi quartic:

$$y^2 = s^2 x^4 - 2rx^3 z + cx^2 z^2 + txz^3 + \tfrac{1}{4}uz^4. \tag{4.23}$$

or equivalently

$$y^2 = -ux^4 - 2tx^3z + cx^2z^2 + rxz^3 - \tfrac{1}{4}s^2z^4. \tag{4.24}$$

Both Jacobi quartics (4.23) and (4.24) admit the same Jacobian.

In a Weierstrass model, each coefficient a_i ($i = 1, 2, 3, 4, 6$) is a section of $\mathscr{L}^i$, where $\mathscr{L}$ is the fundamental line bundle of the elliptic fibration. Assuming that s is a section of a line bundle $\mathscr{M}$, then the different variables r, c, t, u are sections of the following line bundles:

Line bundle	$\mathscr{M}^2$	$\mathscr{L} \otimes \mathscr{M}$	$\mathscr{L}^2$	$\mathscr{L}^3 \otimes \mathscr{M}^{-1}$	$\mathscr{L}^4 \otimes \mathscr{M}^{-2}$
Section	s^2	r	c	t	u

In this table, as we move to the right, we multiply the line bundle by $\mathscr{L} \otimes \mathscr{M}^{-1}$. The dictionary to the notation in the main text is:

$$s = b_2, \quad r = c_3, \quad c = -c_2, \qquad t = -\frac{1}{2}c_1, \quad u = -c_0. \tag{4.25}$$

We see that the line bundle $\mathscr{S}$ corresponds to $\mathscr{L} \otimes \mathscr{M}$. This shows that $\mathscr{S} \otimes \mathscr{L}^{-1}$ is a natural line to consider to discuss the arithmetic properties of the section.

4.2.4 The spectrum of singular fibers

The $\mathrm{Q}_7(\mathscr{L}, \mathscr{S})$ model has all the types of singular cubics with the exception of the triple line as seen on Figure 4.2. In particular, there is a non-Kodaira fiber composed of two rational curves

of multiplicity one and two intersecting transversely[1]. We call it a fiber of type $\mathrm{IV}^{(2)}$. Such a non-Kodaira fiber is very natural from the point of view of degeneration of genus-one curves modeled by cubic curves. It can be understood as a limiting case of a Kodaira fiber of type I_3 or of type IV. See Figure 4.2 and Table 4.2.

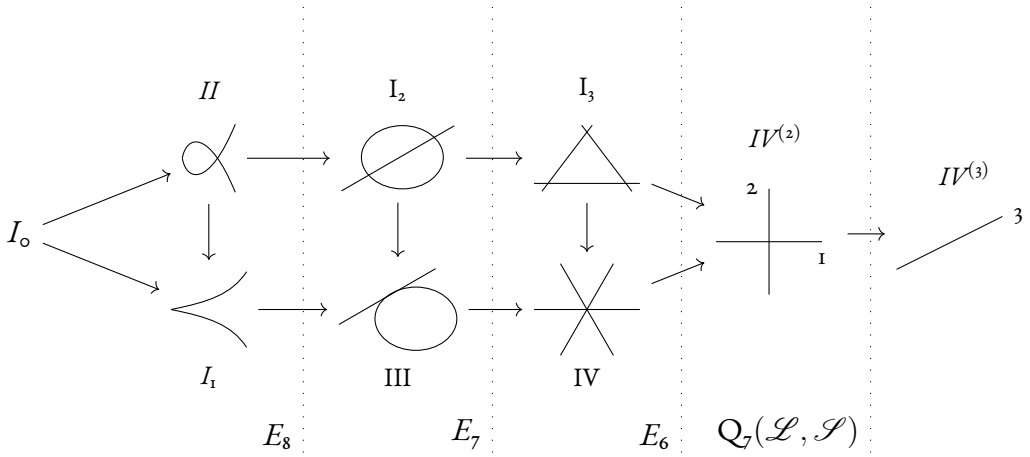

Figure 4.2: Singular fibers of plane cubic curves. There are a total of 8 possible singular fibers including the 6 Kodaira fibers with at most 3 components ($I_1, II, I_2, III, I_3, IV$) and the two non-Kodaira fibers $IV^{(2)}$ and $IV^{(3)}$. All the fibers at the left of a given dotted vertical line are those of a smooth elliptic fibration of the type (E_8, E_7, E_6, Q_7) specified at the bottom left of the dotted line.

4.2.5 Weak coupling limit, tadpole and flux matching condition

From the point of view of F-theory, elliptic fibrations with a Mordell–Weil group of rank one yield an Abelian $U(1)$ gauge symmetry. Depending on the dimension of the base, we are interesting at different geometric properties of the elliptic fibration. If the base is a surface, the compactification of F-theory models a six-dimensional supersymmetric gauge theory in presence of gravity. In that case,

[1]For non-Kodaira fibers in F-theory see [60, 64, 76, 109, 126, 128, 129, 163, 241].

Description	Kodaira fiber	Symbols	E_8	E_7	E_6	Q_7
smooth genus one curve	✓	I_0	✓	✓	✓	✓
a nodal curve	✓	I_1	✓	✓	✓	✓
a cusp	✓	II	✓	✓	✓	✓
a conic and a secant line	✓	I_2		✓	✓	✓
a conic and a tangent line	✓	III		✓	✓	✓
three lines forming a triangle	✓	I_3			✓	✓
three lines meeting at a point	✓	IV			✓	✓
a line and a double line		$IV^{(2)}$				✓
a triple line		$IV^{(3)}$				

Table 4.1: Planar cubic curves.

anomalies cancellations with an $U(1)$ sector are particularly subtle and have a beautiful geometric formulation. If the base is a threefold, F-theory models a type IIB theory with a non-trivial axio-dilaton profile and an Abelian $U(1)$ symmetry. Duality with M-theory gives a simple description of the origin of this $U(1)$ symmetry using the three-form of M-theory. The full F-theory regime is usually strongly coupled and following Sen [277], we can explore the weak coupling limit of F-theory to make contact with well understood type IIB configurations.

The weak coupling limit has a purely geometric description as a degeneration of the elliptic fibration in which the general fiber becomes a semi-stable curve: the elliptic fibration is replaced by a ALE fibration [6, 77]. This description of the weak coupling limit was started in [6] and provides a purely geometric definition of the weak coupling limit that generalizes to any elliptic fibration regardless of the dimension of its base and independent of the Calabi–Yau condition. Interestingly, the topological relations that are expected to hold when F-theory is compared to its weak coupling limit are still true independently of all the string theory setups necessary to make sense of them. For

example, the D3 charge in F-theory depends only on the Euler characteristic of the elliptic fibration and the G_4 flux. In a type IIB orientifold, the same D3 charge depends on the Euler characteristic of the orientifolds, the D7 branes, the DBI fluxes supported on these D7 branes and the fluxes coming from the type IIB three form field strengths.

The weak coupling limit of a Weierstrass model is an orientifold theory [277]. In absence of fluxes in weak and strong coupling, there is a perfect match between the D3 charge computed in type IIB and in F-theory [5, 78]. The same is true for other models of elliptic fibration such as the E_7, E_6 and D_5 elliptic fibrations [6, 109]. After classifying the singular fibers of a $Q_7(\mathscr{L}, \mathscr{S})$ model, it is straightforward to identify its weak coupling limit using a semi-stable degeneration following [6]. The weak coupling limit is given by equation (4.60) which yields the following spectrum:

$$(\star) \quad \text{a } \mathbb{Z}_2 \text{ orientifold} + \text{ a Whitney brane} + \text{an } Sp(1) \text{ stack.}$$

The orientifold, the $Sp(1)$ stack, and the Whitney brane are respectively wrapping the divisors O, D, and D_w. The $Sp(1)$ stack is composed of two smooth invariant branes intersecting the orientifold transversely. We prove that the tadpole matching condition is satisfied for this spectrum:

$$2\chi(Y) = 4\chi(O) + 2\chi(D) + \chi^{\infty}(D_w). \tag{4.26}$$

It follows that the G-flux and the type IIB brane fluxes match aswell [78, 95]:

$$\int_Y G_4 \wedge G_4 = -\frac{1}{2}\sum_i \int_{D_i} tr(F^2). \tag{4.27}$$

The tadpole matching is a by-product of a much more general relation valid at the level of the total homological Chern classes as summarized in the following theorem:

Theorem 4.2.1 (Topological tadpole matching for $Q_7(\mathscr{L},\mathscr{S})$ elliptic fibrations)**.** *A $Q_7(\mathscr{L},\mathscr{S})$ elliptic fibration endowed with the weak coupling limit* (4.60) *satisfies the topological tadpole matching condition at the level of the total Chern class:*

$$2\phi_* c(Y) = 4\rho_* c(O) + 2\rho_* c(D) + \rho_* c^{\infty}(D_w),$$

where the Chern class of the Whitney brane is understood as $\rho_* c^{\infty}(D_w) = \rho_* c(\overline{D}_w) - \rho_* c(S)$, with $\overline{D}_w$ the normalization of D_w and S the cuspidial locus of the Whitney brane.

4.3 Properties of a $Q_7(\mathscr{L},\mathscr{S})$ elliptic fibration

In the section, we will further explain our new model, $Q_7(\mathscr{L},\mathscr{S})$. It is similar to E_6 and E_8 model as it is a model for a cubic. But as we will establish in details, a $Q_7(\mathscr{L},\mathscr{S})$ elliptic fibration has a much richer spectrum of singular fibers. It admits all possible types of singular cubics except for the triple line. In other words, its spectrum of singular fibers is (I_1, II, I_2, III, I_3, IV and $IV^{(2)}$). In particular, it contains a non-Kodaira fiber, a fiber of type $IV^{(2)}$, which consists of two rational curves

of multiplicity 1 and 2 intersecting transversely at a point. To appreciate the difference in the spectrum of singular fibers of smooth elliptic fibrations of type E_8, E_7, E_6, and $Q_7(\mathscr{L}, \mathscr{S})$, we review the singular fibers of cubic plane curves and the elliptic fibrations defined in Table 4.1 and Figure 4.2.

The following lemma is a direct consequence of the use of the adjunction formula to compute the canonical class of an $Q_7(\mathscr{L}, \mathscr{S})$ elliptic fibration:

Theorem 4.3.1 (Calabi–Yau condition). *An $Q_7(\mathscr{L}, \mathscr{S})$ fibration is Calabi–Yau if the line bundle $\mathscr{L}$ is the anti-canonical line bundle of the base B.*

4.3.1 Mordell–Weil group

An E_n elliptic fibration ($n = 8, 7, 6, 5$ with $E_5 = D_5$) has $(9 - n)$ marked points defined by a divisor of degree $(9 - n)$ on each fibers and each of the points defined by such a divisor gives a section of the elliptic fibration as the divisor splits. The elliptic fibration $Q_7(\mathscr{L}, \mathscr{S})$ has a different structure: on each fiber, we have a rational divisor of degree three as it is the case for a E_6 elliptic fibration. However, the divisor does not split into three rational points on every fiber but instead splits into a rational point and a divisor of degree two that does not factorize. This is very clear using the canonical form (4.1). The line at infinity ($z = 0$) cuts every elliptic fiber along the following degree three divisor

$$z = y(x^2 - c_0 y^2) = 0, \tag{4.28}$$

which splits into a closed point $z = y = 0$ and a degree two divisor $z = x^2 - c_0 y^2 = 0$. As we circle around the locus c_0 in the base, the two points defined by $z = x^2 - c_0 y^2 = 0$ are exchanged.

This monodromy is the $\mathbb{Z}_2$ discrete group corresponding to the Galois group of the field extension needed to properly define individually the two points $z = x^2 - c_0 y^2 = 0$ over the base. A $\mathrm{Q}_7(\mathscr{L}, \mathscr{S})$ elliptic fibration has an additional rational section. Consider the intersection with $y = 0$:

$$\begin{gathered} y = 0 \Longrightarrow z^2(b_2 x + c_3 z) = 0 \Longrightarrow 2O + O', \\ \text{where} \quad O : y = z = 0, \quad O' : y = b_2 x + c_3 z = 0. \end{gathered} \tag{4.29}$$

This indicates that $y = 0$ is tangent to the elliptic curve at O and intersects the elliptic curve at an additional point O'. These two sections intersect over the divisor $b_2 = 0$.

Remark 4.3.2. If $\mathscr{S} = \mathscr{L}^{-1}$, b_2 is a constant and thus the two sections do not intersect. In such a case, it is easier to start from the following projective bundle obtained by an overall factor of $\mathscr{S}$:

$$\mathbb{P}[(\mathscr{L} \otimes \mathscr{S}^{-1}) \oplus \mathscr{O}_B \oplus \mathscr{S}^{-1}], \tag{4.30}$$

and the equation is a section of $\mathscr{O}(3) \otimes \pi^* \mathscr{L}^2 \otimes \pi^* \mathscr{S}^{-2}$, which gives for $\mathscr{S} = \mathscr{L}^{-1}$:

$$\mathbb{P}[(\mathscr{L}^2 \oplus \mathscr{O}_B \oplus \mathscr{L}]_{\mathscr{O}(3) \otimes \pi^* \mathscr{L}^4}. \tag{4.31}$$

Theorem 4.3.3 (Mordell–Weil group). *A $\mathrm{Q}_7(\mathscr{L}, \mathscr{S})$ elliptic fibration has a Mordell–Weil group of rank one with generator O' and neutral element O.*

4.3.2 A smooth hypersurface description of an elliptic fibration of rank one

The Jacobian obtained in equation (4.5) is exactly the one describing a general rank one elliptic fibration as discussed in Morrison-Park [239] modulo the following substitution:

$$c_2 \mapsto -c_2. \tag{4.32}$$

This provides an interesting opportunity to obtain a non-singular formulation of the general rank one elliptic fibration as an hypersurface in a projective bundle by generalizing the E_6' fibration to have coefficients that are sections of different line bundles. It is useful to notice that the Jacobian (4.5) is invariant under the following scaling:

$$\alpha \cdot (c_0, c_1, c_2, c_3, b_2^2) = (\alpha^2 c_0, \alpha c_1, c_2, \alpha^{-1} c_3, \alpha^{-2} b_2^2), \tag{4.33}$$

from which we find that the coefficients are sections of the following line bundles[2]:

c_0	c_1	c_2	c_3	b_2^2
$\mathscr{L}^2 \otimes \mathscr{S}^{-2}$	$\mathscr{L}^2 \otimes \mathscr{S}^{-1}$	$\mathscr{L}^2$	$\mathscr{L}^2 \otimes \mathscr{S}$	$\mathscr{L}^2 \otimes \mathscr{S}^2$

(4.34)

where $\mathscr{S}$ is also a line bundle over B. We can then define a projective bundle with coordinates $[x : y : z]$ such that

$$x \in \Gamma[\mathscr{O}(1) \otimes \pi^* \mathscr{L}], \quad y \in \Gamma[\mathscr{O}(1) \otimes \pi^* \mathscr{S}], \quad z \in \Gamma[\mathscr{O}(1)], \tag{4.35}$$

[2] We recall that the Weierstrass model the coefficients F and G are respectively sections of $\mathscr{L}^4$ and $\mathscr{L}^6$.

the corresponding projective bundle is $\mathbb{P}[\mathscr{L} \oplus \mathscr{S} \oplus \mathscr{O}_B]$. With this choice, the defining equation (4.1) will be a section of the line bundle $\mathscr{O}(3) \otimes \pi^*\mathscr{L}^2 \otimes \pi^*\mathscr{S}$. Altogether we have a new family of elliptic fibration characterized by two line bundles $\mathscr{L}$ and $\mathscr{S}$ such that it is an hypersurface of degree $\mathscr{O}(3) \otimes \pi^*\mathscr{L}^2 \otimes \pi^*\mathscr{S}$ in the projective bundle $\mathbb{P}[\mathscr{L} \oplus \mathscr{S} \oplus \mathscr{O}_B]$. We call this model $Q_7(\mathscr{L}, \mathscr{S})$:

$$Q_7(\mathscr{L}, \mathscr{S}): \quad \mathbb{P}[\mathscr{L} \oplus \mathscr{S} \oplus \mathscr{O}_B]_{\mathscr{O}(3)\otimes\pi^*\mathscr{L}^2\otimes\pi^*\mathscr{S}}. \tag{4.36}$$

All elliptic fibrations of rank one can be put in this form since it was obtained form their common Jacobian. For general values of the coefficients, this is a smooth elliptic fibration. A quick calculation with the adjunction formula shows that the Calabi–Yau condition for the family $Q_7(\mathscr{L}, \mathscr{S})$ is $c_1(B) = c_1(\mathscr{L})$.

Theorem 4.3.4. *An elliptic fibration of rank one is always birational to a fibration of type $Q_7(\mathscr{L}, \mathscr{S})$. The fibration is Calabi–Yau when $\mathscr{L}$ is the anti-canonical line bundle of the base.*

4.3.3 Special cases

The special case of $Q_7(\mathscr{L}, \mathscr{O}_B)$ gives the elliptic fibration recently introduced by Cacciatori, Cattaneo, and Van Geemen [64] while the case $Q_7(\mathscr{L}, \mathscr{L})$ is the usual E_6 elliptic fibration [5]. The rational points of a $Q_7(\mathscr{L}, \mathscr{S})$ model are

$$O: y = z = 0 \quad \textit{and} \quad O': y = b_2x + c_3z = 0. \tag{4.37}$$

These two points are on the line $y = 0$ which is tangent to the elliptic curve at O. There is also a degree-two divisor on each fiber given by $z = x^2 - c_0 y^2 = 0$, where c_0 is a section of $\mathscr{L}^2 \otimes \mathscr{S}^{-2}$. In the case of $Q_7(\mathscr{L}, \mathscr{L})$, c_0 is just a constant and we get two additional rational sections, $z = x \pm \sqrt{c_0} y = 0$, which are inverse of each other in the Mordell–Weil group.

If $\mathscr{S} = \mathscr{L}^{-1}$, we start from the following projective bundle obtained by an overall factor of $\mathscr{S}^3$:

$$\mathbb{P}[(\mathscr{L} \otimes \mathscr{S}^{-1}) \oplus \mathscr{O}_B \oplus \mathscr{S}^{-1}], \tag{4.38}$$

and the equation is a section of $\mathscr{O}(3) \otimes \pi^* \mathscr{L}^2 \otimes \pi^* \mathscr{S}^{-2}$, which gives for $\mathscr{S} = \mathscr{L}^{-1}$:

$$\mathbb{P}[(\mathscr{L}^2 \oplus \mathscr{O}_B \oplus \mathscr{L}]_{\mathscr{O}(3) \otimes \pi^* \mathscr{L}^4}. \tag{4.39}$$

4.3.4 Birational map to a Jacobi quartic

We multiply the defining equation 4.1, by y and we replace the variable x by $u = xy$. This can be explained as a birational map in the ambient projective bundle to turn it into a weighted projective bundle:

$$\begin{gathered} \mathbb{P}[\mathscr{L} \oplus \mathscr{S} \oplus \mathscr{O}_B] \to \mathbb{P}_{2,1,1}[\mathscr{M} \oplus \mathscr{S} \oplus \mathscr{O}_B], \quad \mathscr{M} = \mathscr{L} \otimes \mathscr{S} \\ [x : y : z] \mapsto [u : y : z] = [xy : y : z]. \end{gathered} \tag{4.40}$$

[3] Hartshorne Chap II, Lemma 7.9.

The variable u is a section of $\pi^*\mathscr{M} \otimes \mathscr{O}(2)$. The defining equation is a section of $\pi^*\mathscr{M}^2 \otimes \mathscr{O}(4)$:

$$u(u + b_2 z^2) + y(-c_0 y^3 + c_1 z y^2 + c_2 y z^2 + c_3 z^3) = 0. \tag{4.41}$$

This defines an elliptic fibration whose generic fiber is given by a quartic curve with the Newton's polygon given in Figure 4.3. The rational sections are at $y = u = 0$ and $y = u + b_2 z^2 = 0$. The equation is singular at $u = y = b_2 = c_3 = 0$. We can blow up the non-Cartier divisor $u = y = 0$ to resolve with this singularity. The ambient space becomes the blow up of the weighted projective bundle $Bl_{[0:0:1]}\mathbb{P}_{2,1,1}$.

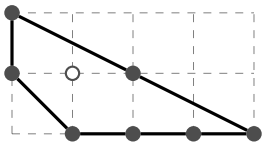

Figure 4.3: Quartic Q_7: a reflexive quadrilateral with seven lattice points on its boundary. This is the Newton's polygon for the quartic in equation (2.8).

4.3.5 A double cover embedded in the $Q_7(\mathscr{L}, \mathscr{S})$ fibration

Inside a $Q_7(\mathscr{L}, \mathscr{S})$ fibration, we can use the divisor of degree 2 along each fiber to define a double cover the base X:

$$X : z = x^2 - c_0 y^2 = 0. \tag{4.42}$$

It admits the following involution:

$$\sigma : \quad x \mapsto -x, \tag{4.43}$$

for which $c_0 = 0$ is the locus of fixed point. In the definition of X, the divisor $z = 0$ cuts $\mathbb{P}(E)$ along a projective bundle $\mathbb{P}(\mathscr{L} \oplus \mathscr{S})$ with coordinates $[x : y]$. The variety X naturally lives in that projective bundle with the defining equation $x^2 + c_0 y^2 = 0$. Along X, the projective coordinate y never vanishes since otherwise we would have $z = y = x = 0$, which is not possible because $[x : y : z]$ are projective coordinates of the projective bundle. It follows that we can just define X in the affine patch $y \neq 0$ by taking the affine coordinate $\xi = x/y$, which is a section of $\mathscr{L} \otimes \mathscr{S}^{-1}$:

$$X : \quad \xi^2 = -c_0, \quad \text{with the involution } \xi \mapsto -\xi, \tag{4.44}$$

which expresses X as the zero locus of a section of $\mathscr{L}^2 \otimes \mathscr{S}^{-2}$. Note that this is not an orientifold. Using adjunction formula, it is easy to see that the elliptic fibration $Y \to B$ is a Calabi–Yau $(n+1)$-fold if and only if $c_1(B) = c_1(\mathscr{L})$ while the double cover $X \to B$ branched on c_0 is a Calabi–Yau n-fold if and only if $c_1(B) = c_1(\mathscr{L}) - c_1(\mathscr{S})$. The two are compatible only when S is trivial, that is for the $\mathrm{Q}_7(\mathscr{L}, \mathscr{O}_B)$ model.

Lemma 4.3.5. *An elliptic fibration of type $\mathrm{Q}_7(\mathscr{L}, \mathscr{O}_B)$ admits a divisor which is a double cover X of the base. The $\mathrm{Q}_7(\mathscr{L}, \mathscr{O}_B)$ elliptic fibration is Calabi–Yau if and only if the double cover X of the base is also Calabi–Yau.*

4.3.6 Spectrum of singular fibers of a $\mathrm{Q}_7(\mathscr{L}, \mathscr{S})$ elliptic fibration

A $\mathrm{Q}_7(\mathscr{L}, \mathscr{S})$ elliptic fibration admits up to 7 different types of singular fibers including the non-Kodaira fiber $\mathrm{IV}^{(2)}$ constituted of two rational curves of multiplicity one and two intersecting

transversally. These 7 different types represent all the different types of singular fibers of a cubic curve with the exception of the triple line, which is the only multiple singular cubic curve.

General picture

The spectrum of singular fibers of a $Q_7(\mathscr{L}, \mathscr{S})$ elliptic fibration can be easily obtained by a direct analysis of its defining equation. We can use the birationally equivalent Weierstrass model to characterize irreducible singular curves (nodal and cuspidial curves). Since the elliptic fibration is nonsingular, to classify reducible singular fibers, we analyze the conditions under which the defining equation factorizes. A cubic curve can factorize into a line and a conic. This corresponds to the fibers of type I_2 if the line and the conic meet at two distinct points or of type III if the line is tangent to the conic. The conic can further splits into two lines so that the singular fiber has the structure of a triangle, Kodaira type I_3, or a star, Kodaira type IV. If the conic specializes to a double line, we have a non-Kodaira fiber that we call a type $IV^{(2)}$. We summarize the condition to have all these fibers in Table 4.2 and Figure 4.2. It is also instructive to look at the spectrum of singular fibers of elliptic fibrations of type $Q_7(\mathscr{L}, \mathscr{S})$, E_7, E_8 and E_6 together since it reveals some beautiful patterns as illustrated in Figure 4.2. In the next subsection, we will methodically derive Table 4.2 .

Irreducible singular fibers

Using the Weierstrass moddel, we can easily determine the irreducible singular fibers or the $Q_7(\mathscr{L}, \mathscr{S})$ fibration: we have a nodal curve at a general point of the discriminant locus and a cuspidial curve at

Fiber	j-invariant	Algebraic Conditions
I_1	∞	$\Delta = 0$
II	0	$F = G = 0$
I_2	∞	$b_2 = c_3 = 0$
III	1728	$c_0 = c_1 = c_2 = c_3 = 0$ or $b_2 = c_2 = c_3 = 0$
I_3	∞	$b_2 = c_3 = c_1^2 + 4c_0c_2 = 0$
IV	0	$b_2 = c_2 = c_1 = c_3 = 0$
$\mathrm{IV}^{(2)}$	undefined "$\frac{0}{0}$"	$b_2 = c_0 = c_1 = c_2 = c_3 = 0$

Table 4.2: Singular fibers of the $\mathrm{Q}_7(\mathscr{L}, \mathscr{S})$ elliptic fibration $x^2y + b_2xz^2 - c_0y^3 + c_1zy^2 + c_2z^2y + c_3z^3$. The fiber I_3 and II (with $b_2 = 0$) are non-split when c_0 is not a perfect square. The fiber III (with $b_2 \neq 0$) can also be non-split when b_2 is a not a perfect square.

a general point of $F = G = 0$:

$$\mathrm{I}_1 : \quad \Delta = 0, \quad \mathrm{II} : \quad F = G = 0. \tag{4.45}$$

Reducible singular fibers

For reducible singular fibers, we can find the condition for factorizing the defining equation (4.1).

Assuming that $b_2 \neq 0$, the only factorization is

$$\mathrm{III} : \quad x(xy + b_2z^2) = 0, \tag{4.46}$$

which requires $c_i = 0$. The fiber is of type III since it is composed of two rational curves (a line and a conic) meeting at a double point. When $b_2 = c_i = 0$, the fiber III enhances to a non-Kodaira fiber

of type $IV^{(2)}$ as the degree two:

$$\mathrm{IV}^{(2)}: \quad x^2 y = 0. \tag{4.47}$$

If we assume that $b_2 = 0$, we have much richer spectrum. In order to be able to factorize a linear term, we have to assume $b_2 = c_3 = 0$, which gives

$$\mathrm{I}_2: \quad y(x^2 - c_0 y^2 + c_1 yz + c_2 z^2) = 0. \tag{4.48}$$

This singular fiber is constituted of two rational curves (a line and a conic) meeting transversally at two distinct points.

Remark 4.3.6. The section O' is now the full line $y = 0$. The zero section O intersect only that line and does not intersect the conic. We also note that the two points of intersection can be seen as the intersection of the conic with the section O'.

We have an enhancement to a fiber of type III when the line becomes tangent to the conic. This happens when $b_2 = c_2 = c_3 = 0$ and the line and the conic intersect at a double point:

$$\mathrm{III}: \quad y(x^2 - c_0 y^2 + c_1 yz) = 0. \tag{4.49}$$

The fiber I_2 can enhance to a fiber I_3 when the conic degenerates into two lines. This requires the additional condition $c_1^2 - 4c_0c_2 = 0$ so that all together we have a I_3 fiber when $b_2 = c_3 = c_1^2 - 4c_0c_2 =$

0 ($c_1 \neq 0$ or $c_2 \neq 0$). The equation of the fiber is:

$$\mathrm{I}_3 : \quad y\left(x^2 - c_0(y - \frac{c_1}{2c_0}z)^2\right) = 0 \quad or \quad y\left(x^2 + c_2(z - \frac{c_1}{2c_2}y)^2\right) = 0. \tag{4.50}$$

This I_3 fiber is split if and only if c_0 is a perfect square, otherwise, we have a non-split fiber with a $\mathbb{Z}_2$ torsion. If $b_2 = c_2 = c_1 = 0$, we have a fiber of type IV^{ns}.

$$\mathrm{IV}^{ns} : \quad y(x^2 - c_0y^2) = 0. \tag{4.51}$$

This fiber is split only if c_0 is a perfect square. Otherwise it is a non-split fiber with a $\mathbb{Z}_2$ torsion. Finally, if $b_2 = c_i = 0$, we have a fiber of type $\mathrm{IV}^{(2)}$.

4.3.7 Generalized Sethi-Vafa-Witten formula

The Sethi-Vafa-Witten formula gives the Euler characteristic of a Calabi–Yau fourfolds defined by a generic Weierstrass model [279]. In this section, we present a generating function for the Euler characteristic of a $\mathrm{Q}_7(\mathscr{L}, \mathscr{S})$ model over a base of arbitrary dimension. We also do not assume the Calabi–Yau condition. This is done using a push-forward formula following [6, 109].

Theorem 4.3.7 (Euler characteristic of $\mathrm{Q}_7(\mathscr{L}, \mathscr{S})$)**.** *Let $L = c_1(\mathscr{L})$, $S = c_1(\mathscr{S})$ and c_k be the k-th Chern class $c_k(TB)$ of the base B. Then, the push-forward of the total homological Chern class of the elliptic fibration Y is:*

$$\begin{aligned}\pi_* c(Y) &= \frac{6(2L + 2L^2 - LS - S^2)}{(1 + 2L - 2S)(1 + 2L + S)} c(B) \\ &= 12Lt + (12c_1L - 36L^2 + 6LS - 6S^2)t^2 + \\ &\quad (12c_2L - 36c_1L^2 + 96L^3 + 6c_1LS - 36L^2S - 6c_1S^2 + 54LS^2 - 6S^3)t^3 + \cdots\end{aligned} \tag{4.52}$$

This gives a generating function for the Euler characteristic: if the base is of dimension d, then the Euler characteristic of Y is given by the coefficient of t^d. If $Y = Q_7(\mathscr{L}, \mathscr{S})$ is a Calabi–Yau variety, we can simplify further the expression by using $L = c_1$.

Lemma 4.3.8. *For Y a Calabi–Yau threefold or fourfold, we get the Euler characteristics respectively as*

$$\chi(Y) = -6(4c_1^2 - c_1S + S^2), \quad \chi(Y) = 6(10c_1^3 + 2c_1c_2 - 5c_1^2S + 8c_1S^2 - S^3) \tag{4.53}$$

Proof of theorem 4.3.7. The ambient space in which we define Y is the following projective bundle

$$\pi : \mathbb{P}(\mathscr{L} \oplus \mathscr{S} \oplus \mathscr{O}_B) \to B. \tag{4.54}$$

We would like to compute the pushforward from its Chow's ring to the Chow's ring of the base. We use the fact that:

$$\pi_*\big(1 + \zeta + \zeta^2 + \cdots\big) = \frac{1}{(1 + L)(1 + S)}. \tag{4.55}$$

It is easy to see that

$$\frac{1}{(1+Lt)(1+St)} = \sum_{k\geq 0}(-1)^k P_k(L,S)t^k, \tag{4.56}$$

where we have inserting a variable t to track the other. We also have:

$$P_k(L,S) = L^k + L^{k-1}S + \cdots + S^k = \frac{L^{k+1} - S^{k+1}}{L-S}.$$

Comparing terms of the same dimension, we get:

$$\pi_* 1 = \pi_* \zeta = 0, \quad \pi_* \zeta^{2+k} = (-1)^k P_k(L,S). \tag{4.57}$$

Then we get

$$\pi_* F(H) = \frac{F(H) - F(0) - H\partial_H F(0)}{(S-L)H}\Big|_{H=-L} - \frac{F(H) - F(0) - H\partial_H F(0)}{(S-L)H}\Big|_{H=-S}. \tag{4.58}$$

Now we apply it to the total homological Chern class of the elliptic fibration $\mathrm{Q}_7(\mathscr{L}, \mathscr{S})$:

$$c(Y) = \frac{(1+H)(1+H+L)(1+H+S)}{(1+3H+2L+S)}(3H+2L+S)c(B), \tag{4.59a}$$

which gives

$$\pi_* c(Y) = \frac{6(2L+2L^2-LS-S^2)}{(1+2L-2S)(1+2L+S)}c(B) \tag{4.59b}$$

□

4.4 Weak coupling limit of a $Q_7(\mathscr{L}, \mathscr{S})$ model

Following [6], we characterize geometrically a weak coupling limit by a transition from a semi-stable to an unstable fiber. See Sections 2.10 and 2.11 for a review of weak coupling limits of an elliptic fibration and its connection with F-theory on elliptic fourfolds. The transition that we will consider is between a fiber of Kodaira type I_2 to a fiber of Kodaira type III. A fiber of type I_2 is composed of a conic intersecting a line at two distinct points. It specializes to a fiber of type III when the line is tangent to the conic, that is, when the two intersection points coincide. As reviewed in Table 4.2, a fiber of type I_2 is characterized by $b_2 = c_3 = 0$ and it specializes to a fiber of typer III when in addition $c_2 = 0$. We will use ε as our deformation parameter and the weak coupling limit ($j \to \infty$) will be reached as ε approaches zero. We will also denote h a section of $\mathscr{L}^2$. We will use it to define the double cover of the base $\rho : X \to B$ as $\xi^2 = h$.

4.4.1 Choice of a weak coupling limit

We will impose the fiber I_2 in the weak coupling limit (that is at $\varepsilon = 0$) and the fiber III over the orientifold at $\varepsilon = h = 0$:

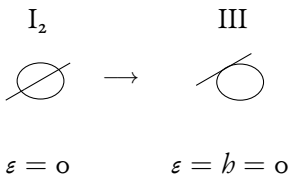

This is done by the following choice:

$$\text{Weak coupling limit: } \mathrm{I}_2 \to \mathrm{III} \quad \begin{cases} b_2 = \varepsilon^2 \rho, & c_3 = \varepsilon k, \\ c_0 = \chi, & c_1 = 2\eta, \quad c_2 = h, \end{cases} \tag{4.60}$$

which leads to the following behavior at leading order in ε

$$\Delta \propto \varepsilon^2 h^2 k^2 (\eta^2 - h\chi), \quad j \propto \frac{h^4}{\varepsilon^2 k^2 (\eta^2 - h\chi)}. \tag{4.61}$$

It is then direct to see that we do have a weak coupling limit since $\lim_{\varepsilon \to 0} j = \infty$ as long as we are away from $h = 0$. Over a general point of h, we have $\lim_{\varepsilon \to 0} j = 0$. But at the intersection of $h = 0$ with $k(\eta^2 - \chi h) = 0$, the j-invariant is not well-defined.

4.4.2 Brane spectrum at weak coupling

Defining the double cover $\rho : X \to B$ branched over the locus $h = 0$:

$$X : \ \xi^2 = h. \tag{4.62}$$

With the weak coupling limit (4.60), we can identify the following spectrum at weak coupling:

1. $O : \xi = 0$: the orientifold,

2. $D : k = 0$: a stack of two invariant D7-branes,

3. $D_w : \eta^2 - \xi^2\chi = 0$, a Whitney-brane.

4.4.3 Topological tadpole matching for $\mathrm{Q}_7(\mathscr{L}, \mathscr{S})$ models

The weak coupling limit (4.60) constructed in the previous subsection naturally leads to the following relation

$$2\chi(Y) = 4\chi(O) + 2\chi(D) + \chi(D_w),$$

which is a direct consequence of the following theorem:

Theorem 4.4.1 (Topological tadpole matching for $\mathrm{Q}_7(\mathscr{L}, \mathscr{S})$ elliptic fibrations)**.** *A $Q_7(\mathscr{L}, \mathscr{S})$ elliptic fibration endowed with the weak coupling limit* (4.60) *satisfies the topological tadpole matching condition at the level of the total Chern class:*

$$2\phi_* c(Y) = 4\rho_* c(O) + 2\rho_* c(D) + \rho_* c^{\infty}(D_w),$$

where the Chern class of the Whitney brane is understood as $\rho_* c^{\infty}(D_w) = \rho_* c(\overline{D}_w) - \rho_* c(S)$, with $\overline{D}_w$ the normalization of D_w and S the cuspidial locus of the Whitney brane.

First we establish the following important lemma that gives the Chern class from which we compute the orientifold Euler characteristic of a Whitney brane.

Lemma 4.4.2. *Consider $\underline{D} : \eta^2 - h\chi = 0$*

$$\rho_* c^{\infty}(D_w) = \frac{4(2L - S)}{(1 + 2L)(1 + 2L - 2S)}. \tag{4.63}$$

Proof. This is a direct calculation following [5]:

$$\begin{aligned}\rho_* c^{\infty}(D_w) &= 2c_{SM}(\underline{D}) - 2i^*(S) \quad \text{(by definition)} \\ &= \frac{4(2L-S)}{(1+2L)(1+2L-2S)}. \end{aligned} \tag{4.64}$$

□

We can now prove the theorem.

Proof. The Chern class of the Whitney brane is understood as $\rho_* c^{\infty}(D_w) = \rho_* c(\overline{D}_w) - \rho_* c(S)$, with $\overline{D}_w$ the normalization of D_w and S the cuspidial locus of the Whitney brane.

$$\pi_* c(Y) = \frac{6(2L+2L^2-LS-S^2)}{(1+2L-2S)(1+2L+S)} c(B), \tag{4.65}$$

$$\rho_* c(O) = \frac{2L}{1+2L} c(B), \tag{4.66}$$

$$\rho_* c(D) = \frac{2(1+L)(2L+S)}{(1+2L)(1+2L+S)} c(B), \tag{4.67}$$

$$c^{\infty}(D_w) = \frac{4(2L-S)}{(1+2L)(1+2L-2S)}, \tag{4.68}$$

The generalized tadpole follows immediately form the following rational identity:

$$\frac{12(2L+2L^2-LS-S^2)}{(1+2L-2S)(1+2L+S)} - \frac{8L(1+2L+S)+4(1+L)(2L+S)}{(1+2L)(1+2L+S)} - \frac{4(2L-S)}{(1+2L)(1+2L-2S)} = 0. \tag{4.69}$$

□

4.4.4 Weak coupling geometry: a second look.

The weak coupling limit we have obtained previously for the elliptic fibration of type $\mathrm{Q}_7(\mathscr{L},\mathscr{S})$ is given by the following family over the ε-line:

$$Y_{(\varepsilon)} : y(x^2+\chi y^2+2\eta yz+hz^2)+\varepsilon(kz^3+\varepsilon\rho xz^2)=0. \tag{4.70}$$

When $\varepsilon \neq 0$, $Y_{(\varepsilon)}$ is a smooth elliptic fibration. When $\varepsilon = 0$, $Y_{(\varepsilon)}$ degenerates into the normal crossing variety

$$Y_{(0)} : \quad y(x^2+\chi y^2+2\eta yz+hz^2)=0, \tag{4.71}$$

which is composed of two smooth varieties Z_1 and Z_2 :

$$Z_1 : y=0, \qquad Z_2 : x^2+\chi y^2+2\eta yz+hz^2=0. \tag{4.72}$$

Z_1 is the bundle $\mathbb{P}^1[\mathscr{L}\oplus\mathscr{O}_B]$ over the base B while Z_2 is a fibration of conics realized as quadric in the $\mathbb{P}^2$-bundle in which the elliptic fibration is defined. The normal crossing variety $Y_{(0)}$ is a fibration of intersecting $\mathbb{P}^1$s whose generic fiber is a fiber of Kodaira type I_2 realized by a line (the fiber of Z_1) intersecting transversally a conic (the fiber of Z_2).

Lemma 4.4.3. *The intersection of the two irreducible components of $Y_{(0)}$ is a smooth variety X which is a double cover $\rho : X \to B$ of the base B.*

Indeed, the intersection is defined by the following complete intersection:

$$X = Z_1 \cap Z_2 : y = x^2 + hz^2 = 0. \tag{4.73}$$

This intersection is completely included in the patch $z \neq 0$ as otherwise $x = y = z = 0$, which is not allowed since $[x : y : z]$ are projective coordinates of a $\mathbb{P}^2$ projective bundle. In order to connect with notations familiar in F-theory, we put $y = z - 1 = 0$ in the definition of $Z_1 \cap Z_2$. We are left only with the affine coordinate x, which is a section of the line bundle $\mathscr{L}$. Introducing $\xi = ix$, the intersection can simply be expressed in the total space of the line bundle $\mathscr{L}$ by the canonical equation $\xi^2 = h$:

$$\rho : X \to B : \quad \xi^2 = h. \tag{4.74}$$

This is a double cover of the base B of the original elliptic fibration branched on the divisor $\underline{O} : h = 0$ in B:

$$\underline{O} : h = 0. \tag{4.75}$$

This divisor of B pulls back to the divisor $O = \rho^* \underline{O}$:

$$O : \xi = 0, \quad \text{in} \quad X. \tag{4.76}$$

It is the divisor $O \subset X$ which is called the *orientifold plane*. One can see X as a type IIB orientifold

weak coupling limit of F-theory on Y. The discriminant locus of the conic fibration Z_2:

$$\underline{D}_w : \eta^2 - h\chi = 0,$$

which is singular at $\eta = h = \chi = 0$. The variety $\underline{D}_w$ pull-back in the double cover X as the Whitney brane $D_w = \rho^\star \underline{D}_w$:

$$D_w : \quad \eta^2 - \xi^2\chi = 0. \tag{4.77}$$

4.4.5 Fiberwise description of the limit

The generic fiber at $\varepsilon \neq 0$ is a smooth elliptic curve. At $\varepsilon = 0$, the fiber degenerates to a singular elliptic fiber of Kodaira type I_2. This I_2 fiber is composed of a line and a conic meeting at two distinct points. The leading order in ε defines a family of elliptic fibration

$$Y_{(\varepsilon)} : x^2 y + \chi y^3 + 2\eta y^2 z + h y z^2 + \varepsilon k z^3 = 0.$$

At leading order in ε, the discriminant locus of $Y_{(0)}$ splits into three components

$$\Delta_{(\varepsilon)} \propto \quad \varepsilon^2 h^2 k^2 \left(\eta^2 - h\chi\right) = 0. \tag{4.78}$$

The first one is the branch locus of the orientifold $h = 0$, the second one $\underline{D} : k = 0$ is a stack of two branes transversal to the orientifold and the last one is a Whitney brane $\underline{D} : \eta^2 - \chi h = 0$. The fibers over $h = 0$ are of type I_1 for $\varepsilon \neq 0$ and of type III for $\varepsilon = 0$. Over $k = 0$, the fibers are of

type I_2. The fiber over the Whitney brane are of type I_1 when $\varepsilon \neq 0$ and of type I_3 when $\varepsilon = 0$. If we consider higher terms in ε, the stack of branes and the Whitney brane recombine into a unique brane:

$$\Delta_{(\varepsilon)} \propto \varepsilon^2 k^2 \left(-4h^2\eta^2 + 4h^3\chi + 32k\varepsilon\eta^3 - 36hk\varepsilon\eta\chi + 27k^2\varepsilon^2\chi^2\right) = 0. \tag{4.79}$$

Interestingly, $Y_{(0)}$ is not an elliptic fibration: the generic fiber is not an elliptic curve but a fiber of type I_2, composed of a line $y = 0$ and a conic $x^2 + \chi y^2 + 2\eta yz + hz^2 = 0$. The fiber I_2 specializes to a fiber of type III when the line becomes tangent to the conic. This happens when $h = 0$:

$$\underline{O}: \quad h = 0 \to \text{III}. \tag{4.80}$$

The fiber I_2 specializes to a triangle I_3 as the conic splits into two lines. This happens when the discriminant of the conic vanishes and corresponds to the Whitney brane:

$$\underline{D_w}: \quad \eta^2 - \chi h = 0 \to I_3. \tag{4.81}$$

The two lines coming from the conics are no individually well defined because of a $\mathbb{Z}_2$ monodromy[4]. When $h = \eta = 0$, the fiber specializes further to a star (a fiber of type IV):

$$\underline{O} \cap \underline{D_w}: \quad h = \eta = 0 \to \text{IV}. \tag{4.82}$$

Finally, when $b = \eta = \chi = 0$, the fiber specializes to a double line $x^2 = 0$ intersecting transversally the line $y = 0$. This is a non-Kodaira fiber of type $\mathrm{IV}^{(2)}$:

$$Sing(\underline{D_w}) : \quad b = \eta = \chi = 0 \to \mathrm{IV}^{(2)}. \tag{4.83}$$

4.5 Conclusion and discussion

In this chapter we introduce a new model for elliptic fibrations with a Mordell–Weil group of rank one using an hypersurface in a projective bundle. Global aspects of this elliptic fibration are controlled by two line bundles $\mathscr{L}$ and $\mathscr{S}$ that are used to define the ambient space $\pi : \mathbb{P}[\mathscr{L} \oplus \mathscr{S} \oplus \mathscr{O}_B] \to B$. The equation is then retrieved as a section of the line bundle $\mathscr{O}(3) \otimes \pi^*\mathscr{L}^2 \otimes \pi^*\mathscr{S}$. The resulting defining equation is a cubic with a Newton's polygon which is a reflexive polytope in a quadrilateral shape with seven lattice points on its boundary. We call it an elliptic fibration of type $\mathrm{Q}_7(\mathscr{L}, \mathscr{S})$. This models generalize both the E_6 elliptic fibration and the elliptic fibration introduced recently by Cacciatori, Cattaneo, and Van Geemen [64]. Using this smooth model we can easily determine the spectrum of singular fibers and compute basic topological invariants. We identify seven possible singular fibers: six Kodaira fibers (type I_1, I_2, I_3, II, III and IV) and the non-Kodaira fiber of type $\mathrm{IV}^{(2)}$. We also get a pushforward formula for the total Chern class. This is a generalized Sethi-Vafa-Witten formula. Using the geometric description of the weak coupling limit developed in [6], we find a weak coupling limit for the $\mathrm{Q}_7(\mathscr{L}, \mathscr{S})$ elliptic fibration. The weak coupling that we consider is based on a specialization to a fiber of type I_2 over a general point of the base. The fiber

specialize further to a fiber of type III over the orientifold $h = 0$:

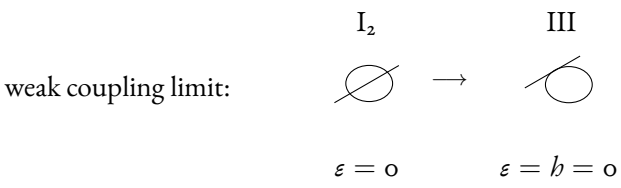

It yields the following brane spectrum at weak coupling:

$$(\star) \quad \text{a } \mathbb{Z}_2 \text{ orientifold} + \text{ a Whitney brane} + \text{an } Sp(1) \text{ stack.}$$

The $Sp(1)$ stack is composed of two smooth and invariant branes intersecting the orientifold transversally. We prove that the tadpole matching condition is satisfied for this spectrum. The singularities of the Whitney brane play an essential role as they contribute to the D3-charge at weak coupling. Such a contribution is already necessary for the usual Sen's limit and for certain weak coupling limits of E_7 elliptic fibrations [5, 6, 78]. The Euler characteristic for the Whitney brane is defined using the *orientifold Euler characteristic* introduced in [78] and mathematically defined in [5]. The weak coupling limit that we have obtained is naturally an ALE degeneration of the elliptic fibration. As the coupling becomes weak, the generic fiber is no longer elliptic but becomes a fiber of type I_2 composed of a conic and a line meeting at two distinct points. As we move over the locus of the orientifold, the conic becomes tangent to the line and we get a fiber of type III.

There are several interesting questions that are not discussed in this chapter. For example, the weak coupling limit discussed here is not unique. But it is not clear that another one would satisfy

the tadpole condition. The fibration discussed in [64] does not satisfy the tadpole condition but seems to admit specializations describing orientifolds with surprising properties. An analysis of these particular cases will be the subject of a companion chapter.

Part III

Topological Invariants and Characteristic Numbers

Introduction

The study of crepant resolutions of Weierstrass models, their fibral structure, and their flop transitions is an area of common interest to algebraic geometers, number theorists, and string theorists [124, 125, 127, 129, 135, 163, 286]. The theory of elliptic surfaces has its beginnings in the 1960s, and was advanced largely by the contributions of mathematicians such as Kodaira [200]; Néron [251]; Mumford and Suominen [246], Deligne [94], and Tate [290]. Miranda studied the desingularization of elliptic threefolds and the phenomenon of collisions of singularities in [236], and Szydlo subsequently generalized Miranda's work to elliptic n-folds [286]; the Picard number (i.e., the rank of the Néron-Severi group) of an elliptic fibration can be obtained using the Shioda–Tate–Wazir theorem [300]; the study of elliptic fibrations having the same Jacobian was developed by Dolgachev and Gross [100]; and Nakayama studied local and global properties of Weierstrass models over bases of arbitrary dimension in [249, 250]. Furthermore, more recent developments have been inspired by string theory (in particular, M-theory and F-theory) constructions that ascribe an interesting physical meaning to various topological and geometric properties of elliptically-fibered Calabi–Yau varieties [37, 96, 176, 243, 244, 292].

A Weierstrass model provides a convenient framework for computing the discriminant, the j-invariant, and the Mordell–Weil group of an elliptic fibration. Weierstrass models are also the setting in which Tate's algorithm is defined [290]. Any elliptic fibration over a smooth base is birational to a (potentially singular) Weierstrass model [94]. Since a Weierstrass model is a hypersurface, it is Gorenstein [105, Corollary 21.19], and hence its canonical class is well-defined as a Cartier divisor.

In practice, it is often necessary to regularize the singularities of Weierstrass models when computing, for example, their topological invariants. Among the possible regularizations of a singular variety, crepant resolutions are particularly desirable as, by definition, they preserve the canonical class and the smooth locus of the variety. In a sense, crepant resolutions modify the variety as mildly as possible while regularizing its singularities. Surfaces with canonical singularities always have a crepant resolution, which is unique up to isomorphism. However, for varieties of dimension three or higher, crepant resolutions do not necessarily exist, and when they do, they may not be unique. Distinct crepant resolutions of the same Weierstrass model are connected by a network of flops.

Example 4.5.1. The quadric cone over a conic surface $V(x_1x_2 - x_3x_4) \subset \mathbb{C}^4$ has two crepant resolutions related by an Atiyah flop. By contrast, the quadric cone $V(x_1^2 + x_2^2 + x_3^2 + x_4^2 + x_5^2) \subset \mathbb{C}^5$ does not have a crepant resolution since it has $\mathbb{Q}$-factorial terminal singularities. The binomial variety $V(x_1x_2 - u_1u_2u_3) \subset \mathbb{C}^5$ has six crepant resolutions whose network of flops forms a hexagon [129]. For additional examples of flops involving Weierstrass models, see [112–115, 118–121, 125, 127].

There is an important subset of singular Weierstrass models that have crepant resolutions and play a central role in string geometry, as they are instrumental in the geometric engineering of gauge theories in F-theory and M-theory. We refer to them as G-models, they are defined in Section 2.3 in the introduction and are typically obtained by the Weierstrass models that appear as outputs of Tate's algorithm [37, 186, 290]. The networks of crepant resolutions of these Weierstrass models are conjectured to be isomorphic to the incidence graph of the chambers of a hyperplane arrangement [110, 111, 163, 176].

In the last few years, there was significant progress in the longstanding problem to describe all crepant resolutions of a given G-model given by a singular Weierstrass model and understand the geography of the flops connecting them, some of which are presented in this thesis [13, 112–115, 118–121, 124, 125, 127, 129, 163, 229]. The number of distinct resolutions associated to a G-model can be rather large [110, 111, 163]. Another natural step in our understanding of these geometries is to explore further their topology and intersection rings. The intersection ring is not invariant under flops as we see already in the study of triple intersection numbers of elliptically fibered threefolds connected by flops [112, 115, 118, 119, 121, 124].

The most convenient invariants to compute are those preserved under crepant birational maps, as they are independent of a choice of a crepant resolution. An example of such a topological invariant is the Euler characteristic—using p-adic integration and Weil conjecture, Batyrev proved that the Betti numbers of smooth varieties connected by a crepant birational map are the same [29], and it therefore follows that the Euler characteristics of any two crepant resolutions are the same.

The purpose of Chapter 5 is to compute the Euler characteristics of G-models obtained by crepant resolutions of Weierstrass models, where G is a simple group. Following [5, 6], we allow the base to be of arbitrary dimension and we do not impose the Calabi–Yau condition. We work relative to a base that we leave arbitrary. In this sense, this chapter is a direct generalization of the work of Fullwood and van Hoeij on stringy invariants of Weierstrass models [135].

The Euler characteristic of an elliptic fibration plays a central role in many physical problems such as the computation of gravitational anomalies of six dimensional supergravity theories [142, 257] and the cancellation of tadpoles in four dimensional theories [5, 6, 44, 78, 109, 120, 279]. Unfortu-

nately, the Euler characteristics of crepant resolutions of Weierstrass models are generally not known, although they have been computed in some special cases for Calabi–Yau threefolds and fourfolds [12, 13, 135, 226]. For instance, the Euler characteristics of G-models for Calabi–Yau threefolds were studied in [142], and there are conjectures for the Euler characteristics of G-models for Calabi–Yau fourfolds based on heterotic string theory/F-theory duality [44].

We continue the work started in Chapter 5 by providing additional characteristic numbers of G-models in Chapter 6. It is mentoned earlier that it is interesting to study topological invariants that do not depend on the choice of a crepant resolution. Such invariants include the Euler characteristic and the Hodge numbers [29, Kontsevich]. In particular, their values for Calabi–Yau fourfolds were subject of conjectured inspired by string dualities [44]. There have been major improvements in the literature that such conjectures are now becoming theorems with even more general assumptions [114]. In particular, the Euler characteristics of G-models of arbitrary dimensions are systematically derived in [114].

In addition, if the variety is at most of complex dimension four, its Chern numbers, and hence all its characteristic numbers that are rational combinations of Chern numbers, are also invariant under crepant birational maps [3, 116]. Only elliptic fibrations of dimension four or less are considered in [116], since crepant birational fivefolds do not necessarily have the same Chern numbers as illustrated by Goresky and MacPherson in [140, Example 2, p221].

Characteristic classes are cohomology classes associated to isomorphic classes of vector bundles [136, 171, 234]. They measure how a vector bundle is twisted or non-trivial. Characteristic classes of a nonsingular variety are defined via its tangent bundle.

Characteristic classes are instrumental in many questions of geometry and theoretical physics. In string theory and in supergravity theories, characteristic classes appear in discussions of anomaly cancellations [7, 8] and tadpole cancellations [78, 96, 279], in the computations of the index of supersymmetry operators, and in the definition of the charges of D-branes [5, 235] and orientifold planes [274].

The characteristic numbers of G-models that are smooth fourfolds obtained by crepant resolutions of Weierstrass models have been determined in Chapter 6. The key to all these developments is a new pushforward theorem in Chapter 5 that streamlines computations in the intersection ring of a blowup with a center that is a smooth complete intersection.

The Chapter 7 is a follow-up to Chapter 6, where we computed characteristic numbers of G-models of complex dimension four for $G = \mathrm{SU}(n)$ ($n = 2, 3, 4, 5, 6, 7$), Spin(7), Spin(8), Spin(10), G_2, F_4, E_6, E_7, and E_8. Each group considered in [116] are simply-connected, which implies that the Mordell–Weil group of the generic fiber of the associated elliptic fibration is trivial. We aim to extend the results of [116] to elliptic fibrations with multisections or a non-trivial Mordell–Weil group.

Lisez Euler, lisez Euler, c'est notre maître à tous.

Pierre-Simon Laplace

5

Euler characteristics of crepant resolutions of Weierstrass models

A crucial ingredient of our results is Theorem 5.0.1, which is a pushforward formula for any analytic function of the class of the exceptional divisor of a blowup of a nonsingular variety along a smooth complete intersection of hypersurfaces meeting transversally. Theorem 5.0.1 is a generalization to

arbitrary analytic functions of a result of Fullwood and van Hoeij [135, Lemma 2.2], which relies on a theorem of Aluffi [4] simplifying the classic formula of Porteous on Chern classes of the tangent bundle of a blowup [261]. Theorem 5.0.1 profoundly simplifies the algebraic manipulations necessary to compute pushforwards, and therefore has a large range of applications independently of the specific applications discussed in this chapter.

For the reader's convenience, we provide tables specializing our results to the cases of elliptic threefolds and fourfolds, and further to the cases of Calabi–Yau threefolds and fourfolds, including an explicit computation of the Hodge numbers in the Calabi–Yau threefold case. We emphasize that our results are insensitive to the particular choice of a crepant resolution due to Batyrev's theorem on the Betti numbers of crepant birational equivalent varieties [29] and Kontsevich's theorem on the Hodge numbers of birational equivalent Calabi–Yau varieties [Kontsevich].

One of our key results in this chapter is a pushforward theorem that streamlines all the computations of this chapter. We present the pushforward theorem in this subsection.

Theorem 5.0.1. *Let the nonsingular variety $Z \subset X$ be a complete intersection of d nonsingular hypersurfaces $Z_1, \cdots, Z_d$ meeting transversally in X. Let E be the class of the exceptional divisor of the blowup $f : \widetilde{X} \longrightarrow X$ centered at Z. Let $\widetilde{Q}(t) = \sum_a f^* Q_a t^a$ be a formal power series with $Q_a \in A_*(X)$. We define the associated formal power series $Q(t) = \sum_a Q_a t^a$ whose coefficients pullback to the coefficients of $\widetilde{Q}(t)$. Then the pushforward $f_* \widetilde{Q}(E)$ is:*

$$f_* \widetilde{Q}(E) = \sum_{\ell=1}^{d} Q(Z_\ell) M_\ell, \quad \text{where} \quad M_\ell = \prod_{\substack{m=1 \\ m \neq \ell}}^{d} \frac{Z_m}{Z_m - Z_\ell}.$$

We call the coefficient M_ℓ the *ℓ-moment* of the blowup f.

Remark 5.0.2. Given a blowup $f : \widetilde{X} \longrightarrow X$, any element α of the Chow ring $A_*(\widetilde{X})$ can be expressed as $\alpha = \sum_{n=0}^{\infty} f^* \alpha_i E^i$ where α_i are elements of the Chow ring $A_*(X)$. So Theorem 5.0.1 can be used to pushforward any element of $A_*(\widetilde{X})$.

Theorem 5.0.1 is proven in §5.4.1. By the projection formula and the linearity of the pushforward, the proof of Theorem 5.0.1 is almost trivial once it is established in the special case of a monic monomial $Q(t) = t^k$. This special case is Lemma 5.4.4 on page 242. The proof of the Lemma 5.4.4 relies on an identity due to Carl Gustave Jacobi that gives a partial fraction formula for homogeneous complete symmetric polynomials:

Lemma 5.0.3 (Jacobi). *Let $h_r(x_1, \ldots, x_d)$ be the homogeneous complete symmetric polynomial of degree r in d variables of an integral domain. Then:*

$$h_r(x_1, \cdots, x_d) = \sum_{\ell=1}^{d} x_\ell^{r+d-1} \prod_{\substack{m=1 \\ m \neq \ell}}^{d} \frac{1}{x_\ell - x_m}.$$

Jacobi first proved this identity in 1825 in a slightly different form in his doctoral thesis[1] as a partial fraction reformulation of the generating function of complete homogeneous polynomials. Lemma 5.0.3 was rediscovered in many different mathematical and physical problems, as discussed elegantly in [154]. For example, a proof using Schur polynomials was proposed as the solution to Exercise

[1] [177, Section III.17, p. 29-30], Jacobi asserts:

$$\prod_i \frac{1}{x - a_i} = \sum_i \frac{1}{x - a_i} \prod_{\ell \neq i} \frac{1}{a_\ell - a_i}$$

7.4 of [283]. For a proof using integrals and residues see Appendix A of [222]; for a proof using matrices, see [81]. We give a short and simple proof of this identity in Section 5.5.

We also make use of a second pushforward theorem that concerns the projection from the ambient projective bundle to the base B over which the Weierstrass model is defined. Let $\mathscr{V}$ be a vector bundle of rank r over a nonsingular variety B. The Chow ring of a projective bundle $\pi : \mathbb{P}(\mathscr{V}) \longrightarrow B$ is isomorphic to the module $A_*(B)[\zeta]$ modded out by the relation [136, Remark 3.2.4, p. 55]

$$\zeta^r + c_1(\pi^*\mathscr{V})\zeta^{r-1} + \cdots + c_i(\pi^*\mathscr{V})\zeta^{r-i} + \cdots + c_r(\pi^*\mathscr{V}) = 0, \quad \zeta = c_1\Big(\mathscr{O}_{\mathbb{P}(\mathscr{V})}(1)\Big).$$

Theorem 5.0.4 (See [5, 6, 134]). *Let $\mathscr{L}$ be a line bundle over a variety B and $\pi : X_0 = \mathbb{P}[\mathscr{O}_B \oplus \mathscr{L}^{\otimes 2} \oplus \mathscr{L}^{\otimes 3}] \longrightarrow B$ a projective bundle over B. Let $\widetilde{Q}(t) = \sum_a \pi^* Q_a t^a$ be a formal power series in t such that $Q_a \in A_*(B)$. Define the auxiliary power series $Q(t) = \sum_a Q_a t^a$. Then*

$$\pi_*\widetilde{Q}(H) = -2\,\frac{Q(H)}{H^2}\bigg|_{H=-2L} + 3\,\frac{Q(H)}{H^2}\bigg|_{H=-3L} + \frac{Q(0)}{6L^2},$$

where $L = c_1(\mathscr{L})$ and $H = c_1(\mathscr{O}_{X_0}(1))$ is the first Chern class of the dual of the tautological line bundle of X_0.

Proof. Using the functoriality of Segre classses, we can write

$$\pi_*\left(\frac{1}{1-H}\right) = \frac{1}{(1+2L)(1+3L)} = \frac{-2}{1+2L} + \frac{3}{1+3L},$$

which can be expanded on the both sides. This gives the following expressions for the pushforward

of each power of H:

$$\pi_* 1 = 0\,,\ \pi_* H = 0\,,\ \pi_* H^{i+2} = \left[-2(-2)^i + 3(-3)^i\right] L^i$$

where i is nonnegative. Then, expanding $Q(H)$ as a power series with coefficients in $A_*(B)$,

$$\widetilde{Q}(H) = \sum_{i=0}^{\infty} \pi^* \alpha_i H^i = \pi^* \alpha_0 + (\pi^* \alpha_1) H + H^2 \sum_{k=0}^{\infty} (\pi^* \alpha_k) H^k,$$

the pushforward of $Q(H)$ can hence be computed as

$$\begin{aligned}
\pi_* \widetilde{Q}(H) &= -2 \sum_{k=0}^{\infty} \alpha_k (-2L)^k + 3 \sum_{k=0}^{\infty} \alpha_k (-3L)^k \\
&= -2 \frac{Q(H) - \alpha_1 H - \alpha_0}{H^2}\Big|_{H=-2L} + 3 \frac{Q(H) - \alpha_1 H - \alpha_0}{H^2}\Big|_{H=-3L} \\
&= -2 \frac{Q(H)}{H^2}\Big|_{H=-2L} + 3 \frac{Q(H)}{H^2}\Big|_{H=-3L} + \frac{Q(0)}{6L^2}.
\end{aligned}$$

□

5.1 Strategy and organization of the chapter

5.1.1 Strategy

We take an intersection theory point of view inspired by Fulton [136] and Aluffi [4], and use explicit crepant resolutions of Tate models to compute their Euler characteristics. Using Chern classes, we evaluate the Euler characteristic without dealing with the combinatorics of the fiber structure. In-

stead, we compute the pushforward of the homological Chern class of the variety to the base of the fibration. Since the Euler characteristics of two crepant resolutions of the same Weierstrass model are the same [29], we do not need to explore the network of all flops to arrive at our conclusions.

Our method for computing the Euler characteristics of G-models is as follows. Given a choice of Lie group G, we first use Tate's algorithm to determine a singular Weierstrass model $Y_0 \longrightarrow B$ such that G is the Lie group attached to the elliptic fibration following the F-theory algorithm discussed in Section 2.3 in the introduction. We then determine a crepant resolution $f : Y \longrightarrow Y_0$ of the singular Weierstrass model to obtain an explicit realization of the G-model as a smooth projective variety. By doing so, we retrieve the data necessary to compute the total homological Chern class of the crepant resolution $f : Y \longrightarrow Y_0$. We apply Theorem 5.0.1 repeatedly to push this class forward to the projective bundle X_0 in which the Weierstrass model is defined. Finally, we use Theorem 5.0.4 to push the total Chern class forward to B. In doing so, we obtain a generating function of the form

$$\chi(Y) = \int_B Q(L,S)c(B), \quad c(B) := c(TB) \cap [B],$$

where $\int_B$ indicates the degree, $Q(L,S)$ is a rational function in L and S such that

$$Q(L,0) = \frac{12L}{1+6L}c(B).$$

$Q(L,0)$ is the generating function for the Euler characteristic of a smooth Weierstrass model [5]. The rational expression $Q(L,S)c(B)$ is defined in the Chow ring $A_*(B)$ of the base. The expression

$\chi(Y)$ is a generating function in the following sense. If the base has dimension d, the Euler characteristic is then given by the coefficient of t^d in a power series expansion in the parameter t:

$$\chi(Y) = [t^d]\left(Q(tL, tS)c_t(TB)\right), \quad \text{where} \quad d := \dim\, B,$$

where $[t^n]g(t) = g_n$ for a formal series $g(t) = \sum_{i=0}^{\infty} g_i t^i$, and

$$c_t(TB) = 1 + c_1(TB)t + \cdots + c_d(TB)t^d,$$

is the Chern polynomial of the tangent bundle of B.

It follows from the adjunction formula that one can further impose the Calabi–Yau condition by setting $L = c_1(TB)$; see Tables 5.5 and 5.6 for the Euler characteristics of elliptic threefold and fourfold G-models.

In Table 5.1, we organize the Lie algebras associated to our choices of Tate models into a network, where an arrow indicates inclusion as a subalgebra.

$$\begin{array}{ccccccccccccc} & & & & & & \mathrm{C}_2 & \longrightarrow & \mathrm{A}_3 & \longrightarrow & \mathrm{A}_4 & \longrightarrow & \mathrm{D}_5 \\ & & & & & & \downarrow & & \downarrow & & & & \downarrow \\ \mathrm{A}_1 & \longrightarrow & \mathrm{A}_2 & \longrightarrow & \mathrm{G}_2 & \longrightarrow & \mathrm{B}_3 & \longrightarrow & \mathrm{D}_4 & \longrightarrow & \mathrm{F}_4 & \longrightarrow & \mathrm{E}_6 & \longrightarrow & \mathrm{E}_7 & \longrightarrow & \mathrm{E}_8 \end{array}$$

$\mathrm{I}_2^{\mathrm{s}}$, $\mathrm{I}_2^{\mathrm{ns}}$, III, $\mathrm{IV}^{\mathrm{ns}}$, $\mathrm{I}_3^{\mathrm{ns}}$	IV^{s}, $\mathrm{I}_3^{\mathrm{s}}$	$\mathrm{I}_4^{\mathrm{s}}$	$\mathrm{I}_4^{\mathrm{ns}}$	$\mathrm{I}_5^{\mathrm{s}}$	$\mathrm{I}_0^{*\mathrm{ns}}$	$\mathrm{I}_0^{*\mathrm{ss}}$	$\mathrm{I}_0^{*\mathrm{s}}$	$\mathrm{IV}^{*\mathrm{ns}}$	$\mathrm{I}_1^{*\mathrm{s}}$	$\mathrm{IV}^{*\mathrm{s}}$	III*	II*
A_1	A_2	A_3	C_2	A_4	G_2	B_3	D_4	F_4	D_5	E_6	E_7	E_8

Table 5.1: Models studied in this section.

As is evident from Table 5.1, the results of this chapter cover all instances of Kodaira fibers with

the exception of the general cases of I_k and I_k^*. In particular, our list contains:

- G-models corresponding to Deligne exceptional series:

$$\{e\} \subset \mathrm{A}_1 \subset \mathrm{A}_2 \subset \mathrm{G}_2 \subset \mathrm{D}_4 \subset \mathrm{F}_4 \subset \mathrm{E}_6 \subset \mathrm{E}_7 \subset \mathrm{E}_8.$$

- G-models for the extended exceptional series[2]:

$$\{e\} \subset \mathrm{A}_1 \subset \mathrm{A}_2 \subset \mathrm{A}_3 \subset \mathrm{E}_4 \subset \mathrm{E}_5 \subset \mathrm{E}_6 \subset \mathrm{E}_7 \subset \mathrm{E}_8.$$

- G-models for simple orthogonal groups of small rank[3]:

$$\{e\} \subset \mathrm{SO}(3) \subset \mathrm{SO}(5) \subset \mathrm{SO}(6).$$

- G-models of the I_0^* series [112]:

$$\{e\} \subset \mathrm{G}_2 \subset \mathrm{Spin}(7) \subset \mathrm{Spin}(8).$$

[2] We recall that the Dynkin diagram of E_n is the same as A_n but with the nth node connected with the third node. In particular, $\mathrm{E}_4 \cong \mathrm{A}_4$, $\mathrm{E}_5 \cong \mathrm{D}_5$, $\mathrm{E}_3 = \mathrm{A}_2 \times \mathrm{A}_1$, $\mathrm{E}_2 = \mathrm{A}_2$, and $\mathrm{E}_1 = \mathrm{A}_1$.

[3] These models require a Mordell–Weil group $\mathbb{Z}/2\mathbb{Z}$.

5.1.2 Organization of the chapter

The remainder of the chapter is organized as follows. In Section 5.2 we discuss some general properties of the Euler characteristic of an elliptic fibration. With this in mind, an explanation of the Euler characteristic as the degree of the top Chern class is given in Section 5.3. In Section 5.4.1 we discuss the pushforward theorem and explain the details of our computation of the Euler characteristic. A proof of Jacobi's partial fraction identity is given in Section 5.5. Section 5.6 then describes how these results can be used to calculate the Hodge numbers of Calabi–Yau threefold G-models. In Section 5.7, we describe the simplest model, the SU(2)-model, as an example of our computation. We present the results of our computation in a series of tables in Section 5.8. Finally, in Section 5.9 we conclude with a discussion of the computation and comment on possible future research directions.

5.2 Euler Characteristic of Elliptic Fibrations

The Euler characteristic of a smooth Weierstrass model $\phi : Y \longrightarrow B$ over a base B is given by the following formula[5, 6]

$$\chi(Y) = \int \frac{12L}{1+6L} c(B),$$

where $c(B) = c(TB) \cap [B]$ is the total homological Chern class and $L = c_1(\mathscr{L})$ is the first Chern class of the fundamental line bundle $\mathscr{L} = (R^1\phi_*\mathscr{O}_Y)^{-1}$ of the elliptic fibration. This expression is the generating function for the Euler characteristic. Assigning weight n to the nth Chern class, the Euler

characteristic of Y is the component of weight $d = \dim B$. A direct expansion gives

$$\chi(Y) = -2\sum_{i=1}^{d}(-6L)^i c_{d-i}(TB) \cap [B].$$

The Euler characteristic of an elliptic surface is given by Kodaira's formula [200, III, Theorem 12.2, p. 14]:

$$\chi(Y) = \sum_i v(\Delta_i),$$

where the discriminant $\Delta = \sum_i \Delta_i$ is a sum of points Δ_i and $v(\Delta_i)$ denotes the valuation of Δ_i. In particular, the Euler characteristic of the resolution of a Weierstrass model over a curve is always $12\int L$:

$$\chi(Y) = \int 12L.$$

There are several different ways to compute the Euler characteristic of an elliptic fibration. The Euler characteristic (with compact support) is multiplicative on local trivial fibrations and satisfies the excision property ($\chi(X/Z) = \chi(X) - \chi(Z)$ for any closed $Z \subset X$); moreover, if $\varphi : M \to N$ is a smooth proper morphism, then $\chi(M) = \chi(N)\chi(N_\eta)$ where $\chi(N_\eta)$ is the Euler characteristic of the generic fiber. It follows from these properties that the Euler characteristic of an elliptic fibrations gets all its contribution from its discriminant locus since the Euler characteristic of a smooth elliptic curve is zero. One can identify a partition of the discriminant locus by subvarieties V_i over which

the generic fiber is constant. The Euler characteristic is then

$$\chi(Y) = \sum_i \chi(V_i)\chi(Y_{\eta_i}),$$

where Y_{η_i} is the fiber over the generic point η_i of V_i. This method increases quickly in complexity when the fiber structure becomes more involved [142].

A more effective way to compute the Euler characteristic is to use the Poincaré–Hopf theorem, which asserts that the Euler characteristic of X equals the degree of the top Chern class of the tangent bundle TX evaluated on the homological class of the variety. In other words, the Euler characteristic is the degree of the total homological Chern class:

$$\chi(X) = \int c(X), \quad c(X) := c(TX) \cap (X).$$

This method is explained in Section 2.8.1 and can also be thought of as an algebraic version of the Chern–Gauss–Bonnet theorem. We give three different proofs in Section 5.3.

5.2.1 Crepant resolutions and flops

Let X be a projective variety with at worst canonical Gorenstein singularities. We denote the canonical class by K_X.

Definition 5.2.1. A birational projective morphism $\rho : Y \longrightarrow X$ is called a *crepant desingularization* of X if Y is smooth and $K_Y = \rho^* K_X$.

Definition 5.2.2. A resolution of singularities of a variety Y is a proper surjective birational morphism $\phi : \widetilde{Y} \longrightarrow Y$ such that $\widetilde{Y}$ is nonsingular and ϕ is an isomorphism away from the singular locus of Y. In other words, $\widetilde{Y}$ is nonsingular and if U is the singular locus of Y, ϕ maps $\phi^{-1}(Y \setminus U)$ isomorphically onto $Y \setminus U$. A *crepant resolution of singularities* is a resolution of singularities such that $K_Y = f^* K_X$.

Remark 5.2.3. In dimension two, there is one and only one crepant resolution of a variety with canonical singularities. In dimension three, crepant resolutions of Gorenstein singularities always exist but are usually not unique. In dimension four or greater, crepant resolutions are not always possible. However, one can always find a crepant birational morphism from a $\mathbb{Q}$-factorial variety with terminal singularities.

Definition 5.2.4 (D-flop (See [228, p. 156-157])). Let $f_1 : X_1 \longrightarrow X$ a small contraction. Let D be a $\mathbb{Q}$-Cartier divisor in X_1. A *D-flop* is a birational morphism $f : X_1 - - \to X_2$ fitting into a triangular diagram where f_1 and f_2 are birational morphisms

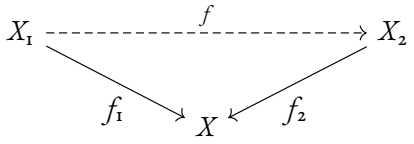

such that

1. X_i are normal varieties with at worst terminal singularities.

2. f_i are small contractions (i.e. their exceptional loci are in codimension two or higher).

3. K_{X_i} is numerically trivial along the fibers of f_i (i.e. $K_{X_i} \cdot \ell = 0$ for any curve ℓ contracted by f_i).

4. The $\mathbb{Q}$-divisor $-D$ is f_1-ample.

5. The strict f-transform D^+ of D is f_2-ample.

Definition 5.2.5 (flop)**.** The morphism $f_2 : X_2 \longrightarrow X$ is said to be a *flop* of $f_1 : X_1 \longrightarrow X$ if there exists a divisor $D \subset X_1$ such that f_2 is a D-flop of f_1.

5.3 The Euler Characteristic as the Degree of the Top Chern Class

The purpose of this section is to explain from different points of view why the Euler characteristic is the degree of the top Chern class. Traditionally, this statement is seen as a generalization of the Poincaré–Hopf theorem that asserts that the total degree of a vector field defined on a smooth manifold M is the Euler characteristic of M. This statement can also be seen as a generalization of the Gauss–Bonnet–Chern Theorem (which is itself is a consequence of Poincaré–Hopf theorem). Here we will review three different approaches. The first one relies on Leftschetz fixed point theorem. The second one uses he Poincaré–Hopf theorem using the interpretation of Chern classes as related to the class of some degenerated loci as discussed in Chapter 3 of Fulton. The third one is an application of the Hirzebruch–Riemann–Roch theorem and the Hodge decomposition theorem.

Let M be a smooth compact manifold. The kth Betti number of M is by definition the dimension of the cohomology group $H^k(M, \mathbb{Q})$. The Euler characteristic of M is denoted by $\chi(X)$ and is

defined as the following alternative sum of Betti numbers of M:

$$\chi(M) := \sum_{k=0}^{\dim M} (-1)^k b_k, \quad b_k := \dim H^i(M, \mathbb{Q}).$$

5.3.1 Lefschetz fixed point theorem and the Euler characteristic as an intersection number

Theorem 5.3.1 (Lefschetz fixed point theorem)**.** *Let M be a compact smooth manifold of dimension m and $f : M \longrightarrow M$ a continuous map. We define the Lefschetz number of f as*

$$L(f) := \sum_{k=0}^{m} (-1)^k \operatorname{tr}\Big(f^* | H^k(M, \mathbb{Q})\Big), \quad f^* : H^k(M, \mathbb{Q}) \longrightarrow H^k(M, \mathbb{Q}).$$

Then $L(f)$ is equal to the intersection number of the graph Γ_f of f and the diagonal Δ in $M \times M$

$$L(f) = \int_{M \times M} \Gamma_f \cdot \Delta.$$

Thus, the Leftschetz number $L(f)$ is the number of fixed points of f counted with multiplicities.

Corollary. *Let M be a compact smooth manifold and Δ be the diagonal of $M \times M$, then the Euler characteristic of M,*

$$\chi(M) = \sum_i (-1)^k \dim H^i(M, \mathbb{Q}),$$

is equal to the self-intersection of Δ *in* $M \times M$*:*

$$\chi(M) = \int_{M\times M} \Delta \cdot \Delta.$$

Proof. Consider the special case of Lefschetz theorem for which f is the identify map on M. Then, the Leftschetz number reduces to the Euler characteristic $\chi(M)$ as the trace $\mathrm{tr}\Big(f^* | H^k(M, \mathbb{Q})\Big)$ becomes the kth Betti number b^k of M and the intersection number $\int_{M\times M} \Gamma_f \cdot \ \Delta$ becomes the self-intersection of the diagonal Δ in $M \times M$. □

Theorem 5.3.2 (Self-intersection formula, see [136, Corollary 6.3, p. 102-103])**.** *Let* $i : Z \to X$ *be a regular imbedding of codimension* d *and normal bundle* N*. Then for any* $\alpha \in A_*(Z)$ *we have the self-intersection formula*

$$i^* i_*(\alpha) = c_d(N) \cap \alpha.$$

Theorem 5.3.3. *If* X *is a nonsingular complete algebraic variety, then the Euler characteristic of* X *is equal to the degree of the total homological Chern class of* X*:*

$$\chi(X) = \int c(X), \quad c(X) := c(TX) \cap [X].$$

Proof. The theorem follows from the previous corollary expressing the Euler characteristic $\chi(X)$ as the self-intersection of the diagonal Δ in $X \times X$, followed by the self-intersection formula expressing $\Delta \cdot \Delta$ as the class $c_{\dim X}(N_\Delta X \times X) \cap [\Delta]$. Since the normal bundle of Δ in $X \times X$ is isomorphic to the tangent bundle of X (see for example [54, Lemma 11.23, p. 127]), it follows that [136, Example 8.1.12,

p. 136], the self-intersection of the diagonal Δ in $X \times X$ is $\int c_{\dim X}(TX) \cap [X] = \int c(TX) \cap [X]$:

$$\chi(X) = \int_{X \times X} \Delta \cdot \Delta = \int c(N_\Delta X \times X) \cap [\Delta] = \int c(TX) \cap [X].$$

□

5.3.2 Poincaré-Hopf theorem and the Euler characteristic

Theorem 5.3.4 (Poincaré-Hopf)**.** *Let M be a smooth compact manifold without boundary and v be a vector field with isolated zeros. Then the sum of the local indices at the zeros of v is equal to the Euler characteristic of M.*

Remark 5.3.5. This theorem can be generalized to manifolds with boundaries by requiring v to point outward. Poincaré proved a two dimensional version of this theorem in 1885. The general version was proven by Hopf in 1926.

Theorem 5.3.6 ([136, Example 3.2.16, p. 61])**.** *Let E be a vector bundle of rank r on a smooth variety X, let s be a section of E, and Z the zero-scheme of s. If X is purely n-dimensional and s is a regular section, then Z is purely $(n - r)$-dimensional, and*

$$[Z] = c_r(E) \cap [X].$$

In particular, if E is the tangent bundle TX of X, then r (i.e. the rank of E) is the dimension of X, and the section s of E is just a vector field. The zero-scheme Z is a 0-cycle that is the sum of the

isolated singularities of s counted with multiplicities. Hence, the degree of the top Chern class of TX gives the index of the vector field s, which is the Euler characteristic of M by the Poincaré–Hopf theorem. Since the degree of $c(X)$ is exactly the degree of $c_r(TX) \cap [X]$, we retrieve Theorem 5.3.3:

$$\chi(X) = \int c(X).$$

5.3.3 Hirzebruch–Riemann–Roch theorem and the Euler characteristic

In this sub-section, using the Hirzebruch–Riemann–Roch theorem and the Hodge decomposition theorem, we prove that the Euler characteristic of a nonsingular projective variety is the degree of its homological total Chern class. We follow Fulton ([136, Example 18.3.7, p. 362] and [136, Example 3.2.5, p. 57]) as presented by D. Rössler [Rössler]. We denote the Todd class, the Chern character, and the dual of a vector bundle E by $\mathrm{td}(E)$ and $\mathrm{ch}(E)$, and $E^\vee$ respectively.

Let X be a projective variety of dimension d and V a coherent sheaf defined over X. We denote by $H^q(X, V)$ the q-th cohomology group of X with coefficients in the sheaf of germs of local sections of V. The cohomology groups $H^q(X, V)$ vanish for $q > d$ and are all finite dimensional for $0 \leq q \leq d$. The Euler characteristic of V in X is by definition the finite number

$$\chi(X, V) := \sum_{q=0}^{d} (-1)^q \dim H^q(X, V).$$

The Hirzebruch–Riemann–Roch theorem provides an expression for $\chi(X, V)$ in terms of characteristic classes of TX and V realizing a conjecture of Serre in a letter to Kodaira and Spencer.

Theorem 5.3.7 (Hirzebruch–Riemann–Roch)**.** *Let V be a coherent sheaf over a nonsingular variety X. Then*

$$\chi(X, V) = \int_X \mathrm{ch}(V)\mathrm{td}(TX).$$

We will also need the following lemma relating the Todd class and the Chern character. This lemma is instrumental in the proof of the Hirzebruch–Riemann–Roch theorem of Borel and Serre [52, Lemma 18, p. 128], and is also discussed by Fulton in [136, Example 3.2.5, p. 57].

Lemma 5.3.8 (Hirzebruch, [171, Theorem 10.1.1, page 92])**.** *Let E be a vector bundle of rank r. Then*

$$\mathrm{ch}\Big(\sum_{q=0}^{r}(-1)^q \bigwedge^q E^\vee\Big)\mathrm{td}(E) = c_r(E).$$

Proof. By the splitting principal, we can always formally factorize the total Chern class of E as $c(E) = \prod_i (1 + a_i)$, where a_i are the Chern roots of E. Then by definition

$$\mathrm{ch}(E) := \sum_{i=1}^{r} e^{a_i}, \quad \mathrm{td}(E) := \prod_i \frac{a_i}{(1 - e^{-a_i})}.$$

We have the classical relations (see [171, Theorem 4.4.3, page 64] or [136, Remark 3.2.3, p. 54–56])

$$c(E^\vee) = \prod_i (1 - a_i), \quad c(\bigwedge^q E) = \prod_{1 \le i_1 < \cdots < i_q \le r} \Big(1 + a_{i_1} + \cdots + a_{i_q}\Big)$$

Hence

$$\mathrm{ch}\Big(\bigwedge^q E^\vee\Big) = \sum_{1 \le i_1 < \cdots < i_q \le r} e^{-(a_{i_1} + \cdots + a_{i_q})}$$

Thus by the additive properties of the Chern character and the definition of the Todd class:

$$\begin{aligned}\mathrm{ch}\Big(\sum_{q=0}^{r}(-1)^q\bigwedge^q E^\vee\Big) &= \sum_{q=0}^{r}(-1)^q\mathrm{ch}\Big(\bigwedge^q E^\vee\Big) = \prod_{i=1}^{r}(1-e^{-a_i})\\ &= (a_1\dots a_r)\prod_{i=1}^{r}\frac{(1-e^{-a_i})}{a_i} = c_r(E)\mathrm{td}^{-1}(E).\end{aligned}$$

□

Theorem 5.3.9. *Let X be a nonsingular complete projective variety defined over the complex numbers. Then the Euler characteristic*

$$\chi(X) = \int c(X).$$

Proof. For X a nonsingular variety of dimension d, we apply Lemma 5.3.8 to the tangent bundle $E = TX$ and we note that $E^\vee = TX^\vee := \Omega_X$, where Ω_X is the sheaf of differentials of X, and by definition, the sheaf of differential p-forms is $\bigwedge^q \Omega_X := \Omega_X^q$. Hence, we get

$$\mathrm{ch}\Big(\sum_{q=0}^{d}(-1)^q\Omega_X^q\Big)\mathrm{td}(TX) = c_r(TX).$$

We rewrite the left hand side of the previous equation as follows

$$\begin{aligned}\int_X \mathrm{ch}\Big(\sum_{q=0}^{d}(-1)^q\Omega_X^q\Big)\mathrm{td}(TX) &= \sum_{q=0}^{d}(-1)^q\int_X \mathrm{ch}(\Omega_X^q)\mathrm{td}(TX) = \sum_{q=0}^{d}(-1)^q\int_X \chi(X,\Omega_X^q)\\ &= \sum_{q=0}^{d}\sum_{p=0}^{d}(-1)^{p+q}\dim \mathrm{H}^{\mathrm{p}}(\mathrm{X},\Omega_{\mathrm{X}}^{\mathrm{q}}) = \sum_{\mathrm{k}=0}^{\mathrm{d}}(-1)^{\mathrm{k}}\sum_{\mathrm{p}+\mathrm{q}=\mathrm{k}}\dim \mathrm{H}^{\mathrm{p}}(\mathrm{X},\Omega_{\mathrm{X}}^{\mathrm{q}}) = \sum_{\mathrm{k}=0}^{\mathrm{d}}(-1)^{\mathrm{k}}\mathrm{b}_{\mathrm{k}} = \chi(\mathrm{X}).\end{aligned}$$

The first equality is a direct consequence of the additive property of the Chern character, the second equality is due to the Hirzebruch–Riemann-Roch theorem applied to Ω^q_X, the third equality follows from the definition of the Euler characteristic of a sheaf, and the fifth equality is a direct application of the Hodge decomposition theorem $\Omega^k = \bigoplus_{p+q=k} \Omega^{p,q}$ and Dolbeault's theorem, which asserts that the Dolbeault cohomology is isomorphic to the sheaf cohomology of the sheaf of differential forms: $H^{p,q}(X) \cong H^p(X, \Omega^q_X)$. In particular, $h^{p,q}(X) = \dim \mathrm{H}^p(\mathrm{X}, \Omega^q_\mathrm{X})$ are the Hodge numbers of X. The last equality is by the definition of the Euler characteristic. Hence, since $\int c(X) = \int c(TX) \cap [X] = \int_X c_r(TX)$, we get

$$\int c(X) = \chi(X).$$

□

5.4 Pushforwards and Computing the Euler Characteristic

We use the definitions and theorems of intersection theory, which are reviewed in Section 2.7.2.

5.4.1 The pushforward theorem

A formula for the Chern classes of blowups of a smooth variety along a smooth center was conjectured by Todd and Segre and proven in the general case by Porteous [261] using the Riemann-Roch theorem. A proof using Riemann-Roch "without denominators" is presented in §15.4 of [136]. A proof without Riemann-Roch was derived by Lascu and Scott [213, 214]. A generalization of the formula to potentially singular varieties was obtained by Aluffi [4].

The blowup formula simplifies dramatically when the center of the blowup is a nonsingular complete intersection of nonsingular hypersurfaces meeting transversally. Aluffi gives an elegant short proof using functorial properties of Chern classes and Chern classes of bundles of tangent fields with logarithmic zeros in Theorem 2.7.11.

Lemma 5.4.1. *Let $f : \widetilde{X} \longrightarrow X$ be the blowup of X centered at Z. We denote the exceptional divisor of f by E. Then*

$$f_* E^n = (-1)^{d+1} h_{n-d}(Z_1, \cdots, Z_d) Z_1 \cdots Z_d,$$

where $h_i(x_1, \cdots, x_k)$ is the complete homogeneous symmetric polynomial of degree i in $(x_1, \cdots, x_k)$ with the convention that h_i is identically zero for $i < 0$ and $h_0 = 1$.

Proof. The exceptional locus of the blowup of X centered at Z is the projective bundle $\mathbb{P}(N_Z X)$. Let $E = c_1(\mathscr{O}_{\mathbb{P}(N_Z X)}(1))$. By the functoriality properties of Segre classes, we have:

$$f_* \frac{1}{1+E} \cap [E] = \frac{1}{c(N_Z X)} \cap [Z] = \prod_{i=1}^{d} \frac{Z_i}{1+Z_i}, \tag{5.1}$$

where $N_Z X$ is the normal bundle of Z in X. The generating function of complete homogeneous symmetric polynomials in $(x_1, \ldots, x_d)$ is $\prod_{\ell=1}^{d} (1 - x_\ell t)^{-1}$:

$$\sum_{n=1}^{\infty} h_n(x_1, \cdots, x_d) t^n = \prod_{\ell=1}^{d} \frac{1}{1 - x_\ell t}.$$

By matching terms of the same dimensions in equation (5.1), we can compute $f_* E^n$ in terms of com-

plete homogeneous symmetric polynomials $h_i(Z_1, \ldots, Z_d)$ in the classes Z_i:

$$f_*E^n = (-1)^{n-1}[t^n]\left(\prod_{i=1}^{d}\frac{tZ_i}{1+tZ_i}\right) = (-1)^{d+1}h_{n-d}(Z_1, \cdots, Z_d)Z_1\cdots Z_d,$$

where $[t^n]g(t) = g_n$ for a formal series $g(t) = \sum_{i=0}^{\infty} g_i t^i$ and h_i is identically zero for $i < 0$ and $h_0 = 1$. □

Example 5.4.2. If $d = 2$, we have

$$f_*E = 0, \quad f_*E^2 = -Z_1Z_2, \quad f_*E^3 = -(Z_1+Z_2)Z_1Z_2, \quad f_*E^4 = -(Z_1^2+Z_2^2+Z_1Z_2)Z_1Z_2.$$

Example 5.4.3. If $d = 3$, we have

$$f_*E = 0, \quad f_*E^2 = 0, \quad f_*E^3 = Z_1Z_2Z_3, \quad f_*E^4 = (Z_1+Z_2)Z_1Z_2Z_3.$$

A direct consequence of Theorem 5.5.2 (Jacobi's identity) and Lemma 2.7.12 is the following push-forward formula (see [135]):

Lemma 5.4.4. *Let $Z \subset X$ be the complete intersection of d nonsingular hypersurfaces $Z_1, \cdots, Z_d$ meeting transversally in X. Let $f : \widetilde{X} \longrightarrow X$ be the blowup of X centered at Z with exceptional divisor E. Then for any integer $n \geq 0$:*

$$f_*E^n = \sum_{\ell=1}^{d} Z_\ell^n M_\ell, \quad M_\ell = \prod_{\substack{m=1\\ m\neq\ell}} \frac{Z_m}{Z_m - Z_\ell}.$$

The coefficient M_ℓ is the ℓ-moment of the blowup f defined after Theorem 5.0.1.

Proof.

$$
\begin{aligned}
f_*E^n &= (-1)^{d+1} h_{n-d}(Z_1, \cdots, Z_d) Z_1 \cdots Z_d && \text{(by Lemma 2.7.12)} \\
&= (-1)^{d+1} \sum_{\ell=1}^{d} Z_\ell^{n-1} \Big(\prod_{\substack{m=1 \\ m\neq\ell}}^{d} \frac{1}{Z_\ell - Z_m} \Big) Z_1 \cdots Z_d && \text{(by Lemma 5.0.3)} \\
&= (-1)^{d+1} \sum_{\ell=1}^{d} Z_\ell^{n} \Big(\prod_{\substack{m=1 \\ m\neq\ell}}^{d} \frac{Z_m}{Z_\ell - Z_m} \Big) && \text{(by the identity } Z_1 \cdots Z_d = Z_\ell \prod_{\substack{m=1 \\ m\neq\ell}}^{d} Z_m) \\
&= \sum_{\ell=1}^{d} Z_\ell^{n} \Big(\prod_{\substack{m=1 \\ m\neq\ell}}^{d} \frac{Z_m}{Z_m - Z_\ell} \Big) && \text{(since } \prod_{\substack{m=1 \\ m\neq\ell}}^{d} \frac{Z_m}{Z_\ell - Z_m} = (-1)^{d-1} \prod_{\substack{m=1 \\ m\neq\ell}}^{d} \frac{Z_m}{Z_m - Z_\ell})
\end{aligned}
$$

□

To compute topological invariants of a blowup, we often have to pushforward analytic expressions of E. Let $\widetilde{Q}(t) = \sum_a f^* Q_a t^a$ be a formal power series with $Q_a \in A_*(X)$. The formal series $Q(E)$ is a well-defined element of $A_*(\widetilde{X})$. We recall Theorem 5.0.1:

Theorem 5.0.1. *Let the nonsingular variety $Z \subset X$ be a complete intersection of d nonsingular hypersurfaces $Z_1, \cdots, Z_d$ meeting transversally in X. Let E be the class of the exceptional divisor of the blowup $f : \widetilde{X} \longrightarrow X$ centered at Z. Let $\widetilde{Q}(t) = \sum_a f^* Q_a t^a$ be a formal power series with $Q_a \in A_*(X)$. We define the associated formal power series $Q(t) = \sum_a Q_a t^a$ whose coefficients pullback to the*

coefficients of $\widetilde{Q}(t)$*. Then the pushforward* $f_*\widetilde{Q}(E)$ *is:*

$$f_*\widetilde{Q}(E) = \sum_{\ell=1}^{d} Q(Z_\ell) M_\ell, \quad \textit{where} \quad M_\ell = \prod_{\substack{m=1 \\ m\neq\ell}}^{d} \frac{Z_m}{Z_m - Z_\ell}.$$

Proof.

$$f_*\widetilde{Q}(E) = f_* \sum_a (f^* Q_a) E^a = \sum_a Q_a f_* E^a = \sum_a Q_a \sum_{\ell=1}^{d} Z_\ell^a M_\ell = \sum_a \sum_{\ell=1}^{d} Q_a Z_\ell^a M_\ell = \sum_{\ell=1}^{d} Q(Z_\ell) M_\ell. \tag{5.2}$$

□

5.4.2 Classes of the blowup centers of crepant resolutions

We denote the projective bundle of the Weierstrass model to be $X_0 = \mathbb{P}[\mathscr{O}_B \oplus \mathscr{L}^{\otimes 2} \oplus \mathscr{L}^{\otimes 3}]$ and the elliptic fibration $\phi : Y_0 \to B$ to be the zero-scheme of a section of $\mathscr{O}(3) \otimes \pi^* \mathscr{L}^{\otimes 6}$. We denote by $\mathscr{O}(1)$ the dual of the tautological line bundle of X_0. We denote by H the first Chern class of $\mathscr{O}(1)$, and by L the first Chern class of $\mathscr{L}$. The elliptic fibration $\phi : Y_0 \longrightarrow B$ is of class $[Y_0] = 3H + 6\pi^* L$. The classes of the generators of the blowup centers are $Z_i^{(n)}$, where n is the number of the blowup map and i is the number of the center. For example, consider the following blowup:

$$X_0 \xleftarrow{(x,y,s|e_1)} X_1 \xleftarrow{(y,e_1|e_2)} X_2 \tag{5.3}$$

where each arrow above denotes a blowup, $V(s)$ is a smooth divisor in X, and where $E_n = V(e_n)$ is the exceptional divisor of the nth blowup. The first exceptional divisor is a projective bundle whose fibers have projective coordinates $[x' : y' : s']$, where

$$x = x'e_1\ ,\ y = y'e_1\ ,\ s = s'e_1.$$

For notational convenience, we drop the prime superscripts ($'$) appearing after each blowup.

The classes associated to the center of the first blowup in (5.3) are:

$$Z_1^{(1)} = [x] = H + 2\pi^*L, \quad Z_2^{(1)} = [y] = H + 3\pi^*L, \quad Z_3^{(1)} = [s] = \pi^*S.$$

Likewise, the classes associated to the center of the second blowup are

$$Z_1^{(2)} = [y] = f_1^*(H + 3\pi^*L) - E_1, \quad Z_2^{(2)} = [e_1] = E_1.$$

Let us adapt the above data into a matrix-inspired notation, such that i denote columns and n denotes rows. This notation allows us to read the classes of the blowup center by each row. In this notation, the above results can be expressed as follows:

$$Z = \begin{pmatrix} Z_1^{(1)} & Z_2^{(1)} & Z_3^{(1)} \\ Z_1^{(2)} & Z_2^{(2)} & \end{pmatrix} = \begin{pmatrix} H + 2\pi^*L & H + 3\pi^*L & \pi^*S \\ f_1^*(H + 3\pi^*L) - E_1 & E_1 & \end{pmatrix}.$$

See Table 5.3 for an exhaustive list of the generator classes associated to the blowup centers of the

crepant resolutions in Table 5.2. Note that we streamline our notation by omitting the explicit pull-back maps from the expressions for the classes appearing in these tables.

5.5 Jacobi's Partial Fraction Identity

In this section, we prove a formula of Jacobi and exploit the theorem to give a simple proof of a formula of Louck and Biedenharn [222, Appendix A, p. 2400] by demonstrating its equivalence with the following theorem of Jacobi.

Theorem 5.5.1 (Jacobi, [177, Section III.17, p. 29-30]). *Let a_i $(i = 1, \ldots, d)$ be d distinct elements of an integral domain. Then*

$$\prod_{i=1}^{d} \frac{1}{x - a_i} = \sum_{i=1}^{d} \frac{1}{x - a_i} \prod_{\substack{j=1 \\ j \neq i}}^{d} \frac{1}{a_i - a_j}. \tag{5.4}$$

Proof. Let

$$F(x) = \prod_{i=1}^{d} \frac{1}{x - a_i}, \tag{5.5}$$

where $a_i \neq a_j$ for $i \neq j$. We would like to find the partial fraction expansion of $F(x)$. That is, we would like to find coefficients A_i $(i = 1, \cdots, d)$ such that

$$F(x) = \sum_{i=1}^{d} \frac{A_i}{x - a_i}. \tag{5.6}$$

We determine A_i by the *method of residues*. Multiplying (5.6) by $(x - a_i)$, simplifying, and evaluating

at $x = a_i$ gives

$$(x - a_j)F(x)\big|_{x=a_j} = A_j.$$

Applying the above formula to (5.5), we get $A_j = \prod_{i \neq j} \frac{1}{a_i - a_j}$, which is the identity of Jacobi:

$$\prod_{i=1}^{d} \frac{1}{x - a_i} = \sum_{i=1}^{d} \frac{1}{x - a_i} \prod_{\substack{j=1 \\ j \neq i}}^{d} \frac{1}{a_i - a_j}. \tag{5.7}$$

□

Theorem 5.5.2 (Jacobi, Louck–Biedenharn, Cornelius)**.** *Let $h_r(x_1, \cdots, x_d)$ be the homogeneous complete symmetric polynomial of degree r in d variables of an integral domain. Then,*

$$h_r(x_1, \cdots, x_d) = \sum_{\ell=1}^{d} x_\ell^{r+d-1} \prod_{\substack{m=1 \\ m \neq \ell}}^{d} \frac{1}{x_\ell - x_m}.$$

This theorem was proven by Louck-Biedenharn [222, Appendix A, p. 2400] and Cornelius [81]. We present a new and much simpler proof below by showing that the theorem is simply a reformulation of Jacobi's identity (Theorem 5.5.1).

Proof. Substituting $x \to 1/t$ in Equation (5.4) gives:

$$\prod_{i=1}^{d} \frac{t}{1 - a_i t} = \sum_{i=1}^{d} \frac{t}{1 - a_i t} \prod_{\substack{j=1 \\ j \neq i}}^{d} \frac{1}{a_i - a_j}.$$

Expanding $1/(1 - a_i t)$ in both side of the equation gives

$$t^d \sum_{r=0}^{\infty} h_r(a_1, \ldots, a_d) t^r = t \sum_{i=1}^{d} \sum_{k=0}^{\infty} a_i^k t^k \prod_{\substack{j=1 \\ j \neq i}}^{d} \frac{1}{a_i - a_j}$$

$$\sum_{r=0}^{\infty} h_r(a_1, \ldots, a_d) t^{r+d-1} = \sum_{k=0}^{\infty} \Big(\sum_{i=1}^{d} a_i^k \prod_{\substack{j=1 \\ j \neq i}}^{d} \frac{1}{a_i - a_j} \Big) t^k.$$

Comparing terms of the same degree in t, we get the final expression of Lemma 5.0.3:

$$h_r(a_1, \ldots, a_d) = \sum_{i=1}^{d} a_i^{r+d-1} \prod_{\substack{j=1 \\ j \neq i}}^{d} \frac{1}{a_i - a_j}.$$

□

5.6 Hodge Numbers of Elliptically Fibered Calabi–Yau Threefolds

Using motivitic integration, Kontsevich shows in his famous "String Cohomology" Lecture at Orsay that birational equivalent Calabi–Yau varieties have the same class in the completed Grothendieck ring [Kontsevich]. Hence, birational equivalent Calabi–Yau varieties have the same Hodge-Deligne polynomial, Hodge numbers, and Euler characteristic. In this section, we compute the Hodge numbers of crepant resolutions of Weierstrass models in the case of Calabi–Yau threefolds.

Theorem 5.6.1 (Kontsevich, (see [Kontsevich])). *Let X and Y be birational equivalent Calabi–Yau varieties over the complex numbers. Then X and Y have the same Hodge numbers.*

Remark 5.6.2. In Kontsevich's theorem, a Calabi–Yau variety is a nonsingular complete projective variety of dimension d with a trivial canonical divisor. To compute Hodge numbers in this section, we use the following stronger definition of a Calabi–Yau variety, which is given in Definition 2.8.6.

We first recall some basic definitions and relevant classical theorems.

Definition 5.6.3. The *Néron-Severi group* $\mathrm{NS}(X)$ of a variety X is the group of divisors of X modulo algebraic equivalence. The rank of the Néron-Severi group of X is called the *Picard number* and is denoted $\rho(X)$.

Theorem 5.6.4 (Lefschetz $(1,1)$-theorem, see [295, Theorem 7.2, p. 157])**.** *If X is compact Kähler manifold, then the map $c_1 : Pic(X) \to H^{1,1}(X,\mathbb{Z}) = H^{1,1}(X,\mathbb{C}) \cap H^2(X,\mathbb{Z})$ is well-defined and surjective. In addition, the Picard number $\rho(X)$ is equal to the Hodge number $h^{1,1}(X) := \dim H^{1,1}(X,\mathbb{Z})$.*

Theorem 5.6.5 (Noether's formula)**.** *If B is a smooth compact, connected, complex surface with canonical class K_B and Euler number c_2:*

$$\chi(\mathscr{O}_B) = 1 - h^{0,1}(B) + h^{0,2}(B), \quad \chi(\mathscr{O}_B) = \frac{1}{12}(K^2 + c_2).$$

When B is a smooth compact rational surface, we have a simple expression of $h^{1,1}(B)$ as a function of K^2 using the Lemma 2.8.8: $h^{1,1}(B) = 10 - K^2$. f We now compute $h^{1,1}(Y)$ using the Shioda-Tate-Wazir theorem using Theorem 2.8.9. Then we can have Thoerem 2.8.10 that we recite and prove below.

Theorem 5.6.6. *Let Y be a smooth Calabi–Yau threefold elliptically-fibered over a smooth variety B with Mordell–Weil group of rank zero. Then,*

$$h^{1,1}(Y) = h^{1,1}(B) + f + 1, \quad h^{2,1}(Y) = h^{1,1}(Y) - \frac{1}{2}\chi(Y),$$

where f is the number of geometrically irreducible fibral divisors not touching the zero section. In particular, if Y is a G-model with G a simple group, f is the rank of G.

Proof. In the statement of the Shioda–Tate–Wazir theorem, we can replace the Picard numbers $\rho(Y)$ and $\rho(B)$ by the Hodge numbers $h^{1,1}(Y)$ and $h^{1,1}(B)$ using Lefschetz's (1,1)-theorem. That gives $h^{1,1}(Y) = h^{1,1}(B) + f + 1$. Since the Euler characteristic of a Calabi–Yau threefold is $\chi(Y) = 2(h^{1,1} - h^{2,1})$, and assuming that both $\chi(Y)$ and $h^{1,1}(Y)$ are known, it follows that $h^{2,1}(Y) = h^{1,1}(Y) - \frac{1}{2}\chi(Y)$. □

Remark 5.6.7. For G-models with G a simple group, f will be the rank of G [244, §4].

5.7 An Illustrative Example: SU(2)-Models

In this section, we discuss in detail the computation of the Euler characteristic of SU(2)-models. Note that the results presented in this section are equivalent for each of the four possible Kodaira fibers (namely, types $\mathrm{I}_2^{\mathrm{s}}$, $\mathrm{I}_2^{\mathrm{s}}$, $\mathrm{I}_3^{\mathrm{s}}$, III, $\mathrm{IV}^{\mathrm{ns}}$) realizing an SU(2)-model; see Section 5.8 for a list of the Weierstrass equations defining the various SU(2)-models. We find

$$c(X_0) = (1 + H)(1 + H + 3\pi^* L)(1 + H + 2\pi^* L)c(B)$$

$$c(Y_0) = (3H + 6\pi^* L)\frac{c(X_0)}{1 + 3H + 6\pi^* L}.$$

The singular elliptic fibration is resolved by a unique blowup with center (x, y, s) [125]. We denote the blowup by $f : X_1 \longrightarrow X_0$ and the exceptional divisor by E_1. The center is a complete intersection of hypersurfaces $V(x)$, $V(y)$, and $V(s)$, whose classes are respectively

$$Z_1 = 2\pi^* L + H, \quad Z_2 = 3\pi^* L + H, \quad Z_3 = \pi^* S.$$

The proper transform of the elliptic fibration Y_0 is denoted Y, and is obtained from the total transform of Y by removing $2E_1$. It follows that the class of Y in X_1 is

$$[Y] = [f^*(3H + 6\pi^* L) - 2E_1] \cap [X_1]$$

Moreover, we have the following Chern classes:

$$c(TX_1) = (1 + E_1)\frac{(1 + f^* Z_1 - E_1)(1 + f^* Z_2 - E_1)(1 + f^* Z_3 - E_1)}{(1 + f^* Z_1)(1 + f^* Z_2)(1 + f^* Z_3)} f^* c(TX_0)$$
$$c(TY) = \frac{(1 + E_1)(1 + f^* Z_1 - E_1)(1 + f^* Z_2 - E_1)(1 + f^* Z_3 - E_1)}{(1 + 3H + 6L - 2E_1)(1 + f^* Z_1)(1 + f^* Z_2)(1 + f^* Z_3)} f^* c(TX_0)$$

By an expansion of $c(TY)$ in first order, we can easily check that the resolution is crepant:

$$c(TY) = f^* c(TY_0).$$

After the blowup, the homological total Chern class is $c(Y) = c(TY) \cap [Y]$:

$$c(Y) = (3f^*H + 6f^*\pi^*L - 2E_1)(1 + E_1)\frac{(1 + f^*Z_1 - E_1)(1 + f^*Z_2 - E_1)(1 + f^*Z_3 - E_1)}{(1 + f^*Z_1)(1 + f^*Z_2)(1 + f^*Z_3)} f^*c(X_0).$$

To compute the Euler characteristic, we have to evaluate

$$\chi(Y) = \int_Y c(Y).$$

The first pushforward requires the following data:

$$M_1 = \frac{Z_2 Z_3}{(Z_2 - Z_1)(Z_3 - Z_1)}, \quad M_2 = \frac{Z_1 Z_3}{(Z_1 - Z_2)(Z_3 - Z_2)}, \quad M_3 = \frac{Z_1 Z_2}{(Z_1 - Z_3)(Z_2 - Z_3)}.$$

Applying the pushforward theorem is now a purely algebraic routine that can be easily implemented in one's favorite algebraic software. Using Theorem 5.0.1, we pushforward $c(Y)$ from the Chow ring $A_*(X_1)$ to the Chow ring $A_*(X_0)$. Using Theorem 5.0.4, we then pushforward $f_*c(Y)$ to the Chow ring of the base. When the dust settles, we find an expression of $\chi(Y)$ in the Chow ring of the base:

$$\chi(Y) = \int_Y c(TY) = \int_{X_0} f_*c(TY) = \int_B \pi_* f_* c(TY) = \int_B 6\frac{2L + 3LS - S^2}{(1 + S)(1 + 6L - 2S)} c(TB).$$

Concretely, we replace $c(TB)$ by the Chern polynomial $c_t(TB) = 1 + c_1 t + c_2 t^2 + c_3 t^3 + \cdots$, L by Lt, and S by St; if d is the dimension of B, the Euler characteristic of Y is given by the coefficient of t^d in

the Taylor expansion centered at $t = 0$ of the generating function:

$$\begin{aligned}\chi(Y) &= 6\frac{2Lt + 3LSt^2 - S^2t^2}{(1+St)(1+6Lt-2St)}c_t(TB)\\ &= 12Lt + 6t^2(2c_1L - 12L^2 + 5LS - S^2) +\\ &\quad + 6t^3(-12c_1L^2 + 5c_1LS - c_1S^2 + 2c_2L + 72L^3 - 54L^2S + 15LS^2 - S^3) + \cdots\end{aligned}$$

Theorem 5.7.1. *If B is a curve, the Euler characteristic of an SU(2) model is $12L$. If B is a surface, the Euler characteristic is $6(2c_1L - 12L^2 + 5LS - S^2)$. If B is a threefold, the Euler characteristic is $6(-12c_1L^2 + 5c_1LS - c_1S^2 + 2c_2L + 72L^3 - 54L^2S + 15LS^2 - S^3)$.*

In order to consider the Calabi–Yau case, we set $L = c_1(TB)$ in the above expression, which gives

$$\chi(Y) = 12c_1t - 6t^2(10c_1^2 - 5c_1S + S^2) + 6t^3(60c_1^3 - 49c_1^2S + 2c_1c_2 + 14c_1S^2 - S^3) + \cdots$$

Note that we retrieve the result for a smooth Weierstrass model if we further impose $S = 0$.

Remark 5.7.2. As a byproduct of the computation of the Euler characteristic of the resolution, we can also easily evaluate the contribution from the singularities to be

$$6\frac{2L + 3LS - S^2}{(1+S)(1+6L-2S)}c(TB) - \frac{12L}{1+6L}c(TB) = 6\frac{(5L + 6L^2 - 2LS - S)S}{(1+6L)(1+6L-2S)(1+S)}c(TB),$$

which can be rewritten as

$$\chi(Y) - \chi(Y_0) = 6\frac{6L^2 - 2LS + 5L - S}{(1+6L)(1+6L-2S)}c(S), \quad c(S) = \frac{S}{1+S}c(TB) \cap [B].$$

In the Calabi–Yau case $L = c_1(TB)$, the above quantity usually has a physical meaning. For example, if Y is a Calabi–Yau fourfold, this expression reduces to $-6S(7c_1 - S)^2 \cap [B]$, which is the contribution of branes to the Euler characteristic. In another limit, the above expression can be understood as the contribution of the G_4-flux in M-theory to the M2-brane flux or brane flux in type IIB string theory:

$$\frac{1}{2}\int_{Y_0} G_4 \wedge G_4 = \frac{1}{2}\int_S F \wedge F = -6\int_S (7c_1 - S)^2.$$

5.8 Tables of Results

The G-models studied in this chapter are all realized as crepant resolutions of the singular Weierstrass model

$$y^2z + a_1xyz + a_3yz^2 - (x^3 + a_2x^2z + a_4xz^2 + a_6z^3) = 0,$$

where the desired singularity structures corresponding to the decorated Kodaira fibers can be specified by the valuation of the coefficients of the Weierstrass equation with respect to the divisor $S = V(s)$. Following Tate's algorithm, we use the notation $a_{i,p} = a_i/s^p$, where the valuations p are the minimal values dictated by Tate's algorithm and we assume that the coefficients $a_{i,p}$ are generic.

We present the results of our computation of the Euler characteristic generating functions for various G-models. The generating functions are the pushforwards of the homological total Chern class of the resolved Weierstrass model to the base B, and are expressed as rational functions of the classes S and L (where $L = c_1(\mathscr{L})$ is the class of the fundamental line bundle and S is the class of the divisor in the base B), multiplied by the total Chern class of the base, $c(B)$—see Table 5.4. Tables 5.5-5.7 specialize the results to (respectively) elliptic threefolds, fourfolds, and elliptic Calabi–Yau fourfolds, while Table 5.8 summarizes the Hodge numbers for Calabi–Yau threefold G-models.

When computing Hodge numbers of a G model which is a Calabi–Yau threefold, we recall that we assume that the base is a rational surface. This is a direct consequence of Definition 2.8.6. For a G-model with G a simple group, the integer f that enters in Theorem 2.8.10 is the rank of G.

For the SO(3), SO(5), and SO(6)-models, the class S is given by:

$$S = 4L \text{ for SO(3)}, \quad S = 2L \text{ for SO(5)}, \quad S = 2L \text{ for SO(6)}.$$

Below we list the various Weierstrass equations we use to compute the G-models, labeled by their Kodaira fiber type and associated Lie group G. It is necessary to specify a crepant resolution in order to actually compute the total Chern class and Euler characteristic of a G-model. There could be several distinct crepant resolutions for a G-model. However, Theorem 2.8.3 assures that the Euler characteristic is insensitive to the choice of crepant resolution and therefore we only need one crepant resolution to compute the Euler characteristic of a G-model defined by the crepant resolution of a

Weierstrass model. The models associated to the groups SU(n) and USp($2n$) are [186]:

$$\mathrm{I}_2^{\mathrm{s}} \quad \mathrm{SU}(2) \quad : \quad y^2z + a_{1,1}xyz + a_{3,1}syz = x^3 + a_{2,1}sx^2z + a_{4,1}sxz^2 + a_{6,2}s^2z^3, \tag{5.8}$$

$$\mathrm{I}_{2n}^{\mathrm{ns}} \quad \mathrm{USp}(2n) \quad : \quad y^2z = x^3 + a_2x^2z + a_{4,n}s^nxz^2 + a_{6,2n}s^{2n}z^3, \tag{5.9}$$

$$\mathrm{I}_{2n+1}^{\mathrm{ns}} \quad \mathrm{USp}(2n) \quad : \quad y^2z = x^3 + a_2x^2z + a_{4,n+1}s^{n+1}xz^2 + a_{6,2n+1}s^{2n+1}z^3, \tag{5.10}$$

$$\mathrm{I}_{2n}^{\mathrm{s}} \quad \mathrm{SU}(2n) \quad : \quad y^2z + a_{1,1}xyz = x^3 + a_{2,1}sx^2z + a_{4,n}s^nxz^2 + a_{6,2n}s^{2n}z^3, \tag{5.11}$$

$$\mathrm{I}_{2n+1}^{\mathrm{s}} \quad \mathrm{SU}(2n+1) \quad : \quad y^2z + a_{1,1}xyz + a_{3,n}s^nyz^2 = x^3 + a_{2,1}sx^2z + a_{4,n+1}s^{n+1}xz^2 + a_{6,2n+1}s^{2n+1}z^3. \tag{5.12}$$

The Weierstrass models for SO(3), SO(5), and SO(6) are discussed; these models require a Mordell–Weil group $\mathbb{Z}/2\mathbb{Z}$. The crepant resolutions of the Weierstrass models for G_2, Spin(7), and Spin(8) models are studied in [112] and require a careful analysis of the Galois group of an associated polynomial. The Weierstrass equations defining these models along with the remaining G-models, with G one of the exceptional groups are given below [186]:

$$\mathrm{I}_2^{\mathrm{ns}} \quad \mathrm{SO}(3) \quad : \quad y^2z = x(x^2 + a_2xz + a_4z^2), \tag{5.13}$$

$$\mathrm{I}_4^{\mathrm{ns}} \quad \mathrm{SO}(5) \quad : \quad y^2z = (x^3 + a_2x^2z + s^2xz^2), \tag{5.14}$$

$$\mathrm{I}_4^{\mathrm{s}} \quad \mathrm{SO}(6) \quad : \quad y^2z + a_1xyz = x^3 + msx^2z + s^2xz^2, \quad m \in \mathbb{C}, \quad m \neq -2, 0, 2, \tag{5.15}$$

$$\mathrm{I}_0^{*\mathrm{ss}} \quad \mathrm{Spin}(7) \quad : \quad y^2z = x^3 + a_{2,1}sx^2z + a_{4,2}s^2xz^2 + a_{6,4}s^4z^3, \tag{5.16}$$

$$\mathrm{I}_0^{*\mathrm{s}} \quad \mathrm{Spin}(8) \quad : \quad y^2z = (x - x_1sz)(x - x_2sz)(x - x_3sz) + s^2rx^2z + s^3qxz^2 + s^4tz^3, \tag{5.17}$$

III	SU(2)	:	$y^2z = x^3 + sa_{4,1}xz^2 + s^2a_{6,2}z^3,$	(5.18)
IV^{ns}	SU(2)	:	$y^2z = x^3 + s^2a_{4,2}xz^2 + s^2a_{6,2}z^3,$	(5.19)
IV^{s}	SU(3)	:	$y^2z + a_{3,1}syz^2 = x^3 + s^2a_{4,2}xz^2 + s^3a_{6,3}z^3,$	(5.20)
I_0^{*ns}	G_2	:	$y^2z = x^3 + s^2a_{4,2}xz^2 + s^3a_{6,3}z^3,$	(5.21)
IV^{*ns}	F_4	:	$y^2z = x^3 + s^3a_{4,3}xz^2 + s^4a_{6,4}z^3,$	(5.22)
IV^{*s}	E_6	:	$y^2z + a_{3,2}s^2yz^2 = x^3 + s^3a_{4,3}xz^2 + s^5a_{6,5}z^3,$	(5.23)
III^{*}	E_7	:	$y^2z = x^3 + s^3a_{4,3}xz + s^5a_{6,5}z^3,$	(5.24)
II^{*}	E_8	:	$y^2z = x^3 + s^4a_{4,4}xz^2 + s^5a_{6,5}z^3.$	(5.25)

Theorem 5.8.1. *Let $Y_0 \to B$ be a singular Weierstrass model of a G-model. If $f : Y \to Y_0$ is a crepant resolution of Y_0 given by one of the sequence of blowups given in Table 5.2, the generating function of the Euler characteristic of any crepant resolution of Y_0 is given by the corresponding entry in Table 5.4.*

Remark 5.8.2. The theorem does not address if the sequence of blowups define a crepant resolution. One usually has to assume some conditions on the coefficients of the Weierstrass equations. See for example [112]. In some cases, the dimension of the base plays a role too [112].

Group	Fiber Type	Crepant Resolution
SU(2)	$\mathrm{I}_2^{\mathrm{s}}, \mathrm{I}_2^{\mathrm{ns}}$ $\mathrm{I}_3^{\mathrm{ns}}, \mathrm{III}$ $\mathrm{IV}^{\mathrm{ns}}$	$X_0 \xleftarrow{(x,y,s\mid e_1)} X_1$
SU(3) USp(4) G_2	$\mathrm{I}_3^{\mathrm{s}}, \mathrm{IV}^{\mathrm{s}}$ $\mathrm{I}_4^{\mathrm{ns}}$ $\mathrm{I}_0^{*\mathrm{ns}}$	$X_0 \xleftarrow{(x,y,s\mid e_1)} X_1 \xleftarrow{(y,e_1\mid e_2)} X_2$
SU(4) Spin(7)	$\mathrm{I}_4^{\mathrm{s}}$ $\mathrm{I}_0^{*\mathrm{ss}}$	$X_0 \xleftarrow{(x,y,s\mid e_1)} X_1 \xleftarrow{(y,e_1\mid e_2)} X_2 \xleftarrow{(x,e_2\mid e_3)} X_3$
Spin(8)	$\mathrm{I}_0^{*\mathrm{s}}$	$X_0 \xleftarrow{(x,y,s\mid e_1)} X_1 \xleftarrow{(y,e_1\mid e_2)} X_2 \xleftarrow{(x-x_isz,e_2\mid e_3)} X_3 \xleftarrow{(x-x_jsz,e_2\mid e_4)} X_4$
F_4	$\mathrm{IV}^{*\mathrm{ns}}$	$X_0 \xleftarrow{(x,y,s\mid e_1)} X_1 \xleftarrow{(y,e_1\mid e_2)} X_2 \xleftarrow{(x,e_2\mid e_3)} X_3 \xleftarrow{(e_3,e_2\mid e_4)} X_4$
SU(5)	$\mathrm{I}_4^{\mathrm{s}}$	$X_0 \xleftarrow{(x,y,s\mid e_1)} X_1 \xleftarrow{(x,y,e_1\mid e_2)} X_2 \xleftarrow{(y,e_1\mid e_3)} X_3 \xleftarrow{(y,e_2\mid e_4)} X_4$
Spin(10)	$\mathrm{I}_1^{*\mathrm{s}}$	$X_0 \xleftarrow{(x,y,s\mid e_1)} X_1 \xleftarrow{(y,e_1\mid e_2)} X_2 \xleftarrow{(x,e_2\mid e_3)} X_3 \xleftarrow{(y,e_3\mid e_4)} X_4 \xleftarrow{(e_2,e_3\mid e_5)} X_5$
E_6	$\mathrm{IV}^{*\mathrm{s}}$	$X_0 \xleftarrow{(x,y,s\mid e_1)} X_1 \xleftarrow{(y,e_1\mid e_2)} X_2 \xleftarrow{(x,e_2\mid e_3)} X_3 \xleftarrow{(e_2,e_3\mid e_4)} X_4$ $X_6 \xrightarrow{(y,e_4\mid e_6)} X_5 \xleftarrow{(y,e_3\mid e_5)}$
E_7	III^*	$X_0 \xleftarrow{(x,y,s\mid e_1)} X_1 \xleftarrow{(y,e_1\mid e_2)} X_2 \xleftarrow{(x,e_2\mid e_3)} X_3 \xleftarrow{(y,e_3\mid e_4)} X_4$ $X_7 \xrightarrow{(e_4,e_5\mid e_7)} X_6 \xrightarrow{(e_2,e_4\mid e_6)} X_5 \xleftarrow{(e_2,e_3\mid e_5)}$
E_8	II^*	$X_0 \xleftarrow{(x,y,s\mid e_1)} X_1 \xleftarrow{(y,e_1\mid e_2)} X_2 \xleftarrow{(x,e_2\mid e_3)} X_3 \xleftarrow{(y,e_3\mid e_4)} X_4$ $X_8 \xrightarrow{(e_4,e_7\mid e_8)} X_7 \xrightarrow{(e_2,e_4,e_6\mid e_7)} X_6 \xrightarrow{(e_4,e_5\mid e_6)} X_5 \xleftarrow{(e_2,e_3\mid e_5)}$
SO(3)	$\mathrm{I}_2^{\mathrm{ns}}$	$X_0 \xleftarrow{(x,y\mid e_1)} X_1$
SO(5)	$\mathrm{I}_4^{\mathrm{ns}}$	$X_0 \xleftarrow{(x,y,s\mid e_1)} X_1 \xleftarrow{(x,y,e_1\mid e_2)} X_2$
SO(6)	$\mathrm{I}_4^{\mathrm{s}}$	$X_0 \xleftarrow{(x,y,s\mid e_1)} X_1 \xleftarrow{(y,e_1\mid e_2)} X_2 \xleftarrow{(x,e_2\mid e_3)} X_3$

Table 5.2: The blowup centers of the crepant resolutions. See the beginning of Section 5.4.2 for an explanation of our notation.

Algebra	Group	Generator classes of the blowup centers $(Z_i^{(n)})$
A_1	$SU(2)$	$\begin{pmatrix} H+2L & H+3L & S \end{pmatrix}$
A_2 C_2 G_2	$SU(3)$ $USp(4)$ G_2	$\begin{pmatrix} H+2L & H+3L & S \\ H+3L-E_1 & E_1 & \end{pmatrix}$
A_3	$SU(4)$ $Spin(7)$	$\begin{pmatrix} H+2L & H+3L & S \\ H+3L-E_1 & E_1 & \\ H+2L-E_1 & E_2 & \end{pmatrix}$
D_4	$Spin(8)$	$\begin{pmatrix} H+2L & H+3L & S \\ H+3L-E_1 & E_1 & \\ H+2L-E_1 & E_2 & \\ H+2L-E_1 & E_2-E_3 & \end{pmatrix}$
F_4	F_4	$\begin{pmatrix} H+2L & H+3L & S \\ H+3L-E_1 & E_1 & \\ H+2L-E_1 & E_2 & \\ E_2-E_3 & E_3 & \end{pmatrix}$
A_4	$SU(5)$	$\begin{pmatrix} H+2L & H+3L & S \\ H+2L-E_1 & H+3L-E_1 & E_1 \\ H+3L-E_1-E_2 & E_1-E_2 & \\ H+3L-E_1-E_2-E_3 & E_2 & \end{pmatrix}$
D_5	$Spin(10)$	$\begin{pmatrix} H+2L & H+3L & S \\ H+3L-E_1 & E_1 & \\ H+2L-E_1 & E_2 & \\ H+3L-E_1-E_2 & E_3 & \\ E_2-E_3 & E_3-E_4 & \end{pmatrix}$
E_6	E_6	$\begin{pmatrix} H+2L & H+3L & S \\ H+3L-E_1 & E_1 & \\ H+2L-E_1 & E_2 & \\ E_2-E_3 & E_3 & \\ H+3L-E_1-E_2 & E_3-E_4 & \\ H+3L-E_1-E_2-E_5 & E_4 & \end{pmatrix}$
E_7	E_7	$\begin{pmatrix} H+2L & H+3L & S \\ H+3L-E_1 & E_1 & \\ H+2L-E_1 & E_2 & \\ H+3L-E_1-E_2 & E_3 & \\ E_2-E_3 & E_3-E_4 & \\ E_2-E_3-E_5 & E_4 & \\ E_4-E_6 & E_5 & \end{pmatrix}$
E_8	E_8	$\begin{pmatrix} H+2L & H+3L & S \\ H+3L-E_1 & E_1 & \\ H+2L-E_1 & E_2 & \\ H+3L-E_1-E_2 & E_3 & \\ E_2-E_3 & E_3-E_4 & \\ E_4 & E_5 & \\ E_2-E_3-E_5 & E_4-E_6 & E_6 \\ E_4-E_6-E_7 & E_7 & \end{pmatrix}$
A_1	$SO(3)$	$\begin{pmatrix} H+2L & H+3L \end{pmatrix}$
B_2	$SO(5)$	$\begin{pmatrix} H+2L & H+3L & 2L \\ H+2L-E_1 & H+3L-E_1 & E_1 \end{pmatrix}$
A_3	$SO(6)$	same as $SU(4)$, with $S = 2L$

Table 5.3: The classes of the centers of the blowups for all G-models

Algebra	Group	Kodaira Fiber	$\chi(Y) = \pi_*\left(f_*c(TY) \cap [Y]\right)$
–	{e}	I_1	$\frac{12L}{1+6L}c(B)$
A_1	SU(2)	$\mathrm{I}_2^{\mathrm{s}}, \mathrm{I}_2^{\mathrm{ns}}$ $\mathrm{I}_3^{\mathrm{ns}}, \mathrm{III}$ $\mathrm{IV}^{\mathrm{ns}}$	$6\frac{2L+3LS-S^2}{(1+S)(1+6L-2S)}c(B)$
A_2 C_2 G_2	SU(3) USp(4) G_2	$\mathrm{I}_3^{\mathrm{s}}, \mathrm{IV}^{\mathrm{s}}$ $\mathrm{I}_4^{\mathrm{ns}}$ $\mathrm{I}_0^{*\mathrm{ns}}$	$12\,\frac{L+2SL-S^2}{(1+S)(1+6L-3S)}c(B)$
A_3 B_3	SU(4) Spin(7)	$\mathrm{I}_4^{\mathrm{s}}$ $\mathrm{I}_0^{*\mathrm{ss}}$	$4\,\frac{3L+12L^2+LS-5S^2+30L^2S-35LS^2+10S^3}{(1+S)(1+6L-4S)(1+4L-2S)}c(B)$
D_4 F_4	Spin(8) F_4	$\mathrm{I}_0^{*\mathrm{s}}$ $\mathrm{IV}^{*\mathrm{ns}}$	$12\,\frac{L+3SL-2S^2}{(1+S)(1+6L-4S)}c(B)$
A_4	SU(5)	$\mathrm{I}_5^{\mathrm{s}}$	$\frac{12L+42L^2S+12L^2-35LS^2+32LS-30S^2}{(1+L)(1+S)(1+6L-5S)}c(B)$
D_5	Spin(10)	$\mathrm{I}_1^{*\mathrm{s}}$	$\frac{4\left(-8(4L+1)S^2+6(4L+1)LS+3(2L+1)L+10S^3\right)}{(S+1)(-2L+S-1)(-6L+5S-1)}c(B)$
E_6	E_6	$\mathrm{IV}^{*\mathrm{s}}$	$3\,\frac{4L+12L^2-12S^2+6SL-81S^2L+54SL^2+30S^3}{(1+S)(1+6L-5S)(1+3L-2S)}c(B)$
E_7	E_7	III^*	$2\,\frac{6L+24L^2+7LS-21S^2+120L^2S-190LS^2+75S^3}{(1+S)(1+6L-5S)(1+4L-3S)}c(B)$
E_8	E_8	II^*	$12\,\frac{L+6LS-5S^2}{(1+S)(1+6L-5S)}c(B)$
A_1	SO(3)	$\mathrm{I}_2^{\mathrm{ns}}$	$\frac{12L}{1+4L}c(B)$
B_2	SO(5)	$\mathrm{I}_4^{\mathrm{ns}}$	$\frac{4L(3+4L)}{(1+2L)^2}c(B)$
A_3	SO(6)	$\mathrm{I}_4^{\mathrm{s}}$	$\frac{12L}{1+2L}c(B)$

Table 5.4: Generating functions of Euler characteristic of crepant resolutions of Tate's models with trivial Mordell–Weil groups. S is the divisor over which the generic fiber is of type given by the Kodaira fiber and $L = c_1(\mathscr{L})$ where $\mathscr{L}$ is the fundamental line bundle of the Weierstrass model.

Models	$\chi(Y_3)$, Euler characteristic
Smooth Weierstrass	$12L(c_1 - 6L)$
SU(2)	$6(2c_1L - 12L^2 + 5LS - S^2)$
SU(3) or USp(4) or G_2	$12(c_1L - 6L^2 + 4LS - S^2)$
SU(4) or Spin(7)	$4(3c_1L - 18L^2 + 16LS - 5S^2)$
Spin(8) or F_4	$12(c_1L - 6L^2 + 6LS - 2S^2)$
SU(5)	$2(6c_1L - 36L^2 + 40LS - 15S^2)$
Spin(10)	$4(3c_1L - 18L^2 + 21LS - 8S^2)$
E_6	$6(2c_1L - 12L^2 + 15LS - 6S^2)$
E_7	$2(6c_1L - 36L^2 + 49LS - 21S^2)$
E_8	$12(c_1L - 6L^2 + 10LS - 5S^2)$
SO(3)	$12L(c_1 - 4L)$
SO(5)	$4L(3c_1 - 8L)$
SO(6)	$12L(c_1 - 2L)$

Table 5.5: Euler characteristic for elliptic threefolds

Models	$\chi(Y_4)$, Euler characteristic
Smooth Weierstrass	$12L(-6c_1L + c_2 + 36L^2)$
SU(2)	$6(-12c_1L^2 + 5c_1LS - c_1S^2 + 2c_2L + 72L^3 - 54L^2S + 15LS^2 - S^3)$
SU(3) or USp(4) or G_2	$12(-6c_1L^2 + 4c_1LS - c_1S^2 + c_2L + 36L^3 - 42L^2S + 17LS^2 - 2S^3)$
SU(4) or Spin(7)	$4(-18c_1L^2 + 16c_1LS - 5c_1S^2 + 3c_2L + 108L^3 - 166L^2S + 89LS^2 - 15S^3)$
SU(5)	$-72c_1L^2 + 80c_1LS - 30c_1S^2 + 12c_2L + 432L^3 - 830L^2S + 555LS^2 - 120S^3$
Spin(10)	$4(-18c_1L^2 + 21c_1LS - 8c_1S^2 + 3c_2L + 108L^3 - 210L^2S + 140LS^2 - 30S^3)$
Spin(8) or F_4	$12(-6c_1L^2 + c_2L + 36L^3 + 6c_1LS - 2c_1S^2 - 60L^2S + 34LS^2 - 6S^3)$
E_6	$3(-24c_1L^2 + 30c_1LS - 12c_1S^2 + 4c_2L + 144L^3 - 288L^2S + 195LS^2 - 42S^3)$
E_7	$2(-36c_1L^2 + 49c_1LS - 21c_1S^2 + 6c_2L + 216L^3 - 454L^2S + 321LS^2 - 72S^3)$
E_8	$12(-6c_1L^2 + 10c_1LS - 5c_1S^2 + c_2L + 36L^3 - 90L^2S + 75LS^2 - 20S^3)$
SO(3)	$12L(16L^2 - 4c_1L + c_2)$
SO(5)	$4L(20L^2 - 8c_1L + 3c_2)$
SO(6)	$12L(4L^2 - 2Lc_1 + c_2)$

Table 5.6: Euler characteristic for elliptic fourfolds

Models	$\chi(Y_4)$, Euler characteristic
Smooth Weierstrass	$12c_1c_2 + 360c_1^3$
SU(2)	$6(2c_1c_2 + 60c_1^3 - 49c_1^2S + 14c_1S^2 - S^3)$
SU(3) or USp(4) or G_2	$12(c_1c_2 + 30c_1^3 - 38c_1^2S + 16c_1S^2 - 2S^3)$
SU(4) or Spin(7)	$12(3c_1c_2 + 30c_1^3 - 50c_1^2S + 28c_1S^2 - 5S^3))$
Spin(8) or F_4	$12(c_1c_2 + 30c_1^3 - 54c_1^2S + 32c_1S^2 - 6S^3)$
SU(5)	$3(4c_1c_2 + 120c_1^3 - 250c_1^2S + 175c_1S^2 - 40S^3)$
Spin(10)	$12(c_1c_2 + 30c_1^3 - 63c_1^2S + 44c_1S^2 - 10S^3)$
E_6	$3(4c_1c_2 + 120c_1^3 - 258c_1^2S + 183c_1S^2 - 42S^3)$
E_7	$6(2c_1c_2 + 60c_1^3 - 135c_1^2S + 100c_1S^2 - 24S^3)$
E_8	$12(c_1c_2 + 30c_1^3 - 80c_1^2S + 70c_1S^2 - 20S^3)$
SO(3)	$12c_1(12c_1^2 + c_2)$
SO(5)	$12c_1(4c_1^2 + c_2)$
SO(6)	$12c_1(2c_1^2 + c_2)$

Table 5.7: Euler characteristic for Calabi–Yau elliptic fourfolds where $c_1 = L$.

Algebra	Group	Kodaira Fiber	$h^{1,1}(Y_3)$	$h^{2,1}(Y_3)$	$\chi(Y_3)$
–	{e}	I_1	$11 - K^2$	$11 + 29K^2$	$-60K^2$
A_1	$SU(2)$	$\mathrm{I}_2^{\mathrm{s}}, \mathrm{I}_2^{\mathrm{ns}}$ $\mathrm{I}_3^{\mathrm{ns}}, \mathrm{III}$ $\mathrm{IV}^{\mathrm{ns}}$	$12 - K^2$	$12 + 29K^2 + 15KS + 3S^2$	$-60K^2 - 30KS - 6S^2$
A_2 C_2 G_2	SU(3) USp(4) G_2	$\mathrm{I}_3^{\mathrm{s}}, \mathrm{IV}^{\mathrm{s}}$ $\mathrm{I}_4^{\mathrm{ns}}$ $\mathrm{I}_0^{*\mathrm{ns}}$	$13 - K^2$	$13 + 29K^2 + 24KS + 6S^2$	$-60K^2 - 48KS - 12S^2$
A_3 B_3	SU(4) Spin(7)	$\mathrm{I}_4^{\mathrm{s}}$ $\mathrm{I}_0^{*\mathrm{ss}}$	$14 - K^2$	$14 + 29K^2 + 32KS + 10S^2$	$-60K^2 - 64KS - 20S^2$
D_4 F_4	Spin(8) F_4	$\mathrm{I}_0^{*\mathrm{s}}$ $\mathrm{IV}^{*\mathrm{ns}}$	$15 - K^2$	$15 + 29K^2 + 36KS + 12S^2$	$-60K^2 - 72KS - 24S^2$
A_4	SU(5)	$\mathrm{I}_5^{\mathrm{s}}$	$15 - K^2$	$15 + 29K^2 + 40KS + 15S^2$	$-60K^2 - 80KS - 30S^2$
D_5	Spin(10)	$\mathrm{I}_1^{*\mathrm{s}}$	$16 - K^2$	$16 + 29K^2 + 42KS + 16S^2$	$-60K^2 - 84KS - 32S^2$
E_6	E_6	$\mathrm{IV}^{*\mathrm{s}}$	$17 - K^2$	$17 + 29K^2 + 45KS + 18S^2$	$-60K^2 - 90KS - 36S^2$
E_7	E_7	III^*	$18 - K^2$	$18 + 29K^2 + 49KS + 21S^2$	$-60K^2 - 98KS - 42S^2$
E_8	E_8	II^*	$19 - K^2$	$19 + 29K^2 + 60KS + 30S^2$	$-60K^2 - 120KS - 60S^2$
A_1	SO(3)	$\mathrm{I}_2^{\mathrm{ns}}$	$12 - K^2$	$12 + 17K^2$	$-36K^2$
B_2	SO(5)	$\mathrm{I}_4^{\mathrm{ns}}$	$14 - K^2$	$14 + 9K^2$	$-20K^2$
A_3	SO(6)	$\mathrm{I}_4^{\mathrm{s}}$	$14 - K^2$	$14 + 5K^2$	$-12K^2$

Table 5.8: Hodge numbers and Euler characteristic of Calabi–Yau threefolds obtained from crepant resolutions of Tate's models.

5.9 Discussion

In this chapter, we have computed the generating functions for the Euler characteristics of G-models obtained by crepant resolutions of Weierstrass models with bases of arbitrary dimension. The case of G-models that are also Calabi–Yau varieties is important in string theory and is treated here as a special case. In particular, we list the Euler characteristic of G-models that are elliptic threefolds and fourfolds. For Calabi–Yau threefolds, we also compute the Hodge numbers. These results are insensitive to the particular choice of resolution due to Batyrev's theorem on the Betti numbers of crepant birational equivalent varieties and Kontsevich's theorem on the Hodge numbers of birational equivalent Calabi–Yau varieties [29, Kontsevich]. We have considered all possible G-models with G a simple Lie group, except for the case of Kodaira fibers $\mathrm{I}_{n>5}$ and $\mathrm{I}^*_{n>1}$.

We start with a G-model given by a singular Weierstrass model $\phi : Y_0 \longrightarrow B$ with a fundamental line bundle $\mathscr{L}$ (in the Calabi–Yau case, $c_1(\mathscr{L}) = c_1(TB)$). Given a crepant resolution $f : Y \longrightarrow Y_0$ determined by a sequence of blowups with smooth centers that are complete intersections with normal crossings, we compute the Euler characteristic of Y as the degree of its total Chern class defined in homology

$$\chi(Y) = \int_Y c(Y).$$

We work relative to a smooth base B of arbitrary dimension. Using the functorial properties of the degree, we pushforward first to the Chow ring of the projective bundle and then to the Chow ring

of the base:

$$\chi(Y) = \int_B \pi_* f_* c(Y).$$

The final result is a generating function for the Euler characteristic.

A key result of this work is Theorem 5.0.1, which has numerous applications in intersection theory. We also provide a simple proof of an identity (Lemma 5.0.3) that can be traced back to Jacobi's thesis and appears in numerous situations in mathematics and physics, which is instrumental in the proof of Theorem 5.0.1.

We also retrieve in a unifying way known results on the Euler characteristics and Hodge numbers of Calabi–Yau threefolds. Furthermore, we have proven *en passant* a conjecture of Blumenhagen, Grimm, Jurke, and Weigand [44] on the Euler characteristics of Calabi–Yau fourfolds that are G-models with G belonging to the exceptional series. One interesting point that is almost trivial from the perspective taken in this chapter is that certain G-models with different G will have the same Euler characteristic just because they are resolved by the same sequence of blowups.

Theoretical physicists accept the need for mathematical beauty as an act of faith... For example, the main reason why the theory of relativity is so universally accepted is its mathematical beauty.

Paul Dirac

6

Characteristic numbers of crepant resolutions of Weierstrass models

We restrict ourselves to the case of elliptic fibrations with a unique divisor over which the generic fiber is reducible. We also consider only elliptic fibration of complex dimension four with a trivial Mordell–Weil group. That corresponds to groups G that are simple and simply-connected. We note

that our techniques apply without subtleties to the cases with non-trivial Mordell–Weil groups or to cases where G is semi-simple. The elliptic fibrations that we analyze are all given explicitly by crepant resolutions of singular Weierstrass models as discussed in section 6.5.

In our analysis, we do not impose the Calabi–Yau condition since it will reduce the problem to a computation of Euler characteristics, which is already addressed in [114]. The Calabi–Yau fourfold case is reviewed in section 6.2.1. We also point out integrality issues for the invariant $\chi_1(Y)$ in the cases of SU(5), SU(6), and E_6 in section 6.2.3. We compute the characteristic numbers by explicitly performing pushforwards after correcting the Chern classes to take into account the effect of the sequence of blowups necessary to define the crepant resolution.

6.1 Strategy and roadmaps of results

The data at the heart of our computations are the lists of blowups that give a crepant resolution for each of these G-models. We can summarize our strategy as follows

1. The G-models considered in this chapter are defined by crepant resolutions of Weierstrass models given in section 2.2.6.

2. They crepant resolutions are obtained by sequence of blowups given in Table 5.2.

3. The Chern numbers and Pontryagin numbers of the G-models are listed respectively in Table 6.4 and Table 6.6.

4. The holomorphic genera are listed in Table 6.5.

5. The invariant $X_8(Y)$, the signature $\sigma(Y)$, and the $\hat{A}$-genus are given in Table 6.7.

Let $\pi : X_0 \to B$ be the projective bundle in which the Weierstrass model Y_0 is defined. We define a crepant resolution $f : Y \to Y_0$ by a composition of k blowups $f_i : X_i \to X_{i-1}$ $i = 1, \cdots, k$ with smooth centers that are transverse complete intersections in X_i. Using Theorem 2.7.11 for each f_i, we compute the Chern classes of each X_i and by adjunction. We then determine the Chern classes of Y by adjunction.

For an element Q of the Chow ring $A^*(Y)$, we compute $\int_Y Q$ as a function of the topology of the base as follows. Using Theorem 5.0.1, we then express the Chern numbers in terms of the Chow ring of the original ambient space X_0 in which the Weierstrass model is defined. Next, we pushforward these to the base B of the elliptic fibration using Theorem 5.0.4. Since we fix the base to be a threefold, we can also simply use Lemmas 2.7.15–2.7.17 for our pushforwards. In summary we get,

$$\int_Y Q = \int_{X_k} Q \cdot [Y] = \int_B \pi_* f_{1*} f_{2*} \cdots f_{k*} \Big(Q \cdot [Y] \Big). \tag{6.1}$$

The following theorem gives the behaviors of intersection numbers involving Chern classes and Pontryagin classes of dimension too small to give Chern or Pontryagin numbers. To give a number, they must be multiplied by an element of the Chow ring of appropriate dimension.

Theorem 6.1.1. *Let $\phi : Y \longrightarrow B$ be an elliptic fibration given by the crepant resolution of a singular Weierstrass model of dimension n. Then,*

$$\int_Y c_1^i(TY) \cdot \alpha \qquad = \int_B (c_1 - L)^i \cdot \phi_* \alpha, \qquad \alpha \in A^*(Y), \tag{6.2}$$

$$\int_Y c_1^i(TY) \cdot \phi^* \beta = \int_B (c_1 - L)^i \beta, \qquad \beta \in A^*(B), \tag{6.3}$$

$$\int_Y c_1^n(TY) = \int_B (c_1 - L)^n = 0, \tag{6.4}$$

$$\int_Y c_3(TY) \cdot \phi^* \beta = \int_B \phi_*(c_3(TY)[Y]) \cdot \beta, \qquad \beta \in A^*(B), \tag{6.5}$$

$$\int_Y c_2(TY) \cdot \phi^* \beta = 12 \int_B L \cdot \beta, \qquad \beta \in A^*(B), \tag{6.6}$$

$$\int_Y p_1(TY) \cdot \phi^* \beta = \int_B (c_1 - L)^2 \beta - 24 \int_B L \cdot \beta \qquad \beta \in A^*(B) \tag{6.7}$$

where $\phi_*(c_3(TY)[Y])$ is given in Table 6.3 for the G-models considered in this chapter and is invariant of a choice of a crepant resolution.

Proof. Since Y is a crepant resolution of a Weierstrass model, we have that the first Chern class of Y is the pullback $c_1(TY) = \phi^*(c_1 - L)$. Equation (6.2) is therefore a direct consequence of the projection formula and the invariance of the degree under a proper map:

$$\int_Y \phi^*(c_1 - L)^i \alpha = \int_B \phi_*(\phi^*(c_1 - L)^i \alpha) = \int_B (c_1 - L)^i \phi_* \alpha.$$

Equations (6.3) and (6.4) are direct specializations of equation (6.2). In particular, if Y is an n-fold, we have $\int_Y \phi^*(c_1 - L)^n = \int_B (c_1 - L)^n = 0$. Equation (6.5) is also a direct consequence of the projection formula. Equation (6.6) follows from Theorem 2.7.18 and the fact that $\int_{Y_0} \pi_* c_2 = 12L$ for a smooth Weierstrass model $\pi : Y_0 \to B$. Theorem 2.7.18, asserts that for any crepant blowup centered at a transverse complete intersection of smooth divisors, we have $f_*(c_2(TY) \cdot [Y]) = c_2(TY_0) \cdot [Y_0]$. We note that these are exactly the types of blowups we use in section 6.5. Equation

(6.7) is derived by linear combination using $p_1 = c_1^2 - 2c_2$ and equations (6.3) and (6.6). □

Algebra	$\mu_G = \int_Y c_2^2(TY) - \int_{Y_o} c_2^2(TY_o)$
A_1	$-2\int_B S(7L-S)^2$
$A_2,\ C_2,\ G_2$	$-8\int_B S\,(19L^2 - 8LS + S^2)$
$A_3,\ B_3$	$-4\int_B S\,(50L^2 - 28LS + 5S^2)$
$D_4,\ F_4$	$-8\int_B S\,(27L^2 - 16LS + 3S^2)$
A_4	$-5\int_B S\,(50L^2 - 35LS + 8S^2)$
D_5	$-4\int_B S\,(63L^2 - 44LS + 10S^2)$
A_5	$-\int_B S\,(298L^2 - 251LS + 70)$
A_6	$-2\int_B S\,(174L^2 - 171LS + 56S^2)$
E_6	$-3\int_B S\,(86L^2 - 61LS + 14S^2)$
E_7	$-\int_B (135L^2 - 100LS + 24S^2)$
E_8	$-\int_B (8L^2 - 7LS + 2S^2)$

Table 6.1: μ_G for all the G-models. Y is the crepant resolution of a singular Weierstrass model corresponding to a G-model, and Y_o is a smooth Weierstrass model over the same base with the same fundamental line bundle $\mathscr{L}$.

Corollary. *Let $\phi : Y \to B$ be an elliptic fibration given by the crepant resolution of a singular Weierstrass model of dimension n with fundamental line bundle $\mathscr{L}$. Then,*

$$\int_Y c_1(TY)^{n-1} c_2(TY) = 12 \int_B (c_1 - L)^{n-1} L. \tag{6.8}$$

The following theorem shows how the dependence of the Pontryagin numbers on the Kodaira type (or better, on the group G) is controlled by the Chern number $\int_Y c_2^2(TY)$.

Theorem 6.1.2. *For a G-model, defined by a crepant resolution of one of the Weierstrass model given in section 2.2.6 and resolved by the sequence of blowups given in Table 5.2, we have*

$$\begin{aligned}
\int_Y c_2^2(TY) &= 24\int_B L(c_2 - c_1 L + 6L^2) + \mu_G,\\
\int_Y p_2(TY) &= 24\int_B L(2c_2 - c_1^2 + 36L^2) + 7\mu_G,\\
\int_Y p_1^2(TY) &= 48\int_B L(2c_2 - c_1^2 + 11L^2) + 4\mu_G,
\end{aligned} \tag{6.9}$$

where $\mu_G = \int_B S(\alpha_0 L^2 + \alpha_1 LS + \alpha_2 S^2)$ is the contribution from the singularities induced by the Kodaira type over S. The different values of μ_G are listed in Table 6.1. The correction for $\lambda_2\int_Y p_2 + \lambda_1\int_Y p_1^2$ is then $(7\lambda_2 + 4\lambda_1)\mu_G$. In particular,

$$\begin{aligned}
\int_Y \left(p_1^2(TY) - 4p_2(TY)\right) &= 48\int_B L\left(c_1^2 - 2c_2 - 61L^2\right) - 24\mu_G,\\
\int_Y \left(7p_2(TY) - p_1^2(TY)\right) &= 120\int_B L\left(2c_2 - c_1^2 + 46L^2\right) + 45\mu_G,\\
\int_Y \left(7p_1^2(TY) - 4p_2(TY)\right) &= 240\int_B L\left(2c_2 - c_1^2 + L^2\right).
\end{aligned} \tag{6.10}$$

Proof. This follows directly from an inspection of Table 6.4, Table 6.6, and Table 6.7. □

6.2 Geometric discussion

6.2.1 The Calabi–Yau fourfold case

In the case of Calabi–Yau fourfolds, knowing the Euler characteristic is enough to also compute other invariants such as the Chern number $c_2(TY)^2$ is a function of the Euler characteristic.

Theorem 6.2.1. *The Chern numbers and Pontryagin numbers of a Calabi–Yau fourfold are topological invariants depending only on its Euler characteristic.*

Proof. The only non-zero Chern numbers of a Calabi–Yau fourfold are $\int_Y c_2^2(TY)$ and $\int_Y c_4(TY) = \chi(Y)$. These two Chern numbers are related linearly as

$$\int_Y c_2^2(TY) = 480 + \frac{1}{3}\chi(Y).$$

Thus, for a Calabi–Yau fourfold, all Chern numbers and Pontryagin numbers are topological invariants as they are functions of the Euler characteristic of Y. □

For more information see section 6.2.1. It follows that in the Calabi–Yau fourfold case, all Chern and Pontryagin numbers can be read from the computation of the Euler characteristic of G-models

in [114] as we have [196, 279]

$$\int_Y c_2^2(TY) = 480 + \frac{1}{3}\chi(Y), \quad \sigma = 32 + \frac{1}{3}\chi(Y),$$
$$\chi_0 = 2, \quad \chi_1 = 8 - \frac{1}{6}\chi(Y), \quad \chi_2 = 12 + \frac{2}{3}\chi(Y),$$
$$X_8 = -\frac{1}{24}\chi(Y), \quad \frac{1}{5760}\int_Y \hat{\mathrm{A}}_2 = 2.$$

For G-models, the Euler characteristic of a Calabi–Yau fourfold is given in Table 10 of [114], which we reproduce here for completeness. We notice that the same table can be obtained from the Euler characteristic $c_4(TY)$ after putting $L = c_1$, which is the condition that ensure that the canonical class of Y is trivial.

Models	$\chi(Y_4)$, Euler characteristic
Smooth Weierstrass	$12\int_B(c_1c_2 + 30c_1^3)$
SU(2)	$6\int_B(2c_1c_2 + 60c_1^3 - 49c_1^2S + 14c_1S^2 - S^3)$
SU(3) or USp(4) or G_2	$12\int_B(c_1c_2 + 30c_1^3 - 38c_1^2S + 16c_1S^2 - 2S^3)$
SU(4) or Spin(7)	$12\int_B(3c_1c_2 + 30c_1^3 - 50c_1^2S + 28c_1S^2 - 5S^3))$
Spin(8) or F_4	$12\int_B(c_1c_2 + 30c_1^3 - 54c_1^2S + 32c_1S^2 - 6S^3)$
SU(5)	$3\int_B(4c_1c_2 + 120c_1^3 - 250c_1^2S + 175c_1S^2 - 40S^3)$
SU(6)	$3\int_B(4c_1c_2 + 120c_1^3 - 298c_1^2S + 251c_1S^2 - 70S^3)$
SU(7)	$6\int_B(2c_1c_2 + 60c_1^3 - 174c_1^2S + 171c_1S^2 - 56S^3)$
Spin(10)	$12\int_B(c_1c_2 + 30c_1^3 - 63c_1^2S + 44c_1S^2 - 10S^3)$
E_6	$3\int_B(4c_1c_2 + 120c_1^3 - 258c_1^2S + 183c_1S^2 - 42S^3)$
E_7	$6\int_B(2c_1c_2 + 60c_1^3 - 135c_1^2S + 100c_1S^2 - 24S^3)$
E_8	$12\int_B(c_1c_2 + 30c_1^3 - 80c_1^2S + 70c_1S^2 - 20S^3)$

Table 6.2: Euler characteristic for Calabi–Yau elliptic fourfolds where $c_1 = L$.

6.2.2 A geometric interpretation of the $\hat{A}$-genus and the Todd-genus of a G-model.

In this section, we will see that the $\hat{A}$-genus of a G-model Y can be understood as the A-genus of the surface W with normal bundle $\mathscr{L}$ in the base B. We call W the *Weierstrass divisor*.

The Â-genus of a G-model is

$$\int_Y \hat{A}(Y) = \frac{1}{5760}\int_Y (7p_1^2 - 4p_2) = \frac{1}{24}\int_B L(-c_1^2 + 2c_2 + L^2) = \int_W \hat{A}_1(W).$$

We compute the Chern classes of W by the adjunction formula:

$$c(TW) = \frac{c(TB)}{1+L} = 1 + (c_1 - L) + (c_2 - c_1 L + L^2).$$

It is then direct to determine the first Pontryagin class of W:

$$p_1(TW) = c_1(TW)^2 - 2c_2(TW) = (c_1 - L)^2 - 2(c_2 - c_1 L + L^2) = c_1^2 - 2c_2 - L^2.$$

Since W is a surface, it has a unique Pontryagin number, namely $\int_W p_1(TW)$:

$$\int_W p_1(TW) = \int_B L(c_1^2 - 2c_2 - L^2) = -24\int_W \hat{A}(W).$$

The last equality uses the fact that $\hat{A}_1 = -p_1/24$. If W is a spin manifold, $\int_W \hat{A}_1(W)$ is an integer

number and so is $\hat{A}(Y)$. We note that Y has a vanishing canonical class if and only if W does too. In other words, Y is Calabi–Yau if and only if W is a K3 surface. In that case, $\hat{A}(Y) = \hat{A}(W) = 2$.

A direct computation shows that the arithmetic genus of Y is the same as the arithmetic genus of the surface W.

$$\chi(W, \mathcal{O}_W) = \int_B (1 - e^{-L})\mathrm{Td}(TB) = \frac{1}{12}\int_W \Big(c_1(TW)^2 + c_2(TW)\Big) \tag{6.11}$$

$$= \frac{1}{12}\int_B L(c_1^2 - 3c_1L + c_2 + 2L^2) = \chi_0(Y). \tag{6.12}$$

6.2.3 Integrability problems for SU(5) and E_6 Calabi–Yau fourfolds.

A Calabi–Yau fourfold Y has a trivial canonical class and therefore satisfies the following relation

$$\chi_1(Y) := \chi(\Omega^1_Y) = \sum_{p=0}^{4}(-)^p h^{1,p}(Y) = 8 - \frac{1}{6}\chi(Y). \tag{6.13}$$

Since $\chi_1(Y)$ is obtained by adding and subtracting Hodge numbers, it is an integer number. Thus, the Euler characteristic $\chi(Y)$ of a Calabi–Yau fourfold should be a multiple of 6. By a direct inspection of Table 6.2, we observe that this is indeed the case for each G-models without any additional condition with the exception of SU(5), SU(6), and E_6.

Lemma 6.2.2. *Let S be the smooth divisor supporting a generic fiber of Kodaira type I_5^s, I_6^s or IV^{*ns} in the* SU(5)*,* SU(6) *or* E_6 *model. The The Euler characteristics of the* SU(5)*-model ,* SU(6)*, and the*

E_6*-model are divisible by* 6 *in the Calabi–Yau case if and only if*

$$\int_B c_1(TB)S^2 \quad \textit{is an even integer number.} \tag{6.14}$$

This condition is clearly not always realized as seen in Example 6.2.3. If $c_1(TB)$ or S is an even class, or if B is a flat fibration with fiber S, the condition is automatically satisfied. A geometric situation naturally realizing the condition that $\int_B c_1(TB)S^2$ is even is presented in Example 6.2.4.

Example 6.2.3. If B is a smooth quadric threefold in $\mathbb{P}^4$ and S is the intersection of a hyperplane of $\mathbb{P}^4$ with B, then, $\int_B c_1(TB)S^2 = (5-2)1^2 = 3$. Note that a smooth quadric threefold is Fano. Thus we can construct a Weierstrass model with $\mathscr{L}$ the anticanonical line bundle of B.

Example 6.2.4. The line bundle $\mathscr{O}_B(S)$ has two distinct sections whose zero loci are smooth transverse divisors in B, then we can compute their complete intersection, which gives a smooth curve in B. By the adjunction formula, the first Chern class of such a curve would be $c_1(TB) - 2S$. It follows that its Euler characteristic is $2 - 2g = \int_B (c_1 - 2S)S^2$. In such a case, we see that $\int_S c_1 S^2 = 2(1 - g + \int_B S^3)$ is an even number.

6.3 Invariance of characteristic numbers

In contrast to Chern numbers, Pontryagin numbers are oriented diffeomorphism invariants. There are even oriented homeomorphic invariants as proven by Novikov in the 1960s [253]. It follows that characteristic classes that are expressed in terms of Pontryagin classes and the Euler characteristic are

both oriented diffeomorphic invariants and oriented homeomorphic invariants. In contrast to the Euler characteristic, Pontryagin numbers change their signs when the variety changes its orientation. Thus, if any Pontryagin class of a variety is non-zero, the variety cannot possess any orientation reversing diffeomorphism (or homeomorphism).

In 1954, Hirzebruch asked in [170] which linear combinations of Chern numbers of a nonsingular projective variety are topological invariants. Since a complex projective variety comes with a special choice of orientation, it is natural to restrict Hirzebruch question to oriented homeomorphism or an oriented diffeomorphism. With that restriction, the question was answered by Kotschick in the following theorem.

Theorem 6.3.1 (Kotschick, [206]). 1. *A rational linear combination of Chern numbers is an oriented diffeomorphism invariant of a smooth complex projective variety if and only if it is a linear combination of the Euler and Pontryagin numbers.*

2. *In complex dimension $n \geq 3$, a rational linear combination of Chern numbers is a diffeomorphism invariant of smooth complex projective varieties if and only if it is a multiple of the Euler characteristic. In complex dimension two, both Chern numbers $\int c_1^2$ and $\int c_2$ are oriented diffeomorphism invariant.*

The statement about surfaces is a consequence of Seiberg-Witten's theory [204, 205].

There are also invariants such as the Euler characteristic, the holomorphic genus, the holomorphic genera, and the signature, which are linear combination of Hodge numbers. Hodge numbers are known to be the same for varieties in the same K-equivalence class. The following theorem char-

acterizes which linear combinations of Chern numbers are also linear combinations of Hodge numbers.

Lemma 6.3.2 (Kotschick, [206]). *A rational linear combination of Chern numbers of a smooth complex projective variety is determined by the Hodge numbers if and only if it is a linear combination of the holomorphic genera χ_p.*

The Euler characteristic is a homotopy invariant while the signature is an oriented homotopy invariant. The following theorem of Kahn characterizes linear combination of Chern numbers that are oriented homotopy invariants.

Theorem 6.3.3 (Kahn, [183]). *A linear rational combination of Chern numbers is an oriented homotopy invariant, for almost-complex manifolds, if and only if it is a rational linear combination of the Euler characteristic and the signature of the manifold.*

6.4 Pushforward of blowups and projective bundles.

We use the pushforward theorems summarized in Section 2.7. Using thses, we can compute characteristic numbers of the fourfolds in the following examples.

6.4.1 Example: Todd class of a flat fibration of genus-g curves.

Theorem 6.4.1 (Esole-Fullwood-Yau, [109, Theorem A.1]). *Let $\phi : X \to B$ be a proper and flat morphism between smooth projective varieties such that the generic fiber of ϕ is a smooth curve of genus*

g. Then

$$\phi_* Td(X) = \Big(1 - ch(\phi_* \omega_{X/B}^{\vee})\Big) Td(B), \tag{6.15}$$

where $\omega_{X/B}$ is the relative dualizing sheaf of the fibration.

When the variety Y is smooth, $\omega_{X/B} = \omega_Y \otimes (\phi^* \omega_B)^{\vee}$. In particular, in the case of an elliptic fibration, we get

$$\phi_* Td(Y) = (1 - e^{-L}) Td(B), \tag{6.16}$$

where $L = c_1(\mathscr{L})$ and $\mathscr{L}$ is the fundamental line bundle of the Weierstrass model.

The previous theorem shows that the holomorphic Euler characteristic depends only on the base and the line bundle $\mathscr{L}$. In particular, for a G-model, it does not depend on the Kodaira type.

the holomorphic arithmetic genus of Y is the same as $\chi(W, \mathscr{O}_W)$ where W is the Weierstrass divisor defined as the zero locus of a smooth section of $\mathscr{L}$. See [109, Appendix A].

$$\chi_0(Y) = \int_Y \phi_* Td(Y) = \chi(W, \mathscr{O}_W). \tag{6.17}$$

6.4.2 Example: Smooth Weierstrass model

The Euler characteristic of a smooth Weierstrass model $Y_0 \to B$ with fundamental line bundle $\mathscr{L}$ is

$$\chi(Y_0) = 12L \int_B \frac{1}{1 + 6L} c(TB), \quad \text{where } L = c_1(\mathscr{L}). \tag{6.18}$$

For an elliptic fourfold given by a smooth Weierstrass model:

$$\chi_0(Y_0) = \frac{1}{12}\int_B L(c_1^2 + c_2 - 3c_1L + 2L^2), \quad \chi_1(Y_0) = -\frac{1}{3}\int_B L(2c_1^2 + 5c_2 - 54c_1L + 232L^2), \tag{6.19}$$

$$\chi_2(Y_0) = -\frac{1}{2}\int_B L(3c_1^2 - 17c_2 + 71c_1L - 554L^2). \tag{6.20}$$

Using the adjunction formula, we have

$$c(TY_0) = \frac{(1+H)(1+H+2L)(1+H+3L)}{(1+3H+6L)}(1 + c_1(TB) + c_2(TB) + c_3(TB)) \tag{6.21}$$

We abuse notation and do not write the pullback. By expanding, we get:

$$\begin{aligned}
c_1(TY_0) &= (c_1 - L), \quad c_2(TY) = c_2 - c_1L + 13HL + 12L^2 + 3H^2, \\
c_3(TY_0) &= -72L^3 + 12c_1L^2 - c_2L + c_3 + H(13c_1L - 108L^2) + H^2(3c_1 - 52L) - 8H^3 \\
c_4(TY_0) &= (-72c_1L^3 + 12c_2L^2 - c_3L + 432L^4) + H(-108c_1L^2 + 13c_2L + 864L^3) \\
&\quad + (-52c_1L + 3c_2 + 636L^2)H^2 + (204L - 8c_1)H^3 + 24H^4.
\end{aligned} \tag{6.22}$$

Theorem 6.4.2 (Chern and Pontryagin numbers of a smooth Weierstrass fourfold)**.** *Let B be a projective threefold and $\phi : Y_0 \to B$ be a smooth Weierstrass model with fundamental line bundle $\mathscr{L}$. Denoting the first Chern class of $\mathscr{L}$ by L and writing the ith Chern class of the base B simply as c_i, the*

Chern and Pontryagin numbers of Y_0 are

$$\int_{Y_0} c_1^4(TY_0) = 0, \tag{6.23}$$

$$\int_{Y_0} c_1^2(TY_0)c_2(TY_0) = 12\int_B L(c_1 - L)^2, \tag{6.24}$$

$$\int_{Y_0} c_2^2(TY_0) = 24\int_B L(6L^2 - c_1L + c_2), \tag{6.25}$$

$$\int_{Y_0} c_1(TY_0)c_3(TY) = 12\int_B L(c_1 - 6L)(c_1 - L), \tag{6.26}$$

$$\int_{Y_0} c_4(TY_0) = 12\int_B L(36L^2 - 6Lc_1 + c_2), \tag{6.27}$$

$$\int_{Y_0} p_2(TY_0) = -24\int_B L(-c_1^2 + 2c_2 + 36L^2), \tag{6.28}$$

$$\int_{Y_0} p_1^2(TY_0) = -48\int_B L(c_1^2 - 2c_2 - 11L^2). \tag{6.29}$$

Proof. For each entries, we use (6.22) and compute

$$\int_{Y_0} A = \int_{X_0} A \cdot (3H + 6L) = 3\int_B \pi_*\Big[A \cdot (H + 2L)\Big].$$

The pushforward is then evaluated using Theorem 5.0.4 or Lemma 2.7.17.

For instance, $\int_{Y_0} c_4(TY_0) = \int_{X_0} c_4(TY_0)(3H + 6L)$. Since terms independent of H or linear in H

will not contribute (see Lemma 2.7.17), we have

$$\begin{aligned}\int_{Y_o} c_4(TY_o) &= \int_{X_o} c_4(TY_o)(3H+6L)\\ &= \int_B \pi_*\Big(H^3(-204c_1L+9c_2+3132L^2)+H^2(-636c_1L^2+57c_2L+6408L^3)+\\ &\qquad H^4(756L-24c_1)+72H^5\Big)\\ &= 12\int_B L(36L^2-6Lc_1+c_2)\end{aligned}$$

Using Lemma 2.7.17, we implement the pushforward with the substitution $H^2 \to 1$, $H^3 \to -5L$, $H^4 \to 19L^2$, $H^5 \to -65L^3$, which gives the final answer. □

As a direct application of Theorem 6.4.2, we compute the following invariants for a smooth Weierstrass model.

Theorem 6.4.3 (L-genus, $\hat{A}$-genus, and X_8 invariant of a smooth Weierstrass model)**.** *Let B be a projective threefold and $\phi : Y_o \to B$ be a smooth Weierstrass model with fundamental line bundle $\mathscr{L}$. Denoting the first Chern class of $\mathscr{L}$ by L and the ith Chern class of the base B simply by c_i, then, we have*

$$45\sigma = \int_{Y_o}\Big(7p_2(TY_o)-p_1^2(TY_o)\Big) = 120\int_B L(-c_1^2+2c_2+46L^2), \tag{6.30}$$

$$5760\int_{Y_o}\hat{A}_2 = \int_{Y_o}\Big(7p_1^2(TY_o)-4p_2(TY_o)\Big) = 240\int_B L(-c_1^2+2c_2+L^2), \tag{6.31}$$

$$192X_8 = \int_{Y_o}\Big(p_1^2(TY_o)-4p_2(TY_o)\Big) = 48\int_B L(c_1^2-2c_2-61L^2). \tag{6.32}$$

Proof. True by linearity from the quantities computed in Theorem 6.4.2. □

6.4.3 Example: the SU(2)-model

In this section, we discuss in detail the computation of Chern numbers of the SU(2)-model. The result is independent of a choice of a possible Kodaira fiber realizing the Dynkin diagram of type A_1 because type I_2 and III are resolved by the same blowup. The Weierstrass equations defining SU(2)-models are given in section 2.2.6. The Weierstrass equation is defined in the ambient space as the projective bundle X_0, where the projection map is $\pi : X_0 = \mathbb{P}_B[\mathscr{O}_B \oplus \mathscr{L}^{\otimes 2} \oplus \mathscr{L}^{\otimes 3}] \to B$ and the defining equation is a section of $\mathscr{O}(3) \otimes \mathscr{L}^{\otimes 6}$. Hence, we find

$$
\begin{aligned}
c(TX_0) &= (1+H)(1+H+3\pi^*L)(1+H+2\pi^*L)\pi^*c(TB), \\
c(TY_0) &= \frac{c(X_0)}{1+3H+6\pi^*L},
\end{aligned}
$$

where $L = c_1(\mathscr{L})$ and $H = c_1(\mathscr{O}_{X_0}(1))$ is the first Chern class of the dual of the tautological line bundle of $\pi : X_0 = \mathbb{P}(\mathscr{O}_B \oplus \mathscr{L}^{\otimes 2} \oplus \mathscr{L}^{\otimes 3}) \to B$. We denote by $S = V(s)$ the Cartier divisor supporting the fiber I_2 or III with dual graph of Dynkin type $\widetilde{A}_1$.

The singular elliptic fibration of an SU(2)-model is resolved by a unique blowup with the center (x, y, s), which we denote as $f : X_1 \longrightarrow X_0$ with the exceptional divisor E_1. The center is a complete intersection of hypersurfaces $V(x)$, $V(y)$, and $V(s)$, whose classes are respectively

$$
Z_1 = 2\pi^*L + H, \quad Z_2 = 3\pi^*L + H, \quad Z_3 = \pi^*S.
$$

The proper transform of the elliptic fibration Y_0 is denoted as Y, and is obtained from the total transform of Y by removing $2E_1$. It follows that the class of Y in X_1 is

$$[Y] = [f^*(3H + 6\pi^*L) - 2E_1] \cap [X_1].$$

Using Theorem 2.7.11, we have the following Chern class for X_1

$$c(TX_1) = (1 + E_1)\frac{(1 + f^*Z_1 - E_1)(1 + f^*Z_2 - E_1)(1 + f^*Z_3 - E_1)}{(1 + f^*Z_1)(1 + f^*Z_2)(1 + f^*Z_3)} f^*c(TX_0).$$

The adjunction formula gives

$$c(TY) = \frac{(1 + E_1)(1 + f^*Z_1 - E_1)(1 + f^*Z_2 - E_1)(1 + f^*Z_3 - E_1)}{(1 + 3f^*H + 6f^*\pi^*L - 2E_1)(1 + f^*Z_1)(1 + f^*Z_2)(1 + f^*Z_3)} f^*c(TX_0).$$

Concretely, we replace $c(TB)$ by the Chern polynomial $c_t(TB) = 1 + c_1t + c_2t^2 + c_3t^3$, L by Lt, and S by St. Then, $c_i(TY)$ is given by the coefficient of t^i in the Taylor expansion centered at $t = 0$. From the expansion, we get the following expression (to ease the notation, we do not write the pullbacks. Thus, by c_i, L, S, and H we mean $f^*\pi^*c_i, f^*\pi^*L, f^*\pi^*S$, and f^*H respectively).

$$c_1(TY) = (c_1 - L), \tag{6.33}$$

$$c_2(TY) = (c_2 - c_1L + 12L^2) + 3H^2 + 13HL + E_1(-4H - 7L + S), \tag{6.34}$$

$$c_3(TY) = 3c_1H^2 + 13c_1HL + 12c_1L^2 - c_2L + c_3 - 8H^3 - 52H^2L - 108HL^2 - 72L^3$$

$$
\begin{aligned}
&+ E_1(-4c_1H - 7c_1L + c_1S + 16H^2 + 66HL + 66L^2 - LS - S^2) \qquad (6.35)\\
&+ E_1^2(-10H - 19L + S) + 2E_1^3,\\
c_4(TY) = (&-8c_1H^3 - 52H^2c_1L - 108c_1HL^2 - 72c_1L^3 + 3c_2H^2 + 13c_2HL\\
&+ 12c_2L^2 - c_3L + 24H^4 + 204H^3L + 636H^2L^2 + 864HL^3 + 432L^4)\\
&+ E_1(16c_1H^2 + 66c_1HL + 66c_1L^2 - c_1LS - c_1S^2 - 4c_2H - 7c_2L + c_2S \qquad (6.36)\\
&- 64H^3 - 398H^2L + 3H^2S - 810HL^2 + 13HLS - 540L^3 + 12L^2S + LS^2 + S^3)\\
&+ E_1^2(-10c_1H - 19c_1L + c_1S + 59H^2 + 239HL - 4HS + 240L^2 - 8LS - S^2)\\
&+ E_1^3(2c_1 - 22H - 45L + S) + 3E_1^4.
\end{aligned}
$$

We can now compute $\int_Y c_2^2(TY)$ and apply the pushforward formula of Lemma 2.7.16

$$
\begin{aligned}
\int_Y c_2^2(TY) = \int_{X_1} c_2^2(TY)[Y] &= \int_{X_1} c_2^2(TY)(f^*(3H + 6\pi^*L) - 2E_1)\\
&= \int_{X_0} f_*\Big(c_2^2(TY)(f^*(3H + 6\pi^*L) - 2E_1)\Big)\\
&= \int_B \pi_* f_*\Big(c_2^2(TY)(f^*(3H + 6\pi^*L) - 2E_1)\Big)\\
&= 24\int_B L(c_2 - c_1L + 6L^2) - 2\int_B S(7L - S)^2.
\end{aligned} \qquad (6.37)
$$

In the second line, we use $\int_Y A = \int_{X_1} A \cap [Y]$. In the third line, we use the functorial property $\int_{X_1} A = \int_{X_0} f_* A$ for a proper map $f : X_1 \to X_0$. In the fourth line, we use again the functional property of the degree, but this time, for the proper map $\pi : X_0 \to B$. In the last line, we use Lemma 2.7.16 to compute the pushforward of f to X_0 and then Lemma 2.7.17 to compute of π to

the base B.

Using the same logic, we now compute $\int_Y c_3(TY) f^*\pi^*\alpha$.

$$\begin{aligned}\int_Y c_3(TY) f^*\pi^*\alpha &= \int_{X_1} c_3(TY)(f^*(3H + 6\pi^*L) - 2E_1) f^*\pi^*\alpha \\ &= \int_{X_0} f_*\Big(c_3(TY)(3H + 6L - 2E_1)\Big)\pi^*\alpha \\ &= \int_B \pi_* f_*\Big(c_3(TY)(3H + 6L - 2E_1)\Big)\alpha \\ &= \int_B 12L(c_1 - 6L)\alpha + 6\int_B (5L - S)S\alpha.\end{aligned} \tag{6.38}$$

In the first line, we use $\int_Y A = \int_{X_1} A \cap [Y]$. The second and third lines are projection formula for f and π. In the last line, we use Lemma 2.7.16 to compute the pushforward of f to X_0 and then Lemma 2.7.17 to compute of π to the base B.

6.5 G-MODELS

The Tate' forms of the G-models considered are listed in the first part of Section 5.8. A crepant resolution of each model are given as a sequence of blowups. The blowup centers of the crepant resolutions of all G-models considered are listed in Table 5.2. The variable s is a section of the line bundle $\mathscr{O}_B(S)$. In other words, the zero locus locus $V(s)$ is the divisor S supporting the singular fiber given in the second column.

Algebra	G	Kodaira	$\phi_*\left(c_3(TY)[Y]\right)$
A_1	$SU(2)$	$I_2^s, I_2^{ns}, I_3^{ns}$ III, IV^{ns}	$12L(c_1 - 6L) + 30LS - 6S^2$
A_2	$SU(3)$	$I_3^s,\ IV^s$	$12L(c_1 - 6L) + 48LS - 12S^2$
C_2	$USp(4)$	I_4^{ns}	
G_2	G_2	I_0^{*ns}	
A_3	$SU(4)$	I_4^s	$12L(c_1 - 6L) + 64LS - 20S^2$
B_3	$Spin(7)$	I_0^{*ss}	
D_4	$Spin(8)$	I_0^{*s}	$12L(c_1 - 6L) + 72LS - 24S^2$
F_4	F_4	IV^{*ns}	
A_4	$SU(5)$	I_5^s	$12L(c_1 - 6L) + 80LS - 30S^2$
D_5	$Spin(10)$	I_1^{*s}	$12L(c_1 - 6L) + 84LS - 32S^2$
A_5	$SU(6)$	I_6^s	$12L(c_1 - 6L) + 96LS - 42S^2$
A_6	$SU(7)$	I_7^s	$12L(c_1 - 6L) + 112LS - 56S^2$
E_6	E_6	IV^{*s}	$12L(c_1 - 6L) + 90LS - 36S^2$
E_7	E_7	III^*	$12L(c_1 - 6L) + 98LS - 42S^2$
E_8	E_8	II^*	$12L(c_1 - 6L) + 120LS - 60S^2$

Table 6.3: Chern numbers after pushforwards to the base. The divisor S is the one supporting the reducible Kodaira fiber corresponding to the type of the Lie algebra $\mathfrak{g}$. By definition, $L = c_1(\mathscr{L})$ and c_i denotes the ith Chern class of the base of the fibration.

Group	$c_1^4(TY)$	$c_1^2(TY)c_2(TY)$	$c_2^2(TY)$	$c_1(TY)c_3(TY)$	$c_4(TY)$
SU(2)	0	$12L(c_1-L)^2$	$24L(L(6L-c_1)+c_2)$ $-2S(7L-S)^2$	$12L(c_1-6L)(c_1-L)$ $+6S(c_1-L)(5L-S)$	$12L(6L(6L-c_1)+c_2)$ $+6LS(5c_1-54L)$ $-6S^2(c_1-15L)-6S^3$
SU(3) USp(4) G_2	0	$12L(c_1-L)^2$	$24L(L(6L-c_1)+c_2)$ $-8S(19L^2-8LS+S^2)$	$12L(c_1-6L)(c_1-L)$ $+12S(c_1-L)(4L-S)$	$12L(6L(6L-c_1)+c_2)$ $+24LS(2c_1-21L)$ $-12S^2(c_1-17L)-24S^3$
SU(4) Spin(7)	0	$12L(c_1-L)^2$	$24L(L(6L-c_1)+c_2)$ $-4S(50L^2-28LS+5S^2)$	$12L(c_1-L)(c_1-6L)$ $+4S(c_1-L)(16L-5S)$	$12L(6L(6L-c_1)+c_2)$ $+8LS(8c_1-83L)$ $+4S^2(89L-5c_1)-60S^3$
Spin(8) F_4	0	$12L(c_1-L)^2$	$24L(L(6L-c_1)+c_2)$ $-8S(27L^2-16LS+3S^2)$	$12L(c_1-L)(c_1-6L)$ $+24S(c_1-L)(3L-S)$	$12L(6L(6L-c_1)+c_2)$ $+72LS(c_1-10L)$ $-24S^2(c_1-17L)-72S^3$
SU(5)	0	$12L(c_1-L)^2$	$24L(L(6L-c_1)+c_2)$ $-5S(50L^2-35LS+8S^2)$	$12L(c_1-L)(c_1-6L)$ $+10S(c_1-L)(8L-3S)$	$12L(6L(6L-c_1)+c_2)$ $+10LS(8c_1-83L)$ $+15S^2(37L-2c_1)-120S^3$
Spin(10)	0	$12L(c_1-L)^2$	$24L(L(6L-c_1)+c_2)$ $-4S(63L^2-44LS+10S^2)$	$12L(c_1-L)(c_1-6L)$ $+4S(c_1-L)(21L-8S)$	$12L(6L(6L-c_1)+c_2)$ $+84LS(c_1-10L)$ $-16S^2(2c_1-35L)-120S^3$
SU(6)	0	$12L(c_1-L)^2$	$24L(L(6L-c_1)+c_2)$ $-S(298L^2-251LS+70S^2)$	$12L(c_1-L)(c_1-6L)$ $+6S(c_1-L)(16L-7S)$	$12L(6L(6L-c_1)+c_2)$ $+6LS(16c_1-165L)$ $-3S^2(14c_1-265L)-210S^3$
SU(7)	0	$12L(c_1-L)^2$	$24L(L(6L-c_1)+c_2)$ $-2S(174L^2-171LS+56S^2)$	$12L(c_1-L)(c_1-6L)$ $+56S(c_1-L)(2L-S)$	$12L(6L(6L-c_1)+c_2)$ $+4LS(28c_1-289L)$ $-2S^2(28c_1-541L)-336S^3$
E_6	0	$12L(c_1-L)^2$	$24L(L(6L-c_1)+c_2)$ $-3S(86L^2-61LS+14S^2)$	$12L(c_1-L)(c_1-6L)$ $+18S(c_1-L)(5L-2S)$	$12L(6L(6L-c_1)+c_2)$ $+18LS(5c_1-48L)$ $-9S^2(4c_1-65L)-126S^3$
E_7	0	$12L(c_1-L)^2$	$24L(L(6L-c_1)+c_2)$ $-2S(135L^2-100LS+24S^2)$	$12L(c_1-L)(c_1-6L)$ $+14S(c_1-L)(7L-3S)$	$12L(6L(6L-c_1)+c_2)$ $+2LS(49c_1-454L)$ $-6S^2(7c_1-107L)-144S^3$
E_8	0	$12L(c_1-L)^2$	$24L(L(6L-c_1)+c_2)$ $-40S(8L^2-7LS+2S^2)$	$12L(c_1-L)(c_1-6L)$ $+60S(c_1-L)(2L-S)$	$12L(6L(6L-c_1)+c_2)$ $+120LS(c_1-9L)$ $-60S^2(c_1-15L)-240S^3$

Table 6.4: Chern numbers of elliptically-fibered fourfolds obtained from crepant resolutions of Tate's models. The divisor S is supporting the reducible Kodaira fiber corresponding to the type of the Lie algebra. We abuse notation and omit the degree $\int$ in the entries of the table. By definition, $L = c_1(\mathscr{L})$ and c_i denotes the ith Chern class of the base of the fibration.

Group	χ_0	χ_1	χ_2
SU(2)	$\frac{1}{12}L\left(c_1^2 - 3c_1L + c_2 + 2L^2\right)$	$-\frac{1}{3}L\left(2c_1^2 - 54c_1L + 5c_2 + 232L^2\right)$ $+\frac{1}{2}S^2(3c_1 - 31L) - \frac{1}{2}LS(15c_1 - 113L) + S^3$	$-\frac{1}{2}L\left(3c_1^2 + 71c_1L - 17c_2 - 554L^2\right)$ $+S^2(59L - 3c_1) + LS(15c_1 - 211L) - 4S^3$
SU(3) USp(4) G_2	$\frac{1}{12}L\left(c_1^2 - 3c_1L + c_2 + 2L^2\right)$	$-\frac{1}{3}L\left(2c_1^2 - 54c_1L + 5c_2 + 232L^2\right)$ $+S^2(3c_1 - 35L) - 4LS(3c_1 - 22L) + 4S^3$	$-\frac{1}{2}L\left(3c_1^2 + 71c_1L - 17c_2 - 554L^2\right)$ $-2S^2(3c_1 - 67L) + 8LS(3c_1 - 41L) - 16S^3$
SU(4) Spin(7)	$\frac{1}{12}L\left(c_1^2 - 3c_1L + c_2 + 2L^2\right)$	$-\frac{1}{3}L\left(2c_1^2 - 54c_1L + 5c_2 + 232L^2\right)$ $+S^2(5c_1 - 61L) - 4LS(4c_1 - 29L) + 10S^3$	$-\frac{1}{2}L\left(3c_1^2 + 71c_1L - 17c_2 - 554L^2\right)$ $-2S^2(5c_1 - 117L) + 16LS(2c_1 - 27L) - 40S^3$
Spin(8) F_4	$\frac{1}{12}L\left(c_1^2 - 3c_1L + c_2 + 2L^2\right)$	$-\frac{1}{3}L\left(2c_1^2 - 54c_1L + 5c_2 + 232L^2\right)$ $+2S^2(3c_1 - 35L) - 18LS(c_1 - 7L) + 12S^3$	$-\frac{1}{2}L\left(3c_1^2 + 71c_1L - 17c_2 - 554L^2\right)$ $-4S^2(3c_1 - 67L) + 36LS(c_1 - 13L) - 48S^3$
SU(5)	$\frac{1}{12}L\left(c_1^2 - 3c_1L + c_2 + 2L^2\right)$	$-\frac{1}{3}L\left(2c_1^2 - 54c_1L + 5c_2 + 232L^2\right)$ $+\frac{5}{2}S^2(3c_1 - 38L) - 5LS(4c_1 - 29L) + 20S^3$	$-\frac{1}{2}L\left(3c_1^2 + 71c_1L - 17c_2 - 554L^2\right)$ $-5S^2(3c_1 - 73L) + 20LS(2c_1 - 27L) - 80S^3$
Spin(10)	$\frac{1}{12}L\left(c_1^2 - 3c_1L + c_2 + 2L^2\right)$	$-\frac{1}{3}L\left(2c_1^2 - 54c_1L + 5c_2 + 232L^2\right)$ $+8S^2(c_1 - 12L) - 21LS(c_1 - 7L) + 20S^3$	$-\frac{1}{3}L\left(2c_1^2 - 54c_1L + 5c_2 + 232L^2\right)$ $+8S^2(c_1 - 12L) - 21LS(c_1 - 7L) + 20S^3$
SU(6)	$\frac{1}{12}L\left(c_1^2 - 3c_1L + c_2 + 2L^2\right)$	$-\frac{1}{3}L\left(2c_1^2 - 54c_1L + 5c_2 + 232L^2\right)$ $+\frac{1}{2}S^2(21c_1 - 272L) - LS(24c_1 - 173L) + 35S^3$	$-\frac{1}{2}L\left(3c_1^2 + 71c_1L - 17c_2 - 554L^2\right)$ $+S^2(523L - 21c_1) + 4LS(12c_1 - 161L) - 140S^3$
SU(7)	$\frac{1}{12}L\left(c_1^2 - 3c_1L + c_2 + 2L^2\right)$	$-\frac{1}{3}L\left(2c_1^2 - 54c_1L + 5c_2 + 232L^2\right)$ $(+S^2)\left(14c_1 - 185L\right) - 2LS(14c_1 - 101L) + 56S^3$	$-\frac{1}{2}L\left(3c_1^2 + 71c_1L - 17c_2 - 554L^2\right)$ $-4S^2(7c_1 - 178L) + 8LS(7c_1 - 94L) - 224S^3$
E_6	$\frac{1}{12}L\left(c_1^2 - 3c_1L + c_2 + 2L^2\right)$	$-\frac{1}{3}L\left(2c_1^2 - 54c_1L + 5c_2 + 232L^2\right)$ $+\frac{3}{2}S^2(6c_1 - 67L) - \frac{3}{2}LS(15c_1 - 101L) + 21S^3$	$-\frac{1}{2}L\left(3c_1^2 + 71c_1L - 17c_2 - 554L^2\right)$ $-6S^2(3c_1 - 64L) + 3LS(15c_1 - 187L) - 84S^3$
E_7	$\frac{1}{12}L\left(c_1^2 - 3c_1L + c_2 + 2L^2\right)$	$-\frac{1}{3}L\left(2c_1^2 - 54c_1L + 5c_2 + 232L^2\right)$ $+\frac{1}{2}S^2(21c_1 - 221L) - \frac{1}{2}LS(49c_1 - 319L) + 24S^3$	$-\frac{1}{2}L\left(3c_1^2 + 71c_1L - 17c_2 - 554L^2\right)$ $+S^2(421L - 21c_1) + LS(49c_1 - 589L) - 96S^3$
E_8	$\frac{1}{12}L\left(c_1^2 - 3c_1L + c_2 + 2L^2\right)$	$-\frac{1}{3}L\left(2c_1^2 - 54c_1L + 5c_2 + 232L^2\right)$ $+5S^2(3c_1 - 31L) + 10LS(19L - 3c_1) + 40S^3$	$\frac{1}{2}L\left(-3c_1^2 - 71c_1L + 17c_2 + 554L^2\right)$ $+10S^2(59L - 3c_1) + 20LS(3c_1 - 35L) - 160S^3$

Table 6.5: Holomorphic genera. The divisor S is the one supporting the reducible Kodaira fiber corresponding to the type of the Lie algebra $\mathfrak{g}$. To ease the notation, we abuse notation and omit the degree $\int$ in the entries of the table. By definition, $L = c_1(\mathscr{L})$ and c_i denotes the ith Chern class of the base of the fibration. The holomorphic Euler characteristic $\chi_0(Y)$ is equal to $\chi_0(W, \mathscr{O}_W)$ where W is the divisor defined by $\mathscr{L}$ in the base (see section 6.4.1).

Group	$\int_Y p_2(TY)$	$\int_Y p_1^2(TY)$
SU(2)	$24L(-c_1^2+2c_2+36L^2)-14S(7L-S)^2$	$-48L(c_1^2-2c_2-11L^2)-8S(7L-S)^2$
SU(3), USp(4), G_2	$24L(-c_1^2+2c_2+36L^2)-56S(19L^2-8LS+S^2)$	$-48L(c_1^2-2c_2-11L^2)-32S(19L^2-8LS+S^2)$
SU(4), Spin(7)	$24L(-c_1^2+2c_2+36L^2)-28S(50L^2-28LS+5S^2)$	$-48L(c_1^2-2c_2-11L^2)-16S(50L^2-28LS+5S^2)$
Spin(8), F_4	$24L(-c_1^2+2c_2+36L^2)-56S(27L^2-16LS+3S^2)$	$-48L(c_1^2-2c_2-11L^2)-32S(27L^2-16LS+3S^2)$
SU(5)	$24L(-c_1^2+2c_2+36L^2)-35S(50L^2-35LS+8S^2)$	$-48L(c_1^2-2c_2-11L^2)-20S(50L^2-35LS+8S^2)$
Spin(10)	$24L(-c_1^2+2c_2+36L^2)-28S(63L^2-44LS+10S^2)$	$-48L(c_1^2-2c_2-11L^2)-16S(63L^2-44LS+10S^2)$
SU(6)	$24L(-c_1^2+2c_2+36L^2)-7S(298L^2-251LS+70S^2)$	$-48L(c_1^2-2c_2-11L^2)-4S(298L^2-251LS+70S^2)$
SU(7)	$24L(-c_1^2+2c_2+36L^2)-14S(174L^2-171LS+56S^2)$	$-48L(c_1^2-2c_2-11L^2)-8S(174L^2-171LS+56S^2)$
E_6	$24L(-c_1^2+2c_2+36L^2)-21S(86L^2-61LS+14S^2)$	$-48L(c_1^2-2c_2-11L^2)-12S(86L^2-61LS+14S^2)$
E_7	$24L(-c_1^2+2c_2+36L^2)-14S(135L^2-100LS+24S^2)$	$-48L(c_1^2-2c_2-11L^2)-8S(135L^2-100LS+24S^2)$
E_8	$24L(-c_1^2+2c_2+36L^2)-280S(8L^2-7LS+2S^2)$	$-48L(c_1^2-2c_2-11L^2)-160S(8L^2-7LS+2S^2)$

Table 6.6: Pontryagin numbers. The divisor S is the one supporting the reducible Kodaira fiber corresponding to the type of the Lie algebra $\mathfrak{g}$. To ease the notation, we abuse notation and omit the degree $\int$ in the entries of the table. By definition, $L = c_1(\mathscr{L})$ and c_i denotes the ith Chern class of the base of the fibration.

Group	$192X_8 = \int_Y (p_1^2 - 4p_2)$	$45\sigma = 45\int_Y L_2 = \int_Y (7p_2 - p_1^2)$	$5760\int_Y \hat{\mathrm{A}}_2 = \int_Y (7p_1^2 - 4p_2)$
SU(2)	$48L\,(c_1^2 - 2c_2 - 61L^2)$ $+48S(7L - S)^2$	$120L\,(-c_1^2 + 2c_2 + 46L^2)$ $-90S(7L - S)^2$	$240L\,(-c_1^2 + 2c_2 + L^2)$
SU(3) USp(4) G_2	$48L\,(c_1^2 - 2c_2 - 61L^2)$ $+192S(19L^2 - 8LS + S^2)$	$120L\,(-c_1^2 + 2c_2 + 46L^2)$ $-360S(19L^2 - 8LS + S^2)$	$240L\,(-c_1^2 + 2c_2 + L^2)$
SU(4) Spin(7)	$48L\,(c_1^2 - 2c_2 - 61L^2)$ $+96S(50L^2 - 28LS + 5S^2)$	$120L\,(-c_1^2 + 2c_2 + 46L^2)$ $-180S(50L^2 - 28LS + 5S^2)$	$240L\,(-c_1^2 + 2c_2 + L^2)$
Spin(8) F_4	$48L\,(c_1^2 - 2c_2 - 61L^2)$ $+192S(27L^2 - 16LS + 3S^2)$	$120L\,(-c_1^2 + 2c_2 + 46L^2)$ $-360S(27L^2 - 16LS + 3S^2)$	$240L\,(-c_1^2 + 2c_2 + L^2)$
SU(5)	$48L\,(c_1^2 - 2c_2 - 61L^2)$ $+120S(50L^2 - 35LS + 8S^2)$	$120L\,(-c_1^2 + 2c_2 + 46L^2)$ $-225S(50L^2 - 35LS + 8S^2)$	$240L\,(-c_1^2 + 2c_2 + L^2)$
Spin(10)	$48L\,(c_1^2 - 2c_2 - 61L^2)$ $+96S(63L^2 - 44LS + 10S^2)$	$120L\,(-c_1^2 + 2c_2 + 46L^2)$ $-180S(63L^2 - 44LS + 10S^2)$	$240L\,(-c_1^2 + 2c_2 + L^2)$
SU(6)	$48L\,(c_1^2 - 2c_2 - 61L^2)$ $+24S(298L^2 - 251LS + 70S^2)$	$120L\,(-c_1^2 + 2c_2 + 46L^2)$ $-45S(298L^2 - 251LS + 70S^2)$	$240L\,(-c_1^2 + 2c_2 + L^2)$
SU(7)	$48L\,(c_1^2 - 2c_2 - 61L^2)$ $+48S(174L^2 - 171LS + 56S^2)$	$120L\,(-c_1^2 + 2c_2 + 46L^2)$ $-90S(174L^2 - 171LS + 56S^2)$	$240L\,(-c_1^2 + 2c_2 + L^2)$
E_6	$48L\,(c_1^2 - 2c_2 - 61L^2)$ $+72S(86L^2 - 61LS + 14S^2)$	$120L\,(-c_1^2 + 2c_2 + 46L^2)$ $-135S(86L^2 - 61LS + 14S^2)$	$240L\,(-c_1^2 + 2c_2 + L^2)$
E_7	$48L\,(c_1^2 - 2c_2 - 61L^2)$ $+48S(135L^2 - 100LS + 24S^2)$	$120L\,(-c_1^2 + 2c_2 + 46L^2)$ $-90S(135L^2 - 100LS + 24S^2)$	$240L\,(-c_1^2 + 2c_2 + L^2)$
E_8	$48L\,(c_1^2 - 2c_2 - 61L^2)$ $+960S(8L^2 - 7LS + 2S^2)$	$120L\,(-c_1^2 + 2c_2 + 46L^2)$ $-1800S(8L^2 - 7LS + 2S^2)$	$240L\,(-c_1^2 + 2c_2 + L^2)$

Table 6.7: Characteristic invariants: the anomaly invariant X_8, the signature σ, and the index of the $\hat{\mathrm{A}}$-genus. The divisor S is the one supporting the reducible Kodaira fiber corresponding to the type of the Lie algebra $\mathfrak{g}$. To ease the notation, we abuse notation and omit the degree $\int$ in the entries of the table. By definition, $L = c_1(\mathscr{L})$ and c_i denotes the ith Chern class of the base of the fibration.

There is no royal road to geometry.

Euclid

7

Characteristic numbers of elliptic fibrations with non-trivial Mordell–Weil groups

Elliptic fibrations with multisections were first studied in string theory in [34, 39, 195] as complete intersections in weighted projective spaces. They were generalized to complete intersections in projective bundles in [6, 109]. Elliptic fibrations with non-trivial Mordell–Weil groups were studied

heavily in F-theory. For examples, see [20, 31, 58, 61, 63, 86, 144, 151, 207, 229–231, 254] and [301, §7] for a review.

7.1 Models with multisections and organization of the chapter

In this chapter, we will focus on the generic models with multisections having trivial Lie algebra $\mathfrak{g}$ with Mordell–Weil groups $\mathbb{Z}/2\mathbb{Z}$, $\mathbb{Z}/3\mathbb{Z}$, and $\mathbb{Z}$. Since the first model has a gauge group SO(3), we also include in our analysis the G-models with G=SO(n) for $n = 3, 4, 5, 6$; they all have the Mordell–Weil group $\mathbb{Z}/2\mathbb{Z}$ and are related to each other by base changes [118]. We also examine the G-model with G=PSU(3), which is the generic model with a Mordell–Weil group $\mathbb{Z}/3\mathbb{Z}$ [20]. Finally, we consider the case of elliptic fibration of rank one. A generic model of an elliptic fibration of rank one was introduced in F-theory by Morrison and Park [239]; a smooth model in the birational class of the Morrison-Park model is given by the Q_7-model introduced in [120], which generalizes a model introduced by Cacciatori, Cattaneo and Geemen in [65] sharing the same Jacobian with the Morrison-Park model.

In particular, we determine the characteristic numbers, that are listed in 2.9.1 as it was in Chapter 6, of elliptic fourfolds $\phi : Y \longrightarrow B$ of the following three types of elliptic fibrations:

1. The generic fiber of Y is a genus-one normal curve of degree d for $d = 1, 2, 3, 4, 5$. Such elliptic fibrations are called models of type E_{9-d}. They are defined in [6, 109], where they are used to provide strong coupling regimes of several systems of intersecting branes and orientifolds preserving a fraction of supersymmetry and satisfying the tadpole constraints

[5, 6, 78].

2. Y is an elliptic fibration of rank one. In this case, we use the smooth model $\mathrm{Q}_7(\mathscr{L}, \mathscr{M})$ introduced in [120], and a generalization of the model of [65], birational to the model of Morrison-Park [239].

3. Y is a G-model with $G = \mathrm{SO}(n)$ with $n = 3, 4, 5$, or 6 or with G=PSU(3). The SO(3)-model is the generic elliptic fibration with a Mordell–Weil group $\mathbb{Z}/2\mathbb{Z}$ [20]. The SO(3)-model is defined by $b_6 = 0$ and has a fiber of type I_2 over the generic point of b_4. The SO(5)-model and SO(6)-model are both derived from the SO(3)-model by the base change $b_4 \to t^2$, which replaces the fiber I_2 by an I_4. The model is an SO(5) (resp. SO(6)) when the generic fiber over $V(t)$ is of type $\mathrm{I}_4^{\mathrm{ns}}$ (resp. $\mathrm{I}_4^{\mathrm{s}}$). The SO(4)-model is a collision of type $A_1 + A_1$ with a Mordell–Weil group $\mathbb{Z}/2\mathbb{Z}$ [121]. Such a collision is not uniquely defined since there are several Kodaira fibers whose dual graph is $\widetilde{\mathrm{A}}_1$. The collisions of kodaira fibers describing the SO(4)-model that have crepant resolutions are I_2^{ns}+I_2^{ns}, I_2^{ns}+I_2^{s}, I_2^{s}+I_2^{s}, III+I_2^{ns}, and III+III [118]. The PSU(3)-model has a fiber of type I_3^{s} with a Mordell–Weil group $\mathbb{Z}/3\mathbb{Z}$ [20].

The Theorem 2.9.6 asserts that the Chern numbers of fourfolds are K-equivalence invariants. The proof is given in Section 2.9.2 and it follows from Theorem 2.9.4 of Aluffi and the birational invariance of the Todd-genus. The Chern number $\int_Y c_1(TY)^2 c_2(TY)$, the $\hat{A}$-genus, and the Todd-genus (the holomorphic Euler characteristic) are invariants of the choice of G. They can all be expressed as invariants of the divisor W defined by the vanishing locus of a smooth section of $\mathscr{L}$.

By expressing χ_0 and $\hat{A}$ in terms of Chern numbers and using the identity $\int_Y c_1^4 = 0$, which holds

Type	Zero scheme of a section of	Ambient space
Q_7	$\mathscr{O}(3) \otimes \pi^*\mathscr{L}^{\otimes 2} \otimes \pi^*\mathscr{M}$	$\mathbb{P}(\mathscr{O}_B \oplus \mathscr{M} \oplus \mathscr{L})$
$E_5 = D_5$	$\mathscr{O}(2) \otimes \pi^*\mathscr{L}^{\otimes 2}, \mathscr{O}(2) \otimes \pi^*\mathscr{L}^{\otimes 2}$	$\mathbb{P}(\mathscr{O}_B \oplus \mathscr{L} \oplus \mathscr{L} \oplus \mathscr{L})$
E_6	$\mathscr{O}(3) \otimes \pi^*\mathscr{L}^{\otimes 3}$	$\mathbb{P}(\mathscr{O}_B \oplus \mathscr{L} \oplus \mathscr{L})$
E_7	$\mathscr{O}(4) \otimes \pi^*\mathscr{L}^{\otimes 4}$	$\mathbb{P}_{1,1,2}(\mathscr{O}_B \oplus \mathscr{L} \oplus \mathscr{L}^{\otimes 2})$
E_7'	$\mathscr{O}(3) \otimes \pi^*\mathscr{L}^{\otimes 4}$	$\mathbb{P}(\mathscr{O}_B \oplus \mathscr{L} \oplus \mathscr{L}^{\otimes 2})$
E_8	$\mathscr{O}(3) \otimes \pi^*\mathscr{L}^{\otimes 6}$	$\mathbb{P}(\mathscr{O}_B \oplus \mathscr{L}^{\otimes 2} \oplus \mathscr{L}^{\otimes 3})$

Table 7.1: The E_8-model is the usual Weierstrass model defined by Deligne and Tate. The E_6 and E_7-models are defined in [5] while the D_5-model is defined in [109]. The E_7' and Q_7 model are respectively introduced in [65] and [120]. The Q_7-model specializes to E_6 and E_7' when $\mathscr{M}$ is $\mathscr{L}$ and $\mathscr{L}^{\otimes 2}$ respectively.

for any elliptic fibration related to a Weierstrass model by a crepant birational map (see Theorem 6.1.1), we get the following expressions of $c_1^2c_2$ and c_1c_3:

$$\int_Y c_1^2c_2 = 96(\chi_0(Y) - \hat{A}(Y)), \quad \int_Y c_1c_3 = 384\hat{A}(Y) + 336\chi_0(Y) + \chi(Y) - 3\int_Y c_2^2. \tag{7.1}$$

For an elliptic fibration that is a crepant birational map away from a Weierstrass model, this shows that $\int_Y c_1^2c_2$ gives the same value as a smooth Weierstrass model with the same fundamental line bundle $\mathscr{L}$. It is therefore enough to compute only $\int_Y c_2^2$ and the Euler characteristic $\chi(Y) = \int_Y c_4$ to know all the Chern numbers.

7.1.1 Organization of the chapter

The rest of the chapter is organized as follows. In Section 7.2, we introduce all the models considered in this chapter. First we explain E_8, E_7, E_6, D_5, and Q_7-models in Section 7.2.1 and 7.2.2. We then explain the G-models considered in this chapter with $G = \mathrm{SO}(n)$ for $n = 3, 4, 5, 6$ in Section 7.2.4

and with $G = \mathrm{PSU}(3)$ in Section 7.2.5. We summarize necessary pushforward theorems used and introduce theorems for the models considered in this chapter in Section 7.3. Finally, we present our results in Section 7.4.

7.2 Descriptions of the elliptic fibrations considered

In this section, we introduce the elliptic fibrations considered in this chapter. Namely, the elliptic fibrations of type E_8, E_7, E_6 [5], D_5 [109], and Q_7 [120], the $\mathrm{SO}(n)$-models for $n = 3, 4, 5, 6$ [118], and the PSU(3)-model [20].

7.2.1 Genus-one normal curves of degree d

The Riemann-Roch theorem for curves famously implies that a genus-one curve with a rational point can be expressed as the zero scheme of a Weierstrass equation [246]. Using some cohomology and base change techniques, the result can also be extended to fibrations of genus-one curves with a rational section [94, 246]. A divisor of degree $d \geq 3$ defines an embedding of the genus-one curve into $\mathbb{P}^{d-1}$, such a curve is a called a *genus-one normal curve of degree d*. For a review on genus-one normal curves, see [173] and [133, §3]. Some of the historical most famous families of elliptic curves are genus-one normal curves of degree 1, 2, 3, and 4. These are precisely the genus-one normal curves that are hypersurfaces or complete intersections in a (weighted) projective space [173]. A rational point is a divisor of degree one on the curve. By the Riemann-Roch theorem, a divisor of degree one on a genus-one curve yields a Weierstrass equation [246]. A divisor of degree two gives a quartic curve that can be embedded as a quartic in a weighted projective space $\mathbb{P}_{1,1,2}$. Since the weighted

projective space $\mathbb{P}_{1,1,2}$ is mapped to a singular quadric surface by a map of degree two, we can also think of quartic in $\mathbb{P}_{1,1,2}$ as a particular case of a complete intersection of quadric surfaces in $\mathbb{P}^3$. A divisor of degree three gives a projective cubic curve in $\mathbb{P}^2$. A divisor of degree four gives the complete intersection of two quadrics surfaces in $\mathbb{P}^3$.

In the string theory literature, an elliptic fibration whose generic fiber is a genus-one normal curve of degree $d = 1, 2, 3, 4$ is called a model of type E_{9-d} (we recall that E_5 is isomorphic to D_5) [6, 109, 196]. They are historically named after some del Pezzo surfaces in which they can be embedded as hyperplane divisors.

A del Pezzo surface is a smooth surface with an ample anticanonical divisor [278]. It follows that the anticanonical model of a del Pezzo surface is isomorphic to the del Pezzo surface. The degree of a del Pezzo surface is the square of its canonical class. In string theory, a del Pezzo surface of degree d is usually called a dP_{9-d}. If X is a del Pezzo surface of degree $d \geq 3$, then its anticanonical model is a smooth surface of degree d in $\mathbb{P}^d$. If X is a del Pezzo surface of degree one, then its anticanonical model is a hypersurface of degree six in the weighted projective space $\mathbb{P}_{1,1,2,3}$. If X is a del Pezzo surface of degree two, then its anticanonical model is a hypersurface of degree four in $\mathbb{P}_{1,1,2,3}$. A del Pezzo surface of degree eight is isomorphic to a quadratic Veronese embedding of a quadric in $\mathbb{P}^3$. A del Pezzo surface of degree $3 \leq d \leq 8$ is isomorphic to $\mathbb{P}^2$ blown up at $(9 - d)$ points in general position.

In the late 1960s, Manin discovered that a del Pezzo surface X of degree $d \leq 6$ is associated with a root system E_{9-d} [225]: the automorphism group of the incidence graph of the exceptional curves on X is the Weyl group $\mathrm{W}(\mathrm{E}_{9-d})$ of the Lie algebra of type E_{9-d}. By Bertini's theorem, a general

hyperplane section on a del Pezzo surface of degree d defines a smooth (normal) elliptic curve of degree d. Such an elliptic curve is said to be of type E_{9-d} when $d = 1, 2, 3, 4, 5$ [6, 109, 196].

Weierstrass model (E_8-type)	$y^2 = x^3 + fx + g$
Legendre family	$y^2 = x(x-1)(x-\lambda)$
Hesse family (E_6-type)	$x^3 + y^3 + 3\mu xy + 1 = 0$
Jacobi's quartic (E_7-type)	$y^2 = x^4 + 2\kappa x^2 + 1$
Jacobi's intersection (D_5-type)	$x^2 + y^2 - z^2 = kx^2 + w^2 - z^2 = 0$
Newton's cubic hyperbola (Q_7 type)	$yx^2 + Ax = By^3 + Cy^2 + Dy + E$

Table 7.2: Some classic families of elliptic curves. The Newton's cubic hyperbola is also than most of these curves but has not been used until recently in [120]. The Weierstrass model was also in Newton's list of cubics.

7.2.2 E_8, E_7, E_6, D_5, AND Q_7-MODELS

The model of type E_8 is the usual Weierstrass model [94, 246]. The E_8-model is often described in string theory by a curve of degree six in the weighted projective space $\mathbb{P}_{1,2,3}$, specially in toric constructions. The Weierstrass equation appears automatically in this form, but it has a major drawback as the ambient space has singularities which require much care, especially when doing intersection theory. In turn, we prefer using the projective bundle $\mathbb{P}[\mathscr{O}_B \oplus \mathscr{L}^{\otimes 2} \oplus \mathscr{L}^{\otimes 3}] \to B$ [114].

Models of type E_7, E_6, and $E_5 = D_5$ were first realized as hypersurfaces in weighted projective spaces [34, 39, 195, 196]. They were generalized to arbitrary bases by using projective bundles in [6, 109]. In [120], we introduced a new family modeled after Newton's cubic hyperbola generalizing the family introduced in [65]. Another generalization would be to consider elliptic surfaces whose generic fiber are defined as hypersurfaces in toric surfaces [61, 144, 197]. There are in total sixteen two dimensional reflexive polyhedra. By the adjunction theorem, each of them can define a genus

one curve as an anticanonical divisor.

For example, the generic equation of an elliptic fibration with Mordell–Weil group $\mathbb{Z}/2\mathbb{Z}$ has a singularity that has a crepant resolution defined by blowing up the point $x = y = 0$. This turns the $\mathbb{P}^2$-bundle $X_0 = \mathbb{P}(\mathscr{O}_B \oplus \mathscr{L}^{\otimes 2} \oplus \mathscr{L}^{\otimes 3})$ into a fibration of dP_1 surfaces. Interestingly, the discriminant locus has a fiber of type I_2, and therefore the gauge group is SO(3) as we have to take the quotient of SU(2) by a central $\mathbb{Z}/2\mathbb{Z}$.

1. The Weierstrass model is a zero scheme of a section of $\mathscr{O}(3) \otimes \pi^* \mathscr{L}^{\otimes 6}$ in $\mathbb{P}(\mathscr{O}_B \oplus \mathscr{L}^{\otimes 2} \oplus \mathscr{L}^{\otimes 3})$. This is the usual Weierstrass model given for example by Tate's form.

2. The elliptic fibration of type E_7 is a zero scheme of a section of $\mathscr{O}(4) \otimes \pi^* \mathscr{L}^{\otimes 4}$ in $\mathbb{P}_{1,1,2}(\mathscr{O}_B \oplus \mathscr{L} \oplus \mathscr{L}^{\otimes 2})$ [6]. Its generic fiber corresponds to a fiber of the Jacobi quartic. The elliptic fibration of type E_7 can be written as a zero scheme of a section of $\mathscr{O}(3) \otimes \pi^* \mathscr{L}^{\otimes 4}$ in $\mathbb{P}(\mathscr{O}_B \oplus \mathscr{L} \oplus \mathscr{L}^{\otimes 2})$ as proven in [65].

3. The elliptic fibration of type E_6 is a zero scheme of a section of $\mathscr{O}(3) \otimes \pi^* \mathscr{L}^{\otimes 3}$ in $\mathbb{P}(\mathscr{O}_B \oplus \mathscr{L} \oplus \mathscr{L})$ [6]. Its generic fiber has a triple section.

4. The elliptic fibration of type D_5 is a zero scheme of two sections of $\mathscr{O}(2) \otimes \pi^* \mathscr{L}^{\otimes 2}$ in $\mathbb{P}(\mathscr{O}_B \oplus \mathscr{L} \oplus \mathscr{L} \oplus \mathscr{L})$ [109]. Its generic fiber corresponds to a Jacobi complete intersection (Intersection of two quadrics in $\mathbb{P}^3$.

5. The elliptic fibration of type $Q_7(\mathscr{L}, \mathscr{M})$ is a zero scheme of a section of $\mathscr{O}(3) \otimes \pi^* \mathscr{L}^{\otimes 2} \otimes \pi^* \mathscr{M}$ in $\mathbb{P}(\mathscr{O}_B \oplus \mathscr{M} \oplus \mathscr{L}^{\otimes 2})$ [120]. Its generic fiber is of the type of "cubic hyperbola"

that appeared in Newton's classification of cubics. It extrapolates between the E_7' family (at $\mathscr{M} = \mathscr{L}^{\otimes 2}$) and the family introduced by Cacciatori, Cattaneo, and van Geemen in [65], which corresponds to $\mathscr{M} = \mathscr{O}_B$.

7.2.3 Newton's cubic hyperbola, Morrison-Park model, and the Q_7-model

Morrison and Park have popularized in the F-theory literature the Jacobian of an elliptic fibration of rank one [239]. The model is also well-known to number theorists since it corresponds to a genus-one normal curve of degree two in the special case where the degree-two divisor splits into two rational points without having to introduce a field extension. A smooth model sharing the same Jacobian appeared in the F-theory literature a year earlier in [65] where Cacciatori, Cattaneo, and Geemen studied tadpole cancellation conditions in the spirit of [5, 6] in a new projective bundle. The Morrison–Park model [239] matches the Jacobian of the new model of Cacciatori, Cattaneo, and Geemen [65] after the change of variables

$$c_0 \to -\frac{1}{6}c_0,\ c_1 \to -c_1,\ c_2 \to -6c_2,\ c_3 \to -36c_3,\ b \to 6\sqrt{6}b_2. \tag{7.2}$$

Both models can be traced directly to Newton's cubic hyperbola as explained in [120], as they can both be written as the following cubic hyperbola:

$$yx^2 + bz^2x = c_0y^3 + c_1y^2z + c_2yz^2 + c_3z^3. \tag{7.3}$$

We call this model a Q_7-model because the Newton's polygon of the defining equation is a quadrilateral with seven points on its boundary and a unique interior point (ensuring that it describes a curve of arithmetic genus one). This Newton's polygon is one of the sixteen reflexive polygons of degree one [28, 201]. Since the genus-one fibration has a rational section at $z = y = 0$, it is birational to a Weierstrass model, which can be determined using the results of [18]. The model of type $Q_7(\mathscr{L}, \mathscr{M})$ is a hypersurface in a projective bundle generalizing the elliptic fibration introduced in [65]. We introduce two line bundles $\mathscr{L}$ and $\mathscr{M}$ and define the ambient space as the projective bundle $X_0 = \mathbb{P}(\mathscr{O}_B \oplus \mathscr{M} \oplus \mathscr{L})$ [120]. We denote by $\mathscr{O}(1)$ the dual of the tautological line bundle of X_0. The projective coordinates $[z : y : x]$ are such that z, y, x are respectively sections of $\mathscr{O}(1)$, $\mathscr{O}(1) \otimes \mathscr{L}$, and $\mathscr{O}(1) \otimes \mathscr{M}$. The defining equation is a section of the line bundle $\mathscr{O}(3) \otimes \pi^* \mathscr{L}^{\otimes 2} \otimes \pi^* \mathscr{M}$. The coefficient c_i is a section of $\mathscr{L}^{\otimes 2} \otimes \mathscr{M}^{\otimes(-2+i)}$ and b is a section of $\mathscr{L} \otimes \mathscr{M}$. At $z = 0$, we also have the degree-two divisor $z = x^2 - c_0 y^2 = 0$. Thus, it follows from Riemann-Roch that the Q_7-model is also birational to a quartic model [120]. The quartic model can be derived by multiplying both side of the defining equation by y and introduce the new variable $u = xy$. This gives the quartic model

$$u(u + bz^2) = y(c_0 y^3 + c_1 y^2 z + c_2 y z^2 + c_3 z^3). \tag{7.4}$$

The variable u is a section of $\mathscr{O}(2) \otimes \pi^* \mathscr{L} \otimes \pi^* \mathscr{M}$. The ambient space is the weighted projective bundle $\pi : \mathbb{P}_{1,2,1}(\mathscr{O}_B \oplus \mathscr{U} \oplus \mathscr{L}) \longrightarrow B$ with $\mathscr{U} = \mathscr{L} \otimes \mathscr{M}$. The defining equation is a section of $\mathscr{O}(4) \otimes \pi^* \mathscr{U}^{\otimes 2}$. The quartic equation has double point singularities at $u = b = y = c_3 = 0$.

7.2.4 G-MODELS FOR $G = \mathrm{SO}(n)$ WITH $n = 3, 4, 5, 6$

The SO(3)-model is the generic case of a Weierstrass model with a $\mathbb{Z}/2\mathbb{Z}$ torsion [20]:

$$y^2 z = x(x^2 + a_2 xz + a_4 z^2). \tag{7.5}$$

There is a fiber of type I_2 over the generic point of $V(a_4)$. The Weierstrass models for the SO(3), SO(5), and SO(6)-models are summarized in Table 7.3.

The SO(5)-model is obtained from the SO(3)-model via a base change that converts the section a_4 to a perfect square $a_4 = t^2$ where t is a section of $\mathscr{L}^{\otimes 2}$. The generic fiber over the generic point of $V(t)$ is of type $\mathrm{I}_4^{\mathrm{ns}}$. Moreover, a_2 must be nonzero, otherwise the Mordell–Weil group becomes $\mathbb{Z}/2\mathbb{Z} \times \mathbb{Z}/2\mathbb{Z}$, which in turn implies $G = \mathrm{PSO}(5)$ rather than SO(5).

The SO(6)-model is subsequently derived from the SO(5)-model by requiring that the section a_2 is a perfect square modulo t so that the fiber type over $V(t)$ is of type $\mathrm{I}_4^{\mathrm{s}}$.

The SO(4)-model is defined by a collision of two Kodaira fibers with dual graph $\widetilde{\mathrm{A}}_1$ with a Mordell–Weil group $\mathbb{Z}/2\mathbb{Z}$ [118]. The simplest SO(4)-model is realized by III+III, the collision of two fibers of type III, in an elliptic fibration with a Mordell–Weil group $\mathbb{Z}/2\mathbb{Z}$. For all the possible realizations of SO(4)-models, see Table 7.3. We give a crepant resolution for each model in Table 7.9.

Group	Kodaira fibers	Mordell–Weil	Weierstrass model
SO(3)	$\mathrm{I}_2^{\mathrm{ns}}$, III	$\mathbb{Z}/2\mathbb{Z}$	$y^2z = x(x^2 + a_2xz + sz^2)$
SO(4)	$\mathrm{I}_2^{\mathrm{ns}} + \mathrm{I}_2^{\mathrm{ns}} \to \mathrm{I}_4^{\mathrm{ns}}$ $\mathrm{I}_2^{\mathrm{ns}} + \mathrm{I}_2^{\mathrm{s}} \to \mathrm{I}_4^{\mathrm{s}}$ $\mathrm{I}_2^{\mathrm{s}} + \mathrm{I}_2^{\mathrm{s}} \to \mathrm{I}_4^{\mathrm{s}}$ $\mathrm{III} + \mathrm{I}_2^{\mathrm{ns}} \to 1 - 2 - 1$ III+III $\to 1 - 2 - 1$	$\mathbb{Z}/2\mathbb{Z}$	$y^2z = x^3 + a_2x^2z + stxz^2$ $y^2z + a_1xyz = x^3 + \widetilde{a}_2tx^2z + stxz^2$ $y^2z + a_1xyz = x^3 + \widetilde{a}_2stx^2z + stxz^2$ $y^2z = x^3 + \widetilde{a}_2sx^2z + stxz^2$ $y^2z = x^3 + \widetilde{a}_2stx^2z + stxz^2$
SO(5)	$\mathrm{I}_4^{\mathrm{ns}}$	$\mathbb{Z}/2\mathbb{Z}$	$y^2z = x(x^2 + a_2xz + t^2z^2)$
SO(6)	$\mathrm{I}_4^{\mathrm{s}}$	$\mathbb{Z}/2\mathbb{Z}$	$y^2z + a_1yxz = x(x^2 + mtxz + t^2z^2)$ $m \neq 0, \pm 2$
PSU(3)	$\mathrm{I}_3^{\mathrm{s}}$	$\mathbb{Z}/3\mathbb{Z}$	$y^2z + a_1xyz + syz^2 = x^3$

Table 7.3: Weierstrass equations for the SO(n)-models for $n = 3, 4, 5, 6$ [118] and the PSU(3)-model [20]. For the SO(3)-model, the divisor supporting the group is $S = V(s)$, where s is a section of $\mathscr{L}^{\otimes 4}$. For the SO(5) and SO(6)-models, the divisor supporting the gauge group is $T = V(t)$, where t is a section of $\mathscr{L}^{\otimes 2}$. For SO(6), m is a constant number different from 0 and ± 2. For the SO(4)-model, the gauge group is semi-simple and we have two divisors $S = V(s)$ and $T = V(t)$, whose classes satisfy the relation $S + T = 4L$. For the PSU(3)-model, the divisor supporting the group is $S = V(s)$, where s is a section of $\mathscr{L}^{\otimes 3}$.

7.2.5 PSU(3)-model

The PSU(3)-model is the generic Weierstrass model with torsion $\mathbb{Z}/3\mathbb{Z}$ [20]:

$$y^2z + a_1xyz + syz^2 = x^3. \tag{7.6}$$

Its discriminant is

$$\Delta = \frac{1}{16}s^3(27s - a_1^3). \tag{7.7}$$

The model has a singular fiber of type $\mathrm{I}_3^{\mathrm{s}}$ over $V(s)$ where s is a smooth section of the line bundle $\mathscr{L}^{\otimes 3}$.

A crepant resolution is an embedded resolution defined by a sequence of blowups with smooth

centers. We denote the blowup $X_{i+1} \longrightarrow X_i$ along the ideal $(f_1, f_2, \ldots, f_n)$ with exceptional divisor E as:

$$X_i \xleftarrow{(f_1, \ldots, f_n | E)} X_{i+1} \ .$$

A crepant resolution of a PSU(3)-model is given by the following sequence of blowups

$$X_0 \xleftarrow{(x, y, s | e_1)} X_1 \xleftarrow{(y, e_1 | e_2)} X_2. \tag{7.8}$$

7.3 Pushforward theorems

In this section, we prove the pushforward theorems that are the heart of our computations.

Theorem 7.3.1 (Fullwood, [134]). *Let $\mathscr{L}$ be a line bundle over a variety B. We denote the first Chern class of $\mathscr{L}$ by $L = c_1(\mathscr{L})$. We define a vector bundle $\mathscr{E} = \mathscr{O}_B \oplus \cdots \oplus \mathscr{L}^{r_n}$ of rank $n+1$ and the projective bundle of lines $\pi : X_0 = \mathbb{P}(\mathscr{E}) \longrightarrow B$. We denote by $\mathscr{O}_{X_0}(1)$ the dual of the tautological line of $\mathbb{P}(\mathscr{E})$. The first Chern class of $\mathscr{O}_{X_0}(1)$ is $c_1(\mathscr{O}_{X_0}(1)) = H$. We assume that the rational fraction expansion of $\frac{1}{c(\mathscr{E})} = \prod_{i=1}^{n} \frac{1}{(1+r_i L)}$ is*

$$\frac{1}{c(\mathscr{E})} = \sum_{i=1}^{m} \sum_{j=1}^{n_i} q_{ij} \frac{1}{(1 + r_i L)^j}. \tag{7.9}$$

Let $F = \pi^* F_0 + \pi^* F_1 H + \pi^* F_2 H^2 + \cdots$ be an analytic function of H with F_i in the Chow ring of B.

Then

$$\pi_*(F) = \sum_{i=1}^{m}\sum_{j=1}^{n_i} q_{ij}\frac{1}{(j-1)!}\frac{d^{j-1}}{dH^{j-1}}\Big[\frac{1}{H^{n-j}}(F - F_0 - F_1H - \cdots - F_{n-1}H^{n-1})\Big]\Big|_{H=-r_iL}. \quad (7.10)$$

Theorem 7.3.2. *Given the projective bundle $\pi : X_0 = \mathbb{P}(\mathscr{O}_B \oplus \mathscr{L} \oplus \mathscr{L}^{\otimes 2} \oplus \mathscr{L}^{\otimes 2}) \to B$, we denoting the first Chern class of $\mathscr{L}$ by L and the first Chern class of the dual of the tautological line bundle of π by H. We have*

$$\begin{aligned}\pi_*F(H) = &\Big(\frac{F - F_0 - F_1H - F_2H^2}{H^3}\Big)\Big|_{H=-L} - 2\Big(\frac{F - F_0 - F_1H - F_2H^2}{H^3}\Big)\Big|_{H=-2L}\\ &+ \partial_H\Big(\frac{F - F_0 - F_1H - F_2H^2}{H^2}\Big)\Big|_{H=-2L}.\end{aligned} \quad (7.11)$$

In particular,

$$\begin{cases}\pi_*1 = 0, \quad \pi_*H = 0, \quad \pi_*H = 0, \quad \pi_*H^2 = 0, \quad \pi_*H^3 = 1,\\ \pi_*H^4 = -5L, \quad \pi_*H^5 = 17L^2, \quad \pi_*H^6 = -49L^3, \quad \pi_*H^7 = 129L^4, \quad H^7 = -321L^5,\\ H^{3+k} = (-L)^k - 2(-2L)^k - (k+1)(-2L)^k.\end{cases} \quad (7.12)$$

Proof. We use Theorem 7.3.1 with the partial fraction decomposition :

$$\frac{1}{(1+L)(1+2L)^2} = \frac{1}{1+L} - \frac{2}{1+2L} + \frac{2}{(1+2L)^2}.$$

The first few terms and the generic term can be computed directly as follows

$$\begin{aligned}\frac{1}{(1+L)(1+2L)^2} &= \frac{1}{1+L} - \frac{2}{1+2L} - \partial_L\Big(\frac{1}{1+2L}\Big)\\ &= \sum_{k=0}^{\infty}\Big((-L)^k - 2(-2L)^k - 2(k+1)(-2L)^k\Big)\\ &= 1 - 5L + 17L^2 - 49L^3 + 129L^4 - 321L^5 + 769L^6 + \cdots.\end{aligned}$$

□

Theorem 7.3.3. *Given the projective bundle $\pi : X_0 = \mathbb{P}(\mathscr{O}_B \oplus \mathscr{L} \oplus \mathscr{L}^{\otimes 2}) \to B$. Denoting the first Chern class of $\mathscr{L}$ by L and the first Chern class of the dual of the tautological line bundle of π by H, we have:*

$$\pi_* F(H) = -\Big(\frac{F - F_0 - F_1 H}{H^2}\Big)\Big|_{H=-L} + 2\Big(\frac{F - F_0 - F_1 H}{H^2}\Big)\Big|_{H=-2L}. \tag{7.13}$$

In particular,

$$\begin{cases}\pi_* 1 = 0, \quad \pi_* H = 0, \quad \pi_* H^2 = 1,\\ \pi_* H^3 = -3L, \quad \pi_* H^4 = +7L^2, \quad \pi_* H^5 = -15L^3, \quad \pi_* H^6 = +31L^4, \quad \pi_* H^7 = -63L^5,\\ \pi_* H^{k+2} = -(-L)^k + 2(-2L)^k \quad (k > 0).\end{cases} \tag{7.14}$$

Proof. We use Theorem 7.3.1 with the partial fraction decomposition:

$$\begin{aligned}\frac{1}{(1+L)(1+2L)} &= -\frac{1}{1+L}+\frac{2}{1+2L}\\ &= \sum_{k=0}^{\infty}\Big(-(-L)^k+2(-2L)^k\Big)\\ &= 1-3L+7L^2-15L^3+31L^4-63L^5+127L^6+\cdots.\end{aligned}$$

□

Theorem 7.3.4. *Given the projective bundle $\pi : X_0 = \mathbb{P}(\mathscr{O}_B \oplus \mathscr{L} \oplus \mathscr{L}) \to B$. Denoting the first Chern class of $\mathscr{L}$ by L and the first Chern class of the dual of the tautological line bundle of π by H, we have:*

$$\pi_* F = \Big(\partial_L \frac{F - F_0 - F_1 H}{H^2}\Big)\Big|_{H=-L}. \tag{7.15}$$

In particular, we have

$$\begin{cases} \pi_* 1 = 0, \quad \pi_* H = 0, \quad \pi_* H^2 = 1, \\ \pi_* H^3 = -2L, \quad \pi_* H^4 = +3L^2, \quad \pi_* H^5 = -4L^3, \quad \pi_* H^6 = +5L^4, \quad \pi_* H^7 = -6L^5, \\ \pi_* H^{k+2} = (k+1)(-L)^k \quad (k > 0). \end{cases} \tag{7.16}$$

Proof. The result for $\pi_* F$ follows directly from Theorem 7.3.1. We can compute the first few terms

by the following expansion:

$$\begin{aligned}\frac{1}{(1+L)^2} &= -\partial_L \frac{1}{1+L} = -\partial_L\Big(\sum_{k=0}^{\infty}(-L)^k\Big)\\ &= 1 - 2L + 3L^2 - 4L^3 + 5L^4 - 6L^5 + 7L^6 + \cdots .\end{aligned}$$

□

Theorem 7.3.5. *Given the projective bundle $\pi : X_0 = \mathbb{P}(\mathscr{O}_B \oplus \mathscr{L} \oplus \mathscr{L} \oplus \mathscr{L}) \to B$. Denoting the first Chern class of $\mathscr{L}$ by L and the first Chern class of the dual of the tautological line bundle of π by H, we have:*

$$\pi_* F = \frac{1}{2}\Big(\partial_L^2 \frac{F - F_0 - F_1 H - F_2 H^2}{H}\Big)_{H=-L}. \tag{7.17}$$

In particular, we have,

$$\begin{cases} \pi_* 1 = 0, \quad \pi_* H = 0, \quad \pi_* H^2 = 0, \quad \pi_* H^3 = 1 \\ \pi_* H^4 = -3L, \quad \pi_* H^4 = +6L^2, \quad \pi_* H^5 = -10L^3, \quad \pi_* H^6 = 15L^4, \quad \pi_* H^7 = -21L^5, \\ \pi_* H^{k+3} = \frac{1}{2}(k+1)(k+2)(-L)^k \quad (k > 0). \end{cases} \tag{7.18}$$

Proof. The result for $\pi_* F$ follows directly from Theorem 7.3.1. We can compute the first few terms

by the following expansion:

$$\frac{1}{(1+L)^3} = \frac{1}{2}\partial_L^2 \frac{1}{(1+L)} = \frac{1}{2}\partial_L^2 \sum_{k=0}^{\infty}(-L)^k$$
$$= 1 - 3L + 6L^2 - 10L^3 + 15L^4 - 21L^5 + 28L^6 + \cdots .$$

□

7.4 Collection of results

The theorem 6.1.1 gives the behaviors of intersection numbers involving Chern and Pontryagin classes of dimension too small to give Chern or Pontryagin numbers [116]. To give a number, they must be multiplied by an element of the Chow ring of appropriate dimension.

Corollary. *Let $\phi : Y \longrightarrow B$ be an elliptic fibration given by the crepant resolution of a singular Weierstrass model of dimension n with fundamental line bundle $\mathscr{L}$. Then,*

$$\int_Y c_1(TY)^{n-1}c_2(TY) = 12\int_B (c_1 - L)^{n-1}L. \tag{7.19}$$

Below are tables summarizing all the results.

The E_8, E_7, E_6, D_5, and Q_7-models are considered in Tables 7.4–7.8. The pushforwards of the third Chern classes are given in Table 7.4, the Chern numbers of the elliptically-fibered fourfolds are given in Table 7.5, the holomorphic genera of the fourfolds are given in Table 7.6, the Pontryagin numbers are given in Table 7.7, and the Hirzebruch signatures σ, the A-genus $\hat{A}_2$, and the curvature

invariants X_8 are given in Table 7.8.

The G-models for $G = \mathrm{SO}(n)$ for $n = 3, 4, 5, 6$ and $G = \mathrm{PSU}(3)$ are considered in Tables 7.9–7.14. The sequence of blowups used to describe a crepant resolution for each G-model is summarized in Table 7.9, the pushforwards of the third Chern classes are given in Table 7.10, the Chern numbers of the elliptically-fibered fourfolds are given in Table 7.11, the holomorphic genera of the fourfolds are given in Table 7.12, the Pontryagin numbers are given in Table 7.13, and the Hirzebruch signatures σ, the A-genus $\hat{A}_2$, and the curvature invariants X_8 are given in Table 7.14.

Type	$\phi_*\left(c_3(TY)[Y]\right)$
Q_7	$6\left(2c_1L - 6L^2 + LS - S^2\right)$
D_5	$4L(3c_1 - 7L)$
E_6	$12L(c_1 - 3L)$
E_7	$12L(c_1 - 4L)$
E_8	$12L(c_1 - 6L)$

Table 7.4: Chern numbers after pushforwards to the base. The divisor S appears in the definition of the Q_7-model, $L = c_1(\mathscr{L})$, and c_i denotes the ith Chern class of the base of the fibration.

Type	$c_1^4(TY)$	$c_1^2(TY)c_2(TY)$	$c_2^2(TY)$	$c_1(TY)c_3(TY)$	$c_4(TY)$
Q_7	0	$12L(c_1-L)^2$	$2(12c_2L-12c_1L^2+22L^3)$ $-2S(5L^2-8LS+S^2)$	$6L(c_1-L)(2c_1-6L)$ $+6S(c_1-L)(L-S)$	$6L(2c_2-6c_1L+16L^2)$ $+6LS(c_1-6L)$ $-6S^2(c_1-9L)-6S^3$
D_5	0	$12L(c_1-L)^2$	$12L(2c_2-2c_1L+3L^2)$	$4L(c_1-L)(3c_1-7L)$	$4L(3c_2-7c_1L+16L^2)$
E_6	0	$12L(c_1-L)^2$	$24L(c_2-c_1L+2L^2)$	$12L(c_1-L)(c_1-3L)$	$12L(c_2-3c_1L+9L^2)$
E_7	0	$12L(c_1-L)^2$	$24L(c_2-c_1L+3L^2)$	$12L(c_1-L)(c_1-4L)$	$12L(c_2-4c_1L+16L^2)$
E_8	0	$12L(c_1-L)^2$	$24L(c_2-c_1L+6L^2)$	$12L(c_1-6L)(c_1-L)$	$12L(c_2-6c_1L+36L^2)$

Table 7.5: Chern numbers of elliptically-fibered fourfolds obtained from crepant resolutions of Tate's models. We abuse notation and omit the degree $\int$ in the entries of the table. The divisor S appears in the definition of the Q_7-model, $L=c_1(\mathscr{L})$, and c_i denotes the ith Chern class of the base of the fibration.

Type	χ_0	χ_1	χ_2
Q_7	$\frac{1}{12}L\left(c_1^2-3c_1L+c_2+2L^2\right)$	$-\frac{1}{3}L\left(2c_1^2-27c_1L+5c_2+55L^2\right)$ $-\frac{1}{2}LS(3c_1-13L)$ $+\frac{1}{2}S^2(3c_1-19L)+S^3$	$-\frac{1}{2}L\left(3c_1^2+35c_1L-17c_2-118L^2\right)$ $+LS(3c_1-23L)$ $-3S^2(c_1-35L)-4S^3$
D_5	$\frac{1}{12}L\left(c_1^2-3c_1L+c_2+2L^2\right)$	$-\frac{1}{3}L\left(2c_1^2-21c_1L+5c_2+37L^2\right)$	$\frac{1}{2}L\left(-3c_1^2-27c_1L+17c_2+78L^2\right)$
E_6	$\frac{1}{12}L\left(c_1^2-3c_1L+c_2+2L^2\right)$	$-\frac{1}{3}L\left(2c_1^2-27c_1L+5c_2+61L^2\right)$	$\frac{1}{2}L\left(-3c_1^2-35c_1L+17c_2+134L^2\right)$
E_7	$\frac{1}{12}L\left(c_1^2-3c_1L+c_2+2L^2\right)$	$-\frac{1}{3}L\left(2c_1^2-36c_1L+5c_2+106L^2\right)$	$\frac{1}{2}L\left(-3c_1^2-47c_1L+17c_2+242L^2\right)$
E_8	$\frac{1}{12}L\left(c_1^2-3c_1L+c_2+2L^2\right)$	$-\frac{1}{3}L\left(2c_1^2-54c_1L+5c_2+232L^2\right)$	$\frac{1}{2}L\left(-3c_1^2-71c_1L+17c_2+554L^2\right)$

Table 7.6: Holomorphic genera. To ease the notation, we omit the degree $\int$ in the entries of the table. The divisor S appears in the definition of the Q_7-model, $L=c_1(\mathscr{L})$, and c_i denotes the ith Chern class of the base of the fibration. The holomorphic Euler characteristic $\chi_0(Y)$ is equal to $\chi_0(W,\mathscr{O}_W)$ where W is the divisor defined by $\mathscr{L}$ in the base.

Type	$\int_Y p_2(TY)$	$\int_Y p_1^2(TY)$
Q_7	$4L\left(-6c_1^2+12c_2+41L^2\right)$ $-14S\left(5L^2-8LS+S^2\right)$	$16L(-3c_1^2+6c_2+8L^2)$ $-8S(5L^2-8LS+S^2)$
D_5	$12L\left(-2c_1^2+4c_2+9L^2\right)$	$48L\left(-c_1^2+2c_2+2L^2\right)$
E_6	$24L\left(-c_1^2+2c_2+8L^2\right)$	$48L\left(-c_1^2+2c_2+3L^2\right)$
E_7	$24L\left(-c_1^2+2c_2+15L^2\right)$	$48L\left(-c_1^2+2c_2+5L^2\right)$
E_8	$24L(-c_1^2+2c_2+36L^2)$	$48L(-c_1^2+2c_2+11L^2)$

Table 7.7: Pontryagin numbers. To ease the notation, we omit the degree $\int$ in the entries of the table. The divisor S appears in the definition of the Q_7-model, $L=c_1(\mathscr{L})$, and c_i denotes the ith Chern class of the base of the fibration.

Type	$192X_8=\int_Y(p_1^2-4p_2)$	$45\sigma=45\int_Y L_2=\int_Y(7p_2-p_1^2)$	$5760\int_Y\hat{\mathrm{A}}_2=\int_Y(7p_1^2-4p_2)$
Q_7	$48(c_1^2L-2c_2L-11L^3)$ $+48S(5L^2-8LS+S^2)$	$60L(-2c_1^2+4c_2+17L^2)$ $-90S(5L^2-8LS+S^2)$	$240L\left(-c_1^2+2c_2+L^2\right)$
D_5	$48L\left(c_1^2-2c_2-7L^2\right)$	$60L\left(-2c_1^2+4c_2+11L^2\right)$	$240L\left(-c_1^2+2c_2+L^2\right)$
E_6	$48L\left(c_1^2-2c_2-13L^2\right)$	$120L\left(-c_1^2+2c_2+10L^2\right)$	$240L\left(-c_1^2+2c_2+L^2\right)$
E_7	$48L\left(c_1^2-2c_2-25L^2\right)$	$120L\left(-c_1^2+2c_2+19L^2\right)$	$240L\left(-c_1^2+2c_2+L^2\right)$
E_8	$48L\left(c_1^2-2c_2-61L^2\right)$	$120L\left(-c_1^2+2c_2+46L^2\right)$	$240L\left(-c_1^2+2c_2+L^2\right)$

Table 7.8: Characteristic invariants: the anomaly invariant X_8, the signature σ, and the index of the $\hat{\mathrm{A}}$-genus. To ease the notation, we abuse notation and omit the degree $\int$ in the entries of the table. The divisor S appears in the definition of the Q_7-model, $L=c_1(\mathscr{L})$, and c_i denotes the ith Chern class of the base of the fibration.

Group	Fiber Type	Crepant Resolution
$\mathrm{SO}(3)$	$\mathrm{I}_2^{\mathrm{ns}},\ \mathrm{III}$	$X_0 \xleftarrow{(x,y\|e_1)} X_1$
$\mathrm{PSU}(3)$	$\mathrm{I}_3^{\mathrm{s}}$	$X_0 \xleftarrow{(x,y,s\|e_1)} X_1 \xleftarrow{(y,e_1\|e_2)} X_2$
$\mathrm{SO}(4)$	$\mathrm{I}_2^{\mathrm{ns}}+\mathrm{I}_2^{\mathrm{s}}$ $\mathrm{I}_2^{\mathrm{s}}+\mathrm{I}_2^{\mathrm{s}}$ $\mathrm{III}+\mathrm{I}_2^{\mathrm{ns}}$ $\mathrm{III}+\mathrm{I}_2^{\mathrm{s}}$ $\mathrm{III}+\mathrm{III}$	$X_0 \xleftarrow{(x,y,s\|e_1)} X_1 \xleftarrow{(x,y,t\|w_1)} X_2$
$\mathrm{SO}(5)$	$\mathrm{I}_4^{\mathrm{ns}}$	$X_0 \xleftarrow{(x,y,s\|e_1)} X_1 \xleftarrow{(x,y,e_1\|e_2)} X_2$
$\mathrm{SO}(6)$	$\mathrm{I}_4^{\mathrm{s}}$	$X_0 \xleftarrow{(x,y,s\|e_1)} X_1 \xleftarrow{(y,e_1\|e_2)} X_2 \xleftarrow{(x,e_2\|e_3)} X_3$

Table 7.9: The blowup centers of the crepant resolutions. The variable s and t is a section of the line bundles $\mathscr{O}_B(S)$ and $\mathscr{O}_B(T)$. The SO(4)-model has reducible Kodaira fibers supported on smooth divisors of classes T and $S = 4L - T$. For the notation, see Section 7.2.5.

Algebra	Mordell–Weil	G	Kodaira	$\phi_*\left(c_3(TY)[Y]\right)$
A_1	$\mathbb{Z}_2$	$SO(3)$	I_2^{ns}, III	$12L(c_1 - 4L)$
A_2	$\mathbb{Z}_3$	$PSU(3)$	I_3^s	$12L(c_1 - 3L)$
$A_1 + A_1$	$\mathbb{Z}_2$	$SO(4)$	$I_2^{ns} + I_2^s$ $I_2^s + I_2^s$ $III + I_2^{ns}$ $III + I_2^s$ $III + III$	$12L(c_1 - 4L) + 16LT - 4T^2$
B_2	$\mathbb{Z}_2$	$SO(5)$	I_4^{ns}	$4L(3c_1 - 8L)$
A_3	$\mathbb{Z}_2$	$SO(6)$	I_4^s	$12L(c_1 - 2L)$

Table 7.10: Chern numbers after pushforwards to the base. The SO(4)-model has reducible Kodaira fibers supported on smooth divisors of classes T and $S = 4L - T$. By definition, $L = c_1(\mathscr{L})$ and c_i denotes the ith Chern class of the base of the fibration.

Type	$c_1^4(TY)$	$c_1^2(TY)c_2(TY)$	$c_2^2(TY)$	$c_1(TY)c_3(TY)$	$c_4(TY)$
SO(3)	0	$12L(c_1-L)^2$	$24L(c_2-c_1L+3L^2)$	$12L(c_1-L)(c_1-4L)$	$12L(c_2-4c_1L+16L^2)$
PSU(3)	0	$12L(c_1-L)^2$	$24L(c_2-c_1L+2L^2)$	$12L(c_1-3L)(c_1-L)$	$12L(c_2-3c_1L+9L^2)$
SO(4)	0	$12L(c_1-L)^2$	$24L(c_2-c_1L+3L^2)$ $-32L^2T+8LT^2$	$12L(c_1-L)(c_1-4L)$ $+16T(c_1-L)(L-4T)$	$12L(c_2-4c_1L+16L^2)$ $-4T(c_1-7L)(T-4L)$
SO(5)	0	$12L(c_1-L)^2$	$8L(3c_2-3c_1L+5L^2)$	$4L(c_1-L)(3c_1-8L)$	$4L(3c_2-8c_1L+20L^2)$
SO(6)	0	$12L(c_1-L)^2$	$8L(3c_2+4L^2-3c_1L)$	$12L(c_1-L)(c_1-2L)$	$12L(c_2-2c_1+4L^2)$

Table 7.11: Chern numbers of elliptically-fibered fourfolds obtained from crepant resolutions of Tate's models. We abuse notation and omit the degree $\int$ in the entries of the table. The SO(4)-model has reducible Kodaira fibers supported on smooth divisors of classes T and $S = 4L - T$. By definition, $L = c_1(\mathscr{L})$ and c_i denotes the ith Chern class of the base of the fibration.

Type	χ_0	χ_1	χ_2
SO(3)	$\frac{1}{12}L(c_1^2+c_2-3c_1L+2L^2)$	$-\frac{1}{3}L(2c_1^2+5c_2-36c_1L+106L^2)$	$\frac{1}{2}L(-3c_1^2+17c_2-47c_1L+242L^2)$
PSU(3)	$\frac{1}{12}L(c_1^2+c_2-3c_1L+2L^2)$	$-\frac{1}{3}L(2c_1^2+5c_2-27c_1L+61L^2)$	$\frac{1}{2}L(-3c_1^2+17c_2-35c_1L+134L^2)$
SO(4)	$\frac{1}{12}L(c_1^2+c_2-3c_1L+2L^2)$	$-\frac{1}{3}L(2c_1^2+5c_2-36c_1L+106L^2)$ $-T(c_1-5L)(4L-T)$	$-\frac{1}{2}L(3c_1^2-17c_2+47c_1L-242L^2)$ $+2T(c_1-9L)(4L-T)$
SO(5)	$\frac{1}{12}L\,(c_1^2-3c_1L+c_2+2L^2)$	$-\frac{1}{3}L\,(2c_1^2-24c_1L+5c_2+46L^2)$	$-\frac{1}{2}L\,(3c_1^2+31c_1L-17c_2-98L^2)$
SO(6)	$\frac{1}{12}L\,(c_1^2-3c_1L+c_2+2L^2)$	$-\frac{1}{3}L\,(2c_1^2-18c_1L+5c_2+28L^2)$	$-\frac{1}{2}L\,(3c_1^2+23c_1L-17c_2-58L^2)$

Table 7.12: Holomorphic genera. To ease the notation, we omit the degree $\int$ in the entries of the table. The SO(4)-model has reducible Kodaira fibers supported on smooth divisors of classes T and $S = 4L - T$. By definition, $L = c_1(\mathscr{L})$ and c_i denotes the ith Chern class of the base of the fibration. The holomorphic Euler characteristic $\chi_0(Y)$ is equal to $\chi_0(W, \mathscr{O}_W)$ where W is the divisor defined by $\mathscr{L}$ in the base.

Type	$\int_Y p_2(TY)$	$\int_Y p_1^2(TY)$
SO(3)	$24L(-c_1^2+2c_2+15L^2)$	$48L(-c_1^2+2c_2+5L^2)$
PSU(3)	$24L(-c_1^2+2c_2+8L^2)$	$48L(-c_1^2+2c_2+3L^2)$
SO(4)	$24L(-c_1^2+2c_2+15L^2)-56LT(4L-T)$	$48L(-c_1^2+2c_2+5L^2)-32LT(4L-T)$
SO(5)	$8L\left(-3c_1^2+6c_2+17L^2\right)$	$16L\left(-3c_1^2+6c_2+7L^2\right)$
SO(6)	$8L\left(-3c_1^2+6c_2+10L^2\right)$	$16L\left(-3c_1^2+6c_2+5L^2\right)$

Table 7.13: Pontryagin numbers. To ease the notation, we omit the degree $\int$ in the entries of the table. The SO(4)-model has reducible Kodaira fibers supported on smooth divisors of classes T and $S=4L-T$. By definition, $L=c_1(\mathscr{L})$ and c_i denotes the ith Chern class of the base of the fibration.

Type	$192X_8=\int_Y(p_1^2-4p_2)$	$45\sigma=45\int_Y L_2=\int_Y(7p_2-p_1^2)$	$5760\int_Y\hat{\mathrm{A}}_2=\int_Y(7p_1^2-4p_2)$
SO(3)	$48L(c_1^2-2c_2-25L^2)$	$120L(-c_1^2+2c_2+19L^2)$	$240L(-c_1^2+2c_2+L^2)$
PSU(3)	$48L(c_1^2-2c_2-13L^2)$	$120L(-c_1^2+2c_2+10L^2)$	$240L(-c_1^2+2c_2+L^2)$
SO(4)	$48L(c_1^2-2c_2-25L^2)$ $+192LT(4L-T)$	$120L(-c_1^2+2c_2+19L^2)$ $-360LT(4L-T)$	$240L(-c_1^2+2c_2+L^2)$
SO(5)	$-48L\left(-c_1^2+2c_2+9L^2\right)$	$120L\left(-c_1^2+2c_2+7L^2\right)$	$240L(-c_1^2+2c_2+L^2)$
SO(6)	$-48L\left(-c_1^2+2c_2+5L^2\right)$	$120L\left(-c_1^2+2c_2+4L^2\right)$	$240L(-c_1^2+2c_2+L^2)$

Table 7.14: Characteristic invariants: the anomaly invariant X_8, the signature σ, and the index of the $\hat{\mathrm{A}}$-genus. To ease the notation, we abuse notation and omit the degree $\int$ in the entries of the table. The SO(4)-model has reducible Kodaira fibers supported on smooth divisors of classes T and $S=4L-T$. By definition, $L=c_1(\mathscr{L})$ and c_i denotes the ith Chern class of the base of the fibration.

Part IV

Geometric Perspective on 5d/6d Supergravity Theories with Simple Gauge Groups

Introduction

A classical problem in the study of elliptic fibrations is understanding the geometry of the crepant resolutions of Weierstrass models and their flop transitions [9, 129]. The constructions of G-models are deeply connected to the classification of singular fibers of Weierstrass models and provide an interesting scene to explore higher dimensional elliptic fibrations with a view inspired by their applications to physics. The framework of G-models naturally includes a geometric formulation of basic notions of representation theory such as the theory of root systems and weights of representations. The data characterizing a G-model can be understood in the framework of gauge theories, which provides a natural language to talk about the geometry of these elliptic fibrations. F-theory enables a description of gauge theories in string theory and M-theory via geometric engineering based on elliptic fibrations [37, 243, 244, 292]. The data of a gauge theory that can be extracted from an elliptic fibration are its Lie algebra, its Lie group, and the set of irreducible representations defining how charged particles transform under the action of the gauge group.

In F-theory, the Lie algebra is determined by the dual graphs of the fibers over the generic points of the irreducible components of the discriminant locus of the elliptic fibration. The Mordell–Weil group of the elliptic fibration is conjectured to be isomorphic to the first homotopy group of the gauge group [90]. Hence, the Lie group depends on both the singular fibers and the Mordell–Weil group of the elliptic fibration. In F-theory, the singular fibers responsible for non-simply laced Lie algebras are not affine Dynkin diagrams, but twisted affine Dynkin diagrams, as presented in Figure 8.1 and Table 2.4, respectively, on pages 324 and 78. These twisted affine Dynkin diagrams are the

Dynkin duals of the corresponding affine Dynkin diagrams. The Dynkin dual of a Dynkin diagram is obtained by inverting all the arrows. In the language of Cartan matrices, two Dynkin diagrams are dual to each other if their Cartan matrices are transposes of each other. The Langlands duality interchanges B_n and C_n, but preserves all the other simple Lie algebras. For affine Dynkin diagrams, only the ADE series are preserved under the Langlands duality. In particular, the Langlands duals of $\widetilde{\mathrm{B}}_n$, $\widetilde{\mathrm{C}}_n$, $\widetilde{\mathrm{G}}_2$, and $\widetilde{\mathrm{F}}_4$ are respectively denoted in the notation of Carter as $\widetilde{\mathrm{B}}_n^t$, $\widetilde{\mathrm{C}}_n^t$, $\widetilde{\mathrm{G}}_2^t$, and $\widetilde{\mathrm{F}}_4^t$.

The purpose of the Chapter 8 is to study the geometry of F_4-models. We define an F_4-model as an elliptic fibration over a smooth variety of dimension two or higher such that the singular fiber over the generic point of a chosen irreducible Cartier divisor S is of type $\mathrm{IV}^{*\mathrm{ns}}$, and the fibers are irreducible (smooth elliptic curves, type II or type I_1) away from S. Such an F_4-model is realized by a crepant resolution of a Weierstrass model, whose coefficients have valuations with respect to S, matching the generic case of Step 8 of Tate's algorithm. An F_4-model can is always birational to a singular short Weierstrass equation whose singularities are due to the valuations $v_S(c_4) \geq 3$ and $v_S(c_6) = 4$ of its coefficients. Such a singular Weierstrass equation can be traced back to Néron's seminal paper [251] where it corresponds to type c6.

The goal of the Chapter 9 is to study the geometry of crepant resolutions of Weierstrass models corresponding to Step 6 of Tate's algorithm [290]. Such a Weierstrass model has a discriminant locus Δ containing a nonsingular and irreducible divisor S of the base B such that the geometric fiber over the generic point of S is of Kodaira type I_0^*, whose dual graph is the affine Dynkin diagram of type $\widetilde{\mathrm{D}}_4$. The divisor S appears with multiplicity six in the discriminant Δ and the remainder of the discriminant $\Delta' = \Delta S^{-6}$ is typically singular. The Kodaira fibers over generic points of Δ' are of

type I_1 and the two divisors S and Δ' do not intersect transversally. At the intersection of S and Δ', we have a "collision of singularities"[1] of type $\mathrm{I}_1+\mathrm{I}_0^*$ yielding non-Kodaira fibers whose structures are explained in detail in later sections. Such a collision is not allowed in Miranda's models since the fiber I_1 has an infinite j-invariant while I_0^* can only take finite values for its j-invariant.

From its application to F-theory and its M-theory dual, we have computed the number of hypermltiplets in five and six-dimensional theories with eight supercharges. As a byproduct, we see that the models we consider from the Kodaira type I_0^* can have "*frozen*" representations. We have found on the conditions when we have frozen representations for all cases in Section 9.6.2.

[1]When two irreducible components Δ_1 and Δ_2 of the discriminant locus intersect, if we denote by T_1 and T_2 the Kodaira type of their respective generic fibers, their intersection is called a collision of singularity of type $T_1 \quad + \quad T_2$. The collision is said to be transverse when Δ_1 and Δ_2 intersect transversally. The type of the generic fiber over their intersection is usually not one of the Kodaira type. The possible types are classified for Miranda's models [236, 286], which are regularizations of Weierstrass models that gives flat elliptic fibrations such that the j-invariant is a morphism. Miranda's models only allow transverse collisions.

There is geometry in the humming of the strings.

Pythagoras

8

The Geometry of F_4-Models

One of the major achievements of F-theory is the geometric engineering of exceptional Lie groups. These elliptic fibrations play an essential role in the study of superconformal field theories even in absence of a Lagrangian description. The study of non-simply laced Lie algebras in F-theory started in May of 1996 during the second string revolution with a paper of Aspinwall and Gross [19], followed shortly afterwards by the classic F-theory paper of Bershadsky, Intriligator, Kachru, Morrison,

Sadov, and Vafa [37]. M-theory compactifications giving rise to non-simply laced gauge groups are studied in [97, 112, 119, 176].

In this chapter, we study the geometry of F_4-models, namely, G-models with $G = \mathrm{F}_4$. F_4 is a simply connected and non-simply laced Lie group with an exceptional simple Lie algebra of rank 4 and dimension 52. Aspects of the physics of F_4-models in M-theory and F-theory are studied in [37, 47, 91, 97, 114, 123, 156, 296].

8.1 Summary of results

8.1.1 F_4-models: definition and first properties

An F_4-model is mathematically constructed as follows. Let B be a smooth projective variety of dimension two or higher. Let S be an effective Cartier divisor in B defined as the zero scheme of a section s of a line bundle $\mathscr{S}$. Since S is smooth, the residue field of its generic point is a discrete valuation ring. We denote the valuation with respect to S as v_S. An F_4-model is defined by the crepant resolution of the following Weierstrass model

$$y^2z = x^3 + s^{3+\alpha}a_{4,3+\alpha}xz^2 + s^4a_{6,4}z^3, \quad \alpha \in \mathbb{Z}_{\geq 0}, \tag{8.1}$$

where $v_S(a_{6,4}) = 0$, and either $v_S(a_{4,3+\alpha}) = 0$ or $a_{4,3+\alpha} = 0$. We assume that $a_{6,4}$ is generic; in particular, $a_{6,4}$ is not a perfect square modulo s. This ensures that the generic fiber is of type IV$^{*\mathrm{ns}}$ rather than IV$^{*\mathrm{s}}$.

The defining equation (8.1) is of type (c6) in Néron's classification of minimal Weierstrass models, defined over a perfect residue field of characteristic different from 2 and 3 [251]. This corresponds to Step 8 of Tate's algorithm [290]. Hence, the geometric fiber over the generic point of S is of Kodaira type IV*. As discussed earlier, the generic fiber over S has a dual graph that is the twisted Dynkin diagram $\widetilde{\mathrm{F}}_4^t$ see Figure 8.1, which is the Langlands dual of the affine Dynkin diagram $\widetilde{\mathrm{F}}_4$. The structure of the generic fiber of the F_4-model is due to the arithmetic restriction that $a_{6,4}$ is not a perfect square modulo s.

The innocent arithmetic condition which characterizes an F_4-model has surprisingly deep topological implications for the elliptic fibration [114, 116]. When $a_{6,4}$ is a perfect square modulo s, the elliptic fibration is called an E_6-model; the generic fiber $\mathrm{IV}^{*\mathrm{ns}}$ is replaced by the fiber $\mathrm{IV}^{*\mathrm{s}}$ whose dual graph is the affine Dynkin diagram $\widetilde{\mathrm{E}}_6$. Both E_6-models and F_4-models share the same geometric fiber over the generic point of S; however, the generic fiber type is different. Both are characterized by Step 8 of Tate's algorithm, but while the generic fiber of an E_6-model is already made of geometrically irreducible components, the generic fiber of an F_4-model requires a quadratic field extension to make all its components geometrically irreducible. The Weierstrass model of an E_6-model has more complicated singularities, and thus requires a more involved crepant resolution. In a sense, the F_4-model is a more rigid version of the E_6-model as some fibral divisors are glued together by the arithmetic condition on $a_{6,4}$. Both have a fiber of Kodaira type IV*, but F_4 is the generic case while E_6 is a special case of a fiber of type IV* since the Weierstrass coefficients have to satisfy additional algebraic constraints. It follows from the Shioda-Tate-Wazir theorem [300] that the Picard number of an E_6-model is bigger than the one for an F_4-model. Furthermore, their Poincaré-Euler charac-

teristics are also different, as was recently analyzed in [114]. A crepant resolution of the Weierstrass model of an E_6-model has fourteen distinct minimal models [163], while that of an F_4-model has only one [110, Theorem 1.27]. An F_4-model is a flat elliptic fibration, while this is not the case for an E_6-model of dimension four or higher, as certain fibers over codimension-three points contain rational surfaces [209].

The discriminant locus of the elliptic fibration (8.1) is

$$\Delta = s^8(4s^{1+3\alpha}a_{4,3+\alpha}^3 + 27a_{6,4}^2).$$

The discriminant is composed of two irreducible components not intersecting transversally. The first one is the divisor S, and the fiber above its generic point is of type $\mathrm{IV}^{*\mathrm{ns}}$. The second component is a singular divisor, and the fiber over its generic point is a nodal curve, i.e. a Kodaira fiber of type I_1. The fiber I_1 degenerates to a cuspidal curve over $a_{4,3+\alpha} = a_{6,4} = 0$. The two components of the discriminant locus collide at $s = a_{6,4} = 0$, where we expect the singular fiber $\mathrm{IV}^{*\mathrm{ns}}$ to degenerate, further producing a non-Kodaira fiber.

8.1.2 Representations associated to an F_4-model and absence of flops

To determine the irreducible representations associated with a given G-model, we adopt the approach of Aspinwall and Gross [19], which is deeply rooted in geometry. The representation associated to a G-model is characterized by its weights, which are geometrically given by the intersection numbers, with a negative sign, of the fibral divisors with curves appearing over codimension-two

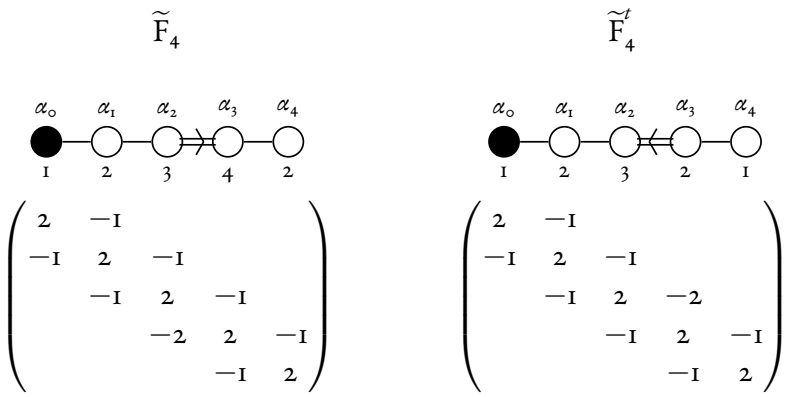

Figure 8.1: Affine Dynkin diagram $\widetilde{F}_4$ vs. twisted affine Dynkin diagram $\widetilde{F}_4^t$. Their Cartan matrices are transposes of each other. Since the matrices are not symmetric, taking the transpose means inverting the arrow of the Dynkin diagram and changing the multiplicities of the nodes. These matrices have rank four and therefore a kernel of dimension one. The normalization of the zero direction in terms of relatively prime integers gives the multiplicities of the nodes of the Dynkin diagram. In the notation of Kac, $\widetilde{F}_4^t$ is denoted as $\widetilde{E}_6^{(2)}$ and $\widetilde{F}_4$ is denoted as $\widetilde{F}_4$, or sometimes $\widetilde{E}_6^{(1)}$. The dual graph that appears in the theory of elliptic fibration is $\widetilde{F}_4^t$ and never $\widetilde{F}_4$

loci over which the generic fiber $\mathrm{IV}^{*\mathrm{ns}}$ degenerates. This approach, also used in [1, 176, 226] and closely related to the approach of [241], transcends its application to physics and allows an intrinsic determination of a representation for any G-model. For more information, see [112, 119]. The representation induced by the weights of vertical curves over codimension-two points is not always physical as it is possible that no hypermultiplet is charged under that representation. In such a case, the representation is said to be "frozen" as discussed in section 8.7.3.

For F_4-models, we find that over $V(s, a_{6,4})$, the fiber $\mathrm{IV}^{*\mathrm{ns}}$ degenerates to a non-Kodaira fiber of type $1 - 2 - 3 - 4 - 2$. This fiber consists of a chain of rational curves intersecting transversally; each number gives the multiplicity of the corresponding rational curve. We refer to this non-Kodaira fiber by the symbol $\mathrm{IV}^*_{(2)}$. The last two nodes, of multiplicities 4 and 2, have weights in the representation 26 of F_4, namely $\boxed{0\ -1\ 2\ -1}$ and $\boxed{0\ 0\ -1\ 2}$ as illustrated in Figure 8.3 on page 350. The

representation 26 is a quasi-minuscule fundamental representation comprised of two zero weights and 24 non-zero weights that form a unique Weyl orbit. The possibility of flops between different crepant resolutions of the same singular Weierstrass model can be explained by the relative minimal model program [228]. All the weights of the 26 are (short) roots of F_4. This explains why there is only one chamber for F_4 with matter in the adjoint representation and the fundamental representation.

For each non-simply laced Lie algebra $\mathfrak{g}_o$, there is a specific quasi-minuscule representation $\mathbf{R}_o$ defined by the branching rule $\mathfrak{g} = \mathfrak{g}_o \oplus \mathbf{R}_o$, where $\mathfrak{g}_o$ is defined by a folding of $\mathfrak{g}$ of degree d. The degree d is the ratio of the squared lengths of long roots and short roots of $\mathbf{R}_o$. In other words, except for G_2, for which $d = 3$, all other non-simply laced Lie algebras have $d = 2$. This branching rule is related to the arithmetic degeneration $K^{\mathrm{ns}} \to K^{\mathrm{s}}$, where K is a Kodaira fiber. For F_4, we have $\mathrm{E}_6 = \mathrm{F}_4 \oplus 26$, and the representation $\mathbf{R}_o$ coincides with the representation 26 we find by computing weights of the curves over $V(s, a_{6,4})$. We note that fiber geometry over $V(s, a_{6,4})$ does not produce a fiber enhancement related to E_6 or more precisely to a Kodaira fiber of type $\mathrm{IV}^{*\mathrm{ns}}$. We discuss more geometrically inspired branching rule in the next subsection.

8.1.3 Arithmetic versus geometric degenerations

Given an elliptic fibration $\phi : Y \to B$, if S is an irreducible component of the discriminant locus, the generic fiber over S can degenerate further over subvarieties of S. We distinguish between two types of degenerations [112]. A degeneration is said to be *arithmetic* if it modifies the type of the fiber without changing the type of the geometric fiber. A degeneration is said to be *geometric* if it

modifies the geometric type of the fiber.

Example 8.1.1 (Arithmetic degeneration)**.** Let K be a Kodaira fiber. Then, $K^{\text{ns}} \to K^{\text{s}}$ or $K^{\text{ns}} \to K^{\text{ss}}$ are arithmetic degenerations.

Example 8.1.2 (Geometric degeneration)**.** Let K be a Kodaira fiber. Consider the non-split fiber K^{ns}. Denote by $K_{(d)}$ the non-Kodaira fibers defined in the limit where d non-split curves of K^{ns} coincide. Then the fiber $K^{\text{ns}} \to K_{(d)}$ is a geometric degeneration.

Arithmetic degenerations and geometric degenerations are respectively responsible for non-localized and localized matter in physics. For example, in the case of an F_4-model over a base of dimension three or higher, we have the degeneration $\text{IV}^{*\text{ns}} \to \text{IV}^{*\text{s}}$ over the intersection of S with any double cover of $a_{6,4}$ as it is clear from the explicit resolution of singularities. Such a double cover has equation $\zeta^2 = a_{6,4}$ where ζ is a section of $\mathscr{L}^{\otimes 3} \otimes \mathscr{S}^{\otimes 2}$. We can have such an arithmetic degeneration over any point of S away from $V(s, a_{6,4})$.

In the case of an F_4-model, we get a fiber of type $1-2-3-4-2$, which is of the type $\text{IV}^*_{(2)}$ discussed in Example 8.1.2. The geometry of the fiber shows explicitly that localized matter fields at $V(s, a_{6,4})$ are in the representation 26 and do not come from an enhancement $\text{F}_4 \to \text{E}_6$. That is because over the locus $V(s, a_{6,4})$, the generic fiber is the non-Kodaira fiber $1-2-3-4-2$. Such a fiber can only be seen as the result of an enhancement of type $\text{IV}^{*\text{ns}}$ (F_4) to either an incomplete III^* (E_7) or an incomplete II^* (E_8), depending on the valuation of the Weierstrass coefficient a_4. We have either the enhancement $\text{F}_4 \longrightarrow \text{E}_7$ if $v(a_4) = 3$, or $\text{F}_4 \longrightarrow \text{E}_8$ if $v(a_4) \geq 4$.[1]

[1]The fiber $1-2-3-4-2$ also appears in Miranda's models at the transverse collision II+IV* where it is presented as a contraction of a fiber of type II^* (E_8), see Table 14.1 on page 130 of [236].

8.1.4 Branching rules and Katz-Vafa method for localized matter in an F_4-model

The Katz-Vafa method [187] is an intuitive way to determine under which representations charged matter fields transform in F-theory. The Katz-Vafa method does not always predict the correct matter content in F-theory as discussed for example in the case of the $SU(2)\times G_2$-model [119]. For this reason, we prefer to determine the representation associated to an elliptic fibration by computing the weights of rational curves appearing over codimension-two points. This is formalized in [112] using the notion of *saturated set of weights* and applied systematically in [113, 115, 118, 119, 121].

The branching rule discussed in [142, 143], namely,

$$E_6 \to F_4 : 78 = 52 \oplus 26, \tag{8.2}$$

is geometrically appropriate to understand the non-localized matter since it corresponds to F_4 enhancing to E_6. However, it is at odds with the structure of the fiber for the localized matter. In the case of a F_4-model, as discussed in the previous subsection, over $V(s, a_{6,4})$, the degenerated fiber is an incomplete fiber of type III* whose dual graph is the affine Dynkin diagram of type $\widetilde{E}_7$ with some nodes contracted. Our goal in this subsection is to provide a branching rule inspired by the geometry of the fiber appearing over the locus where localized matter fields appear in an F_4-model.

Since F_4 is not a maximal subalgebra of E_7, we consider a sequence of maximal subalgebras. Look-

ing at Dynkin's classification of maximal subalgebras of E_7, there are two roads to consider:

$$E_7 \to E_6 \oplus \mathfrak{u}_1 \to F_4 \quad \text{or} \quad E_7 \to A_1 \oplus F_4 \to F_4. \tag{8.3}$$

We note that both roads involving a S-maximal subalgebras ($E_6 \to F_4$ and $E_7 \to A_1 \oplus F_4$). To assess the final representations, the relevant branching rules are [233]:

$$E_7 \to E_6 \oplus \mathfrak{u}_1 \quad : \quad 133 = 27_2 \oplus \overline{27}_{-2} \oplus 78_0 \oplus 1_0, \tag{8.4}$$

$$E_6 \to F_4 \quad : \quad 78 = 52 \oplus 26 \oplus 1, \quad 27 = 26 \oplus 1, \quad \overline{27} = 26 \oplus 1, \tag{8.5}$$

$$E_7 \to A_1 \oplus F_4 \quad : \quad 133 = (3,1) \oplus (1,52) \oplus (3,26). \tag{8.6}$$

In both cases ($E_7 \to E_6 \oplus \mathfrak{u}_1 \to F_4$ or $E_7 \to A_1 \oplus F_4 \to F_4$), we end up with the branching rule:

$$E_7 \to F_4 : \quad 133 = 52 \oplus 26 \oplus 26 \oplus 26 \oplus 1 \oplus 1 \oplus 1, \tag{8.7}$$

which signals matter in the adjoint (52) and the fundamental representation (26) of F_4. The multiplicity observed (three times the fundamental representation) does not give the number of hypermultiplets observed. As we explain in the next subsection, we determine the number of hypermultiplets in an M-theory compactification to $5d$ by comparing the triple intersection numbers and the prepotential and in an F-theory compactification to $6d$ we determine the number of charged hypermultiplets transforming in given representations by solving the local anomaly cancelation con-

ditions.

8.1.5 Counting hypermultiplets: Witten's genus formula

M-theory compactified on an elliptically-fibered Calabi–Yau threefold Y gives rise to a five-dimensional supergravity theory with eight supercharges coupled to $h^{2,1}(Y) + 1$ neutral hypermultiplets and $h^{1,1}(Y) - 1$ vector multiplets [66]. Taking into account the graviphoton, there are a total of $h^{1,1}(Y)$ gauge fields. The kinetic terms, the Chern–Simons coefficients of the vector multiplets, and the graviphoton are all completely determined by the intersection ring of the Calabi–Yau variety.

As it is written in detail in Section 2.12.2 in the introduction, Witten has determined using a quantization argument that the number of hypermultiplets transforming in the adjoint representation is the genus of the curve S over which the gauge group is localized [306]. Aspinwall, Katz, and Morrison subsequently applied Witten's quantization argument to the case of non-simply laced groups in [1], which is known as the Witten's genus formula:

$$n_{\mathbf{R}_0} = (d-1)\Big(g-1\Big) + \frac{1}{2}\deg R, \tag{8.8}$$

g is the genus of S.

For an F_4-model, $\mathbf{R}_0 = 26$, the ramification locus R is $V(s, a_{6,4})$, and its degree is

$$\deg R = 12(1-g) + 2S^2.$$

Hence, by Witten's argument, we expect for a generic F_4-model the following multiplicities:

$$n_{52} = g, \quad n_{26} = 5(1-g) + S^2.$$

We later derive in Theorem 8.7.2 the number of matter representations from a direct comparison of the triple intersection numbers and the one-loop prepotential of a five-dimensional gauge theory with eight supercharges [176]. This matches exactly the number n_{26} derived by Witten's genus formula. This provides a confirmation of the number of charged hypermultiplets from a purely five-dimensional point of view, thereby avoiding a six-dimensional argument based on cancellations of anomalies [142] and the subtleties of the Kaluza-Klein circle compactification [46, 149]. We further check that the number $n_{26} = 5(1-g) + S^2$ and $n_{52} = g$ are also the unique solution for the number of charged hypermultiplets derived from six-dimensional anomaly cancellation conditions when F-theory is compactified on an F_4-model that is a Calabi–Yau threefold with a base B that is a rational surface.

Deriving the number of charged hypermultiplets in $\mathcal{N} = 1$ five-dimensional theories by comparing the triple intersection numbers and the one-loop contribution to the prepotential was advocated in [124, 148] and has been used in [124] for SU(n); in [112] for Spin(7), Spin(8), G_2 models; in [122] for the E_7-model; in [118] for SO(4) and Spin(4); in [119] for SU(2)$\times$ G_2 in [119]; in [113] for SU(2)$\times$SU(3); and in [121] for SU(2)$\times$ SU(4) and SU(2)$\times$ Sp(4).

8.1.6 Frozen representations

As we have explained before, we identify representations by their weights, and we compute the weights geometrically by the intersection of fibral divisors with vertical curves located over codimension-two points on the base. It is important to keep in mind that the presence of a given weight is a necessary condition but not a sufficient condition for the existence of hypermultiplets transforming under the corresponding representation. We always have to keep in mind that the geometric representations deduced by the weights of vertical curves over codimension-two points are not necessarily carried by physical states. A representation **R** deduced geometrically on an elliptic fibration is said to be *frozen* when the elliptic fibration has vertical curves (over a codimension-two locus of the base) carrying the weights of the representation **R**, but no hypermultiplet is charged under the representation **R**.

It is known that the adjoint representation is frozen when the gauge group is on a curve of genus zero [306]. However, it is less appreciated that other representations can also be frozen. A natural candidate is the representation $\mathbf{R}_0$ discussed in Section 8.1.5 for the case of a non-simply laced gauge group. (See Section 2.12.2 for more detail.) We will discuss the existence of a frozen representation for an F_4-model in §8.7.3. In particular, Theorem 8.7.5 asserts that the representation 26 is frozen if and only if the curve S has genus zero and self-intersection -5.

It is a folklore theorem of D-brane model building that the number of representations appearing at the transverse collision of two branes is the number of collision points. In other words, one would expect one hypermultiplet for each intersection points. While this is true for localized matter

fields, it is not usually true when the same representation appears both as localized and non-localized. As a rule of thumb, when localized and non-localized matter fields transforming in the same representation coexist, the number of representations is given by assuming that all the matter is non-localized [240].

The notion of frozen representation discussed in this chapter should not be confused with the frozen singularities of ref. [21, 90, 287].

8.1.7 Roadmap of results

The road map to the rest of the chapter is the following.

In section 8.2, we discuss Step 8 of Tate's algorithm, which characterizes the Weierstrass model of F_4-models.

In section 8.3 (see Theorem 8.3.2 on page 338), we present a crepant resolution of the singular Weierstrass model, giving a flat fibration. The resolution is given by a sequence of four blowups with centers that are regular monomial ideals.

In section 8.4, we analyze in details the degeneration of the singular fiber and determine the geometry of the fibral divisors (see Theorem 8.4.1 on page 345 and Figure 8.2 on page 344). The generic fiber over S degenerates along $V(a_{6,4}) \cap S$ to produce a non-Kodaira fiber of type $1-2-3-4-2$. This non-Kodaira fiber appears as an incomplete Kodaira fiber of type III* or II* resulting from the (non-transverse) collision of the divisor S with the remaining factor of the discriminant locus. Such a collision is not of Miranda-type since it involves two fibers of different j-invariants[236]. Interestingly, the multiplicity of the nodes of this non-Kodaira fibers matches the Dynkin's coefficients

of the highest root of F_4, namely $(1, 2, 3, 4, 2)$ where the first component of multiplicity one corresponds to the affine node.

We show that the fibral divisors D_3 and D_4 corresponding to the root α_3 and α_4 of the F_4 Dynkin diagram are **not** $\mathbb{P}^1$-bundles over the divisor S, but rather double covers of $\mathbb{P}^1$-bundles over S, with ramification locus $V(a_{6,4})$. The geometry of these fibral divisors is illustrated in Figure 8.2. The difference is important since it affects the computation of triple intersection numbers and the degeneration of the fibers in codimension two, which is responsible for the appearance of weights of the representation 26. We use the Stein factorization to have more control on the geometry of D_3 and D_4. Consider the morphism $f : D_3 \to S$. The geometric generic fiber is not connected and consists of two rational curves. Since the morphism is proper, we consider its Stein factorization $D_3 \xrightarrow{f'} S' \xrightarrow{\pi} S$. By definition, the morphism $\pi : S' \to S$ is a finite map of degree two; each geometric point of the fiber represents a connected component of the fiber of $D_3 \to S$. The morphism $f' : D_3 \to S'$ has connected fibers that are all smooth rational curves. Hence, $f' : D_3 \to S'$ gives D_3 the structure of a $\mathbb{P}^1$-bundle over S' rather than over S.

We determine in Section 8.4.3 the geometric weights that identify the representation naturally associated to the degeneration of the generic fiber over the codimension-two loci. The last two nodes of the fiber $1 - 2 - 3 - 4 - 2$ are responsible for generating the representation 26.

In section 8.5, we compute the following topological invariants: the Euler characteristic of the elliptic fibration, the Hodge numbers in the Calabi–Yau threefold case, the double and triple intersection numbers of the fibral divisors (Theorem 8.4.2 on page 347), and the linear form induced in the Chow ring by the second Chern class in the case of a Calabi threefold. To have a complete list of

known results on F_4, in Table 8.3, we reproduce the characteristic numbers of an F_4-model that is an elliptic fourfold as computed in [116]. We note that the F_4-model shares the same characteristic numbers as aSpin(8)-model since they are both computed using the same sequence of blowups and as proven in [116], they are flop invariant and therefore can be computed in any crepant resolution of a Spin(8)-model. Various characteristic classes were computed for F_4-models and Spin(8)-models in Table 8.3.

In section 8.7, we leverage our understanding of the geometry to study aspects of the physics of F_4-gauge theories in different dimensions. When M-theory is computed in a Calabi–Yau threefold Y that is an F4-model, we get a five-dimensional theory with charged hypermultiplets transforming in the adjoint and the fundamental representation. We compute the number of charged hypermultiplets in the adjoint and fundamental representations by matching the five-dimensional quantum prepotential computed at the one-loop level in [176] and the triple intersection numbers that we compute using intersection theory in presence after a sequence of blowups. F-theory compactified on the same Calabi–Yau threefold Y gives a six-dimensional (1,0) theories with neutral tensor multiplets and neutral hypermultiplets counted by the Hodge numbers of Y.

We compute the number of charged hypermultiplets of the 6d theory as a unique solution of the 6d anomaly cancellation conditions. The two independent countings in 5d and 6d perfectly match: this can be interpreted as a consistency check that the 5d theory has a six-dimensional parent theory.

Finally, in Section 8.7.3 we discuss in detail the existence of frozen representations for an F_4-model.

8.2 Step 8 of Tate's algorithm

We follow the notation of Fulton [136]. The terminology is borrowed from [114]. Let $Y_0 \longrightarrow B$ be a Weierstrass model over a smooth base B, in which we choose a smooth Cartier divisor $S \subset B$. The local ring $\mathcal{O}_{B,\eta}$ in B of the generic point η of S is a discrete valuation ring with valuation v_S given by the multiplicity along S. Using Tate's algorithm, the valuation of the coefficients of the Weierstrass model with respect to v_S determines the type of the singular fiber over the generic point of S. Kodaira fibers refer to the type of the geometric fiber over the generic point of irreducible components of the discriminant locus of the Weierstrass model.

An F_4-model describes the generic case of Step 8 of Tate's algorithm, which characterizes the Kodaira fiber of type IV^{*ns} in F-theory notation or IV_2^* in the notation of Liu. By definition, Kodaira fibers classify geometric fibers over the generic point of a component of the discriminant locus of an elliptic fibration. When the elliptic fibration is given by a Weierstrass model, this can be expressed in the language of a discrete valuation ring. Let S be the relevant component. We assume that S is smooth with generic point η. The local ring at η defines a discrete valuation ring with valuation v that is essentially the multiplicity along S. We then have the following characterization:

Theorem 8.2.1 (Tate's algorithm [290], Step 8). *If $v(a_1) \geq 1$, $v(a_2) \geq 2$, $v(a_3) \geq 2$, $v(a_4) \geq 3$, $v(a_6) \geq 4$ and the quadric polynomial $Q(T) = T^2 + a_{3,2}T - a_{6,4}$ has two distinct solutions, then the geometric special fiber is of Kodaira type IV^*. If the roots of $Q(T)$ are rational in the residue field, the generic fiber is of type IV^{*s}, otherwise (if the solutions are not rational in the residue field) the generic fiber is of type IV^{*ns}.*

Remark 8.2.2. The discriminant of the quadric $Q(T) = T^2 + a_{3,2}T - a_{6,4}$, is exactly $b_{6,4}$. It follows that the fiber is of type IV* if and only if $v(b_{6,4}) = 0$. Moreover, the fiber is of either type IV^{*s} or IV^{*ns}, depending respectively on whether or not $b_{6,4}$ is a perfect square.

In view of the multiplicities, we can safely complete the square in y and the cube in x and write the Tate equation of a IV^{*ns} model as

$$y^2z = x^3 + a_{4,3+\alpha}s^{3+\alpha}xz^2 + s^4a_{6,4}z^3, \quad \alpha \in \mathbb{Z}_{\geq 0},$$

where $a_{6,4}$ is **not** a perfect square modulo s.

The simplest way to identify a fiber of type IV^{*ns} is to use the short Weierstrass equation since it does not require performing any translation.

Theorem 8.2.3 (Tate's algorithm[290], Step 8)**.**

$$\begin{cases} v(c_4) \geq 3, \quad v(c_6) = 4 \\ c_6 \quad \textit{not a square modulo } s \end{cases} \iff IV^{*ns}.$$

The conditions on c_4 and c_6 can be traced back to Néron and forces the discriminant to have valuation 8. Néron also points out that a fiber of type IV* is uniquely identified by the valuation of its j-invariant and its discriminant locus:

Theorem 8.2.4 (Néron [251])**.** $v(j) > 0 \quad \textit{and} \quad v(\Delta) = 8 \iff IV^*$.

This implies in particular that a fiber of type IV* has a vanishing j-invariant.

8.3 The crepant resolution

Let $X_0 = \mathbb{P}[\mathscr{O}_B \oplus \mathscr{L}^{\otimes 2} \oplus \mathscr{L}^{\otimes 3}]$ be the projective bundle in which the singular Weierstrass model is defined as a hypersurface. The tautological line bundle of the projective bundle X_0 is denoted $\mathscr{O}(-1)$ and its dual $\mathscr{O}(1)$ has first Chern class $H = c_1\big(\mathscr{O}(1)\big)$.

Let X be a nonsingular variety. Let $Z \subset X$ be a complete intersection defined by the transverse intersection of r hypersurfaces $Z_i = V(g_i)$, where g_i is a section of the line bundle $\mathscr{I}_i$ and $(g_1, \cdots, g_r)$ is a regular sequence. We denote the blowup of a nonsingular variety X along the complete intersection Z by

$$X \xleftarrow{(g_1, \cdots, g_r | e_1)} \widetilde{X}.$$

The blowup of X with center Z is the morphism $f : \widetilde{X} = \mathbf{Proj}_X(\oplus_d \mathscr{I}^d) \to X$. The exceptional divisor of f is the pre-image of the center Z, that is, $\widetilde{Z} = \mathbf{Proj}_X(\oplus_d \mathscr{I}^d / \mathscr{I}^{d+1})$. The exceptional divisor is f-relatively ample. If Z is a complete intersection, then $\mathscr{I}/\mathscr{I}^2$ is locally free. Hence, $\mathbf{Sym}^d(\mathscr{I}/\mathscr{I}^2) = \mathscr{I}^d/\mathscr{I}^{d+1}$ and $\widetilde{Z} = \mathbb{P}_X(\mathscr{I}/\mathscr{I}^2)$. The normal sheaf $N_{\widetilde{Z}|\widetilde{X}}$ is $\mathscr{O}_{\widetilde{Z}}(-1)$, $E_1 = c_1(\mathscr{O}_{\widetilde{Z}}(1))$ is the first Chern class of the exceptional divisor $\widetilde{Z} = V(e_1)$, and $[\widetilde{Z}] = E_1 \cap [\widetilde{X}]$.

We abuse notation and use the same symbols for x, y, s, e_i and their successive proper transforms. We also do not write the obvious pullbacks.

Lemma 8.3.1. *Let $Z \subset X$ be a smooth complete intersection of $n+1$ hypersurfaces meeting transversally. Let Y be a hypersurface in X singular along Z. If Y has multiplicity n along Z, then the blowup of X along Z restricts to a crepant morphism $\overline{Y} \longrightarrow Y$ for the proper transform of Y.*

Proof. Let $\widetilde{X} = Bl_Z X$ be the blowup of X along Z and E be the class of the exceptional divisor. Then $c_1(TX) = f^* c_1(TX) - nE$. Since Y has a multiplicity n along Z, we have $f^* Y = \overline{Y} + nE$, where $\overline{Y}$ is the proper transform of Y. By adjunction formula,

$$c_1(\overline{Y}) = c_1(\widetilde{X}) - \overline{Y} = f^* c_1(X) - f^* Y = f^* c_1(Y).$$

□

Theorem 8.3.2. *Consider the following Weierstrass equation where $S = V(s)$ is a Cartier divisor of the base B:*

$$\mathscr{E}_0 : \quad y^2 z = x^3 + s^{3+\alpha} f x z^2 + s^4 g z^3, \quad \alpha \in \mathbb{Z}_{\geq 0},$$

where f, g, and s are respectively assumed to be generic sections of $\mathscr{L}^{\otimes 4} \otimes \mathscr{S}^{-\otimes(3+\alpha)}$, $\mathscr{L}^{\otimes 6} \otimes \mathscr{S}^{-\otimes 4}$, and $\mathscr{S}$. Let $X_0 = \mathbb{P}_B[\mathscr{O}_B \oplus \mathscr{L}^{\otimes 2} \oplus \mathscr{L}^{\otimes 3}]$ be the ambient space in which $\mathscr{E}_0$ is defined. The following sequence of blowups provides a crepant resolution of the singular Weierstrass model $\mathscr{E}_0$:

$$X_0 \xleftarrow{(x,y,s|e_1)} X_1 \xleftarrow{(y,e_1|e_2)} X_2 \xleftarrow{(x,e_2|e_3)} X_3 \xleftarrow{(e_2,e_3|e_4)} X_4. \tag{8.9}$$

We describe this sequence of blowups starting with the projective bundle X_0, which serves as the ambient space of the Weierstrass equation. The first blowup $X_1 \longrightarrow X_0$ is centered at the regular monomial ideal (x, y, s), where s is a section of $\mathscr{S} = \mathscr{O}_B(S)$. The exceptional divisor E_1 of the first blowup is a

$\mathbb{P}^2$ *bundle. The second blowup* $X_2 \longrightarrow X_1$*, parametrized by* $[x : s]$*, is centered along the fiber of* E_1 *defined by the proper transform of* $V(y)$ *and its exceptional divisor is* E_2*. The third blowup* $X_3 \longrightarrow X_2$ *is centered in* E_2 *along the fiber over* $V(x)$ *and has exceptional divisor* E_3*. The last blowup* $X_4 \longrightarrow X_3$ *is centered in* E_3 *along the fiber given by* $V(e_2)$ *and has exceptional divisor* E_4*.*

Proof. We recall that blowup up of a divisor is an isomorphism away from the singular locus. The Weierstrass model has a singular scheme supported on the ideal (x, y, s).

1. *First blowup.* Since the generic point of this ideal is a double point singularity of the Weierstrass model and the ideal has length 3, blowing up (x, y, s) is a crepant morphism.

2. *Second blowup.* We are in X_1 and the singular locus is supported on (y, x, e_1). At this point, we could choose to blowup again (x, y, e_1) since it is a locus of double points and the ideal has length 3. However, we could also blowup (y, e_1), which is a non-Cartier Weil divisor. This is clearly crepant since (y, e_1) has length 2 and multiplicity one. Blowing up this divisor is not an isomorphism since it contains (x, y, e_1), the support of the singular locus.

3. *Third blowup.* We blowup the ideal (x, e_2), which corresponds to a non-Cartier Weil divisor of multiplicity one.

4. *Fourth blowup.* We finally blowup (e_2, e_3), which is also a non-Cartier Weil divisor of multiplicity one. This is crepant because the ideal has length 2 and the defining equation has multiplicity one along (e_2, e_3).

After the fourth blowup, we check using the Jacobian criterion that there are no singularities

left. We can also simplify computations by noticing that the defining equation is a double cover and therefore, the singularities should be on the branch locus. Moreover, certain variables cannot vanish at the same time due to the centers of the blowups. In particular, each of (x, y, s), (y, e_1), (s, e_3), (s, e_4), (x, e_2), (x, e_4), and (e_2, e_3) corresponds to the empty set in X_4. □

The divisor classes of the different variables in X_i are given in Table 8.1.

	x	y	z	s	e_1	e_2	e_3	e_4
X_0	$2L + H$	$3L + H$	H	S	-	-	-	-
X_1	$2L + H - E_1$	$3L + H - E_1$	H	$S - E_1$	E_1	-	-	-
X_2	$2L + H - E_1$	$3L + H - E_1 - E_2$	H	$S - E_1$	$E_1 - E_2$	E_2	-	-
X_3	$2L + H - E_1 - E_3$	$3L + H - E_1 - E_2$	H	$S - E_1$	$E_1 - E_2$	$E_2 - E_3$	E_3	-
X_4	$2L + H - E_1 - E_3$	$3L + H - E_1 - E_2$	H	$S - E_1$	$E_1 - E_2$	$E_2 - E_3 - E_4$	$E_3 - E_4$	E_4

Table 8.1: The divisor classes of the variables $x, y, z, s, e_1, e_2, e_3$, and e_4 in X_i where X_0 is is the projective bundle and $i = 1, 2, 3, 4$ is the number of the blowups performed.

The proper transform of the Weierstrass model is a smooth elliptic fibration $\phi : Y \longrightarrow B$

$$Y : e_2 y^2 z = e_1(e_3^2 e_4 x^3 + e_1 e_2 e_3 (e_1 e_2 e_3 e_4^2)^{\alpha} s^{3+\alpha} a_{4,3+\alpha} x z^2 + e_1 e_2 s^4 a_{6,4} z^3).$$

The successive relative "projective coordinates" for the fibers of X_i over X_{i-1} are $(i = 1, 2, 3, 4)$

$$[e_1 e_2 e_3^2 e_4^3 x : e_1 e_2^2 e_3^2 e_4^4 y : z],\ [e_3 e_4 x : e_2 e_3 e_4^2 y : s], [y : e_1],\ [x : e_2 e_4],\ [e_2 : e_3]. \tag{8.10}$$

These projective coordinates are not independent of each other, as we have a tower of projective

bundles defined over subvarieties of projective bundles. The interdependence between the different projective bundles are captured by the following scalings:

$$\begin{aligned}
X_0/B &\quad [e_1e_2e_3^2e_4^3x : e_1e_2^2e_3^2e_4^4y : z] \\
X_1/X_0 &\quad [\ell_1(e_3e_4x) : \ell_1(e_3e_4^2e_2y) : \ell_1 s] \\
X_2/X_1 &\quad [\ell_1\ell_2 y : \ell_1^{-1}\ell_2 e_1] \\
X_3/X_2 &\quad [\ell_1\ell_3 x : \ell_2^{-1}\ell_3(e_2e_4)] \\
X_4/X_3 &\quad [\ell_4\ell_3\ell_2^{-1}e_2 : \ell_4\ell_3^{-1}e_3]
\end{aligned}$$

where ℓ_1, ℓ_2, ℓ_3, and ℓ_4 are used to denote the scalings of each blowup.

8.4 Fiber structure

In this section, we explore the geometry of the crepant resolution $Y \to \mathscr{E}_0$ obtained in the previous section. Composing with the projection of $\mathscr{E}_0$ to the base B, we have a surjective morphism $\phi : Y \to B$, which is an elliptic fibration over B. We denote by η a generic point of S. We study in details the generic fiber Y_η of the elliptic fibration and its specialization. Its dual graph is the twisted Dynkin diagram $\widetilde{F}_4^t$, namely, the dual of the affine Dynkin diagram $\tilde{F}_4$. We call C_a the irreducible components of the generic fiber, and D_a the irreducible fibral divisors. We can think of C_a as the generic fiber of D_a over S. Given a section u of a line bundle, we denote by $V(u)$ the vanishing scheme of u. As a set of point, $V(u)$ is defined by the equation $u = 0$. If $\mathcal{I}$ is an ideal sheaf, we also denote by $V(\mathcal{I})$ its zero scheme.

8.4.1 Structure of the generic fiber

After the blowup, the generic fiber over S is composed of five curves since the total transform of s is $se_1e_2e_3e_4^2$. The fibral divisors are:

$$\begin{cases} D_0: & s = e_2y^2 - e_1e_3^2e_4x^3 = 0 \\ D_1: & e_1 = e_2 = 0 \\ D_2: & e_2 = e_4 = 0 \\ D_3: & e_4 = y^2 - e_1^2s^4a_{6,4}z^2 = 0 \\ D_4: & e_3 = y^2 - e_1^2s^4a_{6,4}z^2 = 0 \end{cases} \tag{8.11}$$

Their respective multiplicities are 1, 2, 3, 2, and 1.

The curve C_a is the generic fiber of the fibral divisor D_a ($a = 0, 1, 2, 3, 4$). The fibral divisors can also be defined as the irreducible components of ϕ^*S:

$$\phi^*S = D_0 + 2D_1 + 3D_2 + 2D_3 + D_4. \tag{8.12}$$

Furthermore, we have the following relations:

$$V(s) = D_0, \quad V(e_1) = D_1, \quad V(e_2) = D_1 + D_2, \quad V(e_4) = D_2 + D_3, \quad V(e_3) = D_4. \tag{8.13}$$

Denoting by E_i the exceptional divisor of the ith blowup and by S the class of S, we identify the

classes of the five fibral divisors to be

$$\begin{aligned} &D_0 = S - E_1, \quad D_1 = E_1 - E_2, \quad D_2 = 2E_2 - E_1 - E_3 - E_4, \\ &D_3 = 2E_4 - 2E_2 + E_1 + E_3, \quad D_4 = E_3 - E_4. \end{aligned} \tag{8.14}$$

The curve C_0 is the normalization of a cuspidal curve. The curves C_1 and C_2 are smooth rational curves. The curves C_3 and C_4 are not geometrically irreducible. After a field extension that includes the square root of $a_{6,4}$, they split into two smooth rational curves. Hence, D_0, D_1, and D_2 are $\mathbb{P}^1$-bundles while D_3 and D_4 are double coverings of $\mathbb{P}^1$-bundles. Geometrically, when D_3 and D_4 are seen as families of curves over S, D_3 and D_4 are families of pair of lines.

In the next subsection, we determine what these $\mathbb{P}^1$-bundles are up to an isomorphism.

8.4.2 Fibral divisors

In this section, we study the geometry of the fibral divisors. We recall that for a $\mathbb{P}^1$-bundle, all fibers are smooth projective curves with no multiplicities. A conic bundle has a discriminant locus, over which the fiber is reducible when it is composed of two rational curves meeting transversally or is a double line.

In the case of an F_4-model, the fibral divisors D_0, D_1, and D_2 are $\mathbb{P}^1$-bundles while D_3 and D_4 are double covers of $\mathbb{P}^1$-bundles. The generic fiber of D_3 and D_4 is geometrically composed of two non-intersecting rational curves. D_3 and D_4 have $V(a_{6,4})$ as a discriminant locus. Over the discriminant locus of these double covers, the fiber is composed of a double rational curve.

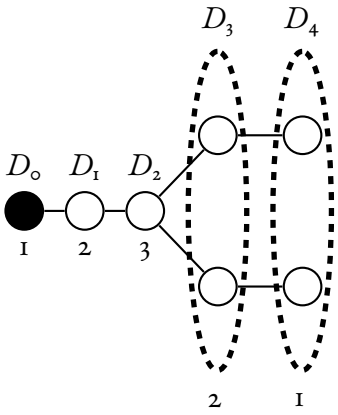

$D_0 : \mathbb{P}_S[\mathscr{L} \oplus \mathscr{O}_S]$

$D_1 : \mathbb{P}_S[\mathscr{L}^{\otimes 2} \oplus \mathscr{S}]$

$D_2 : \mathbb{P}_S[\mathscr{L}^{\otimes 3} \oplus \mathscr{S}^{\otimes 2}]$

D_3: double cover of $\mathbb{P}_S[\mathscr{L}^{\otimes 4} \oplus \mathscr{S}^{\otimes 3}]$

or $\mathbb{P}^1_{S'}[\pi^*(\mathscr{L}^{\otimes 2} \oplus \mathscr{S}^{\otimes 3})]$

D_4: double cover of $\mathbb{P}_S[\mathscr{L}^{\otimes 2} \oplus \mathscr{S}^{\otimes 2}]$

or $\mathbb{P}^1_{S'}[\pi^*(\mathscr{L}^{\otimes 2} \oplus \mathscr{S}^{\otimes 2})]$

(S': double cover of S branched at $V(s, a_{6,4})$)

Figure 8.2: Fibral divisors of an F_4-model as schemes over S. See Theorem 8.4.1. The fibral divisors D_0, D_1, and D_2 are $\mathbb{P}^1$-bundles over S; each of D_3 and D_4 is a double cover of S branched at $V(s, a_{6,4})$. The generic fiber of $f_i : D_i \to S$ (with $i = 3$ or 4) is not connected and consists of two non-intersecting rational curves. The Stein factorization gives a morphism $f'_i : D_i \to S'$ with connected fibers and a finite morphism $\pi : S' \to S$ that is a double cover branched at $V(s, a_{6,4})$. The morphism $f'_3 : D_3 \to S'$ is the $\mathbb{P}^1$-bundle $\mathbb{P}^1_{S'}[\pi^*(\mathscr{L}^{\otimes 2} \oplus \mathscr{S}^{\otimes 3})] \to S'$; the morphism $f'_4 : D_4 \to S'$ is the $\mathbb{P}^1$-bundle $\mathbb{P}^1_{S'}[\pi^*(\mathscr{L}^{\otimes 2} \oplus \mathscr{S}^{\otimes 2})] \to S'$.

We can also simply describe D_3 and D_4 as flat double coverings of $\mathbb{P}^1$-bundles over S or as geomet-

rically reducible conic bundles over S.

Theorem 8.4.1. *The fibral divisors D_0, D_1, and D_2 are $\mathbb{P}^1$-bundles. D_3 and D_4 are double covers of $\mathbb{P}^1$-bundles branched at $V(a_{6,4})$. The corresponding projective bundles are*[2] *(see Figure 8.2)*

- D_0 *is isomorphic to* $\mathbb{P}_S[\mathscr{L} \oplus \mathscr{O}_S]$,
- D_1 *is isomorphic to* $\mathbb{P}_S[\mathscr{L}^{\otimes 2} \oplus \mathscr{S}]$,
- D_2 *is isomorphic to* $\mathbb{P}_S[\mathscr{L}^{\otimes 3} \oplus \mathscr{S}^{\otimes 2}]$,
- D_3 *is isomorphic to a double covering of* $\mathbb{P}_S[\mathscr{L}^{\otimes 4} \oplus \mathscr{S}^{\otimes 3}]$ *ramified in* $V(a_{6,4}) \cap S$,
- D_4 *is isomorphic to a double covering of* $\mathbb{P}_S[\mathscr{L}^{\otimes 2} \oplus \mathscr{S}^{\otimes 2}]$ *ramified in* $V(a_{6,4}) \cap S$,

where $\mathscr{L}$ is the fundamental line bundle of the Weierstrass model and S is the zero scheme of a regular section of the line bundle $\mathscr{S} = \mathscr{O}_B(S)$.

Proof. The strategy for this proof is as follows. We use the knowledge of the explicit sequence of blowups to parametrize each curve. Since each blowup has a center that is a complete intersection with normal crossing, each successive blowup gives a projective bundles. The successive blowups give a tower of projective bundles over projective bundles. We keep track of the projective coordinates of each projective bundle relative to its base. An important part of the proof is to properly normalize the relative projective coordinates when working in a given patch, as they are twisted with

[2] We do not write explicitly the obvious pullback of line bundles. For example, if $\sigma : S \hookrightarrow B$ is the embedding of S in B and $\mathscr{L}$ is a line bundle on B, we abuse notation by writing $\mathbb{P}_S[\mathscr{L} \oplus \mathscr{O}_S]$ for $\mathbb{P}_S[\sigma^* \mathscr{L} \oplus \mathscr{O}_S]$.

respect to previous blowups. We show that D_0, D_1, and D_2 are $\mathbb{P}^1$-bundles over S while D_3 and D_4 are conic bundles defined by a double cover of a $\mathbb{P}^1$-bundle over S.

The fiber C_0 can be studied after the first blowup since the remaining blowups are away from C_0. We can work in the patch $x \neq 0$. We use the defining equation of C_0 to solve for e_1 since x is a unit. We then observe that C_0 has the parametrization

$$C_0 \quad [t^2 : t^3 : 1][1 : t : 0], \quad t = y/x.$$

This is the usual normalization of a cuspidal cubic curve. It follows that C_0 is a rational curve parametrized by t. Since $t = y/x$ is a section of $\mathscr{L}$, it follows that the fibral divisor D_0 is isomorphic to the $\mathbb{P}^1$-bundle $\mathbb{P}_S[\mathscr{L} \oplus \mathscr{O}_S]$ over S.

D_1 is the Cartier divisor $V(e_1)$ in Y, which corresponds to the complete intersection $V(e_1, e_2)$ in X_4. The generic fiber of D_1 over S is the rational curve C_1, which is parametrized as

$$C_1 \quad [0 : 0 : z][\ell_1(e_3e_4x) : 0 : \ell_1 s][\ell_1\ell_2 y : 0][\ell_1\ell_3 x : 0][0 : \ell_4\ell_3^{-1}e_3].$$

We can use ℓ_4, ℓ_3, and ℓ_2 to fix the scalings. But C_1 is parametrized by $[x : s]$ and D_1 is isomorphic to the $\mathbb{P}^1$-bundle $\mathbb{P}_S[\mathscr{L}^{\otimes 2} \oplus \mathscr{S}]$ over S.

C_2 is defined as the generic fiber with $e_2 = e_4 = 0$. This gives

$$C_2 \quad [0 : 0 : z][0 : 0 : \ell_1 s][\ell_1\ell_2 y : \ell_1^{-1}\ell_2 e_1][\ell_1\ell_3 x : 0][0 : \ell_4\ell_3^{-1}e_3].$$

Fixing the scaling as $\ell_1 = s^{-1}, \quad \ell_3 = sx^{-1}$, we see that C_2 is a rational curve parametrized by $[y : s^2]$ and D_2 is isomorphic to $\mathbb{P}_S[\mathscr{L}^{\otimes 3} \oplus \mathscr{S}^{\otimes 2}]$.

For C_3 take $\ell_1 = s^{-1}, \ell_3 = sx^{-1}, \ell_2 = s^{-1}, \ell_3 = sx^{-1}$,

$$C_3 \quad [0:0:1] \quad [0:0:1] \quad [ys^{-2}:1] \qquad [1:0] \quad [\ell_4 s^2 x^{-1} : \ell_4 x s^{-1}].$$

The double cover is $\left(\frac{y}{s^2}\right)^2 = a_{6,4}$. This is clearly a double cover of D_3^+, where D_3^+ is $\mathbb{P}^1$-bundle over S, whose fiber is parametrized by $[s^2x^{-1} : xs^{-1}]$. Such a $\mathbb{P}^1$-bundle is isomorphic to $\mathbb{P}_S[\mathscr{L}^{\otimes 4} \oplus \mathscr{S}^{\otimes 3}]$.

For C_4, take $\ell_1 = s^{-1}, \ell_2 = s^{-1}, \ell_4 = s\ell_3^{-1}$,

$$C_4 \quad [0:0:1] \quad [0:0:1] \quad [ys^{-2}:1] \qquad [s^{-1}x : s] \quad [1:0]$$

The double cover is again $\left(\frac{y}{s^2}\right)^2 = a_{6,4}$. □

Theorem 8.4.2. *The crepant resolution defined in Theorem 8.3.2 has the following properties:*

(i) The resolved variety is a flat elliptic fibration over the base B.

(ii) The fiber over the generic point of S has dual graph $\widetilde{F}_4^t$ and the geometric generic fiber is of Kodaira type IV.*

(iii) The fiber degenerates over $V(s, a_{6,4})$ as

$$V(s, a_{6,4}) \quad \begin{cases} C_3 \longrightarrow 2C_3', \\ C_4 \longrightarrow 2C_4'. \end{cases}$$

where C_3 and C_4 are generic curves defined over S, and C_3' and C_4' are generic curves over $V(s, a_{6,4})$. The generic fiber over $V(s, a_{6,4})$ is a non-Kodaira fiber composed of five geometrically irreducible rational curves. The reduced curves meet transversally with multiplicities $1 - 2 - 3 - 4 - 2$.

Proof. The special fiber is the fiber over the generic point of S. Note that C_2 and C_3 intersect at a divisor of degree two, composed of two points that are non-split. Hence, the dual graph of this fiber is the twisted affine Dynkin diagram of type $\widetilde{\mathrm{F}}_4^t$. All the curves are geometrically irreducible with the exception of C_3 and C_4, which are the double covers of a geometrically irreducible rational curve and the branching locus is $a_{6,4} = 0$. Each of these two curves splits into two geometrically irreducible curves in a field extension that includes a square root of $a_{6,4}$. They degenerate into a double rational curve over $a_{6,4} = 0$. Over the branching locus, the singular fiber is a chain $1 - 2 - 3 - 4 - 2$. The geometric generic fiber has a dual graph that is a $\widetilde{\mathrm{E}}_6$ affine Dynkin diagram. The fibers C_a are fibers of fibral divisors D_a. The matrix of intersection numbers $\deg(D_a \cdot C_a)$ is the opposite of the invariant form of the twisted affine Dynkin diagram of type $\widetilde{\mathrm{F}}_4^t$, normalized in such a way that the

short roots have length square 2:

$$\deg(D_a \cdot C_b) = \left(\begin{array}{c|cccc} -2 & 1 & 0 & 0 & 0 \\ \hline 1 & -2 & 1 & 0 & 0 \\ 0 & 1 & -2 & 2 & 0 \\ 0 & 0 & 2 & -4 & 2 \\ 0 & 0 & 0 & 2 & -4 \end{array}\right)$$

This matrix has a kernel generated by the vector $(1, 2, 3, 2, 1)$. The entries of this vector give the multiplicities of the curve C_a, or equivalently, of the fibral divisors D_a. □

Example 8.4.3. If B is the total space of the line bundle $\mathscr{O}_{\mathbb{P}^1}(-n)$ with $n \in \mathbb{Z}_{\geq 0}$, the Picard group of B is generated by one element, which we call $\mathscr{O}(1)$ and its nth tensor product is $\mathscr{O}(n)$ with dual $\mathscr{O}(-n)$. In particular, the compact curve $\mathbb{P}^1$ is a section of the zero locus of a $\mathscr{O}(-n)$. A local Calabi–Yau threefold can be defined by a Weierstrass model with $\mathscr{L} = \mathscr{O}(2 - n)$. Consider the case of the F_4-model, defined with S a regular section of $\mathscr{S} = \mathscr{O}(-n)$. This requires that $1 \leq n \leq 5$. Denoting the Hirzebruch surface of degree d by $\mathbb{F}_d$, we have $D_0 = \mathbb{F}_{n-2}$, $D_1 = \mathbb{F}_{n-4}$, $D_2 = \mathbb{F}_{n-6}$, D_3 a double cover of $\mathbb{F}_{n-8}$, and D_4 a double cover of $\mathbb{F}_4$. In particular for $n = 5$, the divisors are $D_0 = \mathbb{F}_3$, $D_1 = \mathbb{F}_1$, $D_2 = \mathbb{F}_1$, D_3 a double cover of $\mathbb{F}_3$, and D_4 a double cover of $\mathbb{F}_4$.

8.4.3 Representation associated to the elliptic fibration

In this subsection, we compute the weights of the vertical curves appearing over codimension-two points. There is only one case to consider. The generic fiber over $V(a_{6,4}) \cap S$ is a fiber of type $1-2-3-4-2$ resulting from the following specialization:

$$\begin{cases} C_3 \longrightarrow 2C_3', \\ C_4 \longrightarrow 2C_4'. \end{cases} \tag{8.15}$$

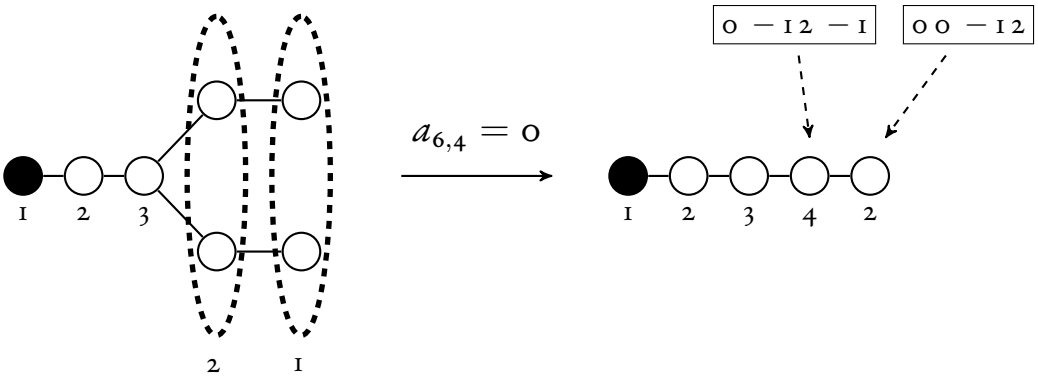

Figure 8.3: Degeneration of the F_4 fiber at the non-transverse collision $IV^{*ns} + I_1$. The nodes represent geometrically irreducible curves. The dashed lines identify the irreducible components of the generic fiber that are geometrically irreducible. They split inside their interior nodes after a $\mathbb{Z}/2\mathbb{Z}$ field extension. The degeneration produces weights $\boxed{0\ -1\ 2\ -1}$ and $\boxed{0\ 0\ -1\ 2}$ that identify 26 as the representation associated with the elliptic fibration. This fiber can be seen as an incomplete Kodaira fiber of type III^* with its dual graph $\tilde{E}_7$ if $\alpha = 0$ or an incomplete Kodaira fiber of type II^* with dual graph $\tilde{E}_8$ if $\alpha > 0$.

Theorem 8.4.4. *1. The intersection numbers of the generic curves C_3' and C_4' with the fibral divi-*

sors D_a for $a = 0, 1, \ldots, 4$ are

$$\varpi(C_3') = (0, 0, -1, 2, -1), \quad \varpi(C_4') = (0, 0, 0, -1, 2).$$

2. *The representation associated to an F_4-model is the quasi-minuscule representation 26 of F_4.*

Proof. By the linearity of the intersection product, the geometric weights $\varpi(C) = -(D_a \cdot C)$ of $C = C_3'$ and $C = C_4'$ are half of the geometric weights of C_3 and C_4':

$$\varpi(C_3') = (0, 0, -1, 2, -1), \quad \varpi(C_4') = (0, 0, 0, -1, 2).$$

Ignoring the weight of D_0, we get the following two weights of F_4:

$$\boxed{0\ -1\ 2\ -1} \quad \boxed{0\ 0\ -1\ 2}.$$

These two weights are quasi-minuscule and are in the same Weyl orbit, which consists of the non-zero weights of the representation 26 of F_4. This is a fundamental representation corresponding to the fundamental weight α_4. This representation is also quasi-minuscule. Since the weight system is invariant under a change of signs, the representation is quaternionic and we can consider half of the representation. Both weights coming from the degeneration of the main fiber are in the same half quaternionic set of weights. □

Remark 8.4.5. An important consequence of Theorem 8.4.4 is that the elliptic fibration does not

have flop transitions to another smooth elliptic fibration since all the curves move in families.

The reduced discriminant has two components, namely $S = V(s)$ and $\Delta' = V(a_{4,3+\alpha}^3 s^{1+3\alpha} + 27a_{6,4}^2)$ intersecting non-transversally at $V(s, a_{6,4})$. Their intersection is exactly the locus over which the fiber $\mathrm{IV}^{*\mathrm{ns}}$ degenerates. The generic fiber over Δ' is of Kodaira fiber I_1. Hence, what we are witnessing is a collision of type $\mathrm{IV}^{*\mathrm{ns}} + \mathrm{I}_1$, leading to an incomplete III^* or an incomplete II^*

$$\mathrm{IV}^{*\mathrm{ns}} + \mathrm{I}_1 \longrightarrow \quad 1 - 2 - 3 - 4 - 2 \quad (\text{incomplete } \mathrm{III}^* \quad \text{or} \quad \text{incomplete } \mathrm{II}^*).$$

This is clearly not a collision of Miranda models since the fibers have different j-invariants and do not intersect transversally. The j-invariants of fibers of type IV^* and I_1 are, respectively, zero and infinity.

By using an elliptic surface whose bases pass through the collision point, the singular fiber at the collision point is of Kodaira type III^* for $\alpha = 0$ and Kodaira type II^* for $\alpha > 0$. Interestingly, we can think of the singular fiber $1 - 2 - 3 - 4 - 2$ as a contraction of a fiber of type III^* or a fiber of type II^*, as expected from the analysis of Cattaneo [76].

8.4.4 Representation theory of F_4

F_4 is studied in Planche VIII of [56, pp 287-288]. The exceptional group F_4 has rank 4, Coxeter number 12, dimension 52, and a trivial center. Its root system consists of 48 roots, half of which are short roots. The Weyl group $W(\mathrm{F}_4)$ of F_4 is the semi-direct product of the symmetric group $\mathfrak{S}_3$ with the semi-direct product of the symmetric group $\mathfrak{S}_4$ and $(\mathbb{Z}/2\mathbb{Z})^3$. Hence, $W(\mathrm{F}_4)$ has dimen-

sion $3!4!2^3 = 2^7 \times 3^2 = 1152$. $W(\mathrm{F}_4)$ is also a solvable group isomorphic to the symmetry group of the 24-cell. The long roots of F_4 form a sublattice of index 4. The outer automorphism group of F_4 is trivial. Hence, F_4 has neither complex nor quaternionic representations, and all its representations are real. Its smallest representation has dimension 26 and is usually called the fundamental representation of F_4. The fundamental representation of F_4 of dimension 26 is a quasi-minuscule representation: all its nonzero weights are in the same orbit of the Weyl group. Moreover, all the nonzero weights of the fundamental representation of F_4 are short roots. Its highest weight is α_4. F_4 is not simply laced and can be described from E_6 by a $\mathbb{Z}/2\mathbb{Z}$ folding.

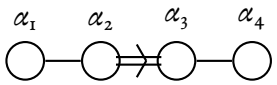

$$\begin{pmatrix} 2 & -1 & 0 & 0 \\ -1 & 2 & -2 & 0 \\ 0 & -1 & 2 & -1 \\ 0 & 0 & -1 & 2 \end{pmatrix}$$

Figure 8.4: Dynkin diagram and Cartan matrix of F_4

Highest weight	Dimension
$(1, 0, 0, 0)$	52
$(0, 1, 0, 0)$	1274
$(0, 0, 1, 0)$	273
$(0, 0, 0, 1)$	26

F_4 contains both B_3 and C_3, as is clear by removing the first or last node. It is less trivial to see that F_4 also contains B_4. One way to see it is to remember that $\mathrm{F}_4 = su(3, \mathbb{O})$ while $\mathfrak{so}_9 = \mathfrak{su}(2, \mathbb{O})$. The coset manifold $\mathrm{F}_4/\mathrm{Spin}(9)$ is the octonionic projective plane $\mathbb{OP}^2$. It follows that we have the

isomorphism [36, 132]

$$\pi_i(\mathrm{F}_4) = \pi_i(\mathrm{Spin}(9)), \quad i \leq 6.$$

The compact real form of F_4 can be described as the automorphism group of the Jordan Lie algebra J_3 of dimension 27 [36]. Maybe a more geometrically familiar picture is to describe the compact real form of F_4 as the *Killing superalgebra* of the 8-sphere S^8 [132]. In this form, the Lie algebra F_4 decomposes (as a vector space) as the direct sum of the Lie algebra $\mathrm{B}_4 \cong \mathfrak{so}_9$ and its spin representation. For more information on the geometry of F_4, we refer to [23] and reference within.

The 48 nonzero roots of F_4 are [56, pp 287]

$$\pm\varepsilon_i \, (1 \leq i \leq 4), \quad \pm\varepsilon_i \pm \varepsilon_j \, (1 \leq i < j \leq 4), \quad \frac{1}{2}(\pm\varepsilon_1 + \pm\varepsilon_2 + \pm\varepsilon_3 + \pm\varepsilon_4), \tag{8.16}$$

where $\varepsilon_i \, (i = 1, 2, 3, 4)$ are respectively $(1, 0, 0, 0)$, $(0, 1, 0, 0)$, $(0, 0, 1, 0)$, and $(0, 0, 0, 1)$. The positive roots are

$$\varepsilon_i \, (1 \leq i \leq 4), \quad \varepsilon_i \pm \varepsilon_j \, (1 \leq i < j \leq 4), \quad \frac{1}{2}(\varepsilon_1 + \pm\varepsilon_2 + \pm\varepsilon_3 + \pm\varepsilon_4). \tag{8.17}$$

A basis of simple positive roots is given by [56, pp 287]

$$\alpha_1 = \varepsilon_2 - \varepsilon_3, \quad \alpha_2 = \varepsilon_3 - \varepsilon_4, \quad \alpha_3 = \varepsilon_4, \quad \alpha_4 = \frac{1}{2}(\varepsilon_1 - \varepsilon_2 - \varepsilon_3 - \varepsilon_4). \tag{8.18}$$

The highest root is $2\alpha_1 + 3\alpha_2 + 4\alpha_3 + 2\alpha_4$. The fundamental weights are [56, pp 288]

$$\begin{aligned} \omega_1 &= 2\alpha_1 + 3\alpha_2 + 4\alpha_3 + 2\alpha_4, \quad \omega_2 = 3\alpha_1 + 6\alpha_2 + 8\alpha_3 + 4\alpha_4, \\ \omega_3 &= 2\alpha_1 + 4\alpha_2 + 6\alpha_3 + 3\alpha_4, \quad \omega_4 = \alpha_1 + 2\alpha_2 + 3\alpha_3 + 2\alpha_4. \end{aligned} \tag{8.19}$$

Roots of F_4	Weight of the representation 26 of F_4
1 0 0 0	0 0 0 1
-1 1 0 0	0 0 1 -1
0 -1 2 0	0 1 -1 0
0 0 0 1	1 -1 1 0
0 0 1 -1 | 0 1 -2 2	-1 0 1 0 | 1 0 -1 1
0 1 -1 0 | 1 -1 0 2	-1 1 -1 1 | 1 0 0 -1
-1 0 0 2 | 0 1 0 -2 | 1 -1 1 0	-1 1 0 -1 | 0 -1 1 1
-1 0 1 0 | 1 -1 2 -2 | 1 0- 1 1	0 -1 2 -1 | 0 0 -1 2
-1 0 2 -2 | -1 1 -1 1 | 1 0 0 -1	0 0 0 0 | 0 0 0 0
-1 1 0 -1 | 0 -1 1 1 | 1 1 -2 0	0 0 1 -2 | 0 1 -2 1
-1 2 -2 0 | 0 -1 2 -1 | 0 0 -1 2 | 2 -1 0 0	0 1 -1 -1 | 1 -1 0 1
0 0 0 0 | 0 0 0 0 | 0 0 0 0 | 0 0 0 0	-1 0 0 1 | 1 -1 1 -1
-2 1 0 0 | 0 0 1 -2 | 0 1 -2 1 | 1 -2 2 0	-1 0 1 -1 | 1 0 -1 0
-1 -1 2 0 | 0 1 -1 -1 | 1 -1 0 1	-1 1 -1 0
-1 0 0 1 | 1 -1 1 -1 | 1 0 -2 2	0 -1 1 0
-1 0 1 -1 | -1 1 -2 2 | 1 0 -1 0	0 0 -1 1
-1 1 -1 0 | 0 -1 0 2 | 1 0 0 -2	0 0 0 -1
-1 1 0 -2 | 0 -1 1 0	
0 -1 2 -2 | 0 0 -1 1	
0 0 0 -1	
0 1 -2 0	
1 -1 0 0	
-1 0 0 0	

Table 8.2: Roots of F_4 and weights of the representation 26 in the basis of fundamental weights.

8.5 Topological invariants

In this section we compute several topological invariants of the crepant resolution. Using the push-forward theorem of [114], we can compute the Euler characteristic of an F_4-model. We need to know the classes of the centers of the sequence of blowups that define the crepant resolution. The center of the nth blowup is a smooth complete intersection of d_n divisors of classes $Z_i^{(n)}$, where $i = 1, 2, \ldots, d_n$.

8.5.1 Intersection theory

To compute intersection numbers, we use Theorems 2.7.11, 5.0.1 and 5.0.4 [4, 114]. In particular, using Theorems 2.7.11 and 5.0.1, we can evaluate the Chern class after the crepant resolution given by the sequence of blowups given in equation (8.9).

In the case of F_4, we recall that $H = c_1(\mathscr{O}(1))$, $L = c_1(\mathscr{L})$, and $S = [S]$. The classes associated to the centers of each blowup are [114]

$$\begin{aligned}
&Z_1^{(1)} = H + 2L && Z_2^{(1)} = H + 3L && Z_3^{(1)} = S \\
&Z_1^{(2)} = Z_2^{(1)} - E_1 && Z_2^{(2)} = E_1 \\
&Z_1^{(3)} = Z_1^{(1)} - E_1 && Z_2^{(3)} = E_2 \\
&Z_1^{(4)} = E_2 - E_3 && Z_2^{(4)} = E_3
\end{aligned} \tag{8.20}$$

8.5.2 Total Chern class and the Euler characteristic

After some algebra, we can express the total Chern class of Y as[3]

$$c(TY) = Z\frac{(1+H)(1+H+3L-E_1-E_2)(1+H+2L-E_1-E_3)}{(1+3H+6L-2E_1-E_2-E_3-E_4)}c(TB), \tag{8.21}$$

where the class of Y in X_4 is $3H+6L-2E_1-E_2-E_3-E_4$.

$$Z = \frac{(1+E_4)(1+S-E_1)(1+E_1-E_2)(1+E_3-E_4)(1+E_2-E_3-E_4)}{1+S}. \tag{8.22}$$

In particular, we have

$$c_1(TY) = (c_1 - L) \tag{8.23}$$

$$\begin{aligned} c_2(TY) = (&-c_1L + c_2 + 2E_1E_2 + E_1E_3 + 2E_1E_4 - 4E_1H - 7E_1L + E_1S - E_2^2 + 2E_2E_3 + \\ &2E_2E_4 - 2E_2H - 3E_2L - E_3^2 + E_3E_4 - 2E_3H - 4E_3L \\ &- E_4^2 - 3E_4H - 6E_4L + 3H^2 + 13HL + 12L^2) \end{aligned} \tag{8.24}$$

In the case of a threefold, the second Chern class defines a linear form on $H^2(Y,\mathbb{Z})$. In particular, for the fibral divisors we have

$$\int_Y c_2(TY)\cdot(\sum_a D_a\varphi_a) = 2S(S-L)(\varphi_0+\varphi_1+\varphi_2) + 4S(2L-S)(\varphi_3+\varphi_4).$$

[3] To simplify notation, we do not write all the pullbacks.

This follows from equation (8.14), equation (8.24), and the pushforward formula of Theorem 5.0.1, and Theorem 5.0.4. Imposing the Calabi–Yau condition, we can rewrite this as

$$\int_Y c_2(TY) \cdot (\sum_a D_a \varphi_a) = 4(g-1)(\varphi_0 + \varphi_1 + \varphi_2) + 4(4 - 4g + S^2)(\varphi_3 + \varphi_4).$$

Theorem 8.5.1 ([114]). *The Euler characteristic of an F_4-model obtained by a crepant resolution of the Weierstrass model $y^2 z = x^3 + s^{3+\alpha} a_{4,3+\alpha} x z^2 + s^4 a_{6,4} z^3 \quad (\alpha \in \mathbb{Z}_{\geq 0})$ over the base B is*

$$\chi(Y) = \int 12 \frac{(L + 3SL - 2S^2)}{(1+S)(1+6L-4S)} c(B),$$

where $L = c_1(\mathscr{L})$ and S is the class of $V(s)$. In particular, denoting $c_i(TB)$ simply as c_i:

Conditions	$\chi(Y)$
$\dim Y = 3$	$12(c_1 L - 6L^2 + 6LS - 2S^2)$
$\dim Y = 3$ *and* $c_1(TY) = 0$	$12(5c_1^2 - 6c_1 S + 2S^2)$
$\dim Y = 4$	$12(-6c_1 L^2 + c_2 L + 36L^3 + 6c_1 LS - 60L^2 S - 2c_1 S^2 + 34LS^2 - 6S^3)$
$\dim Y = 4$ *and* $c_1(TY) = 0$	$12(30c_1^3 + c_1 c_2 - 54c_1^2 S + 32c_1 S^2 - 6S^3)$

The case of a Calabi–Yau fourfold is useful to discuss the cancellation of tadpoles [5, 6, 78, 109, 120].

Theorem 8.5.2 ([114]). *Let Y be a Calabi–Yau threefold that is an F_4-model obtained from a crepant*

resolution. Then the Hodge numbers of Y are

$$h^{1,1}(Y) = 15 - K^2, \quad h^{2,1}(Y) = 15 + 29K^2 + 36SK + 12S^2.$$

8.5.3 Other characteristic numbers for an F_4-model over a three dimensional base

$c_1^4(TY)$	0
$c_1^2(TY)c_2(TY)$	$12L(c_1 - L)^2$
$c_2^2(TY)$	$24L(L(6L - c_1) + c_2) - 8S(27L^2 - 16LS + 3S^2)$
$c_1(TY)c_3(TY)$	$12L(c_1 - L)(c_1 - 6L) + 24S(c_1 - L)(3L - S)$
$c_4(TY)$	$12L(6L(6L - c_1) + c_2) + 72LS(c_1 - 10L)$ $-24S^2(c_1 - 17L) - 72S^3$
$\phi_*(c_3(TY)\phi^*M_1)$	$\left[12L(c_1 - 6L) + 72LS - 24S^2\right] \cdot M_1$
$\chi_0(Y)$	$\frac{1}{12}L\left(c_1^2 - 3c_1L + c_2 + 2L^2\right)$
$\chi_1(Y)$	$-\frac{1}{3}L\left(2c_1^2 - 54c_1L + 5c_2 + 232L^2\right)$ $+2S^2(3c_1 - 35L) - 18LS(c_1 - 7L) + 12S^3$
$\chi_2(Y)$	$-\frac{1}{2}L\left(3c_1^2 + 71c_1L - 17c_2 - 554L^2\right)$ $-4S^2(3c_1 - 67L) + 36LS(c_1 - 13L) - 48S^3$
$p_1^2(TY)$	$24L(-c_1^2 + 2c_2 + 36L^2) - 56S(27L^2 - 16LS + 3S^2)$
$p_2(TY)$	$-48L(c_1^2 - 2c_2 - 11L^2) - 32S(27L^2 - 16LS + 3S^2)$
$192X_8(TY)$	$48L\left(c_1^2 - 2c_2 - 61L^2\right) + 192S(27L^2 - 16LS + 3S^2)$
$45L(TY)$	$120L\left(-c_1^2 + 2c_2 + 46L^2\right) - 360S(27L^2 - 16LS + 3S^2)$
$5760A(TY)$	$240L\left(-c_1^2 + 2c_2 + L^2\right)$

Table 8.3: Characteristic number for an F_4-model or a Spin(8)-model over a base of dimension three [116].

Chern numbers of an elliptically-fibered fourfold $\phi : Y \longrightarrow B$ that is given by the crepant resolution of a Weierstrass model were recently computed in [116]. We recall the result in the case of an F_4-model in Table 8.3. They are the same as those of a Spin(8)-model [116]. These numbers are

computed using the sequence of blowups and the theorems presented in section 8.5.1. Similar results exist for elliptic fibrations that are not given by Weierstrass models [117].

8.5.4 Triple intersection numbers

With an explicit resolution of singularities, it is straightforward to compute intersection numbers of divisors. In particular, we evaluate the triple intersection numbers of the fibral divisors D_a, where $a = 0, 1, 2, 3, 4$. The result is

$$\phi_* \left(\left(\sum D_a \varphi_a \right)^3 \cdot \phi^* M \right) = 6\mathscr{F}(L, S, \varphi) M,$$

where M is an arbitrary element of $A_{d-2}(B)$. In particular, if the base B is a surface, M is just a point.

Theorem 8.5.3. *Let D_a ($a = 0, 1, 2, 3, 4$) be the fibral divisor of an F_4-model obtained by a crepant resolution of singularities. The triple intersection numbers $\phi_* \left((\sum D_a \varphi_a)^3 \cdot \phi^* M \right) = 6\mathscr{F}(L, S, \varphi) M$, where M is an element of $A_{d-2}(B)$ ($d = \dim B$), are given by*

$$\begin{aligned} 6\mathscr{F}(L, S, \varphi) = {} & 4(L - S) S \varphi_0^3 + 3(S - 2L) S \varphi_0^2 \varphi_1 + 3LS \varphi_0 \varphi_1^2 \\ & + 4(L - S) S \varphi_1^3 + 4(L - S) S \varphi_2^3 + 8(S - 2L) S \varphi_3^3 + 8(S - 2L) S \varphi_4^3 \\ & + 3(2S - 3L) S \varphi_1^2 \varphi_2 + 3(2L - S) S \varphi_1 \varphi_2^2 \\ & + 6(3S - 4L) S \varphi_2^2 \varphi_3 + 12(3L - 2S) S \varphi_2 \varphi_3^2 + 12(S - L) S \varphi_3^2 \varphi_4 + 6(4L - 3S) S \varphi_3 \varphi_4^2. \end{aligned}$$

Proof. Use equation (8.14) and successively apply the pushforward formula of Theorem 5.0.1, and Theorem 5.0.4. □

In the case of a Calabi–Yau threefold, we have $L = -K$ (the anticanonical class of B). It follows that we can express the coefficient in terms of the genus of S and its self-intersection using the relation $2 - 2g = -K_B \cdot S - S^2$:

$$\begin{aligned} 6\mathscr{F}(\varphi) = &- 8\,(g-1)\,\varphi_0^3 - 3\,(-4g+4+S^2)\,\varphi_0^2\varphi_1 + 3\,(-2g+2+S^2)\,\varphi_1^2\varphi_0 \\ &- 8(g-1)\varphi_1^3 - 8(g-1)\varphi_2^3 + 8\,(4g-4-S^2)\,\varphi_3^3 + 8\,(4g-4-S^2)\,\varphi_4^3 \\ &+ 3\,(6g-6-S^2)\,\varphi_1^2\varphi_2 + 3\,(-4g+4+S^2)\,\varphi_1\varphi_2^2 + 6\,(8g-8-S^2)\,\varphi_2^2\varphi_3 \\ &+ 12\,(-6g+6+S^2)\,\varphi_2\varphi_3^2 + 24(g-1)\varphi_3^2\varphi_4 + 6\,(-8g+8+S^2)\,\varphi_3\varphi_4^2. \end{aligned} \tag{8.25}$$

Remark 8.5.4 (Comparing with Diaconescu-Entin [97, §2.2])**.** The triple intersection numbers of divisors intersecting as an F_4 Dynkin diagram in a Calabi–Yau threefold were studied by Diaconuscu and Entin in [97, §2.2]. After taking $\varphi_0 = 0$, this result can be compatible with the computation in [97, §2.2]. There is a small normalization typo in [97, §2.2], what is called $\mathcal{F}(\varphi)$ there should be $6\mathcal{F}(\varphi)$. In [97, §2.2], the curve S is assumed to be a rational curve, which implies that $g = 0$. We can immediately see from the explicit crepant resolution that the curve $\gamma_2 = D_2 \cap D_3$: $e_2 = e_4 = y^2 - e_1^2 s^4 a_{6,4} z^2 = 0$ is a double cover of S branched at $2b$ points with $b = -S \cdot (3K + 2S)$

since we are in the patch $zse_1e_3 \neq 0$ as seen by analyzing the projective coordinates given in equation (8.10). Since S is a rational curve, we have $2 = -K \cdot S - S^2$, which gives $b = 6 + S^2$. Using the Riemann-Hurwitz Theorem (see Theorem 2.12.1), we see that the genus of γ_2 is $g(\gamma_2) = 5 + S^2$. The variable g appearing in [97, §2.2] is the genus of γ_2. We get a perfect match between our triple intersection numbers and those of [97, §2.2] if and only if

$$g(S) = 0, \quad g(\gamma_2) = 5 + S^2, \tag{8.26}$$

which is always the case with S is a smooth rational curve. Moreover, if $\gamma_2 = D_2 \cap D_3$ is a rational curve, then $g(\gamma_2) = 0$ and the matching requires necessary that S be a -5-curve since $g(\gamma_2) = 5 + S^2 = 0$. Thus, we get in that special case

$$\begin{aligned} 6\mathscr{F}(\varphi) =& 8\varphi_1^3 + 8\varphi_2^3 + 8\varphi_3^3 + 8\varphi_4^3 - 3\varphi_1^2\varphi_2 - 3\varphi_1\varphi_2^2 - 18\varphi_2^2\varphi_3 + 12\varphi_2\varphi_3^2 - 24\varphi_3^2\varphi_4 + 18\varphi_3\varphi_4^2. \end{aligned} \tag{8.27}$$

8.5.5 Stein factorization and the geometry of non-simply laced G-models

To understand the geometry of a fibral divisor D, it is important to see the divisor D as a relative scheme with respect to the appropriate base. The choice of the base is crucial to having the correct physical interpretation. In particular, to discuss the matter content of the theory, the base has to be a component of the discriminant locus. However, to study the possible contractions of D, the base can be an arbitrary subvariety of the elliptic fibration.

Let S be the irreducible component of the discriminant locus supporting the gauge group. In the case of G-models with G a non-simply laced groups, Stein factorization illuminates the discussion of the geometry of the fibral divisors D, whose generic fibers over S are not geometrically irreducible. The elliptic fibration $\phi : Y \to B$ pulls back to a fibration $D \to S$. If the generic fiber of this fibration is not geometrically irreducible, the generic fiber is not geometrically connected.

We recall the following two classical theorems on morphisms that are consequences of the theorem of formal functions.

Theorem 8.5.5 (Zariski). *Let $f : X \to Y$ be a proper morphism of Noetherian schemes such that $f_*\mathcal{O}_X \cong \mathcal{O}_Y$. Then all fibers are geometrically connected and non-empty.*

Theorem 8.5.6 (Stein factorization [162, Chap III.11.3]). *Let $f : X \to S$ be a proper morphism with S a Noetherian scheme. Then there exists a factorization*

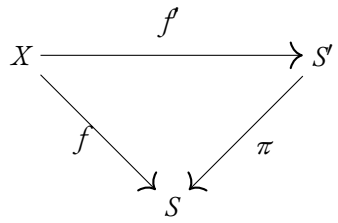

such that

1. *$\pi : S' \to S$ is a finite morphism and $f' : X \to S'$ is a proper morphism with geometrically connected fibers.*

2. *$f'_*\mathcal{O}_X \cong \mathcal{O}_{S'}$.*

3. *S' is the normalization of S in X.*

4. $S' = \underline{\mathrm{Spec}}_S(f_*\mathscr{O}_X)$.

The Stein factorization on $f : D \to S$ is the decomposition $f = \pi' \circ f'$, where $\pi' : \overline{S} \to S$ is a finite map of degree d and $f' : D \to \overline{S}$ is a morphism with connected fibers. We expect $f' : D \to \overline{S}$ to be a $\mathbb{P}^1$-bundle and $\pi' : \overline{S} \to S$ a smooth d-cover of S.

In the case of F_4-models, D is a $\mathbb{P}^1$-bundle for the fibral divisor D_0, D_1, and D_2 (corresponding to the affine root, and the small roots of $\widetilde{F}_4$. The remaining two fibral divisors (namely D_3 and D_4) are not $\mathbb{P}^1$-bundles over S but rather double covers of $\mathbb{P}^1$-bundles over S with a ramification locus $a_{6,4} = 0$. The crepant resolution naturally defines a double cover $\pi : D \to \underline{D}$, where $\underline{D}$ is a $\mathbb{P}^1$-bundle $p : \underline{D} \to S$. Let $f = \pi \circ p : D \to S$ be the composition. The key to understanding the different perspective on the geometry of D is to consider the Stein factorization of f.

Let D be the reduced fibral divisor D_3 or D_4 of an F_4-model. By definition, $f : D \to S$ has a generic fiber that is not geometrically connected. Consider the Stein factorization of the morphism $f : D \to S$. It gives a factorization $f = \pi' \circ f'$ with π' a finite map and f' a proper morphism with geometrically connected fibers.

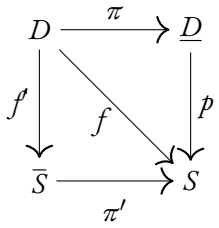

In particular, the morphism $f' : D \to \overline{S}$ endows D the structure of a $\mathbb{P}^1$-bundle over the double cover $\overline{S}$ of S. This structure illustrates that D can contract to $\overline{S}$.

It is important to not confuse the role of the morphisms $f' : D \to \overline{S}$ and $f : D \to S$ in F-theory. One might naively assume that the existence of a $\mathbb{P}^1$-bundle $f' : D \to \overline{S}$ means that the divisor D does not produce new curves leading to localized matter representations. However, it is important to keep in mind that it is the morphism $f : D \to S$ over the curve S that is relevant for studying the singular fibers of the elliptic fibration as S.

The morphism $f : D \to S$ contains singular fibers that are double lines. The intersection numbers of these lines with the fibral divisors give two weights of the representation 26, namely $\boxed{0\ -1\ 2\ -1}$ for D_3 and $\boxed{0\ 0\ -1\ 2}$ for D_4. The same weights are obtained over any closed points away from $a_{6,4}$ and are attributed to non-localized matter.

8.6 A double cover of a ruled surface branch along $2b$ fibers

A ruled surface is by definition a $\mathbb{P}^1$-bundle over a smooth curve of genus g.

Theorem 8.6.1. *Let $p : Y \to S$ be the projection of a ruled surface Y to its base curve S where S is a smooth curve of genus g. There exists a non-negative integer number n such that $\int_Y S^2 = -n$. Consider the double cover $\pi : X \to Y$ of Y branched along $2b$ distinct fibers of p. Then X is smooth and the morphism π is flat. The curve $\overline{S} = \pi^* S$ is a double cover of S branched at $2b$ distinct points. Let f be the*

class of a generic fiber of Y and define ℓ such that $2\ell = \pi^* f$. Then

$$g(\overline{S}) = 2g + b - 1, \tag{8.28}$$

$$\int_X \overline{S}^2 = -2n, \tag{8.29}$$

$$K_X = \pi^* K_Y + b\pi^* f = -2\overline{S} + (2(2g + b - 1) - 2 - 2n)\ell, \tag{8.30}$$

$$K_X^2 = 8(2 - 2g - b), \tag{8.31}$$

$$\chi(X) = 4(2 - 2g - b), \tag{8.32}$$

$$\chi(\mathcal{O}_X) = 2 - 2g - b. \tag{8.33}$$

Proof. X is smooth because the branch locus of π is smooth and π is flat by construction. The genus of $\overline{S}$ follows from Riemann-Hurwitz's formula given in Theorem 2.12.1. The self-intersection of $\overline{S}$ and of K_X follows from the fact that π is a finite map of degree 2. The Euler characteristic of X is computed by using the formula for a branch covering. The holomorphic Euler characteristic is computed from Noether's formula $12\chi(\mathcal{O}_X) = K_X^2 + \chi(X)$. □

Remark 8.6.2. Since the $\mathbb{P}^1$-bundle over S pulls back to a $\mathbb{P}^1$-bundle over $\overline{S}$, X is a ruled surface over the curve $\overline{S}$ of genus $(2g + b - 1)$ and self-intersection $-2n$. By the universal property of the Stein factorization, $X \xrightarrow{f'} \overline{S} \xrightarrow{\pi} S$ is the Stein factorization of $X \to S$.

8.7 Application to M-theory and F-theory in 5 and 6 dimensions

In this section, we study the aspects of five-dimensional gauge theories with gauge group F_4 using the geometry of the F_4-model. We consider an M-theory compactified on an F_4-model $\phi : Y \to B$. We assume then that the variety Y is a Calabi–Yau threefold and the base B is a rational surface. Then, the resulting theory is a five-dimensional $\mathcal{N} = 1$ supersymmetric theory with eight supersymmetric generators, whose matter content contains n_H hypermultiplets and n_V vector multiplets. We have n_H° neutral hypermultiplets, n_{52} hypermultiplets transforming in the adjoint representation, and n_{26} hypermultiplets transforming in the fundamental representation 26. We have n_V vector multiplets whose kinetic terms and Chern–Simons terms are controlled by a cubic prepotential. For the F_4 gauge theory with both adjoint and fundamental matters, there is a unique Coulomb phase because all the weights of the representation 26 are roots of F_4.

Since F_4 does not have a non-trivial third order Casimir, the classical part of the prepotential vanishes, and the quantum corrections fully determine the prepotential. The number of vector multiplets is the dimension of the Lie algebra of F_4. Then, we can determine the quantum contribution to the prepotential and hence determine n_{52} and n_{26}. Since we know the Hodge numbers of F_4-models in the case of Calabi–Yau threefolds [114], we can compute $n_H^\circ = h^{2,1}(Y) - 1$ as well.

We also solve directly the anomaly cancellation conditions of a six-dimensional $\mathcal{N} = (1, 0)$ supergravity theory with a gauge group F_4 resulting from the compactification of F-theory on an F_4-model. We observe that the number of hypermultiplets transforming in the adjoint representation (52) and the fundamental representation (26) matches what we found in the five-dimensional the-

ory obtained from a compactification of M-theory on the same elliptic fibration.

8.7.1 Intriligator-Morrison-Seiberg prepotential

The Intrilligator-Morrison-Seiberg (IMS) prepotential [176] is the quantum contribution to the prepotential of a five-dimensional gauge theory with the matter fields in the representations $\mathbf{R}_i$ of the gauge group. Denoting the simple roots by α, the set of weights of $\mathbf{R}_i$ by W_i, the number of hypermultiplets transforming under the representation $\mathbf{R_i}$ by $n_{\mathbf{R}_i}$, we have

$$6\mathscr{F}_{\text{IMS}} = \frac{1}{2}\left(\sum_{\alpha} |\langle \alpha, \varphi\rangle|^3 - \sum_{\mathbf{R}_i}\sum_{\varpi\in W_i} n_{\mathbf{R}_i} |\langle \varpi, \varphi\rangle|^3\right). \tag{8.34}$$

For more information, see Section 2.12.1 Within each of these subchambers, the prepotential is a cubic polynomial; in particular, it has smooth second derivatives. But as we go from one subchamber to an adjacent one, we have to go through one of the walls defined by the weights and the third derivatives will not be well-defined. Physically, we think of the dual fundamental Weyl chamber as the ambient space and each of the subchambers is called a *Coulomb phase* of the gauge theory. The number of chambers of such a hyperplane arrangement is physically the number of phases of the Coulomb branch of the gauge theory.

In the case of F_4 with the matter fields in the representation $52 \oplus 26$, there is a unique chamber as the hyperplanes $\langle \varpi, \varphi\rangle = 0$ have no intersections with the interior of the dual fundamental Weyl chamber. The explicit computation of $6\mathscr{F}_{\text{IMS}}$ is presented in the theorem below. The weights of the 52 and the 26 are listed in Table 8.2.

Theorem 8.7.1. *The IMS prepotential for an $\mathcal{N} = 1$ five-dimensional (supergravity) gauge theory with the gauge group F_4 coupled to n_{52} hypermultiplets in the adjoint representation and n_{26} hypermultiplets in the fundamental representation 26 is*

$$\begin{aligned} 6\mathcal{F}_{IMS} = &- 8\left(n_{52}-1\right)\varphi_1^3 - 8\left(n_{52}-1\right)\varphi_2^3 - 8\left(n_{52}+n_{26}-1\right)\varphi_3^3 - 8\left(n_{52}+n_{26}-1\right)\varphi_4^3 \\ &- 3\left(-n_{52}+n_{26}+1\right)\varphi_1^2\varphi_2 + 3\left(n_{52}+n_{26}-1\right)\varphi_1\varphi_2^2 \\ &+ 12\left(-n_{52}+n_{26}+1\right)\varphi_2\varphi_3^2 - 6\left(-3n_{52}+n_{26}+3\right)\varphi_2^2\varphi_3 \\ &+ 6\left(-3n_{52}+n_{26}+3\right)\varphi_3\varphi_4^2 + 24\left(n_{52}-1\right)\varphi_3^2\varphi_4 . \end{aligned} \tag{8.35}$$

Proof. Direct computation from equation (8.34) for the Lie algebra of type F_4 and the representations 52 and 26 whose weights are listed in Table 8.2. □

Theorem 8.7.2. *The triple intersection polynomial of the elliptic fibration defined by the crepant resolution of the F_4-model Weierstrass matches the IMS potential if and only if*

$$n_{52} = g, \quad n_{26} = 5(1-g) + S^2. \tag{8.36}$$

Proof. These numbers are obtained by comparing the coefficients of φ_1^3 and φ_4^3 in $\mathscr{F}_{\mathrm{IMS}}$ and $\mathscr{F}$. A direct check shows that all the other coefficients match. □

8.7.2 Cancellations of six-dimensional anomalies for an F_4-model

In this section, we prove that the data we computed on the F_4-model as seen in a M-theory compactification on a Calabi–Yau threefold Y will satisfy the anomaly cancellation conditions of a six-dimensional theory with the same gauge group and same number of vector and hypermultiplets. Moreover, in a six-dimensional $(1, 0)$ gauge theory, we can also have tensor multiplets. We assume here that the tensor multiplets are massless and have numbers $n_T = h^{1,1}(B)$, which is $n_T = 9 - K^2$ since we assume that the base is a rational surface.

Since F_4 does not have a fourth Casimir, $B_{\mathbf{R}} = 0$. We have [22] ,

$$\mathrm{tr}_{52}\, F^2 = 3\mathrm{tr}_{26}\, F^2, \quad \mathrm{tr}_{52}\, F^4 = \frac{5}{12}(\mathrm{tr}_{26} F^2)^2 \quad \mathrm{tr}_{26}\, F^4 = \frac{1}{12}(\mathrm{tr}_{26} F^2)^2. \tag{8.37}$$

From these trace identities, we can immediately read off the coefficients $A_{\mathbf{R}}$, $B_{\mathbf{R}}$, and $C_{\mathbf{R}}$:

$$A_{52} = 3, \quad B_{52} = 0, \quad C_{52} = \frac{5}{12}, \quad A_{26} = 1, \quad B_{26} = 0, \quad C_{26} = \frac{1}{12}. \tag{8.38}$$

For F_4, the normalization factor λ is 6 and the last two anomaly equations are:

$$(3 - 3n_{52} - n_{26}) = K \cdot S, \quad (5 - 5n_{52} - n_{26}) = -S^2. \tag{8.39}$$

Using the identity $2 - 2g = -K \cdot S - S^2$, where g is the arithmetic genus of the curve S, we find:

$$n_{52} = g, \quad n_{26} = 5 - 5g + S^2, \tag{8.40}$$

which matches what we found by comparing the triple intersection numbers with the prepotential in the $\mathcal{N} = 1$ five-dimensional theory obtained by compactifiying M-theory on the same elliptic fibration. Thus,

$$\begin{aligned} &n_T = 9 - K^2, \quad n_V = 52, \\ &n_{52} = g, \quad n_{26} = 5(1-g) + S^2, \quad h^{2,1}(Y) = 15 + 29K^2 + 72(g-1) - 24S^2, \end{aligned} \tag{8.41}$$

We recall that n_V is given by the dimension of the Lie algebra of F_4. The Hodge numbers of Y were computed in [114].

Using the Green-Schwarz mechanism for 6d reviewed in section 2.13.2, we check that the pure gravitational, pure gauge, and mixed gravitational-gauge anomalies are all canceled. We first compute the pure gravitational anomaly. We need to satisfy equation (2.44). Using the data of (2.62b), we compute $n_H = 29K^2 + 64$ and check that the gravitational anomaly cancels:

$$n_H - n_V + 29n_T - 273 = (29K^2 + 64) - 52 + 29(9 - K^2) - 273 = 0.$$

We will now show that the anomaly polynomial I_8 is a perfect square. The forms $X^{(2)}$ and $X^{(4)}$ are

$$X^{(2)} = (3 - 3n_{52} - n_{26})\mathrm{tr}\, F^2, \quad X^{(4)} = \frac{1}{12}\Big(5 - 5n_{52} - n_{26}\Big)(\mathrm{tr}F^2)^2. \tag{8.42}$$

After plugging in the values of n_{52} and n_{26}, we have

$$X^{(2)} = K \cdot S\mathrm{tr}\, F^2, \quad X^{(4)} = -\frac{1}{12}S^2(\mathrm{tr}F^2)^2. \tag{8.43}$$

We can now prove that the anomaly polynomial is a perfect square:

$$I_8 = \frac{K^2}{8}(\mathrm{tr}\, R^2)^2 + \frac{1}{6}K \cdot S(\mathrm{tr}\, F^2)(\mathrm{tr}\, R^2) + \frac{1}{18}S^2(\mathrm{tr}F^2)^2 = \frac{1}{2}\Big(\frac{1}{2}K\mathrm{tr}\, R^2 + \frac{1}{3}S\,\mathrm{tr}F^2\Big)^2. \tag{8.44}$$

This shows that the anomalies can be canceled by the Green-Schwarz mechanism.

8.7.3 Frozen representations

Motivated by the counting of charged hypermultiplets in M-theory compactifications, we introduce the notion of *frozen representations*. When a vertical curve of an elliptic fibration carries the weight of a representation **R**, the representation **R** is said to be the *geometric representation* induced by the vertical curve. The existence of a vertical curve carrying a weight of the representation **R** is a necessary but not sufficient condition for hypermultiplets to be charged under the representation **R**. It is possible that a geometric representation is not physical in the sense that no hypermultiplet is charged under **R**, so that $n_{\mathbf{R}} = 0$.

Definition 8.7.3 (Frozen representation)**.** A geometric representation **R** is said to be *frozen* if it is induced by the weights of vertical curves of the elliptic fibration but no hypermultiplet is charged under **R**.

Witten has proven that a curve of genus g supporting a Lie group produces g hypermultiplets in the adjoint representation. It follows that the adjoint representation is frozen when the genus is zero. This is because the adjoint hypermultiplets are counted by holomorphic forms on the curve S. When the genus is zero, there are no such forms. Hence, even though we clearly witness vertical rational curves carrying the weights of the adjoint representation, no adjoint hypermultiplet are to be seen.

For non-simply laced groups, frozen representations can occur when the curve defined by the Stein factorization has the same genus as the base curve S. The representation is frozen if and only if

$$g = 0 \quad \text{and} \quad \deg R = 2(d-1).$$

The number of points over which the fiber $\mathrm{IV}^{*\mathrm{ns}}$ degenerates to the non-Kodaira fiber IV_2^* is the degree of the ramification divisor R. This is an interesting geometric invariant to keep in mind.

Lemma 8.7.4. *If B is a surface with canonical class K_B and $\mathscr{L} = \mathscr{O}_B(-K_B)$ so that the F_4-model is a Calabi–Yau threefold, then the number of points over which the generic fiber IV^{*ns} over S degenerates further to the non-Kodaira fiber $1-2-3-4-2$ is*

$$\deg R = 12(1-g) + 2S^2.$$

Proof. The number of intersection points is the intersection product of $V(a_{6,4})$ and the curve S.

Note that this is a transverse intersection and the class of $V(a_{6,4})$ is $6L - 4S$. Then using $L = -K_B$ and $2g - 2 = (K + S) \cdot S$, we have $\deg R = (6L - 4S) \cdot S = 12(1 - g) + 2S^2$. □

The degree of the ramification locus R is the number of points in the reduced intersection of the two components of the discriminant locus, namely S and Δ'. The degree of R has to be positive as otherwise D_3 and D_4 are not irreducible and we have an E_6-model rather than an F_4-model. This gives a constraint on the self-intersection of S: $S^2 > 6(g - 1)$. For example, if $B = \mathbb{P}^2$, the bound is respected when S is a smooth curve of degree 1, 2, 3, or 4.

Proposition 8.7.5. *For an F_4-model, the number of charged hypermultiplets are*

$$n_{26} = \frac{1}{2}\deg R + g - 1 \quad n_{52} = g.$$

In particular, the adjoint representation is frozen if and only if $g = 0$. The representation 26 is frozen if and only if $S^2 = -5$ and $g = 0$, which also forces the adjoint representation to be frozen.

Proof. The number of representation n_{26} is computed in Theorem 8.7.2. The representation 26 is frozen if and only if $\deg R = 2(1 - g)$. Since the degree of R has to be positive, we also see that $g = 0$, hence by using Lemma 8.7.4, we conclude that $S^2 = -5$ and $\deg R = 2$. □

We consider two important examples.

Example 8.7.6 (Frozen adjoint representation). $n_{52} = 0$ if and only if $g = 0$. In this case, $\deg R = 12 + 2S^2$ and $n_{26} = 5 + S^2$. This matches what is found in Table 3 of [37] using $n = S^2$ as the instanton number.

Example 8.7.7 (Frozen representation 26). $n_{26} = 0$ if and only if $S^2 = -5$ and $g = 0$. For example, take B to be the quasi-projective surface given by the total space of the line bundle $\mathscr{O}_{\mathbb{P}^1}(-5)$. If B is the total space of the line bundle $\mathscr{O}_{\mathbb{P}^1}(-n)$ with $n \in \mathbb{Z}_{\geq 0}$, the Picard group of B is generated by one element, which we call $\mathscr{O}(1)$ and its nth tensor product is $\mathscr{O}(n)$ with dual $\mathscr{O}(-n)$. In particular, the compact curve $\mathbb{P}^1$ is a section of the zero locus of a $\mathscr{O}(-n)$. To construct a local Calabi–Yau threefold, use $\mathscr{L} = \mathscr{O}(-3)$. This is the non-Higgsable model of [240]. The defining equation of such a Weierstrass model is

$$y^2 z = x^3 + f_3 s^3 x z^2 + g_2 s^4 z^3,$$

where g_2 and f_3 are respectively sections of $\mathscr{O}_{\mathbb{P}^1}(2)$ and $\mathscr{O}_{\mathbb{P}^1}(3)$. The $\mathrm{IV}^{*\mathrm{ns}}$ fiber degenerates further at the two points $g_2 = 0$. Over these points we have the non-Kodaira fiber of type $1 - 2 - 3 - 4 - 2$, each carrying the weights of the representation 26.

8.7.4 Geometry of fibral divisors in the case of frozen representations

The case of an F_4-model with both representations frozen has been recently studied in [91]. Such a model does not have any charged hypermultiplets as explained first in [240]. It follows from the geometry of the crepant resolution, the generic fiber over the base curve S does degenerate at two points $V(g_2)$. Our description is consistent with the analyses of [142, 143, 240] and the Hirzebruch surfaces identified in [91].

We discuss in detail the geometry of the fibral divisors of an F_4-model in the case where all representations are frozen. This means that S is a curve of genus zero and self-intersection -5. For

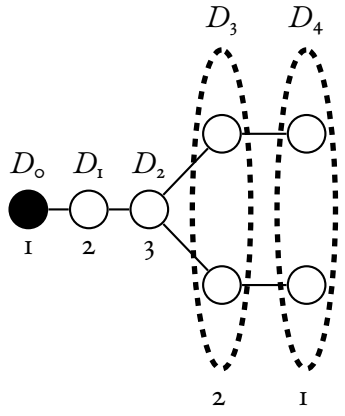

D_0 : $\mathbb{F}_3$ with base S

D_1 : $\mathbb{F}_1$ with base S

D_2 : $\mathbb{F}_1$ with base S

D_3: $\mathbb{F}_6$ with base S'

D_4: $\mathbb{F}_8$ with base S'

(S': double cover of S branched at two points ($g_2 = 0$) with S a -5-curve.)

Figure 8.5: Fibral divisors of an F_4-model as schemes over S a curve of self-intersection -5. See Lemma 8.7.8. The Stein factorization gives a morphism $f_i' : D_i \to S'$ with connected fibers and a finite morphism $\pi : S' \to S$ that is a double cover branched at the two points $g_2 = 0$ of S. Hence S' is also a rational curve. The morphisms $f_3' : D_3 \to S'$ and $f_4' : D_4 \to S'$ define, respectively, an $\mathbb{F}_6$ and an $\mathbb{F}_8$ with base curve S'. The prepotential of the five-dimensional theory is obtained from this geometry by removing the Kahler modulus φ_0 associated to the affine node in the F_4 Dynkin diagram of the elliptic fibration.

example, the base could be $\mathbb{F}_5$ or the total space of $\mathscr{O}_{\mathbb{P}^1}(-5)$. The key is Theorem 8.4.1, which we specialize to this situation in the following lemma.

Lemma 8.7.8. *Let $S \subset B$ be a smooth rational curve of self-intersection -5. An F_4-model over B with gauge group supported on S has fibral divisors D_0, D_1, D_2, D_3 and D_4 such that $D_0 \to S$, $D_1 \to S$, $D_2 \to S$ are respectively, Hirzebruch surfaces $\mathbb{F}_3$, $\mathbb{F}_1$, and $\mathbb{F}_1$. $D_3 \to S$ and $D_4 \to S$ are not Hirzebruch surfaces over S but double covers of $\mathbb{F}_3$ and $\mathbb{F}_4$ Hirzebruch surfaces. Considering the Stein factorization $D_3 \xrightarrow{f} S' \xrightarrow{\pi} S$ and $D_4 \xrightarrow{f} S' \xrightarrow{\pi} S$ where $S' \xrightarrow{\pi} S$ is a double cover of S branched at two points. The morphism $D_3 \xrightarrow{f} S'$ presents D_3 as an Hirzebruch surface $\mathbb{F}_6$ over S' and $D_4 \xrightarrow{f} S'$ presents D_4 as a Hirzebruch surface $\mathbb{F}_8$ over S'.*

Proof. We use Theorem 8.4.1. The Calabi–Yau condition implies that $\mathscr{L} = \mathscr{O}(-K_B)$. D_0, D_1, and D_2 are Hirzebruch surfaces. We compute their degrees by intersection theory as follows. We recall that for a Hirzebruch surface $\mathbb{F}_n = \mathbb{F}_{-n}$. We follow the following strategy. Given two line bundles $\mathscr{L}_1$ and $\mathscr{L}_2$ and a Hirzebruch surface $\mathbb{P}_S[\mathscr{L}_1 \oplus \mathscr{L}_2] \to S$ over a smooth rational curve S, then the degree of the Hirzebruch surface is $\deg\mathscr{L}_1 - \deg\mathscr{L}_2 = \int_S c_1(\mathscr{L}_1) - \int_S c_1(\mathscr{L}_2)$. We know that D_0 is $\mathbb{P}_S[\mathscr{L} \oplus \mathscr{O}_S]$. To compute the degree of this Hirzebruch surface, we compute $\int_S c_1(\mathscr{L}) = -S \cdot K_B = -3$. that is, D_0 is an $\mathbb{F}_3$. We know that D_1 is $\mathbb{P}_S[\mathscr{L}^{\otimes 2} \oplus \mathscr{S}]$, which is isomorphic to $\mathbb{P}_S[\left(\mathscr{L}^{\otimes 2} \otimes \mathscr{S}^{-1}\right) \oplus \mathscr{O}_S]$.

To compute the degree of this Hirzebruch surface, we compute $\int_S [2c_1(\mathscr{L}) - S] = S \cdot (-2K_B - S) = -6 + 5 = -1$. Hence $D_1 \to S$ is an $\mathbb{F}_1$. D_2 is $\mathbb{P}_S[\mathscr{L}^{\otimes 3} \oplus \mathscr{S}^{\otimes 2}]$, which is a Hirzebruch surface of degree $S \cdot (-3K_B - 2S) = -9 + 10 = 1$. Hence, $D_2 \to S$ is also an $\mathbb{F}_1$. As is clear from the crepant resolution, the fibral divisors $D_3 \to S$ and $D_4 \to S$ are not Hirzebruch surfaces over S. Their fibers consist of two generically disconnected rational curves ramified over $R = V(s, g_2)$. They can be respectively described as double covers of a $\mathbb{P}_S[\mathscr{L}^{\otimes 4} \oplus \mathscr{S}^{\otimes 3}]$ and a $\mathbb{P}_S[\mathscr{L}^{\otimes 2} \oplus \mathscr{S}^{\otimes 2}]$; These are isomorphic to, respectively, $\mathbb{F}_3$ and $\mathbb{F}_4$. In each case, the branch locus of the double cover consists of two fibers of the Hirzebruch surface, and these are the fibers over $V(g_2)$.

The absence of charged multiplets is justified by the phenomena of frozen representations rather than the absence of degenerations supporting the weights of the representation 26. The Stein factorization of $D_3 \to S$ is

$$D_3 \xrightarrow{f} S' \xrightarrow{\pi} S,$$

where $S' \xrightarrow{\pi} S$ is a double cover branched at two points and $f : D_3 \to S'$ is a proper morphism with connected fibers. In particular, $f : D_3 \to S'$ is a $\mathbb{P}^1$-bundle. Since S' has genus zero, this is a Hirzebruch surface. The degree of this Hirzebruch surface is $\int_{D_3} S'^2$, which is $2\int_{\mathbb{F}_3} S^2 = 2 \cdot (-3) = -6$. Hence $f : D_3 \to S'$ is an $\mathbb{F}_6$-surface.

We show in the same way that $f : D_3 \to S'$ is an $\mathbb{F}_8$-surface. In other words, while $D_3 \to S$ and $D_4 \to S$ are not $\mathbb{P}^1$-bundles over S, $D_3 \to S'$ and $D_3 \to S'$ are $\mathbb{P}^1$-bundles over S'. As discussed in the appendix, with respect to S', D_3 and D_4 have the structure of an $\mathbb{F}_6$ and an $\mathbb{F}_8$ since the base curve S' has self-intersection. □

8.8 Conclusion

In this chapter, we studied the geometry of F_4-models. Our starting point is a singular Weierstrass model characterized by the valuations with respect to a smooth divisor $S = V(s)$ given by Step 8 of Tate's algorithm:

$$v_S(a_1) \geq 1, \quad v_S(a_2) \geq 2, \quad v_S(a_3) \geq 2, \quad v_S(a_4) \geq 3, \quad v_S(a_6) \geq 3, \qquad v_S(b_6) = 4.$$

The last condition ensures that the polynomial $Q(T) = T^2 + a_{3,2}T - a_{6,4}$ has two distinct solutions modulo s. The F_4 model is characterized by the fact that $Q(T)$ has no rational solutions modulo s. When $Q(T)$ has rational solutions, we have an E_6-model. The generic fiber over S is called a fiber of type IV^{*ns}. Without loss of generality, the Weierstrass model can be written in the following canoni-

cal form:

$$y^2z = x^3 + a_{4,3+\alpha}s^{3+\alpha}xz^2 + a_{6,4}s^4z^3, \quad \alpha \in \mathbb{Z}_{\geq 0}.$$

A crepant resolution of this Weierstrass model is called an F_4-model. Such elliptic fibrations are used to engineer F_4 gauge theories in F-theory and M-theory. While it is common to take $\alpha = 0$ in the F-theory literature, here, we keep α unfixed to keep the geometry as general as possible. This allows us to cover local enhancements of the type $F_4 \to E_7$ and $F_4 \to E_8$ over $s = a_{6,4} = 0$, depending on the valuation of a_4. While the generic fiber is a twisted affine Dynkin diagram $\tilde{F}_4^t$, the geometric fiber is the affine $\tilde{E}_6$ diagram. Thus we have the natural enhancement $F_4 \to E_6$, which is non-local and appears over any closed point of S away from $a_{6,4} = 0$.

The crepant resolution that we have considered consists of a sequence of four blowups centered at regular monomial ideals. We answered several questions regarding the geometry and topology of the resulting smooth elliptic fibration. In particular, we identified the geometry of the fibral divisors of the F_4-model as $\mathbb{P}^1$-bundles for the three divisors D_0, D_1, and D_2, while the remainders, namely D_3 and D_4, are double-coverings of $\mathbb{P}^1$-bundles with discriminant locus $a_{6,4} = 0$. This is illustrated in Figure 8.2. The singular fibers of these conic bundles consist of double lines and play an important role in determining the geometry of the singular fiber over $s = a_{6,4} = 0$, which is a non-Kodaira fiber of type $1 - 2 - 3 - 4 - 2$. This fiber can be thought of as an incomplete E_7 or E_8 if $v(a_4) = 3$ or $v(a_4) \geq 4$, respectively.

To identify the representation associated with this singular fiber over $s = a_{6,4} = 0$, we computed the intersection numbers of the new rational curves with the fibral divisors. These intersection num-

bers are interpreted as weights of F_4. We identified the corresponding representation as the 26 of F_4. We also compute the triple intersection number of the fibral divisors. We finally specialize to the case of Calabi–Yau threefolds. The Euler characteristic of an F_4-model and the Hodge numbers in the Calabi–Yau threefold case have been presented in [114]. We also computed the linear form induced by the second Chern class.

In the final section, we studied details of M-theory compactified on a Calabi–Yau threefold that is an F_4-model, for which the resulting theory is a five-dimensional gauge theory with eight supercharges. Such a theory has vector multiplets characterized by a cubic prepotential. The classical part of the cubic prepotential vanishes but there is a quantum correction coming from an exact one-loop contribution [176]. This one-loop term depends explicitly on the number of charged hypermultiplets. It is known that this correction term matches exactly with the triple intersection numbers of the fibral divisors of the elliptic Calabi–Yau threefold. We computed the number of hypermultiplets in the adjoint representation and in the fundamental representation via a direct comparison:

$$n_{52} = g, \quad n_{26} = 5(1-g) + S^2.$$

We checked that also satisfy the genus formula of Aspinwall-Katz-Morrison– here they are derived from the triple intersection numbers. With the knowledge of the Hodge numbers [114], matter representation, and their multiplicities, we compared this with the unique solution of the number of charged hypermultiplets in a F-theory compactification to a six-dimensional $(1, 0)$ supergravity theory free of gravitational, gauge, and mixed anomalies following Sadov [269]. In the six-dimensional

(1, 0) theory, they they appear as part of the unique solutions to the anomaly cancelation conditions and also match the results in [142].

We also computed the weights of vertical curves of an F_4 models and proved that over the locus $V(s, a_{6,4})$ the generic fiber over the divisor S has weights of the quasi-minuscule representation 26. We introduced the notion of a *frozen representation*, which explains that the existence of geometric weights carried by vertical curves does not imply the existence of hypermultiplets charged under the corresponding representation. If the base is a surface, the divisor S is a curve. The representation 26 is frozen if and only if S has genus zero and self-intersection -5. Frozen representations happen for other G-models as illustrated in [112, 119, 122].

How can it be that mathematics, a product of human thought independent of experience, is so admirably adapted to the objects of reality?

Albert Einstein

9

The Geometry of G_2, Spin(7), and Spin(8)-models

In this chapter, we study the geometry of the Kodaira fiber of type I_0^*, which has at least three unique properties that is distinguishable from all other Kodaira fibers. Firstly, the I_0^* fiber shares with smooth elliptic curves that it can have a j-invariant of any value in the ground field of the elliptic

fibration. On the other hand, all other singular Kodaira fibers have a j-invariant taking the values 0 or 1728, with the exceptions of the Kodaira fiber $\mathrm{I}^*_{n>0}$ and $\mathrm{I}_{n>0}$, whose j-invariant has a pole and takes an infinite value.

Secondly, while all the other Kodaira fibers have at most two splitting types: split and non-split. The fiber I^*_0 distinguishes itself by having three splitting types — split, semi-split, and non-split — corresponding to three distinct Lie algebras, namely G_2, B_3, and D_4. As we assume that the Mordell-Weil group is trivial, these three Lie algebras correspond to the simply-connected groups G_2, Spin(7), and Spin(8). It is also more natural to distinguish two different versions of the non-split case, since there are two possible Galois groups which give rise to distinct fiber degenerations, as we shall explain below.

Lastly, the fiber of type I^*_0 plays a central role in Miranda's models [236] and in the classification of "non-Higgsable clusters" [240]. The fiber I^*_0 appears in collisions of the types $j = 0$ (namely II+I^*_0 and IV+I^*_0) and $j = 1728$ (namely III+I^*_0) [236]. These collisions are building blocks for the non-Higgsable clusters of elliptically-fibered Calabi–Yau threefolds [240]. For example, an isolated curve of self-intersection -4 can support a Kodaira fiber of type I^*_0 and an associated Lie algebra $\mathfrak{so}_8$ with a trivial representation. There are also three building blocks consisting of two or three rational curves of negative self-intersection intersecting transversally. We write $(-n_1, -n_2, -n_3, \ldots, -n_r)$ for a chain of r rational curves C_i, with $1 \leq i \leq r$, where $C_i^2 = -n_i$ and two consecutive curves in the chain intersect transversally. A $(-2, -3)$-chain corresponds to the collision of two Kodaira fibers of type III and I^*_0, yielding a semi-simple Lie algebra $\mathfrak{sp}_1 \oplus \mathfrak{g}_2$ [240]. A $(-2, -2, -3)$-chain corresponds to the chain of Kodaira fibers II+IV+I^*_0, supporting the Lie algebra $\mathfrak{su}_2 \oplus \mathfrak{g}_2$, and the

collisions of this type is studied geometrically in [119]; finally, a $(-2,-3,-2)$-chain corresponds to the chain of Kodaira fibers III+I_0^*+III, yielding a Lie algebra $\mathfrak{su}_2 \oplus \mathfrak{so}_7 \oplus \mathfrak{su}_2$ [240].

Fiber type	Dual graph	Splitting type	Field extension $[\kappa' : \kappa]$
$\mathrm{I}_0^{*\mathrm{ns}}$ $\widetilde{\mathrm{G}}_2^t$	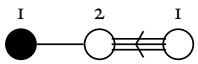	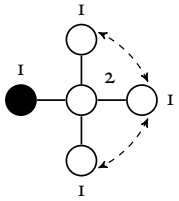	3 or 6
$\mathrm{I}_0^{*\mathrm{ss}}$ $\widetilde{\mathrm{B}}_3^t$	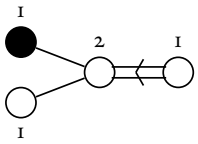	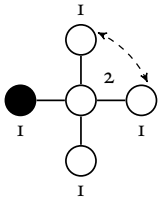	2
$\mathrm{I}_0^{*\mathrm{s}}$ $\widetilde{\mathrm{D}}_4$	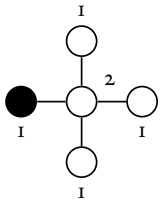	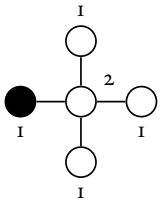	1

Table 9.1: Fibers of type I_0^*. There are three different possible types based on its field extensions, which yield three different Dynkin diagrams respectively.

.

The geometry and topology of an I_0^*-model is subtle. To fully appreciate the geometry of a Weierstrass model describing the fiber I_0^*, one has to take into account the scheme structure of the generic fiber. This scheme structure contains more detailed information than can be seen by the type of the geometric fiber and impacts the values of the topological invariants. Fiber types, generic fibers, and geometric irreducibility play a central role in this chapter. See Appendix C of [114] for a review.

The type of a singular fiber depends on the ground field used to define its scheme structure. For

the fiber over the generic point of an irreducible component of the discriminant locus, the natural ground field is the residue field of the generic point [219, §3.1.2, Remark 1.17]. This is because in scheme theory, the fiber over a point p is by definition $Y \times_B Spec\ \kappa(p)$ [219, §3.1.2, Definition 1.13] and the second projection $Y_p \to Spec\ \kappa(p)$ gives the fiber Y_p the structure of a scheme defined with the residue field $\kappa(p)$ as its ground field. As the residue field $\kappa(p)$ is not necessarily an algebraically closed field, the fiber type of Y_p as a scheme over $\kappa(p)$ does not always match its Kodaira type. We recall that a Kodaira fiber is by definition a geometric fiber.[1] The Kodaira type of Y_p is seen only after a field extension causing all components of the fiber to become geometrically irreducible. In the case of Weierstrass models coming from Tate's algorithm, the required field extension is carefully described in Tate's algorithm to be the splitting field of an appropriate cubic or quadratic polynomial defined from the Weierstrass coefficients. For elliptic fibrations, the type of a generic fiber Y_p that is not geometric is either an affine Dynkin diagram of type $\widetilde{\mathrm{A}}_1$, or a twisted affine Dynkin diagram of type $\widetilde{\mathrm{G}}_2^t$, $\widetilde{\mathrm{B}}_{3+n}^t$, $\widetilde{\mathrm{F}}_4^t$, or $\widetilde{\mathrm{C}}_{2+n}^t$.

A fiber of type I_0^* consists of a rational curve of multiplicity two intersecting transversally with four other rational curves. Its dual graph is the affine Dynkin diagram $\widetilde{\mathrm{D}}_4$. One of the four is the component touching the section of the elliptic fibration. The points of intersection between the central node of multiplicity two and the other three nodes (see Table 9.1 for the Dynkin diagram for these nodes) can be described by a cubic polynomial that is essentially the auxiliary polynomial $P(T)$. The elliptic fibration is called the G_2, Spin(7), or Spin(8)-model, respectively, if $P(T)$ has no

[1] A geometric fiber is such that its components are all geometrically irreducible, i.e. they do not factor into more components even after a field extension [219, §3.2, Definition 2.8].

κ-rational roots, a unique κ-rational root, or three distinct κ-rational roots. The generic fibers over S are then denoted by

$$\mathrm{I}_0^{*\mathrm{ns}},\ \mathrm{I}_0^{*\mathrm{ss}},\ \text{and}\ \mathrm{I}_0^{*\mathrm{s}},$$

where "ns", "ss", and "s" stand for "non-split", "semi-split", and "split" [37]. The fibers $\mathrm{I}_0^{*\mathrm{ns}}$, $\mathrm{I}_0^{*\mathrm{ss}}$, and $\mathrm{I}_0^{*\mathrm{s}}$ defined with respect to the residue field κ are called *arithmetic fibers*; this distinguishes them from their geometric fiber I_0^* defined in the splitting field of $P(T)$.

In fact, the Galois group $\mathrm{Gal}(\kappa'/\kappa)$ is trivial for Spin(8)-models, $\mathbb{Z}/2\mathbb{Z}$ for Spin(7)-models, and can be either the symmetric group S_3 or the cyclic group $\mathbb{Z}/3\mathbb{Z}$ for G_2-models. Thus, the Galois group provides a finer invariant than the number of rational solutions of $P(T)$. We introduce the notion of $\mathrm{G}_2^{S_3}$-models and $\mathrm{G}_2^{\mathbb{Z}/3\mathbb{Z}}$-models to distinguish between the two cases of a G_2-model as they have different fiber structures. One can think of the $\mathrm{G}_2^{\mathbb{Z}/3\mathbb{Z}}$-model as a specialization of the $\mathrm{G}_2^{S_3}$-model in which the discriminant $\Delta(P)$ of the auxiliary polynomial $P(T)$ is a perfect square in the residue field κ. The difference of these two models are easily viewed in algebrac form given in Section 9.2.1.

We show the existance and numbers of of crepant resolutions of each model:

1. Each G_2-model has a unique crepant resolution,
2. Each Spin(7)-model has two crepant resolutions connected by a simple flop,
3. Each Spin(8)-model has six distinct crepant resolutions forming a cycle— under conditions that ensure the existence of crepant resolutions.

Figures 9.2, 9.3, and 9.4 on page 401 depict the structure of the set of crepant resolutions in relationship to the geometry of the Coulomb branch. (For a review of Coulomb branch and flops, see Section 2.4.2 in the introduction.)

When the Weierstrass coefficients vanish to high order along the component S of the discriminant locus, $\mathbb{Q}$-factorial terminal singularities are obstructions to the existence of a crepant resolution depending on the dimension of the base B.[2] See Section 9.3.3 for the case of the G_2-model and Section 9.4.1 for the case of terminal singularities with the Spin(7)-model. In contrast, crepant resolutions were recently shown to exist in [115] for F_4-models for generic coefficients of arbitrary valuations, as long as the restrictions of Step 7 of Tate's algorithm are satisfied. We also show by direct inspection that each of the crepant resolutions we obtained determines a flat fibration.

In this chapter, we consider elliptic fibrations over bases of arbitrary dimensions. For F-theory and M-theory applications, we focus mostly on compactifications yielding five and six-dimensional gauge theories. In particular, we do not discuss Sen's weak coupling limit of these theories. However, we point out that the weak coupling limit of G_2, Spin(7), and Spin(8)-models gives a local $\mathfrak{so}(8)$-gauge theory realized by eight D7 branes on top of an O7 orientifold [123, Table 4]. Such an $\mathfrak{so}(8)$-gauge theory can also be constructed using K-theory as in [78, §4.2.4].

9.0.1 Non-Kodaira fibers and Tate's algorithm in higher codimension

The study of the fiber structure of G_2, Spin(7), and Spin(8)-models is surprisingly rich in non-Kodaira fibers. We get eight types of non-Kodaira fibers in the fiber degenerations of these elliptic

[2] The $\mathbb{Q}$-factorial terminal singularities have been discussed recently in F-theory in [17].

fibrations. They are listed in Figure 9.1. To put this in perspective, we recall that in the theory of Miranda's models, there are only seven non-Kodaira fibers across all possible collisions, while here, the Spin(7)-model on its own already produces six non-Kodaira fibers. Miranda has observed that non-Kodaira fibers of Miranda's models of elliptic threefolds [236] are contractions of Kodaira fibers (see also [76]). Here we see that this is also true in higher codimension for the crepant resolutions of the Weierstrass model resulting from Step 6 of Tate's algorithm.

With a careful study of the crepant resolutions of the Weierstrass models resulting from Step 6 of Tate's algorithm, it is possible to predict (for Step 6) the possible higher codimension fibers from the valuations of the coefficients of Weierstrass equations. In many cases, these valuations do not completely determine the fiber type: different crepant resolutions of the same Weierstrass model can have distinct fiber types over points of codimension two or higher.

9.0.2 Road map to the rest of the chapter

The rest of the chapter is organized as follows. We review Step 6 of Tate's algorithm that characterizes the Kodaira fiberof type I_0^* in Section 9.1. In Section 9.2 we summarize the main mathematical results of the chapter. We first derive canonical forms for G_2, Spin(7), and Spin(8)-models in Section 9.2.1 by scrutinizing Step 6 of Tate's algorithm. We distinguish between two types of G_2-models using the Galois group of the splitting field of the associated polynomial $P(T)$ used in Step 6 of Tate's algorithm. They have distinct fiber structures and j-invariants over S. We also distinguish between two Weierstrass models for Spin(7)-models by their fiber degenerations and their j-invariants over S. We then study the existence of crepant resolutions for these canonical forms and determine the fiber

structure for each resolution. We compute the Chern–Simons coefficients as the triple intersection numbers of the fibral divisors in Section 9.2.6. We study G_2-models in Section 9.3, Spin(7)-models in Section 9.4, and Spin(8)-models in Section 9.5. In Section 9.6, we apply the results collected in the previous sections to describe the physics of the I_o^* models. In Section 9.6.1, we compute the one-loop prepotential and compute the number of hypermultiplets transforming in each irreducible representations of the gauge group. In section 9.6.2, we also count the number of representations of each model by comparing the triple intersection numbers and the cubic prepotential, and show in section 9.6.2 that the number of representations found are identical to the unique solution on the number of hypermultiplets of the anomaly cancellation conditions of the six-dimensional theory; hence, we determine that the five-dimensional theories are compatible with an anomaly-free six-dimensional theories. The counting matches the number found by Grassi and Morrison [142] using six-dimensional anomaly cancellation conditions and Witten's quantization method (as generalized by Aspinwall, Katz and Morrison) [1].

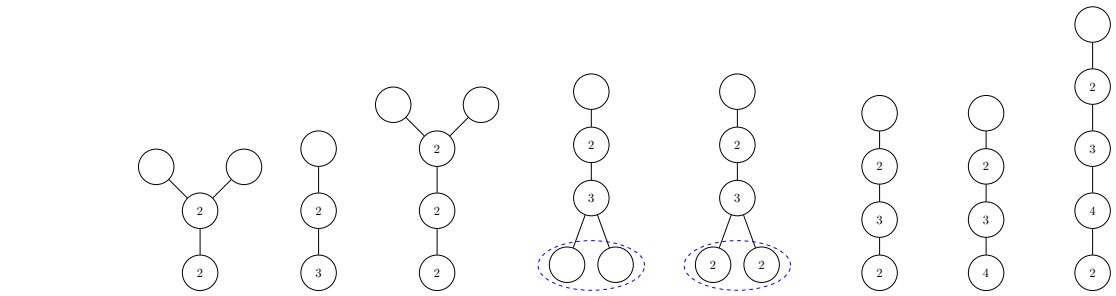

G_2	✓	✓						
Spin(7)	✓		✓	✓	✓	✓	✓	
Spin(8)							✓	✓

Figure 9.1: Non-Kodaira fibers appearing in the fiber structures of G_2, Spin(7), and Spin(8)-models. Certain non-Kodaira fibers appear more than once, and all of them are of the type of contracted nodes.

9.1 Step 6 of Tate's algorithm characterizing the fiber I_0^*

Tate's algorithm consists of eleven steps (see [290], [281, §IV.9], [256], and [286, §4.8]).[3] Step 6 of Tate's algorithm characterizes the fiber of Kodaira type I_0^*. We start with a general Weierstrass equation

$$y^2z + a_1xyz + a_3yz^2 = x^3 + a_2x^2z + a_4xz^2 + a_6z^3.$$

[3] In F-theory, Tate's algorithm is discussed in [37, 186, 244], but usually focuses on the minimal valuations of the coefficients of the Weierstrass equation. Hence, we use instead the original paper of Tate [290], which contains some typos that are listed and corrected in in [256].

Néron proved in [251] that a Weierstrass model over a discrete valuation ring has a special fiber of type I_0^* (denoted by C_4 in Néron's notation) if and only if the discriminant

$$\Delta(x^3 + a_2x^2 + a_4x + a_6) = -4a_2^3a_6 + a_2^2a_4^2 + 18a_2a_4a_6 - 4a_4^3 - 27a_6^2$$

has valuation 6 with respect to S, and the valuation of the Weierstrass coefficients satisfies the following inequalities:

$$v_S(a_1) \geq 1, \quad v_S(a_2) \geq 1, \quad v_S(a_3) \geq 2, \quad v_S(a_4) \geq 2, \quad v_S(a_6) \geq 3. \tag{9.1}$$

This case is further studied by Tate in Step 6 of his algorithm [290]. Tate defines the following auxiliary cubic polynomial in the polynomial ring $\kappa[T]$ to be

$$P(T) = T^3 + a_{2,1}T^2 + a_{4,2}T + a_{6,3}, \tag{9.2}$$

where $a_{i,j} = a_i/s^j$. The splitting field of the cubic $P(T)$ in κ is denoted by κ'. The discriminant $\Delta(P)$ of $P(T)$ is

$$\Delta(P) := 4a_{2,1}^3a_{6,3} - a_{2,1}^2a_{4,2}^2 - 18a_{2,1}a_{4,2}a_{6,3} + 4a_{4,2}^3 + 27a_{6,3}^2.$$

The polynomial $P(T)$ is separable in κ if and only if $P(T)$ has three distinct roots in κ'. This is the case if and only if the discriminant $\Delta(P)$ of $P(T)$ has valuation zero. This condition is equivalent to Néron's requirement discussed above. In view of the inequalities in equation (9.1), the discriminant

of the full Weierstrass equation has valuation 6 if and only if the valuation of $\Delta(P)$ is zero. The type of the geometric fiber is the same as the type of the fiber as seen in the splitting field κ' of the polynomial $P(T)$ in κ. The type of the special fiber as a scheme over κ depends on the degree $[\kappa' : \kappa]$ of the field extension κ'/κ:

- $[\kappa' : \kappa] = 6 \implies \mathrm{I}_0^{*\mathrm{ns}}$ with Galois group S_3 and dual graph $\widetilde{G}_2^t$,
- $[\kappa' : \kappa] = 3 \implies \mathrm{I}_0^{*\mathrm{ns}}$ with Galois group $\mathbb{Z}/3\mathbb{Z}$ and dual graph $\widetilde{G}_2^t$,
- $[\kappa' : \kappa] = 2 \implies \mathrm{I}_0^{*\mathrm{ss}}$ with Galois group $\mathbb{Z}/2\mathbb{Z}$ and dual graph $\widetilde{\mathrm{B}}_3^t$,
- $[\kappa' : \kappa] = 1 \implies \mathrm{I}_0^{*\mathrm{s}}$ with trivial Galois group and dual graph $\widetilde{\mathrm{D}}_4$,

where "*ns*", "*ss*", and "*s*" stand for *non-split*, *semi-split*, and *split*, respectively [37].[4]

If the discriminant of $P(T)$ does not have a κ-rational root, then the fiber is of type $\mathrm{I}_0^{*\mathrm{ns}}$ with dual graph $\widetilde{G}_2^t$. If $P(T)$ has a unique κ-root, then the fiber is of type $\mathrm{I}_0^{*\mathrm{ss}}$ with dual graph $\widetilde{\mathrm{B}}_3^t$. If $P(T)$ has three κ-roots, then the fiber is of type $\mathrm{I}_0^{*\mathrm{s}}$ with dual graph $\widetilde{\mathrm{D}}_4$.

There are two cases of fibers $\mathrm{I}_0^{*\mathrm{ns}}$, depending on whether the Galois group of the field extension κ'/κ is either $\mathbb{Z}/3\mathbb{Z}$ or S_3. The two cases differ by the behavior of the discriminant of $P(T)$ in view of the following well-known theorem.

Lemma 9.1.1 (Galois group of a cubic polynomial)**.** *The Galois group of the splitting field of a separable cubic polynomial $P(T)$, defined over a field κ of characteristic different from 2 and 3, is*

1. *S_3 if and only if the $P(T)$ is κ-irreducible and its discriminant is not a perfect square.*
2. *$\mathbb{Z}/3\mathbb{Z}$ if and only if $P(T)$ is κ-irreducible and its discriminant is a perfect square.*

[4] In the notation of Liu [219, §10.2], the fibers $\mathrm{I}_0^{*\mathrm{ns}}$, $\mathrm{I}_0^{*\mathrm{ss}}$, and $\mathrm{I}_0^{*\mathrm{s}}$ are denoted by $\mathrm{I}_{0,3}^*$, $\mathrm{I}_{0,2}^*$, and I_0^*, respectively.

3. *$\mathbb{Z}/2\mathbb{Z}$ if and only if $P(T)$ factorizes into a linear factor and a κ-irreducible quadric.*

4. *the trivial group if and only if $P(T)$ factorizes into three linear factors over κ.*

Proof. See [212, Chap. VI §2]. □

Lemma 9.1.1 provides a direct route to the classification of fibers of type $\mathrm{I}_0^{*\mathrm{s}}$, $\mathrm{I}_0^{*\mathrm{ss}}$, and $\mathrm{I}_0^{*\mathrm{ns}}$ using the Galois group of the splitting field of $P(T)$. A more refined classification will also take into account the values of the *j*-invariant. In contrast to other singular Kodaira fibers, the fiber of type I_0^* can take any finite value of the *j*-invariant. However, for the arithmetic fibers, there are some restrictions. For example, a fiber of type $\mathrm{I}_0^{*\mathrm{ss}}$ cannot have $j = 0$.

9.2 Summary of results

In this section, we summarize the main mathematical results of the chapter. We first list the obtained canonical forms as well as the values of the j-invariant in Section 9.2.1. We then identify the crepant resolutions of G_2, Spin(7), and Spin(8)-models as sequences of blowups in Section 9.2.2. The hyperplane arrangements of these models — $\mathrm{I}(G_2, 7)$, $\mathrm{I}(B_3, 7 \oplus 8)$, and $\mathrm{I}(D_4, 8_v \oplus 8_c \oplus 8_s)$ — are given in Section 9.2.3. The crepant resolutions and the chambers of the hyperplane arrangements of each model are shown to be matched perfectly, which is described in section sec:matching.

In Section 9.6, we discuss the physical implications of our results for five- and six-dimensional gauge theories obtained from of F-theory and M-theory compactifications.

9.2.1 Canonical forms and crepant resolutions for G_2, Spin(7), and Spin(8)-models

We summarize the canonical forms for G_2, Spin(7), and Spin(8)-models from Step 6 of Tate's algorithm. These forms are derived in Theorems 9.3.1, 9.4.1, and 9.5.1. We assume that the Mordell-Weil group of the elliptic fibrations is trivial. Using Step 6 of Tate's algorithm, we obtain the Weierstrass model describing a Kodaira fiber of type I_0^* over the generic point of $S = V(s)$. This model takes one of the following forms below, which are organized by the fiber type when seen as a scheme over the residue field of S, as well as the value of the j-invariant:

- $\mathrm{G}_2^{S_3}: \quad y^2z - x^3 - s^2fxz^2 - s^3gz^3 = 0, \quad fg \neq 0, \quad j \neq 0, 1728,$ (9.3)

where $4f^3 + 27g^2$ is not a perfect square modulo s.

- $\mathrm{G}_2^{\mathbb{Z}/3\mathbb{Z}}: \quad y^2z - x^3 - s^2fxz^2 - s^3gz^3 = 0, \quad fg \neq 0, \quad j \neq 0, 1728,$ (9.4)

where $4f^3 + 27g^2$ is a perfect square modulo s. In particular, the following $\mathrm{G}_2^{\mathbb{Z}/3\mathbb{Z}}$-model is uniquely specified by the valuations of the coefficients:

- $\mathrm{G}_2^{\mathbb{Z}/3\mathbb{Z}}: \quad y^2z - x^3 - s^{3+\alpha}fxz^2 - s^3gz^3 = 0, \quad \alpha \in \mathbb{Z}_{\geq 0} \quad j = 0,$ (9.5)

where g is not a cube modulo s;

- Spin(7) : $y^2z - (x^3 + a_{2,1}sx^2z + a_{4,2}s^2xz^2 + a_{6,4}s^{4+\beta}z^3) = 0, \quad \beta \in \mathbb{Z}_{\geq 0}, \quad j \neq 0, 1728,$ (9.6)

where $a_{2,1}$ is not proportional to s;

- Spin(7) : $y^2z - x^3 - s^2fxz^2 - s^{4+\beta}gz^3 = 0, \quad \beta \in \mathbb{Z}_{\geq 0}, \qquad j = 1728,$ (9.7)

where f is not a square modulo s;

- Spin(8) : $y^2z = (x - sx_1z)(x - sx_2z)(x + sx_3z) - s^{2+\alpha}Qz, \quad Q = rx^2 + qsxz - s^2tz^2, \quad \alpha \in \mathbb{Z}_{\geq 0},$ (9.8)

where $\quad v_S((x_1 - x_2)(x_1 - x_3)(x_2 - x_3)) = 0$ and $(r, q, t) \neq (0, 0, 0)$.

The j-invariant of a Spin(8)-model is

$$\begin{cases} j = 1728\frac{A^3}{B^3 - C^2} = 1728 - \frac{A^2}{A^3 - B^2}, \\ A = -16(-x_1^2 - x_2^2 - x_3^2 + x_1x_2 + x_1x_3 + x_2x_3), \\ B = 32(-2x_1 + x_2 + x_3)(x_1 - 2x_2 + x_3)(x_1 + x_2 - 2x_3). \end{cases} \tag{9.9}$$

In particular, $j = 0$ when $A = 0$ and $j = 1728$ when $B = 0$.

In contrast to the usual forms seen in the F-theory literature, we do not restrict to the minimal

values for the valuations of the coefficients. Allowing more general valuations enables a richer set of behaviors for the degeneration and the values of the j-invariant. In the case of Spin(7), depending on the dimension of the base, the valuations can become an obstruction to the existence of a crepant resolution when they are too big.

9.2.2 Crepant resolutions

The following sequences of blowups provide crepant resolutions for the Weierstrass models defined in section 9.2.1. These are, however, valid only under some conditions which will be discussed in Theorems 9.3.2, 9.4.2, and 9.5.2. In some cases, the non-minimal valuations obstruct the existence of a crepant resolution. We assume that the coefficients of the Weierstrass models are general except for their valuations with respect to S. To prove smoothness, we also have to impose some light con-

ditions on the coefficients that are usually left unspecified in the F-theory literature.

Goup Crepant resolutions

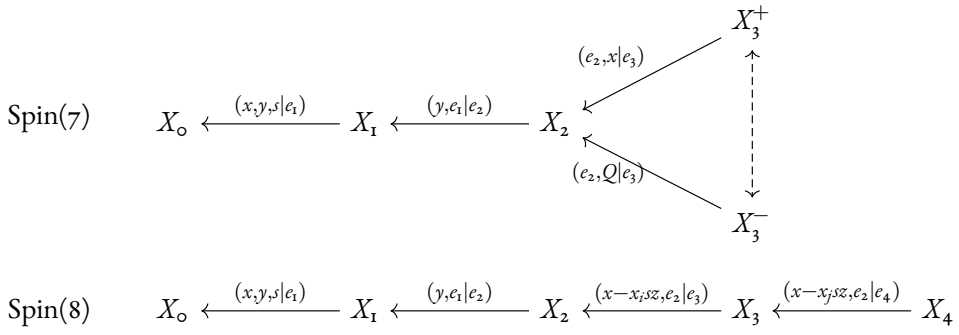

(9.10)

For Spin(8), i, j are two distinct elements of $\{1, 2, 3\}$ and hence define six distinct crepant resolutions. We have two distinct crepant resolutions for Spin(7), and a unique one for G_2.

9.2.3 Hyperplane arrangement $I(\mathfrak{g}, \mathbf{R})$

Let $\mathfrak{g}$ be a semi-simple Lie algebra and $\mathbf{R}$ a representation of $\mathfrak{g}$. The kernel of each weight ϖ of $\mathbf{R}$ defines a hyperplane $\varpi^{\perp}$ through the origin of the Cartan sub-algebra of $\mathfrak{g}$.

Definition 9.2.1. The hyperplane arrangement $I(\mathfrak{g}, \mathbf{R})$ is defined inside the dual fundamental Weyl chamber of $\mathfrak{g}$, i.e. the dual cone of the fundamental Weyl chamber of $\mathfrak{g}$, and its hyperplanes are the set of kernels of the weights of $\mathbf{R}$.

	G_2	Spin(7)		Spin(8)
Locus	$V(s, 4f^3 + 27g^2)$	$V(s, a_{4,2})$	$V(s, a_{2,1}^2 - 4a_{4,2})$	$V(s, d)$
Weights	$\boxed{2\ -1}$	$\boxed{0\ 1\ -2}$	$\pm\boxed{1\ 0\ -1}$	$\boxed{0\ 0\ -1\ 1}$, $\boxed{-1\ 0\ 0\ 1}$, $\boxed{-1\ 0\ 1\ 0}$
$\mathbf{R}$	7	7	8	$8_v \oplus 8_s \oplus 8_c$
$\mathrm{I}(\mathfrak{g}, \mathbf{R})$	$\mathrm{I}(G_2, 7)$	$\mathrm{I}(B_3, 7 \oplus 8)$		$\mathrm{I}(D_4, 8_v \oplus 8_s \oplus 8_c)$
# of Chambers	1	2		6

For each G-model, we associate the hyperplane arrangement $\mathrm{I}(\mathfrak{g}, \mathbf{R})$ using the representation $\mathbf{R}$ induced by the weights of vertical rational curves produced by degenerations of the generic fiber over codimension-two points of the base. We then study the incidence structure of the hyperplane arrangement $\mathrm{I}(\mathfrak{g}, \mathbf{R})$.

Proposition 9.2.2. *The weights of the vertical curves over codimension-two points are given by*

The chambers of G_2, Spin(7), and Spin(8)-models are illustrated in Figures 9.2, 9.3, and 9.4 respectively on page 401 and described in the following theorem.

Theorem 9.2.3. *The hyperplane arrangement* $\mathrm{I}(G_2, 7)$ *has a unique chamber. The hyperplane arrangement* $\mathrm{I}(B_3, 7 \oplus 8)$ *has two chambers whose incidence graph is the Dynkin diagram* A_2*. The hyperplane arrangement* $\mathrm{I}(D_4, 8_v \oplus 8_c \oplus 8_s)$ *has six chambers whose incidence graph is a hexagon (the affine Dynkin diagram* $\widetilde{A}_6$*).*

Proof. A hyperplane $\varpi^\perp$ (the kernel of a weight ϖ) intersects the interior of the dual fundamental Weyl chamber of $\mathfrak{g}$ if and only if when written in the basis of positive simple roots, at least two of its coefficients have different signs. The hyperplane arrangement $\mathrm{I}(G_2, 7)$ has a unique chamber as none of its weights have coefficients of different signs in the basis of positive simple roots. The

hyperplane arrangement $\mathrm{I}(B_3, 7 \oplus 8)$ has two chambers separated by the kernel of the unique (up to a sign) weight of the representation $7 \oplus 8$; this representation is not in the cone generated by the positive simple roots, namely $\boxed{1\ 0\ -1}$. For Spin(8), each of the representations 8_v, 8_c, and 8_s has a unique weight (up to a sign) not in the cone generated by the positive simple roots. These are the following weights, written respectively for 8_v, 8_c, and 8_s in the basis of fundamental weights:

$$\varpi_4^v = \boxed{0\ 0\ -1\ 1}, \quad \varpi_4^c = \boxed{-1\ 0\ 0\ 1}, \quad \varpi_4^s = \boxed{-1\ 0\ 1\ 0}.$$

Let $\varphi = (\varphi_1, \varphi_2, \varphi_3, \varphi_4) \in \mathfrak{h}$ be a vector of the dual fundamental Weyl chamber written in the basis of simple coroots. The linear forms corresponding to the weights ϖ_4^v, ϖ_4^c, and ϖ_r^s are

$$L_1 = (\varpi_4^v, \varphi) = -\varphi_3 + \varphi_4, \quad L_2 = (\varpi_4^c, \varphi) = -\varphi_1 + \varphi_4, \quad L_3 = (\varpi_4^s, \varphi) = -\varphi_1 + \varphi_3.$$

The set of chambers of $\mathrm{I}(D_4, 8_v \oplus 8_c \oplus 8_s)$ is in bijection with the set of all possible signs of (L_1, L_2, L_3). Two chambers are adjacent to each other when the signs of (L_1, L_2, L_3) differ by one entry only. Since $L_1 + L_3 = L_2$, we can neither get the sign vector $(- + -)$ nor $(+ - +)$. It is easy to see that all the six remaining arrangements of signs are possible. In total, there are six chambers determined by the signs of L_1, L_2, and L_3 :

$$\begin{array}{l} 1.\ (- - -)\ \varphi_1 > \varphi_3 > \varphi_4, \quad 2.\ (- - +)\ \varphi_3 > \varphi_1 > \varphi_4, \quad 3.\ (- + +)\ \varphi_3 > \varphi_4 > \varphi_1, \\ 4.\ (+ + +)\ \varphi_4 > \varphi_3 > \varphi_1, \quad 5.\ (+ + -)\ \varphi_4 > \varphi_1 > \varphi_3, \quad 6.\ (+ - -)\ \varphi_1 > \varphi_4 > \varphi_3. \end{array} \tag{9.11}$$

Two chambers are said to be adjacent when they differ by the sign of only one L_i. It follows that there are six chambers organized as in Figure 9.4 on page 401. □

9.2.4 Matching the crepant resolutions and the chambers of the hyperplane arrangement

For each crepant resolution, we study the fiber structure and compute geometrically the weights of vertical curves. These weights uniquely determine a chamber. G_2-models only have one crepant resolution. For Spin(7)-models, the crepant resolution $Y^{\pm}$ corresponds to $\pm\boxed{1, 0, -1}$. For Spin(8)-models, the vertical curves give the weights $\pm L_1$, $\pm L_2$, and $\pm L_3$. The explicit matching of the chambers and the crepant resolutions is given in Table 9.2.

	Resolutions	Chambers
1	$Y^{(2,3)}$	$(---)\quad(\varphi_1 > \varphi_3 > \varphi_4)$
2	$Y^{(3,2)}$	$(--+)\quad(\varphi_3 > \varphi_1 > \varphi_4)$
3	$Y^{(3,4)}$	$(-++)\quad(\varphi_3 > \varphi_4 > \varphi_1)$
4	$Y^{(4,3)}$	$(+++)\quad(\varphi_4 > \varphi_3 > \varphi_1)$
5	$Y^{(4,2)}$	$(++-)\quad(\varphi_4 > \varphi_1 > \varphi_3)$
6	$Y^{(2,4)}$	$(+--)\quad(\varphi_1 > \varphi_4 > \varphi_3)$

Table 9.2: Matching the crepant resolutions of the Spin(8)-model with the chambers of the hyperplane arrangement $\mathsf{I}(\mathsf{D}_3, 8_v \oplus 8_s \oplus 8_c)$.

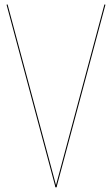

Figure 9.2: Chambers of the hyperplane arrangement $\mathsf{I}(G_2, 7)$ or equivalently, the Coulomb phases of a G_2 gauge theory with matter in the representation 7. There is a unique chamber since the non-zero weights of 7 are the short roots of G_2.

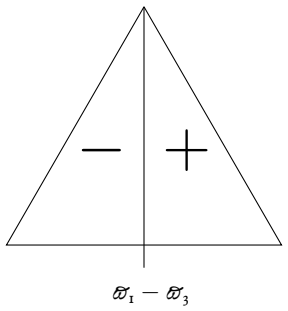

Figure 9.3: Chambers of the hyperplane arrangement $\mathsf{I}(B_3, 8)$ or equivalently, the Coulomb phases of a Spin(7) gauge theory with matter in the representation 8. The only weight defining an interior wall is the weight $\boxed{1\ 0\ -1}$ of the representation 8.

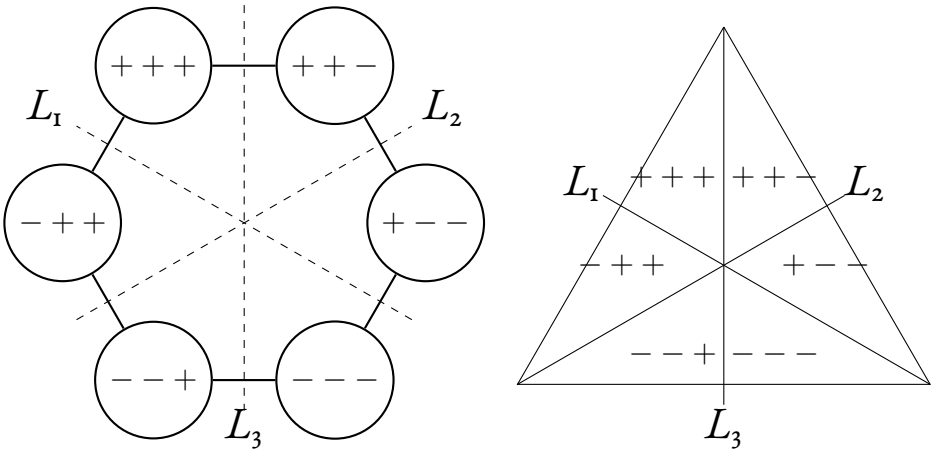

Figure 9.4: Chambers of the hyperplane arrangement $\mathsf{I}(D_4, 8_v \oplus 8_s \oplus 8_c)$ or equivalently, the Coulomb phases of a Spin(8) gauge theory with matter in the representation $8_v \oplus 8_s \oplus 8_c$. The signs in the figure are those of linear forms induced by the weights $L_1 = \boxed{0, 0, -1, 1}$, $L_2 = \boxed{-1, 0, 0, 1}$, and $L_3 = \boxed{-1, 0, 1, 0}$.

9.2.5 Fiber degenerations

The $G_2^{S_3}$-model is the generic case of a fiber of type I_0^* and has the simple fiber structure presented in Figure 9.5. In codimension two, the generic fiber with dual graph $\widetilde{G}_2^t$ degenerates to an incomplete affine Dynkin diagram of type $\widetilde{D}_5$, whose dual graph is a Dynkin diagram of type D_4. The fiber degenerates further in codimension three to a fiber of type $1-2-3$, which can be understood as an incomplete fiber of type $\widetilde{E}_6$. The $G_2^{\mathbb{Z}/3\mathbb{Z}}$-model can be realized in various ways. The model is defined in equation (9.23), and has a fiber structure with an enhancement in codimension two from $\widetilde{G}_2^t$ to an incomplete $\widetilde{E}_6$. This can be understood as a specialization of $G_2^{S_3}$ in which the codimension two fiber $\widetilde{D}_5$ does not appear and the fiber degenerates directly to an incomplete $\widetilde{E}_6$. The fiber structure of the $G_2^{\mathbb{Z}/3\mathbb{Z}}$-model defined in equation (9.24) is presented in Figure 9.6 and has two distinct fibers in codimension-two, in contrast to the other G_2-model, which has only one type of specialization in codimension two.

The generic fiber structure of a Spin(7)-model is presented in Figure 9.7. The fiber structure depends on the valuations ($v_S(a_2) \geq 1$ and $v_S(a_6) \geq 4$) and the choice of a crepant resolution. The valuations can be organized into four different cases, and we have two possible choice of crepant resolutions. Thus, there are eight distinct types of fiber structures. Two resolutions related by a flop have distinct fibers in codimension two, three, or four, depending on the valuations. We organize this information by grouping the flops together. In one of the two possible resolutions, both the C_2 and C_3 components of the generic $\widetilde{B}_3^t$ fiber degenerate, while in the flop, only C_3 degenerates.

The first case is in Figure 9.7, and corresponds to the lowest possible values for the valuations of

a_2 and a_6, namely $v_S(a_2) = 1$ and $v_S(a_6) = 4$. All the other cases are specialization of this case, obtained by skipping some of the intermediate steps in the degenerations as forced by the valuations. The fiber structure in Figure 9.9 is for the case ($v_S(a_2) = 1, v_S(a_6) \geq 5$), Figure 9.10 for the case ($v_S(a_2) = 2, v_S(a_6) = 4$), and finally Figure 9.11 for the case ($v_S(a_2) \geq 2, v_S(a_6) \geq 5$). Each of these Weierstrass models has two possible resolutions related by a flop, and each possible resolution has a different fiber in codimension two or three.

For the Spin(8)-models, the fiber structure is the split case of a fiber of type I_0^* and is presented in Figures 9.12 and 9.13. The most generic case for the Spin(8)-models is when $\alpha = 0$. In such a model, the fiber structure degenerates into $\widetilde{\mathrm{D}}_5$ in codimension two, $\widetilde{\mathrm{E}}_6$ or an incomplete $\widetilde{\mathrm{D}}_6$ in codimension three, and an incomplete $\widetilde{\mathrm{E}}_7$ in codimension four. The fiber structure for $\alpha > 0$ is presented in Figure 9.13, in which the fiber structure skips $\widetilde{\mathrm{D}}_5$ and degenerates directly into either an incomplete $\widetilde{\mathrm{D}}_6$ in codimension two or an incomplete $\widetilde{\mathrm{E}}_7$ in codimension three. In contrast to Spin(7)-models, the fiber type does not depend on the choice of the crepant resolution. Even though different crepant resolutions are differentiated by the way the curves split, they give the same fiber types.

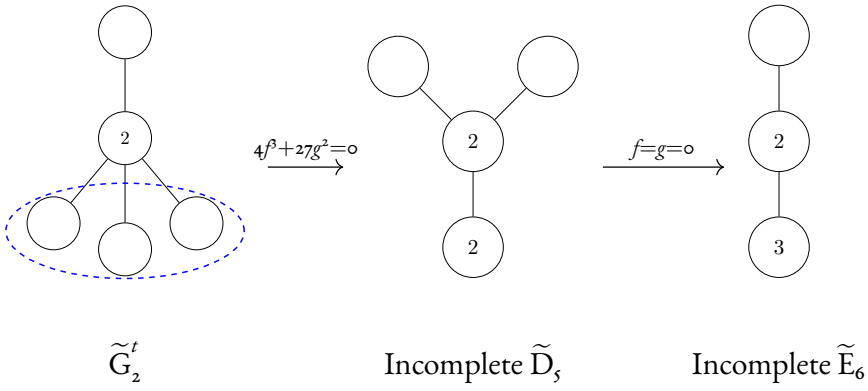

Figure 9.5: Geometric fiber degeneration of $\widetilde{G}_2^{S_3}$-model with valuation $(2, 3, 6)$.

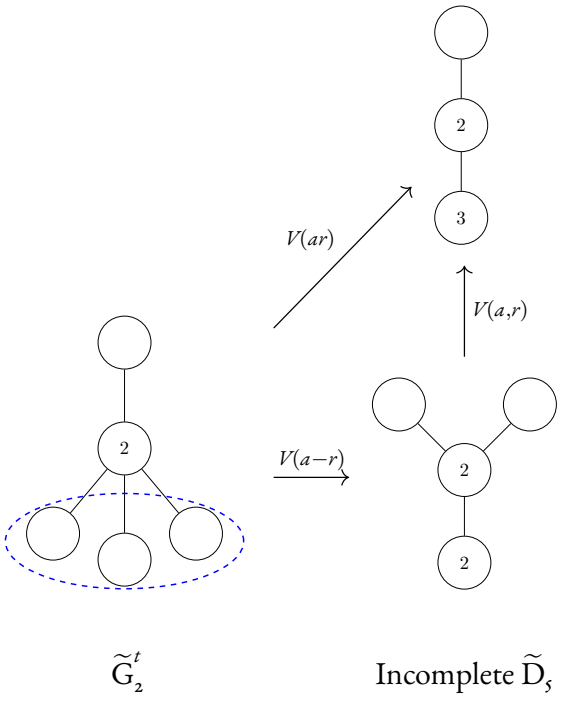

Figure 9.6: Geometric fiber degeneration for a $\widetilde{G}_2^{\mathbb{Z}/\mathbb{Z}_3}$-model with valuation $(2, 3, 6)$ and special configuration for f and g such that $\Delta' = 4f^3 + 27g^2$ is a perfect square in the residue field $\kappa(\eta)$. We assume that the base B is a surface to avoid $\mathbb{Q}$-factorial terminal singularities.

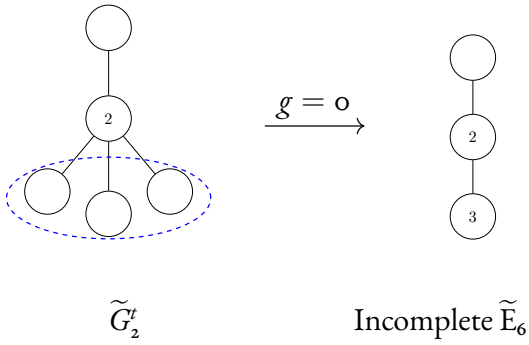

Figure 9.7: Geometric fiber degeneration of $\widetilde{G}_2^{\mathbb{Z}/3\mathbb{Z}}$ with valuation $(\geq 3, 3, 6)$.

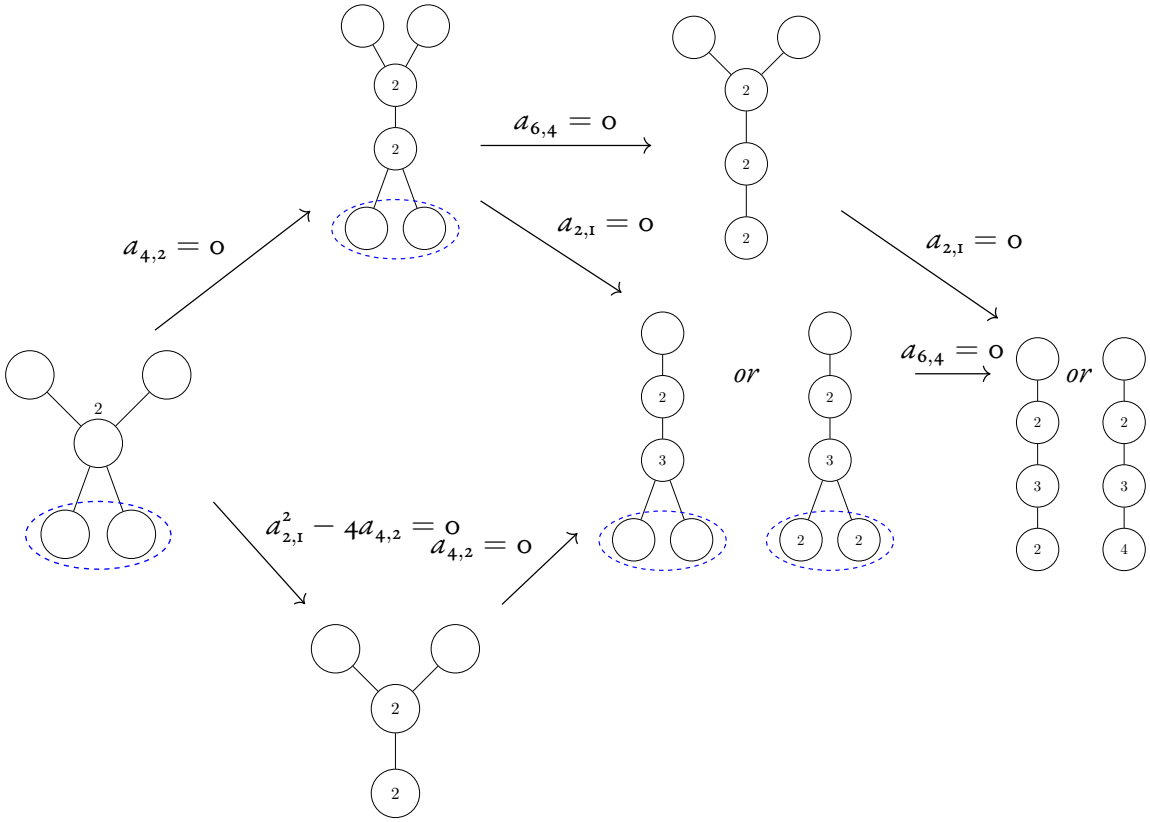

Figure 9.8: Geometric fiber degeneration of a Spin(7)-model with $v_S(a_2) = 1$ and $v_S(a_6) = 4$. When $v_S(a_2) > 1$, the degeneration graph contracts to the middle row. When there are multiple fibers, the one on the left corresponds to the monomial resolution and the one on the right to its flop.

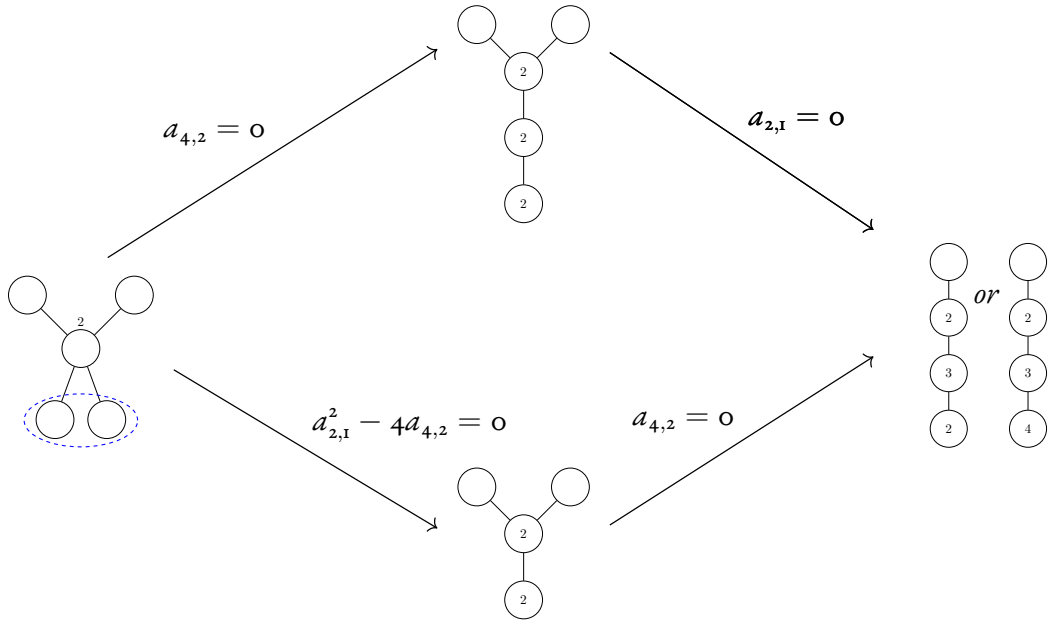

Figure 9.9: Geometric fiber degeneration of a Spin(7)-model with $v_S(a_2) = 1$ and $v_S(a_6) \geq 5$.

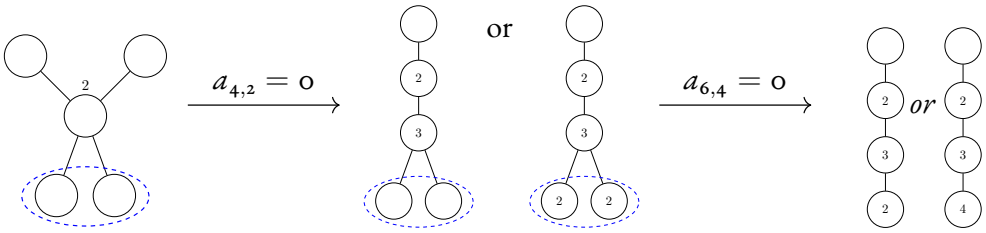

Figure 9.10: Geometric fiber degeneration of a Spin(7)-model with $v_S(a_2) \geq 2$ and $v_S(a_6) = 4$.

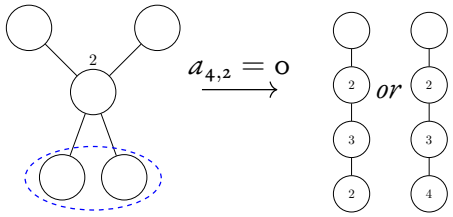

Figure 9.11: Geometric fiber degeneration of a Spin(7)-model with $v_S(a_2) \geq 2$ and $v_S(a_6) \geq 5$.

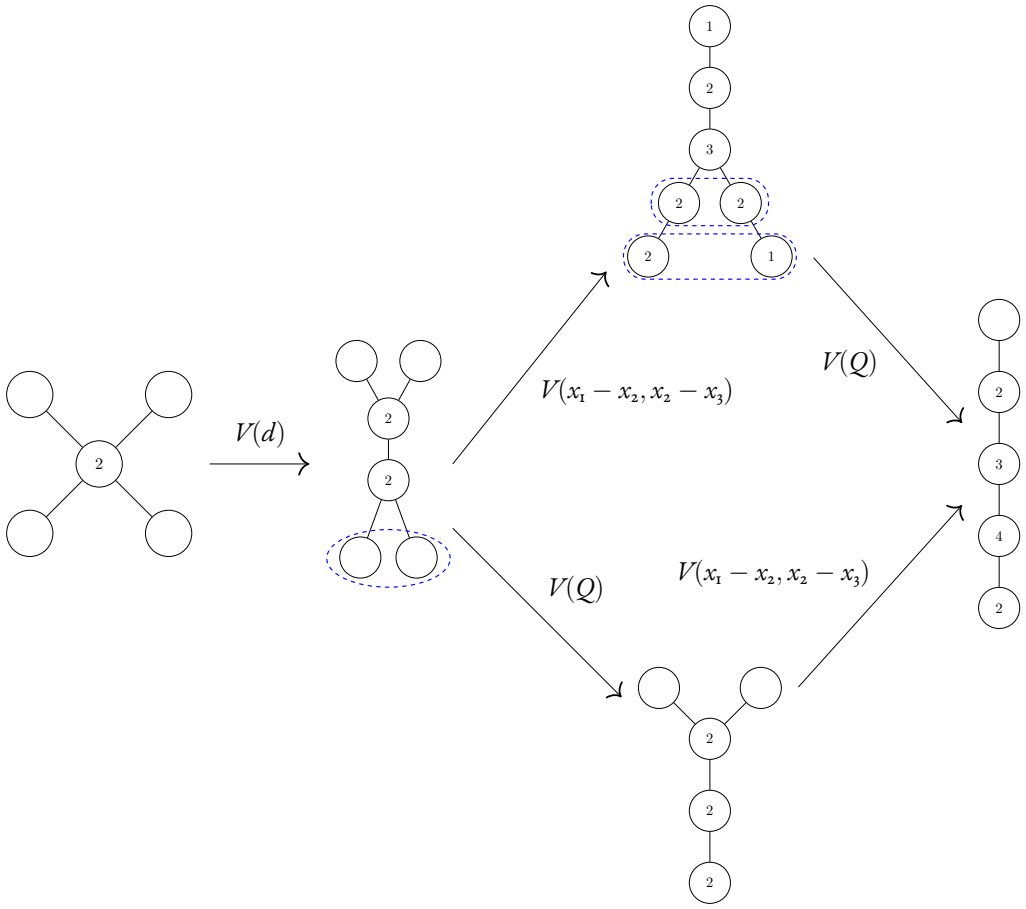

Figure 9.12: Fiber degeneration of a Spin(8)-model with $\alpha = 0$.

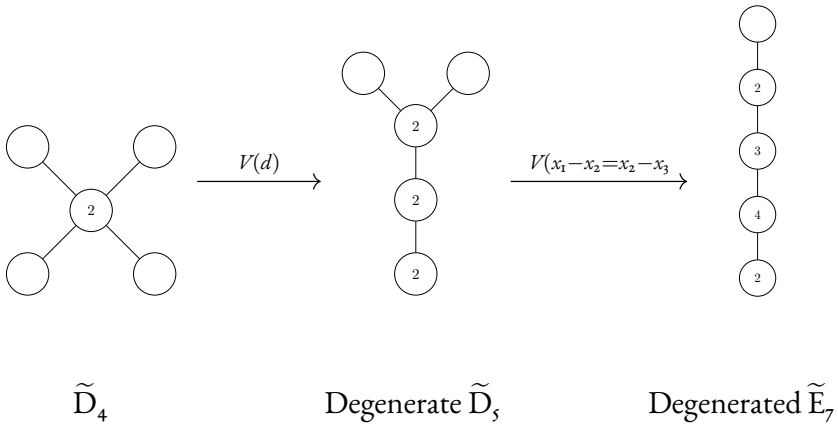

Figure 9.13: Fiber degeneration of a Spin(8)-model with $\alpha > 0$.

9.2.6 Triple intersection numbers

Two crepant resolutions of the same Weierstrass model have the same Euler characteristic [29]. In this subsection, we compute a topological invariant that is dependent on the choice of the crepant resolution. Let $D_0, D_1, \cdots, D_r$ be the fibral divisors of an elliptic fibration over a base B of dimension d. By definition, they are the irreducible components of

$$\phi^* S = m_0 D_0 + m_1 D_1 + \cdots + m_r D_r,$$

where m_i is the multiplicity of D_i and D_0 is the divisor touching the section of the elliptic fibration. It is useful to introduce a polynomial ring $A_*(Y)[\varphi_0, \cdots, \varphi_r]$ over the Chow ring $A_*(Y)$ of Y.

We define the polynomial $\mathscr{F}$ in $A_*(B)[\phi_0, \cdots, \phi_r]$ via a pushforward as

$$\mathscr{F} := \phi_*(D_0\varphi_0 + D_1\varphi_1 + \cdots D_r\varphi_r)^3.$$

Hence, if M is an element of $A_{d-3}(B)$, we have

$$\int_Y (D_0\varphi_0 + D_1\varphi_1 + \cdots D_r\varphi_r)^3 \cdot \phi^* M = \int_B \phi_* \left[(D_0\varphi_0 + D_1\varphi_1 + \cdots D_r\varphi_r)^3\right] \cdot M = \int_B \mathscr{F} \cdot M.$$

Note that the factor of $\phi^* M$ is some number; for the case of a Calabi–Yau threefold, its contribution is simply one. The polynomial $\mathscr{F}$ is called the triple intersection polynomial of the elliptic fibration. When the base is a surface, its coefficients are numbers.

A Weierstrass model of a G_2-model has a unique crepant resolution and therefore a unique possible triple intersection polynomial. There are two distinct crepant resolutions $Y^{\pm}$ for the Weierstrass model corresponding to a Spin(7)-model. These two crepant resolutions also have different triple intersection polynomials $\mathscr{F}^{\pm}_{\text{Spin}(7)}$. The Weierstrass model of a Spin(8)-model has six distinct crepant resolutions $Y^{(i,j)}$ with $\{i, j \neq i\} \subset \{2, 3, 4\}$, and we compute all six different polynomials $\mathscr{F}^{(i,j)}_{\text{Spin}(7)}$.

Theorem 9.2.4. *The triple intersection numbers of a G_2, Spin(7), or Spin(8)-model defined by the sequence of blowups listed in Section 9.2.2 are*

$$\begin{aligned}\mathscr{F}_{G_2} = &-4S(S-L)\varphi_0^3 + 3S(S-2L)\varphi_0^2\varphi_1 + 3LS\varphi_0\varphi_1^2 \\ &- 4S(S-L)\varphi_1^3 + 12S(S-3L)\varphi_2^3 + 9S(2S-3L)\varphi_1^2\varphi_2 - 27S(S-2L)\varphi_1\varphi_2^2,\end{aligned} \tag{9.12}$$

$$\begin{aligned}\mathscr{F}^{+}_{Spin(7)} = &-4S(S-L)\varphi_0^3 + 3S(S-2L)\varphi_0^2\varphi_2 + 3LS\varphi_0\varphi_2^2 \\ &- 3S(S-2L)(\varphi_1^2 + 4\varphi_1\varphi_3 + 4\varphi_3^2)\varphi_2 + 3S(2S-3L)(\varphi_1 + 2\varphi_3)\varphi_2^2 \\ &- 4S(S-L)\varphi_2^3 - 4LS\varphi_1^3 - 8LS\varphi_3^3 + 12S(S-2L)\varphi_1\varphi_3^2,\end{aligned} \tag{9.13}$$

$$\begin{aligned}\mathscr{F}^{-}_{Spin(7)} = &-4S(S-L)\varphi_0^3 + 3S(S-2L)\varphi_0^2\varphi_2 + 3LS\varphi_0\varphi_2^2 \\ &- 3S(S-2L)(4\varphi_1^2 + 4\varphi_1\varphi_3 + \varphi_3^2)\varphi_2 + 3S(2S-3L)(\varphi_3 + 2\varphi_1)\varphi_2^2 \\ &- 4S(S-L)\varphi_2^3 - 4S(S-L)\varphi_3^3 + 4S(S-4L)\varphi_1^3 + 12S(S-2L)\varphi_1\varphi_3^2,\end{aligned} \tag{9.14}$$

$$\begin{aligned}\mathscr{F}^{(i,j)}_{Spin(8)} &= -4S(S-L)\varphi_0^3 + 3S(S-2L)\varphi_0^2\varphi_1 + 3LS\varphi_0\varphi_1^2 \\ &+ 3S(2S-3L)(\varphi_2+\varphi_3+\varphi_4)\varphi_1^2 - 3S(S-2L)\left[(\varphi_2+\varphi_3+\varphi_4)^2 - 4\varphi_k^2\right]\varphi_1 \\ &- 4S(S-L)(\varphi_1^3+\varphi_k^3) - 4LS\varphi_i^3 - 2S^2\varphi_j^3 + 6S(S-2L)(\varphi_j\varphi_k^2+\varphi_i\varphi_j^2+6\varphi_i\varphi_k^2),\end{aligned} \tag{9.15}$$

where (i,j,k) *is a permutation of* $(1,2,3)$.

We see that $\mathscr{F}^{\pm}_{\text{Spin}(7)}$ are related via

$$\mathscr{F}^{-}_{\text{Spin}(7)} = \pi_{13}\mathscr{F}^{+}_{\text{Spin}(7)} + 4S(2L-S)\left(\varphi_1-\varphi_3\right)^3, \tag{9.16}$$

where π_{13} is the permutation $\varphi_1 \leftrightarrow \varphi_3$.

Lemma 9.2.5. *If a G-model is a Calabi–Yau threefold,* $c_1 = L = -K$. *Furthermore, denoting by* g *the genus of* S, *the triple intersection numbers are*

$$\begin{aligned}\mathscr{F}_{G_2} &= -8(g-1)\varphi_0^3 + 3\varphi_1\varphi_0^2\left(4g-4-S^2\right) - 3\varphi_1^2\varphi_0\left(2g-2-S^2\right) \\ &- 8(g-1)\varphi_1^3 + 24\left(3g-3-S^2\right)\varphi_2^3 - 27\left(4g-4-S^2\right)\varphi_1^2\varphi_2 + 9\left(6g-6-S^2\right)\varphi_1\varphi_2^2\end{aligned} \tag{9.17}$$

$$\begin{aligned}\mathscr{F}^{+}_{Spin(7)} = &-8(g-1)\varphi_0^3 + 3(4g-4-S^2)\varphi_0^2\varphi_2 - 3(2g-2-S^2)\varphi_0\varphi_2^2 \\ &- 3(4g-4-S^2)(4\varphi_3^2 + 4\varphi_1\varphi_3 + \varphi_1^2)\varphi_2 + 3(6g-6-S^2)(\varphi_1+2\varphi_3)\varphi_2^2 \\ &- 8(g-1)\varphi_2^3 + 4\varphi_1^3(2g-S^2-2) + 8\varphi_3^3(2g-S^2-2) + 12\varphi_1\varphi_3^2(4g-4-S^2)\end{aligned} \tag{9.18}$$

$$\begin{aligned}\mathscr{F}^{-}_{Spin(7)} = &-8(g-1)\varphi_0^3 + 3(4g-4-S^2)\varphi_0^2\varphi_2 - 3(2g-2-S^2)\varphi_0\varphi_2^2 \\ &- 3(4g-4-S^2)(4\varphi_1^2 + 4\varphi_1\varphi_3 + \varphi_3^2)\varphi_2 + 3(6g-6-S^2)(\varphi_3+2\varphi_1)\varphi_2^2 \\ &- 8(g-1)\varphi_2^3 - 8(g-1)\varphi_3^3 + 4S(S-4L)\varphi_1^3 + 12(4g-4-S^2)\varphi_1\varphi_3^2\end{aligned} \tag{9.19}$$

$$\begin{aligned}\mathscr{F}^{(i,j)}_{Spin(8)} = &-8(g-1)\varphi_0^3 + 3(4g-4-S^2)\varphi_0^2\varphi_1 - 3(2g-2-S^2)\varphi_0\varphi_1^2 \\ &+ 3(6g-g-S^2)(\varphi_2+\varphi_3+\varphi_4)\varphi_1^2 - 3(4g-4-S^2)\left[(\varphi_2+\varphi_3+\varphi_4)^2 - 4\varphi_k^2\right]\varphi_1 \\ &- 8(g-1)(\varphi_1^3+\varphi_k^3) + 4\left(2g-2-S^2\right)\varphi_i^3 - 2S^2\varphi_j^3 + 6(4g-4-S^2)(\varphi_j\varphi_k^2 + \varphi_i\varphi_j^2 + 6\varphi_i\varphi_k^2),\end{aligned} \tag{9.20}$$

where (i,j,k) *is a permutation of* $(1,2,3)$.

Lemma 9.2.5 is a direct specialization of Theorem 9.2.4. Theorem 9.2.4 is proven using Theorems Theorems 5.0.1 and 5.0.4 (see [114] for examples of such computations).

Lemma 9.2.5 is a specialization to the case of Calabi–Yau threefolds and will play an important role in Section 9.6.1. For each model and each irreducible representation $\mathbf{R}_i$ induced by its fiber degeneration, we compute the number of hypermultiplets transforming in the representation $\mathbf{R}_i$.

The results are given by Proposition 9.6.1 by comparing the triple intersection numbers given in Lemma 9.2.5 with the one-loop prepotential computed in Section 9.6.1:

$$\begin{aligned}
\mathrm{G}_2: &\quad n_7 = -10(g-1) + 3S^2, && n_{14} = g, \\
\mathrm{Spin}(7): &\quad n_7 = S^2 - 3(g-1), \quad n_8 = 2S^2 - 8(g-1), && n_{21} = g, \\
\mathrm{Spin}(8): &\quad n_{8_\mathrm{v}} = n_{8_\mathrm{s}} = n_{8_\mathrm{c}} = S^2 - 4(g-1), && n_{28} = g,
\end{aligned} \tag{9.21}$$

where g is the genus of S.

9.2.7 Euler characteristics and Hodge numbers

The results of this subsection are proven in [114] and used in Section 9.6 to check the cancellation of anomalies in the six-dimensional supersymmetric theory.

Theorem 9.2.6 (Euler characteristics). *Smooth elliptic fibrations $Y \to B$ defined as crepant resolutions of the Weierstrass models given in Section 9.2.2 have the following Euler characteristics:*

$$\begin{aligned}
G_2: &\quad \chi(Y) = 12 \int_B \frac{L + 2SL - S^2}{(1+S)(1+6L-3S)}\, c(TB) \\
Spin(7): &\quad \chi(Y) = 4 \int_B \frac{3L + (12L^2 + LS - 5S^2) + 5(3L-2S)(2L-S)S}{(1+S)(-1-6L+4S)(-1-4L+2S)}\, c(TB) \\
Spin(8): &\quad \chi(Y) = 12 \int_B \frac{L + 3SL - 2S^2}{(1+S)(1+6L-4S)}\, c(TB),
\end{aligned}$$

where $L = c_1(\mathscr{L})$, S is the class of the divisor S, $c(TB)$ is the total Chern class of the tangent bundle of the base of the Weierstrass model, and $\int_B A = \int A \cap B$ is the degree in the Chow ring of the base B.

We determine the Euler characteristic for a d-dimensional base B via the coefficient of t^d, after substituting

$$\begin{cases} L & \longrightarrow & tL \\ S & \longrightarrow & tS \\ c(TB) & \longrightarrow & c_t(TB) = 1 + c_1 t + c_2 t^2 + \cdots + c_d t^d, \quad c_i = c_i(TB). \end{cases}$$

We give the results for threefolds and fourfolds below.

Lemma 9.2.7. *If the base is a surface, Y is a threefold, and the Euler characteristic for each model is*

G_2	$12(c_1 L - 6L^2 + 4LS - S^2)$
Spin(7)	$4(3c_1 L - 18L^2 + 16LS - 5S^2)$
Spin(8)	$12(c_1 L - 6L^2 + 6LS - 2S^2)$

We specialize to the Calabi–Yau case by requiring $L = -K_B$. In the case of a Calabi–Yau threefold, we have the following result.

Lemma 9.2.8. *For Calabi–Yau threefolds, let S be the divisor over which we have the fiber I_0^*. If g denotes the genus of S and K denotes the canonical class of the base, then the Euler characteristic for each*

model is

G_2	$-60K^2 + 96(1-g) + 36S^2$
Spin(7)	$-60K^2 + 128(1-g) + 44S^2$
Spin(8)	$-60K^2 + 144(1-g) + 48S^2$

Theorem 9.2.9. *For Calabi–Yau threefolds, let S be the divisor over which we have the fiber I_0^*. If g denotes the genus of S and K denotes the canonical class of the base, then the Hodge numbers $h^{1,1}$ and $h^{1,2}$ for each model are*

	$h^{1,1}$	$h^{1,2}$
G_2	$13 - K^2$	$13 + 29K^2 - 18S^2 + 48(g-1)$
Spin(7)	$14 - K^2$	$14 + 29K^2 - 22S^2 + 64(g-1)$
Spin(8)	$15 - K^2$	$15 + 29K^2 - 24S^2 + 72(g-1)$

Lemma 9.2.10. *If Y is a fourfold, then the Euler characteristic for each model is*

G_2	$12(-6c_1L^2 + 4c_1LS - c_1S^2 + c_2L + 36L^3 - 42L^2S + 17LS^2 - 2S^3)$
Spin(7)	$4(-18c_1L^2 + 16c_1LS - 5c_1S^2 + 3c_2L + 108L^3 - 166L^2S + 89LS^2 - 15S^3)$
Spin(8)	$12(-6c_1L^2 + 6c_1LS - 2c_1S^2 + c_2L + 36L^3 - 60L^2S + 34LS^2 - 6S^3)$

Lemma 9.2.11. *If the base is a threefold and Y is a Calabi–Yau fourfold, the Euler characteristic for*

each model is

G_2	$-12\,(c_2K + 30K^3 + 38K^2S + 16KS^2 + 2S^3)$
Spin(7)	$-12\,(c_2K + 30K^3 + 50K^2S + 28KS^2 + 5S^3)$
Spin(8)	$-12\,(c_2K + 30K^3 + 54K^2S + 32KS^2 + 6S^3)$

9.3 G_2-MODELS

A G_2-model is a Weierstrass model with a geometric fiber of type I_0^* over the generic point of a divisor S of the base such that the auxiliary polynomial $P(T)$ is κ-irreducible. We distinguish two types of G_2-models, depending on the Galois group $\mathrm{Gal}(\kappa'/\kappa)$. If the discriminant $\Delta(P)$ of the associated cubic polynomial $P(T)$ is a perfect square modulo s, then the Galois group is $\mathbb{Z}/3\mathbb{Z}$, and we call such a model a $\mathrm{G}_2^{\mathbb{Z}/3\mathbb{Z}}$-model. Otherwise the Galois group is the symmetric group S_3, and the model is called a $\mathrm{G}_2^{S_3}$-model. Geometrically, these two types have different fiber structures from codimension-two.

Theorem 9.3.1 (Canonical form for G_2-models)**.** *A $G_2^{S_3}$-model can always be written in the following canonical form*

$$G_2^{S_3} \quad y^2z = x^3 + s^2fxz^2 + s^3gz^3, \quad v(f) \geq 0, \quad v(g) = 0.$$

The polynomial $P(T) = T^3 + fT + g$ is an irreducible cubic in $\kappa[T]$ and $\Delta(P) = 4f^3 + 27g^2$ is its discriminant. If $\Delta(P)$ is not a perfect square in κ, the Galois group $Gal(\kappa'/\kappa)$ is S_3. Otherwise, it is

$\mathbb{Z}/3\mathbb{Z}$. *The j-invariant is* $j = 1728\frac{4f^3}{4f^3+27g^2}$, *which varies over S.*

Proof. Directly follows from Step 6 of Tate's algorithm and Lemma 9.1.1. □

The generic case of a fiber of type I_0^* is when the Galois group $\mathrm{Gal}(\kappa'/\kappa)$ is the symmetric group S_3 and requires $v(f) = 0$, i.e.

$$\mathrm{G}_2^{S_3} \quad y^2z = x^3 + s^2fxz^2 + s^3gz^3, \quad v(f) = v(g) = 0. \tag{9.22}$$

If we increase the valuation of f, the Galois group is automatically $\mathbb{Z}/3\mathbb{Z}$ since $\Delta(P)$ will be a perfect square modulo s. Note that g cannot be a perfect cube modulo s because otherwise, $P(T) = T^3 + g$ will have three κ-roots and the model would be a Spin(8)-model instead of a G_2-model. Hence, we have in this case

$$\mathrm{G}_2^{\mathbb{Z}/3\mathbb{Z}} \quad y^2z = x^3 + s^{3+\alpha}fxz^2 + s^3gz^3, \quad \alpha \geq 0, \quad v(f) = v(g) = 0, \quad g \text{ is not a cube modulo } s. \tag{9.23}$$

In Section 9.3.2, we prove that this $\mathrm{G}_2^{\mathbb{Z}/3\mathbb{Z}}$-model is compatible with a crepant resolution after some mild assumptions. Moreover, we allow $\Delta(P)$ to be a perfect square modulo s using more complicated coefficients. For example, a Weierstrass model inspired by well-known examples in number theory is

$$\mathrm{G}_2^{\mathbb{Z}/3\mathbb{Z}} \quad y^2z = x^3 + s^2(-3ar + sq)xz^2 + s^3(a^2r + ar^2 + st)z^3. \tag{9.24}$$

This model suffers from $\mathbb{Q}$-factorial terminal singularities obstructing the existence of a crepant

resolution if the base is of dimension three or higher. When the base is a surface, this model does have a crepant resolution, and its fiber structure (see Figure 9.6) is much richer than that of equation (9.23) (see Figure 9.7). The fiber structure of the crepant resolution of a $G_2^{S_3}$-model described by equation (9.22) is presented in Figure 9.5.

Finally, we point out that all the different G_2-models discussed have (at best) a unique crepant resolution. In other words, a smooth G_2-model does not have flops. This can be explained numerically by studying the vertical curves produced by the codimension-two degenerations. They have intersection numbers with the fibral divisors corresponding to weights of the representation 7 of $\mathfrak{g}_2$; thus, the corresponding hyperplane arrangement $I(\mathfrak{g}_2, 7)$ has only one chamber.

Theorem 9.3.2 (Crepant resolutions for G_2)**.** *Assuming that $V(s)$ and $V(g)$ intersect transversally, the sequence of blowups that define a crepant resolution of the Weierstrass model $\mathscr{E}_0$: $y^2 - (x^3 + s^2fx + s^3g) = 0$ is given to be*

$$X_0 \xleftarrow{(x,y,s|e_1)} X_1 \xleftarrow{(y,e_1|e_2)} X_2.$$

The proper transform of the Weierstrass model is the vanishing locus of

$$F = e_2y^2 - e_1(x^3 + s^{2+\alpha}e_1^\alpha e_2^\alpha fx + s^3g), \quad \alpha \geq 0.$$

The relative projective coordinates are $[e_1e_2x : e_1e_2^2y : z = 1][x : e_2y : s][y : e_1]$.[5]

[5] Without loss of generality, we are in the patch of $z = 1$ for simplicity. This is ok since the section ($z = x = 0$) is always smooth.

Proof. We check smoothness in charts. By our assumptions, (x, y, s, g) forms a regular sequence and can be extended to a local set of coordinates. This will allow us to take derivatives with respect to s and g. The first blowup is done in three charts.

1. $(x, y, s) \to (xy, y, ys)$ The defining equation is

$$F_{(1)} = 1 - y(x^3 + s^{2+\alpha} f x + s^3 g).$$

There are no singularities left in this chart since F and $\partial_y F$ cannot both vanish at the same time. The center of the second blowup is not visible in this chart since $y \neq 0$.

2. $(x, y, s) \to (x, xy, xs)$

$$F_{(2)} = y^2 - x(1 + s^{2+\alpha} f + s^3 g).$$

There is a singularity at $(y, x, 1 + s^{2+\alpha} f + s^3 g)$. The exceptional divisor is $V(x)$. Hence, in this chart, the second blowup has center (x, y) and requires two charts.

   (a) $(x, y) \to (x, yx)$

$$F_{(2,1)} = xy^2 - (1 + s^{2+\alpha} f + s^3 g).$$

$V(F_{(2,1)})$ is smooth in this chart since $\partial_x F_{(2,1)}$, $\partial_f F_{(2,1)}$ (or $\partial_g F_{(2,1)}$), and $F_{(2,1)}$ cannot all vanish at the same time.

   (b) $(x, y) \to (xy, x)$

$$F_{(2,2)} = y - x(1 + s^{2+\alpha} f + s^3 g).$$

$V(F_{(2,2)})$ is smooth since $\partial_y F_{(2,2)}$ is a unit.

3. $(x, y, s) \to (sx, sy, s)$

$$F_{(3)} = y^2 - s(x^3 + s^\alpha fx + g).$$

We have double point singularities at $(y, s, x^3 + fx + g)$. The exceptional divisor is $V(s)$; hence, the second blowup has center (y, s), which requires two charts.

(a) $(y, s) \to (y, ys)$

$$F_{(3,1)} = y - s(x^3 + s^\alpha fx + g).$$

This is smooth, as can be demonstrated by taking the derivative with respect to y.

(b) $(y, s) \to (ys, s)$

$$F_{(3,2)} = sy^2 - (x^3 + s^\alpha fx + g).$$

Since $\partial_g F_{(3,2)}$ is a unit, there are no singularities.

□

9.3.1 $G_2^{S_3}$-MODEL

We recall from Theorem 9.3.2 that, after the blowup, the elliptic fibration is cut out by

$$F = e_2 y^2 - e_1(x^3 + s^{2+\alpha} e_1^\alpha e_2^\alpha fx + s^3 g), \quad \alpha \geq 0.$$

The relative projective coordinates are $[e_1e_2x : e_1e_2^2y : z][x : e_2y : s][y : e_1]$. The irreducible components of the generic fiber over S are C_0, C_1, and C_2. The curve C_a is also the generic fiber of the fibral divisor D_a ($a = 0, 1, 2$), which are given by

$$\begin{aligned} D_0 \quad &: \qquad s = e_2y^2z - e_1x^3 = 0, \\ D_1 \quad &: \qquad e_1 = e_2 = 0, \\ D_2 \quad &: \quad e_2 = x^3 + s^2fxz^2 + s^3gz^3 = 0. \end{aligned} \tag{9.26}$$

In the Chow ring $A(Y)$, the divisors D_a are of classes[6]

$$[D_0] = [S] - [E_1], \quad [D_1] = [E_1] - [E_2], \quad [D_2] = 2[E_2] - [E_1].$$

The curve C_0 is the only one that touches the section of the Weierstrass model. The curves C_0 and C_1 are smooth geometrically irreducible rational curves. Hence, the divisors D_0 and D_1 are $\mathbb{P}^1$-bundles over S:

$$D_0 = \mathbb{P}_S[\mathscr{L} \oplus \mathscr{O}_S], \quad D_1 = \mathbb{P}_S[\mathscr{L}^{\otimes 2} \oplus \mathscr{S}].$$

The curve C_2 splits into three geometrically irreducible rational curves in the splitting field of the polynomial $P(T)$. The divisor D_2 is a triple cover of the $\mathbb{P}^1$-bundle $\mathbb{P}_S[\mathscr{L}^{\otimes 3} \oplus \mathscr{S}^{\otimes 2}]$ ramified over $V(s, 4f^3 + 27g^2)$. Over the generic point of $V(s, 4f^3 + 27g^2)$, the curve C_2 factorizes into a line and a double line. The full geometric generic fiber over $V(s, 4f^3 + 27g^2)$ is an incomplete $\widetilde{D}_5$, while the full

[6] The fibral divisor D_1 is the Cartier divisor $V(e_1)$ while the Cartier divisor $V(e_2)$ is $D_1 + D_2$. Hence to the class of D_2 is $[V(e_2) - V(e_1)] = E_2 - (E_1 - E_2)$.

generic fiber over $V(s, 4f^3 + 27g^2)$ is an incomplete $\widetilde{B}_4'$ if the dimension of the base is three or higher. Over the generic point of $V(s, f, g)$, C_2 degenerates further into a triple line $3C_2'$, where

$$C_2' : e_2 = x = f = g = 0.$$

It follows that the full fiber structure is an incomplete $\widetilde{\mathrm{E}}_6$, formed by three rational curves of multiplicity 1, 2, and 3, namely $C_0 + 2C_{12} + 3C_2'$. The proper morphism $f : D_2 \to S$ has a Stein factorization

$$f : D_2 \xrightarrow{f'} S' \xrightarrow{\pi} S,$$

where $\pi : S' \to S$ is a finite map, as well as a triple cover of S with ramification divisor $4f^3 + 27g^2$. The proper morphism $f' : D_2 \to S'$ has connected fibers, and endows D_2 with the structure of a $\mathbb{P}^1$-bundle over S' such that

$$D_2 \cong \mathbb{P}_{S'}[\pi^*(\mathscr{L}^{\otimes 3} \oplus \mathscr{S}^{\otimes 2})] \to S'.$$

The node C_2' has the quasi-minuscule weight $\boxed{1, -2}$, whose Weyl orbit corresponds to the non-zero weights of the fundamental representation 7 of G_2. It follows that the representation associated with the G_2-model is the direct sum of the adjoint representation (which is always present) and the fundamental representation 7.

9.3.2 $G_2^{\mathbb{Z}/3\mathbb{Z}}$-MODEL

A G_2-model over $S = V(s)$ with Galois group $\mathbb{Z}/3\mathbb{Z}$ is given by the Weierstrass model

$$\mathscr{E}_0 : \quad y^2z = x^3 + s^{3+\alpha}fxz^2 + s^3gz^3, \quad \alpha \geq 0,$$

where g is not a perfect square modulo s. This $G_2^{\mathbb{Z}/3\mathbb{Z}}$ is a specialization of $G_2^{S_3}$, obtained by increasing the valuation of c_4. The $G_2^{\mathbb{Z}/3\mathbb{Z}}$-model distinguishes itself by the behavior of its j-invariant over S and its fiber degeneration.

Lemma 9.3.3. *The value of the j-invariant for the generic fiber over S is* 0.

Proof. An elliptic fibration $y^2z = x^3 + Fxz^2 + Gz^3$ has a j-invariant $j = 1728\frac{4F^3}{(4F^3+27G^2)}$. In this case, since $v_S(F^3) > v_S(G^2), j = 0$ over the generic point of S. □

The crepant resolution of this elliptic fibration follows the same blowup as in the general case. But the proper transform is now

$$Y : \quad e_2y^2 = e_1(x^3 + e_2^{1+\alpha}e_1^{1+\alpha}s^{3+\alpha}fx + s^3g).$$

In X_2, the projective coordinates are

$$[e_1e_2x : e_1e_2^2y : z = 1][x : e_2y : s][y : e_1].$$

The divisor D_2 is now simply

$$D_2 \quad : \quad e_2 = x^3 + s^3 g = 0.$$

The divisor D_2 is still a triple cover of the $\mathbb{P}^1$-bundle $\mathbb{P}_S[\mathscr{L}^{\otimes 3} \oplus \mathscr{S}^{\otimes 2}]$, except now branched at $V(s, g)$. The node C_2 splits into three irreducible components in the splitting field of the polynomial $T^3 - g$. Hence, the Galois group of the splitting field is $\mathbb{Z}/3\mathbb{Z}$.

The arithmetic degeneration only exits to a D_4, while the geometric degeneration to an incomplete $\widetilde{\mathrm{E}}_6$ over $V(s, g)$. The node C_2' has the quasi-minuscule weight $\boxed{2 \ -1}$, whose Weyl orbit corresponds to the non-zero weights of the fundamental representation 7 of G_2. Thus, the representation 7 is quasi-minuscule.

If the base is of dimension three or higher, there is an *arithmetic degeneration*

$$\widetilde{\mathrm{G}}_2 \longrightarrow \widetilde{\mathrm{D}}_4,$$

as the $\widetilde{\mathrm{G}}_2$ becomes a fiber $\widetilde{\mathrm{D}}_4$ over the loci where the polynomial $x^3 + s^3 g$ splits completely. An example of such a loci is over the intersection of s with the locus

$$V(\xi^3 + g + sr),$$

where ξ is a section of the line bundle $\mathscr{L}^2 \otimes \mathscr{S}^{-1}$.

Example 9.3.4. If $B = \mathbb{P}^3$, $\mathscr{L} = \mathscr{O}_{\mathbb{P}^3}(4)$, and $\mathscr{S} = \mathscr{O}_{\mathbb{P}^3}(2)$, then g is a section of $\mathscr{O}(18)$ and ξ is a section of $\mathscr{O}(6)$. Such a curve depends on twenty parameters, and one can easily write a family of

them passing through any arbitrary point of S.

The same weight $\boxed{2\ -1}$ of the representation 7 appears for the arithmetic degeneration, i.e.

$$(\widetilde{G}_2 \longrightarrow \widetilde{\mathrm{D}}_4) \Longrightarrow \quad \text{weight} \quad \boxed{2\ -1} \quad \text{of the representation} \quad 7.$$

We remark that this is one third of the weight corresponding to a generic fiber of D_1.

9.3.3 $G_2^{\mathbb{Z}/3\mathbb{Z}}$ and terminal singularities

The $G_2^{\mathbb{Z}/3\mathbb{Z}}$-model we have considered in the previous section has a crepant resolution for a base of arbitrary dimension. It was uniquely defined by the valuation of the Weierstrass coefficients $(v_S(c_4) \geq 3, v_S(c_6) = 3)$. In this section, we explore an example of a $G_2^{\mathbb{Z}/3\mathbb{Z}}$-model that has the same valuations as the $G_2^{S_3}$ $(v_S(c_4) = 2, v_S(c_6) = 3)$ model. The Galois group $\mathbb{Z}/3\mathbb{Z}$ is enforced by requiring that the discriminant $\Delta(P)$ is a perfect square in the residue field $\kappa(\eta)$. However, we will encounter non-trivial $\mathbb{Q}$-factorial terminal singularities when the base is of dimension three or higher.

Consider the Weierstrass model given by[7]

$$\mathscr{E}_0 : \quad y^2z = x^3 + s^2(-3ar + sq)xz^2 + s^3(a^2r + ar^2 + st)z^3. \tag{9.27}$$

[7] This model is inspired by the family of cubics $F = x^3 - bx + bc$, which has Galois group $\mathbb{Z}/3\mathbb{Z}$ when $4b - 27c^2$ is a perfect square as it ensures that its discriminant $\Delta(F) = b^2(4b - 27c^2)$ is a perfect square. A famous example of this type is the family of cubics $F_m = x^3 + mx^2 + (m-3)x + 1$ introduced by Shank in the definition of the *simplest cubic fields* [280]: after completing the cube in x, F_m takes the form $F = x^3 - bx + bc$ with $b = (m^2 + 3m + 9)/3$ and $c = (2m + 3)/9$.

The auxiliary polynomial $P(T)$ and its discriminant $\Delta(P)$ are given by

$$P(T) = T^3 - 3arT + ar(a+r), \quad \text{with} \quad \Delta(P) = 27a^2r^2(a-r)^2.$$

Note that $P(T)$ is irreducible and $\Delta(P)$ is a perfect square. Hence, the splitting field of $P(T)$ has Galois group $\mathbb{Z}/3\mathbb{Z}$, which means we have a $G_2^{\mathbb{Z}/3\mathbb{Z}}$-model.

Using the same sequence of blowups as in section 9.2.2, we have

$$\mathscr{E}_2: \quad e_2y^2z = e_1\Big(x^3 + s^2(-3ar + se_1e_2q)xz^2 + s^3(a^2r + ar^2 + se_1e_2t)z^3\Big).$$

The irreducible components of the generic fiber over S are

$$\begin{aligned} D_0: &\qquad s = e_2y^2z - e_1x^3 = 0,\\ D_1: &\qquad e_1 = e_2 = 0,\\ D_2: &\qquad \frac{e_2}{e_1} = x^3 - 3ars^2xz^2 + s^3ar(a+r)z^3 = 0. \end{aligned}$$

The curve C_2 (i.e. the generic fiber of D_2) is irreducible over κ. The degeneration of the fibers are characterized by the irreducible components of $\Delta(P) = 27a^2r^2(a-r)^2$. Along $ar = 0$, $P(T)$ specializes to a perfect cube $P(T) = T^3$. This means all three geometric components of C_2 coincide, yielding the fiber of type $1-2-3$, which is an incomplete $\widetilde{\mathrm{E}}_6$. Along $a-r=0$, $P(T) = (T-a)^2(T+2a)$. This means two of the three geometric components of C_2 coincide, giving an incomplete fiber of type $\widetilde{\mathrm{D}}_5$. Finally, along $a+r=0$, $P(T) = T(T^2+3a^2)$. This means $P(T)$ factorizes into a linear

term and an irreducible quadratic term, giving a fiber of type $\mathrm{I}_0^{*\mathrm{ss}}$ $(\widetilde{\mathrm{B}}_3^t)$. We have three codimension two loci over which the fiber C_2 splits into a double curve and a curve. These are geometric degenerations to an incomplete $\widetilde{\mathrm{E}}_6$ along $V(s,a)$, $V(s,r)$, and $V(s,a+r)$. If the base is of dimension three or higher, the loci $V(s,a)$, $V(s,r)$, $V(s,a-r)$, and $V(s,a+r)$ intersect on a codimension three loci at $V(s,a,r)$. Over $V(s,a+r)$, the generic fiber is of type $1-2-3$. If the base B is a surface, $\mathscr{E}_2 \to \mathscr{E}_0$ is a crepant resolution. If the base has dimension three or higher, we can rewrite the equation as

$$\mathscr{E}_2: \quad e_2(y^2 - s^4 e_1^2 t z^2)z = e_1\Big(x^3 + s^2(-3ar + s e_1 e_2 q)xz^2 + s^3 ar(a+r)z^3\Big),$$

where the singularity is in the patch $e_1 s \neq 0$. Analytically, this is a binomial hypersurface of type $V(u_1u_2u_3 - w_1w_2w_3)$.

There are terminal singularities along the codimension four loci $(x, y^2 - e_1^2 s^4 t, e_2, a, r)$. By the Grothendick-Samuel's theorem, $\mathscr{E}_2$ does not have a crepant resolution if the base is of dimension three or higher. This is because $\mathscr{E}_2$ is locally a complete intersection nonsingular up to codimension three with terminal singularities in codimension four.

9.4 Spin(7)-models

We recall that a fiber is of type $\mathrm{I}_0^{*\mathrm{ss}}$ if its dual graph is the Dynkin diagram of type $\widetilde{\mathrm{B}}_3^t$ and its geometric fiber is the Kodaira fiber of type I_0^* (with dual graph $\widetilde{\mathrm{D}}_4$). Tate's algorithm is performed with respect to the valuation ring associated to a smooth divisor $S = V(s)$ with generic point η and residue field κ. The fiber over η is of Kodaira type I_0^* and the auxiliary polynomial of Step 6 is

$P(T) = T^3 + a_{2,1}T^2 + a_{4,2}T + a_{6,3}$. The arithmetic fiber is of type $\mathrm{I}_0^{*\mathrm{ss}}$ when the splitting field of $P(T)$ defines a quadratic field extension κ' of the residue field κ. This means that $P(T)$ has a unique κ-rational solution and that the Galois group $\mathrm{Gal}(\kappa'/\kappa)$ is the cyclic group $\mathbb{Z}/2\mathbb{Z}$.

We give convenient canonical forms for Spin(7)-models in Theorem 9.4.1. All the canonical forms we deal with have the κ-rational point of $P(T)$ at the origin $T = 0$. We distinguish between two cases by the value of the j-invariant at the generic point η in S.

Theorem 9.4.1 (Canonical forms for Spin(7)-models)**.**

- *A Spin(7)-model such that $j(\eta) \neq 0, 1728$ always has a canonical form that can be written as*

$$\mathit{Spin}(7) \quad \mathscr{E}_0 = V(zy^2 - x^3 - a_{2,1}sx^2z - s^2a_{4,2}xz^2 - s^{4+\beta}a_{6,4+\beta}z^3), \quad j \neq 0, 1728, \quad \beta \in \mathbb{Z}_{\geq 0},$$

with

$$P(T) = T(T^2 + a_{2,1}T + a_{4,2}), \quad \Delta(P) = a_{4,2}^2(a_{2,1}^2 - 4a_{4,2}),$$

where $a_{2,1}$ is not zero modulo s and $a_{2,1}^2 - 4a_{4,2}$ is not a perfect square modulo s.

- *A Spin(7)-model with $j(\eta) = 1728$ can always be written in such a way that $v_S(a_1) \geq 1$, $v_S(a_2) \geq 2$, $v_S(a_3) \geq 2$, $v_S(a_4) = 2$, and $v_S(a_6) \geq 4$. Thus, it can be put in the canonical form*

$$\mathit{Spin}(7) \quad \mathscr{E}_0 = V(zy^2 - x^3 - s^2a_{4,2}xz^2 - s^{4+\beta}a_{6,4+\beta}z^3), \quad j = 1728, \quad \beta \in \mathbb{Z}_{\geq 0},$$

with

$$P(T) = T(T^2 + a_{4,2}), \quad \Delta(P) = -4a_{4,2}^3,$$

where $a_{4,2}$ is not a perfect square modulo s.

Proof. Without loss of generality, we can solve the arithmetic condition requiring $P(T)$ to have a κ-rational point, by requiring $v_S(a_6) \geq 4$. This is essentially the same as performing a translation that puts the unique $\kappa(\eta)$-rational root of $P(T)$ at $T = 0$. We then have to restrict the valuation of a_4 to be exactly two; otherwise, $v(a_4) \geq 3$, the discriminant of $P(T)$ will be zero in $\kappa(\eta)$, and $P(T)$ will have a double root.

The discriminant $\Delta(P)$ depends only on $a_{4,2}$ and $a_{2,1}$. Since the valuation of a_4 is fixed, it is interesting to explore how the geometry depends on the valuation of a_2. The valuation of a_2 characterizes two distinct types of Spin(7)-models as the j-invariant and the residual discriminant $\Delta(P)$ have different behavior when $v_S(a_2) = 1$ or $v_S(a_2) \geq 2$. The j-invariant takes the generic value $j = 1728$ over the generic point of S when $v_S(a_2) \geq 2$ and varies over S. Moreover, the residual discriminant $\Delta(P)$ is composed of two distinct components when $v_S(a_2) = 1$, and the two components coincide when $v_S(a_2) \geq 2$. To avoid a trivial Galois group, we assume that the discriminant of the quadratic part of $P(T)$ is not a perfect square. When $v_S(a_2) \geq 2$, we can also complete the cube in x, and take the canonical form to be in a short Weierstrass form without changing the conditions $v_S(a_4) = 2$ and $v_S(a_6) \geq 4$.

□

9.4.1 First crepant resolution of the general Spin(7)

We first consider a resolution of the Spin(7)-model obtained by blowing up reduced monomial ideals. In the following section, we consider a flop of that resolution. We assume the Theorem 9.4.1 hold.

Theorem 9.4.2. *Let $\mathscr{E}_0 \longrightarrow B$ be a Spin(7)-model given in Theorem 9.4.1. Let Y^+ be the proper transform of $\mathscr{E}_0$ after the following sequence of blowups starting with the ambient space $X_0 = \mathbb{P}_B[\mathscr{L}^{\otimes 2} \oplus \mathscr{L}^{\otimes 3} \oplus \mathscr{O}_B]$:*

$$X_0 \xleftarrow{(x,y,s|e_1)} X_1 \xleftarrow{(y,e_1|e_2)} X_2 \xleftarrow{(x,e_2|e_3)} X_3^+ \ .$$

If $V(a_{4,2})$ and $V(a_{6,4})$ are smooth hypersurfaces in B that meet $S = V(s)$ transversally, then $Y^+ \to \mathscr{E}_0$ is either a crepant resolution or a crepant partial resolution with terminal $\mathbb{Q}$-factorial singularities, as indicated in the table below.

	$v_S(a_6) = 4$	$v_S(a_6) = 5$	$v_S(a_6) \geq 6$
$dim B = 2$	*Crepant resolution*	*Crepant resolution*	*Term. $\mathbb{Q}$-factor. Sing.*
$dim B \geq 3$	*Crepant resolution*	*Term. $\mathbb{Q}$-factor. Sing.*	*Term. $\mathbb{Q}$-factor. Sing.*

Proof of the theorem. Assume that $V(s)$ and $V(a_{4,2})$ are smooth varieties intersecting transversally. For notational simplicity, we take $b = a_{4,2}$ and $c = a_{6,4+\beta}$. When $\alpha = 0$, we take $a = a_{2,1}$; however, if $\alpha > 0$, we complete the cube in x such that $a_2 = 0$. To examine singularities, it is enough to work in the patch $z = 1$ since the section $(z = x = 0)$ is always smooth. To check smoothness, we work in

local patches. The defining equation is

$$F = y^2 - (x^3 + asx^2 + bs^2x + cs^{4+\beta}), \quad \beta \geq 0,$$

where $a = 0$ if $v(a_2) \geq 2$. The variable b cannot be identically zero for Spin(7), as otherwise, the polynomial $P(T)$ will have a double root modulo s. The first blowup is centered at (x, y, s) and requires the following three charts:

1. $(x, y, s) \to (xy, y, sy)$

$$F_{(1)} = 1 - y(x^3 + asx^2 + bs^2x + cy^{1+\beta}s^{4+\beta}).$$

$V(F_{(1)})$ is smooth as there is no solution for $F_{(1)} = \partial_b F_{(1)} = \partial_y F_{(1)} = \partial_x F_{(1)} = 0$.

2. $(x, y, s) \to (x, yx, sx)$

$$F_{(2)} = y^2 - x(1 + as + bs^2 + cs^{4+\beta}x^{1+\beta}).$$

$V(F_{(2)})$ has a double point singularity at $(y, x, 1 + as + bs^2)$. The second blowup is centered at (x, y) and is implemented in two charts.

   (a) $(x, y) \to (x, yx)$

$$F_{(2,1)} = xy^2 - (1 + as + bs^2 + cs^{4+\beta}x^{1+\beta}).$$

$V(F_{(2,1)})$ is smooth since $F_{(2,1)} = \partial_y F_{(2,1)} = \partial_b F_{(2,1)} = 0$ does not have a solution.

(b) $(x, y) \to (xy, y)$

$$F_{(2,2)} = y - x(1 + as + bs^2 + cs^{4+\beta} x^{1+\beta} y^{1+\beta}).$$

This is smooth as $\partial_b F_{(2,2)}$ and $\partial_y F_{(2,2)}$ cannot vanish simultaneously.

3. $(x, y, s) \to (sx, sy, s)$

$$F_{(3)} = y^2 - s(x^3 + ax^2 + bx + cs^{1+\beta}), \quad \beta \geq 0.$$

We have a singularity at $(y, s, x(x^2 + ax + b))$. The second blowup is centered at (y, s). We have to perform the next blowup in two patches.

(a) $(y, s) \to (y, ys)$

$$F_{(3,1)} = y - s(x^3 + ax^2 + bx + cy^{1+\beta} s^{1+\beta}), \quad \beta \geq 0.$$

When $\beta > 0$, $V(F_{(3,1)})$ is smooth since $F_{(3,1)} = \partial_y F_{(3,1)} = \partial_b F_{(3,1)} = 0$ cannot vanish simultaneously. When $\beta = 0$, there is a singularity at $x = y = 1 - cs^2 = b = 0$. This singularity has a crepant resolution by blowing up (x, y).

i. $(x, y) \to (x, xy)$

$$F_{(3,1,1)} = y - s(x^2 + ax + b + cx^\beta y^{1+\beta} s^{1+\beta}), \quad \beta \geq 0.$$

$V(F_{(3,1,1)})$ is smooth since $\partial_b F_{(3,1,1)}$ and $\partial_y F_{(3,1,1)}$ cannot vanish at the same time.

ii. $(x, y) \to (xy, y)$

$$F_{(3,1,2)} = 1 - s(y^2 x^3 + ayx^2 + bx + cy^\beta s^{1+\beta}), \quad \beta \geq 0.$$

$V(F_{(3,1,2)})$ is smooth since $F_{(3,1,2)}$, $\partial_b F_{(3,1,2)}$, and $\partial_s F_{(3,1,2)}$ cannot vanish at the same time.

(b) $(y, s) \to (sy, s)$

$$F_{(3,2)} = sy^2 - (x^3 + ax^2 + bx + cs^{1+\beta}).$$

We still have a singularity at (y, s, x, b). The next blowup is centered at (s, x). We again have two patches to consider.

i. $(x, s) \to (x, sx)$.

$$F_{(3,2,1)} = sy^2 - (x^2 + ax + b + cx^\beta s^{1+\beta}).$$

This is smooth as it is linear in b, which can be taken as a local parameter in the base.

ii. $(x, s) \to (xs, s)$.

The proper transform is

$$Y^+ : \quad F_{(3,2,2)} = y^2 - (s^2x^3 + asx^2 + bx + cs^\beta).$$

When $\beta = 0$, Y^+ is smooth as it is linear in c, which can be used as a local parameter of the base, assuming $V(c)$ is smooth. When $\beta > 0$, we have $F|_{s=0} = y^2 - bx$, which is irreducible. If we localize at $V(s)$, $F = 0$ is just a redefinition of c and we trivially have a UFD. It follows by Nagata's criterion of factoriality that Y^+ is factorial.

When $\beta = 1$, Y^+ has terminal singularities at (x, y, b, c, s), which is in codimension 4. When $\beta > 1$, Y^+ has terminal singularities at (x, y, b, s), which is in codimension 3.

We thus have the following conclusions:[8]

1. If $\beta = 0$, Y^+ is smooth if $V(c)$ is smooth.
2. If $\beta = 1$ and dim $B = 2$, Y^+ is smooth.
3. If $\beta = 1$ and dim $B \geq 3$, Y^+ is factorial with terminal singularities at (x, y, b, c, s). Hence, Y^+ does not have a crepant resolution.

[8] We recall that factoriality is an obstruction for crepant resolutions in presence of terminal singularities.

4. If $\beta > 1$ and $\dim B \geq 2$, Y^+ is factorial with terminal singularities at (y, x, b, s). Hence, Y^+ does not have a crepant resolution.

□

The relative projective coordinates of X_0 over B, X_{i+1} over X_i ($i = 0, 1$), and X_3^+ over X_2 are respectively

$$[e_1e_2e_3^2x : e_1e_2^2e_3^2y : z = 1], \quad [e_3x : e_2e_3y : s], \quad [y : e_1], \quad [x : e_2].$$

The proper transform of $\mathscr{E}_0$ is

$$Y^+ : \quad e_2y^2 = e_1(e_3^2x^3 + a_{2,1+\alpha}s^{1+\alpha}e_1^\alpha e_2^\alpha e_3^{1+\alpha}x^2 + a_{4,2}s^2x + a_{6,4+\beta}e_3^\beta e_2^{1+\beta}e_1^{1+\beta}s^{4+\beta}).$$

We now explore the fiber structure of the smooth elliptic fibration $\phi : Y^+ \to B$ obtained by the crepant resolution. Denoting C_a as the irreducible components of the fiber over the generic point η of S, we have

$$\phi^*(\eta) = C_0 + C_1 + 2C_2 + C_3.$$

This curve is a scheme with respect to the residue field $\kappa(\eta)$. The curve C_0 is the one touching the section of the elliptic fibration. These curves are generic fibers for the fibral divisors D_a, which are defined as the irreducible components of

$$\phi^*(S) = D_0 + D_1 + 2D_2 + D_3.$$

The fibral divisors are

$$
\begin{aligned}
D_0 : &\qquad s = e_2 y^2 - e_1 e_3^2 x^3 = 0, \\
D_1 : &\qquad e_3 = e_2(y^2 - a_{6,4} e_1^2 s^4) - a_{4,2} s^2 e_1 x = 0, \\
D_2 : &\qquad e_1 = e_2 = 0, \\
D_3 : &\qquad \frac{e_2}{e_1} = e_3^2 x^2 + a_{2,1} s e_3 x + a_{4,2} s^2 = 0.
\end{aligned}
$$

We observe that D_0 and D_2 are respectively isomorphic to the projective bundles $\mathbb{P}_S[\mathscr{O}_S \oplus \mathscr{L}]$ and $\mathbb{P}_S[\mathscr{L}^2 \oplus \mathscr{S}]$, while the fibers of the divisors D_1 and D_3 can degenerate over higher codimension loci. The generic fiber (over S) of the divisor D_3 is not geometrically irreducible; after a field extension, it splits into two rational curves. The divisor D_3 is a double cover of $\mathbb{P}_S[\mathscr{L}^3 \oplus \mathscr{S}^2]$ branched along $V(s, a_{2,1}^2 - 4a_{4,2})$. We note that $a_{2,1}^2 - 4a_{4,2}$ is one of the components of the discriminant $\Delta(P)$ of the associated polynomial $P(T)$.

The only fiber components that can degenerate are C_1 and C_3. The degeneration of the generic fiber are on the components of $\Delta(P)$, and are given by

$$
V(a_4) \begin{cases} C_3 \to C_{13} + C_3' \\ C_1 \to C_{13} + C_1' \end{cases}, \quad V(a_2^2 - 4a_4) \begin{cases} C_3 \to 2C_3'' \\ C_1 \to C_1 \end{cases},
$$

$$V(a_2,a_4)\begin{cases} C_3 \to 2C_{13} \\ C_1 \to C_{13}+C_1' \end{cases},\ V(a_4,a_6)\begin{cases} C_3 \to C_{13}+C_3' \\ C_1 \to C_{13}+2C_1'' \end{cases},\ V(a_2,a_4,a_6)\begin{cases} C_3 \to 2C_{13} \\ C_1 \to C_{13}+2C_1'' \end{cases},$$

where

$$\begin{cases} C_{13} : e_2 = e_3 = 0, \\ C_3' : e_2 = e_3x + a_2s = 0, \\ C_3'' : e_2 = e_3x + \frac{1}{2}a_2s = 0, \\ C_1' : e_3 = y^2 - a_6e_1^2s^4 = 0 \\ C_1'' : e_3 = y = 0. \end{cases}$$

Since the divisor $D_0, D_i\ (i = 1,2,3)$ satisfy the linear relation $D_0 + D_1 + 2D_2 + D_3 \cong 0$, it is enough to consider the weights with respect to $D_i\ (i = 1,2,3)$. Using the fiber structure, it is easy to evaluate the weights for each curve by solving the linear relations below at the level of intersection numbers.

$$C_{13} \cong C_3'' \cong C_3' \cong \frac{1}{2}C_3, \quad C_1' \cong C_1 - \frac{1}{2}C_3, \quad C_1'' \cong \frac{1}{2}C_1 - \frac{1}{4}C_3.$$

$$\begin{array}{c} \\ D_0 \\ D_1 \\ D_2 \\ D_3 \end{array} \begin{pmatrix} C_0 & C_1 & C_2 & C_3 \\ \hline 2 & 0 & -1 & 0 \\ 0 & 2 & -1 & 0 \\ -1 & -1 & 2 & -2 \\ 0 & 0 & -2 & 4 \end{pmatrix} \begin{pmatrix} C_{13} \\ \hline 0 \\ 0 \\ -1 \\ 2 \end{pmatrix} \begin{pmatrix} C_3' \\ \hline 0 \\ 0 \\ -1 \\ 2 \end{pmatrix} \begin{pmatrix} C_3'' \\ \hline 0 \\ 0 \\ -1 \\ 2 \end{pmatrix} \begin{pmatrix} C_1' \\ \hline 0 \\ 2 \\ 0 \\ -2 \end{pmatrix} \begin{pmatrix} C_1'' \\ \hline 0 \\ 1 \\ 0 \\ -1 \end{pmatrix}.$$

The new weight is $\boxed{1\ 0\ -1}$.

9.4.2 Second crepant resolution of Spin(7)

In this section, we construct a flop of the crepant resolution obtained in the previous subsection. The flop appears after the second blowup. The proper transform of $\mathscr{E}_0$ after the second blowup is $\mathscr{E}_2$, which can be suggestively rewritten as

$$Y^{\frown}: \quad \begin{cases} e_2(y^2 - a_6 e_1 s^4) - e_1 x Q & = 0 \\ Q - (x^2 + a_2 s x + a_4 s^2) & = 0. \end{cases}$$

The first equation emphasizes that $\mathscr{E}_2$ has double point singularities, while the second equation defines Q, which is used in our next blowup so that it formally resembles a blowup of a monomial ideal. The singular scheme of $\mathscr{E}_2$ is supported along $(e_2, e_1 x, Q, y^2 - a_6 e_1 s^4)$, which is in the patch $s e_1 \neq 0$. Recall that for the first resolution, the center of the blowup is the ideal (e_2, x). In the spirit

of Atiyah's flop, this time we blowup the non-Cartier Weil divisor (e_2, Q), i.e. D_3:

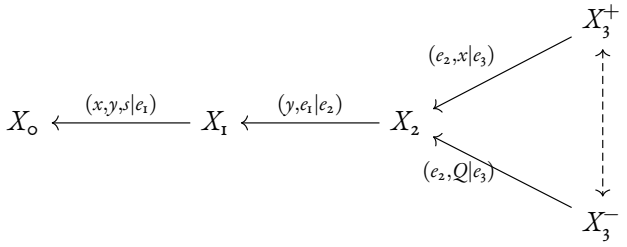

The proper transform is

$$Y^- : \quad \begin{cases} e_2(y^2 - a_6 s^4) - e_1 x Q & = 0 \\ Qe_3 - (x^2 + a_2 sx + a_4 s^2) & = 0; \end{cases}$$

the relative projective coordinates of $X_i \to X_{i-1}$ $(i = 1, 2, 3)$ are

$$[e_1 e_2 e_3 x : e_1 e_2^2 e_3^2 y : z = 1] \quad [x : e_2 e_3 y : s] \quad [y : e_1] \quad [Q : e_2];$$

and the irreducible components of the generic fibers are

$$D_0 \quad C_0 : \quad s = e_2 y^2 - e_1 x Q = Qe_3 - x^2 = 0,$$

$$D_1 \quad C_1 : \quad e_1 = e_2 = 0,$$

$$D_2 \quad C_2 : \quad \frac{e_2}{e_1} = x = Qe_3 - a_4 s^2 = 0,$$

$$D_3 \quad C_3 : \quad e_3 = x^2 + a_2 sx + a_4 s^2 = e_2(y^2 - a_6 e_1 s^4) - e_1 x Q = 0.$$

They degenerate as follows

$$V(a_4)\begin{cases} C_2 \to C_{23} \\ C_3 \to C_{23} + C_3^{(1)} + C_3^{(2)} \end{cases}, \; V(a_2^2 - 4a_4)\begin{cases} C_2 \to C_2 \\ C_3 \to 2C_3' \end{cases}, \; V(a_2, a_4)\begin{cases} C_2 \to C_{23} \\ C_3 \to 2C_{23} + 2C_3^{(1)} \end{cases},$$

$$V(a_4, a_6)\begin{cases} C_2 \to C_{23} \\ C_3 \to C_{23} + 2C_3^{(1')} + C_3^{(2)} \end{cases}, \; V(a_2, a_4, a_6)\begin{cases} C_2 \to C_{23} \\ C_3 \to 2C_{23} + 4C_3^{(1')} \end{cases},$$

where each fibers are given by

$$\begin{cases} C_{23}: & e_2 = e_3 = x = 0, \\ C_3^{(1)}: & e_3 = x = y^2 - a_6 e_1 s^4 = 0, \\ C_3^{(1')}: & e_3 = x = y = 0, \\ C_3^{(2)}: & e_3 = x + a_2 s = e_2(y^2 - a_6 e_1 s^4) + a_2 s e_1 Q = 0, \\ C_3': & e_3 = x + \frac{1}{2} a_2 s = e_2(y^2 - a_6 e_1 s^4) - e_1 x Q = 0. \end{cases}$$

The weights of each of these curves with respect to the divisors D_i $(i = 0, 1, 2, 3)$ are

$$
\begin{array}{c|cccc|c|c|c|c|c}
 & C_0 & C_2 & C_1 & C_3 & C_{23} & C_3' & C_3^{(2)} & C_3^{(1)} & C_3^{(1')} \\
\hline
D_0 & 2 & 0 & -1 & 0 & 0 & 0 & 0 & 0 & 0 \\
D_1 & 0 & 2 & -1 & 0 & 2 & 0 & 0 & -2 & 1 \\
D_2 & -1 & -1 & 2 & -2 & -1 & -1 & -1 & 0 & 0 \\
D_3 & 0 & 0 & -2 & 4 & 0 & 2 & 2 & 2 & -1
\end{array}
$$

9.4.3 Weights and representations

Letting (a, b, c) denote a weight expressed in the basis of simple roots and $\boxed{a\ b\ c}$ denote a weight expressed in the basis of fundamental weights, the weights of the representations 7 and 8 are given below.

Representation 7 of B_3		Representation 8 of B_3	
$\boxed{1\ 0\ 0}$	(1,1,1)	$\boxed{0\ 0\ 1}$	(1/2, 1, 3/2)
$\boxed{-1\ 1\ 0}$	(0,1,1)	$\boxed{0\ 1\ -1}$	(1/2, 1, 1/2)
$\boxed{0\ -1\ 2}$	(0,0,1)	$\boxed{1\ -1\ 1}$	(1/2, 0, 1/2)
$\boxed{0\ 0\ 0}$	(0,0,0)	$\boxed{-1\ 0\ 1}\ \boxed{1\ 0\ -1}$	(-1/2, 0, 1/2)(1/2, 0, -1/2)
$\boxed{0\ 1\ -2}$	(1,-1,0)	$\boxed{-1\ 1\ -1}$	(-1/2, 0, -1/2)
$\boxed{1\ -1\ 0}$	(0,-1,-1)	$\boxed{0\ -1\ 1}$	(-1/2, -1, -1/2)
$\boxed{-1\ 0\ 0}$	(0,0,-1)	$\boxed{0\ 0\ -1}$	(-1/2, -1, -3/2)

For the first crepant resolution, we obtained the following two weights from the fiber degenera-

	Spin(7) with $v_S(a_2) = 1$		Spin(7) with $v_S(a_2) \geq 2$
Locus	$V(a_{4,2})$	$V(a_{2,1}^2 - 4a_{4,2})$	$V(a_{4,2})$
Weights	$\boxed{0\ 1\ -2}$	$\pm\boxed{1\ 0\ -1}$	$\boxed{0\ 1\ -2}$ and $\boxed{-1\ 0\ 1}$
Representations	7	8	7 and 8

Table 9.3: The matter content from the geometry of a Spin(7)-model

tions:

$$\boxed{0\ -1\ 2} \quad \text{and} \quad \boxed{1\ 0\ -1}.$$

The weight $\boxed{0\ -1\ 2}$ is a weight of the representation 7 (the vector representation of B_3). The weight $\boxed{1\ 0\ -1}$ is weight of the representation 8 (the spin representation of B_3). The vector representation of B_3 is quasi-miniscule while the spin representation is minuscule; as their name indicates, they are of dimensions seven and eight, respectively.

9.5 Spin(8)-model

The Weierstrass model of a Spin(8)-model is described by Step 6 of Tate's algorithm with the additional arithmetic condition that $P(T)$ has three distinct κ-rational solutions, where κ is the residue field of the generic point η of $S = V(s)$ and s is a section of $\mathscr{O}_B(S) = \mathscr{S}$.

Theorem 9.5.1 (Canonical form for Spin(8)-models)**.** *The Weierstrass model for a* Spin(8)*-model can be written as*

$$\mathscr{E}_0: \quad y^2z = (x - sx_1z)(x - sx_2z)(x + sx_3z) - s^{2+\alpha}Qz, \quad Q = rx^2 + qsxz - s^2tz^2, \quad \alpha \in \mathbb{Z}_{\geq 0}, \tag{9.30}$$

where $(r, q, t) \neq (0, 0, 0)$ *on the divisor S and the coefficients s,* x_i*, r, q, and t are sections of the line bundles given below.*

s	x_i	r	q	t
$\mathscr{S}$	$\mathscr{L}^{\otimes 2} \otimes \mathscr{S}^{-1}$	$\mathscr{L}^{\otimes 2} \otimes \mathscr{S}^{\otimes(-2-\alpha)}$	$\mathscr{L}^{\otimes 4} \otimes \mathscr{S}^{\otimes(-3-\alpha)}$	$\mathscr{L}^{\otimes 6} \otimes \mathscr{S}^{\otimes(-2\alpha-4)}$

Q cannot be identically zero since otherwise, the Mordell-Weil group will contain at least a torsion subgroup $\mathbb{Z}/2\mathbb{Z} \oplus \mathbb{Z}/2\mathbb{Z}$*. Moreover,* $d = (x_1 - x_2)(x_2 - x_3)(x_3 - x_1)$ *cannot be identically zero on S.*

Proof. By Step 6 of Tate's algorithm, the Weierstrass coefficients have following valuations along S:

$$v_S(a_1) \geq 1, \quad v_S(a_2) \geq 1, \quad v_S(a_3) \geq 2, \quad v_S(a_4) \geq 2, \quad v_S(a_6) \geq 3.$$

By definition, a Spin(8)-model is such that the cubic polynomial $P(T) = T^3 + a_{2,1}T^2 + a_{4,2}T + a_{6,3}$ factorizes in κ. That is,

$$P(T) = (T - x_1)(T - x_2)(T - x_3), \quad x_i \in \kappa.$$

The discriminant of $P(T)$ is a perfect square $\Delta(P) = d^2$ with

$$d = (x_1 - x_2)(x_2 - x_3)(x_3 - x_1).$$

The polynomial $P(T)$ has three distinct roots in κ if and only if d is nonzero modulo s. Working

backwards, from $P(T)$, we can then compute the Weierstrass coefficients a_2, a_4, and a_6 to be

$$a_2 = -(x_1 + x_2 + x_3)s + s^2 r', \quad a_4 = s^2(x_1x_2 + x_1x_3 + x_2x_3) + s^3 q', \quad a_6 = s^3 x_1x_2x_3 + s^4 t'.$$

We complete the square in T and obtain $a_1 = a_3 = 0$; this modifies r', q', and t' accordingly. We then define α to be the highest power of s that we can factor out of r', q', and t', i.e. $r' = s^\alpha r$, $q' = s^\alpha q$, and $t' = t^\alpha q$. This explains the canonical form of the equation. We require Q to be nonzero, as otherwise, the Mordell-Weil group is non-trivial. □

9.5.1 Crepant resolution of singularities

Theorem 9.5.2 (Crepant resolutions for Spin(8)-models)**.** *Assuming that $V(x_i)$ are smooth varieties intersecting two by two transversally, the following sequence of blowups defines a crepant resolution of the normal form of a Spin(8)-model given by Theorem 9.5.1:*

$$X_0 \xleftarrow{(x,y,s|e_1)} X_1 \xleftarrow{(y,e_1|e_2)} X_2 \xleftarrow{(x-x_isz,e_2|e_3)} X_3 \xleftarrow{(x-x_jsz,e_2|e_4)} X_4,$$

where $X_0 = \mathbb{P}_B[\mathscr{O}_B \oplus \mathscr{L}^{\otimes 2} \oplus \mathscr{L}^{\otimes 3}]$. The proper transform of $\mathscr{E}_0$ is

$$Y^{(i+1,j+1)}: \quad \begin{cases} e_2\left(y^2 - e_4^\alpha e_3^\alpha e_2^\alpha e_1^{2+\alpha} s^{2+\alpha} Q\right) = e_1 u_i u_j (x - x_k s) \\ e_3 u_i = (x - x_i s) \\ e_4 u_j = (x - x_j s), \end{cases}$$

where the relative projective coordinates are

$$[e_1e_2e_3^2e_4x : e_1e_2^2e_3^2e_4^2y : z = 1][e_3x : e_3e_2e_4y : s][y : e_1][u_i : e_2e_4][u_j : e_2].$$

Proof. The Kodaira fiber I_0^{*s} over the generic point of S is seen after the first two blowups:

$$X_0 = \mathbb{P}_B[\mathscr{O}_B \oplus \mathscr{L}^{\otimes 2} \oplus \mathscr{L}^{\otimes 3}] \xleftarrow{(x,y,s|e_1)} X_1 \xleftarrow{(y,e_1|e_2)} X_2\,.$$

The proper transform of $\mathscr{E}_0$ is

$$\mathscr{E}_2 : \quad e_2(y^2 - e_2^{\alpha}e_1^{2+\alpha}s^{2+\alpha}Q) = e_1(x - x_1s)(x - x_2s)(x - x_3s).$$

In X_2, the projective coordinates of the fiber of X_0 and the successive blowup maps are

$$[e_1e_2x : e_1e_2^2y : z = 1][x : e_2y : s][y : e_1].$$

After the second blowup, the variety is smooth up to codimension two. The generic fibers of the fibral divisors of this partial resolution are

$$C_0 : \quad s = e_2y^2 - e_1x^3 = 0$$

$$C_1 : \quad e_1 = e_2 = 0$$

$$C_2^{(i)} : \quad e_2 = (x - x_is) = 0, \quad i = 1, 2, 3.$$

Their dual graph is the affine Dynkin diagram $\widetilde{\mathrm{D}}_4$. The component C_1 has multiplicity two, where one comes from the exceptional divisor $e_1 = 0$, and the other from the exceptional divisor $e_2 = 0$. The C_0 component is the proper transform of the original elliptic fiber and is the only one touching the section $x = z = 0$ of the elliptic fibration. The C_1 component is the central node of the affine Dynkin diagram $\widetilde{\mathrm{D}}_4$, and $C_2^{(i)}$ are the remaining nodes. Over $V(x_i - x_j)$, the components of $C_2^{(i)}$ and $C_2^{(j)}$ coincide. These three subvarieties intersect along the subvariety $V(x_1 - x_2, x_2 - x_3)$, over which the three external nodes $C_2^{(i)}$ coincide. There are leftover families of double point singularities in codimension three. $\mathscr{E}_2$ has terminal singularities in codimension three along the three loci

$$S_i^{(3)} = V\Big(y^2 - e_2^{\alpha} e_1^{2+\alpha} s^{2+\alpha} Q, e_2, x - x_j s, x_j - x_k\Big) = V(y^2 - e_2^{\alpha} e_1^{2+\alpha} s^{2+\alpha} Q) \cap C_2^{(j)} \cap C_2^{(k)},$$

where (i, j, k) is a permutation of $(1, 2, 3)$. These singularities are located in the patch $ze_1 s \neq 0$.

These singularities have crepant resolutions obtained by blowing up two of the three Weil divisors $C_2^{(i)}$. Thus, there are six possible choices. Since the singularities are located in the patch $zse_1 \neq 0$, we note that $\mathscr{E}_2$ has the structure of the binomial variety

$$V(v_1 v_2 - w_1 w_2 w_3),$$

which was studied in [129]. This binomial variety has six small resolutions whose flop diagram is a hexagon (a Dynkin diagram of type $\widetilde{\mathrm{A}}_5$) [129]. □

The following is a proof that we have a resolution by inspecting the singularities chart by chart.

Proof in charts.

$$F = y^2 - (x - x_1 s)(x - x_2 s)(x - x_3 s) + s^{2+\alpha}(px^2 + qsx + s^2 t).$$

We assume that $V(x_1)$, $V(x_2)$, and $V(x_3)$ are smooth varieties intersecting two by two transversally. The idea of the proof is the following. Working in charts. The first blowup has center (x, y, s) and requires three charts. If we call the exceptional divisor $E_1 = V(e_1)$, the second blowup is centered at $V(y, e_1)$ and requires two charts. We will show that after two blowups, the proper transform of F describes a smooth variety or a binomial variety of the type $V(u_1 u_2 - w_1 w_2 w_3)$, which will require two more blowups that can be done in six different ways.

1. $(x, y, s) \to (xy, y, sy)$

   $$F_{(1)} = 1 - y(x - x_1 s)(x - x_2 s)(x - x_3 s) + s^{2+\alpha} y^{2+\alpha}(px^2 + qsx + s^2 t).$$

   which is smooth since the system of equations $\partial_x F = \partial_y F = \partial_s F = F = 0$ has no solutions.

2. $(x, y, s) \to (x, yx, sx)$

   $$F_{(2)} = y^2 - x(1 - x_1 s)(1 - x_2 s)(1 - x_3 s) + s^{2+\alpha} x^{2+\alpha}(p + qs + s^2 t).$$

   The exceptional divisor is $V(x)$. Hence the second blowup is centered at (x, y) and requires two charts.

(a) $(x, y) \to (x, yx)$

$$F_{(2,1)} = x(y^2 + s^{2+\alpha}x^\alpha(p + qs + s^2t)) - (1 - x_1s)(1 - x_2s)(1 - x_3s).$$

This has the singularities of the binomial variety $V(u_1u_2 - w_1w_2w_3)$.

(b) $(x, y) \to (xy, y)$

$$F_{(2,2)} = y\Big(1 + s^{2+\alpha}x^{2+\alpha}y^\alpha(p + qs + s^2t)\Big) - x(1 - x_1s)(1 - x_2s)(1 - x_3s).$$

When $\alpha > 0$, there are no singularities left. However, when $\alpha = 0$, we still have double point singularities in the patch $x \neq 0$, and $F_{(2,2)}$ can be replaced by $V(u_1u_2 - w_1w_2w_3)$.

3. $(x, y, s) \to (xs, ys, s)$

$$F_{(3)} = y^2 - s(x - x_1)(x - x_2)(x - x_3) + s^{2+\alpha}(px^2 + qx + t).$$

The exceptional divisor is $V(s)$. Hence, the second blowup is centered at (y, s) in this chart. We then blowup (y, s), which requires two charts.

(a) $(y, s) \to (y, sy)$.

$$F_{(3,1)} = y(1 + s^{2+\alpha}y^\alpha(px^2 + qx + t)) - (x - x_1)(x - x_2)(x - x_3).$$

$F_{(3,1)}$ has the singularities of the binomial variety $V(u_1u_2 - w_1w_2w_3)$.

(b) $(y, s) \to (ys, s)$.

$$F_{(3,2)} = s(y^2 + s^\alpha(px^2 + qx + t)) - (x - x_1)(x - x_2)(x - x_3),$$

which is again of the binomial variety $V(u_1u_2 - w_1w_2w_3)$.

After two blowups, if there are singularities left, they are those of the binomial variety

$$V(u_1u_2 - w_1w_2w_3),$$

whose toric description is a triangular prism. A crepant resolution of this binomial variety is given by a sequence of two blowups corresponding to the subdivision of the triangular prism into two tetrahedrons [129]. Blowup of (u_1, w_i) with $(u_1, w_i) \to (u_1w_i, w_i)$ gives

$$u_1u_2 - w_jw_k = 0.$$

The other patch $(u_1, w_i) \to (u_1, w_iu_1)$ is trivially smooth. Likely, blowing up (u_1, w_j) with $(u_1, w_j) \to (u_1w_j, w_j)$ gives

$$u_1u_2 - w_k = 0,$$

which is smooth. The other patch is also trivially smooth. This resolution is $Y^{i+1,j+1}$. The graph of their flops is an affine Dynkin diagram $\widetilde{A}_5$ (a hexagon). □

9.5.2 Fiber structure and degenerations

The fibral divisors of the elliptic fibration $Y^{(i+1,j+1)}$ for $\alpha = 0$ are

$$\begin{aligned}
D_0 \quad C_0 \quad &: \quad s = e_2 y^2 - e_1 x^3 = 0, \\
D_1 \quad C_1 \quad &: \quad e_1 = e_2 = e_3 u_1 - (x - x_1 s) = e_4 u_2 - (x - x_2 s) = 0, \\
D_{i+1} \quad C_2^{(i)} \quad &: \quad e_3 = x - x_i s = e_4 u_j - (x_i - x_j) s = z e_2 (y^2 - e_1^2 s^2 Q) - e_1 u_i u_j (x - x_k s) = 0, \\
D_{j+1} \quad C_2^{(j)} \quad &: \quad e_4 = x - x_j s = e_3 u_i - (x_j - x_i) s = z e_2 (y^2 - e_1^2 s^2 Q) - e_1 u_i u_j (x - x_k s) = 0, \\
D_{k+1} \quad C_2^{(k)} \quad &: \quad e_2 = x - x_k s = e_3 u_i - (x_k - x_i) s = e_4 u_2 - (x_k - x_j) s = 0.
\end{aligned} \tag{9.32}$$

If $\alpha > 0$, Q is replaced by $e_4^\alpha e_3^\alpha e_2^\alpha e_1^{2+\alpha} s^{2+\alpha} Q$, which is zero for all the fibral divisors D_a. Note that this will carry through equations (9.32), (9.33), (9.34) and (9.35). Even though the generic fiber over S has geometric components, this is not necessarily carried over to its degenerations.

When $\alpha = 0$, the generic point of $V(x_i - x_j) \cap S$ (see equation (9.33)) contains the irreducible component $C_2^{(i')}$, which is not geometrically irreducible but splits into two geometrically irreducible curves after a quadratic field extension. The fiber is of type $\mathrm{I}_1^{*\mathrm{ns}}$ with its dual graph of type $\widetilde{B}_4^t$.

Over codimension-two points (the three irreducible components of $V(d)$), we have

$$\begin{array}{ccc}
V(x_i - x_j) \cap S & V(x_i - x_k) \cap S & V(x_j - x_k) \cap S \\
\begin{cases} C_2^{(i)} \longrightarrow C_2^{(i,j)} + C_2^{(i')} \\ C_2^{(j)} \longrightarrow C_2^{(i,j)} \end{cases} &
\begin{cases} C_2^{(i)} \longrightarrow C_2^{(i,k)} + C_2^{(i'')} \\ C_2^{(k)} \longrightarrow C_2^{(i,k)} \end{cases} &
\begin{cases} C_2^{(j)} \longrightarrow C_2^{(j,k)} + C_2^{(j')} \\ C_2^{(k)} \longrightarrow C_2^{(j,k)} \end{cases}
\end{array} . \tag{9.33}$$

Over codimension-three points (the common intersection of the three components of $V(d)$), we have the following splittings of the curves

$$V(x_1 - x_2, x_2 - x_3) \cap S \begin{cases} C_2^{(i)} \longrightarrow C_2^{(1,2,3)} + C_2^{(i,j)'} + C_2^{(i''')} \\ C_2^{(j)} \longrightarrow C_2^{(1,2,3)} + C_2^{(i,j)'} \\ C_2^{(k)} \longrightarrow C_2^{(1,2,3)} \end{cases}, \tag{9.34}$$

with the components of the fiber defined as

$$\begin{cases} C_2^{(i')}: & e_3 = x_i - x_j = x - x_i s = u_j = y^2 - e_1^2 s^2 Q = 0, \\ C_2^{(i,j)}: & e_3 = e_4 = x_i - x_j = x - x_i s = e_2(y^2 - e_1^2 s^2 Q) - e_1 u_i u_j (x_i - x_k)s = 0, \\ C_2^{(i,j)'}: & e_3 = e_4 = x_i - x_j = x_j - x_k = x - x_i s = y^2 - e_1^2 s^2 Q = 0, \\ C_2^{(i'')}: & e_3 = x_1 - x_k = x - x_1 s = e_4 u_j - (x_i - x_j)s = y^2 - e_1^2 s^2 Q = 0, \\ C_2^{(i''')}: & e_3 = x_1 - x_k = x_i - x_j = x - x_i s = u_2 = y^2 - e_1^2 s^2 Q = 0, \\ C_2^{(i,k)}: & e_3 = e_2 = x_i - x_j = x - x_i s = e_4 u_2 - (x_1 - x_2)s = 0, \\ C_2^{(j,k)}: & e_4 = e_2 = x_j - x_k = x - x_j s = e_3 u_i - (x_j - x_i)s = 0, \\ C_2^{(j')}: & e_4 = x_j - x_k = x - x_i s = y^2 - e_1^2 s^2 Q = 0, \\ C_2^{(1,2,3)}: & e_2 = e_3 = e_4 = x - x_k s = x_i - x_j = x_j - x_k = 0. \end{cases} \tag{9.35}$$

Over $V(x_i - x_j) \cap S$, we have a fiber of type $\mathrm{I}_1^{*\mathrm{ns}}$ with dual graph of type $\widetilde{\mathrm{B}}_4^t$. The non-geometrically

irreducible node is $C_2^{(i')}$ whereas the geometric fiber is a full $\widetilde{\mathrm{D}}_5$. Over $V(x_1 - x_2, x_2 - x_3) \cap S$, the fiber is of type IV$^{*\mathrm{ns}}$ with dual graph of type $\widetilde{\mathrm{F}}_4^t$ and geometric dual graph of type $\widetilde{\mathrm{E}}_6$. When $Q(x_i, s, z) = 0$, the fibers $\mathrm{I}_1^{*\mathrm{ns}}$ and IV$^{*\mathrm{ns}}$ degenerate further along the codimension three locus $V(s, x_i - x_j, x_i^2 + x_i r + t)$ in the base B when the curve is $C_2^{(i')}$. The degenerations are illustrated in Figure 9.12 for $\alpha = 0$ and Figure 9.13 for $\alpha > 0$, respectively.

9.5.3 Flops and representations

For $Y^{2,3}$, the curves obtained by analyzing the fiber structure have the following geometric weights.

$$
\begin{array}{cc}
 & \left(\begin{array}{ccccc|cccccc}
C_0 & C_1 & C_2^{(1)} & C_2^{(2)} & C_2^{(3)} & C_2^{(1,2)} & C_2^{(1')} & C_2^{(1,3)} & C_2^{(1'')} & C_2^{(2,3)} & C_2^{(2')} \\ \hline
2 & -1 & 0 & 0 & 0 & 0 & 0 & 0 & 0 & 0 & 0 \\
-1 & 2 & -1 & -1 & -1 & -1 & 0 & -1 & 0 & -1 & 0 \\
0 & -1 & 2 & 0 & 0 & 0 & 2 & 0 & 2 & 0 & 0 \\
0 & -1 & 0 & 2 & 0 & 2 & -2 & 0 & 0 & 0 & 2 \\
0 & -1 & 0 & 0 & 2 & 0 & 0 & 2 & -2 & 2 & -2
\end{array}\right) \\
\begin{array}{cc} \alpha_0 & D_0 \\ \alpha_2 & D_1 \\ \alpha_1 & D_2 \\ \alpha_3 & D_3 \\ \alpha_4 & D_4 \end{array} &
\end{array}
\,. \tag{9.36}
$$

To express the intersection numbers with the fibral divisors, we introduce the convention

$$
\begin{gathered}
\varepsilon_0 = (1,0,0,0,0), \quad \varepsilon_1 = (0,1,0,0,0), \quad \varepsilon_2 = (0,0,1,0,0), \\
\varepsilon_3 = (0,0,0,1,0), \quad \varepsilon_4 = (0,0,0,0,1).
\end{gathered} \tag{9.37}
$$

Since the central node of the D_4 diagram corresponds to the node C_1 of the resolution, in order to match the convention we use for weights, the intersection numbers (w_0, w_1, w_2, w_3) correspond to the weight $[w_2, w_1, w_3]$ of D_4:

$$(w_0, w_1, w_2, w_3, w_4) = \sum_{a=0}^{4} w_a \varepsilon_a \to \boxed{w_2\, w_1\, w_3\, w_4}. \tag{9.38}$$

Since weights with their appropriate multiplicities sum to zero, i.e. $w_0 + 2w_1 + w_2 + w_3 + w_4 = 0$, we have a bijection with the inverse map

$$\boxed{\varpi_1\, \varpi_2\, \varpi_3\, \varpi_4} \to (-2\varpi_2 - \varpi_1 - \varpi_3 - \varpi_4, \varpi_2, \varpi_1, \varpi_3, \varpi_4).$$

For the resolution $Y^{(i+1,j+1)}$, by a direct generalization from equation (9.36), we have the geometric weights

$$C_2^{(i,j)} \to -\varepsilon_1 + 2\varepsilon_{j+1}, \qquad C_2^{(i')} \to 2\varepsilon_{i+1} - 2\varepsilon_{j+1}, \quad C_2^{(i,k)} \to -\varepsilon_1 + 2\varepsilon_{k+1},$$
$$C_2^{(i'')} \to 2\varepsilon_{i+1} - 2\varepsilon_{k+1}, \quad C_2^{(j,k)} \to -\varepsilon_1 + 2\varepsilon_{k+1}, \qquad C_2^{(j')} \to 2\varepsilon_{j+1} - 2\varepsilon_{k+1}.$$

When $\alpha = 0$, these curves are not geometrically irreducible, as each curve splits into two irreducible curves, each having the same intersection numbers as the fibral divisors corresponding to half of those of $C_2^{(i')}$, $C_2^{(i'')}$, and $C_2^{(j')}$. When $\alpha > 0$, the curves $C_2^{(i')}$, $C_2^{(i'')}$, and $C_2^{(j')}$ are double curves and the intersection numbers of the corresponding reduced curves are also half of those of $C_2^{(i')}$, $C_2^{(i'')}$,

and $C_2^{(j')}$. Hence, for any α, we end up with the following intersection numbers:

$$\varepsilon_{i+1} - \varepsilon_{j+1}, \quad \varepsilon_{i+1} - \varepsilon_{k+1}, \quad \varepsilon_{j+1} - \varepsilon_{k+1}.$$

These are, up to a sign, permutations of

$$(0,0,0,1,-1) \quad (0,0,1,0,-1), \quad (0,0,1,-1,0).$$

Following the dictionary given by equation (9.38), we get

$$\boxed{0\,0\,1\,-1}, \quad \boxed{1\,0\,0\,-1}, \quad \boxed{1\,0\,-1\,0},$$

which are the weights of the minuscule representations 8_v, 8_c, and 8_s, respectively. Hence, each resolution gives the representation $8_v \oplus 8_c \oplus 8_s$.

The hexagon of crepant resolutions is isomorphic to the chamber structure of the hyperplane arrangement

$$\mathrm{I}(D_4, 8_v \oplus 8_c \oplus 8_s),$$

where 8_v is the vector representation, and 8_c and 8_s are the two irreducible spinor representations. Each of these three irreducible representations is minuscule of dimension eight, and their highest weights are respectively $\boxed{1\,0\,0\,0}$, $\boxed{0\,0\,1\,0}$, and $\boxed{0\,0\,0\,1}$. Note that these weights are related by simple involutions: $8_v \leftrightarrow 8_c$ by the involution $(\varpi_1 \leftrightarrow \varpi_3)$, and $8_v \leftrightarrow 8_c$ by the involution $(\varpi_3 \leftrightarrow \varpi_4)$.

Weight system of 8_v of D_4	Weight system of 8_c of D_4	Weight system of 8_s of D_4
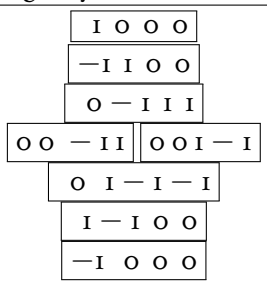	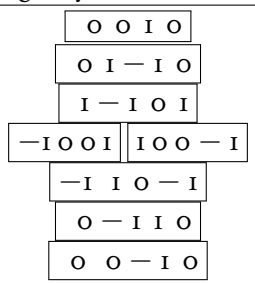	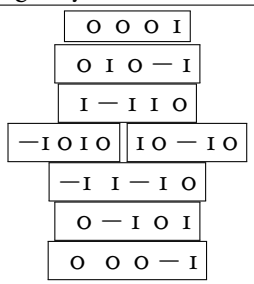
$(1, 1, \frac{1}{2}, \frac{1}{2})$	$(\frac{1}{2}, 1, 1, \frac{1}{2})$	$(\frac{1}{2}, 1, \frac{1}{2}, 1)$
$(0, 1, \frac{1}{2}, \frac{1}{2})$	$(\frac{1}{2}, 1, 0, \frac{1}{2})$	$(\frac{1}{2}, 1, \frac{1}{2}, 0)$
$(0, 0, \frac{1}{2}, \frac{1}{2})$	$(\frac{1}{2}, 0, 0, \frac{1}{2})$	$(\frac{1}{2}, 0, \frac{1}{2}, 0)$
$(0, 0, -\frac{1}{2}, \frac{1}{2})(0, 0, \frac{1}{2}, -\frac{1}{2})$	$(-\frac{1}{2}, 0, 0, \frac{1}{2})(\frac{1}{2}, 0, 0, -\frac{1}{2})$	$(-\frac{1}{2}, 0, \frac{1}{2}, 0)(\frac{1}{2}, 0, -\frac{1}{2}, 0)$
$(0, 0, -\frac{1}{2}, -\frac{1}{2})$	$(-\frac{1}{2}, 0, 0, -\frac{1}{2})$	$(-\frac{1}{2}, 0, -\frac{1}{2}, 0)$
$(0, -1, -\frac{1}{2}, -\frac{1}{2})$	$(-\frac{1}{2}, -1, 0, -\frac{1}{2})$	$(-\frac{1}{2}, -1, -\frac{1}{2}, 0)$
$(-1, -1, -\frac{1}{2}, -\frac{1}{2})$	$(-\frac{1}{2}, -1, -1, -\frac{1}{2})$	$(-\frac{1}{2}, -1, -\frac{1}{2}, -1)$

Table 9.4: The weight systems of$mathbf{8}_v$, $mathbf{8}_c$,and $mathbf{8}_s$ of$\mathbf{D}_4$.

The weights of the representations 8_v, 8_c and 8_s are given below with the following conventions: (a, b, c, d) is a weight of D_4 expressed in the basis of simple roots while $\boxed{a\ b\ c\ d}$ is a weight of D_4 written in the basis of fundamental weights.

9.6 Application to five-dimensional and six-dimensional supergravity theories

In this section, we use the information we gathered from the geometry of G_2, Spin(7), and Spin(8)-models to explore the corresponding gauge theories in M-theory and F-theory compactifications. We first consider M-theory compactified on a Calabi–Yau threefold Y elliptically-fibered over a smooth rational surface B of canonical class K. The divisor S over which the generic fiber is of Ko-

daira type I_0^* is now a smooth curve of genus g and self-intersection S^2.

By matching the triple intersection numbers and the 5d prepotential, we determined the number of hypermultiplets charged in each irreducible component of the representations. (See Section 2.12 for the details.)The number of representations we find using this procedure satisfy the anomaly cancellation equations of a six-dimensional gauge theory with eight supercharges and the same matter content. One can also determine them geometrically using either Witten's genus formula for the G_2 and Spin(7)-models, or the usual intersecting brane methods for the Spin(8)-model. (See Section 2.12.2 for Witten's genus formula.)

9.6.1 Coulomb branches of 5d $\mathcal{N} = 1$ theories with gauge groups G_2, Spin(7), and Spin(8)

The Intrilligator–Morrison–Seiberg (IMS) prepotential is the one-loop quantum contribution to the prepotential of a five-dimensional gauge theory with the matter fields in the representations $\mathbf{R}_i$ of the gauge group. See Section 2.12.1 for more details.

For G_2 with the adjoint representation 14 and the fundamental representation 7, the one-loop prepotential is

$$6\mathscr{F}_{\text{IMS}} = -8\varphi_1^3(n_{14}+n_7-1)+9\varphi_2\varphi_1^2(-2n_{14}+n_7+2)+3\varphi_2^2\varphi_1(8n_{14}-n_7-8)-8(n_{14}-1)\varphi_2^3. \quad (9.39)$$

For Spin(7) with the adjoint representation 21, the vector representation 7, and the spin representa-

tion 8, the prepotential depends on the choice of $sign(\varphi_1 - \varphi_3) = \pm$, and is given by

$$\begin{aligned}
6\mathscr{F}^{\pm}_{\text{IMS}} = &- \left(n_8 \pm n_8 + 8n_{21} - 8\right)\varphi_1^3 - \left(8n_7 + n_8 \mp n_8 + 8n_{21} - 8\right)\varphi_3^3 - 3n_8(1 \mp 1)\varphi_1^2\varphi_3 - 3n_8(1 \pm 1)\varphi_1\varphi_3^2 \\
&+ 3\left(-n_7 + n_8 + n_{21} - 1\right)\varphi_1^2\varphi_2 + 3\left(n_7 - n_8 + n_{21} - 1\right)\varphi_1\varphi_2^2 + 6n_8\varphi_1\varphi_2\varphi_3 \\
&- 8\left(n_{21} - 1\right)\varphi_2^3 + 12\left(n_7 - n_{21} + 1\right)\varphi_2\varphi_3^2 - 6\left(n_7 - 3n_{21} + 3\right)\varphi_2^2\varphi_3.
\end{aligned} \tag{9.40}$$

Finally, for Spin(8) with the adjoint representation 28, the vector representation 8_v, and the two spin representations 8_s and 8_c, we have six chambers. Each chamber is uniquely defined by the ordering of $(\varphi_1, \varphi_3, \varphi_4)$. For example, the first chamber is defined by $\varphi_1 > \varphi_3 > \varphi_4$, and the prepotential is

$$\begin{aligned}
6\mathscr{F}^{(1)}_{\text{IMS}} = &- 2\left(n_{8_c} + n_{8_s} + 4n_{28} - 4\right)\varphi_1^3 - 2\left(n_{8_v} + 4n_{28} - 4\right)\varphi_3^3 - 8\left(n_{28} - 1\right)\varphi_4^3 - 8\left(n_{28} - 1\right)\varphi_2^3 \\
&+ 3\varphi_2\left(\left(-n_{8_v} + n_{8_s} + n_{8_c}\right)\varphi_1^2 + \left(n_{8_v} + n_{8_s} - n_{8_c}\right)\varphi_3^2 + \left(n_{8_v} - n_{8_s} + n_{8_c}\right)\varphi_4^2\right) \\
&+ 6\left(n_{8_c}\varphi_1\varphi_4 + n_{8_s}\varphi_1\varphi_3 + n_{8_v}\varphi_3\varphi_4\right)\varphi_2 - 6\left(n_{8_c}\varphi_1\varphi_4^2 + n_{8_s}\varphi_1\varphi_3^2 + n_{8_v}\varphi_3\varphi_4^2\right) \\
&+ 3\left(n_{8_v} - n_{8_c} - n_{8_s} + 2n_{28} - 2\right)\varphi_2^2\varphi_1 + 3\left(-n_{8_v} + n_{8_c} - n_{8_s} + 2n_{28} - 2\right)\varphi_2^2\varphi_3 \\
&+ 3\left(-n_{8_v} - n_{8_c} + n_{8_s} + 2n_{28} - 2\right)\varphi_2^2\varphi_4.
\end{aligned} \tag{9.41}$$

The other five chambers have the same one-loop prepotential up to a permutation of φ_1, φ_2, and φ_3, as in equation (9.11).

9.6.2 Counting hypermultiplets with triple intersection numbers

Proposition 9.6.1. *In the case of a Calabi–Yau threefold, the number of each representations derived by matching the triple intersection numbers of a G_2, Spin(7), or Spin(8)-model and the one-loop prepotential does not depend on the choice of a crepant resolution and are given by*

$$\begin{aligned}
G_2: &\quad n_7 = 3S^2 - 10(g-1), && n_{14} = g,\\
\text{Spin}(7): &\quad n_7 = S^2 - 3(g-1), \quad n_8 = 2S^2 - 8(g-1), && n_{21} = g,\\
\text{Spin}(8): &\quad n_{8_v} = n_{8_s} = n_{8_c} = S^2 - 4(g-1), && n_{28} = g,
\end{aligned}$$

where g is the genus of S.

Proof. Direct comparison of eqs. (9.39) to (9.41) with Lemma 9.2.5 after imposing $\varphi_0 = 0$. □

We checked that the numbers computed in Proposition 9.6.1 satisfy the genus formula of Aspinwall–Katz–Morrison, here they are derived from the triple intersection numbers. The same numbers were computed by Grassi and Morrison using Witten's genus formula.

The advantage of our method is that we do not use the degeneration loci of the curves and hence the computation is the same even if the fiber degeneration is not generic. This method also provides the number of charged hypermultiplets from a purely fivedimensional point of view, thereby avoiding a six-dimensional argument based on cancellations of anomalies and the subtleties of the Kaluza-Klein circle compactification [149]. The same method was used in [124] for SU(N)-models and in [115] for F_4-models.

The representation induced by the weights of vertical curves over codimension-two points is not always physical as it is possible that no hypermultiplet is charged under that representation. In such a case, the representation is said to be "*frozen*" [115].

In all cases, the adjoint representation is always frozen when the curve S is a smooth rational curve ($g = 0$) [306]. For a G_2-model, the fundamental representation is frozen if and only if $g = 3k + 1$ and $S^2 = 10k$ with k in $\mathbb{Z}_{\geq 0}$. For a Spin(7)-model, the vector representation is frozen when $S^2 = 3(g-1)$, whereas the spin representation is frozen when $S^2 = 4(g-1)$, and both representations are simultaneously frozen when $S^2 = n(g-1) = 0$ for any nonnegative integer n. For a Spin(8)-model, all representations are frozen if and only if $g = 0$ and $S^2 = -4$. In this case, one can check that there are no curves carrying the weights of the representations: this corresponds to the well-known non-Higgsable model with a rational curve of self-intersection -4 [240].

9.6.3 Anomaly cancellations for 6d (1,0) theories with gauge groups G_2, Spin(7), and Spin(8)

Consider a six-dimensional $\mathcal{N} = (1, 0)$ theory coupled to n_T tensor multiplets, n_V vectors, and n_H hypermultiplets. We assume that there is a simple gauge group G, with Lie algebra $\mathfrak{g}$. The action of the gauge group on a hypermultiplet is characterized by a weight vector determining the charge of the hypermultiplet. It follows that hypermultiplets are organized into representations of the Lie algebra $\mathfrak{g}$. In our convention, a neutral hypermultiplet has a zero weight. The number of zero

weights of a representation $\mathbf{R}$ is denoted by $\dim \mathbf{R}_0$. The difference

$$(\dim \mathbf{R} - \dim \mathbf{R}_0)$$

is called the *charge dimension* of the representation $\mathbf{R}$ [142]. The charge dimensions of G_2, Spin(7), or Spin(8)-models are listed in Table 9.5.

$\mathfrak{g}$	G_2		B_3			D_4			
$\mathbf{R}$	14	7	21	7	8	28	8_v	8_s	8_c
$\dim\mathbf{R} - \dim\mathbf{R}_0$	12	6	18	6	8	24	8	8	8
$A_\mathbf{R}$	4	1	5	1	1	6	1	1	1
$B_\mathbf{R}$	0	0	−1	1	$-\frac{1}{2}$	0	$-\frac{1}{2}$	$-\frac{1}{2}$	$-\frac{1}{2}$
$C_\mathbf{R}$	$\frac{5}{2}$	$\frac{1}{4}$	3	0	$\frac{3}{8}$	3	$\frac{3}{8}$	$\frac{3}{8}$	$\frac{3}{8}$

Table 9.5: Charge dimensions and coefficients ($A_\mathbf{R}$, $B_\mathbf{R}$, $C_\mathbf{R}$) of the irreducible representations for G_2, Spin(7), or Spin(8)-model appearing in this chapter. The coefficients $A_\mathbf{R}$, $B_\mathbf{R}$, and $C_\mathbf{R}$ (see [22]) are defined by the trace identities $\mathrm{tr}_\mathbf{R}\, F^2 = A_\mathbf{R}\mathrm{tr}_V F^2$, $\mathrm{tr}\, F^4 = B_\mathbf{R}\mathrm{tr}_V F^4 + C_\mathbf{R}(\mathrm{tr}_V F^2)^2$. When a representation $\mathbf{R}$ has a unique quartic invariant, we take $B_\mathbf{R} = 0$. In this chapter, the reference representation V will always be the vector representation.

From the charge dimensions, we can compute the degeneracies of the charged hypermutiplets in each irreducible representations.

Following Section 2.13.2, the conditions to ensure a factorization can be summarized by the fol-

lowing set of equations

$$n_T = 9 - K^2, \tag{9.42a}$$

$$n_H - n_V^{(6)} + 29 n_T - 273 = 0, \tag{9.42b}$$

$$\left(B_{\mathbf{adj}} - \sum_i n_{\mathbf{R}_i} B_{\mathbf{R}_i} \right) = 0, \tag{9.42c}$$

$$\lambda \left(A_{\mathbf{adj}} - \sum_i n_{\mathbf{R}_i} A_{\mathbf{R}_i} \right) = 6K \cdot S, \tag{9.42d}$$

$$\lambda^2 \left(C_{\mathbf{adj}} - \sum_i n_{\mathbf{R}_i} C_{\mathbf{R}_i} \right) = -3S^2, \tag{9.42e}$$

where λ is the normalization factor depending on the gauge algebra as in Table 2.9. In particular, for G_2, Spin(7), and Spin(8), λ takes the same value

$$\lambda = 2. \tag{9.43}$$

Solving these equations is a simple problem of linear algebra. In each case, we get a unique solution[9]:

$$\begin{aligned}
G_2: &\quad n_7 = -10(g-1) + 3S^2, && n_{14} = g, \\
\text{Spin}(7): &\quad n_7 = S^2 - 3(g-1), \quad n_8 = 2S^2 - 8(g-1), && n_{21} = g, \\
\text{Spin}(8): &\quad n_{8_v} = n_{8_s} = n_{8_c} = S^2 - 4(g-1), && n_{28} = g.
\end{aligned} \tag{9.44}$$

[9]For the Spin(8), we use the fact from the triality that the number of representations in 8_v, 8_s, and 8_c are identical.

These matches the number of representations in Proposition 9.6.1 derived by matching the triple intersection numbers and the one-loop prepotential of the 5d theory. This confirms that the five-dimensional theory with gauge groups G_2, Spin(7), and Spin(8) may be uplifted to an anomaly-free six-dimensional theory with the gauge groups G_2, Spin(7), and Spin(8) respectively.

For each model, when we feed the numbers of representations presented in equation (9.44) into the anomaly polynomial, we get

$$X^{(2)} = 3K \cdot S \operatorname{tr}_{\mathbf{V}} F^2, \quad X^{(4)} = -\frac{3}{4} S^2 \left(\operatorname{tr}_{\mathbf{V}} F^2\right)^2, \tag{9.45}$$

and the anomaly cancellation polynomial factorizes as [269]

$$\begin{aligned} I_8 &= \frac{K^2}{8} (\operatorname{tr} R^2)^2 + \frac{1}{2} K \cdot S \operatorname{tr}_{\mathbf{V}} F^2 \left(\operatorname{tr} R^2\right) + \frac{1}{2} S^2 \left(\operatorname{tr}_{\mathbf{V}} F^2\right)^2 \\ &= \frac{1}{2} \left(\frac{1}{2} c_1(B) \operatorname{tr} R^2 - S \operatorname{tr}_{\mathbf{V}} F^2 \right)^2 . \end{aligned} \tag{9.46}$$

Since I_8 factorizes, the anomaly can be canceled by the Green-Schwarz mechanism.

Part V

5d and 6d Spectra and Anomalies of Semi-simple Gauge Group Models

Introduction

Semi-simple Lie groups appear naturally in compactifications of M-theory and F-theory on elliptic fibrations [37, 38]. The Lie group G is semi-simple (but non-simple) when the discriminant of the elliptic fibration contains at least two irreducible components Δ_1 and Δ_2 for which the dual graph of the singular fiber over the generic point of Δ_i ($i = 1, 2$) is reducible. These are called *collisions of singularities* and were first studied in string theory by Bershadsky and Johanson [38] using Miranda's regularization of singular Weierstrass models [236]. The gauge group G depends on the gauge algebra $\mathfrak{g}$ and the Mordell–Weil group of the elliptic fibration [229]. When the Mordell–Weil group is trivial, the gauge group G is the unique simple, compact, connected, and simply-connected Lie group with Lie algebra $\mathfrak{g}$. If the fiber over the generic point of Δ_i is a Kodaira fiber of type T_i, the collision is called a $T_1 + T_2$-model. If T_i has dual graph with Langlands dual $\widetilde{\mathfrak{g}}_i$, where $\mathfrak{g}_i$ is the Lie algebra of a compact simply-connected group G_i (assuming that the Mordell–Weil group is trivial), the model is also called a $G_1 \times G_2$-model. See Section 2.6 for the collisions of singularities and semi-simple groups in F-theory.

We consider various semi-simple Lie groups of a form $\mathrm{SU}(2) \times G$ or $(\mathrm{SU}(2) \times G)/\mathbb{Z}_2$ where G is a simple group. All the cases considered are listed as following with the designated chapters.

1. Chapter 10: $\mathrm{SO}(4) \simeq \mathrm{SU}(2) \times \mathrm{SU}(2)$ and $\mathrm{Spin}(4) \simeq (\mathrm{SU}(2) \times \mathrm{SU}(2))/\mathbb{Z}_2$,
2. Chapter 11: $\mathrm{SU}(2) \times \mathrm{G}_2$,
3. Chapter 12: $\mathrm{SU}(2) \times \mathrm{SU}(3)$,

4. Chapter 13: $SU(2) \times Sp(4)$, $(SU(2) \times Sp(4))/\mathbb{Z}_2$, $SU(2) \times SU(4)$, and $(SU(2) \times SU(4))/\mathbb{Z}_2$.

This is arranged in terms of their ranks. We first consider the case of the simplest semi-simple group by considering two copies of SU(2). We further consider replcing an SU(2) with another group of rank 2 such as G_2, SU(3), and Sp(4). We also consider a case by replacing a copy of SU(2) into a group of rank three such as an SU(4).

For these various cases, we compute topological invariants such as the Euler characteristic of each model over a base of arbitrary dimension in the spirit of [114]. The Euler characteristic of the elliptically-fibered Calabi–Yau threefold Y is instrumental in the discussion of the gravitational anomalies of the six-dimensional supergravity theory when F-theory is compactified on such Y [142]. The Hodge numbers of Y determines the number of vector multiplets and neutral hypermultiplets in an M-theory compactification on Y [66]. We have determined the Hodge numbers of each model in the case of the Calabi–Yau threefolds and the triple intersection numbers of its fibral divisors. In the case of Calabi–Yau fourfolds, the Euler characteristic is relevant to the cancellation of the D3-brane tadpole [5, 6, 78, 279].

Some topological invariants, such as the Euler characteristic and the Betti numbers, are independent of the choice of a crepant resolution as shown by Batyrev [29]. But others, such as the triple intersection numbers of fibral divisors used for computing Chern–Simons terms of an M-theory compactification on a Calabi–Yau threefold, do depend on a choice of a crepant resolution [176].

We analyze the physics of the compactifications of M-theory and F-theory on elliptically-fibered Calabi–Yau threefolds corresponding to each model. These give five and six-dimensional gauged

supergravity theories with eight supercharges respectively. For the five-dimensional supergravity theory, we compute the one-loop prepotential in the Coulomb branch, and determine the Chern–Simons couplings, the number of vector multiplets, tensor multiplets, and hypermultiplets. The Chern–Simons couplings are computed geometrically as triple intersection numbers of fibral divisors in each Coulomb chamber.

The Chern–Simons levels are given by triple intersection numbers of divisors of the Calabi–Yau threefolds and determine the prepotential of a five-dimensional supergravity theory from an M-theory compactification on such Calabi–Yau threefolds [66]. Using such relation, we match the triple intersection polynomial with the one-loop prepotential in each Coulomb chamber to obtain constraints on the number of charged hypermultiplets. In many cases, such a method will completely fix the number of multiplets [112, 115, 118, 121, 124]; however for some models, we get linear constraints that does not fully determine the number of multiplets. More precisely, when we consider a model with a semi-simple Lie algebra and a trivial Mordell–Weil group, we always get linear constraints that does not fully determine the number of multiplets by matching the prepotential and the triple intersection polynomial [113, 118, 119, 121]. However, they can completely be fixed by using Witten's genus formula, which is a five-dimensional result. In the five-dimensional theory, we also determine the structure of the Coulomb chambers. Each chamber corresponds to a specific crepant resolution that we determine explicitly.

In Chapter 10, we study the geometry of SO(4) and Spin(4)-models. The SO(n) and Spin(n)-models for $n \neq 4, n \geq 3$ are associated with gauge theories with simple gauge groups and do not require a collision of singularities. The SO(4) and Spin(4)-models are associated with the semi-

simple Lie algebra of type D_2, which is the unique reducible semi-simple Lie algebra $\mathfrak{g}$ of rank two, and the direct sum of two Lie algebras of type A_1:

$$D_2 \cong A_1 \oplus A_1.$$

In this sense, the SO(4) and Spin(4)-models are the simplest G-models with G a semi-simple group.[10]

The aim of the Chapter 11 is to study the geometry and physics of $SU(2) \times G_2$-models realized by the collision of singularities of type $III + I_0^{*ns}$, which has the associated Lie algebra

$$A_1 \oplus \mathfrak{g}_2. \tag{9.47}$$

We observe that in the case of an $SU(2) \times G_2$-model, the representation $\mathbf{R}$ cannot be derived by the Katz–Vafa method (see Section 11.4.1) but can be deduced using the method of saturations of weights obtained geometrically by intersection of fibral divisors and irreducible components of singular fibers over codimension-two points in the base (see Section 11.4.2). We write the tensor product of a representation $\mathbf{r}_1$ of SU(2) and $\mathbf{r}_2$ of G_2 as $(\mathbf{r}_1, \mathbf{r}_2)$.[11] The 2 and the 3 of SU(2) are respectively the fundamental and the adjoint representation of SU(3); the 7 and the 14 of G_2 are respectively the fundamental and the adjoint representation of G_2. The representations $(3, 1)$, $(1, 14)$, and $(1, 7)$ are

[10] There are also other compact groups with Lie algebra D_2, namely the half-spin groups $HSpin^{\pm}(4)$ which are isomorphic to $SO(3) \times SU(2)$ and $SU(2) \times SO(3)$. However, these groups are not compatible with the typical representation $(2, 2)$ observed at the collisions of two fibers with dual graphs $\widetilde{A}_1$. For futher discussions, see Section 10.1.1.

[11] We follow the usual tradition in physics of writing a representation by its dimension as there is no room for ambiguity with the representations used in this chapter.

real while the representation $(2,1)$ and $(2,7)$ are pseudo-real.

The matter representation is then the following direct sum of irreducible representations(see Section 11.4)

$$\mathbf{R} = (3,1) \oplus (1,14) \oplus (2,7) \oplus (2,1) \oplus (1,7). \tag{9.48}$$

In contrast to the traditional approach [69, 240, 269], we derive this representation $\mathbf{R}$ purely geometrically without using the anomaly cancellation conditions of the six-dimensional theory nor a dual heterotic model. This method is valid for both five and six-dimensional theories and has the advantage to work in situations where the Katz–Vafa method is not applicable (see Section 11.4.1). In the 5d theory, it also has the benefit of not depending on the existence of a 6d uplift. For the six-dimensional theory, we check explicitly that the anomaly cancellation conditions are satisfied. We also point out that the fundamental representation $(1,7)$ is a *frozen representation* when the curve supporting G_2 is a -3-curve intersecting the curve supporting SU(2) transversally and at a unique point. This explains the absence of the representation $(1,7)$ in [69]. The number of charged hypermultiplets in each of these representations are given in equation (11.1), which generalizes the spectrum $\frac{1}{2}(2,7) \oplus \frac{1}{2}(2,1)$ expected in a six-dimensional theory when a $\mathrm{SU}(2) \times \mathrm{G}_2$-model is locally defined at the collision of a -2-curve and a -3-curve intersecting transversally at one point and supporting respectively an SU(2) and a G_2 Lie group [69, 240].

The purpose of the Chapter 12 is to study the crepant resolutions of Weierstrass models giving $\mathrm{SU}(2) \times \mathrm{SU}(3)$-models. We show that there are six possible types of collisions of singularities that define Weierstrass models for $\mathrm{SU}(2) \times \mathrm{SU}(3)$-models; we show that each Weierstrass model of

$\mathrm{SU}(2) \times \mathrm{SU}(3)$-models has eight distinct crepant resolutions. In total, we have a network of 48 distinct elliptic fibrations connected by deformations and flops. By studying their crepant resolutions, we find a rich structure of non-Kodaira fibers, some of which are observed for the very first time. We determine the geography of all the crepant resolutions of the $\mathrm{SU}(2) \times \mathrm{SU}(3)$-model, compute their (topological) invariants, and analyze aspects of F-theory and M-theory compactified on such varieties when they are Calabi–Yau threefolds. We study the resulting 5d prepotential in the Coulomb branch of the theory and check that the six-dimensional theory is anomaly-free and compatible with a 6d uplift from a 5d theory.

In Chapter 13, we explore non-trivial models of semi-simple Lie algebra with Mordell–Weil group $\mathbb{Z}_2 := \mathbb{Z}/2\mathbb{Z}$. Specifically, we study the geometry and physics of elliptic fibrations corresponding to the following collisions[12]

$$\mathrm{I}_2^{\mathrm{ns}} + \mathrm{I}_4^{\mathrm{ns}} \quad \text{and} \quad \mathrm{I}_2^{\mathrm{ns}} + \mathrm{I}_4^{\mathrm{s}}, \tag{9.49}$$

with a Mordell–Weil group that is either trivial or $\mathbb{Z}_2$. The corresponding Lie algebras are

$$\mathrm{A}_1 \oplus \mathrm{C}_2, \quad \mathrm{A}_1 \oplus \mathrm{A}_3. \tag{9.50}$$

Such collisions correspond to semi-simple gauge groups (see Table 13.1):

$$(\mathrm{SU}(2) \times \mathrm{Sp}(4))/\mathbb{Z}_2, \quad \mathrm{SU}(2) \times \mathrm{Sp}(4), \quad \mathrm{SU}(2) \times \mathrm{SU}(4))/\mathbb{Z}_2, \quad \mathrm{SU}(2) \times \mathrm{SU}(4).$$

[12] Given two Kodaira types T_1 and T_2, a model of type $T_1 + T_2$ is an elliptic fibration such that the discriminant locus contains two intersecting divisors Δ_1 and Δ_2, where the generic fiber of Δ_i is T_i and the generic fiber of any other component of the discriminant locus is an irreducible fiber (such as Kodaira type I_1 or II).

These models are uniquely defined for the following reasons. Since a $\mathbb{Z}_2$ Mordell–Weil group always induces at least an I_2 fiber, the collision I_2+I_4 is the simplest case with Mordell–Weil group $\mathbb{Z}_2$ and a semi-simple Lie algebra that is not $A_1 \oplus A_1$. We consider the two possible generic fibers of Kodaira type I_4, namely I_4^s and I_4^{ns}. We use a fiber of type I_2^{ns} because it is the generic reducible fiber induced by the $\mathbb{Z}_2$ Mordell–Weil group (see Section 2.2.4). For comparison, we also study the same collisions with a trivial Mordell–Weil group. These considerations completely fix our models once we use Weierstrass models [107] and assume minimal valuations for all Weierstrass coefficients with respect to the divisors supporting the simple components of the gauge group.

I am coming more and more to the conviction that the necessity of our geometry cannot be demonstrated, at least neither by, nor for, the human intellect.

Carl Friedrich Gauss

10

Flopping and Slicing: SO(4) and Spin(4)-models

10.1 Models considered

Geometrically, SO(4) and Spin(4)-models are elliptic fibrations whose discriminant locus contains two smooth irreducible components (S and T) such that the dual graphs of the fibers over the

generic points of S and T is the affine Dynkin diagram $\widetilde{A}_1$, while the fiber over other generic points of the discriminant locus are irreducible singular fibers. Since Spin(4) has a trivial fundamental group and the fundamental group of SO(4) is $\mathbb{Z}/2\mathbb{Z}$, the Mordell–Weil group of a Spin(4)-model is trivial while the one of an SO(4)-model is $\mathbb{Z}/2\mathbb{Z}$.

The SO(4)-model as a collision $\mathrm{I}_2^{\mathrm{ns}} + \mathrm{I}_2^{\mathrm{ns}}$ in an elliptic fibration with Mordell–Weil group $\mathbb{Z}/2\mathbb{Z}$ has been discussed in [242] in the case of a Calabi–Yau threefold elliptically-fibered over a $\mathbb{P}^2$ base. The SO(4)-model was studied in more detail using toric methods in [229]. The first appearing of elliptic fibrations with a $\mathbb{Z}/2\mathbb{Z}$ Mordell–Weil group in F-theory is in [39] in relation to the CHL model (see also [276]) and shortly after in [20] in the study of non-simply connected Lie groups in F-theory.

In this chapter, we add to previous work on SO(4) and Spin(4)-models in many ways. We consider other collisions than $\mathrm{I}_2^{\mathrm{ns}} + \mathrm{I}_2^{\mathrm{ns}}$ and before to specialize to the case of Calabi–Yau threefolds, we study these geometries over a base arbitrary dimension. Geometrically, SO(4) and Spin(4)-models are characterized by the collision of two Kodaira fibers whose dual graphs are of type $\widetilde{A}_1$. While the Kodaira fiber of type I_2 has dual graph $\widetilde{A}_1$, it is not the only one. That means there are many more ways to realize geometrically a model of type SO(4) or Spin(4) than a collision of type I_2+I_2. In fact, the dual graph $\widetilde{\mathrm{A}}_1$ is the most versatile one as it can be realized geometrically by five distinct types of singular fibers, namely

$$\text{Fibers with dual graph } \widetilde{A}_1: \quad \mathrm{I}_2^{\mathrm{ns}}, \quad \mathrm{I}_2^{\mathrm{s}}, \quad \mathrm{III}, \quad \mathrm{I}_3^{\mathrm{ns}}, \quad \mathrm{IV}^{\mathrm{ns}}. \tag{10.1}$$

We avoid realizing A_1 with fibers of type I_3^{ns} to stay away from terminal singularities. The elliptic fibrations that we consider are constructed by crepant resolutions of Weierstrass models corresponding to the following collisions of singularities

$$I_2^{ns} + I_2^{ns}, \quad I_2^{s} + I_2^{ns}, \quad I_2^{s} + I_2^{s}, \quad III + I_2^{ns}, \quad III + I_2^{s}, \quad III + III, \quad IV^{ns} + I_2^{s}, \quad IV^{ns} + I_2^{ns}. \tag{10.2}$$

These collisions define a gauge theory with Lie algebra $A_1 \oplus A_1$. There are many gauge groups with this Lie algebra, but as we will explain, we only get SO(4) or Spin(4) in this case respectively when the Mordell–Weil group is $\mathbb{Z}/2\mathbb{Z}$ or trivial. It is important to distinguish between I_2^{s} and I_2^{ns} and to fix the Mordell–Weil group as they lead to completely different fiber structures as seen by comparing Figures 10.3 to 10.12.

The models considered in this chapter are given by Weierstrass equations listed in Table 10.1. The fiber at the collisions are listed in Table 10.4. For the SO(4)-model, the Mordell–Weil condition forces the class of the two divisors S and T to satisfy the linear relation

$$S + T = 4L,$$

where $L = c_1(\mathscr{L})$ is the first Chern class of the fundament line bundle $\mathscr{L}$ of the Weierstrass model (see Definition 2.2.1). In the Calabi–Yau case, $L = -K$ where K is the canonical class of the base B of the elliptic fibration.

Each of the Weierstrass models listed in Table 10.1 has two crepant resolutions connected by an

Atiyah flop. Using the main theorem of [114], we determine a generating function for the Euler characteristic of SO(4) and Spin(4)-models (see Theorem 10.2.3 and Theorem 10.2.1). We study in detail the fiber degeneration of each of these elliptic fibrations and identify new non-Kodaira fibers (see Figures 10.2, 10.3, 10.4, 10.5, 10.6, 10.7, 10.8, 10.9, 10.10, 10.11, and 10.12).

When the elliptic fibration is a threefold, we compute the triple intersection numbers of the fibral divisors (see Theorem 10.4.3). Assuming the Calabi–Yau condition, we can also compute the Hodge numbers of the elliptic fibration. The five-dimensional theory has two distinct Coulomb phases separated by a wall defined by a weight of the vector representation corresponding to the difference of the fundamental weights of each A_1 forming the Lie algebra of type D_2. When the elliptic fibration is a Calabi–Yau threefold, the triple intersection numbers of the fibral divisors give the Chern-Simons levels of the theory in a Calabi–Yau compactification of M-theory to a five-dimensional supergravity theory with eight supercharges. In such a five-dimensional theory, we can constrain the number of charged hypermultiplets by comparing the triple intersection numbers of fibral divisors of the elliptic fibration with the cubic $5d$ prepotential. This point of view was presented in [149] and explicitly implemented in [112, 115, 121, 124]. For an SO(4)-model this is enough to completely fix the number of charged hypermultiplets. But for a Spin(4)-model, this only gives two unresolved linear relations. The number of charged multiplets are fixed by using intersecting-brane techniques or anomaly cancellations from an uplift to a chiral six-dimensional gauged supergravity theory, coming from a Calabi–Yau compactification of F-theory. In all cases, we check that the matter content we obtained is compatible with an anomaly free six-dimensional supergravity theory.

10.1.1 Spin groups, orthogonal groups, and half-spin groups

Assuming that a Lie group G is complex and connected, we only need to know its fundamental group $\pi_1(G)$ and the type of its Lie algebra $\mathfrak{g}$ to determine G up to isomorphism. The Lie algebra only determines the local structure of the group G. In F-theory, the Mordell–Weil group of the elliptic fibration is isomorphic to the fundamental group of the Lie group. Assuming that the Mordell–Weil group has a trivial rank, and is therefore purely a torsion group T, we can then retrieve the group G as the quotient $G = \widetilde{G}/\widetilde{T}$, where $\widetilde{G} = \exp(\mathfrak{g})$ is the simply connected and compact connected group with Lie algebra $\mathfrak{g}$ and $\widetilde{T}$ is a normal subgroup of the center $Z(\widetilde{G})$ of $\widetilde{G}$ isomorphic to T. Note that different isomorphic subgroups $\widetilde{T}_1$ and $\widetilde{T}_2$ of the center $Z(\widetilde{G})$ can give non-isomorphic quotient $\widetilde{G}/\widetilde{T}_1$ and $\widetilde{G}/\widetilde{T}_2$. The fundamental group $\pi_1(G)$ and the center $Z(G)$ of G are respectively isomorphic to T and the quotient $Z(\widetilde{G})/\widetilde{T}$.

$$G = \widetilde{G}/\widetilde{T}, \quad \widetilde{G} := \exp(\mathfrak{g}), \quad T \cong \widetilde{T} \subset Z(\widetilde{G}), \quad \pi_1(G) \cong T, \quad Z(G) = Z(\widetilde{G})/\widetilde{T}. \tag{10.3}$$

In our case of interest, we recall that the universal covering of a compact gauge group with Lie algebra of type $\mathrm{D}_2 \cong \mathrm{A}_1 \oplus \mathrm{A}_1$ is Spin(4)

$$\widetilde{G} = \mathrm{Spin}(4) \cong \mathrm{SU}(2) \times \mathrm{SU}(2). \tag{10.4}$$

The center of $\mathrm{Spin}(4+4n)$ is the Klein's four-group $\mathbb{Z}/2\mathbb{Z}\times\mathbb{Z}/2\mathbb{Z}$:

$$Z=\mathbb{Z}/2\mathbb{Z}\times\mathbb{Z}/2\mathbb{Z}\cong\{\pm\mathbb{I},\pm\Gamma_*\}. \tag{10.5}$$

where $\mathbb{I}$ is the identity and Γ_* is the product of all gamma matrices and squares to the identity $\Gamma_*^2=\mathbb{I}$. The matrix Γ_* is used to define Weyl spinors of $\mathrm{Spin}(4+4n)$. Each non-neutral element g of $\mathbb{Z}/2\mathbb{Z}\times\mathbb{Z}/2\mathbb{Z}$ generates a subgroup $\langle g\rangle$ isomorphic to $\mathbb{Z}/2\mathbb{Z}$ and the three possibilities account for all the possible embedding of $\mathbb{Z}/2\mathbb{Z}$ in $\mathbb{Z}/2\mathbb{Z}\times\mathbb{Z}/2\mathbb{Z}$. Each of the corresponding quotient $Z/\langle g\rangle$ is isomorphic to $\mathbb{Z}/2\mathbb{Z}$. But each quotient $\mathrm{Spin}(4)/\langle g\rangle$ is a different group as expressed by the following exact sequences.

$$\begin{aligned}
&1\longrightarrow\langle-\mathbb{I}\rangle\cong\mathbb{Z}/2\mathbb{Z}\longrightarrow\mathrm{Spin}(4+4n)\longrightarrow\mathrm{SO}(4+4n)\longrightarrow 1\\
&1\longrightarrow\langle+\Gamma_*\rangle\cong\mathbb{Z}/2\mathbb{Z}\longrightarrow\mathrm{Spin}(4+4n)\longrightarrow\mathrm{HSpin}^+(4+4n)\longrightarrow 1\\
&1\longrightarrow\langle-\Gamma_*\rangle\cong\mathbb{Z}/2\mathbb{Z}\longrightarrow\mathrm{Spin}(4+4n)\longrightarrow\mathrm{HSpin}^-(4+4n)\longrightarrow 1
\end{aligned} \tag{10.6}$$

The group $\mathrm{SO}(4+4n)$ is the $\mathbb{Z}/2\mathbb{Z}$ quotient of $\mathrm{Spin}(4+4n)$ when $\mathbb{Z}/2\mathbb{Z}$ is generated by minus the identity of $\mathrm{Spin}(4+4n)$. When $\mathbb{Z}/2\mathbb{Z}$ is generated by Γ_* or $-\Gamma_*$, we get a *half-spin group*. In the case of $\mathrm{SO}(4)$, we have

$$\mathrm{HSpin}^+(4)\cong\mathrm{SO}(3)\times\mathrm{SU}(2),\quad \mathrm{HSpin}^-(4)\cong\mathrm{SU}(2)\times\mathrm{SO}(3). \tag{10.7}$$

Half-spin groups are called *semi-spin group* in Bourbaki [57, Chap 8,§13.4]. The quotient of Spin$(4+4n)$ by its center is the adjoint group PSO$(4+4n)$. Hence, there are four compact groups of type D_{2+2n}, namely the simply connected group Spin$(4+4n)$, the adjoint group PSO$(4+4n)$, the half-spin groups HSpin$^{\pm}(4+4n)$, and the orthogonal group SO$(4+4n)$.

10.1.2 The simplest SO(4)-model as a Miranda model

The simplest SO(4)-model is realized by III+III, the collision of two fibers of type III, in an elliptic fibration with Mordell–Weil group $\mathbb{Z}/2\mathbb{Z}$. Its defining equation is

$$y^2z = x(x^2 + stz^2). \tag{10.8}$$

As an illustration, we quickly derive this equation. First, the general elliptic fibration with Mordell–Weil group $\mathbb{Z}/2\mathbb{Z}$ is [20, 175]

$$y^2z = x(x^2 + a_2z^2 + a_4z^3). \tag{10.9}$$

The generator of the Mordell–Weil group is the section $x = y = 0$ and the neutral element is $x = z = 0$. A fiber of type III over the generic point of $S = V(S)$ requires that the valuation of a_2 and a_4 be:

$$v_S(a_2) \geq 1, \quad v_S(a_4) = 1.$$

Hence, we should have

$$y^2z = x(x^2 + \tilde{a}_2 s^{1+m} z^2 + \tilde{a}_4 s z^3), \quad m \in \mathbb{Z}_{\geq 0}. \tag{10.10}$$

The discriminant is $\tilde{a}_4^2 s^3(4\tilde{a}_4 - \tilde{a}_2^2 s)$. We can therefore take $\tilde{a}_4 = t$ to have a collision of type III+$\mathrm{I}_2^{\mathrm{ns}}$ on the divisors $S = V(s)$ and $T = V(t)$. Since $a_4 = st$, we have the linear relation $S + T = 4L$. The fiber $\mathrm{I}_2^{\mathrm{ns}}$ is replaced by a fiber of type III when $v_T(\tilde{a}_2) \geq 1$. That would give

$$y^2z = x(x^2 + \tilde{a}_2 s^{1+m} t^{1+n} z^2 + stz^3), \quad m, n \in \mathbb{Z}_{\geq 0}. \tag{10.11}$$

If we take the lowest valuations ($m = n = 0$), the coefficient $\tilde{a}_2$ has to be section of $\mathscr{L}^{-\otimes 2}$ while a_2 is a section of $\mathscr{L}^{\otimes 2}$. A general solution is simply to take $\tilde{a}_2 = 0$, which gives[1]

$$y^2z = x(x^2 + stz^2). \tag{10.12}$$

The reduced discriminant $\Delta_{red} = st$ is a normal transverse divisor and the j-invariant is a constant morphism taking the value $j = 1728$ everywhere. After a crepant resolution defined by a sequence of two blow-ups, we get a fiber of type III over the generic point of $S = V(s)$ and the generic point of $T = V(t)$. Over the generic point of their intersection $S \cap T$, the fiber degenerates to The fiber III degenerates to a non-Kodaira fiber of type $1 - 2 - 1$, which is a contraction of a fiber of type

[1] For example, if the base is $\mathbb{P}^r$, this is the only possibility as a line bundle of $\mathbb{P}^r$ and its inverse cannot have non-trivial sections.

I_0^*. There are no other singular fibers. This model satisfies all the conditions of a Miranda model. In Miranda regularization, the collision III+III is replaced by a chain of collisions of type III+I_0^*+III (see [236, Table 13.1]) by blowing up the intersection of the two divisors. The intersection becomes an exceptional divisor of the base over which the generic fiber is of type I_0^{*ss}. Here, we avoid such a blowup of the base since it modifies the canonical class and introduce an additional component in the gauge algebra changing the gauge algebra from type $A_1 \oplus A_1$ to type $A_1 \oplus B_3 \oplus A_1$

10.2 Summary of results

In this section, we categorize all the possible collisions of the fibers that yield SO(4) and Spin(4)-models, and summarize the results of the chapter. We first state the geometrical setup and results including Euler characteristics, Hodge numbers, and the triple intersection polynomials in section 10.2.1, and describe their application to the five-dimensional supergravity theories and their six-dimensional uplifted theories in section 10.2.2. We then list the collision of singularities in section 10.2.3.

10.2.1 Geometry

Weierstrass equations for SO(4) and Spin(4)-models with minimal valuations of the coefficients are given by Table 10.1.

Let Y_0 be one of the Weierstrass models considered in Table 10.1. Then Y_0 has two distinct crepant resolutions $f^{\pm} : Y^{\pm} \to Y_0$. One is given by the sequence of two blowups f^+. The other crepant res-

Group	Collision	Mordell–Weil	Weierstrass model
SO(4)	$\mathrm{I}_2^{\mathrm{ns}}+\mathrm{I}_2^{\mathrm{ns}}\to\mathrm{I}_4^{\mathrm{ns}}$ $\mathrm{I}_2^{\mathrm{ns}}+\mathrm{I}_2^{\mathrm{s}}\to\mathrm{I}_4^{\mathrm{s}}$ $\mathrm{I}_2^{\mathrm{s}}+\mathrm{I}_2^{\mathrm{s}}\to\mathrm{I}_4^{\mathrm{s}}$ $\mathrm{III}+\mathrm{I}_2^{\mathrm{ns}}\to \mathrm{I}-2-\mathrm{I}$ $\mathrm{III}+\mathrm{III}\to \mathrm{I}-2-\mathrm{I}$	$\mathbb{Z}/2\mathbb{Z}$	$y^2z=x^3+a_2x^2z+stxz^2$ $y^2z+a_1xyz=x^3+\widetilde{a}_2tx^2z+stxz^2$ $y^2z+a_1xyz=x^3+\widetilde{a}_2stx^2z+stxz^2$ $y^2z=x^3+\widetilde{a}_2sx^2z+stxz^2$ $y^2z=x^3+\widetilde{a}_2stx^2z+stxz^2$
Spin(4)	$\mathrm{I}_2^{\mathrm{ns}}+\mathrm{I}_2^{\mathrm{ns}}\to\mathrm{I}_4^{\mathrm{ns}}$ $\mathrm{I}_2^{\mathrm{ns}}+\mathrm{I}_2^{\mathrm{s}}\to\mathrm{I}_4^{\mathrm{s}}$ $\mathrm{I}_2^{\mathrm{s}}+\mathrm{I}_2^{\mathrm{s}}\to\mathrm{I}_4^{\mathrm{s}}$ $\mathrm{III}+\mathrm{I}_2^{\mathrm{ns}}\to \mathrm{I}-2-\mathrm{I}$ $\mathrm{III}+\mathrm{III}\to \mathrm{I}-2-\mathrm{I}$ $\mathrm{IV}^{\mathrm{ns}}+\mathrm{I}_2^{\mathrm{ns}}\to \mathrm{I}-2-(1,1)$	trivial	$y^2z=x^3+a_2x^2z+\widetilde{a}_4stxz^2+\widetilde{a}_6s^2t^2$ $y^2z+a_1xyz=x^3+\widetilde{a}_2tx^2z+\widetilde{a}_4stxz^2+\widetilde{a}_6s^2t^2$ $y^2z+a_1xyz=x^3+\widetilde{a}_2stx^2z+\widetilde{a}_4stxz^2+\widetilde{a}_6s^2t^2$ $y^2z=x^3+\widetilde{a}_2sx^2z+\widetilde{a}_4stxz^2+\widetilde{a}_6s^2t^2$ $y^2z=x^3+\widetilde{a}_2stx^2z+\widetilde{a}_4stxz^2+\widetilde{a}_6s^2t^2$ $y^2z=x^3+\widetilde{a}_2sx^2z+\widetilde{a}_4s^2txz^2+\widetilde{a}_6s^2t^2z^3$

Table 10.1: Weierstrass equations and collision rules

olution is obtained by exchanging the order of the blowups.

$$f^+:\quad X_0 \xleftarrow{(x,y,s|e_1)} X_1^+ \xleftarrow{(x,y,t|w_1)} X_2^+. \tag{10.13}$$

$$f^-:\quad X_0 \xleftarrow{(x,y,t|w_1)} X_1^- \xleftarrow{(x,y,s|e_1)} X_2^-. \tag{10.14}$$

The two resolutions are connected by an Atiyah flop. These two resolutions are not isomorphic to each other as the triple intersection numbers are not symmetric under the permutation of S and T.

Theorem 10.2.1. *The generating polynomial of the Euler characteristic of a Spin(4)-model obtained by a crepant resolution of a Weierstrass model given in Table 10.1 is*

$$\chi(Y)=2\left(\frac{S(-6L^2(4T+3)+L(8(T-1)T-9)+T(5T+4))}{(2L+1)(S+1)(T+1)(-6L+2S+2T-1)}\right.$$
$$\left.+\frac{S^2(L(8T+6)+5T+3)+3(2L+1)\,(T^2-L(3T+2))}{(2L+1)(S+1)(T+1)(-6L+2S+2T-1)}\right)c(B).$$

In particular, in the case of a Calabi–Yau threefold that is also a Spin(4)-model we have

$$\chi(Y) = -2\left(30K^2 + 15K(S+T) + 3S^2 + 3T^2 + 4ST\right).$$

Theorem 10.2.2. *The Hodge numbers of a Spin(4)-model given by the crepant resolution of a Weierstrass model given in Table 10.1 are*

$$h^{1,1}(Y) = 13 - K^2, \quad h^{2,1}(Y) = 13 + 29K^2 + 15K(S+T) + 3S^2 + 4ST + 3T^2.$$

For the Euler characteristic and the Hodge numbers of the Spin(4)-models, see their proof and detailed description in section 10.4.2.

Theorem 10.2.3. *The generating polynomial of the Euler characteristic of an SO(4)-model given by the crepant resolution of a Weierstrass model given in Table 10.1 is*

$$\chi(Y) = \frac{4(3L + 4TL - T^2)}{(1+T)(1+4L-T)}c(B).$$

In particular, if the SO(4)-model is a Calabi–Yau threefold,we have

$$\chi(Y) = -4(9K^2 + 4KT + T^2).$$

Theorem 10.2.4. *The Hodge numbers of an SO(4)-model given by the crepant resolution of a Weier-*

strass model given in Table 10.1 are

$$h^{1,1}(Y) = 13 - K^2, \quad h^{2,1}(Y) = 13 + 17K^2 + 8KT + 2T^2.$$

For the Euler characteristic and the Hodge numbers of the SO(4)-models, see their proof and detailed description in section 10.3.3.

Theorem 10.2.5. *Let $f^+ : Y^+ \to Y_0$ be the crepant resolution where Y_0 is any of the Spin(4)-model listed in Table 10.1. The triple intersection polynomial of Y^+ is*

$$\begin{aligned}
\mathscr{F}^+_{trip} &= \int_Y \pi_* f_* \left[\left(\psi_0 D_0^s + \psi_1 D_1^s + \varphi_0 D_0^t + \varphi_1 D_1^t \right)^3 \right] \\
&= 2T(-2L + S - T)\varphi_1^3 - 6ST\psi_1\varphi_1^2 - 2S(2L + S)\psi_1^3 \\
&\quad + 2T(2L - S - 2T)\varphi_0^3 + 6T\varphi_0^2 \left(\varphi_1(-2L + S + T) - S\psi_1 \right) - 4S(S - L)\psi_0 \left(\psi_0 - \psi_1 \right)^2 \\
&\quad - 2S(2L + S)\psi_0\psi_1 \left(\psi_0 - \psi_1 \right) + 6T\varphi_0 \left(\varphi_1^2(2L - S) - 2S \left(\psi_0 - \psi_1 \right)^2 + 2S\psi_1\varphi_1 \right).
\end{aligned}$$

The triple intersection polynomial in the fibration Y^- defined by exchanging the order of the blowup is $\mathscr{F}^-_{trip}$ and is obtained from $\mathscr{F}^-_{trip}$ by the involution $\psi \leftrightarrow \varphi$.

The triple intersection polynomial for the Spin(4)-models are derived in section 10.4.3. The triple intersection for an SO(4)-model is then derived from the one of a Spin(4)-model by the specialization $S \to -4K - T$.

Theorem 10.2.6. *Let $f^+ : Y^+ \to Y_0$ be the crepant resolution where Y_0 is any of the SO(4)-model*

listed in Table 10.1. The triple intersection polynomial of Y^+ is

$$\begin{aligned}\mathscr{F}^+_{trip} =& \pi_* f_* \left(\psi_0 D^s_0 + \psi_1 D^s_1 + \varphi_0 D^t_0 + \varphi_1 D^t_1\right)^3 \\ =& -2T\varphi_0^3(2L+T) - 2(4L-T)\left(\psi_0-\psi_1\right)^2\left(\psi_0(6L-2T)+\psi_1(6L-T)\right) \\ &+ 6T\varphi_0\left(-\left(\psi_0-\psi_1\right)^2(4L-T) + 2\psi_1\varphi_1(4L-T) + \varphi_1^2(T-2L)\right) + 6T\varphi_0^2\left(\psi_1(T-4L)+2L\varphi_1\right) \\ &- 2\left(24L^2-10LT+T^2\right)\psi_1^3 + 6T(T-4L)\psi_1\varphi_1^2 + 4T(L-T)\varphi_1^3.\end{aligned}$$

This triple intersection model of an SO(4)-model is described in detail in section 10.3.4.

10.2.2 Applications to 5*d* and 6*d* supergravity theories

The $\mathbb{Z}/2\mathbb{Z}$ quotients of Spin(4) can be SO(4), or the half-spin groups SO(3)×SU(2) and SU(2)× SO(3). But which one is realized by the collisions presented in Table 10.1? This question is answered by scrutinizing the representation **R** associated with the elliptic fibration.

We recall that a representation of $A_1 \oplus A_1$ is given by two spins (j_1, j_2) where j_1 is in $\frac{1}{2}\mathbb{Z}_{\geq 0}$. It we name the representation by two numbers indicating the dimension of each projection, (j_1, j_2) is the same as $(2\mathbf{j}_1 + 1, 2\mathbf{j}_2 + 1)$. Each representation (j_1, j_2) is a valid representation of Spin(4). But is only a projective representation of the three possible $\mathbb{Z}/2\mathbb{Z}$ quotient of Spin(4). More explicitly, the representations of the semi-spin group SU(2)× SO(3) are those with spin (j_1, j_2) where j_2 an integer, while the representations of the semi-spin group SO(3)× SU(2) have spin (j_1, j_2) where j_1 an integer, and the representations of SO(4) have spin (j_1, j_2) such that $j_1 + j_2$ an integer.

Group	Representation (j_1, j_2) or $(2\mathbf{j}_1 + 1, 2\mathbf{j}_2 + 1)$
Spin(4)	$j_1, j_2 \in \frac{1}{2}\mathbb{Z}_{\geq 0}$
$\text{Spin}^+(4)$	$j_1 \in \mathbb{Z}_{\geq 0}$, $j_2 \in \frac{1}{2}\mathbb{Z}_{\geq 0}$
$\text{Spin}^-(4)$	$j_1 \in \frac{1}{2}\mathbb{Z}_{\geq 0}$, $j_2 \in \mathbb{Z}_{\geq 0}$
SO(4)	$j_1, j_2 \in \frac{1}{2}\mathbb{Z}_{\geq 0}, j_1 + j_2 \in \mathbb{Z}_{\geq 0}$

Table 10.2: Representations for SO(4) and Spin(4) groups.

The determination of the representation $\mathbf{R}$ associated to an elliptic fibration is explained in section 2.3. In the present case, we find that [2]:

$$\text{SO(4)-model:} \qquad \mathbf{R} = (3,1) \oplus (1,3) \oplus (2,2)$$

$$\text{Spin(4)-model:} \qquad \mathbf{R} = (3,1) \oplus (1,3) \oplus (2,2) \oplus (2,1) \oplus (1,2)$$

The representation $(3,1) \oplus (1,3)$ is the adjoint representation of the Lie algebra of type $D_2 \cong A_1 \oplus A_1$ and the representation $(2,1) \oplus (1,2)$ is the spin representation of D_2. The representation $(2,2)$ is the vector representation of D_2. The collisions listed in Table 10.1 always produce the bifundamental representation $(2,2)$ of spin $(\frac{1}{2}, \frac{1}{2})$ of the Lie algebra of type D_2. Such a representation is incompatible with the half-spin groups and left only SO(4) and Spin(4) as possible options. [3]

[2] We denote a representation by the dimensions $(\mathbf{d}_1, \mathbf{d}_2)$ of its two projections.

[3] The bifundamental representation $(2,2)$ of $A_1 \oplus A_1$ is the vector representation of SO(4) of dimension 4, which, in terms of spins of the two SU(2) forming a Spin(4), is the representation $(\frac{1}{2}, \frac{1}{2})$. The bifundamental representation rules out the groups $SU(2) \times SO(3)$ and $SO(3) \times SU(2)$, but is a valid representation of both SO(4) and Spin(4).

From the point of view of the elliptic fibration, the group Spin(4) requires a trivial Mordell–Weil group while the group SO(4) requires a Mordell–Weil group $\mathbb{Z}/2\mathbb{Z}$. We are not aware of any F-theory construction of a gauge theory with the semi-spin group SU(2)×SO(3).

We denote by g_S and g_T the genus of S and T. The SO(4)-model only has adjoint representations ($\mathbf{Adj}^- = (3,1)$ and $\mathbf{Adj}^+ = (1,3)$) and the vector representation $\mathbf{V} = (2,2)$. For the Spin(4)-model, there are additional hypermultiplets transforming in the two semi-spin representations ($\mathbf{Spin}^-$ $(2,1)$ and $\mathbf{Spin}^+$ $(1,2)$) of $\mathrm{D}_2 \cong \mathfrak{so}(4)$. If we denote by Δ' the third component of the discriminant locus, then the number of hypermultiplets transforming in the semi-spin representations $\mathbf{Spin}^\pm$ of $\mathrm{D}_2 \cong \mathfrak{so}(4)$ are given by the intersection numbers $S\cdot\Delta'$ and $T\cdot\Delta'$. The class of Δ' is $-2(4K+T+S)$. In particular, it is zero when we specialize to the SO(4)-model.

We show that for an SO(4)-model and a Spin(4)-model with the matter content discussed above and summarized on Table 10.3, all anomalies are canceled in a six-dimensional $\mathcal{N} = (1,0)$ supergravity theory. Comparing the triple intersection numbers of an SO(4)-model with the prepotential of a five-dimensional $\mathcal{N} = 1$ theory with matter charged under the same representation $\mathbf{R}$ completely fixes the numbers of charged hypermultiplets. However this is not the case for a Spin(4)-model, since there are more representations involved; the comparison with the triple intersection numbers only give two linear relations. Using additional information from intersecting branes, we check that the six-dimensional uplifted theory can be anomaly-free by the Green-Schwarz mechanism.

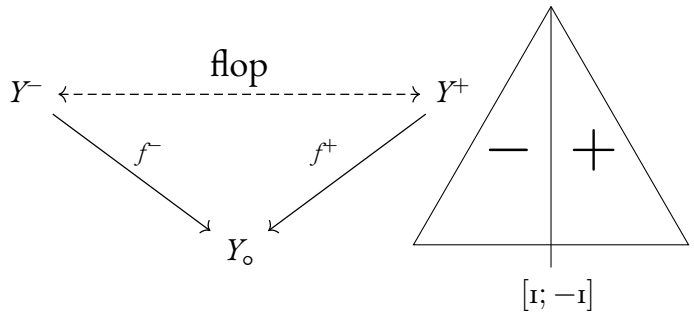

Figure 10.1: Coulomb phases of an SO(4)-model or a Spin(4)-model with matter in the representation $(2,2)$. The addition of the representation $(3,1)$, $(1,3)$, $(2,1)$, or $(1,2)$ do not change the chamber structure.The only weight defining an interior wall is the weight $[1;-1]$ of the representation $(2,2)$. Geometrically, the chambers are identified by the presence of a curve with weights $\pm[1,-1]$ with respect to the fibral divisors D_1^s and D_1^t that project respectively to the divisors S and T and do not touch the zero section of the elliptic fibration.

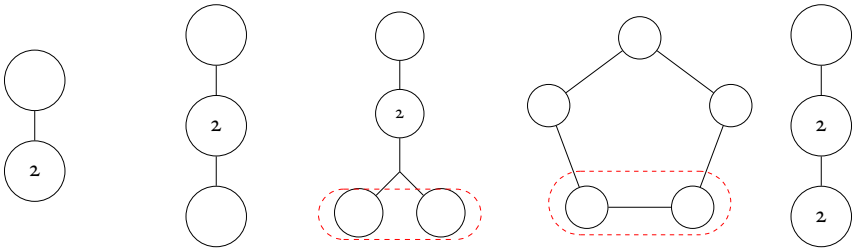

Figure 10.2: Non-Kodaira fibers. Nodes surrounded by a red ellipsis are obtained only after a field extension. For example, all these fibers appear in the collision $I_2^s+I_2^s$.

SO(4)	$\mathbf{R} = (3,1) \oplus (1,3) \oplus (2,2)$ $\chi(CY_3) = -4(9K^2 + 4KT + T^2)$ $h^{1,1}(CY_3) = 13 - K^2, \quad h^{2,1}(CY_3) = 13 + 17K^2 + 8KT + 2T^2$ $\mathscr{F}^+_{triple} = -2\left(24L^2 - 10LT + T^2\right)\psi_1^3 + 6T(T-4L)\psi_1\varphi_1^2 + 4T(L-T)\varphi_1^3$ $n_{1,3} = g_T, \quad n_{3,1} = g_S, \quad n_{2,2} = S \cdot T$
Spin(4)	$\mathbf{R} = (3,1) \oplus (1,3) \oplus (2,2) \oplus (2,1) \oplus (1,2)$ $\chi(CY_3) = -2\left(30K^2 + 15KS + 15KT + 3S^2 + 4ST + 3T^2\right)$ $\mathscr{F}^+_{triple} = 2T(-2L + S - T)\varphi_1^3 - 6ST\psi_1\varphi_1^2 - 2S(2L+S)\psi_1^3$ $h^{1,1}(CY_3) = 13 - K^2, \quad h^{2,1}(CY_3) = 13 + 29K^2 + 15KS + 15KT + 3S^2 + 4ST + 3T^2$ $n_{3,1} = g_S, \quad n_{1,3} = g_T, \quad n_{2,2} = S \cdot T, \quad n_{2,1} = S \cdot V(\tilde{b}_8), \quad n_{1,2} = T \cdot V(\tilde{b}_8)$

Table 10.3: Data of the low energy effective theory of a SO(4) and a Spin(4)-model compactified on a Calabi–Yau threefolds. $\mathbf{R}$ is the representation, χ is the Euler characteristic of the Calabi–Yau threefold, S and T are the two divisors supporting the reducible fibers, g_S and g_T are the genus of these divisors. The number of representations in the irreducible representation $\mathbf{R}_i$ is denoted $n_{\mathbf{R}_i}$. $\mathscr{F}^+_{triple}$ is the triple intersection polynomial for the variety Y^+ defined by the crepant resolution of equation (10.13). In the resolution Y^-, we have a distinct $\mathscr{F}^-_{triple}$ obtained by exchanging ψ_1 and φ_1, which corresponds to the crepant resolution of equation 10.14.

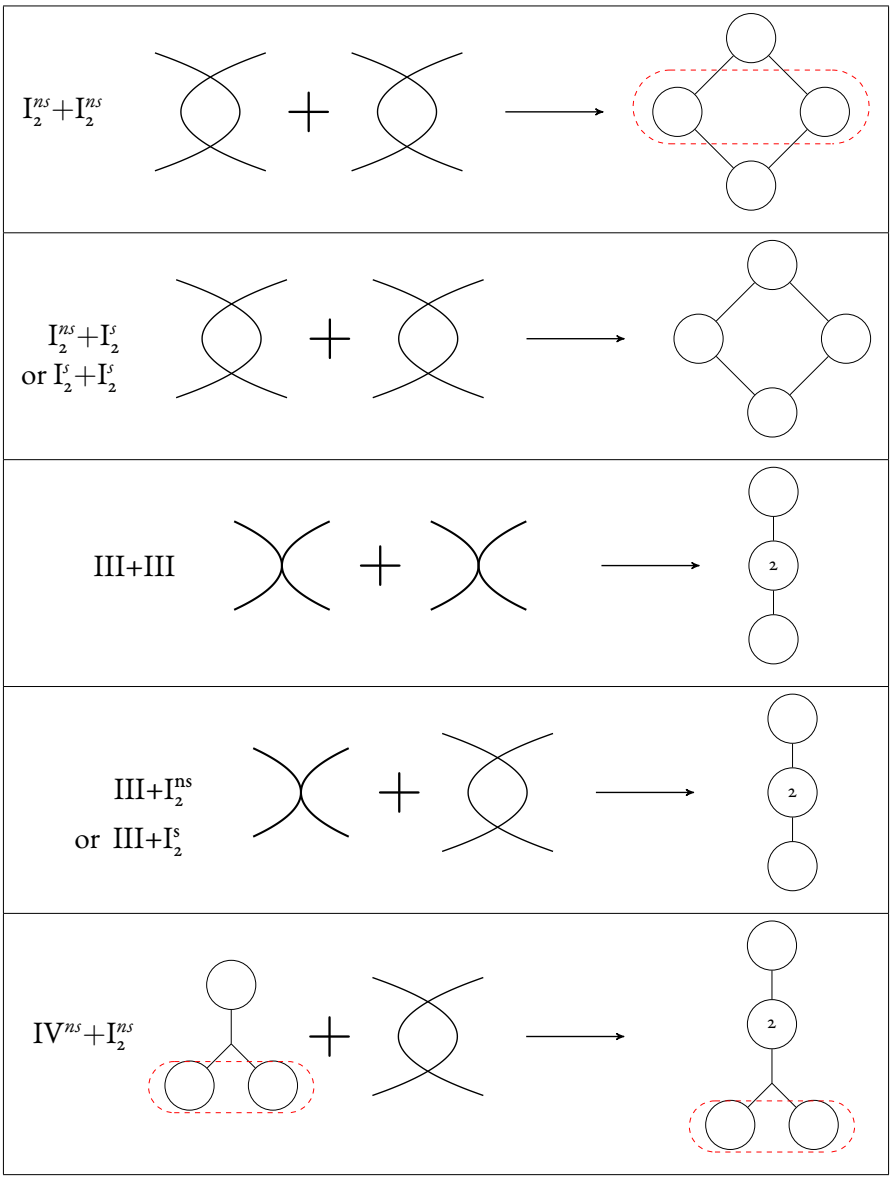

Table 10.4: Collisions at the intersections of two Kodaira fibers with dual graph $\widetilde{A}_1$. The representation produced is always the bifundamental representation $(2, 2)$ of $A_1 \oplus A_1$. Nodes surrounded by a red ellipse form a non-split node and are obtained individually only after a field extension (they are "related by monodromies").

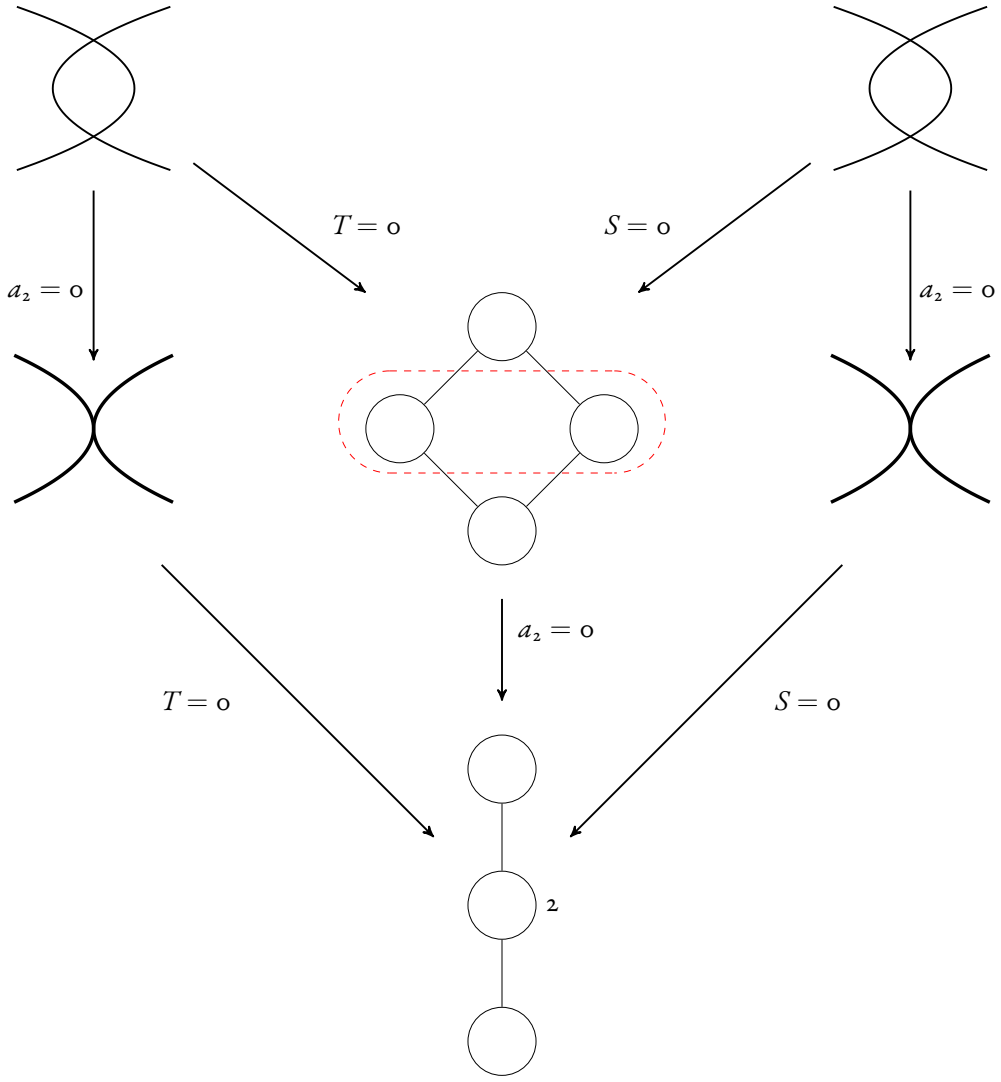

Figure 10.3: Fiber structure of an SO(4)-model with collision $\mathrm{I}_2^{\mathrm{ns}} + \mathrm{I}_2^{\mathrm{ns}}$ and Mordell–Weil group $\mathbb{Z}/2\mathbb{Z}$.

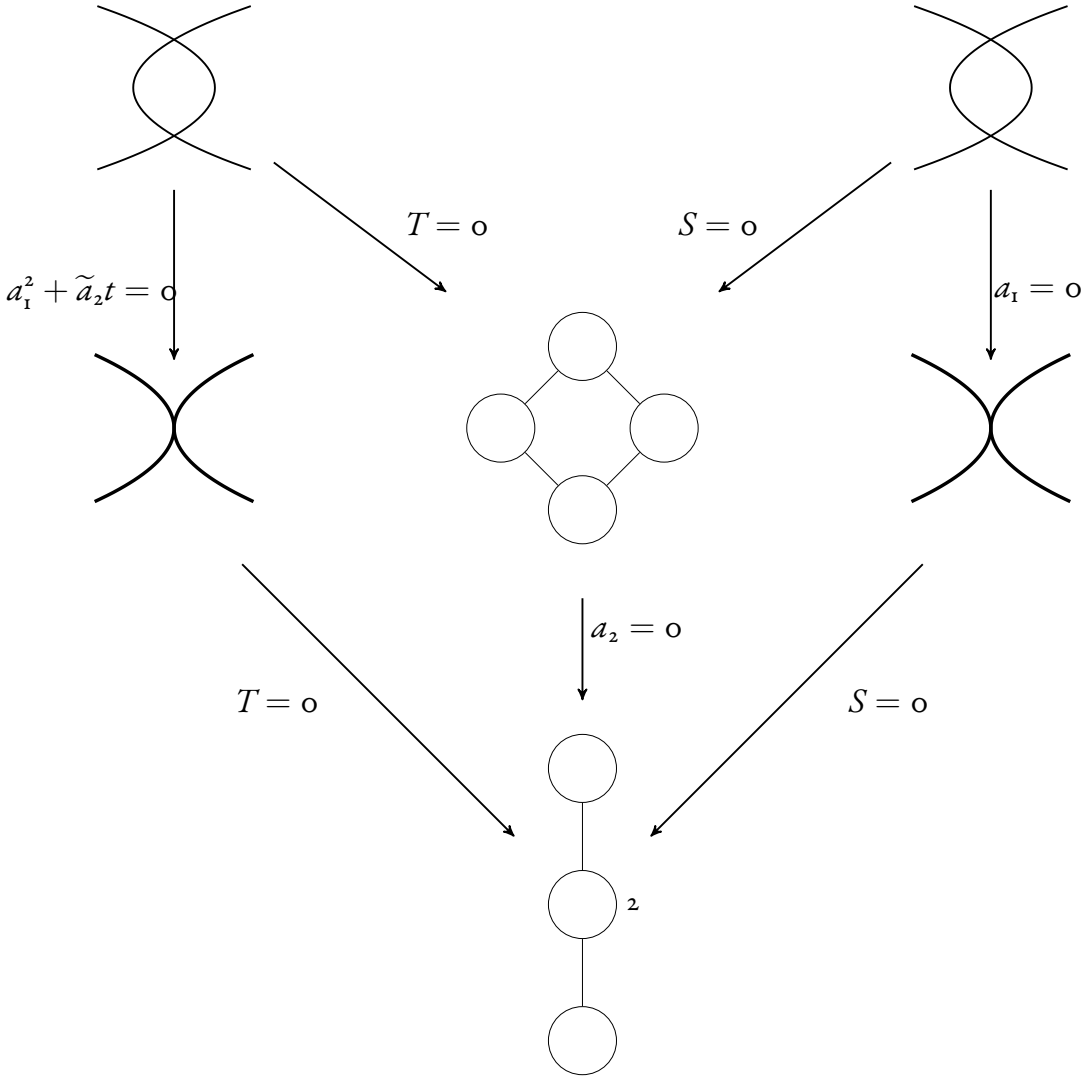

Figure 10.4: Fiber structure of an SO(4)-model with collision $\mathrm{I}_2^{\mathrm{ns}} + \mathrm{I}_2^{\mathrm{s}}$ and Mordell–Weil group $\mathbb{Z}/2\mathbb{Z}$.

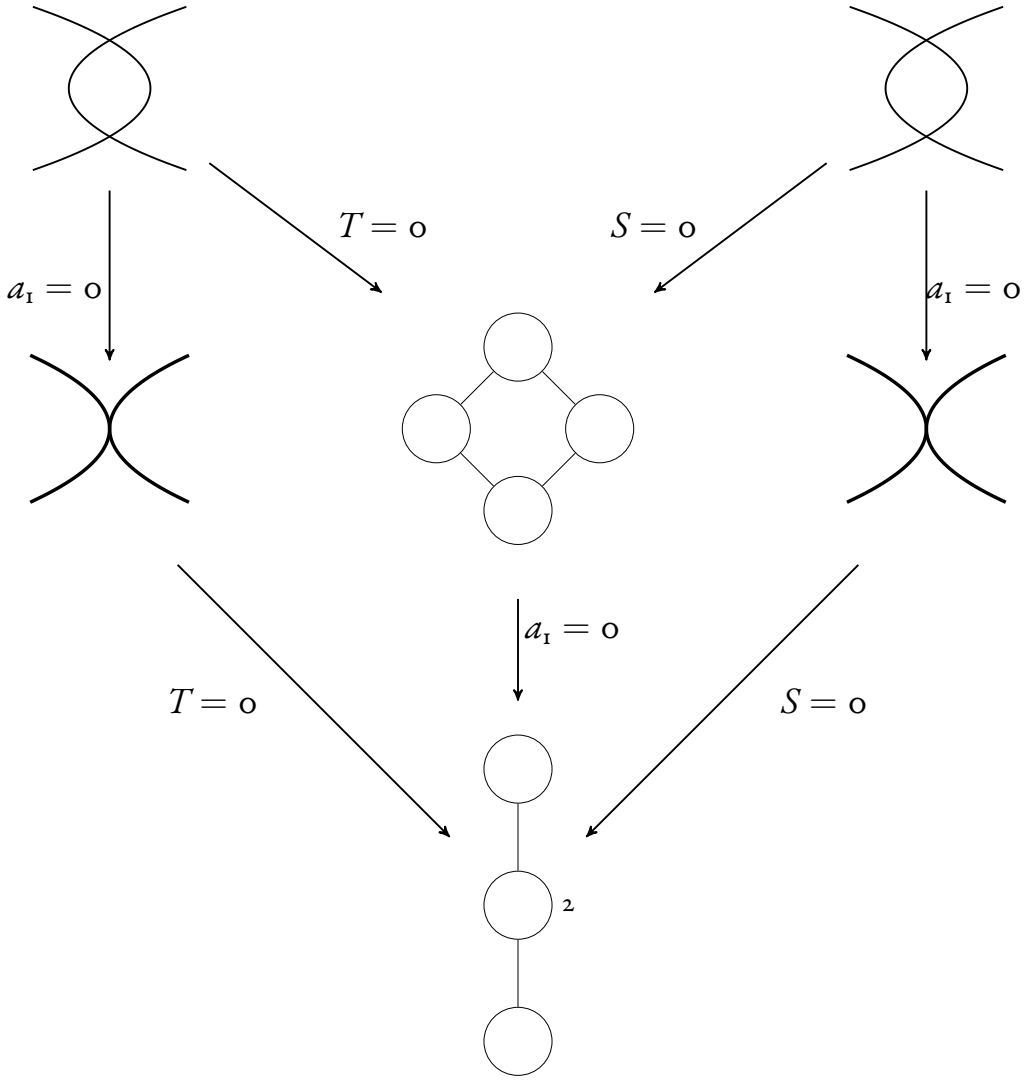

Figure 10.5: Fiber structure of an SO(4)-model with collision $I_2^s + I_2^s$ and Mordell–Weil group $\mathbb{Z}/2\mathbb{Z}$.

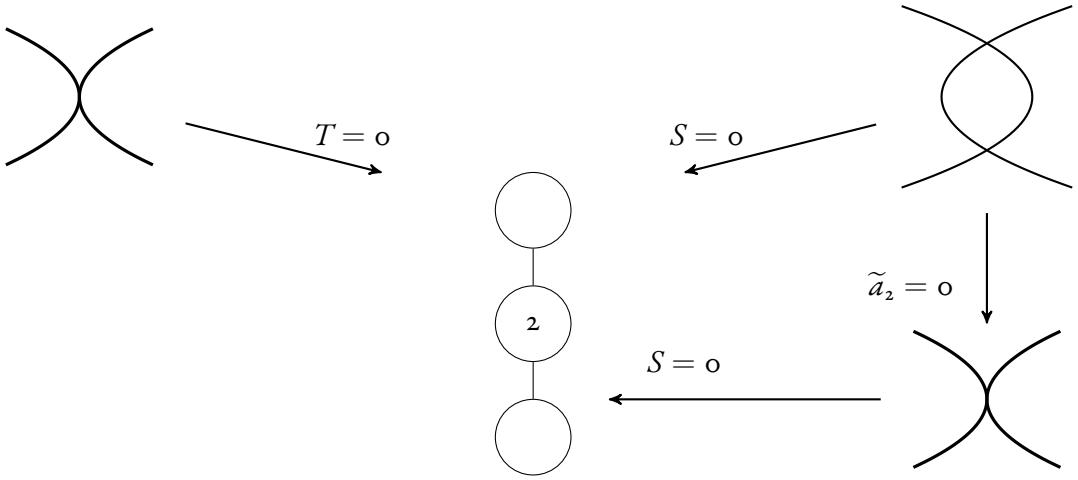

Figure 10.6: Fiber structure of an SO(4)-model with III+I_2^{ns}. The Weierstrass equation is $y^2z = x^3 + a_2st^2z + stxz^2$.

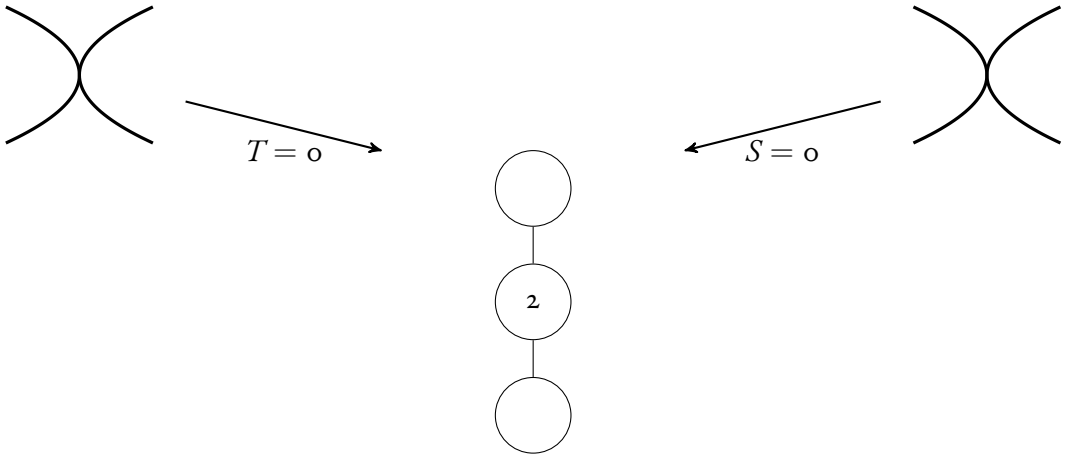

Figure 10.7: Fiber structure of an SO(4)-model with III+III. The Weierstrass equation is $y^2z = x^3 + stxz^2$ and there are moduli coming from the Weierstrass coefficients since we necessary have $S + T = 4L$ and $a_2 = 0$. The discriminant $\Delta \propto s^3t^3$ is a divisor with simple normal crossing and the j-invariant is constant and equal to 1728.

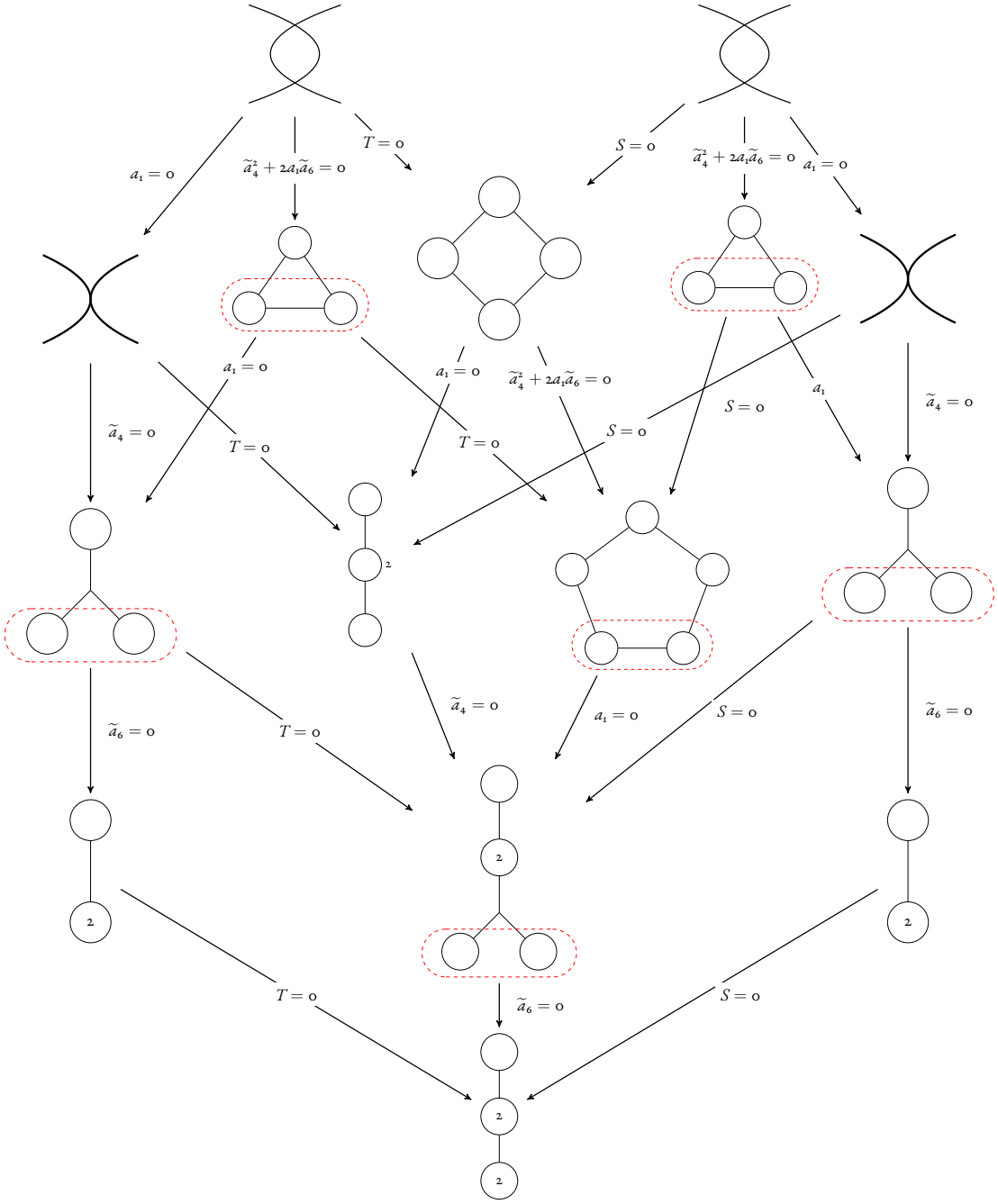

Figure 10.8: Fiber structure of a Spin(4)-model with $I_2^s + I_2^s$.

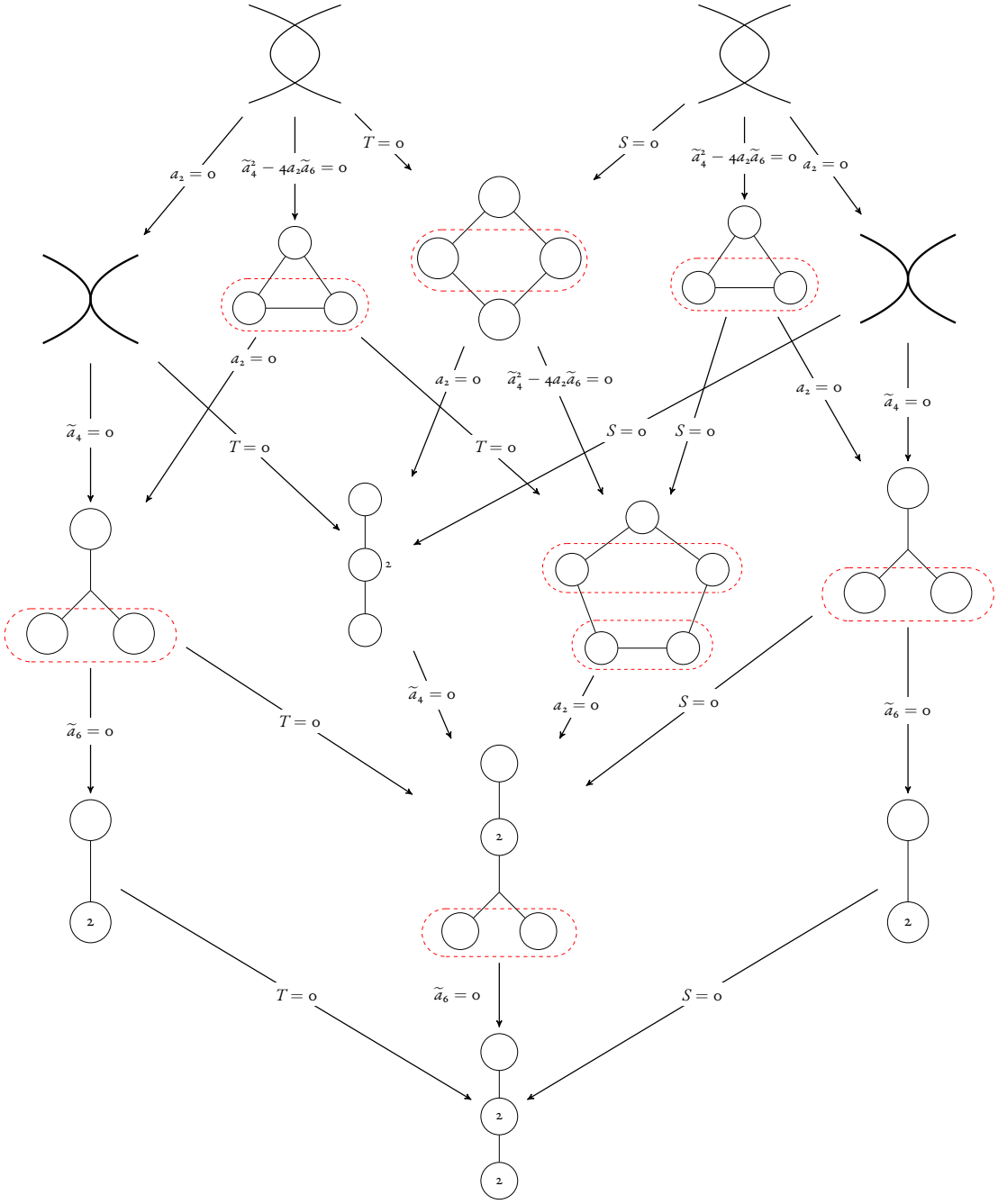

Figure 10.9: Fiber structure of a Spin(4)-model with $\mathrm{I}_2^{\mathrm{ns}} + \mathrm{I}_2^{\mathrm{ns}}$.

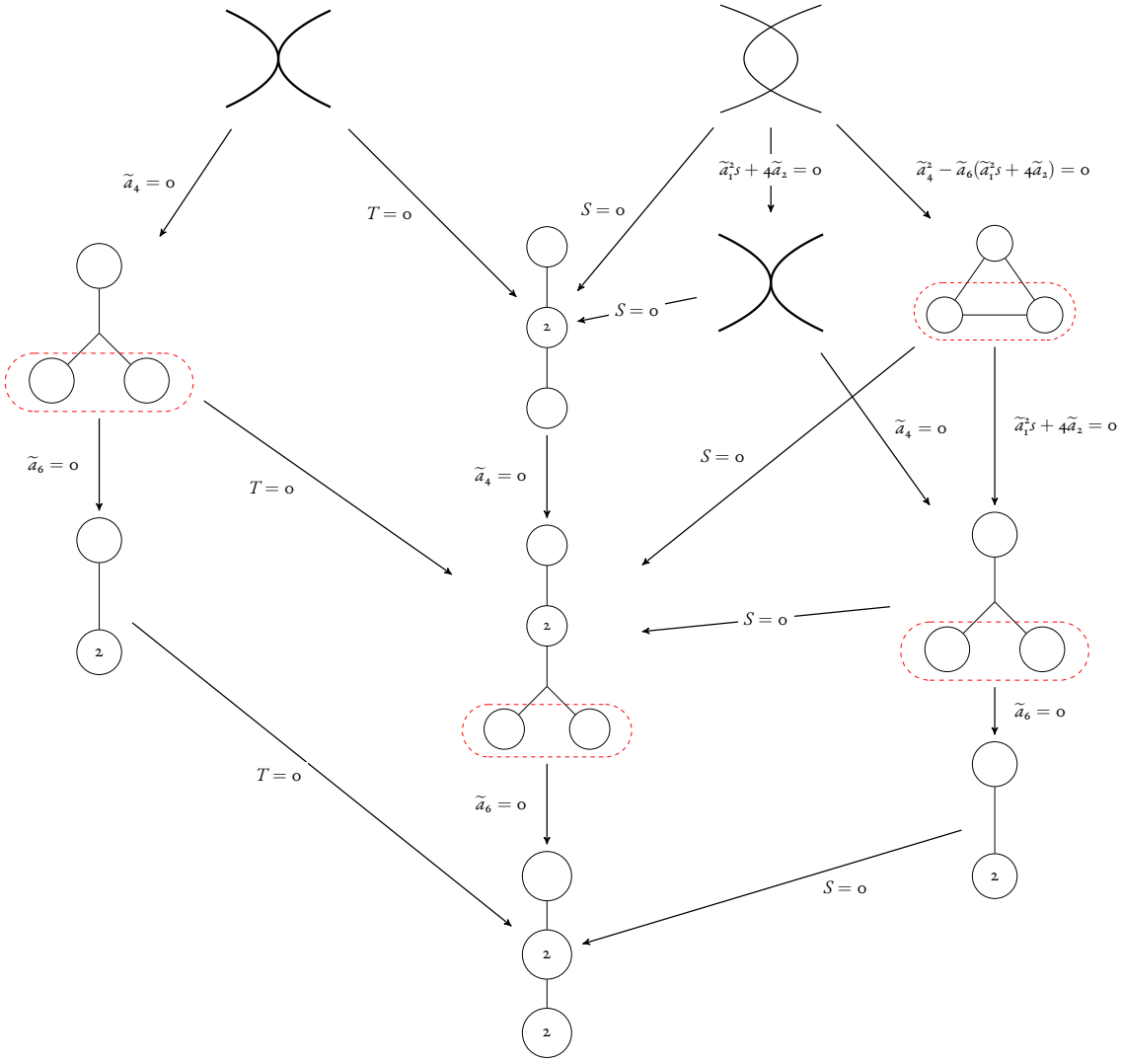

Figure 10.10: Fiber structure of a Spin(4)-model with III+I_2^{ns}.

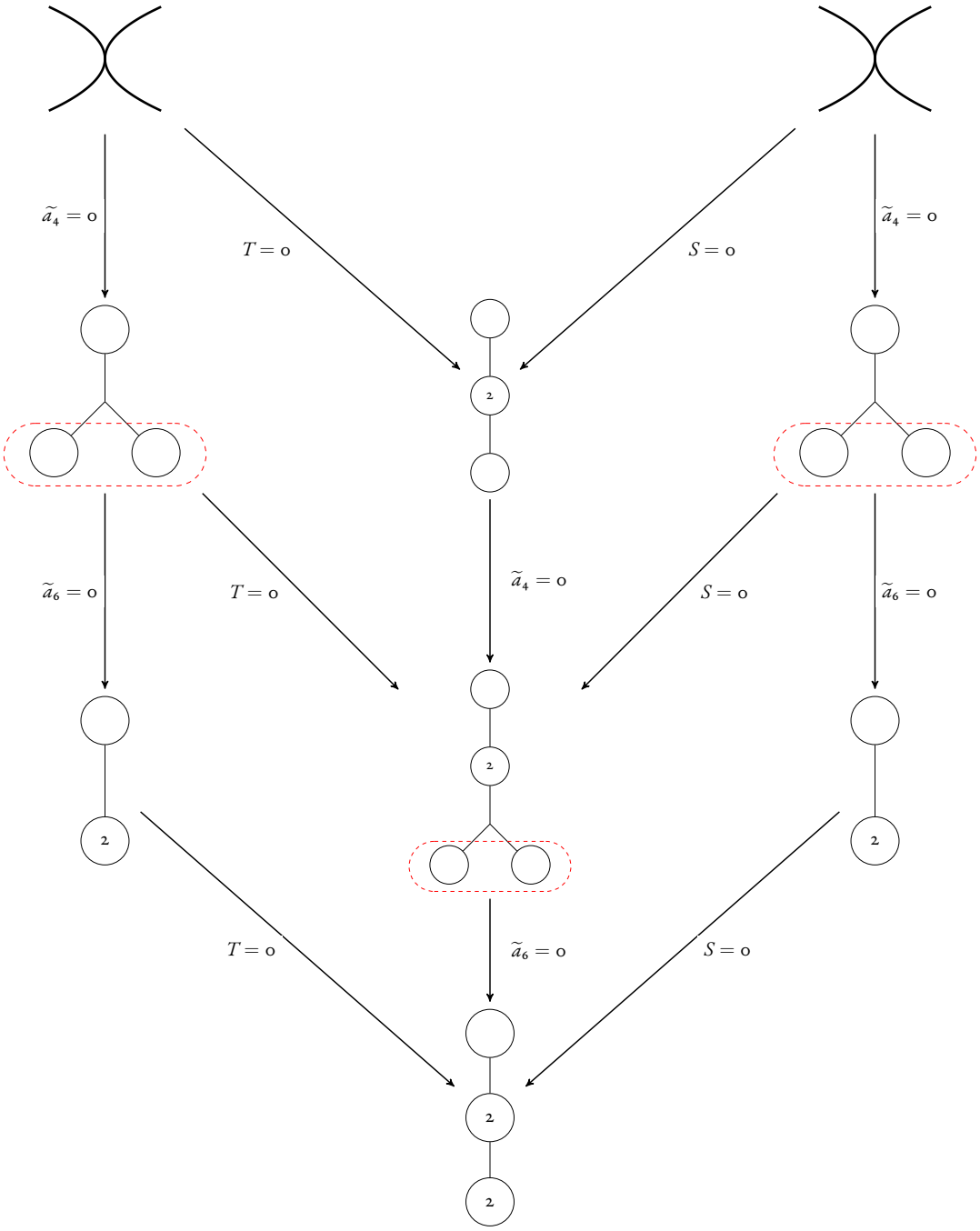

Figure 10.11: Fiber structure of a Spin(4)-model with III+III.

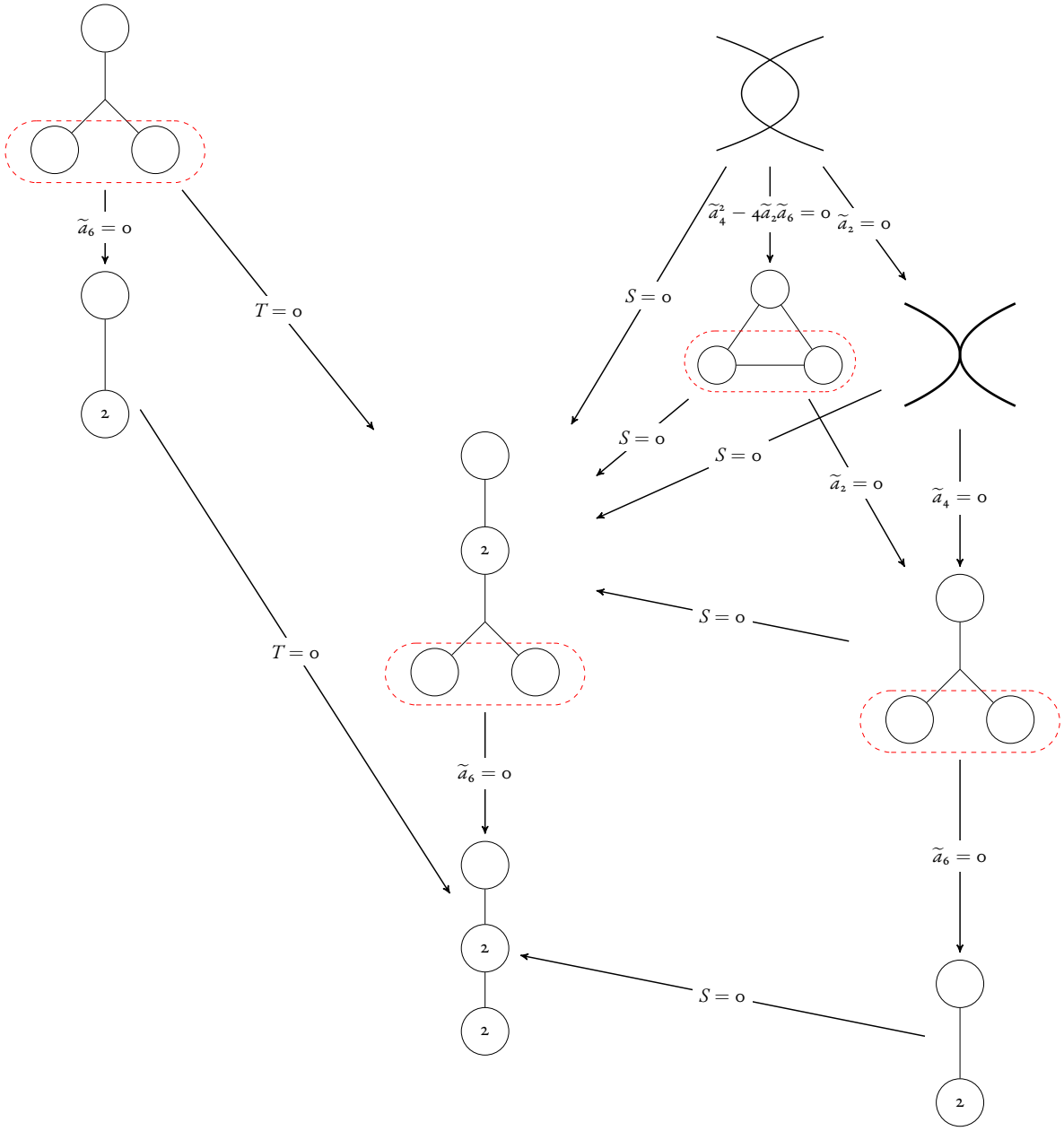

Figure 10.12: Fiber structure of a Spin(4)-model with $\mathrm{IV}^{ns} + \mathrm{I}_2^{\mathrm{ns}}$.

10.3 SO(4)-model

The generic SO(4)-model is defined as an $\mathrm{I}_2^{\mathrm{ns}} + \mathrm{I}_2^{\mathrm{ns}}$-model with a $\mathbb{Z}/2\mathbb{Z}$ Mordell–Weil group. We assume that the first and second $\mathrm{I}_2^{\mathrm{ns}}$ are the generic fibers of two smooth divisors $S = V(s)$ and $T = V(t)$ intersecting transversally. Using the work of Miranda or Nakayama, we expect a geometric fiber of type I_4 at the collision of S and T. All the other SO(4)-model are then obtained as degenerations of this one.

10.3.1 Weierstrass equation, crepant resolutions and flops

We recall that the generic Weierstrass model with a $\mathbb{Z}/2\mathbb{Z}$ Mordell–Weil group is

$$y^2z = x^3 + a_2x^2z + a_4xz^2, \tag{10.15}$$

where a_2 and a_4 are respectively sections of $\mathscr{L}^{\otimes 2}$ and of $\mathscr{L}^{\otimes 4}$. The discriminant locus of this elliptic fibration is $\Delta = 16a_4^2(a_2^2 - 4a_4)$. The generic fiber over $V(a_4)$ is of type $\mathrm{I}_2^{\mathrm{ns}}$ while the generic fiber over $V(a_2^2 - 4a_4)$ is of type I_1. An SO(4)-model is obtained by requiring a_4 to factor into two irreducible components

$$a_4 = st. \tag{10.16}$$

We assume that $S = V(s)$ and $T = V(t)$ are two smooth divisors intersecting transversally. Since a_4 is a section of $\mathscr{L}^{\otimes 4}$, the equation $a_4 = st$ imposes the following linear constraint on the class of S

and T:

$$S + T = 4L, \tag{10.17}$$

where we denote the first Chern class of $\mathscr{L}$ as $L = c_1(\mathscr{L})$. The Weierstrass model of this SO(4)-model is then

$$y^2 z = x^3 + a_2 x^2 z + stxz^2. \tag{10.18}$$

Its discriminant locus is

$$\Delta = 16 s^2 t^2 \left(a_2^2 - 4st\right), \tag{10.19}$$

which consists of three components

$$S = V(s), \quad T = V(t), \text{ and } \Delta' = a_2^2 - 4st. \tag{10.20}$$

When the base is of dimension three or higher, the divisor Δ' has double point singularities at $V(a_2, s, t)$. The divisors S and T do not intersect Δ' transversally as the intersection is non-reduced.

We can easily deform the elliptic fibration to produce other fibers still giving an SO(4)-model.

$$\mathrm{I}_2^{\mathrm{ns}} + \mathrm{I}_2^{\mathrm{s}}: \quad y^2 z + a_1 yxz = x^3 + \widetilde{a}_2 tx^2 z + stxz^2 \tag{10.21}$$

$$\mathrm{I}_2^{\mathrm{s}} + \mathrm{I}_2^{\mathrm{s}}: \quad y^2 z + a_1 yxz = x^3 + \widetilde{a}_2 stx^2 z + stxz^2 \tag{10.22}$$

$$\mathrm{III} + \mathrm{I}_2^{\mathrm{s}}: \quad y^2 z = x^3 + \widetilde{a}_2 sx^2 z + stxz^2 \tag{10.23}$$

$$\mathrm{III} + \mathrm{I}_2^{\mathrm{s}}: \quad y^2 z + \widetilde{a}_1 sxyz = x^3 + \widetilde{a}_2 sx^2 z + stxz^2 \tag{10.24}$$

$$\text{III} + \text{III}: \quad y^2 z = x^3 + \widetilde{a}_2 s t x^2 z + s t x z^2. \tag{10.25}$$

We give a crepant resolution via following sequence of two blowups

$$X_0 \xleftarrow{(x,y,s|e_1)} X_1 \xleftarrow{(x,y,t|w_1)} X_2. \tag{10.26}$$

The other crepant resolution connected by a flop is obtained by exchanging S and T. For that reason, we work with the current resolution as the other one is described by a simple exchange of S and T. The relative "projective coordinates" of X_2 are then given by

$$[e_1 w_1 x : e_1 w_1 y : z = 1][w_1 x : w_1 y : s][x : y : t]. \tag{10.27}$$

The proper transform of the original Weierstrass model is

$$y^2 z = e_1 w_1 x^3 + a_2 x^2 z + s t x z^2. \tag{10.28}$$

By the Jacobian criterion, assuming that S and T are transverse is enough to prove that this proper transform is smooth since (x, y, st) is an empty ideal after the two blowups.

In the SO(4)-model, the Atiyah flop is easily seen by considering a partial resolution that is a

common blowdown for both resolutions.

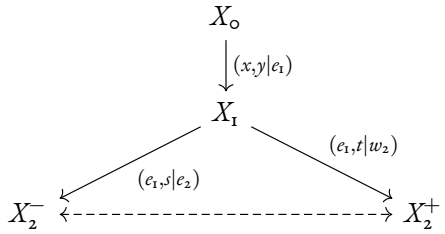

(10.29)

After the first blow-up, we get the partial resolution

$$\mathscr{E}_1 : \quad e_1(y^2 - e_1x^3 - a_2x^2) = stx. \tag{10.30}$$

Since (x, y) cannot vanish at the same time, the previous equation is of the type $u_1u_2 - u_3u_4 = 0$, which is exactly the equation of the singularity whose resolutions determine the Atiyah's flop. The two crepant resolutions are then obtained by blowing up (e_1, s) or (e_1, t).

10.3.2 Fiber structure

We can now study the fiber structure of this elliptic fibration. We assume that the base is of arbitrary dimension. We have four fibral divisors:

$$\begin{cases} D_0^s & : \quad s = y^2 - e_1 w_1 x^3 - a_2 x^2 = 0, \\ D_1^s & : \quad e_1 = y^2 - a_2 x^2 - stx = 0, \\ D_0^t & : \quad t = y^2 - e_1 w_1 x^3 - a_2 x^2 = 0, \\ D_1^t & : \quad w_1 = y^2 - a_2 x^2 - stx = 0. \end{cases} \tag{10.31}$$

The divisors D_0^s and D_1^s (resp. D_0^t and D_1^t) project to S (resp. T). All these divisors are conic bundles. Over the generic point of S, we have two fibers C_0^s and C_1^s intersecting at

$$C_0^s \cap C_1^s : s = e_1 = y^2 - a_2 x^2 = 0. \tag{10.32}$$

The intersection points are the two roots of $y^2 - a_2 x^2 = 0$. Thus, this is does represent an I_2^{ns} since computing the roots requires taking the square root of a_2, the two points coincide when $a_2 = 0$ yielding a fiber of type III. The same is true over T, where the generic fiber $\mathrm{I}_2^{\mathrm{ns}}$ degenerates to a fiber

III over $T \cap V(a_2)$. At the intersection of S and T, we get

$$\begin{cases} D_0^s \cap D_0^t & : s = t = y^2 - e_1 w_1 x^3 - a_2 x^2 = 0 \to \eta^{00}, \\ D_1^s \cap D_0^t & : e_1 = t = y^2 - a_2 x^2 = 0 \to \eta^{10\pm}, \\ D_1^s \cap D_1^t & : e_1 = w_1 = y^2 - a_2 x^2 - stx = 0 \to \eta^{11}, \end{cases} \tag{10.33}$$

where the intersections of the new fibers are given by

$$\eta^{00} \cap \eta^{10\pm} : s = e_1 = t = y^2 - a_2 x^2 = 0, \tag{10.34}$$

$$\eta^{10\pm} \cap \eta^{11} : e_1 = t = w_1 = y^2 - a_2 x^2 = 0. \tag{10.35}$$

This gives a fiber of type $\mathrm{I}_4^{\mathrm{ns}}$ (see Figure 10.7). Over $V(S, T, a_2)$, the fiber $\mathrm{I}_4^{\mathrm{ns}}$ degenerates further to a non-Kodaira fiber of type $1 - 2 - 1$ as the two rational curves $\eta^{10\pm}$ coincide. There are no other degenerations.

At the collision $S \cap T$, the splitting of the curves C_0^s, C_1^s, C_0^t, and C_1^t are given by

$$\begin{cases} C_0^s \to \eta^{00}, \\ C_1^s \to \eta^{10+} + \eta^{10-} + \eta^{11}, \\ C_0^t \to \eta^{00} + \eta^{10+} + \eta^{10-}, \\ C_1^t \to \eta^{11}, \end{cases} \tag{10.36}$$

This induces linear relations that we exploit to compute the intersection numbers between the curves of the collision and the fibral divisors

	D_0^s	D_1^s	D_0^t	D_1^t
η^{00}	-2	2	0	0
$\eta^{10+} + \eta^{10-}$	2	-2	-2	2
$\eta^{10\pm}$	1	-1	-1	1
η^{11}	0	0	2	-2.

(10.37)

Hence, we see that we get the weight $[1; -1]$ from the curves $\eta^{10\pm}$. Since both $[1]$ and $[-1]$ are from the representation 2 of $\mathfrak{su}(2)$, we can deduce that the matter content we get is a bifundamental, $(2, 2)$, corresponding to the vector representation of SO(4). Hence the matter contents of the $\mathrm{I}_2^{ns}+\mathrm{I}_2^{ns}$-model with a $\mathbb{Z}/2\mathbb{Z}$ Mordell–Weil group is given by

$$\mathbf{R} = (3, 1) \oplus (1, 3) \oplus (2, 2). \tag{10.38}$$

10.3.3 Euler characteristic

Now we compute the Euler characteristic using the blowup maps for getting this crepant resolution. The following theorems are direct specializations of Theorem 10.2.1 and 10.2.2 for Spin(4)-models after imposing the condition $S + T = 4L$.

Theorem 10.2.3. *The generating polynomial of the Euler characteristic of an SO(4)-model given by*

the crepant resolution of a Weierstrass model given in Table 10.1 is

$$\chi(Y) = \frac{4(3L + 4TL - T^2)}{(1+T)(1+4L-T)}c(B).$$

In particular, if the SO(4)-model is a Calabi–Yau threefold,we have

$$\chi(Y) = -4(9K^2 + 4KT + T^2).$$

Theorem 10.2.4. *The Hodge numbers of an SO(4)-model given by the crepant resolution of a Weierstrass model given in Table 10.1 are*

$$h^{1,1}(Y) = 13 - K^2, \quad h^{2,1}(Y) = 13 + 17K^2 + 8KT + 2T^2.$$

10.3.4 Triple Intersection and the Prepotential

In this subsection, we compute the triple intersection polynomial of the SO(4)-model.

$$\begin{aligned}
\mathscr{F}^{+}_{trip} =& \pi_* f_* \left(\psi_0 D^s_0 + \psi_1 D^s_1 + \varphi_0 D^t_0 + \varphi_1 D^t_1\right)^3 \\
=& -2T\varphi_0^3(2L+T) - 2(4L-T)\left(\psi_0 - \psi_1\right)^2\left(\psi_0(6L-2T) + \psi_1(6L-T)\right) \\
&+ 6T\varphi_0\left(-\left(\psi_0 - \psi_1\right)^2(4L-T) + 2\psi_1\varphi_1(4L-T) + \varphi_1^2(T-2L)\right) + 6T\varphi_0^2\left(\psi_1(T-4L) + 2L\varphi_1\right) \\
&- 2\left(24L^2 - 10LT + T^2\right)\psi_1^3 + 6T(T-4L)\psi_1\varphi_1^2 + 4T(L-T)\varphi_1^3.
\end{aligned} \tag{10.39}$$

In the flop, $\mathscr{F}^{-}_{trip}$ is obtained by the involution $\psi \leftrightarrow \varphi$. Using the Intrilligator-Morrison-Seiberg approach, we compute the prepotential of the five-dimensional theory to be

$$6\mathscr{F}_{\text{IMS}} = -8(n_{1,3}-1)\left|\varphi_1\right|^3 - n_{2,2}\Big(\left|\varphi_1-\psi_1\right|^3 - \left|\varphi_1+\psi_1\right|^3\Big) - 8(n_{3,1}-1)\left|\psi_1\right|^3. \tag{10.40}$$

In the chamber $\varphi_1 - \psi_1 > 0$, the prepotential is

$$6\mathscr{F}^{+}_{\text{IMS}} = -8(n_{1,3}-1)\varphi_1^3 - 2(n_{2,2}+4n_{3,1}-4)\psi_1^3 - 6n_{2,2}\varphi_1^2\psi_1. \tag{10.41}$$

In the chamber $\varphi_1 - \psi_1 < 0$, the prepotential is

$$6\mathscr{F}^{-}_{\text{IMS}} = -8(n_{1,3}-1)\psi_1^3 - 2(n_{2,2}+4n_{3,1}-4)\varphi_1^3 - 6n_{2,2}\psi_1^2\varphi_1. \tag{10.42}$$

10.3.5 Counting charged hypermultiplets in $5d$

Matching the $5d$ prepotential with the triple intersection numbers, we can determine the number of representations. We find a perfect match between the triple intersection number and the prepotential when

$$n_{2,2} = -T(-4L+T), \quad n_{1,3} = \frac{1}{2}\left(-LT+T^2+2\right), \quad n_{3,1} = \frac{1}{2}\left(12L^2-7LT+T^2+2\right) \tag{10.43}$$

Using the relation $T + S = 4L$, we can rewrite these numbers as

$$n_{2,2} = TS, \quad n_{1,3} = g_T, \quad n_{3,1} = g_S, \tag{10.44}$$

where g_T and g_S are respectively the genus of T and S.

10.3.6 Anomaly cancellations

The number of vector multiplets $n_V^{(6)}$, tensor multiplets n_T, and hypermultiplets n_H are (see equations (2.42)):

$$\begin{aligned} &n_V^{(6)} = 6, \quad n_T = 9 - K^2, \\ &n_H = h^{2,1}(Y) + 1 + n_{3,1}(3-1) + n_{2,2}(4-0) + n_{1,3}(3-1) = 18 + 29K^2. \end{aligned} \tag{10.45}$$

Thus, we can conclude that the purely gravitational anomaly is canceled:

$$n_H - n_V^{(6)} + 29n_T - 273 = 0. \tag{10.46}$$

Now consider the remaining parts of the anomaly polynomial

$$I_8 = \frac{9 - n_T}{8}(\mathbf{tr}R^2)^2 + \frac{1}{6}(X_1^{(2)} + X_2^{(2)})\mathbf{tr}R^2 - \frac{2}{3}(X_1^{(4)} + X_2^{(4)}) + 4Y_{12}, \tag{10.47}$$

where

$$X_1^{(2)} = (A_3(1-n_3) - n_2 A_2)\,\mathbf{tr}_2 F_1^2 = -6K(4K+T)\mathbf{tr}_2 F_1^2 \tag{10.48}$$

$$\begin{aligned} X_1^{(4)} &= (B_3(1-n_3) - n_2 B_2)\,\mathbf{tr}_2 F_1^4 + (C_3(1-n_3) - n_2 C_2)\,(\mathbf{tr}_2 F_1^2)^2 \\ &= -3(4K+T)^2(\mathbf{tr}_2 F_1^2)^2 \end{aligned} \tag{10.49}$$

$$X_2^{(2)} = (A_3(1-n_3) - n_2 A_2)\,\mathbf{tr}_2 F_1^2 = 6KT\mathbf{tr}_2 F_1^2 \tag{10.50}$$

$$\begin{aligned} X_2^{(4)} &= (B_3(1-n_3) - n_2 B_2)\,\mathbf{tr}_2 F_1^4 + (C_3(1-n_3) - n_2 C_2)\,(\mathbf{tr}_2 F_1^2)^2 \\ &= -3T^2(\mathbf{tr}_2 F_1^2)^2 \end{aligned} \tag{10.51}$$

$$Y_{12} = (n_{2,4} + n_{2,\bar{4}})\mathbf{tr}_2 F_1^2 \mathbf{tr}_4 F_2^2 = -T(4K+T)\mathbf{tr}_2 F_1^2 \mathbf{tr}_4 F_2^2. \tag{10.52}$$

Hence the anomaly polynomial becomes simply

$$I_8 = \frac{1}{2}\left(\frac{1}{2}K\mathbf{tr}R^2 + 2S\mathbf{tr}_2 F_1^2 + 2T\mathbf{tr}_2 F_2^2\right)^2, \tag{10.53}$$

where $S + T = -4K$. Since the anomaly polynomial is a perfect square, we can conclude that the anomalies are all canceled.

10.4 Spin(4)-model

A Weierstrass equation for Spin(4) is given by the collision of type $\mathrm{I}_2^{ns}+\mathrm{I}_2^{ns}$ in an elliptic fibration with a trivial Mordell–Weil group.

$$Y_0: \quad y^2z = x^3 + a_2x^2z + \widetilde{a}_4stxz^2 + \widetilde{a}_6s^2t^2z^3. \tag{10.54}$$

This is a good starting point as the other possibilities (see Table 10.1) can be described as degenerations of it. The discriminant locus of this model is

$$\Delta = -s^2t^2\left(4a_2^3\widetilde{a}_6 - a_2^2\widetilde{a}_4^2 - 18a_2\widetilde{a}_4\widetilde{a}_6st + 4\widetilde{a}_4^3st + 27\widetilde{a}_6^2s^2t^2\right). \tag{10.55}$$

Theorem 10.4.1. *Assuming that $S = V(s)$ and $T = V(t)$ intersect transversally, the Weierstrass model*

$$Y_0: \quad y^2z = x^3 + a_2x^2z + \widetilde{a}_4stxz^2 + \widetilde{a}_6s^2t^2z^3.$$

has two distinct crepant resolutions $Y^{\pm}$. One is given by the sequence of blowups

$$X_0 \xleftarrow{(x,y,s|e_1)} X_1^+ \xleftarrow{(x,y,t|w_1)} X_2^+. \tag{10.56}$$

The other crepant resolution is obtained by exchanging the order of the blowup.

$$X_0 \xleftarrow{(x,y,t|w_1)} X_1^- \xleftarrow{(x,y,s|e_1)} X_2^-. \tag{10.57}$$

The proper transforms of the Weierstrass model Y_0 is then a smooth elliptic fibration Y^+ or Y^- are crepant resolutions of Y_0 connected by an Atiyah flop.

The proper transforms are

$$Y^{\pm}: \quad y^2 z = e_1 w_1 x^3 + a_2 x^2 z + \widetilde{a}_4 s t x z^2 + \widetilde{a}_6 s^2 t^2 z^3. \tag{10.58}$$

The relative projective coordinates for $X_2^{\pm}$ are then given by

$$X_2^+ \quad [e_1 w_1 x : e_1 w_1 y : z = 1][w_1 x : w_1 y : s][x : y : t]. \tag{10.59}$$

and for the second sequence of blowups:

$$X_2^- \quad [e_1 w_1 x : e_1 w_1 y : z = 1][e_1 x : e_1 y : t][x : y : s]. \tag{10.60}$$

The same blowups are also giving crepant resolutions connected by an Atiyah flop.

10.4.1 Fiber structure

We have four fibral divisors where two (D_0^s and D_1^s) are over S and the other two (D_0^t and D_1^t) are over T:

$$D_0^s : s = y^2 - e_1 w_1 x^3 - a_2 x^2 = 0, \tag{10.61}$$

$$D_1^s : e_1 = y^2 - a_2 x^2 - \widetilde{a}_4 s t x - \widetilde{a}_6 s^2 t^2 = 0 \tag{10.62}$$

$$D_0^t : t = y^2 - e_1 w_1 x^3 - a_2 x^2 = 0, \tag{10.63}$$

$$D_1^t : w_1 = y^2 - a_2 x^2 - \widetilde{a}_4 stx - \widetilde{a}_6 s^2 t^2 = 0. \tag{10.64}$$

First we can understand the fiber structure of this chamber. Over S, we have two fibers C_0^s and C_1^s, where they intersect at two points given by

$$C_0^s \cap C_1^s : s = e_1 = y^2 - a_2 x^2 = 0. \tag{10.65}$$

This is the same intersection from the $\mathrm{I}_2^{ns}+\mathrm{I}_2^{ns}$-model with $\mathbb{Z}/2\mathbb{Z}$. This enhances to a type III fiber when $a_2 = 0$ as well. This has another enhancement over S when $\widetilde{a}_4^2 - 4a_2\widetilde{a}_6 = 0$, because the conic curve D_1^s splits into two curves

$$C_1^s \to C_{1+}^s + C_{1-}^s, \tag{10.66}$$

which yields the fiber I_3^{ns}. The intersection numbers between the new curves and the fibral divisors are given by

	D_0^s	D_1^s	D_0^t	D_1^t
C_0^s	-2	2	0	0
C_{1+}^s	1	-1	0	0
C_{1-}^s	1	-1	0	0

. (10.67)

From the intersection numbers, we get the weight $[1;0]$ from both curves $C_{1\pm}^s$. Since $[1]$ corresponds to the representation 2 of $\mathfrak{su}(2)$ and it is only charged over S, we get the matter content in the repre-

sentation $(2,1)$.

Over T, the same enhancements $\mathrm{I}_2 \to \mathrm{I}_3$ and $\mathrm{I}_2 \to \mathrm{III}$ exist as the two divisors are the same when $s \leftrightarrow t$ and $e_1 \leftrightarrow w_1$. For the former enhancement, the intersection numbers between the new curves via the splitting

$$C_1^t \to C_{1+}^t + C_{1-}^t, \tag{10.68}$$

and the fibral divisors are given by

	D_0^s	D_1^s	D_0^t	D_1^t
C_0^t	0	0	-2	2
C_{1+}^t	0	0	1	-1
C_{1-}^t	0	0	1	-1

. (10.69)

From these intersection numbers of the curves $C_{1\pm}^t$, we get the weight $[0;1]$. Since $[1]$ corresponds to the representation 2 of $\mathfrak{su}(2)$ and it is only charged over T, we get the matter content in the representation $(1,2)$.

Over both S and T, we get four following curves:

$$\begin{cases} D_0^s \cap D_0^t & : s = t = y^2 - e_1 w_1 x^3 - a_2 x^2 = 0 \to \eta^{00}, \\ D_1^s \cap D_0^t & : e_1 = t = y^2 - a_2 x^2 = 0 \to \eta^{10}, \\ D_1^s \cap D_1^t & : e_1 = w_1 = y^2 - a_2 x^2 - \widetilde{a}_4 stx - \widetilde{a}_6 s^2 t^2 = 0 \to \eta^{11}. \end{cases} \tag{10.70}$$

The curve $\eta^{\mathrm{I}0}$ is not geometrically irreducible and consists of two geometrically irreducible curves $\eta^{\mathrm{I}0\pm}$ that requires taking the square-root of a_2. Clearly, if in the Weierstrass equation, a_2 was a perfect square modulo t or s, the fiber $\eta^{\mathrm{I}0}$ will factorize into $\eta^{\mathrm{I}0\pm}$ without the need of a field extension. The intersections of the new curves are

$$\eta^{\mathrm{o}\mathrm{o}} \cap \eta^{\mathrm{I}0\pm} : s = e_1 = t = y^2 - a_2 x^2 = 0, \tag{10.71}$$

$$\eta^{\mathrm{I}0\pm} \cap \eta^{\mathrm{II}} : e_1 = t = w_1 = y^2 - a_2 x^2 = 0. \tag{10.72}$$

This gives a fiber of type $\mathrm{I}_4^{\mathrm{ns}}$. When $a_2 = 0$, this specializes into a new fiber, as represented in Figure 10.9, where the nonsplit curves $\eta^{\mathrm{I}0\pm}$ become a single curve $\eta^{\mathrm{I}0y}$ with degeneracy two, where

$$\eta^{\mathrm{I}0y} : e_1 = t = y = 0. \tag{10.73}$$

From these splittings of the curve,

$$\begin{cases} C_{\mathrm{o}}^{s} \to \eta^{\mathrm{o}\mathrm{o}}, \\ C_{\mathrm{I}}^{s} \to \eta^{\mathrm{I}0+} + \eta^{\mathrm{I}0-} + \eta^{\mathrm{II}}, \\ C_{\mathrm{o}}^{t} \to \eta^{\mathrm{o}\mathrm{o}} + \eta^{\mathrm{I}0+} + \eta^{\mathrm{I}0-}, \\ C_{\mathrm{I}}^{t} \to \eta^{\mathrm{II}}, \end{cases} \tag{10.74}$$

we compute the intersection numbers between the curves on the collision with the divisors of two

I_2^{ns} fibers to be

	D_0^s	D_1^s	D_0^t	D_1^t
η^{00}	-2	2	0	0
$\eta^{10+} + \eta^{10-}$	2	-2	-2	2
$\eta^{10\pm}$	1	-1	-1	1
η^{11}	0	0	2	-2

(10.75)

Hence we see that we get the weight $[1; -1]$ from the curves $\eta^{10\pm}$. Since both $[1]$ and $[-1]$ is from the representation 2 of $\mathfrak{su}(2)$, we can deduce that the matter content we get is a bifundamental, $(2, 2)$.

Hence, the matter content of the $\mathrm{I}_2^{ns}+\mathrm{I}_2^{ns}$-model with a trivial Mordell–Weil group is

$$\mathbf{R} = (3, 1) \oplus (1, 3) \oplus (2, 1) \oplus (2, 2) \oplus (1, 2). \tag{10.76}$$

10.4.2 Euler characteristic and Hodge numbers

We compute the Euler characteristic using the blowup maps and the pushforward theorems of [114]. Let $S = V(s)$, $T = V(t)$ be the two smooth divisors that support the fibers with dual graph $\widetilde{\mathrm{A}}_1$. We assume that S and T intersect transversally. Let us recall that $L = c_1(\mathscr{L})$ is the first Chern class of the fundamental line bundle of the Weierstrass model.

Theorem 10.2.1. *The generating polynomial of the Euler characteristic of a Spin(4)-model obtained*

by a crepant resolution of a Weierstrass model given in Table 10.1 is

$$\chi(Y) = 2\left(\frac{S\left(-6L^2(4T+3)+L(8(T-1)T-9)+T(5T+4)\right)}{(2L+1)(S+1)(T+1)(-6L+2S+2T-1)}\right.$$
$$\left.+\frac{S^2(L(8T+6)+5T+3)+3(2L+1)\left(T^2-L(3T+2)\right)}{(2L+1)(S+1)(T+1)(-6L+2S+2T-1)}\right)c(B).$$

In particular, in the case of a Calabi–Yau threefold that is also a Spin(4)-model we have

$$\chi(Y) = -2\left(30K^2+15K(S+T)+3S^2+3T^2+4ST\right).$$

Proof. The Euler characteristic of a variety Y is the degree of its homological total Chern class. The homological Chern class of a Weierstrass model is

$$\frac{(1+H)(1+H+2\pi^*L)(1+H+3\pi^*L)}{1+3H+6\pi^*L}\pi^*c(TB).$$

The ambient space for the Weierstrass model is the projective bundle is $\pi : X_0 \to B$. We denote by $f_1 : X_1^+ \to X_0$ the first blowup with center (x, y, s) and by $f_2 : X_2^+ \to X_1^+$ the second blowup with center (x, y, t). The center of the first and second blowups have centered of class:

$$Z_1^{(1)} = H+2\pi^*L, \qquad Z_2^{(1)} = H+3\pi^*L, \qquad Z_3^{(1)} = S$$
$$Z_1^{(2)} = f_1^*H+2f_1^*\pi^*L-E_1, \qquad Z_2^{(2)} = f_1^*H+3f_1^*\pi^*L-E_1, \qquad Z_3^{(2)} = T$$

The total Chern class of X_0, X_1, and X_2 are

$$\begin{aligned}
c(TX_0) &= (1+H)(1+H+2\pi^*L)(1+H+3\pi^*L)\pi^*c(TB),\\
c(TX_1^+) &= (1+E_1)\frac{(1+Z_1^{(1)})(1+Z_2^{(1)})(1+Z_3^{(1)})}{(1+Z_1^{(1)})(1+Z_2^{(1)})(1+Z_3^{(1)})}f_1^*c(TX_0),\\
c(TX_2^+) &= (1+W_1)\frac{(1+Z_1^{(2)})(1+Z_2^{(2)})(1+Z_3^{(2)})}{(1+Z_1^{(2)})(1+Z_2^{(2)})(1+Z_3^{(2)})}f_2^*c(TX_1^+).
\end{aligned}$$

After each blowup, we can pull out two powers of the exceptional divisor. It follows that the defining equation is a section of a line bundle whose first Chern class is

$$3f_1^*H + 6f_1^*\pi^*L - 2E_1.$$

After the second blowup, the proper transform of the defining equation is a section of a line bundle whose first Chern class is

$$3f_2^*f_1^*H + 6f_2^*f_1^*\pi^*L - 2f_2^*E_1 - 2W_1$$

It follows that the total Chern class of the proper transform of the elliptic fibration is

$$c(TY_2^+) = \frac{c(TX_2^+)}{1+3f_2^*f_1^*H + 6f_2^*f_1^*\pi^*L - 2f_2^*E_1 - 2W_1}.$$

The Euler characteristic is then

$$\chi(Y_2^+) = \int \frac{(3f_2^*f_1^*H + 6f_2^*f_1^*\pi^*L - 2f_2^*E_1 - 2W_1)}{1+3f_2^*f_1^*H + 6f_2^*f_1^*\pi^*L - 2f_2^*E_1 - 2W_1}c(TX_1^+),$$

where $\int A$ is the degree of A. Since the degree is invariant under a pushforward, we get

$$\chi(Y_2^+) = \int \pi_* f_{1*} f_{2*} \frac{(3f_2^* f_1^* H + 6f_2^* f_1^* \pi^* L - 2f_2^* E_1 - 2W_1)}{1 + 3f_2^* f_1^* H + 6f_2^* f_1^* \pi^* L - 2f_2^* E_1 - 2W_1} c(TX_2^+).$$

The pushforwards f_{1*} and f_{2*} are computed using Theorem 5.0.1. The final pushforward π_* is computed using Theorem 5.0.4. These three pushforwards are purely algebraic computations.

In the Calabi–Yau case, we have $L = -K$. For a Calabi–Yau threefold, we just keep the terms of degree two in the base. □

Theorem 10.2.2. *The Hodge numbers of a Spin(4)-model given by the crepant resolution of a Weierstrass model given in Table 10.1 are*

$$h^{1,1}(Y) = 13 - K^2, \quad h^{2,1}(Y) = 13 + 29K^2 + 15K(S+T) + 3S^2 + 4ST + 3T^2.$$

Proof. For a Calabi–Yau threefold, we have $h^{1,0} = 0$ and $\chi(Y) = 2\Big(h^{1,1}(Y) - h^{2,1}(Y)\Big)$. Since the variety is elliptically-fibered, we can compute $h^{1,1}(Y)$ by the Shioda–Tate–Wazir theorem (see Theorem 2.8.10) and Noether's formula. We then have $h^{1,1}(Y) = h^{1,1}(B) + f + 1$ with $f = 2$ and $h^{1,1}(B) = 10 - K^2$ (see Lemma 2.8.8). Finally, $h^{2,1}(Y) = h^{1,1}(Y) - \chi(Y)/2$, where $\chi(Y)$ is given in Theorem 10.2.1. □

10.4.3 Triple Intersection numbers

In this subsection, we compute the triple intersection polynomial of the Spin(4)-model. In contrast to the Euler characteristic, the triple intersection polynomial does depend on the choice of a crepant resolution. In particular, the two varieties $Y^{\pm}$ have distinct topologies as they have distinct triple intersection numbers.

Theorem 10.2.5. *Let $f^+ : Y^+ \to Y_0$ be the crepant resolution where Y_0 is any of the Spin(4)-model listed in Table 10.1. The triple intersection polynomial of Y^+ is*

$$\begin{aligned}\mathscr{F}^+_{trip} &= \int_Y \pi_* f_* \left[\left(\psi_0 D_0^s + \psi_1 D_1^s + \varphi_0 D_0^t + \varphi_1 D_1^t \right)^3 \right] \\ &= 2T(-2L + S - T)\varphi_1^3 - 6ST\psi_1\varphi_1^2 - 2S(2L + S)\psi_1^3 \\ &\quad + 2T(2L - S - 2T)\varphi_0^3 + 6T\varphi_0^2 \left(\varphi_1(-2L + S + T) - S\psi_1 \right) - 4S(S - L)\psi_0 \left(\psi_0 - \psi_1 \right)^2 \\ &\quad - 2S(2L + S)\psi_0\psi_1 \left(\psi_0 - \psi_1 \right) + 6T\varphi_0 \left(\varphi_1^2(2L - S) - 2S \left(\psi_0 - \psi_1 \right)^2 + 2S\psi_1\varphi_1 \right).\end{aligned}$$

The triple intersection polynomial in the fibration Y^- defined by exchanging the order of the blowup is $\mathscr{F}^-_{trip}$ and is obtained from $\mathscr{F}^-_{trip}$ by the involution $\psi \leftrightarrow \varphi$.

Proof. The ambient space for the Weierstrass model is the projective bundle is $\pi : X_0 \to B$. We denote by $f_1 : X_1^+ \to X_0$ the first blowup with center (x, y, s) and by $f_2 : X_2^+ \to X_1^+$ the second blowup with center (x, y, t).

The class of the fibral divisors D^s_0, D^s_1, D^t_0, D^t_1 are

$$[D^s_0] = f_2^* f_1^* \pi^* S - f_2^* E_1, \quad [D^s_1] = f_2^* E_1, \quad [D^t_0] = f_2^* f_1^* \pi^* T - W_1, \quad [D^s_1] = W_1.$$

$$\begin{aligned}\int_Y (f_2^* E_1 a + W_1 b + f_2^* f_1^* H b)^3 &= \int_{X_2} (f_2^* E_1 a + W_1 b + f_2^* f_1^* H c)^3 (3 f_2^* f_1^* H + 6 f_2^* f_1^* \pi^* L - 2 f_2^* E_1 - 2 W_1) \\ &= -2S(S+2L)a^3 - 6STab^2 + 2(S-2L-T)Tb^3 + 27L^2c^3\end{aligned}$$

which gives the following non-vanishing triple intersection numbers

$$\int_Y f_2^* E_1^3 = -2S(S+2L), \quad \int_Y f_2^* E_1 W_1^2 = -2ST, \quad \int_Y W_1^3 = 2T(S-2L-T), \quad \int_Y f_2^* f_1^* H^3 = 27L^2.$$

The triple intersection numbers of the fibral divisors are then computed from these equations. □

10.4.4 Counting charged hypermultiplets in $5d$

M-theory compactified on a Calabi–Yau threefold yields a five-dimensional theory with eight supercharges. This is reviewed in section 2.12. The dynamics of the vector fields and the scalar fields of the vector multiplets depends on the prepotential $\mathscr{F}$, which gets a one-loop correction protected from additional corrections by supersymmetry. In the present case, the Lie algebra is $\mathrm{D}_2 = \mathrm{A}_1 \oplus \mathrm{A}_1$ and charged hypermultiplets transform in the representation $\mathbf{R} = (3,1) \oplus (1,3) \oplus (2,2) \oplus (2,1) \oplus (1,2)$ of D_2. In the Coulomb phase, all massive particles have been integrated out; in particular, the prepotential depends only on fields in the Cartan sub algebra of the Lie algebra.

Let (ψ_1, φ_1) be a parametrization of the coroots written in the basis of simple coroots of the Lie

algebra $D_2 = A_1 \oplus A_1$. The prepotential of the five-dimensional supergravity theory with Lie algebra D_2 and matter in the representation $\mathbf{R}$ defined above is [176]

$$6\mathscr{F}_{\text{IMS}} = -(8n_{1,3}+n_{1,2}-8)\left|\varphi_1\right|^3 - n_{2,2}\Big(\left|\varphi_1-\psi_1\right|^3 - \left|\varphi_1+\psi_1\right|^3\Big) - (8n_{3,1}+n_{2,1}-8)\left|\psi_1\right|^3, \quad (10.77)$$

where $n_{\mathbf{R}_1,\mathbf{R}_2}$ is the number of hypermultiplets transforming in the irreducible representation $(\mathbf{R}_1, \mathbf{R}_2)$ of D_2. The dual fundamental Weyl chamber is $\psi_1 > 0$ and $\varphi_1 > 0$. The only weights of the representation $\mathbf{R}$ are the weights $\pm[1; -1]$. It follows that there are two Coulomb chambers, each characterized by the sign of $\varphi_1 - \psi_1$.

In the chamber $\varphi_1 - \psi_1 > 0$, the prepotential is

$$6\mathscr{F}^{+}_{\text{IMS}} = \varphi_1^3(-n_{1,2} - 8n_{1,3} - 2n_{2,2} + 8) + \psi_1^3(-n_{2,1} - 8n_{3,1} + 8) - 6n_{2,2}\psi_1^2\varphi_1. \quad (10.78)$$

In the chamber $\varphi_1 - \psi_1 < 0$, the prepotential is

$$6\mathscr{F}^{-}_{\text{IMS}} = \varphi_1^3(-n_{1,2} - 8n_{1,3} + 8) + \psi_1^3(-n_{2,1} - 2n_{2,2} - 8n_{3,1} + 8) - 6n_{2,2}\psi_1\varphi_1^2. \quad (10.79)$$

Matching the $5d$ prepotential with the triple intersection numbers gives constraints on the number of representations that are sometimes enough to completely fix them. However, in the present case, they do determine only the number of bifundamental $(2, 2)$ while giving two linear relations

for the four other numbers:

$$n_{1,2} + 8n_{1,3} = T(4L - 2S + 2T) + 8, \quad n_{2,1} + 8n_{3,1} = S(4L - 2T + 2S) + 8. \tag{10.80}$$

This can be fixed using two different methods.

Firstly, by using the intersecting brane picture, we compute the number of fundamentals as the number of intersection points between appropriate components of the reduced discriminant. Since the split curve that gives the representation $(2, 1)$ is from $s = a_4^2 - 4a_2a_6 = 0$, whose class is $[s](2[a_4]) = 2S(4L - S - T)$, we deduce that $n_{2,1} = 2S(4L - S - T)$. Likely, for the representation $(1, 2)$ is from $t = a_4^2 - 4a_2a_6 = 0$, whose class is $[t](2[a_4]) = 2T(4L - S - T)$, we can also deduce that $n_{1,2} = T(4L - S - T)$. This fixes all the number of representations to be

$$\begin{aligned} &n_{1,2} = 2T(4L - S - T), && n_{2,1} = 2S(4L - S - T), && n_{2,2} = ST, \\ &n_{1,3} = \tfrac{1}{2}\left(-LT + T^2 + 2\right) = g_T, && n_{3,1} = \tfrac{1}{2}\left(-LS + S^2 + 2\right) = g_S, \end{aligned} \tag{10.81}$$

where $g_C = (K \cdot C + C^2 + 2)/2$ is the arithmetic genus of a curve C.

Secondly, using that Witten's genus formula holds in this context, the number of adjoint representations $n_{3,1}$ and $n_{1,3}$ are given respectively by the genus of the supporting curve S and T as in the last two equations of (10.81). We then determine $n_{2,1}$ and $n_{1,2}$ using the linear relations (10.80) and thereby reproducing (10.81) after imposing the Calabi–Yau condition $-K = L$.

The vanishing of the coefficients of $\mathbf{tr}R^4$ and $\mathbf{tr}F_i^4$ are necessary conditions for ensuring that the six-dimensional supergravity theory is anomaly free. Since here we are dealing with two SU(2), we

never have a fourth Casimir.

10.4.5 Counting hypermultiplets in $6d$ and anomaly cancellations

Sadov's F-theory geometric interpretation of the Green-Schwarz anomaly conditions gives the following system of five equations

$$\begin{cases} A_3(1-n_{3,1}) - A_2(n_{2,1}+2n_{2,2}) = 6K\cdot S, \quad C_3(1-n_{3,1}) - C_2(n_{2,1}+2n_{2,2}) = -3S^2, \\ A_3(1-n_{1,3}) - A_2(n_{1,2}+2n_{2,2}) = 6K\cdot T, \quad C_3(1-n_{1,3}) - C_2(n_{1,2}+2n_{2,2}) = -3T^2, \\ A_1A_1n_{2,2} = S\cdot T, \end{cases} \tag{10.82}$$

which give[4]

$$4(1-n_{3,1}) - (n_{2,1}+2n_{2,2}) = 6K\cdot S, \quad 16(1-n_{3,1}) - (n_{2,1}+2n_{2,2}) = -6S^2, \tag{10.83}$$

$$4(1-n_{1,3}) - (n_{1,2}+2n_{2,2}) = 6K\cdot T, \quad 16(1-n_{1,3}) - (n_{1,2}+2n_{2,2}) = -6T^2, \tag{10.84}$$

$$n_{2,2} = S\cdot T, \tag{10.85}$$

The solutions of these linear equations provide a direct computation of the numbers of representations (see equation (10.81)) from a purely six-dimensional perspective.

Witten's genus formula for S and T states that the number of hypermultiplets transforming in

[4] For the Lie algebra of SU(2), we recall that $A_3 = 4, \quad B_3 = B_2 = 0, \quad A_2 = 1, \quad C_3 = 8, \quad C_2 = \frac{1}{2}$. See [22, 106, 272].

the adjoint representation is the arithmetic genus of the curve supporting the corresponding fiber. Here it becomes a direct consequence of equations (10.83) and (10.84). Equation (10.85) is equivalent to the condition obtained by comparing the triple intersection numbers and the one-loop prepotential (the coefficient of $\psi_1^2\varphi_1$ of $\varphi_1^2\psi_1$) depending on the chamber) or by counting the number of intersection points of S and T.

Since we have geometrically computed the Hodge numbers and the number of representations, we can check if the anomalies are canceled in the uplifted six-dimensional supergravity theory. The number of vector multiplets $n_V^{(6)}$, tensor multiplets n_T, and hypermultiplets n_H are

$$\begin{aligned} &n_V^{(6)} = 6, \quad n_T = 9 - K^2, \\ &n_H = h^{2,1}(Y) + 1 + n_{3,1}(3-1) + n_{2,1}(2-0) + n_{2,2}(4-0) + n_{1,2}(2-0) + n_{1,3}(3-1) \\ &\quad = 29K^2 + 15KS + 15KT + 3S^2 + 4ST + 3T^2 + 13. \end{aligned} \tag{10.86}$$

Thus, a direct computation shows that the purely gravitational anomalies are also canceled:

$$n_H - n_V^{(6)} + 29n_T - 273 = 0. \tag{10.87}$$

The remaining parts of the anomaly polynomial is

$$I_8 = \frac{K^2}{8}(\mathbf{tr}R^2)^2 + \frac{1}{6}(X_1^{(2)} + X_2^{(2)})\mathbf{tr}R^2 - \frac{2}{3}(X_1^{(4)} + X_2^{(4)}) + 4Y_{12}. \tag{10.88}$$

Since A_1 does not have quartic Casimir invariants, the coefficients of $\mathbf{tr}F_1^4$ and $\mathbf{tr}F_2^4$ vanish. We also

have

$$X_1^{(2)} = (A_3(1 - n_{3,1}) - (n_{2,1} + 2n_{2,2})A_2)\,\mathbf{tr}_2 F_1^2 = 6KS\mathbf{tr}_2 F_1^2, \tag{10.89}$$

$$X_2^{(2)} = (A_3(1 - n_{1,3}) - (n_{1,2} + 2n_{2,2})A_2)\,\mathbf{tr}_2 F_2^2 = 6KT\mathbf{tr}_2 F_2^2, \tag{10.90}$$

$$X_1^{(4)} = (C_3(1 - n_3) - (n_{2,1} + 2n_{2,2})C_2)\,(\mathbf{tr}_2 F_1^2)^2 = -3S^2(\mathbf{tr}_2 F_1^2)^2, \tag{10.91}$$

$$X_2^{(4)} = (C_3(1 - n_3) - (n_{1,2} + 2n_{2,2})C_2)\,(\mathbf{tr}_2 F_1^2)^2 = -3T^2(\mathbf{tr}_2 F_1^2)^2, \tag{10.92}$$

$$Y_{12} = n_{2,2}\mathbf{tr}_2 F_1^2 \mathbf{tr}_4 F_2^2 = ST\mathbf{tr}_2 F_1^2 \mathbf{tr}_2 F_2^2. \tag{10.93}$$

It follows that the anomaly polynomial becomes

$$I_8 = \frac{K^2}{8}(\mathbf{tr}R^2)^2 + K(S\mathbf{tr}_2 F_1^2 + T\mathbf{tr}_2 F_2^2)\mathbf{tr}R^2 + 2S^2(\mathbf{tr}_1 F_1^2)^2(\mathbf{tr}_2 F_1^2)^2 + 4ST\mathbf{tr}_2 F_1^2 \mathbf{tr}_2 F_2^2, \tag{10.94}$$

which is a perfect square

$$I_8 = \frac{1}{2}\left(\frac{1}{2}K\mathbf{tr}R^2 + 2S\mathbf{tr}_2 F_1^2 + 2T\mathbf{tr}_2 F_2^2\right)^2. \tag{10.95}$$

Since the anomaly polynomial is a perfect square, we can safely deduce that all the anomalies are canceled by the Green–Schwarz mechanism.

There is a certain sense in which I would say the universe

has a purpose. It's not there by chance.

Roger Penrose

11

The Geometry of $SU(2) \times G_2$-models

The aim of this article is to study the geometry and physics of $SU(2) \times G_2$-models realized by the collision of singularities of type $III + I_0^{*ns}$:

$$SU(2) \times G_2 \quad \text{from} \quad III + I_0^{*ns}.$$

The $III + I_0^{*ns}$-model was first discussed in string theory in the early days of F-theory in [38, 68,

69] and was already considered in mathematics in the early 1980's by Miranda [236]. The $SU(2)\times G_2$-model appears naturally in the study of *non-Higgsable clusters* [240]. Over non-compact bases, collisions of singularities are used to classify *6d* $\mathcal{N} = (1, 0)$ superconformal field theories using elliptic fibrations. For example, for elliptic threefolds, such a non-Higgsable model is produced when the discriminant locus contains two rational curves with self-intersection -3 and -2 intersecting transversally or three rational curves which form a chain of curves intersecting transversally at a point with self-intersections $(-3, -2, -2)$ [92, 168, 240].

Surprisingly, despite receiving a significant amount of attention in the last few years for their role in the study of superconformal field theories, many properties of the $\mathrm{III} + \mathrm{I}_0^{*\mathrm{ns}}$ model remain unknown. For example, the structure of its Coulomb branch is not known. We show that the Coulomb branch consists of four chambers arranged as a Dynkin diagram of type A_4 illustrated on Figure 11.1. We also compute the four corresponding prepotentials. Geometrically, each Coulomb chamber corresponds to a different crepant resolution of the Weierstrass model. We present for the first time these four crepant resolutions, we study their fiber structures (see Figures 11.3 and Tables 11.9-11.13) and determine the triple intersection numbers of their fibral divisors in Theorem 11.2.7. By comparing the triple intersection numbers with the prepotential, we determine the number of charged hypermultiplets in a five-dimensional supergravity theory defined by a compactification of M-theory on a threefold given by an $SU(2) \times G_2$-model. We then show that these numbers are also consistent with an anomaly-free six-dimensional theory, which corresponds to a compactification of F-theory on the same variety.

We work with an arbitrary base of dimension n and specialize to the case of Calabi-Yau threefolds

only when necessary to connect with the physics. Since the resolution of singularities is a local process, the base can be either compact or non-compact. The compactness of the base will matter when considering anomaly cancellations.

11.1 Summary and organization of the chapter

Let S and T be the divisors supporting SU(2) and G_2 respectively. Let Δ' be the third component of the discriminant locus. Then, the number of charged hypermultiplets are (see Section 11.5)

$$\begin{aligned} n_{2,7} = \frac{1}{2} S \cdot T, \qquad n_{3,1} = g(S), \qquad n_{2,1} &= -S \cdot (8K + 2S + \frac{7}{2} T), \\ n_{1,14} = g(T), \qquad n_{1,7} &= -T \cdot (5K + 2T + S). \end{aligned} \tag{11.1}$$

The numbers $n_{2,7}$ and $n_{2,1}$ can be half-integer numbers since the representations $(2,7)$ and $(2,1)$ are both pseudo-real and thus can have half-hypermultiplets charged under them. As a sanity check, when S and T are respectively -2 and -3-curves intersecting transversally at a unique point, we retrieve the familiar spectrum(see Remark 11.1.1 below)

$$\mathbf{R} = \tfrac{1}{2}(2,7) \oplus \tfrac{1}{2}(2,1).$$

It is also useful to express $n_{2,1}$ and $n_{1,7}$ in terms of the genus[1] and the self-intersection of T and S

$$n_{2,1} = 16 - 16g(S) + 6S^2 - \frac{7}{2} S \cdot T, \quad n_{1,7} = 10 - 10g(T) + 3T^2 - S \cdot T. \tag{11.2}$$

[1] We recall that the genus g of a curve C in a surface of canonical class K satisfies the relation $2 - 2g = -C \cdot K - C^2$.

The Hodge numbers of a compact Calabi-Yau threefold that is an $\mathrm{SU}(2) \times \mathrm{G}_2$-model are (see Section 11.2.4)

$$h^{1,1}(Y) = 14 - K^2, \quad h^{2,1}(Y) = 29K^2 + 15K \cdot S + 24K \cdot T + 3S^2 + 6S \cdot T + 6T^2 + 14, \qquad (11.3)$$

where K is the canonical class of the base of the elliptic fibration Y. In the six-dimensional supergravity theory, using Sadov's techniques [269], we check that anomalies are canceled explicitly by the Green–Schwarz–Sagnotti-West mechanism. The anomaly polynomial I_8 factors as a perfect square:

$$I_8 = \frac{1}{2}\left(\frac{1}{2}K\mathrm{tr}R^2 + 2S\mathrm{tr}_2F_1^2 + T\mathrm{tr}_7F_2^2\right)^2,$$

where F_1 and F_2 are the field strengths for $\mathrm{SU}(2)$ and G_2 respectively.

Remark 11.1.1. the $\mathrm{SU}(2) \times \mathrm{G}_2$-model, the fundamental representation $(1, 7)$ is often ignored because it is localized away from the collision of the curves supporting G_2 and $\mathrm{SU}(2)$. However, it is expected from the study of the G_2-model as discussed in detail [112]. In the case of an $\mathrm{SU}(2) \times \mathrm{G}_2$-model for which $\mathrm{SU}(2)$ is supported on a curve S and G_2 is supported on a -3-curve T, such that S and T intersect transversally at one point, we see using equation (11.2) that the fundamental representation $(1, 7)$ is a *frozen representation*: there are vertical curves carrying the weights of such a representation, whereas the number of hypermultiplets $n_{1,7}$ charged under that representation vanishes. If S and T are smooth rational curves, the adjoint representation is frozen ($n_{3,1} = n_{1,14} = 0$). If T is and S are respectively -3 and -2 curves intersecting transversally at a point, we retrieve

the famous spectrum $\frac{1}{2}(2,7) \oplus \frac{1}{2}(2,1)$ first observed in [69] by Candelas, Perevalov and Rajesh; and popularized in recent years with the study of non-Higgsable clusters [240].

Remark 11.1.2. In an $\mathcal{N} = (1,0)$ six-dimensional theory, the cancellations of anomalies of an $\mathrm{SU}(2) \times \mathrm{G}_2$-model show that the number of hypermultiplets charged in the representation $(2,1)$ receives a contribution $S \cdot T/2$, which suggests that there are curves carrying the weights of that representation at the intersection of S and T. The formula for $n_{2,1}$ derived using anomaly cancellations of the six-dimensional theory is consistent with the triple intersection numbers of the $\mathrm{SU}(2) \times \mathrm{G}_2$-model. However, we do not see any evidence of such a representation in the weights carried by curves composing the singular fibers over $S \cap T$. They carry instead the weights of the representation $(2,7)$ which contain as a subset the weights of the representation $(2,1)$. We note that if S and Δ' have a non-empty intersection, there are rational curves carrying the weight of the representation $(2,1)$ away from the intersection of S and T, exactly over the points where the fiber III degenerates to a fiber of type IV. We discuss this further in Section 11.6.

11.1.1 Organization of the chapter

In the rest of the introduction, we will motivate the model by an argument of simplicity, spell out the questions that we aim to answer, and summarize the key results of the chapter for the convenience of the reader. We discuss the definition of the model, explain the structure of its Coulomb branch (and the geometric derivation of its matter content), present the non-Kodaira fibers produced by the four crepant resolutions of the $\mathrm{SU}(2) \times \mathrm{G}_2$-model, and discuss aspects of compactifi-

cations of M-theory and F-theory on an $SU(2) \times G_2$-model that is a Calabi-Yau threefold. We also summarize the counting of its charged hypermultiplets, and the cancellations of anomalies of the six-dimensional theory.

The rest of the chapter is a detailed development of these points and is structured as follows. In Section 11.2, we collect our geometric results. In Section 11.2.1, we introduce the model that we study in this chapter, define its Weierstrass model, its crepant resolutions, compute the Euler characteristic of the crepant resolutions and the triple intersection of the fibral divisors. In the case of a Calabi-Yau threefold, we also compute the Hodge numbers. We compute the adjacency graph of the hyperplane arrangement associated with an $SU(2) \times G_2$-model, and finally match the structure of the hyperplane arrangement with the flopping curves of the crepant resolutions. In Section 11.5, we study the consequences of our geometric results for the physics of F-theory and M-theory compactified on an $SU(2) \times G_2$-model. We discuss the subtleties of counting the number of hypermultiplets in presence of singularities in Section 11.6.

11.1.2 The simplest collisions of singularities

The $SU(2) \times G_2$-model is an important model not only in F-theory and M-theory but also in birational geometry. Mathematically, it will appear naturally as a key model of collision of singularities solely based on the simplicity of its fiber structure. It is natural to organize elliptic fibrations describing collision of singularities by the rank of the associated Lie algebra derived from F-theory. Geometrically, the rank of G counts the number of fibral divisors produced by a crepant resolution and relates to the relative Picard number of the elliptic fibration via the Shioda–Tate–Wazir theorem

[300, Corollary 4.1].

If we organize the collisions of singularities by the rank of the associated Lie algebra, the simplest collisions will correspond to the collision of two singular fibers with dual graphs $\widetilde{A}_1$ and the associated gauge group is either

$$\mathrm{Spin}(4)=\mathrm{SU}(2)\times\mathrm{SU}(2) \quad \text{or} \quad \mathrm{SO}(4)=\mathrm{SU}(2)\times\mathrm{SU}(2)/(\mathbb{Z}/2\mathbb{Z}),$$

when the Mordell–Weil group is trivial or $\mathbb{Z}/2\mathbb{Z}$, respectively. These models are studied in detail in [118].

The next simplest case has an associated Lie group of the type $\mathrm{SU}(2)\times G$, where G is a simple Lie group of rank two. There are three possibilities when G is a compact simple and simply connected Lie group of rank two:

$$\mathrm{SU}(2)\times \mathrm{SU}(3), \quad \mathrm{SU}(2)\times \mathrm{Sp}(4), \quad \text{or} \quad \mathrm{SU}(2)\times \mathrm{G}_2.$$

The $\mathrm{SU}(2)\times\mathrm{SU}(3)$-model is interesting for its connection to the non-Abelian sector of the Standard Model and is studied in [113]. The others are QCD-like theories obtained by replacing $\mathrm{SU}(3)$ by another simple and simply connected group of rank two. The $\mathrm{SU}(2)\times \mathrm{Sp}(4)$-model is studied in [121]. The group G_2 is the smallest simply connected Lie group with a trivial center and all its representation are real. The G_2-model is analyzed in detail in [112].

In Miranda's regularization, the collisions of singularities are organized by their values of the *j*-

invariant as only Kodaira fibers sharing the same j-invariant are considered in Miranda's model [236]. The III + $\mathrm{I}_0^{*\mathrm{ns}}$ is a collision of fibers for which the j-invariant is 1728. The fiber over the generic point of the collision is a non-Kodaira fiber composed of a chain of five rational curves intersecting transversally with multiplicities 1-2-3-2-1. This fiber is a contraction of a Kodaira fiber of type III* whose dual graph is the affine Dynkin diagram of type $\widetilde{\mathrm{E}}_7$.

Rank	G-Model
2	Spin(4)
2	SO(4)
3	SU(2)× SU(3)
3	SU(2)× Sp(4)
3	SU(2)× G_2

Table 11.1: Simplest collisions of singularities. We assume that G is a semi-simple non-simply connected group of rank 2 or 3. The Spin(4) and SO(4)-models are studied in [118]. The G =SU(2)× SU(3) is studied in [113], the G =SU(2)× Sp(4) is studied in [121], and the G =SU(2)× G_2 is the subject of the present chapter.

11.1.3 Defining the $\mathrm{SU}(2)\times\mathrm{G}_2$-model

Given a morphism $X \to B$ and an irreducible divisor S of B, the generic fiber over S is by definition the fiber over its generic point η. Such a fiber X_η is a scheme over the residue field κ of η. The residue field κ is not necessarily geometrically closed. Some components of X_η can be irreducible as a κ-scheme but will decompose further after a field extension $\kappa \to \kappa'$. We denote the cyclic group (resp. the group of permutations) of n distinct elements by $\mathbb{Z}_n$ (resp. S_n). In the case of a flat elliptic fibration, the Galois group of the minimal field extension that allows all the irreducible components of X_η to be geometrically irreducible is $\mathbb{Z}_2$ for all non-split Kodaira fibers with the exception of I_0^* for

which the Galois group could also be S_3 or $\mathbb{Z}_3$ [112].

Kodaira fibers classify geometric generic fibers of an elliptic fibration (the fiber defined over the algebraic closure of the residue field). The generic fiber (defined over the residue field κ) is classified by the Kodaira type of the corresponding geometric generic fiber together with the Galois group of the minimal field extension necessary to make all irreducible components of the fiber geometrically irreducible. The Galois group is always $\mathbb{Z}_2$ unless in the case of the fiber I_0^* where it can also be $\mathbb{Z}_3$ or S_3. Thus, there are two distinct fibers with dual graph $\widetilde{\mathrm{G}}_2^{\mathrm{t}}$ as the Galois group of an irreducible cubic can be the symmetric group S_3 or the cyclic group $\mathbb{Z}_3$ [112]. When we specify the type of Galois group, we write $\mathrm{I}_0^{*\mathrm{ns}}$ as $\mathrm{I}_0^{*S_3}$ or $\mathrm{I}_0^{*\mathbb{Z}_3}$. An $\mathrm{I}_0^{*\mathbb{Z}_3}$-model is very different from an $\mathrm{I}_0^{*\mathbb{S}_3}$-model already at the level of the fiber geometry as discussed in [112] and reflected in the Tables of section §11.3.5 of this chapter. Elliptically fibered threefolds corresponding to an $\mathrm{I}_0^{*\mathbb{Z}_3}$-model or an $\mathrm{I}_0^{S_3}$-model give the same gauge group, matter representations and number of charged hypermultiplets. The $\mathrm{I}_0^{*\mathbb{S}_3}$-model is the more general one and behaves better with respect to resolutions of singularities. We refer to [112] for more information. In the rest of the chapter, when we write $\mathrm{I}_0^{*\mathrm{ns}}$ without further explanation, we always mean the generic $\mathrm{I}_0^{*S_3}$.

There are five different Kodaira fibers with dual graph $\widetilde{\mathrm{A}}_1$ and thus producing an SU(2), namely $\mathrm{I}_2^{\mathrm{ns}}$, $\mathrm{I}_2^{\mathrm{s}}$, III, $\mathrm{IV}^{\mathrm{ns}}$, and $\mathrm{I}_3^{\mathrm{ns}}$. The $\mathrm{SU}(2)\times\mathrm{G}_2$ could be realized by any of the following ten models

$$\mathrm{I}_2^{\mathrm{ns}}+\mathrm{I}_0^{*\mathrm{ns}},\ \mathrm{I}_2^{\mathrm{s}}+\mathrm{I}_0^{*\mathrm{ns}},\ \mathrm{III}+\mathrm{I}_0^{*\mathrm{ns}},\ \mathrm{I}_3^{\mathrm{ns}}+\mathrm{I}_0^{*\mathrm{ns}},\ \text{or}\ \mathrm{IV}^{\mathrm{ns}}+\mathrm{I}_0^{*\mathrm{ns}}\ ,$$

where $\mathrm{I}_0^{*\mathrm{ns}}$ could be either $\mathrm{I}_0^{*\mathbb{Z}_3}$ or $\mathrm{I}_0^{*S_3}$. For example, the non-Higgsable models of type $\mathrm{SU}(2)\times\mathrm{G}_2$

studied in the literature are typically of the type $\mathrm{III} + \mathrm{I}_0^{*\mathbb{S}_3}$.

A Weierstrass model for the collision $\mathrm{III} + \mathrm{I}_0^{*S_3}$ is [236]

$$\mathrm{III} + \mathrm{I}_0^{*S_3}: \quad y^2 z = x^3 + fst^2 xz^2 + gs^2 t^3 z^3. \tag{11.4}$$

The discriminant locus is composed of three irreducible components S, T, and Δ':

$$\Delta = s^3 t^6 (4f^3 + 27g^2 s), \tag{11.5}$$

where $S = V(s)$ and $T = V(t)$ are two smooth Cartier divisors supporting respectively the fiber of type III and of type $\mathrm{I}_0^{*\mathrm{ns}}$. We assume that S and T intersect transversally. The fiber over the generic point of the leftover discriminant $\Delta' = 4f^3 + 27g^2 s$ is a nodal curve (Kodaira type I_1). Following Tate's algorithm, the type of the decorated Kodaira fibers depends on the Galois group of the associated associated cubic polynomial

$$P(q) = q^3 + fsq + gs^2. \tag{11.6}$$

Assuming that $P(q)$ is irreducible, the Galois group is $\mathbb{Z}_3$ if the discriminant of $P(q)$, $\Delta(P) = s^3(4f^3 + 27g^2 s)$, is a perfect square in the residue field of the generic point of T [112]. A simple way to have a $\mathbb{Z}_3$ Galois group is to increase the valuation of f along T [112]:

$$\mathrm{III} + \mathrm{I}_0^{*\mathbb{Z}_3}: \quad y^2 z = x^3 + fst^3 xz^2 + gs^2 t^3 z^3. \tag{11.7}$$

In this case, the j-invariant will be zero over the generic point of T in contrast to the case of equation (11.4) where the j-invariant is 1728 on both S and T. The fact that the Galois group of $P(q)$ is $\mathbb{Z}_3$ is clear as it now takes the form

$$P(q) = q^3 + gs^2. \tag{11.8}$$

11.1.4 Representations, Coulomb branches, hyperplane arrangements, and flops

In F-theory, we associate to an elliptic fibration a group G with Lie algebra $\mathfrak{g}$, and a representation $\mathbf{R}$ of $\mathfrak{g}$. In the case of an $\mathrm{SU}(2) \times \mathrm{G}_2$-model, the representation $\mathbf{R}$ is the direct sum of the following irreducible representations (see Section 11.3)

$$\mathbf{R} = (3,1) \oplus (1,14) \oplus (2,7) \oplus (2,1) \oplus (1,7). \tag{11.9}$$

The $(3,1)$ is the adjoint representation of $\mathrm{SU}(2)$ and the $(1,14)$ is the adjoint representation of G_2. The $(2,7)$ is the bifundamental representation of $\mathrm{SU}(2) \times \mathrm{G}_2$ supported at the intersection $S \cap T$ of the two divisors supporting G_2 and $\mathrm{SU}(2)$. The representation $(2,1)$ (resp. $(1,7)$) is the fundamental representation of $\mathrm{SU}(2)$ (resp. G_2) supported at the collision of the third component of the discriminant locus $\Delta' = (4f^3 + 27g^2s)$ with the divisor S (resp. T).

The study of the Coulomb branch of the gauge theory geometrically engineered by an elliptic fibration is the study of the minimal models over the Weierstrass model and how they flop to each other. This can also be described through the hyperplane arrangement $\mathrm{I}(\mathfrak{g}, \mathbf{R})$ with hyperplanes that are kernels of the weights of $\mathbf{R}$ restricted inside the dual fundamental Weyl chamber of

$\mathfrak{g}$ [110, 111, 125, 127]. In the case of the $\mathrm{SU}(2) \times \mathrm{G}_2$-model, it is interesting to notice that the generic $\mathrm{SU}(2)$-model and G_2-model do not have any flops [112, 125]. However, the $\mathrm{SU}(2) \times \mathrm{G}_2$-model has the bifundamental representation $(2, 7)$, which contains several weights whose kernels are hyperplanes intersecting the open dual Weyl chamber of $\mathrm{A}_1 \oplus \mathfrak{g}_2$ and giving four chambers, whose incidence graph is a chain illustrated in Figure 11.1. In this way, we see that the hyperplane arrangement $\mathrm{I}(\mathfrak{g}, \mathbf{R})$ does not care about the fundamental and adjoint representations, namely $(2, 1)$, $(1, 7)$, $(3, 1)$, and $(1, 14)$, since only the weights ϖ of the bifundamental representation $(2, 7)$ define the hyperplanes $\varpi^{\perp}$ intersecting the interior of the dual Weyl chamber of $\mathfrak{g} = \mathrm{A}_1 \oplus \mathfrak{g}_2$; hence, it is enough to study only $\mathrm{I}(\mathrm{A}_1 \oplus \mathfrak{g}_2, (2, 7))$.

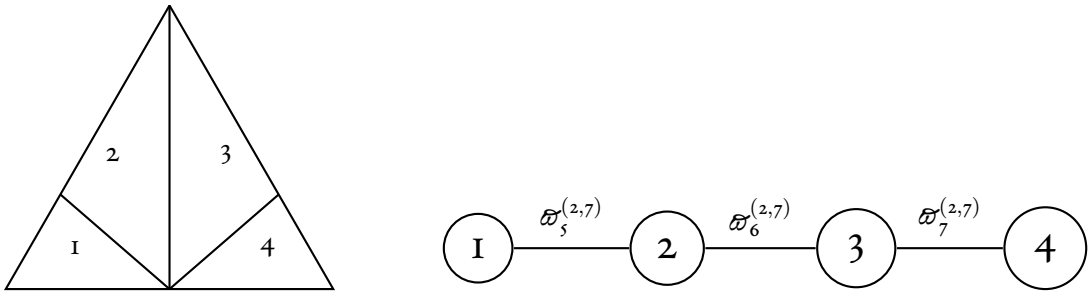

Figure 11.1: The chamber structure of $\mathrm{I}(\mathrm{A}_1 \oplus \mathfrak{g}_2, (2, 7))$ and its adjacency graph. This also represents the structure of the extended Kähler cone of an $\mathrm{SU}(2) \times \mathrm{G}_2$-model. Replacing $(2, 7)$ with $\mathbf{R} = (3, 1) \oplus (1, 14) \oplus (2, 7) \oplus (2, 1) \oplus (1, 7)$ does not change the adjacency graph since the adjoint and fundamental representations do not intersect the interior of the Weyl chamber of $\mathrm{A}_1 \oplus \mathfrak{g}_2$. The interior walls are given by the weights $\varpi_5^{(2,7)} = (1; -2, 1), \varpi_6^{(2,7)} = (1; 1, -1)$, and $\varpi_7^{(2,7)} = (1; -1, 0)$.

11.1.5 Non-Kodaira fibers

Three rational curves that are transverse to each other and meet at the same point (such as the Kodaira fiber of type IV) are represented by three nodes connected to the same point. We write $\widetilde{\mathrm{G}}_2$ and

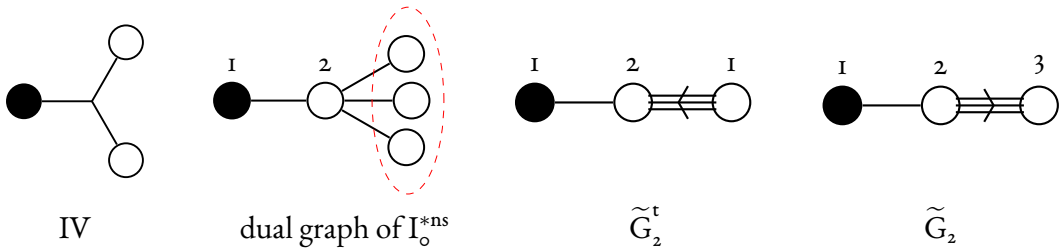

Figure 11.2: Conventions for dual graphs. The black node represents the extra node of the affine Dynkin diagram. The affine Dynkin diagrams $\widetilde{G}_2$ and $\widetilde{G}_2^t$ are Langlands dual of each other. But only $\widetilde{G}_2^t$ is the dual graph of a singular fiber over the generic point of a component of the discriminant locusof an elliptic fibrations. Specifically, $\widetilde{G}_2^t$ is the dual graph of the fiber I_0^{*ns}.

$\widetilde{G}_2^t$ for the affine Dynkin diagram of type $\widetilde{G}_2$ and its Langlands dual, respectively. In Kac's notation [182], they are denoted respectively $G_2^{(1)}$ and $D_4^{(3)}$. The dual graph of the fiber I_0^{*ns} is of type $\widetilde{G}_2^t$ and not $\widetilde{G}_2$ as often stated in the F-theory literature but clear from Figure 11.2.

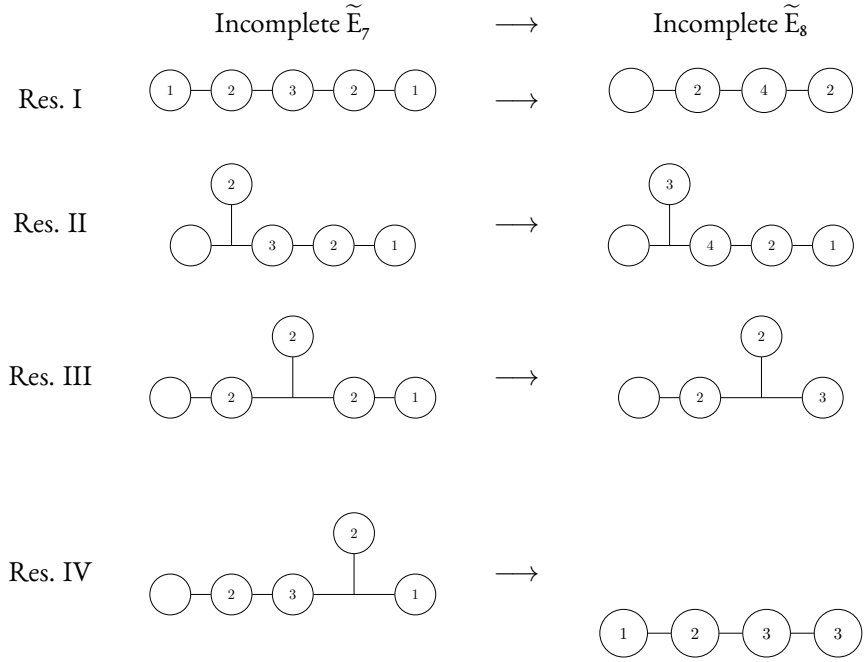

Figure 11.3: Non-Kodaira Fibers for the $SU(2) \times G_2$-model. On the left, we have the generic fiber over the collision $S \cap T$. On the right, we have its specialization when $f = 0$. This specialization is seen only when the base is at least a threefold or if we change the valuation of t along a_4.

There are many examples of non-Kodaira fibers in the literature [76, 109, 129, 163, 236, 286]. Over the generic point of $s = f = g = 0$, the III-model has a non-Kodaira fiber that are contractions of a fiber of type I_0^*. The G_2-model has non-Kodaira fibers that are contractions of an I_1^* and a IV* fiber [112]. At the collision III+I_0^{*ns}, we get a non-Kodaira fiber that is an incomplete III* and specializes further to an incomplete II*. The fibers found by Miranda at the collision III+I_0^{*ns} match the ones we find in the resolution I for the generic fiber over $S \cap T$. Miranda has already noticed in [236] that the non-Kodaira fibers of Miranda's model were always contractions of Kodaira fibers. The same is true for Miranda's models of arbitrary dimension [286] and for flat elliptic threefolds [76].

11.1.6 Compactifications of F-theory and M-theory on an $SU(2) \times G_2$-model

The crepant resolutions of the Weierstrass model of an $SU(2) \times G_2$-model are listed in equation (11.11). The Euler characteristic of an $SU(2) \times G_2$-model obtained by one of these crepant resolutions is derived in Theorem 11.2.1. As explained in the previous subsections, the hyperplane arrangements $I(\mathfrak{g}, \mathbf{R})$ has four chambers whose adjacency graph is represented in Figure 11.1. Each chamber corresponds to a specific crepant resolution that we determine explicitly. While three of the crepant resolutions (namely, Resolutions I, III, and IV) are obtained by blowing up smooth centers, one (resolution II) is defined by a blowup with a non-smooth center. For each chamber, we match an explicit crepant resolution of the Weierstrass model, so that the graph of flops matches the adjacency graph of the hyperplane arrangement.

We analyze the physics of compactifications of M-theory and F-theory on elliptically fibered Calabi-Yau threefolds corresponding to $SU(2) \times G_2$-models. These give five- and six-dimensional gauged supergravity theories with eight supercharges with the gauge group $SU(2) \times G_2$. We determine the matter content of these compactifications and study anomaly cancellations of the six-dimensional theory and their Chern-Simons terms.

In the five-dimensional theory [66, 176], the structure of the Coulomb chambers is isomorphic to the adjacency graph of the hyperplane arrangement $I(\mathfrak{g}, \mathbf{R})$. We compute the one-loop prepotential in each Coulomb chamber as a function of the number of hypermultiplets in each irreducible representations that add up to $\mathbf{R}$. The Chern-Simons couplings are computed geometrically as triple intersection numbers of the fibral divisors (see Theorem 11.2.7). We match the triple intersection

polynomial with the prepotential to obtain constraints on the number of charged hypermultiplets (see equation (11.42)). In many cases, such a method will completely fix the number of multiplets, but here, the numbers $n_{2,1}$ and $n_{3,1}$ are left unfixed but related by a linear relation. However, they are completely fixed once we use Witten's genus formula, which asserts that the number of multiplets in the adjoint representation is given by the genus of curve supporting the gauge group [306].

In the six-dimensional theory obtained by compactification of F-theory on an $\mathrm{SU}(2)\times \mathrm{G}_2$-model, we solve the anomaly equations and deduce the number of hypermultiplets. They match perfectly what we found independently in the M-theory compactification (see equation (11.51)).

11.2 Geometric Results

In this section, we collect key geometric results on $\mathrm{SU}(2)\times \mathrm{G}_2$-models.

11.2.1 Geometric description

We consider the following defining equation for an $\mathrm{SU}(2)\times \mathrm{G}_2$-model:

$$\mathrm{III}+\mathrm{I}_0^{*\mathrm{ns}}: \quad y^2z = x^3 + fst^2xz^2 + gs^2t^3z^3. \tag{11.10}$$

We assume that the coefficients f and g are algebraically independent and $S = V(s)$ and $T = V(t)$ are smooth divisors intersecting transversally. The Kodaira fiber over the generic point of S (resp. T) has a respective dual graph $\widetilde{\mathrm{A}}_1$ (resp. $\widetilde{\mathrm{G}}_2^{\mathrm{t}}$).

11.2.2 Crepant resolutions

We use the following convention. Let X be a nonsingular variety. Let $Z \subset X$ be a complete intersection defined by the transverse intersection of r hypersurfaces $Z_i = V(g_i)$, where g_i is a section of the line bundle $\mathscr{I}_i$ and $(g_1, \cdots, g_r)$ is a regular sequence. We denote the blowup of a nonsingular variety X along the complete intersection Z by

$$X \xleftarrow{(g_1, \cdots, g_r | e_1)} \widetilde{X}.$$

The exceptional divisor is $E_1 = V(e_1)$. We abuse notation and use the same symbols for x, y, s, e_i and their successive proper transforms. We also do not write the obvious pullbacks.

Each of the following four sequences of blowups is a different crepant resolution of the $\mathrm{SU}(2) \times \mathrm{G}_2$-model given by the Weierstrass model of equation (11.10).

$$\begin{aligned}
&\textbf{Resolution I:} \quad X_0 \xleftarrow{(x,y,s|e_1)} X_1 \xleftarrow{(x,y,t|w_1)} X_2 \xleftarrow{(y,w_1|w_2)} X_3 \ , \\
&\textbf{Resolution II:} \quad X_0 \xleftarrow{(x,y,p_0|p_1)} X_1 \xleftarrow{(y,p_1,t|w_1)} X_2 \xleftarrow{(p_0,t|w_2)} X_3 \ , \\
&\textbf{Resolution III:} \quad X_0 \xleftarrow{(x,y,t|w_1)} X_1 \xleftarrow{(x,y,s|e_1)} X_2 \xleftarrow{(y,w_1|w_2)} X_3 \ , \\
&\textbf{Resolution IV:} \quad X_0 \xleftarrow{(x,y,t|w_1)} X_1 \xleftarrow{(y,w_1|w_2)} X_2 \xleftarrow{(x,y,s|e_1)} X_3 \ .
\end{aligned} \tag{11.11}$$

These are embedded resolutions and $X_0 = \mathbb{P}(\mathscr{O}_B \oplus \mathscr{L}^{\otimes 2} \oplus \mathscr{L}^{\otimes 3})$.

11.2.3 Intersection theory

All of our intersection theory computations come down to Theorems Theorems 2.7.11, 5.0.1 and 5.0.4 [4, 114].

11.2.4 Euler characteristics and Hodge numbers

In the spirit of [114], the Euler characteristic depends only on the sequence of blowups. Using p-adic integration and the Weil conjecture, Batyrev proved Theorem 2.8.2 [29].

Theorem 11.2.1. *The generating polynomial of the Euler characteristic of an $SU(2) \times G_2$-model obtained by a crepant resolution of a Weierstrass model given in Section 11.2.2:*

$$\chi(Y) = 6\,\frac{S^2 - 2L - 3SL + 2(S^2 - 3SL + S - 2L)T + (3S + 2)T^2}{(1+S)(1+T)(-1 - 6L + 2S + 3T)}\,c(TB).$$

Proof. The total Chern class of $X_0 = \mathbb{P}_B[\mathscr{O}_B \oplus \mathscr{L}^{\otimes 2} \oplus \mathscr{L}^{\otimes 3}]$ is

$$c(TX_0) = (1+H)(1+H+2\pi^*L)(1+H+3\pi^*L)\pi^*c(TB).$$

where $L = c_1(\mathscr{L})$ and $H = c_1\Big(\mathscr{O}_{X_0}(1)\Big)$. The class of the Weierstrass equation is $[Y_0] = 3H + 6L$. Since all the resolutions are crepant, it is enough to do the computation in one of them. We consider Resolution I. We denote the blowups by

$$f_1 : X_1 \to X_0, \quad f_2 : X_2 \to X_1, \quad \text{and} \quad f_3 : X_3 \to X_2,$$

where E_1, W_1 and W_2 are respectively the classes of the first, second, and third blowups. The center of the three blowups have respectively classes:

$$Z_1^{(1)} = H + 2\pi^*L, \qquad Z_2^{(1)} = H + 3\pi^*L, \qquad Z_3^{(1)} = \pi^*S,$$
$$Z_1^{(2)} = f_1^*H + 2f_1^*\pi^*L - E_1, \qquad Z_2^{(2)} = f_1^*H + 3f_1^*\pi^*L - E_1, \quad Z_3^{(2)} = f_1^*\pi^*T,$$
$$Z_1^{(3)} = f_2^*f_1^*H + 3f_2^*f_1^*\pi^*L - f_2^*E_1 - W_1, \quad Z_2^{(3)} = W_1.$$

The successive blowups give (see Theorem 2.7.11)

$$c(TX_1) = \frac{(1+E_1)(1+Z_1^{(1)}-E_1)(1+Z_2^{(1)}-E_1)(1+Z_3^{(1)}-E_1)}{(1+Z_1^{(1)})(1+Z_2^{(1)})(1+Z_3^{(1)})} f_1^*c(TX_0),$$
$$c(TX_2) = \frac{(1+W_1)(1+Z_1^{(2)}-W_1)(1+Z_2^{(2)}-W_1)(1+Z_3^{(2)}-W_1)}{(1+Z_1^{(2)})(1+Z2^{(2)})(1+Z3^{(2)})} f_2^*c(TX_1),$$
$$c(TX_3) = \frac{(1+W_2)(1+Z_1^{(3)}-W_2)(1+Z_2^{(3)}-W_2)}{(1+Z_1^{(3)})(1+Z_2^{(1)})} f_3^*c(TX_2).$$

After the first blowup, the proper transform of Y_0 is of class $Y_1 = f_1^*Y_0 - 2E_1$. After the second blowup, the proper transform of Y_1 is of class $Y_2 = f_2^*Y_1 - 2W_1$. And finally, after the third blowup, the proper transform of Y_2 is $Y = f_3^*Y_2 - W_2$. Altogether, we have

$$[Y] = (f_3^*f_2^*f_1^*(3H + 6\pi^*L) - 2f_3^*f_2^*E_1 - 2f_3^*W_1 - W_2) \cap [X_3].$$

We also have that $c_1(X_3) = f_3^*f_2^*f_1^*c_1(X_0) - 2f_3^*f_2^*E_1 - 2f_3^*W_1 - W_2$. Hence $c_1(Y) = f_3^*f_2^*f_1^*c_1(Y_0)$,

which prove that the resolution is crepant. The total Chern class of Y is (see Theorem 2.7.11)

$$c(TY) \cap [Y] = \frac{f_3^* f_2^* f_1^* (3H + 6\pi^* L) - 2 f_3^* f_2^* E_1 - 2 f_3^* W_1 - W_2}{1 + f_3^* f_2^* f_1^* (3H + 6\pi^* L) - 2 f_3^* f_2^* E_1 - 2 f_3^* W_1 - W_2} c(TX_3) \cap [X_3].$$

Then,

$$\chi(Y) = \int_Y c(TY) \cap [Y] = \int_B \pi_* f_{1*} f_{2*} f_3^* c(TY) \cap [Y]$$

The final formula for the Euler characteristic follows directly from the pushforward Theorems 5.0.1 and 5.0.4. □

By direct expansion and specialization, we have the following three lemmas:

Lemma 11.2.2. *For an elliptic threefold, the Euler characteristic of of an $SU(2) \times G_2$-model obtained by a crepant resolution of a Weierstrass model given in Section 11.2.2 is:*

$$\chi(Y_3) = -6(-2c_1 \cdot L + 12L^2 + S^2 - 5S \cdot L + 2S \cdot T - 8L \cdot T + 2T^2).$$

By applying $c_1 = L = -K$, we have the following Lemma.

Lemma 11.2.3. *In the case of a Calabi-Yau threefold, The Euler characteristic of an $SU(2) \times G_2$-model obtained by a crepant resolution of a Weierstrass model given in Section 11.2.2 is:*

$$\chi(Y_3) = -6(10K^2 + S^2 + 5S \cdot K + 2S \cdot T + 8K \cdot T + 2T^2).$$

Lemma 11.2.4. *The Euler characteristic for an elliptic fourfold, the Euler characteristic of an $SU(2)\times G_2$-model obtained by a crepant resolution of a Weierstrass model given in Section 11.2.2 is given by*

$$\chi(Y_4) = -6\left(-2c_2\cdot L - 72L^3 + 12c_1\cdot L^2 + c_1\cdot S^2 - 5c_1\cdot S\cdot L + 2c_1\cdot S\cdot T - 8c_1\cdot L\cdot T + 2c_1\cdot T^2\right.$$
$$\left. + S^3 - 15S^2\cdot L + 6S^2\cdot T + 54S\cdot L^2 - 44S\cdot L\cdot T + 9S\cdot T^2 + 84L^2\cdot T - 34L\cdot T^2 + 4T^3\right).$$

Again, by the Calabi-Yau condition $c_1 = L = -K$, we have the following Lemma.

Lemma 11.2.5. *In the case of a Calabi-Yau fourfold, the Euler characteristic of an $SU(2)\times G_2$-model obtained by a crepant resolution of a Weierstrass model given in Section 11.2.2 is*

$$\chi(Y_4) = -6\left(2c_2K + 60K^3 + S^3 + 14S^2K + 6S^2T + 49SK^2 + 42SKT + 9ST^2 + 76K^2T + 32KT^2 + 4T^3\right).$$

Theorem 11.2.6. *In the Calabi-Yau case, the Hodge numbers of an $SU(2)\times G_2$-model obtained by the crepant resolution of a Weierstrass model given in Section 11.2.2 are*

$$h^{1,1}(Y) = 14 - K^2, \quad h^{2,1}(Y) = 29K^2 + 15KS + 24KT + 3S^2 + 6ST + 6T^2 + 14.$$

There are three fibral divisors not touching the section of the elliptic fibration. This number is exactly the rank of $\mathrm{SU}(2)\times \mathrm{G}_2$. Hence, using the Shioda-Tata-Wazir theorem (see Theorems 2.8.9 and 2.8.10), we have

$$h^{1,1}(Y) = 10 + 1 + 3 - K^2, \quad h^{2,1}(Y) = h^{1,1}(Y) - \frac{1}{2}\chi(Y).$$

11.2.5 Triple intersection numbers

Let $f : Y \to Y_0$ be one of the crepant resolutions of a Weierstrass model given in Section 11.2.2. Assuming that Y is a threefold, we collect the triple intersection numbers $(D_a \cdot D_b \cdot D_c) \cap [Y]$ of the fibral divisors as the coefficient of a cubic polynomial in ψ_0, ψ_1, φ_0, φ_1, and φ_2 that couples respectively with the fibral divisors D^s_0, D^s_1, D^t_0, D^t_1, and D^t_2. We pushforward to the Chow ring of X_0 and then to the base B. We recall that $\pi : X_0 \to B$ is the projective bundle in which the Weierstrass model is defined. Then,

$$\mathscr{F}_{trip} = \int_Y \left[\left(\psi_0 D^s_0 + \psi_1 D^s_1 + \varphi_0 D^t_0 + \varphi_1 D^t_1 + \varphi_2 D^t_2\right)^3\right] = \int_B \pi_* f_* \left[\left(\psi_0 D^s_0 + \psi_1 D^s_1 + \varphi_0 D^t_0 + \varphi_1 D^t_1 + \varphi_2 D^t_2\right)^3\right].$$

Once the classes of the fibral divisors are determined, we compute the pushforward of the triple intersection numbers using Theorem 5.0.1 successively for each blowups $X_{i+1} \to X_i$ $(i = 2, 1, 0)$. We are then in the Chow ring of X_0 and we use Theorem 5.0.4 to push forward to the Chow ring of B using the projective bundle map $\pi : X_0 \to B$. We can then take the degree to end up with a number.

Theorem 11.2.7. *The triple intersection polynomial of an $SU(2) \times G_2$-model depends on the choice of a crepant resolution (they are listed in Section 11.2.2) and are as follows:*

Resolution I:

$$\begin{aligned}\mathscr{F}^{(I)}_{trip} =& -9T\varphi_1\varphi_2\left(\varphi_2(-6L+S+3T)-2S\psi_1\right)+3T\varphi_1^2\left(\varphi_2(-9L+S+6T)-2S\psi_1\right)\\&-2\left(2T\varphi_2^3(9L-2S-3T)+S\left(\psi_0-\psi_1\right)^2\left(2\psi_0(S-L)+\psi_1(2L+S)\right)+9ST\psi_1\varphi_2^2\right)\\&+3T\varphi_0\left(\varphi_1^2(L-S)+2S\varphi_1\left(\psi_1+\varphi_2\right)-2S\left(\left(\psi_0-\psi_1\right)^2+\varphi_2^2\right)\right)\\&+2T\varphi_0^3(2L-S-2T)+3T\varphi_0^2\left(\varphi_1(-2L+S+T)-2S\psi_1\right),\end{aligned}$$

Resolution II:

$$\begin{aligned}\mathscr{F}^{(II)}_{trip} =& S\psi_1^3(-4L-2S+T)+T\varphi_2^3(-36L+7S+12T)+4T\varphi_1^3(L-T)-15ST\psi_1\varphi_2^2-3ST\psi_1^2\varphi_2\\&+3T(-9L+S+6T)\varphi_1^2\varphi_2-6ST\varphi_1^2\psi_1+9T\varphi_1\varphi_2\left(2S\psi_1-(-6L+S+3T)\varphi_2\right)\\&-T\varphi_0^3(-4L+S+4T)+3T\varphi_0^2\left(\varphi_1(-2L+S+T)-S\left(\psi_0+\psi_1+\varphi_2\right)\right)\\&-3T\varphi_0\left(\varphi_1^2(S-L)-2S\varphi_1\left(\psi_1+\varphi_2\right)+S\left(-\psi_0+\psi_1+\varphi_2\right)^2\right)+6ST\psi_0\psi_1\varphi_2-3ST\psi_0\varphi_2^2\\&-3ST\psi_0^2\varphi_2+3S\psi_1\psi_0^2(-4L+2S+T)++3S\psi_1^2\psi_0(4L-T)-S\psi_0^3(-4L+4S+T),\end{aligned}$$

Resolution III:

$$\begin{aligned}\mathscr{F}^{(III)}_{trip} =& -3T(9L-2(S+3T))\varphi_1^2\varphi_2 - 3T\varphi_1\varphi_2^2(-18L+4S+9T) - 3ST\psi_1\varphi_1^2 - 12ST\psi_1\varphi_2^2 \\ &+ T\varphi_1^3(4L-S-4T) - 4ST\varphi_2^3(9L-2S-3T) - 3ST\psi_1^2\varphi_1 + 12ST\psi_1\varphi_1\varphi_2 - 2S(2L+S-T)\psi_1^3 \\ &+ 3T\varphi_0^2\left(\varphi_1(T-2L) - 2S\psi_0\right) + 3T\varphi_0\varphi_1\left(L\varphi_1 + 2S\psi_0\right) - 3ST\psi_0\varphi_1^2 + 6ST\psi_0\varphi_1\varphi_2 \\ &+ 6ST\psi_0\psi_1\varphi_1 - 3ST\psi_0^2\varphi_1 - 2S(-2L+2S+T)\psi_0\left(\psi_0^2 - 2\psi_0^1\psi_1 + \psi_1^2\right) \\ &- 2S(2L+S-T)\psi_0(\psi_0\psi_1 - 2\psi_1^2) - 6ST\psi_0\varphi_2^2 + 4T\varphi_0^3(L-T),\end{aligned}$$

Resolution IV:

$$\begin{aligned}\mathscr{F}^{(IV)}_{trip} =& S(-4L-2S+3T)\psi_1^3 + 4T(L-T)\varphi_1^3 + 9T(2T-3L)\varphi_1^2\varphi_2 + 27T(2L-T)\varphi_1\varphi_2^2 \\ &+ 12T(T-3L)\varphi_2^3 - 6ST\psi_1^2\varphi_2 \\ &+ S\psi_0^3(4L-4S-3T) + 4T\varphi_0^3(L-T) + \varphi_0^2\left(3T\varphi_1(T-2L) - 6ST\psi_0\right) \\ &+ \psi_0^2\left(3S(-4L+2S+3T)\psi_1 - 6ST\varphi_2\right) + 3T\varphi_0\varphi_1\left(L\varphi_1 + 2S\psi_0\right) \\ &+ 3S\psi_0\left(\psi_1^2(4L-3T) + 4T\psi_1\varphi_2 - 2T\varphi_1^2 + 6T\varphi_1\varphi_2 - 6T\varphi_2^2\right).\end{aligned}$$

Proof. We give the proof for the case of resolution I discussed in detail in Section 11.3.1; the other

cases follow the same pattern.

$$\begin{aligned}\mathscr{F}_{trip} &= \int_Y \left[\left(\psi_0 D_0^s + \psi_1 D_1^s + \varphi_0 D_0^t + \varphi_1 D_1^t + \varphi_2 D_2^t\right)^3\right] \\ &= \int_{X_3} \left[\left(\psi_0 D_0^s + \psi_1 D_1^s + \varphi_0 D_0^t + \varphi_1 D_1^t + \varphi_2 D_2^t\right)^3 (3H + 6L - 2E_1 - 2W_1 - W_2)\right] \\ &= \int_{X_0} f_{1*}f_{2*}f_{3*}\left[\left(\psi_0 D_0^s + \psi_1 D_1^s + \varphi_0 D_0^t + \varphi_1 D_1^t + \varphi_2 D_2^t\right)^3 (3H + 6L - 2E_1 - 2W_1 - W_2)\right] \\ &= \int_B \pi_* f_{1*}f_{2*}f_{3*}\left[\left(\psi_0 D_0^s + \psi_1 D_1^s + \varphi_0 D_0^t + \varphi_1 D_1^t + \varphi_2 D_2^t\right)^3 (3H + 6L - 2E_1 - 2W_1 - W_2)\right].\end{aligned}$$

The classes of the fibral divisors in the Chow ring of X_3 are

$$[D_0^s] = S - E_1, \quad [D_1^s] = E_1, \quad [D_0^t] = T - W_1, \quad [D_1^t] = W_1 - W_2, \quad [D_2^t] = 2W_2 - W_1.$$

Denoting by M an arbitrary divisor in the class of the Chow ring of the base, The nonzero product intersection numbers of M, H, E_1, W_1, and W_2 are

$$\begin{aligned}&\int_Y H^3 = 27L^2, \quad \int_Y E_1^3 = -2S(2L + S), \quad \int_Y W_1^3 = -2T(2L - S + T), \\ &\int_Y W_2^3 = -T(5L - 2S + T), \quad \int_Y W_1^2 E_1 = -2ST, \quad \int_Y W_1^2 W_2 = T(-2L + S - T), \\ &\int_Y W_2^2 E_1 = -2ST, \quad \int_Y W_2^2 W_1 = T(-L + S - 2T), \\ &\int_Y H^2 M = -9LM, \quad \int_Y HM^2 = 3M^2, \quad \int_Y E_1 W_1 W_2 = -ST, \\ &\int_Y MH^2 = -9LM, \quad \int_Y ME_1^2 = -2SM, \quad \int_Y MW_1^2 = -2TM, \quad \int_Y MW_2^2 = -2TM.\end{aligned}$$

The triple intersection numbers of the fibral divisors follow from these by simple linearity.

□

The triple intersection polynomials computed in Theorem 11.2.7 are very different from each other in chambers I, II, III, and IV.

11.2.6 Hyperplane arrangement

We consider the semi-simple Lie algebra

$$\mathfrak{g} = \mathrm{A}_1 \oplus \mathfrak{g}_2.$$

An irreducible representation of $\mathrm{A}_1 \oplus \mathfrak{g}_2$ is always a tensor product $\mathbf{R}_1 \otimes \mathbf{R}_2$, where $\mathbf{R}_1$ and $\mathbf{R}_2$ are respectively irreducible representations of A_1 and $\mathfrak{g}_2$. Following a common convention in physics, we denote a representation by its dimension in bold character. The weights are denoted by ϖ_j^I where the upper index I denotes the representation $\mathbf{R_I}$ and the lower index j denotes a particular weight of the representation $\mathbf{R_I}$. A weight of a representation of $\mathrm{A}_1 \oplus \mathfrak{g}_2$ is denoted by a triple $(a; b, c)$ such that (a) is a weight of A_1 and (b, c) is a weight of $\mathfrak{g}_2$, all in the basis of fundamental weights. A vector φ of the coroot space of $\mathrm{A}_1 \oplus \mathfrak{g}_2$ is written as $\varphi = (\psi_1; \varphi_1, \varphi_2)$, where ψ_1 is the projection of φ on the fundamental coroot of A_1 and (φ_1, φ_2) are the coordinates of the projection of φ along the coroot of G_2 expressed in the basis of fundamental coroots. Each weight ϖ defines a linear form by the natural evaluation on coroot vectors. We recall that fundamental coroots are dual to fundamental weights.

We attach to an $\mathrm{SU}(2) \times \mathrm{G}_2$-model the representation

$$\mathbf{R} = (3,1) \oplus (1,14) \oplus (2,7) \oplus (2,1) \oplus (1,7). \tag{11.12}$$

The weights ϖ_j^I of each summand are listed in Table 11.2.

Representation	Weights		
$(2,1)$	$\varpi_1^{(2,1)} = (1;0,0)$	$\varpi_2^{(2,1)} = (-1;0,0)$	
$(1,7)$	$\varpi_1^{(1,7)} = (0;1,0)$	$\varpi_2^{(1,7)} = (0;-1,1)$	$\varpi_3^{(1,7)} = (0;2,-1)$
		$\varpi_4^{(1,7)} = (0;0,0)$	
	$\varpi_5^{(1,7)} = (0;-2,1)$	$\varpi_6^{(1,7)} = (0;1,-1)$	$\varpi_7^{(1,7)} = (0;-1,0)$
$(2,7)$	$\varpi_1^{(2,7)} = (1;1,0)$	$\varpi_2^{(2,7)} = (1;-1,1)$	$\varpi_3^{(2,7)} = (1;2,-1)$
		$\varpi_4^{(2,7)} = (1;0,0)$	
	$\varpi_5^{(2,7)} = (1;-2,1)$	$\varpi_6^{(2,7)} = (1;1,-1)$	$\varpi_7^{(2,7)} = (1;-1,0)$
	$\varpi_8^{(2,7)} = (-1;1,0)$	$\varpi_9^{(2,7)} = (-1;-1,1)$	$\varpi_{10}^{(2,7)} = (-1;2,-1)$
		$\varpi_{11}^{(2,7)} = (-1;0,0)$	
	$\varpi_{12}^{(2,7)} = (-1;-2,1)$	$\varpi_{13}^{(2,7)} = (-1;1,-1)$	$\varpi_{14}^{(2,7)} = (-1;-1,0)$

Table 11.2: Weights of the representations of $\mathrm{A}_1 \oplus \mathfrak{g}_2$.

We would like to study the arrangement of hyperplanes perpendicular to the weights of the representation $\mathbf{R}$ inside the dual fundamental Weyl chamber of $\mathrm{A}_1 \oplus \mathfrak{g}_2$. The only representation that

will contribute to the interior walls is the bifundamental $(2,7)$.

Theorem 11.2.8. *The hyperplane arrangement $I(A_1 \oplus \mathfrak{g}_2, \mathbf{R})$ with $\mathbf{R} = (2,7)$ has four chambers whose sign vectors and whose adjacency graph is given in Figure 11.1. A choice of a sign vector is $(\varpi_5^{(2,7)}, \varpi_6^{(2,7)}, \varpi_7^{(2,7)})$. With respect to it, the chambers are listed in Table 11.3.*

Proof. The open dual fundamental Weyl chamber is the half cone defined by the the positivity of the linear form induced by the simple roots:

$$\psi_1 > 0, \quad 2\varphi_1 - \varphi_2 > 0, \quad -3\varphi_1 + 2\varphi_2 > 0. \tag{11.13}$$

There are only three hyperplanes intersecting the interior of the fundamental Weyl chamber:

$$\varpi_5^{(2,7)},\ \varpi_6^{(2,7)},\ \varpi_7^{(2,7)}.$$

We use them in the order $(\varpi_5^{(2,7)}, \varpi_6^{(2,7)}, \varpi_7^{(2,7)})$, the sign vector is

$$(\psi_1 - 2\varphi_1 - \varphi_2, \psi_1 + \varphi_1 - \varphi_2, \psi_1 - \varphi_2).$$

First we consider when $\psi_1 - \varphi_1 > 0$. Then $\varpi_5^{2,7} = \psi_1 - \varphi_1 > 0$, $\varpi_6^{2,7} = \psi_1 + \varphi_1 - c = (\psi_1 - \varphi_1) + (2\varphi_1 - c) > 0$, and $\varpi_7^{2,7} = \psi_1 - 2\varphi_1 + \varphi_2 = (\psi_1 - \varphi_1) + (2\varphi_1 - \varphi_2) + (-3\varphi_1 + 2\varphi_2) = \varpi_6^{2,7} + (-3\varphi_1 + 2\varphi_2) > 0$.

When $\psi_1 - \varphi_1 < 0$, $\varpi_5^{2,7} = \psi_1 - \varphi_1 < 0$. Then we have either $\varpi_6^{2,7} = \psi_1 + \varphi_1 - \varphi_2 =$

$(\psi_1 - \varphi_1) + (2\varphi_1 - \varphi_2) > 0$, or $\varpi_6^{2,7} = \psi_1 + \varphi_1 - \varphi_2 = (\psi_1 - \varphi_1) + (2\varphi_1 - \varphi_2) < 0$. If $\varpi_6^{2,7} > 0$, it follows that $\varpi_7^{2,7} = \varpi_6^{2,7} + (-3\varphi_1 + 2\varphi_2) > 0$. When $\varpi_6^{2,7} = \psi_1 + \varphi_1 - \varphi_2 = (\psi_1 - \varphi_1) + (2\varphi_1 - \varphi_2) < 0$, we can have both $\varpi_7^{2,7} > 0$ and $\varpi_7^{2,7} < 0$. See Table 11.3. □

Subchambers	$\varpi_5^{(2,7)}$	$\varpi_6^{(2,7)}$	$\varpi_7^{(2,7)}$	Explicit description
①	+	+	+	$0 < \frac{1}{2}\varphi_2 < \varphi_1 < \frac{2}{3}\varphi_2, \qquad \varphi_1 < \psi_1$
②	+	+	−	$0 < \frac{1}{2}\varphi_2 < \varphi_1 < \frac{2}{3}\varphi_2, \quad \varphi_2 - \varphi_1 < \psi_1 < \varphi_1$
③	+	−	−	$0 < \frac{3}{2}\varphi_1 < \varphi_2 < 2\varphi_1, \quad 2\varphi_1 - \varphi_2 < \psi_1 < \varphi_2 - \varphi_1$
④	−	−	−	$0 < \frac{3}{2}\varphi_1 < \varphi_2 < 2\varphi_1, \quad 0 < \psi_1 < 2\varphi_1 - \varphi_2$

Table 11.3: Chambers of the hyperplane arrangement $I(A_1 \oplus G_2, \mathbf{R})$ with $\mathbf{R} = (2, 7)$. The wall between the chamber i and $i + 1$ ($i = 1, 2, 3$) is given by the weight $\varpi_{8-i}^{(2,7)}$.

11.2.7 Flops

In this section, we discuss the flops between the resolutions I, II, III, IV. We identify the flopping curves in Table 11.4. These are curves whose weights differ only by a sign.

Flopping curves										Weight
Resolution I:	$\eta_1^{\circ A}$	$[1;-1,0]$	$(2,7)$	$\leftrightarrow$	Resolution II:	η_{01}^{2}	$[-1;1,0]$	$(2,7)$		$\omega_7^{(2,7)}$
Resolution II:	η_1^{02}	$[1;1,-1]$	$(2,7)$	$\leftrightarrow$	Resolution III:	η_0^{12}	$[-1;-1,1]$	$(2,7)$		$\omega_6^{(2,7)}$
Resolution III:	η_1^{12}	$[1;-2,1]$	$(2,7)$	$\leftrightarrow$	Resolution IV:	η_0^{2B}	$[-1;2,-1]$	$(2,7)$		$\omega_5^{(2,7)}$

Table 11.4: Flopping curves between different crepant resolutions of the $\mathrm{SU}(2)\times \mathrm{G}_2$-model.

11.3 The Crepant Resolutions and Fiber Structures

In this section, we study the fibral structure of the elliptic fibrations obtained by the crepant resolutions of the $\mathrm{SU}(2)\times \mathrm{G}_2$-model given by the Weierstrass model

$$Y_0: \quad y^2 = x^3 + fst^2x + gs^2t^3. \tag{11.14}$$

The resolutions are given by the sequence of blowups listed in Section 11.2.1. We analyze the fiber structure of each of these crepant resolutions and determine the weights of the rational curves produced by the degeneration over codimension-two points. These weights are important to determine the representation $\mathbf{R}$. We denote the fibral divisors over S and T by $D_a^{\mathfrak{s}}$ and $D_a^{\mathfrak{t}}$ respectively. Their generic fibers are respectively written as $C_a^{\mathfrak{s}}$ and $C_a^{\mathfrak{t}}$. We will focus on analyzing the collision III+I_0^{*ns} as we already know the behavior of the III-model and the G_2-model.

11.3.1 Resolution I

Resolution I is given by the following sequence of blowups:

$$X_0 \xleftarrow{(x,y,s|e_1)} X_1 \xleftarrow{(x,y,t|w_1)} X_2 \xleftarrow{(y,w_1|w_2)} X_3 \tag{11.15}$$

The proper transform of the Weierstrass model is

$$Y: \quad w_2 y^2 = w_1(e_1 x^3 + f s t^2 x + g s^2 t^3). \tag{11.16}$$

The projective coordinates are then given by

$$[e_1 w_1 w_2 x\,;\; e_1 w_1 w_2^2 y\,;\; z = 1][w_1 w_2 x\,;\; w_1 w_2^2 y\,;\; s][x\,;\; w_2 y\,;\; t][y\,;\; w_1]. \tag{11.17}$$

The fibral divisors are given by $se_1 = 0$ for type III and $tw_1 w_2 = 0$ for type I_0^{*ns}:

$$\mathrm{III}: \begin{cases} D_0^{\mathrm{s}}: & s = w_2 y^2 - w_1 e_1 x^3 = 0, \\ D_1^{\mathrm{s}}: & e_1 = w_2 y^2 - s t^2 w_1 (f x + g s t) = 0. \end{cases} \qquad \mathrm{I}_0^{*ns}: \begin{cases} D_0^{\mathrm{t}}: & t = w_2 y^2 - w_1 e_1 x^3 = 0, \\ 2D_1^{\mathrm{t}}: & w_1 = w_2 = 0, \\ D_2^{\mathrm{t}}: & w_2 = e_1 x^3 + f s t^2 x + g s^2 t^3 = 0. \end{cases} \tag{11.18}$$

On the intersection of S and T, we see the following curves:

$$\text{On } S\cap T: \begin{cases} D_0^s\cap D_0^t \to & \eta_0^0 : s=t=w_2y^2-w_1e_1x^3=0, \\ D_1^s\cap D_0^t \to & \eta_1^{02} : e_1=t=w_2=0, \quad \eta_1^{0A} : e_1=t=y=0, \\ D_1^s\cap D_1^t \to & \eta_1^{12} : e_1=w_1=w_2=0, \\ D_1^s\cap D_2^t \to & \eta_1^{02} : e_1=w_2=t=0, \quad \eta_1^{2} : e_1=w_2=fx+gst=0. \end{cases} \tag{11.19}$$

Hence we can deduce that the five fibral divisors split in the following way to produce the fiber in Figure 11.4, which is a fiber of type IV* with contracted nodes.

$$\text{On } S\cap T: \begin{cases} C_0^s \longrightarrow \eta_0^0, \\ C_1^s \longrightarrow 2\eta_1^{0A}+3\eta_1^{02}+2\eta_1^{12}+\eta_1^2, \\ C_0^t \longrightarrow \eta_0^0+\eta_1^{02}+2\eta_1^{0A}, \\ C_1^t \longrightarrow \eta_1^{12}, \\ C_2^t \longrightarrow 2\eta_1^{02}+\eta_1^2. \end{cases} \tag{11.20}$$

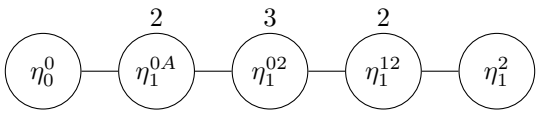

Figure 11.4: Codimension-two Collision of $\mathrm{SU}(2) \times \mathrm{G}_2$-model at $S \cap T$, Resolution I. This fiber is of type III* (with dual graph $\widetilde{\mathrm{E}}_7$) with contracted nodes.

In order to get the weights of the curves, the intersection numbers are computed between the codimension-two curves and the fibral divisors.

	D_0^s	D_1^s	D_0^t	D_1^t	D_2^t	Weight	Representation
η_0^0	-2	2	0	0	0	[-2;0,0]	$(3,1)$
η_1^{0A}	1	-1	-1	0	1	[1;-1,0]	$(2,7)$
η_1^{02}	0	0	0	1	-2	[0;2,-1]	$(1,7) \subset (1,14)$
η_1^{12}	0	0	1	-2	3	[0;-3,2]	$(1,14)$
η_1^2	0	0	0	1	-2	[0;2,-1]	$(1,7) \subset (1,14)$

Table 11.5: Weights and representations of the components of the generic curve over $S \cap T$ in Resolution I of the $\mathrm{SU}(2) \times \mathrm{G}_2$-model. See Section 11.4.2 for more information on the interpretation of these representations.

The fiber of Figure 11.4 specializes further when $f = 0$:

$$\eta_1^2 \longrightarrow \eta_1^{02}. \tag{11.21}$$

This corresponds to the non-Kodaira diagram in Figure 11.5, which is a fiber of type II* with con-

tracted nodes.

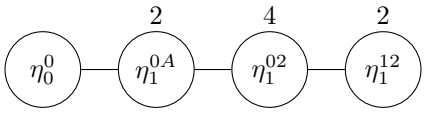

Figure 11.5: Codimension-three enhancement of $\mathrm{SU}(2) \times \mathrm{G}_2$-model at $S \cap T \cap V(f)$, Resolution I. This fiber is of type II^* (with dual graph $\widetilde{\mathrm{E}}_8$) with contracted nodes.

11.3.2 Resolution II

In this section, we study Resolution II in detail. Resolution II requires a first blowup that does not have a smooth center; it is useful to rewrite equation (11.10) as

$$Y_0 : \begin{cases} y^2 = x^3 + fp_0tx + gp_0^2t, \\ \\ p_0 = st. \end{cases} \tag{11.22}$$

Resolution II is given by the following sequence of blowups

$$X_0 \xleftarrow{(x,y,p_0|p_1)} X_1 \xleftarrow{(y,t,p_1|w_1)} X_2 \xleftarrow{(t,p_0|w_2)} X_3 \ , \tag{11.23}$$

where $X_0 = \mathbb{P}[\mathscr{O}_B \oplus \mathscr{L}^{\otimes 2} \oplus \mathscr{L}^{\otimes 3}]$. The projective coordinates are then

$$[p_1w_1x \,:\, p_1w_1^2y \,:\, z = 1][x \,:\, w_1y \,:\, p_0w_2][y \,:\, tw_2 \,:\, p_1][t \,:\, p_0], \tag{11.24}$$

and the proper transform is

$$Y: \begin{cases} w_1 y^2 = p_1 x^3 + f p_0 t w_2^2 x + g p_0^2 t w_2^3, \\ p_0 p_1 = st. \end{cases} \tag{11.25}$$

$X_1 = Bl_{(x,y,p_0)} X_0$ has double point singularities at the ideal (p_0, p_1, s, t). Recall that we have two curves from III and three curves from I_0^* individually. We denote by D_a^{s} and D_a^{t} the fibral divisors that project to S and T:

$$\begin{aligned} \mathrm{III}: & \begin{cases} D_0^{\mathrm{s}}: s = p_0 = w_1 y^2 - p_1 x^3 = 0 \\ D_1^{\mathrm{s}}: s = p_1 = w_1 y^2 - (p_1 x^3 + p_0 t w_2^2 (fx + g p_0 w_2) = 0 \end{cases} \\ \mathrm{I}_0^*: & \begin{cases} D_0^{\mathrm{t}}: w_2 = p_0 p_1 - st = w_1 y^2 - p_1 x^3 = 0 \\ D_1^{\mathrm{t}}: t = p_1 = w_1 = 0 \\ D_2^{\mathrm{t}}: w_1 = p_0 p_1 - st = p_1 x^3 + p_0 t w_2^2 (fx + g p_0 w_2) = 0 \end{cases} \end{aligned} \tag{11.26}$$

At the intersection of S and T, the fiber enhances to a non-Kodaira fiber presented in Figure 11.6, which is a fiber of type III* with contracted nodes. This is realized by the following splitting of

curves.

$$\text{On } S \cap T : \begin{cases} C_0^s \longrightarrow \eta_0^0 + \eta_{01}^2 \\ C_1^s \longrightarrow \eta_{01}^2 + 3\eta_1^{02} + 2\eta_1^{12} + \eta_1^2 \\ C_0^t \longrightarrow \eta_0^0 + \eta_1^{02} \\ C_1^t \longrightarrow \eta_1^{12} \\ C_2^t \longrightarrow 2\eta_{01}^2 + 2\eta_1^{02} + \eta_1^{12} + \eta_1^2 \end{cases} \tag{11.27}$$

The curves at the intersection are given by

$$\text{On } S \cap T : \begin{cases} D_0^s \cap D_1^t \to & \eta_0^0 : s = p_0 = w_2 = w_1 y^2 - p_1 x^3 = 0, \\ D_0^s \cap D_2^t \to & \eta_{01}^2 : s = p_0 = w_1 = p_1 = 0, \\ D_1^s \cap D_0^t \to & \eta_1^{02} : s = p_1 = w_2 = w_1 = 0, \\ D_1^s \cap D_1^t \to & \eta_1^{12} : s = p_1 = t = w_1 = 0, \\ D_1^s \cap D_2^t \to & \eta_1^2 : s = p_1 = w_1 = fx + gp_0 w_2 = 0, \quad \eta_{01}^2 : s = p_1 = w_1 = p_0 = 0, \\ & \eta_1^{12} : s = p_1 = w_1 = t = 0, \qquad\qquad \eta_1^{02} : s = p_1 = w_1 = w_2 = 0. \end{cases} \tag{11.28}$$

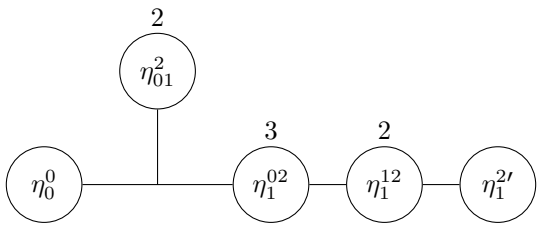

Figure 11.6: Codimension-two Collision of $\mathsf{SU}(2) \times \mathsf{G}_2$-model at $S \cap T$, Resolution II. This fiber is of type III* (with dual graph $\widetilde{\mathsf{E}}_7$) with contracted nodes.

	D_0^s	D_1^s	D_0^t	D_1^t	D_2^t	Weight	Representation
η_0^0	-1	1	-1	0	1	[-1;-1,0]	$(2,7)$
η_{01}^2	-1	1	1	0	-1	[-1;1,0]	$(2,7)$
η_1^{02}	1	-1	-1	1	-1	[1;1,-1]	$(2,7)$
η_1^{12}	0	0	1	-2	3	[0;-3,2]	$(1,14)$
η_1^2	0	0	0	1	-2	[0;2,-1]	$(1,7) \subset (1,14)$

Table 11.6: Weights and representations of the components of the generic curve over $S \cap T$ in Resolution II of the $\mathsf{SU}(2) \times \mathsf{G}_2$-model. See Section 11.4.2 for more information on the interpretation of these representations.

The fiber enhances further over $f = 0$:

$$\eta_1^2 \longrightarrow \eta_{01}^2 + \eta_1^{02} \ . \tag{11.29}$$

For this codimension-three enhancement, we get a non-Kodaira fiber corresponding to Figure 11.7, which is a fiber of type II* with contracted nodes.

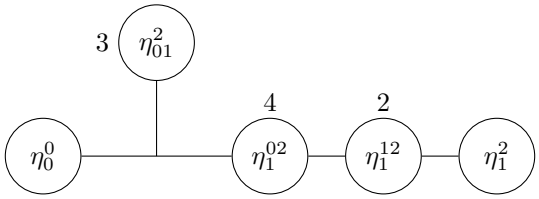

Figure 11.7: Codimension-three enhancement of $\mathsf{SU}(2)\times\mathsf{G}_2$-model at $S\cap T\cap V(f)$, Resolution II. This fiber is of type II^* (with dual graph $\widetilde{\mathsf{E}}_8$) with contracted nodes.

11.3.3 Resolution III

Consider the following sequence of blowups:

$$X_0 \xleftarrow{(x,y,t|w_1)} X_1 \xleftarrow{(x,y,s|e_1)} X_2 \xleftarrow{(y,w_1|w_2)} X_3 \ . \tag{11.30}$$

The projective coordinates are then given by

$$[e_1w_1w_2x\,;\ e_1w_1w_2^2y\,;\ z=1][e_1x\,;\ e_1w_2y\,;\ t][x\,;\ w_2y\,;\ s][y\,;\ w_1]. \tag{11.31}$$

The proper transform is identical to equation (11.16). It follows that the fibral divisors are also identical to equation (11.18).

On the intersection of S and T, we see the following curves:

$$\text{On } S \cap T : \begin{cases} D^{s}_{0} \cap D^{t}_{0} \to & \eta^{0}_{0} : s = t = w_2 y^2 - w_1 e_1 x^3 = 0, \\ D^{s}_{0} \cap D^{t}_{1} \to & \eta^{12}_{0} : s = w_1 = w_2 = 0, \\ D^{s}_{0} \cap D^{t}_{2} \to & \eta^{2}_{01} : s = w_2 = e_1 = 0, \quad \eta^{12}_{0} : s = w_2 = w_1 = 0, \\ D^{s}_{1} \cap D^{t}_{1} \to & \eta^{12}_{1} : e_1 = w_1 = w_2 = 0, \\ D^{s}_{1} \cap D^{t}_{2} \to & \eta^{2}_{1} : e_1 = w_2 = fx + gst = 0, \quad \eta^{2}_{01} : e_1 = w_2 = s = 0. \end{cases} \tag{11.32}$$

The resulting fiber is a non-Kodaira fiber illustrated in Figure 11.8 and corresponding to a fiber of type III* with three contracted nodes.

$$\text{On } S \cap T : \begin{cases} C^{s}_{0} \longrightarrow \eta^{0}_{0} + 2\eta^{12}_{0} + \eta^{2}_{01}, \\ C^{s}_{1} \longrightarrow \eta^{2}_{01} + 2\eta^{12}_{1} + \eta^{2}_{1}, \\ C^{t}_{0} \longrightarrow \eta^{0}_{0}, \\ C^{t}_{1} \longrightarrow \eta^{12}_{0} + \eta^{12}_{1}, \\ C^{t}_{2} \longrightarrow 2\eta^{2}_{01} + \eta^{2}_{1}. \end{cases} \tag{11.33}$$

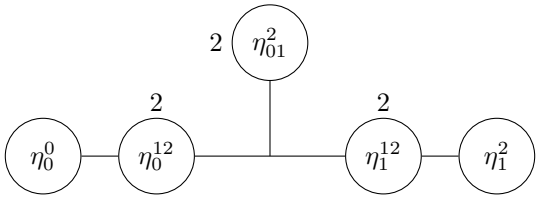

Figure 11.8: Codimension-two Collision of $\mathrm{SU}(2)\times\mathrm{G}_2$-model at $S\cap T$, Resolution III. This fiber is of type III* (with dual graph $\widetilde{\mathrm{E}}_7$) with contracted nodes.

In order to get the weights of the curves, the intersection numbers are computed between the codimension-two curves and the fibral divisors.

	D_0^s	D_1^s	D_0^t	D_1^t	D_2^t	Weight	Representation
η_0^0	0	0	-2	1	0	[0;0,-1]	$(1,7)\subset(1,14)$
η_0^{12}	-1	1	1	-1	1	[-1;-1,1]	$(2,7)$
η_1^{12}	1	-1	0	-1	2	[1;-2,1]	$(2,7)$
η_1^2	0	0	0	1	-2	[0;2,-1]	$(1,7)\subset(1,14)$
η_{01}^2	0	0	0	1	-2	[0;2,-1]	$(1,7)\subset(1,14)$

Table 11.7: Weights and representations of the components of the generic curve over $S\cap T$ in Resolution III of the $\mathrm{SU}(2)\times\mathrm{G}_2$-model. See Section 11.4.2 for more information on the interpretation of these representations.

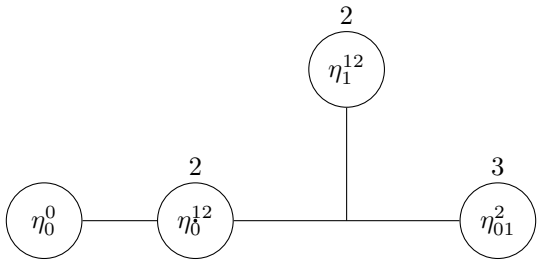

Figure 11.9: Codimension-three enhancement of $\mathrm{SU}(2)\times \mathrm{G}_2$-model at $S\cap T\cap V(f)$, Resolution III. This fiber is of type II^* (with dual graph $\widetilde{\mathrm{E}}_8$) with contracted nodes.

We have a further enhancement when $f = 0$ as the rational curve η_1^2 coincides with η_{01}^2:

$$\eta_1^2 \longrightarrow \eta_{01}^2. \tag{11.34}$$

This corresponds to the codimension-three enhancement in Figure 11.9, which is a fiber of type III^* with contracted nodes.

11.3.4 Resolution IV

The last crepant resolution of the $\mathrm{SU}(2)\times \mathrm{G}_2$-model is given by the following sequence of blowups:

$$X_0 \xleftarrow{(x,y,t|w_1)} X_1 \xleftarrow{(y,w_1|w_2)} X_2 \xleftarrow{(x,y,s|e_1)} X_3. \tag{11.35}$$

Its projective coordinates are then given by

$$[e_1w_1w_2x\,;\,e_1w_1w_2^2y\,;\,z=1][e_1x\,;\,e_1w_2y\,;\,t][e_1y\,;\,w_1][x\,;\,y\,;\,s]. \tag{11.36}$$

The proper transform is identical to equation (11.16). It follows that the divisors are also identical to equation (11.18). On the intersection of S and T, we see the following curves:

$$\text{On } S\cap T: \begin{cases} D^s_0\cap D^t_0 \to & \eta^0_0 : s=t=w_2y^2-w_1e_1x^3=0, \\ D^s_0\cap D^t_1 \to & \eta^{12}_0 : s=w_1=w_2=0, \\ D^s_0\cap D^t_2 \to & \eta^B_{02} : s=w_2=x=0, \quad \eta^2_{01} : s=w_2=e_1=0, \quad \eta^{12}_0 : s=w_2=w_1=0, \\ D^s_1\cap D^t_2 \to & \eta^2_1 : e_1=w_2=fx+gst=0, \quad \eta^2_{01} : e_1=w_2=s=0. \end{cases} \tag{11.37}$$

Hence, we can deduce that the five fibral divisors split in the following way to produce the fiber in Figure 11.10, which is a fiber of type III* with contracted nodes.

$$\text{On } S\cap T: \begin{cases} C^s_0 \longrightarrow \eta^0_0+2\eta^{12}_0+3\eta^{2B}_0+\eta^2_{01}, \\ C^s_1 \longrightarrow \eta^2_{01}+\eta^2_1, \\ C^t_0 \longrightarrow \eta^0_0, \\ C^t_1 \longrightarrow \eta^{12}_0, \\ C^t_2 \longrightarrow 3\eta^{2B}_0+2\eta^2_{01}+\eta^2_1. \end{cases} \tag{11.38}$$

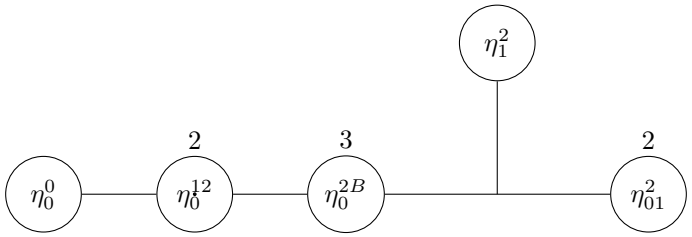

Figure 11.10: Codimension-two Collision of $\mathrm{SU}(2) \times \mathrm{G}_2$-model at $S \cap T$, Resolution IV. This fiber is of type III* (with dual graph $\widetilde{\mathrm{E}}_7$) with contracted nodes.

In order to get the weights of the curves, the intersection numbers are computed between the codimension-two curves and the fibral divisors.

	D_0^s	D_1^s	D_0^t	D_1^t	D_2^t	Weight	Representation
η_0^0	0	0	-2	1	0	[0;0,-1]	$(1,7) \subset (1,14)$
η_0^{12}	0	0	1	-2	3	[0;-3,2]	$(1,14)$
η_0^{2B}	-1	1	0	1	-2	[-1;2,-1]	$(2,7)$
η_{01}^2	1	-1	0	0	0	[1;0,0]	$(2,1) \subset (2,7)$
η_1^2	1	-1	0	0	0	[1;0,0]	$(2,1) \subset (2,7)$

Table 11.8: Weights and representations of the components of the generic curve over $S \cap T$ in Resolution IV of the $\mathrm{SU}(2) \times \mathrm{G}_2$-model. See Section 11.4.2 for more information on the interpretation of these representations.

For the codimension-three fiber enhancement, consider when $f = 0$. Note that only the fiber η_1^2 changes under this condition:

$$\eta_1^2 \to \eta_{01}^2. \tag{11.39}$$

Even though only a single curve changed, we get a completely different fiber as a result. The codimension-three enhancement is represented in Figure 11.11, which is a fiber of type III* with contracted nodes.

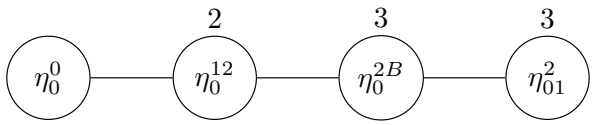

Figure 11.11: Codimension-three enhancement of $\mathrm{SU}(2) \times \mathrm{G}_2$-model at $S \cap T \cap V(f)$, Resolution IV. This fiber is of type II^* (with dual graph $\widetilde{\mathrm{E}}_8$) with contracted nodes.

11.3.5 Fiber structure

In this section, we describe codimension-one and codimension-two fiber enhancements of all the resolutions (Resolutions I, II, III, IV) of the $\mathrm{SU}(2) \times \mathrm{G}_2$-model. We consider two different ways of realizing the $\mathrm{SU}(2) \times \mathrm{G}_2$-model: the collision of the fibers of type III+$\mathrm{I}_0^{*S_3}$ and III + $\mathrm{I}_0^{*\mathbb{Z}_3}$ depending on the Galois group of the fiber $\mathrm{I}_0^{*\mathrm{ns}}$. The Weierstrass equation of type III+$\mathrm{I}_0^{*S_3}$ is given by $y^2 = x^3 + fst^2x + gs^2t^3$, whereas that of type III + $\mathrm{I}_0^{*\mathbb{Z}_3}$ is given by $y^2 = x^3 + fst^{3+\alpha}x + gs^2t^3$. Resolutions I, II, III, and IV of the collision of the type III+$\mathrm{I}_0^{*S_3}$ are respresented in Tables 11.9, 11.10, 11.11, and 11.12 respectively. Resolutions I, II, III, and IV of the collision of type III + $\mathrm{I}_0^{*\mathbb{Z}_3}$ are represented in Table 11.13.

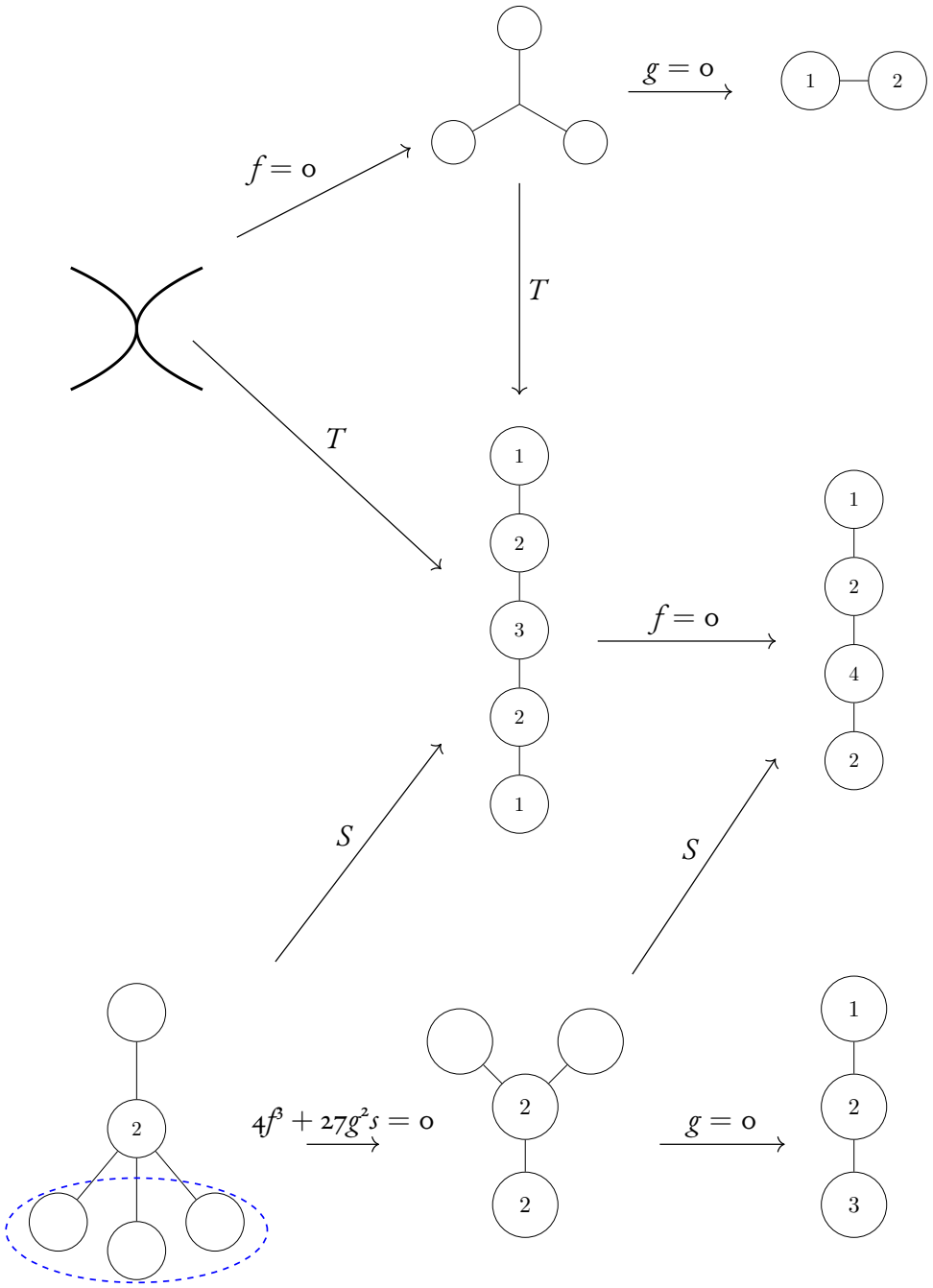

Table 11.9: III + $I_0^{*S_3}$, Resolution I.

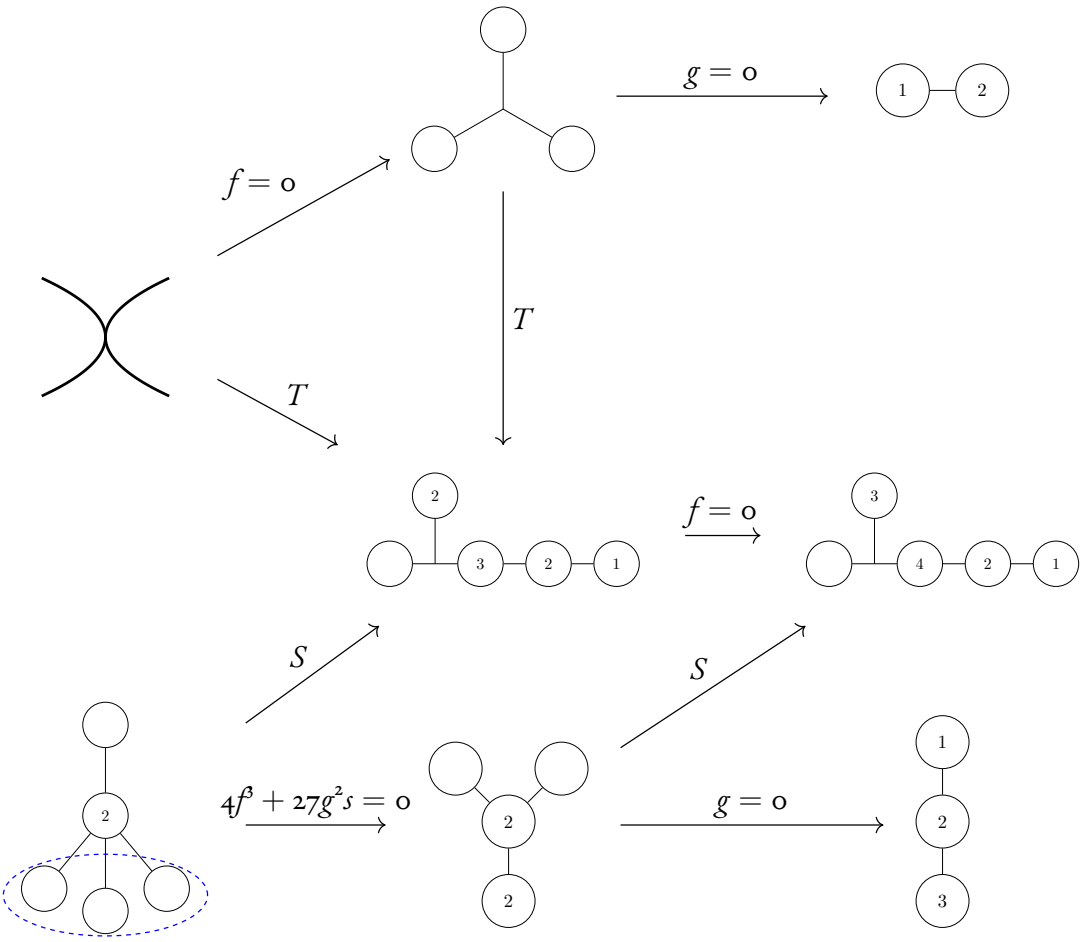

Table 11.10: III + I_0^{*,S_3}, Resolution II.

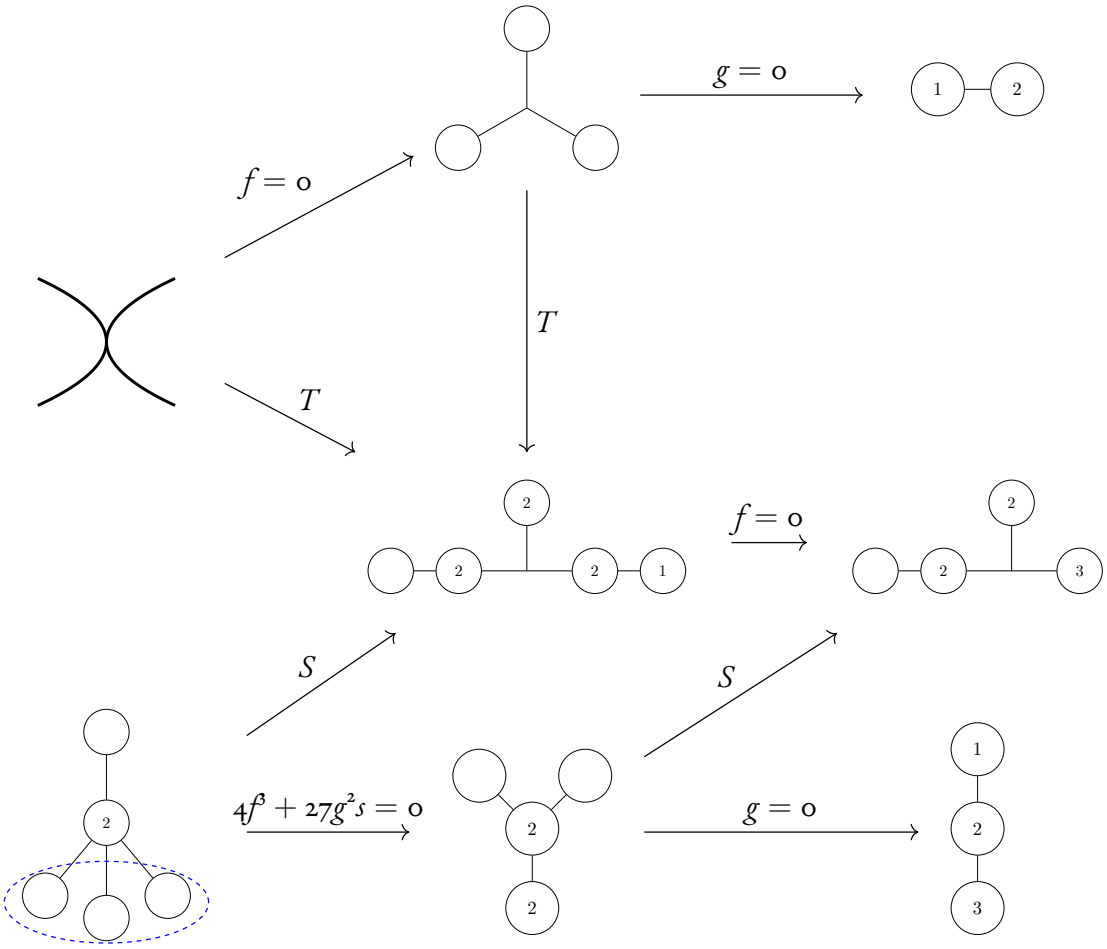

Table 11.11: III + I_0^{*,S_3}, Resolution III.

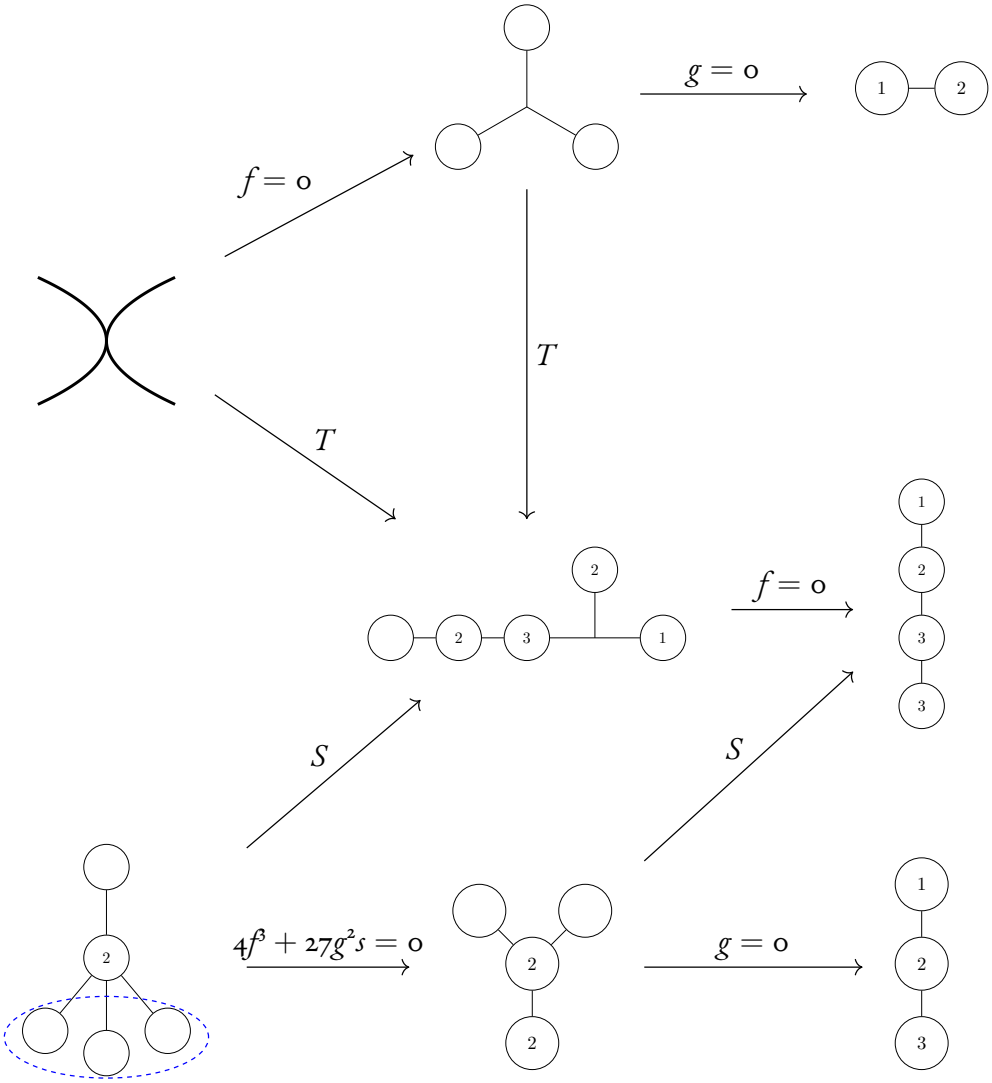

Table 11.12: III + $I_0^{*S_3}$, Resolution IV.

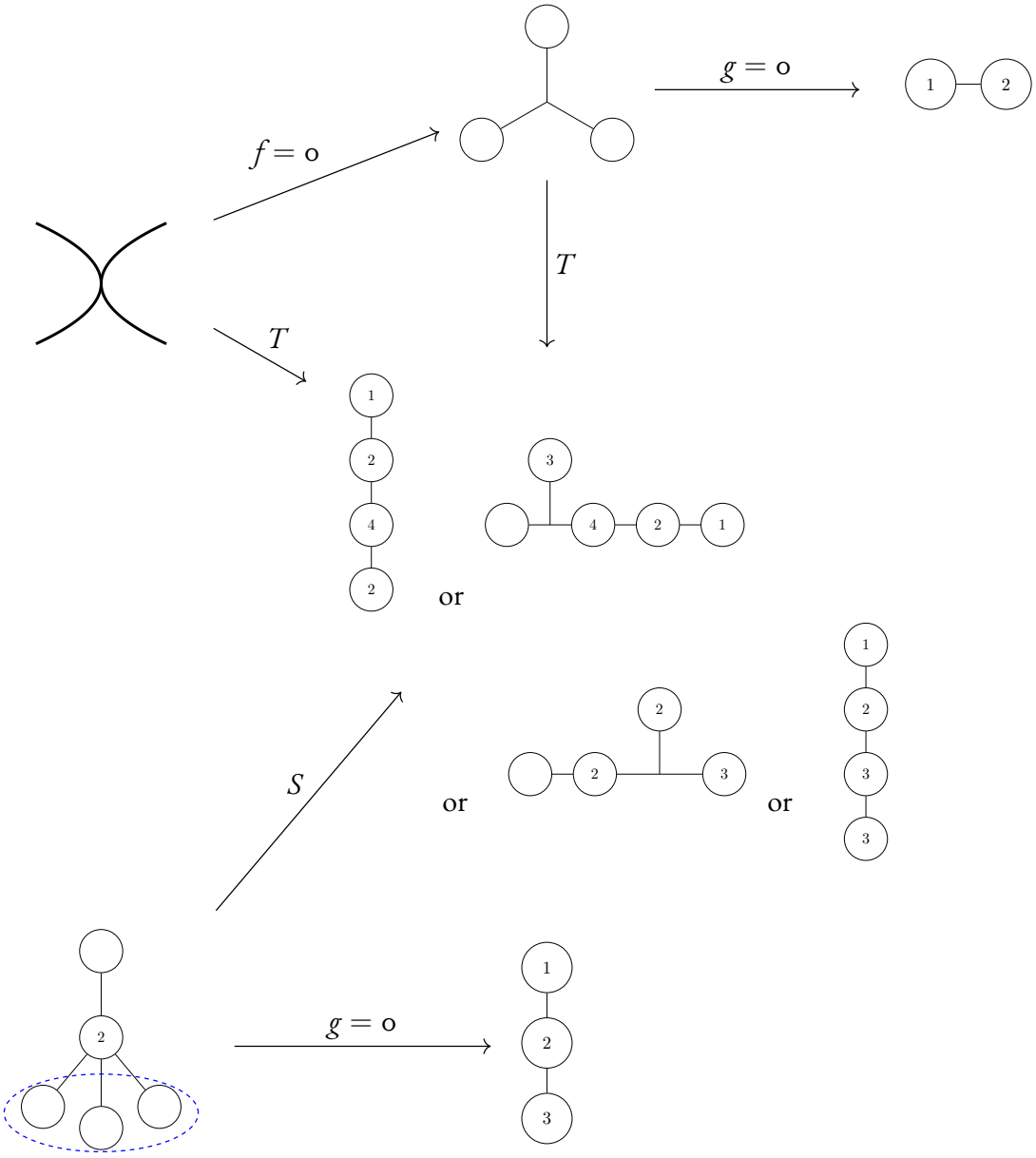

Table 11.13: III + $I_0^{*\mathbb{Z}_3}, y^2 = x^3 + fst^{3+\alpha}x + gs^2t^3$. Resolution I, II, III, and IV. The fibers in codimension-two are arranged in the order of the resolution. There are no more enhancements in higher codimension.

11.4 Deriving the matter representation of an $SU(2) \times G_2$-model

In this section, we explain how to derive the representation attached to an $SU(2) \times G_2$-model. We first explain how the Katz-Vafa method does not give the correct representation for the $SU(2) \times G_2$-model. We use instead the notion of saturation of weights starting with a set of weights derived geometrically by intersecting the fibral divisors by the irreducible components of singular fibers over codimension-two points.

11.4.1 Failing of the Katz–Vafa method for the $SU(2) \times G_2$-model

The Katz–Vafa method was defined for rank-one enhancements between Lie algebras of type ADE [187]. For a G-model with a simple Lie group G, the Katz–Vafa method provides an elegant derivation of the matter content. This method had enabled the F-theory constructions to be independent from the existence of a Heterotic dual to explain their matter content. In collision of singularities, given two simple groups G_1 and G_2, we can determine the group G that corresponds to their collision by considering an elliptic surface whose discriminant locus pass by one of the points of intersection of the divisors supporting G_1 and G_2.

The Katz–Vafa method uses as input a triple (G_1, G_2, G) of Lie groups such that $G_1 \otimes G_2 \subset G$ and returns representations $\mathbf{R}_i$ appearing in the branching rule for the decomposition of the adjoint of $\mathfrak{g} = \mathrm{Lie}(G)$ in terms of representations of $G_1 \times G_2$.

$$\mathfrak{g} = \mathfrak{g}_1 \oplus \mathfrak{g}_2 \oplus R_1 \oplus \cdots \oplus R_n,$$

where $\mathbf{R}_i$ are representations of $G_1 \times G_2$.

The branching rules for $G \supset G_1 \otimes G_2$ provide the Katz–Vafa representations $\mathbf{R}_i = (r_i^{(1)}, r_i^{(2)})$ for the collision of G_1 and G_2 :

$$adj(\mathfrak{g}) = adj(\mathfrak{g}_1) \oplus adj(\mathfrak{g}_2) \oplus \bigoplus_i (r_i^{(1)}, r_i^{(2)}). \tag{11.40}$$

The original motivation for Katz–Vafa was to give an intrinsic derivation of the matter content of F-theory without relying on the duality with the Heterotic string theory. In six-dimensional theories, anomaly cancellations are a sanity check for the identification of the correct representations. But a direct derivation is still necessary as anomalies do not uniquely identify the matter content. In explicit examples, we often have a rank-one enhancement with $G_1 \times U(1) \subset G$ with G_1 given via the fiber structure and G to be determined.

The Katz-Vafa method does not always produce the correct matter content, in particular, the matter content of the $SU(2) \times G_2$-model cannot be derived by the Katz-Vafa method. The geometry of the fibration shows that at the collision of S and T, the fibers are contractions of fibers of type III* whose dual graph is the affine Dynkin diagram of type $\widetilde{E}_7$. The Lie algebra of $SU(2) \times G_2$ is a maximal subalgebra of type S of E_7. The branching rule for the adjoint representation of E_7 in terms of the representation of $SU(2) \times G_2$ is as follows [233] :

$$133 = (3,1) \oplus (1,14) \oplus (5,7) \oplus (3,27). \tag{11.41}$$

The two summands $(3,1)$ and $(1,14)$ are the two components of the adjoint representation of $\mathrm{SU}(2)\times \mathrm{G}_2$. Thus, the remaining parts $(5,7)\oplus(3,27)$ should give the matter content of the $\mathrm{SU}(2)\times \mathrm{G}_2$-model according to the Katz–Vafa method. However, the representations $(5,7)$ and $(3,27)$ are incompatible with the weights from the geometry after resolving the singularities of the $\mathrm{SU}(2)\times \mathrm{G}_2$-model, as they do not contain the weights of the bifundamental representation $(2,7)$.

11.4.2 Saturation of weights and representations

To determine the representation $\mathbf{R}$ attached to a given elliptic fibration, over each codimension-two point, we identify a subset of weights of $\mathfrak{g}$ using intersection theory. This process can be explained in the following steps:

1. We first identify all the fibral divisors[2] of the elliptic fibration. Each fibral divisor is a fibration over an irreducible component of the discriminant locus.

2. Then, we collect all the singular fibers over codimension-two points of the base where the generic fibers of the fibral divisors degenerate further. Assuming that the fibration is equidimensional up to codimension-two points, all the irreducible components of the singular fibers are necessarily rational curves that we call *rational vertical curves*.

3. We compute the intersection numbers of these rational vertical curves with the fibral divisors. In this way, we attach to each irreducible components of a singular fiber over a codimension-

[2] Under mild assumptions, the discriminant locus of an elliptic fibration $\phi : Y \to B$ is a divisor Δ. The *fibral divisors* are by definition the irreducible components of the pullback $\phi^*(\Delta_{red})$ where Δ_{red} is the reduced discriminant.

two point a vector with integer entries. If we consider only the fibral divisors not touching the section of the elliptic fibration, we get a vector of dimension equal to the rank of the Lie algebra $\mathfrak{g}$; we identify the negative of such a vector with an element of the weight lattice of $\mathfrak{g}$.

4. We determine the representation **R** attached to the weights of the rational vertical curves over each codimension-two points. The representation **R** has to necessarily contain all the weights that we have identified by intersections of rational vertical curves with the fibral divisors.

In the last step, the goal is then to determine the minimal representation generated by the subset of weights given to us by the geometry. A systematic way to do so is to use the notion of *saturation of weights* introduced by Bourbaki (see [57, Chap.VIII.§7. Sect. 2]). The identification of a representation using weights obtained by intersection numbers can be traced back to Aspinwall and Gross [19]; it is based on the M-theory picture of M2-branes wrapping chains of curves and becoming massless when the curve shrinks to a point. The use of saturation of weights in this context was first explained in [112] and inspired directly by [19] and [57]. See also [226, 241].

Definition 11.4.1. A set Π of integral weights is said to be *saturated* if for all $\mu \in \Pi$, for all roots α, and for all t between 0 and $\langle \mu, \alpha \rangle$, we have $\mu - t\alpha \in \Pi$. The *saturation* of a set of weights Π is the smallest saturated set containing Π.

We refer to Bourbaki [57, Chap.VIII.§7. Sect.2] for more information on saturated sets of weights. A direct consequence of the definition is that a saturated set of weights is invariant under the Weyl group. Given a representation **R**, its set of weights $\Phi_{\mathbf{R}}$ is a saturated set of weights.

Theorem 11.4.2 (See Corollary of Proposition 5 of [57, Chap.VIII.§7. Sect.2]). *For any finite saturated set of weights* Π*, there exists a finite-dimensional representation* $\mathbf{R}$ *such that* Π *is the set of weights of* $\mathbf{R}$.

Thus, the saturation of weights attaches a representation $\mathbf{R}$ to a finite set of weights Π in a systematic way: $\mathbf{R}$ is the unique representation whose set of weights is the saturation of Π. In other words, $\mathbf{R}$ is the representation generated by the set of weights Π. There can be other representations containing the saturation of Π as a proper subset of their set of weights.

We determine the representation $\mathbf{R}$ attached to an elliptic fibration by first interpreting the negative of the intersection of vertical curves (over codimension-two points) with the fibral divisors as elements of the weight lattice. We then associate a representation to these weights using the notion of saturation of weights [112, 115, 121].

We illustrate the method with Resolution I. In Resolution I, the curve C_1^s degenerates as follows over $S \cap T$:

$$C_1^s \longrightarrow 3\eta_1^{o2} + 2\eta_1^{oA} + 2\eta_1^{12} + \eta_1^2,$$

where η_1^{o2} and η_1^2 have weight $[0; 2, -1]$, which is a weight of the fundamental representation $(1, 7) \subset (1, 14)$, η_1^{oA} has weight $[1; -1, 0]$ of the bifundamental representation $(2, 7) \subset (2, 14)$, and η_1^{12} has weight $[0; -3, 2]$ of the adjoint representation $(1, 14)$.

In Resolution IV, the curve C_1^s undergoes the following degeneration over $S \cap T$:

$$C_1^s \longrightarrow \eta_{o1}^2 + \eta_1^2,$$

where both η^2_{01} and η^2_1 have weight $[1; 0, 0]$, which is a weight of the representation $(2, 1) \subset (2, 7)$. There is another curve (η^{2B}_0) coming from the degeneration of C^s_0 that carries the weight $[-1, 2, -1]$ of the bifundamental $(2, 7)$ of $SU(2) \times G_2$.

To make sense of the representation we should attach to these degenerations, we recall first few fact about the weights involved. The adjoint representation of G_2 consists of fourteen weights that split into four orbits under the action of the Weyl group: each of the two zero weights form an orbit on its own, the six short roots form an orbit, and the six long weights form the fourth orbit. The short roots of the adjoint of G_2 are the nonzero weights of the fundamental representation 7 of G_2. The highest weight of the adjoint representation is a long root; thus, the adjoint representation is the smallest representation containing the saturation set of any subset of long roots. The bifundamental representation of $SU(2) \times G_2$ $(2, 7)$ consists of the following Weyl orbits: the two weights $[\pm 1; 0, 0]$ form an orbit corresponding to the representation $(2, 1)$, and the other twelve weights form a unique orbit. Thus we can conclude the saturations from the weights are given by Table 11.14.

Set of weights Π	Saturation of Π
$\{[0; 2, -1]\}$	the fundamental rep. $(1, 7)$
$\{[1; -1, 0]\}$	the bifundamental rep. $(2, 7)$
$\{[0; -3, 2]\}$	the adjoint representation $(1, 14)$
$\{[1; 0, 0]\}$	the fundamental rep. $(2, 1)$
$\{[0; -3, 2], [0; 2, -1]\}$	the adjoint representation $(1, 14)$
$\{[-1; 0, 0], [-1; 2, -1]\}$	the bifundamental rep. $(2, 7)$

Table 11.14: Representations derived from saturation of weights.

11.5 5*d* and 6*d* Supergravity Theories with Eight Supercharges

In this section, we determine the prepotential in each Coulomb branch of the five-dimensional supergravity theory with eight supercharges and match with the triple intersection polynomial for each corresponding crepant resolution. We determine the number of multiplets of the corresponding uplifted six-dimensional theory and check if the anomalies can be canceled using Green-Schwarz mechanism. We also explain the numerical oddities we encounter while counting the number of hypermultiplets.

11.5.1 5*d* $\mathcal{N} = 1$ prepotentials

We compute $\mathscr{F}_{\text{IMS}}$ for each of the four chambers of an $\mathrm{SU}(2)\times \mathrm{G}_2$-model. The chambers are defined by Table 11.3.

Theorem 11.5.1. *The prepotential of an $SU(2)\times G_2$-model in the four phases defined by the chambers of Table 11.3.*

Chamber 1:

$$\begin{aligned} 6\mathscr{F}^{(1)}_{IMS} = &-4\varphi_2^3(2n_{1,14}+n_{1,7}-2)+9\varphi_1\varphi_2^2(-2n_{1,14}+n_{1,7}+2)-8(n_{1,14}-1)\varphi_1^3 \\ &+3\varphi_1^2\varphi_2(8n_{1,14}-n_{1,7}-8)+\psi_1^3(-n_{2,1}-7n_{2,7}-8n_{3,1}+8) \\ &+12\psi_1\left(-3n_{2,7}\varphi_2^2+3n_{2,7}\varphi_1\varphi_2-n_{2,7}\varphi_1^2\right), \end{aligned}$$

Chamber 2:

$$\begin{aligned}6\mathscr{F}^{(2)}_{IMS} =& -2\varphi_2^3(4(n_{1,14}+n_{1,7}-1)+n_{2,7}) + 9\varphi_1\varphi_2^2(-2n_{1,14}+n_{1,7}+2) - 8(n_{1,14}-1)\varphi_1^3 \\ &+ 3\varphi_1^2\varphi_2(8n_{1,14}-n_{1,7}-8) + \psi_1^3(-n_{2,1}-5n_{2,7}-8n_{3,1}+8) - 6n_{2,7}\psi_1^2\varphi_2 \\ &+ \psi_1\left(-30n_{2,7}\varphi_2^2+36n_{2,7}\varphi_1\varphi_2-12n_{2,7}\varphi_1^2\right),\end{aligned}$$

Chamber 3:

$$\begin{aligned}6\mathscr{F}^{(3)}_{IMS} =& 3\varphi_1\varphi_2^2(-6n_{1,14}+3n_{1,7}-2n_{2,7}+6) + 3\varphi_1^2\varphi_2(8n_{1,14}-n_{1,7}+2n_{2,7}-8) \\ &- 8\varphi_2^3(n_{1,14}+n_{1,7}-1) - 2\varphi_1^3(4n_{1,14}+n_{2,7}-4) + \psi_1^3(-n_{2,1}-3n_{2,7}-8n_{3,1}+8) \\ &+ \psi_1\left(-24n_{2,7}\varphi_2^2+24n_{2,7}\varphi_1\varphi_2-6n_{2,7}\varphi_1^2\right) - 6n_{2,7}\psi_1^2\varphi_1,\end{aligned}$$

Chamber 4:

$$\begin{aligned}6\mathscr{F}^{(4)}_{IMS} =& -8(n_{1,14}-1)\varphi_1^3 + 9\varphi_1\varphi_2^2(-2n_{1,14}+n_{1,7}+2n_{2,7}+2) - 8\varphi_2^3(n_{1,14}+n_{1,7}+2n_{2,7}-1) \\ &+ 3\varphi_2\varphi_1^2(8n_{1,14}-n_{1,7}-2n_{2,7}-8) + \psi_1^3(-n_{2,1}-n_{2,7}-8n_{3,1}+8) - 12n_{2,7}\psi_1^2\varphi_2.\end{aligned}$$

Proof. Direct computation starting with equation (2.39) and using Table 11.3 to remove the absolute values. □

The number of hypermultiplets are computed by comparing the prepotential and the intersection polynomial. Comparing the triple intersection numbers obtained in the Resolutions I, II, III,

IV with the prepotentials computed respectively in Chambers 1,2,3,4, we get

$$\begin{aligned} n_{2,1} + 8n_{3,1} &= S \cdot \left(4L + 2S - \frac{7}{2}T\right) + 8, \qquad & n_{1,14} &= \frac{1}{2}(-L \cdot T + T^2 + 2), \\ n_{2,7} &= \frac{1}{2}S \cdot T, & n_{1,7} &= T \cdot (5L - S - 2T). \end{aligned} \tag{11.42}$$

We see in particular that the numbers $n_{2,1}$ and $n_{3,1}$ are not completely fixed by this method but restricted by a linear relation. The same is true for the SU(2)-model in [124]. Using Witten's genus formula to restrict $n_{3,1}$ with $K = -L$, we get that $n_{3,1}$ and $n_{1,14}$ become respectively the arithmetic genus of the curves S and T:

$$n_{3,1} = g(S), \quad n_{1,14} = g(T), \quad n_{2,1} = -S \cdot \left(8K + 2S + \frac{7}{2}T\right), \quad n_{1,7} = -T \cdot (5K + S + 2T). \tag{11.43}$$

The geometric origin of the number $n_{1,7}$ is as follows. The G_2 fiber contains a non-split curve that splits into three curves after an appropriate field extension. Over T, this non-split curve defines a triple cover of T with a branch locus given by its discriminant $s^3t^6(4f^3 + 27g^2s)$. The reduced discriminant is $s(4f^3 + 27g^2s)$ as t is a unit. Using Witten's genus formula [1, 306, 306], we get

$$n_{1,7} = (d-1)(g-1) + \frac{1}{2}R, \tag{11.44}$$

where $d = 3, g = \frac{1}{2}(KT + T^2 + 2)$, and the class of R is the class of the reduced discriminant, i.e. $R = [t][s(4f^3 + 27g^2s)] = -3T \cdot (4K + S + 2T) + S \cdot T$.

As explained in Remark 11.1.1, the representation $n_{1,7}$ is frozen when S and T intersect transver-

sally at one point and T is a -3-curve. The meaning of $n_{2,1}$ is much more complicated. One would expect it to be just an intersection number, but that is not the case as will discuss in section 11.6.

11.5.2 Anomalies cancellations for an $\mathrm{SU}(2)\times \mathrm{G}_2$-model

In this section, we check that the gravitational, gauged, and mixed anomalies of the six-dimensional supergravity are all canceled when the Lie algebra and the representation are

$$\mathfrak{g} = \mathrm{A}_1 \oplus \mathrm{G}_2, \quad \mathbf{R} = (3,1) \oplus (1,14) \oplus (2,1) \oplus (1,7) \oplus (2,7).$$

First, we recall that for the case of a Calabi-Yau threefold (defined as a crepant resolution of the Weierstrass model of an $\mathrm{SU}(2)\times \mathrm{G}_2$-model), the Euler characteristic is (see Lemma 11.2.3)

$$\chi(Y) = -6(10K^2 + 5K\cdot S + 8K\cdot T + S^2 + 2S\cdot T + 2T^2), \tag{11.45}$$

where S and T are the curves supporting A_1 and G_2 respectively. The Hodge numbers are

$$h^{1,1}(Y) = 14 - K^2, \quad h^{2,1}(Y) = 29K^2 + 15K\cdot S + 24K\cdot T + 3S^2 + 6S\cdot T + 6T^2 + 14. \tag{11.46}$$

The numbers of vector multiplets and tensor multiplets, and neutral hypermultiplets are

$$\begin{aligned} &n_T = 9 - K^2, \quad n_V = \dim G = \dim\ \mathrm{SU}(2) + \dim\ \mathrm{G}_2 = 3 + 14 = 17, \\ &n_H^\circ = h^{2,1}(Y) + 1 = 29K^2 + 15K\cdot S + 24K\cdot T + 3S^2 + 6S\cdot T + 6T^2 + 15. \end{aligned} \tag{11.47}$$

We will use the anomaly cancellation conditions to explicitly compute the number of hypermultiplets transforming in each representation by requiring all anomalies to cancel. We will see that they are the same as those found in five-dimensional supergravity by comparing the triple intersection numbers of the fibral divisors of a given crepant resolution and the cubic prepotential of the corresponding Coulomb chamber.

The Lie algebra of type A_1 (resp. G_2) only has a unique quartic Casimir invariant so that we do not have to impose the vanishing condition for the coefficients of $\mathrm{tr}\, F_1^4$ (resp. $\mathrm{tr}\, F_2^4$). We have the following trace identities for SU(2) and G_2 [22, 106]:

$$\begin{aligned} &\mathrm{tr}_3 F_1^2 = 4\mathrm{tr}_2 F_2^2, \quad \mathrm{tr}_3 F_1^4 = 8(\mathrm{tr}_3 F_1^2)^2, \quad \mathrm{tr}_2 F_1^4 = \frac{1}{2}(\mathrm{tr}_2 F_1^2)^2, \\ &\mathrm{tr}_{14} F_2^2 = 4\mathrm{tr}_7 F_2^2, \quad \mathrm{tr}_{14} F_2^4 = \frac{5}{2}(\mathrm{tr}_7 F_2^2)^2, \quad \mathrm{tr}_7 F_2^4 = \frac{1}{4}(\mathrm{tr}_7 F_2^2)^2, \end{aligned} \tag{11.48}$$

which give

$$\begin{aligned} X_1^{(2)} &= (4 - 4n_{3,1} - n_{2,1} - 7n_{2,7})\,\mathrm{tr}_2 F_1^2, \quad X_2^{(2)} = (4 - 4n_{1,14} - n_{1,7} - 2n_{2,7})\,\mathrm{tr}_7 F_2^2, \\ X_1^{(4)} &= (8 - 8n_{3,1} - \frac{1}{2}n_{2,1} - \frac{7}{2}n_{2,7})(\mathrm{tr}_2 F_1^2)^2, \quad X_2^{(4)} = (\frac{5}{2} - \frac{5}{2}n_{1,14} - \frac{1}{4}n_{1,7} - \frac{2}{4}n_{2,7})(\mathrm{tr}_7 F_2^2)^2, \\ Y_{27} &= n_{2,7}\,\mathrm{tr}_2 F_1^2\,\mathrm{tr}_7 F_7^2. \end{aligned} \tag{11.49}$$

Following Table 2.9, we take $\lambda_1 = 1$ for A_1 and $\lambda_2 = 2$ for G_2. If the pure gravitational anomaly

vanishes, the anomaly cancellation conditions are

$$\begin{gathered}
2(4-4n_{1,14}-n_{1,7}-2n_{2,7})=6K\cdot T,\quad (4-4n_{3,1}-n_{2,1}-7n_{2,7})=6K\cdot S,\\
(10-10n_{1,14}-n_{1,7}-2n_{2,7})=-3T^2,\quad (8-8n_{3,1}-\frac{1}{2}n_{2,1}-\frac{7}{2}n_{2,7})=-3S^2,\\
2n_{2,7}=S\cdot T.
\end{gathered}\tag{11.50}$$

These linear equations have the following unique solution

$$\begin{gathered}
n_{2,7}=\frac{1}{2}S\cdot T,\qquad n_{3,1}=\frac{1}{2}(K\cdot S+S^2+2)\qquad n_{2,1}=-S\cdot(8K+2S+\frac{7}{2}T),\\
n_{1,14}=\frac{1}{2}(K\cdot T+T^2+2),\qquad n_{1,7}=-T\cdot(5K+S+2T).
\end{gathered}\tag{11.51}$$

We note that the numbers of charged hypermultiplets match exactly the values found in the five-dimensional theory (see equation (11.43)) after using Witten's genus formula which asserts that the number of adjoint hypermultiplets $n_{3,1}$ is the genus of the curve S supporting the group SU(2) [306].

We can now check that the pure gravitational anomaly is cancelled. The total number of hypermultiplets is the sum of the neutral hypermultiplets coming from the compactification and the charged hypermultiplets transforming under the different irreducible summands of the representation **R**. Since the charge of a hypermultiplet is given by a weight of a representation, we remove

the zero weights when counting charged hypermultiplets [142]. In the present case, we have:

$$\begin{aligned} n_H &= n_H^{\circ} + n_H^{ch} \\ &= (h^{2,1}(Y) + 1) + 2n_{2,1} + (7-1)n_{1,7} + 14n_{2,7} + (3-1)n_{3,1} + (14-2)n_{1,14} = 29K^2 + 29. \end{aligned} \tag{11.52}$$

Using equation (11.47), we check that the coefficient of tr R^4 vanishes as required by the cancellation of the pure gravitational anomaly [262]:

$$n_H - n_V + 29n_T - 273 = 0. \tag{11.53}$$

Finally, we show that the anomaly polynomial I_8 factors as a perfect square:

$$\begin{aligned} I_8 &= \frac{K^2}{8}(\mathrm{tr}R^2)^2 + \frac{1}{6}(X_1^{(2)} + X_2^{(2)})\mathrm{tr}R^2 - \frac{2}{3}(X_1^{(4)} + X_2^{(4)}) + 4Y_{27}, \\ &= \frac{1}{2}\left(\frac{1}{2}K\mathrm{tr}R^2 + 2S\mathrm{tr}_2F_1^2 + T\mathrm{tr}_7F_2^2\right)^2. \end{aligned} \tag{11.54}$$

Hence, we conclude that all the local anomalies are canceled via the Green–Schwarz–Sagnotti–West mechanism [147, 270].

11.6 Counting hypermultiplets: numerical oddities

The physics of D-branes in presence of singularities is full of subtleties [5, 78, 123]. The situations that are well understood rely on fundamental physical properties such as the cancellations of anoma-

lies and tadpoles or string dualities. For example, the induced D3-charge of a singular D7-brane is derived from a tadpole cancellation condition [5, 78].

The numbers of charged hypermultiplets we get from the triple intersection numbers of the five-dimensional theory match the numbers of hypermultiplets we get by solving the six-dimensional theory anomaly cancellation conditions. The number of fundamental $n_{1,7}$ can be explained using Witten's genus formula and the number of bifundamental $n_{2,7}$ is given by an intersection number as expected by the usual D-brane picture.

We point out an interesting observation about the number of hypermultiplets charged in the representation $(2, 1)$ in the $SU(2) \times G_2$-model. One would expect that the number of fundamental matter $n_{2,1}$ is also given by a direct intersection number, but that is not the case. We cannot explain the number $n_{2,1}$ by looking at the D-brane configuration attached to this geometry.

11.6.1 Determining $n_{2,1}$ from $5d$ and/or $6d$

If we evaluate the number of multiplets in a five-dimensional supergravity theory with eight supercharges resulting from a compactification of M-theory on an elliptically fibered Calabi-Yau threefold obtained by one of the resolution of the $SU(2) \times G_2$-model, we can compare the triple intersection numbers of the divisors of the Calabi-Yau with the one-loop prepotential and deduce the number of multiplets. Moreover, in a compactification of F-theory on the same variety, we get a six-dimensional supergravity theory and we can use anomaly cancellation conditions to determine the

number of hypermultiplets. In both cases, we find that $n_{2,1}$ is given by

$$n_{2,1} = -2S \cdot (4K + S + \frac{7}{4}T) = -2S \cdot (4K + S + 2T) + \frac{1}{2}S \cdot T.$$

11.6.2 Localization of hypermultiplets charged under $(2, 1)$

We recall that the discriminant of the $SU(2) \times G_2$-model is supported on three divisors, namely, S (which supports SU(2)), T (which supports G_2) and $\Delta' = 4f^3 + 27g^2s$ (which does not support any gauge group). While S has a transverse intersection with T, S intersects Δ' non-transversally along triple points located at $s = f = 0$. The hypermultiplets transforming in the representation $(2, 1)$ are localized at these non-transverse intersection points of S and Δ'. The divisor Δ' has cuspidal singularities at $V(f, g)$. However, since the divisor S intersects it along its smooth locus, the cuspdical points should not affect the discussion of the hypermultiplets charged under $(2, 1)$.

The reduced locus of the intersection of S and Δ' is $V(s, f)$. One might think that following the usual D-brane picture, the number of hypermultiplets $n_{2,1}$ will just be the intersection number

$$S \cdot [f] = -S \cdot (4K + S + 2T). \tag{11.55}$$

We might also think that since the intersection of S and Δ' is given by the non-reduced scheme (s, f^3), we might take the multiplicity seriously and have

$$S \cdot [\Delta'] = -3S \cdot (4K + S + 2T). \tag{11.56}$$

But what we get is

$$n_{2,1} = -2S \cdot (4K + S + 2T) + \frac{1}{2} S \cdot T. \tag{11.57}$$

As discussed in Remark 11.1.1, this formula reproduces what is known for the case when T and S are rational curves of self-intersection -2 and -3 intersecting transversally at one point [69, 240].

Remark 11.6.1. There are two surprising numerical oddities about this formula (equation 11.57).

1. The first oddity is the coefficient of 2 in the first term $-2S \cdot (4K + S + 2T)$.

2. The second numerical oddity is the presence of the second term as it predicts a nonzero number of hypermultiplets charged in the representation $(2, 1)$ even when the fiber of type III does not intersect the component Δ' and therefore does not enhance to a fiber of type IV.

We will discuss these two points further below using the geometric point of view of this chapter, namely, the fiber geometry in a crepant resolution and the notion of saturations of weights.

11.6.3 Mismatch between the brane and the anomaly picture?

We can justify the contribution $-2S \cdot (4K + S + 2T)$ to $n_{2,1}$ by analyzing the crepant resolution. To be specific, we consider the case of the Resolution I studied in Section 11.3.1. The fiber III consists of two curves, a projective line (C_0^s) and a conic (C_1^s):

$$C_1^s : e_1 = w_2 y^2 - t^2 s w_1 (fx + gts) = 0. \tag{11.58}$$

The matrix of this conic is (with respect to the projective coordinates $[y : s : x]$):

$$M = \begin{pmatrix} w_2 & 0 & 0 \\ 0 & 0 & -\frac{1}{2} w_1 t^2 f \\ 0 & -\frac{1}{2} t^2 f w_1 & -t^3 g w_1 \end{pmatrix}. \tag{11.59}$$

The determinant of this matrix is

$$\det M = -\frac{1}{4} w_2 w_1^2 t^4 f^2. \tag{11.60}$$

The determinant of M vanishes over two distinct loci in the base: the intersection $T \cap S$ (in particular $V(e_1, w_1 w_2 t)$) and the intersection of S and $V(f)$ (located on S and away from T).

At $f = 0$, M has rank two and the conic splits into two lines inducing an enhancement III $\to$ IV. Each of the two line has weight $[1; 0, 0]$ since they are both away from the intersection with T and each of them intersects D_0^s transversally at one point (and therefore by linearity has intersection -1 with D_1^s).

The rank of the matrix M collapses to two when $w_2 = 0$ and one when $w_1 = 0$. We recall that after the three blowups, the divisor T has total transform $w_1 w_2 t$. Over $S \cap T$, the generic fiber C_1^s of D_1^s degenerates to a collection of four distinct rational curve with multiplicities. We are at the intersection of S and T and the fiber III collides with the fiber I_0^* to produce a non-Kodaira fiber corresponding to a Kodaira fiber of type III* (whose dual graph $\widetilde{\mathrm{E}}_7$) with some components contracted

to points.

$$\mathrm{III} + \mathrm{I}_0^* \to \mathrm{III}^* \text{ with contracted components.} \tag{11.61}$$

Over $S \cap T$, the weights produced are in the adjoint representation $(1, 14)$ and the bifundamental representation $(2, 7)$. When $f = 0$, C_1^5 produces weights of the fundamental representation $(2, 1)$ of $\mathrm{SU}(2) \times \mathrm{G}_2$. One should keep in mind that the nonzero weights of the $(1, 7)$ are the short nonzero weights of the adjoint representation.

The discriminant of the conic indicates that the number of hypermultiplets in the representation $(2, 1)$ of $\mathrm{SU}(2) \times \mathrm{G}_2$ at points away from T might be (taking into account the multiplicity of f in $\det M$)

$$S \cdot [\det M] = -2S \cdot (4K + S + 2T). \tag{11.62}$$

In the expression of $n_{2,1}$ in equation (11.57), the first term $-2S \cdot (4K + S + 2T)$ is exactly the contribution from the discriminant of the conic away from the divisor T seen in equation (11.62) when we take into account the multiplicity of f^2 in $\det M$. This explains the first numerical oddity mentioned in Remark 11.6.1.

11.6.4 Hypers in the representation $(2, 1)$ at $S \cap T$?

The second term $\frac{1}{2}S \cdot T$ in equation (11.57) is a correction term that is equal to $n_{2,7}$, the number of hypermultiplets transforming in the bi-fundamental representation $(2, 7)$. This correction term gives an explicit mismatch with the number of hypermultiplets in the fundamental representation $n_{2,1}$ from what we expect from the D-brane picture which should be proportional to the intersection

number computed in equation (11.62).

One might argue that this second term $\frac{1}{2}S \cdot T$ is an evidence of the existence of extra hypermultiplets transforming in the representation $(2, 1)$ that is localized at the intersection of S and T. This argument is in direct conflict with the fibral geometry of the $\mathrm{SU}(2) \times \mathrm{G}_2$-model, since at the collision of S and T, the geometry only predicts bifundamental matters in the representation $(2, 7)$.

Remark 11.6.2. The representation 2 is a minuscule representation of SU(2) and 7 is a quasi-minuscule representation of G_2, in particular, the representation 7 of G_2 has a zero weight and all the six remaining nonzero weights are in the same orbit of the Weyl group. The representation $(2, 7)$ is not a (quasi)-minuscule representation of $\mathrm{SU}(2) \times \mathrm{G}_2$ but its set of weights contains all the weights of the minuscule representation $(2, 1)$ of $\mathrm{SU}(2) \times \mathrm{G}_2$. We note that the set of weights of the representation $(2, 1)$ is a maximal subweight system of the set of weights of the representation $(2, 7)$. The weights of the representation $(2, 7)$ consists of two orbits under the Weyl group. One of the orbits has twelve elements that are the products of the weights of the 2 of SU(2) with the non-zero weights of the 7 of G_2. There also exists an orbit that is consisted of exactly of the weights of the representation $(2, 1)$ and is obtained by the direct product of the weights of the 2 of SU(2) with the zero weight of the 7 of G_2. It follows that the weights of the fundamental representation $(2, 1)$ are exactly the short weights of the bifundamental representation $(2, 7)$. They form an orbit under the action of the Weyl group and the unique sub-system of weights of the representation $(2, 7)$.

In the Resolution I, II, and III, the geometric weights in the representation $(2, 7)$ are always weights of the representation $(2, 7)$ that are not weights of the representation $(2, 1)$. In contrast,

in the Resolution IV, some of the rational curves that compose the singular fibers over $S \cap T$ have weights $[1; 0, 0]$, which is a weight of the representation $(2, 1)$. However, on the same locus, we also get a rational curve with the weight $[-1; 2, -1]$, which belongs to the representation $(2, 7)$. As summarized on Table 11.8, the saturation of these two weights, $\{[1; 0, 0],\ [-1; 2, -1]\}$, is the full set of weights of the representation $(2, 7)$ as can be seen directly by computing their Weyl orbits (see Remark 11.6.2). We note that the representation $(2, 7)$ was derived in all the three other chambers. Hence, finding $(2, 7)$ on $S \cap T$ in Resolution IV is expected since the representations seen in F-theory should not depend on a choice of a crepant resolution, as each crepant resolution corresponds to a distinct Coulomb chamber of the same gauge theory.

In conclusion, the number of SU(2) fundamental hypermultiplets $n_{2,1}$ is not given by an intersection number. It has a correction that is at odd with the fibral geometry. While we see only the representation $(2, 7)$ at the intersection $S \cap T$, we note that the representation $(2, 1)$ is a minuscule representation of $\mathrm{SU}(2) \times \mathrm{G}_2$ and its weights form a subset of the weights of the representation $(2, 7)$. In that sense, the weights of the representation $(2, 1)$ are visible in all chambers even though they appear explicitly only as weights of vertical irreducible curves in the Resolution IV. It would be interesting to check if this phenomena occurs in other models with semi-simple Lie groups.

Throughout my work, I have assumed that the standard model is correct, and hence, the Higgs boson should be found. Although this is not directly connected to string theory, the discovery of the Higgs boson demonstrated the power of theoretical reasoning.

Ashoke Sen

12

48 crepant paths to $\mathrm{SU}(2) \times \mathrm{SU}(3)$

The compact simply connected semi-simple Lie groups with rank 2 or 3 are

$$\mathrm{SU}(2) \times \mathrm{SU}(2), \quad \mathrm{SU}(2) \times \mathrm{G}_2, \quad \mathrm{SU}(2) \times \mathrm{Sp}(4), \quad \text{and} \quad \mathrm{SU}(2) \times \mathrm{SU}(3).$$

The $\mathrm{SU}(2) \times \mathrm{SU}(2)$-, $\mathrm{SU}(2) \times \mathrm{G}_2$-, and $\mathrm{SU}(2) \times \mathrm{SU}(3)$-models could be realized by non-Higgsable clusters [240] as in [118, 119, 141]. There are subtleties in realizing an $\mathrm{SU}(3)$ as a non-Higgsable group

as discussed in Remark 12.2.1. The $\mathrm{SU}(2) \times \mathrm{SU}(2)$-model, the $\mathrm{SU}(2) \times \mathrm{G}_2$-model, and the $\mathrm{Sp}(4)$-model are studied respectively in [118], [119], and [121]. The individual $\mathrm{SU}(2)$ and $\mathrm{SU}(3)$-models are studied in [124, 125] and the $\mathrm{SU}(2)\times\mathrm{SU}(3)$-model (realized by the collision III+IV^s) has been studied from the point of view of string junctions in [141]. While the group $\mathrm{SU}(2) \times \mathrm{SU}(3)$ is famously the non-Abelian gauge sector of the Standard Model of particle physics [24, §2.4], the $\mathrm{SU}(2) \times \mathrm{SU}(3)$-model has never been constructed explicitly as a nonsingular variety.

The purpose of this chapter is to study the $\mathrm{SU}(2) \times \mathrm{SU}(3)$-model with associated Lie algebra

$$\mathrm{E}_3 = \mathrm{A}_1 \oplus \mathrm{A}_2.$$

We define elliptic fibrations with collisions of singularities corresponding to a Lie algebra of type E_3, we study their geometry and topology, and explore the physics of compactifications of M-theory and F-theory on such varieties when the elliptic fibration is a Calabi–Yau threefold. By definition, an $\mathrm{SU}(2) \times \mathrm{SU}(3)$-model is an elliptic fibration with a trivial Mordell–Weil group and a discriminant locus containing two irreducible smooth components S and T such that the generic fiber over S and T have respectively dual graphs of affine Dynkin type $\widetilde{\mathrm{A}}_1$ and $\widetilde{\mathrm{A}}_2$, while the Kodaira type of the fiber over the generic point of any other irreducible component of the discriminant locus is of type I_1 or II. The $\mathrm{SU}(2) \times \mathrm{SU}(3)$-models examined in this chapter are defined by singular Weierstrass models, given in Section 12.2, for which we construct explicit crepant resolutions in Section 12.3.1. Weierstrass models provide convenient canonical birational models for elliptic fibrations since any elliptic fibration over a smooth base is birational to a possibly singular Weierstrass model [94, 108,

246].

We show that there are six distinct types of *collisions of singularities* that define Weierstrass models for $\mathrm{SU}(2)\times\mathrm{SU}(3)$-models with crepant resolutions, namely:

$$\mathrm{I}_2^{\mathrm{s}}+\mathrm{I}_3^{\mathrm{s}},\quad \mathrm{I}_2^{\mathrm{ns}}+\mathrm{I}_3^{\mathrm{s}},\quad \mathrm{III}+\mathrm{I}_3^{\mathrm{s}},\quad \mathrm{I}_2^{\mathrm{s}}+\mathrm{IV}^{\mathrm{s}},\quad \mathrm{I}_2^{\mathrm{ns}}+\mathrm{IV}^{\mathrm{s}},\quad \mathrm{III}+\mathrm{IV}^{\mathrm{s}}.$$

We show that each of the corresponding Weierstrass models has eight distinct crepant resolutions.

These six $\mathrm{SU}(2)\times\mathrm{SU}(3)$-models are deformation of each other, where the deformations commute with the resolutions in a way such that the same eight sequences of three blowups are used for each of the six realizations of the $\mathrm{SU}(2)\times\mathrm{SU}(3)$-model. In total, we have a network of 48 distinct elliptic fibrations connected by deformations and flops. All the crepant resolutions of the $\mathrm{SU}(2)\times\mathrm{SU}(3)$-models are listed in Section (12.3.1).

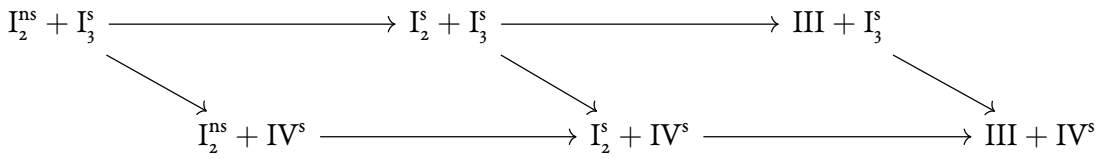

Figure 12.1: The six collisions of singularities that give Weierstrass models whose crepant resolutions are smooth $\mathrm{SU}(2)\times\mathrm{SU}(3)$-models. In this graph, each arrow indicates a specialization of a Weierstrass model to another. The only collision that correspond to a non-Higgsable model is $\mathrm{III}+\mathrm{IV}^{\mathrm{s}}$.

12.1 Summary and organization of this chapter

12.1.1 Matter representation and connection to the Standard Model

The gauge group of the $\mathrm{SU}(2)\times\mathrm{SU}(3)$-model is the non-Abelian sector of the Standard Model of particle physics [24, §2.4]. In this chapter, we consider this gauge theory in the context of five and six-dimensional supergravity theories with minimal supersymmetry resulting from a compactification of M-theory or F-theory on a Calabi–Yau threefold Y that corresponds to an elliptic fibration giving an $\mathrm{SU}(2)\times\mathrm{SU}(3)$-model. The representation $\mathbf{R}$ of the resulting 5d and 6d theory is reminiscent of the representations of fermions of the Standard Model once we ignore the Abelian sector.

The weights of vertical curves over codimension-one loci of the discriminant locus determine a representation $\mathbf{R}$ of $\mathfrak{g}$ called the *matter representation*. See [112] and reference therein for details on Weierstrass models, weights of curves, dual graphs, and G-models. We show that $\mathrm{SU}(2)\times\mathrm{SU}(3)$-models, defined over a base of dimension-two or higher, have vertical rational curves carrying the weights of the following quaternionic representation $\mathbf{R}$ reminiscent of the representation $\mathbf{F}$ of fermions of the Standard Model transforming non-trivially under $\mathrm{SU}(2)\times\mathrm{SU}(3)$:

$$\mathbf{R} = (2,1)\oplus(1,3)\oplus(1,\overline{3})\oplus(2,3)\oplus(2,\overline{3})\oplus(3,1)\oplus(1,8),$$

$$\mathbf{F} = (2,1)\oplus(1,3)\oplus(1,\overline{3})\oplus(2,3)\oplus(2,\overline{3}),$$

where $(\mathbf{r}_1,\mathbf{r}_2)$ is the product of the representation $\mathbf{r}_1$ of the Lie algebra of type A_1 and the representation $\mathbf{r}_2$ of A_2, and $\overline{\mathbf{r}}$ is the complex conjugate representation of $\mathbf{r}$. In particular, $(3,1)$ is the adjoint

representation of A_1, $(1, 8)$ is the adjoint representation of A_2, $(2, 1)$ is the fundamental representation of A_1, $(1, 3)$ is the fundamental representation of A_2, and $(2, 3)$ is the bifundamental representation of $A_1 \oplus A_2$.

In the Standard Model, left-handed leptons transform in the representation $(2, 1)$ of $SU(2) \times SU(3)$, left-handed quarks transform in the representation $(2, 3)$, and right-handed up and down quarks transform in the representation $(1, 3)$. Right-handed leptons are neutral under $SU(2) \times SU(3)$ in the Standard Model, and we also have $n_H^\circ = h^{2,1}(Y) + 1$ neutral hypermultiplets in the $SU(2) \times SU(3)$-model (see equation (12.86)).

There are also differences: the $SU(2) \times SU(3)$-model has hypermultiplets transforming under the adjoints representations $(3, 1)$ and $(1, 8)$ while the Standard Model does not have fermions transforming in adjoint representations.

12.1.2 Geography of crepant resolutions of G-models and $\mathrm{I}(\mathfrak{g}, \mathbf{R})$ hyperplane arrangements

A crepant resolution is a resolution of singularities that preserves the canonical class. In the case of surfaces, a crepant resolution is necessarily unique and always exists for du Val singularities. Starting from dimension-three, crepant resolutions (when they exist) are not necessarily unique. For normal threefolds with canonical singularities, the number of crepant resolutions is finite [191] and two crepant resolutions are connected by flops [190]. A substitute for crepant resolutions are terminal varieties and they always exist for varieties with canonical singularities [42]. In light of the result of Kawamata [190], it follows from the celebrated results of [42] that minimal models are connected

by flops. $\mathbb{Q}$-factorial terminal singularities are obstructions to the existence of crepant resolutions as $\mathbb{Q}$-factoriality implies that the exceptional set of any birational map is a divisor, and being terminal implies that all the discrepancies are positive [172]. Canonical singularities, $\mathbb{Q}$-factorial singularities, terminal singularities, crepant resolutions, and flops are defined for example in [202, 228].

For G-models, the geography of flops can be described by the hyperplane arrangement $\mathrm{I}(\mathfrak{g}, \mathbf{R})$ defined inside the dual fundamental Weyl chamber of $\mathfrak{g}$ and whose hyperplanes are the kernel of the weights of the representation $\mathbf{R}$ [110, 111, 163]. In stringy geometry, this is a conjecture motivated by the structure of the Coulomb branches of a five-dimensional $\mathcal{N} = 1$ supergravity theory with a gauge group G and matter transforming in the representation $\mathbf{R}$ [176]. As each Coulomb phase corresponds to a unique crepant resolution of the Weierstrass model, flops corresponds to phase transitions [306], and the different Coulomb phases correspond to the different connected domains in which the prepotential is differentiable; the study of the structure of the 5d Coulomb branches boils down to identifying the chambers of a hyperplane arrangement (see Section 12.7.1). Mathematically, this fact can be understood by subdivision of a relative movable cone of any of the crepant resolution over the Weierstrass model of a G-model into nef cones of each particular crepant resolution in the spirit of [188, 189, 227] and [228, Theorem 12-2-7].

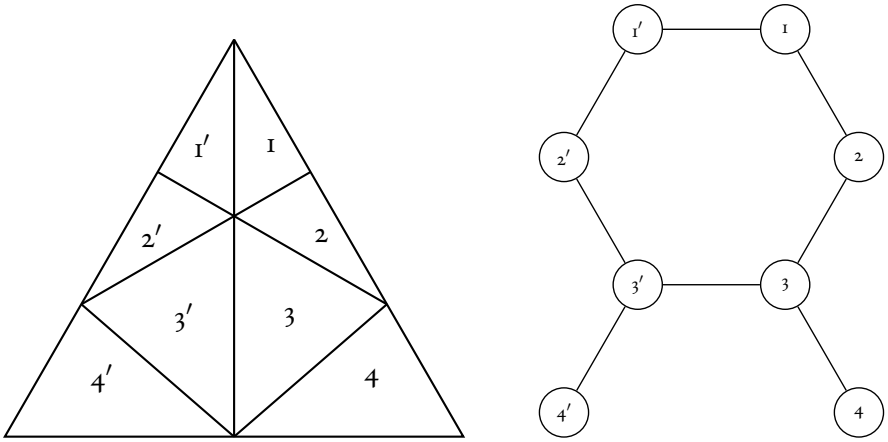

Figure 12.2: The chamber structure of $\mathrm{I}(\mathrm{E}_3 = \mathrm{A}_1 \oplus \mathrm{A}_2, (1,3) \oplus (2,3))$ and its adjacency graph. This also represents the structure of the extended Kähler cone of an $\mathrm{SU}(2) \times \mathrm{SU}(3)$-model. See Figure 12.3 for more details on the walls separating the chambers.

The network of flops of the $\mathrm{SU}(2) \times \mathrm{SU}(3)$-model matches the hyperplane arrangement $\mathrm{I}(\mathrm{E}_3 = \mathrm{A}_1 \oplus \mathrm{A}_2, (1,3) \oplus (2,3))$, where $(1,3) \oplus (2,3)$ is the direct sum of the bifundamental representation of $\mathrm{SU}(2) \times \mathrm{SU}(3)$ and the fundamental representation of $\mathrm{SU}(3)$. The chamber structure of this hyperplane arrangement is represented in Figure 12.2.

12.1.3 Topological invariants

The Euler characteristic of the elliptically-fibered Calabi–Yau threefold Y is instrumental in the discussion of the gravitational anomalies of the six-dimensional supergravity theory when F-theory is compactified on such Y [142]. The Hodge numbers of Y determines the number of vector multiplets and neutral hypermultiplets in an M-theory compactification on Y [66]. In the case of Calabi–Yau fourfolds, the Euler characteristic is relevant to the cancellation of the D3-brane tadpole [5, 6, 78, 279]. The triple intersection numbers of divisors of a Calabi–Yau threefold Y give the Chern–

Simons terms of an M-theory compactification on Y.

While the Euler characteristic and the Betti numbers, are independent of the choice of a crepant resolution as shown by Batyrev [29], the triple intersection numbers are not preserved by flops and depend on a choice of a crepant resolution [176]. We compute the Euler characteristic of an $\mathrm{SU}(2) \times \mathrm{SU}(3)$-model over a base of arbitrary dimension in Theorem 12.3.2 in the spirit of [114, 116, 117]. Denoting by B the base of the fibration, by S and T the divisors supporting respectively the fiber with dual graphs $\widetilde{\mathrm{A}}_1$ and $\widetilde{\mathrm{A}}_2$, and by L the first Chern class of the line bundle $\mathscr{L}$ of the Weierstrass model (see Theorem 5.0.4), we have

$$\chi(Y) = 6 \, \frac{S^2 - 2L - 3SL + 2(S^2 - 3SL + S - 2L)T + (3S + 2)T^2}{(1 + S)(1 + T)(-1 - 6L + 2S + 3T)} \, c(TB).$$

We also determine the Hodge numbers of an $\mathrm{SU}(2) \times \mathrm{SU}(3)$-model and the triple intersection numbers in the case of the Calabi–Yau threefolds. Since the triple intersection numbers depend on a choice of a resolution, we compute them for each of the crepant resolutions in Theorem 12.3.3.

$$h^{1,1}(Y) = 14 - K^2, \quad h^{2,1}(Y) = 29K^2 + 15KS + 24KT + 3S^2 + 6ST + 6T^2 + 14,$$

where K is the canonical class of the base B.

12.1.4 Compactification of M-theory to $5d$ $\mathcal{N} = 1$ supergravity

We analyze the physics of the compactifications of M-theory and F-theory on elliptically-fibered Calabi–Yau threefolds corresponding to $\mathrm{SU}(2) \times \mathrm{SU}(3)$-models. These give five and six-dimensional

gauge theories coupled to supergravity theories with eight supercharges respectively. For the five-dimensional supergravity theory, we compute the one-loop prepotential in the Coulomb branch (see Theorem 12.7.1), and determine the Chern–Simons couplings, the number of vector multiplets, tensor multiplets, and hypermultiplets. The Chern–Simons couplings are computed geometrically as triple intersection numbers of fibral divisors in each Coulomb chamber (see Theorem 12.3.8).

The Chern–Simons levels are given by triple intersection numbers of divisors of the Calabi–Yau threefolds and determine the prepotential of a five-dimensional supergravity theory from an M-theory compactification on such Calabi–Yau threefolds [66]. Using such relation, we match the triple intersection polynomial with the one-loop prepotential in each Coulomb chamber to obtain constraints on the number of charged hypermultiplets (see equation (12.75)). In many cases, such a method will completely fix the number of multiplets [112, 115, 118, 121, 124]; however for the $\mathrm{SU}(2) \times \mathrm{SU}(3)$-model, we get linear constraints that does not fully determine the number of multiplets.[1] However, they can completely be fixed by using Witten's genus formula, which is a five-dimensional result. In the five-dimensional theory, we also determine the structure of the Coulomb chambers. Each chamber corresponds to a specific crepant resolution that we determine explicitly.

If we denote the number of hypermultiplets transforming in the irreducible representation $\mathbf{R}$ as $n_{\mathbf{R}}$ and denote the curve supporting the gauge group SU(2) and SU(3) by S and T respectively, and

[1] When we consider a model with a semisimple Lie algebra and a trivial Mordell–Weil group, we always get linear constraints that does not fully determine the number of multiplets by matching the prepotential and the triple intersection polynomial [118, 118, 119, 121].

write K for the canonical class of the base of the elliptic threefold,[2] we have:

$$n_{3,1} = \frac{1}{2}(K \cdot S + S^2 + 2), \qquad n_{1,8} = \frac{1}{2}(K \cdot T + T^2 + 2),$$

$$n_{2,1} = -S \cdot (8K + 2S + 3T), \qquad n_{1,3} + n_{1,\bar{3}} = -T \cdot (9K + 3T + 2S), \qquad n_{2,3} + n_{2,\bar{3}} = S \cdot T.$$

Interpreting the number of charged hypermultiplets with the genus of the supporting curves of S and T, denoted as $g(S)$ and $g(T)$ respectively, we get

$$n_{3,1} = g(S), \qquad n_{1,8} = g(T),$$

$$n_{2,1} = 16(1 - g(S)) + 6S^2 - 3S \cdot T, \qquad n_{1,3} + n_{1,\bar{3}} = 18(1 - g(T)) + 6T^2 - 2S \cdot T, \quad n_{2,3} \quad + n_{2,\bar{3}} = S \cdot T.$$

12.1.5 Compactification of F-theory to $6d\ \mathcal{N} = (1, 0)$ supergravity and cancellation of anomalies

We also study in detail the anomaly cancellations of the six-dimensional theory. Considering the set of equations from requiring the local anomalies in the six-dimensional theory to cancel, we determine the unique solution of the number of charged hypermultiplets in each irreducible representation. Using Sadov's techniques [269], we check that anomalies are canceled explicitly by the Green-Schwarz mechanism. The number of hypermultiplets in each irreducible representations for an anomaly-free six-dimensional theory matches with those we get from the five-dimensional theories (see Section 12.7.2 for the discussion). This ensures that the five-dimensional theory can be

[2] The genus $g(S)$ of a supporting curve of S in a surface of canonical class K satisfies $2-2g(S) = -S\cdot K - S^2$. The same holds for the case of T as well.

uplifted to an anomaly-free six-dimensional theory.

Furthermore, in this chapter we show that the matter content of the 6d gauge theory is anomaly-free. This theory can be still anomaly-free after an additional compactification on a Riemann surface to four-dimensions if we impose the condition $n_3 = n_{\bar{3}}$, which will naturally follow from the CPT condition. For local gauge anomalies in four-dimensional spacetime, SU(2) is always anomaly-free as all its representation are (pseudo)-real whereas the triangle diagram of SU(3) is anomaly-free only when the number of matter transforming in the 3 and $\bar{3}$ are equal to each other, which will naturally be satisfied if the CPT invariance is respected.

For global anomalies in four spacetime dimensions, one has to worry about SU(2) as it is subject to Witten anomaly [303]. This is a direct consequence of the fact that the fourth homotopy group for SU(N) is zero for N greater than two whereas for SU(2) it is a $\mathbb{Z}_2$. Thus, Witten anomalies from SU(2) only vanishes when there is an even number of SU(2) doublet. Similarly, the global anomaly contributions from SU(2) and SU(3) in six-dimensions can be discussed by looking into the sixth homotopy group for SU(2) and SU(3), which are given by $\mathbb{Z}_{12}$ and $\mathbb{Z}_6$ respectively. Bershadsky and Vafa has shown that this yields the linear constraints on the number of hypermultiplets [40]. Considering these conditions only give a constraint on the genus of the curve S supporting the SU(2) group: $g(S) = 0 \mod 3$, as derived in Section 12.7.2.

12.1.6 Organization of this chapter

The rest of the chapter is structured as follows. In Section 12.2, we introduce the possible collisions of fibers that produce SU(2) $\times$ SU(3)-models and define their Weierstrass models. In Section 12.3,

we describe the eight crepant resolutions of each of the six Weierstrass models introduced in Section 12.2. We also compute the Euler characteristic of the crepant resolutions and the triple intersection of the fibral divisors. In the case of Calabi–Yau threefolds, we also compute the Hodge numbers. In Section 12.4, we discuss the matter representations of the five and six-dimensional supergravity theories with a gauge group $\mathrm{SU}(2)\times\mathrm{SU}(3)$, compute the adjacency graph of the hyperplane arrangement associated with an $\mathrm{SU}(2)\times\mathrm{SU}(3)$-model, and match the structure of the hyperplane arrangement with the flopping curves of the crepant resolutions. In Sections 12.5 and 12.6, we study in detail the crepant resolutions of the $\mathrm{I}_2^{\mathrm{s}}+\mathrm{I}_3^{\mathrm{s}}$-models and the $\mathrm{III}+\mathrm{IV}^{\mathrm{s}}$-models respectively. In Section 12.7, we study the consequences of our geometric results for the physics of F-theory and M-theory compactified on an $\mathrm{SU}(2)\times\mathrm{SU}(3)$-model. We first explain the number of multiplets of the five-dimensional theory using geometric data. We further derive the unique number of charged hypers in each irreducible representations in the uplifted six-dimensional theory canceling the local anomalies and show that it matches that of the five-dimensional theory. We also study the gobal anomaly contributions of the gauge group $\mathrm{SU}(2)\times\mathrm{SU}(3)$[40].

12.2 The many faces of the $\mathrm{SU}(2)\times\mathrm{SU}(3)$-model

In algebraic geometry, the notion of an irreducible variety depends on the choice of the underlying field. A variety is said to be *geometrically irreducible* when it stays irreducible after any field extension. Kodaira has introduced symbols to classify the type of the singular fibers of a minimal elliptic surface [200]. Kodaira symbols can be used more generally to classify the geometric fibers over

generic points of the discriminant locus of an elliptic fibration of arbitrary dimension. The types of the fibers over generic points of the discriminant locus of an elliptic fibration are classified by decorated Kodaira fibers, as the Kodaira type classifies only the geometric fiber [108, §7.4.2]. The decoration tracks the minimal field extension under which all fiber components of the generic fiber become geometrically irreducible. Following [37], we use the decoration *non-split* ("ns"), *semi-split* ("ss"), and *split* ("s"). The fibers of type I_1, II, III, II*, and III* are always well-defined without the need of a field extension. The fiber of type I_n ($n \geq 2$), IV, IV*, and I_n^* can be split or non-split. The Kodaira fiber of type I_0^* can come from three distinct type: I_0^{*s}, I_0^{*ss}, and I_0^{*ns} with respective dual graphs $\widetilde{\mathrm{D}}_4$, $\widetilde{\mathrm{B}}_3$, and $\widetilde{\mathrm{G}}_2$. The fiber I_0^{*ns} comes in two types as the minimal field extension can be the cyclic group $\mathbb{Z}_3$ or the permutation group of three elements S_3 [112].

There is a subtlety about the fiber I_2: the fiber $\mathrm{I}_2^{\mathrm{s}}$ and $\mathrm{I}_2^{\mathrm{ns}}$ both have two geometrically irreducible components intersecting at two geometric points forming a divisor of degree two on the curve. The fiber $\mathrm{I}_2^{\mathrm{ns}}$ corresponds to the case where the two distinct points are well defined defined only after a a quadratic field extension while the fiber of type $\mathrm{I}_2^{\mathrm{s}}$ does not require a field extension to define the two points of intersection.

There are several inequivalent decorated Kodaira fibers that have the same dual graph. The $\mathrm{SU}(2) \times \mathrm{SU}(3)$-model involves the only two root systems that are dual graphs of several distinct Kodaira fibers. The dual graph of type $\widetilde{\mathrm{A}}_1$ is shared by two different Kodaira fibers, while there are five different Kodaira fibers with the dual graph $\widetilde{\mathrm{A}}_2$, which is presented in Table 12.1.

Fibers	Dual graph
$\mathrm{I}_2^{\mathrm{s}}$, $\mathrm{I}_2^{\mathrm{ns}}$, $\mathrm{I}_3^{\mathrm{ns}}$, III, $\mathrm{IV}^{\mathrm{ns}}$	$\widetilde{\mathrm{A}}_1$
$\mathrm{I}_3^{\mathrm{s}}$, IV^{s}	$\widetilde{\mathrm{A}}_2$

Table 12.1: Decorated Kodaira fibers with dual graph of $\widetilde{\mathrm{A}}_1$ or $\widetilde{\mathrm{A}}_2$.

The affine root system $\widetilde{\mathrm{A}}_1 \oplus \widetilde{\mathrm{A}}_2$ is the dual graph of ten different pairs of decorated Kodaira fibers. It follows that there are ten distinct ways to realize an $\mathrm{SU}(2) \times \mathrm{SU}(3)$-model. Using Tate's algorithm, we realize these collisions as singular Weierstrass models by introducing specific valuations of the coefficients with respect to the divisors over which the singular fibers are defined. The minimal multiplicities for the coefficients a_i are reproduced in Table 12.2.

	a_1	a_2	a_3	a_4	a_6	Δ
$\mathrm{I}_2^{\mathrm{s}}$	0	1	1	1	2	2
$\mathrm{I}_2^{\mathrm{ns}}$	0	0	1	1	2	2
$\mathrm{I}_3^{\mathrm{ns}}$	0	0	2	2	3	3
III	1	1	1	1	2	3
$\mathrm{IV}^{\mathrm{ns}}$	1	1	1	2	2	4
$\mathrm{I}_3^{\mathrm{s}}$	0	1	1	2	3	3
IV^{s}	1	1	1	2	3	4

Table 12.2: Valuations of the coefficients of the Weierstrass models used in this chapter for the Kodaira fibers of type $\mathrm{I}_2^{\mathrm{s}}$, $\mathrm{I}_2^{\mathrm{ns}}$, $\mathrm{I}_3^{\mathrm{ns}}$, III, $\mathrm{IV}^{\mathrm{ns}}$, $\mathrm{I}_3^{\mathrm{s}}$, and IV^{s} to define SU(2) and SU(3)-models [37, 108, 186, 290]. The valuation of the discriminant Δ follows from the other valuations.

However, not all corresponding Weierstrass models have a crepant resolution. In this chapter, we

only consider those Weierstrass models that have crepant resolutions. In particular, we do not use $\mathrm{I}_3^{\mathrm{ns}}$ or $\mathrm{IV}^{\mathrm{ns}}$ to realize $\widetilde{\mathrm{A}}_1$, as the Kodaira fibers of type $\mathrm{I}_3^{\mathrm{ns}}$ and $\mathrm{IV}^{\mathrm{ns}}$ have $\mathbb{Q}$-factorial terminal singularities. Such singularities are obstructions for the existence of crepant resolutions[3] (this follows, for example, from [42, Lemma 3.6.2]). Thus, we consider only the following six cases of collisions:

$$\mathrm{I}_2^{\mathrm{s}} + \mathrm{I}_3^{\mathrm{s}}, \quad \mathrm{I}_2^{\mathrm{ns}} + \mathrm{I}_3^{\mathrm{s}}, \quad \mathrm{III} + \mathrm{I}_3^{\mathrm{s}}, \quad \mathrm{I}_2^{\mathrm{s}} + \mathrm{IV}^{\mathrm{s}}, \quad \mathrm{I}_2^{\mathrm{ns}} + \mathrm{IV}^{\mathrm{s}}, \quad \mathrm{III} + \mathrm{IV}^{\mathrm{s}}.$$

The corresponding Weierstrass models are listed in equation (12.1):

$$\begin{aligned}
\mathrm{I}_2^{\mathrm{ns}} + \mathrm{I}_3^{\mathrm{s}} : &\quad y(y + a_1 x + \widetilde{a}_3 st) = x^3 + \widetilde{a}_2 t x^2 + \widetilde{a}_4 s t^2 x + \widetilde{a}_6 s^2 t^3, \\
\mathrm{I}_2^{\mathrm{s}} + \mathrm{I}_3^{\mathrm{s}} : &\quad y(y + a_1 x + \widetilde{a}_3 st) = x^3 + \widetilde{a}_2 s t x^2 + \widetilde{a}_4 s t^2 x + \widetilde{a}_6 s^2 t^3, \\
\mathrm{I}_2^{\mathrm{s}} + \mathrm{IV}^{\mathrm{s}} : &\quad y(y + \widetilde{a}_1 t x + \widetilde{a}_3 st) = x^3 + \widetilde{a}_2 s t x^2 + \widetilde{a}_4 s t^2 x + \widetilde{a}_6 s^2 t^3, \\
\mathrm{I}_2^{\mathrm{ns}} + \mathrm{IV}^{\mathrm{s}} : &\quad y(y + \widetilde{a}_1 t x + \widetilde{a}_3 st) = x^3 + \widetilde{a}_2 t x^2 + \widetilde{a}_4 s t^2 x + \widetilde{a}_6 s^2 t^3, \\
\mathrm{III} + \mathrm{I}_3^{\mathrm{s}} : &\quad y(y + \widetilde{a}_1 s x + \widetilde{a}_3 st) = x^3 + \widetilde{a}_2 s t x^2 + \widetilde{a}_4 s t^2 x + \widetilde{a}_6 s^2 t^3, \\
\mathrm{III} + \mathrm{IV}^{\mathrm{s}} : &\quad y(y + \widetilde{a}_1 s t x + \widetilde{a}_3 st) = x^3 + \widetilde{a}_2 s t x^2 + \widetilde{a}_4 s t^2 x + \widetilde{a}_6 s^2 t^3.
\end{aligned} \tag{12.1}$$

We assume that the coefficients a_1 and $\widetilde{a}_i$ ($i = 1, 2, 3, 4, 6$) are algebraically independent and $S = V(s)$ and $T = V(t)$ are smooth divisors intersecting transversally. The variables s (resp. t) is a section of the normal bundle of the divisor S (resp. T). In each case, the Kodaira fiber over the generic point of S (resp. T) has a dual graph of type $\widetilde{\mathrm{A}}_1$ (resp. $\widetilde{\mathrm{A}}_2$). The difference between these models are the

[3] The possible physical relevance of $\mathbb{Q}$-factorial terminal singularities in F-theory is explored in [17, 145].

valuations of the Weierstrass coefficients a_1 and a_2 with respect to S and T, which are listed in Table 12.2. The discriminant locus of each Weierstrass model is given by

$$\Delta = s^{2+a}t^{3+b}(\cdots),$$

where a is related to $S = V(s)$ and b to $T = V(t)$, $a = 0$ for Kodaira fibers of types $\mathrm{I}_2^{\mathrm{s}}$ and $\mathrm{I}_2^{\mathrm{ns}}$, $a = 1$ for Kodaira fibers of type III, $b = 0$ for Kodaira fibers of type $\mathrm{I}_3^{\mathrm{s}}$, and $b = 1$ for Kodaira fibers of type IV^{s}. We observe that the reduced discriminant locus is composed of three irreducible components. The fiber degenerates further at the intersection of these three components and we study them to determine the type of matter.

Remark 12.2.1. As seen on Table 12.2, the fiber IV^{s} becomes the fiber $\mathrm{IV}^{\mathrm{ns}}$ when the Weierstrass coefficient a_6 is deformed by a term of valuation two. Such a deformation does not commute with the resolution and changes the gauge group from SU(3) to SU(2). However, the resulting SU(2) has $\mathbb{Q}$-factorial terminal singularities. Moreover, these groups SU(2) and SU(3) coming from fibers $\mathrm{IV}^{\mathrm{ns}}$ and IV^{s} are strongly coupled and related to Argyres-Douglas theories [16, 244], both give in the weak coupling limit of type IIB string theory an SO(6) gauge theory [123]. The non-Higgsable group corresponding to a fiber of type IV is SU(2) as generically a fiber of type IV is a $\mathrm{IV}^{\mathrm{ns}}$. A non-Higgsable model of type IV^{s} will require a very particular setting to avoid the existence of a deformation to the fiber $\mathrm{IV}^{\mathrm{ns}}$ as it will break the gauge group from SU(3) to SU(2).

12.3 Geometry

In this section, we collect the geometric data – crepant resolutions, Euler characteristic, Hodge numbers, triple intersection numbers– of the $\mathrm{SU}(2) \times \mathrm{SU}(3)$-models. In Section 12.3.1, we present eight sequences of blowups that each give crepant resolutions of all six Weierstrass models from equation (12.1). In total, this results in 48 distinct $\mathrm{SU}(2)\times\mathrm{SU}(3)$-models. Since two smooth n-dimensional projective algebraic variety over $\mathbb{C}$ connected by a crepant birational map have the same Betti numbers [29, Theorem 4.2], all the crepant resolutions of Weierstrass models of an $\mathrm{SU}(2)\times\mathrm{SU}(3)$-model have the same Euler characteristic. In Section 12.3.2, we give a generating function for the Euler characteristic of an $\mathrm{SU}(2) \times \mathrm{SU}(3)$-model. In the case of Calabi–Yau threefolds, we also compute the Hodge numbers of the $\mathrm{SU}(2) \times \mathrm{SU}(3)$-models. In the case of a threefold, we also compute the Hodge numbers and the triple intersection numbers in Section 12.3.3. In Section 12.3.4, we discuss the various non-Kodaira fibers obtain from the resolutions of the $\mathrm{SU}(2)\times\mathrm{SU}(3)$-models, we summarize them in Table 12.3.

12.3.1 Crepant resolutions

We use the following convention. Let X be a nonsingular variety. Let $Z \subset X$ be a complete intersection defined by the transverse intersection of r hypersurfaces $Z_i = V(g_i)$, where g_i is a section of the line bundle $\mathscr{I}_i$ and $(g_1, \cdots, g_r)$ is a regular sequence. We denote the blowup of a nonsingular

variety X along the complete intersection Z by

$$X \xleftarrow{(g_1, \cdots, g_r | e_1)} \widetilde{X}.$$

The exceptional divisor is $E_1 = V(e_1)$. We abuse notation and use the same symbols for x, y, s, e_i and their successive proper transforms. We also do not write the obvious pullbacks.

Assuming some mild regularity conditions on the coefficients of the Weierstrass equations, each of the following eight sequences of blowups gives a different crepant resolution of any of the $\mathrm{SU}(2) \times \mathrm{SU}(3)$-model given by the Weierstrass models in equation (12.1):

$$\begin{aligned}
\text{Resolution I}: &\quad X_0 \xleftarrow{(x,y,s|e_1)} X_1 \xleftarrow{(x,y,t|w_1)} X_2 \xleftarrow{(y,w_1|w_2)} X_3 \ , \\
\text{Resolution II}: &\quad X_0 \xleftarrow{(x,y,p_0|p_1)} X_1 \xleftarrow{(y,p_1,t|w_1)} X_2 \xleftarrow{(p_0,t|w_2)} X_3 \ , \\
\text{Resolution III}: &\quad X_0 \xleftarrow{(x,y,t|w_1)} X_1 \xleftarrow{(x,y,s|e_1)} X_2 \xleftarrow{(y,w_1|w_2)} X_3 \ , \\
\text{Resolution IV}: &\quad X_0 \xleftarrow{(x,y,t|w_1)} X_1 \xleftarrow{(y,w_1|w_2)} X_2 \xleftarrow{(x,y,s|e_1)} X_3 \ , \\
\text{Resolution I}': &\quad X_0 \xleftarrow{(x,q,s|e_1)} X_1 \xleftarrow{(x,q,t|w_1)} X_2 \xleftarrow{(q,w_1|w_2)} X_3 \ , \\
\text{Resolution II}': &\quad X_0 \xleftarrow{(x,q,p_0|p_1)} X_1 \xleftarrow{(q,p_1,t|w_1)} X_2 \xleftarrow{(p_0,t|w_2)} X_3 \ , \\
\text{Resolution III}': &\quad X_0 \xleftarrow{(x,q,t|w_1)} X_1 \xleftarrow{(x,q,s|e_1)} X_2 \xleftarrow{(q,w_1|w_2)} X_3 \ , \\
\text{Resolution IV}': &\quad X_0 \xleftarrow{(x,q,t|w_1)} X_1 \xleftarrow{(q,w_1|w_2)} X_2 \xleftarrow{(x,q,s|e_1)} X_3 \ ,
\end{aligned} \tag{12.2}$$

where $q = y + a_1 x + a_3$ and $p_0 = st$.

We observe that the sequences of blowups that define the first four resolutions are exactly the same as the sequence of blowups that define the resolutions of the $\mathrm{SU}(2) \times \mathrm{G}_2$-model [119].

The birational map connecting the resolution I to I′ (resp. II to II′, III to III′, and IV to IV′) is induced by the involution $\sigma : [x : y : z] \to [-q : x : z]$ of the Weierstrass model. Fiberwise, the involution σ is the inverse map of the Mordell–Weil group: it maps a point P to its opposite $-P$ with respect to the Mordell–Weil group law. This is familiar from [125, 127, 129]. The birational maps induced by σ are *pseudo-isomorphisms* of the crepant resolutions over the Weierstrass model, as they are isomorphisms in codimension-one.

With the exceptions of resolutions II and II', all of the resolutions are defined by sequences of blowups around centers that are smooth, complete intersections. The resolutions II and II′ are also defined by a sequence of blowups; however, one of the blowups does not have a smooth center but still defines a regular sequence. Fortunately, this condition is enough to use the pushforward theorems and compute the topological invariants as in the other cases.

12.3.2 Euler characteristics and Hodge numbers

When an elliptic fibration is defined by the resolution of a singular Weierstrass model by a sequence of blowups with smooth centers defining regular embeddings, there are powerful pushforward theorems to compute its Euler characteristic in few simple algebraic manipulations [114].

Remark 12.3.1. All the Weierstrass models of the $\mathrm{SU}(2)\times\mathrm{SU}(3)$-models and the $\mathrm{SU}(2)\times\mathrm{G}_2$-models [119] share four crepant resolutions that are given by the same sequences of blowups (Resolutions I,

II, III, and IV). Hence, the $\mathrm{SU}(2)\times\mathrm{SU}(3)$-model for a choice of $(B, S, T, \mathscr{L})$ and the $\mathrm{SU}(2)\times\mathrm{G}_2$-model defined with the same choice of $(B, S, T, \mathscr{L})$, have the same the same Euler characteristics as formal expressions in S, T, L, $c(TB)$. Likewise, since $\mathrm{SU}(2)\times\mathrm{SU}(3)$ and $\mathrm{SU}(2)\times\mathrm{G}_2$ have the same rank, their Hodge numbers are also identical in the Calabi–Yau threefold case.

Theorem 12.3.2. *The generating polynomial of the Euler characteristic of an $SU(2)\times SU(3)$-model obtained by a crepant resolution of a Weierstrass model given in Section 12.3.1:*

$$\chi(Y) = 6\,\frac{S^2 - 2L - 3SL + 2(S^2 - 3SL + S - 2L)T + (3S+2)T^2}{(1+S)(1+T)(-1-6L+2S+3T)}\,c(TB).$$

Proof. See [119, Theorem 2.5]. □

By direct expansion and specialization, we have the following three lemmas [119]:

Lemma 12.3.3. *For an elliptic threefold, the Euler characteristic is*

$$\chi(Y_3) = -6(-2c_1L + 12L^2 + S^2 - 5SL + 2ST - 8LT + 2T^2).$$

Lemma 12.3.4. *In the case of a Calabi–Yau threefold, by applying $c_1 = L = -K$, we have*

$$\chi(Y_3) = -6(10K^2 + S^2 + 5SK + 2ST + 8KT + 2T^2).$$

Lemma 12.3.5. *The Euler characteristic for an elliptic fourfold is given by*

$$\chi(Y_4) = -6\,(-2c_2L - 72L^3 + 12c_1L^2 + c_1S^2 - 5c_1SL + 2c_1ST - 8c_1LT + 2c_1T^2 \\ +S^3 - 15S^2L + 6S^2T + 54SL^2 - 44SLT + 9ST^2 + 84L^2T - 34LT^2 + 4T^3)\,.$$

Lemma 12.3.6. *The same Calabi–Yau condition $c_1 = L = -K$ is applied to get the Euler characteristic for a Calabi–Yau fourfold:*

$$\chi(Y_4) = -6\,(2c_2K + 60K^3 + S^3 + 14S^2K + 6S^2T + 49SK^2 + 42SKT \\ +9ST^2 + 76K^2T + 32KT^2 + 4T^3)\,.$$

Theorem 12.3.7. *In the Calabi–Yau case, the Hodge numbers of an $SU(2)\times SU(3)$-model given by the crepant resolution of a Weierstrass model given in Section 12.3.1 are*

$$h^{1,1}(Y) = 14 - K^2, \quad h^{2,1}(Y) = 29K^2 + 15KS + 24KT + 3S^2 + 6ST + 6T^2 + 14.$$

Proof. See [119, Theorem 2.10]. □

12.3.3 Triple intersection numbers

Let Y be a crepant resolution of an $\mathrm{SU}(2)\times\mathrm{SU}(3)$-model defined by one of the crepant resolutions $f\colon Y \to Y_0$ given in Section 12.3.1. Assuming that Y is a threefold, the triple intersection polynomial of Y is a polynomial containing the divisors $(D_a \cdot D_b \cdot D_c) \cap [Y]$. We express a triple intersection polynomial of the $\mathrm{SU}(2)\times\mathrm{SU}(3)$-model as a polynomial in ψ_0, ψ_1, φ_0, φ_1, and φ_2 that couples re-

spectively with the fibral divisors D^s_0, D^s_1, D^t_0, D^t_1, and D^t_2. The pushforward is expressed in the base by pushing forward to the Chow ring of X_0 and then to the base B. We recall that $\pi : X_0 \to B$ is the projective bundle in which the Weierstrass model is defined. Then,

$$\begin{aligned}\mathscr{F}_{trip} &= \int_Y \left[\left(\psi_0 D^s_0 + \psi_1 D^s_1 + \varphi_0 D^t_0 + \varphi_1 D^t_1 + \varphi_2 D^t_2\right)^3\right] \\ &= \int_B \pi_* f_* \left[\left(\psi_0 D^s_0 + \psi_1 D^s_1 + \varphi_0 D^t_0 + \varphi_1 D^t_1 + \varphi_2 D^t_2\right)^3\right].\end{aligned} \tag{12.3}$$

Once the classes of the fibral divisors are determined, all that is left is to compute the pushforward to the base B using the pushforward theorems of Section 2.7.

Theorem 12.3.8. *The triple intersection polynomial of an $SU(2)\times SU(3)$-model defined by the crepant resolutions in Section 12.3.1 is*

- *Resolution I:*

$$\begin{aligned}\mathscr{F}^{(I)}_{trip} = &-2S(2L+S)\psi_1^3 - 6ST\psi_1\left(\varphi_1^2 - \varphi_2\varphi_1 + \varphi_2^2\right) - 4T(T-L)\varphi_1^3 \\ &- 3T(5L-S-2T)\varphi_1^2\varphi_2 - 3T(-4L+S+T)\varphi_1\varphi_2^2 - T(5L-2S+T)\varphi_2^3 \\ &+ 4S(L-S)\psi_0^3 + 6S(S-2L)\psi_0^2\psi_1 + 12LS\psi_0\psi_1^2 \\ &- 2T\varphi_0^3(-2L+S+2T) + \varphi_0^2\left(3T\left(\varphi_1+\varphi_2\right)(-2L+S+T) - 6ST\psi_1\right) \\ &+ 3T\varphi_0\left(2\varphi_1\left(L\varphi_2 + S\psi_1\right) + \varphi_1^2(L-S) + \varphi_2^2(L-S) - 2S\left(\psi_0-\psi_1\right)^2 + 2S\psi_1\varphi_2\right)\end{aligned}$$

- *Resolution II:*

$$\begin{aligned}\mathscr{F}^{(II)}_{trip} =& -S(4L+2S-T)\psi_1^3+3T(-5L+S+2T)\varphi_1^2\varphi_2-3T(-4L+S+T)\varphi_1\varphi_2^2\\&+4T(L-T)\varphi_1^3+T(-5L+S-T)\varphi_2^3-3ST\psi_1^2\varphi_2-3ST\psi_1\left(2\varphi_1^2-2\varphi_1\varphi_2+\varphi_2^2\right)\\&-S(-4L+4S+T)\psi_0^3+3S(-4L+2S+T)\psi_0^2\psi_1+3S(4L-T)\psi_0\psi_1^2\\&+3T\varphi_0^2\left(-S(\psi_0+\psi_1)-(2L-T)\varphi_2\right)+3T\varphi_0\left(L\varphi_2^2-S\left(\psi_0-\psi_1\right)^2+2S\psi_0\varphi_2\right)\\&-T(-4L+S+4T)\varphi_0^3+3T\varphi 0^2\varphi 1(-2L+S+T)\\&+3T\varphi 0\varphi 1\left(\varphi 1(L-S)+2L\varphi 2+2S\psi 1\right)-3ST\psi 0\varphi 2\left(\psi 0-2\psi 1+\varphi 2\right).\end{aligned}$$

- *Resolution III:*

$$\begin{aligned}\mathscr{F}^{(III)}_{trip} =& -2S(2L+S-T)\psi_1^3-T(-4L+S+4T)\varphi_1^3-3ST\psi_1\left(\left(\varphi_1-\varphi_2\right)^2+\psi_1\left(\varphi_1+\varphi_2\right)\right)\\&-3T(-4L+S+T)\varphi_1\varphi_2^2-T(5L-S+T)\varphi_2^3-3T(5L-S-2T)\varphi_1^2\varphi_2\\&-2S(-2L+2S+T)\psi_0^3+\psi_0^2\left(6S\psi_1(-2L+S+T)-3ST\left(\varphi_1+\varphi_2\right)\right)\\&+\psi_0\left(-6S\psi_1^2(T-2L)+6ST\psi_1\left(\varphi_1+\varphi_2\right)-3ST\left(\varphi_1^2+\varphi_2^2\right)\right)+4T\varphi_0^3(L-T)\\&+\varphi_0^2\left(3T\left(\varphi_1+\varphi_2\right)(T-2L)-6ST\psi_0\right)+3T\varphi_0\left(\varphi_1+\varphi_2\right)\left(L\left(\varphi_1+\varphi_2\right)+2S\psi_0\right)\end{aligned}$$

- *Resolution IV:*

$$\begin{aligned}\mathscr{F}^{(IV)}_{trip} = {} & S(-4L-2S+3T)\psi_1^3 - 4T(T-L)\varphi_1^3 - 3T(5L-2T)\varphi_1^2\varphi_2 \\ & - 3T(T-4L)\varphi_1\varphi_2^2 - T(5L+T)\varphi_2^3 - 6ST\psi_1^2\varphi_2 \\ & + \psi_0^2\left(3S\psi_1(-4L+2S+3T) - 6ST\varphi_2\right) + 3S\psi_0\left(\psi_1^2(4L-3T) + 4T\psi_1\varphi_2\right) \\ & - 6ST\psi_0\left(\varphi_1^2 - \varphi_2\varphi_1 + \varphi_2^2\right) + S(4L-4S-3T)\psi_0^3 + 4T\varphi_0^3(L-T) \\ & + \varphi_0^2\left(3T\left(\varphi_1+\varphi_2\right)(T-2L) - 6ST\psi_0\right) + 3T\varphi_0\left(\varphi_1+\varphi_2\right)\left(L\left(\varphi_1+\varphi_2\right) + 2S\psi_0\right)\end{aligned}$$

The triple intersection polynomials for the resolutions I′, II′, III′, *and* IV′ *are respectively derived from those of the resolutions* I, II, III, *and* IV *by the involution* $\varphi_1 \leftrightarrow \varphi_2$.

Proof. We give the proof for the case of Resolution I discussed in detail in Section 12.5.1, the other cases follow the same pattern.

$$\begin{aligned}\mathscr{F}_{trip} &= \int_Y \left[\left(\psi_0 D^s_0 + \psi_1 D^s_1 + \varphi_0 D^t_0 + \varphi_1 D^t_1 + \varphi_2 D^t_2\right)^3\right] \\ &= \int_{X_3} \left[\left(\psi_0 D^s_0 + \psi_1 D^s_1 + \varphi_0 D^t_0 + \varphi_1 D^t_1 + \varphi_2 D^t_2\right)^3 (3H + 6L - 2E_1 - 2W_1 - W_2)\right] \\ &= \int_{X_0} f_{1*}f_{2*}f_{3*}\left[\left(\psi_0 D^s_0 + \psi_1 D^s_1 + \varphi_0 D^t_0 + \varphi_1 D^t_1 + \varphi_2 D^t_2\right)^3 (3H + 6L - 2E_1 - 2W_1 - W_2)\right] \\ &= \int_B \pi_* f_{1*}f_{2*}f_{3*}\left[\left(\psi_0 D^s_0 + \psi_1 D^s_1 + \varphi_0 D^t_0 + \varphi_1 D^t_1 + \varphi_2 D^t_2\right)^3 (3H + 6L - 2E_1 - 2W_1 - W_2)\right].\end{aligned}$$

The classes of the fibral divisors in the Chow ring of X_3 are

$$[D^s_0] = S - E_1, \quad [D^s_1] = E_1, \quad [D^t_0] = T - W_1, \quad [D^t_1] = W_1 - W_2, \quad [D^t_2] = W_2.$$

Denoting by M an arbitrary divisor in the class of the Chow ring of the base B, the nonzero intersection numbers of the products of M, H, E_1, W_1, and W_2 are

$$\int_Y E_1^3 = -2S(2L+S), \quad \int_Y W_1^3 = -2T(2L-S+T), \quad \int_Y MW_1^2 = -2TM,$$
$$\int_Y W_2^3 = -T(5L-2S+T), \quad \int_Y W_1^2 E_1 = -2ST, \quad \int_Y W_1^2 W_2 = T(-2L+S-T),$$
$$\int_Y ME_1^2 = -2SM, \quad \int_Y W_2^2 E_1 = -2ST, \quad \int_Y W_2^2 W_1 = T(-L+S-2T), \quad \int_Y E_1 W_1 W_2 = -ST,$$
$$\int_Y HM = 3M, \quad \int_Y H^2 M = -9LM, \quad \int_Y H^3 = 27L^2, \quad \int_Y MW_2^2 = -2TM,$$

where the right-hand-side of each equality is computed in the Chow ring of the base B, the pushforward for f_{i*} ($i = 1, 2, 3$) are obtained via Theorem 5.0.1, the pushforward for π_* uses Theorem 5.0.4. The triple intersection numbers of the fibral divisors follow from these by simple linearity. □

The triple intersection polynomials computed in Theorem 12.3.8 are very different from each other in chambers I, II, III, and IV. In chamber III, we get all possible ten homogeneous monomials in ψ_1, φ_1 and φ_2. In chamber II, we get nine of them ($\psi_1^2\varphi_1$ is missing); in chamber I, we are missing two ($\psi_1^2\varphi_1$ and $\psi_1^2\varphi_2$); in chamber IV, we are missing four ($\psi_1^2\varphi_1$, $\psi_1\varphi_1^2$, $\psi_1\varphi_2^2$ and $\psi_1\varphi_1\varphi_2$). These facts become handy when comparing the triple intersection polynomials with the prepotentials in Section 12.7.1.

12.3.4 Non-Kodaira fibers

The $\mathrm{SU}(2)\times\mathrm{SU}(3)$-models have a particularly rich fiber structure with various types of non-Kodaira fibers. We have identified a total of thirteen non-Kodaira fibers over points in codimension-two or

three in the base, which are all summarized in Table 12.3.

The fiber structure of each models studied in this chapter is described in Section 12.8. Two of these non-Kodaira fibers appear for the first time in the literature. They are contraction of the fiber I_2^* appearing over codimension codimension-three points in the base in the crepant resolution II or IV of the collision I_2+IV^s. They are related to the sequence A_1+$\mathrm{A}_2 \to \mathrm{D}_5 \to \mathrm{D}_6$. All the non-Kodaira fibers obtained at the collision of S and T can be derived by removing certain nodes on the Kodaira fibers I_0^*, I_1^*, I_2^*, IV^*, or III^*. Away from $S \cap T$, there is also a non-Kodaira fiber that appears in the specialization of the fiber of type III. The phenomena that non-Kodaira fibers of a flat fibration are contractions of Kodaira fibers has been noticed by Miranda in the particular case of his regularization of elliptic threefolds [236] and also in generalizations of Miranda's models to n-folds as studied by Szydlo [286]. Cattaneo argues in [76] that this is always the case for flat elliptic threefolds that are crepant resolutions of Weierstrass models. The study of crepant resolutions of singular Weierstrass models and the geography of their flops is an essential endeavor in stringy geometry and has been studied for many models producing in this way most of the known non-Kodaira fibers [76, 109, 112, 115, 118–122, 125, 127, 129, 207, 215, 236, 241, 286, 289].

12.4 Hyperplane arrangements and geography of flops

In Section 12.4.1, we discuss matter representations of the $\mathrm{SU}(2) \times \mathrm{SU}(3)$-model in five and six-dimensional theories with eight supercharges from Katz-Vafa method and confirm its perfect match with the representations computed from the geometry.

In Section 12.4.2, we study the hyperplane arrangement $\mathrm{I}(\mathrm{A}_1 \oplus \mathrm{A}_2, (1,3) \oplus (2,3))$. The full representation of the SU(2) × SU(3)-model is $\mathbf{R} = (2,1) \oplus (1,3) \oplus (1,\bar{3}) \oplus (2,3) \oplus (2,\bar{3}) \oplus (3,1) \oplus (1,8)$. However, the hyperplane arrangement $\mathrm{I}(\mathrm{A}_1 \oplus \mathrm{A}_2, \mathbf{R})$ has the same chamber structure as $\mathrm{I}(\mathrm{A}_1 \oplus \mathrm{A}_2, (1,3) \oplus (2,3))$ since the adjoints only define the exterior walls of the dual fundamental Weyl chamber, taking care of the redundancy, and noticing that $((2,1))$ does not contribute interior walls, it is sufficient to consider $(1,3) \oplus (2,3)$ only.

In Section 12.4.3, we match the chamber of the hyperplane arrangement $\mathrm{I}(\mathrm{A}_1 \oplus \mathrm{A}_2, (1,3) \oplus (2,3))$ with the crepant resolutions as inspired by their interpretation as Coulomb branches of a five-dimensional gauge theory discussed in Section 12.7.1.

12.4.1 Geometric weights and matter representations

An important geometric data is the representation $\mathbf{R}$ under which the matter fields transform. This representation is characterized by its weights, which are computed geometrically by intersection numbers of fibral divisors with vertical curves over codimension-two points. We do not add by hand the chiral conjugates of representations; all representations are seen explicitly by their weights via fibers given by the geometry. Starting from a collection of weights, we determine the representation by using the notion of *saturated set of weights* borrowed from Bourbaki. See [112, 115] for more information.

The representation $\mathbf{R}$ that we obtain from purely geometric considerations is consistent with what one would indirectly guess using the Katz-Vafa method [187]. But the Katz-Vafa method can fail for certain models such as the SU(2)× G_2 model, while the method of saturations of weight still

provides the correct representation **R** as discussed in [119]. The sector of **R** that does not contain fundamental representations can be derived from the branching rule of the adjoint representation of maximal embedding $\mathrm{A}_1 \oplus \mathrm{A}_2 \to \mathrm{A}_4$ while the fundamental representations follow from the branching rule of the adjoints of the maximal embedding $\mathrm{A}_1 \to \mathrm{A}_2$ and $\mathrm{A}_2 \to \mathrm{A}_3$:

$$\begin{cases} 24 & \longrightarrow (3,1) \oplus (1,8) \oplus (2,3) \oplus (2,\bar{3}) \oplus (1,\bar{1}), \\ 15 & \longrightarrow 8 \oplus 3 \oplus \bar{3} \oplus 1, \\ 8 & \longrightarrow 3 \oplus 2 \oplus \bar{2} \oplus 1. \end{cases} \tag{12.4}$$

A frozen representation is a representation ρ whose weights are carried by certain curves of the elliptic fibration over codimension-two points in the base, but no hypermultiplet is charged under ρ [115, 119]. When compactified to a five-dimensional or six-dimensional supergravity theory with eight supercharges, matter in these adjoint representations are frozen when the curves supporting the components of the gauge group are smooth rational curves since the number of adjoint hypermultiplets is given by the arithmetic genus of the curve supporting the gauge group.

12.4.2 Hyperplane arrangement

We consider the semi-simple Lie algebra

$$\mathfrak{g} = \mathrm{A}_1 \oplus \mathrm{A}_2.$$

An irreducible representation of $A_1 \oplus A_2$ is the tensor product $\mathbf{r}_1 \otimes \mathbf{r}_2$, where $\mathbf{r}_1$ and $\mathbf{r}_2$ are respectively irreducible representations of A_1 and A_2. Following a common convention in physics, we denote a representation of A_n by its dimension in bold character. The weights are denoted by ϖ_j^I where the upper index I denotes the representation $\mathbf{R_I}$ and the lower index j denotes a particular weight of the representation $\mathbf{R_I}$. A weight of a representation of $A_1 \oplus A_2$ is denoted by a triple $(a; b, c)$ such that (a) is a weight of A_1 and (b, c) is a weight of A_2, all in the basis of fundamental weights. We use the same notation for coroots. Let $\varphi = (\psi_1; \varphi_1, \varphi_2)$ be a vector of the coroot space of $A_1 \oplus A_2$ in the basis of the fundamental coroots. Each weight ϖ defines a linear form $\varphi \cdot \varpi$ defined by the natural evaluation on a coroot. We recall that fundamental coroots are dual to fundamental weights. Hence, with our choice of conventions, $\varphi \cdot \varpi$ is the usual Euclidian scalar product.

To study the hyperplane arrangement, it is not necessary to consider the full representation $\mathbf{R} = (2,1) \oplus (1,3) \oplus (1,\bar{3}) \oplus (2,3) \oplus (2,\bar{3}) \oplus (3,1) \oplus (1,8)$ since the adjoints only define the dual fundamental Weyl chamber and 3 and $\bar{3}$ defer only by a sign. Thus, we use without loss of generality the representation $\mathbf{R}$ as:

$$\mathbf{R} = (2,1) \oplus (1,3) \oplus (2,3), \tag{12.5}$$

which is the sum of the fundamental of A_1, the fundamental of A_2, and the bifundamental representations of A_1 and A_2. We study the arrangement of hyperplanes perpendicular to the weights of the representation $\mathbf{R}$ inside the dual fundamental Weyl chamber of $A_1 \oplus A_2$.

The open dual fundamental Weyl chamber is the half cone defined by the the positivity of the

linear form induced by the simple roots:

$$\psi_1 > 0, \quad 2\varphi_1 - \varphi_2 > 0, \quad -\varphi_1 + 2\varphi_2 > 0. \tag{12.6}$$

The weight system of the representation **2** of A_1 and the representation **3** of A_2 are

$$2: \quad \varpi_1^2 = 1, \quad \varpi_2^2 = -1 \tag{12.7}$$

$$3: \quad \varpi_1^3 = (1,0), \quad \varpi_2^3 = (-1,1), \quad \varpi_3^3 = (0,-1). \tag{12.8}$$

The weights of the representation $(2,1)$, $(1,3)$ and $(2,3)$ are (in the Cartan's basis of fundamental weights). All the relevant weights are given in Table 12.4.

Theorem 12.4.1. *The hyperplane arrangement* $\mathrm{I}(A_1 \oplus A_2, (1,3) \oplus (2,3))$ *has eight chambers whose sign vectors (with respect to the forms* $(\varpi_2^{(1,3)}, \varpi_5^{(2,3)}, \varpi_4^{(2,3)}, \varpi_3^{(2,3)}, \varpi_2^{(2,3)})$*) are as listed in Table 12.5. The corresponding adjacency graph is given in Figure 12.3.*

Proof. There are five hyperplanes intersecting the interior of the dual fundamental Weyl chamber: $\varpi_2^{(1,3)}$, $\varpi_2^{(2,3)}$, $\varpi_3^{(2,3)}$, $\varpi_4^{(2,3)}$, and $\varpi_5^{(2,3)}$. We use them in the order $(\varpi_2^{(1,3)}, \varpi_5^{(2,3)}, \varpi_4^{(2,3)}, \varpi_3^{(2,3)}, \varpi_2^{(2,3)})$, the sign vector is $(-\varphi_1 + \varphi_2, -\psi_1 - \varphi_1 + \varphi_2, -\psi_1 + \varphi_1, \psi_1 - \varphi_2, \psi_1 - \varphi_1 + \varphi_2)$. Keeping in mind the conditions in equation (12.6) defining the open dual fundamental Weyl chamber, the results follow from a direct check of all possible signs and the chambers are listed on Table 12.5. □

12.4.3 Correspondence between the geometry and the representation theory

In this section, we match the crepant resolutions of Section 12.3.1 and the chambers of the hyperplane arrangement $\mathrm{I}(\mathfrak{g}, \mathbf{R})$ of Table 12.5. The graph of flops between the crepant resolutions is isomorphic to the adjacency graph of the chambers of the hyperplane arrangement, but the isomorphism is not canonical since the graph has a $\mathbb{Z}_2$ automorphism. A simple way to fix the identification is to compare the triple intersection numbers in each resolution, which are given by Theorem 12.3.8, and the prepotentials computed in each chamber, which are given by Theorem 12.7.1.

In Section 12.3, we described eight different possible resolutions. There is a $\mathbb{Z}_2$ symmetry in the the structures of the resolutions mapping resolutions I, II, III, IV and the resolutions I′, II′, III′, IV′ and induced by the inverse map of the Mordell–Weil group. Similarly, we see the $\mathbb{Z}_2$ symmetry in the adjacent graph of the chambers between the chambers 1, 2, 3, 4 and the chambers 1′, 2′, 3′, 4′. This can be observed easily in Figure 12.3.

We see the explicit correspondence between the chambers and the resolutions as

$$\begin{gathered} \mathrm{I} \leftrightarrow 1, \quad \mathrm{II} \leftrightarrow 2, \quad \mathrm{III} \leftrightarrow 3, \quad \mathrm{IV} \leftrightarrow 4, \\ \mathrm{I}' \leftrightarrow 1', \quad \mathrm{II}' \leftrightarrow 2', \quad \mathrm{III}' \leftrightarrow 3', \quad \mathrm{IV}' \leftrightarrow 4'. \end{gathered} \tag{12.9}$$

We can also compute the weight of the flopping curve between pairs of resolutions connected by a flop, and compare it with the weight of the wall between the adjacent chambers. As an illustration, we treat the case of $\mathrm{I}_2^{\mathrm{s}}+\mathrm{I}_3^{\mathrm{s}}$-models and show that that the weights of the flopping curves, which are derived in Section 12.5.5, match the weights of the walls in Figure 12.3. This solidifies the duality

between the chambers and the resolutions, which is represented by the complete structure of the resolutions and the adjacent graph of the chambers juxtaposed in Figure 12.3.

The dual fundamental Weyl chamber is identified with the relative movable cone of a crepant resolution $Y \to Y_0$ over the Weierstrass model Y_0. This cone is an invariant of minimal models in the same birational class [228, §12-2]. The nef cone of any crepant resolution is then identified with a chamber of the hyperplane arrangement $\mathrm{I}(\mathfrak{g}, \mathbf{R})$. In particular, two nef cones whose interior coincide represent the same crepant resolution. An interior walls of $\mathrm{I}(\mathfrak{g}, \mathbf{R})$ corresponds to a geometric weight observed up to a sign between two distinct crepant resolutions separated by a flop. Two crepant resolutions have nef cones separated by an interior wall they they are connected by an extremal flop [228, Propostion 12-2-2].

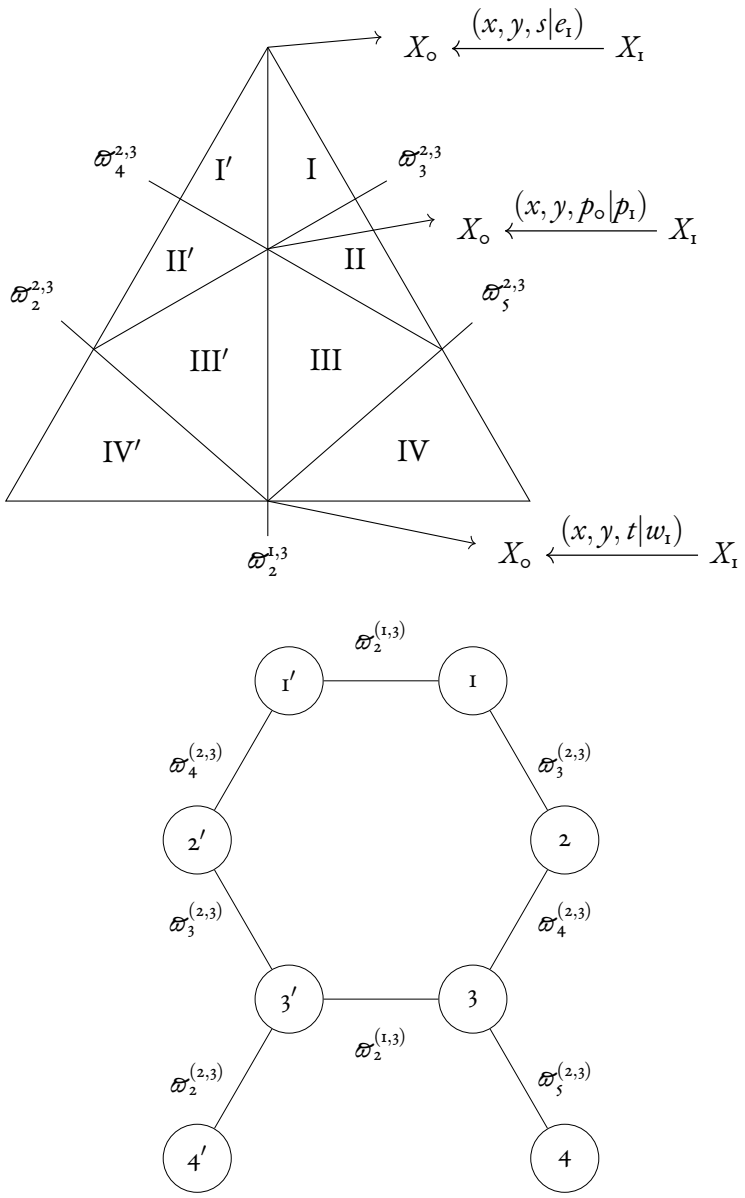

Figure 12.3: Left: the complete structure of the resolutions of $\mathrm{SU}(2) \times \mathrm{SU}(3)$. This is a two-dimensional patch of the entire three-dimensional cones. Hence, every point (resp. line) on this picture represents a line (resp. surface). Accordingly, these eight triangles are the three-dimensional triangular cones. The point in the top of the triangle is the resolution that resolves the SU(2), and the bottom-middle point of the triangle is the first resolution that resolves SU(3) only. The point in the middle of the triangle is the point that describes the blow-up that mixes both SU(2) and SU(3). All these three points are connected as expected and it works as the plane of the mirrors. **Right:** the adjacent graph of the eight chambers of $\mathsf{I}(\mathfrak{g}, \mathbf{R})$ with $\mathfrak{g} = \mathsf{A}_1 \oplus \mathsf{A}_2$ and $\mathbf{R} = (1,3) \oplus (2,3)$.

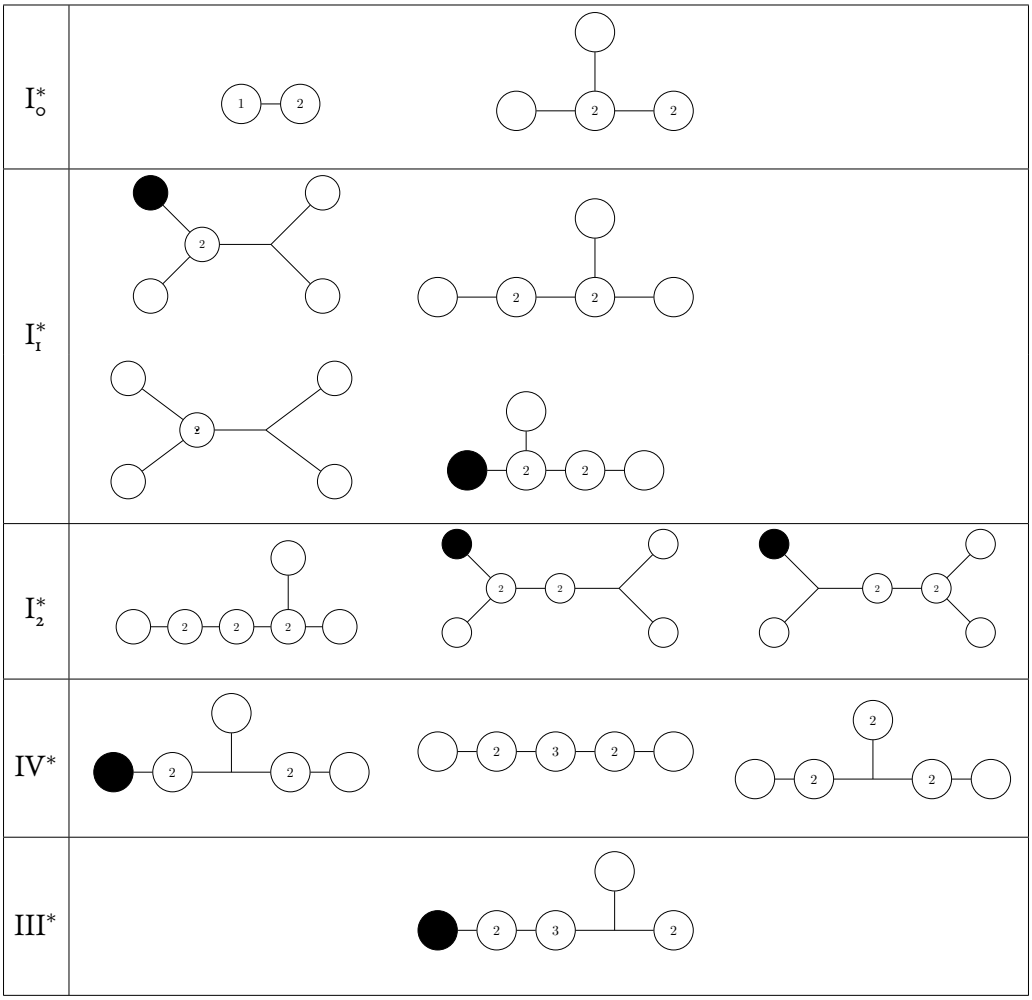

Table 12.3: These are the non-Kodaira fibers observed for the $SU(2) \times SU(3)$-models organized by the type of the resulting Kodaira fibers with contracted nodes. When there is a possible ambiguity, the node that touches the zero section is colored in black. The last two fibers in the row of I_2^* are observed for the first time.

Representation	Weights
$(2,1)$	$\varpi_1^{(2,1)} = (1;0,0)$ $\quad \varpi_2^{(2,1)} = (-1;0,0)$
$(1,3)$	$\varpi_1^{(1,3)} = (0;1,0)$ $\quad \varpi_2^{(1,3)} = (0;-1,1)$ $\quad \varpi_3^{(2,1)} = (0;0,-1)$
$(2,3)$	$\varpi_1^{(2,3)} = (1;1,0)$ $\quad \varpi_2^{(2,3)} = (1;-1,1)$ $\quad \varpi_3^{(2,3)} = (1;0,-1)$ $\varpi_4^{(2,3)} = (-1;1,0)$ $\quad \varpi_5^{(2,3)} = (-1;-1,1)$ $\quad \varpi_6^{(2,3)} = (-1;0,-1)$

Table 12.4: Weights of the representations

Subchambers	$\varpi_2^{(1,3)}$	$\varpi_5^{(2,3)}$	$\varpi_4^{(2,3)}$	$\varpi_3^{(2,3)}$	$\varpi_2^{(2,3)}$	Explicit description
①	$+$	$-$	$-$	$+$	$+$	$0 < \varphi_2 - \varphi_1 < \varphi_1 < \varphi_2 < \psi_1$
②	$+$	$-$	$-$	$-$	$+$	$0 < \varphi_2 - \varphi_1 < \varphi_1 < \psi_1 < \varphi_2$
③	$+$	$-$	$+$	$-$	$+$	$0 < \varphi_2 - \varphi_1 < \psi_1 < \varphi_1 < \varphi_2$
④	$+$	$+$	$+$	$-$	$+$	$0 < \psi_1 < \varphi_2 - \varphi_1 < \varphi_1 < \varphi_2$
①′	$-$	$-$	$-$	$+$	$+$	$0 < \varphi_1 - \varphi_2 < \varphi_2 < \varphi_1 < \psi_1$
②′	$-$	$-$	$+$	$+$	$+$	$0 < \varphi_1 - \varphi_2 < \varphi_2 < \psi_1 < \varphi_1$
③′	$-$	$-$	$+$	$-$	$+$	$0 < \varphi_1 - \varphi_2 < \psi_1 < \varphi_2 < \varphi_1$
④′	$-$	$-$	$+$	$-$	$-$	$0 < \psi_1 < \varphi_1 - \varphi_2 < \varphi_2 < \varphi_1$

Table 12.5: Chambers of the hyperplane arrangement $I(A_1 \oplus A_2, \mathbf{R})$ with $\mathbf{R} = (1,3) \oplus (2,3)$. We will get exactly the same structure if we take the representation $\mathbf{R} = (2,1) \oplus (1,3) \oplus (2,3)$ since the representation $(2,1)$ does not contribute any hyperplane intersecting the interior of the dual fundamental Weyl chamber.

12.5 The $I_2^s+I_3^s$ Model

In this section, we study the fiber structure of the crepant resolutions of the $I_2^s+I_3^s$ model defined by the following Weierstrass equation:

$$Y_0 : \; y^2 + a_1xy + \widetilde{a}_3sty = x^3 + \widetilde{a}_2stx^2 + \widetilde{a}_4st^2x + \widetilde{a}_6s^2t^3. \tag{12.10}$$

12.5.1 Resolution I

Resolution I is defined by the following sequence of blowups:

$$X_0 = \mathbb{P}(\mathscr{O}_B \oplus \mathscr{L}^{\otimes 2} \oplus \mathscr{L}^{\otimes 3}) \xleftarrow{(x,y,s|e_1)} X_1 \xleftarrow{(x,y,t|w_1)} X_2 \xleftarrow{(y,w_1|w_2)} X_3 \;, \tag{12.11}$$

where X_0 is the projective bundle in which the Weierstrass model is defined; each successive blowup produces a projective bundle over the center of the blowup. The projective coordinates of the fibers of the successive projective bundles are

$$[e_1w_1w_2x\,;\; e_1w_1w_2^2y\,;\; z=1][w_1w_2x\,;\; w_1w_2^2y\,;\; s][x\,;\; w_2y\,;\; t][y\,;\; w_1]. \tag{12.12}$$

The proper transform of Y_0 is denoted Y and is a smooth elliptic fibration:

$$Y : \; y(w_2y + a_1x + \widetilde{a}_3st) = w_1(e_1x^3 + \widetilde{a}_2se_1tx^2 + \widetilde{a}_4st^2x + \widetilde{a}_6s^2t^3). \tag{12.13}$$

We denote by $\mathrm{D}^{\mathrm{s}}_a$ and D^{t}_a the irreducible fibral divisors that project to S and T:

$$\mathrm{I}^{\mathrm{s}}_2 : \begin{cases} D^{\mathrm{s}}_{\mathrm{o}} : s = y(w_2 y + a_1 x) - w_1 e_1 x^3 = 0 \\ D^{\mathrm{s}}_{\mathrm{I}} : e_1 = y(w_2 y + a_1 x + \widetilde{a}_3 st) - w_1(\widetilde{a}_4 st^2 x + \widetilde{a}_6 s^2 t^3) = 0 \end{cases} \tag{12.14}$$

$$\mathrm{I}^{\mathrm{s}}_3 : \begin{cases} D^{\mathrm{t}}_{\mathrm{o}} : t = y(w_2 y + a_1 x) - w_1 e_1 x^3 = 0 \\ D^{\mathrm{t}}_{\mathrm{I}} : w_1 = w_2 y + a_1 x + \widetilde{a}_3 st = 0 \\ D^{\mathrm{t}}_2 : w_2 = y(a_1 x + \widetilde{a}_3 st) - w_1(e_1 x^3 + \widetilde{a}_2 s e_1 t x^2 + \widetilde{a}_4 st^2 x + \widetilde{a}_6 s^2 t^3) = 0 \end{cases} \tag{12.15}$$

The generic fiber of D^{s}_a (resp. D^{t}_a) over S (resp. T) is denoted as C^{s}_a (resp. C^{t}_a). The fiber structure away from the intersection $S \cap T$ is well understood from the study of the individual SU(2) and SU(3)-models [125]. The generic fiber over the intersection of S and T is of type $\mathrm{I}^{\mathrm{s}}_5$ as in Figure 12.4, which is produced by the following splittings of C^{s}_a and C^{t}_a.

$$\text{On } S \cap T : \begin{cases} C^{\mathrm{s}}_{\mathrm{o}} \longrightarrow \eta^{\circ}_{\mathrm{o}} \\ C^{\mathrm{s}}_{\mathrm{I}} \longrightarrow \eta^{\circ A}_{\mathrm{I}} + \eta^{\circ B}_{\mathrm{I}} + \eta^{\mathrm{I}}_{\mathrm{I}} + \eta^{2}_{\mathrm{I}} \\ C^{\mathrm{t}}_{\mathrm{o}} \longrightarrow \eta^{\circ A}_{\mathrm{I}} + \eta^{\circ B}_{\mathrm{I}} + \eta^{\circ}_{\mathrm{o}} \\ C^{\mathrm{t}}_{\mathrm{I}} \longrightarrow \eta^{\mathrm{I}}_{\mathrm{I}} \\ C^{\mathrm{t}}_{2} \longrightarrow \eta^{2}_{\mathrm{I}} \end{cases} \tag{12.16}$$

$$\text{On } S \cap T : \begin{cases} C_{\circ}^{\mathfrak{s}} \cap C_{\circ}^{\mathfrak{t}} \to & \eta_{\circ}^{\circ} : s = t = y(w_2 y + a_1 x) - w_1 e_1 x^3 = 0 \\ C_{\mathrm{I}}^{\mathfrak{s}} \cap C_{\circ}^{\mathfrak{t}} \to & \eta_{\mathrm{I}}^{\circ A} : e_1 = t = y = 0, \quad \eta_{\mathrm{I}}^{\circ B} : e_1 = t = w_2 y + a_1 x = 0 \\ C_{\mathrm{I}}^{\mathfrak{s}} \cap C_{\mathrm{I}}^{\mathfrak{t}} \to & \eta_{\mathrm{I}}^{\mathrm{I}} : e_1 = w_1 = w_2 y + a_1 x + \widetilde{a}_3 s t = 0 \\ C_{\mathrm{I}}^{\mathfrak{s}} \cap C_{2}^{\mathfrak{t}} \to & \eta_{\mathrm{I}}^{2} : e_1 = w_2 = y(a_1 x + \widetilde{a}_3 s t) - s t^2 w_1 (\widetilde{a}_4 x + \widetilde{a}_6 s t) = 0 \end{cases} \tag{12.17}$$

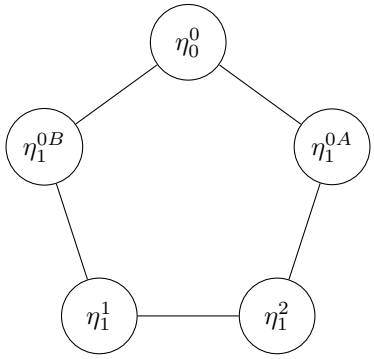

Figure 12.4: Fiber over the generic point of the locus $S \cap T$ in Resolution I of the $\mathrm{I}_2^{\mathfrak{s}}$+$\mathrm{I}_3^{\mathfrak{s}}$-model.

The curves $\eta_{\circ}^{\circ}$, $\eta_{\mathrm{I}}^{\mathrm{I}}$, and η_{I}^{2} have the same weights as $C_{\circ}^{\mathfrak{s}}$, $C_{\mathrm{I}}^{\mathfrak{t}}$, and $C_{2}^{\mathfrak{t}}$, respectively. The curves $\eta_{\mathrm{I}}^{\circ A}$ (resp. $\eta_{\mathrm{I}}^{\circ B}$) has zero intersection with $D_{\mathrm{I}}^{\mathfrak{t}}$ (resp. $D_{2}^{\mathfrak{t}}$). The intersection of the curves composing the fiber $\mathrm{I}_5^{\mathfrak{s}}$ with the fibral divisors are listed on Table 12.6.

The weights of the curves $\eta_{\circ}^{\circ}$, η_{I}^{2}, and $\eta_{\mathrm{I}}^{\mathrm{I}}$ are are among the weights of the adjoint representation while the weights of the curves $\eta_{\mathrm{I}}^{\circ A}$ and $\eta_{\mathrm{I}}^{\circ B}$ are respectively in the bifundamental representation $(2, 3)$ and $(2, \overline{3})$.

	D_0^s	D_1^s	D_0^t	D_1^t	D_2^t	Weight	Representation
η_0°	-2	2	0	0	0	[-2;0,0]	$(3,1)$
η_1^2	0	0	1	1	-2	[0;-1,2]	$(1,8)$
η_1^{I}	0	0	1	-2	1	[0;2-1]	$(1,8)$
$\eta_1^{\circ A}$	1	-1	-1	0	1	[1;0,-1]	$(2,3)$
$\eta_1^{\circ B}$	1	-1	-1	1	0	[1;-1,0]	$(2,\bar{3})$

Table 12.6: Weights of vertical curves and representations in the resolution I of the $\mathrm{I}_2^s+\mathrm{I}_3^s$-model.

The fiber I_5^s can degenerate in two different ways by following the degenerations of $\eta_1^{\circ B}$ and η_1^2. The curve $\eta_1^{\circ B}$ degenerates at $V(a_1)$, and η_1^2 is a conic that degenerates at the zero locus of its discriminant. The generic fiber over $S \cap T \cap V(a_1)$ is a non-Kodaira fiber corresponding to a contracted fiber of type IV* described in Figure 12.5. The generic fiber over $S \cap T \cap V(a_1\widetilde{a}_6 - \widetilde{a}_3\widetilde{a}_4)$ is an I_6^s fiber obtained by the degeneration of the conic η_1^2 into two lines intersecting transversally (see Figure 12.6).

$$\text{On } S\cap T\cap V(a_1): \begin{cases} \eta_0^\circ & \longrightarrow & \eta_0^\circ : s = t = w_2y^2 - w_1e_1x^3 = 0 \\ \eta_1^{\circ A} & \longrightarrow & \eta_1^{\circ A} : e_1 = t = y = 0 \\ \eta_1^{\circ B} & \longrightarrow & \eta_1^{\circ A} : e_1 = t = y = 0,\ \eta_1^{\circ 2} : e_1 = t = w_2 = 0 \\ \eta_1^{\mathrm{I}} & \longrightarrow & \eta_1^{\mathrm{I}} : e_1 = w_1 = w_2y + \widetilde{a}_3st = 0 \\ \eta_1^2 & \longrightarrow & \eta_1^{\circ 2} : e_1 = w_2 = t = 0,\ \eta_1^2 : e_1 = w_2 = \widetilde{a}_3y - tw_1(\widetilde{a}_4x + \widetilde{a}_6st) = 0 \end{cases} \tag{12.18}$$

$$\text{On } S \cap T \cap V(a_1\widetilde{a}_6 - \widetilde{a}_3\widetilde{a}_4) : \eta_1^2 \longrightarrow \begin{cases} \eta_1^{2A} : a_1 x + \widetilde{a}_3 s t = 0, \\ \eta_1^{2B} : \widetilde{a}_3 y - \widetilde{a}_6 s t^2 w_1 = 0 \end{cases} \tag{12.19}$$

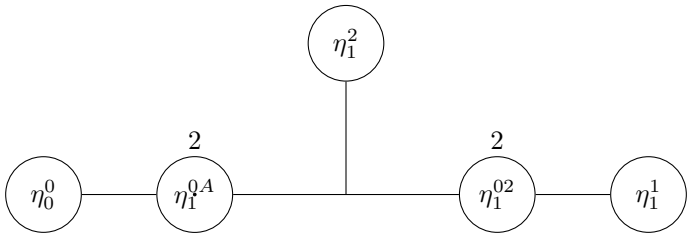

Figure 12.5: Fiber over the generic point of the locus $S \cap T \cap V(a_1)$ in Resolution I of the I_2^s+I_3^s-model.

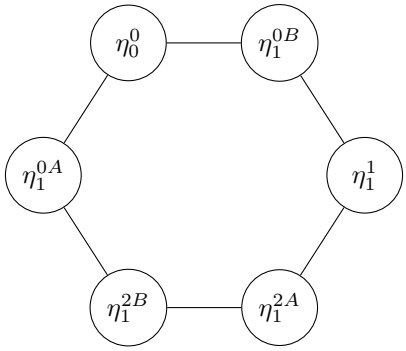

Figure 12.6: Fiber over the generic point of the locus $S \cap T \cap V(a_1\widetilde{a}_6 - \widetilde{a}_3\widetilde{a}_4)$ in Resolution I of the I_2^s+I_3^s-model.

As it is clear from equation (12.19), the curve η_1^{2A} will degenerate to a surface over $S \cap T \cap V(a_1, \widetilde{a}_3)$. For that reason, we assume that the base is at most a threefold to ensure that the fibration is flat.

12.5.2 Resolution II

In this section, we study the resolution II. In contrast to the other resolutions, some of the centers of the blowups that define resolutions II and II' are singular. In particular, the first blowup in the sequence of blowups that defines resolution II has a singular center. In order to describe the first blowup, it is useful to rewrite the equation (12.10) as

$$Y_0 : \begin{cases} y(y + a_1 x + \widetilde{a}_3 p_0) = x^3 + \widetilde{a}_2 p_0 x^2 + \widetilde{a}_4 p_0 t x + \widetilde{a}_6 p_0^2 t \\ p_0 = st \end{cases} . \tag{12.20}$$

The resolution II is then given by the following sequence of blowups

$$X_0 \xleftarrow{(x,y,p_0|p_1)} X_1 \xleftarrow{(y,t,p_1|w_1)} X_2 \xleftarrow{(t,p_0|w_2)} X_3 , \tag{12.21}$$

where $X_0 = \mathbb{P}[\mathscr{O}_B \oplus \mathscr{L}^{\otimes 2} \oplus \mathscr{L}^{\otimes 3}]$. The projective coordinates on X_3 are then

$$[p_1 w_1 x : p_1 w_1^2 y : z = 1][x : w_1 y : p_0 w_2][y : t w_2 : p_1][t : p_0], \tag{12.22}$$

and the proper transform is

$$Y : \begin{cases} y(w_1 y + a_1 x + \widetilde{a}_3 p_0 w_2) = p_1 x^3 + \widetilde{a}_2 p_0 p_1 w_2 x^2 + \widetilde{a}_4 p_0 t w_2^2 x + \widetilde{a}_6 p_0^2 t w_2^3 \\ p_0 p_1 = st \end{cases} . \tag{12.23}$$

The variety $X_1 = Bl_{(x,y,p_0)}X_0$ has double point singularities at $p_0 = p_1 = s = t = 0$. The fibral divisors of Y are

$$\mathrm{I}_2^{\mathfrak{s}}: \begin{cases} D_0^{\mathfrak{s}} : s = p_0 = y(w_1 y + a_1 x) - p_1 x^3 = 0 \\ D_1^{\mathfrak{s}} : s = p_1 = y(w_1 y + a_1 x + \widetilde{a}_3 p_0 w_2) - t w_2^2(\widetilde{a}_4 p_0 x + \widetilde{a}_6 p_0^2 w_2) = 0 \end{cases} \tag{12.24}$$

$$\mathrm{I}_3^{\mathfrak{s}}: \begin{cases} D_0^{\mathfrak{t}} : w_2 = p_0 p_1 - st = y(w_1 y + a_1 x) - p_1 x^3 = 0 \\ D_1^{\mathfrak{t}} : t = p_1 = w_1 y + a_1 x + \widetilde{a}_3 p_0 w_2 = 0 \\ D_2^{\mathfrak{t}} : w_1 = p_0 p_1 - st = y(a_1 x + \widetilde{a}_3 p_0 w_2) - (p_1 x^3 + \widetilde{a}_2 p_0 p_1 w_2 x^2 + \widetilde{a}_4 p_0 t w_2^2 x + \widetilde{a}_6 p_0^2 t w_2^3) = 0 \end{cases} \tag{12.25}$$

At the intersection of S and T the fiber enhances to an $\mathrm{I}_5^{\mathfrak{s}}$. This is realized by the following splittings of the curves.

$$\text{On } S \cap T: \begin{cases} C_0^{\mathfrak{s}} \longrightarrow \eta_0^{\circ} + \eta_0^2 \\ C_1^{\mathfrak{s}} \longrightarrow \eta_1^{\circ} + \eta_1^{\mathrm{I}} + \eta_1^2 \\ C_0^{\mathfrak{t}} \longrightarrow \eta_0^{\circ} + \eta_1^{\circ} \\ C_1^{\mathfrak{t}} \longrightarrow \eta_1^{\mathrm{I}} \\ C_2^{\mathfrak{t}} \longrightarrow \eta_0^2 + \eta_1^2 \end{cases} \tag{12.26}$$

The curves at the intersection are given by

$$\text{On } S\cap T: \begin{cases} C_0^s\cap C_0^t & \to \quad \eta_0^0 : s=p_0=w_2=y(w_1y+a_1x)-p_1x^3=0, \\ C_0^s\cap C_2^t & \to \quad \eta_0^2 : s=p_0=w_1=a_1y-p_1x^2=0, \\ C_1^s\cap C_0^t & \to \quad \eta_1^0 : s=p_1=w_2=w_1y+a_1x=0, \\ C_1^s\cap C_1^t & \to \quad \eta_1^1 : s=p_1=t=w_1y+a_1x+\widetilde{a}_3p_0w_2=0, \\ C_1^s\cap C_2^t & \to \quad \eta_1^2 : s=p_1=w_1=y(a_1x+\widetilde{a}_3p_0w_2)-p_0tw_2^2(\widetilde{a}_4x+\widetilde{a}_6p_0w_2)=0. \end{cases} \tag{12.27}$$

This corresponds to I_5^s as in Figure 12.7. The curve η_1^2 is quadratic in x, y, and p_0 with the discriminant $a_1(a_1\widetilde{a}_6-\widetilde{a}_3\widetilde{a}_4)$.

	D_0^s	D_1^s	D_0^t	D_1^t	D_2^t	Weight	Representation
η_0^0	-1	1	-1	0	1	[-1;0,-1]	$(2,3)$
η_0^2	-1	1	1	0	-1	[-1;0,1]	$(2,\overline{3})$
η_1^1	0	0	1	-2	1	[0;2,-1]	$(1,8)$
η_1^0	1	-1	-1	1	0	[1;-1,0]	$(2,\overline{3})$
η_1^2	1	-1	0	1	-1	[1;-1,1]	$(2,3)$

Table 12.7: Weights of vertical curves and representations in the resolution II of the $\mathrm{I}_2^s+\mathrm{I}_3^s$-model.

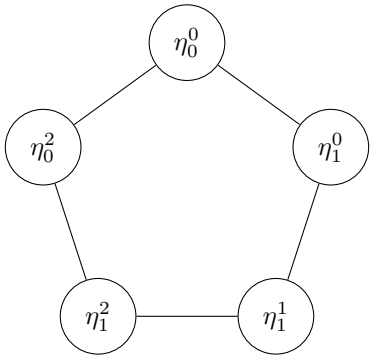

Figure 12.7: Fiber over the generic point of the locus $S \cap T$ in Resolution II of the I_2^s+I_3^s-model.

There are two enhancements when the discriminant of the curve η_1^2 vanishes. First enhancement is when $a_1 = 0$:

$$\text{On } S \cap T \cap V(a_1): \begin{cases} \eta_0^2 \longrightarrow \eta_{01}^2 \\ \eta_1^0 \longrightarrow \eta_1^{02} \\ \eta_1^2 \longrightarrow \eta_{01}^2 + \eta_1^{02} + \eta_1^2 \end{cases}, \tag{12.28}$$

where the new curves are given by

$$\begin{cases} \eta_{01}^2: & s = p_0 = p_1 = w_1 = 0 \\ \eta_1^{02}: & s = p_1 = w_2 = w_1 = 0 \\ \eta_1^2: & s = p_1 = w_1 = \widetilde{a}_3 y - \widetilde{a}_4 t w_2 x - \widetilde{a}_6 p_0 t w_2^2 = 0 \end{cases}. \tag{12.29}$$

For this codimension-three enhancement, we get a non-Kodaira fiber that is an incomplete fiber of type IV*, as illustrated in Figure 12.8.

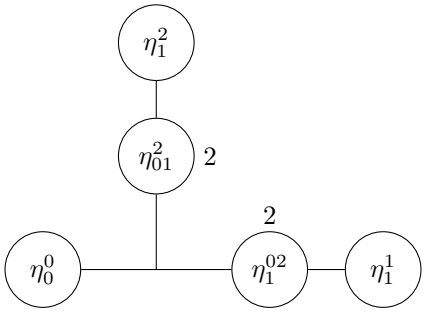

Figure 12.8: Fiber over the generic point of the locus $S \cap T \cap V(a_1)$ in Resolution II of the I_2^s+I_3^s-model.

The other specialization is when $(a_1\widetilde{a}_6 - \widetilde{a}_3\widetilde{a}_4)$, where η_1^2 splits into two curves that intersect each other such that

$$\text{on } S \cap T \cap V(a_1\widetilde{a}_6 - \widetilde{a}_3\widetilde{a}_4) : \ \eta_1^2 \longrightarrow \eta_1^{2A} + \eta_1^{2B}, \tag{12.30}$$

while all the other fibers are the same. except η_1^2. The resulting fiber is a Kodaira fiber of type I_6 as in Figure 12.9.

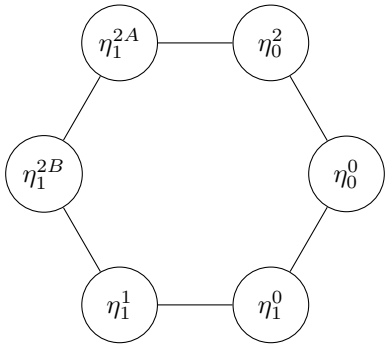

Figure 12.9: Fiber over the generic point of the locus $S \cap T \cap V(a_1\widetilde{a}_6 - \widetilde{a}_3\widetilde{a}_4)$ in Resolution II of the I_2^s+I_3^s-model.

12.5.3 Resolution III

The resolution III is defined by the following sequence of blowups:

$$X_0 \xleftarrow{(x,y,t|w_1)} X_1 \xleftarrow{(x,y,s|e_1)} X_2 \xleftarrow{(y,w_1|w_2)} X_3 \tag{12.31}$$

The projective coordinates are then given by

$$[e_1w_1w_2x\,;\, e_1w_1w_2^2y\,;\, z=1][e_1x\,;\, e_1w_2y\,;\, t][x\,;\, w_2y\,;\, s][y\,;\, w_1]. \tag{12.32}$$

The proper transform of the elliptic fibration for the resolution III is the same as equation (12.13) and the five fibral divisors are thus identical to those listed on the equation (12.15).

As before, we have a fiber of type I_2^s over the generic point of S and fiber of type I_3^s over the generic point of T. At the collision of S and T, the different curves are

$$\text{On } S\cap T: \begin{cases} C_0^s\cap C_0^t \to & \eta_0^0 : s=t=y(w_2y+a_1x)-w_1e_1x^3=0 \\ C_0^s\cap C_1^t \to & \eta_0^1 : s=w_1=w_2y+a_1x=0 \\ C_0^s\cap C_2^t \to & \eta_0^2 : s=w_2=a_1y-e_1w_1x^2=0 \\ C_1^s\cap C_1^t \to & \eta_1^1 : e_1=w_1=w_2y+a_1x+\widetilde{a}_3st=0 \\ C_1^s\cap C_2^t :\to & \eta_1^2 : e_1=w_2=y(a_1x+\widetilde{a}_3st)-st^2w_1(\widetilde{a}_4x+\widetilde{a}_6st)=0 \end{cases} \tag{12.33}$$

The splittings of curves are

$$\text{On } S \cap T: \begin{cases} C_0^s \longrightarrow \eta_0^0 + \eta_0^1 + \eta_0^2 \\ C_1^s \longrightarrow \eta_1^1 + \eta_1^2 \\ C_0^t \longrightarrow \eta_0^0 \\ C_1^t \longrightarrow \eta_0^1 + \eta_1^1 \\ C_2^t \longrightarrow \eta_0^2 + \eta_1^2 \end{cases} \tag{12.34}$$

This corresponds to I_5^s, which is represented in Figure 12.10.

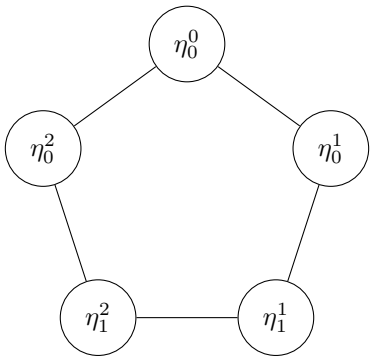

Figure 12.10: Fiber over the generic point of the locus $S \cap T$ in Resolution III of the I_2^s+I_3^s-model.

From the splittings of the curves, we compute the intersection numbers to get the weight vectors and further deduce the representations.

This has two further specializations when the discriminant of η_1^2 vanishes. The first enhancement

	D_0^s	D_1^s	D_0^t	D_1^t	D_2^t	Weight	Representation
η_0^0	0	0	-2	1	1	[0;-1,-1]	$(1, 8)$
η_0^1	-1	1	1	-1	0	[-1;1,0]	$(2, 3)$
η_1^1	1	-1	0	-1	1	[1;1,-1]	$(2, \bar{3})$
η_1^2	1	-1	0	1	-1	[1;-1,1]	$(2, 3)$
η_0^2	-1	1	1	0	-1	[-1;0,1]	$(2, \bar{3})$

Table 12.8: Weights of vertical curves and representations in the resolution III of the $I_2^s+I_3^s$-model.

is when $a_1 = 0$. We observe the following splittings for the elliptical fibrations:

$$\text{On } S \cap T \cap V(a_1): \begin{cases} \eta_0^0 & \longrightarrow & \eta_0^0 : s = t = w_2 y^2 - w_1 e_1 x^3 = 0 \\ \eta_0^1 & \longrightarrow & \eta_0^{12} : s = w_1 = w_2 = 0 \\ \eta_0^2 & \longrightarrow & \eta_0^{12} : s = w_2 = w_1 = 0,\ \eta_{01}^2 : s = w_2 = e_1 = 0 \\ \eta_1^1 & \longrightarrow & \eta_1^1 : e_1 = w_1 = w_2 y + \widetilde{a}_3 st = 0 \\ \eta_1^2 & \longrightarrow & \eta_{01}^2 : e_1 = w_2 = s = 0, \eta_1^2 : e_1 = w_2 = \widetilde{a}_3 y - t w_1(\widetilde{a}_4 x + \widetilde{a}_6 st) = 0 \end{cases} \tag{12.35}$$

The splittings from the five divisors to the codimension-three enhancement when $a_1 = 0$ is

$$\text{On } S \cap T \cap V(a_1): \begin{cases} C_0^s \longrightarrow \eta_0^0 + \eta_0^{12} + \eta_{01}^2 \\ C_1^s \longrightarrow \eta_{01}^2 + \eta_1^1 + \eta_1^2 \\ C_0^t \longrightarrow \eta_0^0 \\ C_1^t \longrightarrow \eta_0^{12} + \eta_1^1 \\ C_2^t \longrightarrow \eta_0^{12} + \eta_{01}^2 + \eta_1^2. \end{cases} \tag{12.36}$$

The generic fiber over $S \cap T \cap V(a_1)$ is a non-Kodaira fiber illustrated in Figure 12.11 and corresponding to an incomplete fiber of type IV*.

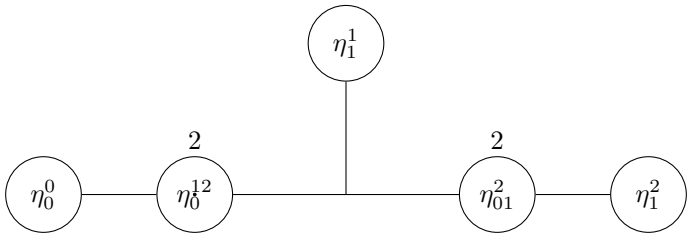

Figure 12.11: Fiber over the generic point of the locus $S \cap T \cap V(a_1)$ in Resolution III of the I_2^s+I_3^s-model.

Now consider the other condition, $a_1\widetilde{a}_6 = \widetilde{a}_3\widetilde{a}_4$, to get the other specialization. The curve η_1^2 splits into two fibers intersecting each other:

$$\text{on } S \cap T \cap V(a_1\widetilde{a}_6 - \widetilde{a}_3\widetilde{a}_4): \quad \eta_1^2 \longrightarrow \eta_1^{2A} + \eta_1^{2B}. \tag{12.37}$$

Thus, we get a fiber enhancement of type $\mathrm{I}_6^{\mathrm{s}}$, which is represented in Figure 12.12.

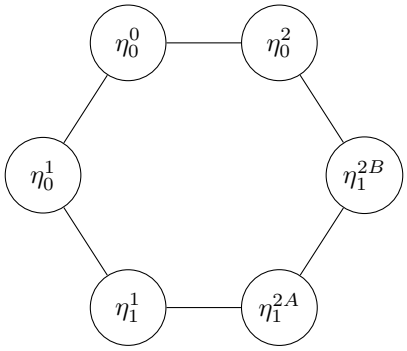

Figure 12.12: Fiber over the generic point of the locus $S \cap T \cap V(a_1\widetilde{a}_6 - \widetilde{a}_3\widetilde{a}_4)$ in Resolution III of the $\mathrm{I}_2^{\mathrm{s}}$+$\mathrm{I}_3^{\mathrm{s}}$-model.

12.5.4 Resolution IV

The resolution IV is given by the following sequence of blowups:

$$X_0 \xleftarrow{(x,y,t|w_1)} X_1 \xleftarrow{(y,w_1|w_2)} X_2 \xleftarrow{(x,y,s|e_1)} X_3 \ . \tag{12.38}$$

Its projective coordinates are then given by

$$[e_1w_1w_2x\,;\ e_1w_1w_2^2y\,;\ z=1][e_1x\,;\ e_1w_2y\,;\ t][e_1y\,;\ w_1][x\,;\ y\,;\ s]. \tag{12.39}$$

The proper transform of the elliptic fibration for the resolution III is the same as equation (12.13) and the five fibral divisors are thus identical to the equation (12.15). At the intersection of both divi-

sors S and T, we get the following curves:

$$\text{On } S \cap T \cap V(a_1) : \begin{cases} C_0^s \cap C_0^t \longrightarrow & \eta_0^0 : s = t = y(w_2 y + a_1 x) - w_1 e_1 x^3 = 0, \\ C_0^s \cap C_1^t \longrightarrow & \eta_0^1 : s = w_1 = w_2 y + a_1 x = 0, \\ C_0^s \cap C_2^t \longrightarrow & \eta_0^{2A} : s = w_2 = x = 0,\ \eta_0^{2B} : s = w_2 = a_1 y - w_1 e_1 x^2 = 0, \\ C_1^s \cap C_2^t \longrightarrow & \eta_1^2 : e_1 = w_2 = y(a_1 x + \widetilde{a}_3 s t) - s t^2 w_1 (\widetilde{a}_4 x + \widetilde{a}_6 s t) = 0. \end{cases} \tag{12.40}$$

From the five fibral divisors, we summarize the splittings of the curves to be the following.

$$\text{On } S \cap T \cap V(a_1) : \begin{cases} C_0^s \longrightarrow \eta_0^0 + \eta_0^1 + \eta_0^{2A} + \eta_0^{2B} \\ C_1^s \longrightarrow \eta_1^2 \\ C_0^t \longrightarrow \eta_0^0 \\ C_1^t \longrightarrow \eta_0^1 \\ C_2^t \longrightarrow \eta_0^{2A} + \eta_0^{2B} + \eta_1^2. \end{cases} \tag{12.41}$$

This corresponds to I_5^s as it is represented in Figure 12.13.

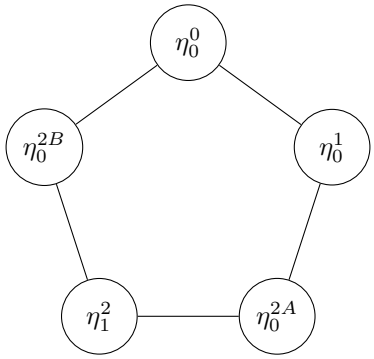

Figure 12.13: Fiber over the generic point of the locus $S \cap T$ in Resolution IV of the I_2^s+I_3^s-model.

The intersection numbers are computed using the equation (12.41) to get the weights and the representations of the curves.

	D_0^s	D_1^s	D_0^t	D_1^t	D_2^t	Weight	Representation
η_0^0	0	0	-2	1	1	[0;-1,-1]	$(1, 8)$
η_0^1	0	0	1	-2	1	[0;2,-1]	$(1, 8)$
η_0^{2A}	-1	1	0	1	-1	[-1;-1,1]	$(2, 3)$
η_1^2	2	-2	0	0	0	[2;0,0]	$(3, 1)$
η_0^{2B}	-1	1	1	0	-1	[-1;0,1]	$(2, \bar{3})$

Table 12.9: Weights of vertical curves and representations in the resolution IV of the $I_2^s+I_3^s$-model.

This has two further specializations in codimension-three. The first specialization is when $a_1 = 0$.

We observe the following splittings for the elliptical fibrations

$$\text{on } S\cap T\cap V(a_1):\ \begin{cases} \eta_o^{\circ} & \longrightarrow & \eta_o^{\circ}: s=t=w_2y^2-w_1e_1x^3=0, \\ \eta_o^{\mathrm{I}} & \longrightarrow & \eta_o^{12}: s=w_1=w_2=0, \\ \eta_o^{2A} & \longrightarrow & \eta_o^{2A}: s=w_2=x=0, \\ \eta_o^{2B} & \longrightarrow & \eta_o^{12}: s=w_2=w_1=0,\ \eta_{o1}^{2}: s=w_2=e_1=0,\ \eta_o^{2A}: s=w_2=x=0, \\ \eta_1^{2} & \longrightarrow & \eta_{o1}^{2}: e_1=w_2=s=0,\ \eta_1^{2}: e_1=w_2=\widetilde{a}_3y-tw_1(\widetilde{a}_4x+\widetilde{a}_6st)=0. \end{cases} \tag{12.42}$$

For this codimension-three fiber enhancement, we get a specialization of E_6, as it is represented in Figure 12.14.

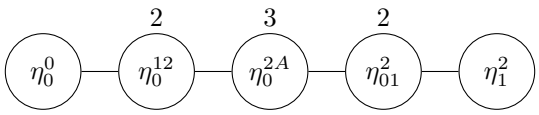

Figure 12.14: Fiber over the generic point of the locus $S\cap T\cap V(a_1)$ in Resolution IV of the $\mathrm{I}_2^{\mathrm{s}}$+$\mathrm{I}_3^{\mathrm{s}}$-model.

The other specialization is when $a_1\widetilde{a}_6 = \widetilde{a}_3\widetilde{a}_4$. Then all the other fibers are the same except η_1^2, which splits into two curves intersecting each other:

$$\text{on } S\cap T\cap V(a_1\widetilde{a}_6-\widetilde{a}_3\widetilde{a}_4):\quad \eta_1^2 \longrightarrow \eta_1^{2A}+\eta_1^{2B}. \tag{12.43}$$

For this codimension-three enhancement, we get a fiber of type $\mathrm{I}_6^{\mathrm{s}}$ as in Figure 12.15.

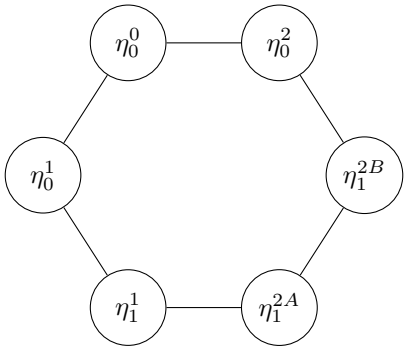

Figure 12.15: Fiber over the generic point of the locus $S \cap T \cap V(a_1\widetilde{a}_6 - \widetilde{a}_3\widetilde{a}_4)$ in Resolution IV of the $\mathrm{I}_2^{\mathrm{s}}$+$\mathrm{I}_3^{\mathrm{s}}$-model.

12.5.5 Flops

In this section, we discuss the flops between the resolutions I, II, III, and IV. We recall that the resolutions I′, II′, III′, IV′ are their mirrors under the birational map induced by the involution of the Mordell–Weil group. We consider the case of the $\mathrm{I}_2^{\mathrm{s}}$+$\mathrm{I}_3^{\mathrm{s}}$ model analyzed in Section 12.5. The other case follows the same scheme. When there is a simple flop between two resolutions, if the flopping curve has weights ω in one of the resolutions, is replaced in the other by a curve of weights $-\omega$. Each resolution corresponds to a minimal model over the Weierstrass model. Hence, in the hyperplane arrangement, each resolution corresponds to a specific chamber. When two resolutions are connected by a flop of a curve of weight ω, the hyperplane separating the corresponding chamber is exactly the hyperplane $\omega^{\perp}$ perpendicular to ω. It follows that a chamber is uniquely defined by its possible flopping curves. We determine in Table 12.10 all the flopping curves and show that their weights coincide with the hyperplanes separating two chambers of the hyperplane arrangement. These curves are

identified with their corresponding weights from Table 12.4. This result matches with the analysis in Figure 12.3, which completes the correspondence between the geometry and the representation theory.

Flopping curves									Weight
Resolution I:	$\eta_1^{\circ A}$	$[1;0,-1]$	$(2,3)$	$\leftrightarrow$	Resolution II:	η_0^2	$[-1;0,1]$	$(2,\bar{3})$	$\omega_3^{(2,3)}$
Resolution II:	η_1^{I}	$[1;-1,0]$	$(2,\bar{3})$	$\leftrightarrow$	Resolution III:	η_0^{I}	$[-1;1,0]$	$(2,3)$	$\omega_4^{(2,3)}$
Resolution III:	η_1^{I}	$[1;1,-1]$	$(2,\bar{3})$	$\leftrightarrow$	Resolution IV:	η_0^{2A}	$[-1;-1,1]$	$(2,3)$	$\omega_5^{(2,3)}$

Table 12.10: The fibers that is the one that separates between the chambers and thus responsible for flops in the $\mathrm{I}_2^{\mathrm{s}}+\mathrm{I}_3^{\mathrm{s}}$-model. The weight of the contracted curve in a (terminal) flop connecting two resolutions is normal to the facet common to the closures of the corresponding chambers in the hyperplane arrangement.

12.6 The III+IV$^{\mathrm{s}}$ Model

In this section, we study the fiber structure of the crepant resolutions of the III + IV$^{\mathrm{s}}$-model defined by the following Weierstrass equation:

$$Y_0 : y^2 + \widetilde{a}_1 stxy + \widetilde{a}_3 sty = x^3 + \widetilde{a}_2 stx^2 + \widetilde{a}_4 st^2 x + \widetilde{a}_6 s^2 t^3, \tag{12.44}$$

where the fiber III and IV$^{\mathrm{s}}$ are the fibers over the generic point of $S = V(s)$ and $T = V(t)$ respectively. It corresponds to the low-right corner of Figure 12.1. In particular, the fiber over S and T can-

not specialize further while preserving their dual graphs (and hence, the gauge group $\mathrm{SU}(2)\times\mathrm{SU}(3)$). In [141], this model was explored using the point of view of string junctions.

Here, we analyze the geometry of the crepant resolutions of the III + IV^{s}-model. The triple intersection numbers are the same as those of the $\mathrm{I}_2^{\mathrm{s}}$+$\mathrm{I}_3^{\mathrm{s}}$-model. The fiber over the generic point of $S\cap T$ is a non-Kodaira fiber corresponding to a fiber of type IV^* with some nodes contracted. Such a fiber enhances further over $S\cap T\cap V(\widetilde{a}_3)$ to a non-Kodaira fiber corresponding to a fiber of type III^* with some nodes contracted. The non-Kodaira fibers observed for the III+IV^{s}-model were already seen in the $\mathrm{I}_2^{\mathrm{s}}$+$\mathrm{I}_3^{\mathrm{s}}$-model but one codimension higher.

12.6.1 Resolution I

The resolution I is defined by the following sequence of blowups:

$$X_0 \xleftarrow{(x,y,s|e_1)} X_1 \xleftarrow{(x,y,t|w_1)} X_2 \xleftarrow{(y,w_1|w_2)} X_3 \tag{12.45}$$

The proper transform of the III+IV^{s}-model is

$$Y : y(w_2y + \widetilde{a}_1se_1tw_1w_2x + \widetilde{a}_3st) = w_1(e_1x^3 + \widetilde{a}_2se_1tx^2 + \widetilde{a}_4st^2x + \widetilde{a}_6s^2t^3). \tag{12.46}$$

The projective coordinates are then given by

$$[e_1w_1w_2x\,;\ e_1w_1w_2^2y\,;\ z=1][w_1w_2x\,;\ w_1w_2^2y\,;\ s][x\,;\ w_2y\,;\ t][y\,;\ w_1]. \tag{12.47}$$

The fibral divisors are

$$\mathrm{I}_2^s:\begin{cases} D_0^s: & s = w_2y^2 - w_1e_1x^3 = 0, \\ D_1^s: & e_1 = y(w_2y + \widetilde{a}_3st) - st^2w_1(\widetilde{a}_4x + \widetilde{a}_6st) = 0, \end{cases} \tag{12.48}$$

$$\mathrm{I}_3^s:\begin{cases} D_0^t: & t = w_2y^2 - w_1e_1x^3 = 0, \\ D_1^t: & w_1 = w_2y + \widetilde{a}_3st = 0, \\ D_2^t: & w_2 = \widetilde{a}_3sty - w_1(e_1x^3 + \widetilde{a}_2se_1tx^2 + \widetilde{a}_4st^2x + \widetilde{a}_6s^2t^3) = 0. \end{cases} \tag{12.49}$$

Over the generic point of the intersection of S and T, we get the following irreducible curves

$$\text{On } S\cap T:\begin{cases} C_0^s\cap C_0^t & \to & \eta_0^0 : s = t = w_2y^2 - w_1e_1x^3 = 0, \\ C_1^s\cap C_0^t & \to & \eta_1^{02} : e_1 = t = w_2 = 0,\ \eta_1^{0A} : e_1 = t = y = 0, \\ C_1^s\cap C_1^t & \to & \eta_1^{1} : e_1 = w_1 = w_2y + \widetilde{a}_3st = 0, \\ C_1^s\cap C_2^t & \to & \eta_1^{02} : e_1 = w_2 = t = 0,\ \eta_1^{2} : e_1 = w_2 = \widetilde{a}_3y - tw_1(\widetilde{a}_4x + \widetilde{a}_6st) = 0. \end{cases} \tag{12.50}$$

The fiber over the generic point of $S\cap T$ has a structure given by Figure 12.16, and corresponds to a fiber of type IV* with contracted nodes. At the collision $S\cap T$, the components of the fibers III and

IV^{s} degenerate as follows.

$$\text{On } S \cap T : \begin{cases} C_{0}^{s} \longrightarrow \eta_{0}^{0}, \\ C_{1}^{s} \longrightarrow 2\eta_{1}^{02} + 2\eta_{1}^{0A} + \eta_{1}^{1} + \eta_{1}^{2}, \\ C_{0}^{t} \longrightarrow \eta_{0}^{0} + \eta_{1}^{02} + 2\eta_{1}^{0A}, \\ C_{1}^{t} \longrightarrow \eta_{1}^{1}, \\ C_{2}^{t} \longrightarrow \eta_{1}^{02} + \eta_{1}^{2}. \end{cases} \tag{12.51}$$

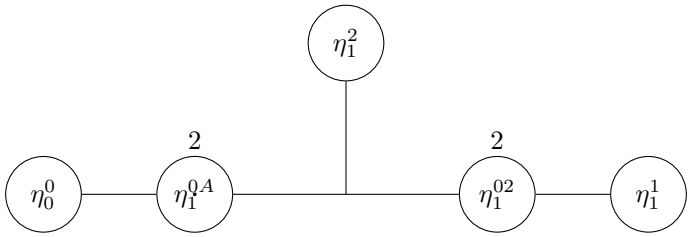

Figure 12.16: Fiber over the generic point of the locus $S \cap T$ in Resolution I of the III+IV^{s}-model.

We observe that this is identical to the fiber in the resolution I of the $\mathrm{I}_{2}^{s} + \mathrm{I}_{3}^{s}$-model in codimension-three over $S \cap T \cap V(a_{1})$.

In order to get the weights of the curves, the intersection numbers are computed between the codimension-two curves and the fibral divisors.

	D_0^s	D_1^s	D_0^t	D_1^t	D_2^t	Weight	Representation
η_0°	-2	2	0	0	0	[-2;0,0]	$(3,1)$
$\eta_1^{\circ A}$	1	-1	-1	0	1	[1;0,-1]	$(2,3)$
η_1^2	0	0	1	0	-1	[0;0,1]	$(1,\bar{3})$
$\eta_1^{\circ 2}$	0	0	0	1	-1	[0;-1,1]	$(1,3)$
η_1^1	0	0	1	-2	1	[0;2,-1]	$(1,8)$

Table 12.11: Weights of vertical curves and representations in the resolution I of the III+IV^s-model.

We note that the sum of the two curves $\eta_1^{\circ 2} + \eta_1^{\circ A}$ produce the weight $[1;-1,0]$ of the representation $(2,\bar{3})$. In the resolution I of the $I_2^s + I_3^s$-model, the weight $[1;-1,0]$ corresponds to $\eta_1^{\circ B}$ in codimension-two, which splits into the two curves in codimension-three with the same weights as $\eta_1^{\circ 2}$ and $\eta_1^{\circ A}$.

The fiber over the generic point of $S \cap T$ shown on Figure 12.16 specializes further when $\widetilde{a}_3 = 0$:

$$\text{on } S \cap T \cap V(\widetilde{a}_3) : \begin{cases} \eta_1^1 \longrightarrow \eta_1^{12}, \\ \eta_1^2 \longrightarrow \eta_1^{\circ 2} + \eta_1^{12} + \eta_1^2, \end{cases} \tag{12.52}$$

where the new curves are given by

$$\begin{cases} \eta_1^{12}: & e_1 = w_1 = w_2 = 0, \\ \eta_1^{02}: & e_1 = w_2 = t = 0, \\ \eta_1^{2}: & e_1 = w_2 = \widetilde{a}_4 x + \widetilde{a}_6 st = 0. \end{cases} \tag{12.53}$$

The fiber over the generic point $S \cap T \cap V(\widetilde{a}_3)$ is illustrated in Figure 12.17, and corresponds to a fiber of type III* with contracted nodes.

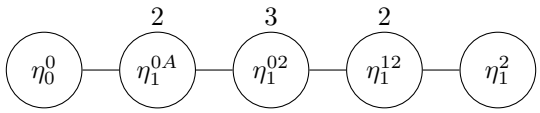

Figure 12.17: Fiber over the generic point of the locus $S \cap T \cap V(\widetilde{a}_3)$ in Resolution I of the III+IV^s-model.

12.6.2 Resolution II

In this section, we study the resolution II in detail. As the resolution II requires making a first blowup around a singular center, it is useful to rewrite equation (12.44) as

$$Y_0: \begin{cases} y(y + \widetilde{a}_1 p_0 x + \widetilde{a}_3 p_0) = x^3 + \widetilde{a}_2 p_0 x^2 + \widetilde{a}_4 p_0 t x + \widetilde{a}_6 p_0^2 t \\ p_0 = st \end{cases}. \tag{12.54}$$

The resolution II is then given by the following sequence of blowups

$$X_0 \xleftarrow{(x,y,p_0|p_1)} X_1 \xleftarrow{(y,t,p_1|w_1)} X_2 \xleftarrow{(t,p_0|w_2)} X_3 \ . \tag{12.55}$$

Where $X_0 = \mathbb{P}[\mathscr{O}_B \oplus \mathscr{L}^{\otimes 2} \oplus \mathscr{L}^{\otimes 3}]$. The projective coordinates are then

$$[p_1 w_1 x \ : \ p_1 w_1^2 y \ : \ z = 1][x \ : \ w_1 y \ : \ p_0 w_2][y \ : \ t w_2 \ : \ p_1][t \ : \ p_0], \tag{12.56}$$

and the proper transform is

$$Y : \begin{cases} y(w_1 y + \widetilde{a}_1 p_0 w_2 x + \widetilde{a}_3 p_0 w_2) = p_1 x^3 + \widetilde{a}_2 p_0 p_1 w_2 x^2 + \widetilde{a}_4 p_0 t w_2^2 x + \widetilde{a}_6 p_0^2 t w_2^3 \\ p_0 p_1 = st \end{cases} . \tag{12.57}$$

The variety $X_1 = Bl_{(x,y,p_0)} X_0$ has double point singularities on $p_0 = p_1 = s = t = 0$. The fibral divisors are:

$$\text{III} : \begin{cases} D_0^s : \quad s = p_0 = w_1 y^2 - p_1 x^3 = 0 \\ D_1^s : \quad s = p_1 = y(w_1 y + \widetilde{a}_1 p_0 w_2 x + \widetilde{a}_3 p_0 w_2) - (p_1 x^3 + \widetilde{a}_4 p_0 t w_2^2 x + \widetilde{a}_6 p_0^2 t w_2^3) = 0 \end{cases} \tag{12.58}$$

$$\mathrm{IV}^{s}:\begin{cases} D_0^t: & w_2 = p_0p_1 - st = w_1y^2 - p_1x^3 = 0 \\ D_1^t: & t = p_1 = w_1y + \widetilde{a}_1p_0w_2x + \widetilde{a}_3p_0w_2 = 0 \\ D_2^t: & w_1 = p_0p_1 - st = y(\widetilde{a}_1p_0w_2x + \widetilde{a}_3p_0w_2) - (p_1x^3 + \widetilde{a}_2p_0p_1w_2x^2 + \widetilde{a}_4p_0tw_2^2x + \widetilde{a}_6p_0^2tw_2^3) = 0 \end{cases} \tag{12.59}$$

At the intersection of S and T, the fiber enhances to a non-Kodaira fiber presented in Figure 12.18. This is realized by the following splitting of curves.

$$\text{On } S\cap T:\begin{cases} C_0^s \longrightarrow \eta_0^0 + \eta_{01}^2 \\ C_1^s \longrightarrow \eta_{01}^2 + 2\eta_1^{02} + \eta_1^{I} + \eta_1^2 \\ C_0^t \longrightarrow \eta_0^0 + \eta_1^{02} \\ C_1^t \longrightarrow \eta_1^{I} \\ C_2^t \longrightarrow 2\eta_{01}^2 + \eta_1^{02} + \eta_1^2 \end{cases} \tag{12.60}$$

The curves at the intersection are given by

$$\text{On } S \cap T: \begin{cases} C_0^s \cap C_1^t & \longrightarrow \quad \eta_0^0 : s = p_0 = w_2 = w_1 y^2 - p_1 x^3 = 0 \\ C_0^s \cap C_2^t & \longrightarrow \quad \eta_0^2 : s = p_0 = w_1 = p_1 = 0 \\ C_1^s \cap C_0^t & \longrightarrow \quad \eta_1^{02} : s = p_1 = w_2 = w_1 = 0 \\ C_1^s \cap C_1^t & \longrightarrow \quad \eta_1^1 : s = p_1 = t = w_1 y + \widetilde{a}_3 p_0 w_2 = 0 \\ C_1^s \cap C_2^t & \longrightarrow \quad \eta_1^{02} : s = p_1 = w_1 = w_2 = 0,\ \eta_{01}^2 : s = p_1 = w_1 = p_0 = 0, \\ & \qquad\quad \eta_1^2 : s = p_1 = w_1 = \widetilde{a}_3 y - \widetilde{a}_4 t w_2 x + \widetilde{a}_6 p_0 t w_2^2 = 0 \end{cases} \tag{12.61}$$

Note that we had the same fiber earlier in the resolution I of the $\mathrm{I}_2^s + \mathrm{I}_3^s$-model in codimension-three with a condition $a_1 = 0$.

	D_0^s	D_1^s	D_0^t	D_1^t	D_2^t	Weight	Representation
η_0^0	-1	1	-1	0	1	[-1;0,-1]	$(2, 3)$
η_{01}^2	-1	1	1	0	-1	[-1;0,1]	$(2, \overline{3})$
η_1^1	0	0	1	-2	1	[0;2,-1]	$(1, 8)$
η_1^{02}	1	-1	-1	1	0	[1;-1,0]	$(2, \overline{3})$
η_1^2	1	-1	0	0	0	[1;0,0]	$(2, 1)$

Table 12.12: Weights of vertical curves and representations in the resolution II of the III+IV^s-model.

The chain $\eta_1^{02} + \eta_{01}^2 + \eta_1^2$ produces the weight $[1; -1, 1]$ of the representation $(2, 3)$. In the case of the resolution II of the $\mathrm{I}_2^s + \mathrm{I}_3^s$-model, the sum of the curves corresponds to η_1^2 in codimension-two, which splits into the three curves in codimension-three.

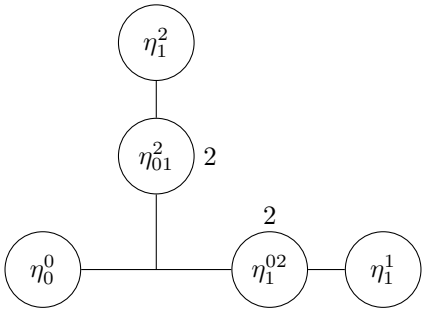

Figure 12.18: Fiber over the generic point of the locus $S \cap T$ in Resolution II of the III+IV^s-model.

There is an enhancement when $\widetilde{a}_3$ as the two curves $\eta_{\text{I}}^{\text{I}}$ and η_{I}^2 degenerate as follows:

$$\text{on } S \cap T \cap V(\widetilde{a}_3): \begin{cases} \eta_{\text{I}}^{\text{I}} \longrightarrow \eta_{\text{I}}^{\text{I2}}, \\ \eta_{\text{I}}^2 \longrightarrow \eta_{\text{I}}^{\text{O2}} + \eta_{\text{I}}^{\text{I2}} + \eta_{\text{I}}^2, \end{cases} \tag{12.62}$$

where the new curves are given by

$$\begin{cases} \eta_{\text{I}}^{\text{I2}}: & s = p_{\text{I}} = t = w_{\text{I}} = 0, \\ \eta_{\text{I}}^{\text{O2}}: & s = p_{\text{I}} = w_{\text{I}} = w_2 = 0, \\ \eta_{\text{I}}^2: & s = p_{\text{I}} = w_{\text{I}} = \widetilde{a}_4 x - \widetilde{a}_6 p_0 w_2 = 0. \end{cases} \tag{12.63}$$

For this codimension-three enhancement, we get a non-Kodaira fiber corresponding to a non-Kodaira fiber corresponding to a contracted fiber of type IV* as in Figure 12.19.

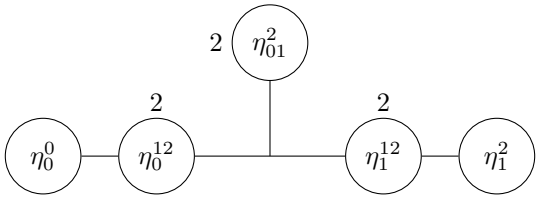

Figure 12.19: Fiber over the generic point of the locus $S \cap T \cap V(\widetilde{a}_3)$ in Resolution II of the III+IV^s-model.

12.6.3 Resolution III

The Resolution III is defined by the following sequence of blowups:

$$X_0 \xleftarrow{(x,y,t|w_1)} X_1 \xleftarrow{(x,y,s|e_1)} X_2 \xleftarrow{(y,w_1|w_2)} X_3 \tag{12.64}$$

The projective coordinates are then given by

$$[e_1 w_1 w_2 x\,;\, e_1 w_1 w_2^2 y\,;\, z = 1][e_1 x\,;\, e_1 w_2 y\,;\, t][x\,;\, w_2 y\,;\, s][y\,;\, w_1]. \tag{12.65}$$

The proper transform is identical to equation (12.46).

On the intersection of S and T, we see the following curves:

$$\text{On } S \cap T : \begin{cases} C_{\text{o}}^{\text{s}} \cap C_{\text{o}}^{\text{t}} & \longrightarrow \eta_{\text{o}}^{\text{o}} : s = t = w_2 y^2 - w_1 e_1 x^3 = 0, \\ C_{\text{o}}^{\text{s}} \cap C_{\text{I}}^{\text{t}} & \longrightarrow \eta_{\text{o}}^{\text{I2}} : s = w_1 = w_2 = 0, \\ C_{\text{o}}^{\text{s}} \cap C_{2}^{\text{t}} & \longrightarrow \eta_{\text{oI}}^{2} : s = w_2 = e_1 = 0,\ \eta_{\text{o}}^{\text{I2}} : s = w_2 = w_1 = 0, \\ C_{\text{I}}^{\text{s}} \cap C_{\text{I}}^{\text{t}} & \longrightarrow \eta_{\text{I}}^{\text{I}} : e_1 = w_1 = w_2 y + \widetilde{a}_3 s t = 0, \\ C_{\text{I}}^{\text{s}} \cap C_{2}^{\text{t}} & \longrightarrow \eta_{\text{oI}}^{2} : e_1 = w_2 = s = 0, \eta_{\text{I}}^{2} : e_1 = w_2 = \widetilde{a}_3 y - t w_1 (\widetilde{a}_4 x + \widetilde{a}_6 s t) = 0. \end{cases} \tag{12.66}$$

Hence, we can deduce that the five fibral divisors split in the following way to produce the fiber in codimension-two, which is presented in Figure 12.20.

$$\text{On } S \cap T : \begin{cases} C_{\text{o}}^{\text{s}} & \longrightarrow \eta_{\text{o}}^{\text{o}} + 2\eta_{\text{o}}^{\text{I2}} + \eta_{\text{oI}}^{2}, \\ C_{\text{I}}^{\text{s}} & \longrightarrow \eta_{\text{oI}}^{2} + \eta_{\text{I}}^{\text{I}} + \eta_{\text{I}}^{2}, \\ C_{\text{o}}^{\text{t}} & \longrightarrow \eta_{\text{o}}^{\text{o}}, \\ C_{\text{I}}^{\text{t}} & \longrightarrow \eta_{\text{o}}^{\text{I2}} + \eta_{\text{I}}^{\text{I}}, \\ C_{2}^{\text{t}} & \longrightarrow \eta_{\text{o}}^{\text{I2}} + 2\eta_{\text{oI}}^{2} + \eta_{\text{I}}^{2}. \end{cases} \tag{12.67}$$

We observe that we had the same fiber earlier in the resolution III of the $\text{I}_2^{\text{s}} + \text{I}_3^{\text{s}}$-model in codimension-three with a condition $a_1 = 0$.

In order to get the weights of the curves, the intersection numbers are computed between the codimension-two curves and the fibral divisors.

	D_0^s	D_1^s	D_0^t	D_1^t	D_2^t	Weight	Representation
η_0^0	0	0	-2	1	1	[0;-1,-1]	$(1, 8)$
η_0^{12}	-1	1	1	-1	0	[-1;1,0]	$(2, 3)$
η_1^1	1	-1	0	-1	1	[1;1,-1]	$(2, \bar{3})$
η_{01}^2	0	0	0	1	-1	[0;-1,1]	$(1, 3)$
η_1^2	1	-1	0	0	0	[1;0,0]	$(2, 1)$

Table 12.13: Weights of vertical curves and representations in the resolution III of the III+IV^s-model at the III+IV^s collision.

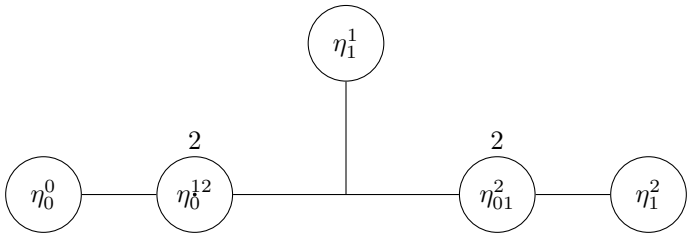

Figure 12.20: Fiber over the generic point of the locus $S \cap T$ in Resolution III of the III+IV^s-model.

The sum of the two curves $\eta_0^{12} + \eta_{01}^2$ produce the weight $[-1; 0, 1]$ of the representation $(2, \bar{3})$. Moreover, the sum of $\eta_{01}^2 + \eta_1^2$ produce the weight $[1; -1, 1]$, which corresponds to a representation $(2, 3)$. In the case of the resolution III of the $\mathrm{I}_2^s + \mathrm{I}_3^s$-model, the former sum corresponds to η_0^2 and the latter sum corresponds to η_1^2 in codimension-two.

Over $S \cap T \cap V(\widetilde{a}_3)$ the curve η_1^2 splits as:

$$\text{on } S \cap T \cap V(\widetilde{a}_3): \begin{cases} \eta_1^{\mathrm{I}} \longrightarrow \eta_1^{\mathrm{I2}}, \\ \eta_1^2 \longrightarrow \eta_1^{\mathrm{I2}} + \eta_1^2, \end{cases} \tag{12.68}$$

where the new curves are given by

$$\begin{cases} \eta_1^{\mathrm{I2}}: \quad e_1 = w_1 = w_2 = 0, \\ \eta_1^2: \quad e_1 = w_2 = \widetilde{a}_4 x + \widetilde{a}_6 st = 0. \end{cases} \tag{12.69}$$

This corresponds to the codimension-three enhancement in Figure 12.21.

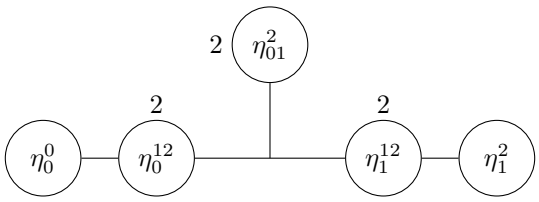

Figure 12.21: Fiber over the generic point of the locus $S \cap T \cap V(\widetilde{a}_3)$ in Resolution III of the III+IV^s-model.

12.6.4 Resolution IV

The Resolution IV is defined by the following sequence of blowups

$$X_0 \xleftarrow{(x,y,t|w_1)} X_1 \xleftarrow{(y,w_1|w_2)} X_2 \xleftarrow{(x,y,s|e_1)} X_3. \tag{12.70}$$

Its projective coordinates are then given by

$$[e_1w_1w_2x\,;\,e_1w_1w_2^2y\,;\,z=1][e_1x\,;\,e_1w_2y\,;\,t][e_1y\,;\,w_1][x\,;\,y\,;\,s]. \tag{12.71}$$

The proper transform is identical to equation (12.46).

Over the generic point of the intersection of S and T, we see the following irreducible vertical curves.

$$\text{On } S\cap T: \begin{cases} C_0^s\cap C_0^t & \longrightarrow \quad \eta_0^0 : s=t=w_2y^2-w_1e_1x^3=0, \\ C_0^s\cap C_1^t & \longrightarrow \quad \eta_0^{12} : s=w_1=w_2=0, \\ C_0^s\cap C_2^t & \longrightarrow \quad \eta_0^{2A} : s=w_2=x=0,\ \eta_{01}^2 : s=w_2=e_1=0,\ \eta_0^{12} : s=w_2=w_1=0 \\ C_1^s\cap C_2^t & \longrightarrow \quad \eta_{01}^2 : e_1=w_2=s=0, \eta_1^2 : e_1=w_2=\widetilde{a}_3y-tw_1(\widetilde{a}_4x+\widetilde{a}_6st)=0. \end{cases} \tag{12.72}$$

The collision gives the following splitting of curves from the fiber III and IV^s resulting in the fiber

illustrated in Figure 12.22:

$$\text{On } S \cap T: \begin{cases} C_0^{\mathfrak{s}} \longrightarrow \eta_0^0 + 2\eta_0^{12} + 3\eta_0^{2A} + \eta_{01}^2, \\ C_1^{\mathfrak{s}} \longrightarrow \eta_{01}^2 + \eta_1^2, \\ C_0^{\mathfrak{t}} \longrightarrow \eta_0^0, \\ C_1^{\mathfrak{t}} \longrightarrow \eta_0^{12}, \\ C_2^{\mathfrak{t}} \longrightarrow \eta_0^{12} + 3\eta_0^{2A} + 2\eta_{01}^2 + \eta_1^2. \end{cases} \tag{12.73}$$

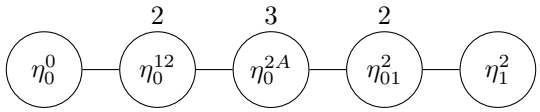

Figure 12.22: Fiber over the generic point of the locus $S \cap T$ in Resolution IV of the III+IV$^{\mathfrak{s}}$-model.

Note that we had the same fiber earlier in the resolution III of the $\mathrm{I}_2^{\mathfrak{s}} + \mathrm{I}_3^{\mathfrak{s}}$-model in codimension-three with a condition $a_1 = 0$.

The weights of these vertical curves and the corresponding representations are collected in Table 12.14. In order to get the weights of the curves, the intersection numbers are computed between the codimension-two curves and the fibral divisors.

The sum of the three curves $\eta_1^{02} + \eta_{01}^2 + \eta_1^2$ produce the weight $[1; -1, 1]$, which yields a representation $(2, 3)$. In the case of the resolution IV of the $\mathrm{I}_2^{\mathfrak{s}} + \mathrm{I}_3^{\mathfrak{s}}$-model, the sum of the curves corresponds

	D^s_0	D^s_1	D^t_0	D^t_1	D^t_2	Weight	Representation
η^0_0	0	0	-2	1	1	[0;-1,-1]	$(1, 8)$
η^{12}_0	0	0	1	-2	1	[0;2,-1]	$(1, 8)$
η^{2A}_0	-1	1	0	1	-1	[-1;-1,1]	$(2, 3)$
η^2_{01}	1	-1	0	0	0	[1;0,0]	$(2, 1)$
η^2_1	1	-1	0	0	0	[1;0,0]	$(2, 1)$

Table 12.14: Weights of vertical curves and representations in the resolution IV of the III+IV^s.

to η^2_1 in codimension-two, which splits into the three curves in codimension-three.

The fiber specialize further over $S \cap T \cap V(\widetilde{a}_3)$ as the curve η^2_1 becomes

$$\text{on } S \cap T \cap V(\widetilde{a}_3) : \ \eta^2_1 \to \eta^2_1 : \ e_1 = w_2 = \widetilde{a}_4 x + \widetilde{a}_6 st = 0. \tag{12.74}$$

What is now different from other points of $S \cap T$ is that the curve η^2_1 now intersect both η^2_{01} and η^{2A}_0 at the same point resulting in a different fiber structure represented in Figure 12.23.

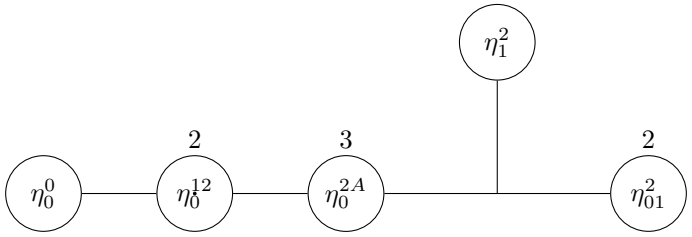

Figure 12.23: Fiber over the generic point of the locus $S \cap T \cap V(\widetilde{a}_3)$ in Resolution IV of the III+IV^s-model.

12.7 5*d* and 6*d* supergravity theories with eight supercharges

In this section, we discuss the five and six-dimensional theories with eight supercharges via Calabi–Yau compactification of M-theory and F-theory on an $\mathrm{SU}(2) \times \mathrm{SU}(3)$-model. We first compute the one-loop prepotentials of the $\mathrm{SU}(2) \times \mathrm{SU}(3)$-model in all eight chambers and match them with the triple intersection numbers of the corresponding crepant resolutions to get the number of charged hypermultiplets in each irreducible representations (fundamentals, adjoints, and bifundamental) in Section 12.7.1. Recall from Section 2.13.2 how the anomaly cancellation conditions in six-dimensional theory with a gauge group can be derived with geometric data with number of charged hypermultiplets as the unknowns. We return to our case for the gauge group $\mathrm{SU}(2) \times \mathrm{SU}(3)$ in Section 12.7.2 and show that we get a unique solution of number of hypers for the six-dimensional theory and find it to match with the result we got for the five-dimensional theory in Section 12.7.1.

12.7.1 5*d* $\mathcal{N} = 1$ supergravity theory with a gauge group $\mathrm{SU}(2) \times \mathrm{SU}(3)$

M-theory (an eleven-dimensional supergravity theory) compactified on a Calabi–Yau threefold yields a low energy physics that describes five-dimensional $\mathcal{N} = 1$ supergravity. The prepotential depends on the choice of a Coulomb chamber to get rid of the absolute values. We compute it for each of the eight chambers of an $\mathrm{SU}(2) \times \mathrm{SU}(3)$-model. The chambers are defined by Table 12.5.

Theorem 12.7.1. *The prepotential of an $SU(2) \times SU(3)$-model in the eight phases defined by the chambers of Table 12.5 are*

- *Chamber 1*

$$\begin{aligned}6\mathscr{F}^{(1)}_{IMS} = &-8(n_{1,8}-1)\varphi_1^3 - \frac{3}{2}(n_{1,3}+n_{1,\bar{3}}-2n_{1,8}+2)\varphi_1^2\varphi_2 \\ &+\frac{3}{2}(n_{1,3}+n_{1,\bar{3}}+2n_{1,8}-2)\varphi_1\varphi_2^2 + (-n_{1,3}-n_{1,\bar{3}}-8n_{1,8}+8)\varphi_2^3 \\ &-(n_{2,1}+3n_{2,3}+3n_{2,\bar{3}}+8n_{3,1}-8)\psi_1^3 - 6(n_{2,3}+n_{2,\bar{3}})\psi_1\left(\varphi_1^2-\varphi_1\varphi_2+\varphi_2^2\right)\end{aligned}$$

- *Chamber 2*

$$\begin{aligned}6\mathscr{F}^{(2)}_{IMS} = &-8(n_{1,8}-1)\varphi_1^3 - \frac{3}{2}(n_{1,3}+n_{1,\bar{3}}-2n_{1,8}+2)\varphi_1^2\varphi_2 + \frac{3}{2}(n_{1,3}+n_{1,\bar{3}}+2n_{1,8}-2)\varphi_1\varphi_2^2 \\ &-(n_{1,3}+n_{1,\bar{3}}+8n_{1,8}+n_{2,3}+n_{2,\bar{3}}-8)\varphi_2^3 - (n_{2,1}+2(n_{2,3}+n_{2,\bar{3}}+4n31-4))\psi_1^3 \\ &-3(n_{2,3}+n_{2,\bar{3}})\psi_1^2\varphi_2 - 3(n_{2,3}+n_{2,\bar{3}})\psi_1\left(2\varphi_1^2-2\varphi_1\varphi_2+\varphi_2^2\right)\end{aligned}$$

- *Chamber 3*

$$\begin{aligned}6\mathscr{F}^{(3)}_{IMS} = &-(8n_{1,8}+n_{2,3}+n_{2,\bar{3}}-8)\varphi_1^3 - \frac{3}{2}(n_{1,3}+n_{1,\bar{3}}-2n_{1,8}+2)\varphi_1^2\varphi_2 \\ &+\frac{3}{2}(n_{1,3}+n_{1,\bar{3}}+2n_{1,8}-2)\varphi_1\varphi_2^2 + (-n_{1,3}-n_{1,\bar{3}}-8n_{1,8}-n_{2,3}-n_{2,\bar{3}}+8)\varphi_2^3 \\ &+(-n_{2,1}-n_{2,3}-n_{2,\bar{3}}-8n_{3,1}+8)\psi_1^3 - 3(n_{2,3}+n_{2,\bar{3}})\psi_1^2\left(\varphi_1+\varphi_2\right) \\ &-3(n_{2,3}+n_{2,\bar{3}})\psi_1\left(\varphi_1^2-2\varphi_1\varphi_2+\varphi_2^2\right)\end{aligned}$$

- *Chamber 4*

$$\begin{aligned}
6\mathscr{F}^{(4)}_{IMS} = &-8(n_{1,8}-1)\varphi_1^3 - \frac{3}{2}(n_{1,3}+n_{1,\bar{3}}-2n_{1,8}+2n_{2,3}+2n_{2,\bar{3}}+2)\varphi_1^2\varphi_2 \\
&+\frac{3}{2}(n_{1,3}+n_{1,\bar{3}}+2n_{1,8}+2n_{2,3}+2n_{2,\bar{3}}-2)\varphi_1\varphi_2^2 \\
&-(n_{1,3}+n_{1,\bar{3}}+8n_{1,8}+2n_{2,3}+2n_{2,\bar{3}}-8))\varphi_2^3 \\
&-(n_{2,1}+8n_{3,1}-8)\psi_1^3 - 6(n_{2,3}+n_{2,\bar{3}})\psi_1^2\varphi_2
\end{aligned}$$

The prepotential $\mathscr{F}^{(i')}_{IMS}$ (for $i = 1, 2, 3, 4$) is obtained from $\mathscr{F}^{(i)}_{IMS}$ by the involution $\varphi_1 \leftrightarrow \varphi_2$.

Proof. Direct computation starting with equation (2.39) and using Table 12.5 to remove the absolute values. □

Following [129], the number of hypermultiplets are computed by comparing the prepotential and the triple intersection polynomial given in Theorem 12.3.8. Comparing the triple intersection numbers obtained in the resolutions I, II, III, IV with the prepotentials computed respectively in chambers 1, 2, 3, 4, we get

$$\begin{aligned}
&n_{2,1}+8n_{3,1} = 4LS+2S^2-3ST+8, \qquad && n_{1,8} = \frac{1}{2}(-LT+T^2+2), \\
&n_{2,3}+n_{2,\bar{3}} = ST, && n_{1,3}+n_{1,\bar{3}} = T(9L-2S-3T).
\end{aligned} \tag{12.75}$$

We see in particular that the numbers $n_{2,1}$ and $n_{3,1}$ are restricted by a linear relation but are not fixed by this method. In the case of Calabi–Yau threefolds, the vanishing of the first Chern class yields

$K = -L$ where K is the canonical class of the base B. Using Witten's genus formula [306], we get

$$n_{2,1} = -S(8K + 2S + 3T), \quad n_{3,1} = \frac{1}{2}(KS + S^2 + 2). \tag{12.76}$$

We notice that the number of (bi)fundamental matter is compatible with what is expected from the technique of intersecting branes, and when the threefold is Calabi–Yau, $K = -L$ and $n_{1,8}$ becomes the arithmetic genus of the curve T as expected from Witten's genus formula.

12.7.2 Anomaly cancellations in $6d$ $\mathcal{N} = (1, 0)$ supergravity theory

In this section, we check that the gravitational, gauge, and mixed gravitational-gauge anomalies of the six-dimensional supergravity are all canceled when the Lie algebra and the representation are

$$\mathfrak{g} = \mathrm{A}_1 \oplus \mathrm{A}_2, \quad \mathbf{R} = (2,1) \oplus (1,3) \oplus (1,\bar{3}) \oplus (2,3) \oplus (2,\bar{3}) \oplus (3,1) \oplus (1,8).$$

We follow the approach of Sadov [269] (see also [142] and [237]) and use the notation of [121]. The six-dimensional anomaly cancellation conditions put linear constraints on the number of charged hypermultiplets transforming in each irreducible representations.

First, we recall that the Euler characteristic of a Calabi–Yau threefold defined as a crepant resolution of the Weierstrass model of an $\mathrm{SU}(2) \times \mathrm{SU}(3)$-model is

$$\chi(Y) = -6(10K^2 + 5KS + 8KT + S^2 + 2ST + 2T^2), \tag{12.77}$$

where S supports A_1 and T supports A_2. We also assume that S and T are smooth divisors intersecting transversally.

We will use the anomaly cancellation conditions to explicitly compute the number of hypermultiplets transforming in each representation by requiring all anomalies to cancel. We will see that they are the same as those found in five-dimensional supergravity by comparing the triple intersection numbers of the fibral divisors and the cubic prepotentials in the Coulomb phase.

The Lie algebra of type A_1 (resp. A_2) only has a unique quartic Casimir invariant so that we don't have to impose the vanishing condition for the coefficients of $\mathrm{tr}\, F_1^4$ (resp. $\mathrm{tr}\, F_2^4$). We have the following trace identities

$$\mathrm{tr}_3 F_1^2 = 4\mathrm{tr}_2 F_2^2, \quad \mathrm{tr}_3 F_1^4 = 8(\mathrm{tr}_3 F_1^2)^2, \quad \mathrm{tr}_2 F_1^4 = \frac{1}{2}(\mathrm{tr}_2 F_1^2)^2, \tag{12.78}$$

$$\mathrm{tr}_8 F_2^2 = 6\mathrm{tr}_3 F_2^2, \quad \mathrm{tr}_8 F_2^4 = 9(\mathrm{tr}_3 F_2^2)^2, \quad \mathrm{tr}_3 F_2^4 = \frac{1}{2}(\mathrm{tr}_3 F_2^2)^2, \tag{12.79}$$

which give

$$\begin{aligned}
X_1^{(2)} &= (4 - 4n_{3,1} - n_{2,1} - 3n_{2,3} - 3n_{2,\bar{3}})\,\mathrm{tr}_2 F_1^2, \\
X_2^{(2)} &= (6 - 6n_{1,8} - n_{1,3} - n_{1,\bar{3}} - 2n_{2,3} - 2n_{2,\bar{3}})\,\mathrm{tr}_3 F_2^2, \\
X_1^{(4)} &= (8 - 8n_{3,1} - \frac{1}{2}n_{2,1} - \frac{3}{2}n_{2,3} - \frac{3}{2}n_{2,\bar{3}})(\mathrm{tr}_2 F_1^2)^2, \\
X_2^{(4)} &= (9 - 9n_{1,8} - \frac{1}{2}n_{1,3} - \frac{1}{2}n_{1,\bar{3}} - n_{2,3} - n_{2,\bar{3}})(\mathrm{tr}_3 F_2^2)^2, \\
Y_{23} &= (n_{2,3} + n_{2,\bar{3}})\,\mathrm{tr}_3 F_2^2\,\mathrm{tr}_2 F_1^2.
\end{aligned} \tag{12.80}$$

Following Sadov, the anomaly cancellation conditions are [269]:

$$\begin{aligned} &X_1^{(2)} = 6KS\,\mathrm{tr}_2 F_1^2, \qquad X_2^{(2)} = 6KT\,\mathrm{tr}_3 F_2^2, \\ &X_1^{(4)} = -3S^2(\mathrm{tr}_2 F_1^2)^2, \quad X_2^{(4)} = -3T^2(\mathrm{tr}_3 F_2^2)^2, \quad Y_{23} = ST\,\mathrm{tr}_3 F_2^2\,\mathrm{tr}_2 F_1^2. \end{aligned} \tag{12.81}$$

Comparing the coefficients, we get the following linear equations

$$\begin{gathered} 6(1-n_{1,8}) - (n_{1,3}+n_{1,\bar{3}}) - 2(n_{2,3}+n_{2,\bar{3}}) = 6KT, \quad 4(1-n_{3,1}) - n_{2,1} - 3(n_{2,3}+n_{2,\bar{3}}) = 6KS, \\ 9(1-n_{1,8}) - \frac{1}{2}(n_{1,3}+n_{1,\bar{3}}) - (n_{2,3}+n_{2,\bar{3}}) = -3T^2, \quad 8(1-n_{3,1}) - \frac{1}{2}n_{2,1} - \frac{3}{2}(n_{2,3}+n_{2,\bar{3}}) = -3S^2, \\ n_{2,3}+n_{2,\bar{3}} = ST. \end{gathered} \tag{12.82}$$

These linear equations have the following unique solution[4]

$$\begin{aligned} &n_{1,8} = \frac{1}{2}(KT+T^2+2), \qquad n_{3,1} = \frac{1}{2}(KS+S^2+2), \\ &n_{2,1} = -S(8K+2S+3T), \qquad n_{1,3}+n_{1,\bar{3}} = -T(9K+2S+3T), \qquad n_{2,3}+n_{2,\bar{3}} = ST. \end{aligned} \tag{12.83}$$

These numbers have simple geometric interpretations. The numbers $n_{1,8}$ and $n_{3,1}$ are respectively the genus of the curves T and S. The number $n_{2,3}+n_{2,\bar{3}}$ is the degree of $S\cdot T$ (intersection number of S and T). The number $n_{2,1}$ is the intersection number of S and the discriminant of the generic fiber of D_1^s. The number $n_{1,3}+n_{1,\bar{3}}$ is the intersection number of T and the discriminant of D_2^t.

[4] We recall that Witten's genus formula asserts that the number of hypermultiplets charged under the adjoint representation is given by the genus of the curve supporting the corresponding gauge group.

From here we can get the numbers of hypermultiplets n_2 and $n_3 + n_{\bar{3}}$ tracing back from equation (2.47):

$$n_2 = -2(4K + S), \quad n_3 + n_{\bar{3}} = -3T(3K + T). \tag{12.84}$$

We recall that the Hodge numbers of a crepant resolution of an $\mathrm{SU}(2) \times \mathrm{SU}(3)$-model are (see Theorem 12.3.7)

$$h^{1,1}(Y) = 14 - K^2, \quad h^{2,1}(Y) = 29K^2 + 15KS + 24KT + 3S^2 + 6ST + 6T^2 + 14. \tag{12.85}$$

The total number of hypermultiplets is the sum of the number of neutral hypermultiplets ($n_H^\circ = h^{2,1}(Y) + 1$) and the number of charged hypermultiplets[5].

$$n_H^\circ = h^{2,1}(Y) + 1 = 29K^2 + 15KS + 24KT + 3S^2 + 6ST + 6T^2 + 15, \tag{12.86}$$

$$n_H^{ch} = 2n_{2,1} + 6(n_{2,3} + n_{2,\bar{3}}) + 3(n_{1,3} + n_{1,\bar{3}}) + (8-2)n_{1,8} + (3-1)n_{3,1}. \tag{12.87}$$

Thus, the total number of hypermultiplets is

$$n_H = n_H^\circ + n_H^{ch} = 29K^2 + 23. \tag{12.88}$$

[5] To count the charged hypermultiplets, each irreducible representation $\mathbf{R}$ contributes $\dim^{ch} \mathbf{R} \times n_{\mathbf{R}}$ where $\dim^{ch} \mathbf{R}$ is the number of non-zero weights of the representation $\mathbf{R}$ and $n_{\mathbf{R}}$ is the number of hypermultiplets transforming in the representation $\mathbf{R}$ [142].

The numbers of vector multiplets and tensor multiplets are

$$n_T = 9 - K^2, \quad n_V = \dim G = \dim\ \mathrm{SU}(2) + \dim\ \mathrm{SU}(3) = 3 + 8 = 11. \tag{12.89}$$

We can now check that the coefficient of tr R^4 vanishes [262]:

$$n_H - n_V + 29 n_T - 273 = 0. \tag{12.90}$$

Finally, we show that the anomaly polynomial I_8 indeed factors as a perfect square:

$$\begin{aligned} I_8 &= \frac{K^2}{8}(\mathrm{tr}R^2)^2 + \frac{1}{6}(X_1^{(2)} + X_2^{(2)})\mathrm{tr}R^2 - \frac{2}{3}(X_1^{(4)} + X_2^{(4)}) + 4Y_{23}, \\ &= \frac{1}{2}\left(\frac{1}{2}K\,\mathrm{tr}R^2 + 2S\,\mathrm{tr}_2 F_1^2 + 2T\,\mathrm{tr}_3 F_2^2\right)^2. \end{aligned} \tag{12.91}$$

Hence, we conclude that all the local anomalies are canceled via Green-Schwarz mechanism.

The global anomalies for the Standard Model in 4d was discussed in Section 12.1.1 by examining the fourth homotopy group of SU(2) and SU(3). Similarly, the global anomaly contributions from SU(2) and SU(3) in six-dimensions can be discussed by looking into the sixth homotopy group for SU(2) and SU(3), which are given by $\mathbb{Z}_{12}$ and $\mathbb{Z}_6$ respectively. Bershadsky and Vafa has shown that this yields the linear constraints on the number of hypermultiplets [40]. In the case of SU(2) and

SU(3), we have:

$$\begin{cases} \mathrm{SU}(2): & 4 - n_2 = 0 \mod 6, \\ \mathrm{SU}(3): & n_3 = 0 \mod 6, \end{cases} \tag{12.92}$$

where n_2 and n_3 are the number of hypermultiplets transforming in the fundamental representation of SU(2) and SU(3) respectively. Using equation (12.83), we immediately compute geometrically the number of charged hypermultiplets as

$$\begin{cases} n_2 = n_{2,1} + 3(n_{2,3} + n_{2,\bar{3}}) = -16(g(S) - 1) + 6S^2, \\ n_3 = n_{1,3} + n_{1,\bar{3}} + 2(n_{2,3} + n_{2,\bar{3}}) = -18(g(T) - 1) + 6T^2, \end{cases} \tag{12.93}$$

where $g(S)$ and $g(T)$ are the genus of the curves supporting S and T respectively. By using these conditions we find that the global anomalies of SU(3) always vanishes whereas SU(2) global anomaly canceling condition is found to be

$$g(S) = 0 \mod 3. \tag{12.94}$$

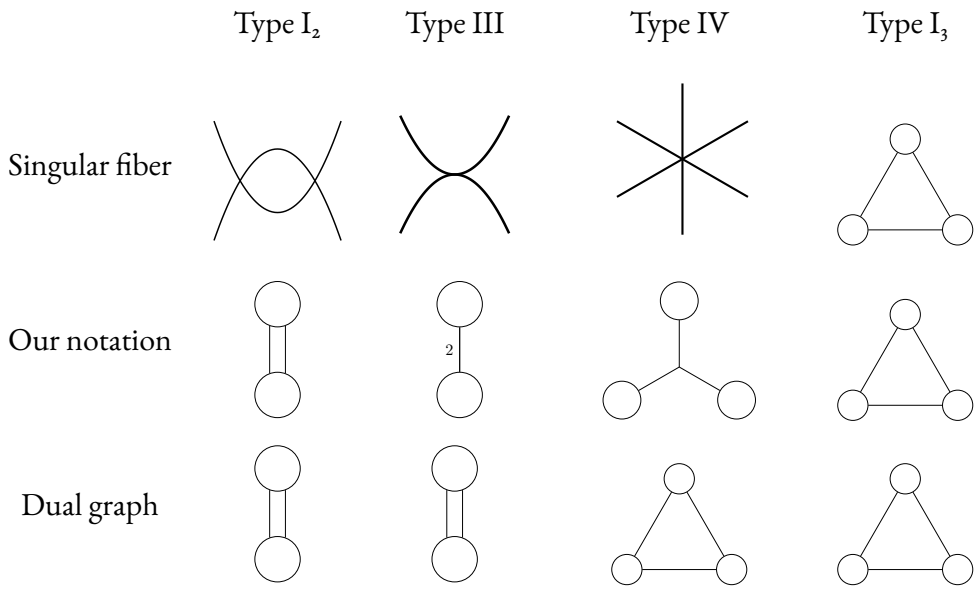

Figure 12.24: Convention for Kodaira fibers of type I_2, III, IV, and I_3.

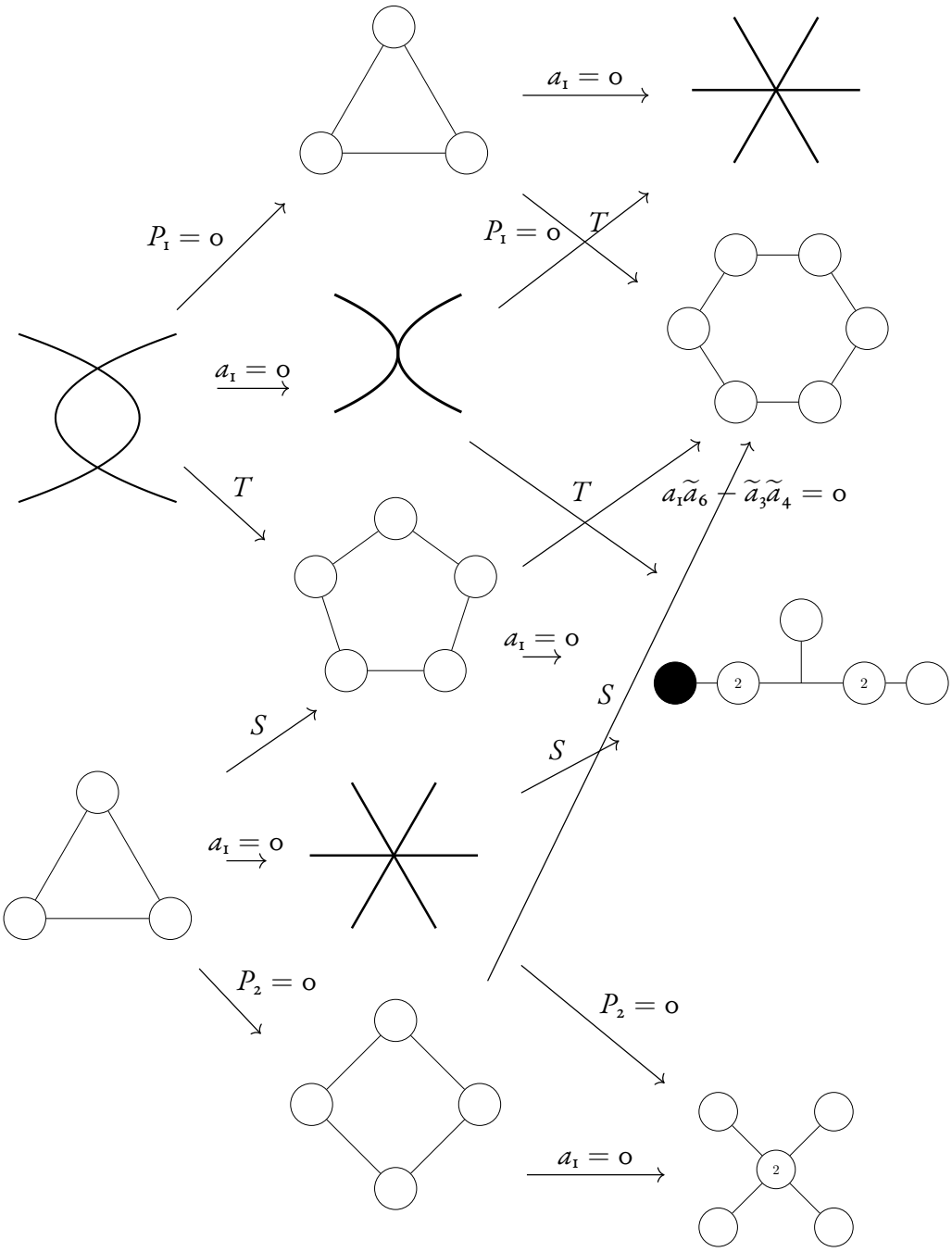

Table 12.15: $\mathrm{I}_2^s + \mathrm{I}_3^s$, Resolution I, II, and III. $P_1 = \widetilde{a}_4^2 t - a_1^2\widetilde{a}_6$ and $P_2 = \widetilde{a}_3^3 s - a_1\widetilde{a}_2\widetilde{a}_3^2 s + a_1^2\widetilde{a}_3\widetilde{a}_4 - a_1^3\widetilde{a}_6$. The non-Kodaira fiber in codimension-three is a contraction of a IV^*.

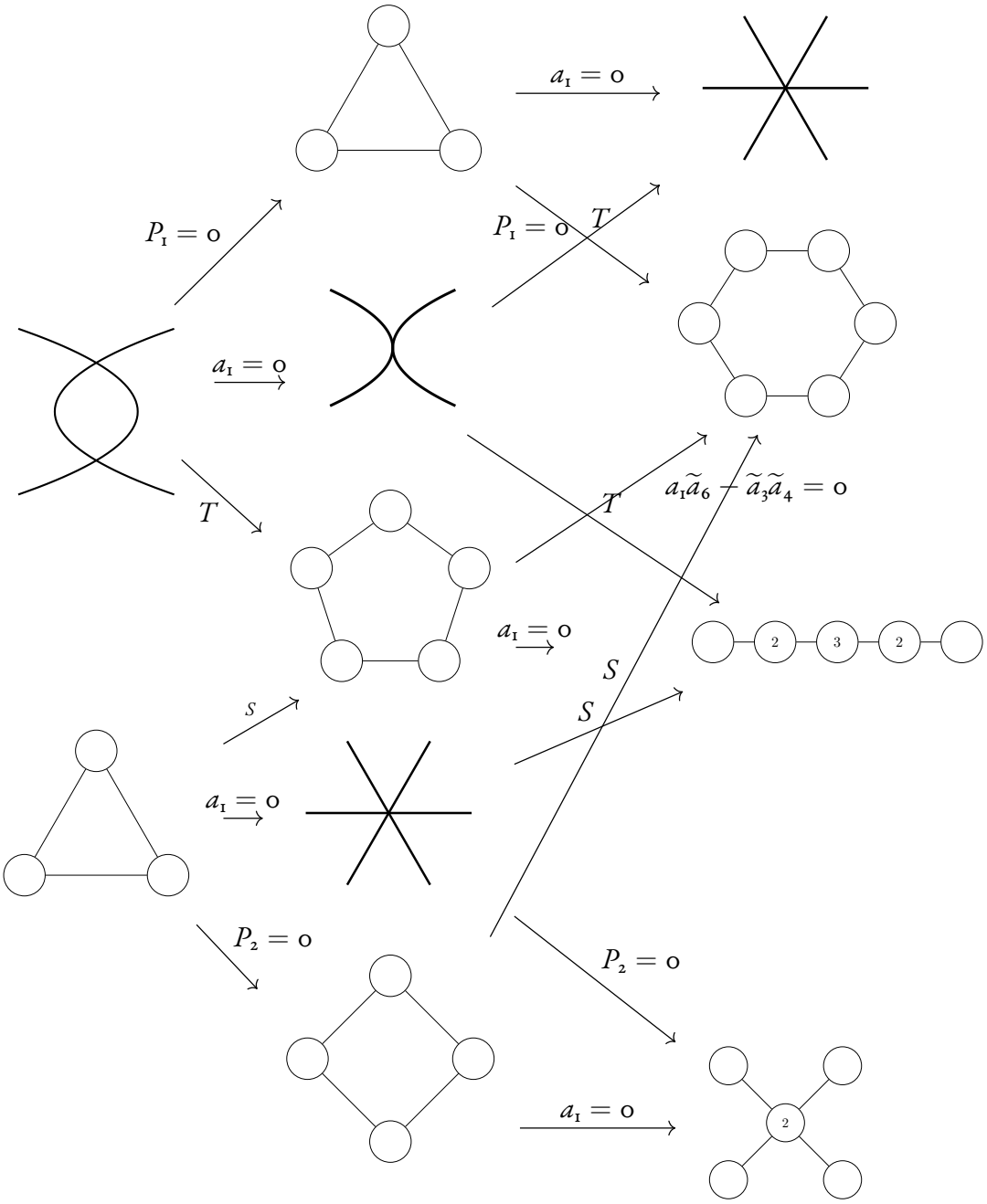

Table 12.16: $\mathrm{I}_2^s + \mathrm{I}_3^s$, Resolution IV. $P_1 = \widetilde{a}_4^2 t - a_1^2\widetilde{a}_6$ and $P_2 = \widetilde{a}_3^3 s - a_1\widetilde{a}_2\widetilde{a}_3^2 s + a_1^2\widetilde{a}_3\widetilde{a}_4 - a_1^3\widetilde{a}_6$. The non-Kodaira fiber is a contracted fiber of type IV*.

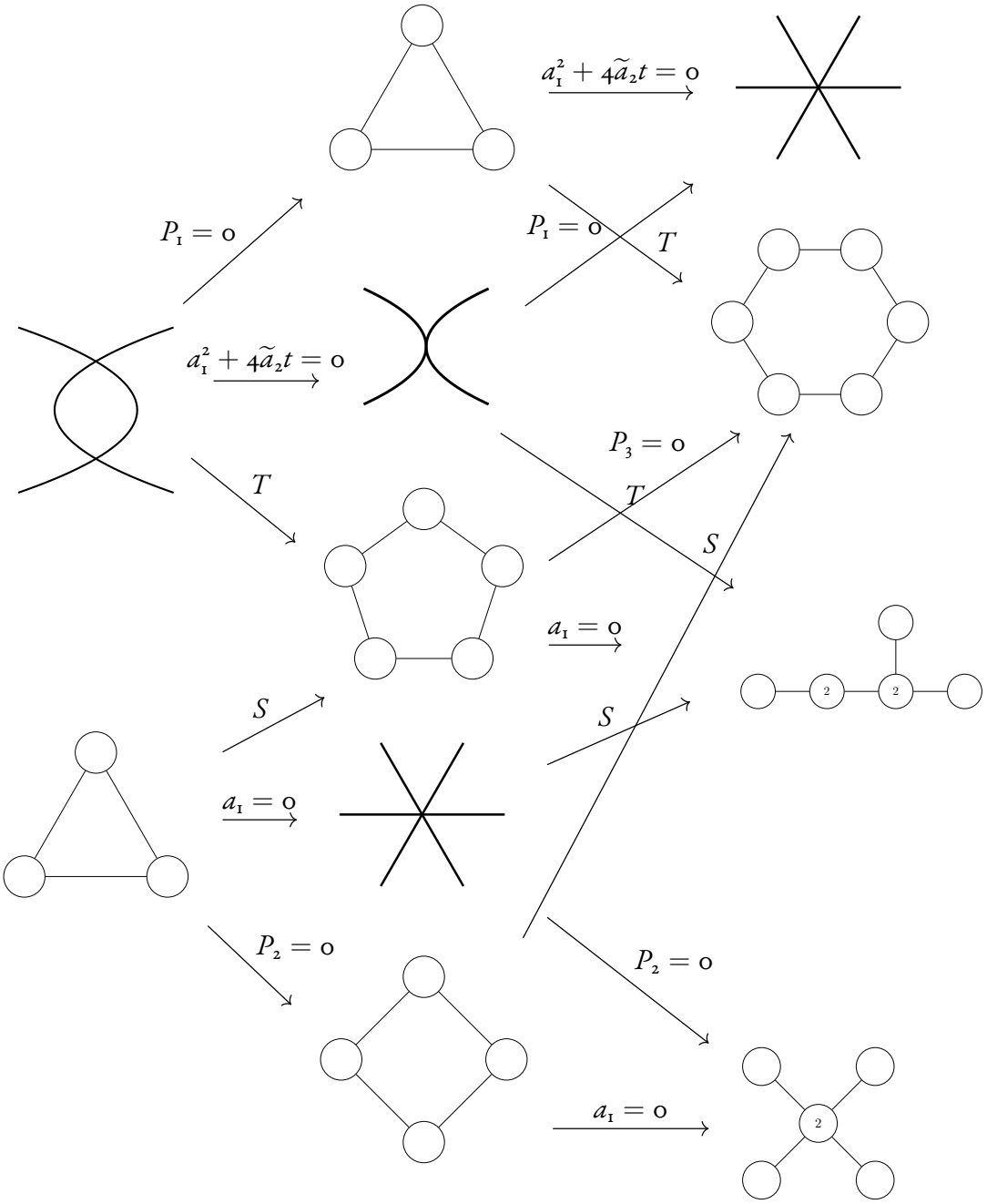

Table 12.17: $\mathrm{I}_2^{\mathrm{ns}} + \mathrm{I}_3^{\mathrm{s}}$ Resolution I and IV. $P_1 = -2\widetilde{a}_4^2 t + 4\widetilde{a}_2\widetilde{a}_6 t + a_1^2\widetilde{a}_6 - 2\widetilde{a}_2\widetilde{a}_3^2, P_2 = \widetilde{a}_3^3 s - a_1\widetilde{a}_2\widetilde{a}_3^2 + a_1^2\widetilde{a}_3\widetilde{a}_4 - a_1^3\widetilde{a}_6$, and $P_3 = \widetilde{a}_2\widetilde{a}_3^2 s - a_1(a_1\widetilde{a}_6 - \widetilde{a}_3\widetilde{a}_4)$. The non-Kodaira fiber is a contraction of an I_1^*.

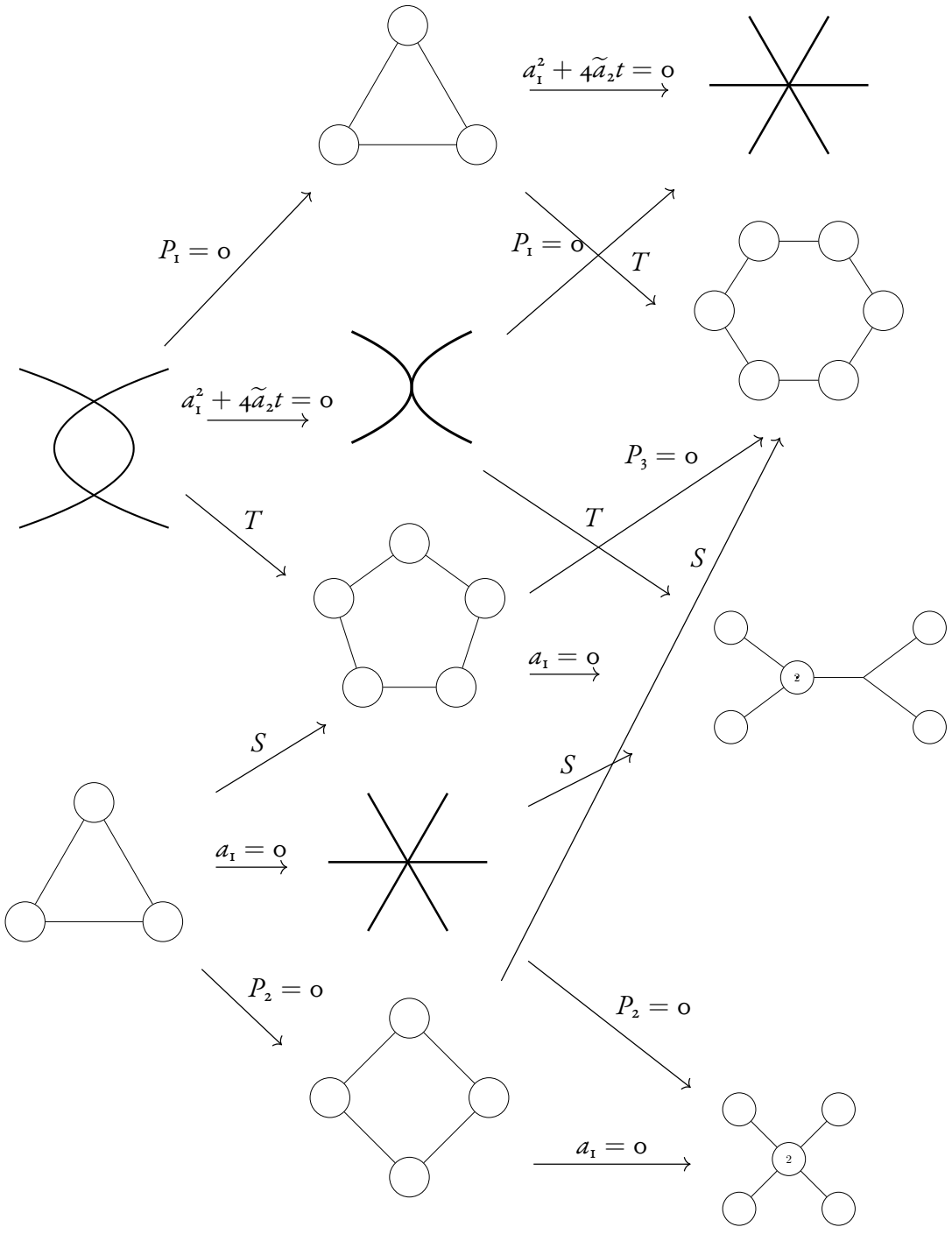

Table 12.18: $\mathrm{I}_2^{\mathrm{ns}} + \mathrm{I}_3^{\mathrm{s}}$ Resolution II. $P_1 = -2\widetilde{a}_4^2 t + 4\widetilde{a}_2\widetilde{a}_6 t + a_1^2\widetilde{a}_6 - 2\widetilde{a}_2\widetilde{a}_3^2$, $P_2 = \widetilde{a}_3^3 s - a_1\widetilde{a}_2\widetilde{a}_3^2 + a_1^2\widetilde{a}_3\widetilde{a}_4 - a_1^3\widetilde{a}_6$, and $P_3 = \widetilde{a}_2\widetilde{a}_3^2 s - a_1(a_1\widetilde{a}_6 - \widetilde{a}_3\widetilde{a}_4)$. The non-Kodaira fiber is a contraction of an I_1^*.

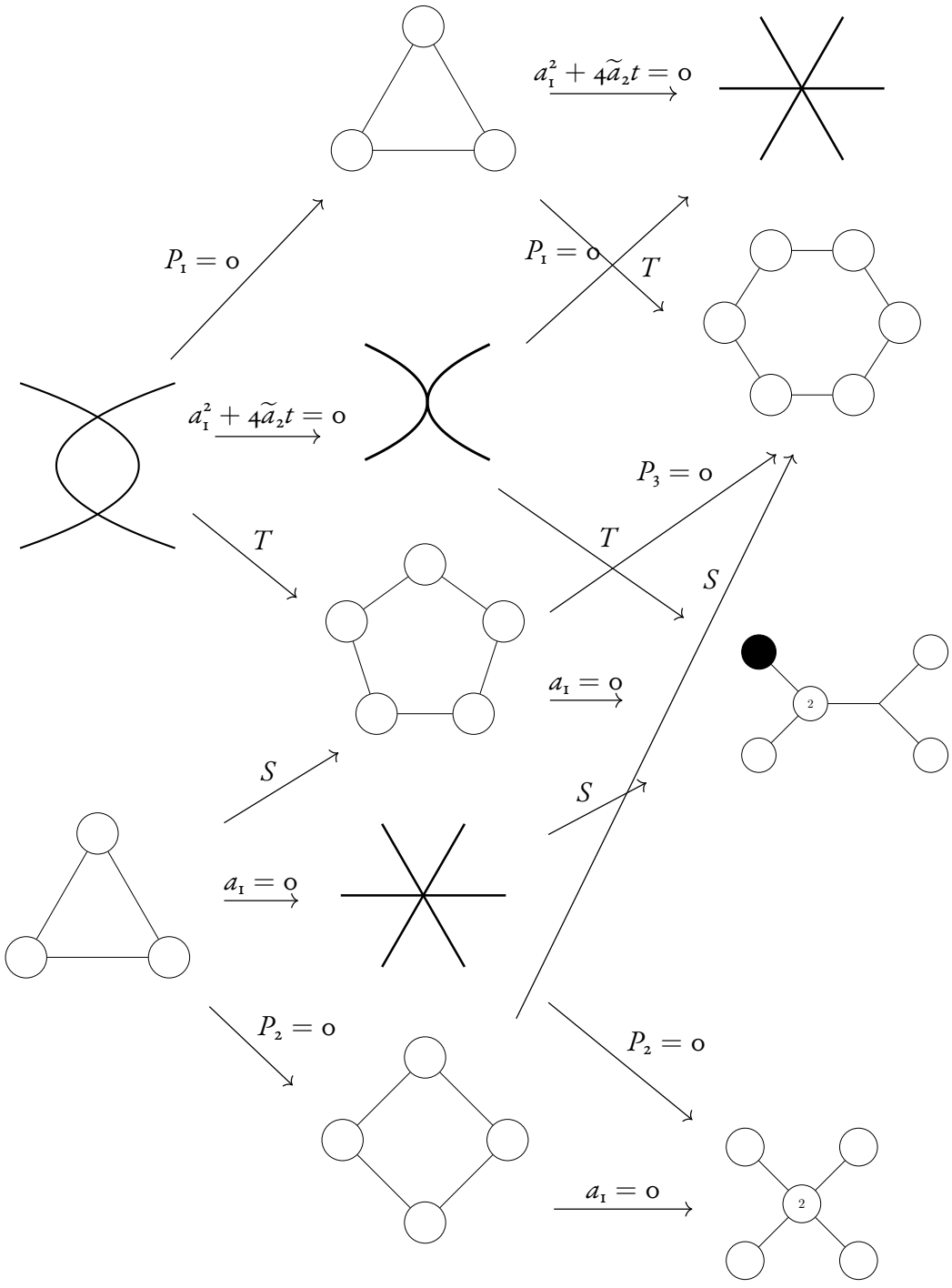

Table 12.19: $\mathrm{I}_2^{\mathrm{ns}} + \mathrm{I}_3^{\mathrm{s}}$ Resolution III. $P_1 = -2\widetilde{a}_4^2 t + 4\widetilde{a}_2\widetilde{a}_6 t + a_1^2\widetilde{a}_6 - 2\widetilde{a}_2\widetilde{a}_3^2$, $P_2 = \widetilde{a}_3^3 s - a_1\widetilde{a}_2\widetilde{a}_3^2 + a_1^2\widetilde{a}_3\widetilde{a}_4 - a_1^3\widetilde{a}_6$, and $P_3 = \widetilde{a}_2\widetilde{a}_3^2 s - a_1(a_1\widetilde{a}_6 - \widetilde{a}_3\widetilde{a}_4)$. The non-Kodaira fiber is a contraction of an I_1^*.

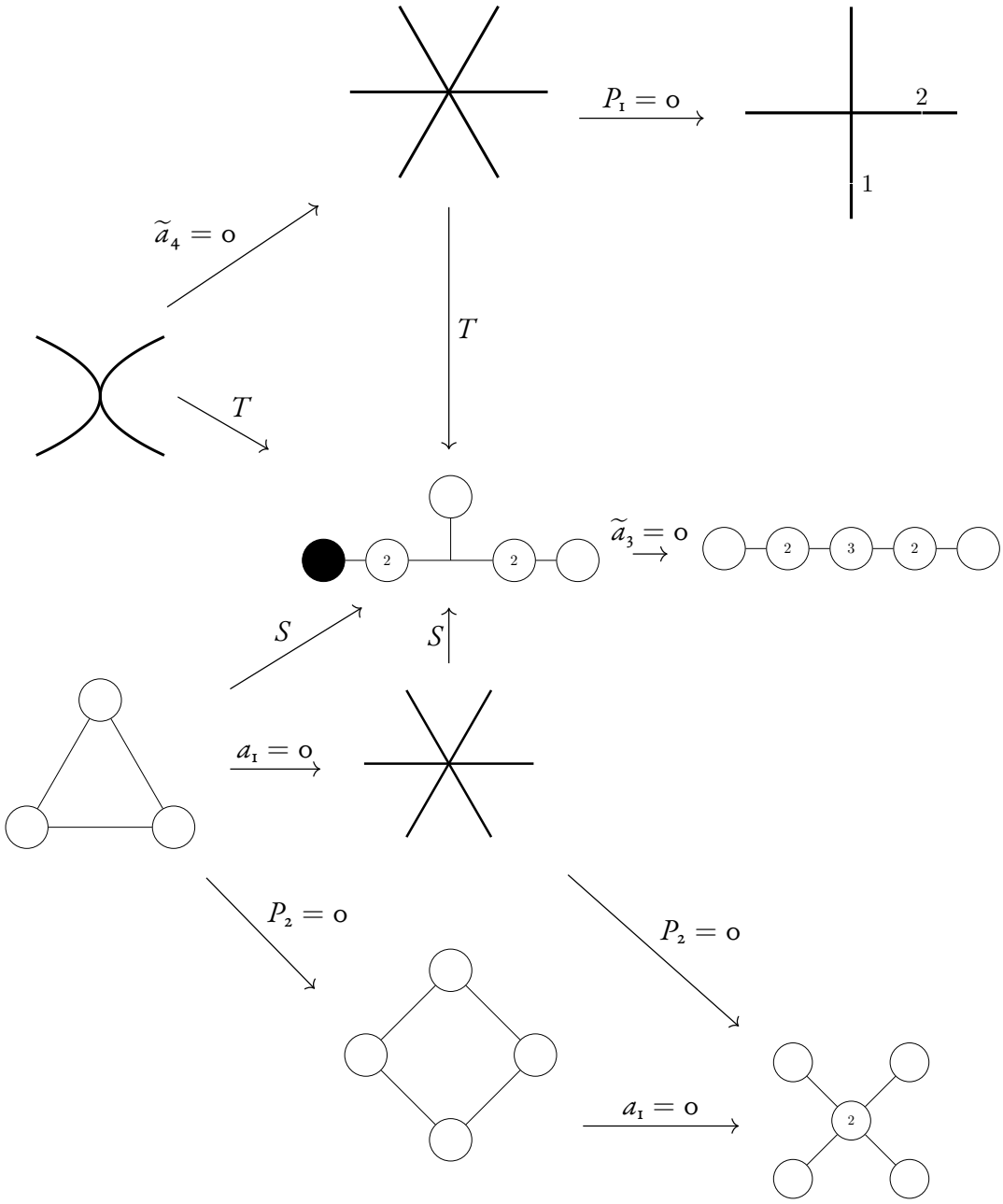

Table 12.20: III + I_3^s Resolution I. $P_1 = \widetilde{a}_3^2 + 4\widetilde{a}_6 t$ and $P_2 = \widetilde{a}_3^3 - \widetilde{a}_1\widetilde{a}_2\widetilde{a}_3^2 s + \widetilde{a}_1^2\widetilde{a}_3\widetilde{a}_4 s - \widetilde{a}_1^3\widetilde{a}_6 s^2$

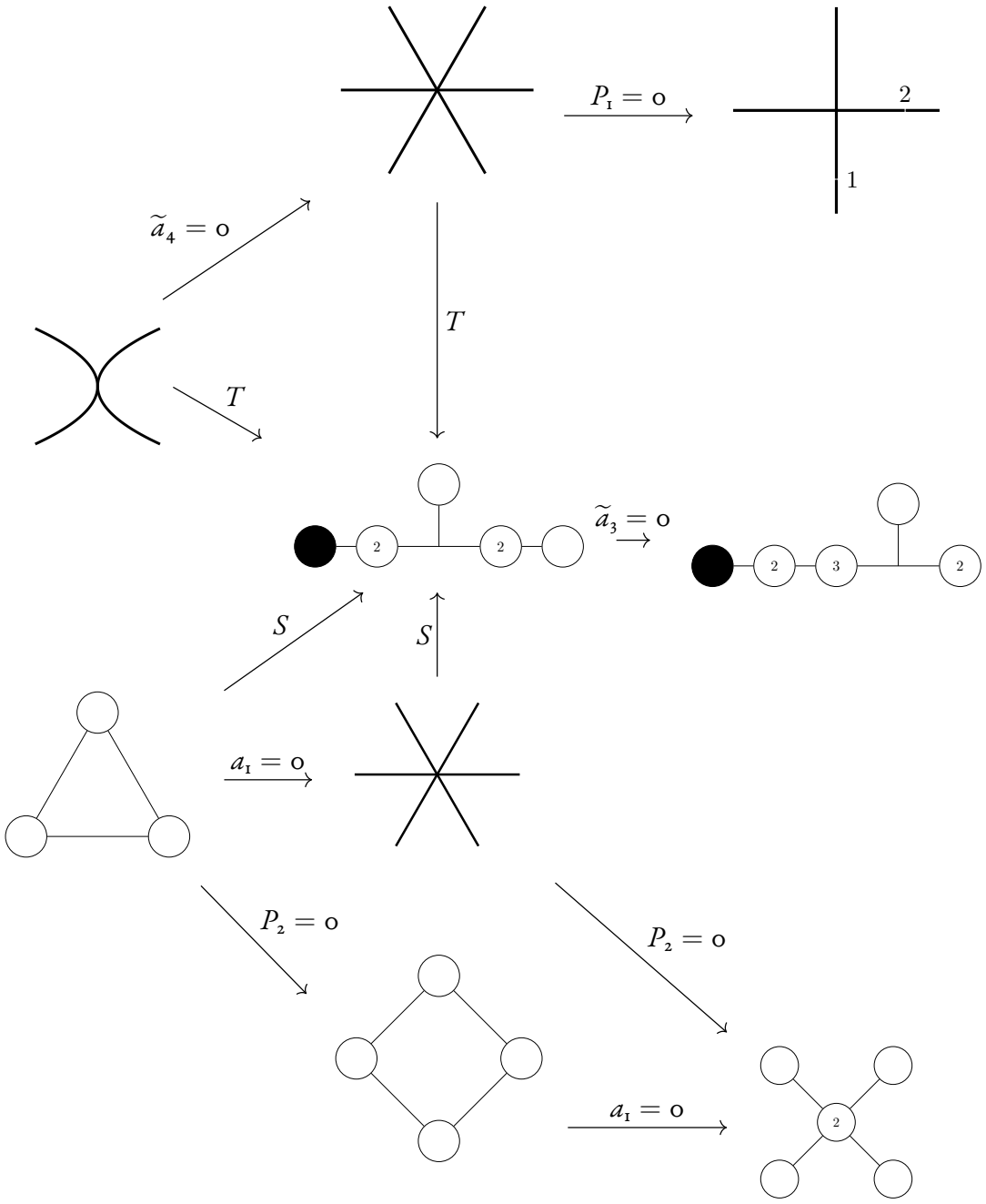

Table 12.21: III + I_3^s Resolution II. $P_1 = \widetilde{a}_3^2 + 4\widetilde{a}_6 t$ and $P_2 = \widetilde{a}_3^3 - \widetilde{a}_1\widetilde{a}_2\widetilde{a}_3^2 s + \widetilde{a}_1^2\widetilde{a}_3\widetilde{a}_4 s - \widetilde{a}_1^3\widetilde{a}_6 s^2$

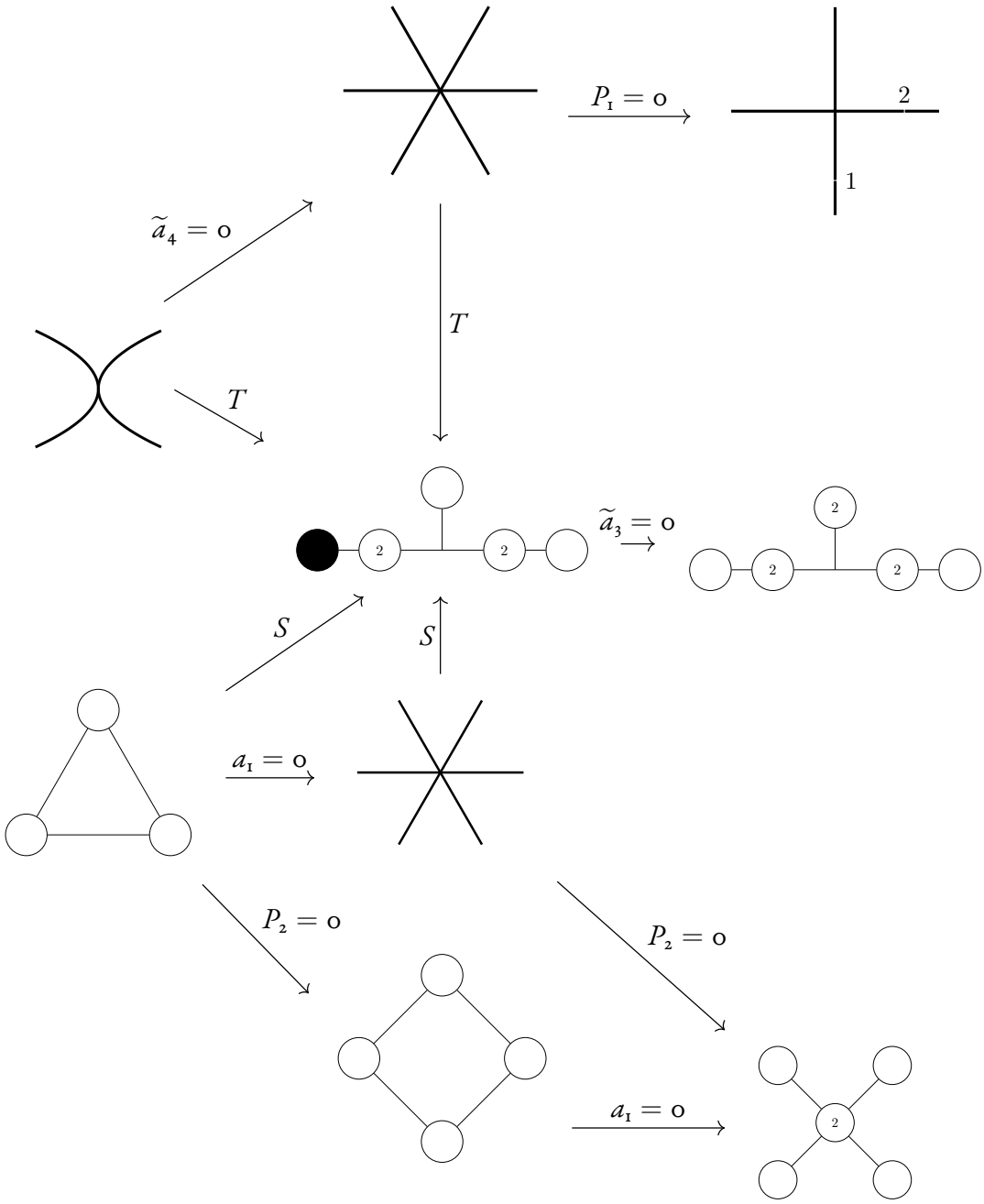

Table 12.22: III + I_3^s Resolution III. $P_1 = \widetilde{a}_3^2 + 4\widetilde{a}_6 t$ and $P_2 = \widetilde{a}_3^3 - \widetilde{a}_1\widetilde{a}_2\widetilde{a}_3^2 s + \widetilde{a}_1^2\widetilde{a}_3\widetilde{a}_4 s - \widetilde{a}_1^3\widetilde{a}_6 s^2$

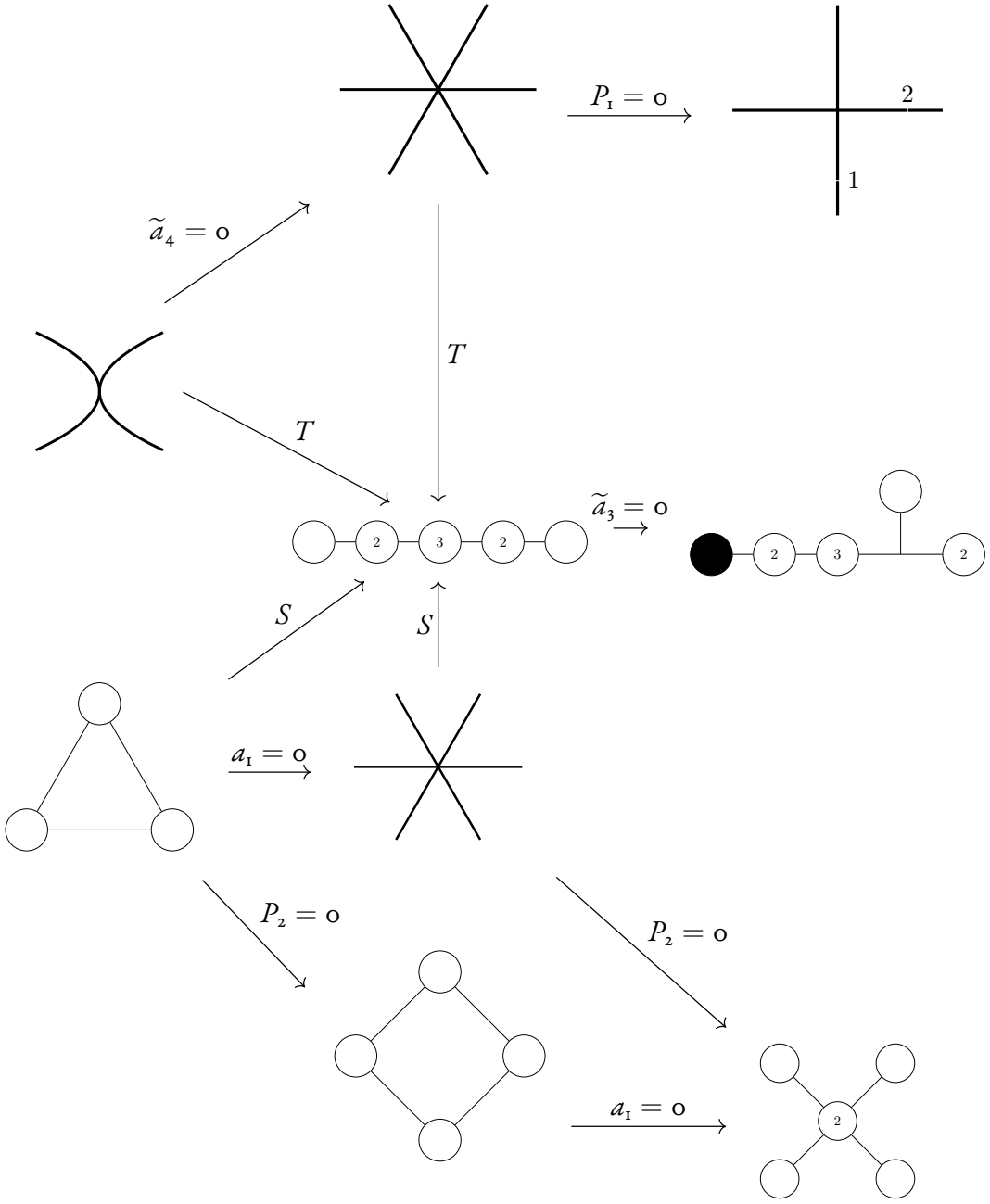

Table 12.23: III + I_3^5 Resolution IV. $P_1 = \widetilde{a}_3^2 + 4\widetilde{a}_6 t$ and $P_2 = \widetilde{a}_3^3 - \widetilde{a}_1\widetilde{a}_2\widetilde{a}_3^2 s + \widetilde{a}_1^2\widetilde{a}_3\widetilde{a}_4 s - \widetilde{a}_1^3\widetilde{a}_6 s^2$

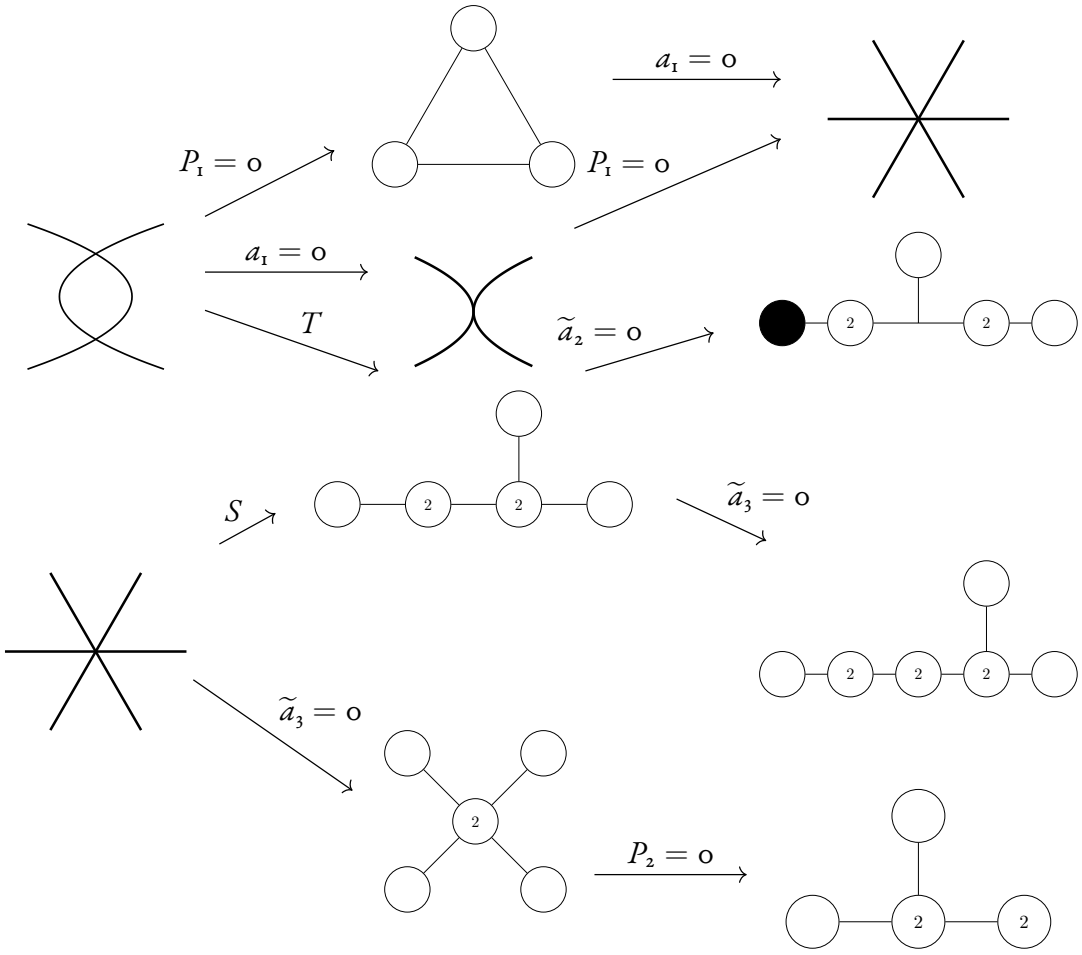

Table 12.24: $\mathsf{I}_2^{ns}+\mathsf{IV}^s$ or $\mathsf{I}_2^s+\mathsf{IV}^s$, Resolution I. $P_1 = \widetilde{a}_4^2 - \widetilde{a}_1^2\widetilde{a}_6 t$ and $P_2 = \widetilde{a}_2^2\widetilde{a}_4^2 - 4\widetilde{a}_4^3 s - 4\widetilde{a}_2^3\widetilde{a}_6 + 18\widetilde{a}_2\widetilde{a}_4\widetilde{a}_6 s - 27\widetilde{a}_6^2 s^2$ for $\mathsf{I}_2^{ns}+\mathsf{IV}^s$, $P_2 = \widetilde{a}_2^2\widetilde{a}_4^2 s - 4\widetilde{a}_4^3 - 4\widetilde{a}_2^3\widetilde{a}_6 s^2 + 18\widetilde{a}_2\widetilde{a}_4\widetilde{a}_6 s^2 - 27\widetilde{a}_6^2 s$ for $\mathsf{I}_2^s+\mathsf{IV}^s$.

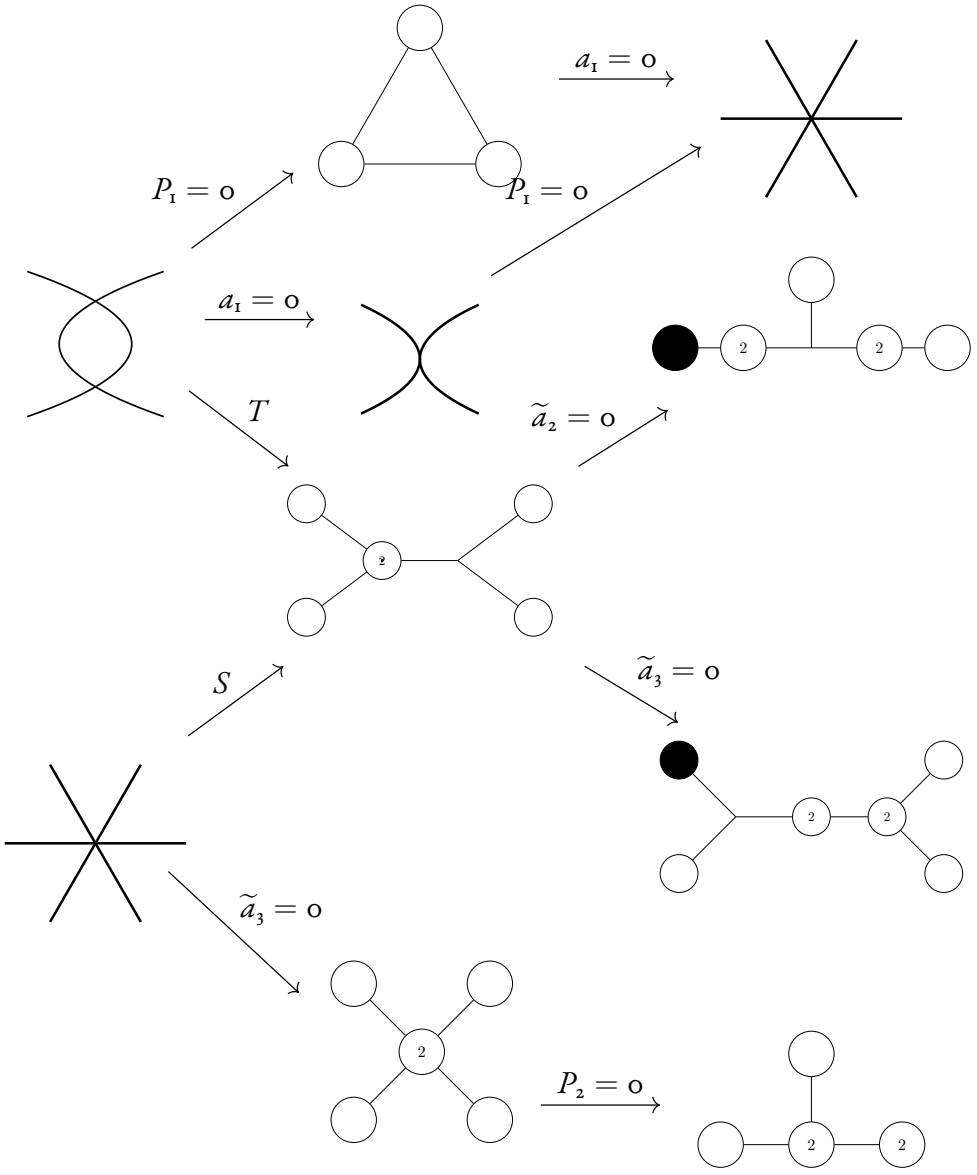

Table 12.25: $\mathrm{I}_2^{\mathrm{s}}+\mathrm{IV}^{\mathrm{s}}$ or $\mathrm{I}_2^{\mathrm{ns}}+\mathrm{IV}^{\mathrm{s}}$, Resolution II. $P_1 = \widetilde{a}_4^2 t - a_1^2 \widetilde{a}_6$ and $P_2 = \widetilde{a}_2^2\widetilde{a}_4^2 - 4\widetilde{a}_4^3 s - 4\widetilde{a}_2^3\widetilde{a}_6 + 18\widetilde{a}_2\widetilde{a}_4\widetilde{a}_6 s - 27\widetilde{a}_6^2 s^2$ for $\mathrm{I}_2^{\mathrm{ns}}+\mathrm{IV}^{\mathrm{s}}$, $P_2 = \widetilde{a}_2^2\widetilde{a}_4^2 s - 4\widetilde{a}_4^3 - 4\widetilde{a}_2^3\widetilde{a}_6 s^2 + 18\widetilde{a}_2\widetilde{a}_4\widetilde{a}_6 s^2 - 27\widetilde{a}_6^2 s$ for $\mathrm{I}_2^{\mathrm{s}}+\mathrm{IV}^{\mathrm{s}}$.

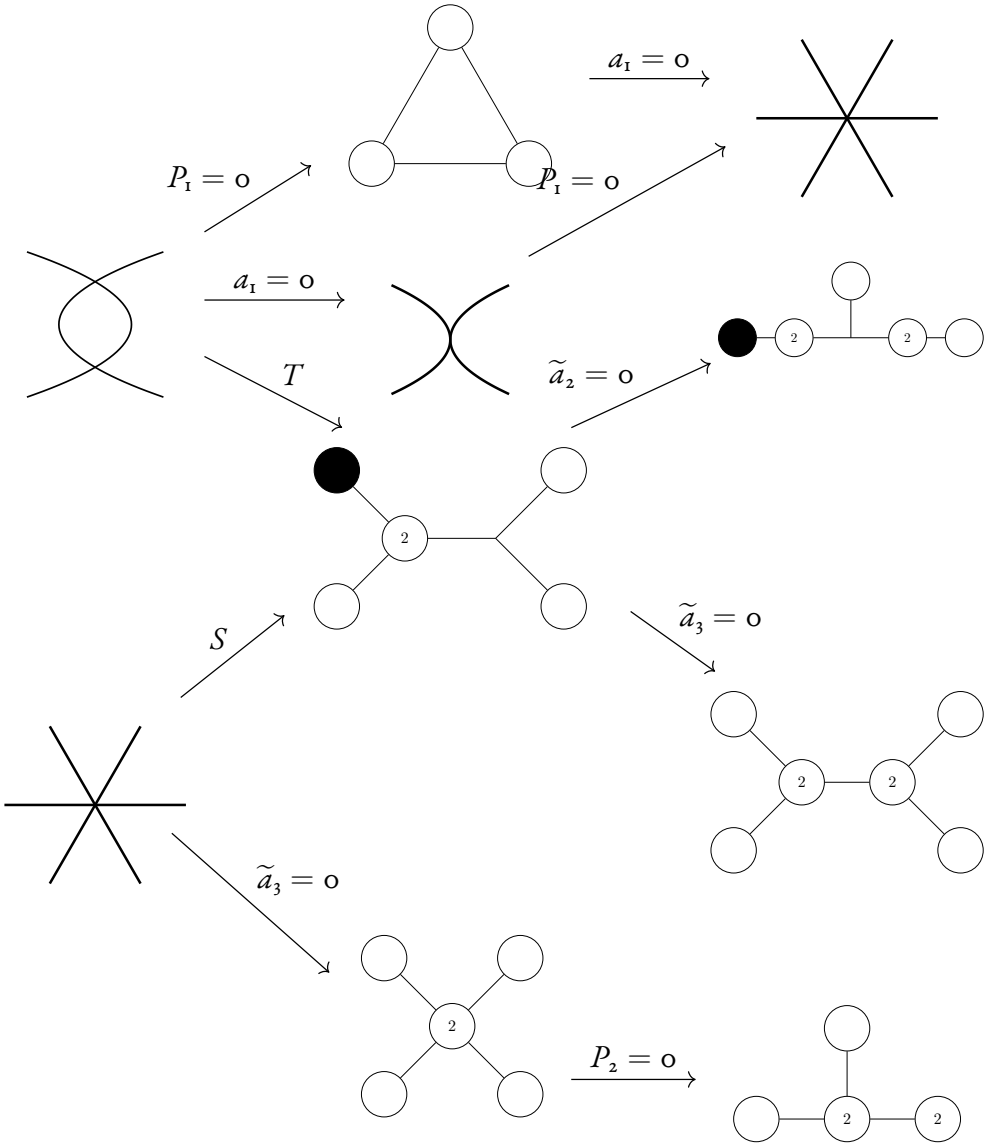

Table 12.26: $I_2^{ns}+IV^s$ or $I_2^s+IV^s$, Resolution III. $P_1 = \widetilde{a}_4^2 t - a_1^2\widetilde{a}_6$ and $P_2 = \widetilde{a}_2^2\widetilde{a}_4^2 - 4\widetilde{a}_4^3 s - 4\widetilde{a}_2^3\widetilde{a}_6 + 18\widetilde{a}_2\widetilde{a}_4\widetilde{a}_6 s - 27\widetilde{a}_6^2 s^2$ for $I_2^{ns}+IV^s$, $P_2 = \widetilde{a}_2^2\widetilde{a}_4^2 s - 4\widetilde{a}_4^3 - 4\widetilde{a}_2^3\widetilde{a}_6 s^2 + 18\widetilde{a}_2\widetilde{a}_4\widetilde{a}_6 s^2 - 27\widetilde{a}_6^2 s$ for $I_2^s+IV^s$.

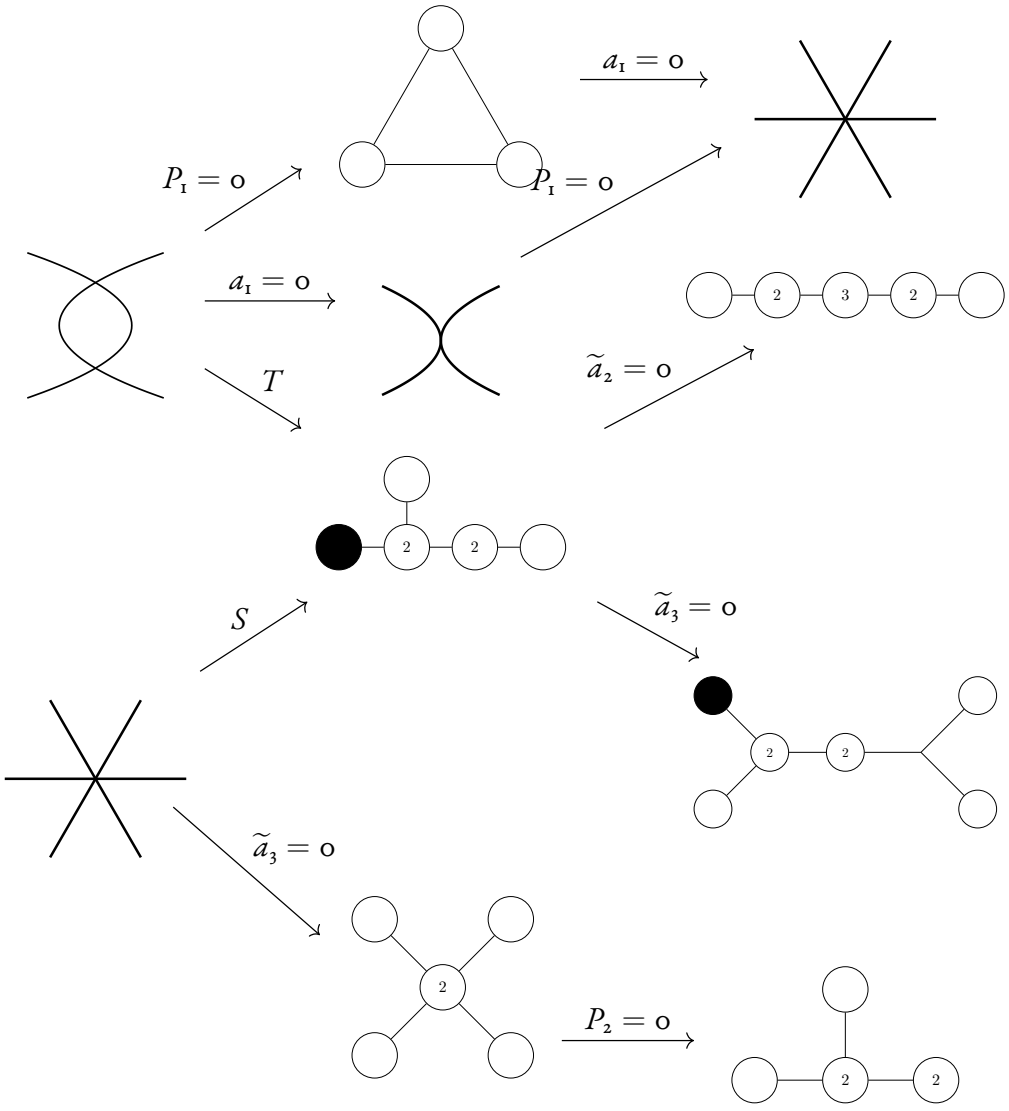

Table 12.27: I_2^s+IV^s or I_2^{ns}+IV^s, Resolution IV. $P_1 = \widetilde{a}_4^2 t - a_1^2 \widetilde{a}_6$ and $P_2 = \widetilde{a}_2^2\widetilde{a}_4^2 - 4\widetilde{a}_4^3 s - 4\widetilde{a}_2^3\widetilde{a}_6 + 18\widetilde{a}_2\widetilde{a}_4\widetilde{a}_6 s - 27\widetilde{a}_6^2 s^2$ for I_2^{ns}+IV^s, $P_2 = \widetilde{a}_2^2\widetilde{a}_4^2 s - 4\widetilde{a}_4^3 - 4\widetilde{a}_2^3\widetilde{a}_6 s^2 + 18\widetilde{a}_2\widetilde{a}_4\widetilde{a}_6 s^2 - 27\widetilde{a}_6^2 s$ for I_2^s+IV^s.

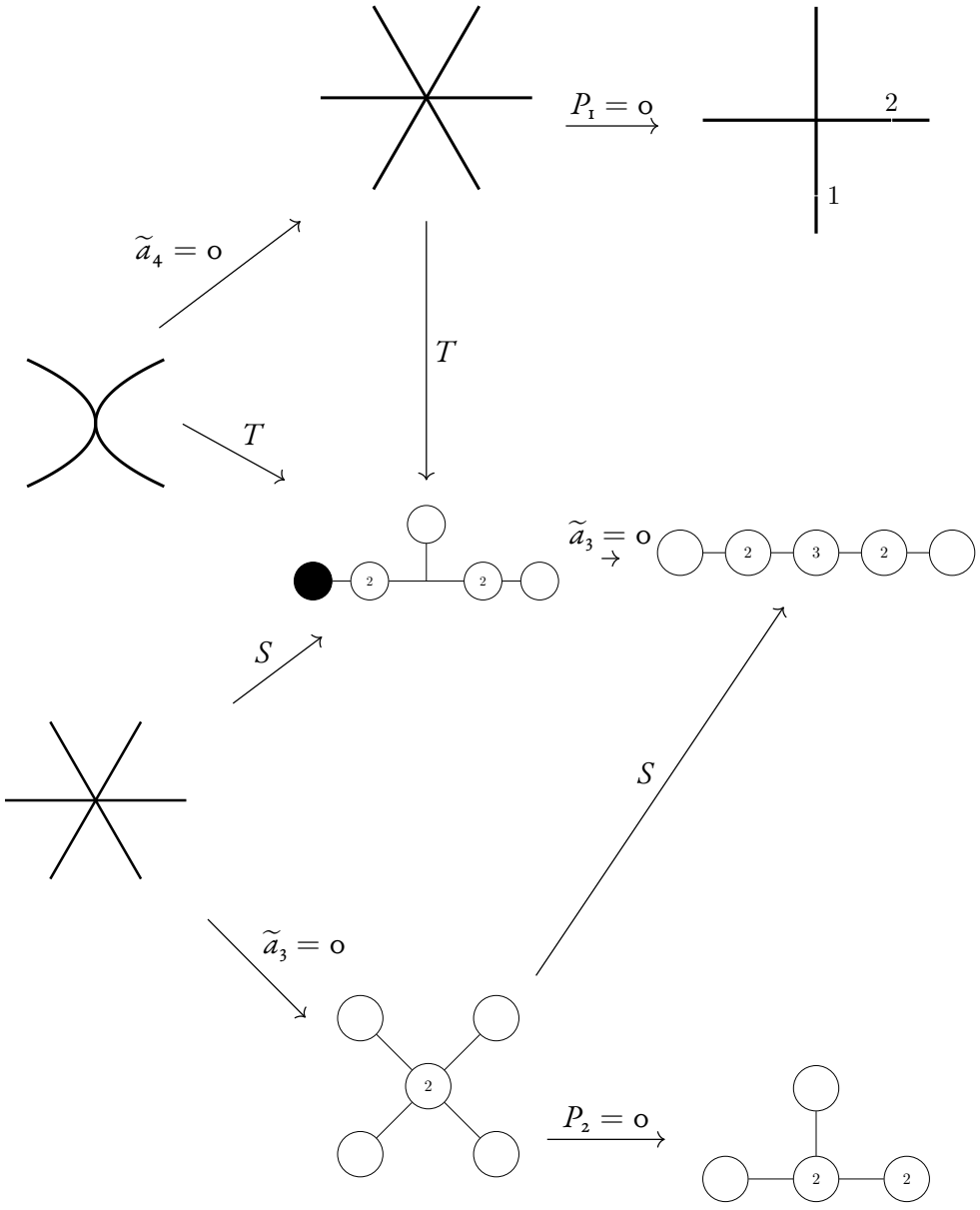

Table 12.28: III + IV^s, Resolution I. $P_1 = \widetilde{a}_3^2 + 4\widetilde{a}_6 t$ and $P_2 = \widetilde{a}_2^2\widetilde{a}_4^2 s - 4\widetilde{a}_4^3 - 4\widetilde{a}_2^3\widetilde{a}_6 s^2 + 18\widetilde{a}_2\widetilde{a}_4\widetilde{a}_6 s - 27\widetilde{a}_6^2 s$.

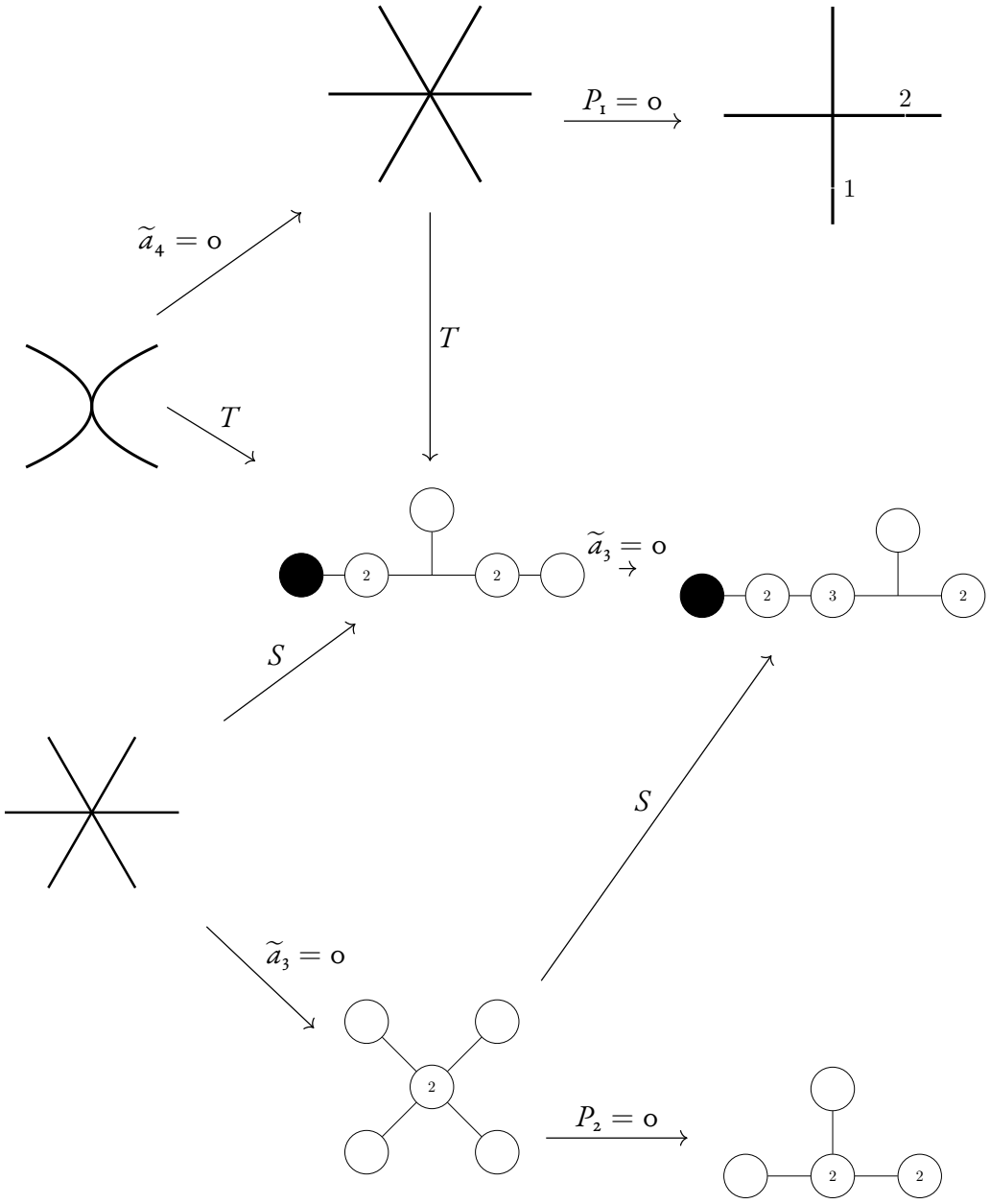

Table 12.29: III + IV^s Resolution II. $P_1 = \widetilde{a}_3^2 + 4\widetilde{a}_6 t$ and $P_2 = \widetilde{a}_2^2\widetilde{a}_4^2 s - 4\widetilde{a}_4^3 - 4\widetilde{a}_2^3\widetilde{a}_6 s^2 + 18\widetilde{a}_2\widetilde{a}_4\widetilde{a}_6 s - 27\widetilde{a}_6^2 s$.

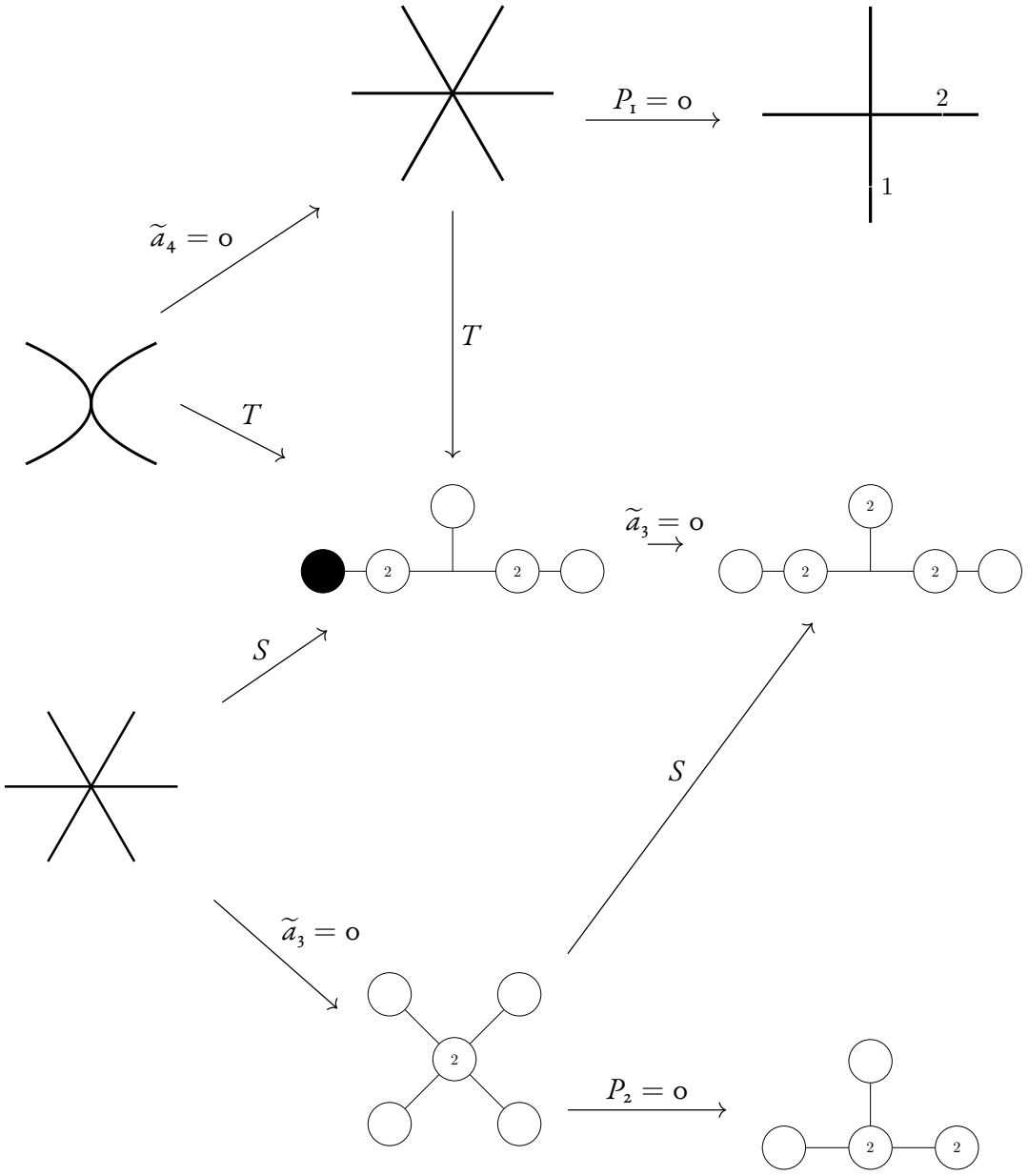

Table 12.30: III + IV^s, Resolution III. $P_1 = \widetilde{a}_3^2 + 4\widetilde{a}_6 t$ and $P_2 = \widetilde{a}_2^2\widetilde{a}_4^2 s - 4\widetilde{a}_4^3 - 4\widetilde{a}_2^3\widetilde{a}_6 s^2 + 18\widetilde{a}_2\widetilde{a}_4\widetilde{a}_6 s - 27\widetilde{a}_6^2 s$. The non-Kodaira fiber in codimension-two is a contraction of a IV* and its specialization in codimension three is a contraction of a III*.

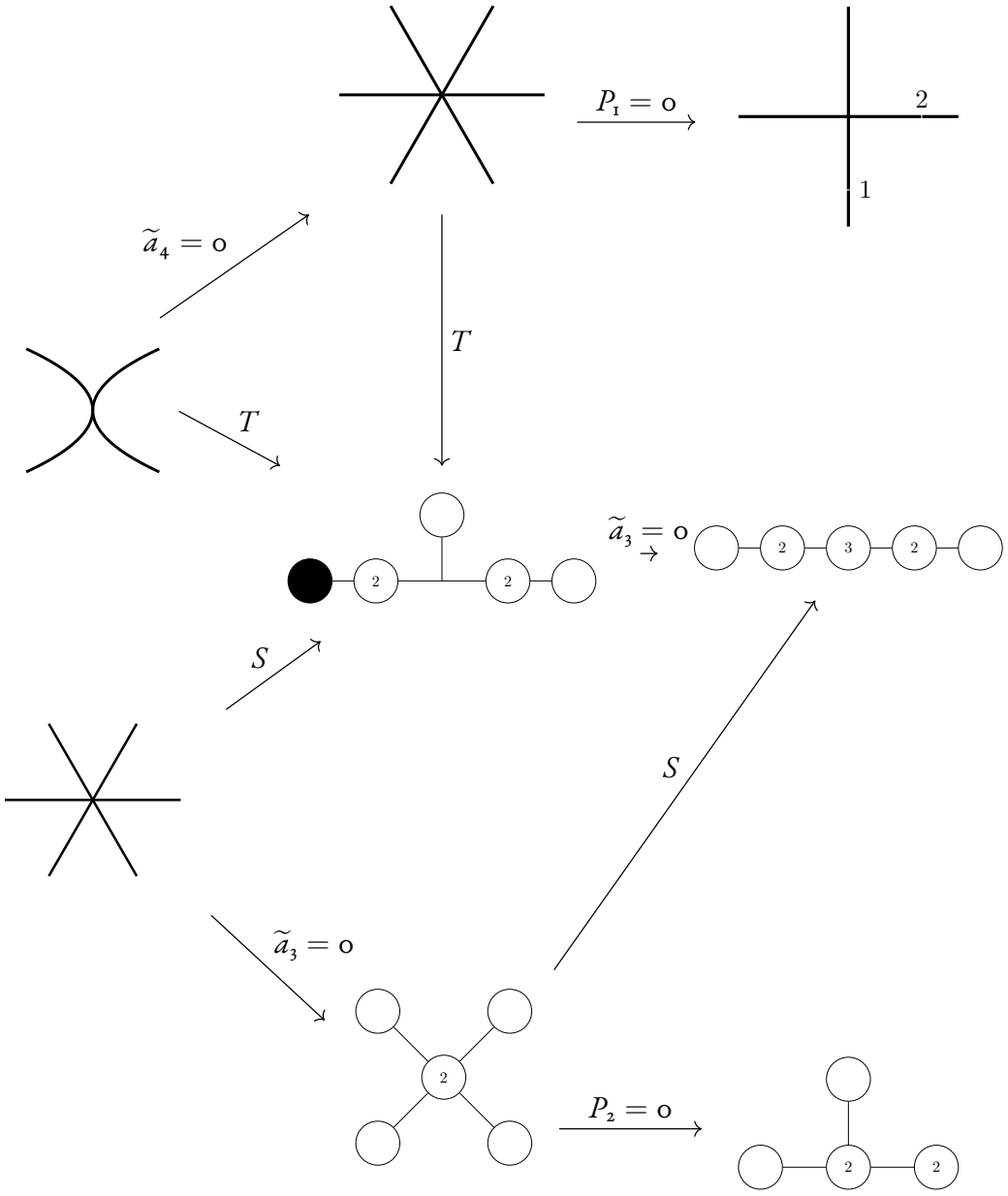

Table 12.31: III + IV^s, Resolution IV. $P_1 = \widetilde{a}_3^2 + 4\widetilde{a}_6 t$ and $P_2 = \widetilde{a}_2^2\widetilde{a}_4^2 s - 4\widetilde{a}_4^3 - 4\widetilde{a}_2^3\widetilde{a}_6 s^2 + 18\widetilde{a}_2\widetilde{a}_4\widetilde{a}_6 s - 27\widetilde{a}_6^2 s$. The non-Kodaira fiber in codimension-two is a contraction of a IV* and its specialization in codimension three is a contraction of a III*.

We have patches that have been put together, but we are not quite sure how all pieces will fit together into a coherent whole.

Benjamin Whisoh Lee (이휘소)

13

Mordell-Weil Torsion, Anomalies, and Phase Transitions

The $(\mathrm{SU}(2) \times \mathrm{SU}(4))/\mathbb{Z}_2$-model has been studied in [229] using toric ambient spaces for the fiber, the SU(2) and the SU(4) models are individually studied in [124, 125]. A specialization of the SU(2) × SU(4)-model is studied in [11] in relation to T-branes and also in [10]. For each of these

models, the representation **R** is uniquely determined by the geometry of the corresponding elliptic fibrations and are listed on Table 13.1.

A representation **R** is sometimes enough to completely identity the group G once we know its Lie algebra $\mathfrak{g}$ and its fundamental group. We illustrate this point with two examples that will be the focus of this chapter. In both cases, the Lie algebra is derived from an elliptic fibration with collisions of the type I_2+I_4 and a Mordell-Weil group $\mathbb{Z}_2$. In the case of the Lie algebra $\mathfrak{g} = A_1 \oplus A_3$, which corresponds to the simply connected compact group $SU(2) \times SU(4)$, the center is $\mathbb{Z}_2 \times \mathbb{Z}_4$. Since there is a unique $\mathbb{Z}_2$ subgroup in $\mathbb{Z}_4$, there are three possibilities for embedding $\mathbb{Z}_2$ in the center $\mathbb{Z}_2 \times \mathbb{Z}_4$, namely

$$(\mathbb{Z}_2, 1), \quad (1, \mathbb{Z}_2), \quad \text{diagonal } \mathbb{Z}_2. \tag{13.1}$$

Hence, the possible quotient groups are

$$SO(3) \times SU(4), \quad SU(2) \times SO(5), \quad (SU(2) \times SU(4))/\mathbb{Z}_2. \tag{13.2}$$

These three groups have the same Lie algebra $A_1 \oplus A_3$, the same universal cover $SU(2) \times SU(4)$, the same first homotopy group, but different centers

$$\mathbb{Z}_4, \quad \mathbb{Z}_2 \times \mathbb{Z}_2, \quad \mathbb{Z}_2. \tag{13.3}$$

The bifundamental representation $(2, 4)$ of $A_1 \oplus A_3$ is only compatible with the group $(SU(2) \times SU(4))/\mathbb{Z}_2$.

For the case of the Lie algebra $\mathfrak{g} = A_1 \oplus C_2$, which corresponds to the simply connected compact group $SU(2) \times Sp(4)$, the center is $\mathbb{Z}_2 \times \mathbb{Z}_2$. Equation (13.1) gives the three possible ways to embed a $\mathbb{Z}_2$ in $\mathbb{Z}_2 \times \mathbb{Z}_2$. In this case, the possible quotient groups are

$$SO(3) \times Sp(4), \quad SU(2) \times SO(6), \quad (SU(2) \times Sp(4))/\mathbb{Z}_2. \tag{13.4}$$

These three groups have the same universal cover $SU(2) \times Sp(4)$, the same fundamental group $\mathbb{Z}_2$, and the same center $\mathbb{Z}_2$. But the center $\mathbb{Z}_2$ is given by a different embedding in $\mathbb{Z}_2 \times \mathbb{Z}_2$. Once again, the bifundamental $(2, 4)$ representation of $A_1 \oplus C_2$ is only compatible with the last one.

Our convention for counting the multiplicity of representations is inspired by the geometry and ease the comparison with the intersecting brane picture. In the case of the $SU(2)\times SU(4)$-model, the matter representation contains the reducible quarternionic representation $(1, 4) \oplus (1, \overline{4})$ with the multiplicity $n_{1,4} = n_{1,\overline{4}} = -T(4K + S + 2T)$. The total multiplicity corresponds to the number of intersection points between the divisor T supporting $SU(4)$ and the irreducible component Δ' of the discriminant not supporting any gauge group. At collision the fiber I_4^s enhances to an I_5^s, producing the weight $\boxed{0, 1, -1}$ of the fundamental representation 4 of $\mathfrak{su}(4)$ and the weight $\boxed{-1, 1, 0}$ of the anti-fundamental representation 4 of $\mathfrak{su}(4)$. See Tables 13.2, 13.14, and 13.12. The representation $(2, 1)$ is pseudo-real and $n_{2,1} = -2S(4K+S+2T)$, which is geometrically the number of intersection $S \cdot V(\tilde{b}_8)$.

Models	Algebraic data	# Flops
$\mathrm{I}_2^{\mathrm{ns}}+\mathrm{I}_4^{\mathrm{ns}}$ $\mathrm{MW}=\mathbb{Z}_2$	$F=y^2z-(x^3+a_2x^2z+st^2xz^2)$ $\Delta=s^2t^4(a_2^2-4st^2)$	3
	$G=(\mathrm{SU}(2)\times\mathrm{Sp}(4))/\mathbb{Z}_2$ $\mathbf{R}=(3,1)\oplus(1,10)\oplus(2,4)\oplus(1,5)$ $\chi=-4(9K^2+8K\cdot T+3T^2)$	
$\mathrm{I}_2^{\mathrm{ns}}+\mathrm{I}_4^{\mathrm{ns}}$ $\mathrm{MW}=\{1\}$	$F=y^2z-(x^3+a_2x^2z+\widetilde{a}_4st^2xz^2+\widetilde{a}_6s^2t^4z^3)$ $\Delta=s^2t^4(4a_2^3\widetilde{a}_6-a_2^2\widetilde{a}_4^2-18a_2\widetilde{a}_4\widetilde{a}_6st^2+4a_4^3st^2+27\widetilde{a}_6^2s^2t^4)$	3
	$G=\mathrm{SU}(2)\times\mathrm{Sp}(4)$ $\mathbf{R}=(3,1)\oplus(1,10)\oplus(2,4)\oplus(1,5)\oplus(2,1)\oplus(1,4)$ $\chi=-2(30K^2+15K\cdot S+30K\cdot T+3S^2+8S\cdot T+10T^2)$	
$\mathrm{I}_2^{\mathrm{ns}}+\mathrm{I}_4^{\mathrm{s}}$ $\mathrm{MW}=\mathbb{Z}_2$	$F=y^2z+a_1xyz-(x^3+\widetilde{a}_2tx^2z+st^2xz^2)$ $\Delta=s^2t^4\,(a_1^4+8a_1^2\widetilde{a}_2t+16\widetilde{a}_2^2t^2-64st^2)$	12
	$G=(\mathrm{SU}(2)\times\mathrm{SU}(4))/\mathbb{Z}_2$ $\mathbf{R}=(3,1)\oplus(1,15)\oplus(2,4)\oplus(2,\overline{4})\oplus(1,6)$ $\chi=-12\,(3K^2+3K\cdot T+T^2)$	
$\mathrm{I}_2^{\mathrm{ns}}+\mathrm{I}_4^{\mathrm{s}}$ $\mathrm{MW}=\{1\}$	$F=y^2z+a_1xyz-(x^3+\widetilde{a}_2tx^2z+\widetilde{a}_4st^2xz^2+\widetilde{a}_6s^2t^4z^3)$ $\Delta=s^2t^4\,(a_1^4+8a_1^2\widetilde{a}_2t+16\widetilde{a}_2^2t^2-64st^2)$	20
	$G=\mathrm{SU}(2)\times\mathrm{SU}(4)$ $\mathbf{R}=(3,1)\oplus(1,15)\oplus(2,4)\oplus(2,\overline{4})\oplus(1,6)$ $\oplus(2,1)\oplus(1,4)\oplus(1,\overline{4})$ $\chi=-2\,(30K^2+15K\cdot S+32K\cdot T+3S^2+8S\cdot T+10T^2)$	

Table 13.1: Weierstrass models, discriminant loci, gauge groups and representations. F is the defining equation of the Weierstrass model, Δ is its discriminant, G is the gauge group, $Z(G)$ is the center of G (isomorphic to the Mordell-Weil group MW of the elliptic fibration), $\mathbf{R}$ is the matter representation, and χ is the Euler characteristic of a crepant resolution of a Calabi-Yau that is elliptically fibered with a defining equation $F=0$. The column "# Flops" gives the number of distinct crepant resolutions , or equivalently, the number of chambers in the hyperplane arrangement $\mathrm{I}(\mathfrak{g},\mathbf{R})$. The number of flops also corresponds to the number of Coulomb phases of a five-dimensional supergravity theory with eight supercharges obtained by a compactification of M-theory on this elliptic fibration. The Euler characteristic of the models with trivial Mordell–Weil groups specializes to those of the models with $\mathbb{Z}_2$ Mordell–Weil groups after imposing the relation $S=-4K-2T$.

G	Adjoint	Bifundamental	Antisymmetric, Fundamental
$(\mathrm{SU}(2)\times\mathrm{Sp}(4))/\mathbb{Z}_2$	$n_{3,1}=g_S \quad n_{1,10}=g_T$	$n_{2,4}=S\cdot T$	$n_{1,5}=g_T-1+\frac{1}{2}T\cdot V(a_2)$
$\mathrm{SU}(2)\times\mathrm{Sp}(4)$	$n_{3,1}=g_S \quad n_{1,10}=g_T$	$n_{2,4}=S\cdot T$	$n_{1,5}=g_T-1+\frac{1}{2}T\cdot V(a_2)$ $n_{2,1}=S\cdot V(\tilde{b}_8)$, $n_{1,4}=T\cdot V(\tilde{b}_8)$
$(\mathrm{SU}(2)\times\mathrm{SU}(4))/\mathbb{Z}_2$	$n_{3,1}=g_S \quad n_{1,15}=g_T$	$n_{2,4}+n_{2,\overline{4}}=S\cdot T$	$n_{1,6}=T\cdot V(a_1)$
$\mathrm{SU}(2)\times\mathrm{SU}(4)$	$n_{3,1}=g_S \quad n_{1,15}=g_T$	$n_{2,4}+n_{2,\overline{4}}=S\cdot T$	$n_{1,6}=T\cdot V(a_1)$ $n_{2,1}=S\cdot V(\tilde{b}_8)$, $n_{1,4}+n_{1,\overline{4}}=T\cdot V(\widetilde{b}_8)$

Table 13.2: Geometrical interpretation of the number of representations of the matter content. In the last column, $n_{1,5}$ is the number of traceless antisymmetric matter in Sp(4), $n_{1,6}$ is the number of antisymmetric matter in SU(4), $n_{1,4}$ is the fundamental representation of SU(4), and $n_{2,1}$ is the number of fundamental representation in SU(2). For SU(4) theories, we have $[V(\tilde{b}_8)]=2(-4T-S-2T)$. In presence of a $\mathbb{Z}_2$, with our choice of Weierstrass models, we have $S=-4K-2T$.

13.1 Summary of results

In this section, we summarize the results of this chapter.

13.1.1 Crepant resolutions

The models we consider in this chapter are given by the following Weierstrass models.

$$(\mathrm{SU}(2)\times\mathrm{Sp}(4))/\mathbb{Z}_2: \qquad y^2z-(x^3+a_2x^2z+st^2xz^2)=0 \tag{13.5}$$

$$\mathrm{SU}(2)\times \mathrm{Sp}(4): \qquad y^2z-(x^3+a_2x^2z+\widetilde{a}_4st^2xz^2+\widetilde{a}_6s^2t^4z^3)=0 \tag{13.6}$$

$$(\mathrm{SU}(2)\times \mathrm{SU}(4))/\mathbb{Z}_2: \qquad y^2z+a_1xyz-(x^3+\widetilde{a}_2tx^2z+st^2xz^2)=0 \tag{13.7}$$

$$\mathrm{SU}(2)\times \mathrm{SU}(4): \qquad y^2z+a_1xyz-(x^3+\widetilde{a}_2tx^2z+\widetilde{a}_4st^2xz^2+\widetilde{a}_6s^2t^4z^3)=0 \tag{13.8}$$

Given a complete intersection Z of hypersurfaces $Z_i = V(z_i)$ in a variety X, we denote the blowup of $\widetilde{X}\to X$ along Z with exceptional divisor $E=V(e)$ as

$$\widetilde{X}\xleftarrow{(z_1,\dots,z_n|e)} X.$$

We use the following sequence of blowups to determine a crepant resolution of each models.

$(\mathrm{SU}(2)\times \mathrm{Sp}(4))/\mathbb{Z}_2$ $\mathrm{SU}(2)\times \mathrm{Sp}(4)$	$X_0 \xleftarrow{(x,y,s\|e_1)} X_1 \xleftarrow{(x,y,t\|w_1)} X_2 \xleftarrow{(x,y,w_1\|w_2)} X_3.$
$(\mathrm{SU}(2)\times \mathrm{SU}(4))/\mathbb{Z}_2$ $\mathrm{SU}(2)\times \mathrm{SU}(4)$	$X_0 \xleftarrow{(x,y,s\|e_1)} X_1 \xleftarrow{(x,y,t\|w_1)} X_2 \xleftarrow{(y,w_1\|w_2)} X_3 \xleftarrow{(x,w_2\|w_3)} X_4$

Table 13.3: Sequence of blowups for crepant resolutions used in the chapter.

The class of the fibral divisors are given as follows.

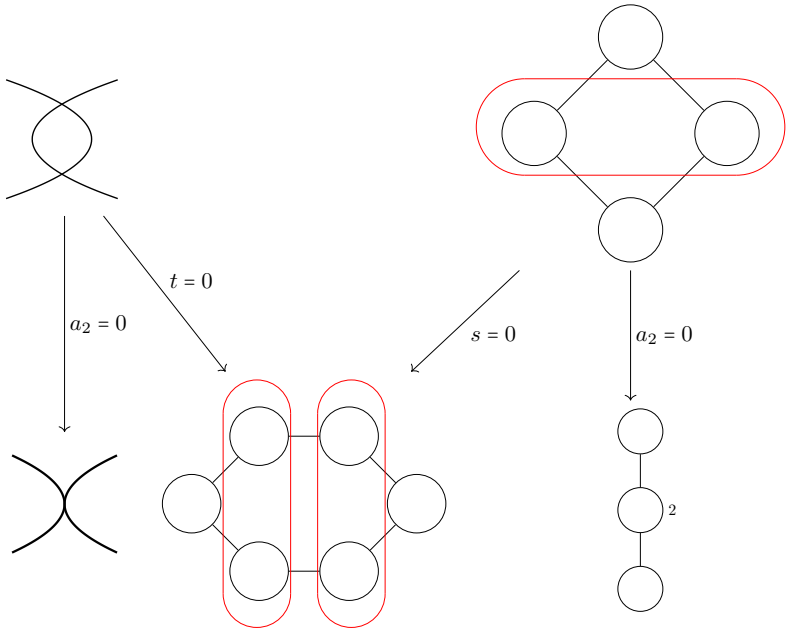

Figure 13.1: This is the fiber structure of $G = (\mathrm{SU}(2) \times \mathrm{Sp}(4))/\mathbb{Z}_2$ uptil codimension two for the Calabi-Yau threefolds.

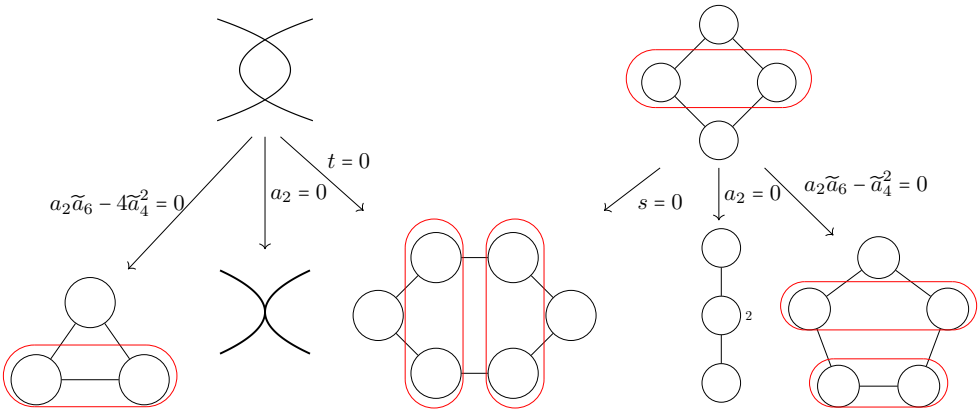

Figure 13.2: This is the fiber structure of $G = \mathrm{SU}(2) \times \mathrm{Sp}(4)$ uptil codimension two for the Calabi-Yau threefolds.

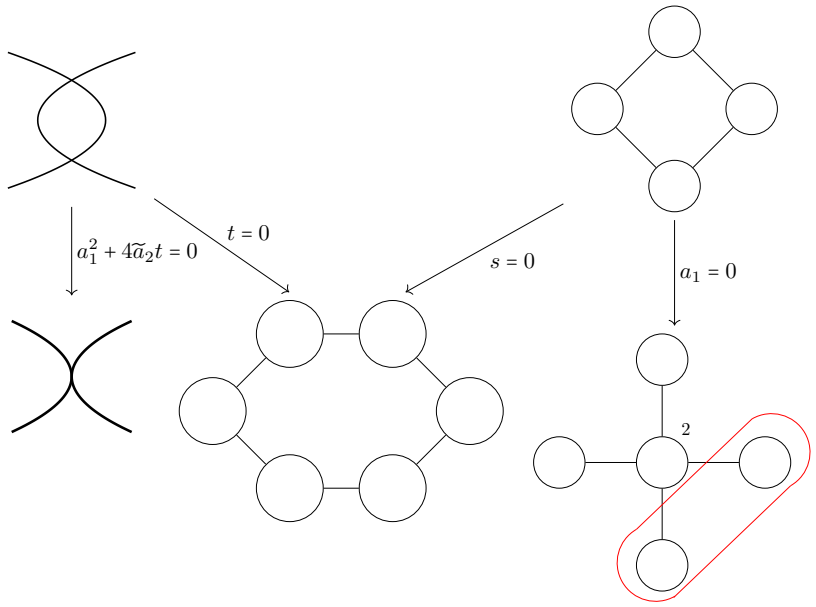

Figure 13.3: This is the fiber structure of $G = (\mathrm{SU}(2) \times \mathrm{SU}(4))/\mathbb{Z}_2$ uptil codimension two for the Calabi-Yau threefolds.

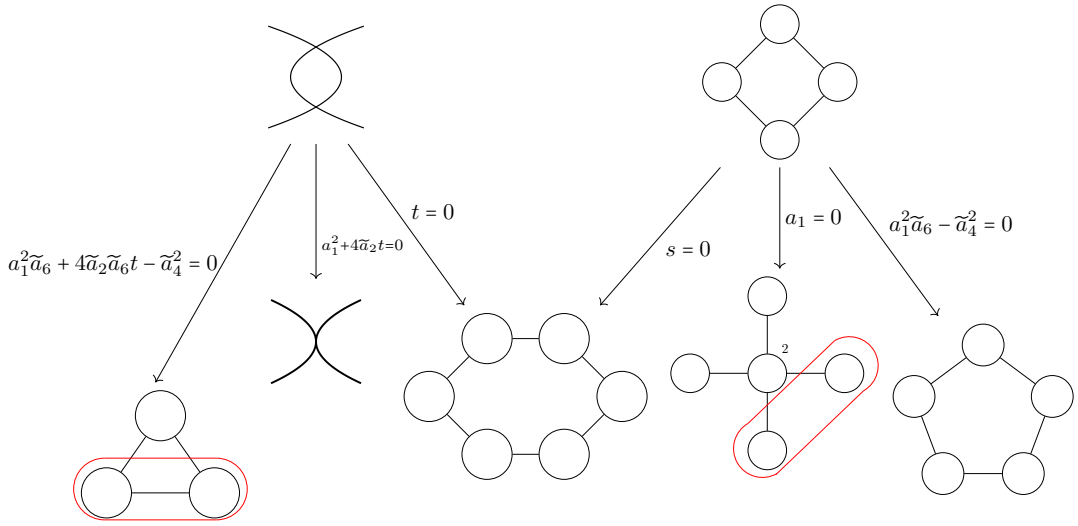

Figure 13.4: This is the fiber structure of $G = \mathrm{SU}(2) \times \mathrm{SU}(4)$ uptil codimension two for the Calabi-Yau threefolds.

	D_0^s	D_1^s	D_0^t	D_1^t	D_2^t	D_3^t
$(\mathrm{SU}(2)\times\mathrm{Sp}(4))/\mathbb{Z}_2$ $\mathrm{SU}(2)\times\mathrm{Sp}(4)$	$S-E_1$	E_1	W_0-W_1	W_1-W_2	W_2	
$(\mathrm{SU}(2)\times\mathrm{SU}(4))/\mathbb{Z}_2$ $\mathrm{SU}(2)\times\mathrm{SU}(4)$	$S-E_1$	E_1	W_0-W_1	W_1-W_2	W_2-W_3	W_3

Table 13.4: Class of the fibral divisors

13.1.2 Euler characteristics

In view of Theorem 2.8.2, this Euler characteristic is independent of the choice of a crepant resolution. We compute the Euler characteristic for each model by considering a particular crepant resolution as listed in Table 13.3. For the models with Mordell-Weil group $\mathbb{Z}_2$, the divisors S and T satisfy the following linear relation since $a_4 = st^2$:

$$4L = S + 2T. \tag{13.9}$$

The generating function of the Euler characteristics are presented in Table 13.5, which produce the Euler characteristics for elliptic threefolds and fourfolds as listed in 13.8 and 13.9. The Calabi-Yau condition imposes $L = -K$. For each model, we present the Euler characteristic of Calabi-Yau threefolds and fourfolds respectively in Table 13.6 and 13.7.

Models	Generating Function
$(\mathrm{SU}(2)\times\mathrm{Sp}(4))/\mathbb{Z}_2$	$\frac{4(2L^2(5T+3)+L(3-5(T-1)T)-3T^2)}{(2L+1)(T+1)(4L-2T+1)}c[B]$
$\mathrm{SU}(2)\times\mathrm{Sp}(4)$	$\frac{2(T(-6L^2(5S+4)+L(2S-3)(5S+4)+S(7S+8)))}{(2L+1)(S+1)(T+1)(-6L+2S+4T-1)}c[B]$ $+\frac{2(3(2L+1)(S^2-L(3S+2))+2T^2(2L(5S+4)+7S+5))}{(2L+1)(S+1)(T+1)(-6L+2S+4T-1)}c[B]$
$(\mathrm{SU}(2)\times\mathrm{SU}(4))/\mathbb{Z}_2$	$\frac{12(2LT+L-T^2)}{(T+1)(4L-2T+1)}c[B]$
$\mathrm{SU}(2)\times\mathrm{SU}(4)$	$\frac{4T^3(7S+5)+4T^2(14S^2-7(7S+5)L+6S-5)}{(S+1)(T+1)(S-4L+2T-1)(2S-6L+4T-1)}c[B]$ $+\frac{2T(12(7S+5)L^2+(2-S(49S+43))L+(7S(S+1)-8)S)}{(S+1)(T+1)(S-4L+2T-1)(2S-6L+4T-1)}c[B]$ $+\frac{6(S-4L-1)(S^2-3SL-2L)}{(S+1)(T+1)(S-4L+2T-1)(2S-6L+4T-1)}c[B]$

Table 13.5: Generating function for Euler Characteristics

Models	Euler Characteristics
$(\mathrm{SU}(2)\times\mathrm{Sp}(4))/\mathbb{Z}_2$	$-4(9K^2+8K\cdot T+3T^2)$
$\mathrm{SU}(2)\times\mathrm{Sp}(4)$	$-2(30K^2+15K\cdot S+30K\cdot T+3S^2+8S\cdot T+10T^2)$
$(\mathrm{SU}(2)\times\mathrm{SU}(4))/\mathbb{Z}_2$	$-12\,(3K^2+3K\cdot T+T^2)$
$\mathrm{SU}(2)\times\mathrm{SU}(4)$	$-2\,(30K^2+15K\cdot S+32K\cdot T+3S^2+8S\cdot T+10T^2)$

Table 13.6: Calabi-Yau threefolds

Models	Euler Characteristics
$(\mathrm{SU}(2)\times\mathrm{Sp}(4))/\mathbb{Z}_2$	$-12\left(c_2K+12K^3+16K^2T+8KT^2+T^3\right)$
$\mathrm{SU}(2)\times\mathrm{Sp}(4)$	$-6\left(2c_2K+60K^3+49K^2S+98K^2T+14KS^2\right.$ $\left.+56KST+56KT^2+S^3+8S^2T+16ST^2+10T^3\right)$
$(\mathrm{SU}(2)\times\mathrm{SU}(4))/\mathbb{Z}_2$	$-12\left(c_2K+12K^3+17K^2T+8KT^2+T^3\right)$
$\mathrm{SU}(2)\times\mathrm{SU}(4)$	$-6\left(2c_2K+60K^3+49K^2S+100K^2T+14KS^2\right.$ $\left.+56KST+56KT^2+S^3+8S^2T+16ST^2+10T^3\right)$

Table 13.7: Calabi-Yau fourfolds

Models	Euler Characteristics
$(\mathrm{SU}(2)\times\mathrm{Sp}(4))/\mathbb{Z}_2$	$4\left(3c_1L-12L^2+8LT-3T^2\right)$
$\mathrm{SU}(2)\times\mathrm{Sp}(4)$	$2\left(6c_1L-36L^2+15LS+30LT-3S^2-8ST-10T^2\right)$
$(\mathrm{SU}(2)\times\mathrm{SU}(4))/\mathbb{Z}_2$	$12\left(c_1L-4L^2+3LT-T^2\right)$
$\mathrm{SU}(2)\times\mathrm{SU}(4)$	$2\left(6c_1L-36L^2+15LS+32LT-3S^2-8ST-10T^2\right)$

Table 13.8: Elliptic threefolds

Models	Euler Characteristics
$(\mathrm{SU}(2)\times\mathrm{Sp}(4))/\mathbb{Z}_2$	$4\,(-12c_1L^2+8c_1LT-3c_1T^2+3c_2L+48L^3$ $-56L^2T+27LT^2-3T^3)$
$\mathrm{SU}(2)\times\mathrm{Sp}(4)$	$2\,(-36c_1L^2+15c_1LS+30c_1LT-3c_1S^2-8c_1ST$ $-10c_1T^2+6c_2L+216L^3-162L^2S-324L^2T+45LS^2T$ $+176LS+178LT^2-3S^3-24S^2T-48ST^2-30T^3)$
$(\mathrm{SU}(2)\times\mathrm{SU}(4))/\mathbb{Z}_2$	$12\,(-4c_1L^2+3c_1LT-c_1T^2+c_2L+16L^3$ $-20L^2T+9LT^2-T^3)$
$\mathrm{SU}(2)\times\mathrm{SU}(4)$	$2\,(-36c_1L^2+15c_1LS+32c_1LT-3c_1S^2-8c_1ST$ $-10c_1T^2+6c_2L+216L^3-162L^2S-332L^2T+45LS^2$ $+176LST+178LT^2-3S^3-24S^2T-48ST^2-30T^3)$

Table 13.9: Elliptic fourfolds

13.1.3 Hodge numbers for Calabi-Yau elliptic threefolds

Hodge numbers of $(\mathrm{SU}(2)\times\mathrm{Sp}(4))/\mathbb{Z}_2$, $\mathrm{SU}(2)\times\mathrm{Sp}(4)$, $(\mathrm{SU}(2)\times\mathrm{SU}(4))/\mathbb{Z}_2$, and $\mathrm{SU}(2)\times\mathrm{SU}(4)$-models are given in Table 13.10.

Models	$h^{1,1}(Y)$	$h^{2,1}(Y)$
$(\mathrm{SU}(2)\times\mathrm{Sp}(4))/\mathbb{Z}_2$	$14-K^2$	$17K^2+16K\cdot T+6T^2+14$
$\mathrm{SU}(2)\times\mathrm{Sp}(4)$	$14-K^2$	$29K^2+15K\cdot S+30K\cdot T+3S^2+8S\cdot T+10T^2+14$
$(\mathrm{SU}(2)\times\mathrm{SU}(4))/\mathbb{Z}_2$	$15-K^2$	$17K^2+18K\cdot T+6T^2+15$
$\mathrm{SU}(2)\times\mathrm{SU}(4)$	$15-K^2$	$29K^2+8T\cdot(4K+S)+15K\cdot S+3S^2+10T^2+15$

Table 13.10: Hodge Numbers

13.1.4 Hyperplane arrangements

Let $\mathfrak{g}$ be a semi-simple Lie algebra and $\mathbf{R}$ a representation of $\mathfrak{g}$. The kernel of each weight ϖ of $\mathbf{R}$ defines a hyperplane $\varpi^{\perp}$ through the origin of the Cartan sub-algebra of $\mathfrak{g}$. The hyperplane arrangements of the considered models are given in Figures 13.5 to 13.7.

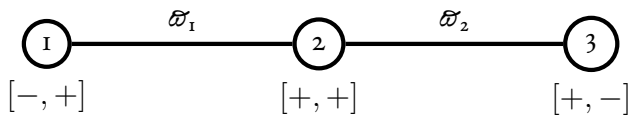

Figure 13.5: There are three chambers in $\mathrm{I}_2^{\mathrm{ns}}+\mathrm{I}_4^{\mathrm{ns}}$-model with a Mordell-Weil group $\mathbb{Z}_2$. Each chamber is noted as the signs of $[\varpi_1,\varpi_2]$ where $\varpi_1=\varphi_1-\psi_1$ and $\varpi_2=\psi_1+\varphi_1-\varphi_2$. For chamber 1, $\varpi_1<0$, $\varpi_2>0$; for chamber 2, $\varpi_1>0$, $\varpi_2>0$; and for chamber 3, $\varpi_1>0$, $\varpi_2<0$.

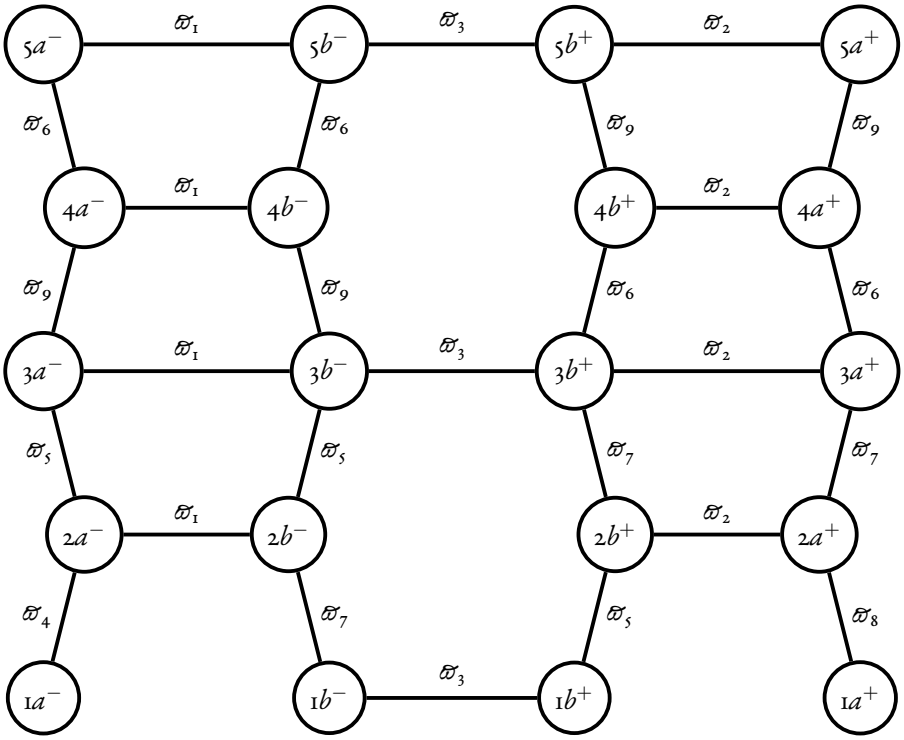

The weights corresponding to the 9 entries are $v = (\varpi_1, \varpi_2, \varpi_3, \varpi_4, \varpi_5, \varpi_6, \varpi_7, \varpi_8, \varpi_9)$, where $\varpi_1 = [0; -1, 1, 0], \varpi_2 = [0; 0, 1, -1], \varpi_3 = [0; -1, 0, 1], \varpi_4 = [1; -1, 1, 0]$, $\varpi_5 = [1; 0, -1, 1], \varpi_6 = [-1; 1, 0, 0], \varpi_7 = [-1; -1, 1, 0], \varpi_8 = [-1; 0, -1, 1], \varpi_9 = [-1; 0, 0, 1]$.

$5a^-$ (010110000)	$5b^-$ (110110000)	$5b^+$ (111100000)	$5a^+$ (101100000)
$4a^-$ (010111000)	$4b^-$ (110111000)	$4b^+$ (111100001)	$4a^+$ (101100001)
$3a^-$ (010111001)	$3b^-$ (110111001)	$3b^+$ (111110001)	$3a^+$ (101110001)
$2a^-$ (010101001)	$2b^-$ (110101001)	$2b^+$ (111111001)	$2a^+$ (101111001)
$1a^-$ (010001001)	$1b^-$ (110101101)	$1b^+$ (111011101)	$1a^+$ (101111111)

Figure 13.6: Chambers of the hyperplane arrangement $\mathsf{I}(A_1 \oplus A_2, \mathbf{R})$ with $\mathbf{R} = (3,1) \oplus (1,15) \oplus (1,6) \oplus (2,4) \oplus (2,\overline{4}) \oplus (1,4) \oplus (1,\overline{4})$. Each circle corresponds to a chamber. The label on the edge connecting two chambers is the wall separating them. In the sign vector, an entry s means a sign $(-1)^{s+1}$ for the corresponding form, that is, $s = 0$ (resp. $s = 1$) means that the corresponding linear form is negative (resp. positive). For example, the chamber $1a^-$ corresponds to (010001001), which gives the sign vector $(-1, 1, -1, -1, -1, 1, -1, -1)$.

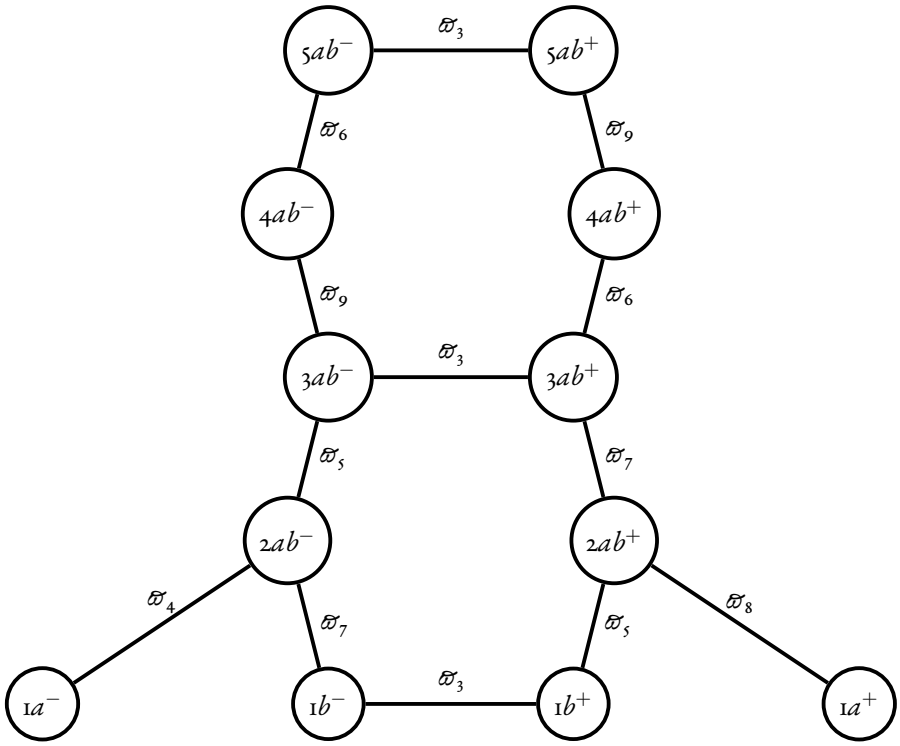

The weights corresponding to the 7 entries are $v = (\varpi_3, \varpi_4, \varpi_5, \varpi_6, \varpi_7, \varpi_8, \varpi_9)$, where $\varpi_3 = [0; -1, 0, 1]$, $\varpi_4 = [1; -1, 1, 0]$, $\varpi_5 = [1; 0, -1, 1]$, $\varpi_6 = [-1; 1, 0, 0]$, $\varpi_7 = [-1; -1, 1, 0]$, $\varpi_8 = [-1; 0, -1, 1]$, $\varpi_9 = [-1; 0, 0, 1]$.

	$5ab^-$ (0110000)	$5ab^+$ (1110000)	
	$4ab^-$ (0111000)	$4ab^+$ (1110001)	
	$3ab^-$ (0111001)	$3ab^+$ (1111001)	
	$2ab^-$ (0101001)	$2ab^+$ (1111101)	
$1a^-$ (0001001)	$1b^-$ (0101101)	$1b^+$ (1101101)	$1a^+$ (1111111)

Figure 13.7: Chambers of the hyperplane arrangement $\mathsf{I}(A_1 \oplus A_2, \mathbf{R})$ with $\mathbf{R} = (3,1) \oplus (1,15) \oplus (2,4) \oplus (2,\overline{4}) \oplus (1,6)$. Each circle corresponds to a chamber. The label on the edge connecting two chambers is the wall separating them. In the sign vector, an entry s means a sign $(-1)^{s+1}$ for the corresponding form, that is, $s = 0$ (resp. $s = 1$) means that the corresponding linear form is negative (resp. positive). For example, the chamber $1a^-$ corresponds to (010001001), which gives the sign vector $(-1, 1, -1, -1, -1, 1, -1, -1)$.

13.1.5 Triple intersection numbers

In contrast to the Euler characteristic, the triple intersection polynomial do depend on the choice of a crepant resolution. Those presented here corresponds to the crepant resolutions given by the sequence of blowups listed in Table 13.3. For each model, we compute the triple intersection numbers of the fibral divisors. We start with the Weierstrass models $\phi : Y \to B$ listed in Table 13.1 and consider the crepant resolution $f : \widetilde{Y} \to Y$ induced by the sequence of blowups in Table 13.3. The crepant resolution produces fibral divisors D_a^s and D_a^t whose classes are listed in Table 13.4. Here, the index a runs through $\{1, 2\}$ for Sp(4) and $\{1, 2, 3\}$ for SU(4). The class of the proper transform $\tilde{Y}$ of Y is

$$(\mathrm{SU}(2) \times \mathrm{Sp}(4))/\mathbb{Z}_2,\ \mathrm{SU}(2) \times \mathrm{Sp}(4) : \quad [\widetilde{Y}] = 3H + 6L - 2E_1 - 2W_1 - 2W_2, \tag{13.10}$$

$$(\mathrm{SU}(2) \times \mathrm{SU}(4))/\mathbb{Z}_2,\ \mathrm{SU}(2) \times \mathrm{SU}(4) : \quad [\widetilde{Y}] = 3H + 6L - 2E_1 - 2W_1 - W_2 - W_3. \tag{13.11}$$

The triple intersection numbers are then given by

$$\mathscr{F}_{trip} = \phi_* f_* \left(\left(D_1^s \psi_1 + \sum_a D_a^t \varphi_a \right)^3 [\widetilde{Y}] \right). \tag{13.12}$$

The pushforwards are computed using theorems 5.0.1 and 5.0.4. We specialize to the Calabi-Yau case by imposing the condition $L = -K$ which ensures that the canonical class of Y is trivial. The triple intersection polynomial of the Calabi-Yau threefold obtained by the resolutions listed in Table 13.3

are

$$\mathscr{F}_{trip}^{(\mathrm{SU}(2)\times\mathrm{Sp}(4))/\mathbb{Z}_2} = -8(T+3K)(T+2K)\psi_1^3 - 8T^2\varphi_1^3 - 4T(K+T)\varphi_2^3 - 12KT\varphi_1^2\varphi_2 + 6T(T+2K)\varphi_1\varphi_2^2 + 12T(T+2K)\psi_1(2\varphi_1^2 - 2\varphi_2\varphi_1 + \varphi_2^2). \tag{13.13}$$

$$\mathscr{F}_{trip}^{\mathrm{SU}(2)\times\mathrm{Sp}(4)} = -2S(S-2K)\psi_1^3 - 8T^2\varphi_1^3 + 2T(2K+S)\varphi_2^3 + 6T(S+2T+2K)\varphi_1^2\varphi_2 - 6T(2K+S+T)\varphi_1\varphi_2^2 - 6ST\psi_1\left(2\varphi_1^2 - 2\varphi_2\varphi_1 + \varphi_2^2\right). \tag{13.14}$$

$$\mathscr{F}_{trip}^{(\mathrm{SU}(2)\times\mathrm{SU}(4))/\mathbb{Z}_2} = -8\left(6K^2+5KT+T^2\right)\psi_1^3 - 4T(K+T)\left(\varphi_1^3+\varphi_2^3\right) - 2T(K+2T)\varphi_3^3 + 6KT\varphi_1^2\varphi_3 - 6KT\varphi_1\varphi_2\varphi_3 + 3T(T+2K)\varphi_2^2\left(\varphi_1+\varphi_3\right) - 3KT\varphi_2\left(\varphi_1^2+\varphi_3^2\right) + 12T(T+2K)\psi_1\left(\varphi_1^2 - \varphi_2\varphi_1 + \varphi_2^2 + \varphi_3^2 - \varphi_2\varphi_3\right). \tag{13.15}$$

$$\mathscr{F}_{trip}^{\mathrm{SU}(2)\times\mathrm{SU}(4)} = -2S(S-2K)\psi_1^3 - 4T(K+T)\varphi_1^3 + 2T(S+2K)\varphi_2^3 - 2T(K+2T)\varphi_3^3 + 6KT\varphi_1^2\varphi_3 - 6KT\varphi_1\varphi_2\varphi_3 - 3T(2K+S+T)\varphi_2^2\left(\varphi_1+\varphi_3\right) + 3T(3K+S+2T)\varphi_2\left(\varphi_1^2+\varphi_3^2\right) - 6ST\psi_1\left(\varphi_1^2 - \varphi_2\varphi_1 + \varphi_2^2 + \varphi_3^2 - \varphi_2\varphi_3\right). \tag{13.16}$$

13.1.6 The prepotential of the five-dimensional theories

Following Intrilligator, Morrison, and Seiberg [176], we compute the quantum contribution to the prepotential of a five-dimensional gauge theory ($6.\mathscr{F}_{IMS}$) with the matter fields in the representations $\mathbf{R}_i$ of the gauge group. Let φ be in the Cartan subalgebra of a Lie algebra $\mathfrak{g}$. We denote by $\varphi = \{\psi_1, \varphi_1, \varphi_2\}$ for the cases with $\mathfrak{g} = \mathfrak{su}(2) + \mathfrak{sp}(4)$, and we denote by $\varphi = \{\psi_1, \varphi_1, \varphi_2, \varphi_3\}$ for the cases with $\mathfrak{g} = \mathfrak{su}(2) + \mathfrak{su}(4)$. The weights are in the dual space of the Cartan subalgebra. We denote the evaluation of a weight on φ as a scalar product $\langle \mu, \varphi \rangle$. We recall that the roots are the weights of the adjoint representation of $\mathfrak{g}$. Denoting the fundamental roots by α and the weights of $\mathbf{R}_i$ by ϖ we have

$$\mathscr{F}_{\text{IMS}} = \frac{1}{12}\left(\sum_{\alpha} |\langle \alpha, \varphi \rangle|^3 - \sum_{\mathbf{R}_i} \sum_{\varpi \in W_i} n_{\mathbf{R}_i} |\langle \varpi, \varphi \rangle|^3\right). \tag{13.17}$$

The representations $\mathbf{R}$ for each group are determined geometrically by using the splittings of the curves. The prepotential is computed in a particular chamber of the five-dimensional theory that matches with the crepant resolution in which the triple intersection polynomial is computed.

For the case of $G = (\mathrm{SU}(2) \times \mathrm{Sp}(4))/\mathbb{Z}_2$, we first determine that matching chamber is given by

$$\text{Chamber } [-,+] : 2\varphi_2 > 2\varphi_1 > \varphi_2 > 0 \wedge \psi_1 > \varphi_1,$$

which is the left chamber in Figure 13.5. The prepotential in this chamber $[-,+]$ is given by

$$\begin{aligned} 6\mathscr{F}_{\text{IMS}} = &-4(n_{2,4}+2n_{3,1}-2)\psi_1^3-8(n_{1,10}-1)\varphi_1^3+(-8n_{1,10}-n_{1,5}+8)\varphi_2^3 \\ &-3\varphi_1^2\varphi_2(4n_{1,10}+n_{1,5}-4)+3(6n_{1,10}+n_{1,5}-6)\varphi_1\varphi_2^2 \\ &+\psi_1\left(-12n_{2,4}\varphi_1^2+12n_{2,4}\varphi_2\varphi_1-6n_{2,4}\varphi_2^2\right). \end{aligned} \tag{13.18}$$

For the case of $G=\text{SU}(2)\times\text{Sp}(4)$, we find the matching chamber to be

$$\text{Chamber}\,[-,+]: 2\varphi_2>2\varphi_1>\varphi_2>0\wedge\psi_1>\varphi_1,$$

which is the very same chamber with the one above with a trivial Mordell-Weil group. Due to its different representations, the prepotential is given by

$$\begin{aligned} 6\mathscr{F}_{\text{IMS}} = &-(n_{2,1}-4n_{2,4}+8n_{3,1}-8)\psi_1^3-8(n_{1,10}+n_{1,5}-1)\varphi_1^3-(8n_{1,10}+n_{1,4}-8)\varphi_2^3 \\ &-3\varphi_1^2\varphi_2(4n_{1,10}+n_{1,4}-4n_{1,5}-4)+3(6n_{1,10}+n_{1,4}-2n_{1,5}-6)\varphi_1\varphi_2^2 \\ &+\psi_1\left(-12n_{2,4}\varphi_1^2+12n_{2,4}\varphi_1\varphi_2-6n_{2,4}\varphi_2^2\right). \end{aligned} \tag{13.19}$$

For the case of $G=(\text{SU}(2)\times\text{SU}(4))/\mathbb{Z}_2$, we find the matching chamber to be

$$\text{Chamber}\,5ab+: \varphi_1>\varphi_2>0\wedge\psi_1>\varphi_1\wedge\psi_1>\varphi_3>\varphi_2-\psi_1, \tag{13.20}$$

which is a chamber on the top right of Figure 13.7. The prepotential in this chamber is given by

$$\begin{aligned}
6\mathscr{F}_{\text{IMS}} = & -4(n_{2,4}+n_{2,\bar{4}}+2n_{3,1}-2)\psi_1^3-8(n_{1,15}-1)\varphi_1^3-(8n_{1,15}-8)\varphi_2^3 \\
& -2(4n_{1,15}+n_{1,6}-4)\varphi_3^3-6n_{1,6}\varphi_1^2\varphi_3+6n_{1,6}\varphi_1\varphi_2\varphi_3+\frac{3}{2}(4n_{1,15}-2n_{1,6}-4)\varphi_2^2(\varphi_1+\varphi_3) \\
& -\frac{3}{2}(-2n_{1,6})\varphi_2(\varphi_1^2+\varphi_3^2)-6(n_{2,4}+n_{2,\bar{4}})\psi_1\left(\varphi_1^2-\varphi_1\varphi_2+\varphi_2^2+\varphi_3^2-\varphi_2\varphi_3\right).
\end{aligned} \tag{13.21}$$

For the case of $G = \mathrm{SU}(2)\times\mathrm{SU}(4)$, we find the matching chamber to be

$$\text{Chamber } 5b+ : 2\varphi_1 > \varphi_2 > 0 \wedge \varphi_2 > \varphi_3 > \varphi_1 \wedge \psi_1 > \varphi_3, \tag{13.22}$$

which is represented in Figure 13.6. The prepotential in this chamber is given by

$$\begin{aligned}
6\mathscr{F}_{\text{IMS}} = & -(n_{3,1}+4(n_{2,4}+n_{2,\bar{4}}+2n_{3,1}-2))\psi_1^3-8(n_{1,15}-1)\varphi_1^3 \\
& -(8n_{1,15}+n_{1,4}+n_{1,\bar{4}}-8)\varphi_2^3-2(4n_{1,15}+n_{1,6}-4)\varphi_3^3-6n_{1,6}\varphi_1^2\varphi_3+6n_{1,6}\varphi_1\varphi_2\varphi_3 \\
& +\frac{3}{2}(4n_{1,15}+n_{1,4}+n_{1,\bar{4}}-2n_{1,6}-4)\varphi_2^2(\varphi_1+\varphi_3)-\frac{3}{2}(n_{1,4}+n_{1,\bar{4}}-2n_{1,6})\varphi_2(\varphi_1^2+\varphi_3^2) \\
& -6(n_{2,4}+n_{2,\bar{4}})\psi_1\left(\varphi_1^2-\varphi_1\varphi_2+\varphi_2^2+\varphi_3^2-\varphi_2\varphi_3\right).
\end{aligned} \tag{13.23}$$

13.1.7 Number of charged hypermultiplets.

The number of charged hypermultiplets under each representation is obtained by comparing the triple intersection numbers and the one-loop prepotential:

$$\mathscr{F}_{trip} = 6\mathscr{F}_{IMS}. \tag{13.24}$$

The comparison is enough to completely determine the number $n_{\mathbf{R}_i}$ for the models with a $\mathbb{Z}_2$ Mordell-Weil group, that is, $(\mathrm{SU}(2) \times \mathrm{Sp}(4))/\mathbb{Z}_2$ and $(\mathrm{SU}(2) \times \mathrm{SU}(4))/\mathbb{Z}_2$. We see that the introduction of a $\mathbb{Z}_2$ Mordell-Weil group removes the fundamental representation, but does not affect the (traceless) antisymmetric representation, the adjoint, or bifundamental matters since they are self-dual representations. However, for the models $\mathrm{SU}(2) \times \mathrm{Sp}(4)$ and $\mathrm{SU}(2) \times \mathrm{SU}(4)$, comparing the triple intersection numbers and the one-loop prepotential is not enough to fix all the multiplicities and we are left with some linear relations between the number of representations. This is because without the $\mathbb{Z}_2$, we get additional matter content but the non-zero triple intersection numbers are unchanged. The remaining linear relations can be solved in many ways. For example, we can use Witten's genus formula to count the number of adjoint matters as the genus of the curve supporting the gauge group [306]. Another possibility is to direct count the number of bi-fundamental representations as intersection numbers between the divisors S and T. We can also use the vanishing of anomalies in the six dimensional uplift to fix the remaining linear equations. For example, the gravitational anomaly or the vanishing of the terms $\mathbf{tr}F_a^4$ are enough in addition to the linear relations left

from the triple intersection numbers. The result is spelled out in Table 13.2.

13.2 $(\mathrm{SU}(2)\times \mathrm{Sp}(4))/\mathbb{Z}_2$-model

The fiber geometry of the collision of $\mathrm{I}_2^{\mathrm{ns}}$ and $\mathrm{I}_4^{\mathrm{ns}}$ is described in detail. The Weierstrass equation of $\mathrm{I}_2^{\mathrm{ns}}+\mathrm{I}_4^{\mathrm{ns}}$ is given by

$$y^2z = x^3 + a_2x^2z + st^2xz^2, \tag{13.25}$$

where $S = V(s)$ is the divisor supporting $\mathrm{I}_2^{\mathrm{ns}}$ and $T = V(t)$ is the divisor supporting $\mathrm{I}_4^{\mathrm{ns}}$. The discriminant of this model is

$$\Delta = 16s^2t^4(a_2^2 - 4st^2). \tag{13.26}$$

The corresponding simply connected group G and the representation $\mathbf{R}$, which is computed geometrically in the next section, are

$$G = (\mathrm{SU}(2)\times \mathrm{Sp}(4))/\mathbb{Z}_2, \quad \mathbf{R} = (3,1)\oplus(1,10)\oplus(2,4)\oplus(1,5). \tag{13.27}$$

The following sequence of blowups gives a crepant resolution of the elliptic fibration:

$$X_0 \xleftarrow{(x,y,s|e_1)} X_1 \xleftarrow{(x,y,t|w_1)} X_2 \xleftarrow{(x,y,w_1|w_2)} X_3. \tag{13.28}$$

The proper transform is

$$y^2 = e_1w_1w_2^2x^3 + a_2x^2 + st^2w_1x, \tag{13.29}$$

and the relative projective "coordinates" are

$$[e_1 w_1 w_2^2 x : e_1 w_1 w_2^2 y : z = 1][w_1 w_2^2 x : w_1 w_2^2 y : s][w_2 x : w_2 y : t][x : y : w_1]. \tag{13.30}$$

To show that we have a resolution of singularities, it is enough to assume that $V(a_2)$, $V(s)$, and $V(t)$ are smooth divisors intersecting transversally. In particular, working in patches using (x, y, a_2) as a part of the local coordinates, the absence of singularities follows from the Jacobian criterion. From applying the adjunction formula after each blowup, we conclude that the resolution is crepant.

13.2.1 Fiber structure and representations

We denote by D_i^s $(i = 0, 1)$, D_j^t $(j = 0, 1, 2)$ the fibral divisors; by C_i^s $(i = 0, 1)$ and C_j^t $(j = 0, 1, 2)$ the generic fibers of D_i^s over S and D_j^t over T, respectively. The fibral divisors for this model are

$$\begin{cases} D_0^s & : s = y^2 - e_1 w_1 w_2^2 x^3 - a_2 x^2 = 0, \\ D_1^s & : e_1 = y^2 - a_2 x^2 - s t^2 w_1 x = 0, \\ D_0^t & : t = y^2 - e_1 w_1 w_2^2 x^3 - a_2 x^2 = 0, \\ D_1^t & : w_1 = y^2 - a_2 x^2 = 0, \text{ (two roots } C_1 = C_{1+}^t + C_{1-}^t), \\ D_2^t & : w_2 = y^2 - a_2 x^2 - s t^2 w_1 x = 0. \end{cases} \tag{13.31}$$

The only components that touch the generator of $\mathbb{Z}_2$ are C_1^s and C_2^t. The only sections that touch the zero section are D_0^s and D_0^t.

Over $S = V(s)$, we have a generic fiber of type $\mathrm{I}_2^{\mathrm{ns}}$ with two geometric components C_0^s and C_1^s. The fiber $\mathrm{I}_2^{\mathrm{ns}}$ specializes to a fiber of type III over $V(a_2)$. Over $T = V(t)$, on the other hand, we have a generic fiber of type $\mathrm{I}_4^{\mathrm{ns}}$, whose geometric components are C_0^t, C_{1+}^t, C_{1-}^t, and C_2^t. The fiber $\mathrm{I}_4^{\mathrm{ns}}$ further enhances over $V(a_2)$, where two non-split curves $C_{1\pm}^t$ degenerate, which is represented on the right side of Figure 13.8.

At the collision of S and T, we produce the following curves:

$$\begin{cases} C_0^s \cap C_0^t & : s = t = y^2 - e_1 w_1 w_2^2 x^3 - a_2 x^2 = 0 \to \eta^{00}, \\ C_1^s \cap C_0^t & : e_1 = t = y^2 - a_2 x^2 = 0 \to \eta^{10\pm}, \text{ (two roots for each curve,)} \\ C_1^s \cap C_1^t & : e_1 = w_1 = y^2 - a_2 x^2 = 0 \to \eta^{11\pm}, \text{ (two roots for each curve,)} \\ C_1^s \cap C_2^t & : e_1 = w_2 = y^2 - a_2 x^2 - s t^2 w_1 x = 0 \to \eta^{12}. \end{cases} \tag{13.32}$$

The fiber structure is represented in Figure 13.8. As expected, the collision of the divisors of the two fibers (type $\mathrm{I}_2^{\mathrm{ns}}$ and $\mathrm{I}_4^{\mathrm{ns}}$) is naturally enhanced into an $\mathrm{I}_6^{\mathrm{ns}}$.

The fibers of the collisions can be described from the splitting of the curves C_i^s ($i = 0, 1$) and C_i^t ($i = 0, 1, 2$) from $\mathrm{I}_2^{\mathrm{ns}}$ and $\mathrm{I}_4^{\mathrm{ns}}$, respectively:

$$\begin{cases} C_0^s & \to \eta^{00}, \quad C_1^s \to \eta^{10+} + \eta^{10-} + \eta^{11+} + \eta^{11-} + \eta^{12}, \\ C_0^t & \to \eta^{00} + \eta^{10+} + \eta^{10-}, \quad C_1^t \to \eta^{11+} + \eta^{11-}, \quad C_2^t \to \eta^{12}. \end{cases} \tag{13.33}$$

From these splittings of the curves, we compute the intersection numbers between the curves and

the fibral divisors of $\mathrm{I}_2^{\mathrm{ns}}$ and $\mathrm{I}_4^{\mathrm{ns}}$ on the collision to be

	D_0^s	D_1^s	D_0^t	D_1^t	D_2^t
η^{00}	-2	2	0	0	0
$\eta^{10+} + \eta^{10-}$	2	-2	-2	2	0
$\eta^{10\pm}$	1	-1	-1	1	0
$\eta^{11+} + \eta^{11-}$	0	0	2	-4	2
$\eta^{11\pm}$	0	0	1	-2	1
η^{12}	0	0	0	2	-2

(13.34)

The physical weight are minus the intersection numbers. We recall that the curve $\eta^{10\pm}$ carries the weight $[1]$ on the $\mathfrak{su}(2)$ side and the weight $[-1, 0]$ on the $\mathfrak{sp}(4)$ side. This gives $[1; -1, 0]$, which yields the representation $(2, 4)$. These non-split curves join together to produce $\eta^{10+} + \eta^{10-}$ with weight $[2; -2, 0]$, and the corresponding representation is $(3, 10)$. Hence, the representation for the $\mathrm{I}_2^{\mathrm{ns}}+\mathrm{I}_4^{\mathrm{ns}}$-model with Mordell-Weil group $\mathbb{Z}_2$ is $\mathbf{R} = (3, 1) \oplus (1, 10) \oplus (3, 10) \oplus (2, 4) \oplus (1, 5)$. We note that for the case of threefolds, the curves $\eta^{10\pm}$ are always split since all curve can split over a codimension-two point. Hence, the bi-adjoint $(3, 10)$ does not show up geometrically. Hence for the Calabi-Yau threefolds, the representation is then

$$\mathbf{R} = (3, 1) \oplus (1, 10) \oplus (2, 4) \oplus (1, 5). \tag{13.35}$$

The only group that is consistent with this representation R is

$$G = (\mathrm{SU}(2) \times \mathrm{Sp}(4))/\mathbb{Z}_2, \tag{13.36}$$

where $\mathbb{Z}_2$ is minus the identity.

The representations with respect to $(\mathfrak{su}(2), \mathfrak{sp}(4))$ from this $\mathrm{I}_2^{\mathrm{ns}}+\mathrm{I}_4^{\mathrm{ns}}$-model with the Mordell-Weil group $\mathbb{Z}_2$ are summarized in Table 13.11 below. Here we denoted weights as $[\psi; \phi_1, \phi_2]$ where $[\psi]$ is the weight for the $\mathfrak{su}(2)$ and $[\phi_1, \phi_2]$ is the weight for the $\mathfrak{sp}(4)$.

Locus	$tw_1w_2 = 0$	$se_1 = tw_1w_2 = 0$	
Curves	$C_1^{\prime\prime\prime}$	$\eta^{10\pm}$	$\eta^{10+} + \eta^{10-}$
Weights	$[0; 2, -1]$	$[1; -1, 0]$	$[2; -2, 0]$
Representations	$(1, 5)$	$(2, 4)$	$(3, 10)$

Table 13.11: Weights and representations for the $\mathrm{I}_2^{\mathrm{ns}}+\mathrm{I}_4^{\mathrm{ns}}$-model with a Mordell-Weil group $\mathbb{Z}_2$

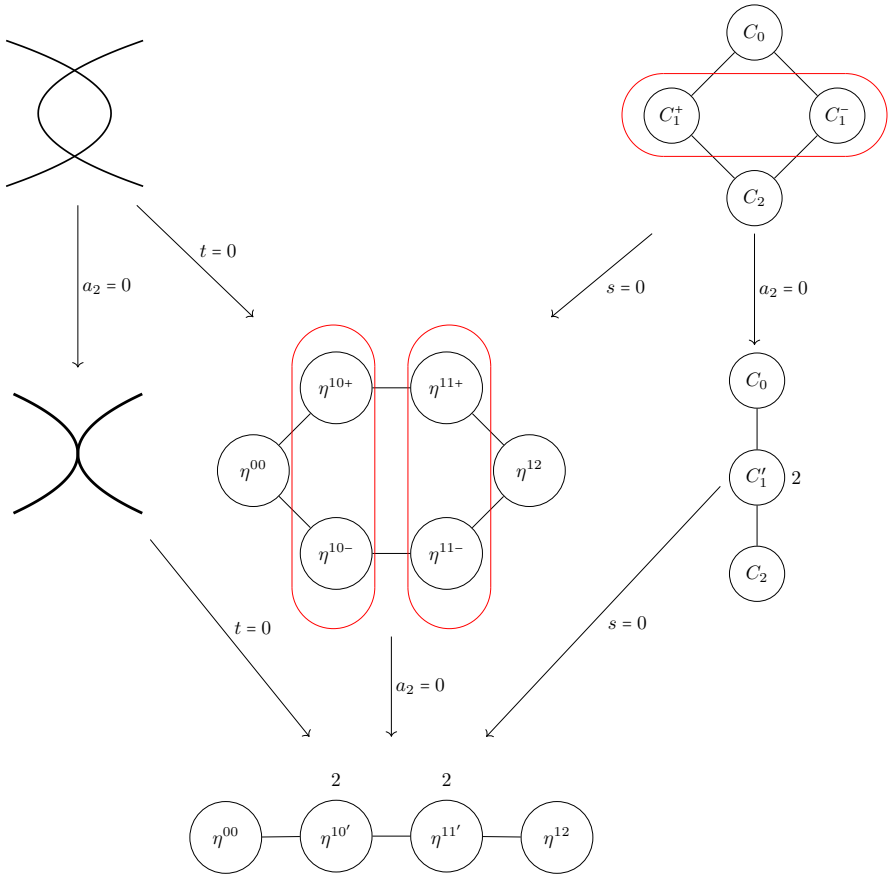

Figure 13.8: Fiber structure of $I_2^{ns}+I_4^{ns}$ with a Mordell-Weil group $\mathbb{Z}_2$. The diagrams on the top are the Kodaira fibers of type I_2^{ns} and I_4^{ns}. When $a_2 = 0$, I_2^{ns} specializes to III, as seen in the middle left diagram, and I_4^{ns} specializes to the diagram on the middle right. When I_2^{ns} and I_4^{ns} collide on the locus $se_1 = tw_1w_2w_3 = 0$, we get the fiber structure of the collision of I_2^{ns} and I_4^{s} as the hexagon drawn in the middle. This enhancement has two newly split curves η^{10+} and η^{10-} that are of non-split type. When $a_2 = 0$, this hexagon further specializes to the diagram on the bottom.

13.2.2 Coulomb phases

In this section, we show that the $I_2^{ns}+I_4^{ns}$-model with a Mordell-Weil group $\mathbb{Z}_2$ has three chambers.

Denote $\mathfrak{su}(2)$ by $[\psi]$ and $\mathfrak{sp}(4)$ by $[\phi_1, \phi_2, \phi_3]$. Then the Weyl chamber of the $I_2^{ns}+I_4^{ns}$-model with

$\mathbb{Z}_2$ is defined with three hyperplanes given by

$$\psi_1 > 0, \quad \varphi_2 - \varphi_1 > 0, \quad 2\varphi_1 - \varphi_2 > 0. \tag{13.37}$$

In addition, the subchambers are defined by the weights of the representation $(2, 4)$,

$$\varpi_1 = \varphi_1 - \psi_1, \quad \varpi_2 = \psi_1 + \varphi_1 - \varphi_2, \tag{13.38}$$

where the summation of these is positive from the first two hyperplanes in equation (13.37):

$$\varpi_1 + \varpi_2 = (2\varphi_1 - \varphi_2) + \psi_1 > 0. \tag{13.39}$$

Hence, ϖ_1 and ϖ_2 cannot be both negative. It follows there are a total of three chambers, which are denoted by the signs of $[\varpi_1, \varpi_2]$:

$$[-,+] : \varphi_2 > 0 \wedge \frac{\varphi_2}{2} < \varphi_1 < \varphi_2 \wedge \psi_1 > \varphi_1, \tag{13.40}$$

$$[+,+] : \varphi_2 > 0 \wedge \frac{\varphi_2}{2} < \varphi_1 < \varphi_2 \wedge \varphi_2 - \varphi_1 < \psi_1 < \varphi_1, \tag{13.41}$$

$$[+,-] : \varphi_1 > 0 \wedge \varphi_1 < \varphi_2 < 2\varphi_1 \wedge 0 < \psi_1 < \varphi_2 - \varphi_1. \tag{13.42}$$

The chambers are flop related by ϖ_1 and ϖ_2, as shown in Figure 13.5.

13.2.3 $5d\,\mathcal{N}=1$ PREPOTENTIALS AND THE TRIPLE INTERSECTION POLYNOMIALS

The triple intersection polynomial is computed for the $\mathrm{I}_2^{\mathrm{ns}}+\mathrm{I}_4^{\mathrm{ns}}$-model with the Mordell-Weil group $\mathbb{Z}_2$ in the crepant resolution:

$$\begin{aligned}\mathscr{F}_{trip} =& -8(T-3L)(T-2L)\psi_1^3-8T^2\varphi_1^3+4T(L-T)\varphi_2^3+12LT\varphi_1^2\varphi_2+6T(T-2L)\varphi_1\varphi_2^2\\&+\psi_1(24T(T-2L)\varphi_1^2-24T(T-2L)\varphi_2\varphi_1+12T(T-2L)\varphi_2^2)\\&-8\psi_0^3(3L-2T)(2L-T)+6T(2L-T)\varphi_0^2\left(\varphi_1-2\psi_1\right)-4LT\varphi_0^3\\&+2\varphi_0\left(6T\psi_1^2(T-2L)+12T\psi_1\varphi_1(2L-T)+6T\varphi_1^2(T-L)\right)\\&+\psi_0^2\left(2\left(8\psi_1(3L-2T)(2L-T)-4\psi_1(2L-T)(3L-T)\right)+12T\varphi_0(T-2L)\right)\\&+\psi_0\left(2\left(8\psi_1^2(2L-T)(3L-T)-4\psi_1^2(3L-2T)(2L-T)\right)-24T\psi_1\varphi_0(T-2L)\right).\end{aligned}\tag{13.43}$$

For Calabi-Yau threefolds, the representation for this $\mathrm{I}_2^{\mathrm{ns}}+\mathrm{I}_4^{\mathrm{ns}}$-model is geometrically computed as

$$\mathbf{R}=(3,1)\oplus(1,10)\oplus(2,4)\oplus(1,5).\tag{13.44}$$

Using these representations, the $5d$ prepotential in the chamber $[-,+]$ is

$$\begin{aligned}6\mathscr{F}_{\mathrm{IMS}} =& -4(n_{2,4}+2n_{3,1}-2)\psi_1^3-8(n_{1,10}-1)\varphi_1^3+(-8n_{1,10}-n_{1,5}+8)\varphi_2^3\\&-3\varphi_1^2\varphi_2(4n_{1,10}+n_{1,5}-4)+3(6n_{1,10}+n_{1,5}-6)\varphi_1\varphi_2^2\\&+\psi_1\left(-12n_{2,4}\varphi_1^2+12n_{2,4}\varphi_2\varphi_1-6n_{2,4}\varphi_2^2\right).\end{aligned}\tag{13.45}$$

Using the triple intersection polynomials that are independent from ψ_0 and φ_0 to match the prepotential, the numbers of representations n_R are computed to be

$$\begin{aligned} &n_{3,1} = 6L^2 - 7LT + 2T^2 + 1 = g_S, \quad n_{2,4} = -2T(T-2L) = 2(-4g_T + T^2 + 4), \\ &n_{1,5} = \frac{1}{2}(LT + T^2) = -g_T + T^2 + 1, \quad n_{1,10} = \frac{1}{2}(-LT + T^2 + 2) = g_T. \end{aligned} \tag{13.46}$$

13.2.4 $6d\,\mathcal{N} = (1,0)$ ANOMALY CANCELLATION

In this section, we consider an $\mathrm{I}_2^{\mathrm{ns}}+\mathrm{I}_4^{\mathrm{ns}}$-model with the Mordell-Weil group $\mathbb{Z}_2$. Then, the gauge algebra is given by

$$\mathfrak{g} = A_1 + C_2, \tag{13.47}$$

and the representation is geometrically computed in Section 13.2 to be

$$\mathbf{R} = (3,1) \oplus (1,10) \oplus (2,4) \oplus (1,5). \tag{13.48}$$

Then the number of vector multiplets $n_V^{(6)}$, tensor multiplets n_T, and hypermultiplets n_H are computed to be

$$\begin{aligned} &n_V^{(6)} = 13, \quad n_T = 9 - K^2, \\ &n_H = h^{2,1}(Y) + 1 + n_{3,1}(3-1) + n_{2,4}(10-2) + n_{1,5}(5-1) + n_{1,10}(10-2) \\ &\quad = 17K^2 + 16KT + 6T^2 + 14. \end{aligned} \tag{13.49}$$

We recall the number of representations from the earlier subsection:

$$\begin{aligned} &n_{3,1} = (2K+T)(3K+2T)+1,\ n_{2,4} = -2T(2K+T), \\ &n_{1,5} = \frac{1}{2}T(T-K), \quad n_{1,10} = \frac{1}{2}(KT+T^2+2). \end{aligned} \tag{13.50}$$

Thus, we see that

$$n_H - n_V^{(6)} + 29n_T - 273 = 0, \tag{13.51}$$

which means that the pure gravitational anomalies are canceled.

By using the trace identities for SU(2), we first compute the SU(2) side of the anomaly polynomials. First, we can determine that

$$n_3 = n_{3,1}, \quad n_2 = 4n_{2,4}. \tag{13.52}$$

For SU(2) with the adjoint representation 3 and the fundamental representation $\mathbf{F} = 2$ as the reference representation,

$$\mathrm{tr}_3 F_1^2 = 4\mathrm{tr}_2 F_1^2, \quad \mathrm{tr}_3 F_1^4 = 8(\mathrm{tr}_2 F_1^2)^2, \quad \mathrm{tr}_2 F_1^4 = \frac{1}{2}(\mathrm{tr}_2 F_1^2)^2. \tag{13.53}$$

Hence, $X_1^{(2)}$ and $X_1^{(4)}$ are given by

$$X_1^{(2)} = (A_3(1-n_3) - n_2 A_2)\,\mathbf{tr}_2 F_1^2 = -12K(2K+T)\mathbf{tr}_2 F_1^2 \tag{13.54}$$

$$\begin{aligned} X_1^{(4)} &= (B_3(1-n_3) - n_2 B_2)\,\mathbf{tr}_2 F_1^4 + (C_3(1-n_3) - n_2 C_2)\,(\mathbf{tr}_2 F_1^2)^2 \\ &= -12(2K+T)^2(\mathbf{tr}_2 F_1^2)^2. \end{aligned} \tag{13.55}$$

Now consider the Sp(4) side of the anomaly cancellation by using the trace identities for Sp(4). We first determine that

$$n_{10} = n_{1,10}, \quad n_5 = n_{1,5}, \quad n_4 = 2n_{2,4}. \tag{13.56}$$

The trace identities for Sp(4) is given by

$$\begin{aligned} \mathrm{tr}_{10}\, F_2^2 &= 6\mathrm{tr}_4\, F_2^2, \quad \mathrm{tr}_{10}\, F_2^4 = 12\mathrm{tr}_4\, F_2^4 + 3(\mathrm{tr}_4\, F_2^2)^2, \\ \mathrm{tr}_5\, F_2^2 &= 2\mathrm{tr}_4\, F_2^2, \quad \mathrm{tr}_5\, F_2^4 = -4\mathrm{tr}_4\, F_2^4 + 3(\mathrm{tr}_4\, F_2^2)^2. \end{aligned} \tag{13.57}$$

Hence, $X_2^{(2)}$ and $X_2^{(4)}$ are given by

$$X_2^{(2)} = (A_{10}(1 - n_{10}) - n_5 A_5 - n_4 A_4)\, \mathbf{tr}_4 F_2^2 = 6KT\mathbf{tr}_4 F_2^2 \tag{13.58}$$

$$\begin{aligned} X_2^{(4)} &= (B_{10}(1 - n_{10}) - n_5 B_5 - n_4 B_4)\, \mathbf{tr}_4 F_2^4 + (C_{10}(1 - n_{10}) - n_5 C_5 - n_4 C_4)\, (\mathbf{tr}_4 F_2^2)^2 \\ &= -3T^2 (\mathbf{tr}_4 F_2^2)^2. \end{aligned} \tag{13.59}$$

Now we further include on both the SU(2) and Sp(4) sides the additional mixed term

$$Y_{12} = n_{2,4} \mathbf{tr}_2 F_1^2 \mathbf{tr}_4 F_2^2; \tag{13.60}$$

this is necessary to fully consider the bifundamental representation $(2, 4)$. Then the full anomaly

polynomial is given by

$$\begin{aligned} I_8 &= \frac{9-n_T}{8}(\mathbf{tr}R^2)^2 + \frac{1}{6}(X_1^{(2)} + X_2^{(2)})\mathbf{tr}R^2 - \frac{2}{3}(X_1^{(4)} + X_2^{(4)}) + 4Y_{12} \\ &= \frac{1}{8}\left(K\mathbf{tr}R^2 - 16K\mathbf{tr}_4F_2^2 - 8T\mathbf{tr}_4F_2^2 + 4T\mathbf{tr}_2F_1^2\right)^2, \end{aligned} \tag{13.61}$$

which is a perfect square. This means that the total anomalies are canceled.

13.3 SU(2) × Sp(4)-model

In this section we consider the $\mathrm{I}_2^{\mathrm{ns}}+\mathrm{I}_4^{\mathrm{ns}}$-model with a trivial Mordell-Weil group. The Weierstrass model is

$$y^2z = x^3 + a_2x^2z + \widetilde{a}_4st^2xz^2 + \widetilde{a}_6s^2t^4z^3. \tag{13.62}$$

The discriminant is

$$\Delta = -16s^2t^4(4a_2^3\widetilde{a}_6 - a_2^2\widetilde{a}_4^2 - 18a_2\widetilde{a}_4\widetilde{a}_6st^2 + 4\widetilde{a}_4^3st^2 + 27\widetilde{a}_6^2s^2t^4). \tag{13.63}$$

The corresponding simply connected group G and the representation $\mathbf{R}$, which is computed geometrically in the next section, are

$$G = \mathrm{SU}(2)\times\mathrm{Sp}(4), \quad \mathbf{R} = (3,1)\oplus(1,10)\oplus(2,1)\oplus(2,4)\oplus(1,5)\oplus(2,1)\oplus(1,4). \tag{13.64}$$

The following sequence of blowups is a crepant resolution of the Weierstrass model:

$$X_0 \xleftarrow{(x,y,s|e_1)} X_1 \xleftarrow{(x,y,t|w_1)} X_2 \xleftarrow{(x,y,w_1|w_2)} X_3. \tag{13.65}$$

The proper transform is

$$y^2 = e_1 w_1 w_2^2 x^3 + a_2 x^2 + \widetilde{a}_4 s t^2 w_1 x + \widetilde{a}_6 s^2 t^4, \tag{13.66}$$

and the relative projective coordinates are

$$[e_1 w_1 w_2^2 x : e_1 w_1 w_2^2 y : z = 1][w_1 w_2^2 x : w_1 w_2^2 y : s][w_2 x : w_2 y : t][x : y : w_1]. \tag{13.67}$$

To prove that this is a crepant resolution, it is enough to assume that $V(a_2)$, $V(\widetilde{a}_6)$, $S = V(s)$, and $T = V(t)$ are smooth divisors intersecting two by two transversally.

13.3.1 Fiber structure and representations

The fibral divisors for this model are

$$\begin{cases} D_0^s & : s = y^2 - x^2(e_1 w_1 w_2^2 x + a_2) = 0, \\ D_1^s & : e_1 = y^2 - a_2 x^2 - \widetilde{a}_4 s t^2 w_1 x - \widetilde{a}_6 s^2 t^4 w_1^2 = 0, \\ D_0^t & : t = y^2 - x^2(e_1 w_1 w_2^2 x + a_2) = 0, \\ D_1^t & : w_1 = y^2 - a_2 x^2 = 0, \\ D_2^t & : w_2 = y^2 - a_2 x^2 - \widetilde{a}_4 s t^2 w_1 x - \widetilde{a}_6 s^2 t^4 w_1^2 = 0. \end{cases} \tag{13.68}$$

The fiber $\mathrm{I}_2^{\mathrm{ns}}$ specializes to a fiber of type III over $V(a_2)$ and a fiber of type $\mathrm{I}_3^{\mathrm{ns}}$ over $V(a_2\widetilde{a}_6 - 4\widetilde{a}_4^2)$ as the generic fiber of D_1^s degenerates into two lines $C_{1\pm}^s$. The intersection numbers between the curves and the fibral divisors of $\mathrm{I}_2^{\mathrm{ns}}$ are

	D_0^s	D_1^s	D_0^t	D_1^t	D_2^t
C_0^s	-2	2	0	0	0
$C_{1\pm}^s$	1	-1	0	0	0
$C_{1+}^s + C_{1-}^s$	2	-2	0	0	0

(13.69)

We get the weight $[-1]$ from each copy of $C_{1\pm}^s$. This is in the representation 2 of A_1 and uncharged from $\mathfrak{sp}(4)$ as it is away from its locus. Hence, the charged matter is in the representation $(2,1)$.

Over $T = V(t)$, we have a generic fiber of type $\mathrm{I}_4^{\mathrm{ns}}$, whose geometric components are C_0^s, C_{1+}^s,

C^t_{1-}, and C^t_2. The curve C^t_2 is a conic that splits into two lines over $V(4a_2\widetilde{a}_6 - \widetilde{a}_4^2)$,

$$C^t_2 \to C^t_{2+} + C^t_{2-}, \tag{13.70}$$

which results in the degeneration $\mathrm{I}^{\mathrm{ns}}_4 \to \mathrm{I}^{\mathrm{ns}}_5$. Then we get an enhancement of type $\mathrm{I}^{\mathrm{ns}}_5$, which is represented in Figure 13.9. Based on the splitting of the curve C^t_2, with C^t_0, C^t_1, and C^t_3 remaining the same, the intersection numbers between these curves and the fibral divisors of $\mathrm{I}^{\mathrm{ns}}_4$ are computed to find the weights of the new curves:

	D^s_0	D^s_1	D^t_0	D^t_1	D^t_2
C^t_0	0	0	-2	2	0
C^t_{1+}	0	0	1	-2	1
C^t_{2+}	0	0	0	1	-1
C^t_{2-}	0	0	0	1	-1
C^t_{1-}	0	0	1	-2	1

(13.71)

From the new splittings of the curves, each produce the weight $[-1, 1]$, which corresponds to the representation 4 of $\mathfrak{sp}(4)$. Since this is away from the locus of $se_1 = 0$, the weight produced is simply $[0; -1, 1]$. Thus, the charged matter is in the representation $(1, 4)$ of $(\mathfrak{su}(2), \mathfrak{sp}(4))$.

At the collision of S and T, we get the following curves:

$$\begin{cases} C_0^s \cap C_0^t & : s = t = y^2 - x^2(e_1 w_1 w_2^2 x + a_2) = 0 \to \eta^{00}, \\ C_1^s \cap C_0^t & : e_1 = t = y^2 - a_2 x^2 = 0 \to \eta^{10\pm}, \text{ (two roots for each curve,)} \\ C_1^s \cap C_1^t & : e_1 = w_1 = y^2 - a_2 x^2 = 0 \to \eta^{11\pm}, \text{ (two roots for each curve,)} \\ C_1^s \cap C_2^t & : e_1 = w_2 = y^2 - a_2 x^2 - \widetilde{a}_4 s t^2 w_1 x - \widetilde{a}_6 s^2 t^4 w_1^2 = 0 \to \eta^{12}. \end{cases} \tag{13.72}$$

The fiber structure is presented in Figure 13.9. As expected, we get a natural enhancement of an $\mathrm{I}_6^{\mathrm{ns}}$. The fibers of the collisions can be described from the splitting of the curves $C_i^s\,(i = 0, 1)$ from $\mathrm{I}_2^{\mathrm{ns}}$ and the curves $C_i^t\,(i = 0, 1, 2)$ fom $\mathrm{I}_4^{\mathrm{ns}}$. From these splittings of the curves, we compute the intersection numbers between the curves and the fibral divisors of $\mathrm{I}_2^{\mathrm{ns}}$ and $\mathrm{I}_4^{\mathrm{ns}}$. The splitting of the curves C_a^s and their intersection numbers with the fibral divisors are computed to be

	D_0^s	D_1^s	D_0^t	D_1^t	D_2^t
η^{00}	-2	2	0	0	0
$\eta^{10+} + \eta^{10-}$	2	-2	-2	2	0
$\eta^{10\pm}$	1	-1	-1	1	0
$\eta^{11+} + \eta^{11-}$	0	0	2	-4	2
$\eta^{11\pm}$	0	0	1	-2	1
η^{12}	0	0	0	2	-2

$$\begin{cases} C_0^s & \to \eta^{00} \\ C_1^s & \to \eta^{10+} + \eta^{10-} + \eta^{11+} + \eta^{11-} + \eta^{12} \\ C_0^t & \to \eta^{00} + \eta^{10+} + \eta^{10-} \\ C_1^t & \to \eta^{11+} + \eta^{11-} \\ C_2^t & \to \eta^{12} \end{cases}$$

(13.73)

The curve $\eta^{10\pm}$ yields the representation $(2,4)$. These nonsplit curves together $\eta^{10+}+\eta^{10-}$ produce the weight $[2;-2,0]$, the corresponding representation is $(3,10)$. Hence, the representation for the $\mathrm{I}_2^{\mathrm{ns}}+\mathrm{I}_4^{\mathrm{ns}}$-model with a trivial Mordell-Weil group is $\mathbf{R} = (3,1)\oplus(1,10)\oplus(3,10)\oplus(2,4)\oplus(1,5)\oplus(2,1)\oplus(1,4)$. We note that for the case of threefolds, the curves $\eta^{10\pm}$ are always split since all curve can split over a codimension-two point. Hence, the bi-adjoint $(3,10)$ does not show up geometrically, and the representation is then

$$\mathbf{R} = (3,1)\oplus(1,10)\oplus(2,4)\oplus(1,5)\oplus(2,1)\oplus(1,4). \tag{13.74}$$

We summarize the representations and the weights of this model with their locus in Table 13.12.

Locus	$tw_1w_2=0$		$se_1=tw_1w_2=0$		$se_1=0$
Curves	$C_1^{t'}$	$C_{2\pm}^{t}$	$\eta^{10\pm}$	$\eta^{10+}+\eta^{10-}$	$C_{1\pm}$
Weights	$[0;2,-1]$	$[0;-1,1]$	$[1;-1,0]$	$[2;-2,0]$	$[-1;0,0,0]$
Representations	$(1,5)$	$(1,4)$	$(2,4)$	$(3,10)$	$(2,1)$

Table 13.12: Weights and representations for the $\mathrm{I}_2^{\mathrm{ns}}+\mathrm{I}_4^{\mathrm{ns}}$-model with a trivial Mordell-Weil group.

When $a_2=0$, $\eta^{10\pm}$ becomes a degenerate node $\eta^{10'}$ with degeneracy two and $\eta^{11\pm}$ also degenerates into a single node $\eta^{11'}$ of degeneracy two:

$$\eta^{10\pm}\to\eta^{10'},\quad \eta^{11\pm}\to\eta^{11'}, \tag{13.75}$$

where the two new types of the curves are given by

$$\eta^{\mathrm{I0}'} : e_1 = t = y = 0, \text{ and } \eta^{\mathrm{II}'} : e_1 = w_1 = y = 0. \tag{13.76}$$

This new fiber structure for $a_2 = 0$ is the bottom left diagram of Figure 13.9. When $\widetilde{a}_4^2 - a_2\widetilde{a}_6 = 0$ instead, η^{I2} is geometrically reducible, and thus becomes two nonsplit curves

$$\eta^{\mathrm{I2}} \to \eta^{\mathrm{I2}+'} + \eta^{\mathrm{I2}-'}. \tag{13.77}$$

Therefore, we get the bottom right diagram in Figure 13.9. When $a_2 = \widetilde{a}_4 = 0$, η^{I2} geometrically reduces into two nonsplit curves

$$\eta^{\mathrm{I2}} \to \eta^{\mathrm{I2}+''} + \eta^{\mathrm{I2}-''} : e_1 = w_2 = y^2 - \widetilde{a}_6 s^2 t^4 w_1^2 = 0, \tag{13.78}$$

whereas from the other specialization when $\widetilde{a}_4^2 - a_2\widetilde{a}_6 = \widetilde{a}_4 = 0$,

$$\begin{cases} \eta^{\mathrm{I0}} & \to \eta^{\mathrm{I0}'}, \\ \eta^{\mathrm{II}} & \to \eta^{\mathrm{II}'}, \\ \eta^{\mathrm{I2}} & \to \eta^{\mathrm{I2}+''} + \eta^{\mathrm{I2}-''}. \end{cases} \tag{13.79}$$

When $a_2 = \widetilde{a}_4 = \widetilde{a}_6 = 0$, the nonsplit fibers become $\eta^{12'''}$ with degeneracy two:

$$\eta^{12\pm''} \to \eta^{12'''} : e = w_2 = y = 0, \tag{13.80}$$

which gives the fiber structure to be the very bottom diagram in Figure 13.9.

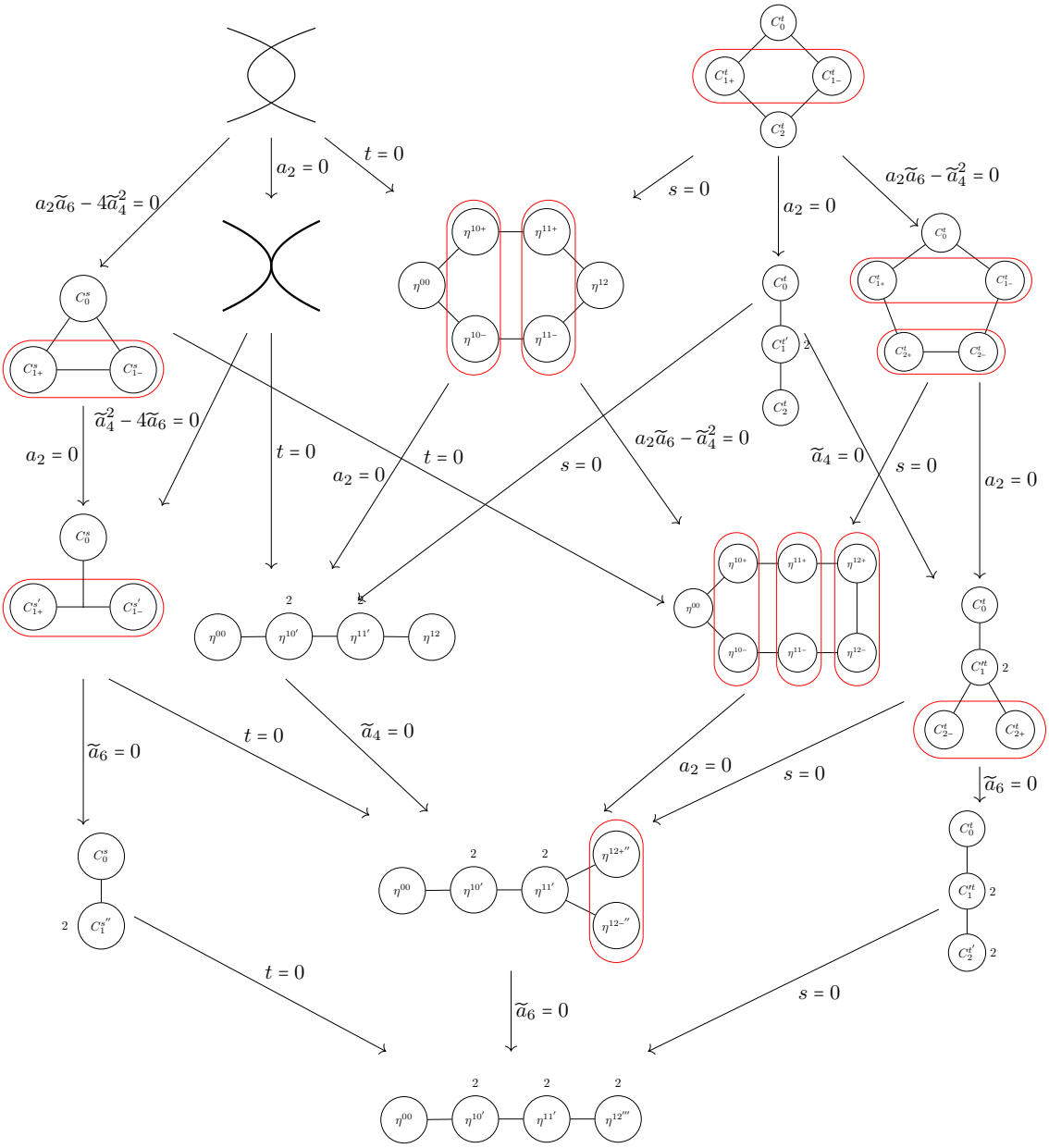

Figure 13.9: Fiber structure of $\mathrm{I}_2^{\mathrm{ns}}+\mathrm{I}_4^{\mathrm{ns}}$ with a trivial Mordell-Weil group. The diagrams on the top are the Kodaira fibers of type $\mathrm{I}_2^{\mathrm{ns}}$ and $\mathrm{I}_4^{\mathrm{ns}}$. When $a_2 = 0$, $\mathrm{I}_2^{\mathrm{ns}}$ specializes to III as seen in the middle left diagram, and $\mathrm{I}_4^{\mathrm{ns}}$ specializes to the diagram on the middle right. When $\mathrm{I}_2^{\mathrm{ns}}$ and $\mathrm{I}_4^{\mathrm{ns}}$ collide on the locus $se_1 = tw_1w_2w_3 = 0$, we get the fiber structure as an hexagon drawn in the middle. This enhancement has two newly split curves $\eta^{\mathrm{IO}+}$ and $\eta^{\mathrm{IO}-}$ that are of non-split type. When $a_2 = 0$, this hexagon further specializes to the diagram on the bottom left, but when $\widetilde{a}_4^2 - a_2\widetilde{a}_6 = 0$, the hexagon becomes a heptagon.

13.3.2 Coulomb phases

The groups SU(2) and Sp(4) individually have a unique Coulomb chamber. Their product with the bifundamental representation introduces an interior wall inside the Weyl chamber, which yields three chambers. Since we have the same Lie algebra with the bifundamental representation $(2, 4)$, the chamber structure does not change under the change of the Mordell-Weil group.

13.3.3 $5d\,\mathcal{N} = 1$ prepotentials and the triple intersection polynomials

The $\mathrm{I}_2^{\mathrm{ns}}+\mathrm{I}_4^{\mathrm{ns}}$-model with a trivial Mordell-Weil group has the identical blowups with the nonsplit model with the Mordell-Weil group $\mathbb{Z}_2$, and the fiber structure in codimension two is the same for the hexagon. Hence, the triple intersection polynomial and the prepotential are the same with the $\mathrm{I}_2^{\mathrm{ns}}+\mathrm{I}_4^{\mathrm{ns}}$-model with the $\mathbb{Z}_2$, without the relation between two divisors of class S and T. Thus, the triple intersection polynomial is given by

$$\begin{aligned}\mathscr{F}_{trip} =& -2S(2L+S)\psi_1^3 - 8T^2\varphi_1^3 - 2T(2L-S)\varphi_2^3 \\ &+ 6T(S+2T-2L)\varphi_1^2\varphi_2 - 6T(-2L+S+T)\varphi_1\varphi_2^2 - 6ST\psi_1\left(2\varphi_1^2 - 2\varphi_2\varphi_1 + \varphi_2^2\right) \\ &+ 6T\varphi_0^2\left((S+T-2L)\varphi_1 - S\psi_1\right) + 6T\varphi_0\left((2L-S)\varphi_1^2 - S\left(\psi_0-\psi_1\right)^2 + 2S\psi_1\varphi_1\right) \\ &- 2T(-2L+S+2T)\varphi_0^3 + 4S\psi_0^3(L-S) + 6S(S-2L)\psi_0^2\psi_1 + 12LS\psi_0\psi_1^2.\end{aligned} \tag{13.81}$$

The representations we achieve geometrically are

$$\mathbf{R} = (3,1) \oplus (2,1) \oplus (2,4) \oplus (1,4) \oplus (1,5) \oplus (1,10). \tag{13.82}$$

Using these representations, the $5d$ prepotential is computed for chamber 1, which is $[-,+]$, to be

$$\begin{aligned} 6\mathscr{F}_{\text{IMS}} = &-(n_{2,1} - 4n_{2,4} + 8n_{3,1} - 8)\psi_1^3 - 8(n_{1,10} + n_{1,5} - 1)\varphi_1^3 - (8n_{1,10} + n_{1,4} - 8)\varphi_2^3 \\ &- 3\varphi_1^2\varphi_2(4n_{1,10} + n_{1,4} - 4n_{1,5} - 4) + 3(6n_{1,10} + n_{1,4} - 2n_{1,5} - 6)\varphi_1\varphi_2^2 \\ &+ \psi_1\left(-12n_{2,4}\varphi_1^2 + 12n_{2,4}\varphi_1\varphi_2 - 6n_{2,4}\varphi_2^2\right) \end{aligned} \tag{13.83}$$

The triple intersection numbers that are independent from ψ_0 and φ_0, which are the first two lines of the equation (13.81), are matched with the $5d$ prepotential term by term. This fixes the linear combination of the number of representations $n_{\mathbf{R}}$:

$$\begin{aligned} &8n_{3,1} + n_{2,1} = 2S(2L + S - 2T) + 8, \\ &8n_{1,10} + n_{1,4} = 2(2LT - ST + 4), \quad n_{1,10} + n_{1,5} = T^2 + 1. \end{aligned} \tag{13.84}$$

However, we need further information in order to fix the number of representations.

Using the fact that the charged matter in the representation $(1,4)$ is from the splittings of the curve $C_2^t \to C_{2+}^t + C_{2-}^t$ when $4a_2\widetilde{a}_6 - \widetilde{a}_4^2 = 0$, whose class is given by twice of $[\widetilde{a}_4] = (4L - S - 2T)$, in the locus of $tw_1w_2 = 0$, we can safely see that this gives the class $n_{1,4} = 2T(4L - S - 2T)$. With this specified $n_{1,4}$, we can fix the number of representations for $n_{1,5}$ and $n_{1,10}$. Moreover, $n_{2,1}$ and $n_{3,1}$

terms are both only in ψ_1^3 term. In order to fix these representations, we look into the specialization of the curve $C_1^s \to C_{1+}^s + C_{1-}^s$ that produces the charged matter in the representation $(2,1)$. This specialization was when $4a_2\widetilde{a}_6 - \widetilde{a}_4^2 = 0$, whose class is then the same as twice the class of $[\widetilde{a}_4] = 4L - S - 2T$. Since the splittings happen when $se_1 = 4a_2\widetilde{a}_6 - \widetilde{a}_4^2 = 0$, we can safely see that this gives the class $n_{2,1} = 2S(4L - S - 2T)$. Hence, the number of representations $n_{\mathbf{R}}$ can all be computed, which are listed below:

$$\begin{aligned} &n_{3,1} = \frac{1}{2}\left(-LS + S^2 + 2\right), \quad n_{2,1} = 2S(4L - S - 2T), \quad n_{2,4} = ST, \\ &n_{1,4} = 2T(4L - S - 2T) \quad n_{1,5} = \frac{1}{2}T(L + T), \quad n_{1,10} = \frac{1}{2}\left(-LT + T^2 + 2\right). \end{aligned} \tag{13.85}$$

When we impose the Calabi-Yau condition, $L = -K$, $n_{3,1} = g_S$ and $n_{1,10} = g_T$.

13.3.4 $6d\,\mathcal{N} = (1,0)$ anomaly cancellation

To compute the number of hypermultiplets, we recall the number of representations from Section 13.3.2:

$$\begin{aligned} &n_{3,1} = \frac{1}{2}\left(KS + S^2 + 2\right), \quad n_{2,1} = -2S(4K + S + 2T), \quad n_{2,4} = ST, \\ &n_{1,4} = -2T(4K + S + 2T), \quad n_{1,5} = -\frac{1}{2}(KT - T^2), \quad n_{1,10} = \frac{1}{2}\left(KT + T^2 + 2\right). \end{aligned} \tag{13.86}$$

The number of vector multiplets $n_V^{(6)}$, tensor multiplets n_T, and hypermultiplets n_H are

$$\begin{aligned} n_V^{(6)} &= 13, \quad n_T = 9 - K^2, \\ n_H &= h^{2,1}(Y) + 1 + n_{2,1}(2-0) + n_{3,1}(3-1) + n_{2,4}(8-0) + n_{1,4}(4-0) \\ &\quad + n_{1,5}(5-1) + n_{1,10}(10-2) = 29K^2 + 25. \end{aligned} \tag{13.87}$$

The coefficients of the $\mathbf{tr}R^4$ vanishes as $n_H - n_V^{(6)} + 29n_T - 273 = 0$, so we can conclude that the pure gravitational anomalies are canceled out.

The terms $X_1^{(2)}, X_2^{(2)}, X_1^{(4)}, X_2^{(4)}$, and Y_{12} are obtained as[1]

$$X_1^{(2)} = (A_3(1-n_3) - n_2A_2)\,\mathbf{tr}_2F_1^2 = 6KS\mathbf{tr}_2F_1^2, \tag{13.88}$$

$$X_2^{(2)} = (A_{10}(1-n_{10}) - n_5A_5 - n_4A_4)\,\mathbf{tr}_4F_2^2 = 6KT\mathbf{tr}_4F_2^2, \tag{13.89}$$

$$Y_{12} = n_{2,4}\mathbf{tr}_2F_2^2\mathbf{tr}_4F_2^2 = ST\mathbf{tr}_2F_2^2\mathbf{tr}_4F_2^2, \tag{13.90}$$

$$X_1^{(4)} = (B_3(1-n_3) - n_2B_2)\,\mathbf{tr}_2F_1^4 + (C_3(1-n_3) - n_2C_2)\,(\mathbf{tr}_2F_1^2)^2 = -3S^2(\mathbf{tr}_2F_1^2)^2, \tag{13.91}$$

$$X_2^{(4)} = (B_{10}(1-n_{10}) - n_5B_5 - n_4B_4)\,\mathbf{tr}_4F_2^4 \tag{13.92}$$

$$+ (C_{10}(1-n_{10}) - n_5C_5 - n_4C_4)\,(\mathbf{tr}_4F_2^2)^2 = -3T^2(\mathbf{tr}_4F_2^2)^2, \tag{13.93}$$

[1] A key point of the computation is that along SU(2), a hypermultiplet transforming in the representation $(2, 4)$ is seen as 4 hypermultiplets in the representation 2 of SU(2). In the same way, the same hypermultiplet in the representation $(2, 4)$ is seen from the group Sp(4) as 2 hypermultiplets in the representation 4 of Sp(4). It follows that we use

$$n_3 = n_{3,1}, \quad n_2 = n_{2,1} + 4n_{2,4}, \quad n_{10} = n_{1,10}, \quad n_5 = n_{1,5}, \quad n_4 = n_{1,4} + 2n_{2,4}.$$

Since we have a theory with two quartic Casimirs, to satisfy the anomaly cancellation conditions, the coefficients of the $\mathbf{tr}_2 F_1^4$ and $\mathbf{tr}_4 F_2^4$ must vanish. These terms are coming from $X_1^{(4)}$ and $X_2^{(4)}$. We can observe from the equations above that the coefficients of $\mathbf{tr}_2 F_1^4$ and $\mathbf{tr}_2 F_1^4$ indeed vanish.

Using the terms above, we compute the anomaly polynomial as

$$I_8 = \frac{1}{2}\left(\frac{1}{2}K\mathbf{tr}R^2 + 2S\mathbf{tr}_4 F_2^2 + 2T\mathbf{tr}_2 F_1^2\right)^2, \tag{13.94}$$

which is a perfect square. Hence we conclude that the anomalies are all canceled when lifted to the six-dimensional theories.

13.4 $(\mathrm{SU}(2)\times\mathrm{SU}(4))/\mathbb{Z}_2$-MODEL

In this section, we study the $\mathrm{I}_2^{\mathrm{ns}}$+$\mathrm{I}_4^{\mathrm{s}}$ with a $\mathbb{Z}_2$ Mordell-Weil group. The Weierstrass model is

$$y^2z + a_1xyz = x^3 + \widetilde{a}_2 tx^2z + st^2xz^2. \tag{13.95}$$

The discriminant for this model is

$$\Delta = s^2t^4\left(a_1^4 + 8a_1^2\widetilde{a}_2 t + 16\widetilde{a}_2^2t^2 - 64st^2\right). \tag{13.96}$$

The corresponding simply connected group G and the representation $\mathbf{R}$, which is computed geometrically in the next section, are

$$G = (\mathrm{SU}(2) \times \mathrm{SU}(4))/\mathbb{Z}_2, \quad \mathbf{R} = (3,1) \oplus (1,15) \oplus (1,6) \oplus (2,4) \oplus (2,\overline{4}). \tag{13.97}$$

We consider the following sequence of blowups for a crepant resolution:

$$X_0 \xleftarrow{(x,y,s|e_1)} X_1 \xleftarrow{(x,y,t|w_1)} X_2 \xleftarrow{(y,w_1|w_2)} X_3 \xleftarrow{(x,w_2|w_3)} X_4 \ . \tag{13.98}$$

The proper transform is

$$w_2 y^2 + a_1 xy = w_1 x(e_1 w_3^2 x^2 + \widetilde{a}_2 w_3 t x + s t^2), \tag{13.99}$$

where the relative projective coordinates are given by

$$[e_1 w_1 w_2 w_3^2 x : e_1 w_1 w_2^2 w_3^2 y : z = 1][w_1 w_2 w_3^2 x : w_1 w_2^2 w_3^2 y : s][w_3 x : w_2 w_3 y : t][y : w_1][x : w_2]. \tag{13.100}$$

13.4.1 Fiber structure

This model has the following fibral divisors that corresponds to their curves:

$$\begin{cases} D_0^s & : s = w_2y^2 + a_1xy - w_1w_3x^2(e_1w_3x + \widetilde{a}_2t) = 0, \\ D_1^s & : e_1 = w_2y^2 + a_1xy - w_1tx(\widetilde{a}_2w_3x + st) = 0, \\ D_0^t & : t = w_2y^2 + a_1xy - e_1w_1w_3^2x^3 = 0, \\ D_1^t & : w_1 = w_2y + a_1x = 0 \\ D_2^t & : w_3 = w_2y^2 + x(a_1y - w_1st^2) = 0 \\ D_3^t & : w_2 = a_1y - w_1(e_1w_3^2x^2 + \widetilde{a}_2w_3tx + st^2) = 0. \end{cases} \tag{13.101}$$

The fiber of type I_2^{ns} consists of two curves C_i^s $(i = 0, 1)$ with their intersection point given by

$$C_0^s \cap C_1^s : s = e_1 = w_2y^2 + a_1xy - \widetilde{a}_2tw_1w_3x^2 = 0. \tag{13.102}$$

Hence it specializes to a type III fiber over $V(a_1^2 + 4\widetilde{a}_2t)$.

On the other hand, over $T = V(t)$, we have a generic fiber of type I_4^s with its geometric components C_0^t, C_1^t, C_2^t, and C_3^t. This fiber I_4^s enhances into a fiber of type I_0^{*ss} over $V(a_1)$, which is presented in Figure 13.10. The curve C_1^t specializes into the central node C_{13}^t where

$$C_1^t \to C_{13}^t : w_1 = w_2 = 0. \tag{13.103}$$

The curve C_3^t splits into three curves C_{12}^t, which is the central node, and $C_{3\pm}^{t'}$, which is given by the two roots of the curve:

$$C_3^t \to C_{13}^t + C_{3+}^{t'} + C_{3-}^{t'} \qquad (C_{3\pm}^{t'} : w_2 = e_1 w_3^2 x^2 + \widetilde{a}_2 t w_3 x + s t^2 = 0). \tag{13.104}$$

From this specialization, we can compute the weights of the curves to see what charged matter we have in the five-dimensional theory.

	D_0^s	D_1^s	D_0^t	D_1^t	D_2^t	D_3^t
C_0^t	0	0	-2	2	0	0
$2\,C_{13}^t$	0	0	2	-4	2	0
C_2^t	0	0	0	0	-2	2
$C_{3+}^{t'} + C_{3-}^{t'}$	0	0	0	2	0	-2

(13.105)

For the curve C_{13}^t, the weight is computed to be $[2, -1, 0]$, and this corresponds to the representation 15, which is the adjoint representation of $\mathfrak{su}(4)$. The curves $C_{3\pm}^{t'}$ each carries the weight $[-1, 0, 1]$ that corresponds to the representation 6, which is the antisymmetric representation of $\mathfrak{su}(4)$. Since these two curves are nonsplit, when we compute the weight of them together as $C_3^{t'} = C_{3+}^{t'} + C_{3-}^{t'}$, the representation is $20'$. Since the locus is away from $se_1 = 0$, it is uncharged on the side for $\mathfrak{su}(2)$ and hence the representation for the whole product group $\mathfrak{su}(2) \times \mathfrak{su}(4)$ is $(1, 6)$.

At the collision of both S and T,

$$\begin{cases} C_0^s \cap C_0^t : & s = t = w_2 y^2 + a_1 xy - w_1 w_3^2 e_1 x^3 = 0 \to \eta^{00}, \\ C_1^s \cap C_0^t : & e_1 = t = w_2 y + a_1 x = 0 \to \eta^{10}, \\ & e_1 = t = y = 0 \to \eta^{10y}, \\ C_1^s \cap C_1^t : & e_1 = w_1 = w_2 y + a_1 x = 0 \to \eta^{11}, \\ C_1^s \cap C_2^t : & e_1 = w_3 = w_2 y^2 + x(a_1 y - w_1 s t^2) = 0 \to \eta^{12}, \\ C_1^s \cap C_3^t : & e_1 = w_2 = a_1 y - w_1 t(\widetilde{a}_2 w_3 x + st) = 0 \to \eta^{13}. \end{cases} \tag{13.106}$$

The fiber structure for this collision is an I_6^s fiber, as depicted in Figure 13.10.

In order to compute the weights for this collision of $\mathfrak{su}(2) \times \mathfrak{su}(4)$, we need to investigate the splittings of the curves from $C_i^s\,(i = 0, 1)$ and $C_i^t\,(i = 0, 1, 2, 3)$. We find that

$$\begin{cases} C_0^s & \to \eta^{00}, \\ C_1^s & \to \eta^{10} + \eta^{11} + \eta^{12} + \eta^{13}, \\ C_0^t & \to \eta^{00} + \eta^{10} + \eta^{10y}, \\ C_1^t & \to \eta^{11}, \\ C_2^t & \to \eta^{12}, \\ C_3^t & \to \eta^{13}. \end{cases} \tag{13.107}$$

Using linear relations, the intersection numbers between the curves and the Cartan divisors are computed below. Since η^{00}, η^{11}, η^{12}, and η^{13} are obtained directly from C_0^s, C_1^t, C_2^t, and C_3^t without modifications, the only curves in consideration are η^{10} and η^{10y} and we get

	D_0^s	D_1^s	D_0^t	D_1^t	D_2^t	D_3^t
η^{00}	-2	2	0	0	0	0
η^{10}	1	-1	-1	1	0	0
η^{10y}	1	-1	-1	0	0	1
η^{11}	0	0	1	-2	1	0
η^{12}	0	0	0	1	-2	1
η^{13}	0	0	1	0	1	-2

(13.108)

Note that for $\mathfrak{su}(2)$, we only get the weight $[1]$, which is in the representation 2. On the other hand, for $\mathfrak{su}(4)$, η^{10} gives the weight $[-1, 0, 0]$ and η^{10y} gives the weight $[0, 0, -1]$. These are in representations $\overline{4}$ and 4 respectively. Thus, we get the bifundamentals $(2, 4) \oplus (2, \overline{4})$ for our product group $\mathfrak{su}(2) \times \mathfrak{su}(4)$.

The representations with respect to $(\mathfrak{su}(2), \mathfrak{su}(4))$ from this $\mathrm{I}_2^{ns}+\mathrm{I}_4^s$-model with the Mordell-Weil group $\mathbb{Z}_2$ are summarized in Table 13.13 below. Here we denoted weights as $[\psi; \phi_1, \phi_2, \phi_3]$, where $[\psi]$ is the weight for the $\mathfrak{su}(2)$ and $[\phi_1, \phi_2, \phi_3]$ is the weight for the $\mathfrak{su}(4)$.

Locus	$tw_1w_2 = 0$		$se_1 = tw_1w_2 = 0$	
Curves	C_{13}^{t}	$C_{3\pm}^{t'}$	$\eta^{1\mathrm{o}}$	$\eta^{1\mathrm{o}y}$
Weights	$[0; 2, -1, 0]$	$[0; -1, 0, 1]$	$[1; -1, 0, 0]$	$[1; 0, 0, -1]$
Representations	$(1, 15)$	$(1, 6)$	$(2, \overline{4})$	$(2, 4)$

Table 13.13: Weights and representations for the $\mathrm{I}_2^{\mathrm{ns}}+\mathrm{I}_4^{\mathrm{s}}$-model with the Mordell-Weil group $\mathbb{Z}_2$.

We have identified the charged matters for the product group $\mathfrak{g} = \mathfrak{su}(2) \times \mathfrak{su}(4)$ to be

$$\mathbf{R} = (3, 1) \oplus (1, 15) \oplus (2, 4) \oplus (2, \overline{4}) \oplus (1, 6). \tag{13.109}$$

When $a_1 = 0$, $\eta^{1\mathrm{o}}$ and η^{13} split and η^{11} produces a curve that intersects with three curves. The splittings of the curves when $a_1 = 0$ is

$$\begin{cases} \eta^{1\mathrm{o}} \to & \eta^{1\mathrm{o}3} + \eta^{1\mathrm{o}y}, \\ \eta^{11} \to & \eta^{11\mathrm{3}}, \\ \eta^{13} \to & \eta^{1\mathrm{o}3} + \eta^{11\mathrm{3}} + \eta^{13'}, \end{cases} \qquad \begin{cases} \eta^{1\mathrm{o}3} & : e_1 = t = w_2 = 0, \quad \eta^{1\mathrm{o}y} : e_1 = t = y = 0, \\ \eta^{11\mathrm{3}} & : e_1 = w_1 = w_2 = 0, \quad \eta^{13'} : e_1 = w_2 = \widetilde{a}_2 w_3 x + st = 0. \end{cases} \tag{13.110}$$

This new fiber structure when $a_1 = 0$ is the diagram in the third row of Figure 13.10. The intersection numbers between the new curves of this enhancement and the fibral divisors of $\mathrm{I}_2^{\mathrm{ns}}$ and $\mathrm{I}_4^{\mathrm{s}}$ are

	D_0^s	D_1^s	D_0^t	D_1^t	D_2^t	D_3^t
η^{00}	-2	2	0	0	0	0
η^{103}	0	0	0	1	0	-1
η^{10y}	1	-1	-1	0	0	1
η^{113}	0	0	1	-2	1	0
η^{12}	0	0	0	1	-2	1
$\eta^{13'}$	0	0	0	1	0	-1

(13.111)

The weight of the curve η^{103} is $[0; -1, 0, 1]$, which corresponds to the representation $(1, 6)$. The curve η^{10y} is the same as before but with a degeneracy of two, with the weight $[1; 0, 0, -1]$ that corresponds to the representation $(2, 4)$. The curve η^{113} carries the same weight as the curve η^{11} earlier due to the linear relation, yielding the weight $[0; 2, -1, 0]$, which corresponds to the representation $(1, 15)$. The weight of the curve $\eta^{13'}$ is then computed as $[0; -1, 0, 1]$, which corresponds to the representation $(1, 6)$. Interestingly, all the new curves are in the adjoint representation of $\mathfrak{su}(4)$ and uncharged under $\mathfrak{su}(2)$. Consider when $a_1 = \widetilde{a}_2 = 0$, which produces a codimension-four specialization. The only curve that transforms is

$$\eta^{13'} \to \eta^{103} : e_1 = t = w_2 = 0, \tag{13.112}$$

which changes the geometry into the bottom diagram of Figure 13.10.

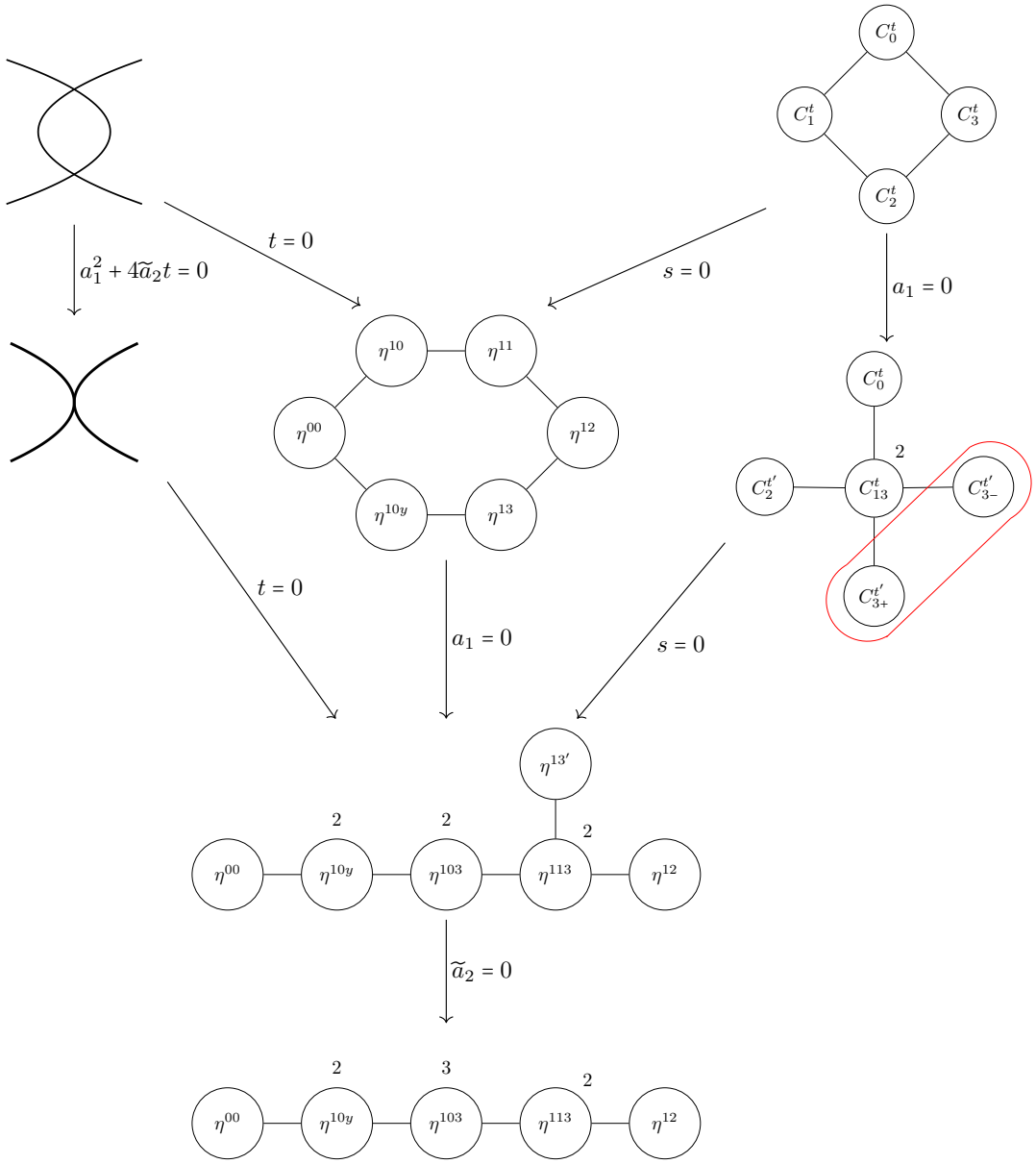

Figure 13.10: Fiber structure of $I_2^{ns}+I_4^s$ with a Mordell-Weil group $\mathbb{Z}_2$.The diagrams on the top are the Kodaira fibers of type I_2^{ns} and I_4^s. When they collide on the locus $se_1 = tw_1w_2w_3 = 0$, we get the fiber structure of the collision of I_2^{ns} and I_4^s as a hexagon drawn in the middle. This enhancement has two newly split curves η^{IO} and η^{IOy} that give the representations $(2,4) \oplus (2,\overline{4})$. When $a_1 = 0$, this hexagon further specializes to the diagram on the third row. When $a_1 = \widetilde{a}_2 = 0$, this further specializes into the diagram on the bottom.

13.4.2 Coulomb phases

We determine the chamber structures by considering the weights that are sign indefinite. First we find the weights that constrain the chamber structures. Denote $\mathfrak{su}(2)$ by $[\psi]$ and denote $\mathfrak{su}(4)$ by $[\phi_1, \phi_2, \phi_3]$. For $(1, 6)$, there is nothing charged under $\mathfrak{su}(2)$ and thus we only have one relation coming from the representation 6:

$$-\phi_1 + \phi_3. \tag{13.113}$$

From the representation $(2, 4)$, we have the following relations:

$$\psi - \phi_1 + \phi_2, \quad \psi - \phi_2 + \phi_3, \quad \psi - \phi_3, \quad -\psi + \phi_1, \quad -\psi - \phi_1 + \phi_2, \quad -\psi - \phi_2 + \phi_3. \tag{13.114}$$

Lastly, the representation $(2, \overline{4})$ gives the following relations:

$$\psi + \phi_2 - \phi_3, \quad \psi + \phi_1 - \phi_2, \quad \psi - \phi_1, \quad -\psi + \phi_3, \quad -\psi + \phi_2 - \phi_3, \quad -\psi + \phi_1 - \phi_2. \tag{13.115}$$

Compositing all these relations, we have a total of seven independent relations that are given by

$$-\phi_1 + \phi_3, \quad \psi - \phi_1 + \phi_2, \quad \psi - \phi_2 + \phi_3, \quad -\psi + \phi_1, \quad -\psi - \phi_1 + \phi_2, \quad -\psi - \phi_2 + \phi_3, \quad -\psi + \phi_3. \tag{13.116}$$

We can compute the region of the Weyl chamber from the Cartan Matrix:

ψ
2
-2

,

ϕ_1	ϕ_2	ϕ_3
2	-1	0
-1	2	-1
0	-1	2

.

Thus the Weyl chamber is defined by the hyperplanes

$$\psi > 0, \quad 2\phi_1 - \phi_2 > 0, \quad -\phi_1 + 2\phi_2 - \phi_3 > 0, \quad -\phi_2 + 2\phi_3 > 0. \tag{13.117}$$

The weights corresponding to the seven entries in equation (13.116) are composited into a vector

$$v = (\varpi_3, \varpi_4, \varpi_5, \varpi_6, \varpi_7, \varpi_8, \varpi_9), \tag{13.118}$$

where each weight is written in the form of a sign vector $[\psi_1; \varphi_1, \varphi_2, \varphi_3]$:

$$\varpi_3 = [0; -1, 0, 1], \quad \varpi_4 = [1; -1, 1, 0], \quad \varpi_5 = [1; 0, -1, 1], \quad \varpi_6 = [-1; 1, 0, 0], \tag{13.119}$$

$$\varpi_7 = [-1; -1, 1, 0], \quad \varpi_8 = [-1; 0, -1, 1], \quad \varpi_9 = [-1; 0, 0, 1], \tag{13.120}$$

with 1 denoting the entry to be positive and 0 denoting the entry to be negative. Then we get total

twelve different chambers, which are denoted by their weight vector:

	$5ab^-$ (011000)	$5ab^+$ (111000)	
	$4ab^-$ (011100)	$4ab^+$ (111001)	
	$3ab^-$ (011001)	$3ab^+$ (111001)	
	$2ab^-$ (010100)	$2ab^+$ (111101)	
$1a^-$ (000100)	$1b^-$ (010110)	$1b^+$ (110110)	$1a^+$ (111111)

. (13.121)

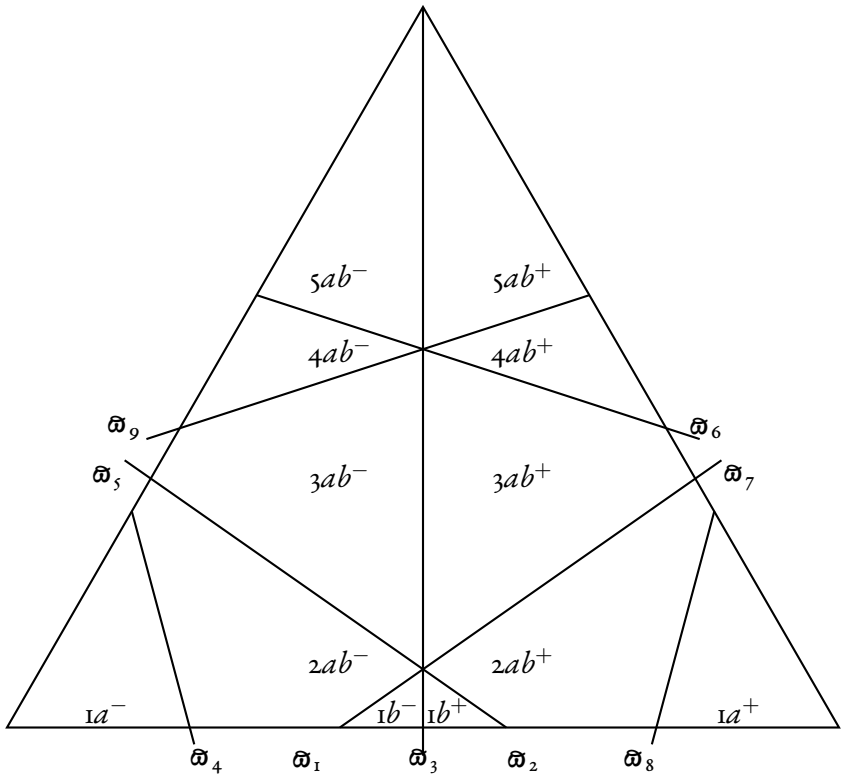

Figure 13.11: This is the chamber structure of the $I_2^{ns}+I_4^s$-model with a Mordell-Weil group $\mathbb{Z}_2$ in a planar diagram.

13.4.3 $5d\,\mathcal{N}=1$ PREPOTENTIALS AND THE TRIPLE INTERSECTION POLYNOMIALS

The triple intersection polynomial is computed for the $\mathrm{I}_2^{\mathrm{ns}}+\mathrm{I}_4^{\mathrm{s}}$-model with the Mordell-Weil group $\mathbb{Z}_2$ in the crepant resolution that we geometrically obtained earlier. We note that the triple intersection is identical to the one we computed for the $\mathrm{I}_2^{\mathrm{ns}}+\mathrm{I}_4^{\mathrm{s}}$-model with a trivial Mordell-Weil group:

$$\begin{aligned}\mathscr{F}_{trip} =& -8\left(6L^2-5LT+T^2\right)\psi_1^3+4T(L-T)\left(\varphi_1^3+\varphi_2^3\right)+2T(L-2T)\varphi_3^3\\
&+3T(T-2L)\varphi_2^2\left(\varphi_1+\varphi_3\right)+3LT\varphi_2\left(\varphi_1^2+\varphi_3^2\right)\\
&-6LT\varphi_1^2\varphi_3+6LT\varphi_1\varphi_2\varphi_3+12T(T-2L)\psi_1\left(\varphi_1^2-\varphi_2\varphi_1+\varphi_2^2+\varphi_3^2-\varphi_2\varphi_3\right)\\
&-8(2L-T)(3L-2T)\psi_0^3-24(2L-T)(T-L)\psi_0^2\psi_1+24L(2L-T)\psi_0\psi_1^2-4LT\varphi_0^3\\
&+3T\varphi_0\left(2\varphi_1\left(L\varphi_3+2(2L-T)\psi_1\right)+(2T-3L)\varphi_1^2+(2T-3L)\varphi_3^2-4(2L-T)\left(\psi_0-\psi_1\right)^2\right)\\
&+12T(2L-T)\varphi_0\psi_1\varphi_3+(2L-T)\varphi_0^2\left(-4\psi_1+\varphi_1+\varphi_3\right).\end{aligned}\tag{13.122}$$

For this split model with $\mathbb{Z}_2$, the representation is

$$\mathbf{R}=(3,1)\oplus(2,4)\oplus(2,\overline{4})\oplus(1,6)\oplus(1,15).\tag{13.123}$$

Then the prepotential for this model in the chamber $5ab+$ is given as

$$\begin{aligned}
6\mathscr{F}_{\text{IMS}} = & -8(n_{1,15}-1)\varphi_1^3-(8n_{1,15}-8)\varphi_2^3-2(4n_{1,15}+n_{1,6}-4)\varphi_3^3 \\
& -4(n_{2,4}+n_{2,\bar{4}}+2n_{3,1}-2)\psi_1^3+\frac{3}{2}(4n_{1,15}-2n_{1,6}-4)\varphi_2^2(\varphi_1+\varphi_3) \\
& -\frac{3}{2}(-2n_{1,6})\varphi_2(\varphi_1^2+\varphi_3^2)-6n_{1,6}\varphi_1^2\varphi_3+6n_{1,6}\varphi_1\varphi_2\varphi_3 \\
& -6(n_{2,4}+n_{2,\bar{4}})\psi_1\left(\varphi_1^2-\varphi_1\varphi_2+\varphi_2^2+\varphi_3^2-\varphi_2\varphi_3\right).
\end{aligned} \tag{13.124}$$

In order to compute the number of representations n_R, we take the triple intersection number to be the same as the prepotential. This fixes every $n_{\mathbf{R}}$ except $n_{2,4}$ and $n_{2,\bar{4}}$, as only their sum is fixed by

$$n_{2,4}+n_{2,\bar{4}}=ST. \tag{13.125}$$

Using the fact that $n_{2,4}=n_{2,\bar{4}}$, we conclude the number of representations to be

$$\begin{aligned}
& n_{3,1}=\frac{1}{4}\left(2LS+S^2-2ST+4\right)=6L^2-7LT+2T^2+1, \quad n_{2,4}=n_{2,\bar{4}}=\frac{1}{2}ST=T(2L-T), \\
& n_{1,6}=-3LT+ST+2T^2=LT, \quad n_{1,15}=\frac{1}{2}\left(-LT+T^2+2\right).
\end{aligned} \tag{13.126}$$

When the Calabi-Yau condition, $L=-K$,

$$n_{3,1}=g_S, \quad n_{1,15}=g_T. \tag{13.127}$$

13.4.4 $6d\,\mathcal{N}=(1,0)$ ANOMALY CANCELLATION

In this section, we consider an $\mathrm{I}_2^{\mathrm{ns}}+\mathrm{I}_4^{\mathrm{s}}$-model with the Mordell-Weil group $\mathbb{Z}_2$. Then, the gauge algebra is given by

$$\mathfrak{g}=A_1+A_3, \tag{13.128}$$

and the representation is geometrically computed in Section 13.4 to be

$$\mathbf{R}=(3,1)\oplus(1,15)\oplus(2,4)\oplus(2,\overline{4})\oplus(1,6). \tag{13.129}$$

Then, the number of vector multiplets $n_V^{(6)}$, tensor multiplets n_T, and hypermultiplets n_H are

$$\begin{aligned}
&n_V^{(6)}=18,\quad n_T=9-K^2,\\
&n_H=h^{2,1}(Y)+1+n_{3,1}(3-1)+n_{2,4}(8-0)+n_{2,\overline{4}}(8-0)+n_{1,6}(6-0)+n_{1,15}(15-3)\\
&\quad=17K^2+18KT+6T^2+15.
\end{aligned} \tag{13.130}$$

We see that

$$n_H-n_V^{(6)}+29n_T-273=0, \tag{13.131}$$

so we can conclude that the pure gravitational anomalies are canceled. We recall that the number of representations are

$$\begin{aligned} n_{3,1} &= (2K+T)(3K+2T)+1, \quad n_{2,4} = n_{2,\bar{4}} = -T(2K+T), \\ n_{1,6} &= -KT, \quad n_{1,15} = \frac{1}{2}(KT+T^2+2). \end{aligned} \tag{13.132}$$

We use the trace identities for SU(2), given by equations (13.53), and the trace identities for SU(4) to compute the remainder terms of the anomaly polynomial. For SU(4), the trace identities are given by

$$\begin{aligned} \mathrm{tr}_{15}\, F_2^2 &= 8\mathrm{tr}_4\, F_2^2, \quad \mathrm{tr}_{15}\, F_2^4 = 8\mathrm{tr}_4\, F_2^4 + 6(\mathrm{tr}_4\, F_2^2)^2, \\ \mathrm{tr}_6\, F_2^2 &= 2\mathrm{tr}_4\, F_2^2, \quad \mathrm{tr}_6\, F_2^4 = -4\mathrm{tr}_4\, F_2^4 + 3(\mathrm{tr}_4\, F_2^2)^2. \end{aligned} \tag{13.133}$$

We first compute the SU(2) side contribution of the anomaly polynomials. The number of representations $n_{\mathbf{R}}$ are then identified as

$$n_3 = n_{3,1}, \quad n_2 = 4(n_{2,4} + n_{2,\bar{4}}). \tag{13.134}$$

Hence, $X_1^{(2)}$ and $X_1^{(4)}$ are given by

$$X_1^{(2)} = (A_3(1-n_3) - n_2 A_2)\,\mathbf{tr}_2 F_1^2 = -12K(2K+T)\mathbf{tr}_2 F_1^2 \tag{13.135}$$

$$
\begin{aligned}
X_1^{(4)} &= (B_3(1-n_3) - n_2 B_2)\,\mathbf{tr}_2 F_1^4 + (C_3(1-n_3) - n_2 C_2)\,(\mathbf{tr}_2 F_1^2)^2 \\
&= -12(2K+T)^2(\mathbf{tr}_2 F_1^2)^2.
\end{aligned}
\tag{13.136}
$$

Now consider the contribution from the SU(4) side of the anomaly cancellation. We determine the number of representations to be

$$
n_4 = 2(n_{2,4} + n_{2,\bar{4}}), \quad n_6 = n_{6,1}, \quad n_{15} = n_{15,1}. \tag{13.137}
$$

Hence, $X_2^{(2)}$ and $X_2^{(4)}$ are given by

$$
X_2^{(2)} = (A_{15}(1-n_{15}) - n_6 A_6 - n_4 A_4)\,\mathbf{tr}_4 F_2^2 = 6KT\mathbf{tr}_4 F_2^2 \tag{13.138}
$$

$$
\begin{aligned}
X_2^{(4)} &= (B_{15}(1-n_{15}) - n_6 B_6 - n_4 B_4)\,\mathbf{tr}_4 F_2^4 + (C_{15}(1-n_{15}) - n_6 C_6 - n_4 C_4)\,(\mathbf{tr}_4 F_2^2)^2 \\
&= -3T^2(\mathbf{tr}_4 F_2^2)^2
\end{aligned}
\tag{13.139}
$$

Since we have a semisimple group with two simple components, we must include the additional mixed term

$$
Y_{12} = (n_{2,4} + n_{2,\bar{4}})\mathbf{tr}_2 F_1^2 \mathbf{tr}_4 F_2^2 \tag{13.140}
$$

to fully consider the bifundamental representation $(2, 4)$. As a result, the full anomaly polynomial is

given by

$$\begin{aligned} I_8 &= \frac{9-n_T}{8}(\mathbf{tr}R^2)^2 + \frac{1}{6}(X_1^{(2)}+X_2^{(2)})\mathbf{tr}R^2 - \frac{2}{3}(X_1^{(4)}+X_2^{(4)}) + 4Y_{12} \\ &= \frac{1}{8}\left(K\mathbf{tr}R^2 - 16K\mathbf{tr}_4F_2^2 - 8T\mathbf{tr}_4F_2^2 + 4T\mathbf{tr}_2F_1^2\right)^2, \end{aligned} \tag{13.141}$$

which is a perfect square. Hence, we can conclude that the anomalies are all canceled when uplifted to a six-dimensional $\mathcal{N}=(1,0)$ theory.

13.5 SU(2) × SU(4)-model

We consider an SU(2) × SU(4)-model with a trivial Mordell-Weil group. The Weierstrass equation for $\mathrm{I}_2^{\mathrm{ns}}+\mathrm{I}_4^{\mathrm{s}}$ is

$$y^2z + a_1xyz = x^3 + \widetilde{a}_2tx^2z + \widetilde{a}_4st^2xz^2 + \widetilde{a}_6s^2t^4z^3. \tag{13.142}$$

The discriminant for this model is

$$\Delta = -s^2t^4\left[(a_1^2+4\widetilde{a}_2t)^2(a_1^2\widetilde{a}_6+4\widetilde{a}_2\widetilde{a}_6t-\widetilde{a}_4^2) - 8st^2(9a_1^2\widetilde{a}_4\widetilde{a}_6+36\widetilde{a}_2\widetilde{a}_4\widetilde{a}_6t-8\widetilde{a}_4^3-54\widetilde{a}_6^2st^2)\right]. \tag{13.143}$$

The corresponding gauge group G and the representation $\mathbf{R}$ are respectively

$$G=\mathrm{SU}(2)\times\mathrm{SU}(4), \quad \mathbf{R}=(3,1)\oplus(1,15)\oplus(2,4)\oplus(2,\overline{4})\oplus(1,6)\oplus(2,1)\oplus(1,4)\oplus(1,\overline{4}). \tag{13.144}$$

The representation **R** is derived geometrically in the next subsection. The following sequence of blowups gives a crepant resolution:

$$X_0 \xleftarrow{(x,y,s|e_1)} X_1 \xleftarrow{(x,y,t|w_1)} X_2 \xleftarrow{(y,w_1|w_2)} X_3 \xleftarrow{(x,w_2|w_3)} X_4. \tag{13.145}$$

Note that unlike other models, this required one more blowup to fully resolve the singularities. The proper transform is

$$w_2y^2 + a_1xy = w_1(e_1w_3^2x^3 + \widetilde{a}_2w_3tx^2 + \widetilde{a}_4st^2x + \widetilde{a}_6w_1w_2s^2t^4), \tag{13.146}$$

where the relative projective coordinates are given by

$$[e_1w_1w_2w_3^2x : e_1w_1w_2^2w_3^2y : z = 1][w_1w_2w_3^2x : w_1w_2^2w_3^2y : s][w_3x : w_2w_3y : t][y : w_1][x : w_2]. \tag{13.147}$$

13.5.1 Fiber structure

This model has the following fibral divisors that correspond to their curves:

$$\begin{cases} D_0^s & : s = w_2y^2 + a_1xy - w_1w_3x^2(e_1w_3x + \widetilde{a}_2t) = 0, \\ D_1^s & : e_1 = w_2y^2 + a_1xy - w_1t(\widetilde{a}_2w_3x^2 + \widetilde{a}_4stx + \widetilde{a}_6w_1w_2s^2t^3) = 0, \\ D_0^t & : t = w_2y^2 + a_1xy - e_1w_1w_3^2x^3 = 0, \\ D_1^t & : w_1 = w_2y + a_1x = 0, \\ D_2^t & : w_3 = w_2y^2 + a_1xy - w_1st^2(\widetilde{a}_4x + \widetilde{a}_6w_1w_2st^2) = 0, \\ D_3^t & : w_2 = a_1y - w_1(e_1w_3^2x^2 + \widetilde{a}_2w_3tx + \widetilde{a}_4st^2) = 0. \end{cases} \tag{13.148}$$

The generic fiber of D_1^s is a conic that degenerates into two lines over its discriminant locus $V(a_1^2\widetilde{a}_6 + 4\widetilde{a}_2\widetilde{a}_6t - \widetilde{a}_4^2)$. The the resulting fiber is of type $\mathrm{I}_3^{\mathrm{ns}}$ and the curves $C_1^s \to C_{1+}^s + C_{1-}^s$ yield weights of the fundamental representation of A_1. The intersection numbers between the curves and the fibral divisors of $\mathrm{I}_2^{\mathrm{ns}}$ are

$C_1^s \to C_{1+}^s + C_{1-}^s,$

	D_0^s	D_1^s	D_0^t	D_1^t	D_2^t	D_3^t
C_0^s	-2	2	0	0	0	0
$C_{1\pm}^s$	1	-1	0	0	0	0
$C_{1+}^s + C_{1-}^s$	2	-2	0	0	0	0

. (13.149)

At the intersection of S and T, we get a fiber of type I_6^s. Its components are

$$\begin{cases} C_0^t \cap C_1^t & : t = w_1 = w_2 y + a_1 x = 0, \\ C_1^t \cap C_2^t & : w_1 = w_3 = w_2 y + a_1 x = 0, \\ C_2^t \cap C_3^t & : w_2 = w_3 = a_1 y - \widetilde{a}_4 w_1 s t^2 = 0, \\ C_3^t \cap C_0^t & : t = w_2 = a_1 y - e_1 w_1 w_3^2 x^2 = 0. \end{cases} \tag{13.150}$$

This specializes to an I_0^{ss} when $a_1 = 0$, just like the other model (with the Mordell-Weil group $\mathbb{Z}_2$) in the previous section. The curve C_1^t specializes into the central node C_{13}^t where

$$C_{13}^t : w_1 = w_2 = 0. \tag{13.151}$$

The curve C_3^t splits into the three curves C_{13}^t, which is the central node, and $C_{3\pm}^{t'}$, which is given by the two roots of the curve

$$C_{3\pm}^{t'} : w_2 = e_1 w_3^2 x^2 + \widetilde{a}_2 w_3 t x + \widetilde{a}_4 s t^2 = 0. \tag{13.152}$$

Thus we establish a Kodaira fiber of type I_0^{*ss} when $a_1 = 0$. This is expected as this is exactly the specialization under the same condition from the other model.

Since the locus of this specialization happens when $t w_1 w_2 w_3 = 0$ but away from the locus of $s e_1 = 0$, there is no charged matter under $\mathfrak{su}(2)$. Then we can compute the intersection numbers

between the curves and the fibral divisors of I_4^s, from the splitting of the curves

$$\begin{cases} C_1^t & \to C_{13}^t, \\ C_3^t & \to C_{13}^t + C_{3+}^{t'} + C_{3-}^{t'}, \end{cases} \tag{13.153}$$

where $C_{3\pm}^{t'}$ are of a non-split type:

	D_0^s	D_1^s	D_0^t	D_1^t	D_2^t	D_3^t
C_0^t	0	0	-2	1	0	1
C_{13}^t	0	0	1	-2	1	0
C_2^t	0	0	0	1	-2	1
$C_{3+}^{t'} + C_{3-}^{t'}$	0	0	0	2	0	-2

.

For the curve C_{13}^t, the weight is computed to be $[2, -1, 0]$, which corresponds to the representation 15. The curves $C_{3\pm}^{t'}$ each carries the weight $[-1, 0, 1]$ that yields the representation 6, which is the fundamental representation of $\mathfrak{so}(6)$. Since these two curves are nonsplit, when we compute the weight of them together as $C_3^{t'} = C_{3+}^{t'} + C_{3-}^{t'}$, the weight is given by $[-2, 0, 2]$; the representation is then computed as $20'$. Since the locus is away from $se_1 = 0$, it is uncharged on the side for $\mathfrak{su}(2)$ and hence the representation for the whole product group $\mathfrak{su}(2) \times \mathfrak{su}(4)$ is $(1, 6)$. It is important to note that the representation we get from the specialization to an I_0^{*ss} is the same for all 6, 15, and $20'$ with the previous model (with the Mordell-Weil group $\mathbb{Z}_2$). This has a codimension-three specialization

when $a_1 = \widetilde{a}_4 = 0$. The curves split as

$$\begin{cases} C_2^t & \to C_{23}^t + C_{2\pm}^{t'}, \\ C_{3\pm}^{t'} & \to C_{23}^t + C_3^{t'}, \end{cases} \tag{13.154}$$

where the new curves are given by

$$\begin{cases} C_{23}^t & : w_2 = w_3 = 0, \\ C_{2\pm}^{t'} & : w_3 = y^2 - \widetilde{a}_6 w_1^2 s^2 t^4 = 0, \\ C_3^{t'} & : w_2 = e_1 w_3 x + \widetilde{a}_2 t = 0. \end{cases} \tag{13.155}$$

This gives the codimension three enhancement, which has a different fiber structure as presented in Figure 13.12. Using these splittings of the curve, we compute the intersection numbers between the curves and the fibral divisors of I_4^s to be

	D_0^s	D_1^s	D_0^t	D_1^t	D_2^t	D_3^t
$C_0^{t'}$	0	0	-2	2	0	0
$C_3^{t'}$	0	0	0	2	0	-2
$2\,C_{13}^t$	0	0	2	-4	0	2
$2\,C_{23}^t$	0	0	0	0	2	-2
$C_{2+}^{t'} + C_{2-}^{t'}$	0	0	0	0	-2	2

(13.156)

The new curves are $C_3^{t'}$, which gives the weight $[-2, 0, 2]$, C_{23}^t, which gives the weight $[0, -1, 1]$, and $C_{2\pm}^{t'}$, which individually gives the weight $[0, 1, -1]$. They respectively correspond to the representations $20'$, $\overline{4}$, and 4. When we consider the two non-split type curves together as $C_2^{t'} = C_{2+}^{t'} + C_{2-}^{t'}$, the weight is then $[0, 2, -2]$ which yields the representation $\overline{10}$.

This model with a trivial Mordell-Weil group has an additional specialization from I_4^s to an I_5^s when $a_1^2\widetilde{a}_6 - \widetilde{a}_4^2 = 0$. Under this condition, the curve C_2^t splits into two curves $C_2^{t'}$ and $C_2^{t''}$ as

$$\begin{cases} C_2^t : w_3 & = w_2y^2 + a_1xy - w_1st^2(\widetilde{a}_4x + \widetilde{a}_6w_1w_2st^2) \\ & = \frac{1}{a_1^2}(a_1y - \widetilde{a}_4w_1st^2)(a_1w_2y + a_1^2x - w_1w_2st^2) = 0; \\ C_2^{t'} : w_3 & = a_1y - \widetilde{a}_4w_1st^2 = 0, \\ C_2^{t''} : w_3 & = a_1w_2y + a_1^2x - w_1w_2st^2 = 0. \end{cases} \tag{13.157}$$

Thus, the fiber structure becomes an I_5^s, which is represented in Figure 13.12.

Based on the splitting of the curve C_2^t where C_0^t, C_1^t, and C_3^t remain the same, the intersection numbers between the curves and the fibral divisors of I_4^s are computed to determine the weights of the new curves:

	D_0^s	D_1^s	D_0^t	D_1^t	D_2^t	D_3^t
C_0^t	0	0	-2	1	0	1
C_1^t	0	0	1	-2	1	0
$C_2^{t''}$	0	0	0	1	-1	0
$C_2^{t'}$	0	0	0	0	-1	1
C_3^t	0	0	1	0	1	-2

.

The weights of the curves are $[-1, 1, 0]$ for the curve $C_2^{t'}$ and $[0, 1, -1]$ for the curve $C_2^{t''}$. They give the representations 4 and $\overline{4}$ respectively. Since this collision is away from the locus of $se_1 = 0$, where the divisors of $\mathfrak{su}(2)$ sit, there is no matter is charged under $\mathfrak{su}(2)$. We therefore get $(1, 4) \oplus (1, \overline{4})$ for the charged matter.

In order to consider the collision of two types of Kodaira fibers, we need to enforce both $se_1 = tw_1w_2 = 0$. Then we can get the following curves:

$$\begin{cases} C_0^s \cap C_0^t : & s = t = w_2y^2 + a_1xy - e_1w_1w_3^2x^3 = 0 \to \eta^{00}, \\ C_1^s \cap C_0^t : & e_1 = t = w_2y + a_1x = 0 \to \eta^{10}, \\ & e_1 = t = y = 0 \to \eta^{10y}, \\ C_1^s \cap C_1^t : & e_1 = w_1 = w_2y + a_1x = 0 \to \eta^{11}, \\ C_1^s \cap C_2^t : & e_1 = w_3 = w_2y^2 + a_1xy - w_1st^2(\widetilde{a}_4x + \widetilde{a}_6w_1w_2st^2) = 0 \to \eta^{12}, \\ C_1^s \cap C_3^t : & e_1 = w_2 = a_1y - w_1t(\widetilde{a}_2w_3x + \widetilde{a}_4st) = 0 \to \eta^{13}. \end{cases} \tag{13.158}$$

The fiber structure is given by the diagram in the second row of Figure 13.12. This has identical structure to the $\mathrm{I}_2^{\mathrm{ns}} \cap \mathrm{I}_4^{\mathrm{s}}$-model with the $\mathbb{Z}_2$ Mordell-Weil group.

The representations with respect to $(\mathfrak{su}(2), \mathfrak{su}(4))$ from this $\mathrm{I}_2^{\mathrm{ns}} + \mathrm{I}_4^{\mathrm{s}}$-model with a trivial Mordell-Weil group are summarized in Table 13.14 below. Here we denote weights as $[\psi; \phi_1, \phi_2, \phi_3]$, where $[\psi]$ is the weight for the $\mathfrak{su}(2)$ and $[\phi_1, \phi_2, \phi_3]$ is the weight for the $\mathfrak{su}(4)$.

Locus	$tw_1w_2 = 0$				$se_1 = tw_1w_2 = 0$		$se_1 = 0$
Curves	C^{t}_{13}	$C^{\mathrm{t}'}_{3\pm}$	$C^{\mathrm{t}'}_{2}$	$C^{\mathrm{t}''}_{2}$	η^{10}	η^{10y}	$C^{\mathrm{s}}_{1\pm}$
Weights	$[0; 2, -1, 0]$	$[0; -1, 0, 1]$	$[0; 0, 1, -1]$	$[0; -1, 1, 0]$	$[1; -1, 0, 0]$	$[1; 0, 0, -1]$	$[-1; 0, 0, 0]$
Rep	$(1, 15)$	$(1, 6)$	$(1, 4)$	$(1, \overline{4})$	$(2, \overline{4})$	$(2, 4)$	$(2, 1)$

Table 13.14: Weights and representations for the $\mathrm{I}_2^{\mathrm{ns}} + \mathrm{I}_4^{\mathrm{s}}$-model with a trivial Mordell-Weil group.

This model has an additional $(2, 1) \oplus (1, 4) \oplus (1, \overline{4})$ compared to the representations of the $\mathrm{I}_2^{\mathrm{ns}} + \mathrm{I}_4^{\mathrm{s}}$-model with the $\mathbb{Z}_2$ Mordell-Weil group:

$$\mathbf{R} = (3, 1) \oplus (1, 15) \oplus (2, 4) \oplus (2, \overline{4}) \oplus (1, 6) \oplus (2, 1) \oplus (1, 4) \oplus (1, \overline{4}). \tag{13.159}$$

When $a_1 = 0$, η^{10} and η^{13} split and η^{11} produces a curve that intersects with three curves. The

splittings of the curves when $a_1 = 0$ are

$$\begin{cases} \eta^{10} \to & \eta^{103} + \eta^{10y}, \\ \eta^{11} \to & \eta^{113}, \\ \eta^{13} \to & \eta^{103} + \eta^{113} + \eta^{13'}, \end{cases} \tag{13.160}$$

where the new fibers are given by

$$\begin{cases} \eta^{103} & : e_1 = t = w_2 = 0, \\ \eta^{10y} & : e_1 = t = y = 0, \\ \eta^{113} & : e_1 = w_1 = w_2 = 0, \\ \eta^{13'} & : e_1 = w_2 = \widetilde{a}_2 w_3 x + \widetilde{a}_4 st = 0. \end{cases} \tag{13.161}$$

This new fiber structure when $a_1 = 0$ is the diagram in the third row of Figure 13.12 as it is the same with the $\mathrm{I}_2^{\mathrm{ns}}+\mathrm{I}_4^{\mathrm{s}}$-model with the Mordell-Weil group $\mathbb{Z}_2$.

Consider when $a_1 = \widetilde{a}_2 = 0$, which produces a codimension-four specialization. The only curve that transforms is

$$\eta^{13'} \to \eta^{103} : e_1 = t = w_2 = 0, \tag{13.162}$$

thus changing the geometry into the bottom left diagram of Figure 13.12.

Consider when $a_1 = \widetilde{a}_4 = 0$, which produces a codimension-four specialization. The only curve

that transforms is

$$\eta^{13'} \to \eta^{123}, \text{ and } \eta^{13'} \to \eta^{123} + \eta^{12'} + \eta^{12''}, \tag{13.163}$$

where the three new curves are given by

$$\eta^{123} : e_1 = w_2 = w_3 = 0, \quad \eta^{12'} : e_1 = w_3 = y + w_1 s t^2 = 0, \quad \eta^{12''} : e_1 = w_3 = y - w_1 s t^2 = 0. \tag{13.164}$$

thus changing the geometry into the bottom right diagram of Figure 13.12.

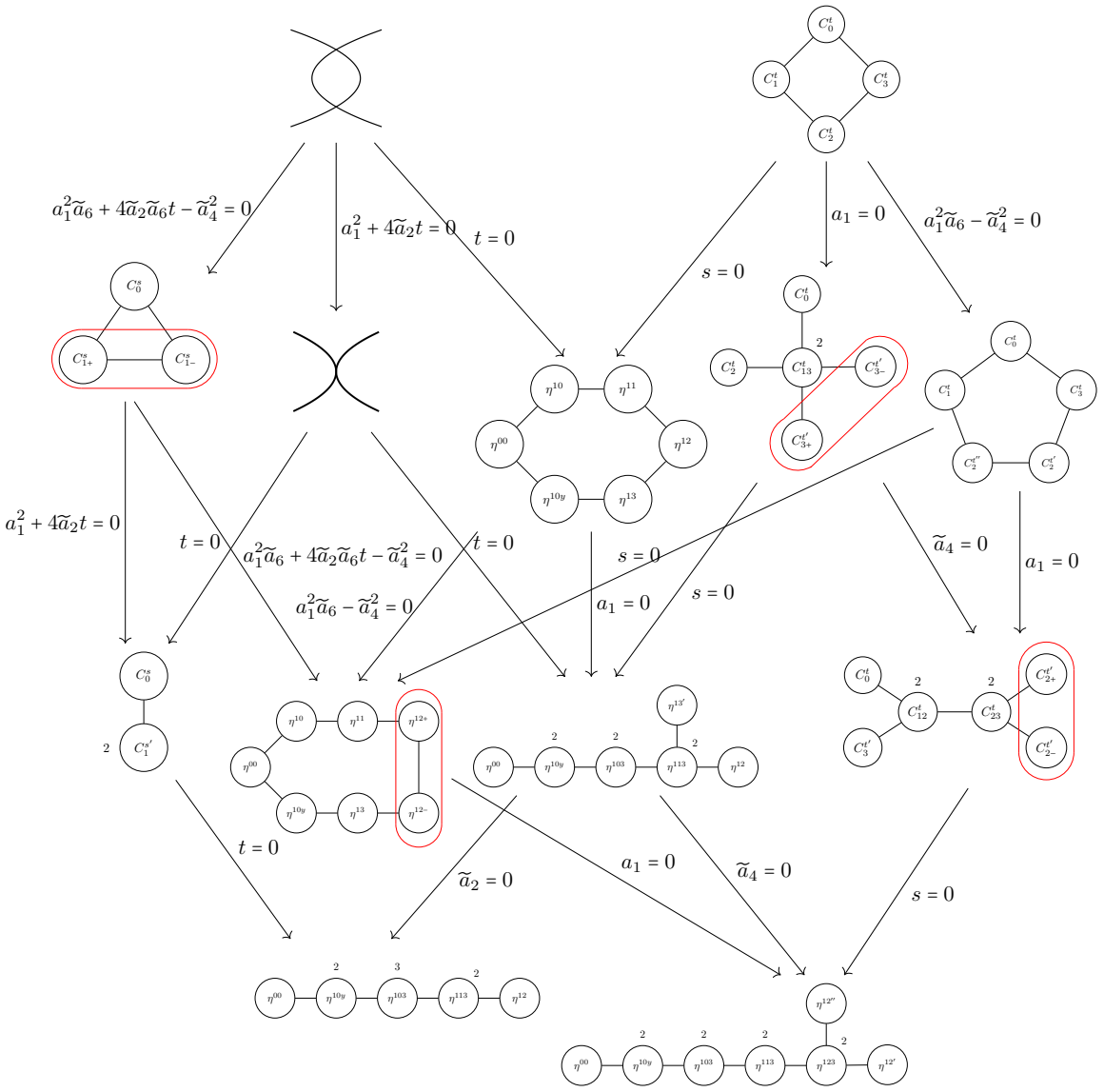

Figure 13.12: Fiber structure of $\mathrm{I}_2^{\mathrm{ns}}+\mathrm{I}_4^{\mathrm{ns}}$ with a trivial Mordell-Weil group. This is the fiber structure of the collision of $\mathrm{I}_2^{\mathrm{ns}}$ and $\mathrm{I}_4^{\mathrm{s}}$, which are drawn on the top, with a trivial Mordell-Weil group. The hexagon on the locus $se_1 = tw_1w_2w_3 = 0$ from the $\mathrm{I}_2^{\mathrm{ns}}+\mathrm{I}_4^{\mathrm{s}}$-model with the Mordell-Weil group $\mathbb{Z}_2$ is identical to the hexagon for this model. This enhancement has two newly split curves η^{IO} and $\eta^{\mathrm{IO}y}$, giving the representations $(2,4)\oplus(2,\overline{4})$. When $a_1 = 0$, this hexagon specializes to the diagram on the third row. When $a_1 = \widetilde{a}_2 = 0$, this further specializes into the diagram on the bottom left. When $a_1 = \widetilde{a}_4 = 0$, we get the diagram on the bottom right.

13.5.2 Coulomb phases

Using the notation of $[\psi; \phi_1, \phi_2, \phi_3]$, the nine independent weights for these representations are given by

$$\begin{aligned}
&\varpi_1 = [0; -1, 1, 0], \quad \varpi_2 = [0; 0, 1, -1], \quad \varpi_3 = [0; -1, 0, 1], \\
&\varpi_4 = [1; -1, 1, 0], \quad \varpi_5 = [1; 0, -1, 1], \quad \varpi_6 = [-1; 1, 0, 0], \\
&\varpi_7 = [-1; -1, 1, 0], \quad \varpi_8 = [-1; 0, -1, 1], \quad \varpi_9 = [-1; 0, 0, 1].
\end{aligned} \tag{13.165}$$

The first two weights are from $(1, 4) \oplus (1, \overline{4})$, the third weight is from $(1, 6)$, and the remaining six weights are from $(2, 4) \oplus (2, \overline{4})$. More specifically, the first weight is $(1, 4)$, the second weight is $(1, \overline{4})$,the third weight is $(1, 6)$, the fourth to eighth weights are $(2, 4)$, and the ninth weight is $(2, \overline{4})$.

For convenience, we denote these relations as a vector of weights v,

$$\begin{aligned}
v =&(-\phi_1 + \phi_2,\ \phi_2 - \phi_3,\ -\phi_1 + \phi_3,\ \psi_1 - \phi_1 + \phi_2,\ \psi_1 - \phi_2 + \phi_3, \\
&-\psi_1 + \phi_1,\ -\psi_1 - \phi_1 + \phi_2,\ -\psi_1 - \phi_2 + \phi_3,\ -\psi_1 + \phi_3).
\end{aligned} \tag{13.166}$$

The chambers structures of these are computed, which is drawn in Figure 13.6. There are in total 20 chambers. The chambers are denoted as a set of signs of the nine relations that determine the chamber, where 1 denotes the relation to be positive and -1 denotes the relation to be negative.

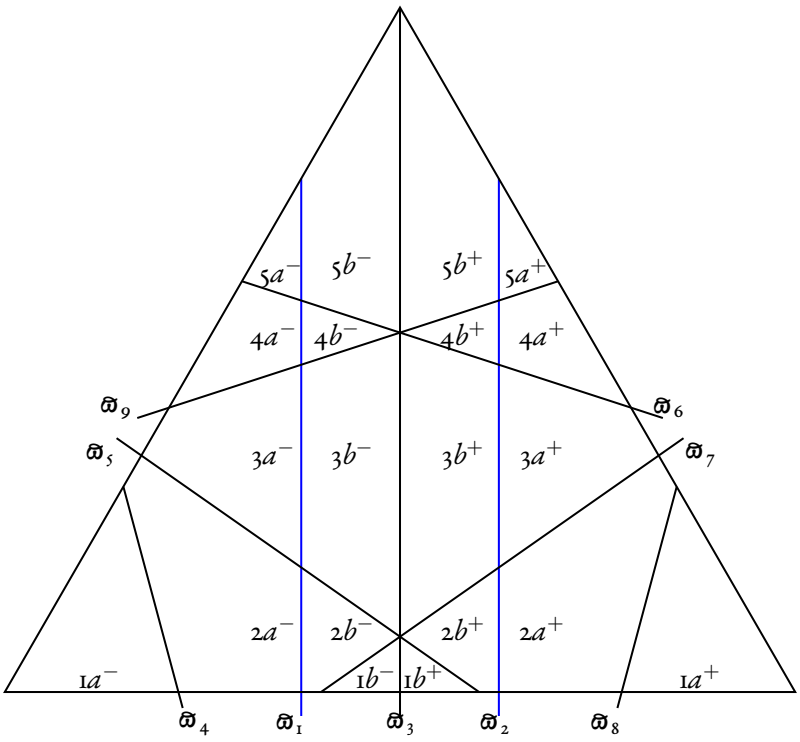

Figure 13.13: This is the chamber structure of the $\mathrm{I}_2^{\mathrm{ns}}+\mathrm{I}_4^{\mathrm{s}}$-model with a trivial Mordell-Weil group in a planar diagram.

13.5.3 $5d\,\mathcal{N}=1$ PREPOTENTIALS AND THE TRIPLE INTERSECTION POLYNOMIALS

The triple intersection polynomial is computed for the $\mathrm{I}_2^{\mathrm{ns}}+\mathrm{I}_4^{\mathrm{s}}$-model with a trivial Mordell-Weil group defined by the crepant resolution we determined earlier [REF]:

$$\begin{aligned}\mathscr{F}_{trip} =& -2S(2L+S)\psi_1^3+4T(L-T)\varphi_1^3+2T(S-2L)\varphi_2^3+2T(L-2T)\varphi_3^3\\
&+3T(2L-S-T)\varphi_2^2\left(\varphi_1+\varphi_3\right)+3T(-3L+S+2T)\varphi_2\left(\varphi_1^2+\varphi_3^2\right)\\
&-6LT\varphi_1^2\varphi_3+6LT\varphi_1\varphi_2\varphi_3-6ST\psi_1\left(\varphi_1^2-\varphi_2\varphi_1+\varphi_2^2+\varphi_3^2-\varphi_2\varphi_3\right)\\
&+4S(L-S)\psi_0^3+6S(S-2L)\psi_0^2\psi_1+12LS\psi_0\psi_1^2-2T(-2L+S+2T)\varphi_0^3\\
&+3T\varphi_0\left(2\varphi_1\left(L\varphi_3+S\psi_1\right)+\varphi_1^2(L-S)+\varphi_3^2(L-S)-2S\left(\psi_0-\psi_1\right)^2+2S\psi_1\varphi_3\right)\\
&+\varphi_0^2\left(3T\left(\varphi_1+\varphi_3\right)(-2L+S+T)-6ST\psi_1\right).\end{aligned}\tag{13.167}$$

The bottom three lines have terms depending on ψ_0 and φ_0, which will not be contributing to the prepotential term that is computed below, and the prepotential is compared with the triple intersection polynomial explicitly. The triple intersection number is different for different crepant resolutions, so the correct chamber has to be identified.

The Intrilligator-Morrison-Seiberg prepotential is computed in the same chamber that corresponds to $5b+$ in Figure 13.6. This is determined from the weights computed from the curves, which is summarized in Table 13.14. The chamber that we geometrically computed has positive relations for the first three entries of the sign vector v in Figure 13.6. Also, the sixth entry is negative and the ninth

entry is negative in the sign vector v as well. The only chamber that satisfies $v = (111xxoxxo)$, where x denotes an unknown sign, is the chamber $5b+$, which has $v = (11110000)$. Using the representation for this split model with $\mathbb{Z}_2$,

$$\mathbf{R} = (3,1 \oplus (1,15)) \oplus (2,4) \oplus (2,\overline{4}) \oplus (1,6) \oplus (2,1) \oplus (1,4) \oplus (1,\overline{4}), \tag{13.168}$$

the prepotential in the chamber $5b+$ is

$$\begin{aligned} 6\mathscr{F}_{\text{IMS}} = & -8(n_{1,15}-1)\varphi_1^3 - (8n_{1,15}+n_{1,4}+n_{1,\overline{4}}-8)\varphi_2^3 - 2(4n_{1,15}+n_{1,6}-4)\varphi_3^3 \\ & - (n_{2,1}+4(n_{2,4}+n_{2,\overline{4}}+2n_{3,1}-2))\psi_1^3 + \frac{3}{2}(4n_{1,15}+n_{1,4}+n_{1,\overline{4}}-2n_{1,6}-4)\varphi_2^2(\varphi_1+\varphi_3) \\ & - \frac{3}{2}(n_{1,4}+n_{1,\overline{4}}-2n_{1,6})\varphi_2(\varphi_1^2+\varphi_3^2) - 6n_{1,6}\varphi_1^2\varphi_3 + 6n_{1,6}\varphi_1\varphi_2\varphi_3 \\ & - 6(n_{2,4}+n_{2,\overline{4}})\psi_1\left(\varphi_1^2 - \varphi_1\varphi_2 + \varphi_2^2 + \varphi_3^2 - \varphi_2\varphi_3\right). \end{aligned} \tag{13.169}$$

Using the dictionary that the triple intersection polynomial is identical to the prepotential, we can fix $n_{1,6}$ and $n_{1,15}$ completely, and determine the following linear relations for the remainder $n_{\mathbf{R}}$:

$$n_{1,4}+n_{1,\overline{4}} = 2T(4L-S-2T),\ n_{2,4}+n_{2,\overline{4}} = ST,\ n_{2,1}+8n_{3,1} = 2S(2L+S-2T)+8. \tag{13.170}$$

In order to compute individual $n_{\mathbf{R}}$, we recall that the representation $(2,1)$ was computed from the splittings of the curve $C_1^{\mathrm{s}} \to C_{1+}^{\mathrm{s}} + C_{1-}^{\mathrm{s}}$ in Section 13.5. These splittings are from the condition of the coefficients such that $a_1^2\widetilde{a}_6 + 4\widetilde{a}_2\widetilde{a}_6 t - \widetilde{a}_4^2 = 0$. The class of this condition is then twice that of the

class of $\widetilde{a}_4$, which is $2(4L-S-2T)$. Then these splittings happen when $s = a_1^2\widetilde{a}_6 + 4\widetilde{a}_2\widetilde{a}_6 t - \widetilde{a}_4^2 = 0$, which yields the class $2S(4L - S - 2T)$. Hence, $n_{2,1} = 2S(4L - S - 2T)$. Moreover, we also use $n_{1,4} = n_{1,\overline{4}}$ and $n_{2,4} = n_{2,\overline{4}}$. Thus, we can now fix all the $n_{\mathbf{R}}$ to be

$$\begin{aligned} &n_{3,1} = \frac{1}{2}(-LS + S^2 + 2), \quad n_{2,1} = 2S(4L - S - 2T), \quad n_{2,4} = n_{2,\overline{4}} = \frac{1}{2}ST, \\ &n_{1,6} = LT, \quad n_{1,15} = \frac{1}{2}\left(-LT + T^2 + 2\right), \quad n_{1,4} = n_{1,\overline{4}} = T(4L - S - 2T). \end{aligned} \tag{13.171}$$

Using the genus of the curve, let g_S and g_T be the curves such that $2 - 2g_S = S(L-S)$ and $2 - 2g_T = T(L - T)$. Also we use the Calabi-Yau condition $L = -K$. Then we can interpret the prepotential in terms of these genus as

$$\begin{aligned} \mathscr{F}_{trip} = &- (8 - 8g_S + 6S^2)\psi_1^3 + (8 - 8g_T)\varphi_1^3 + (-8 + 8g_T + 2T(S - 2T))\varphi_2^3 - 2(2g_T + T^2 - 2)\varphi_3^3 \\ &+ 3\left(-4g_T - ST + T^2 + 4\right)\varphi_2^2\left(\varphi_1 + \varphi_3\right) + 3\left(6g_T + T(S - T) - 6\right)\varphi_2\left(\varphi_1^2 + \varphi_3^2\right) \\ &- 6\left(-2g_T + T^2 + 2\right)\varphi_1^2\varphi_3 + 6\left(-2g_T + T^2 + 2\right)\varphi_1\varphi_2\varphi_3 \\ &- 6ST\psi_1\left(\varphi_1^2 - \varphi_2\varphi_1 + \varphi_2^2 + \varphi_3^2 - \varphi_2\varphi_3\right). \end{aligned} \tag{13.172}$$

13.5.4 $6d\,\mathcal{N}=(1,0)$ ANOMALY CANCELLATION

In this section, we consider an $\mathrm{I}_2^{\mathrm{ns}}+\mathrm{I}_4^{\mathrm{s}}$-model with the trivial Mordell-Weil group. Then, the gauge algebra and the representations, which are computed geometrically in Section 13.5, are given by

$$\mathfrak{g}=\mathcal{A}_1+\mathcal{A}_3,\quad \mathbf{R}=(3,1)\oplus(2,4)\oplus(2,\overline{4})\oplus(1,4)\oplus(1,\overline{4})\oplus(1,6)\oplus(1,15). \tag{13.173}$$

The number of representations are computed above:

$$\begin{aligned} &n_{3,1}=\frac{1}{2}(KS+S^2+2)=g_S,\quad n_{2,1}=-2S(4K+S+2T),\quad n_{2,4}=n_{2,\overline{4}}=\frac{1}{2}ST\\ &n_{1,6}=-KT,\quad n_{1,15}=\frac{1}{2}\,(KT+T^2+2)=g_T,\quad n_{1,4}=n_{1,\overline{4}}=-T(4K+S+2T). \end{aligned} \tag{13.174}$$

Then, the number of vector multiplets $n_V^{(6)}$, tensor multiplets n_T, and hypermultiplets n_H are

$$\begin{aligned} &n_V^{(6)}=18,\quad n_T=9-K^2,\\ &n_H=h^{2,1}(Y)+1+n_{3,1}(3-1)+n_{2,1}(2-0)+n_{2,4}(8-0)+n_{2,\overline{4}}(8-0)\\ &\qquad+n_{1,6}(6-0)+n_{1,15}(15-3)+n_{1,4}(4-0)+n_{1,\overline{4}}(4-0)=30+29K^2. \end{aligned} \tag{13.175}$$

Then we see that

$$n_H-n_V^{(6)}+29n_T-273=0, \tag{13.176}$$

which vanishes. The pure gravitational anomalies are thus canceled.

In order to check the remainder terms of the anomaly polynomial, the number of representations

are then identified as

$$
\begin{aligned}
n_3 = n_{3,1}, \quad n_2 = n_{2,1} + 4(n_{2,4} + n_{2,\bar{4}}), \\
n_4 = n_{1,4} + n_{1,\bar{4}} + 2(n_{2,4} + n_{2,\bar{4}}), \quad n_6 = n_{6,1}, \quad n_{15} = n_{15,1}.
\end{aligned}
\tag{13.177}
$$

Hence, using the trace identities os SU(2) and SU(4) given by the equations (13.53) and (13.133), $X_1^{(2)}$, $X_1^{(4)}$, $X_2^{(2)}$, $X_2^{(4)}$, and Y_{ab} are given by

$$
X_1^{(2)} = (A_3(1 - n_3) - n_2 A_2)\,\mathbf{tr}_2 F_1^2 = 6KT\mathbf{tr}_2 F_1^2 \tag{13.178}
$$

$$
\begin{aligned}
X_1^{(4)} &= (B_3(1 - n_3) - n_2 B_2)\,\mathbf{tr}_2 F_1^4 + (C_3(1 - n_3) - n_2 C_2)\,(\mathbf{tr}_2 F_1^2)^2 \\
&= -3T^2(\mathbf{tr}_2 F_1^2)^2
\end{aligned}
\tag{13.179}
$$

$$
X_2^{(2)} = (A_{15}(1 - n_{15}) - n_6 A_6 - n_4 A_4)\,\mathbf{tr}_4 F_2^2 = 6KS\mathbf{tr}_4 F_2^2 \tag{13.180}
$$

$$
\begin{aligned}
X_2^{(4)} &= (B_{15}(1 - n_{15}) - n_6 B_6 - n_4 B_4)\,\mathbf{tr}_4 F_2^4 + (C_{15}(1 - n_{15}) - n_6 C_6 - n_4 C_4)\,(\mathbf{tr}_4 F_2^2)^2 \\
&= -3S^2(\mathbf{tr}_4 F_2^2)^2
\end{aligned}
\tag{13.181}
$$

$$
Y_{12} = (n_{2,4} + n_{2,\bar{4}})\mathbf{tr}_2 F_1^2 \mathbf{tr}_4 F_2^2 = ST\mathbf{tr}_2 F_1^2 \mathbf{tr}_4 F_2^2. \tag{13.182}
$$

The remainder terms of anomaly polynomial are then given by

$$
\begin{aligned}
I_8 &= \frac{9 - n_T}{8}(\mathbf{tr}R^2)^2 + \frac{1}{6}(X_1^{(2)} + X_2^{(2)})\mathbf{tr}R^2 - \frac{2}{3}(X_1^{(4)} + X_2^{(4)}) + 4Y_{12} \\
&= \frac{1}{8}\left(K\mathbf{tr}R^2 + 4S\mathbf{tr}_2 F_1^2 + 4T\mathbf{tr}_4 F_2^2\right)^2,
\end{aligned}
\tag{13.183}
$$

which is a perfect square. Hence, all the six-dimensional anomalies are canceled.

Part VI

Entanglement Entropy, Holography, and Infinite-dimensional von Neumann Algebra

Introduction

Quantum error correcting codes with finite dimensional Hilbert spaces have yielded new insights on bulk reconstruction in AdS/CFT. In this part of the thesis, we discuss the formalism to understand holography in the context of infinite-dimensional Hilbert spaces with Reeh-Shlieder theorem in mind. We use infinite–dimensional von Neumann Algebra to characterise a causal spacetime.

In Chapter 14, we prove that in the context of quantum error correction with infinite-dimensional Hilbert spaces, the equivalence of bulk and boundary relative entropies is a necessary and sufficient condition for entanglement wedge reconstruction.

Along the way, we show that the bulk and boundary modular operators act on the code subspace in the same way. For holographic theories with a well-defined entanglement wedge, this result provides a well-defined notion of holographic relative entropy. See Chapter 14 forthe proof and discussions.

In Chapter 15, we give an explicit construction of a quantum error correcting code where the code and physical Hilbert spaces are infinite dimensional. We define a type II_1 von Neumann algebra acting on the code Hilbert space and show how it is mapped to a von Neumann algebra of type II_1 acting on the physical Hilbert space. This toy model demonstrates the equivalence of entanglement wedge reconstruction and the exact equality of bulk and boundary relative entropies in infinite-dimensional Hilbert spaces. In particular, we first show that our QECC satisfies entanglement wedge reconstruction for a particular choice of von Neumann algebras acting on the code and physical Hilbert spaces, and then we invoke Theorem 1.1 in [185] to argue that our QECC also

satisfies the JLMS formula.

Furthermore, we show that relative entropies defined with respect to the infinite-dimensional von Neumann algebras we consider can be expressed as limits of relative entropies defined with respect to finite-dimensional subalgebras. Thus, another way to see that our QECC satisfies the JLMS formula is to note that our QECC satisfies the JLMS formula with respect to finite-dimensional von Neumann algebras. The JLMS formula for finite-dimensional algebras is studied in [159].

The technical assumptions that connect entanglement wedge reconstruction and the JLMS formula are presented in Theorem 3.0.1 in Chapter 14.

The infinite! No other question has ever moved so profoundly the spirit of man.

David Hilbert

14

Holographic Relative Entropy in Infinite-dimensional Hilbert Spaces

We reformulate entanglement wedge reconstruction in the language of operator-algebra quantum error correction with infinite-dimensional physical and code Hilbert spaces. Von Neumann algebras are used to characterize observables in a boundary subregion and its entanglement wedge. Assum-

ing that the infinite-dimensional von Neumann algebras associated with an entanglement wedge and its complement may both be reconstructed in their corresponding boundary subregions, we prove that the relative entropies measured with respect to the bulk and boundary observables are equal. We also prove the converse: when the relative entropies measured in an entanglement wedge and its complement equal the relative entropies measured in their respective boundary subregions, entanglement wedge reconstruction is possible. This is presented more precisely in Theorem 3.0.1.

14.1 The Main Theorem: Bulk Reconstruction and Relative Entropy

The following Theorem 3.0.1 provides in a setting of the infinite-dimensional Hilbert space that the two statements are equivalent: the bulk reconstruction and the equivalence of the relative entropy between the boundary and the bulk. We define cyclic and separating states in Definitions 3.5.1 and 3.5.2, and relative entropy in Definition 3.5.6.

Theorem 3.0.1. Let $u : \mathcal{H}_{code} \to \mathcal{H}_{phys}$ be an isometry[1] between two Hilbert spaces. Let M_{code} and M_{phys} be von Neumann algebras on $\mathcal{H}_{code}$ and $\mathcal{H}_{phys}$ respectively. Let M'_{code} and M'_{phys} respectively be the commutants of M_{code} and M_{phys}. Suppose that the set of cyclic and separating vectors with respect to M_{code} is dense in $\mathcal{H}_{code}$. Also suppose that if $|\Psi\rangle \in \mathcal{H}_{code}$ is cyclic and separating with respect to M_{code}, then $u|\Psi\rangle$ is cyclic and separating with respect to M_{phys}. Then the following two statements are equivalent:

[1] This means that u is a norm-preserving map. The map u need not be a bijection. In general, $u^\dagger u$ is the identity on $\mathcal{H}_{code}$ and $uu^\dagger$ is a projection on $\mathcal{H}_{phys}$.

1. Bulk reconstruction

$$\forall \mathcal{O} \in M_{code}\, \forall \mathcal{O}' \in M'_{code}, \quad \exists \tilde{\mathcal{O}} \in M_{phys}\, \exists \tilde{\mathcal{O}}' \in M'_{phys} \quad \text{such that}$$

$$\forall\, |\Theta\rangle \in \mathcal{H}_{code} \quad \begin{cases} u\mathcal{O}\,|\Theta\rangle = \tilde{\mathcal{O}} u\,|\Theta\rangle\,, & u\mathcal{O}'\,|\Theta\rangle = \tilde{\mathcal{O}}' u\,|\Theta\rangle\,, \\ u\mathcal{O}^\dagger\,|\Theta\rangle = \tilde{\mathcal{O}}^\dagger u\,|\Theta\rangle\,, & u\mathcal{O}'^\dagger\,|\Theta\rangle = \tilde{\mathcal{O}}'^\dagger u\,|\Theta\rangle\,. \end{cases}$$

2. Boundary relative entropy equals bulk relative entropy

For any $|\Psi\rangle, |\Phi\rangle \in \mathcal{H}_{code}$ with $|\Psi\rangle$ cyclic and separating with respect to M_{code},

$$\mathcal{S}_{\Psi|\Phi}(M_{code}) = \mathcal{S}_{u\Psi|u\Phi}(M_{phys}), \text{ and } \mathcal{S}_{\Psi|\Phi}(M'_{code}) = \mathcal{S}_{u\Psi|u\Phi}(M'_{phys}),$$

where $\mathcal{S}_{\Psi|\Phi}(M)$ is the relative entropy.

The proof of Theorem 3.0.1 requires two parts: statement 1 implies statement 2, and statement 2 implies statement 1 as well. Unlike the other direction, our proof that statement 1 implies statement 2 does not requite all of the assumptions of the theorem. We highlight this by presenting Theorem 14.1.1:

Theorem 14.1.1. *Let $u : \mathcal{H}_{code} \to \mathcal{H}_{phys}$ be an isometry between two Hilbert spaces. Let M_{code} and M_{phys} be von Neumann algebras on $\mathcal{H}_{code}$ and $\mathcal{H}_{phys}$ respectively. Let M'_{code} and M'_{phys} respectively be the commutants of M_{code} and M_{phys}.*

Suppose that

- *There exists some state $|\Omega\rangle \in \mathcal{H}_{code}$ such that $u\,|\Omega\rangle \in \mathcal{H}_{phys}$ is cyclic and separating with*

respect to M_{phys}.

- $\forall \mathcal{O} \in M_{code}\, \forall \mathcal{O}' \in M'_{code}, \quad \exists \tilde{\mathcal{O}} \in M_{phys}\, \exists \tilde{\mathcal{O}}' \in M'_{phys}$ *such that*

$$\forall\, |\Theta\rangle \in \mathcal{H}_{code} \quad \begin{cases} u\mathcal{O}\,|\Theta\rangle = \tilde{\mathcal{O}} u\,|\Theta\rangle\,, & u\mathcal{O}'\,|\Theta\rangle = \tilde{\mathcal{O}}' u\,|\Theta\rangle\,, \\ u\mathcal{O}^\dagger\,|\Theta\rangle = \tilde{\mathcal{O}}^\dagger u\,|\Theta\rangle\,, & u\mathcal{O}'^\dagger\,|\Theta\rangle = \tilde{\mathcal{O}}'^\dagger u\,|\Theta\rangle\,. \end{cases}$$

Then, for any $|\Psi\rangle, |\Phi\rangle \in \mathcal{H}_{code}$ *with* $|\Psi\rangle$ *cyclic and separating with respect to* M_{code},

- $u\,|\Psi\rangle$ *is cyclic and separating with respect to* M_{phys} *and* M'_{phys},

- $\mathcal{S}_{\Psi|\Phi}(M_{code}) = \mathcal{S}_{u\Psi|u\Phi}(M_{phys}), \quad \mathcal{S}_{\Psi|\Phi}(M'_{code}) = \mathcal{S}_{u\Psi|u\Phi}(M'_{phys}),$

where $\mathcal{S}_{\Psi|\Phi}(M)$ *is the relative entropy.*

Theorem 3.0.1, our main result, has a natural interpretation in the context of AdS/CFT. As the notation suggests, $\mathcal{H}_{code}$ may be interpreted as a code subspace of the physical Hilbert space $\mathcal{H}_{phys}$ that consists of states with semi-classical bulk duals. The von Neumann algebra M_{phys} denotes an algebra of boundary operators associated with a subregion on the boundary, and M_{code} denotes an algebra of bulk operators associated with the dual entanglement wedge. The commutant algebra M'_{phys} is associated with the complementary boundary subregion, and M'_{code} is associated with the complement of the entanglement wedge of M_{code}.

Theorem 3.0.1 provides a necessary and sufficient criterion for a subalgebra of bulk operators and its commutant to respectively be reconstructed in a subregion in the boundary and its complement.

We need [178] to argue that M_{code} and M'_{code} are associated with entanglement wedges. While Theorem 3.0.1 may not come as a surprise to readers familiar with [102, 159], we emphasize that studying the infinite-dimensional case can potentially yield new physical insights in AdS/CFT. As an example in quantum field theory, the Reeh–Schlieder Theorem [265] cannot be anticipated by studying a finite-dimensional spin-lattice model where the Hilbert space factorizes as $\mathcal{H} = \mathcal{H}_1 \otimes \mathcal{H}_2 \otimes \cdots \otimes \mathcal{H}_N$ where $\mathcal{H}_i$ denotes the finite-dimensional Hilbert space at each site.

While proving Theorem 14.1.1, we show in equation (14.35) that the modular operators associated with the bulk and boundary subregions act the same way on $\mathcal{H}_{code}$. Furthermore, while proving bulk reconstruction in Theorem 3.0.1, we explicitly show how to define a boundary operator that represents a given bulk operator on the code subspace. In Section 14.4, we discuss the implications of the Reeh–Schlieder Theorem for infinite- and finite-dimensional quantum error correction and make contact with the results of [159].

An outline of our proof of Theorem 14.1.1 is the following.

- We prove that for any $|\Psi\rangle \in \mathcal{H}_{code}$ which is cyclic and separating with respect to M_{code}, $u|\Psi\rangle$ is cyclic and separating with respect to M_{phys}.[2] If such is false, the relative entropy between $u|\Psi\rangle$ and $u|\Phi\rangle$ would not be possible to be defined, as the relative modular operator requires that $u|\Psi\rangle$ be cyclic and separating with respect to M_{phys}.

- Using the fact that M_{phys} and M'_{phys} are commutants of each other , we show that for any $\mathcal{P} \in M_{phys}$, $u^\dagger \mathcal{P} u \in M_{code}$.

[2] This is because we may act with an operator in M_{code} to send $|\Psi\rangle$ to a vector arbitrarily close to $|\Omega\rangle$, and we may act with an operator in M_{phys} to send $u|\Omega\rangle$ arbitrarily close to any vector in $\mathcal{H}_{phys}$.

- Let $S^c_{\Psi|\Phi}$ and $S^p_{u\Psi|u\Phi}$ denote relative Tomita operators defined with respect to M_{code} and M_{phys} respectively. We relate $S^c_{\Psi|\Phi}$ and $S^p_{u\Psi|u\Phi}$ and derive $uS^c_{\Psi|\Phi} = S^p_{u\Psi|u\Phi}u$ for generically unbounded operators. In particular, we show that their domains are equal and $S^p_{u\Psi|u\Phi}$ restricted to the vector space $(\text{Im } u)^\perp$ has a range contained within $(\text{Im } u)^\perp$.

- We derive a relation for the relative modular operators associated with $S^c_{\Psi|\Phi}$ and $S^p_{u\Psi|u\Phi}$.[3] This is related to the physical notion that bulk modular flow is dual to boundary modular flow. Likewise, we show that $\Delta^p_{u\Psi|u\Phi}$ restricted to the vector space $(\text{Im } u)^\perp$ has a range contained within $(\text{Im } u)^\perp$.

- Using the spectral theorem, we show that the spectral projections commute with the projector $uu^\dagger$.[4] We derive that the spectral projections of $\Delta^c_{\Psi|\Phi}$ are given by $u^\dagger P^p_\Omega u$, where P^p_Ω denotes the spectral projections of $\Delta^p_{u\Psi|u\Phi}$.[5]

- Any function of $\Delta^p_{u\Psi|u\Phi}$ or $\Delta^c_{\Psi|\Phi}$ can be constructed once the spectral projections are known. It follows that $\langle\Psi| \log \Delta^c_{\Psi|\Phi} |\Psi\rangle = \langle u\Psi| \log \Delta^p_{u\Psi|u\Phi} |u\Psi\rangle$, and thus the relative entropies are equal.

We note that Theorem 14.1.1 dictates that statement 1 of Theorem 3.0.1 implies statement 2 of Theorem 3.0.1. A sketch of our proof of the converse is the following. This completes the proof of Theorem 3.0.1.

[3] With the relation for the Tomita operators we derived above, we obtain a relation for the relative modular operators $\Delta^c_{\Psi|\Phi}$ and $\Delta^p_{u\Psi|u\Phi}$ to be $u\Delta^c_{\Psi|\Phi} = \Delta^p_{u\Psi|u\Phi}u$.

[4] We apply the spectral theorem separately for the restriction of $\Delta^p_{u\Psi|u\Phi}$ to Im u and $(\text{Im } u)^\perp$.

[5] We use the relation $\Delta^c_{\Psi|\Phi} = u^\dagger \Delta^p_{u\Psi|u\Phi} u$. For the projections, Ω denotes a measurable subset of $\mathbb{R}$

- For any $|\Phi\rangle \in \mathcal{H}_{code}$ that is cyclic and separating with respect to M_{code}, and for any unitary $U' \in M'_{code}$, the properties of relative entropy and the assumptions of the theorem imply that $0 = \mathcal{S}_{\Phi|U'\Phi}(M_{code}) = \mathcal{S}_{u\Phi|uU'\Phi}(M_{phys})$.

- Following the logic of [307], one may show that $\langle uU'\Phi|\mathcal{P}uU'\Phi\rangle = \langle u\Phi|\mathcal{P}|u\Phi\rangle$ for all $\mathcal{P} \in M_{phys}$. Using the assumption that cyclic and separating states with respect to M_{code} are dense in $\mathcal{H}_{code}$, it follows that $u^\dagger \mathcal{P} u U' = U' u^\dagger \mathcal{P} u$. The same logic also implies that for $\mathcal{P}' \in M'_{phys}$ and any unitary $U \in M_{code}$, $u^\dagger \mathcal{P}' u U = U u^\dagger \mathcal{P}' u$.

- We define a linear map $X'^{\Phi\, U'} : \mathcal{H}_{phys} \to \mathcal{H}_{phys}$ by $X'^{\Phi\, U'} \mathcal{P} u\, |\Phi\rangle := \mathcal{P} u U' |\Phi\rangle \quad \forall \mathcal{P} \in M_{phys}$, and we show that $X'^{\Phi\, U'}$ is unitary and that $X'^{\Phi\, U'} \in M'_{phys}$.

- Since $u^\dagger X'^{\Phi\, U'} u U = U u^\dagger X'^{\Phi\, U'} u$ and any operator in M_{code} may be written as a linear combination of four unitary operators in M_{code}, we show that $u^\dagger X'^{\Phi\, U'} u = U'$. We also show that $X'^{\Phi\, U'}$ maps the vector space $\text{Im}\, u \to \text{Im}\, u$. Hence, $X'^{\Phi\, U'} u = u U'$

- Using similar methods, we then show that $(X'^{\Phi\, U'})^\dagger u = u (U')^\dagger$. Thus, the unitary operator $U' \in M_{code}$ may be reconstructed as $X'^{\Phi\, U'}$ for some choice of $|\Phi\rangle \in \mathcal{H}_{code}$ that is cyclic and separating with respect to M_{code}.

- Since any operator in M_{code} may be written as a linear combination of four unitary operators in M_{code}, we have a way to represent any operator in M_{code} as an operator in M_{phys}. The same logic applies to show that any operator in M'_{code} may be represented as an operator in M'_{phys}.

The rest of this chapter is summarized as follows. In Section 2, we define von Neumann algebras

and functions of operators, and we review the spectral theorem (for unbounded operators). In Section 3, we review the relative modular operator from Tomita-Takesaki theory, and define the relative entropy. In Section 4, we prove that when the bulk reconstruction is satisfied, the relative entropy is equivalent between the boundary and the bulk (Theorem 14.1.1). In Section 14.3, we prove the converse, completing the proof of Theorem 3.0.1. In Section 14.4, we physically interpret Theorem 3.0.1 and relate our work to previous work on finite-dimensional quantum error correction and holography.

14.2 Proof of Theorem 14.1.1

This section contains the proof of Theorem 14.1.1. In Lemma 14.2.1, we show that cyclic and separating states in $\mathcal{H}_{code}$ are mapped to cyclic and separating states in $\mathcal{H}_{phys}$. In Lemma 14.2.2, we relate operators in M_{phys} to operators in M_{code}. In Section 14.2.1, we consider Theorem 14.1.1 in a special case where the relative Tomita operators are bounded. In Section 14.2.2, we prove Theorem 14.1.1 in full generality.

Lemma 14.2.1. *Under the assumptions of Theorem 14.1.1, for every $|\Psi\rangle \in \mathcal{H}_{code}$ that is cyclic and separating with respect to M_{code}, $u|\Psi\rangle$ is cyclic and separating with respect to M_{phys}.*

Proof. Let $|\Omega\rangle$ be defined as in Theorem 14.1.1. We will first show that $u|\Psi\rangle$ is cyclic with respect to M_{phys}. That is, we can act on $u|\Psi\rangle$ with an operator in M_{phys} to get a state arbitrarily close to any state in $\mathcal{H}_{phys}$. Given any $|\Phi\rangle \in \mathcal{H}_{phys}$ and $\varepsilon > 0$, we need to choose $\mathcal{P} \in M_{phys}$ such that $|| \, |\Phi\rangle - \mathcal{P}u|\Psi\rangle \, || < \varepsilon$. Choose $\hat{\mathcal{P}} \in M_{phys}$ such that $||\hat{\mathcal{P}}u|\Omega\rangle - |\Phi\rangle \, || < \frac{\varepsilon}{2}$ and $\hat{\mathcal{P}} \neq 0$. Since

$|\Psi\rangle$ is cyclic with respect to M_{code}, choose $\mathcal{O} \in M_{code}$ such that $||\mathcal{O}|\Psi\rangle - |\Omega\rangle|| < \frac{\varepsilon}{2||\hat{\mathcal{P}}||}$. Let $\tilde{\mathcal{O}} \in M_{phys}$ be an operator that satisfies $\tilde{\mathcal{O}}u|\Theta\rangle = u\mathcal{O}|\Theta\rangle \, \forall \, |\Theta\rangle \in \mathcal{H}_{code}$. Then, note that

$$|\Phi\rangle - \hat{\mathcal{P}}\tilde{\mathcal{O}}u|\Psi\rangle = |\Phi\rangle - \hat{\mathcal{P}}u\mathcal{O}|\Psi\rangle = |\Phi\rangle - \hat{\mathcal{P}}u|\Omega\rangle - \hat{\mathcal{P}}u(\mathcal{O}|\Psi\rangle - |\Omega\rangle). \tag{14.1}$$

By the triangle inequality,

$$||\,|\Phi\rangle - \hat{\mathcal{P}}\tilde{\mathcal{O}}u|\Psi\rangle\,|| \leq ||\,|\Phi\rangle - \hat{\mathcal{P}}u|\Omega\rangle\,|| + ||\hat{\mathcal{P}}|| \cdot ||\mathcal{O}|\Psi\rangle - |\Omega\rangle||. \tag{14.2}$$

By choosing $\mathcal{P} = \hat{\mathcal{P}}\tilde{\mathcal{O}}$, we see that $u|\Psi\rangle$ is cyclic with respect to M_{phys}. The same logic shows that $u|\Psi\rangle$ is cyclic with respect to M'_{phys} and hence separating for M_{phys}. □

Lemma 14.2.2. *Under the assumptions of Theorem 14.1.1, for any $\mathcal{P} \in M_{phys}$, $u^\dagger \mathcal{P} u \in M_{code}$.*

Proof. Choose any $\mathcal{O}' \in M'_{code}$. For any $|\Psi\rangle, |\Phi\rangle \in \mathcal{H}_{code}$, we have that

$$\begin{aligned}\langle\Psi|u^\dagger\mathcal{P}u\mathcal{O}'|\Phi\rangle = \langle\Psi|u^\dagger\mathcal{P}\tilde{\mathcal{O}}'u|\Phi\rangle = \langle\Psi|u^\dagger\tilde{\mathcal{O}}'\mathcal{P}u|\Phi\rangle = \langle\tilde{\mathcal{O}}'^\dagger u\Psi|\mathcal{P}u|\Phi\rangle \\ = \langle u\mathcal{O}'^\dagger\Psi|\mathcal{P}u|\Phi\rangle = \langle\Psi|\mathcal{O}'u^\dagger\mathcal{P}u|\Phi\rangle\,.\end{aligned} \tag{14.3}$$

Hence, $u^\dagger\mathcal{P}u \in M''_{code} = M_{code}$. □

14.2.1 Special case of bounded relative Tomita operator

We will first prove Theorem 14.1.1 in the special case where the relative Tomita operators with respect to M_{code} and M_{phys}, denoted respectively by $S^c_{\Psi|\Phi}$ and $S^p_{\Psi|\Phi}$, are bounded operators. In this special

case, we do not have to keep track of their domains. The proof of the general case is similar, but technically more complicated.

For any $\mathcal{O} \in M_{code}$,

$$uS^{c}_{\Psi|\Phi}\mathcal{O}\left|\Psi\right\rangle = u\mathcal{O}^{\dagger}\left|\Phi\right\rangle = \tilde{\mathcal{O}}^{\dagger}u\left|\Phi\right\rangle = S^{p}_{u\Psi|u\Phi}\tilde{\mathcal{O}}u\left|\Psi\right\rangle = S^{p}_{u\Psi|u\Phi}u\mathcal{O}\left|\Psi\right\rangle, \tag{14.4}$$

Hence

$$\left(uS^{c}_{\Psi|\Phi} - S^{p}_{u\Psi|u\Phi}u\right)\mathcal{O}\left|\Psi\right\rangle = 0. \tag{14.5}$$

$\left(uS^{c}_{\Psi|\Phi} - S^{p}_{u\Psi|u\Phi}u\right)$ is a bounded operator that annihilates a dense subspace of $\mathcal{H}_{code}$, since $\left|\Psi\right\rangle$ is cyclic with respect to M_{code}. It follows from the fact that the kernel of $\left(uS^{c}_{\Psi|\Phi} - S^{p}_{u\Psi|u\Phi}u\right)$ is closed that

$$uS^{c}_{\Psi|\Phi} = S^{p}_{u\Psi|u\Phi}u. \tag{14.6}$$

Likewise, for any $\mathcal{P} \in M_{phys}$,

$$u^{\dagger}S^{p}_{u\Psi|u\Phi}\mathcal{P}\left|u\Psi\right\rangle = u^{\dagger}\mathcal{P}^{\dagger}u\left|\Phi\right\rangle = S^{c}_{\Psi|\Phi}u^{\dagger}\mathcal{P}\left|u\Psi\right\rangle, \tag{14.7}$$

$$\left(u^{\dagger}S^{p}_{u\Psi|u\Phi} - S^{c}_{\Psi|\Phi}u^{\dagger}\right)\mathcal{P}\left|u\Psi\right\rangle = 0. \tag{14.8}$$

As $u\left|\Psi\right\rangle$ is cyclic with respect to M_{phys} by assumption, we have that

$$u^{\dagger}S^{p}_{u\Psi|u\Phi} = S^{c}_{\Psi|\Phi}u^{\dagger}, \quad S^{p\,\dagger}_{u\Psi|u\Phi}u = uS^{c\,\dagger}_{\Psi|\Phi}. \tag{14.9}$$

Equations (14.6) and (14.9) imply that the subspace Im u is mapped to itself under $S^p_{u\Psi|u\Phi}$ and ${S^p_{u\Psi|u\Phi}}^\dagger$. Thus, the subspace Im u is mapped to itself under $\Delta^p_{u\Psi|u\Phi}$. From the fact that $\Delta^p_{u\Psi|u\Phi}$ is self-adjoint and bounded, it follows that the subspace $(\text{Im } u)^\perp$ is mapped to itself under $\Delta^p_{u\Psi|u\Phi}$. Equations (14.6) and (14.9) also imply that

$$\Delta^c_{\Psi|\Phi} = u^\dagger \Delta^p_{u\Psi|u\Phi} u. \tag{14.10}$$

Note that $\Delta^p_{u\Psi|u\Phi}$ and $\Delta^c_{\Psi|\Phi}$ are positive, self-adjoint, bounded operators. Thus, we may use the spectral theorem to study them. We will apply the spectral theorem to $(\Delta^p_{u\Psi|u\Phi})|_{\text{Im } u}$ and $(\Delta^p_{u\Psi|u\Phi})|_{(\text{Im } u)^\perp}$ separately.[6] We write

$$(\Delta^p_{u\Psi|u\Phi})|_{\text{Im } u} = \int_{\mathbb{R}} \lambda \, d(P_\lambda^{\text{Im } u}), \; (\Delta^p_{u\Psi|u\Phi})|_{(\text{Im } u)^\perp} = \int_{\mathbb{R}} \lambda \, d(P_\lambda^{(\text{Im } u)^\perp}). \tag{14.11}$$

For a Borel set $\Omega \subset \mathbb{R}$, the projections $P_\Omega^{\text{Im } u}$ and $P_\Omega^{(\text{Im } u)^\perp}$ commute with $uu^\dagger$ because $uu^\dagger$ is the projection onto Im u. The spectral decomposition of $\Delta^p_{u\Psi|u\Phi}$ is given by

$$\Delta^p_{u\Psi|u\Phi} = \int_{\mathbb{R}} \lambda \, d(P^p_\lambda). \tag{14.12}$$

By the uniqueness of the spectral decomposition, we have that $P^p_\Omega = P_\Omega^{\text{Im } u} + P_\Omega^{(\text{Im } u)^\perp}$. Thus, P^p_Ω

[6] $(\Delta^p_{u\Psi|u\Phi})|_{\text{Im } u}$ denotes the restriction of $\Delta^p_{u\Psi|u\Phi}$ to the closed subspace Im u.

commutes with $uu^\dagger$. Let Ω_1 and Ω_2 be two Borel sets. Then

$$u^\dagger P^p_{\Omega_1} u u^\dagger P^p_{\Omega_2} u = u^\dagger P^p_{\Omega_1} P^p_{\Omega_2} u. \tag{14.13}$$

One can then check that the family of projections $u^\dagger P^p_\Omega u = u^\dagger P^{\mathrm{Im}\, u}_\Omega u$ is a projection valued measure on $\mathcal{H}_{code}$. We will now show that this is the projection valued measure associated with $\Delta^c_{\Upsilon|\Phi}$. From equation (14.10), it follows that for any $|\Theta\rangle \in \mathcal{H}_{code}$, we have that

$$\Delta^c_{\Upsilon|\Phi}\,|\Theta\rangle = u^\dagger \Delta^p_{u\Upsilon|u\Phi} u\,|\Theta\rangle = \int_{\mathbb{R}} \lambda\, d(u^\dagger P^p_\lambda u\,|\Theta\rangle). \tag{14.14}$$

By the uniqueness of the spectral decomposition of $\Delta^c_{\Upsilon|\Phi}$, we conclude that $u^\dagger P^p_\Omega u$ is the projection valued measure associated with $\Delta^c_{\Upsilon|\Phi}$. It follows that

$$\begin{aligned} -\langle\Upsilon|\log(\Delta^c_{\Upsilon|\Phi})|\Upsilon\rangle &= -\int_0^\infty \log(\lambda)\, d(\langle\Upsilon|u^\dagger P^p_\lambda u|\Upsilon\rangle) \\ &= -\int_0^\infty \log(\lambda)\, d(\langle u\Upsilon|P^p_\lambda|u\Upsilon\rangle) = -\langle u\Upsilon|\log(\Delta^p_{u\Upsilon|u\Phi})|u\Upsilon\rangle\,. \end{aligned} \tag{14.15}$$

The same logic can be applied to the commutant algebras $\mathcal{M}'_{code}$ and $\mathcal{M}'_{phys}$. Hence,

$$\mathcal{S}_{\Upsilon|\Phi}(\mathcal{M}_{code}) = \mathcal{S}_{u\Upsilon|u\Phi}(\mathcal{M}_{phys}), \quad \mathcal{S}_{\Upsilon|\Phi}(\mathcal{M}'_{code}) = \mathcal{S}_{u\Upsilon|u\Phi}(\mathcal{M}'_{phys}). \tag{14.16}$$

14.2.2 General proof of Theorem 14.1.1

Lemma 14.2.3. *Let $S^{c}_{\Psi|\Phi}$ denote the relative Tomita operator defined with respect to M_{code}. Let $S^{p}_{u\Psi|u\Phi}$ denote the relative Tomita operator defined with respect to M_{phys}. Let $S^{c\,\prime}_{\Psi|\Phi}$ and $S^{p\,\prime}_{u\Psi|u\Phi}$ denote the relative Tomita operators defined with respect to M'_{code} and M'_{phys}. Then $uS^{c}_{\Psi|\Phi} = S^{p}_{u\Psi|u\Phi}u$ and $uS^{c\,\prime}_{\Psi|\Phi} = S^{p\,\prime}_{u\Psi|u\Phi}u$.*

Proof. $D(S^{c}_{\Psi|\Phi})$ is given by all $|x\rangle \in \mathcal{H}_{code}$ that may be written as

$$|x\rangle = \lim_{n\to\infty} \mathcal{O}_n |\Psi\rangle \tag{14.17}$$

for some sequence $\{\mathcal{O}_n\} \in \mathcal{M}_{code}$ such that the limit

$$|y\rangle := \lim_{n\to\infty} \mathcal{O}_n^{\dagger} |\Phi\rangle \tag{14.18}$$

exists. By definition, $S^{c}_{\Psi|\Phi} |x\rangle := |y\rangle$. Given $|x\rangle$ and $|y\rangle$ defined as above, it follows that

$$u|x\rangle = \lim_{n\to\infty} \tilde{\mathcal{O}}_n u |\Psi\rangle\,, \quad u|y\rangle = \lim_{n\to\infty} \tilde{\mathcal{O}}_n^{\dagger} u |\Phi\rangle\,. \tag{14.19}$$

Hence, $u|x\rangle \in D(S^{p}_{u\Psi|u\Phi})$. It follows that for all $|x\rangle \in D(S^{c}_{\Psi|\Phi})$,

$$uS^{c}_{\Psi|\Phi} |x\rangle = S^{p}_{u\Psi|u\Phi} u |x\rangle\,,$$

which means that $S^{p}_{u\Psi|u\Phi}u$ is an extension of $uS^{c}_{\Psi|\Phi}$. To see that $S^{p}_{u\Psi|u\Phi}u$ is not a proper extension, suppose $|w\rangle \in D(S^{p}_{u\Psi|u\Phi}u)$. Then $u\,|w\rangle \in D(S^{p}_{u\Psi|u\Phi})$, meaning that there exists a sequence $\{\mathcal{P}_n\} \in \mathcal{M}_{phys}$ such that

$$u\,|w\rangle = \lim_{n\to\infty} \mathcal{P}_n u\,|\Psi\rangle\,, \text{ and } \lim_{n\to\infty} \mathcal{P}_n^{\dagger} u\,|\Psi\rangle \text{ exists.} \tag{14.20}$$

We may also write $|w\rangle = \lim_{n\to\infty} u^{\dagger}\mathcal{P}_n u\,|\Psi\rangle$. From Lemma 14.2.2, $u^{\dagger}\mathcal{P}_n u \in \mathcal{M}_{code}$. Hence, $|w\rangle \in D(S^{c}_{\Psi|\Phi})$; so we may write $uS^{c}_{\Psi|\Phi} = S^{p}_{u\Psi|u\Phi}u$ as an operator equality because the operators on both sides have the same domain and act the same way on vectors in the domain. The same logic establishes that $uS^{c\prime}_{\Psi|\Phi} = S^{p\prime}_{u\Psi|u\Phi}u$. □

Lemma 14.2.4. *Let* $\Delta^{p}_{u\Psi|u\Phi} := S^{p\,\dagger}_{u\Psi|u\Phi}S^{p}_{u\Psi|u\Phi}$ *be the relative modular operator associated with* $S^{p}_{u\Psi|u\Phi}$. *Then,*

- $\Delta^{p}_{u\Psi|u\Phi}$ *maps the vector space* $(Im\,u) \cap D(\Delta^{p}_{u\Psi|u\Phi})$ *into* $(Im\,u)$, *and* $(\Delta^{p}_{u\Psi|u\Phi})|_{(Im\,u)}$ *is densely defined on* $(Im\,u)$.
- $\Delta^{p}_{u\Psi|u\Phi}$ *maps the vector space* $(Im\,u)^{\perp} \cap D(\Delta^{p}_{u\Psi|u\Phi})$ *into* $(Im\,u)^{\perp}$, *and* $(\Delta^{p}_{u\Psi|u\Phi})|_{(Im\,u)^{\perp}}$ *is densely defined on* $(Im\,u)^{\perp}$.

Proof. Let $|x\rangle \in D(S^{p}_{u\Psi|u\Phi})$. Then there exists a sequence $\{\mathcal{P}_n\} \in \mathcal{M}_{phys}$ such that

$$|x\rangle = \lim_{n\to\infty} \mathcal{P}_n\,|u\Psi\rangle\,, \text{ and } \lim_{n\to\infty} \mathcal{P}_n^{\dagger}\,|u\Phi\rangle \text{ exists.} \tag{14.21}$$

Then $u^\dagger |x\rangle \in D(S^c_{\Psi|\Phi})$. We may write

$$S^c_{\Psi|\Phi} u^\dagger |x\rangle = u^\dagger S^p_{u\Psi|u\Phi} |x\rangle . \tag{14.22}$$

The fact that $u^\dagger |x\rangle \in D(S^c_{\Psi|\Phi})$ and Lemma 14.2.3 together imply that $uu^\dagger |x\rangle \in D(S^p_{u\Psi|u\Phi})$.

We may uniquely decompose $|x\rangle$ into the sum

$$|x\rangle = |a\rangle + |b\rangle \tag{14.23}$$

where $|a\rangle \in \operatorname{Im} u$ and $|b\rangle \in (\operatorname{Im} u)^\perp$. We know that $|a\rangle = uu^\dagger |x\rangle \in D(S^p_{u\Psi|u\Phi})$. As $D(S^p_{u\Psi|u\Phi})$ is a vector space, this implies that $|b\rangle \in D(S^p_{u\Psi|u\Phi})$.

It follows from the above that

$$D(S^p_{u\Psi|u\Phi}) = \operatorname{Im} u \cap D(S^p_{u\Psi|u\Phi}) \oplus (\operatorname{Im} u)^\perp \cap D(S^p_{u\Psi|u\Phi}). \tag{14.24}$$

From equation (14.22),

$$uu^\dagger S^p_{u\Psi|u\Phi} |b\rangle = 0, \tag{14.25}$$

which means that $S^p_{u\Psi|u\Phi}$ maps the vector space $(\operatorname{Im} u)^\perp \cap D(S^p_{u\Psi|u\Phi}) \to (\operatorname{Im} u)^\perp$.

From Lemma 14.2.3 we may write, for all $|x\rangle \in D(S^p_{u\Psi|u\Phi})$,

$$uS^c_{\Psi|\Phi} u^\dagger |x\rangle = S^p_{u\Psi|u\Phi} uu^\dagger |x\rangle . \tag{14.26}$$

It follows from $uu^\dagger |x\rangle = |a\rangle$ that

$$uS^{c}_{\Psi|\Phi}u^\dagger |x\rangle = S^{p}_{u\Psi|u\Phi} |a\rangle . \tag{14.27}$$

It follows from $u^\dagger |b\rangle = 0$ that

$$uS^{c}_{\Psi|\Phi}u^\dagger |a\rangle = S^{p}_{u\Psi|u\Phi} |a\rangle , \tag{14.28}$$

which means that $S^{p}_{u\Psi|u\Phi}$ maps the vector space $(\text{Im } u) \cap D(S^{p}_{u\Psi|u\Phi}) \to (\text{Im } u)$.

We will now show that $(\text{Im } u) \cap D(S^{p}_{u\Psi|u\Phi})$ is dense in $(\text{Im } u)$. Given any $|A\rangle \in (\text{Im } u)$, choose $|X\rangle \in \mathcal{H}_{phys}$ such that $uu^\dagger |X\rangle = |A\rangle$. Next, choose a sequence $\{|x_n\rangle\} \in D(S^{p}_{u\Psi|u\Phi})$ that converges to $|X\rangle$. We then have that $\lim_{n\to\infty} uu^\dagger |x_n\rangle = |A\rangle$. Since $|x_n\rangle \in D(S^{p}_{u\Psi|u\Phi})$, we know from earlier that $uu^\dagger |x_n\rangle \in D(S^{p}_{u\Psi|u\Phi})$. Hence, $(\text{Im } u) \cap D(S^{p}_{u\Psi|u\Phi})$ is dense in $(\text{Im } u)$. The same logic shows that $(\text{Im } u)^\perp \cap D(S^{p}_{u\Psi|u\Phi})$ is dense in $(\text{Im } u)^\perp$.

Furthermore, $(S^{p}_{u\Psi|u\Phi})|_{(\text{Im } u)}$ is a closed operator because $(\text{Im } u)$ is a closed subspace.

We can apply all of the above logic to the commutant algebras. To summarize,

- $S^{p}_{u\Psi|u\Phi}$ maps the vector space $(\text{Im } u)^\perp \cap D(S^{p}_{u\Psi|u\Phi}) \to (\text{Im } u)^\perp$, and $(S^{p}_{u\Psi|u\Phi})|_{(\text{Im } u)^\perp}$ is closed and densely defined on $(\text{Im } u)^\perp$.

- $S^{p}_{u\Psi|u\Phi}$ maps the vector space $(\text{Im } u) \cap D(S^{p}_{u\Psi|u\Phi}) \to (\text{Im } u)$, and $(S^{p}_{u\Psi|u\Phi})|_{(\text{Im } u)}$ is closed and densely defined on $(\text{Im } u)$.

- $S^{p\prime}_{u\Psi|u\Phi}$ maps the vector space $(\text{Im } u)^\perp \cap D(S^{p\prime}_{u\Psi|u\Phi}) \to (\text{Im } u)^\perp$, and $(S^{p\prime}_{u\Psi|u\Phi})|_{(\text{Im } u)^\perp}$ is

closed and densely defined on $(\mathrm{Im}\, u)^\perp$.

- $S^{p\prime}_{u\Psi|u\Phi}$ maps the vector space $(\mathrm{Im}\, u) \cap D(S^{p\prime}_{u\Psi|u\Phi}) \to (\mathrm{Im}\, u)$, and $(S^{p\prime}_{u\Psi|u\Phi})|_{(\mathrm{Im}\, u)}$ is closed and densely defined on $(\mathrm{Im}\, u)$.

It directly follows that the above statements also hold for the adjoints $S^{p\,\dagger}_{u\Psi|u\Phi}$ and $S^{p\prime\,\dagger}_{u\Psi|u\Phi}$. Recall that $\Delta^p_{u\Psi|u\Phi} = S^{p\,\dagger}_{u\Psi|u\Phi} S^p_{u\Psi|u\Phi}$. We may compute $(\Delta^p_{u\Psi|u\Phi})|_{(\mathrm{Im}\, u)}$ from $(S^p_{u\Psi|u\Phi})|_{(\mathrm{Im}\, u)}$ and $(\Delta^p_{u\Psi|u\Phi})|_{(\mathrm{Im}\, u)^\perp}$ from $(S^p_{u\Psi|u\Phi})|_{(\mathrm{Im}\, u)^\perp}$. In particular, $(\Delta^p_{u\Psi|u\Phi})|_{(\mathrm{Im}\, u)}$ is given by

$$(\Delta^p_{u\Psi|u\Phi})|_{(\mathrm{Im}\, u)} = (S^{p\,\dagger}_{u\Psi|u\Phi}|_{(\mathrm{Im}\, u)})(S^p_{u\Psi|u\Phi}|_{(\mathrm{Im}\, u)}) = (S^p_{u\Psi|u\Phi}|_{(\mathrm{Im}\, u)})^\dagger (S^p_{u\Psi|u\Phi}|_{(\mathrm{Im}\, u)}). \tag{14.29}$$

It follows that $(\Delta^p_{u\Psi|u\Phi})|_{(\mathrm{Im}\, u)}$ is densely defined and self-adjoint on $(\mathrm{Im}\, u)$. The same logic can be applied to $(\Delta^p_{u\Psi|u\Phi})|_{(\mathrm{Im}\, u)^\perp}$. □

Having established Lemmas 14.2.1 to 14.2.4, we can now prove Theorem 14.1.1, which shows that entanglement wedge reconstruction implies the equivalence of bulk and boundary relative entropies.

Theorem 14.1.1. Let $u : \mathcal{H}_{code} \to \mathcal{H}_{phys}$ be an isometry between two Hilbert spaces. Let M_{code} and M_{phys} be von Neumann algebras on $\mathcal{H}_{code}$ and $\mathcal{H}_{phys}$ respectively. Let M'_{code} and M'_{phys} respectively be the commutants of M_{code} and M_{phys}.

Suppose that

- There exists some state $|\Omega\rangle \in \mathcal{H}_{code}$ such that $u|\Omega\rangle \in \mathcal{H}_{phys}$ is cyclic and separating with respect to M_{phys}.

- $\forall \mathcal{O} \in M_{code}\, \forall \mathcal{O}' \in M'_{code}, \quad \exists \tilde{\mathcal{O}} \in M_{phys}\, \exists \tilde{\mathcal{O}}' \in M'_{phys}$ such that

$$\forall\, |\Theta\rangle \in \mathcal{H}_{code} \quad \begin{cases} u\mathcal{O}\,|\Theta\rangle = \tilde{\mathcal{O}} u\,|\Theta\rangle\,, & u\mathcal{O}'\,|\Theta\rangle = \tilde{\mathcal{O}}' u\,|\Theta\rangle\,, \\ u\mathcal{O}^\dagger\,|\Theta\rangle = \tilde{\mathcal{O}}^\dagger u\,|\Theta\rangle\,, & u\mathcal{O}'^\dagger\,|\Theta\rangle = \tilde{\mathcal{O}}'^\dagger u\,|\Theta\rangle\,. \end{cases}$$

Then, for any $|\Psi\rangle, |\Phi\rangle \in \mathcal{H}_{code}$ with $|\Psi\rangle$ cyclic and separating with respect to M_{code},

- $u\,|\Psi\rangle$ is cyclic and separating with respect to M_{phys} and M'_{phys},

- $\mathcal{S}_{\Psi|\Phi}(M_{code}) = \mathcal{S}_{u\Psi|u\Phi}(M_{phys}), \quad \mathcal{S}_{\Psi|\Phi}(M'_{code}) = \mathcal{S}_{u\Psi|u\Phi}(M'_{phys}),$

where $\mathcal{S}_{\Psi|\Phi}(M)$ is the relative entropy.

Proof. $\Delta^p_{u\Psi|u\Phi}$ and $\Delta^c_{\Psi|\Phi}$ are positive, densely defined, self-adjoint operators that are generically unbounded. Thus, we may use the spectral theorem to study them. We will apply the spectral theorem to $(\Delta^p_{u\Psi|u\Phi})|_{\mathrm{Im}\, u}$ and $(\Delta^p_{u\Psi|u\Phi})|_{(\mathrm{Im}\, u)^\perp}$ separately. We write

$$(\Delta^p_{u\Psi|u\Phi})|_{\mathrm{Im}\, u} = \int_{\mathbb{R}} \lambda\, d(P^{\mathrm{Im}\, u}_\lambda),\ (\Delta^p_{u\Psi|u\Phi})|_{(\mathrm{Im}\, u)^\perp} = \int_{\mathbb{R}} \lambda\, d(P^{(\mathrm{Im}\, u)^\perp}_\lambda). \tag{14.30}$$

For a Borel set $\Omega \subset \mathbb{R}$, the projections $P^{\mathrm{Im}\, u}_\Omega$ and $P^{(\mathrm{Im}\, u)^\perp}_\Omega$ commute with $uu^\dagger$ because $uu^\dagger$ is the projection onto Im u. The spectral decomposition of $\Delta^p_{u\Psi|u\Phi}$ is given by

$$\Delta^p_{u\Psi|u\Phi} = \int_{\mathbb{R}} \lambda\, d(P^p_\lambda). \tag{14.31}$$

By the uniqueness of the spectral decomposition, we have that $P^p_\Omega = P^{\mathrm{Im}\, u}_\Omega + P^{(\mathrm{Im}\, u)^\perp}_\Omega$. Thus, P^p_Ω

commutes with $uu^\dagger$. Let Ω_1 and Ω_2 be two Borel sets. Then

$$u^\dagger P^p_{\Omega_1} u u^\dagger P^p_{\Omega_2} u = u^\dagger P^p_{\Omega_1} P^p_{\Omega_2} u. \tag{14.32}$$

One can then check that the family of projections $u^\dagger P^p_\Omega u = u^\dagger P^{\mathrm{Im}\, u}_\Omega u$ is a projection valued measure on $\mathcal{H}_{code}$. We will now show that this is the projection valued measure associated with $\Delta^c_{\Psi|\Phi}$. From Lemma 14.2.3 we have that

$$u S^c_{\Psi|\Phi} u^\dagger = S^p_{u\Psi|u\Phi} u u^\dagger = (S^p_{u\Psi|u\Phi})|_{(\mathrm{Im}\, u)}. \tag{14.33}$$

We may take the adjoint of the above equation to obtain

$$u S^{c\,\dagger}_{\Psi|\Phi} u^\dagger = (S^{p\,\dagger}_{u\Psi|u\Phi})|_{(\mathrm{Im}\, u)}, \tag{14.34}$$

from which it follows that

$$u \Delta^c_{\Psi|\Phi} u^\dagger = (\Delta^p_{u\Psi|u\Phi})|_{(\mathrm{Im}\, u)}, \quad \Delta^c_{\Psi|\Phi} = u^\dagger \Delta^p_{u\Psi|u\Phi} u. \tag{14.35}$$

For any $|\Theta\rangle \in D(\Delta^c_{\Psi|\Phi})$, we have that

$$\Delta^c_{\Psi|\Phi} |\Theta\rangle = u^\dagger \Delta^p_{u\Psi|u\Phi} u |\Theta\rangle = \int_{\mathbb{R}} \lambda \, d(u^\dagger P^p_\lambda u |\Theta\rangle). \tag{14.36}$$

By the uniqueness of the spectral decomposition of $\Delta^{c}_{\Psi|\Phi}$, we conclude that $u^\dagger P^{p}_{\Omega} u$ is the projection valued measure associated with $\Delta^{c}_{\Psi|\Phi}$.

It follows that

$$\begin{aligned} -\langle\Psi|\log(\Delta^{c}_{\Psi|\Phi})|\Psi\rangle &= -\int_{0}^{\infty}\log(\lambda)\, d(\langle\Psi|u^\dagger P^{p}_{\lambda} u|\Psi\rangle) \\ &= -\int_{0}^{\infty}\log(\lambda)\, d(\langle u\Psi|P^{p}_{\lambda}|u\Psi\rangle) = -\langle u\Psi|\log(\Delta^{p}_{u\Psi|u\Phi})|u\Psi\rangle\,. \end{aligned} \tag{14.37}$$

The same logic can be applied to the commutant algebras M'_{code} and M'_{phys}. Hence,

$$\mathcal{S}_{\Psi|\Phi}(M_{code}) = \mathcal{S}_{u\Psi|u\Phi}(M_{phys}), \quad \mathcal{S}_{\Psi|\Phi}(M'_{code}) = \mathcal{S}_{u\Psi|u\Phi}(M'_{phys}). \tag{14.38}$$

□

14.3 Proof of Theorem 3.0.1

Theorem 3.0.1. Let $u : \mathcal{H}_{code} \to \mathcal{H}_{phys}$ be an isometry between two Hilbert spaces. Let M_{code} and M_{phys} be von Neumann algebras on $\mathcal{H}_{code}$ and $\mathcal{H}_{phys}$ respectively. Let M'_{code} and M'_{phys} respectively be the commutants of M_{code} and M_{phys}. Suppose that the set of cyclic and separating vectors with respect to M_{code} is dense in $\mathcal{H}_{code}$. Also suppose that if $|\Psi\rangle \in \mathcal{H}_{code}$ is cyclic and separating with respect to M_{code}, then $u|\Psi\rangle$ is cyclic and separating with respect to M_{phys}. Then the following two statements are equivalent:

1. Bulk reconstruction $\forall \mathcal{O} \in M_{code}\, \forall \mathcal{O}' \in M'_{code}, \quad \exists \tilde{\mathcal{O}} \in M_{phys}\, \exists \tilde{\mathcal{O}}' \in M'_{phys}$ such that

$$\forall\, |\Theta\rangle \in \mathcal{H}_{code} \quad \begin{cases} u\mathcal{O}\,|\Theta\rangle = \tilde{\mathcal{O}} u\,|\Theta\rangle\,, & u\mathcal{O}'\,|\Theta\rangle = \tilde{\mathcal{O}}' u\,|\Theta\rangle\,, \\ u\mathcal{O}^\dagger\,|\Theta\rangle = \tilde{\mathcal{O}}^\dagger u\,|\Theta\rangle\,, & u\mathcal{O}'^\dagger\,|\Theta\rangle = \tilde{\mathcal{O}}'^\dagger u\,|\Theta\rangle\,. \end{cases}$$

2. Relative entropy equals bulk relative entropy For any $|\Psi\rangle, |\Phi\rangle \in \mathcal{H}_{code}$ with $|\Psi\rangle$ cyclic and separating with respect to M_{code},

$$\mathcal{S}_{\Psi|\Phi}(M_{code}) = \mathcal{S}_{u\Psi|u\Phi}(M_{phys}), \text{ and } \mathcal{S}_{\Psi|\Phi}(M'_{code}) = \mathcal{S}_{u\Psi|u\Phi}(M'_{phys}),$$

where $\mathcal{S}_{\Psi|\Phi}(\mathcal{M})$ is the relative entropy.

Proof. Given the proof of Theorem 14.1.1, we only need to show that statement 2 implies statement 1. Let $|\Phi\rangle \in \mathcal{H}_{code}$ be cyclic and separating with respect to M_{code}, and let $U \in M_{code}$ and $U' \in M'_{code}$ be unitary operators. We can easily see that

$$0 = \mathcal{S}_{\Phi|U'\Phi}(M_{code}) = \mathcal{S}_{u\Phi|uU'\Phi}(M_{phys}). \tag{14.39}$$

Due to Theorem 3.1.26, this implies that

$$\Delta^{p}_{u\Phi|uU'\Phi}\,|u\Phi\rangle = |u\Phi\rangle\,, \tag{14.40}$$

where $\Delta^{p}_{u\Phi|uU'\Phi} = S^{p\,\dagger}_{u\Phi|uU'\Phi} S^{p}_{u\Phi|uU'\Phi}$ and $S^{p}_{u\Phi|uU'\Phi}$ is the relative modular operator defined with

respect to $\mathcal{M}_{phys}$. It follows that for any $\mathcal{P} \in \mathcal{M}_{phys}$,

$$\langle uU'\Phi|\mathcal{P}uU'\Phi\rangle = \langle S^{p}_{u\Phi|uU'\Phi}u\Phi|S^{p}_{u\Phi|uU'\Phi}\mathcal{P}^{\dagger}u\Phi\rangle = \langle \mathcal{P}^{\dagger}u\Phi|S^{p\,\dagger}_{u\Phi|uU'\Phi}S^{p}_{u\Phi|uU'\Phi}u\Phi\rangle = \langle u\Phi|\mathcal{P}|u\Phi\rangle\,. \tag{14.41}$$

This implies that

$$\langle\Phi|U'^{\dagger}u^{\dagger}\mathcal{P}uU' - u^{\dagger}\mathcal{P}u|\Phi\rangle = 0. \tag{14.42}$$

We now use the assumption that cyclic and separating vectors with respect to $\mathcal{M}_{code}$ are dense in $\mathcal{H}_{code}$. For any $|\Psi\rangle \in \mathcal{H}_{code}$, choose a sequence $\{|\Phi_n\rangle\} \in \mathcal{H}_{code}$ such that each $|\Phi_n\rangle$ is cyclic and separating with respect to $\mathcal{M}_{code}$, and $|\Psi\rangle = \lim_{n\to\infty}|\Phi_n\rangle$. Then,

$$\langle\Psi|U'^{\dagger}u^{\dagger}\mathcal{P}uU' - u^{\dagger}\mathcal{P}u|\Psi\rangle = \lim_{n\to\infty}\langle\Phi_n|U'^{\dagger}u^{\dagger}\mathcal{P}uU' - u^{\dagger}\mathcal{P}u|\Phi_n\rangle = 0. \tag{14.43}$$

Hence, this implies that the operators that are measured in the limit itself is zero, i.e. $U'^{\dagger}u^{\dagger}\mathcal{P}uU' - u^{\dagger}\mathcal{P}u = 0$. This then gives the following identity involving the isometry u, an arbitrary operator $\mathcal{P} \in \mathcal{M}_{phys}$, and a unitary operator $U' \in \mathcal{M}'_{code}$:

$$u^{\dagger}\mathcal{P}uU' = U'u^{\dagger}\mathcal{P}u. \tag{14.44}$$

The same logic can be applied to the commutant algebras; thus, for any $\mathcal{P}' \in \mathcal{M}'_{phys}$, $U \in \mathcal{M}_{code}$

with U unitary, we have a similar relation:

$$u^\dagger \mathcal{P}' u U = U u^\dagger \mathcal{P}' u. \tag{14.45}$$

Another consequence of equation (14.41) is that for any $\mathcal{P}_1, \mathcal{P}_2 \in \mathcal{M}_{phys}$, we have that

$$\langle \mathcal{P}_1 u U' \Phi | \mathcal{P}_2 u U' \Phi \rangle = \langle \mathcal{P}_1 u \Phi | \mathcal{P}_2 u \Phi \rangle \,. \tag{14.46}$$

Naturally, we define a linear map $X'^{\Phi\, U'} : \mathcal{H}_{phys} \to \mathcal{H}_{phys}$. We define $X'^{\Phi\, U'}$ by

$$X'^{\Phi\, U'} \mathcal{P} u \,|\Phi\rangle := \mathcal{P} u U' \,|\Phi\rangle \quad \forall \mathcal{P} \in \mathcal{M}_{phys}. \tag{14.47}$$

Then we see that $X'^{\Phi\, U'}$ is densely defined. From equation (14.46), we see that $X'^{\Phi\, U'}$ preserves the norm of all vectors in its domain. Hence, $X'^{\Phi\, U'}$ may be uniquely extended to a bounded operator, which is unitary. By definition, $X'^{\Phi\, U'}$ commutes with all operators in $\mathcal{M}_{phys}$; hence, we deduce that $X'^{\Phi\, U'} \in \mathcal{M}'_{phys}$. (The superscripts on $X'^{\Phi\, U'}$ remind us that it depends on the choice of $|\Phi\rangle$ and U' and that it is in the commutant of $\mathcal{M}_{phys}$.)

Next, we use equations (14.45) and (14.47) with $\mathcal{P}' = X'^{\Phi\, U'}$. We find that

$$u^\dagger X'^{\Phi\, U'} u U |\Phi\rangle = U u^\dagger X'^{\Phi\, U'} u \,|\Phi\rangle = U u^\dagger u U' \,|\Phi\rangle = U U' \,|\Phi\rangle = U' U |\Phi\rangle \,. \tag{14.48}$$

The first equality follows from equation (14.45), the second equality follows from (14.47), the third

equality follows from the fact that $u^\dagger u$ is the identity on $\mathcal{H}_{code}$, and the last equality follows because $U \in M_{code}$ and $U' \in M'_{code}$. Recall that U is an arbitrary unitary operator in M_{code}. We now need Theorem 3.1.14, which states that any operator in M_{code} may be written as a linear combination of four unitary operators in M_{code} [180]. The above equation implies that for any $\mathcal{O} \in M_{code}$, we have that

$$(u^\dagger X'^{\Phi U'} u - U')\mathcal{O}\,|\Phi\rangle = 0. \tag{14.49}$$

Note that $(u^\dagger X'^{\Phi U'} u - U')$ is a bounded operator, so its kernel is closed. Recall that $|\Phi\rangle$ is cyclic with respect to M_{code}. Since any vector in the Hilbert space may be written as $\lim_{n\to\infty} \mathcal{O}_n\,|\Phi\rangle$ for some sequence of operators $\{\mathcal{O}_n\} \in M_{code}$, it follows that $(u^\dagger X'^{\Phi U'} u - U')$ annihilates every vector in $\mathcal{H}_{code}$. In other words,

$$u^\dagger X'^{\Phi U'} u = U'. \tag{14.50}$$

Choose an arbitrary $|\Upsilon\rangle \in \mathcal{H}_{code}$ with $\langle\Upsilon|\Upsilon\rangle = 1$. We may uniquely write $X'^{\Phi U'} u\,|\Upsilon\rangle$ as

$$X'^{\Phi U'} u\,|\Upsilon\rangle = |a\rangle + |b\rangle\,, \tag{14.51}$$

where $|a\rangle \in \text{Im}\, u$, and $|b\rangle \in (\text{Im u})^\perp$. Note that $X'^{\Phi U'}$ is unitary; hence, we can decompose as

$$\langle u\Upsilon|X'^{\Phi U'\,\dagger} X'^{\Phi U'}|u\Upsilon\rangle = 1 = \langle a|a\rangle + \langle b|b\rangle\,. \tag{14.52}$$

Next, note that

$$u^\dagger |a\rangle = u^\dagger(|a\rangle + |b\rangle) = u^\dagger X'^{\Phi U'} u |\Psi\rangle = U' |\Psi\rangle . \tag{14.53}$$

Hence,

$$\langle a|a\rangle = \langle u^\dagger a|u^\dagger a\rangle = \langle U'\Psi|U'\Psi\rangle = 1. \tag{14.54}$$

This implies that $\langle b|b\rangle = 0$; hence $|b\rangle = 0$. Hence, $X'^{\Phi U'}$ maps the vector space Im u to itself. We may then use equation (14.50) to find that

$$X'^{\Phi U'} u = uu^\dagger X'^{\Phi U'} u = uU'. \tag{14.55}$$

Next, we define a linear map $X'^{(U'\Phi)(U'^\dagger)} : \mathcal{H}_{phys} \to \mathcal{H}_{phys}$. We define $X'^{(U'\Phi)(U'^\dagger)}$ by

$$X'^{(U'\Phi)(U'^\dagger)} \mathcal{P} u U' |\Phi\rangle := \mathcal{P} u |\Phi\rangle \quad \forall \mathcal{P} \in \mathcal{M}_{phys}. \tag{14.56}$$

It is easy to see that $U' |\Phi\rangle$ is cyclic and separating with respect to $\mathcal{M}_{code}$ given that $|\Phi\rangle$ is cyclic and separating with respect to $\mathcal{M}_{code}$ and that $U' \in \mathcal{M}'_{code}$ is unitary. It follows that $X'^{(U'\Phi)(U'^\dagger)}$ is densely defined and uniquely extends to a bounded operator, which is unitary. Since equation (14.55) is true for any $|\Phi\rangle \in \mathcal{H}_{code}$ that is cyclic and separating with respect to $\mathcal{M}_{code}$ and any unitary $U' \in \mathcal{M}'_{code}$,

$$X'^{(U'\Phi)(U'^\dagger)} u = uU'^\dagger. \tag{14.57}$$

This relation can be used to see that for any $\mathcal{P} \in M_{phys}$,

$$X'^{(U'\Phi)(U'^{\dagger})} X'^{\Phi U'} \mathcal{P} u |\Phi\rangle = \mathcal{P} u |\Phi\rangle . \tag{14.58}$$

Thus, we deduce that the two operators we defined are adjoints of each other:

$$(X'^{\Phi U'})^{\dagger} = X'^{(U'\Phi)(U'^{\dagger})}. \tag{14.59}$$

We have thus shown that for every unitary operator $U' \in M'_{code}$, there exists a unitary operator $X' \in M'_{phys}$ such that

$$X' u = u U', \text{ and } X'^{\dagger} u = u U'^{\dagger}. \tag{14.60}$$

The same logic applies to show that for every unitary operator $U \in M_{code}$, there exists a unitary operator $X \in M_{phys}$ such that

$$X u = u U, \text{ and } X^{\dagger} u = u U^{\dagger}. \tag{14.61}$$

We conclude the proof by noting that any operator in a von Neumann algebra M may be written as a linear combination of four unitary operators in M (Theorem 3.1.14). □

Our proof provides an explicit formula for reconstructing an operator in M_{code} as an operator in M_{phys}. Given $\mathcal{O} \in M_{code}$, we define the operator $\tilde{\mathcal{O}} \in M_{phys}$ by

$$\tilde{\mathcal{O}} \mathcal{P}' u |\Phi\rangle := \mathcal{P}' u \mathcal{O} |\Phi\rangle \quad \forall \mathcal{P}' \in M'_{phys}, \tag{14.62}$$

where $|\Phi\rangle \in \mathcal{H}_{code}$ is a fiducial state that is cyclic and separating with respect to M_{code} and M'_{code}. This formula follows from writing $\mathcal{O}$ as a linear combination of four unitary operators in M_{code} and using equation (14.47) on each unitary operator. The arguments in our proof then establish that $\tilde{\mathcal{O}}u = u\mathcal{O}$. Note that $\tilde{\mathcal{O}}$ does not depend on the choice of the fiducial state $|\Phi\rangle$. To see this, we define $\tilde{\mathcal{O}}_\star \in M_{code}$ by

$$\tilde{\mathcal{O}}_\star \mathcal{P}' u \,|\Phi_\star\rangle := \mathcal{P}' u \mathcal{O} \,|\Phi_\star\rangle \quad \forall \mathcal{P}' \in M'_{phys}, \tag{14.63}$$

where $|\Phi_\star\rangle \in \mathcal{H}_{code}$ is a different fiducial state. Since $\tilde{\mathcal{O}}u \,|\Phi_\star\rangle = u\mathcal{O} \,|\Phi_\star\rangle$, it follows that

$$\tilde{\mathcal{O}}\mathcal{P}' u \,|\Phi_\star\rangle = \mathcal{P}'\tilde{\mathcal{O}}u \,|\Phi_\star\rangle = \mathcal{P}' u\mathcal{O} \,|\Phi_\star\rangle = \tilde{\mathcal{O}}_\star \mathcal{P}' u \,|\Phi_\star\rangle \quad \forall \mathcal{P}' \in M'_{phys}. \tag{14.64}$$

Hence, $\tilde{\mathcal{O}}$ and $\tilde{\mathcal{O}}_\star$ are equal because they are both bounded operators that act the same way on a dense subspace of $\mathcal{H}_{code}$.

14.4 Discussion

In this section, we discuss the physical implications of Theorem 3.0.1. In particular, we explain in physical settings the validity of the technical assumptions of the theorem. In Section 14.4.1, we motivate our use of von Neumann algebras by explaining how they arise in quantum field theory, with an approach inspired by [155]. In Section 14.4.2, we summarize reasons why Theorem 3.0.1 should only be true in an approximate sense in quantum gravity. In Section 14.4.3, we summarize

the Reeh–Schlieder theorem. In Section 14.4.4, we use the Reeh–Schlieder theorem to physically motivate the assumptions of Theorem 3.0.1. In Section 14.4.6, we compare Theorem 3.0.1 with previous work on finite-dimensional error correction [159].

14.4.1 Von Neumann algebras in quantum field theory

Quantum field theories are characterized by algebras of operators acting on a Hilbert space $\mathcal{H}$. For every open region in spacetime, there is an associated algebra [155]. We will assume that there is a unique ground state $|\Omega\rangle \in \mathcal{H}$. The closure of the set of states obtained by acting on $|\Omega\rangle$ with all operators in the algebra associated with the entire spacetime is defined to be the vacuum superselection sector, $\mathcal{H}_0$. By definition, each superselection sector of the theory is an invariant subspace of this algebra.

Theories with lagrangian descriptions have a notion of an elementary field. Given an open region of spacetime $\mathcal{U}$, we can define an associated operator algebra $\mathcal{A}(\mathcal{U})$ by smearing the elementary fields with functions supported only in $\mathcal{U}$.[7] The operator algebra $\mathcal{A}(\mathcal{U})$ generically contains unbounded operators. Given $\mathcal{A}(\mathcal{U})$, we may obtain a von Neumann algebra $\mathcal{M}(\mathcal{U})$, which only consists of bounded operators, as follows [155]. For every unbounded operator (which we assume to be closed) in $\mathcal{A}(\mathcal{U})$, we may perform a polar decomposition to obtain a partial isometry and a self-adjoint positive operator, which is canonically associated with a set of projections by the spectral theorem. The von Neumann algebra $\mathcal{M}(\mathcal{U})$ is generated by the set of all spectral projections and par-

[7] Assuming that the time-slice axiom [155] holds, $\mathcal{A}(\mathcal{U})$ should really be associated with the domain of dependence of $\mathcal{U}$, as operators in the domain of dependence are related to operators in $\mathcal{U}$ via an equation of motion. Note that the time-slice axiom does not hold for generalized free fields [104], which we consider in Section 14.4.2.

tial isometries associated with the operators in $\mathcal{A}(\mathcal{U})$.[8] We assume that the operators in $\mathcal{A}(\mathcal{U})$ may be approximated by operators in $\mathcal{M}(\mathcal{U})$. As shown in [307], the Reeh–Schlieder theorem implies that states with bounded energy-momentum are cyclic with respect to $\mathcal{A}(\mathcal{U})$ for any open subregion of spacetime $\mathcal{U}$. We assume that this is also true for $\mathcal{M}(\mathcal{U})$.

14.4.2 Approximate entanglement wedge reconstruction

Throughout the chapter, we have used von Neumann algebras to denote subregions in the bulk and the boundary. In AdS/CFT, the boundary theory is a quantum field theory, so the discussion in Section 14.4.1 directly applies. However, the bulk theory is a theory of quantum gravity (string theory). For states with a semi-classical bulk dual, the bulk theory may be effectively described using quantum field theory on an asymptotically AdS background that might contain black holes. The applicability of quantum field theory motivates us to use von Neumann algebras to describe operators associated with covariantly defined subregions in the bulk, like the entanglement wedge of a boundary subregion.[9] Since entanglement wedges are causally complete, they naturally have an associated von Neumann algebra.

Since the long-distance bulk physics is only approximately described by quantum field theory, we need a generalization of Theorem 3.0.1 that relates the approximate bulk reconstruction to the approximate equivalence of relative entropies between the boundary and the bulk. We want to note

[8] If a subalgebra $\mathcal{S}$ of bounded operators contains the identity and is closed under hermitian conjugation, then its double commutant, $\mathcal{S}''$, is the von Neumann algebra generated by $\mathcal{S}$. Von Neumann algebras are naturally associated with causally complete subregions [180, 307].

[9] Associating a set of operators with a subregion in the bulk is highly nontrivial due to nonlocal effects in the bulk [138]. This is addressed in [139], which studies information measures for sets of operators that are not closed under multiplication. We do not consider this subtlety in our analysis.

that our formulation of bulk reconstruction in Theorem 3.0.1 is exact in the sense that correlation functions of operators in $\mathcal{M}_{code}$ exactly equal correlation functions computed on the boundary with the corresponding operators in $\mathcal{M}_{phys}$.

To be more precise, Theorem 3.0.1 is only valid for certain choices of the code subspace. If the code subspace consists of states with semi-classically distinct geometries, it is not clear how von Neumann algebras can be associated with subregions in a state independent way. For Theorem 3.0.1 to be relevant, we could choose $\mathcal{H}_{code}$ to be a subspace describing long wavelength modes in quantum field theory on a fixed background and the entanglement wedge to be the classical minimal area surface corresponding to a boundary subregion. To order G_N^0, the bulk dual of entanglement entropy is given by the bulk entanglement entropy of the entanglement wedge plus a local integral on the minimal area surface [130]. This was used to relate the bulk and boundary modular hamiltonians [178]. Since the bulk and boundary modular hamiltonians only differ by operators localized on the minimal surface, the bulk and boundary relative entropies are equivalent up to $\mathcal{O}(G_N)$ corrections [178]. The bulk dual of relative entropy beyond order G_N^0 involves bulk modular hamiltonians evaluated with respect to different bulk surfaces [103].[10] Since the formula for the bulk dual of relative entropy in Theorem 3.0.1 is only valid to order G_N^0, the two main statements in Theorem 3.0.1 can only be true in quantum gravity in an approximate sense. Theorem 4 of [82] proves that in the case of finite-dimensional von Neumann algebras, the approximate equivalence of bulk and boundary relative entropies implies approximate bulk reconstruction. Furthermore, [165] proves that entanglement

[10] It will be interesting to generalize equation (5.4) in [103] to an expression that uses infinite-dimensional von Neumann algebras.

wedge reconstruction can be exact to all orders in perturbation theory.[11]

It is possible for both statements in Theorem 3.0.1 to be exactly true in the limit $G_N \to 0$. In this case, the AdS/CFT duality relates a $(d+1)$-dimensional quantum field theory in AdS and a d-dimensional generalized free field theory, for which all connected n-point correlation functions vanish when $n \geq 3$.[12] We may set $\mathcal{H}_{code} = \mathcal{H}_{phys}$ because every state in the boundary theory has a geometric dual. The case where the bulk theory is a free scalar is studied in [104]. The authors of [104] work in Poincaré coordinates, which has d-dimensional Minkowski space as its conformal boundary. They argue that in the boundary generalized free field theory, the algebra associated with the domain of dependence of any ball-shaped region in a spatial slice of Minkowski space is equal to the algebra associated with the causal wedge in the bulk.[13] This statement is expressed in equation (5.7) of [104]. This implies that M_{code} and M_{phys} are isomorphic, i.e. $M_{code} = M_{phys}$, which means that the bulk and boundary relative entropies are equal.

14.4.3 The Reeh–Schlieder theorem

In the previous subsection, we explained how we use von Neumann algebras to approximately characterize bulk physics. Before we physically motivate the assumption in Theorem 3.0.1 that the set of cyclic and separating vectors with respect to M_{code} is dense in $\mathcal{H}_{code}$, we outline the conclusions of the Reeh–Schlieder theorem. Our discussion of the Reeh–Schlieder theorem follows the spirit of

[11] However, in certain contexts, the entanglement wedge reconstruction proposal must be nonperturbatively approximate (see [165, 192]).

[12] The fact that all correlation functions may be expressed in terms of two-point functions arises from large-N factorization in the boundary CFT.

[13] This statement is also true for conformal transformations of such regions. For these boundary regions, the causal wedge is the same as the entanglement wedge [263].

[307].

For the purposes of presenting the Reeh–Schlieder theorem, we restrict ourselves to quantum field theory in d-dimensional Minkowski space. Let P^μ be the energy-momentum operator. Each component of P^μ is a self-adjoint operator with its own set of spectral projections. Let S_Λ be the subset of momentum space defined by

$$S_\Lambda = \{p^\mu : |p^\mu| < \Lambda \quad \forall \mu \in \{0, 1, \cdots, d-1\}\}$$

for some cutoff energy Λ. Using the spectral projections of each P^μ, we may construct a projection operator Π_{S_Λ} that projects onto the subspace of states with energy-momentum in S_Λ. As P^μ is defined by smearing the local operator $T^{0\mu}$ (where $T^{\mu\nu}$ is the stress tensor) over an entire spatial slice,[14] Π_{S_Λ} leaves each superselection sector invariant. Furthermore, for every $|\Psi\rangle \in \mathcal{H}$,

$$\lim_{\Lambda\to\infty} \Pi_{S_\Lambda} |\Psi\rangle = |\Psi\rangle .$$

Thus, the set of states of bounded energy-momentum in a given superselection sector is dense in that superselection sector.

The Reeh–Schlieder theorem may be applied to states of bounded energy-momentum. Let $|\Xi\rangle$ denote such a state. Let Σ denote a spatial slice. Given an open proper subregion $\mathcal{V} \subset \Sigma$, let $\mathcal{U}_\mathcal{V}$ be a small neighborhood in spacetime containing $\mathcal{V}$. The Reeh–Schlieder theorem tells us that the closure of the set of states obtained by acting on $|\Xi\rangle$ with operators in the algebra $\mathcal{A}(\mathcal{U}_\mathcal{V})$ is equal

[14] Technically, a spatial slice is not an open subregion of spacetime.

to the closure of the set of states obtained by acting on $|\Xi\rangle$ with all local operators, which is the superselection sector of $|\Xi\rangle$.

Let us restrict our attention to a single superselection sector. Then $|\Xi\rangle$ is cyclic with respect to $\mathcal{A}(\mathcal{U}_\mathcal{V})$ and $\mathcal{M}(\mathcal{U}_\mathcal{V})$. Since $\mathcal{V}$ is a proper subregion of Σ, the Reeh–Schlieder theorem may also be applied to the subregion $\mathcal{U}_{\mathcal{V}'}$, where $\mathcal{V}'$ is the complement of the closure of $\mathcal{V}$ in Σ. The result is that $|\Xi\rangle$ is also separating with respect to $\mathcal{M}(\mathcal{U}_\mathcal{V})$ [307]. Thus, in quantum field theory in Minkowski space restricted to a single superselection sector, the fact that the set of states of bounded energy-momentum is dense implies that the set of cyclic and separating vectors with respect to $\mathcal{M}(\mathcal{U}_\mathcal{V})$ is dense.

14.4.4 Physical motivation for the assumptions of Theorem 3.0.1

We now use the Reeh–Schlieder theorem to understand the assumptions in Theorem 3.0.1 in a physical context. Without loss of generality, we assume that the bulk-to-boundary isometry u in Theorem 3.0.1 maps $\mathcal{H}_{code}$ into a single superselection sector of $\mathcal{H}_{phys}$. That is, the code subspace lies within a single superselection sector. If this is not the case, then we can decompose $\mathcal{H}_{code}$ into orthogonal subspaces that each are mapped into different superselection sectors of the boundary theory, and we can study Theorem 3.0.1 separately for each orthogonal subspace.

In Theorem 3.0.1, we assume that the set of cyclic and separating vectors with respect to $\mathcal{M}_{code}$ is dense in $\mathcal{H}_{code}$. If the bulk theory was quantum field theory in Minkowski space, then the discussion in Section 14.4.3 directly applies. However, the discussion in Section 14.4.3 does not directly imply this because the bulk theory is only approximately described by quantum field theory and

the background spacetime is asymptotically AdS. In [245], a version of the Reeh–Schlieder theorem is proved for free scalar fields in global AdS. The theorem is valid for the vacuum state of the field quantized in global AdS, the vacuum state of the field quantized in any causal wedge, and finite-energy excitations of these vacua. If we choose to ignore the gravitational backreaction in the bulk and take $\mathcal{H}_{code}$ to consist of finite-energy excitations of the global AdS vacuum, the results of [245] suggest to us that it is plausible that the set of cyclic and separating vectors with respect to $\mathcal{M}_{code}$, where $\mathcal{M}_{code}$ is associated with an entanglement wedge, is dense in the bulk vacuum superselection sector $\mathcal{H}_0$. If $\mathcal{H}_0$ is a proper subset of $\mathcal{H}_{code}$, we should redefine $\mathcal{H}_{code}$ to be $\mathcal{H}_0$ for Theorem 3.0.1 to apply.

It would be interesting to investigate the plausibility of the assumption that the set of cyclic and separating states with respect to $\mathcal{M}_{code}$ is dense in $\mathcal{H}_{code}$ when $\mathcal{H}_{code}$ contains black hole microstates. For a sufficiently large boundary subregion, the entanglement wedge of $\mathcal{M}_{code}$ will contain the black hole, and the operators in $\mathcal{M}_{code}$ correspond to local operators associated with the field degrees of freedom outside of the black hole as well as operators that act on the black hole microstates, whose description involves quantum gravity at the Planck scale. In quantum field theory, it is possible to generate the whole Hilbert space by acting on the vacuum with operators in a small subregion because the vacuum is highly entangled. It would be interesting to understand how the presence of a black hole changes the structure of spacetime entanglement outside the horizon. Holographic tensor network models suggest that entanglement wedge reconstruction is possible in the presence of a black hole [160]; operators outside the black hole can in fact be "pushed through" the black hole tensor [165]. However, tensor network models of holography involve finite dimensional Hilbert

spaces and thus cannot capture the pattern of entanglement that makes the Reeh–Schlieder theorem work.

Finally, we address the assumption in Theorem 3.0.1 that for all states $|\Psi\rangle \in \mathcal{H}_{code}$ that are cyclic and separating with respect to $\mathcal{M}_{code}$, $u|\Psi\rangle$ is cyclic and separating with respect to $\mathcal{M}_{phys}$. In [245], the Reeh–Schlieder theorem holds for the vacuum of global AdS, implying that the vacuum is cyclic and separating with respect to the local operator algebra associated with a bulk subregion. The image of the bulk vacuum state under the bulk-to-boundary isometry is the boundary vacuum state, which is cyclic and separating with respect to the local operator algebras associated with boundary subregions. Likewise, finite-energy excited states in the bulk map to states in the boundary CFT of bounded energy-momentum, which are also cyclic and separating. This supports the assumption of Theorem 3.0.1 that the cyclic and separating states with respect to $\mathcal{M}_{code}$ map to the cyclic and separating states with respect to $\mathcal{M}_{phys}$.

14.4.5 von Neumann algbegra with type III_1 factors as a special case

Our main physical justification of the assumption that cyclic and separating states with respect to $\mathcal{M}_{code}$ are dense in $\mathcal{H}_{code}$ is the fact that the Reeh-Schlieder theorem applies to states of bounded energy-momentum, which are dense in the Hilbert space. When considering a generic local quantum field theory, the von Neumann algebra of a type III_1 factor[15] is associated with a causal subregion of the spacetime. When $\mathcal{M}_{code}$ and $\mathcal{M}'_{code}$ are type III_1 factors, the assumption of Theorem 3.0.1 that cyclic and separating states with respect to $\mathcal{M}_{code}$ are dense in $\mathcal{H}_{code}$ also follows from a result of

[15] The definition of a type III_1 factor is given in [184].

Connes-Størmer, which is presented below.

Theorem 14.4.1 (Connes-Størmer [80]). *A factor M is of type III_1 if and only if the action of its unitary group on its state space by inner automorphisms is topologically transitive in the norm topology.*

Let $|\Psi\rangle$ be a cyclic and separating vector with respect to M. The above theorem implies that the set of vectors that can be written as $UU'|\Psi\rangle$, where $U \in M$ and $U' \in M'$ are both unitary operators, is dense in $\mathcal{H}$. Given that $|\Psi\rangle$ is cyclic and separating with respect to M, $UU'|\Psi\rangle$ is also cyclic and separating. The existence of one cyclic and separating vector $|\Psi\rangle$ in Theorem 3.0.1 guarantees, for a factor of type III_1, that the set of cyclic and separating vectors with respect to M_{code} is dense in $\mathcal{H}_{code}$.

14.4.6 Finite-dimensional quantum error correction

In this section, we explain Theorem 3.0.1 in the context of previous work on finite-dimensional error correction [102, 159, 259]. First, we interpret the assumption that cyclic and separating vectors with respect to M_{code} map to cyclic and separating vectors with respect to M_{phys} in the case that $\mathcal{H}_{code}$ and $\mathcal{H}_{phys}$ are finite dimensional. As discussed in [159], a finite dimensional M_{code} induces a decomposition of the code subspace,

$$\mathcal{H}_{code} = \oplus_\alpha \mathcal{H}_{a_\alpha} \otimes \mathcal{H}_{\bar{a}_\alpha}, \tag{14.65}$$

such that any $\mathcal{O} \in M_{code}$ may be written in block-diagonal form:

$$\mathcal{O} = \begin{pmatrix} \mathcal{O}_{a_1} \otimes I_{\bar{a}_1} & 0 & \cdots \\ 0 & \mathcal{O}_{a_2} \otimes I_{\bar{a}_2} & \cdots \\ \vdots & \vdots & \ddots \end{pmatrix}. \tag{14.66}$$

In the setup of [159], $\mathcal{H}_{phys}$ may be written in the factorized form $\mathcal{H}_{phys} = \mathcal{H}_A \otimes \mathcal{H}_{\overline{A}}$ where each factor corresponds to a boundary subregion and its complement. Let M_{phys} induce the factorization $\mathcal{H}_{phys} = \mathcal{H}_A \otimes \mathcal{H}_{\overline{A}}$ such that operators in M_{phys} act trivially on $\mathcal{H}_{\overline{A}}$. As [159] points out, subalgebra codes with complementary recovery are especially relevant for AdS/CFT as they display a Ryu–Takayanagi formula with a nontrivial area operator. For such codes, an orthonormal basis of $\mathcal{H}_{a_\alpha} \otimes \mathcal{H}_{\bar{a}_\alpha}$ may be written as

$$u \left|\alpha, ij\right\rangle_{\text{code}} = U_A U_{\overline{A}} \left(\left|\alpha, i\right\rangle_{A_1^\alpha} \left|\alpha, j\right\rangle_{\overline{A}_1^\alpha} \left|\chi_\alpha\right\rangle_{A_2^\alpha \overline{A}_2^\alpha} \right), \tag{14.67}$$

for a decomposition of $\mathcal{H}_A$ given by

$$\mathcal{H}_A = \oplus_\alpha (\mathcal{H}_{A_1^\alpha} \otimes \mathcal{H}_{A_2^\alpha}) \oplus \mathcal{H}_{A_3}, \tag{14.68}$$

and similarly for $\mathcal{H}_{\overline{A}}$. Also,

$$\dim \mathcal{H}_{A_1^\alpha} = \dim \mathcal{H}_{a_\alpha} \text{ and } \dim \mathcal{H}_{\overline{A}_1^\alpha} = \dim \mathcal{H}_{\bar{a}_\alpha}.$$

For each α, i and j are indices that denote basis vectors in $\mathcal{H}_{a_\alpha}$ and $\mathcal{H}_{\bar{a}_\alpha}$ respectively. We have explicitly included u, the isometry from the code subspace to the physical Hilbert space. U_A, $U_{\overline{A}}$ are unitary matrices that act on $\mathcal{H}_A$, $\mathcal{H}_{\overline{A}}$, and $|\chi\rangle_{A_2^\alpha \overline{A}_2^\alpha}$ is a state that depends on the specific code under consideration. It is important that in the state $|\chi\rangle_{A_2^\alpha \overline{A}_2^\alpha}$, subsystems A_2^α and $\overline{A}_2^\alpha$ are entangled. If $|\chi\rangle_{A_2^\alpha \overline{A}_2^\alpha}$ were a factorized state for every α, then it would not be possible to express $|\alpha, ij\rangle_{\text{code}}$ as in (14.67) for arbitrary choices of the factorization $\mathcal{H}_{phys} = \mathcal{H}_A \otimes \mathcal{H}_{\overline{A}}$. That is, the code would not be useful for studying bulk reconstruction for arbitrary choices of boundary subregions. Furthermore, equation (5.26) of [159] would imply that the area operator vanishes.

We now discuss the implications of Theorem 3.0.1 for the state $|\chi_\alpha\rangle_{A_2^\alpha \overline{A}_2^\alpha}$. Let us assume that $\dim \mathcal{H}_A = \dim \mathcal{H}_{\overline{A}}$ and that for every α, $\dim \mathcal{H}_{a_\alpha} = \dim \mathcal{H}_{\bar{a}_\alpha}$. Otherwise, there do not exist any cyclic and separating vectors with respect to M_{code} or M_{phys}. A vector in $\mathcal{H}_{phys}$ is cyclic and separating with respect to M_{phys} if and only if it has maximal Schmidt number with respect to $\mathcal{H}_{phys} = \mathcal{H}_A \otimes \mathcal{H}_{\overline{A}}$. The assumption that cyclic and separating vectors with respect to M_{code} map to cyclic and separating vectors with respect to M_{phys} implies that $|\chi\rangle_{A_2^\alpha \overline{A}_2^\alpha}$ must have maximal Schmidt number with respect to the factorization $\mathcal{H}_{A_2^\alpha} \otimes \mathcal{H}_{\overline{A}_2^\alpha}$ and that $\dim \mathcal{H}_{A_2^\alpha} = \dim \mathcal{H}_{\overline{A}_2^\alpha}$. To see why, note that a cyclic and separating vector $|\Phi\rangle \in \mathcal{H}_{code}$ with respect to M_{code} may be written as

$$|\Phi\rangle = \sum_{\alpha,i,j} c_{ij}^\alpha \, |\alpha, ij\rangle_{\text{code}} \,, \tag{14.69}$$

where c_{ij}^α is a full-rank square matrix for each α. Using equation (14.67) to map $|\Phi\rangle$ to $u\,|\Phi\rangle \in \mathcal{H}_{phys}$, we see that if $|\chi_{\hat{\alpha}}\rangle_{A_2^{\hat{\alpha}} \overline{A}_2^{\hat{\alpha}}}$ does not have maximal Schmidt number for some $\hat{\alpha}$, then we can annihilate

$u\,|\Phi\rangle$ with an operator that, up to conjugation by U_A, acts as the identity on $\mathcal{H}_{\overline{A}}$, annihilates $\mathcal{H}_{A_3}$, annihilates $\mathcal{H}_{A_1^\alpha} \otimes \mathcal{H}_{A_2^\alpha}$ for $\alpha \neq \hat{\alpha}$, and acts nontrivially on $\mathcal{H}_{A_1^\alpha} \otimes \mathcal{H}_{A_2^\alpha}$. This implies that $u\,|\Phi\rangle$ is not separating with respect to M_{phys}, which contradicts the assumption. Another consequence of the assumption is that $\mathcal{H}_{A_3}$ and $\mathcal{H}_{\overline{A}_3}$ must be trivial. Previous work on finite-dimensional error correction [159, 259] has highlighted the crucial role of entanglement in bulk reconstruction. We have shown that the Reeh–Schlieder theorem suggests that cyclic and separating vectors with respect to M_{code} are mapped via the bulk-to-boundary isometry to vectors that are cyclic and separating with respect to M_{phys}. In the context of finite-dimensional subalgebra codes, this implies that the area term in the Ryu–Takayangi formula cannot vanish.

Our proof of entanglement wedge reconstruction in Theorem 3.0.1 is constructive. Given a bulk operator $\mathcal{O} \in M_{code}$, equation (14.62) provides an explicit formula for a boundary operator $\tilde{\mathcal{O}} \in M_{phys}$. In order to understand our formula in the finite dimensional case, we use the decomposition $\mathcal{H}_A = \oplus_\alpha (\mathcal{H}_{A_1^\alpha} \otimes \mathcal{H}_{A_2^\alpha})$ (and similarly for $\mathcal{H}_{\overline{A}}$) and let $|\Phi\rangle$ (defined in equation (14.69)) be our fiducial state. The action of $\mathcal{O} \in M_{code}$ on a code subspace basis vector is

$$\mathcal{O}\,|\Phi\rangle = \sum_{\alpha,i,\hat{i},j} c_{ij}^{\alpha}\, \langle \hat{i}|\mathcal{O}_{a_\alpha}|i\rangle\, |\alpha, \hat{i}j\rangle_{\text{code}}\,, \tag{14.70}$$

where $\mathcal{O}_{a_\alpha}$ is defined in equation (14.66). By equation (14.67) we then have that

$$u\,|\Phi\rangle = \sum_{\alpha,i,j} c_{ij}^{\alpha} U_A U_{\overline{A}} \left(|\alpha, i\rangle_{A_1^\alpha}\, |\alpha, j\rangle_{\overline{A}_1^\alpha}\, |\chi_\alpha\rangle_{A_2^\alpha \overline{A}_2^\alpha} \right), \tag{14.71}$$

$$u\mathcal{O}\,|\Phi\rangle = \sum_{\alpha,i,\hat{i},j} c_{ij}^{\alpha}\,\langle\hat{i}|\mathcal{O}_{a_\alpha}|i\rangle\; U_A U_{\overline{A}}\left(|\alpha,\hat{i}\rangle_{A_1^\alpha}\,|\alpha,j\rangle_{\overline{A}_1^\alpha}\,|\chi_\alpha\rangle_{A_2^\alpha\overline{A}_2^\alpha}\right). \tag{14.72}$$

Equation (14.62) then defines $\tilde{\mathcal{O}} \in M_{phys}$ by

$$\begin{aligned}\tilde{\mathcal{O}}\,\mathcal{P}' U_A U_{\overline{A}} \sum_{\alpha,i,j} c_{ij}^{\alpha}\left(|\alpha,i\rangle_{A_1^\alpha}\,|\alpha,j\rangle_{\overline{A}_1^\alpha}\,|\chi_\alpha\rangle_{A_2^\alpha\overline{A}_2^\alpha}\right)& \\ := \sum_{\alpha,i,\hat{i},j} c_{ij}^{\alpha}\,\langle\hat{i}|\mathcal{O}_{a_\alpha}|i\rangle\;\mathcal{P}' U_A U_{\overline{A}}\left(|\alpha,\hat{i}\rangle_{A_1^\alpha}\,|\alpha,j\rangle_{\overline{A}_1^\alpha}\,|\chi_\alpha\rangle_{A_2^\alpha\overline{A}_2^\alpha}\right),&\end{aligned} \tag{14.73}$$

where $\mathcal{P}' \in M_{phys}$ can be any operator that acts as the identity on $\mathcal{H}_A$. With a suitable choice of $\mathcal{P}'$, we may show that for any α, i, j,

$$\tilde{\mathcal{O}}\;U_A U_{\overline{A}}\left(|\alpha,i\rangle_{A_1^\alpha}\,|\alpha,j\rangle_{\overline{A}_1^\alpha}\,|\chi_\alpha\rangle_{A_2^\alpha\overline{A}_2^\alpha}\right) = U_A U_{\overline{A}}\left(\sum_{\hat{i}}\langle\hat{i}|\mathcal{O}_{a_\alpha}|i\rangle\,|\alpha,\hat{i}\rangle_{A_1^\alpha}\,|\alpha,j\rangle_{\overline{A}_1^\alpha}\,|\chi_\alpha\rangle_{A_2^\alpha\overline{A}_2^\alpha}\right). \tag{14.74}$$

Thus, Theorem 3.0.1 along with the reconstruction formula in equation (14.62) is an appropriate infinite-dimensional generalization of the finite-dimensional subalgebra codes with complementary recovery studied in [159].

14.4.7 Outlook for holographic relative entropy

The entanglement wedge reconstruction proposal is an example of bulk reconstruction. It asserts that for holographic theories, local operators in the entanglement wedge of a boundary subregion A can be written in terms of CFT operators localized on A [102, 160, 178]. Assuming that the operators

in $\mathcal{M}_{code}$ and $\mathcal{M}'_{code}$ in Theorem 3.0.1 lie respectively in an entanglement wedge and its complement, Theorem 3.0.1 establishes entanglement wedge reconstruction from the equivalence of bulk and boundary relative entropies and vice versa. Thus, it has been suggested that the entanglement wedge is "dual" to its corresponding boundary subregion [178]. Another interesting result of [178] is that bulk modular flow is dual to boundary modular flow, which we have captured in equation (14.35). The bulk and boundary modular operators act on the code subspace in the same way.

Quantum error correction in finite dimensional Hilbert spaces has been crucially used to argue for the entanglement wedge reconstruction proposal [102, 159]. When $\mathcal{H}_{code}$ and $\mathcal{H}_{phys}$ are finite-dimensional, Theorem 3.0.1 has parallels to Theorem 1.1 of [159]. In Theorem 3.0.1, we assume that cyclic and separating vectors with respect to $\mathcal{M}_{code}$ are dense in $\mathcal{H}_{code}$, which is essentially a bulk version of the Reeh–Schlieder Theorem [245]. We also assume that cyclic and separating states with respect to $\mathcal{M}_{code}$ map to cyclic and separating states with respect to $\mathcal{M}_{phys}$, the algebra corresponding to a boundary subregion. These assumptions guarantee that the subalgebra codes studied in [159] have a nonzero area operator. [159] defines relative entropy in the boundary theory as $S(\rho, \sigma) = \mathrm{Tr}\, \rho(\log \rho - \log \sigma)$. The definition of relative entropy we use in the bulk and boundary is appropriate for infinite-dimensional Hilbert spaces and reduces to the aforementioned formula in the finite-dimensional case [15]. Thus, we have shown that the relative entropy formula in [15] naturally describes the holographic relative entropy in quantum field theory to order G_N^0.

Entropy is time's arrow.

Arthur Stanley Eddington

15

Entanglement Wedge Reconstruction of Infinite-dim von Neumann Algebras

Tensor networks with a finite number of nodes have been used to construct QECC for finite dimensional Hilbert spaces [159, 160]. However, the use of tensor networks in quantum error correction can be generalized to the case of infinite-dimensional Hilbert spaces.

In our toy model, the infinite-dimensional code and physical Hilbert spaces are constructed by tensoring together the Hilbert spaces of a countably infinite number of qutrits and then restricting to a countably infinite-dimensional subspace. Finite collections of qutrits are related by a tensor network as represented in Figure 15.1. Each connected graph defines an isometry from the state of two code qutrits (denoted as black nodes) to the state of four physical qutrits (denoted as white nodes). Our toy model explores how tensor networks with a repeated pattern can be generalized to define a QECC with infinite-dimensional Hilbert spaces. This model does not capture the negatively curved geometry of AdS; however, we believe that our construction can be generalized to encapsulate the holographic setup.

A more detailed summary of our construction is given as follows.

- The code pre-Hilbert space $p\mathcal{H}_{code}$ is defined to be the Hilbert space of a countably infinite collection of qutrit pairs, where all but finitely many qutrit pairs are in the maximally entangled state $|\lambda\rangle = \frac{1}{\sqrt{3}}(|00\rangle + |11\rangle + |22\rangle)$. Each code qutrit pair is represented by two vertically-aligned black nodes in Figure 15.1. The code Hilbert space $\mathcal{H}_{code}$ is the completion of $p\mathcal{H}_{code}$. The physical pre-Hilbert space $p\mathcal{H}_{phys}$ and physical Hilbert space $\mathcal{H}_{phys}$ are constructed the same way. Each qutrit pair in the physical Hilbert space is represented by two vertically-aligned white nodes in Figure 15.1.

- We construct a bulk-to-boundary isometry from $p\mathcal{H}_{code}$ to $p\mathcal{H}_{phys}$ using the tensor network in Figure 15.1. The tensor network is comprised of infinite copies of connected diagrams, where a single connected diagram is represented in Figure 3.3. Each trivalent vertex is asso-

ciated with the rank-four perfect tensor[1] of the three qutrit code $T_{i\tilde{a}\tilde{b}\tilde{c}}$. Our tensor network maps the states of the black qutrits to the states of the white qutrits. Using these notations, the isometry associated with a connected diagram is explicitly given by

$$|p\rangle_i |q\rangle_j \to \sum_{\tilde{x},\tilde{y},\tilde{z},\tilde{c},\tilde{w}} \sqrt{3} T_{p\tilde{x}\tilde{y}\tilde{c}} T_{q\tilde{z}\tilde{w}\tilde{c}} |\tilde{x}\rangle_{\tilde{a}} |\tilde{y}\rangle_{\tilde{b}} |\tilde{z}\rangle_{\tilde{d}} |\tilde{w}\rangle_{\tilde{e}} ,$$

where the qutrits are labeled as in Figure 15.1. The indices $p, q, \tilde{x}, \tilde{y}, \tilde{z}, \tilde{w}, \tilde{c}$ are all valued in $\{0, 1, 2\}$. The isometry from $p\mathcal{H}_{code}$ to $p\mathcal{H}_{phys}$ may be naturally extended to an isometry that maps $\mathcal{H}_{code}$ to $\mathcal{H}_{phys}$.

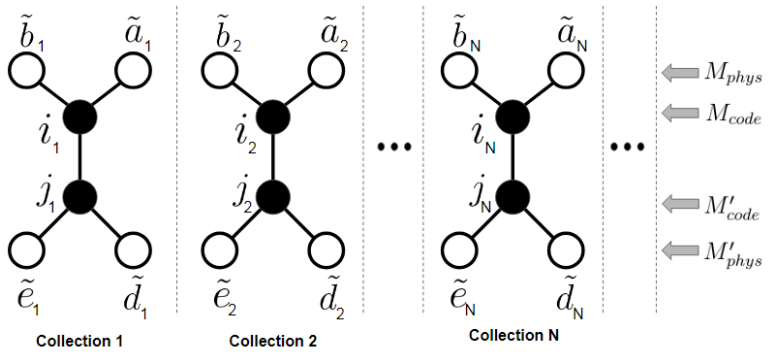

Figure 15.1: Our setup consists of infinitely many collections of code (black) qutrit pairs which are related to physical (white) qutrits via a tensor network that consists of infinitely many disconnected graphs. The von Neumann algebra M_{phys} acts on the first row of qutrits. The algebras M_{code}, M'_{code}, and M'_{phys} act on the second, third, and fourth rows of qutrits respectively.

- Using the code and physical Hilbert spaces and an isometry relating them, we define von Neumann algebras M_{code} and M_{phys}. The $\star$-algebra A_{code} is defined to be the algebra of operators that only act nontrivially on a finite number of qutrits in the top row of black qutrits in

[1] A *perfect tensor* is an even-rank tensor that naturally defines an isometric map from up to half of its indices to the remaining indices. For a more detailed discussion of perfect tensors, see [259].

Figure 15.1. The double commutant of A_{code} defines M_{code}, the von Neumann algebra acting on the top row of black qutrits. We explicitly show that the commutant M'_{code} is the analogously defined algebra that acts on the bottom row of black qutrits. We also define M_{phys} and M'_{phys} which respectively act on the top and bottom row of white qutrits in Figure 15.1. To show that M_{code} is a type II_1 factor, we define a linear function $T : M_{code} \to \mathbb{C}$, which is given by

$$T(\mathcal{O}) := \langle \lambda \cdots | \mathcal{O} | \lambda \cdots \rangle , \quad \mathcal{O} \in M_{code},$$

where $|\lambda \cdots\rangle \in p\mathcal{H}_{code}$ is the state where all black qutrit pairs are in the state $|\lambda\rangle$. We demonstrate that $T(\mathcal{O})$ is a trace and invoke Theorem 3.4.13 to prove that M_{code} is a type II_1 factor. Likewise, M'_{code}, M_{phys}, and M'_{phys} are also type II_1 factors.

- We determine a map from M_{code} to M_{phys} that explicitly shows how operators that act on black qutrits may be reconstructed as operators that act on white qutrits. First, note that an operator $\mathcal{O}$ that acts on a black qutrit i in Figure 3.3 may be expressed as an operator $\tilde{\mathcal{O}}$ that acts on the white qutrits $\tilde{a}, \tilde{b}$. The relation between $\mathcal{O}$ and $\tilde{\mathcal{O}}$ is given by

$$\tilde{\mathcal{O}} = \sum_{p,q} \langle p | \mathcal{O} | q \rangle_i \left[U_{\tilde{a}\tilde{b}} \, |p\rangle_{\tilde{a}} \, \langle q|_{\tilde{a}} \, U^{\dagger}_{\tilde{a}\tilde{b}} \otimes I_{\tilde{d}\tilde{e}} \right],$$

where $U_{\tilde{a}\tilde{b}}$ is a unitary matrix that acts only on white qutrits $\tilde{a}, \tilde{b}$. By applying the above formula finitely many times, we may construct a map from A_{code} into M_{phys} which we call the

tensor network map. We then show that there is a natural way to extend the tensor network map to a map from M_{code} into M_{phys}. We demonstrate that the image under the tensor network map of an operator $\mathcal{O} \in M_{code}$ acts on the code subspace in the same way as $\mathcal{O}$. The same statement holds for the commutant M'_{code}. This demonstrates that our QECC satisfies statement 1 of Theorem 3.0.1.

- To show that our QECC satisfies the assumptions of Theorem 3.0.1, we find a dense subset of $\not{p}\mathcal{H}_{code}$ that consists of cyclic and separating vectors with respect to M_{code}. For example, a state in $\not{p}\mathcal{H}_{code}$ where each black qutrit pair is in a pure state with maximal Schmidt number (such as $|\lambda\rangle$) is cyclic and separating with respect to M_{code}. We also prove that any cyclic and separating state with respect to M_{code} is mapped via the bulk-to-boundary isometry to a cyclic and separating state with respect to M_{phys}. Thus, our QECC satisfies all assumptions and statements of Theorem 3.0.1.

An outline of this chapter is given as follows. First, we describe in detail our construction of an infinite-dimensional QECC in Section 15.1. Tensor networks play an important role in our toy model. In Section 15.2 we define von Neumann algebras $M_{code} \subset \mathcal{B}(\mathcal{H}_{code})$ and $M_{phys} \subset \mathcal{B}(\mathcal{H}_{phys})$.[2] In Sections 15.3 and 15.4, we show that our example satisfies the properties of bulk reconstruction in Theorem 3.0.1. In Section 15.5 we show that cyclic and separating vectors with respect to M_{code} (M_{phys}) are dense in $\mathcal{H}_{code}$ ($\mathcal{H}_{phys}$). We also show that cyclic and separating vectors with respect to M_{code} are mapped via the bulk-to-boundary isometry u to cyclic and separating vectors with respect

[2] The set of bounded operators on a Hilbert space $\mathcal{H}$ is denoted by $\mathcal{B}(\mathcal{H})$. See Definition 3.3.3.

to M_{phys}. It follows that our tensor network model satisfies both statements in Theorem 3.0.1. In Section 15.6, we prove that M_{code} and M_{phys} are type II_1 factors.[3] In section 15.8, we show that the relative entropy of two cyclic and separating states may be computed by tracing over the entire Hilbert space except the Hilbert space of the first N qutrit pairs, computing the relative entropy of the reduced density matrices with the finite-dimensional relative entropy formula, and taking the limit as $N \to \infty$.

15.1 The isometry between two infinite-dimensional Hilbert spaces

In this section, we show how a tensor network with infinitely many nodes can be used to define an isometry (i.e. a norm preserving map) from one infinite-dimensional Hilbert space to another. The isometry will be denoted by $u : \mathcal{H}_{code} \to \mathcal{H}_{phys}$. We use the same notation in Section 3.6 where we have the reviewed some preliminary facts about the three qutrit code.

15.1.1 The code and physical Hilbert spaces

Our general setup is depicted in Figure 15.1. In our construction of an infinite-dimensional QECC, the code and physical Hilbert spaces, $\mathcal{H}_{code}$ and $\mathcal{H}_{phys}$, are each defined as the completions of pre-Hilbert spaces, $p\mathcal{H}_{code}$ and $p\mathcal{H}_{phys}$. As Figure 15.1 shows, we may intuitively think of either the code or physical pre-Hilbert space as an infinite tensor product of two black qutrits or four white qutrits. From now on, whenever we say *collection* we are referring to the qutrits in a single connected dia-

[3] In Section 3.5, we demonstrate that the relative Tomita operator defined with respect to M_{code} or M_{phys} may be bounded or unbounded, depending on the choice of states. In quantum field theory, the Tomita operators defined with respect to local operator algebras are generically unbounded [307].

gram in Figure 15.1. Within each collection we will label the individual qutrits as shown in Figure 3.3.

The pre-Hilbert space $p\mathcal{H}_{code}$ is defined to include states of black qutrits where all but finitely many pairs of black qutrits are in the state $|\lambda\rangle$, defined in equation (3.52), which we sometimes also refer to as the *code reference state*. Any vector in $p\mathcal{H}_{code}$ is a finite linear combination of vectors in an overcomplete basis, where each basis vector may be written as

$$|M, p_1, p_2, \cdots, p_M, q_1, q_2, \cdots, q_M\rangle := \left[|p_1\rangle_{i_1} |q_1\rangle_{j_1}\right] \otimes \left[|p_2\rangle_{i_2} |q_2\rangle_{j_2}\right] \otimes \cdots \otimes \left[|p_M\rangle_{i_M} |q_M\rangle_{j_M}\right] \otimes |\lambda\rangle \cdots \tag{15.1}$$

where each p_k or q_k index (for $k \in \{1, 2, \ldots, M\}$) is valued in $\{0, 1, 2\}$ and specifies an orthonormal basis vector of a black qutrit. The index M can be any natural number. The qutrits in each collection are contained in square brackets. To shorten notation, we will refer to the above basis vector as $|M, \{p, q\}\rangle$. The $\otimes |\lambda\rangle \cdots$ means that all the black qutrit pairs in the $(M+1)$th collection and beyond are in the reference state $|\lambda\rangle$. Note that these basis vectors are not all linearly independent.

Given two basis vectors $|M_1, \{p, q\}_1\rangle$ and $|M_2, \{p, q\}_2\rangle$, their inner product is calculated by ignoring all collections beyond the collection $\max(M_1, M_2)$ and then taking the usual inner product on the remaining $9^{\max(M_1, M_2)}$-dimensional Hilbert space. Note that the basis vectors $|M, \{p, q\}\rangle$ are not all mutually orthogonal, but they are all normalized. With an inner product, we can define Cauchy sequences. The Hilbert space $\mathcal{H}_{code}$ is defined as the closure of $p\mathcal{H}_{code}$ so that all Cauchy sequences in $\mathcal{H}_{code}$ converge. We start from $p\mathcal{H}_{code}$ and include all Cauchy sequences to define $\mathcal{H}_{code}$. If the difference of two Cauchy sequences converges to zero, then we identify the two Cauchy se-

quences for the purposes of defining $\mathcal{H}_{code}$.

The physical pre-Hilbert and Hilbert spaces are defined in a completely analogous way. Each collection consists of four white qutrits. The *physical reference state* for four white qutrits is given by $|\lambda\lambda\rangle := |\lambda\rangle_{\tilde{a}\tilde{d}} |\lambda\rangle_{\tilde{b}\tilde{c}}$ where we are referring to Figure 3.3 to label the qutrits. We choose this reference state for the white qutrits because it is the image of $|\lambda\rangle_{ij}$ under the isometry given by equation (3.50).

15.1.2 The tensor network of isometries

The bulk-to-boundary isometry u is given by a linear norm preserving map $u : \mathcal{H}_{code} \to \mathcal{H}_{phys}$. First, we define its action on $p\mathcal{H}_{code}$ and then use Theorem 3.3.6 to extend its domain to $\mathcal{H}_{code}$. Each vector in $p\mathcal{H}_{code}$ is mapped to a vector in $p\mathcal{H}_{phys}$. The isometry u acts on the basis vector $|M, \{p, q\}\rangle$ by applying the isometry given in equation (3.50) to each collection separately. The state of each black qutrit pair is mapped to a state of four white qutrits. The code reference state is mapped to the physical reference state. Because the map u is linear and norm-preserving, a Cauchy sequence in $p\mathcal{H}_{code}$ is mapped to a Cauchy sequence in $p\mathcal{H}_{phys}$. Thus, we can define u on all of $\mathcal{H}_{code}$.

15.2 Defining von Neumann algebras

Now that we have defined $\mathcal{H}_{code}$ and $\mathcal{H}_{phys}$ and the isometry $u : \mathcal{H}_{code} \to \mathcal{H}_{phys}$, we want to define von Neumann algebras on these Hilbert spaces.

15.2.1 Definition of $\mathcal{M}_{code}$

We now define $\mathcal{M}_{code} \subset \mathcal{B}(\mathcal{H}_{code})$. First, we define a $\star$-algebra called $\mathcal{A}_{code}$ which acts on $p\mathcal{H}_{code}$. Referring to Figure 3.3 for qutrit labels, every operator $a \in \mathcal{A}_{code}$ may be written as

$$a^{(N)} = \sum_{p_1 p_2 \cdots p_N q_1 q_2 \cdots q_N} a_{p_1 p_2 \cdots p_N q_1 q_2 \cdots q_N} \times \left[|p_1\rangle_{i_1} \langle q_1|_{i_1} \otimes I_{j_1} \right] \otimes \left[|p_2\rangle_{i_2} \langle q_2|_{i_2} \otimes I_{j_2} \right] \otimes \cdots \otimes \left[|p_N\rangle_{i_N} \langle q_N|_{i_N} \otimes I_{j_N} \right] \otimes I \cdots , \tag{15.2}$$

where $a_{p_1 p_2 \cdots p_N q_1 q_2 \cdots q_N}$ are the matrix elements of the operator. Each p_k, q_k index ($k \in \{1, 2, \cdots, N\}$) is valued in $\{0, 1, 2\}$ and specifies an orthonormal basis vector of one black qutrit. The $\otimes I \cdots$ means that $a^{(N)}$ acts as the identity on all collections beyond the Nth collection. Each collection is represented by square brackets. The label N may be any natural number. The (N) superscript reminds us of the value of N for this operator. The operator $a^{(N)}$ maps $p\mathcal{H}_{code} \to p\mathcal{H}_{code}$. Because there exists a $K > 0$ such that $||a^{(N)} |\psi\rangle || \leq K || |\psi\rangle ||$ for all $|\psi\rangle \in p\mathcal{H}_{code}$, $a^{(N)}$ is bounded. Thus, $a^{(N)}$ maps Cauchy sequences in $p\mathcal{H}_{code}$ into Cauchy sequences in $p\mathcal{H}_{code}$, and Theorem 3.3.6 implies that $a^{(N)}$ is uniquely defined as a bounded operator acting on $\mathcal{H}_{code}$. The $\star$-algebra $\mathcal{A}_{code}$ is closed under hermitian conjugation and contains the identity.

A sequence of operators $\{a_n\} \in \mathcal{A}_{code}$ converges strongly to an operator in $\mathcal{B}(\mathcal{H}_{code})$ if and only if $\lim_{n\to\infty} a_n |\Psi\rangle$ converges for all $|\Psi\rangle \in \mathcal{H}_{code}$. The $\star$-algebra $\mathcal{A}_{code}$ is not closed under strong limits. The von Neumann algebra $\mathcal{M}_{code}$ is defined to be the closure of $\mathcal{A}_{code}$ in the strong operator topology. We construct $\mathcal{M}_{code}$ from all strongly converging limits of sequences in $\mathcal{A}_{code}$. In topology,

to construct the closure of a set, it is necessary, but generally *not* sufficient, to include limits of converging sequences [264]. We must also include limits of nets, which are more general than sequences. However, it is possible to show that every operator in M_{code} can be written as a strong limit of a sequence in A_{code}. In the next section, we show that the set $S \subset \mathcal{B}(\mathcal{H}_{code})$ of bounded operators that are strong limits of sequences in A_{code} is the smallest strongly closed subset of $\mathcal{B}(\mathcal{H}_{code})$ that contains A_{code}, which implies that $M_{code} = S$. This is because

- S is equal to the commutant of a $\star$-algebra that contains the identity, which is a von Neumann algebra [307]. Because S is a von Neumann algebra, S is strongly closed.
- Any strongly closed subset of $\mathcal{B}(\mathcal{H}_{code})$ that contains A_{code} must contain S because S is defined to only contain all strongly convergent sequences in A_{code}.

We provide explicit details in the next subsection.

15.2.2 The commutant of A_{code} and M_{code}

In this section, we explicitly describe the commutant of A_{code}, which is denoted by A'_{code}. Then, we demonstrate that every operator in M_{code} may be written as a strongly convergent sequence of operators in A_{code}.

An orthonormal basis of $p\mathcal{H}_{code}$ is an orthonormal basis of $\mathcal{H}_{code}$. To see this, let $|\Phi\rangle \in \mathcal{H}_{code}$. Let $\{|\varphi_n\rangle\} \in p\mathcal{H}_{code}$ be a sequence that converges to $|\Phi\rangle$. Suppose that $|\Phi\rangle$ is orthogonal to every orthonormal basis vector of $p\mathcal{H}_{code}$. Using Definition 3.3.2, we need to show that $|\Phi\rangle = 0$. Indeed, $\langle\varphi_n|\Phi\rangle = 0 \ \forall n \in \mathbb{N}$, so $\langle\Phi|\Phi\rangle = 0$. Hence, $|\Phi\rangle = 0$.

Thus, we may define an orthonormal basis of $\mathcal{H}_{code}$ where each basis vector is a finite linear combination of the vectors given in equation (15.1). We will choose an orthonormal basis $|e_i\rangle$, $i \in \mathbb{N}$ such that the first 9^ℓ orthonormal basis vectors in the sequence $\{|e_i\rangle\}$ span the subspace of $p\mathcal{H}_{code}$ where the qutrit pairs in the $(\ell+1)$th collection and beyond are in the reference state $|\lambda\rangle$.

A consequence of Theorem 3.3.9 is that any operator $\mathcal{O} \in \mathcal{B}(\mathcal{H}_{code})$ may be written as the following strong limit:

$$\mathcal{O} = \text{s-lim}_{n\to\infty} \mathcal{O}_n, \quad \mathcal{O}_n := \sum_{i=1}^{9^n} \sum_{j=1}^{9^n} \langle e_i|\mathcal{O}|e_j\rangle \, |e_i\rangle \langle e_j| \, . \tag{15.3}$$

Each operator $\mathcal{O}_n$ acts as the projector onto $|\lambda\rangle$ on the qutrits in the $(n+1)$th collection and beyond. Each $\mathcal{O}_n$ may be written as

$$\begin{aligned} \mathcal{O}_n = \sum_{p_1\cdots p_n q_1\cdots q_n r_1\cdots r_n s_1\cdots s_n} \Big(& \mathcal{O}^n_{p_1\cdots p_n q_1\cdots q_n r_1\cdots r_n s_1\cdots s_n} \\ & \times \left[|p_1\rangle_{i_1} \langle q_1|_{i_1} \otimes |r_1\rangle_{j_1} \langle s_1|_{j_1} \right] \otimes \cdots \otimes \left[|p_n\rangle_{i_n} \langle q_n|_{i_n} \otimes |r_n\rangle_{j_n} \langle s_n|_{j_n} \right] \otimes |\lambda\rangle \langle\lambda| \cdots \Big) \, , \end{aligned} \tag{15.4}$$

where the coefficient of each term of the sum is defined as

$$\begin{aligned} & \mathcal{O}^n_{p_1\cdots p_n q_1\cdots q_n r_1\cdots r_n s_1\cdots s_n} := \\ & \left(\left[\langle p_1|_{i_1} \langle r_1|_{j_1} \right] \otimes \cdots \otimes \left[\langle p_n|_{i_n} \langle r_n|_{j_n} \right] \otimes \langle\lambda| \cdots \right) \mathcal{O} \left(\left[|q_1\rangle_{i_1} |s_1\rangle_{j_1} \right] \otimes \cdots \otimes \left[|q_n\rangle_{i_n} |s_n\rangle_{j_1} \right] \otimes |\lambda\rangle \cdots \right) . \end{aligned} \tag{15.5}$$

The $\otimes |\lambda\rangle \langle\lambda| \cdots$ means that in all collections past the nth collection, $\mathcal{O}_n$ acts as the projector

$|\lambda\rangle\langle\lambda|$. Likewise, $\otimes|\lambda\rangle\cdots$ means that in every collection past the nth collection, the qutrits are in the state $|\lambda\rangle$. Each of the indices p_k,q_k,r_k,s_k ($k \in \{1, 2, \ldots, n\}$) are valued in $\{0, 1, 2\}$ and denote an orthonormal basis vector of a single qutrit.

For each $\mathcal{O}_n$, define the following:

$$\begin{aligned}\hat{\mathcal{O}}_n := \sum_{p_1\cdots p_n q_1\cdots q_n r_1\cdots r_n s_1\cdots s_n} \Big(&\mathcal{O}^n_{p_1\cdots p_n q_1\cdots q_n r_1\cdots r_n s_1\cdots s_n} \\ &\times \left[|p_1\rangle_{i_1}\langle q_1|_{i_1} \otimes |r_1\rangle_{j_1}\langle s_1|_{j_1}\right] \otimes \cdots \otimes \left[|p_n\rangle_{i_n}\langle q_n|_{i_n} \otimes |r_n\rangle_{j_n}\langle s_n|_{j_n}\right] \otimes I \cdots\Big).\end{aligned} \tag{15.6}$$

The projector $|\lambda\rangle\langle\lambda|$ in equation (15.4) has been replaced by the identity operator. For any vector $|\psi\rangle \in p\mathcal{H}_{code}$, we have $\lim_{n\to\infty}\mathcal{O}_n|\psi\rangle = \lim_{n\to\infty}\hat{\mathcal{O}}_n|\psi\rangle$. Also, $||\mathcal{O}_n|| = ||\hat{\mathcal{O}}_n|| \,\forall n \in \mathbb{N}$, so the sequence of norms $\{||\hat{\mathcal{O}}_n||\}$ is bounded because the sequence of norms $\{||\mathcal{O}_n||\}$ is bounded. Because $p\mathcal{H}_{code}$ is dense in $\mathcal{H}_{code}$, $\lim_{n\to\infty}\hat{\mathcal{O}}_n$ converges strongly to $\mathcal{O}$ by Theorem 3.3.5.

Now, we assume that $\mathcal{O} \in \mathcal{A}'_{code}$. The commutant $\mathcal{A}'_{code}$ is a von Neumann algebra because it is the commutant of a $\star$-algebra containing the identity. This assumption restricts what the matrix elements of equation (15.5) can be. By considering the commutator of $\mathcal{O}$ with operators in $\mathcal{A}_{code}$, one finds that $\hat{\mathcal{O}}_n$ can be written as

$$\hat{\mathcal{O}}_n = \sum_{r_1\cdots r_n s_1\cdots s_n} \left(\hat{\mathcal{O}}^n_{r_1\cdots r_n s_1\cdots s_n} \times \left[I_{i_1} \otimes |r_1\rangle_{j_1}\langle s_1|_{j_1}\right] \otimes \cdots \otimes \left[I_{i_n} \otimes |r_n\rangle_{j_n}\langle s_n|_{j_n}\right] \otimes I \cdots\right), \tag{15.7}$$

for some coefficients $\hat{\mathcal{O}}^n_{r_1\cdots r_n s_1\cdots s_n}$. Thus, we have demonstrated that every operator $\mathcal{O} \in \mathcal{A}'_{code}$ can be expressed as $\mathcal{O} = \text{s-}\lim_{n\to\infty}\hat{\mathcal{O}}_n$ where each $\hat{\mathcal{O}}_n$ may be written as above. Furthermore, every such

strong limit is clearly in A'_{code}.

By comparing equation (15.7) with equation (15.2), it is clear the set of operators in A_{code} together with strong limits of sequences in A_{code} (which we called S in the previous subsection) is a von Neumann algebra. In fact, it is the smallest strongly closed subset of $\mathcal{B}(\mathcal{H}_{code})$ containing A_{code}, which is M_{code} by definition. This is because the strong closure of A_{code} must at least contain all strongly convergent sequences of operators in A_{code}. Hence, every operator in M_{code} may be written as a strong limit of a sequence in A_{code}.

Because $M_{code} = \overline{A_{code}} = A''_{code}$, we have that $M'_{code} = A'''_{code} = \overline{A'_{code}} = A'_{code}$. Thus, we see that M'_{code} may be constructed in the same way as M_{code}, except operators in M'_{code} only act nontrivially on the j qutrit in Figure 3.3.

From our explicit construction of M'_{code}, we see that M_{code} and M'_{code} are both factors as $M_{code} \cap M'_{code}$ only consists of scalar multiples of the identity.

15.2.3 Definition of M_{phys} and M'_{phys}

Recall that under the isometry in equation (3.50), the code reference state $|\lambda\rangle$ on the black qutrits i, j in Figure 3.3 is mapped to the state of four white qutrits where the qutrit pairs $\tilde{a}, \tilde{d}$ and $\tilde{b}, \tilde{e}$ are each in the state $|\lambda\rangle$. Thus, both the physical and code pre-Hilbert spaces consist of states of infinitely many qutrit pairs, all but finitely many of which are in the reference state $|\lambda\rangle$. It follows that $\mathcal{H}_{code}$ and $\mathcal{H}_{phys}$ are constructed in the exact same way. We can define a von Neumann algebra $M_{phys} \subset \mathcal{B}(\mathcal{H}_{phys})$ acting on the white qutrits $\tilde{a}, \tilde{b}$ in each collection in the same way we defined M_{code} to act on the black qutrit i. Likewise, the commutant of M_{phys}, denoted by M'_{phys}, acts on white qutrits

$\tilde{d}, \tilde{e}$. Our setup is summarized in Figure 15.1.

15.3 Definition of the tensor network map

Having defined M_{code} and M_{phys}, we define a linear map from M_{code} into M_{phys}. An operator $\mathcal{O} \in M_{code}$ is mapped to $\tilde{\mathcal{O}} \in M_{phys}$. We want the following to hold for all $|\Psi\rangle \in \mathcal{H}_{code}$:

$$u\mathcal{O}\,|\Psi\rangle = \tilde{\mathcal{O}} u\,|\Psi\rangle\,, \quad u\mathcal{O}^\dagger\,|\Psi\rangle = \tilde{\mathcal{O}}^\dagger u\,|\Psi\rangle\,. \tag{15.8}$$

We now describe how to construct this map (which we call the "tensor network map," not to be confused with the map u).

15.3.1 How the tensor network map acts on A_{code}

We first define how the tensor network map acts on operators in A_{code} before generalizing its definition to M_{code}. The operator $a^{(N)}$ in equation (15.2) is mapped to $\tilde{a}^{(N)}$, an operator that acts on $\mathcal{H}_{phys}$. The result is

$$\begin{aligned}\tilde{a}^{(N)} = \sum_{p_1\cdots p_N q_1\cdots q_N} a_{p_1\cdots p_N q_1\cdots q_N} \times \Big[U_{\tilde{a}_1\tilde{b}_1}\,|p_1\rangle_{\tilde{a}_1}\,\langle q_1|_{\tilde{a}_1}\,U^\dagger_{\tilde{a}_1\tilde{b}_1} \otimes I_{\tilde{d}_1\tilde{e}_1}\Big] \\ \otimes\cdots\otimes \Big[U_{\tilde{a}_N\tilde{b}_N}\,|p_N\rangle_{\tilde{a}_N}\,\langle q_N|_{\tilde{a}_N}\,U^\dagger_{\tilde{a}_N\tilde{b}_N} \otimes I_{\tilde{d}_N\tilde{e}_N}\Big] \otimes I\cdots\,,\end{aligned} \tag{15.9}$$

where U is defined in equation (3.51), and the subscripts refer to the specific white qutrits that U is acting on (see Figure 3.3). Given equation (15.9), which shows how $\tilde{a}^{(N)}$ acts on vectors in $p\mathcal{H}_{phys}$, the domain of $\tilde{a}^{(N)}$ may be extended to all of $\mathcal{H}_{phys}$ by demanding that $\tilde{a}^{(N)}$ is a bounded operator

and invoking Theorem 3.3.6. Because $\tilde{a}^{(N)}$ acts trivially on the qutrits $\tilde{d}, \tilde{e}$ in each collection, $\tilde{a}^{(N)} \in \mathcal{M}_{phys}$.

Equation (15.9) simply amounts to applying the map in equation (3.54) for a finite number of collections. It follows that for $a, b \in \mathcal{A}_{code}$, $\alpha, \beta \in \mathbb{C}$, and $|\Upsilon\rangle \in \mathcal{H}_{code}$, the tensor network map has the following properties:

$$\text{1. Bulk Reconstruction :} \quad ua\,|\Upsilon\rangle = \tilde{a}u\,|\Upsilon\rangle\,, \tag{15.10}$$

$$\text{2. Commutativity with hermitian conjugation :} \quad \widetilde{a^\dagger} = \tilde{a}^\dagger, \tag{15.11}$$

$$\text{3. Commutativity with multiplication :} \quad \widetilde{ab} = \tilde{a}\tilde{b}, \tag{15.12}$$

$$\text{4. Linearity :} \quad \widetilde{\alpha a + \beta b} = \alpha\tilde{a} + \beta\tilde{b}, \tag{15.13}$$

$$\text{5. Norm preservation :} \quad ||a|| = ||\tilde{a}||. \tag{15.14}$$

We will prove these properties for all operators in $\mathcal{M}_{code}$ in Section 15.4.

15.3.2 How the tensor network map acts on $\mathcal{M}_{code}$

Now that we specified how the tensor network map acts on $\mathcal{A}_{code}$, we need to specify how it acts on $\mathcal{M}_{code}$. Let $\{a_n\} \in \mathcal{A}_{code}$ be a strongly convergent sequence of operators. The image of each a_n under the tensor network map is $\tilde{a}_n \in \mathcal{B}(\mathcal{H}_{phys})$. We will show that $\{\tilde{a}_n\}$ is a strongly convergent sequence. Then, we will extend the definition of the tensor network map by saying that the strong limit $(\text{s-lim}_{n\to\infty} a_n) \in \mathcal{M}_{code}$ is mapped to the strong limit $(\text{s-lim}_{n\to\infty} \tilde{a}_n) \in \mathcal{M}_{phys}$. We will then prove that this map satisfies equation (15.8).

The fact that s-$\lim_{n\to\infty} a_n$ converges means that the sequence of norms $\{||\tilde{a}_n||\}$ is bounded from above because $||a_n|| = ||\tilde{a}_n|| \, \forall n \in \mathbb{N}$. From Theorem 3.3.5, if $\lim_{n\to\infty} \tilde{a}_n |\psi\rangle$ converges for all $|\psi\rangle \in p\mathcal{H}_{phys}$, then $\lim_{n\to\infty} \tilde{a}_n |\Psi\rangle$ converges for all $|\Psi\rangle \in \mathcal{H}_{phys}$ since $p\mathcal{H}_{phys}$ is dense in $\mathcal{H}_{phys}$. The next theorem is necessary to show that $\lim_{n\to\infty} \tilde{a}_n |\psi\rangle$ converges for all $|\psi\rangle \in p\mathcal{H}_{phys}$.

Theorem 15.3.1. *For any two vectors $|\tilde{\psi}_1\rangle, |\tilde{\psi}_2\rangle \in p\mathcal{H}_{phys}$, we may define a finite number of vectors $|\eta_i\rangle, |\chi_i\rangle \in p\mathcal{H}_{code}$, ($i \in \{1, 2, \ldots, Q\}$ for some $Q \in \mathbb{N}$) such that for any operator $\tilde{a}^{(N)} \in \mathcal{M}_{phys}$ that may be written as the tensor network map image of some $a^{(N)} \in \mathcal{A}_{code}$, we have that*

$$\langle\tilde{\psi}_1|\tilde{a}^{(N)}|\tilde{\psi}_2\rangle = \sum_{i=1}^{Q} \langle\eta_i|a^{(N)}|\chi_i\rangle \, . \tag{15.15}$$

Furthermore, if $|\tilde{\psi}_1\rangle = |\tilde{\psi}_2\rangle$, then we may take $|\eta_i\rangle = |\chi_i\rangle \;\; \forall i$.

Proof. Choose $M \in \mathbb{N}$ such that for both $|\tilde{\psi}_1\rangle$ and $|\tilde{\psi}_2\rangle$, the qutrits in the $(M+1)$th collection and beyond are in the reference state $|\lambda\rangle$. Consider the following set of orthonormal vectors:

$$\begin{aligned} |\{r, \ell, s\}\rangle = &\left[U_{\tilde{a}_1\tilde{b}_1} U_{\tilde{d}_1\tilde{e}_1} |r_1\rangle_{\tilde{a}_1} |\ell_1\rangle_{\tilde{d}_1} |s_1\rangle_{\tilde{b}_1\tilde{e}_1}\right] \otimes \\ &\cdots \otimes \left[U_{\tilde{a}_M\tilde{b}_M} U_{\tilde{d}_M\tilde{e}_M} |r_M\rangle_{\tilde{a}_M} |\ell_M\rangle_{\tilde{d}_M} |s_M\rangle_{\tilde{b}_M\tilde{e}_M}\right] \otimes |\lambda\lambda\rangle \cdots \, , \end{aligned} \tag{15.16}$$

where the labels $\tilde{a}_k$,$\tilde{b}_k$,$\tilde{d}_k$,$\tilde{e}_k$ ($k \in \{1, 2, \ldots, M\}$) refer to the qutrits in the kth collection (see Figure 3.3). Each r_k and ℓ_k index is valued in $\{0, 1, 2\}$ and specifies an orthonormal basis vector of one qutrit. Each s_k index is valued in $\{0, 1, 2, \ldots, 8\}$ and specifies an orthonormal basis vector of two qutrits. The $|\lambda\lambda\rangle \cdots$ means that in all collections past the Mth collection, the qutrits are in the

physical reference state $|\lambda\rangle_{\tilde{a}\tilde{d}} |\lambda\rangle_{\tilde{b}\tilde{e}}$.

We may then write $|\tilde{\psi}_1\rangle$, $|\tilde{\psi}_2\rangle$ as finite linear combinations of the above vectors:

$$|\tilde{\psi}_1\rangle = \sum_{\{s\}} \sum_{\{r,\ell\}} c^1_{\{r,\ell,s\}} \, |\{r,\ell,s\}\rangle \, , \quad |\tilde{\psi}_2\rangle = \sum_{\{s\}} \sum_{\{r,\ell\}} c^2_{\{r,\ell,s\}} \, |\{r,\ell,s\}\rangle \, , \tag{15.17}$$

where $c^1_{\{r,\ell,s\}}$ and $c^2_{\{r,\ell,s\}}$ are $\mathbb{C}$-valued coefficients. Note that $\langle\{r,\ell,s\}|\tilde{a}^{(N)}|\{r',\ell',s'\}\rangle = 0$ if $s_k \neq s'_k$ for any $k \in \{1, 2, \ldots, M\}$. Thus, we write

$$\langle\tilde{\psi}_1|\tilde{a}^{(N)}|\tilde{\psi}_2\rangle = \sum_{\{s\}} \sum_{\{r',\ell'\}} \sum_{\{r,\ell\}} (c^1_{\{r',\ell',s\}})^* \, \langle\{r',\ell',s\}|\tilde{a}^{(N)}|\{r,\ell,s\}\rangle \, c^2_{\{r,\ell,s\}} . \tag{15.18}$$

To calculate $\langle\{r',\ell',s\}|\tilde{a}^{(N)}|\{r,\ell,s\}\rangle$, we must calculate how each term in the sum in equation (15.9) acts on each collection separately. The next three equations apply for a single collection (for simplicity we have suppressed the subscripts labeling the collection).

1. $$\begin{aligned} &\left[U_{\tilde{a}\tilde{b}} U_{\tilde{d}\tilde{e}} \, |r'\rangle_{\tilde{a}} \, |\ell'\rangle_{\tilde{d}} \, |s'\rangle_{\tilde{b}\tilde{e}}\right]^\dagger \left[U_{\tilde{a}\tilde{b}} \, |p\rangle_{\tilde{a}} \, \langle q|_{\tilde{a}} \, U^\dagger_{\tilde{a}\tilde{b}} \otimes I_{\tilde{d}\tilde{e}}\right] \left[U_{\tilde{a}\tilde{b}} U_{\tilde{d}\tilde{e}} \, |r\rangle_{\tilde{a}} \, |\ell\rangle_{\tilde{d}} \, |s\rangle_{\tilde{b}\tilde{e}}\right] \\ &\quad = \left[\langle r'|_{\tilde{a}} \, \langle\ell'|_{\tilde{d}} \, \langle s'|_{\tilde{b}\tilde{e}}\right] \left[|p\rangle_{\tilde{a}} \, \langle q|_{\tilde{a}} \otimes I_{\tilde{b}\tilde{d}\tilde{e}}\right] \left[|r\rangle_{\tilde{a}} \, |\ell\rangle_{\tilde{d}} \, |s\rangle_{\tilde{b}\tilde{e}}\right] , \end{aligned} \tag{15.19}$$

2. $$\left[U_{\tilde{a}\tilde{b}} U_{\tilde{d}\tilde{e}} \, |r'\rangle_{\tilde{a}} \, |\ell'\rangle_{\tilde{d}} \, |s'\rangle_{\tilde{b}\tilde{e}}\right]^\dagger I_{\tilde{a}\tilde{b}\tilde{d}\tilde{e}} \left[U_{\tilde{a}\tilde{b}} U_{\tilde{d}\tilde{e}} \, |r\rangle_{\tilde{a}} \, |\ell\rangle_{\tilde{d}} \, |s\rangle_{\tilde{b}\tilde{e}}\right] = \left[\langle r'|_{\tilde{a}} \, \langle\ell'|_{\tilde{d}} \, \langle s'|_{\tilde{b}\tilde{e}}\right] \left[|r\rangle_{\tilde{a}} \, |\ell\rangle_{\tilde{d}} \, |s\rangle_{\tilde{b}\tilde{e}}\right] , \tag{15.20}$$

3. $$\langle\lambda|_{\tilde{a}\tilde{d}} \, \langle\lambda|_{\tilde{b}\tilde{e}} \left[U_{\tilde{a}\tilde{b}} \, |p\rangle_{\tilde{a}} \, \langle q|_{\tilde{a}} \, U^\dagger_{\tilde{a}\tilde{b}} \otimes I_{\tilde{d}\tilde{e}}\right] |\lambda\rangle_{\tilde{a}\tilde{d}} \, |\lambda\rangle_{\tilde{b}\tilde{e}} = \langle\lambda|_{\tilde{a}\tilde{d}} \left[|p\rangle_{\tilde{a}} \, \langle q|_{\tilde{a}} \otimes I_{\tilde{b}\tilde{d}\tilde{e}}\right] |\lambda\rangle_{\tilde{a}\tilde{d}} \, . \tag{15.21}$$

Next, we define the following vectors in $p\mathcal{H}_{code}$

$$|\{r,\ell\}\rangle := \left[|r_1\rangle_{i_1}|\ell_1\rangle_{j_1}\right] \otimes \left[|r_2\rangle_{i_2}|\ell_2\rangle_{j_2}\right] \otimes \cdots \otimes \left[|r_M\rangle_{i_M}|\ell_M\rangle_{j_M}\right] \otimes |\lambda\rangle \cdots . \tag{15.22}$$

It follows that

$$\langle\tilde{\psi}_1|\tilde{a}^{(N)}|\tilde{\psi}_2\rangle = \sum_{\{s\}}\sum_{\{r',\ell'\}}\sum_{\{r,\ell\}} (c^1_{\{r',\ell',s\}})^* \langle\{r',\ell'\}|a^{(N)}|\{r,\ell\}\rangle c^2_{\{r,\ell,s\}}. \tag{15.23}$$

Then, we can define the new vectors in $p\mathcal{H}_{code}$

$$|\chi_{\{s\}}\rangle := \sum_{\{r\}\{\ell\}} |\{r,\ell\}\rangle c^2_{\{r,\ell,s\}}, \quad |\eta_{\{s\}}\rangle := \sum_{\{r\}\{\ell\}} |\{r,\ell\}\rangle c^1_{\{r,\ell,s\}}, \tag{15.24}$$

so that $\langle\tilde{\psi}_1|\tilde{a}^{(N)}|\tilde{\psi}_2\rangle$ can be expressed as

$$\langle\tilde{\psi}_1|\tilde{a}^{(N)}|\tilde{\psi}_2\rangle = \sum_{\{s\}} \langle\eta_{\{s\}}|a^{(N)}|\chi_{\{s\}}\rangle . \tag{15.25}$$

This demonstrates that we can express $\langle\tilde{\psi}_1|\tilde{a}^{(N)}|\tilde{\psi}_2\rangle$ as in equation (15.15) for $Q = 9^M$. □

Given any $|\tilde{\psi}\rangle \in p\mathcal{H}_{phys}$, Theorem 15.3.1 asserts that we may choose a finite family of vectors $|\psi_i\rangle \in p\mathcal{H}_{code}$ ($i \in \{1, 2, \ldots, Q\}$ for some $Q \in \mathbb{N}$) such that, for any $n, m \in \mathbb{N}$,

$$||(\tilde{a}_n - \tilde{a}_m)|\tilde{\psi}\rangle||^2 = \sum_{i=1}^{Q} ||(a_n - a_m)|\psi_i\rangle||^2. \tag{15.26}$$

This means that if $\{a_n |\psi_i\rangle\}$ is a Cauchy sequence for each i, (which it is by assumption) then $\{\tilde{a}_n |\tilde{\psi}\rangle\}$ is also a Cauchy sequence. This shows that $\lim_{n\to\infty} \tilde{a}_n |\tilde{\psi}\rangle$ converges for any $|\tilde{\psi}\rangle \in p\mathcal{H}_{phys}$. Thus, the strong limit s-$\lim_{n\to\infty} \tilde{a}_n$ exists and defines an operator, which is the *definition* of the image under the tensor network map of the strong limit s-$\lim_{n\to\infty} a_n$. By the definition of $\mathcal{M}_{phys}$, it follows that s-$\lim_{n\to\infty} \tilde{a}_n \in \mathcal{M}_{phys}$.

Suppose that the sequences $\{a_n\} \in \mathcal{A}_{code}$ and $\{b_n\} \in \mathcal{A}_{code}$ converge strongly to the same operator $\mathcal{O}$. Suppose that s-$\lim_{n\to\infty} \tilde{a}_n = \tilde{\mathcal{O}}_1$ and s-$\lim_{n\to\infty} \tilde{b}_n = \tilde{\mathcal{O}}_2$. Then s-$\lim_{n\to\infty}(a_n - b_n) =$ 0, which implies that s-$\lim_{n\to\infty} \widetilde{a_n - b_n}$ = s-$\lim_{n\to\infty}(\tilde{a}_n - \tilde{b}_n) = 0$. Hence, $\tilde{\mathcal{O}}_1 - \tilde{\mathcal{O}}_2 = 0$. Thus, the tensor network map is a well-defined map from $\mathcal{M}_{code}$ into $\mathcal{M}_{phys}$.

15.3.3 How the tensor network map acts on $\mathcal{M}'_{code}$

By construction, the tensor network map is a map from operators in $\mathcal{M}_{code}$ into $\mathcal{M}_{phys}$. Due to the symmetry of the tensor network in Figure 3.3, we can also define the tensor network map on operators in $\mathcal{M}'_{code}$, which are mapped into $\mathcal{M}'_{phys}$ in a completely analogous way.

15.4 Properties of the tensor network map

In this section, we prove that equations (15.10) to (15.14) hold for all operators in $\mathcal{M}_{code}$.

15.4.1 Theorems on strong and weak convergence

The following theorems will be useful in proving some properties of the tensor network map.

Theorem 15.4.1. *Suppose that for a sequence* $\{a_n\} \in \mathcal{A}_{code}$, $\lim_{n\to\infty} \langle \Psi | a_n | \Phi \rangle = 0$ *for any* $|\Psi\rangle, |\Phi\rangle \in \mathcal{H}_{code}$. *Suppose that the sequence of norms* $\{||a_n||\}$ *is bounded from above. Let* $\tilde{a}_n$ *be the image under the tensor network map of* a_n. *Then* $\lim_{n\to\infty} \langle \tilde{\Theta} | \tilde{a}_n | \tilde{\Phi} \rangle = 0$ *for any* $|\tilde{\Theta}\rangle, |\tilde{\Phi}\rangle \in \mathcal{H}_{phys}$.

Proof. Let $\{|\tilde{\theta}_\ell\rangle\}, \{|\tilde{\varphi}_m\rangle\} \in p\mathcal{H}_{phys}$ be Cauchy sequences that converge to $|\tilde{\Theta}\rangle, |\tilde{\Phi}\rangle \in \mathcal{H}_{phys}$ respectively. We may compute

$$|\langle \tilde{\Theta} | \tilde{a}_n | \tilde{\Phi} \rangle| \leq |\langle \tilde{\Theta} | \tilde{a}_n | \tilde{\Phi} - \tilde{\varphi}_m \rangle| + |\langle \tilde{\Theta} - \tilde{\theta}_\ell | \tilde{a}_n | \tilde{\varphi}_m \rangle| + |\langle \tilde{\theta}_\ell | \tilde{a}_n | \tilde{\varphi}_m \rangle|, \tag{15.27}$$

$$|\langle \tilde{\Theta} | \tilde{a}_n | \tilde{\Phi} \rangle| \leq ||\,|\tilde{\Theta}\rangle|| \cdot ||\tilde{a}_n|| \cdot ||\,|\tilde{\Phi}\rangle - |\tilde{\varphi}_m\rangle|| + ||\,|\tilde{\Theta}\rangle - |\tilde{\theta}_\ell\rangle|| \cdot ||\tilde{a}_n|| \cdot ||\,|\tilde{\varphi}_m\rangle|| + |\langle \tilde{\theta}_\ell | \tilde{a}_n | \tilde{\varphi}_m \rangle|, \tag{15.28}$$

$$|\langle \tilde{\Theta} | \tilde{a}_n | \tilde{\Phi} \rangle| \leq K_1 ||\,|\tilde{\Phi}\rangle - |\tilde{\varphi}_m\rangle|| + K_2 ||\,|\tilde{\Theta}\rangle - |\tilde{\theta}_\ell\rangle|| + |\langle \tilde{\theta}_\ell | \tilde{a}_n | \tilde{\varphi}_m \rangle|, \tag{15.29}$$

where K_1, K_2 are some positive real numbers and we used the fact that the sequence $\{||\tilde{a}_n||\}$ is bounded from above. First, fix m, ℓ large enough so that the first two norms on the r.h.s. of equation (15.29) are each less than $\frac{\varepsilon}{3}$. Due to Theorem 15.3.1 and the assumption that w-$\lim_{n\to\infty} a_n = 0$, we have that $\lim_{n\to\infty} \langle \tilde{\theta}_\ell | \tilde{a}_n | \tilde{\varphi}_m \rangle = 0$. Hence, we can choose $N \in \mathbb{N}$ such that for $n > N$, the third norm on the r.h.s. of equation (15.29) is less than $\frac{\varepsilon}{3}$. We conclude that $\lim_{n\to\infty} \langle \tilde{\Theta} | \tilde{a}_n | \tilde{\Phi} \rangle = 0$. □

Theorem 15.4.2. *Let* $\{a_n\} \in \mathcal{A}_{code}$ *be a strongly convergent sequence of operators. Suppose that*

s-$\lim_{n\to\infty} a_n = \mathcal{O}$ *for some* $\mathcal{O} \in M_{code}$. *Then* w-$\lim_{n\to\infty} a_n^\dagger = \mathcal{O}^\dagger$.

Proof. Let $|\Psi\rangle, |\Phi\rangle \in \mathcal{H}_{code}$. Then

$$\langle\Psi|\mathcal{O}^\dagger|\Phi\rangle = \langle\Phi|\mathcal{O}|\Psi\rangle^* = \lim_{n\to\infty} \langle\Phi|a_n|\Psi\rangle^* = \lim_{n\to\infty} \langle\Psi|a_n^\dagger|\Phi\rangle\,, \tag{15.30}$$

so the sequence of operators $\{a_n^\dagger\}$ converges weakly to $\mathcal{O}^\dagger$. Recalling Theorem 3.4.3, we see explicitly that M_{code} is closed under hermitian conjugation. □

15.4.2 The tensor network map is linear

We now demonstrate the linearity of the tensor network map. Consider two sequences of operators in A_{code}, $\{a_n\}$ and $\{b_n\}$, converging strongly to $\mathcal{O}_1$ and $\mathcal{O}_2$ respectively. Then for $\alpha, \beta \in \mathbb{C}$, s-$\lim_{n\to\infty}(\alpha a_n + \beta b_n) = \alpha\mathcal{O}_1 + \beta\mathcal{O}_2$. The image of each a_n is $\tilde{a}_n$ and the image of each b_n is $\tilde{b}_n$. The image of $\alpha\mathcal{O}_1 + \beta\mathcal{O}_2$ under the tensor network map is thus given by $\alpha\tilde{\mathcal{O}}_1 + \beta\tilde{\mathcal{O}}_2$. Hence, the tensor network map is linear when acting on all operators in M_{code}.

15.4.3 The tensor network map commutes with hermitian conjugation

If $\{a_n\} \in A_{code}$ strongly converges to $\mathcal{O}$, then w-$\lim_{n\to\infty} a_n^\dagger = \mathcal{O}^\dagger$ by Theorem 15.4.2. Each a_n is mapped to $\tilde{a}_n$ under the tensor network map, and $\{\tilde{a}_n\}$ strongly converges to $\tilde{\mathcal{O}} \in \mathcal{B}(\mathcal{H}_{phys})$. Each $a_n^\dagger$ is mapped to $\widetilde{a_n^\dagger} = \tilde{a}_n^\dagger$, and w-$\lim_{n\to\infty} \tilde{a}_n^\dagger = (\tilde{\mathcal{O}})^\dagger$. Since M_{code} is defined from A_{code} by taking strong limits, there must exist a sequence $\{b_n\} \in A_{code}$ that converges strongly to $\mathcal{O}^\dagger$. Then, s-$\lim_{n\to\infty} \tilde{b}_n = \widetilde{\mathcal{O}^\dagger}$. Note that, for any two $|\Psi\rangle, |\Phi\rangle \in \mathcal{H}_{code}$, $\lim_{n\to\infty} \langle\Psi|(a_n^\dagger - b_n)|\Phi\rangle = 0$.

The sequence of norms $\{||a_n^\dagger - b_n||\}$ is bounded above because $||a_n^\dagger|| = ||a_n|| \; \forall n \in \mathbb{N}$ and $\{a_n\}$ and $\{b_n\}$ converge strongly. Furthermore, for any $|\tilde{\Psi}\rangle, |\tilde{\Phi}\rangle \in \mathcal{H}_{phys}$, $\lim_{n\to\infty} \langle\tilde{\Psi}|\widetilde{(a_n^\dagger - b_n)}|\tilde{\Phi}\rangle = \langle\tilde{\Psi}|(\tilde{\mathcal{O}}^\dagger - \widetilde{\mathcal{O}^\dagger})|\tilde{\Phi}\rangle$. Applying Theorem 15.4.1, $\langle\tilde{\Psi}|(\tilde{\mathcal{O}}^\dagger - \widetilde{\mathcal{O}^\dagger})|\tilde{\Phi}\rangle = 0$, hence $\tilde{\mathcal{O}}^\dagger = \widetilde{\mathcal{O}^\dagger}$.

15.4.4 The tensor network map commutes with multiplication

Given $\mathcal{O}_1, \mathcal{O}_2 \in M_{code}$, we now show that $\widetilde{\mathcal{O}_1\mathcal{O}_2} = \tilde{\mathcal{O}}_1\tilde{\mathcal{O}}_2$. Let $\{a_n\} \in A_{code}$ converge strongly to $\mathcal{O}_1^\dagger$. Let $\{b_n\} \in A_{code}$ converge strongly to $\mathcal{O}_2$. Let $\{c_n\} \in A_{code}$ converge strongly to $\mathcal{O}_1\mathcal{O}_2$. For any $|\Psi\rangle, |\Phi\rangle \in \mathcal{H}_{code}$,

$$\lim_{n\to\infty} \langle(a_n - \mathcal{O}_1^\dagger)\Psi|(b_n - \mathcal{O}_2)\Phi\rangle = 0, \tag{15.31}$$

which implies that

$$\lim_{n\to\infty} \langle\Psi|a_n^\dagger b_n - c_n|\Phi\rangle = 0. \tag{15.32}$$

The sequence of norms $\{||a_n^\dagger b_n - c_n||\}$ is bounded. By Theorem 15.4.1, we have that, for all $|\tilde{\Psi}\rangle, |\tilde{\Phi}\rangle \in \mathcal{H}_{phys}$,

$$\lim_{n\to\infty} \langle\tilde{\Psi}|\tilde{a}_n^\dagger\tilde{b}_n - \tilde{c}_n|\tilde{\Phi}\rangle = 0. \tag{15.33}$$

It follows that

$$\langle\tilde{\Psi}|\tilde{\mathcal{O}}_1\tilde{\mathcal{O}}_2|\tilde{\Phi}\rangle = \langle\tilde{\Psi}|\widetilde{\mathcal{O}_1\mathcal{O}_2}|\tilde{\Phi}\rangle. \tag{15.34}$$

15.4.5 The tensor network map preserves the norm

Consider any $|\tilde{\psi}\rangle \in p\mathcal{H}_{phys}$. By Theorem 15.3.1, there exists a finite family of vectors $|\psi_i\rangle \in p\mathcal{H}_{code}$, ($i \in \{1, 2, \ldots, Q\}$ for some $Q \in \mathbb{N}$) such that for any $a \in \mathcal{A}_{code}$,

$$\langle\tilde{\psi}|\tilde{a}|\tilde{\psi}\rangle = \sum_{i=1}^{Q} \langle\psi_i|a|\psi_i\rangle \,. \tag{15.35}$$

Consider a sequence $\{a_n\} \in \mathcal{A}_{code}$ that strongly converges to $\mathcal{O} \in \mathcal{M}_{code}$. Then we have

$$\lim_{n\to\infty} \langle\tilde{\psi}|\tilde{a}_n|\tilde{\psi}\rangle = \sum_{i=1}^{Q} \lim_{n\to\infty} \langle\psi_i|a_n|\psi_i\rangle \,, \tag{15.36}$$

$$\langle\tilde{\psi}|\tilde{\mathcal{O}}|\tilde{\psi}\rangle = \sum_{i=1}^{Q} \langle\psi_i|\mathcal{O}|\psi_i\rangle \,. \tag{15.37}$$

In particular, for any $\mathcal{O} \in \mathcal{M}_{code}$, we have that

$$\langle\tilde{\mathcal{O}}\tilde{\psi}|\tilde{\mathcal{O}}\tilde{\psi}\rangle = \sum_{i=1}^{Q} \langle\mathcal{O}\psi_i|\mathcal{O}\psi_i\rangle \,. \tag{15.38}$$

The norms of $|\tilde{\psi}\rangle$ and $\tilde{\mathcal{O}}\,|\tilde{\psi}\rangle$ may be expressed as

$$||\,|\tilde{\psi}\rangle\,|| = \sqrt{\sum_{i=1}^{Q} ||\,|\psi\rangle_i\,||^2}, \quad ||\tilde{\mathcal{O}}\,|\tilde{\psi}\rangle\,|| = \sqrt{\sum_{i=1}^{Q} ||\mathcal{O}\,|\psi_i\rangle\,||^2}. \tag{15.39}$$

Thus,

$$||\tilde{\mathcal{O}}\,|\tilde{\psi}\rangle\,|| \leq ||\mathcal{O}||\sqrt{\sum_{i=1}^{Q} ||\,|\psi_i\rangle\,||^2} = ||\mathcal{O}|| \cdot ||\,|\tilde{\psi}\rangle\,||. \tag{15.40}$$

Note that we may choose $|\tilde{\psi}\rangle$ such that $Q = 1$ and $||\mathcal{O}\,|\psi_1\rangle\,|| - ||\mathcal{O}|| \cdot ||\,|\psi_1\rangle\,||$ is arbitrarily close to zero. Hence, we may choose $|\tilde{\psi}\rangle$ such that $||\tilde{\mathcal{O}}\,|\tilde{\psi}\rangle\,|| - ||\mathcal{O}|| \cdot ||\,|\tilde{\psi}\rangle\,||$ is arbitrarily close to zero. It follows from the fact that $p\mathcal{H}_{phys}$ is dense in $\mathcal{H}_{phys}$ and Theorem 3.3.6 that

$$||\tilde{\mathcal{O}}|| = ||\mathcal{O}||. \tag{15.41}$$

15.4.6 The tensor network map satisfies bulk reconstruction

Theorem 15.4.3. *Let $\mathcal{O} \in M_{code}$. Let $\tilde{\mathcal{O}} \in M_{phys}$ be the image of $\mathcal{O}$ under the tensor network map. Let $|\Psi\rangle \in \mathcal{H}_{code}$. Then*

$$u\mathcal{O}\,|\Psi\rangle = \tilde{\mathcal{O}}u\,|\Psi\rangle\,. \tag{15.42}$$

Proof. Let $\{a_n\} \in A_{code}$ be a sequence that converges strongly to $\mathcal{O} \in M_{code}$. Let $\tilde{a}_n \in M_{phys}$ be the image under the tensor network map of a_n for every $n \in \mathbb{N}$. By the definition of the tensor network map, s-$\lim_{n\to\infty} \tilde{a}_n = \tilde{\mathcal{O}}$. It follows that

$$\tilde{\mathcal{O}}u\,|\Psi\rangle = \lim_{n\to\infty} \tilde{a}_n u\,|\Psi\rangle = \lim_{n\to\infty} ua_n\,|\Psi\rangle = u \lim_{n\to\infty} a_n\,|\Psi\rangle = u\mathcal{O}\,|\Psi\rangle\,. \tag{15.43}$$

□

This theorem demonstrates the bulk reconstruction property of the tensor network map. We can

linearly map a given operator $\mathcal{O} \in M_{code}$ to an operator $\tilde{\mathcal{O}} \in M_{phys}$ such that for all $|\Psi\rangle \in \mathcal{H}_{code}$,

$$u\mathcal{O}\,|\Psi\rangle = \tilde{\mathcal{O}}u\,|\Psi\rangle\,, \quad u\mathcal{O}^\dagger\,|\Psi\rangle = \widetilde{\mathcal{O}^\dagger}u\,|\Psi\rangle = \tilde{\mathcal{O}}^\dagger u\,|\Psi\rangle\,. \tag{15.44}$$

By the symmetry of the tensor network in Figure 3.3, any operator $\mathcal{O}' \in M'_{code}$ can be linearly mapped to $\tilde{\mathcal{O}}' \in M'_{phys}$ such that for all $|\Psi\rangle \in \mathcal{H}_{code}$,

$$u\mathcal{O}'\,|\Psi\rangle = \tilde{\mathcal{O}}'u\,|\Psi\rangle\,, \quad u\mathcal{O}'^\dagger\,|\Psi\rangle = \widetilde{\mathcal{O}'^\dagger}u\,|\Psi\rangle = \tilde{\mathcal{O}}'^\dagger u\,|\Psi\rangle\,. \tag{15.45}$$

15.5 Cyclic and separating vectors

In this section we identify a set of cyclic and separating vectors with respect to M_{code} that is dense in $\mathcal{H}_{code}$. Then, we prove that all cyclic and separating vectors with respect to M_{code} are mapped to cyclic and separating vectors with respect to M_{phys} via the isometry u. This shows that our infinite-dimensional QECC satisfies the assumptions of Theorem 3.0.1.

Theorem 15.5.1. *Cyclic and separating vectors with respect to M_{code} are dense in $\mathcal{H}_{code}$.*

Proof. Since $p\mathcal{H}_{code}$ is dense in $\mathcal{H}_{code}$, any vector in $\mathcal{H}_{code}$ is arbitrarily close to a vector in $p\mathcal{H}_{code}$, which may be denoted as $|\psi\rangle \otimes |\lambda\rangle \cdots$, where $|\psi\rangle$ is a vector in a finite dimensional Hilbert space $\mathcal{H}$ that consists of finitely many pairs of qutrits. We may write $\mathcal{H} = \mathcal{H}_i \otimes \mathcal{H}_j$ where $\mathcal{H}_i$ consists of the black qutrits labeled by i (see Figures 3.3 and 15.1), and $\mathcal{H}_j$ consists of the black qutrits labeled by j. The vector $|\psi\rangle$ is arbitrarily close to a vector of maximal Schmidt number (with respect to this factorization), which we will denote by $|\psi'\rangle$. Hence, any vector in $\mathcal{H}_{code}$ is arbitrarily close to a vector

of the form $|\psi'\rangle \otimes |\lambda\rangle \cdots \in \mathcal{H}_{code}$ where $|\psi'\rangle$ has maximal Schmidt number under the factorization $\mathcal{H} = \mathcal{H}_i \otimes \mathcal{H}_j$, so we just need to show that such vectors are cyclic and separating.

The vector $|\psi'\rangle \otimes |\lambda\rangle \cdots \in \mathcal{H}_{code}$ is cyclic with respect to M_{code} because operators in $A_{code} \subset M_{code}$ may act on it to obtain any vector in $p\mathcal{H}_{code}$, and $p\mathcal{H}_{code}$ is dense in $\mathcal{H}_{code}$. Furthermore, $|\psi'\rangle \otimes |\lambda\rangle \cdots$ is certainly separating with respect to A_{code} as one can see from the definition of A_{code} in equation (15.2). To see that $|\psi'\rangle \otimes |\lambda\rangle \cdots$ is separating with respect to all of M_{code}, note that the same logic as above implies that $|\psi'\rangle \otimes |\lambda\rangle \cdots$ is cyclic with respect to M'_{code}. Hence, $|\psi'\rangle \otimes |\lambda\rangle \cdots$ is separating with respect to M_{code}. □

Alternative Proof. We now give an alternative and more explicit proof of the fact that $|\psi'\rangle \otimes |\lambda\rangle \cdots$ is separating with respect to all of M_{code}. Given a sequence $\{a_n\} \in A_{code}$ that strongly converges to $\mathcal{O} \in M_{code}$ we need to show that $\mathcal{O}(|\psi'\rangle \otimes |\lambda\rangle \cdots) = 0$ implies that $\mathcal{O}$ annihilates every vector in $p\mathcal{H}_{code}$ (which would imply that $\mathcal{O}$ annihilates every Cauchy sequence and hence every vector in $\mathcal{H}_{code}$).

First, we will construct a suitable (yet overcomplete) basis of $p\mathcal{H}_{code}$. Let us assume that $|\psi'\rangle$ is a state of the black qutrits in the first M collections. Since $|\psi'\rangle$ is a vector in a finite dimensional factorized Hilbert space with maximal Schmidt number, we may write it as

$$|\psi'\rangle = \sum_{k=1}^{3^M} \alpha_k |e_k\rangle_i \otimes |f_k\rangle_j , \tag{15.46}$$

where α_k are nonzero coefficients that satisfy $\sum_{k=1}^{3^M} |\alpha_k|^2 = 1$, $|e_k\rangle_i$ is an orthonormal basis of the i black qutrits in the first M collections and $|f_k\rangle_j$ is an orthonormal basis of the j black qutrits in the

first M collections.

We consider the following vectors in $p\mathcal{H}_{code}$, which form a basis. Assume that $L \geq M$.

$$\begin{aligned} &|L, k, k', p_{M+1}, \cdots, p_L, q_{M+1}, \cdots, q_L\rangle = \\ &\quad |e_k\rangle_i \otimes |f_{k'}\rangle_j \otimes \left[|p_{M+1}\rangle_{i_{M+1}} |q_{M+1}\rangle_{j_{M+1}}\right] \otimes \cdots \otimes \left[|p_L\rangle_{i_L} |q_L\rangle_{j_L}\right] \otimes |\lambda\rangle \cdots \end{aligned} \tag{15.47}$$

where k and k' each label a basis vector for their respective black qutrits in the first M collections, and p_ℓ and q_ℓ ($\ell \in \{1, 2, \ldots, M\}$) each run over the three orthonormal basis vectors of their respective black qutrits in the ith collection. All black qutrit pairs past the Lth collection are in the reference state $|\lambda\rangle$.

We first consider the basis vectors that satisfy $L = M$. The vectors $|M, k, k'\rangle$ and $|M, \hat{k}, \hat{k}'\rangle$ are orthogonal for $k' \neq \hat{k}'$. This is also true for the vectors $\mathcal{O}|M, k, k'\rangle$ and $\mathcal{O}|M, \hat{k}, \hat{k}'\rangle$ since $\mathcal{O}$ is a limit of operators which act as the identity on $|f_{k'}\rangle$ in equation (15.47). Since $\sum_{k=1}^{3^M} \alpha_k |M, k, k\rangle = |\psi'\rangle \otimes |\lambda\rangle \cdots$, then $\mathcal{O}(|\psi'\rangle \otimes |\lambda\rangle \cdots) = 0$ implies that $\mathcal{O}|M, k, k\rangle = 0$ for all k. Let $\mathcal{U} \in A_{code}$ be an operator that acts as the identity operator on every vector in the tensor product in equation (15.47) except that it may act arbitrarily on $|f_{k'}\rangle$. We can choose $\mathcal{U}$ to send $|f_k\rangle$ to $|f_w\rangle$ for $w \neq k$. Because $\mathcal{U}$ commutes with $\mathcal{O}$, we have that $0 = \mathcal{U}\mathcal{O}|M, k, k\rangle = \mathcal{O}|M, k, w\rangle$ and hence $\mathcal{O}$ annihilates every basis vector with $L = M$. This argument can be repeated in a completely analogous way for the case $L > M$ (since $|\psi'\rangle \otimes |\lambda\rangle \cdots = (|\psi'\rangle \otimes |\lambda\rangle) \otimes |\lambda\rangle \cdots$ and $|\psi'\rangle \otimes |\lambda\rangle$ has maximal Schmidt number) to show that $\mathcal{O}$ annihilates all vectors in $p\mathcal{H}_{code}$, and hence all of $\mathcal{H}_{code}$.

□

Recall that a vector is cyclic and separating for M_{code} if and only if it is cyclic and separating for M'_{code} [307]. Hence, cyclic and separating vectors for M'_{code} are also dense in $\mathcal{H}_{code}$.

Theorem 15.5.2 ([185]). *If $|\Psi\rangle \in \mathcal{H}_{code}$ is cyclic and separating with respect to M_{code}, then $u|\Psi\rangle \in \mathcal{H}_{phys}$ is cyclic and separating with respect to M_{phys}.*

Proof. To show that $u|\Psi\rangle$ is cyclic, we need to show that given any $|\tilde{\Phi}\rangle \in \mathcal{H}_{phys}$ and $\varepsilon > 0$, we can choose an operator $\mathcal{P} \in M_{phys}$ such that $||\mathcal{P}u|\Psi\rangle - |\tilde{\Phi}\rangle|| < \varepsilon$.

Choose $|\tilde{\varphi}\rangle \in p\mathcal{H}_{phys}$ such that $||\,|\tilde{\varphi}\rangle - |\tilde{\Phi}\rangle\,|| < \frac{\varepsilon}{2}$. Let $|\tilde{\lambda}\cdots\rangle \in p\mathcal{H}_{phys}$ denote the vector for which all boundary qutrit pairs are in the reference state $|\lambda\rangle$. Choose an operator $\hat{\mathcal{P}} \in M_{phys}$ such that $\hat{\mathcal{P}}|\tilde{\lambda}\cdots\rangle = |\tilde{\varphi}\rangle$. Choose $\mathcal{O} \in M_{code}$ such that $||\mathcal{O}|\Psi\rangle - |\lambda\cdots\rangle|| < \frac{\varepsilon}{2||\hat{\mathcal{P}}||}$, where $|\lambda\cdots\rangle \in p\mathcal{H}_{code}$ is the vector for which all qutrit pairs are in the reference state $|\lambda\rangle$. Let $\tilde{\mathcal{O}}$ denote the image of $\mathcal{O}$ under the tensor network map.

Note that

$$|\tilde{\Phi}\rangle - \hat{\mathcal{P}}\tilde{\mathcal{O}}u|\Psi\rangle = |\tilde{\Phi}\rangle - |\tilde{\varphi}\rangle - \hat{\mathcal{P}}u(\mathcal{O}|\Psi\rangle - |\lambda\cdots\rangle). \tag{15.48}$$

Hence,

$$||\,|\tilde{\Phi}\rangle - \hat{\mathcal{P}}\tilde{\mathcal{O}}u|\Psi\rangle\,|| \leq ||\,|\tilde{\Phi}\rangle - |\tilde{\varphi}\rangle\,|| + ||\hat{\mathcal{P}}u(\mathcal{O}|\Psi\rangle - |\lambda\cdots\rangle)||, \tag{15.49}$$

$$||\,|\tilde{\Phi}\rangle - \hat{\mathcal{P}}\tilde{\mathcal{O}}u|\Psi\rangle\,|| \leq ||\,|\tilde{\Phi}\rangle - |\tilde{\varphi}\rangle\,|| + ||\hat{\mathcal{P}}|| \cdot ||(\mathcal{O}|\Psi\rangle - |\lambda\cdots\rangle)||, \tag{15.50}$$

$$||\,|\tilde{\Phi}\rangle - \hat{\mathcal{P}}\tilde{\mathcal{O}}u|\Psi\rangle\,|| < \varepsilon. \tag{15.51}$$

We take $\mathcal{P} = \hat{\mathcal{P}}\tilde{\mathcal{O}}$. This shows that $u\,|\Upsilon\rangle$ is cyclic with respect to M_{phys}. A completely analogous argument shows that $u\,|\Upsilon\rangle$ is cyclic with respect to M'_{phys}, so it is also separating with respect to M_{phys}. □

15.6 M_{code} is a hyperfinite type II_1 factor

In this section, we prove that M_{code} satisfies the assumptions of Theorem 3.4.13, from which it follows that M_{code} is a type II_1 factor. The same argument shows that M'_{code}, M_{phys}, and M'_{phys} are also type II_1 factors.

For $\mathcal{O} \in M_{code}$, define the following linear function from $M_{code} \to \mathbb{C}$:

$$T(\mathcal{O}) := \langle \lambda \cdots | \mathcal{O} | \lambda \cdots \rangle \,, \tag{15.52}$$

where $|\lambda \cdots\rangle \in \mathcal{H}_{code}$ is the vector for which all pairs of black qutrits are in the state $|\lambda\rangle$. This clearly satisfies $T(\mathcal{O}^\dagger \mathcal{O}) \geq 0$, $T(I) = 1$, and $T(\mathcal{O}^\dagger) = T^*(\mathcal{O})$.[4]

For any operator $\mathcal{O}_1 \in M_{code}$, it is possible to choose a neighborhood $\mathcal{N}$ of $\mathcal{O}_1$ in the ultraweak operator topology such that $|T(\mathcal{O}_2) - T(\mathcal{O}_1)| < \varepsilon$ for all $\mathcal{O}_2 \in \mathcal{N}$. We may pick the neighborhood to be

$$\mathcal{N} = \{\mathcal{O}_2 \in M_{code} : |\, \langle \lambda \cdots | (\mathcal{O}_1 - \mathcal{O}_2) | \lambda \cdots \rangle \,| < \varepsilon\}. \tag{15.53}$$

Hence, T is ultraweakly continuous.

For $a, b \in A_{code}$, it is easy to check that $T(ab) = T(ba)$. Since operators in M_{code} may be written

[4] The identity operator is denoted by I.

as strong limits of operators in A_{code}, $T(\mathcal{O}_1\mathcal{O}_2) = T(\mathcal{O}_2\mathcal{O}_1) \quad \forall \mathcal{O}_1, \mathcal{O}_2 \in M_{code}$.

For $\mathcal{O} \in M_{code}$, $T(\mathcal{O}^\dagger\mathcal{O}) = 0$ implies that $\mathcal{O} = 0$ because $|\lambda \cdots\rangle$ is separating with respect to M_{code}. Hence, T is faithful.

On a finite dimensional Hilbert space $\mathcal{H}$, any linear map $F : \mathcal{B}(\mathcal{H}) \to \mathbb{C}$ that satisfies $F(\mathcal{O}_1\mathcal{O}_2) = F(\mathcal{O}_2\mathcal{O}_1)\ \forall \mathcal{O}_1,\ \mathcal{O}_2 \in \mathcal{B}(\mathcal{H})$ is proportional to the trace on $\mathcal{H}$. It follows that for any linear map $\mathcal{T} : M_{code} \to \mathbb{C}, \mathcal{T}(a)$ for $a \in A_{code}$ is completely determined by the conditions such that $\mathcal{T}$ is linear, $\mathcal{T}(ab) = \mathcal{T}(ba)$ for $a, b \in A_{code}$, and $\mathcal{T}(I) = 1$. If $\mathcal{T}(a)$ is known for $a \in A_{code}$ and $\mathcal{T}$ is ultraweakly continuous, then the fact that M_{code} is the strong closure of A_{code} completely determines $\mathcal{T}(\mathcal{O})$ for all $\mathcal{O} \in M_{code}$. Hence, T is the only ultraweakly continuous normalized linear functional from $M_{code} \to \mathbb{C}$ that satisfies $T(\mathcal{O}_1\mathcal{O}_2) = T(\mathcal{O}_2\mathcal{O}_1)$ for all $\mathcal{O}_1, \mathcal{O}_2 \in M_{code}$.

Now, we may apply Theorem 3.4.13, where $\mathrm{tr}(\mathcal{O}) = T(\mathcal{O})$ for $\mathcal{O} \in M_{code}$. Thus, M_{code} is a type II_1 factor.

Recall that a von Neumann algebra M is *hyperfinite* if $M = (\cup_n M_n)''$ where, for each $n \in \mathbb{N}$, each von Neumann subalgebra $M_n \subset M$ is finite-dimensional and $M_n \subset M_{n+1}$. The von Neumann algebra M_{code} is hyperfinite because $M_{code} = A''_{code}$, and $A_{code} = \cup_N A_N$ where A_N is the algebra of operators that can be written as $a^{(N)}$ in equation (15.2). Each A_N is a finite dimensional algebra consisting of operators that act nontrivially on finitely many qutrits.

15.6.1 More on the uniqueness of $T : M_{code} \to \mathbb{C}$

Now, we explicitly show that for an ultraweakly continuous linear map $\mathcal{T} : M_{code} \to \mathbb{C}, \mathcal{T}(\mathcal{O})$ for $\mathcal{O} \in M_{code}$ is completely determined given the value of $\mathcal{T}(a)$ for every $a \in A_{code}$.

The statement that $\mathcal{T}(\mathcal{O})$ is an ultraweakly continuous function of $\mathcal{O} \in M_{code}$ implies that for any $\mathcal{O}_1 \in M_{code}$ and any $\varepsilon > 0$, there exists a neighborhood $\mathcal{N}$ of $\mathcal{O}_1$ in the ultraweak operator topology such that for all operators $\mathcal{O}_2 \in \mathcal{N}$, $|\mathcal{T}(\mathcal{O}_2) - \mathcal{T}(\mathcal{O}_1)| < \varepsilon$. We may assume that $\mathcal{N}$ is given by

$$\mathcal{N} = \{\mathcal{O}_2 \in M_{code} : \sum_{i=1}^{\infty} |\langle \eta_i | (\mathcal{O}_1 - \mathcal{O}_2) | \xi_i \rangle| < \varepsilon\}, \tag{15.54}$$

for some $\varepsilon > 0$ and some choice of sequences $\{|\xi_i\rangle\}$ and $\{|\eta_i\rangle\}$ satisfying

$$\sum_{i=1}^{\infty} (|| \, |\xi_i\rangle \, ||^2 + || \, |\eta_i\rangle \, ||^2) < \infty. \tag{15.55}$$

Given $\mathcal{O}_1 \in M_{code}$, let $\{a_n\} \in A_{code}$ be a sequence of operators that converges strongly to $\mathcal{O}_1$. We need to show that for any choice of ε and $\{|\xi_i\rangle\}, \{|\eta_i\rangle\}$, there exists an $N \in \mathbb{N}$ such that $n > N \implies a_n \in \mathcal{N}$. We calculate

$$\begin{aligned}
&\sum_{i=1}^{\infty} |\langle \eta_i | (\mathcal{O}_1 - a_n) | \xi_i \rangle| = \sum_{i=1}^{M-1} |\langle \eta_i | (\mathcal{O}_1 - a_n) | \xi_i \rangle| + \sum_{i=M}^{\infty} |\langle \eta_i | (\mathcal{O}_1 - a_n) | \xi_i \rangle|, \\
&\sum_{i=M}^{\infty} |\langle \eta_i | (\mathcal{O}_1 - a_n) | \xi_i \rangle| \leq \sum_{i=M}^{\infty} \frac{||\mathcal{O}_1 - a_n||}{2} (|| \, |\xi_i\rangle \, ||^2 + || \, |\eta_i\rangle \, ||^2) \leq K \sum_{i=M}^{\infty} (|| \, |\xi_i\rangle \, ||^2 + || \, |\eta_i\rangle \, ||^2),
\end{aligned} \tag{15.56}$$

for some $K > 0$. We used the fact that the sequence of norms $\{||\mathcal{O}_1 - a_n||\}$ is bounded. First, choose M so that

$$K \sum_{i=M}^{\infty} (|| \, |\xi_i\rangle \, ||^2 + || \, |\eta_i\rangle \, ||^2) < \frac{\varepsilon}{2}. \tag{15.57}$$

Then, choose N so that for all $n > N$,

$$\sum_{i=1}^{M-1} |\langle \eta_i | (\mathcal{O}_1 - a_n) | \xi_i \rangle| < \frac{\varepsilon}{2}. \tag{15.58}$$

Hence for any $\varepsilon > 0$, it is possible to choose an $N \in \mathbb{N}$ such that for $n > N$, $|\mathcal{T}(\mathcal{O}_1) - \mathcal{T}(a_n)| < \varepsilon$. Then we can conclude that

$$\lim_{n\to\infty} \mathcal{T}(a_n) = \mathcal{T}(\mathcal{O}_1). \tag{15.59}$$

If $\mathcal{T}(a)$ is known for all $a \in \mathcal{A}_{code}$, then $\mathcal{T}(\mathcal{O})$ is known for all $\mathcal{O} \in \mathcal{M}_{code}$.

15.7 The relative Tomita operator

In this section, we study the relative Tomita operator defined on $\mathcal{H}_{code}$. See Section 3 of [185] for a review of Tomita-Takesaki theory. Given $|\Psi\rangle, |\Phi\rangle \in \mathcal{H}_{code}$, the relative Tomita operator with respect to $\mathcal{M}_{code}$ is denoted by $S^c_{\Psi|\Phi}$. For $\mathcal{O} \in \mathcal{M}_{code}$,

$$S^c_{\Psi|\Phi} \mathcal{O} |\Psi\rangle = \mathcal{O}^\dagger |\Phi\rangle . \tag{15.60}$$

The vector $|\Psi\rangle$ must be cyclic and separating with respect to $\mathcal{M}_{code}$, but $|\Phi\rangle$ can be anything. In this section, we show that $S^c_{\Psi|\Phi}$ can be bounded or unbounded, depending on the choice of $|\Psi\rangle$ and $|\Phi\rangle$. In Section 15.7.1, we compute the norm of the relative Tomita operator for a general, finite-dimensional Hilbert space. In Sections 15.7.2 and 15.7.3, we provide one example in our setup where $S^c_{\Psi|\Phi}$ is bounded, and one example where $S^c_{\Psi|\Phi}$ is unbounded.

15.7.1 Norm of the Tomita operator in a finite-dimensional Hilbert space

In this section we consider a Hilbert space $\mathcal{H} = \mathcal{H}_1 \otimes \mathcal{H}_2$ for finite dimensional Hilbert spaces $\mathcal{H}_1$ and $\mathcal{H}_2$ with equal dimension D. We want to compute the norm of the relative Tomita operator $S_{\Psi|\Phi}$ defined with respect to the algebra of operators acting on $\mathcal{H}_1$. First, we perform Schmidt decompositions of $|\Psi\rangle$ and $|\Phi\rangle$:

$$|\Psi\rangle = \sum_{k=1}^{D} \alpha_k |e_k\rangle \otimes |f_k\rangle , \quad |\Phi\rangle = \sum_{k=1}^{D} \beta_k |g_k\rangle \otimes |h_k\rangle , \tag{15.61}$$

where $|e_k\rangle$ and $|g_k\rangle$ ($k \in \{1, 2, \ldots, D\}$) are orthonormal bases of $\mathcal{H}_1$ and $|f_k\rangle$ and $|h_k\rangle$ are orthonormal bases of $\mathcal{H}_2$. All of the α_k coefficients must be nonzero. The action of $S_{\Psi|\Phi}$ on any normalized state is given by

$$S_{\Psi|\Phi} \sum_{i=1,j=1}^{D} c_{ij} |e_j\rangle \otimes |f_i\rangle = \sum_{i=1,j=1,k=1}^{D} \frac{c_{ij}^*}{\alpha_i^*} \beta_k \langle e_j|g_k\rangle |e_i\rangle \otimes |h_k\rangle , \tag{15.62}$$

where $\sum_{i=1,j=1}^{D} |c_{ij}|^2 = 1$. The norm of $S_{\Psi|\Phi}$ is found by maximizing the norm of the right hand side above with respect to the coefficients c_{ij}, subject to the normalization constraint. One finds that

$$||S_{\Psi|\Phi}|| = \frac{\max_{k=1}^{D} |\beta_k|}{\min_{k=1}^{D} |\alpha_k|}. \tag{15.63}$$

15.7.2 Example where $S^c_{\Upsilon|\Phi}$ is bounded

In this section, we show that it is possible to choose states for which the relative Tomita operator is bounded. We consider as a special case $S^c_{\psi|\varphi}$ for $|\psi\rangle, |\varphi\rangle \in p\mathcal{H}_{code}$. Suppose that for $|\psi\rangle$ (resp. $|\varphi\rangle$), the qutrit pairs in the n_ψth (resp. n_φth) collection and beyond are in the reference state $|\lambda\rangle$. We note that there are many choices of n_ψ and n_φ, but our argument is independent of the choice we make.

We consider a finite case of n by letting $n = \max(n_\Psi, n_\Phi)$. By considering equation (15.60) for the case that $\mathcal{O}$ can be written as $a^{(N)}$ in equation (15.2) with $N = n - 1$, we may see how $S^c_{\psi|\varphi}$ acts on any vector in $p\mathcal{H}_{code}$ for which the qutrit pairs in the nth collection and beyond are in the reference state $|\lambda\rangle$. Let us temporarily restrict our attention to the 9^{n-1}-dimensional Hilbert subspace spanned by these vectors, which may be written as $\mathcal{H}_i \otimes \mathcal{H}_j$, where $\mathcal{H}_i$ and $\mathcal{H}_j$ are the 3^{n-1}-dimensional Hilbert spaces containing the states of the qutrits labeled by i and j respectively in $n-1$ copies of Figure 3.3. Doing the Schmidt decomposition as in equation (15.61) (where we set $D = 3^{n-1}$), we find that the maximum value of $||S^c_{\psi|\varphi}|\chi\rangle||$ for a normalized vector $|\chi\rangle \in \mathcal{H}_i \otimes \mathcal{H}_j$ is

$$\frac{\max_{k=1}^{3^{n-1}} |\beta_k|}{\min_{k=1}^{3^{n-1}} |\alpha_k|}. \tag{15.64}$$

It is crucial that none of the α_k coefficients vanish.

Let us now restrict our attention to the larger subspace of $p\mathcal{H}_{code}$ where all qutrit pairs in the $(n+1)$th collection and beyond are in the reference state $|\lambda\rangle$. We want to do Schmidt decompositions of $|\psi\rangle$ and $|\varphi\rangle$ in this 9^n dimensional Hilbert subspace. Let α_k,β_k,$|e_k\rangle$,$|g_k\rangle$,$|f_k\rangle$,$|h_k\rangle$ for

$k \in \{1, 2, \ldots, 3^{n-1}\}$ be defined as in equation (15.61) for the Schmidt decomposition in the 9^{n-1} dimensional subspace considered in the previous paragraph. Next, define

$$|\hat{e}_p\rangle := \begin{cases} |e_p\rangle \otimes |0\rangle\,, & p = 1, \ldots, 3^{n-1} \\ |e_{p-3^{n-1}}\rangle \otimes |1\rangle\,, & p = 3^{n-1}+1, \ldots, 2\cdot 3^{n-1} \\ |e_{p-2\cdot 3^{n-1}}\rangle \otimes |2\rangle\,, & p = 2\cdot 3^{n-1}+1, \ldots, 3^n \end{cases}, \tag{15.65}$$

where $|0\rangle\,, |1\rangle\,, |2\rangle$ are states of the nth black qutrit labeled i. The vectors $|\hat{g}_p\rangle$,$|\hat{f}_p\rangle$, and $|\hat{h}_p\rangle$ are defined analogously. Furthermore, define

$$\hat{\alpha}_p := \begin{cases} \frac{1}{\sqrt{3}}\alpha_p, & p = 1, \ldots, 3^{n-1} \\ \frac{1}{\sqrt{3}}\alpha_{p-3^{n-1}}, & p = 3^{n-1}+1, \ldots, 2\cdot 3^{n-1} \\ \frac{1}{\sqrt{3}}\alpha_{p-2\cdot 3^{n-1}}, & p = 2\cdot 3^{n-1}+1, \ldots, 3^n \end{cases}. \tag{15.66}$$

We define $\hat{\beta}_p$ analogously. The Schmidt decomposition is then given by

$$|\psi\rangle = \sum_{p=1}^{3^n} \hat{\alpha}_p\, |\hat{e}_p\rangle \otimes |\hat{f}_p\rangle\,, \tag{15.67}$$

$$|\varphi\rangle = \sum_{p=1}^{3^n} \hat{\beta}_p\, |\hat{g}_p\rangle \otimes |\hat{h}_p\rangle\,. \tag{15.68}$$

If $|\chi\rangle$ is a normalized vector in the 9^n dimensional subspace, then the maximum value of $||S^{\kappa}_{\psi|\varphi}\,|\chi\rangle\,||$ is

$$\frac{\max_{p=1}^{3^n} |\hat{\beta}_p|}{\min_{p=1}^{3^n} |\hat{\alpha}_p|} = \frac{\max_{k=1}^{3^{n-1}} |\beta_k|}{\min_{k=1}^{3^{n-1}} |\alpha_k|}. \tag{15.69}$$

Iterating the procedure of doing the Schmidt decompositions in larger subspaces of the code pre-Hilbert space, we see that for any vector $|\eta\rangle \in p\mathcal{H}_{code}$,

$$||S^{c}_{\psi|\varphi}\,|\eta\rangle\,|| \leq \frac{\max_{k=1}^{3^{n-1}}|\beta_k|}{\min_{k=1}^{3^{n-1}}|\alpha_k|}||\,|\eta\rangle\,||. \tag{15.70}$$

Choose any $|\Theta\rangle \in \mathcal{H}_{code}$. Let $\{|\theta_\ell\rangle\} \in p\mathcal{H}_{code}$ be a sequence that converges to $|\Theta\rangle$. Define a sequence of operators $\{a_\ell\} \in \mathcal{A}_{code}$ such that $|\theta_\ell\rangle = a_\ell\,|\psi\rangle\ \forall \ell \in \mathbb{N}$. Note that $a^\dagger_\ell\,|\varphi\rangle = S^{c}_{\psi|\varphi}\,|\theta_\ell\rangle\ \forall \ell \in \mathbb{N}$. For any $\ell, m \in \mathbb{N}$, we then have that

$$||(a^\dagger_\ell - a^\dagger_m)\,|\varphi\rangle\,|| \leq \frac{\max_{k=1}^{3^{n-1}}|\beta_k|}{\min_{k=1}^{3^{n-1}}|\alpha_k|}||\,|\theta_\ell\rangle - |\theta_m\rangle\,||. \tag{15.71}$$

Hence, $\lim_{\ell\to\infty} a^\dagger_\ell\,|\varphi\rangle$ exists. Thus, $S^{c}_{\psi|\varphi}$ is a bounded operator defined on all of $\mathcal{H}_{code}$.

15.7.3 Example where $S^{c}_{\Psi|\Phi}$ is unbounded

In this section, we show that for a particular choice of $|\Psi\rangle\,, |\Phi\rangle \in \mathcal{H}_{code}$, $S^{c}_{\Psi|\Phi}$ is unbounded. Let $|\Psi\rangle$ be the vector for which all qutrit pairs are in the reference state $|\lambda\rangle$. $|\Phi\rangle$ will be constructed as a limit of a sequence of vectors $\{|\varphi_n\rangle\} \in p\mathcal{H}_{code}$. Let $\{\delta_i\}$ be a sequence of positive real numbers such that $\sum_{i=1}^{\infty}\delta_i$ is finite. For $N \in \mathbb{N}$, let $|e^N_a\rangle$, $a \in \{1, 2, \ldots, 3^N\}$, denote an orthonormal basis vector of the qutrits labeled i (see Figure 3.3) in the first N collections. In particular,

$$|e^1_1\rangle := |0\rangle_{i_1}\,,\ |e^1_2\rangle := |1\rangle_{i_1}\,,\ |e^1_3\rangle := |2\rangle_{i_1}\,. \tag{15.72}$$

$$|e_a^N\rangle := \begin{cases} |e_a^{N-1}\rangle_{i_1\cdots i_{N-1}} \otimes |0\rangle_{i_N}, & a = 1, \ldots, 3^{N-1} \\ |e_{a-3^{N-1}}^{N-1}\rangle_{i_1\cdots i_{N-1}} \otimes |1\rangle_{i_N}, & a = 3^{N-1}+1, \ldots, 2\cdot 3^{N-1} \\ |e_{a-2\cdot 3^{N-1}}^{N-1}\rangle_{i_1\cdots i_{N-1}} \otimes |2\rangle_{i_N}, & a = 2\cdot 3^{N-1}+1, \ldots, 3^N \end{cases} . \tag{15.73}$$

Let $|f_a^N\rangle, a \in \{1, 2, \ldots, 3^N\}$, denote an orthonormal basis vector of the qutrits labeled j in the first N collections, defined in the same way as above. Each $|\varphi_n\rangle$ is defined by

$$|\varphi_n\rangle := \sum_{a=1}^{3^n} \sum_{b=1}^{3^n} c_{ab}^n \, |e_a^n\rangle \, |f_b^n\rangle \otimes |\lambda\rangle \cdots , \tag{15.74}$$

where c_{ab}^n is a $3^n \times 3^n$ matrix to be specified. The $\otimes |\lambda\rangle \cdots$ indicates that all black qutrit pairs in the $(n+1)$th collection and beyond are in the reference state $|\lambda\rangle$. Choose an arbitrary $x \in \mathbb{R}$ such that $x > 0$. Each c_{ab}^n is defined by

$$c_{ab}^1 := \frac{1}{\sqrt{3}} \begin{pmatrix} x & 0 & 0 \\ 0 & x & 0 \\ 0 & 0 & x \end{pmatrix}_{ab} + \begin{pmatrix} \delta_1 & 0 & 0 \\ 0 & 0 & 0 \\ 0 & 0 & 0 \end{pmatrix}_{ab} , \tag{15.75}$$

$$c_{ab}^2 := \frac{1}{\sqrt{3}} \begin{pmatrix} c^1 & 0_{3\times 3} & 0_{3\times 3} \\ 0_{3\times 3} & c^1 & 0_{3\times 3} \\ 0_{3\times 3} & 0_{3\times 3} & c^1 \end{pmatrix}_{ab} + \begin{pmatrix} \delta_2 & 0_{1\times 8} \\ 0_{8\times 1} & 0_{8\times 8} \end{pmatrix}_{ab} , \tag{15.76}$$

$$\vdots \tag{15.77}$$

$$c^n_{ab} := \frac{1}{\sqrt{3}} \begin{pmatrix} c^{n-1} & 0_{3^{n-1}\times 3^{n-1}} & 0_{3^{n-1}\times 3^{n-1}} \\ 0_{3^{n-1}\times 3^{n-1}} & c^{n-1} & 0_{3^{n-1}\times 3^{n-1}} \\ 0_{3^{n-1}\times 3^{n-1}} & 0_{3^{n-1}\times 3^{n-1}} & c^{n-1} \end{pmatrix}_{ab} + \begin{pmatrix} \delta_n & 0_{1\times(3^n-1)} \\ 0_{(3^n-1)\times 1} & 0_{(3^n-1)\times(3^n-1)} \end{pmatrix}_{ab}. \tag{15.78}$$

Assuming $n > m$, we see that $||\varphi_n - \varphi_m|| \leq \sum_{i=m+1}^{n} \delta_i$. Thus, $|\Phi\rangle := \lim_{n\to\infty} |\varphi_n\rangle$ exists.

To demonstrate that $S^{\epsilon}_{\Psi|\Phi}$ is unbounded, we will construct a sequence of bounded operators $\{a_n\} \in \mathcal{A}_{code}$ such that $\lim_{n\to\infty} a_n |\Psi\rangle = 0$ while $\lim_{n\to\infty} a_n^\dagger |\Phi\rangle$ does not converge. For $n \in \mathbb{N}$, define

$$a_n := \varepsilon_n \sqrt{3^n} (|e^n_1\rangle \langle e^n_1|_{i_1\cdots i_n} \otimes I_{j_1\cdots j_n}) \otimes I \cdots, \tag{15.79}$$

where $\{\varepsilon_n\}$ is a sequence of positive real numbers that we will specify later. Note that

$$a_n |\Psi\rangle = \varepsilon_n (|e^n_1\rangle_{i_1\cdots i_n} \otimes |f^n_1\rangle_{j_1\cdots j_n}) \otimes |\lambda\rangle \cdots, \tag{15.80}$$

$$||a_n |\Psi\rangle|| = \varepsilon_n. \tag{15.81}$$

Hence, $\lim_{n\to\infty} a_n |\Psi\rangle = 0$ when $\lim_{n\to\infty} \varepsilon_n = 0$.

Next, we will consider the sequence $\{a_n^\dagger |\Phi\rangle\}$. Note that, for $n \in \mathbb{N}$,

$$a_n^\dagger |\varphi_n\rangle = \varepsilon_n \sqrt{3^n} c^n_{11} |e^n_1\rangle |f^n_1\rangle \otimes |\lambda\rangle \cdots, \tag{15.82}$$

$$||a_n^\dagger |\varphi_n\rangle|| = \varepsilon_n \sqrt{3^n} c_{11}^n = \varepsilon_n (x + \sum_{i=1}^{n} \sqrt{3^i} \delta_i). \tag{15.83}$$

One can verify that $||a_n^\dagger |\varphi_n\rangle|| \leq ||a_n^\dagger |\Phi\rangle||$. Hence,

$$||a_n^\dagger |\Phi\rangle|| \geq \varepsilon_n (x + \sum_{k=1}^{n} \sqrt{3^k} \delta_k). \tag{15.84}$$

We may set $\delta_k = \frac{1}{k^2}$. Then $(x + \sum_{k=1}^{n} \sqrt{3^k} \delta_k)$ grows without bound. We may choose ε_n to go to zero slowly enough so that $\varepsilon_n (x + \sum_{k=1}^{n} \sqrt{3^k} \delta_k)$ also grows without bound. Hence, $||a_n^\dagger |\Phi\rangle||$ grows without bound, so $S^x_{\Psi|\Phi}$ is an unbounded operator.

15.8 Computing relative entropy for hyperfinite von Neumann algebras

While the definition of relative entropy for infinite-dimensional von Neumann algebras is elegant, it is difficult to use in practice. To compute the relative entropy, one in principle needs to explicitly perform a spectral decomposition of the relative modular operator. However, because our setup involves hyperfinite von Neumann algebras, we can show that there is a more practical method to compute relative entropy. Recall that a hyperfinite von Neumann algebra M may be written as $M = (\cup_{n=1}^{\infty} M_n)''$ where each M_n denotes a finite-dimensional subalgebra of M and $M_n \subset M_{n+1} \forall n \in \mathbb{N}$. We will show that given a hyperfinite von Neumann algebra M and two cyclic and separating vectors, the relative entropy of the two vectors may be computed by computing their relative entropy with respect to M_n and then taking the limit $n \to \infty$. This result parallels

the result of [15], but our explanation is better suited for studying our setup.[5] Computing the relative entropy with respect to M_n intuitively amounts to performing a partial trace and using the finite-dimensional relative entropy formula on the reduced density matrices. In the next subsection, we precisely describe how to use the finite-dimensional relative entropy formula to compute the relative entropy defined with respect to a finite-dimensional subalgebra of a hyperfinite algebra. In particular, we will write the entropy in a form that is convenient for taking the limit $n \to \infty$. In section 15.8.2, we review the monotonicity of relative entropy, which we use later. In section 15.8.3, we fully explain why the limit of finite-dimensional entropies equals the infinite-dimensional entropy.

15.8.1 Defining relative entropy with respect to a finite-dimensional subalgebra

The purpose of this section is to describe the relative entropy defined with respect to a finite-dimensional subalgebra of a hyperfinite algebra in a way that will be useful when we consider the limit of larger and larger subalgebras. Let M be a hyperfinite von Neumann algebra on $\mathcal{H}$, and let M_n be a finite-dimensional subalgebra of M. Let $|\Psi\rangle, |\Phi\rangle \in \mathcal{H}$ be cyclic and separating with respect to M. Suppose that we want to compute the relative entropy of $|\Phi\rangle$ and $|\Psi\rangle$ with respect to M_n. Note that while $|\Phi\rangle$ and $|\Psi\rangle$ are separating with respect to M_n, they need not be cyclic. However, they may still be thought of as cyclic if we restrict our attention to subspaces of $\mathcal{H}$ denoted by $\overline{M_n |\Psi\rangle}$ and

[5] In particular, [15] shows that the relative entropy of two linear functionals on a von Neumann algebra is a limit of relative entropies computed with respect to finite-dimensional subalgebras. However, we are more interested in the relative entropy of two vectors in the Hilbert space. Given a Hilbert space vector, we show how to compute a finite-dimensional density matrix. This allows us to express the infinite-dimensional relative entropy of two vectors as a limit of finite-dimensional entropies.

$\overline{M_n |\Phi\rangle}$.

Definition 15.8.1. Given a Hilbert space $\mathcal{H}$, a von Neumann algebra $M \subset \mathcal{B}(\mathcal{H})$, and a vector $|\Psi\rangle \in \mathcal{H}$, let $\overline{M|\Psi\rangle}$ denote the closure of the set of vectors generated by acting on $|\Psi\rangle$ with all operators in M. That is,

$$\overline{M|\Psi\rangle} := \{|\chi\rangle \in \mathcal{H} : \exists \{\mathcal{O}_n\} \in M, \lim_{n\to\infty} \mathcal{O}_n |\Psi\rangle = |\chi\rangle\}.$$

We now explain how to compute the relative entropy of $|\Psi\rangle$ and $|\Phi\rangle$ with respect to M_n. First, the relative Tomita operator $S^n_{\Psi|\Phi}$ is defined to map $\mathcal{O}|\Psi\rangle$ to $\mathcal{O}^\dagger|\Phi\rangle$ for all $\mathcal{O} \in M_n$. The Tomita operator should be viewed as a map between two different Hilbert spaces, $\overline{M_n|\Psi\rangle}$ and $\overline{M_n|\Phi\rangle}$. Since M_n is finite dimensional, $S^n_{\Psi|\Phi}$ is a bounded operator on $\overline{M_n|\Psi\rangle}$. The relative modular operator $\Delta^n_{\Psi|\Phi} = S^{n\,\dagger}_{\Psi|\Phi} S^n_{\Psi|\Phi}$ is a self-adjoint operator on $\overline{M_n|\Psi\rangle}$, and it may be defined to act as the identity operator on the orthogonal complement $\left(\overline{M_n|\Psi\rangle}\right)^\perp$. Then, the relative entropy is defined as

$$\mathcal{S}_n = -\langle\Psi| \log \Delta^n_{\Psi|\Phi} |\Psi\rangle \,. \tag{15.85}$$

Equation (15.85) will appear again when we consider the limit of larger subalgebras. We now relate $\mathcal{S}_n$ to the more familiar finite-dimensional relative entropy formula. Because M_n is a finite-dimensional von Neumann algebra that acts on the finite dimensional Hilbert space $\overline{M_n|\Psi\rangle}$, we

note that $\overline{M_n |\Psi\rangle}$ may be written as [159]

$$\overline{M_n |\Psi\rangle} = \oplus_\alpha \left(\mathcal{H}_{A_\alpha} \otimes \mathcal{H}_{\overline{A}_\alpha} \right), \tag{15.86}$$

while M_n may be written as

$$M_n = \{ \oplus_\alpha \left(\mathcal{O}_{A_\alpha} \otimes I_{\overline{A}_\alpha} \right) : \mathcal{O}_{A_\alpha} \in \mathcal{B}(\mathcal{H}_{A_\alpha}) \}. \tag{15.87}$$

Restricting our attention to $\overline{M_n |\Psi\rangle}$, the vector $|\Psi\rangle$ is cyclic and separating with respect to M_n. This implies that for each α, $\dim \mathcal{H}_{A_\alpha} = \dim \mathcal{H}_{\overline{A}_\alpha}$ [307].

We now explain how to obtain a density matrix on $\overline{M_n |\Psi\rangle}$ from $|\Psi\rangle$. Intuitively, one simply needs to perform a partial trace on $|\Psi\rangle \langle\Psi|$, since $|\Psi\rangle \in \overline{M_n |\Psi\rangle}$. However, we follow a different procedure that will also allow us to obtain a density matrix on $\overline{M_n |\Psi\rangle}$ from $|\Phi\rangle$, even though we might have that $|\Phi\rangle \notin \overline{M_n |\Psi\rangle}$. Let us define a linear map $T_\Psi : M_n \to \mathbb{C}$ such that $T_\Psi(\mathcal{O}) = \langle\Psi|\mathcal{O}|\Psi\rangle \ \forall \mathcal{O} \in M_n$. The map T_Ψ is positive. Assuming that $|\Psi\rangle$ is normalized, $T_\Psi(I) = 1$. The map T_Ψ is also faithful because $|\Psi\rangle$ is separating with respect to M_n. If we restrict the domain of T_Ψ to the set of operators in M_n that annihilate $\mathcal{H}_{A_\alpha} \otimes \mathcal{H}_{\overline{A}_\alpha}$ for all $\alpha \neq 1$, then we can naturally define a hermitian, positive operator on $\mathcal{H}_{A_1}$ as follows. Let $|i\rangle, \quad i \in \{1, 2, \cdots, \dim \mathcal{H}_{A_1}\}$ denote an orthonormal basis of $\mathcal{H}_{A_1}$. Any operator in $\mathcal{B}(\mathcal{H}_{A_1})$ may be written as a linear combination of the operators $|i\rangle \langle j| \quad \forall i, j \in \{1, 2, \cdots, \dim \mathcal{H}_{A_1}\}$. To treat $|i\rangle \langle j|$ as an operator in M_n that acts on all of $\overline{M_n |\Psi\rangle}$, we define $|i\rangle \langle j|$ to act as the identity on $\mathcal{H}_{\overline{A}_1}$ and to annihilate the subspaces $\mathcal{H}_{A_\alpha} \otimes$

$\mathcal{H}_{\bar{A}_\alpha}$ $\forall \alpha \neq 1$. Then, we define the operator $\rho_\Psi^{(1)} \in \mathcal{B}(\mathcal{H}_{A_1})$ by $\langle i|\rho_\Psi^{(1)}|j\rangle = T_\Psi(|j\rangle\langle i|)$. We then extend the definition of $\rho_\Psi^{(1)}$ to an operator on $\mathcal{H}_{A_1} \otimes \mathcal{H}_{\bar{A}_1}$ by defining $\rho_\Psi^{(1)}$ to act as the identity on $\mathcal{H}_{\bar{A}_1}$. In this way, we can define an operator $\rho_\Psi^{(\alpha)}$ acting on each $\mathcal{H}_{A_\alpha} \otimes \mathcal{H}_{\bar{A}_\alpha}$. Then, we define the density matrix $\rho_\Psi \in M_n$ to be the direct sum of all the $\rho_\Psi^{(\alpha)}$ for all values of α. That is,

$$\rho_\Psi = \oplus_\alpha \rho_\Psi^{(\alpha)}. \tag{15.88}$$

Note that $\sum_\alpha \mathrm{Tr}_{A_\alpha}\rho_\Psi^{(\alpha)} = 1$ by construction and that ρ_Ψ only depends on $|\Psi\rangle$ through the linear map T_Ψ. Also, $|\Psi\rangle$ must be a purification of ρ_Ψ on $\overline{M_n|\Psi\rangle}$.

Even though $|\Phi\rangle$ is not necessarily in $\overline{M_n|\Psi\rangle}$, we can still define a density matrix ρ_Φ on $\overline{M_n|\Psi\rangle}$ with the linear map T_Φ, which is defined analogously to T_Ψ. Let $|\tilde{\Phi}\rangle \in \overline{M_n|\Psi\rangle}$ be a purification of ρ_Φ. We want to ask how $|\Phi\rangle$ is related to $|\tilde{\Phi}\rangle$. Note that $\langle\Phi|\mathcal{O}|\Phi\rangle = \langle\tilde{\Phi}|\mathcal{O}|\tilde{\Phi}\rangle$ $\forall \mathcal{O} \in M_n$. Define the linear map $U' : \overline{M_n|\Phi\rangle} \to \overline{M_n|\Psi\rangle}$ such that $U'\mathcal{O}|\Phi\rangle = \mathcal{O}|\tilde{\Phi}\rangle$ $\forall \mathcal{O} \in M_n$. Because M_n is finite dimensional, U' is a bounded operator, and U' has trivial kernel because $|\Psi\rangle$ is separating with respect to M_n. Because $||\mathcal{O}|\Phi\rangle|| = ||\mathcal{O}|\tilde{\Phi}\rangle|| \,\forall \mathcal{O} \in M_n$, U' is an isometry. Because U' is invertible, U' satisfies $U'^\dagger U' = I$, and from its definition we can see that U' commutes with all operators in M_n. Because $|\tilde{\Phi}\rangle = U'|\Phi\rangle$, we see that the relative modular operator $\Delta^n_{\Psi|\Phi}$ defined at the beginning of this section equals the relative modular operator $\Delta^n_{\Psi|\tilde{\Phi}}$. Then, the relative entropy of $|\Psi\rangle$ and $|\Phi\rangle$ computed with respect to M_n is given by

$$\mathcal{S}_n = -\langle\Psi|\log\Delta^n_{\Psi|\tilde{\Phi}}|\Psi\rangle\,. \tag{15.89}$$

Since $|\Psi\rangle$ and $|\tilde{\Phi}\rangle$ are both vectors in the same finite-dimensional Hilbert space $\overline{M_n\,|\Psi\rangle}$, it is straightforward to see [307] that $\mathcal{S}_n$, defined in equation (15.85), is given by equation (A.21) of [159] for $\rho = \rho_\Psi, \sigma = \rho_\Phi, M = M_n$, which is the finite-dimensional relative entropy formula.

The relative entropy defined with respect to M_n of the vectors $|\Psi\rangle$ and $|\Phi\rangle$ only depends on $|\Psi\rangle$ and $|\Phi\rangle$ through the linear maps T_Ψ and T_Φ. As long as we can represent M_n on a finite-dimensional Hilbert space with a cyclic and separating vector, we can decompose the Hilbert space as in (15.86) (see [159] for the details) and compute the relative entropies using ρ_Ψ and ρ_Φ, which are defined from T_Ψ and T_Φ.

Applying the above discussion to our tensor network model, we let $M_n \subset M_{code}$ be a finite-dimensional subalgebra of M_{code} that consists of operators that act on the black qutrits labeled i (see Figure 3.3) in the first n collections. Let $|\Psi\rangle, |\Phi\rangle \in \mathcal{H}_{code}$ be cyclic and separating with respect to M_{code}. To compute the relative entropy with respect to M_n of $|\Psi\rangle$ and $|\Phi\rangle$, we consider the action of M_n on the Hilbert space associated with the first n qutrit pairs. The relative entropy may be computed from the density matrices ρ_Ψ and ρ_Φ, which are constructed using the linear maps T_Ψ and T_Φ. This intuitively amounts to performing a partial trace on $|\Psi\rangle\langle\Psi|$ and $|\Phi\rangle\langle\Phi|$ over all of $\mathcal{H}_{code}$ except the Hilbert space of the first n qutrits. In this subsection, we have shown that the result is equivalent to equation (15.85). In the remainder of this section we will show that the infinite n limit of equation (15.85) yields the relative entropy of $|\Psi\rangle$ and $|\Phi\rangle$ with respect to M_{code}.

15.8.2 Monotonicity of Relative Entropy

To show that the limit of finite-dimensional relative entropies equals the infinite-dimensional relative entropy, we use the monotonicity of relative entropy, which is nicely explained using a graph argument in [49, 307]. However, our proof of the monotonicity of relative entropy is slightly different, as we do not assume that cyclic states remain cyclic after restricting the von Neumann algebra to a subalgebra. In the remainder of section 15.8, we make use of definitions and theorems given in [185], such as the spectral theorem.

Let $\mathcal{H}$ be a separable Hilbert space with an orthonormal basis $\{|e_i\rangle\}$. Any $|\chi\rangle \in \mathcal{H}$ may be written as

$$|\chi\rangle = \sum_{i=1}^{\infty} |e_i\rangle \langle e_i|\chi\rangle \,. \tag{15.90}$$

Define the operator $K : \mathcal{H} \to \mathcal{H}$ as

$$K|\chi\rangle := \sum_{i=1}^{\infty} |e_i\rangle \langle \chi|e_i\rangle \,. \tag{15.91}$$

The sum in equation (15.91) is convergent because the sum in equation (15.90) is convergent. The operator K satisfies the following properties:

- $K^2 = I$,
- $K|\alpha\psi + \beta\chi\rangle = \alpha^* K|\psi\rangle + \beta^* K|\chi\rangle \quad \forall \alpha, \beta \in \mathbb{C} \quad \forall |\psi\rangle, |\chi\rangle \in \mathcal{H}$,
- Given a sequence $\{|\psi_n\rangle\} \in \mathcal{H}$ and a vector $|\psi\rangle \in \mathcal{H}$, $\lim_{n\to\infty} |\psi_n\rangle = |\psi\rangle$ if and only if

$\lim_{n\to\infty} K|\psi_n\rangle = K|\psi\rangle$,

- $\langle K\psi|K\chi\rangle = \langle\chi|\psi\rangle \quad \forall\, |\psi\rangle, |\chi\rangle \in \mathcal{H}$,

- $\langle\psi|K|\chi\rangle = \langle\chi|K|\psi\rangle \quad \forall\, |\psi\rangle, |\chi\rangle \in \mathcal{H}$.

Definition 15.8.2. Let X be a linear operator on $\mathcal{H}$. The *graph* of X is a subset of the Hilbert space $\mathcal{H}\oplus\mathcal{H}$, given by

$$\Gamma_X := \left\{ \begin{pmatrix} |\psi\rangle \\ X|\psi\rangle \end{pmatrix} \in \mathcal{H}\oplus\mathcal{H} : |\psi\rangle \in D(X) \right\}.$$

Let S be a closed, densely defined, antilinear operator on $\mathcal{H}$. Define $X := KS$. Note that $X^\dagger X = S^\dagger S$ and that X is a closed, densely defined, linear operator on $\mathcal{H}$. The graph Γ_X is thus a closed linear subspace of the Hilbert space $\mathcal{H}\oplus\mathcal{H}$. We define Π_X to be the projection operator onto Γ_X, which satisfies $\Pi_X^2 = \Pi_X^\dagger = \Pi_X$. Since any vector in $\mathcal{H}\oplus\mathcal{H}$ can be represented as a column vector

$$\begin{pmatrix} |\psi\rangle \\ |\varphi\rangle \end{pmatrix} \quad \text{for } |\psi\rangle, |\varphi\rangle \in \mathcal{H}, \tag{15.92}$$

we may represent Π_X as a two by two matrix:

$$\Pi_X = \begin{pmatrix} p_{11} & p_{12} \\ p_{21} & p_{22} \end{pmatrix}, \tag{15.93}$$

where each p_{ij} $(i,j \in \{1,2\})$ is a bounded linear operator on $\mathcal{H}$ (since Π_X is bounded). For any

$|\psi\rangle, |\chi\rangle \in \mathcal{H}$, we have that $X(p_{11}|\psi\rangle + p_{12}|\chi\rangle) = p_{21}|\psi\rangle + p_{22}|\chi\rangle$. Hence,

$$Xp_{11} = p_{21}, \quad Xp_{12} = p_{22}. \tag{15.94}$$

The condition $\Pi_X = \Pi_X^\dagger$ implies that $p_{ij}^\dagger = p_{ji} \quad \forall i,j \in \{1,2\}$, and the condition $\Pi_X^2 = \Pi_X$ implies that $\sum_{k=1}^{2} p_{ik}p_{kj} = p_{ij} \quad \forall i,j \in \{1,2\}$. With these relations, one may show that

$$p_{i1}(X^\dagger X + 1)p_{1j} = p_{ij} \quad \forall i,j \in \{1,2\}, \tag{15.95}$$

which implies that

$$p_{11}(X^\dagger X + 1)(p_{11}|\psi\rangle + p_{12}|\chi\rangle) = (p_{11}|\psi\rangle + p_{12}|\chi\rangle). \tag{15.96}$$

Note that the domain of X is given by

$$D(X) = \{p_{11}|\psi\rangle + p_{12}|\chi\rangle : |\psi\rangle, |\chi\rangle \in \mathcal{H}\}. \tag{15.97}$$

Because $D(X)$ is a dense subset of $\mathcal{H}$, it follows that

$$p_{11} = (1 + X^\dagger X)^{-1}. \tag{15.98}$$

Then, we see that

$$p_{21} = X(1 + X^\dagger X)^{-1}, \quad p_{12} = (1 + X^\dagger X)^{-1} X^\dagger, \quad p_{22} = X(1 + X^\dagger X)^{-1} X^\dagger. \tag{15.99}$$

In the following theorem, we study modular operators as opposed to relative modular operators. We will make an explicit connection to monotonicity of relative entropy later.

Theorem 15.8.3. *Let M be a von Neumann algebra that acts on a Hilbert space $\mathcal{H}$. Let $|\Psi\rangle \in \mathcal{H}$ be cyclic and separating with respect to M. Let S_Ψ^M be the Tomita operator defined with respect to M and $|\Psi\rangle$. Let N be a von Neumann subalgebra of M (we do not assume that $|\Psi\rangle$ is cyclic with respect to N). On the closed subspace $\overline{N|\Psi\rangle} \subset \mathcal{H}$, let S_Ψ^N be the Tomita operator defined with respect to N and $|\Psi\rangle$. On the orthogonal complement $\overline{N|\Psi\rangle}^\perp \subset \mathcal{H}$, let $S_\Psi^N = K$, where K is given in equation (15.91). Then for all $|\Phi\rangle \in \overline{N|\Psi\rangle}$ and all $s > 0$,*

$$\langle \Phi | \frac{1}{s + (S_\Psi^M)^\dagger S_\Psi^M} |\Phi\rangle \geq \langle \Phi | \frac{1}{s + (S_\Psi^N)^\dagger S_\Psi^N} |\Phi\rangle \, .$$

Proof. Let $X^M = KS_\Psi^M$ and $X^N = KS_\Psi^N$. Let $\Gamma_{X^M} \subset \mathcal{H} \oplus \mathcal{H}$ and $\Gamma_{X^N} \subset \mathcal{H} \oplus \mathcal{H}$ be the graphs of X^M and X^N respectively, with projections Π_{X^M} and Π_{X^N}. Let $\Pi_{N\Psi}$ denote the projection onto the closed subspace $\Pi_{N\Psi}(\mathcal{H} \oplus \mathcal{H})$, which is defined by

$$\Pi_{N\Psi}(\mathcal{H} \oplus \mathcal{H}) := \left\{ \begin{pmatrix} |\psi\rangle \\ \\ |\chi\rangle \end{pmatrix} \in \mathcal{H} \oplus \mathcal{H} : |\psi\rangle, |\chi\rangle \in \overline{N|\Psi\rangle} \right\}. \tag{15.100}$$

Note that the closed subspace $\Gamma_{X^N} \cap \Pi_{N\Psi}(\mathcal{H} \oplus \mathcal{H})$ is completely determined by the Tomita operator defined with respect to $|\Psi\rangle$ and N on the subspace $\overline{N|\Psi\rangle}$. Because N is a subalgebra of M, it follows that

$$\Gamma_{X^M} \supset (\Gamma_{X^N} \cap \Pi_{N\Psi}(\mathcal{H} \oplus \mathcal{H})). \tag{15.101}$$

The projection onto the closed subspace $(\Gamma_{X^N} \cap \Pi_{N\Psi}(\mathcal{H} \oplus \mathcal{H}))$ is given by $\Pi_{X^N}\Pi_{N\Psi} = \Pi_{N\Psi}\Pi_{X^N}$. It follows that

$$\Pi_{X^M} \geq \Pi_{X^N}\Pi_{N\Psi}. \tag{15.102}$$

If we evaluate the expectation value of the above equation in the state $\begin{pmatrix} |\Phi\rangle \\ 0 \end{pmatrix}$ for $|\Phi\rangle \in \overline{N|\Psi\rangle}$, we find that

$$\langle\Phi| \frac{1}{1 + (X^M)^\dagger X^M} |\Phi\rangle \geq \langle\Phi| \frac{1}{1 + (X^N)^\dagger X^N} |\Phi\rangle \,, \tag{15.103}$$

which implies

$$\langle\Phi| \frac{1}{1 + (S_\Psi^M)^\dagger S_\Psi^M} |\Phi\rangle \geq \langle\Phi| \frac{1}{1 + (S_\Psi^N)^\dagger S_\Psi^N} |\Phi\rangle \,. \tag{15.104}$$

By repeating the above logic with $X^M = \frac{1}{\sqrt{s}} K S_\Psi^M$ and $X^N = \frac{1}{\sqrt{s}} K S_\Psi^N$ for $s > 0$, we have that

$$\langle\Phi| \frac{1}{s + (S_\Psi^M)^\dagger S_\Psi^M} |\Phi\rangle \geq \langle\Phi| \frac{1}{s + (S_\Psi^N)^\dagger S_\Psi^N} |\Phi\rangle \,. \tag{15.105}$$

□

Theorem 15.8.4. *Let Δ_1, Δ_2 be operators on $\mathcal{H}$ that are densely defined, closed, self-adjoint and posi-*

tive. Assume that, for some $|\Phi\rangle \in D(\Delta_1) \cap D(\Delta_2)$ *and all* $s > 0$,

$$\langle\Phi|\frac{1}{s+\Delta_1}|\Phi\rangle \geq \langle\Phi|\frac{1}{s+\Delta_2}|\Phi\rangle\,.$$

Also assume that $\langle\Phi|\log\Delta_1|\Phi\rangle$ *and* $\langle\Phi|\log\Delta_2|\Phi\rangle$ *are finite. Then*

$$-\langle\Phi|\log\Delta_1|\Phi\rangle \geq -\langle\Phi|\log\Delta_2|\Phi\rangle\,.$$

Proof. Let P^1_Ω, P^2_Ω denote the projection-valued measures associated with Δ_1, Δ_2. We use the spectral theorem[6] to write

$$-\langle\Phi|\log\Delta_1|\Phi\rangle = -\int_0^\infty \log\lambda\, d(\langle\Phi|P^1_\lambda|\Phi\rangle) = \int_0^\infty\int_0^\infty ds\left(\frac{1}{s+\lambda}-\frac{1}{s+1}\right) d(\langle\Phi|P^1_\lambda|\Phi\rangle). \tag{15.106}$$

By Fubini's Theorem ([264], page 26), we may interchange the order of integration above if the following integral converges:

$$\begin{aligned}\int_0^\infty\int_0^\infty ds\left|\frac{1}{s+\lambda}-\frac{1}{s+1}\right| d(\langle\Phi|P^1_\lambda|\Phi\rangle) &= \int_0^\infty |\log\lambda|\, d(\langle\Phi|P^1_\lambda|\Phi\rangle)\\ &= \left|\int_0^1 \log\lambda\, d(\langle\Phi|P^1_\lambda|\Phi\rangle)\right| + \int_1^\infty \log\lambda\, d(\langle\Phi|P^1_\lambda|\Phi\rangle).\end{aligned} \tag{15.107}$$

[6] See [185] for an explanation of the notation.

Note that

$$0 \leq \int_1^\infty \log\lambda \, d(\langle\Phi|P_\lambda^1|\Phi\rangle) \leq \int_1^\infty (\lambda - 1)\, d(\langle\Phi|P_\lambda^1|\Phi\rangle) = \langle\Phi|\Delta_1|\Phi\rangle - \langle\Phi|\Phi\rangle\,, \tag{15.108}$$

which implies that

$$\int_1^\infty \log\lambda \, d(\langle\Phi|P_\lambda^1|\Phi\rangle) \tag{15.109}$$

is finite. Because $\langle\Phi|\log\Delta_1|\Phi\rangle$ is finite by assumption, it follows that

$$\int_0^1 \log\lambda \, d(\langle\Phi|P_\lambda^1|\Phi\rangle) \tag{15.110}$$

is finite. Thus, equation (15.107) is finite, which implies that the integrals in equation (15.106) may be interchanged. Thus,

$$\begin{aligned} -\langle\Phi|\log\Delta_1|\Phi\rangle &= \int_0^\infty ds \quad \left(\langle\Phi|\frac{1}{s+\Delta_1}|\Phi\rangle - \frac{\langle\Phi|\Phi\rangle}{s+1}\right) \geq \int_0^\infty ds \quad \left(\langle\Phi|\frac{1}{s+\Delta_2}|\Phi\rangle - \frac{\langle\Phi|\Phi\rangle}{s+1}\right) \\ &= \int_0^\infty ds \int_0^\infty \left(\frac{1}{s+\lambda} - \frac{1}{s+1}\right) d(\langle\Phi|P_\lambda^2|\Phi\rangle). \end{aligned} \tag{15.111}$$

We may switch the order of integration above for the same reason as in equation (15.106). Thus,

$$-\langle\Phi|\log\Delta_1|\Phi\rangle \geq -\langle\Phi|\log\Delta_2|\Phi\rangle\,. \tag{15.112}$$

□

15.8.3 The infinite-dimensional relative entropy as a limit of finite-dimensional relative entropies

In this section, we use the above theorems to show how one could compute the relative entropy of two cyclic and separating vectors of a hyperfinite von Neumann algebra as a limit of finite-dimensional relative entropies.

Theorem 15.8.5. *Let M be a von Neumann algebra acting on a Hilbert space $\mathcal{H}$ such that M is generated by $\cup_{n=1}^{\infty} M_n$, where $\{M_n\}$ is a sequence of finite-dimensional von Neumann subalgebras of M satisfying $M_n \subset M_{n+1}$ $\forall n \in \mathbb{N}$. Let $|\Psi\rangle, |\Phi\rangle \in \mathcal{H}$ both be cyclic and separating with respect to M. Let S_n denote the relative entropy of $|\Psi\rangle$ and $|\Phi\rangle$ defined with respect to M_n (see equation* (15.85) *for details). Let S denote the relative entropy defined with respect to M. Then*

$$\lim_{n\to\infty} S_n = S.$$

In particular, if the limit does not converge, then S is infinity.

Proof. We mostly follow the logic of the proof of Lemma 3 of [15]. We consider the tensor product Hilbert space $\mathcal{H} \otimes \mathcal{K}$, where $\mathcal{K}$ is a four-dimensional Hilbert space spanned by orthonormal basis vectors $|e_{ij}\rangle$ $(i, j \in \{1, 2\})$. Let $M_{2\times 2}$ be a four-dimensional von Neumann algebra spanned by the operators u_{ij} $(i, j \in \{1, 2\})$, which act on the basis vectors of $\mathcal{K}$ as $u_{ij}|e_{k\ell}\rangle = \delta_{jk}|e_{i\ell}\rangle$. It follows that

$u_{ij}^\dagger = u_{ji}$. Define $\hat{M} := M \otimes M_{2\times 2}$ and $\hat{M}_n := M_n \otimes M_{2\times 2}$. Let

$$|\hat{\Phi}\rangle = |\Phi\rangle \otimes |e_{11}\rangle + |\Psi\rangle \otimes |e_{22}\rangle .$$

Note that $|\hat{\Phi}\rangle$ is cyclic and separating with respect to $\hat{M}$. Let $\hat{\Delta}$ denote the modular operator defined with respect to $\hat{M}$ and $|\hat{\Phi}\rangle$. Let the operator $\hat{\Delta}_n$ act on $\overline{\hat{M}_n |\hat{\Phi}\rangle}$ as the modular operator defined with respect to $|\hat{\Phi}\rangle$ and $\hat{M}_n$, and let $\hat{\Delta}_n$ act as the identity on $\overline{\hat{M}_n |\hat{\Phi}\rangle}^\perp$. Note that

$$\begin{aligned} \hat{\Delta}(|\Theta\rangle \otimes |e_{12}\rangle) &= (\Delta_{\Psi|\Phi} |\Theta\rangle) \otimes |e_{12}\rangle , \quad |\Theta\rangle \in D(\Delta_{\Psi|\Phi}), \\ (\log \hat{\Delta})(|\Theta\rangle \otimes |e_{12}\rangle) &= ((\log \Delta_{\Psi|\Phi}) |\Theta\rangle) \otimes |e_{12}\rangle , \quad |\Theta\rangle \in D(\log \Delta_{\Psi|\Phi}), \end{aligned} \tag{15.113}$$

where $\Delta_{\Psi|\Phi}$ is the relative modular operator defined with respect to M, $|\Psi\rangle$, and $|\Phi\rangle$. We also have that

$$\begin{aligned} \hat{\Delta}_n |\Theta\rangle \otimes |e_{12}\rangle &= (\Delta_{\Psi|\Phi}^n |\Theta\rangle) \otimes |e_{12}\rangle , \quad |\Theta\rangle \in \overline{M_n |\Psi\rangle}, \\ (\log \hat{\Delta}_n)(|\Theta\rangle \otimes |e_{12}\rangle) &= ((\log \Delta_{\Psi|\Phi}^n) |\Theta\rangle) \otimes |e_{12}\rangle , \quad |\Theta\rangle \in \overline{M_n |\Psi\rangle}, \end{aligned} \tag{15.114}$$

where $\Delta_{\Psi|\Phi}^n$ is the relative modular operator defined with respect to the finite-dimensional algebra M_n (see the paragraph before equation (15.85) for details). Thus,

$$\begin{aligned} \langle u_{12}\hat{\Phi}| \log \hat{\Delta} |u_{12}\hat{\Phi}\rangle &= \langle \Psi| \log \Delta_{\Psi|\Phi} |\Psi\rangle = -\mathcal{S}, \\ \langle u_{12}\hat{\Phi}| \log \hat{\Delta}_n |u_{12}\hat{\Phi}\rangle &= \langle \Psi| \log \Delta_{\Psi|\Phi}^n |\Psi\rangle = -\mathcal{S}_n. \end{aligned} \tag{15.115}$$

Thus, we need to show that

$$\lim_{n\to\infty} \langle u_{12}\hat{\Phi}| \log \hat{\Delta}_n |u_{12}\hat{\Phi}\rangle = \langle u_{12}\hat{\Phi}| \log \hat{\Delta} |u_{12}\hat{\Phi}\rangle \,. \tag{15.116}$$

Note that Theorems 15.8.3 and 15.8.4 imply relations between the finite dimensional relative entropies $\mathcal{S}_n$. That is, $\mathcal{S}_n \leq \mathcal{S}_{n+1} \quad \forall n \in \mathbb{N}$ because $\mathcal{M}_n \subset \mathcal{M}_{n+1}$. Also $\mathcal{S}_n \leq \mathcal{S}\, \forall n \in \mathbb{N}$. Thus, if $\lim_{n\to\infty} \mathcal{S}_n$ does not converge, then $\mathcal{S}$ must be infinity. For the remainder of the proof, we will thus assume that $\lim_{n\to\infty} \mathcal{S}_n$ converges to a quantity that is less than or equal to $\mathcal{S}$.

Given the definitions of $\hat{\Delta}$ and $\hat{\Delta}_n$, it follows that (see [15] and references therein)

$$\lim_{n\to\infty} \langle u_{12}\hat{\Phi}| g_N(\hat{\Delta}_n) |u_{12}\hat{\Phi}\rangle = \langle u_{12}\hat{\Phi}| g_N(\hat{\Delta}) |u_{12}\hat{\Phi}\rangle \,, \tag{15.117}$$

where $g_N(\lambda)$ is a continuous, bounded function on $\mathbb{R}$, defined for any $N \geq 1$, such that

$$g_N(\lambda) = \begin{cases} -\log N & \lambda \leq \frac{1}{N} \\ \log \lambda & \frac{1}{N} \leq \lambda \leq N \\ \log N & \lambda \geq N. \end{cases} \tag{15.118}$$

Let P_Ω denote the spectral projections of $\hat{\Delta}$, and let P^n_Ω denote the spectral projections of $\hat{\Delta}_n$. By definition,

$$\langle u_{12}\hat{\Phi}| \log \hat{\Delta} |u_{12}\hat{\Phi}\rangle = \int_0^\infty \log \lambda \, d(\langle u_{12}\hat{\Phi}| P_\lambda |u_{12}\hat{\Phi}\rangle). \tag{15.119}$$

Note that

$$\begin{aligned}\langle u_{12}\hat{\Phi}|g_N(\hat{\Delta})|u_{12}\hat{\Phi}\rangle = &\int_0^{\frac{1}{N}} (-\log N)\, d(\langle u_{12}\hat{\Phi}|P_\lambda|u_{12}\hat{\Phi}\rangle) \\ &+ \int_{\frac{1}{N}}^{N} \log\lambda\, d(\langle u_{12}\hat{\Phi}|P_\lambda|u_{12}\hat{\Phi}\rangle) + \int_N^\infty \log N d(\langle u_{12}\hat{\Phi}|P_\lambda|u_{12}\hat{\Phi}\rangle).\end{aligned} \tag{15.120}$$

Next, note that

$$\begin{aligned}0 &\leq \int_N^\infty (\log\lambda - \log N)\, d(\langle u_{12}\hat{\Phi}|P_\lambda|u_{12}\hat{\Phi}\rangle) = \int_N^\infty (\lambda\lambda^{-1}\log\frac{\lambda}{N})\, d(\langle u_{12}\hat{\Phi}|P_\lambda|u_{12}\hat{\Phi}\rangle) \\ &\leq (Ne)^{-1}\int_N^\infty (\lambda)\, d(\langle u_{12}\hat{\Phi}|P_\lambda|u_{12}\hat{\Phi}\rangle) \\ &\leq (Ne)^{-1}\int_0^\infty (\lambda)\, d(\langle u_{12}\hat{\Phi}|P_\lambda|u_{12}\hat{\Phi}\rangle) = (Ne)^{-1}\langle u_{12}\hat{\Phi}|\hat{\Delta}|u_{12}\hat{\Phi}\rangle\,.\end{aligned} \tag{15.121}$$

We have used the inequality $\lambda^{-1}\log\frac{\lambda}{N} \leq (Ne)^{-1}$. Note that $\langle u_{12}\hat{\Phi}|\hat{\Delta}|u_{12}\hat{\Phi}\rangle = \langle\Psi|\Delta_{\Psi|\Phi}|\Psi\rangle = \langle\Phi|\Phi\rangle$ is a finite quantity [307]. Likewise, we have that

$$0 \leq \int_N^\infty (\log\lambda - \log N)\, d(\langle u_{12}\hat{\Phi}|P_\lambda^n|u_{12}\hat{\Phi}\rangle) \leq (Ne)^{-1}\langle u_{12}\hat{\Phi}|\hat{\Delta}_n|u_{12}\hat{\Phi}\rangle = (Ne)^{-1}\langle\Phi|\Phi\rangle\,. \tag{15.122}$$

From equation (15.117), we have that

$$\begin{aligned}\lim_{n\to\infty}\Bigg[\langle u_{12}\hat{\Phi}|\log\hat{\Delta}_n|u_{12}\hat{\Phi}\rangle - \int_N^\infty (\log\lambda - \log N) d(\langle u_{12}\hat{\Phi}|P_\lambda^n|u_{12}\hat{\Phi}\rangle) \\ - \int_0^{\frac{1}{N}} (\log\lambda + \log N) d(\langle u_{12}\hat{\Phi}|P_\lambda^n|u_{12}\hat{\Phi}\rangle)\Bigg] \\ = \int_0^{\frac{1}{N}} (-\log N)\, d(\langle u_{12}\hat{\Phi}|P_\lambda|u_{12}\hat{\Phi}\rangle) + \int_{\frac{1}{N}}^\infty \log\lambda\, d(\langle u_{12}\hat{\Phi}|P_\lambda|u_{12}\hat{\Phi}\rangle) \\ - \int_N^\infty (\log\lambda - \log N)\, d(\langle u_{12}\hat{\Phi}|P_\lambda|u_{12}\hat{\Phi}\rangle).\end{aligned} \tag{15.123}$$

Note that for $N \geq 1$,

$$\int_0^{\frac{1}{N}} (-\log N)\, d(\langle u_{12}\hat{\Phi}|P_\lambda|u_{12}\hat{\Phi}\rangle) \leq 0 \quad \text{and} \quad \int_0^{\frac{1}{N}} (\log\lambda + \log N) d(\langle u_{12}\hat{\Phi}|P_\lambda^n|u_{12}\hat{\Phi}\rangle) \leq 0. \tag{15.124}$$

Thus,

$$\begin{aligned}\lim_{n\to\infty}\left[\langle u_{12}\hat{\Phi}|\log\hat{\Delta}_n|u_{12}\hat{\Phi}\rangle - \int_N^\infty (\log\lambda - \log N) d(\langle u_{12}\hat{\Phi}|P_\lambda^n|u_{12}\hat{\Phi}\rangle)\right] \\ \leq \int_{\frac{1}{N}}^\infty \log\lambda\, d(\langle u_{12}\hat{\Phi}|P_\lambda|u_{12}\hat{\Phi}\rangle) - \int_N^\infty (\log\lambda - \log N)\, d(\langle u_{12}\hat{\Phi}|P_\lambda|u_{12}\hat{\Phi}\rangle).\end{aligned} \tag{15.125}$$

Note that

$$\lim_{N\to\infty} \int_{\frac{1}{N}}^\infty \log\lambda\, d(\langle u_{12}\hat{\Phi}|P_\lambda|u_{12}\hat{\Phi}\rangle) = \langle u_{12}\hat{\Phi}|\log\hat{\Delta}|u_{12}\hat{\Phi}\rangle\,. \tag{15.126}$$

Using equations (15.121) and (15.122), we can take the large N limit of equation (15.125) to obtain

$$\lim_{n\to\infty} \langle u_{12}\hat{\Phi}|\log\hat{\Delta}_n|u_{12}\hat{\Phi}\rangle \leq \langle u_{12}\hat{\Phi}|\log\hat{\Delta}|u_{12}\hat{\Phi}\rangle\,, \tag{15.127}$$

which implies that

$$\lim_{n\to\infty} \mathcal{S}_n \geq \mathcal{S}, \tag{15.128}$$

which implies that $\mathcal{S}$ is finite. Using the monotonicity properties proved earlier, it follows that

$$\lim_{n\to\infty} \mathcal{S}_n = \mathcal{S}. \tag{15.129}$$

□

15.9 Conclusion and outlook

To summarize, our strategy for constructing an infinite-dimensional QECC is to first construct a QECC that relates a code pre-Hilbert space to a physical pre-Hilbert space. Tensor networks with a repeating pattern provide a natural way to do this. In [259] a tensor network constructed from a pentagonal tiling of hyperbolic space was used to construct a QECC (the "HaPPY Code") with a natural AdS/CFT interpretation. We plan to apply our strategy to the HaPPY code, as the HaPPY tensor network can be naturally extended to an arbitrarily large size. The explicit example described in this chapter uses multiple disconnected tensor networks, but it would be more satisfying to use a connected tensor network such as the HaPPY code. If we can generalize the HaPPY code to a QECC with infinite-dimensional Hilbert spaces, we will be able to construct a more accurate toy model of entanglement wedge reconstruction.

An important aspect of AdS/CFT that our toy model captures is that subregions in the boundary

theory are associated with von Neumann algebras. In our example, we study type II_1 factors acting on both the bulk and boundary Hilbert spaces. However, the local operator algebras that arise in quantum field theory are generically of type III [137, 307, Landsman]. Thus, it would be satisfying to have a toy model of entanglement wedge reconstruction where the von Neumann algebras are of type III.

Our infinite-dimensional QECC satisfies both statements in Theorem 3.0.1 [185]. The assumptions and statements in Theorem 3.0.1 are physically motivated by the Reeh-Schlieder Theorem [265] and previous work on error correction and AdS/CFT [2, 102, 159, 178]. Toy models with infinite-dimensional Hilbert spaces should allow us to better understand the physics of entanglement wedge reconstruction and holographic relative entropy, including the role that the Reeh-Schlieder theorem plays.

In light of the fact that the equivalence between bulk and boundary relative entropies is only approximately correct at large N, approximate entanglement wedge reconstruction has been studied in [82] using finite dimensional von Neumann algebras and universal recovery channels. It would be interesting to see if an appropriate generalization of the explicit formulas given for finite dimensional entanglement wedge reconstruction can be checked in an infinite-dimensional toy example. In the future, we want to apply the study of infinite-dimensional von Neumann algebras to entanglement wedge reconstruction beyond the planar/semiclassical limit.

While our primary motivation has been in understanding the bulk reconstruction in AdS/CFT, we note that infinite tensor networks may also be useful in studying two-dimensional conformal field theories. In the algebraic approach to 2d conformal field theory, every interval I on the circle is

assigned a von Neumann algebra $\mathcal{A}$, and if $I_1 \subset I_2$ for two intervals I_1 and I_2, the associated algebras $\mathcal{A}_1$ and $\mathcal{A}_2$ satisfy $\mathcal{A}_1 \subset \mathcal{A}_2$. In the case of 2d chiral conformal field theory studied in [137], each algebra is isomorphic to the unique hyperfinite type III_1 factor. Furthermore, note that there is also a unique hyperfinite type II_1 factor [Landsman]. In our setup, we use an infinite tensor network to characterize the type II_1 factor $\mathcal{M}_{code}$ as a particular subalgebra of $\mathcal{M}_{phys}$ on $\mathcal{H}_{phys}$. By using infinite tensor networks to relate the algebra associated with an interval to a subalgebra associated with a subinterval, we may be able to probe some aspects in 2d conformal field theory. If infinite tensor networks arise naturally in 2d conformal field theory, it would be interesting to see how they are related to quantities such as primary operator dimensions or three-point function coefficients.

Part VII

Conclusion

L'algèbre n'est qu'une géometrie écrite; la géometrie n'est qu'une algèbre figurée.

Sophie Germain

16

Conclusion

String theory has provided powerful framework to understand the theory of quantum gravity, which encapsulates both the viewpoints of top-down approach to an emergent gravity in lower-dimensions. The holistic perspective from string theory innately carries down to understanding various aspects of gravity from the spectrum and dynamics to information residing in black holes and entanglement.

In this thesis we have been concerned with contructing and understanding theories of gravity, in particular of quantum gravity, using mathematical frameworks. The focus has been two-fold; in the first half of this thesis we have considered the study of supergravity theories in three to six dimensions, as constructed via M-theory and F-theory compactified on elliptically-fibered Calabi–Yau manifolds, as well as the topological and geometric properties of such compactifying spaces. In a different vein, the latter half of this thesis has been oriented towards the study of infinite dimensional von Neumann alegbras of various types, which are used to understand the algebra of local operators in quantum field theories. We have been focused on understanding holographic quantum field theories and their gravity duals by studying quantum error correction using such von Neumann algebras. We now reiterate the central results that have appeared throughout this thesis.

Calabi–Yau compactifications and spectra

M-theory and F-theory compactifications enable the geometric engineering of numerous gauge theories using elliptically-fibered Calabi–Yau varieties. Studying the geometric properties of such Calabi–Yau varieties determines the physical properties of the resulting three to six-dimensional field theories. In particular, non-abelian gauge groups and matter contents of such gauge theories are encoded in singular fibers of the elliptic fibration. Understanding these singular fibers necessitates the study of resolutions of singularities of the Weierstrass model that underlies every elliptic fibration. In addition, the study of crepant resolutions of Weierstrass models, their fibral structure, and their flop transitions is an area of common interest to string theorists, algebraic geometers, and number theorists. In this thesis we have investigated the structure of all such possible crepant resolutions and the graph of flops connecting them. From such geometric analysis, we have determined

the matter in the five-dimensional and six-dimensional gauge theories for various gauge groups, such as

1. Chapter 9: G_2, Spin(7), and Spin(8) [112],
2. Chapter 8: F_4 [115],

and for semi-simple groups of forms $SU(2) \times G$ and $(SU(2) \times G)/\mathbb{Z}_2$ such as

1. Chapter 10: SO(4) and Spin(4) [118]
2. Chapter 11: $SU(2) \times G_2$ [119],
3. Chapter 12: $SU(2) \times SU(3)$ [113],
4. Chapter 13: $SU(2) \times Sp(4)$, $(SU(2) \times Sp(4))/\mathbb{Z}_2$, $SU(2) \times SU(4)$, and $(SU(2) \times SU(4))/\mathbb{Z}_2$ [121].

In particular, in five-dimensions, the Chern–Simons levels and the prepotential are determined after the resolution by the triple intersection numbers of divisors.

Semi-simple Lie groups can be studied geometrically via colliding singular fibers. The simplest examples are those with gauge groups of low rank; in particular, we have studied the resolutions of the $SU(2) \times G$ and $(SU(2) \times G)/\mathbb{Z}_2$ with $\text{rank}(G) \leq 3$ in Chapters 10 to 13 [113, 118, 119, 121]. The case of $G = SU(3)$ is interesting for its connection to the non-Abelian sector of the Standard Model. The $SU(2) \times G_2$-model appears naturally in the study of non-Higgsable clusters, which, over non-compact bases, are used as building blocks to classify 6d $\mathcal{N} = (1, 0)$ superconformal field theories. Extending the results from compact models to incorporate non-compactness is the subject of

ongoing work. For example, such a non-Higgsable model is produced when the discriminant locus contains two rational curves with self-intersection -3 and -2 intersecting transversally or three rational curves which form a chain of curves intersecting transversally at a point with self-intersections $(-3,-2,-2)$.

Anomaly cancellation

It is conjectured that the five-dimensional $\mathcal{N}=1$ theory from an M-theory compactification is compatible with an uplift to an anomaly free six-dimensional $\mathcal{N}=(1.0)$ theory. We have checked this explicitly for G_2, Spin(7), and Spin(8)-models in Chapter 9 [112], F_4-models in Chapter 8 [115] and various semi-simple groups such as SO(4) and Spin (4)-models in Chapter 10 [118], $SU(2)\times G_2$-models in Chapter 11 [119], $SU(2)\times SU(3)$-models in Chapter 12 [113], and $SU(2)\times Sp(4)$, $(SU(2)\times Sp(4))/\mathbb{Z}_2$, $SU(2)\times SU(4)$, and $(SU(2)\times SU(4))/\mathbb{Z}_2$-models in Chapter 13 [121].

Furthermore, we have shown that by comparing the triple intersection numbers and the prepotentials, the number of 6d charged multiplets is completely fixed in all studied models except for the semi-simple groups without a $\mathbb{Z}_2$ quotient. We illustrate the role of Mordell–Weil torsion by comparing the models with a trivial Mordell-Weil group on the geometric data of such corresponding elliptic fibration and matter contents of the resulting theories in five and six-dimensions. For the models with the Mordell–Weil group $\mathbb{Z}_2$ completely fix the number of charged hypermultiplets, whereas the corresponding models with a trivial Mordell–Weil group do not fix the number of charged hypermultiplets entirely but instead give a linear relation between the fundamentals and the adjoints.

We have further checked that the number of multiplets is fixed by six-dimensional anomaly can-

cellations using the Green-Schwarz mechanism. We first derive a unique solution of number of multiplets satisfying anomaly cancellation conditions in six-dimensions and confirm it scompatibility with the result from M-theory compactification to five-dimensions. This implies that these 5d theories, which have 6d anomaly-free uplifts, have their natural description from F-theory. This result gives a nontrivial check of M/F-theory duality.

Topological and geometric properties of Calabi–Yau varieties

The Euler characteristic of an elliptic fibration plays a central role in many physics problems, including the gravitational anomalies of 6d theories and the cancellation of tadpoles in 4d theories. This motivates for computing the closed form formulas for the Euler characteristics of elliptic fibrations that are used to geometrically engineer many gauge theories, which is presented in

1. Chapter 5 : Generating functions of Euler characteristics, the Euler characteristics of the eliptically-fibered threefolds and fourfolds, and Hodge numbers of Calabi–Yau threefolds realizing various simple groups [114].

As a byproduct, for Calabi–Yau fourfolds the Euler characteristics match perfectly with the results from heterotic compactifications. As a byproduct, we computed the Euler characteristics of Calabi–Yau fourfolds and showed that they match perfectly with the predictions in [44], where heterotic string theory compactifications were used. Thus, this result gives a nontrivial check of the heterotic/F-theory duality. Moreover, we generalized this to compute the Euler characteristics of many elliptic n-folds without the Calabi–Yau condition [114]. From the Euler characteristic, we have computed the Hodge numbers of the elliptically-fibered Calabi–Yau threefolds for various gauge

groups.

Moreover, we polished our methods to compute the topological invariants of the elliptic fourfolds. In contrast to the case of fivefolds, Chern and Pontryagin numbers of fourfolds are invariant under crepant birational maps; thus are independent of a choice of a crepant resolution. We computed for a large collection of elliptically-fibered fourfolds the closed form expressions for the characteristic classes in

1. Chapter 6 : Characteristic numbers of the eliptically-fibered fourfolds realizing various simple groups [116].

Hence, Chern numbers, Pontryagin numbers, Euler characteristics, all holomorphic genera of the fourfolds, the Todd genus, Hirzebruch signature, A-genus (and in turn, the index of the Dirac operator), and the curvature invariant eight-form were all computed. Furthermore, we showed that the arithmetic genus and the A-genus (and in turn, the index of a Dirac operator) are independent on the choice of a gauge group.

With the same perspective in mind, we computed characteristic numbers of elliptically-fibered fourfolds with multisections or non-trivial Mordell–Weil groups in

1. Chapter 7 : Characteristic numbers of elliptically-fibered fourfolds with multisections or non-trivial Mordell–Weil groups [117].

An elliptic fibration whose generic fiber is a genus-one normal curve of degree up to four is called an E_{9-d}-model, which is named after del Pezzo surfaces dP_{9-d}. We computed all the same characteristic numbers for these models and also for the Q_7-model, which provides a smooth model for elliptic

fibrations of rank one and generalizes E_5, E_6, and E_7-models. This Q_7-model is a generalized model we derived in Chapter 4 based on Newton's polygon with a quadrilateral defining equation with seven points on its boundary and a unique interior point [120]. In addition, we examined the same characteristic numbers of G-models with $G = \mathrm{SO}(n)$ with $n = 3, 4, 5, 6$ and $G = \mathrm{PSU}(3)$, whose Mordell–Weil groups are respectively $\mathbb{Z}_2$ and $\mathbb{Z}_3$.

We have also computed geometric properties of the Calabi–Yau varieties such as the triple intersection numbers in each Coulomb branch for various models [112, 113, 115, 118, 119, 121]. Such geometric properties are particularly more interesting for the models with semi-simple Lie groups. For example, the $\mathrm{SU}(2) \times \mathrm{G}_2$-model is an important model not only in F-theory and M-theory but also in birational geometry. Mathematically, it will appear naturally as a key model of collision of singularities solely based on the simplicity of its fiber structure. It is natural to organize elliptic fibrations describing collision of singularities by the rank of the associated Lie algebra derived from F-theory. Geometrically, the rank of G counts the number of fibral divisors produced by a crepant resolution and relates to the relative Picard number of the elliptic fibration via the Shioda–Tate–Wazir theorem.

Weak coupling limit and an abelian U(1) symmetry

Another important aspect of studying F-theory using elliptic fibrations is that we can study both the strong and weak coupling limits. Using toric geometry, we constructed a Q_7-model with a rank one Mordell–Weil group that gives a weak coupling limit broader than Sen's limit in

1. Chapter 4: Q_7-Model – a new model for elliptic fibrations with a rank one Mordell–Weil

group [120],

thereby solving the problem of the nonexistence of Sen's limit satisfying the tadpole condition for some cases such as the G_2-model [112] and the model considered in [76]. This model was investigated in [117] for its topological properties of the fourfolds. Additionally, despite its simple setup, this model gives an abelian $U(1)$ symmetry, which is desired for phenomenological reasons [120].

Quantum Error Correction and Infinite-dimensional von Neumann Algebras

In recent years, the study of entanglement entropy has utilized results in the mathematical field of operator algebras. Since AdS/CFT implies that information in the bulk is encoded redundantly in the boundary, quantum error correction is a natural framework that elucidates the connection between holographic quantum field theories and their gravity duals. Quantum error correcting codes using operator algebras were studied in finite-dimensional Hilbert spaces, where the bulk reconstruction is shown to be identical to the equivalence of bulk and boundary relative entropies [159]. Such quantum error correcting codes involve von Neumann algebras of type I_n. In order to study a more realistic toy model with infinite-dimensional Hilbert spaces, we are required to consider the action of different types of von Neumann algebras such as type II or III. In fact, a local quantum field theory in general carries a von Neumann algebra of type III as demonstrated in Chapter 15.

We have reformulated entanglement wedge reconstruction in the language of operator-algebra quantum error correction with infinite-dimensional physical and code Hilbert spaces in

1. Chapter 14: Holographic relative entropy in infinite-dimensional Hilbert spaces [185].

Assuming that the infinite-dimensional von Neumann algebras associated with an entanglement

wedge and its complement may both be reconstructed in their corresponding boundary subregions, we have proven that the relative entropies measured with respect to the bulk and boundary observables are equal. Furthermore, we have shown that the converse is also true: when the relative entropies measured in an entanglement wedge and its complement equal the relative entropies measured in their respective boundary subregions, entanglement wedge reconstruction is possible. For holographic theories with a well-defined entanglement wedge, this result provides a well-defined notion of holographic relative entropy.

Based on this theorem, we give an explicit construction of a quantum error correcting code where the code and physical Hilbert spaces are infinite-dimensional in

1. Chapter 15: Entanglement Wedge Reconstruction of Infinite-dimensional von Neumann algebras using Tensor Networks [184]

Following the approach of [307], we built a von Neumann algebra of type II_1 acting on the code Hilbert space and showed how it is mapped to the physical Hilbert space. We believe that the methods used in defining my construction can be extended to define an infinite-dimensional analog of the HaPPY code, yielding a holographic interpretation. Infinite-dimensional quantum error correcting codes, such as the one we have constructedin Chapter 15, should help better understand the connection between entanglement wedge reconstruction and the JLMS formula, which states that the relative entanglement entropy of the boundary gives the bulk relative entropy [178].

Throughout the thesis we have adhered to the philosophy that one can learn about different features of quantum gravity by studying string theory and string theory inspired constructions. With

two very different views using geometric engineering of F-theory and holography, we have discovered fruitful ways to enwiden our understanding of gravitational theories. We expect that the results contained herein, and more generally the research program evident in these nine-hundred pages, can be further utilized to learn much more about this, still, mysterious force, gravity.

References

[1] (2000). Lie groups, Calabi-Yau threefolds, and F theory. *Adv. Theor. Math. Phys.*, 4, 95–126. 2.12.2, 2.12.2, II, 8.1.2, 8.1.5, 9.0.2, II.5.1

[2] Almheiri, A., Dong, X., & Harlow, D. (2015). Bulk Locality and Quantum Error Correction in AdS/CFT. *JHEP*, 04, 163. 3, 3, 3, 15.9

[3] Aluffi, P. (2004). Chern classes of birational varieties. *Int. Math. Res. Not.*, (63), 3367–3377. 2.9.2, 2.9.4, 2.9.5, III

[4] Aluffi, P. (2010). Chern classes of blow-ups. *Math. Proc. Cambridge Philos. Soc.*, 148(2), 227–242. 2.7.1, 2.7.II, 2.7.12, 5, 5.1.1, 5.4.1, 8.5.1, II.2.3

[5] Aluffi, P. & Esole, M. (2009). Chern class identities from tadpole matching in type IIB and F-theory. *J. High Energy Phys.*, (3), 032, 29. 1.6, 2.3.6, 2.6, 2.7.1, 2.7.1, 2.II.1, 2.II.1, 2.II.2, 2.II.2, 4.1, 4.2.1, 4.2.5, 4.3.3, 4.4.3, 4.5, III, 5.0.4, 5.1.1, 5.2, 1, 7.1, 7.2, 7.2.3, 8.5.2, V, II.6, 12.1.3

[6] Aluffi, P. & Esole, M. (2010). New orientifold weak coupling limits in F-theory. *J. High Energy Phys.*, (2), 020, i, 52. 1.6, 2.3.6, 2.6, 2.7.1, 2.10.1, 2.II.1, 2.II.1, 2.II.2, 4.1, 4.2.5, 4.3.7, 4.4, 4.5, III, 5.0.4, 5.2, 7, 1, 7.2.1, 7.2.2, 2, 3, 7.2.3, 8.5.2, V, 12.1.3

[7] Alvarez-Gaume, L. & Ginsparg, P. H. (1985). The Structure of Gauge and Gravitational Anomalies. *Annals Phys.*, 161, 423. [,423(1984)]. III

[8] Alvarez-Gaume, L. & Witten, E. (1984). Gravitational Anomalies. *Nucl. Phys.*, B234, 269. [,269(1983)]. III

[9] Anderson, L. B., Esole, M., Fredrickson, L., & Schaposnik, L. P. (2018). Singular Geometry and Higgs Bundles in String Theory. *SIGMA*, 14, 037. 1.6, 2, IV

[10] Anderson, L. B., Gray, J., Raghuram, N., & Taylor, W. (2016). Matter in transition. *JHEP*, 04, 080. 2.3.3, 13

[11] Anderson, L. B., Heckman, J. J., Katz, S., & Schaposnik, L. P. (2017). T-Branes at the Limits of Geometry. *JHEP*, 10, 058. [JHEP17,058(2020)]. 1.6, 13

[12] Andreas, B. & Curio, G. (1999). On discrete twist and four flux in N=1 heterotic / F theory compactifications. *Adv. Theor. Math. Phys.*, 3, 1325–1413. 2.7.1, III

[13] Andreas, B. & Curio, G. (2010). From Local to Global in F-Theory Model Building. *J. Geom. Phys.*, 60, 1089–1102. 2.3.2, III

[14] Apruzzi, F., Heckman, J. J., Morrison, D. R., & Tizzano, L. (2018). 4D Gauge Theories with Conformal Matter. *JHEP*, 09, 088. 1.6

[15] Araki, H. (1976). Relative Entropy of States of Von Neumann Algebras. *Publ. Res. Inst. Math. Sci. Kyoto*, 1976, 809–833. 3, 3.5, 3.5.6, 14.4.7, 15.8, 5, 15.8.3, 15.8.3

[16] Argyres, P. C. & Douglas, M. R. (1995). New phenomena in SU(3) supersymmetric gauge theory. *Nucl. Phys.*, B448, 93–126. 12.2.1

[17] Arras, P., Grassi, A., & Weigand, T. (2018). Terminal Singularities, Milnor Numbers, and Matter in F-theory. *J. Geom. Phys.*, 123, 71–97. 2, 3

[18] Artin, M., Rodriguez-Villegas, F., & Tate, J. (2005). On the Jacobians of plane cubics. *Adv. Math.*, 198(1), 366–382. 2.2.3, 4.2.2, 7.2.3

[19] Aspinwall, P. S. & Gross, M. (1996). The SO(32) heterotic string on a K3 surface. *Phys. Lett.*, B387, 735–742. 2.3.3, 8, 8.1.2, 11.4.2

[20] Aspinwall, P. S. & Morrison, D. R. (1998). Nonsimply connected gauge groups and rational points on elliptic curves. *JHEP*, 07, 012. 2, 2, 2.2.4, 7, 7.1, 3, 7.2, 7.2.4, 7.3, 7.2.5, 10.1, 10.1.2

[21] Atiyah, M. & Witten, E. (2003). M theory dynamics on a manifold of G(2) holonomy. *Adv. Theor. Math. Phys.*, 6, 1–106. 8.1.6

[22] Avramis, S. D. & Kehagias, A. (2005). A Systematic search for anomaly-free supergravities in six dimensions. *JHEP*, 10, 052. 2, 2.13.2, 8.7.2, 9.5, 4, 11.5.2

[23] Baez, J. C. (2002). The octonions. *Bull. Amer. Math. Soc. (N.S.)*, 39(2), 145–205. 8.4.4

[24] Baez, J. C. & Huerta, J. (2010). The Algebra of Grand Unified Theories. *Bull. Am. Math. Soc.*, 47, 483–552. 12, 12.1.1

[25] Balakrishnan, S., Faulkner, T., Khandker, Z. U., & Wang, H. (2017). A General Proof of the Quantum Null Energy Condition. 3

[26] Ball, W. W. R. (1890/91). On Newton's Classification of Cubic Curves. *Proc. Lond. Math. Soc.*, 22, 104–143. II

[27] Banks, T., Fischler, W., Shenker, S. H., & Susskind, L. (1997). M theory as a matrix model: A Conjecture. *Phys. Rev.*, D55, 5112–5128. [,435(1996)]. 1

[28] Batyrev, V. V. (1984). *Higher-dimensional toric varieties with ample anticanonical class*. PhD thesis, Ph. D. thesis, Moscow State University, Moscow, Russia. 7.2.3

[29] Batyrev, V. V. (1999). Birational Calabi-Yau n-folds have equal Betti numbers. In *New trends in algebraic geometry (Warwick, 1996)*, volume 264 of *London Math. Soc. Lecture Note Ser.* (pp. 1–11). Cambridge Univ. Press, Cambridge. 2.8.2, 2.9.2, III, 5, 5.1.1, 5.9, 9.2.6, V, 11.2.4, 12.1.3, 12.3

[30] Batyrev, V. V. & Dais, D. I. (1996). Strong McKay correspondence, string-theoretic Hodge numbers and mirror symmetry. *Topology*, 35(4), 901–929. 2.8.1, 2.8.1

[31] Baume, F., Cvetic, M., Lawrie, C., & Lin, L. (2018). When rational sections become cyclic — Gauge enhancement in F-theory via Mordell-Weil torsion. *JHEP*, 03, 069. 1.6, 2, 7

[32] Baumgärtel, H. & Wollenberg, M. (1992). *Causal nets of operator algebras*, volume 80 of *Mathematische Lehrbücher und Monographien, II. Abteilung: Mathematische Monographien [Mathematical Textbooks and Monographs, Part II: Mathematical Monographs]*. Akademie-Verlag, Berlin. Mathematical aspects of algebraic quantum field theory. 3.5

[33] Beisert, N. et al. (2012). Review of AdS/CFT Integrability: An Overview. *Lett. Math. Phys.*, 99, 3–32. 1

[34] Berglund, P., Klemm, A., Mayr, P., & Theisen, S. (1999). On type IIB vacua with varying coupling constant. *Nucl. Phys.*, B558, 178–204. 7, 7.2.2

[35] Bernard, C. W., Christ, N. H., Guth, A. H., & Weinberg, E. J. (1977). Instanton Parameters for Arbitrary Gauge Groups. *Phys. Rev.*, D16, 2967. [,153(1977)]. 2.13.2

[36] Bernardoni, F., Cacciatori, S. L., Cerchiai, B. L., & Scotti, A. (2008). Mapping the geometry of the F_4 group. *Adv. Theor. Math. Phys.*, 12(4), 889–944. 8.4.4

[37] Bershadsky, M., Intriligator, K. A., Kachru, S., Morrison, D. R., Sadov, V., & Vafa, C. (1996). Geometric singularities and enhanced gauge symmetries. *Nucl. Phys.*, B481, 215–252. 2, 2.2.6, 2.3.2, III, III, IV, 8, 8.7.6, 9, 3, 9.1, V, 12.2, 12.2

[38] Bershadsky, M. & Johansen, A. (1997). Colliding singularities in F theory and phase transitions. *Nucl. Phys.*, B489, 122–138. 2, 2.6, V, 11

[39] Bershadsky, M., Pantev, T., & Sadov, V. (1999). F theory with quantized fluxes. *Adv. Theor. Math. Phys.*, 3, 727–773. 7, 7.2.2, 10.1

[40] Bershadsky, M. & Vafa, C. (1997). Global anomalies and geometric engineering of critical theories in six-dimensions. 12.1.5, 12.1.6, 12.7.2

[41] Bies, M. (2018-02). *Cohomologies of coherent sheaves and massless spectra in F-theory*. PhD thesis, Heidelberg U. 1.6

[42] Birkar, C., Cascini, P., Hacon, C. D., & McKernan, J. (2006). Existence of minimal models for varieties of log general type. *arXiv Mathematics e-prints*, (pp. math/0610203). 12.1.2, 12.2

[43] Bisognano, J. J. & Wichmann, E. H. (1976). On the Duality Condition for Quantum Fields. *J. Math. Phys.*, 17, 303–321. 3

[44] Blumenhagen, R., Grimm, T. W., Jurke, B., & Weigand, T. (2010). Global F-theory GUTs. *Nucl. Phys.*, B829, 325–369. III, 5.9, 16

[45] Bonetti, F. & Grimm, T. W. (2012). Six-dimensional (1,0) effective action of F-theory via M-theory on Calabi-Yau threefolds. *JHEP*, 05, 019. 1.6, 2

[46] Bonetti, F., Grimm, T. W., & Hohenegger, S. (2013). One-loop Chern-Simons terms in five dimensions. *JHEP*, 07, 043. 8.1.5

[47] Bonora, L. & Savelli, R. (2010). Non-simply-laced Lie algebras via F theory strings. *JHEP*, 11, 025. 8

[48] Borcherds, R. E. (1992). Monstrous moonshine and monstrous Lie superalgebras. *Invent. Math.*, 109(2), 405–444. 1

[49] Borchers, H. J. (2000). On revolutionizing quantum field theory with Tomita's modular theory. *J. Math. Phys.*, 41(6), 3604–3673. 15.8.2

[50] Borchmann, J., Mayrhofer, C., Palti, E., & Weigand, T. (2013). Elliptic fibrations for $SU(5) \times U(1) \times U(1)$ F-theory vacua. *Phys. Rev.*, D88(4), 046005. 4.1

[51] Borchmann, J., Mayrhofer, C., Palti, E., & Weigand, T. (2014). SU(5) Tops with Multiple U(1)s in F-theory. *Nucl. Phys.*, B882, 1–69. 4.1

[52] Borel, A. & Serre, J.-P. (1958). Le théorème de Riemann-Roch. *Bull. Soc. Math. France*, 86, 97–136. 5.3.3

[53] Bosch, S., Lütkebohmert, W., & Raynaud, M. (1990). *Néron models*, volume 21 of *Ergebnisse der Mathematik und ihrer Grenzgebiete (3) [Results in Mathematics and Related Areas (3)]*. Springer-Verlag, Berlin. 4.2.2

[54] Bott, R. & Tu, L. W. (1982). *Differential forms in algebraic topology*, volume 82 of *Graduate Texts in Mathematics*. Springer-Verlag, New York-Berlin. 5.3.1

[55] Bourbaki, N. (1998). *Lie groups and Lie algebras. Chapters 1–3*. Elements of Mathematics (Berlin). Springer-Verlag, Berlin. Translated from the French, Reprint of the 1989 English translation. 2.5, 2.5

[56] Bourbaki, N. (2002). *Lie groups and Lie algebras. Chapters 4–6*. Elements of Mathematics (Berlin). Springer-Verlag, Berlin. Translated from the 1968 French original by Andrew Pressley. 8.4.4, 8.4.4, 8.4.4, 8.4.4

[57] Bourbaki, N. (2005). *Lie groups and Lie algebras. Chapters 7–9*. Elements of Mathematics (Berlin). Springer-Verlag, Berlin. Translated from the 1975 and 1982 French originals by Andrew Pressley. 2.3.3, 2.3.3, 2.4.2, 10.1.1, 11.4.2, 11.4.2, 11.4.2

[58] Braun, A. P., Collinucci, A., & Valandro, R. (2012). G-flux in F-theory and algebraic cycles. *Nucl. Phys.*, B856, 129–179. 4.1, 7

[59] Braun, A. P., Collinucci, A., & Valandro, R. (2014). The fate of U(1)'s at strong coupling in F-theory. *JHEP*, 07, 028. 2.2.2, 4.1

[60] Braun, A. P. & Watari, T. (2013). On Singular Fibres in F-Theory. *JHEP*, 07, 031. 1

[61] Braun, V., Grimm, T. W., & Keitel, J. (2013a). Geometric Engineering in Toric F-Theory and GUTs with U(1) Gauge Factors. *JHEP*, 12, 069. 4.1, 7, 7.2.2

[62] Braun, V., Grimm, T. W., & Keitel, J. (2013b). New Global F-theory GUTs with U(1) symmetries. *JHEP*, 09, 154. 4.1

[63] Braun, V., Grimm, T. W., & Keitel, J. (2015). Complete Intersection Fibers in F-Theory. *JHEP*, 03, 125. 7

[64] Cacciatori, S. L., Cattaneo, A., & Geemen, B. (2011a). A new CY elliptic fibration and tadpole cancellation. *JHEP*, 10, 031. 4, 4.2.1, 1, 4.3.3, 4.5

[65] Cacciatori, S. L., Cattaneo, A., & Geemen, B. (2011b). A new CY elliptic fibration and tadpole cancellation. *JHEP*, 10, 031. 7.1, 2, 7.1, 7.2.2, 2, 5, 7.2.3, 7.2.3

[66] Cadavid, A. C., Ceresole, A., D'Auria, R., & Ferrara, S. (1995). Eleven-dimensional supergravity compactified on Calabi-Yau threefolds. *Phys. Lett.*, B357, 76–80. 2, 2.12, 2.12.2, 2.13.1, 8.1.5, V, 11.1.6, 12.1.3, 12.1.4

[67] Candelas, P., De La Ossa, X. C., Green, P. S., & Parkes, L. (1991). A Pair of Calabi-Yau manifolds as an exactly soluble superconformal theory. *Nucl. Phys.*, B359, 21–74. [AMS/IP Stud. Adv. Math.9,31(1998)]. 1

[68] Candelas, P. & Font, A. (1998). Duality between the webs of heterotic and type II vacua. *Nucl. Phys.*, B511, 295–325. 11

[69] Candelas, P., Perevalov, E., & Rajesh, G. (1998). Matter from toric geometry. *Nucl. Phys.*, B519, 225–238. V, 11, 11.1.1, 11.6.2

[70] Carter, R. W. (2005). *Lie algebras of finite and affine type*, volume 96 of *Cambridge Studies in Advanced Mathematics*. Cambridge University Press, Cambridge. 2, 2.1.1, 2.3.1, 8

[71] Casini, H. (2008). Relative entropy and the Bekenstein bound. *Class. Quant. Grav.*, 25, 205021. 3.5

[72] Casini, H. & Huerta, M. (2007). A c-theorem for the entanglement entropy. *J. Phys.*, A40, 7031–7036. 3

[73] Casini, H., Huerta, M., Myers, R. C., & Yale, A. (2015). Mutual information and the F-theorem. *JHEP*, 10, 003. 3

[74] Casini, H., Teste, E., & Torroba, G. (2017). Relative entropy and the RG flow. *JHEP*, 03, 089. 3.5

[75] Cassels, J. W. S. (1991). *Lectures on elliptic curves*, volume 24 of *London Mathematical Society Student Texts*. Cambridge University Press, Cambridge. 2.2.3

[76] Cattaneo, A. (2013). Crepant resolutions of Weierstrass threefolds and non-Kodaira fibres. 1, 8.4.3, 9.0.1, 11.1.5, 12.3.4, 16

[77] Clingher, A., Donagi, R., & Wijnholt, M. (2014). The Sen Limit. *Adv. Theor. Math. Phys.*, 18(3), 613–658. 4.2.5

[78] Collinucci, A., Denef, F., & Esole, M. (2009). D-brane Deconstructions in IIB Orientifolds. *JHEP*, 02, 005. 2.7.1, 2.10, 2.10, 2.11.2, 2.11.2, 4.1, 4.2.5, 4.2.5, 4.5, III, 1, 8.5.2, 9, V, 11.6, 12.1.3

[79] Collinucci, A., Fazzi, M., & Valandro, R. (2018). Geometric engineering on flops of length two. *JHEP*, 04, 090. 1.6

[80] Connes, A. & Stø rmer, E. (1978). Homogeneity of the state space of factors of type III_1. *J. Functional Analysis*, 28(2), 187–196. 3.0.2, 14.4.1

[81] Cornelius, Jr., E. F. (2011). Identities for complete homogeneous symmetric polynomials. *JP J. Algebra Number Theory Appl.*, 21(1), 109–116. 5, 5.5

[82] Cotler, J., Hayden, P., Penington, G., Salton, G., Swingle, B., & Walter, M. (2017). Entanglement Wedge Reconstruction via Universal Recovery Channels. 14.4.2, 15.9

[83] Cremmer, E., Julia, B., & Scherk, J. (1978). Supergravity Theory in Eleven-Dimensions. *Phys. Lett.*, B76, 409–412. [,25(1978)]. 2

[84] Cvetic, M., Klevers, D., & Piragua, H. (2013). F-Theory Compactifications with Multiple U(1)-Factors: Constructing Elliptic Fibrations with Rational Sections. *JHEP*, 06, 067. 4.1

[85] Cvetic, M., Klevers, D., Piragua, H., & Song, P. (2014). Elliptic fibrations with rank three Mordell-Weil group: F-theory with U(1) x U(1) x U(1) gauge symmetry. *JHEP*, 03, 021. 4.1

[86] Cvetič, M., Donagi, R., Klevers, D., Piragua, H., & Poretschkin, M. (2015). F-theory vacua with $\mathbb{Z}_3$ gauge symmetry. *Nucl. Phys.*, B898, 736–750. 7

[87] Cvetič, M., Grassi, A., Klevers, D., & Piragua, H. (2014). Chiral Four-Dimensional F-Theory Compactifications With SU(5) and Multiple U(1)-Factors. *JHEP*, 04, 010. 4.1

[88] Cvetič, M., Klevers, D., & Piragua, H. (2013). F-Theory Compactifications with Multiple U(1)-Factors: Addendum. *JHEP*, 12, 056. 4.1

[89] Czech, B., Karczmarek, J. L., Nogueira, F., & Van Raamsdonk, M. (2012). The Gravity Dual of a Density Matrix. *Class. Quant. Grav.*, 29, 155009. 3

[90] de Boer, J., Dijkgraaf, R., Hori, K., Keurentjes, A., Morgan, J., Morrison, D. R., & Sethi, S. (2002). Triples, fluxes, and strings. *Adv. Theor. Math. Phys.*, 4, 995–1186. 2.3.2, IV, 8.1.6

[91] Del Zotto, M., Heckman, J. J., & Morrison, D. R. (2017). 6D SCFTs and Phases of 5D Theories. *JHEP*, 09, 147. 8, 8.7.4

[92] Del Zotto, M., Heckman, J. J., Tomasiello, A., & Vafa, C. (2015). 6d Conformal Matter. *JHEP*, 02, 054. 11

[93] Del Zotto, M. & Lockhart, G. (2018). Universal Features of BPS Strings in Six-dimensional SCFTs. *JHEP*, 08, 173. 1.6

[94] Deligne, P. (1975). Courbes elliptiques: formulaire d'après J. Tate. (pp. 53–73. Lecture Notes in Math., Vol. 476). 2, 2, 2.2, 2.2.1, 2.2.1, 2.2.1, 4.2.2, III, 7.2.1, 7.2.2, 12

[95] Denef, F. (2008a). Les Houches Lectures on Constructing String Vacua. *Les Houches*, 87, 483–610. 4.1, 4.2.5

[96] Denef, F. (2008b). Les Houches Lectures on Constructing String Vacua. *Les Houches*, 87, 483–610. III, III

[97] Diaconescu, D.-E. & Entin, R. (1999). Calabi-Yau spaces and five-dimensional field theories with exceptional gauge symmetry. *Nucl. Phys.*, B538, 451–484. 2.4.2, 8, 8.5.4

[98] Dixon, L. J., Harvey, J. A., Vafa, C., & Witten, E. (1986). Strings on Orbifolds. 2. *Nucl. Phys.*, B274, 285–314. 2.8.1

[99] Dokchitser, T. & Dokchitser, V. (2013). A remark on Tate's algorithm and Kodaira types. *Acta Arith.*, 160(1), 95–100. 2.2.6

[100] Dolgachev, I. & Gross, M. (1994). Elliptic threefolds. I. Ogg-Shafarevich theory. *J. Algebraic Geom.*, 3(1), 39–80. 2.6, III

[101] Dolgačev, I. V. (1969). On the purity of the degeneration loci of families of curves. *Invent. Math.*, 8, 34–54. 2, 2.1.2

[102] Dong, X., Harlow, D., & Wall, A. C. (2016). Reconstruction of Bulk Operators within the Entanglement Wedge in Gauge-Gravity Duality. *Phys. Rev. Lett.*, 117(2), 021601. 3, 3, 3.5, 14.1, 14.4.6, 14.4.7, 15.9

[103] Dong, X. & Lewkowycz, A. (2018). Entropy, Extremality, Euclidean Variations, and the Equations of Motion. *JHEP*, 01, 081. 14.4.2, 10

[104] Duetsch, M. & Rehren, K.-H. (2003). Generalized free fields and the AdS - CFT correspondence. *Annales Henri Poincare*, 4, 613–635. 7, 14.4.2

[105] Eisenbud, D. (1995). *Commutative algebra*, volume 150 of *Graduate Texts in Mathematics*. Springer-Verlag, New York. With a view toward algebraic geometry. III

[106] Erler, J. (1994). Anomaly cancellation in six-dimensions. *J. Math. Phys.*, 35, 1819–1833. 2, 2.13.2, 4, 11.5.2

[107] Esole, M. (2017a). Introduction to elliptic fibrations. In *Quantization, geometry and noncommutative structures in mathematics and physics*, Math. Phys. Stud. (pp. 247–276). Springer, Cham. 1.6, 2.2.6, V

[108] Esole, M. (2017b). Introduction to Elliptic Fibrations. In *Proceedings, 9th Summer School on Geometric, Algebraic and Topological Methods for Quantum Field Theory: Villa de Leyva, Colombia, July 20-31, 2015* (pp. 247–276). 12, 12.2, 12.2

[109] Esole, M., Fullwood, J., & Yau, S.-T. (2015a). D_5 elliptic fibrations: non-Kodaira fibers and new orientifold limits of F-theory. *Commun. Number Theory Phys.*, 9(3), 583–642. 2.3.6, 2.6, 2.7.1, 2.7.3, 2.10.1, 2.11.1, 2.11.1, 2.11.2, 4.1, 1, 4.2.5, 4.3.7, III, 6.4.1, 6.4.1, 7, 1, 7.1, 7.2, 7.2.1, 7.2.2, 4, 8.5.2, 11.1.5, 12.3.4

[110] Esole, M., Jackson, S. G., Jagadeesan, R., & Noël, A. G. (2015b). Incidence Geometry in a Weyl Chamber I: GL_n. 1, 2.4.1, 2.4.2, 2.9.2, III, 8.1.1, 11.1.4, 12.1.2

[111] Esole, M., Jackson, S. G., Jagadeesan, R., & Noël, A. G. (2016a). Incidence Geometry in a Weyl Chamber II: SL_n. 1, 2.4.2, 2.9.2, III, 11.1.4, 12.1.2

[112] Esole, M., Jagadeesan, R., & Kang, M. J. (2017a). The Geometry of G_2, Spin(7), and Spin(8)-models. 1.6, 2, 2, 2, 2.2.6, 2.3.2, 2.4.1, 2.6, 2.12, 4.5.1, III, 5.1.1, 5.8, 5.8.2, 8, 8.1.2, 8.1.3, 8.1.4, 8.1.5, 8.8, V, 10.1, 11.1.1, 11.1.2, 11.1.3, 11.1.3, 11.1.4, 11.1.5, 11.4.2, 11.4.2, 12.1.1, 12.1.4, 12.2, 12.3.4, 12.4.1, 1, 16, 16, 16

[113] Esole, M., Jagadeesan, R., & Kang, M. J. (2019). 48 Crepant Paths to $\mathrm{SU}(2) \times \mathrm{SU}(3)$. 1.6, 5, 2.6, 2.12, 8.1.4, 8.1.5, V, 11.1.2, 11.1, 3, 16, 16

[114] Esole, M., Jefferson, P., & Kang, M. J. (2017b). Euler Characteristics of Crepant Resolutions of Weierstrass Models. 1.6, 5, 1, 2, 2.3.2, 2.7.1, 2.7.2, 2.7.12, 2.7.13, 2.7.14, 2.7.17, III, 6, 6.2.1, 7.2.2,

8, 8.1.1, 8.2, 8.5, 8.5.1, 8.5.1, 8.5.2, 8.7, 8.7.2, 8.8, 9, 9.2.6, 9.2.7, V, 10.1, 10.4.2, 11.2.3, 11.2.4, 12.1.3, 12.3.2, 1, 16

[115] Esole, M., Jefferson, P., & Kang, M. J. (2017c). The Geometry of F_4-Models. 1.6, 2, 2, 1, 2.4.1, 2.6, 2.12, 4.5.1, III, 8.1.4, 9, 9.6.2, V, 10.1, 11.4.2, 12.1.4, 12.3.4, 12.4.1, 12.4.1, 2, 16, 16

[116] Esole, M. & Kang, M. J. (2018a). Characteristic numbers of crepant resolutions of Weierstrass models. 2, 2.9.6, III, 7.4, 8.1.1, 8.1.7, 8.3, 8.5.3, 12.1.3, 1

[117] Esole, M. & Kang, M. J. (2018b). Characteristic numbers of elliptic fibrations with non-trivial Mordell-Weil groups. 3, 8.5.3, 12.1.3, 1, 16

[118] Esole, M. & Kang, M. J. (2018c). Flopping and Slicing: SO(4) and Spin(4)-models. 1.6, 3, 2.3.2, 2.4.2, 2.6, 2.7.1, 2.12, 4.5.1, III, 7.1, 3, 7.2, 7.2.4, 7.3, 8.1.4, 8.1.5, V, 11.1.2, 11.1, 12, 12.1.4, 1, 12.3.4, 1, 16, 16

[119] Esole, M. & Kang, M. J. (2019). The Geometry of the SU(2)$\times$ G_2-model. *JHEP*, 02, 091. 1.6, 4, 2.4.2, 2.12, III, 8, 8.1.2, 8.1.4, 8.1.5, 8.8, 9, V, 12, 1, 12.3.1, 12.3.1, 12.3.2, 12.3.2, 12.4.1, 12.4.1, 2, 16, 16

[120] Esole, M., Kang, M. J., & Yau, S.-T. (2014). A New Model for Elliptic Fibrations with a Rank One Mordell-Weil Group: I. Singular Fibers and Semi-Stable Degenerations. 1.6, 2.3.6, 2.6, 2.7.1, 2.7.4, III, 7.1, 2, 7.1, 7.2, 7.2, 7.2.2, 5, 7.2.3, 7.2.3, 8.5.2, 16, 1, 16

[121] Esole, M., Kang, M. J., & Yau, S.-T. (2017d). Mordell-Weil Torsion, Anomalies, and Phase Transitions. 1.6, 6, 2.3.2, 2.4.2, 2.6, 2.7.1, 2.12, 2.13.2, 4.5.1, III, 3, 8.1.4, 8.1.5, V, 10.1, 11.1.2, 11.1, 11.4.2, 12, 12.1.4, 1, 12.7.2, 4, 16, 16

[122] Esole, M. & Pasterski, S. (2018). D_4-flops of the E_7-model. 8.1.5, 8.8, 12.3.4

[123] Esole, M. & Savelli, R. (2013). Tate Form and Weak Coupling Limits in F-theory. *JHEP*, 06, 027. 4.1, 8, 9, 11.6, 12.2.1

[124] Esole, M. & Shao, S.-H. (2015). M-theory on Elliptic Calabi-Yau Threefolds and 6d Anomalies. 1.6, 1.6, 2, 2, 2.3.2, 2.6, 2.7.1, 2.12, III, III, 8.1.5, 9.6.2, V, 10.1, 11.5.1, 12, 12.1.4, 13

[125] Esole, M., Shao, S.-H., & Yau, S.-T. (2015c). Singularities and Gauge Theory Phases. *Adv. Theor. Math. Phys.*, 19, 1183–1247. 1.6, 2, 1, 2.3.2, 2.4.2, 2.6, III, 4.5.1, III, 5.7, 11.1.4, 12, 12.3.1, 12.3.4, 12.5.1, 13

[126] Esole, M., Shao, S.-H., & Yau, S.-T. (2015d). Singularities and Gauge Theory Phases. *Adv. Theor. Math. Phys.*, 19, 1183–1247. 1

[127] Esole, M., Shao, S.-H., & Yau, S.-T. (2016b). Singularities and Gauge Theory Phases II. *Adv. Theor. Math. Phys.*, 20, 683–749. 1.6, 2, 1, 2.3.2, 2.4.2, 2.6, III, 4.5.1, III, 11.1.4, 12.3.1, 12.3.4

[128] Esole, M., Shao, S.-H., & Yau, S.-T. (2016c). Singularities and Gauge Theory Phases II. *Adv. Theor. Math. Phys.*, 20, 683–749. 1

[129] Esole, M. & Yau, S.-T. (2013). Small resolutions of SU(5)-models in F-theory. *Adv. Theor. Math. Phys.*, 17(6), 1195–1253. 1.6, 1.6, 2, 2.3.2, 2.6, 2.7.1, 1, III, 4.5.1, III, IV, 9.5.1, 11.1.5, 12.3.1, 12.3.4, 12.7.1

[130] Faulkner, T., Lewkowycz, A., & Maldacena, J. (2013). Quantum corrections to holographic entanglement entropy. *JHEP*, 11, 074. 14.4.2

[131] Ferrara, S., Minasian, R., & Sagnotti, A. (1996). Low-energy analysis of M and F theories on Calabi-Yau threefolds. *Nucl. Phys.*, B474, 323–342. 2

[132] Figueroa-O'Farrill, J. (2008). A geometric construction of the exceptional Lie algebras F_4 and E_8. *Comm. Math. Phys.*, 283(3), 663–674. 8.4.4

[133] Fisher, T. (2008). The invariants of a genus one curve. *Proc. Lond. Math. Soc. (3)*, 97(3), 753–782. 7.2.1

[134] Fullwood, J. (2011). On generalized Sethi-Vafa-Witten formulas. *J. Math. Phys.*, 52, 082304. 2.7.17, 5.0.4, 7.3.1

[135] Fullwood, J. & van Hoeij, M. (2013). On stringy invariants of GUT vacua. *Commun. Num. Theor Phys.*, 07, 551–579. 2.7.1, III, III, 5, 5.4.1

[136] Fulton, W. (1998). *Intersection theory*, volume 2 of *Ergebnisse der Mathematik und ihrer Grenzgebiete. 3. Folge. A Series of Modern Surveys in Mathematics [Results in Mathematics and Related Areas. 3rd Series. A Series of Modern Surveys in Mathematics]*. Springer-Verlag, Berlin, second edition. 2, 2.1.2, 4, 2.3.3, 2.7.1, 2.7.2, 2.7.5, 2.7.6, 2.7.7, 2.9, III, 5, 5.1.1, 5.3.2, 5.3.1, 5.3.6, 5.3.3, 5.3.3, 5.3.3, 5.4.1, 8.2

[137] Gabbiani, F. & Fröhlich, J. (1993). Operator algebras and conformal field theory. *Comm. Math. Phys.*, 155(3), 569–640. 3, 15.9

[138] Ghosh, S. & Raju, S. (2017). Loss of locality in gravitational correlators with a large number of insertions. *Phys. Rev.*, D96(6), 066033. 9

[139] Ghosh, S. & Raju, S. (2018). Quantum information measures for restricted sets of observables. *Phys. Rev.*, D98(4), 046005. 9

[140] Goresky, M. & MacPherson, R. (1984). Problems and bibliography on intersection homology. In *Intersection cohomology (Bern, 1983)*, volume 50 of *Progr. Math.* (pp. 221–233). Birkhäuser Boston, Boston, MA. 2.9.1, 2.9.2, III

[141] Grassi, A., Halverson, J., Shaneson, J., & Taylor, W. (2015). Non-Higgsable QCD and the Standard Model Spectrum in F-theory. *JHEP*, 01, 086. 12, 12.6

[142] Grassi, A. & Morrison, D. R. (2000). Group representations and the Euler characteristic of elliptically fibered Calabi-Yau threefolds. 2.12.2, 2.13.2, 2.13.2, 2.13.2, III, 5.2, 8.1.4, 8.1.5, 8.7.4, 8.8, 9.0.2, 9.6.3, V, 11.5.2, 12.1.3, 12.7.2, 5

[143] Grassi, A. & Morrison, D. R. (2012). Anomalies and the Euler characteristic of elliptic Calabi-Yau threefolds. *Commun. Num. Theor. Phys.*, 6, 51–127. 11, 8.1.4, 8.7.4

[144] Grassi, A. & Perduca, V. (2013). Weierstrass models of elliptic toric $K3$ hypersurfaces and symplectic cuts. *Adv. Theor. Math. Phys.*, 17(4), 741–770. 7, 7.2.2

[145] Grassi, A. & Weigand, T. (2018). On topological invariants of algebraic threefolds with ($\mathbb{Q}$-factorial) singularities. 3

[146] Green, M. B. & Schwarz, J. H. (1984). Anomaly Cancellation in Supersymmetric D=10 Gauge Theory and Superstring Theory. *phys. Lett.*, 149B, 117–122. 1.1

[147] Green, M. B., Schwarz, J. H., & West, P. C. (1985). Anomaly Free Chiral Theories in Six-Dimensions. *Nucl. Phys.*, B254, 327–348. 2, 2.13, 2.13.2, 2.13.2, 11.5.2

[148] Grimm, T. W. & Hayashi, H. (2012). F-theory fluxes, Chirality and Chern-Simons theories. *JHEP*, 03, 027. 1.6, 1, 2.12, 8.1.5

[149] Grimm, T. W. & Kapfer, A. (2016). Anomaly Cancelation in Field Theory and F-theory on a Circle. *JHEP*, 05, 102. 2, 8.1.5, 9.6.2, 10.1

[150] Grimm, T. W., Kapfer, A., & Keitel, J. (2013). Effective action of 6D F-Theory with U(1) factors: Rational sections make Chern-Simons terms jump. *JHEP*, 07, 115. 4.1

[151] Grimm, T. W. & Weigand, T. (2010). On Abelian Gauge Symmetries and Proton Decay in Global F-theory GUTs. *Phys. Rev.*, D82, 086009. 7

[152] Guicciardini, N. (2009). *Isaac Newton on Mathematical Certainty and Method*. Mit Press. II

[153] Gukov, S., Vafa, C., & Witten, E. (2000). CFT's from Calabi-Yau four folds. *Nucl. Phys.*, B584, 69–108. [Erratum: Nucl. Phys.B608,477(2001)]. 2.10

[154] Gustafson, R. A. & Milne, S. C. a. (1983). Schur functions, Good's identity, and hypergeometric series well poised in SU(n). *Adv. in Math.*, 48(2), 177–188. 5

[155] Haag, R. (1992). *Local quantum physics: Fields, particles, algebras*. 3, 9, 14.4, 14.4.1, 7

[156] Haghighat, B., Klemm, A., Lockhart, G., & Vafa, C. (2015). Strings of Minimal 6d SCFTs. *Fortsch. Phys.*, 63, 294–322. 8

[157] Hamilton, A., Kabat, D. N., Lifschytz, G., & Lowe, D. A. (2006a). Holographic representation of local bulk operators. *Phys. Rev.*, D74, 066009. 3, 3

[158] Hamilton, A., Kabat, D. N., Lifschytz, G., & Lowe, D. A. (2006b). Local bulk operators in AdS/CFT: A Boundary view of horizons and locality. *Phys. Rev.*, D73, 086003. 3, 3

[159] Harlow, D. (2017). The Ryu–Takayanagi Formula from Quantum Error Correction. *Commun. Math. Phys.*, 354(3), 865–912. 3, 3, VI, 14.1, 14.4, 14.4.6, 14.4.6, 14.4.6, 14.4.6, 14.4.6, 14.4.7, 15, 15.8.1, 15.8.1, 15.9, 16

[160] Harlow, D. (2018). TASI Lectures on the Emergence of Bulk Physics in AdS/CFT. *PoS*, TASI2017, 002. 3, 3, 14.4.4, 14.4.7, 15

[161] Harris, J. (1704). *Lexicon Technicum, Or, An Universal English Dictionary of Arts and Sciences: Explaining Not Only the Terms of Art But the Arts Themselves*. Lexicon Technicum. D. Brown. II

[162] Hartshorne, R. (1977). *Algebraic geometry*. Springer-Verlag, New York-Heidelberg. Graduate Texts in Mathematics, No. 52. 2, 2.12.1, 8.5.6

[163] Hayashi, H., Lawrie, C., Morrison, D. R., & Schafer-Nameki, S. (2014). Box Graphs and Singular Fibers. *JHEP*, 05, 048. 1, 2.4.1, 2.4.2, 2.9.2, 1, III, III, 8.1.1, 11.1.5, 12.1.2

[164] Hayden, P., Nezami, S., Qi, X.-L., Thomas, N., Walter, M., & Yang, Z. (2016). Holographic duality from random tensor networks. *JHEP*, 11, 009. 3

[165] Hayden, P. & Penington, G. (2018). Learning the Alpha-bits of Black Holes. 14.4.2, 11, 14.4.4

[166] Hayden, P. & Preskill, J. (2007). Black holes as mirrors: Quantum information in random subsystems. *JHEP*, 09, 120. 1

[167] Headrick, M., Hubeny, V. E., Lawrence, A., & Rangamani, M. (2014). Causality & holographic entanglement entropy. *JHEP*, 12, 162. 3, 3

[168] Heckman, J. J., Morrison, D. R., & Vafa, C. (2014). On the Classification of 6D SCFTs and Generalized ADE Orbifolds. *JHEP*, 05, 028. [Erratum: JHEP06,017(2015)]. 11

[169] Heckman, J. J. & Rudelius, T. (2019). Top Down Approach to 6D SCFTs. *J. Phys.*, A52(9), 093001. 1.6, 2.3.2

[170] Hirzebruch, F. (1954). Some problems on differentiable and complex manifolds. *Ann. of Math. (2)*, 60, 213–236. 6.3

[171] Hirzebruch, F. (1995). *Topological methods in algebraic geometry*. Classics in Mathematics. Springer-Verlag, Berlin. Translated from the German and Appendix One by R. L. E. Schwarzenberger, With a preface to the third English edition by the author and Schwarzenberger, Appendix Two by A. Borel, Reprint of the 1978 edition. 2.9, III, 5.3.8, 5.3.3

[172] (https://mathoverflow.net/users/10076/s Quotient singularities with no crepant resolution? MathOverflow. URL:https://mathoverflow.net/q/66702 (version: 2011-06-03). 12.1.2

[173] Hulek, K. (1983). Projective geometry of elliptic curves. In *Algebraic geometry—open problems (Ravello, 1982)*, volume 997 of *Lecture Notes in Math.* (pp. 228–266). Springer, Berlin. 7.2.1

[174] Humphreys, J. E. (1978). *Introduction to Lie algebras and representation theory*, volume 9 of *Graduate Texts in Mathematics*. Springer-Verlag, New York-Berlin. Second printing, revised. 2.3.3

[175] Husemöller, D. (2004). *Elliptic curves*, volume 111 of *Graduate Texts in Mathematics*. Springer-Verlag, New York, second edition. With appendices by Otto Forster, Ruth Lawrence and Stefan Theisen. 2.2.4, 10.1.2

[176] Intriligator, K. A., Morrison, D. R., & Seiberg, N. (1997). Five-dimensional supersymmetric gauge theories and degenerations of Calabi-Yau spaces. *Nucl. Phys.*, B497, 56–100. 2, I, 2.4.2, 2.12.I, III, III, 8, 8.I.2, 8.I.5, 8.I.7, 8.7.I, 8.8, V, I0.4.4, II.I.6, I2.I.2, I2.I.3, I3.I.6

[177] Jacobi, C. G. J. (1825). *Disquisitiones Analyticae de Fractionibus Simplicibus*. apud F. A. Herbig. I, 5.5.I

[178] Jafferis, D. L., Lewkowycz, A., Maldacena, J., & Suh, S. J. (2016). Relative entropy equals bulk relative entropy. *JHEP*, 06, 004. 3, 3, 3, 3.5, 3.5, I4.I, I4.4.2, I4.4.7, I5.9, I6

[179] Jefferson, P., Katz, S., Kim, H.-C., & Vafa, C. (2018). On Geometric Classification of 5d SCFTs. *JHEP*, 04, I03. I.6

[180] Jones, V. F. (2015). von neumann algebras. 3.I.I, 3.I.I4, 3.3, 3.3.2, 3.4.2, 3.4.3, 3.4.I3, 3.4.I4, 3.4.I5, 3.5, 3.5.4, I4.3, 8

[181] Joyce, D. D. (2000). *Compact manifolds with special holonomy*. Oxford University Press on Demand. I.3

[182] Kac, V. G. (1990). *Infinite-dimensional Lie algebras*. Cambridge University Press, Cambridge, third edition. 2.3.I, II.I.5

[183] Kahn, P. J. (1965). Characteristic numbers and homotopy type. *Michigan Math. J.*, I2, 49–60. 6.3.3

[184] Kang, M. J. & Kolchmeyer, D. (To appear). Entanglement wedge reconstruction of infinite-dim von neumann algebras. 3, I5, I

[185] Kang, M. J. & Kolchmeyer, D. K. (2018). Holographic Relative Entropy in Infinite-dimensional Hilbert Spaces. 3, I0, VI, I5.5.2, I5.7, I5.8.2, 6, I5.9, I

[186] Katz, S., Morrison, D. R., Schafer-Nameki, S., & Sully, J. (2011). Tate's algorithm and F-theory. *JHEP*, 08, 094. 2.2.6, 2.3.2, III, 5.8, 5.8, 3, I2.2

[187] Katz, S. H. & Vafa, C. (1997). Matter from geometry. *Nucl. Phys.*, B497, I46–I54. 8.I.4, II.4.I, I2.4.I

[188] Kawamata, Y. (1988). Crepant blowing-up of 3-dimensional canonical singularities and its application to degenerations of surfaces. *Ann. of Math. (2)*, I27(I), 93–I63. I2.I.2

[189] Kawamata, Y. (1997). On the cone of divisors of Calabi-Yau fiber spaces. *arXiv e-prints*, (pp. alg–geom/9701006). 12.1.2

[190] Kawamata, Y. (2008). Flops connect minimal models. *Publ. Res. Inst. Math. Sci.*, 44(2), 419–423. 12.1.2

[191] Kawamata, Y. & Matsuki, K. (1987). The number of the minimal models for a 3-fold of general type is finite. *Math. Ann.*, 276(4), 595–598. 12.1.2

[192] Kelly, W. R. (2017). Bulk Locality and Entanglement Swapping in AdS/CFT. *JHEP*, 03, 153. 11

[193] Kitaev, A. & Preskill, J. (2006). Topological entanglement entropy. *Phys. Rev. Lett.*, 96, 110404. 1, 3

[194] Klebanov, I. R., Kutasov, D., & Murugan, A. (2008). Entanglement as a probe of confinement. *Nucl. Phys.*, B796, 274–293. 3

[195] Klemm, A., Lerche, W., & Mayr, P. (1995). K3 Fibrations and heterotic type II string duality. *Phys. Lett.*, B357, 313–322. 7, 7.2.2

[196] Klemm, A., Lian, B., Roan, S. S., & Yau, S.-T. (1998). Calabi-Yau fourfolds for M theory and F theory compactifications. *Nucl. Phys.*, B518, 515–574. 2, 6.2.1, 7.2.1, 7.2.2

[197] Klevers, D., Mayorga Pena, D. K., Oehlmann, P.-K., Piragua, H., & Reuter, J. (2015). F-Theory on all Toric Hypersurface Fibrations and its Higgs Branches. *JHEP*, 01, 142. 4.1, 7.2.2

[198] Klevers, D., Morrison, D. R., Raghuram, N., & Taylor, W. (2017). Exotic matter on singular divisors in F-theory. *JHEP*, 11, 124. 1.6

[199] Klevers, D. & Taylor, W. (2016). Three-Index Symmetric Matter Representations of SU(2) in F-Theory from Non-Tate Form Weierstrass Models. *JHEP*, 06, 171. 2.3.3

[200] Kodaira, K. (1963). On compact analytic surfaces. II, III. *Ann. of Math. (2) 77 (1963), 563–626; ibid.*, 78, 1–40. 2, 2, 2.1.1, 2.1.1, 2.1.6, 2.1, 2.6, III, 5.2, 12.2

[201] Koelman, R. J. (1991). *The number of moduli of families of curves on toric surfaces*. [Sl: sn]. 7.2.3

[202] Kollár, J. & Mori, S. (1998). *Birational Geometry of Algebraic Varieties*. Cambridge Tracts in Mathematics. Cambridge University Press. 12.1.2

[Kontsevich] Kontsevich, M. String cohomology. 2.8.3, 2.8.2, 2.8.4, 2.9.2, III, 5, 5.6, 5.6.1, 5.9

[204] Kotschick, D. (2008). Chern numbers and diffeomorphism types of projective varieties. *J. Topol.*, 1(2), 518–526. 6.3

[205] Kotschick, D. (2009). Characteristic numbers of algebraic varieties. *Proc. Natl. Acad. Sci. USA*, 106(25), 10114–10115. 6.3

[206] Kotschick, D. (2012). Topologically invariant Chern numbers of projective varieties. *Adv. Math.*, 229(2), 1300–1312. 6.3.1, 6.3.2

[207] Krause, S., Mayrhofer, C., & Weigand, T. (2012). G_4 flux, chiral matter and singularity resolution in F-theory compactifications. *Nucl. Phys.*, B858, 1–47. 7, 12.3.4

[208] Kumar, V., Morrison, D. R., & Taylor, W. (2010). Global aspects of the space of 6D N = 1 supergravities. *JHEP*, 11, 118. 2.13.2, 2.13.2, 2.9

[209] Kuntzler, M. & Schafer-Nameki, S. (2012). G-flux and Spectral Divisors. *JHEP*, 11, 025. 8.1.1

[210] Kuntzler, M. & Schafer-Nameki, S. (2014). Tate Trees for Elliptic Fibrations with Rank one Mordell-Weil group. 4.1

[Landsman] Landsman, N. Lecture notes on operator algebras. 3.3, 15.9

[212] Lang, S. (2002). *Algebra*, volume 211 of *Graduate Texts in Mathematics*. Springer-Verlag, New York, third edition. 9.1

[213] Lascu, A. T. & Scott, D. B. (1975). An algebraic correspondence with applications to projective bundles and blowing up Chern classes. *Ann. Mat. Pura Appl. (4)*, 102, 1–36. 5.4.1

[214] Lascu, A. T. & Scott, D. B. (1978). A simple proof of the formula for the blowing up of Chern classes. *Amer. J. Math.*, 100(2), 293–301. 5.4.1

[215] Lawrie, C. & Schafer-Nameki, S. (2013). The Tate Form on Steroids: Resolution and Higher Codimension Fibers. *JHEP*, 04, 061. 2.3.2, 12.3.4

[216] Lee, S.-J., Regalado, D., & Weigand, T. (2018). 6d SCFTs and U(1) Flavour Symmetries. *JHEP*, 11, 147. 1.6

[217] Levin, M. & Wen, X.-G. (2006). Detecting Topological Order in a Ground State Wave Function. *Phys. Rev. Lett.*, 96, 110405. 3

[218] Libgober, A. S. & Wood, J. W. (1990). Uniqueness of the complex structure on Kähler manifolds of certain homotopy types. *J. Differential Geom.*, 32(1), 139–154. 2.9.3

[219] Liu, Q. (2002). *Algebraic geometry and arithmetic curves*, volume 6 of *Oxford Graduate Texts in Mathematics*. Oxford University Press, Oxford. Translated from the French by Reinie Erné, Oxford Science Publications. 2.1.2, 9, 1, 4

[220] Longo, R. & Xu, F. (2018a). Comment on the Bekenstein bound. *J. Geom. Phys.*, 130, 113–120. 3

[221] Longo, R. & Xu, F. (2018b). Relative Entropy in CFT. *Adv. Math.*, 337, 139–170. 3

[222] Louck, J. D. & Biedenharn, L. C. (1970). Canonical unit adjoint tensor operators in u(n). *J. Math. Phys.*, 11, 2368–2414. 5, 5.5, 5.5

[223] Macdonald, I. G. (1972). Affine root systems and Dedekind's η-function. *Invent. Math.*, 15, 91–143. 2.3.1

[224] Maldacena, J. M. (1999). The Large N limit of superconformal field theories and supergravity. *Int. J. Theor. Phys.*, 38, 1113–1133. [Adv. Theor. Math. Phys.2,231(1998)]. 1

[225] Manin, Y. I. (1986). *Cubic forms*, volume 4 of *North-Holland Mathematical Library*. North-Holland Publishing Co., Amsterdam, second edition. Algebra, geometry, arithmetic, Translated from the Russian by M. Hazewinkel. 7.2.1

[226] Marsano, J. & Schafer-Nameki, S. (2011). Yukawas, G-flux, and Spectral Covers from Resolved Calabi-Yau's. *JHEP*, 11, 098. 2.7.1, III, 8.1.2, 11.4.2

[227] Matsuki, K. (1995). Weyl groups and birational transformations among minimal models. *Mem. Amer. Math. Soc.*, 116(557), vi+133. 2, 2.4.2, 12.1.2

[228] Matsuki, K. (2002). *Introduction to the Mori program*. Universitext. Springer-Verlag, New York. 5.2.4, 8.1.2, 12.1.2, 12.4.3

[229] Mayrhofer, C., Morrison, D. R., Till, O., & Weigand, T. (2014a). Mordell-Weil Torsion and the Global Structure of Gauge Groups in F-theory. *JHEP*, 10, 16. 2, 2, 2.3.2, 2.3.2, 4.1, III, 7, V, 10.1, 13

[230] Mayrhofer, C., Palti, E., Till, O., & Weigand, T. (2014b). Discrete Gauge Symmetries by Higgsing in four-dimensional F-Theory Compactifications. *JHEP*, 12, 068.

[231] Mayrhofer, C., Palti, E., Till, O., & Weigand, T. (2015). On Discrete Symmetries and Torsion Homology in F-Theory. *JHEP*, 06, 029. 7

[232] Mayrhofer, C., Palti, E., & Weigand, T. (2013). U(1) symmetries in F-theory GUTs with multiple sections. *JHEP*, 03, 098. 4.1

[233] McKay, W. G. & Patera, J. (1981). *Tables of dimensions, indices, and branching rules for representations of simple Lie algebras*, volume 69 of *Lecture Notes in Pure and Applied Mathematics*. Marcel Dekker, Inc., New York. 8.1.4, 11.4.1

[234] Milnor, J. W. & Stasheff, J. D. (1974). *Characteristic classes*. Princeton University Press, Princeton, N. J.; University of Tokyo Press, Tokyo. Annals of Mathematics Studies, No. 76. 2.9, 4, III

[235] Minasian, R. & Moore, G. W. (1997). K theory and Ramond-Ramond charge. *JHEP*, 11, 002. III

[236] Miranda, R. (1983). Smooth models for elliptic threefolds. In *The birational geometry of degenerations (Cambridge, Mass., 1981)*, volume 29 of *Progr. Math.* (pp. 85–133). Birkhäuser, Boston, Mass. 2, 2.6, III, 1, 1, 8.1.7, 9, 9.0.1, V, 10.1.2, 11, 11.1.2, 11.1.3, 11.1.5, 12.3.4

[237] Monnier, S., Moore, G. W., & Park, D. S. (2018). Quantization of anomaly coefficients in 6D $\mathcal{N} = (1, 0)$ supergravity. *JHEP*, 02, 020. 2.13.2, 12.7.2

[238] Montonen, C. & Olive, D. I. (1977). Magnetic Monopoles as Gauge Particles? *Phys. Lett.*, 72B, 117–120. 1.1

[239] Morrison, D. R. & Park, D. S. (2012). F-Theory and the Mordell-Weil Group of Elliptically-Fibered Calabi-Yau Threefolds. *JHEP*, 10, 128. 2, 4.1, 4.2.2, 4.2.3, 4.3.2, 7.1, 2, 7.2.3

[240] Morrison, D. R. & Taylor, W. (2012a). Classifying bases for 6D F-theory models. *Central Eur. J. Phys.*, 10, 1072–1088. 8.1.6, 8.7.7, 8.7.4, 9, 9.6.2, V, 11, 11.1.1, 11.6.2, 12

[241] Morrison, D. R. & Taylor, W. (2012b). Matter and singularities. *JHEP*, 01, 022. 1, 8.1.2, 11.4.2, 12.3.4

[242] Morrison, D. R. & Taylor, W. (2014). Sections, multisections, and U(1) fields in F-theory. 4.1, 10.1

[243] Morrison, D. R. & Vafa, C. (1996a). Compactifications of F theory on Calabi-Yau threefolds. 1. *Nucl. Phys.*, B473, 74–92. 2, 2.3.2, 2.6, III, IV

[244] Morrison, D. R. & Vafa, C. (1996b). Compactifications of F theory on Calabi-Yau threefolds. 2. *Nucl. Phys.*, B476, 437–469. 2, III, 5.6.7, IV, 3, 12.2.1

[245] Morrison, I. A. (2014). Boundary-to-bulk maps for AdS causal wedges and the Reeh-Schlieder property in holography. *JHEP*, 05, 053. 14.4.4, 14.4.7

[246] Mumford, D. & Suominen, K. (1972). Introduction to the theory of moduli. (pp. 171–222). 2, 2.2, III, 7.2.1, 7.2.2, 12

[247] Nakayama, N. (1988). On Weierstrass models. In *Algebraic geometry and commutative algebra, Vol. II* (pp. 405–431). Kinokuniya, Tokyo. 2

[248] Nakayama, N. (1991). Elliptic fibrations over surfaces. I. In *Algebraic geometry and analytic geometry (Tokyo, 1990)*, ICM-90 Satell. Conf. Proc. (pp. 126–137). Springer, Tokyo. 2.6

[249] Nakayama, N. (2002a). Global structure of an elliptic fibration. *Publ. Res. Inst. Math. Sci.*, 38(3), 451–649. III

[250] Nakayama, N. (2002b). Local structure of an elliptic fibration. In *Higher dimensional birational geometry (Kyoto, 1997)*, volume 35 of *Adv. Stud. Pure Math.* (pp. 185–295). Math. Soc. Japan, Tokyo. III

[251] Néron, A. (1964). Modèles minimaux des variétés abéliennes sur les corps locaux et globaux. *Inst. Hautes Études Sci. Publ.Math. No.*, 21, 128. 2, 2.1.1, 2.1, 2.6, III, IV, 8.1.1, 8.2.4, 9.1

[252] Newton, I. & Talbot, C. (1860). *Sir Isaac Newton's Enumeration of Lines of the Third Order, Generation of Curves by Shadows, Organic Description of Curves, and Construction of Equations by Curves*. Bohn. II

[253] Novikov, S. P. (1965). Topological invariance of rational classes of Pontrjagin. *Dokl. Akad. Nauk SSSR*, 163, 298–300. 6.3

[254] Oehlmann, P.-K., Reuter, J., & Schimannek, T. (2016). Mordell-Weil Torsion in the Mirror of Multi-Sections. *JHEP*, 12, 031. 7

[255] Osborn, H. (1979). Topological charges for N = 4 supersymmetric gauge theories and monopoles of spin 1. *Physics Letters B*, 83, 321–326. 1.1

[256] Papadopoulos, I. (1993). Sur la classification de Néron des courbes elliptiques en caractéristique résiduelle 2 et 3. *J. Number Theory*, 44(2), 119–152. 2.2.6, 9.1, 3

[257] Park, D. S. (2012). Anomaly Equations and Intersection Theory. *JHEP*, 01, 093. 2.13.2, 2.13.2, 4.1, III

[258] Park, D. S. & Taylor, W. (2012). Constraints on 6D Supergravity Theories with Abelian Gauge Symmetry. *JHEP*, 01, 141. 4.1

[259] Pastawski, F., Yoshida, B., Harlow, D., & Preskill, J. (2015). Holographic quantum error-correcting codes: Toy models for the bulk/boundary correspondence. *JHEP*, 06, 149. 14.4.6, 14.4.6, 1, 15.9

[260] Petz, D. (1986). Sufficient subalgebras and the relative entropy of states of a von Neumann algebra. *Commun. Math. Phys.*, 105(1), 123–131. 3

[261] Porteous, I. R. (1960). Blowing up Chern classes. *Proc. Cambridge Philos. Soc.*, 56, 118–124. 2.7.1, 5, 5.4.1

[262] Randjbar-Daemi, S., Salam, A., Sezgin, E., & Strathdee, J. A. (1985). An Anomaly Free Model in Six-Dimensions. *Phys. Lett.*, 151B, 351–356. 2.13.2, 11.5.2, 12.7.2

[263] Rangamani, M. & Takayanagi, T. (2017). Holographic Entanglement Entropy. *Lect. Notes Phys.*, 931, pp.1–246. 13

[264] Reed, M. & Simon, B. (1980). *Methods of modern mathematical physics. I.* Academic Press, Inc. [Harcourt Brace Jovanovich, Publishers], New York, second edition. Functional analysis. 3.1, 3.1.1, 3.1.10, 3.1.12, 3.1.13, 3.1.1, 3.1.17, 3.1.22, 3.1.3, 3.1.24, 3.1.3, 3.1.3, 3.3, 3.3.6, 15.2.1, 15.8.2

[265] Reeh, H. & Schlieder, S. (1961). Bemerkungen zur unitäräquivalenz von lorentzinvarianten feldern. *Il Nuovo Cimento (1955-1965)*, 22(5), 1051–1068. 14.1, 15.9

[266] Romans, L. J. (1986). Selfduality for Interacting Fields: Covariant Field Equations for Six-dimensional Chiral Supergravities. *Nucl. Phys.*, B276, 71. [,71(1986)]. 2

[Rössler] Rössler, D. Top chern class = euler characteristic. MathOverflow. URL:https://mathoverflow.net/q/73474 (version: 2011-08-23). 5.3.3

[268] Ryu, S. & Takayanagi, T. (2006). Holographic derivation of entanglement entropy from AdS/CFT. *Phys. Rev. Lett.*, 96, 181602. 3

[269] Sadov, V. (1996). Generalized Green-Schwarz mechanism in F theory. *Phys. Lett.*, B388, 45–50. 2, 2, 2.13, 2.13.2, 2.13.2, 2.13.2, 8.8, 9.6.3, V, 11.1, 12.1.5, 12.7.2, 12.7.2

[270] Sagnotti, A. (1992). A Note on the Green-Schwarz mechanism in open string theories. *Phys. Lett.*, B294, 196–203. 2, 2.13.2, 11.5.2

[271] Sathiapalan, B. (1987). Duality in Statistical Mechanics and String Theory. *Phys. Rev. Lett.*, 58, 1597. 1.1

[272] Schwarz, J. H. (1996). Anomaly - free supersymmetric models in six-dimensions. *Ph. Lett.*, B371, 223–230. 2, 2.13.2, 4

[273] Schwarz, J. H. (2001). Introduction to superstring theory. *NATO Sci. Ser. C*, 566, 143–187. 1.2, 1.2

[274] Scrucca, C. A. & Serone, M. (1999). Anomalies and inflow on D-branes and O - planes. *Nucl. Phys.*, B556, 197–221. III

[275] Sen, A. (1994). Strong - weak coupling duality in four-dimensional string theory. *Int. J. Mod. Phys.*, A9, 3707–3750. 1.1

[276] Sen, A. (1997a). F theory and the Gimon-Polchinski orientifold. *Nucl. Phys.*, B498, 135–155. 10.1

[277] Sen, A. (1997b). Orientifold limit of F theory vacua. *Phys. Rev.*, D55, R7345–R7349. 4.1, 4.2.5

[278] Serganova, V. V. & Skorobogatov, A. N. (2007). Del Pezzo surfaces and representation theory. *Algebra Number Theory*, 1(4), 393–419. 7.2.1

[279] Sethi, S., Vafa, C., & Witten, E. (1996). Constraints on low dimensional string compactifications. *Nucl. Phys.*, B480, 213–224. 2.7.1, 6, 4.3.7, III, 6.2.1, V, 12.1.3

[280] Shanks, D. (1974). The simplest cubic fields. *Math. Comp.*, 28, 1137–1152. 7

[281] Silverman, J. H. (1994). *Advanced topics in the arithmetic of elliptic curves*, volume 151 of *Graduate Texts in Mathematics*. Springer-Verlag, New York. 2.2.6, 9.1

[282] Sokal, A. D. (2011). A really simple elementary proof of the uniform boundedness theorem. *Amer. Math. Monthly*, 118(5), 450–452. 3.3.4

[283] Stanley, R. P. (1999). *Enumerative combinatorics. Vol. 2*, volume 62 of *Cambridge Studies in Advanced Mathematics*. Cambridge University Press, Cambridge. With a foreword by Gian-Carlo Rota and appendix 1 by Sergey Fomin. 5

[284] Strominger, A. & Vafa, C. (1996). Microscopic origin of the Bekenstein-Hawking entropy. *Phys. Lett.*, B379, 99–104. 1

[285] Summers, S. J. (2003). Tomita-Takesaki modular theory. 3.4.21

[286] Szydlo, M. G. (1999). *Flat regular models of elliptic schemes*. ProQuest LLC, Ann Arbor, MI. Thesis (Ph.D.)–Harvard University. 2.6, III, 1, 9.1, 11.1.5, 12.3.4

[287] Tachikawa, Y. (2016). Frozen singularities in M and F theory. *JHEP*, 06, 128. 8.1.6

[288] Takesaki, M. (1970). *Tomita's theory of modular Hilbert algebras and its applications*. Lecture Notes in Mathematics, Vol. 128. Springer-Verlag, Berlin-New York. 3.5.8

[289] Tatar, R. & Walters, W. (2012). GUT theories from Calabi-Yau 4-folds with SO(10) Singularities. *JHEP*, 12, 092. 12.3.4

[290] Tate, J. (1975). Algorithm for determining the type of a singular fiber in an elliptic pencil. (pp. 33–52. Lecture Notes in Math., Vol. 476). 2, 2, 2.2.6, III, III, IV, 8.1.1, 8.2.1, 8.2.3, 9.1, 3, 9.1, 12.2

[291] Tate, J. T. (1974). The arithmetic of elliptic curves. *Invent. Math.*, 23, 179–206. 4.2.2

[292] Vafa, C. (1996). Evidence for F theory. *Nucl. Phys.*, B469, 403–418. 2, 2.3.2, 2.6, III, IV

[293] Vafa, C. & Witten, E. (1995). A One loop test of string duality. *Nucl. Phys.*, B447, 261–270. 6

[294] van Ritbergen, T., Schellekens, A. N., & Vermaseren, J. A. M. (1999). Group theory factors for Feynman diagrams. *Int. J. Mod. Phys.*, A14, 41–96. 2.13.2

[295] Voisin, C. (2007). *Hodge theory and complex algebraic geometry. I*, volume 76 of *Cambridge Studies in Advanced Mathematics*. Cambridge University Press, Cambridge, english edition. Translated from the French by Leila Schneps. 5.6.4

[296] Volker, B. & Morrison, D. R. (2014). F-theory on Genus-One Fibrations. *JHEP*, 08, 132. 4.1, 4.2.3, 8

[297] Wall, A. C. (2014). Maximin Surfaces, and the Strong Subadditivity of the Covariant Holographic Entanglement Entropy. *Class. Quant. Grav.*, 31(22), 225007. 3

[298] Wang, C.-L. (2002). Cohomology theory in birational geometry. *J. Differential Geom.*, 60(2), 345–354. 2.9.2

[299] Wang, C.-L. (2003). *K*-equivalence in birational geometry and characterizations of complex elliptic genera. *J. Algebraic Geom.*, 12(2), 285–306. 2.9.2

[300] Wazir, R. (2004). Arithmetic on elliptic threefolds. *Compos. Math.*, 140(3), 567–580. 5, 2.8.2, 2.8.9, III, 8.1.1, 11.1.2

[301] Weigand, T. (2018). TASI Lectures on F-theory. 1.6, 7

[302] Weil, A. (1954). Remarques sur un mémoire d'Hermite. *Arch. Math. (Basel)*, 5, 197–202. 2.2.3

[303] Witten, E. (1982). An SU(2) Anomaly. *phys. Lett.*, B117, 324–328. [,230(1982)]. 12.1.5

[304] Witten, E. (1988). Topological Sigma Models. *Commun. Math. Phys.*, 118, 411. 1

[305] Witten, E. (1995). String theory dynamics in various dimensions. *Nucl. Phys.*, B443, 85–126. [,333(1995)]. 1.1, 1.2

[306] Witten, E. (1996). Phase transitions in M theory and F theory. *Nucl. Phys.*, B471, 195–216. 2, 2.12.2, 8.1.5, 8.1.6, 9.6.2, 11.1.6, 11.5.1, 11.5.2, 12.1.2, 12.7.1, 13.1.7

[307] Witten, E. (2018). APS Medal for Exceptional Achievement in Research: Invited article on entanglement properties of quantum field theory. *Rev. Mod. Phys.*, 90(4), 045003. 3, 3, 3.4.1, 3.5, 3.5, 12, 14.1, 14.4.1, 8, 14.4.3, 3, 15.2.1, 15.5, 15.8.1, 15.8.1, 15.8.2, 15.8.3, 15.9, 16